Topics in Geobiology 50

Andrzej Kaim
J. Kirk Cochran
Neil H. Landman *Editors*

Ancient Hydrocarbon Seeps

Springer

Topics in Geobiology 50

The Topics in Geobiology series covers the broad discipline of geobiology that is devoted to documenting life history of the Earth. A critical theme inherent in addressing this issue and one that is at the heart of the series is the interplay between the history of life and the changing environment. The series aims for high quality, scholarly volumes of original research as well as broad reviews.

Geobiology remains a vibrant as well as a rapidly advancing and dynamic field. Given this field's multidiscipline nature, it treats a broad spectrum of geologic, biologic, and geochemical themes all focused on documenting and understanding the fossil record and what it reveals about the evolutionary history of life. The Topics in Geobiology series was initiated to delve into how these numerous facets have influenced and controlled life on Earth.

Recent volumes have showcased specific taxonomic groups, major themes in the discipline, as well as approaches to improving our understanding of how life has evolved.

Taxonomic volumes focus on the biology and paleobiology of organisms – their ecology and mode of life – and, in addition, the fossil record – their phylogeny and evolutionary patterns – as well as their distribution in time and space.

Theme-based volumes, such as predator-prey relationships, biomineralization, paleobiogeography, and approaches to high-resolution stratigraphy, cover specific topics and how important elements are manifested in a wide range of organisms and how those dynamics have changed through the evolutionary history of life.

Comments or suggestions for future volumes are welcomed.

Neil H. Landman Department of Paleontology American Museum of Natural History New York, USA E-mail: landman@amnh.org

Peter J. Harries Department of Marine, Earth and Atmospheric Sciences North Carolina State University Raleigh, USA E-mail: pjharrie@ncsu.edu

Andrzej Kaim • J. Kirk Cochran
Neil H. Landman
Editors

Ancient Hydrocarbon Seeps

Springer

Editors
Andrzej Kaim
Institute of Paleobiology
Polish Academy of Sciences
Warszawa, Poland

J. Kirk Cochran
School of Marine and Atmospheric Sciences
Stony Brook University
Stony Brook, NY, USA

Neil H. Landman
Department of Invertebrate Paleontology
American Museum of Natural History
New York, NY, USA

Department of Invertebrate Paleontology
American Museum of Natural History
New York, NY, USA

ISSN 0275-0120
Topics in Geobiology
ISBN 978-3-031-05621-5 ISBN 978-3-031-05623-9 (eBook)
https://doi.org/10.1007/978-3-031-05623-9

This Springer imprint is published by the registered company Springer Nature Switzerland AG
The registered company address is: Gewerbestrasse 11, 6330 Cham, Switzerland

Artistic reconstruction of Early Cretaceous hydrocarbon seep. (Artist: Aleksandra Hołda-Michalska)

Preface

Chemoautotrophic communities in the modern oceans were discovered only relatively recently when Lonsdale (1977) reported the first hydrothermal vent communities at the Galapagos spreading center in the Pacific Ocean. Immediately afterwards, paleontologists started to look for fossil analogs of such communities. The first fossil counterpart of hydrothermal vents was described from the Cretaceous of Oman (Haymon et al. 1984). It turns out, however, that hydrothermal vents, especially those with preserved megafauna, are exceptionally rare in the fossil record. Much more common are fossil deposits and fossilized remains of the animals associated with hydrocarbon cold seeps. Modern hydrocarbon seeps were discovered in 1984 (Paull et al. 1984) and shortly thereafter were identified in the fossil record (Gaillard and Rollin 1986). Since then, the number of hydrocarbon seep sites across the globe and geological time has grown and now there are several dozen localities identified. By 2005, the number of ancient hydrocarbon seep sites reached 75 in Japan alone (Majima et al. 2005) and is still growing.

The first attempt to summarize our knowledge on fossil hydrocarbon seep and hydrothermal vent faunal associations was by Campbell et al. (2006), followed by a book edited by Steffen Kiel published in 2010. The latter volume, entitled *The Vent and Seep Biota*, mostly covered topics related to modern seeps and vents, and fossil seeps constituted only a small part. In the 11 years since that volume was published, new important seep sites have been discovered, spanning many parts of the geologic record (e.g., Peckmann et al. 2011, 2013; Kiel et al. 2017) and including little-known environments and geographical regions (e.g., Hammer et al. 2011; Hryniewicz et al. 2012, 2015, 2019, 2021; Landman et al. 2012; Agirrezabala et al. 2013; Kaim et al. 2013; Kiel et al. 2013, 2020; Kiel and Hansen 2015; Meehan and Landman 2016; Nobuhara et al. 2016). As well, many known seep localities have been studied in much greater detail. As a result, it seemed an appropriate time for a new volume focusing on ancient hydrocarbon seeps.

As we began to assemble the present volume, we asked regional geologists, stratigraphers, and paleontologists whether they had ever seen hydrocarbon seep deposits and their associated fauna during their fieldwork. They were mostly unfamiliar with what we were talking about, and we had to explain in detail the nature

of seep communities and how to recognize them. The same usually was true for undergraduates and graduate students. This reinforced our thinking that there was a need for a book that would not only summarize the available knowledge for specialists but also explain the topic to students as well as to the wider community of geologists and paleontologists and, at the same time, would be comprehensible to educated lay readers. We thought that a volume explaining the geochemical, geological, diagenetic, and evolutionary aspects of ancient chemoautotrophic communities would also be much appreciated by biologists and oceanographers researching modern hydrothermal vents and hydrocarbon seeps.

In this book, we review the biogeochemical processes involved in seep formation and describe the groups of organisms that lived in these communities. We cover the most common and widespread inhabitants of ancient hydrocarbon seeps (e.g., bivalves, brachiopods, and gastropods) as well as organisms that have not been comprehensively reviewed before (e.g., ammonoids, crustaceans, and sponges). We examine the evolution of seeps over time and document well-known and little-known occurrences of seep deposits around the world. Last but not least, we include a glossary with the most important terms in the investigation and description of ancient hydrocarbon seeps to make this subject more comprehensible to non-specialists. We hope that this book will facilitate further developments in the research of chemosynthesis-based communities.

Many people have helped in the production of this volume. Individual authors have added acknowledgments at the end of their respective chapters. Each chapter was reviewed by two scientists, and the editors are extremely grateful for their helpful reviews. We thank all the contributors to this book and in particular the referees Luis M. Agirrezabala, Kazutaka Amano, Denis Audo, Barbara Cavalazzi, J. Kirk Cochran, Selina R. Cole, Magdalena N. Georgieva, William Halligan, Liz Harper, Krzysztof Hryniewicz, Matúš Hyžný, Michał Jakubowicz, Dorte Janussen, Andrzej Kaim, Steffen Kiel, Tomáš Kočí, Crispin T.S. Little, Marcello Natalicchio, Miguel O. Manceñido, Royal H. Mapes, Yusuke Miyajima, Kristian P. Saether, Rossana Sanfilippo, Simon Schneider, Russell S. Shapiro, Daniel Smrzka, Olev Vinn, James D. Witts, Jennifer Zwicker, and one anonymous reviewer. The editors also thank Paula M. Mikkelsen for her excellent editorial assistance. Without all of you, this book would not have been possible.

We would also like to thank those individuals involved in the organization of two International Workshops on Ancient Hydrocarbon Seep and Cognate Communities held in Warsaw (Kaim et al. 2016) and Sapporo (Jenkins et al. 2019), which greatly facilitated the development of this book. Finally, the editors thank the publisher, in the persons of Zachary Romano and Kala Palanisamy, for their patience and cooperation in seeing this project through, especially during the difficult period of the Covid-19 pandemic.

References

Agirrezabala LM, Kiel S, Blumenberg M, Schäfer N, Reitner J (2013) Outcrop analogues of pockmarks and associated methane-seep carbonates: a case study from the Lower Cretaceous (Albian) of the Basque-Cantabrian Basin, western Pyrenees. Palaeogeogr Palaeoclimatol Palaeoecol 390:94–115

Campbell KA (2006) Hydrocarbon seep and hydrothermal vent paleoenvironments and paleontology: Past developments and future research directions. Palaeogeogr Palaeoclimatol Palaeoecol 232:362–407

Gaillard C, Rolin Y (1986) Paléobiocoenoses susceptibles d'être liées à des sources sous-marines en milieu sédimentaire. L'exemple des pseudobiohermes des Terres Noires (S. E. France) et des tepee buttes de la Pierre Shale Formation (Colorado, U.S.A.). CR Acad Sci Paris 303:1503–1508

Hammer Ø, Nakrem HA, Little CTS, Hryniewicz K, Sandy M., Hurum JH, Druckenmiller P, Knutsen EM, Høyberget M (2011) Hydrocarbon seeps from close to the Jurassic-Cretaceous boundary, Svalbard. Palaeogeogr Palaeoclimatol Palaeoecol 306:15–26

Haymon RM, Koski R, Sinclair C (1984) Fossils of hydrothermal vent worms from Cretaceous sulfide ores of the Samail ophiolite, Oman. Science 223:1407–1409

Hryniewicz K, Hammer Ø, Nakrem HA, Little CTS (2012) Microfacies of the Volgian–Ryazanian (Jurassic–Cretaceous) hydrocarbon seep carbonates from Sassenfjorden, central Spitsbergen, Svalbard. Norw J Geol 92:113–131

Hryniewicz K, Hagström J, Hammer Ø et al (2015) Late Jurassic–Early Cretaceous hydrocarbon seep boulders from Novaya Zemlya and their faunas. Palaeogeogr Palaeoclimatol Palaeoecol 436:231–244

Hryniewicz K, Amano K, Bitner MA et al (2019) A late Paleocene fauna from shallow-water chemosynthesis-based ecosystems, Spitsbergen, Svalbard. Acta Pal Pol 64:101–141

Hryniewicz K, Miyajima Y, Amano K et al (2021) Formation, diagenesis and fauna of cold seep carbonates from the Miocene Taishu Group of Tsushima (Japan). Geological Magazine 158: 964–984.

Jenkins RG, Kaim A, Kobayashi Y et al (2019) 2nd International Workshop on Ancient Hydrocarbon Seep and Cognate Communities. 13-15 June 2019, Sapporo, Japan. Abstract Book. Hokkaido University Museum, Japan

Kaim A, Skupien P, Jenkins RG (2013) A new Lower Cretaceous hydrocarbon seep locality from the Czech Carpathians and its fauna. Palaeogeogr Palaeoclimatol Palaeoecol 390:42–51

Kaim A, Bitner MA, Cochran JK et al (2016) 1st International Workshop on Ancient Hydrocarbon Seep and Cognate Communities. 13–17 June 2016, Warsaw, Poland. Abstract Book. Institute of Paleobiology, Warsaw

Kiel S (ed) (2010) The Vent and Seep Biota. Springer, Heidelberg

Kiel S, Tyler PA (2010) Chemosynthetically-driven ecosystems in the deep sea. In: Kiel S (ed) The Vent and Seep Biota. Topics in Geobiology, vol. 33. Springer, Heidelberg, pp. 1–14

Kiel S, Hansen BT (2015) Cenozoic Methane-Seep Faunas of the Caribbean Region. PLoS ONE 10(10):e0140788

Kiel S, Birgel D, Campbell KA, Crampton JS, Schiøler P, Peckmann P (2013) Cretaceous methane-seep deposits from New Zealand and their fauna. Palaeogeogr Palaeoclimatol Palaeoecol 390:17–34

Kiel S, Krystyn L, Demirtaş F et al (2017) Late Triassic mollusk-dominated hydrocarbon-seep deposits from Turkey. Geol 45: 751–754

Kiel, S, Hybertsen, F, Hyžný et al (2020) Mollusks and a crustacean from early Oligocene methane-seep deposits in the Talara Basin, northern Peru. Acta Palaeontol Pol 65:109–138

Landman NH, Cochran JK, Larson NL et al (2012) Methane seeps as ammonite habitats in the U.S. Western Interior Seaway revealed by isotopic analyses of well-preserved shell material. Geology 40:507–510

Lonsdale P (1977) Clustering of suspension-feeding macrobenthos near abyssal hydrothermal vents at oceanic spreading centers. Deep-Sea Res 24:857–863.

Majima R, Nobuhara T, Kitazaki T (2005) Review of fossil chemosynthetic assemblages in Japan. Palaeogeogr Palaeoclimatol Palaeoecol 227:86–123

Meehan KC, Landman NH (2016) Faunal associations in cold-methane seep deposits from the Upper Cretaceous Pierre Shale, South Dakota. Palaios 31:291–301

Nobuhara T, Onda D, Sato T et al (2016) Mass occurrence of the enigmatic gastropod *Elmira* in the Late Cretaceous Sada Limestone seep deposit in southwestern Shikoku, Japan. Paläontologische Zeitschrift 90:701–722

Paull CK, Hecker B, Commeau R, Freeman-Lynde RP, Neumann C, Corso WP, Golubic S, Hook JE, Sikes E, Curray J (1984) Biological communities at the Florida Escarpment resemble hydrothermal vent taxa. Science 226:965–967

Peckmann J, Kiel S, Sandy MR, Taylor DG, Goedert JL (2011) Mass occurrences of the brachiopod *Halorella* in Late Triassic methane-seep deposits, Eastern Oregon. J Geol 119:207-220

Peckmann J, Sandy MR, Taylor DG, Gier S, Bach W (2013) An Early Jurassic brachiopod-dominated seep deposit enclosed by serpentinite, eastern Oregon, USA. Palaeogeogr Palaeoclimatol Palaeoecol 390:4–16.

Warszawa, Poland — Andrzej Kaim
Stony Brook, NY, USA — J. Kirk Cochran
New York, NY, USA — Neil H. Landman

Contents

Contributors

Kazutaka Amano Department of Geoscience, Joetsu University of Education, Joetsu, Japan

Yusuke Ando Mizunami Fossil Museum, Mizunami, Gifu, Japan

Andrzej Baliński Institute of Paleobiology, Polish Academy of Sciences, Warszawa, Poland

Zdzisław Belka Isotope Research Unit, Adam Mickiewicz University, Poznań, Poland

Błażej Berkowski Institute of Geology, Adam Mickiewicz University, Poznań, Poland

Maria Aleksandra Bitner Institute of Paleobiology, Polish Academy of Sciences, Warszawa, Poland

Jamie Brezina Department of Mining Engineering & Management, South Dakota School of Mines and Technology, Rapid City, SD, USA

Kathleen A. Campbell School of Environment, Faculty of Science, University of Auckland, Auckland, New Zealand

J. Kirk Cochran School of Marine & Atmospheric Sciences, Stony Brook University, Stony Brook, NY, USA

Department of Invertebrate Paleontology, American Museum of Natural History, New York, NY, USA

David A. Francis Geological Research Ltd, Lower Hutt, New Zealand

Matthew P. Garb Department of Earth and Environmental Sciences, Brooklyn College, Brooklyn, NY, USA

Magdalena N. Georgieva Department of Life Sciences, Natural History Museum, London, UK

Fiona L. Gill School of Earth & Environment, University of Leeds, Leeds, UK

Krzysztof Hryniewicz Institute of Paleobiology, Polish Academy of Sciences, Warszawa, Poland

Michał Jakubowicz Isotope Research Unit, Adam Mickiewicz University, Poznań, Poland

Robert G. Jenkins Faculty of Geosciences and Civil Engineering, Institute of Science and Engineering, Kanazawa University, Kanazawa, Japan

Andrzej Kaim Institute of Paleobiology, Polish Academy of Sciences, Warszawa, Poland

Steffen Kiel Department of Palaeobiology, Swedish Museum of Natural History, Stockholm, Sweden

Adiël A. Klompmaker Department of Museum Research and Collections & Alabama Museum of Natural History, The University of Alabama, Tuscaloosa, AL, USA

Neil H. Landman Department of Invertebrate Paleontology, American Museum of Natural History, New York, NY, USA

Neal L. Larson Larson Paleontology Unlimited, Keystone, SD, USA

Crispin T. S. Little School of Earth and Environment, University of Leeds, Leeds, UK

Kimberly C. Meehan Department of Geology, University at Buffalo, Buffalo, NY, USA

Yusuke Miyajima Research Institute for Geo-Resources and Environment, Geological Survey of Japan, National Institute of Advanced Industrial Science and Technology (AIST), Tsukuba, Japan

Corinne Myers Department of Earth and Planetary Sciences, University of New Mexico, Albuquerque, NM, USA

Jone Naujokaityte Department of Earth and Environmental Sciences, Brooklyn College, Brooklyn, NY, USA

Department of Earth and Planetary Sciences, University of New Mexico, Albuquerque, NM, USA

Campbell S. Nelson School of Science (Earth Sciences), University of Waikato, Hamilton, New Zealand

Torrey Nyborg Department of Earth and Biological Sciences, Loma Linda University, Loma Linda, CA, USA

Andrzej Pisera Institute of Paleobiology, Polish Academy of Sciences, Warszawa, Poland

Ana Rashkova Department of Invertebrate Paleontology, American Museum of Natural History, New York, NY, USA

Kristian P. Saether Hull, UK

Russell S. Shapiro Department of Geological and Environmental Sciences, CSU, Chico, CA, USA

Tina Treude Department of Earth, Planetary, and Space Sciences, Department of Atmospheric and Oceanic Sciences, University of California, Los Angeles (UCLA), Los Angeles, CA, USA

Olev Vinn Institute of Ecology and Earth Sciences, University of Tartu, Tartu, Estonia

James D. Witts School of Earth Sciences, University of Bristol, Bristol, UK

Part I
Biogeochemical Processes

Chapter 1
Geochemistry of Cold Hydrocarbon Seeps: An Overview

J. Kirk Cochran, Neil H. Landman, Michał Jakubowicz, Jamie Brezina, Jone Naujokaityte, Ana Rashkova, Matthew P. Garb, and Neal L. Larson

J. K. Cochran (✉)
School of Marine and Atmospheric Sciences, Stony Brook University, Stony Brook, NY, USA

Department of Invertebrate Paleontology, American Museum of Natural History, New York, NY, USA
e-mail: kirk.cochran@stonybrook.edu

N. H. Landman · A. Rashkova
Department of Invertebrate Paleontology, American Museum of Natural History, New York, NY, USA
e-mail: landman@amnh.org; arashkova@amnh.org

M. Jakubowicz
Isotope Research Unit, Adam Mickiewicz University, Poznań, Poland
e-mail: mjakub@amu.edu.pl

J. Brezina
Department of Mining Engineering and Management, South Dakota School of Mines and Technology, Rapid City, SD, USA

J. Naujokaityte
Department of Earth and Planetary Sciences, University of New Mexico, Albuquerque, NM, USA
e-mail: jnaujokaityte@unm.edu

M. P. Garb
Department of Earth and Environmental Sciences, Brooklyn College, Brooklyn, NY, USA
e-mail: mgarb@brooklyn.cuny.edu

N. L. Larson
Larson Paleontology Unlimited, Keystone, SD, USA
e-mail: neal@larsonpaleo.com

A. Kaim et al. (eds.), *Ancient Hydrocarbon Seeps*, Topics in Geobiology 50,
https://doi.org/10.1007/978-3-031-05623-9_1

1.1 Introduction

Cold methane or hydrocarbon seeps have been documented throughout the Phanerozoic, with the oldest deposits dating to ~635 Ma (Bristow and Grotzinger 2013; Shields et al. 2007; Kennedy et al. 2008; Fig. 1.1). They are typically recognized by unusual carbonate concretionary deposits with isotopically low $\delta^{13}C$ signatures (<−30‰ VPDB), mineralogies ranging from Mg-calcite to aragonite, and unusual morphologies (e. g., pipes, crusts, isolated masses). The fundamental process operating at seeps is the anaerobic oxidation of methane (AOM), mediated by a consortium of anaerobic methanotrophic archaea (ANME) and sulfate-reducing bacteria (SRB; Boetius et al. 2000). This chapter explores in detail the conditions and pathways by which AOM occurs and the related co-occurring biogeochemical processes, including methanogenesis, organoclastic sulfate reduction, iron reduction, and sedimentary pyrite formation, that lead to the features observed at present-day methane seeps and aid in the interpretation of similar features at fossil seeps. As well, we discuss the application of selected isotope (C, O, Sr, Nd) and elemental systems (rare earth elements, Fe, Mn, Sr, Mg) to seep carbonates. These data provide critical information about the composition of the fluids feeding the hydrocarbon system, validation of methane-derived carbon in the system, temperature of carbonate formation, and constraints on fluid circulation.

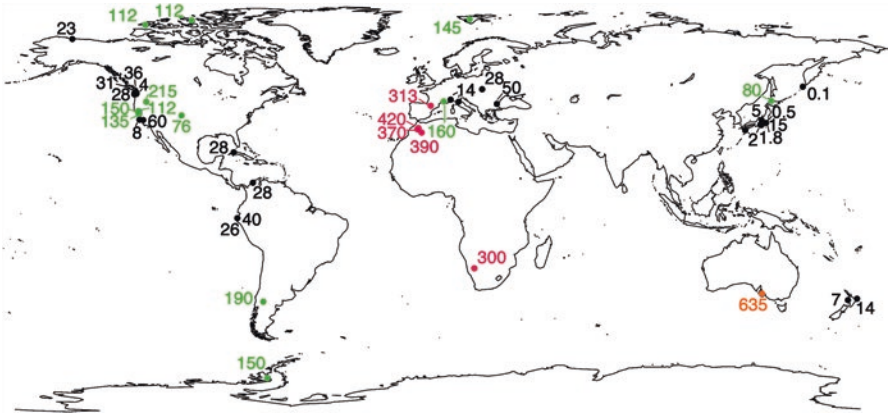

Fig. 1.1 Map of ancient methane seep locations and ages (in Ma). Precambrian cold seep carbonates lack the distinctive low $\delta^{13}C$ signatures that are characteristic of younger seeps (<200 Ma), likely due to lower seawater sulfate and higher dissolved inorganic carbon concentrations. Color coding of ages: Precambrian, *orange*; Paleozoic, *red*; Mesozoic, *green*; Cenozoic, *black*. Some dots represent multiple seeps. (Modified from Bristow and Grotzinger (2013) and reprinted with permission of the Geological Society of America. For a more complete listing of the global distribution of seeps, see Hryniewicz this volume-b)

1.2 The Redox Cascade

Microbes oxidize the carbon in organic matter (herein represented as CH_2O) in marine sediments during early diagenesis using a sequence of electron acceptors: O_2, NO_3^-, Mn^{4+} (as MnO_2), Fe^{3+} (e.g., as FeOOH), and SO_4^{2-}, in what is termed the "redox cascade." The sequence is determined by the standard state free energy change associated with each reaction, with aerobic oxidation producing the greatest energy yield (Berner 1980). An important reaction in this sequence is the organoclastic reduction of pore water sulfate by sulfate-reducing bacteria (e.g., *Desulfovibrio* sp.) to produce bicarbonate ions and hydrogen sulfide (Fig. 1.2):

$$SO_4^{2-} + 2CH_2O \rightarrow 2HCO_3^- + H_2S \tag{1.1}$$

Sulfate reduction via Reaction 1.1 occurs in the upper decimeters to meters of the sediment, depending on the amount and lability of organic matter in the sediment, as well as the sulfate concentration. Figure 1.3a shows how the depth of sulfate reduction varies globally. Organic-rich coastal and ocean margin sediments show depletion of sulfate at shallower depths in the sediment column relative to organic-poor deep-sea sediments.

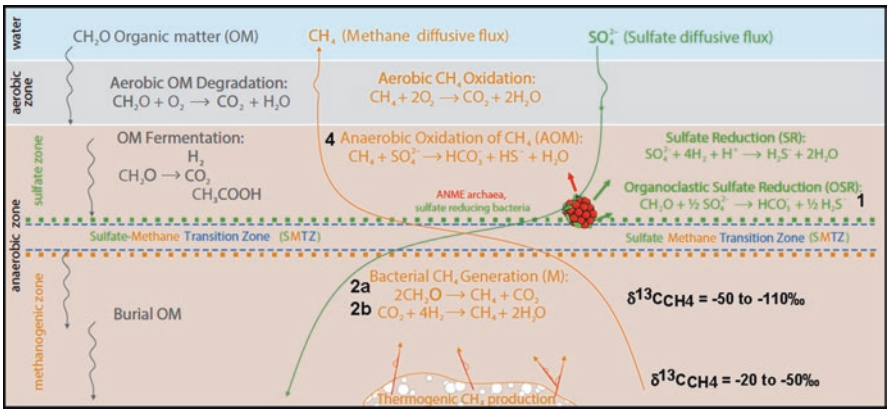

Fig. 1.2 Schematic diagram showing microbially mediated processes of organic matter transformation in marine sediments. Methane is produced at depth in the sediments (biogenically via Reactions 1.2a, 1.2b, and 1.2c) and 1.3 or thermogenically), while organoclastic sulfate reduction (Reaction 1.1) is a major pathway by which organic matter is oxidized in the "sulfate zone." Methane diffuses upward (orange arrow), encounters residual sulfate in the "sulfate-methane transition zone" (SMTZ), and promotes anaerobic oxidation of methane (AOM) (Reaction 1.4). Production of bicarbonate via AOM drives precipitation of authigenic seep carbonates (text Reaction 1.5, not shown in figure). Methane that escapes oxidation via AOM can be oxidized aerobically in the aerobic zone or in overlying oxic waters. Bold numbers refer to Reactions (1.x) in text. (Modified from Matveeva et al. 2015; Used under Creative Commons License; https://creativecommons.org/licenses/by/4.0/)

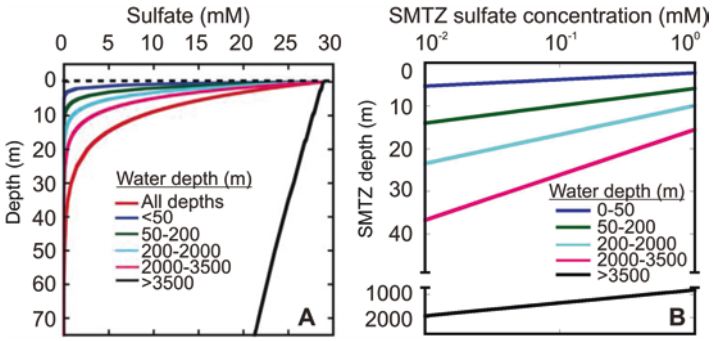

Fig. 1.3 (**a**) Pore water sulfate vs. depth in sediment deposited at different depths of water. The variation reflects the rate of sulfate reduction, in turn a function of the availability of organic matter (OM) and alternate electron acceptors that drive OM oxidation. (**b**) Average depth (m) of the sulfate-methane transition zone (SMTZ) as a function of SMTZ sulfate concentrations (in mM). In shallow-water, organic-rich sediments, the SMTZ is located close to the sediment-water interface, while in deeper water, it may be 10s of meters below. (Reprinted from Bowles et al. 2014 with permission from AAAS)

As sulfate is depleted in sediment pore water, a final step in organic matter decomposition involves the production of methane via a net reaction that is effectively the disproportionation of carbon in organic matter (represented here as CH_2O) by methanogenic archaea:

$$2CH_2O \rightarrow CO_2 + CH_4 \tag{1.2a}$$

Reaction 1.2a involves the coupling of organic matter oxidation to CO_2 and hydrogen in fermentation with the reaction of CO_2 with H_2 to yield methane (Berner 1980; Fig. 1.2):

$$2CH_2O + 2H_2O \rightarrow 2CO_2 + 4H_2 \tag{1.2b}$$

$$4H_2 + CO_2 \rightarrow CH_4 + 2H_2O \tag{1.2c}$$

An alternate pathway for methane production involves acetate disproportionation (Sansone and Martens 1981; Ferry 1992; Burdige 2006):

$$CH_3COOH \rightarrow CO_2 + CH_4 \tag{1.3}$$

Methane produced by Reactions 1.2a, b, c and 1.3 is termed "biogenic" to differentiate it from the production of "thermogenic" methane from deeply buried organic matter subjected to elevated temperatures and pressures (Fig. 1.2). Reactions 1.2 and 1.3 involve a large fractionation in stable carbon isotopes between marine organic matter ($\delta^{13}C \sim -20‰$) and the products CO_2 and CH_4. The methane so produced has a carbon isotope composition that is lower than that of the organic matter ($\delta^{13}C \sim -20$ to $-50‰$ for thermogenic methane and -50 to $-110‰$ for biogenic methane; Whiticar 1999), while the CO_2 has $\delta^{13}C$ values ranging from +5 to +24‰.

Under certain combinations of pressure (elevated) and temperature (low), methane can become incorporated into methane hydrates, a combination of water and methane molecules in a solid cage-like structure (Matsumoto 2001; Bohrmann and Torres 2006). Methane hydrates are stable under conditions of low temperature and high pressure, such as encountered in sediments accumulating in several hundred meters of water or deeper, as well as at depth in deep-sea sediments (Matsumoto 2001; Bohrmann and Torres 2006). Outside of the zone of gas hydrate stability (e.g., in shallow shelf sediments), methane is not present associated with hydrates and is dissolved in the pore water or perhaps is exsolved as gas bubbles.

1.3 Methane Oxidation

The upward migration of dissolved methane in sediments by advective or diffusive transport makes it susceptible to oxidation. This can be carried out aerobically if methane diffuses into the oxic zone of the sediments (Fig. 1.2), or anaerobically by the process of anaerobic methane oxidation (AOM), which involves a symbiotic consortium between several clades of anaerobic methanotrophic archaea (ANME; ANME-1, ANME-2, and ANME-3) and sulfate-reducing bacteria (Knittel and Boetius 2009) via the reaction:

$$CH_4 + SO_4^{2-} \rightarrow HCO_3^- + HS^- + H_2O \tag{1.4}$$

As noted above, the methane oxidized via AOM has a low $\delta^{13}C$ value, and this is imprinted on the produced HCO_3^- and, thus, on the dissolved inorganic carbon (DIC) reservoir of the pore fluids. Modern and ancient seep carbonates typically show low $\delta^{13}C$ values as a consequence of precipitation from this ^{12}C-enriched DIC reservoir (see Sect. 1.6.1).

Sulfate is a necessary reactant for AOM via Reaction 1.4, and given the independent organoclastic reduction of sulfate to oxidize organic matter (Reaction 1.1; Figs. 1.2 and 1.3a), AOM takes place in a region termed the "sulfate-methane transition zone" (SMTZ; Fig. 1.2), i.e., the depth region in the sediment column in which both sulfate and methane co-exist. For seeps occurring in relatively shallow water, this is likely to be close (within a few meters) to the sediment-water interface; conversely, sediments in deeper water have deeper SMTZ depths in the sediment (Fig. 1.3b; Bowles et al. 2014). This is due to lower concentrations of labile organic matter and slower rates of methane production and sulfate reduction. The depth and thickness of the SMTZ also depend on the transport mechanisms for sulfate and methane in the pore fluid. Figures 1.2 and 1.3 depict the situation when molecular diffusion controls the transport of these chemical species – downward diffusion (+ reaction) of sulfate from its source in the overlying water and upward diffusion (+ reaction) of methane produced at depth in the sediment. Advective (or effusive) transport of pore fluid in the sediment may also occur, for example, through extensive bio-irrigation of burrows by infauna. Tectonic activity such as faulting (Sample

et al. 1993) or sediment compaction and dewatering at subduction zones (Han et al. 2004) may also facilitate transport of pore fluids through the deposit and displace the SMTZ upward toward the sediment-water interface.

In addition to AOM via a consortium of ANME and sulfate-reducing bacteria, several alternative pathways of microbial AOM have been documented (Joye 2012). These include AOM via reduction of manganese (or iron) oxide (Beal et al. 2009), bacterial AOM by disproportionation of nitrite (NO_2^-; Ettwig et al. 2010), and AOM by ANME-2 accompanied by disproportionation of sulfate to disulfide (Milucka et al. 2012). The significance of the latter process is that it can be carried out by methanotrophic archaea alone, without the associated bacteria. However, most AOM in marine sediments takes place via Reaction 1.4 with the consortium of methanotrophic archaea and sulfate-reducing bacteria.

The concentration of seawater sulfate has varied with time over Earth history (Planavsky et al. 2012), and the dependence of AOM on sulfate may in part account for the abundance of seeps over time (Bristow and Grotzinger 2013). In particular, seawater sulfate concentrations have been >5 mM in the last ~350 Ma, and seep abundance is more evident over this time (Planavsky et al. 2012). Indeed, Kiel (2015) has proposed that variable seawater sulfate concentrations are responsible for the evolution of deep-sea seep ecosystems over the past 150 Ma. This was a

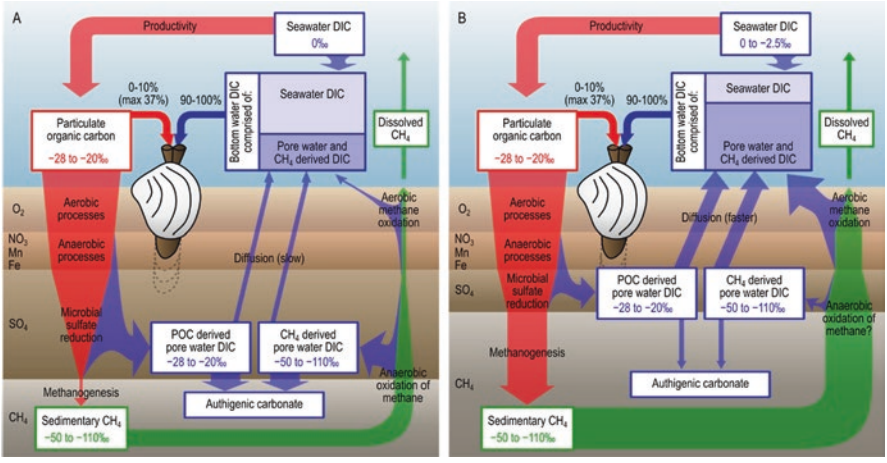

Fig. 1.4 Conceptual model of the sedimentary carbon cycle under high and low sulfate conditions. Conceptual diagram of fluxes of POC (red), DIC (blue), and methane (green) under (**a**) modern high sulfate conditions and (**b**) Cretaceous lower sulfate conditions. Thickness of arrows represents relative strength of flux to each reservoir (not to scale). Depth scales are arbitrary; bottom-water reservoir refers to the benthic boundary layer sampled by bivalves and is likely to be only 5–10 cm in depth. The depth of the sulfate reduction zone is variable in modern marine sediments, depending on factors such as diffusion and bioturbation (see Fig. 1.3). Bivalves, living on or in the sediment, incorporate carbon from both the DIC (90–100%), and metabolic carbon (0–10%) reservoirs into their shells. Reactions corresponding to the processes illustrated are shown in Fig. 1.2 and given in the text. (From Hall et al. 2018; used under Creative Commons License, https://creativecommons.org/licenses/by/4.0/)

period over which seawater sulfate concentrations more than doubled from ~10 mM to the present value of 28 mM. Lower concentrations of sulfate in the past (e.g., Cretaceous) may have shifted the redox cascade in favor of methanogenesis and possibly allowed the SMTZ to move closer to the sediment-water interface (Hall et al. 2018). Figure 1.4 shows this effect, through a comparison of two seep systems with different seawater sulfate concentrations representing the modern and Cretaceous ocean (Hall et al. 2018).

1.4 Seep Carbonate Formation

A consequence of AOM is an increase in the dissolved inorganic carbon reservoir (through production of HCO_3^-) leading to supersaturation with respect to $CaCO_3$ and the precipitation of authigenic carbonates:

$$2HCO_3^- + Ca^{2+} \rightarrow CaCO_3 + CO_2 + H_2O \quad (1.5)$$

The carbonate minerals formed via Reaction 1.5 include microcrystalline high-Mg (>5% Mg) calcite, as well as dolomite, aragonite, and iron-rich carbonates (Stakes et al. 1999; Campbell et al. 2002; Greinert et al. 2002; Luff and Wallmann 2003; Mazzini et al. 2004; Reitner et al. 2005; Naehr et al. 2007; Pierre et al. 2014; Hryniewicz this volume-a). Transformations during burial and later in diagenesis can yield low-Mg calcite (Joseph et al. 2013).

Morphologies of the precipitated carbonates vary widely and include crusts (Luff et al. 2004), strata-bound carbonate layers (Natalicchio et al. 2012), small rod- and dumbbell-shaped concretions (Reitner et al. 2005), tubes and pipes (Cochran et al. 2015; Cavagna et al. 2015), and massive limestones (Michaelis et al. 2002; Reitner et al. 2005; Wiese et al. 2015; Smrzka et al. 2017; Miyajima et al. 2018; Hryniewicz this volume-a). These variations reflect the nature of methane transport through the sediment (diffusive vs. advective transport), rates of transport, rates of AOM, position of the SMTZ, and the temporal evolution of a seep system (Stakes et al. 1999; Naehr et al. 2007; Luff and Wallmann 2003; Luff et al. 2004; Pierre et al. 2014; Miyajima et al. 2018).

1.5 Iron and Sulfur Cycling at Seeps

As noted above, Fe^{3+} is used as an electron acceptor utilized by bacteria to oxidize organic matter during early diagenesis (Berner 1980):

$$CH_2O + 7H^+ + 4FeOOH \rightarrow 4Fe^{2+} + HCO_3^- + 6H_2O \quad (1.6)$$

As a consequence, dissolved hydrogen sulfide and reduced Fe^{2+} (produced via Reactions 1.1, 1.4, and 1.6) can react to form iron monosulfides and, subsequently, phases such as pyrite (FeS_2) and greigite (Fe_3S_4). Indeed, if Fe reduction and AOM occur in close proximity in the sediment column, Peckmann et al. (2003) and Peckmann and Thiel (2004) have proposed that Reactions 1.4 and 1.6 can be coupled:

$$4CH_4 + CH_2O + 4SO_4^{2-} + 4FeOOH + 3H^+ \rightarrow 5HCO_3^- + 4FeS + 10H_2O \quad (1.7)$$

The combined reaction promotes carbonate precipitation (via Reaction 1.5) as well as FeS formation and may help explain the presence of iron sulfides within carbonate nodules in some seep deposits (e.g., Peckmann and Thiel 2004).

AOM is by definition an anaerobic process and, thus, not one that occurs in oxic water columns above seep sites. The formation of carbonates at most modern cold seeps is, thus, confined to the sediments, although often near the sediment-water interface. Carbonate build-ups (i.e., chemoherms; Aharon 1994) in the water column are mostly limited to anoxic basins such as the Black Sea (Michaelis et al. 2002). Where carbonate crusts, pinnacles, or chimneys are presently observed in oxic water columns, as at the Amon mud volcano on the Nile deep-sea fan in the Mediterranean, they are hypothesized to have formed at a time when the bottom water was suboxic or anoxic (Bayon et al. 2013) or, as in the Adriatic Sea, at an earlier time with subsequent exhumation (Angeletti et al. 2015).

An alternate mechanism for the development of chemoherms above the sediment-water interface in oxic waters has been proposed by Teichert et al. (2005). Their observations of such deposits on Hydrate Ridge on the Cascadia margin show the presence of sulfur-oxidizing bacterial mats (of the genus *Beggiatoa*) covering the deposit. The intense production of hydrogen sulfide via AOM, as well as from organoclastic sulfate reduction, provides a source of sulfide for such bacteria. Indeed, *Beggiatoa* sp. can use dissolved O_2 to oxidize sulfide and form organic matter (Jørgensen and Nelson 2004; Schwedt et al. 2012) as:

$$4H_2S + 7O_2 + CO_2 + H_2O \rightarrow 4SO_4^{2-} + CH_2O + 8H^+ \quad (1.8)$$

Although Reaction 1.8 produces acid (H^+) that might inhibit AOM-produced carbonate precipitation (or indeed dissolve carbonates so produced; Peckmann et al. 2004), Teichert et al. (2005) proposed that *Beggiatoa* mats form a microenvironment below which the AOM consortium can operate above the sediment-water interface and carbonate chimneys can, thus, form within an oxic water column. Such microenvironments might permit spatial decoupling of the protons from Reaction 1.8 and the alkalinity produced by AOM (Reaction 1.4), as proposed by Bailey et al. (2009). Peckmann et al. (2004) also documented seep carbonates associated with *Beggiatoa* in a Miocene seep limestone in Italy and concluded that rapid changes from oxic to anoxic conditions facilitated precipitation.

Alternatively, sulfide-oxidizing bacteria can use nitrite (Ettwig et al. 2010) or nitrate as an oxidant (Sayama 2001; Jørgensen and Nelson 2004; Preisler et al. 2007; Himmler et al. 2018):

$$HS^- + NO_3^- + H^+ + H_2O \rightarrow SO_4^{2-} + NH_4^+ \quad (1.9)$$

Reaction 1.9 has been linked to the sulfide-oxidizing bacterium *Thioploca*, and, because it increases the pH, its coupling with the increase in alkalinity produced by AOM (Reaction 1.4) can lead to precipitation of carbonate with a microbial stromatolitic fabric (Himmler et al. 2018).

1.6 Isotope Geochemistry of Cold Seeps

1.6.1 Carbon and Oxygen Isotopes in Seep Carbonates

The delta (δ)-notation for expressing carbon and oxygen isotope ratios involves measurement of the abundance ratios $^{13}C/^{12}C$ or $^{18}O/^{16}O$ in a sample (R_{sample}) and referring them to those of a standard ($R_{standard}$), with values expressed as permil (‰):

$$\delta = \left(R_{sample} / R_{standard} - 1\right) \times 1000 \quad (1.10)$$

The standard used for carbonate O and C isotope notation is historically "Pee Dee Belemnite" or PDB, a fossil cephalopod from the Pee Dee Formation in South Carolina. Once this standard was used up, the measurements were calibrated against standards referable to its laboratory equivalent, Vienna Pee Dee Belemnite (VPDB). Temperature applications express the $\delta^{18}O$ of the water in terms of the seawater standard, Standard Mean Ocean Water or SMOW.

As noted earlier in this chapter, the production of methane by methanogens (Reaction 1.2a) is accompanied by a large C isotope fractionation relative to the carbon isotope composition of the original organic matter (Campbell 2006). The methane so produced is enriched in ^{12}C ($\delta^{13}C = -50$ to -110‰), and the residual CO_2 is enriched in ^{13}C ($\delta^{13}C = +5$ to $+24$‰). Thermogenic methane is enriched in ^{12}C as well but to a lesser extent ($\delta^{13}C = -20$ to -50‰). AOM transfers carbon from methane to the DIC reservoir, imprinting it with low $\delta^{13}C$ values. Carbonates at modern seeps that precipitate from AOM-derived DIC typically have low $\delta^{13}C$ values, and low $\delta^{13}C$ values in presumed fossil seep carbonates are taken as prima facie evidence that the sites indeed represent fossil cold seeps. Additional evidence comes from the molecular fossil inventory in seep-associated carbonates that attest to the presence of lipid biomarkers diagnostic for archaea and bacteria involved in AOM, whose compound-specific carbon isotopes show $\delta^{13}C$ values as low as −120‰ (Peckmann et al. 1999, 2002; Greinert et al. 2002; Elvert et al. 2005: Birgel et al. 2006; Hagemann et al. 2012; Little et al. 2015; Miyajima et al. 2018). A detailed

review of biomarkers at ancient hydrocarbon seeps is beyond the scope of this overview, but the reader is referred to the review by Miyajima and Jenkins (this volume).

During the precipitation of seep carbonates close to the sediment-water interface, other sources of C can contribute to the DIC reservoir and be reflected in the $\delta^{13}C$ values of authigenic carbonates. These additional sources include seawater DIC (−2 to +2‰), C from decomposition of sedimentary organic matter (~−20‰), and a residual CO_2 pool from methanogenesis (+5 to +24‰). The admixture of these sources can produce seep carbonates with a wide range of $\delta^{13}C$ signatures (Natalicchio et al. 2012). For example, Campbell et al. (2002) tabulated $\delta^{13}C$ values ranging from −61‰ to +9‰ in authigenic carbonates from 14 modern seeps. $\delta^{13}C$ values significantly greater than that of ambient DIC likely indicate the incorporation of C from residual CO_2 produced by methanogenesis (Naehr et al. 2007; Roberts et al. 2010). Peckmann and Thiel (2004) suggested that this might occur later in the diagenetic sequence of seep carbonate formation.

The isotope composition of oxygen in seep carbonates also can provide information on the origin of the carbonates. A principal control on $\delta^{18}O$ is the temperature of formation via the well-established temperature-dependent isotope equilibria between O in the water and the precipitated carbonates (Anderson and Arthur 1983; Grossman and Ku 1986; Hudson and Anderson 1989; Stakes et al. 1999), where

$$T(°C) = 16.0 - 4.14\left(\delta^{18}O_c - \delta^{18}O_w\right) + 0.13\left(\delta^{18}O_c - \delta^{18}O_w\right)^2 \quad (1.11)$$

is the temperature equation used for calcite (c) (Anderson and Arthur 1983) and

$$T(°C) = 19.7 - 4.34\left(\delta^{18}O_a - \delta^{18}O_w\right) \quad (1.12)$$

is that for aragonite (a) (Grossman and Ku 1986, as modified by Hudson and Anderson 1989 to express $\delta^{18}O_w$ in terms of SMOW).

The values of $\delta^{18}O_{c,a}$ in Eqs. 1.11 and 1.12 are expressed relative to the VPDB standard (see Eq. 1.10), while that of the water ($\delta^{18}O_w$) is relative to Standard Mean Ocean Water (SMOW). Thus, both mineralogy and fluid composition are factors in these isotope temperature equations. In the case of methane seeps, deep formation waters, including clay dewatering, and water released from the destabilization of methane hydrates can be enriched in ^{18}O and can imprint carbonates with higher $\delta^{18}O$ values than might be predicted from equilibrium precipitation at the ambient temperature of bottom seawater (e.g., Naehr et al. 2007).

An example of the variation in $\delta^{13}C$ and $\delta^{18}O$ observed in ancient seeps is shown in the cross-plot in Fig. 1.5. These data are from authigenic carbonates from seep deposits in the Upper Cretaceous (Campanian) Pierre Shale of North America, which formed in the Western Interior Seaway (WIS) (see Landman et al. this volume, for a list of site localities and more detail on these seeps deposits; data are given in Appendix Table 1.1. These data reveal a broad range in $\delta^{13}C$ values from −5 to −48‰ and a more restricted range in $\delta^{18}O$ values (−0.2 to −1.2‰). The mineralogy is dominated by high-Mg calcite and occasional sparry calcite veins that are the

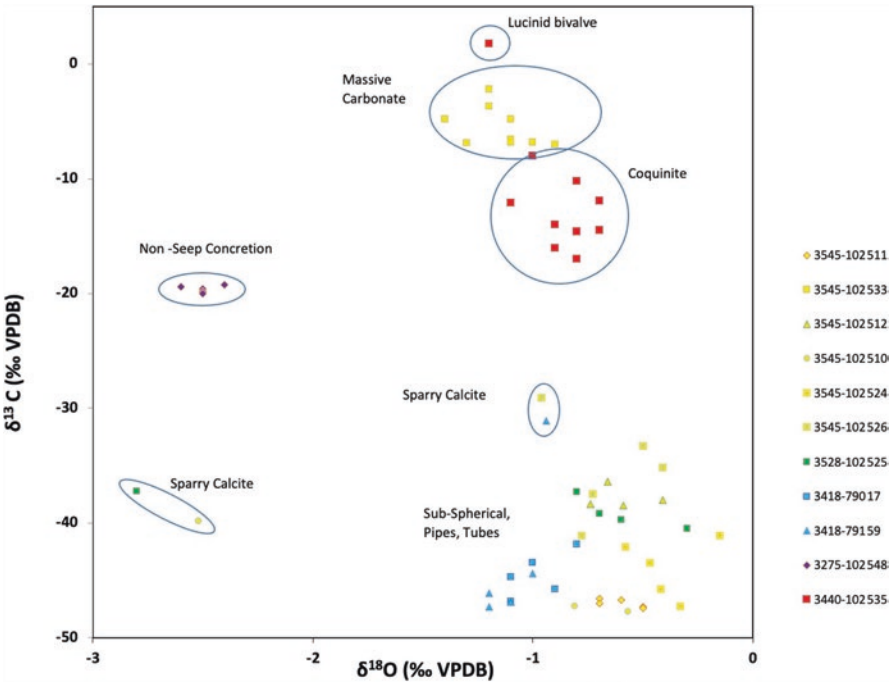

Fig. 1.5 Cross-plot of $\delta^{13}C$ and $\delta^{18}O$ in well-preserved authigenic carbonates from seep deposits collected in the Upper Cretaceous (Campanian) Pierre Shale, South Dakota, USA (Appendix Table 1.1). Seep concretions show a range of $\delta^{13}C$ from ~−48‰ to ~−2‰ (VPDB), reflecting mixtures of different sources of DIC to the precipitated carbonate. Sparry calcite veins in the carbonates are products of later-stage diagenesis. Also plotted are values from a non-seep concretion (AMNH loc. 3275) and lucinid bivalve (AMNH loc. 3440). See text for discussion and Landman et al. (this volume) for information on AMNH localities. Symbols are numbered according to the four-digit AMNH locality, followed by the specimen number. AMNH loc. 3418 is in the *Didymoceras cheyennense* Zone ~74.7 Ma; locs. 3275, 3528, and 3545 are in the *Baculites compressus-B. cuneatus* Zone (~73.5 Ma); and loc. 3440 is in the *Baculites scotti-Didymoceras nebrascense* Zone (~75.6–75.2 Ma)

product of later diagenesis (Handle 2014; Landman et al. 2012; Cochran et al. 2015). Many of the data in Fig. 1.5 were obtained by sequential sampling of seep concretions from the outer surface inward (see Appendix Table 1.1. Variations can be explained by a paragenetic sequence of precipitation as noted by Zwicker et al. (2015; see below). Also shown in Fig. 1.5 are values of $\delta^{13}C$ and $\delta^{18}O$ from a concretion from an age-equivalent non-seep site in the Pierre Shale. These values are distinctly different from those of the seep carbonates and suggest different mechanisms of formation, with precipitation in non-seep concretions associated with organic matter decomposition (e.g., Berner 1968). Concretions with the lowest $\delta^{13}C$ values in Fig. 1.5 are from small, sub-spherical concretions and pipes. Pipes likely formed as AOM proceeded and carbonates precipitated around burrows or methane bubble tubes (Krause et al. 2009; Zwicker et al. 2015), and the high concentration of

methane ensured a strong imprint of methane-derived bicarbonate in the DIC reservoir and precipitated carbonates (Zwicker et al. 2015).

In contrast, massive concretionary bodies and coquinites consisting of cemented layers of *Inoceramus* shells from seep deposits in the Pierre Shale likely formed at or close to the sediment-water interface. As a result, the DIC reservoir from which they formed reflects a mixture of methane-derived DIC and overlying water DIC. Landman et al. (2018) used the $\delta^{13}C$ in well-preserved shells of seep and non-seep ammonites to estimate that the $\delta^{13}C$ of the DIC in the overlying water was +2.7‰ at non-seep sites but was several permil lower, ~ −0.7‰, at seep sites. Additional sources of ^{13}C-enriched DIC include those linked to methanogenesis. The $\delta^{18}O$ values of all the seep carbonates illustrated in Fig. 1.5 suggest precipitation at temperatures typical of bottom water in the WIS, ~20 to 27 °C.

Naehr et al. (2007) observed similar $\delta^{13}C$ and $\delta^{18}O$ patterns in authigenic carbonates found at five continental margin seep sites. They attributed the low $\delta^{13}C$ of many of the high-Mg calcite and aragonite samples to an AOM-derived C source. However, unlike the WIS seep carbonates discussed above, the continental margin seep carbonates studied by Naehr et al. (2007) have $\delta^{18}O$ values that are higher than expected from equilibrium precipitation at bottom-water temperatures and thus suggest an ^{18}O-enriched source, presumably from methane hydrate destabilization. The carbon isotope compositions of dolomites from Monterey Bay and the Santa Barbara and Eel River Basins with higher $\delta^{13}C$ were likely influenced by a ^{13}C-enriched DIC reservoir linked to methanogenesis (Naehr et al. 2007).

Zwicker et al. (2015) demonstrated that a broad range of $\delta^{13}C$ values can occur in a single concretion. Their sampling of pipes from an Oligocene seep deposit (Washington, USA) showed a paragenetic sequence of early-diagenetic carbonate precipitation of matrix micrite and aragonite with very low $\delta^{13}C$ values (<−40‰) that precipitated in the SMTZ as a result of AOM, transitioning to higher $\delta^{13}C$ (>−2.3‰) in later-stage calcite that precipitated in the zone of methanogenesis. Values of $\delta^{18}O$ showed likely equilibrium precipitation with overlying seawater near the sediment-water interface in the early carbonate phases, with more negative values suggesting deeper burial in the later phases.

The rate of methane flux toward the sediment-water interface, position of the SMTZ, pore water-sediment or water-rock interactions, and methane hydrate formation or destabilization can all influence the morphologies and isotopic composition of the precipitated carbonates (Han et al. 2004; Dela Pierre et al. 2010). Methane fluxes can be characterized as effusive (or advective, characterized by high fluid flow) or diffusive (Miyajima et al. 2018). Some of the possible combinations of fluid pathways and sources can be broken down as follows:

- *High methane flux, deep-sourced methane, rapid effusive ascent toward the sediment-water interface (SWI)*: The $\delta^{13}C$ of the DIC of these deep fluids can reflect DIC enriched in ^{13}C from formation of biogenic methane (Reaction 1.2a; $\delta^{13}C$ +8 to +20‰; Han et al. 2004) or with $\delta^{13}C_{DIC}$ closer to 0‰ if from thermogenic methane generation. Such fluids have a high methane concentration (near or at saturation), with a likely $\delta^{13}C_{methane}$ <−50‰. The oxygen isotope composi-

tion of deep fluids can be affected by clay dewatering or reactions with rocks at depth producing ^{18}O-enriched pore fluid, especially for thermogenic sources of methane. Methane hydrate destabilization also would produce ^{18}O-enriched pore fluids. Reactions of the methane-bearing pore water with rock at depth also may alter the Sr or Nd isotope composition of the pore fluid (see Sect. 1.6.4).

The rapid transport of these deep fluids toward and even across the SWI may be facilitated by tectonic activity (such as faulting that opens pathways for deep fluids to flow). Such transport can displace the SMTZ upward, result in the formation of methane bubbles that can escape the sediment through burrows or bubble tubes, and impact the DIC reservoir of the overlying water above the seep. Anaerobic oxidation of methane in the SMTZ results in ^{12}C-enriched DIC that mixes with deep DIC enriched in ^{13}C to produce a higher $\delta^{13}C_{DIC}$ than from AOM alone. Carbonates precipitating near the SWI under these circumstances, thus, may have higher $\delta^{13}C$, and their $\delta^{18}O$ may reflect precipitation at ambient bottom-water temperature and $\delta^{18}O$ composition. Examples of such precipitation are the coquinites and massive carbonates from Late Cretaceous seep deposits of the Pierre Shale (Fig. 1.5). Carbonate precipitation also may occur along fluid escape conduits such as bubble tubes (Krause et al. 2009) or crustacean burrows (Wiese et al. 2015; Zwicker et al. 2015). Methane diffusion away from the main effusive pathway(s) may lead to slower precipitation of smaller sub-spherical concretions with lower $\delta^{13}C$ values resulting from AOM.

- *Deep-sourced methane, slow diffusive flux of methane toward the SWI:* Slow transport of methane in deep-sourced fluids that initially have the characteristics described above provides longer time for the DIC to be influenced by AOM and thus to become more isotopically enriched in ^{12}C. The SMTZ may be displaced to greater sediment depths than in the case of rapid effusive rates of fluid. The $\delta^{18}O$ of the isotopically altered deep pore fluid mixes with that near the sediment-water interface (SWI) pore water and bottom water. Provided that AOM under such conditions is intensive enough to drive local carbonate supersaturation in pore waters, carbonates precipitating under these conditions may have lower $\delta^{13}C$ than those formed from rapid ascent of deep-sourced fluids, as well as $\delta^{18}O$ that more nearly reflects precipitation in equilibrium with near-SWI pore water.
- *Shallow-sourced fluids, rapid effusive transport toward the SWI:* Shallow-sourced fluids likely contain methane dominated by biogenic production, and, therefore, the methane is isotopically highly enriched in ^{12}C ($\delta^{13}C = -50$ to $-110‰$). Rapid ascent can serve to displace the SMTZ toward the SWI, and AOM produces a DIC reservoir that is isotopically enriched in ^{12}C. The $\delta^{18}O$ composition of such fluids reflects that of the shallow sediment pore water. Carbonates precipitated near the SWI under such conditions show perhaps the lowest $\delta^{13}C$ values of the four scenarios described here. The $\delta^{18}O$ of the carbonates reflects precipitation at ambient bottom-water temperatures and oxygen isotope composition.
- *Shallow-sourced fluids, slow diffusive transport of methane toward the SWI:* The methane in these fluids is dominantly biogenic and, thus, strongly enriched in

^{12}C. Because the transport is slow, the SMTZ may be deeper in the sediments. Extensive AOM during diffusion-controlled transport toward the SWI results in a strongly ^{12}C-enriched DIC reservoir. During transport, this can mix with DIC produced from the decomposition of organic matter (e.g., Reaction 1.1) or overlying seawater ($\delta^{13}C_{DIC}$ ~ 0‰), increasing the $\delta^{13}C_{DIC}$. Carbonates precipitated under these conditions may have small sub-spherical morphologies, with low $\delta^{13}C$. Miyajima et al. (2018) described seep deposits from the Neogene of Japan that appear to fit this category. The seeps were characterized by scattered small micritic concretions with $\delta^{13}C$ values ranging from ~ −23 to −46‰. Miyajima et al. (2018) also tabulated other comparable seeps from the Lower Cretaceous to the present day, with $\delta^{13}C$ of micrites ranging from ~ −3 to –50‰.

1.6.2 Carbonate-Clumped Isotopes

As the foregoing illustrates, fluid composition and precipitation temperature are important factors controlling the $\delta^{18}O$ of seep carbonates. The C-O-clumped isotope signature of the carbonates may help resolve these factors for any given seep. Clumped isotope values (Δ_{47}, expressed as ‰) represent the temperature-dependent departure of the abundance of co-occurring ^{13}C and ^{18}O in carbonate relative to that dictated by the statistically predicted abundance of these isotopes in nature. The values of Δ_{47} are independent of fluid composition and, thus, can be used to independently determine the temperature of carbonate precipitation. Together with the carbonate $\delta^{18}O$ signature, this can be used to calculate the $\delta^{18}O$ of the water from which the carbonate precipitated. Loyd et al. (2016) attempted to do this initially for modern seeps for which the temperature and $\delta^{18}O$ of the water were constrained. They found that temperatures determined by the clumped isotope thermometer were up to 50 °C higher than ambient temperatures. Similarly, elevated temperatures were calculated for ancient cold seeps. Loyd et al. (2016) concluded that the clumped isotopes were in disequilibrium relative to the Δ_{47} temperature dependence determined for equilibrium precipitation of calcium carbonate (e.g., Henkes et al. 2013). Possible reasons include mixtures of DIC from distinctly different sources (e.g., DIC from seawater mixed with DIC from AOM), kinetics associated with AOM, or heterogeneous mixtures of carbonate phases in seep carbonates.

More recently, Zhang et al. (2019) measured Δ_{47} values in authigenic carbonates at seeps in the Sea of Japan and Northwest Pacific. They observed that the calculated temperatures were consistent with those of bottom waters at the 300–900-m-deep sites and concluded, in contrast to Loyd et al. (2016), that the carbonates were deposited in clumped isotope equilibrium. Zhang et al. (2019) also calculated $\delta^{18}O$ of the water in which the carbonates precipitated and found that the values were elevated above the ambient bottom water $\delta^{18}O$. They suggested that the oxygen isotope composition of the seep carbonates was influenced by ^{18}O-enriched water released by the destabilization of methane gas hydrates.

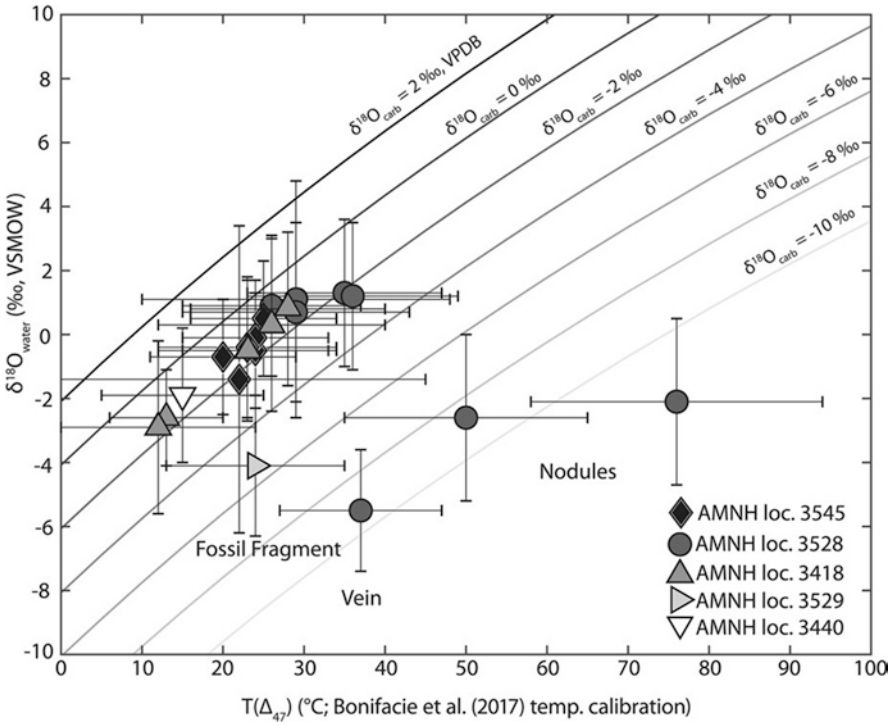

Fig. 1.6 Calculated water oxygen isotope values ($\delta^{18}O_w$) vs. calculated clumped isotope temperatures ($T(\Delta_{47})$) for 21 methane-derived authigenic carbonates from five methane seep deposits in the Upper Cretaceous (Campanian) Pierre Shale, South Dakota, USA. Gray lines represent equilibrium iso-$\delta^{18}O_w$ contours calculated from equilibrium calcite-water oxygen isotope fractionation (Kim and O'Neil 1997). Error bars are calculated based on the propagation of standard deviation of replicate measurements. VSMOW, Vienna standard mean ocean water; VPDB, Vienna Pee Dee Belemnite; AMNH loc., American Museum of Natural History locality (see Landman et al. this volume for details). (Reprinted from Gao et al. 2021 with permission of the Geological Society of America)

Gao (2019) and Gao et al. (2021) documented similar results in seep deposits from the Upper Cretaceous (Campanian) Pierre Shale of North America (Fig. 1.6). Calculated temperatures (23 ± 7 °C) were consistent with other estimates from the Western Interior Seaway, and the authors concluded that the carbonates were precipitated in clumped isotope equilibrium. The calculated $\delta^{18}O$ of the water was −0.5 ± 1.7‰, within error of previous estimates for the WIS and consistent with a time of ice-free conditions on Earth (Shackleton and Kennett 1975). These studies suggest that carbonate-clumped isotopes have a great potential in understanding seep carbonate formation mechanisms, but, clearly, further research is needed.

1.6.3 C and O Isotopes in Shells of Seep Fauna

As described in the preceding section, the carbonates precipitated at cold seeps reflect the different sources of C to the DIC reservoir, from which the carbonate is precipitated. Chief among these is the low $\delta^{13}C_{DIC}$ produced by AOM. Virtually all studies of ancient seeps use the $\delta^{13}C$ of the carbonates to validate that the site was in fact a seep environment. Additional information on the seep environment may be gained through isotope analyses of the shells of mollusks and other carbonate-secreting fauna found at seeps (Lietard and Pierre 2009; Landman et al. 2012, 2018; Cochran et al. 2015). For modern seeps, this is straightforward in that the shells are well-preserved (Lietard and Pierre 2009). Equilibrium precipitation of molluscan shell material from ambient DIC produces $\delta^{13}C$ in the shell carbonate that is ~1‰ and ~2.7‰ greater than that of the DIC for calcite and aragonite, respectively (at 20 °C; McConnaughey 1989). In addition, McConnaughey and Gillikin (2008) showed that metabolically derived (respired) carbon is incorporated into the shell and can account for up to ~30% of the carbon, depending on the mollusk. Lietard and Pierre (2009) measured the O and C isotope composition of bivalves of the genera *Bathymodiolus*, *Calyptogena*, *Vesicomya*, and *Lucina* from both modern cold seeps and hydrothermal vents and also summarized previous measurements from the literature. All the studied bivalves harbored sulfide-oxidizing or methanotrophic bacteria in their tissues (Lietard and Pierre 2009). The values of $\delta^{13}C$ ranged as low as −14‰, and Lietard and Pierre (2009) concluded that ^{12}C-enriched DIC from AOM was partly responsible for the low $\delta^{13}C$ of the shells. Other factors included the mode of life of the bivalves (e.g., infaunal vs. epifaunal) and the influence of the chemosymbionts in the tissues of the organisms. Similarly, Greinert et al. (2002) measured low $\delta^{13}C$ values (−1.83 to −6.50‰) in the solemyid bivalve *Acharax* collected at 4850 m water depth on the Aleutian margin. They acknowledged the possibility of incorporation of low $\delta^{13}C$ metabolic carbon into the shell but concluded that the shells were incorporating carbon from a DIC reservoir that was a mixture of bottom-water DIC and ~4–13% seep fluid DIC. Paull et al. (2008) studied the mussel *Bathymodiolus* from a methane seep and measured $\delta^{13}C$ in both the tissue and shell. They concluded that the shell $\delta^{13}C$ reflected the ambient DIC (which had low $\delta^{13}C$ as a result of AOM) but that the tissue reflected methane-derived C incorporated by methanotrophic bacteria.

Poor preservation of fossil shell material at ancient methane seeps commonly precludes meaningful O and C isotope measurements. However, Landman et al. (2012, 2018), Cochran et al. (2015), and Rowe et al. (2020) reported results on well-preserved shell material from methane seep deposits in the Upper Cretaceous (Campanian) Pierre Shale of South Dakota, USA (see Landman et al. this volume). Preservation was rigorously assessed using scanning electron microscopy (SEM) according to the Preservation Index scale of Cochran et al. (2010), and only the best-preserved shell material was used. Most of the analyses were on ammonites, which lived in the water column above the seeps, and showed $\delta^{13}C$ values as low as −14‰ (Landman et al. 2012).

Cochran et al. (2015) also performed limited sclerochronological sampling of specimens of the Late Cretaceous (Campanian) ammonite *Baculites compressus* collected at seep sites. The low values of $\delta^{13}C$ of these specimens relative to specimens of the same species collected at coeval non-seep sites suggested that the seep ammonites lived and precipitated their shells at the seeps. Other non-isotopic evidence for this conclusion is presented in Landman et al. (this volume). Landman et al. (2018) performed additional sclerochronological sampling of specimens of *B. compressus* from coeval seep and non-seep sites in the same formation (Fig. 1.7). Their results showed a significant offset between the specimens from seep and non-seep sites. Significantly, the C isotope data for the seep ammonites implied that the low $\delta^{13}C_{DIC}$ produced in the sediments from AOM was imprinted on the overlying water column in which the animals lived. An active food web likely developed at the seeps, and the ammonites were attracted to the abundant food there. Indeed, juvenile specimens of *B. compressus* preserved at the seep sites also showed low $\delta^{13}C$ values (Rowe et al. 2020). Both the DIC and the carbon in the food web were likely enriched in ^{12}C, and either DIC- or metabolically-derived carbon (or both) incorporated into the shells produced the lower $\delta^{13}C$ in the seep ammonites relative to non-seep ammonites. The sclerochronological data (Fig. 1.7) support the hypothesis that these animals spent extended time at the seeps. The isotope data, as well as the large number of ammonites collected at seeps from the relatively shallow WIS (Fig. 15.16 in Landman et al. this volume), demonstrate that ammonites, although not seep-obligate fauna, were nevertheless an important component of the Late Cretaceous WIS seep ecosystems.

1.6.4 Strontium and Neodymium Isotopes

Clues to the origin and transport of methane-bearing fluids at seep sites have been gained from the measurement of strontium and neodymium isotopes in seep carbonates. Seeps that occur in tectonically and magmatically active areas can display patterns of $^{87}Sr/^{86}Sr$ and $^{143}Nd/^{144}Nd$ ratios in the authigenic carbonates that indicate the involvement of deep-sourced fluids (Greinert et al. 2002; Joseph et al. 2012; Jakubowicz et al. 2015a, 2019, 2020, 2021). This is particularly the case for active plate margins, at which igneous materials with distinct Sr and Nd isotope signatures are commonly present in the plumbing systems feeding seeps. For example, Greinert et al. (2002) measured $^{87}Sr/^{86}Sr$ values less than the seawater value in seep carbonates from a deep-water seep on the Aleutian margin. They hypothesized that interactions between deep-sourced fluids and oceanic crust produced fluids with low $^{87}Sr/^{86}Sr$ as well as low $\delta^{18}O$, as ^{18}O was preferentially incorporated into altered volcanic glass. Similarly, Hein et al. (2007) observed low $^{87}Sr/^{86}Sr$ in barites and host rocks (dolomites) from the Southern California Borderland. The fluids were likely hydrothermal in origin and exchanged Sr with a less radiogenic strontium source. The low ratios were evident in authigenic carbonates even in cold seep portions of the system. Carbonates with $^{87}Sr/^{86}Sr$ lower than ambient seawater were

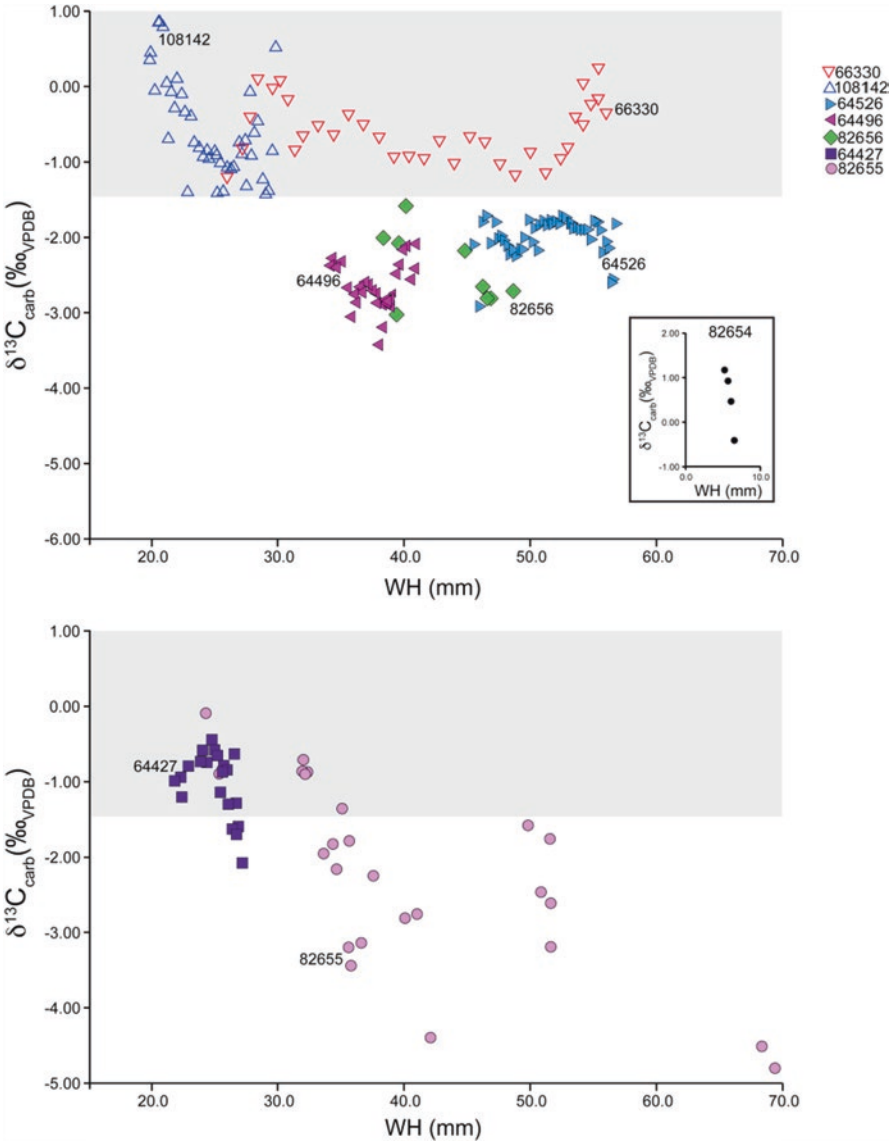

Fig. 1.7 $\delta^{13}C$ (‰ VPDB) from sclerochronological sampling of specimens of *Baculites compressus* from seep deposits (AMNH locs. 3545 and 3528) and coeval non-seep deposits (AMNH locs. 3383 and 3415) in the Upper Cretaceous (Campanian) Pierre Shale, plotted against whorl height (WH). Upper panel: Solid symbols = seep specimens; open symbols = non-seep specimens. Gray area demarcates the isotope values characteristic of the non-seep environment. Lower panel: Seep specimens in which the values of $\delta^{13}C$ in early ontogeny suggest that the animals lived in a non-seep environment (gray area) but migrated into a seep environment as ontogeny progressed (as indicated by increasing whorl height). (Reprinted from Landman et al. 2018 with permission of the American Journal of Science)

found in authigenic carbonates from the Cascadia convergent margin by Joseph et al. (2012), who hypothesized that these involved deep-sourced fluids had exchanged with oceanic-type crust making up the Siletzia terrane, which comprises the basement for much of the Cascadia forearc. The presence of exotic, ^{87}Sr-depleted fluids that interacted with Siletzia apparently characterized the Cascadia subduction zone from an early stage of its activity, as implied by Sr isotope analyses of mid-Eocene (Jakubowicz et al. 2019) and Oligocene (Joseph et al. 2012) seep carbonates of this area. In other instances, the $^{87}Sr/^{86}Sr$ of seep carbonates provides evidence for shallow, near-SWI precipitation. For example, Joseph et al. (2012) also found $^{87}Sr/^{86}Sr$ comparable to coeval seawater in Cascadia margin carbonates, indicating multiple sources and flow paths of fluids in that system. A similar, shallow precipitation of seep carbonates was hypothesized by Peckmann et al. (2001) for seeps in the northwestern Black Sea, in which the $^{87}Sr/^{86}Sr$ of the carbonates was comparable to the $^{87}Sr/^{86}Sr$ of ambient seawater.

In Upper Cretaceous seep deposits in North America, well-preserved authigenic carbonates also display $^{87}Sr/^{86}Sr$ different from coeval seawater, but in contrast to the studies cited above, the values are elevated. Figure 1.8 shows $^{87}Sr/^{86}Sr$ values relative to the coeval seawater value for the WIS (McArthur et al. 1994), expressed as

$$\varepsilon_{Sr} = \left[\left(\frac{87Sr}{86Sr} \right)_{\text{sample}} - \left(\frac{87Sr}{86Sr} \right)_{\text{seawater}} \right] \times 10^6 \tag{1.13}$$

Cochran et al. (2015) hypothesized that the source of the elevated $^{87}Sr/^{86}Sr$ was due to equilibration/exchange of seep fluids at depth with granitic rocks that now comprise the Black Hills. For example, the Harney Peak granite has $^{87}Sr/^{86}Sr$ ratios of 0.833520 ± 50 to 2.104340 ± 130 (Walker et al. 1986) or, expressed as ε_{Sr} values, 1.259×10^5 to 1.3067×10^6. In contrast, the Pierre Shale sediments through which the seep fluids transited have low $^{87}Sr/^{86}Sr$ values, generally <0.7075 (or $\varepsilon_{Sr} = -200$; Cochran et al. 2003). As the seep fluids ascended through the deposit, they mixed with pore water and, near the sediment-water interface, with seawater ($\varepsilon_{Sr} = 0$). Without knowledge of end-member Sr concentrations, it is not possible to discern the relative proportions of the different source contributions at these sites. However, ε_{Sr} values as high as +800 in the seep carbonates (Fig. 1.8; Appendix Table 1.1) indicate the involvement of deep fluids in the seep system. Lower $^{87}Sr/^{86}Sr$ ratios are evident in sparry calcite filling veins in the carbonates (Fig. 1.8), suggesting that the calcitic veins precipitated later in diagenesis. Lesser, but still significant, elevations in $^{87}Sr/^{86}Sr$ ratios (ε_{Sr} = ~+50 to +100) were observed in the shells of some ammonites and bivalves collected at the same sites (Cochran et al. 2015). These data, taken together, suggest that deep-sourced fluids were transported through the muddy sediments of the WIS, likely controlled by tectonic activity. Overall, the potential presence of fluid end-members with Sr isotope compositions deviating notably from that of coeval seawater places important constraints on using this isotope system as a stratigraphic tool (cf. Naehr et al. 2007; Kiel et al. 2014; Argentino et al. 2019). Given that many fossil seep deposits formed along former active plate margins, the

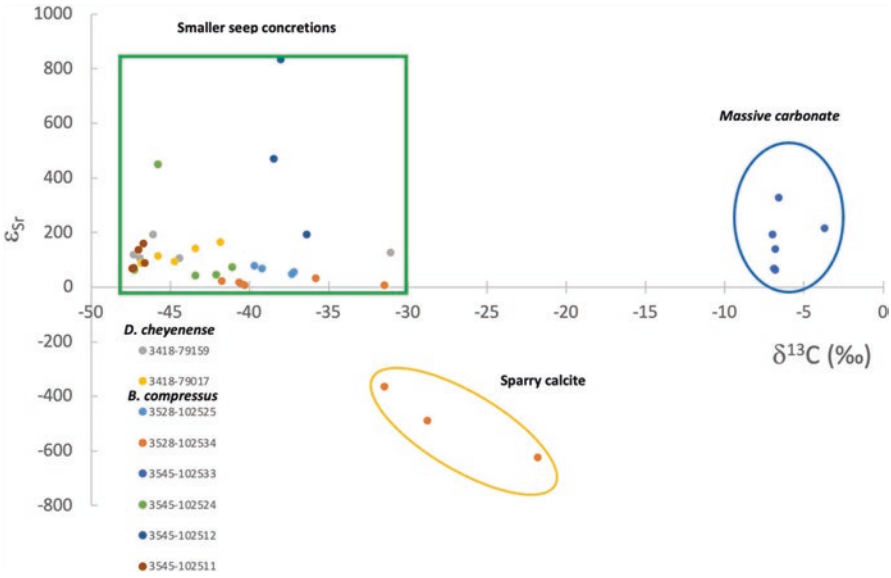

Fig. 1.8 Cross-plot of $^{87}Sr/^{86}Sr$ and $\delta^{13}C$ (‰ VPDB) in well-preserved seep carbonates from the Upper Cretaceous (Campanian) Pierre Shale, South Dakota (Appendix Table 1.1). Sr isotope ratios are plotted as ε_{Sr} (ppm) relative to coeval seawater $^{87}Sr/^{86}Sr$ (see Eq. 1.13). Values of ε_{Sr} >0 ppm suggest that deep fluids interacted with ^{87}Sr-rich granitic rock at depth and were involved in carbonate formation near the sediment-water interface. Sparry calcite veins in the concretions represent later-stage diagenesis. Uncertainty in the ε_{Sr} values is ~±15–20 ppm. Numbers refer to AMNH locality and specimen numbers. See Fig. 1.4 and Appendix Table 1.1 for $\delta^{18}O$ data and the age of the *Didymoceras cheyennense* (AMNH loc. 3418) and *Baculites compressus* (AMNH locs. 3545 and 3528) Zones

likelihood of such deep-seated, exotic Sr involvement must always be evaluated on a case-by-case basis.

Neodymium isotopes ($^{143}Nd/^{144}Nd$) can provide information on the source and nature of transport of seep fluids in a fashion much like $^{87}Sr/^{86}Sr$. Neodymium is a rare earth element, and ^{143}Nd, like ^{87}Sr, is a radiogenic isotope, derived from radioactive decay of ^{147}Sm. The $^{143}Nd/^{144}Nd$ ratio is commonly expressed relative to a standard (CHUR, Chondritic Uniform Reservoir), as ε_{Nd}:

$$\varepsilon_{Nd} = \frac{\left(\frac{143Nd}{144Nd}\right)_{sample} - \left(\frac{143Nd}{144Nd}\right)_{CHUR}}{\left(\frac{143Nd}{144Nd}\right)_{CHUR}} \times 10^4 \tag{1.14}$$

Continental and oceanic crustal rocks have different ε_{Nd} signatures, with low values in continental crust and higher values in oceanic basalts. In the modern ocean, ε_{Nd} varies from ocean basin to ocean basin as a consequence of weathering of different types of source rocks, ranging from −26.6 to +2.7 (Tachikawa et al.

2017). For most basins, ε_{Nd} values are, however, low, globally averaging −8.8 (Lacan et al. 2012). As a tracer of fluid flow at seeps, ε_{Nd} can thus be applied much like ε_{Sr}, with the proviso that, unlike for Sr, establishment of the background seawater ε_{Nd} signature must be made separately for each sedimentary basin, either by direct measurements on water (Bayon et al. 2011; Freslon et al. 2014) or based on mineral proxies (Jakubowicz et al. 2015a, 2019). Considering the dominant sources of rare earth elements, including Nd, to marine pore fluids (see Sect. 1.7.1), for most settings, the pore water ε_{Nd} values can be expected to resemble either the signal from the overlying bottom water (Bayon et al. 2011; Freslon et al. 2014), reflecting dissolution of authigenic, seawater-derived minerals and remineralization of organic matter, or can be expected to be shifted toward higher values, indicative of alteration of silicates (Ge et al. 2020). Therefore, the greatest utility of the Nd isotope system is at seeps overlying mafic volcanic rocks that have an ε_{Nd} signature distinctly different from that of coeval seawater.

Jakubowicz et al. (2015a) made the first such application of Nd isotopes to fossil seeps. They measured rare earth elements (REEs) and $^{143}Nd/^{144}Nd$ ratios in Devonian-age seep carbonates from the Anti-Atlas Mountains of Morocco. They observed that microspar carbonates have higher radiogenic $^{143}Nd/^{144}Nd$ signatures (higher ε_{Nd}) than the coeval seawater value reconstructed from conodonts. They postulated that interactions between ascending seep fluids and a Lower Devonian volcaniclastic unit enriched the fluid in ^{143}Nd. Similar to the observations concerning the Sr isotopes in the sparry calcite veins in the Upper Cretaceous seep carbonates cited above, Jakubowicz et al. (2015a) found less radiogenic Nd isotope signatures in sparry calcite crystals in the Devonian seep carbonates and suggested that these formed under conditions of reduced fluid seepage.

More recently, Jakubowicz et al. (2019) measured ε_{Nd} (as well as $^{87}Sr/^{86}Sr$ and $\delta^{13}C$) in micritic carbonates from a Lower Cretaceous (Barremian) seep deposit that was underlain shallowly by mafic volcanic rocks. The results clearly showed that the carbonates were influenced by mafic signatures of ε_{Nd} and $^{87}Sr/^{86}Sr$, relative to coeval seawater values (Fig. 1.9). Seep fluids that interacted with the rocks displayed an imprint of elevated ε_{Nd} and lower $^{87}Sr/^{86}Sr$ than coeval seawater. Jakubowicz et al. (2021) also showed departures of ε_{Nd} from seawater values in middle Cretaceous seep deposits from the Basque-Cantabrian Basin. The seeps were underlain by igneous intrusions, and Jakubowicz et al. (2021) used the patterns of ε_{Nd} and $\delta^{13}C$ to discern the variety of spatial and temporal differences in fluid flow and composition, as described in Sect. 1.6.1. Thus, both Nd and Sr isotopes help inform the nature of fluid systems at seeps and provide important information not easily obtained from C or O isotope analyses.

1.6.5 Sulfur Isotopes

Fractionation among sulfur isotopes offers clues to sulfur cycling and iron sulfide formation at seeps. The δ-notation used for sulfur is similar to that for C and O:

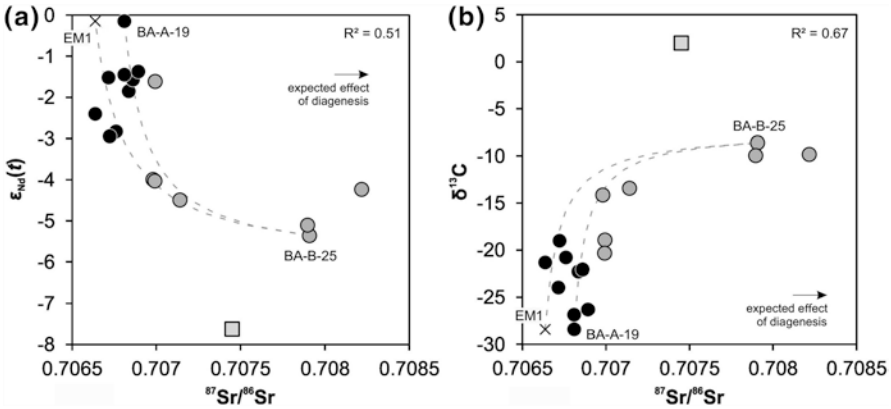

Fig. 1.9 Cross-plots of (**a**) $^{143}Nd/^{144}Nd$ (as ε_{Nd}; Eq. 1.14) vs. $^{87}Sr/^{86}Sr$ and (**b**) $\delta^{13}C$ vs. $^{87}Sr/^{86}Sr$ in Early Cretaceous (Barremian) seep carbonates from the Czech Republic. Also plotted are values corresponding to the isotope composition of contemporaneous local seawater. Coeval seawater values are indicated by the solid gray square. Dashed lines are calculated mixing curves with a mafic rock end-member that has high ε_{Nd} and low $^{87}Sr/^{86}Sr$. Two hypothetical simple mixing scenarios between seep and diagenetic carbonates are shown. The assumed end-members are samples BA-A-19 and BA-A-25, and a hypothetical seep carbonate end-member having the highest ε_{Nd} and lowest $^{87}Sr/^{86}Sr$, $\delta^{13}C$, and $\delta^{18}O$ values observed among the samples. Arrows show trends in which the primary signals shift for diagenetic alteration involving isotopic exchange during fluid-rock interaction, rather than mixing between different cement generations. (Reprinted from Jakubowicz et al. 2019 with permission of Elsevier)

$$\delta^{34}S = \left(R_{sample} / R_{standard} - 1\right) \times 1000 \tag{1.15}$$

where R_{sample} is the $^{34}S/^{32}S$ ratio measured in the sample and $R_{standard}$ is the $^{34}S/^{32}S$ of the standard (Canyon Diablo Troilite; CDT). Organoclastic sulfate reduction produces elevated $\delta^{34}S$ in the residual sulfate reservoir. The sulfide produced has a lower $\delta^{34}S$, and precipitation of iron sulfides generally reflects the $\delta^{34}S$ of the dissolved sulfide. Factors influencing the fractionation include availability of an organic substrate and the sulfate concentration. Maximum fractionations between the sulfate and sulfide reservoirs produced by organoclastic sulfate reduction are ~45‰ (Kaplan and Rittenberg 1964). Higher values likely reflect sulfide oxidation and bacterially mediated disproportionation of reduced sulfur intermediates. Thus, $\delta^{34}S$ values in pyrite ranging down to −45‰ and lower suggest sulfide production from organoclastic sulfate reduction and subsequent reactions (Peckmann et al. 2001; Peckmann and Thiel 2004: Jenkins et al. 2007). In contrast, higher $\delta^{34}S$ in seep pyrite values reflects a ^{34}S-enriched dissolved sulfide reservoir such as might occur in low concentrations of sulfate in the SMTZ (Lin et al. 2016). Indeed, detailed sampling of pyrite from seeps in the South China Sea by SIMS reveals a range of $\delta^{34}S$ value that suggests both organoclastic sulfate reduction and sulfate reduction via AOM are affecting the values during different stages of diagenesis (Lin et al. 2017a, b).

1.7 Elemental Geochemistry of Cold Seeps

1.7.1 Rare Earth Elements

Aside from studies utilizing isotopes of Nd in seeps, a number of new insights have been gained recently by analyzing concentration patterns of rare earth elements [REEs = lanthanides, i.e., elements with atomic numbers 57–71: light REE (LREE) – La, Ce, Pr, Nd; middle REE (MREE) – Sm, Eu, Gd, Tb; heavy REE (HREE) – Dy, Ho, Er, Tm, Yb, Lu]. In terms of their chemical parameters, REEs form a coherent set of elements with similar electronegativities, effective ionic radii decreasing systematically from La to Lu, and, with the exception of Ce and Eu, exist in the trivalent oxidation state (Elderfield 1988; Byrne and Sholkovitz 1996). Changes in REE concentrations across the lanthanide series, as well as variations in the contents of individual REEs, most notably the redox-sensitive Ce and Eu, therefore offer clues to the environmental conditions at which seep carbonates form, including the redox-driven biogeochemical reactions (with implications for the precipitation depth and flow regime; Feng et al. 2009a, b; Ge et al. 2010; Birgel et al. 2011; Wang et al. 2014), and the potential presence of fluid end-members enriched in volcanic-derived components (Jakubowicz et al. 2015a). To facilitate comparison of general trends, REE contents are typically normalized to concentrations found in an average shale (most commonly, Post-Archean Australian Shale – PAAS; McLennan 1989).

Seep carbonates show a broad variability of both total REE concentrations ($\sum$REE) and shale-normalized REE patterns. The highest $\sum$REE are usually shown by microcrystalline cements (micrite/microspar), with an order-of-magnitude lower value typifying sparry crystals (e.g., Himmler et al. 2010; Birgel et al. 2011; Jakubowicz et al. 2015a). Both these features can be attributed to differences in, on the one hand, the environment of carbonate precipitation and, on the other, textural influences on REE acquisition. Being precipitated within pore spaces of background deep-water, typically argillaceous sediments, the microcrystalline carbonates are subjected to high, early-diagenetic influx of REE from reduction of Fe-Mn oxyhydroxide coatings on mineral grains and from remineralization of sedimentary organic matter (Himmler et al. 2010, 2013; Rongemaille et al. 2011; Bayon et al. 2011). A large part of REE uptake by calcite takes place via adsorption onto the crystals, rather than direct substitution for Ca^{2+} in the crystal lattice (Stipp et al. 2003; Lakshtanov and Stipp 2004; Hellebrandt et al. 2016), and thus incorporation of increased REE contents is favored by the high surface-area-to-volume ratio typical of micritic crystals. Indeed, the trend toward increasing REE concentrations with decreasing crystal size is typical also for non-seep carbonates (e.g., Pichler and Veizer 2004; Nothdurft et al. 2004; Webb et al. 2009). Finally, adsorption of larger quantities of REE is facilitated by the kinetic effect associated with the relatively slow precipitation rates typical of micritic carbonates (Ge et al. 2010). Among the sparry carbonate phases, early fibrous cements are most characteristic of areas with focused fluid flow, commonly occluding open spaces present within the micritic

matrix. This, in combination with their rapid growth rate, results in incorporation of lower REE contents (e.g., Feng et al. 2009a; Birgel et al. 2011; Crémière et al. 2016). The lowest ∑REE are typically observed in blocky spar crystals that infill central parts of cavities found in many ancient seep deposits (e.g., Feng et al. 2009b; Jakubowicz et al. 2015a), reflecting the decreasing REE contents of pore fluids with increasing burial, together with progressive REE uptake by precipitating authigenic minerals (cf. Soyol-Erdene and Huh, 2013).

Unlike the case of open-marine and biogenic carbonates precipitated from oxic seawater and usually typified by low ∑REE, the generally high primary REE contents of early-diagenetic seep carbonates make them much less susceptible to significant alteration of their original signatures under marine-burial diagenesis (see discussion in Jakubowicz et al. 2015b). As a result, the REE patterns observed in modern and fossil seep carbonates share notable similarities (Feng et al. 2009b; Jakubowicz et al. 2015a; Wang et al. 2018). Nevertheless, the complex sedimentary environment of seep deposits, including the possible multistage modes of their formation, may make disentangling the signatures imposed by different biogeochemical redox processes difficult (Zwicker et al. 2018; Smrzka et al. 2020).

The shale-normalized REE patterns of seep precipitates are typically distinct from those of oxygenated seawater, characterized by significant HREE-enrichment and strong negative Ce anomalies (Elderfield 1988). The REE incorporation into seep carbonates is controlled by a succession of anaerobic microbial redox processes, involving gradual decomposition of organic matter by the use of progressively less energetically favorable electron acceptors (see Sect. 1.2) and associated intense element remobilization from both mineral and organic substrates (Smrzka et al. 2020). The most common are flattish-to-MREE-enriched patterns, the latter commonly referred to as the "MREE bulge" (Fig. 1.10). This can be attributed

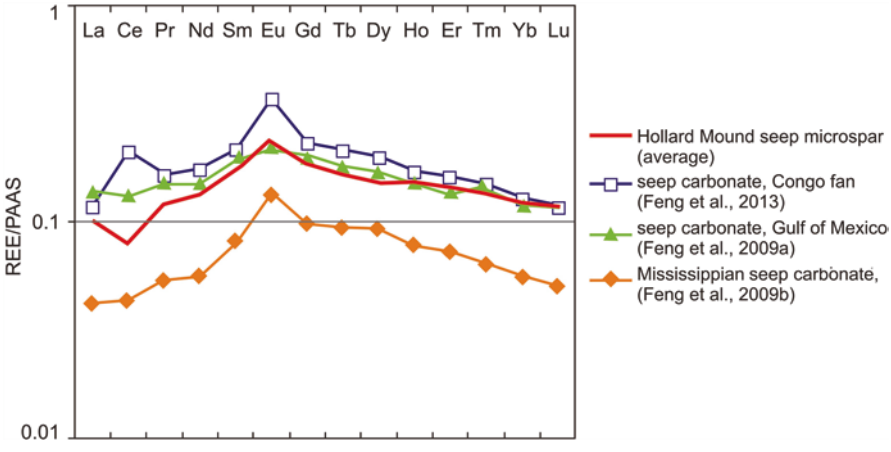

Fig. 1.10 Comparison of the PAAS (post-Archean Australian Shale)-normalized REE patterns in the Holland Mound seep (Middle Devonian, Morocco; average pattern for the microsparitic samples) with selected modern seep carbonates. See text for discussion. (Reprinted from Jakubowicz et al. 2015a, with permission of Elsevier)

mostly to the typical seep carbonate precipitation from anoxic sediment pore waters, rather than open, oxygen-rich seawater. As a result, the main phase of seep carbonate precipitation corresponds to the moment at which large quantities of REEs are released to pore fluids by reduction of Fe-Mn oxides, with their characteristic MREE enrichment (Himmler et al. 2010; Rongemaille et al. 2011; cf. Haley et al. 2004; Kim et al. 2012; Abbott et al. 2016). More rarely, LREE enrichment has been reported, a feature possibly reflecting preferential release of LREE from early-diagenetic decomposition of organic matter (Zwicker et al. 2018, Smrzka et al. 2019; cf. Sholkovitz et al. 1989; Haley et al. 2004; Kim et al. 2012). Finally, HREE enrichment resembling that of seawater has occasionally been observed in some sparry carbonate phases (Zwicker et al. 2018), as well as in pore fluids below the zone of anaerobic oxidation of methane (Kim et al. 2012; Soyol-Erdene and Huh 2013). The origin of the latter pattern, documented relatively recently, remains unclear; possibly, it reflects LREE complexation by increasingly altered organic matter during remineralization of particulate organic carbon and carbonate precipitation from residual, relatively HREE-enriched pore fluids (Himmler et al. 2010; Kim et al. 2012; Zwicker et al. 2018; cf. Haley et al. 2004; Pourret et al. 2008). Other explanations include continuous reduction of Fe oxyhydroxides, complexation by carbonate species, as well as silicate mineral diagenesis (Soyol-Erdene and Huh 2013). For ancient seeps, such HREE-enriched patterns have been observed in texturally and chemically altered carbonates interpreted as a product of early-diagenetic calcification of organic-rich aragonite and may represent a signature imposed on pre-existing carbonates during their early neomorphism, most likely in the zone of methanogenesis (Zwicker et al. 2018).

Because of the small, gradually changing differences in chemical properties among most REEs, they share general similarities in their complexation and surface adsorption behavior in geochemical reactions in modern oceans and sediment pore waters (Elderfield 1988; Byrne and Sholkovitz 1996). Two notable exceptions are Ce and Eu, which can undergo active redox cycling associated with changes in their valence state under near-surface conditions, resulting in their decoupling from the other invariably trivalent REEs. Because under oxic conditions, Ce is rapidly oxidized to reactive Ce^{4+} ions and scavenged by Fe-Mn oxides, a characteristic feature of phases derived from oxygenated seawater is their Ce depletion relative to the neighboring REEs (Byrne and Sholkovitz 1996). Under anoxic conditions, Ce is reduced to soluble Ce^{3+} ions and released into solution, resulting in the Ce enrichment commonly observed in anoxic pore waters (Sholkovitz et al. 1989; German and Elderfield 1990; Tostevin et al. 2016). Indeed, the presence of positive Ce anomalies has been reported for some seep carbonates (Feng et al. 2010; Birgel et al. 2011; Argentino et al. 2019) and pore fluids (Bayon et al. 2011; Himmler et al. 2013), providing insights into spatial and temporal variability of redox conditions in seepage-affected environments. This enrichment is, however, not universal; at many seeps, negative Ce anomalies have been documented in otherwise non-seawater REE patterns, and for some seep deposits, no phases with marked Ce enrichment have been observed (Jakubowicz et al. 2015a and references therein; Fig. 1.10). Factors preventing development of positive Ce anomalies in an environment

apparently favorable for pore water Ce enrichment are the subject of active debate. Among possible explanations are the possible roles of episodic decrease in the flux of methane-rich fluids and associated carbonate precipitation under oxic conditions (Feng et al. 2009b), regular recharge of seawater required for AOM as a source of sulfate (Jakubowicz et al. 2015a), or high alkalinity combined with increased complexation of Ce by organic compounds (Pourret et al. 2008; Himmler et al. 2010; Birgel et al. 2011; Kim et al. 2012).

Cycling of Eu is less understood, and, hence, interpretation of Eu anomalies is commonly problematic. Development of a positive Eu anomaly in a fluid during fluid-rock interactions can proceed through reduction of Eu^{3+} to Eu^{2+}, which is more soluble than trivalent REEs. Such a reduction requires typically high-temperature conditions (>200 °C; Sverjensky 1984), and, therefore, this origin of Eu enrichment is most characteristic of hydrothermal fluids and precipitates (Bau et al. 2010). At relatively low temperatures typifying most hydrocarbon discharges, a more likely source of Eu enrichment is dissolution of Eu-enriched minerals found in mafic igneous rocks, such as plagioclase, provided that such igneous materials are present in the plumbing systems feeding the seeps (Fig. 1.10; Kim et al. 2012; Jakubowicz et al. 2015a). Aside from igneous Eu sources, positive Eu anomalies may develop in authigenic minerals precipitating in non-hydrothermal environments under very strongly reducing, alkaline conditions (Sverjensky 1984; MacRae et al. 1992). For seeps, the latter scenario is facilitated by the high influx of reduced compounds and shallow depth of the sulfate reduction zone, which often results in development of extremely reducing conditions in interstitial waters (Jakubowicz et al. 2015a). Distinguishing these possible sources of Eu enrichment that appear in shale-normalized REE patterns of seep carbonates is additionally hampered by the possibility of developing Eu anomalies as analytical artifacts, because of an interfering effect of BaO on Eu in the course of ICP-MS measurements (Dulski 1994). This possibility should always be considered for seep deposits, which commonly contain an admixture of barite; ideally, REE analyses should be accompanied by measurements of Ba concentrations. Aside from the efforts to constrain mechanisms governing the incorporation of Ce and Eu in seep carbonates, the main focus of recent research in seep-related REE studies includes using REE to better understand the pathways of early-diagenetic processes recorded by different authigenic phases present at seeps (Zwicker et al. 2018), as well as to provide means for identifying fossil seeps discharging a significant amount of longer-chain hydrocarbons (Smrzka et al. 2016, 2019).

1.7.2 Non-lanthanide Elements

In addition to REE, a number of different elemental systems have been measured in seep deposits. Traditionally, minor elements, notably Fe, Mn, Sr, and Mg, have been used as tracers of post-depositional processes and, in particular, to assess the level of diagenetic alteration (with progressive alteration marked by an increase in Fe and Mn and decrease in Sr and Mg concentrations; e.g., Popp et al. 1986; Denison et al. 1994; Brand 2004; Jakubowicz et al. 2015b). However, for methane seeps, application of these elements to constrain diagenetic modifications of primary signatures is

considerably complicated by the complex, mostly anoxic environment of seep carbonate authigenesis. For normal-marine, oxic seawater-derived carbonates, Fe and Mn concentrations are typically very low (<200 ppm for Mn and 600 ppm for Fe; Denison et al. 1994; Brand et al. 2003), because Fe(III) and Mn(IV) must be anaerobically reduced to Fe(II) and Mn(II), respectively, in order to be incorporated into the carbonate crystal lattice. As a result, the enrichment of normal-marine carbonates in Mn and Fe is typically indicative of their post-depositional alteration (Denison et al. 1994; Brand 2004; Boggs and Krinsley 2006). Because seep carbonates precipitate from anoxic interstitial waters in the SMTZ, typically underlying the zones of active microbial Fe(III) and Mn(IV) reduction, the enrichment of seep carbonates in Mn(II) and/or Fe(II) can be a primary feature (e.g., Ritger et al. 1987; Kelly et al. 1995; Buggisch and Krumm 2005; Campbell et al. 2002; Joseph et al. 2013; Tribovillard et al. 2013; Kiel et al. 2014; Zwicker et al. 2018; Argentino et al. 2019). This is especially the case for calcite, which has a rhombohedral crystal structure that is more favorable for incorporation of Mn^{2+} than that of orthorhombic aragonite (Reeder 1983; Tucker and Wright 1990). Mn^{2+} and Fe^{2+} ions also can be directly supplied to the precipitating carbonates due to AOM itself because, in addition to sulfate, Mn(IV) and Fe(III) can also serve as oxidants in this process (see Sect. 1.3; Beal et al. 2009).

One important, yet rarely acknowledged consequence of this is that cathodoluminescence, commonly applied as a cost- and time-effective test of the alteration level of normal-marine limestones, cannot be applied in an analogously simple manner for seep carbonates. The main activator of luminescence in carbonate minerals is Mn(II) (Machel 2000; Boggs and Krinsley 2006), and, consequently, the presence of distinct red-to-yellow luminescence may represent an original characteristic of many seep deposits, especially those dominated by calcite. Accordingly, except for the case of neomorphic alteration, primary mineralogical differences may play a role in the observed differences between cathodoluminescence patterns shown by microcrystalline seep carbonates (most often of original high-Mg calcite and commonly showing red-to-orange luminescence) and isopachous-fibrous cements (commonly primarily aragonitic and more often non-luminescent; e.g., Kiel et al. 2014). For fossil seep deposits that underwent long burial histories, the problem of disentangling the primary and diagenetic controls on the carbonate Mn and Fe contents poses major limitations to more advanced applications of these systems, such as reconstructing past redox zonations, imprints of methanogenesis, or element circulation associated with the formation, oxidation, and dissolution of Fe- and Mn-bearing minerals (see Smrzka et al. 2020 and references therein).

Compared with Fe and Mn, primary mineralogical differences are of even greater importance for the variability of Sr and Mg concentrations observed in unaltered seep carbonates (Bayon et al. 2007; Nöthen and Kasten 2011; Tong et al. 2019). The Sr and Mg contents can also be substantially modified by fluid-rock interactions in the course of diagenetic alteration. Both of the main $CaCO_3$ polymorphs making up seep carbonates, aragonite and high-Mg calcite, are metastable and normally stabilize to low-Mg calcite in the course of diagenesis. This process is accompanied by loss of both Sr and Mg (Tucker and Wright 1990). The scales of these alteration effects are different depending upon the original mineralogies of seep carbonate phases, because the crystal lattice of aragonite is favorable for substitution of Sr^{2+},

but not Mg^{2+} into Ca^{2+} structural sites, whereas the opposite applies to high-Mg calcite (Reeder 1983; Finch and Allison 2007). Among the most common applications of Sr and Mg concentration analyses in fossil seep studies is discrimination between the aragonite and high-Mg calcite precursors of low-Mg calcites that comprise the bulk of most ancient seep deposits. This, in turn, provides constraints on paleoenvironmental conditions, most notably former pore water sulfate concentrations and, by inference, fluid flow rates and precipitation depths (e.g., Greinert et al. 2001; Naehr et al. 2007; Nöthen and Kasten 2011; for a general conceptual background, see Burton 1993). The method relies on the assumption that increased concentrations of Sr in low-Mg calcite are indicative of its originally aragonitic mineralogy, whereas low Sr and elevated Mg contents suggest a high-Mg calcite precursor, consistent with the results of many case studies involving a combination of elemental and petrographic analyses (e.g., Savard et al. 1996; Campbell et al. 2002; Buggisch and Krumm 2005; Kiel et al. 2014).

Interpretation of the Sr and Mg concentration data is further hampered by variable diagenetic pathways experienced by different seep deposits and the disparate alteration responses expected for different $CaCO_3$ polymorphs. For example, some post-aragonite calcites that experienced extensive alteration may display Sr contents even lower than those of unaltered low-Mg calcites, whereas diagenetic calcites precipitated from fluids derived from aragonite calcification may show increased Sr concentrations (Banner 1995). In addition, during recrystallization of high-Mg calcite, Sr can be released from Sr-rich mineral impurities, such as aragonite inclusions, which, even if volumetrically small, may have a substantial effect on the bulk Sr concentrations of the alteration product (Banner 1995). For aragonite, diagenetic exchange may, on the other hand, even result in some increase in its Mg contents (cf. Zwicker et al. 2018). The difficulties with unequivocally distinguishing between former aragonite and high-Mg calcite, or mixtures of the two, based on either geochemical or petrographic criteria may hamper conclusive interpretation of the Mg/Sr ratios when these are applied as a measure of the degree of diagenetic alteration (e.g., Zwicker et al. 2018). Therefore, the Sr and Mg isotope analyses of ancient seep carbonates must be carried out in combination with petrological observations, which remain the primary method of reconstructing former fabrics and mineralogies at fossil seeps (cf., Campbell et al. 2002; Peckmann et al. 2007; Joseph et al. 2013).

Aside from the minor elements, seep studies have also applied trace elements. Many of these applications have been made in the past decade but are yet to develop their full potential to allow for their broader use in investigations of fossil seeps. Among the trace elements that may potentially provide insights into the paleoenvironment, a particular focus has recently been on those offered by redox-sensitive elements, such as Mo, U, Cd, Sb, and As. Concentrations of these elements have been used to provide constraints on fluid flux and the dynamics of redox conditions (Mo and Mo/U ratios: Cangemi et al. 2010; Peketi et al. 2012; Hu et al. 2014, 2020; Chen et al. 2016; Williscroft et al. 2017; Deng et al. 2020; Cd: Smrzka et al. 2017; Ba: Torres et al. 2002; Nöthen and Kasten 2011; Hu et al. 2020; Y/Mo ratios: Himmler et al. 2010; Jakubowicz et al. 2015a; Wang et al. 2018). Applications include (a) distinguishing between sulfate-driven AOM and organoclastic sulfate reduction (Mo, As, Sb; Smrzka et al. 2020), (b) identifying seeps with significant involvement of heavy hydrocarbons (Mo/U ratios; Smrzka et al. 2016, 2019), (c)

discriminating between different primary carbonate mineralogies (Mo, U, Cd; Feng and Chen 2015), and (d) tracing elemental recycling associated with the formation and dissolution of Fe- and Mn-bearing mineral phases (As, Sb, Mo, U; Bayon et al. 2011; Tribovillard et al. 2013; Hu et al. 2014; Wang et al. 2019).

As well as these applications, a more traditional approach has been to use conservative lithogenic elements, such as Al, Ti, Sc, Zr, Th, and Hf, to identify elemental release from a terrigenous fraction, either upon seep carbonate precipitation or as contamination during laboratory leaching procedures, and also to use them for normalization of other elements to calculate their authigenic fractions, as they are applied in general carbonate sedimentology (e.g., Nothdurft et al. 2004; Algeo and Li 2020; Smrzka et al. 2020). In general, however, because many trace elements undergo active cycling in various zones of redox processes and may be subject to repeated remobilization, and diagenetic alteration associated with organic matter and clay-mineral diagenesis, interpretation of trace element data in ancient carbonates remains challenging (Algeo and Liu 2020 and references therein). This problem is especially pertinent for studies of hydrocarbon seeps, given their complex and dynamic redox conditions, spatial and temporal fluctuations in the fluid flux, and migration pathways and composition of the seeping fluids. Accordingly, further research is required before the redox-sensitive trace elements can be more broadly applied to address specific, case study-based questions (for an overview, see Smrzka et al. 2020; general reappraisals of the use of trace elements as redox proxies have recently been published by Algeo and Liu 2020; Algeo and Li 2020; and Bennett and Canfield 2020).

1.8 Summary

A fundamental geochemical process operating at methane seeps is the anaerobic oxidation of methane (AOM) by which methane is oxidized and sulfate is reduced. Because both reactants are necessary for AOM to proceed, this process takes place in the sulfate-methane transition zone, generally located below the sediment-water interface. Methane produced biogenically or thermogenically has a low $\delta^{13}C$ signature, and this is transferred to the dissolved inorganic carbon (DIC) reservoir during AOM. As a consequence of the increase in alkalinity from AOM, calcium carbonate supersaturation can occur, and various carbonate minerals can precipitate with low $\delta^{13}C$. Indeed, very low $\delta^{13}C$ values of ancient calcium carbonates are taken as prima facie evidence that the carbonates formed in a cold hydrocarbon seep environment.

Other chemical reactions typical of early diagenesis of organic matter in marine sediments occur at seeps. Two reactions, organoclastic reduction of sulfate (ORS) and Fe(III) reduction, in addition to AOM, provide links between the iron and sulfur cycles. Dissolved sulfide produced by AOM or ORS can react with reduced iron (Fe^{2+}) to form iron monosulfides and eventually pyrite, a mineral frequently associated with carbonates at methane seeps.

Numerous isotope systems have been applied to studies of methane seeps. Carbon isotopes ($\delta^{13}C$) in authigenic seep carbonates provide evidence of the source of the methane (biogenic or thermogenic) and the possibility of admixtures of other sources of DIC that contribute to seep carbonate formation (DIC from overlying

water, ORS, etc.). Carbon isotope measurements of lipid biomarkers in the molecular fossil inventory in seep-associated carbonates provide evidence for the archaea and bacteria involved in AOM. Oxygen isotopes ($\delta^{18}O$) provide information on the temperature of seep formation, the possible influence of methane hydrates on seep development, and seep fluid-rock or fluid-sediment interactions. The application of carbonate-clumped isotopes to seep systems is at a very early stage but offers the possibility of resolving both the temperature of seep carbonate formation and aspects of fluid source and composition. Fractionation among sulfur isotopes, as expressed by $\delta^{34}S$ in sulfide phases, helps reveal the relative importance of reduced sulfur from OSR and AOM in sulfide formation. Strontium ($^{87}Sr/^{86}Sr$) and neodymium ($^{143}Nd/^{144}Nd$) isotopes help clarify the involvement of deep-sourced fluids and fluid pathways in transferring methane to the SMTZ.

New insights into seeps also have been gained by analyzing concentration patterns of rare earth elements (REEs) in seep carbonates. Changes in REE concentrations across the lanthanide series as well as variations of individual REE, notably the redox-sensitive Ce and Eu, provide clues to the environmental conditions under which seep carbonates formed, including the redox-driven biogeochemical reactions involved (with implications for the precipitation depth and flow regime) and the potential presence of fluid end-members enriched in volcanic-derived components.

Concentrations of the minor elements Fe, Mn, Sr, and Mg in seep carbonates reflect mineralogical differences, although the possibility of diagenetic alteration during burial must be considered in their interpretation. Concentration of redox-sensitive trace elements (e.g., Mo, U, Cd, Sb, As) has been used to provide constraints on fluid flux and the dynamics of redox conditions to identify seeps with significant involvement of heavy hydrocarbons, to aid in discrimination between different primary carbonate mineralogies, and to trace elemental recycling associated with the formation and dissolution of Fe- and Mn-bearing mineral phases. Future research into fossil seep systems should maximize the information to be gained by incorporating multiple isotopic and elemental approaches.

Acknowledgments This chapter has benefited enormously from the helpful reviews by Marcello Natalicchio (University of Torino, Italy) and Daniel Smrzka (Universität Wien, Austria). The authors are grateful for the assistance from Shannon Brophy, Alison Rowe, and Remy Rovelli in the field and Bushra Hussaini, Kathleen Sarg, and Mariah Slovacek in the laboratory. Stephen Thurston provided graphic support. The strontium isotope measurements reported in Appendix Table 1.1 were made at the Stony Brook University FIRST Laboratory. We thank Katie Wooton, Troy Rasbury, and Tyler Levitsky for their efforts. We have benefited from stimulating discussions with Corinne Myers and James Witts. This work was partially supported by the Norman D. Newell Fund and the Landman Research Fund of the American Museum of Natural History.

Appendix

Appendix Table 1.1 gives oxygen, carbon, and strontium isotope data measured on seep concretions from three ammonite zones in the Late Cretaceous Western Interior Seaway (WIS) of North America. These data are plotted in Figs. 1.5 and 1.8. The location information (AMNH loc.) is given in Landman et al. (this volume).

Appendix Table 1.1 Oxygen, carbon, and strontium isotope data for Western Interior Seaway seep concretions

AMNH loc.	Ammonite zone	AMNH ID	Concretion type	Mineralogy	Sample number	$\delta^{18}O$ (‰ VPDB)	$\delta^{13}C$ (‰ VPDB)	$^{87}Sr/^{86}Sr$	ε_{Sr}
3545	*Baculites compressus*	102511	~3 cm; spherical	Micrite	1	−0.5	−47.3	0.707747	72
	(73.79 ± 0.36 Ma)			Micrite	2	−0.7	−46.6	0.707765	90
				Micrite	3	−0.5	−47.4	0.707744	69
				Micrite	4	−0.7	−47.0	0.707811	136
				Micrite	5	−0.6	−46.7	0.707835	160
3545	*B. compressus*	102533	Massive carbonate	Micrite	1	−1.3	−6.9	0.707744	69
				Micrite	2	−1.1	−6.6	0.708002	327
				Sparry calcite	3	−1.4	−4.8	0.707810	135
				Sparry calcite	4	−1.2	−2.2	0.707717	42
				Micrite	5	−1.2	−3.7	0.707890	215
				Micrite	6	−0.9	−7.0	0.707869	194
				Sparry calcite	7	−1.1	−4.8	0.707774	99
				Micrite	8	−1.0	−6.8	0.707738	63
				Micrite	9	−1.1	−6.8	0.707816	141
3545	*B. compressus*	102512	~3 cm; spherical	Micrite	1	−0.7	−36.4	0.707868	193
				Micrite	2	−0.4	−38.0	0.708508	833
				Micrite	3	−0.7	−38.3	–	–
				Micrite	4	−0.6	−38.5	0.708146	471
3545	*B. compressus*	102510	~1 cm; tubular	Micrite	1	−0.8	−47.3	–	–
				Sparry calcite	2	−2.5	−39.9	–	–
				Micrite	3	−0.6	−47.7	–	–
3545	*B. compressus*	102524	~7 cm; tubular	Micrite	1	−0.5	−43.4	0.707718	43
				Micrite	2	−0.6	−42.1	0.707721	46
				Micrite	3	−0.4	−45.8	0.708124	449

(continued)

Appendix Table 1.1 (continued)

AMNH loc.	Ammonite zone	AMNH ID	Concretion type	Mineralogy	Sample number	$\delta^{18}O$ (‰ VPDB)	$\delta^{13}C$ (‰ VPDB)	$^{87}Sr/^{86}Sr$	ε_{Sr}
				Micrite	4	−0.3	−47.3	0.707739	64
				Vug	5	−0.2	−41.1	0.707749	74
3545	*B. compressus*	102526	~10 cm; elongate	Sparry calcite	1	−3.1	1.9	–	–
				Micrite	2	−1.0	−29.1	–	–
				Micrite	3	−0.5	−33.3	–	–
				Micrite	4	−0.8	−41.1	–	–
				Micrite	5	−0.7	−37.4	–	–
				Micrite	6	−0.4	−35.1	–	–
3528	*B. compressus*	102525	~10 cm; tubular	Micrite	1	−0.8	−37.3	0.707717	47
				Micrite	2	−0.3	−40.5	0.707682	12
				Sparry calcite	3	−2.8	−37.2	0.707725	55
				Micrite	4	−0.7	−39.2	0.707737	67
				Micrite	5	−0.6	−39.7	0.707750	80
3528	*B. compressus*	102534	~7 cm; elongate pipe	Micrite	1	−6.6	−28.8	0.707181	−489.2
				Micrite	2	−2.0	−35.8	0.707703	33.2
				Micrite	3	−2.0	−40.3	0.707677	7.0
				Micrite	4	−1.8	−31.5	0.707677	6.6
				Spar	5	−13.9	−21.8	0.707047	−623.0
				Micrite/spar	6	−13.6	−31.5	0.707306	−364.5
				Micrite	7	−1.8	−40.6	0.707688	18.1
				Micrite	8	−1.4	−41.7	0.707692	22.4
3275	*B. compressus*	102548	~6 cm; non-seep	Micrite	1	−2.4	−19	–	–

AMNH loc.	Ammonite zone	AMNH ID	Concretion type	Mineralogy	Sample number	$\delta^{18}O$ (‰ VPDB)	$\delta^{13}C$ (‰ VPDB)	$^{87}Sr/^{86}Sr$	ε_{Sr}
				Micrite	2	−2.6	−19	–	–
				Micrite	3	−2.6	−19	–	–
				Micrite	4	−2.5	−20	–	–
				Micrite	5	−2.5	−20	–	–
				Micrite	6	−2.5	−20	–	–
				Micrite	7	−2.5	−20	–	–
3418	*Didymoceras cheyennense*	79159	~10 cm; elongate	Micrite	1	−1.2	−46.1	0.707829	113
	(74.67 ± 0.15 Ma)			Micrite	2	−1.1	−46.9	0.707741	93
				Micrite	3	−1.2	−47.3	0.707755	142
				Micrite	4	−0.9	−31.1	0.707761	89
				Micrite	5	−1.0	−44.4	0.707741	166
3418	*D. cheyennense*	79017	~5 cm; sub-spherical	Micrite	1	−0.9	−45.8	0.707748	113
				Micrite	2	−1.1	−44.7	0.707728	93
				Micrite	3	−1.0	−43.4	0.707777	142
				Micrite	4	−1.1	−46.8	0.707724	89
				Micrite	5	−0.8	−41.8	0.707801	166
3440	*Didymoceras nebrascense*	102535	~10 cm; coquinite	Micrite w/shell material	1	−1.1	−12.1	–	–
	(75.19 ± 0.28 Ma)			Micrite w/shell material	2	−0.9	−16.0	–	–
				Micrite w/shell material	3	−0.8	−17.0	–	–
				Micrite w/shell material	4	−0.7	−14.5	–	–

(continued)

Appendix Table 1.1 (continued)

AMNH loc.	Ammonite zone	AMNH ID	Concretion type	Mineralogy	Sample number	$\delta^{18}O$ (‰ VPDB)	$\delta^{13}C$ (‰ VPDB)	$^{87}Sr/^{86}Sr$	ε_{Sr}
				Micrite w/shell material	5	−0.8	−14.6	–	–
				Micrite w/shell material	6	−0.9	−14.0	–	–
				Micrite w/shell material	7	−1.0	−8.0	–	–
				Lucinid bivalve	8	−1.2	1.8	–	–
				Micrite w/shell material	9	−0.8	−10.2	–	–
				Micrite w/shell material	10	−0.7	−11.9	–	–

Methods Details on the analytical methods are given in Cochran et al. (2003, 2015) and Landman et al. (2012, 2018). Concretions were sampled sequentially from the outside inward, on a scale of approximately 3 mm, with Sample Number = 1 corresponding to the surface of the concretion. Oxygen and carbon isotopes are reported as permil $\delta^{18}O$ and $\delta^{13}C$ as relative to the VPDB standard. Values of ε_{Sr} are calculated from

$$\varepsilon_{Sr} = \left[\left(\frac{87Sr}{86Sr} \right)_{\text{sample}} - \left(\frac{87Sr}{86Sr} \right)_{\text{seawater}} \right] \times 10^6 \tag{1.13}$$

where $(^{87}Sr/^{86}Sr)_{seawater}$ represents the coeval seawater dissolved $^{87}Sr/^{86}Sr$ for the WIS reconstructed by McArthur et al. (1994). Photos of examples of the types of concretions analyzed here are given in Landman et al. (this volume) Figs. 15.12 and 15.13.

References

Abbott AN, Haley BA, McManus J (2016) The impact of sedimentary coatings on the diagenetic Nd flux. Earth Planet Sci Lett 449:217–227

Aharon P (1994) Geology and biology of modern ad ancient submarine seeps and vents: an introduction. Geo-Mar Lett 14:69–73

Algeo TJ, Li C (2020) Redox classification and calibration of redox thresholds in sedimentary systems. Geochim Cosmochim Acta 287:8–26

Algeo TJ, Liu J (2020) A re-assessment of elemental proxies for paleoredox analysis. Chem Geol 540(2):119549. https://doi.org/10.1016/j.chemgeo.2020.119549

Anderson TF, Arthur MA (1983) Stable isotopes of oxygen and carbon and their application to sedimentologic and environmental problems. In: Arthur MA, Anderson TF, Kaplan IR et al (eds) Stable isotopes in sedimentary geology. Society of Economic Paleontologists and Mineralogists Short Course, vol no. 10. Society of Economic Paleontologists and Mineralogists, Tulsa, pp 1–151

Angeletti L, Canese S, Franchi F et al (2015) The 'chimney forest' of the deep Montenegrin margin, south-eastern Adriatic Sea. Mar Pet Geol 66:542–554

Argentino C, Lugli F, Cipriani A et al (2019) A deep fluid source of radiogenic Sr and highly dynamic seepage conditions recorded in Miocene seep carbonates of the northern Apennines (Italy). Chem Geol 522:135–147

Bailey JV, Orphan VJ, Joye SB et al (2009) Chemotrophic microbial mats and their potential preservation in the rock record. Astrobiology 9(9):843–859

Berner RA (1968) Calcium carbonate concretions formed by the decomposition of organic matter. Science 159(3811):195–197

Banner JL (1995) Application of the trace element and isotope geochemistry of strontium to studies of carbonate diagenesis. Sedimentology 42:805–824

Bau M, Balan S, Schmidt K, Koschinsky A (2010) Rare earth elements in mussel shells of the Mytilidae family as tracers for hidden and fossil high-temperature hydrothermal systems. Earth Planet Sci Lett 299(3–4):310–316

Bayon G, Pierre C, Etoubleau J et al (2007) Sr/Ca and Mg/Ca ratios in Niger Delta sediments: implications for authigenic carbonate genesis in cold seep environments. Mar Geol 241(1−4):93–109

Bayon G, Birot D, Ruffine L et al (2011) Evidence for intense REE scavenging at cold seeps from the Niger Delta margin. Earth Planet Sci Lett 312(3/4):443–452
Bayon G, Dupré S, Ponzevera E et al (2013) Formation of carbonate chimneys in the Mediterranean Sea linked to deep-water oxygen depletion. Nat Geosci 6:755–760. https://doi.org/10.1038/NGEO1888
Beal EJ, House CH, Orphan VJ (2009) Manganese- and iron-dependent marine methane oxidation. Science 325:184–187
Bennett WW, Canfield DE (2020) Redox-sensitive trace metals as paleoredox proxies: a review and analysis of data from modern sediments. Earth-Sci Rev 204:103175
Berner RA (1980) Early diagenesis—a theoretical approach. Princeton University Press, Princeton
Birgel D, Peckmann J, Klautzsch S et al (2006) Anaerobic and aerobic oxidation of methane at Late Cretaceous seeps in the Western Interior Seaway, USA. Geomicrobiol J 23:565–577
Birgel D, Feng D, Roberts HH et al (2011) Changing redox conditions at cold seeps as revealed by authigenic carbonates from Alaminos Canyon, northern Gulf of Mexico. Chem Geol 285(1−4):82–96
Boetius A, Ravenschlag K, Schubert CJ et al (2000) A marine consortium apparently mediating anaerobic oxidation of methane. Nature 407:623–625
Boggs S, Krinsley D (2006) Application of cathodoluminescence imaging to the study of sedimentary rocks. Cambridge University Press, Cambridge
Bohrmann G, Torres ME (2006) Gas hydrates in marine sediments. In: Schulz HD, Zabel M (eds) Marine geochemistry. Springer, Heidelberg, pp 481–512
Bonifacie M, Calmels D, Eiler JM et al (2017) Calibration of the dolomite clumped isotope thermometer from 25 to 350° C, and implications for a universal calibration for all (Ca, Mg, Fe) CO_3 carbonates. Geochim Cosmochim Acta 200:255–279. https://doi.org/10.1016/j.gca.2016.11.028
Bowles MW, Mogollon JM, Kasten S et al (2014) Global rates of marine sulfate reduction and implications for sub-sea-floor metabolic activities. Science 344:889–891
Brand U (2004) Carbon, oxygen and strontium isotopes in Paleozoic carbonate components: an evaluation of original seawater-chemistry proxies. Chem Geol 204(1/2):23–44
Brand U, Logan A, Hiller N et al (2003) Geochemistry of modern brachiopods: applications and implications for oceanography and paleoceanography. Chem Geol 198:305–334
Bristow TF, Grotzinger JP (2013) Sulfate availability and the geological record of cold-seep deposits. Geology 41:811–814
Buggisch W, Krumm S (2005) Palaeozoic cold seep carbonates from Europe and North Africa—an integrated isotopic and geochemical approach. Facies 51(1−4):566–583
Burdige DJ (2006) Geochemistry of marine sediments. Princeton University Press, Princeton
Burton EA (1993) Controls on marine carbonate cement mineralogy: review and reassessment. Chem Geol 105:163–179
Byrne RH, Sholkovitz ER (1996) Marine chemistry and geochemistry of the lanthanides. In: Gschneidner KA Jr, Eyring L (eds) Handbook on the physics and chemistry of rare earths. Elsevier Science, Amsterdam, pp 497–593
Campbell KA (2006) Hydrocarbon seep and hydrothermal vent paleoenvironments and paleontology: past developments and future research directions. Palaeogeogr Palaeoclimatol Palaeoecol 232:362–407
Campbell KA, Farmer JD, Des Marais D (2002) Ancient hydrocarbon seeps from the Mesozoic convergent margin of California: carbonate geochemistry, fluids and palaeoenvironments. Geofluids 2:63–94
Cangemi M, Di Leonardo R, Bellanca A et al (2010) Geochemistry and mineralogy of sediments and authigenic carbonates from the Malta Plateau, Strait of Sicily (central Mediterranean): relationships with mud/fluid release from a mud volcano system. Chem Geol 276(3/4):294–308
Cavagna S, Clari P, Dela Pierre F et al (2015) Sluggish and steady focussed flows through fine-grained sediments: the methane-derived cylindrical concretions of the Tertiary Piedmont Basin (NW Italy). Mar Pet Geol 66:596–605

Chen F, Hu Y, Feng D et al (2016) Evidence of intense methane seepages from molybdenum enrichments in gas hydrate-bearing sediments of the northern South China Sea. Chem Geol 443:173–181

Cochran JK, Landman NH, Turekian KK et al (2003) Paleoceanography of the Late Cretaceous (Maastrichtian) Western Interior Seaway of North America: evidence from Sr and O isotopes. Palaeogeogr Palaeoclimatol Palaeoecol 191:45–64

Cochran JK, Kallenberg K, Landman NH et al (2010) Effect of diagenesis on the Sr, O, and C isotope composition of Late Cretaceous mollusks from the Western Interior Seaway of North America. Am J Sci 310:69–88

Cochran JK, Landman NH, Larson NL et al (2015) Geochemical evidence (C and Sr isotopes) for methane seeps as ammonite habitats in the Late Cretaceous (Campanian) Western Interior Seaway. Swiss J Palaeontol 134:153–165

Crémière A, Lepland A, Chand S et al (2016) Fluid source and methane-related diagenetic processes recorded in cold seep carbonates from the Alvheim channel, central North Sea. Chem Geol 432:16–33

Dela Pierre F, Martire L, Natalicchio M et al (2010) Authigenic carbonates in upper Miocene sediments of the Tertiary Piedmont Basin (NW Italy): vestiges of an ancient gas hydrate stability zone? Geol Soc Am Bull 122(7/8):994–1010

Deng Y, Chen F, Hu Y et al (2020) Methane seepage patterns during the middle Pleistocene inferred from molybdenum enrichments of seep carbonates in the South China Sea. Ore Geol Rev 125:103701. https://doi.org/10.1016/j.oregeorev.2020.103701

Denison RE, Koepnick RB, Fletcher A et al (1994) Criteria for the retention of original seawater $^{87}Sr/^{86}Sr$ in ancient shelf limestones. Chem Geol 112(1/2):131–143

Dulski P (1994) Interferences of oxide, hydroxide and chloride analyte species in the determination of rare earth elements in geological samples by inductively coupled plasma-mass spectrometry. J Anal Chem 350:194–203

Elderfield H (1988) The oceanic chemistry of the rare-earth elements. Phil Trans Roy Soc Lond A 325:105–126

Elvert M, Hopmans EC, Treude T et al (2005) Spatial variations of menthanotrophic consortia at cold methane seeps: implications from a high-resolution molecular and isotopic approach. Geobiology 3:195–209

Ettwig KF, Butler MK, Le Pasilier D et al (2010) Nitrite-driven anaerobic methane oxidation by oxygenic bacteria. Nature 464:543–548

Feng D, Chen D (2015) Authigenic carbonates from an active cold seep of the northern South China Sea: new insights into fluid sources and past seepage activity. Deep-Sea Res II 122:74–83

Feng D, Chen D, Roberts HH (2009a) Petrographic and geochemical characterization of seep carbonate from Bush Hill (GC 185) gas vent and hydrate site of the Gulf of Mexico. Mar Pet Geol 26(7):1190–1198

Feng D, Chen D, Peckmann J (2009b) Rare earth elements in seep carbonates as tracers of variable redox conditions at ancient hydrocarbon seeps. Terra Nova 21(1):49–56

Feng D, Chen D, Peckmann J et al (2010) Authigenic carbonates from methane seeps of the northern Congo fan: microbial formation mechanism. Mar Pet Geol 27(4):748–756

Feng D, Lin Z, Bian Y et al (2013) Rare earth elements of seep carbonates: indication for redox variations and microbiological processes at modern seep sites. J Asian Earth Sci 65:27–33

Ferry JG (1992) Methane from acetate. J Bacteriol 174(17):5489–5495

Finch AA, Allison N (2007) Coordination of Sr and Mg in calcite and aragonite. Mineral Mag 71(5):539–552

Freslon N, Bayon G, Toucanne S et al (2014) Rare earth elements and neodymium isotopes in sedimentary organic matter. Geochim Cosmochim Acta 140:177–198

Gao Y (2019) Clumped isotope paleothermometry of authigenic carbonates from Late Cretaceous (Campanian) methane seeps in the Western Interior Seaway, South Dakota, USA. Thesis, Stony Brook University

Gao Y, Henkes GA, Cochran JK et al (2021) Temperatures of Late Cretaceous (Campanian) methane-derived authigenic carbonates from the Western Interior Seaway, South Dakota, USA, using clumped isotopes. Geol Soc Am Bull 133(11/12):2524–2534. https://doi.org/10.1130/B35846.1

Ge l, Chen W, Zhu B, Fan M, Yang T, Jiang S (2020) Sr and Nd isotopes of cold seep carbonates from the northern South China sea as proxies for fluid sources. Mar Pet Geol 115:104284

Ge L, Jiang S-Y, Swennen R et al (2010) Chemical environment of cold seep carbonate formation on the northern continental slope of South China Sea: evidence from trace and rare earth element geochemistry. Mar Geol 277(1–4):21–30

German CR, Elderfield H (1990) Application of the Ce anomaly as a paleoredox indicator: the ground rules. Paleoceanographica 5(5):823–833

Greinert J, Bohrmann G, Suess E (2001) Gas hydrate-associated carbonates and methane-venting at Hydrate Ridge: classification, distribution, and origin of authigenic lithologies. In: Paull CK, Dillon PW (eds) Natural gas hydrates: occurrence, distribution, and detection. American Geophysical Union, Washington, DC, pp 99–113

Greinert J, Bohrmann G, Elvert M (2002) Stromatolitic fabric of authigenic carbonate crusts: result of anaerobic methane oxidation at cold seeps in 4,850 m water depth. Int J Earth Sci 91(4):698–711

Grossman EL, Ku T-L (1986) Carbon and oxygen isotopic fractionation in biogenic aragonite: temperature effects. Chem Geol 59:59–74

Hagemann A, Leefmann T, Peckmann J et al (2012) Biomarkers from individual carbonate phases of an Oligocene cold-seep deposit. Lethaia 46(1):7–18. https://doi.org/10.1111/j.1502-3931.2012.00316.x

Haley BA, Klinkhammer GP, McManus J (2004) Rare earth elements in pore waters of marine sediments. Geochim Cosmochim Acta 68(6):1265–1279

Hall JLO, Newton RJ, Witts JD et al (2018) High benthic methane flux in low sulfate oceans: evidence from carbon isotopes in Late Cretaceous Antarctic bivalves. Earth Planet Sci Lett 497:113–122

Han X, Suess E, Sahling H et al (2004) Fluid activity on the Costa Rica margin: new results from authigenic carbonates. Int J Earth Sci 93:596–611

Handle KC (2014) Paleoecology of Late Cretaceous methane cold seeps of the Pierre Shale, South Dakota. Dissertation, City University of New York

Hein JR, Zierenberg RA, Maynard JB et al (2007) Barite-forming environments along a rifted continental margin, southern California borderland. Deep-Sea Res II 54:1327–1349

Hellebrandt SE, Hofmann S, Jordan N et al (2016) Incorporation of Eu(III) into calcite under recrystallization conditions. Sci Rep 6:33137. https://doi.org/10.1038/srep33137

Henkes GA, Passey BH, Wanamaker AD et al (2013) Carbonate clumped isotope compositions of modern marine mollusk and brachiopod shells: Geochim Cosmochim Acta 106:307–325

Himmler T, Bach W, Bohrmann G et al (2010) Rare earth elements in authigenic methane-seep carbonates as tracers for fluid composition during early diagenesis. Chem Geol 277(1/2):126–136

Himmler T, Haley BA, Torres ME et al (2013) Rare earth element geochemistry in cold-seep pore waters of Hydrate Ridge, northeast Pacific Ocean. Geo-Mar Lett 33(5):369–379

Himmler T, Smrzka D, Zwicker J et al (2018) Stromatolites below the photic zone in the northern Arabian Sea formed by calcifying chemotrophic microbial mats. Geology 46(4):339–342

Hryniewicz K (this volume-a) Ancient seep carbonates: from outcrop appearance to microscopic petrography. In: Kaim A, Cochran JK, Landman NH (eds) Ancient hydrocarbon seeps. Topics in geobiology, vol 50. Springer, New York

Hryniewicz K (this volume-b) Seeps around the world. In: Kaim A, Cochran JK, Landman NH (eds) Ancient hydrocarbon seeps. Topics in geobiology, vol 50. Springer, New York

Hu Y, Feng D, Peckmann J et al (2014) New insights into cerium anomalies and mechanisms of trace metal enrichment in authigenic carbonate from hydrocarbon seeps. Chem Geol 381:55–66

Hu Y, Feng D, Peckmann J et al (2020) The impact of diffusive transport of methane on pore-water and sediment geochemistry constrained by authigenic enrichments of carbon, sulfur, and trace

elements: a case study from the Shenhu area of the South China Sea. Chem Geol 553:119805. https://doi.org/10.1016/j.chemgeo.2020.119805

Hudson JD, Anderson TF (1989) Ocean temperatures and isotopic compositions through time. Trans R Soc Edinb Earth Sci 80:183–192

Jakubowicz M, Dopieralska J, Belka Z (2015a) Tracing the composition and origin of fluids at an ancient hydrocarbon seep (Holland Mound, Middle Devonian, Morocco): a Nd, REE and stable isotope study. Geochim Cosmochim Acta 156:50–74

Jakubowicz M, Berkpwski B, Correa ML et al (2015b) Stable Isotope Signatures of Middle Palaeozoic ahermatypic rugose corals—deciphering secondary alteration, vital fractionation effects, and palaeoecological implications. PLoS One 10(9):e0136289. https://doi.org/10.1371/journal.pone.0136289

Jakubowicz M, Dopieralska J, Kaim A et al (2019) Nd isotope composition of seep carbonates: towards a new approach for constraining subseafloor fluid circulation at hydrocarbon seeps. Chem Geol 503:40–51

Jakubowicz M, Kiel S, Goedert JL et al (2020) Fluid expulsion system and tectonic architecture of the incipient Cascadia convergent margin as revealed by Nd, Sr and stable isotope composition of mid-Eocene methane seep carbonates. Chem Geol 558:119872. https://doi.org/10.1016/j.chemgeo.2020.119872

Jakubowicz M, Agirrezabala LM, Dopieralska J et al (2021) The role of magmatism in hydrocarbon generation in sedimented rifts: a Nd isotope perspective from mid-Cretaceous methane-seep deposits of the Basque-Cantabrian Basin, Spain. Geochim Cosmochim Acta 393:223–248

Jenkins RG, Kaim A, Hikida Y et al (2007) Methane-flux-dependent lateral faunal changes in a Late Cretaceous chemosymbiotic assemblage from the Nakagawa area of Hokkaido, Japan. Geobiology 6:127–139

Jørgensen BB, Nelson DC (2004) Sulfide oxidation in marine sediments: geochemistry meets microbiology. In: Amend JP, Edwards KJ, Lyons TW (eds) Sulfur biogeochemistry—past and present, Geological Society of America Special Paper 379. Geological Society of America, Boulder, pp 63–81

Joseph C, Torres ME, Martin RA et al (2012) Using the $^{87}Sr/^{86}Sr$ of modern and paleoseep carbonates from northern Cascadia to link modern fluid flow to the past. Chem Geol 334:122–130

Joseph C, Campbell KA, Torres ME et al (2013) Methane-derived authigenic carbonates from modern and paleoseeps on the Cascadia margin: mechanisms of formation and diagenetic signals. Palaeogeogr Palaeoclimatol Palaeoecol 390:52–67

Joye S (2012) A piece of the methane puzzle. Nature 491:538–539

Kaplan IR, Rittenberg SC (1964) Microbiological fractionation of sulphur isotopes. J Gen Microbiol 34:195–212

Kelly SRA, Ditchfield PW, Doubleday PA et al (1995) An Upper Jurassic methane-seep limestone from the Fossil Bluff Group fore-arc basin of Alexander Island, Antarctica. J Sediment Res A 65(2):274–282

Kennedy M, Mrofka D, von der Borch C (2008) Snowball Earth termination by destabilization of equatorial permafrost methane clathrate. Nature 453:642–645

Kiel S (2015) Did shifting seawater sulfate concentrations drive the evolution of methane-seep ecosystems? Proc R Soc B 282(1804):20142908. https://doi.org/10.1098/rspb.2014.2908

Kiel S, Hansen C, Nitzsche KN et al (2014) Using $^{87}Sr/^{86}Sr$ ratios to date fossil methane seep deposits: methodological requirements and an example from the Great Valley Group, California. J Geol 122(4):353–366

Kim S, O'Neil JR (1997) Equilibrium and nonequilibrium oxygen isotope effects in synthetic carbonates. Geochim Cosmochim Acta 61:3461–3475. https://doi.org/10.1016/S0016-7037(97)00169-5

Kim J-H, Torres ME, Haley BA et al (2012) The effect of diagenesis and fluid migration on rare earth element distribution in pore fluids of the northern Cascadia accretionary margin. Chem Geol 291:152–165

Knittel K, Boetius A (2009) Anaerobic oxidation of methane: progress with an unknown process. Annu Rev Microbiol 63:311–334

Krause FF, Clark J, Sayegh SG et al (2009) Tube worm fossils or relic methane expulsing conduits? Palaios 24:41–50

Lacan F, Tachikawa K, Jeandel C (2012) Neodymium isotope composition of the oceans: a compilation of seawater data. Chem Geol 300(301):177–184

Lakshtanov LZ, Stipp SLS (2004) Experimental study of europium (III) coprecipitation with calcite. Geochim Cosmochim Acta 68(4):819–827

Landman NH, Cochran JK, Larson NL et al (2012) Methane seeps as ammonite habitats in the U.S. Western Interior Seaway revealed by isotopic analyses of well-preserved shell material. Geology 40(6):507–510. https://doi.org/10.1130/G32782.1

Landman NH, Cochran JK, Slovacek M et al (2018) Isotope sclerochronology of ammonites (*Baculites compressus*) from methane seep and non-seep sites in the Late Cretaceous Western Interior Seaway, USA: implications for ammonite habitat and mode of life. Am J Sci 318:603–639

Landman NH, Cochran JK, Brezina J et al (this volume) Methane seeps in the Late Cretaceous Western Interior Seaway. In: Kaim A, Cochran JK, Landman NH (eds) Ancient hydrocarbon seeps. Topics in geobiology, vol. 50, Springer, New York

Lietard C, Pierre C (2009) Isotopic signatures ($\delta^{18}O$ and $\delta^{13}C$) in bivalve shells from cold seeps and hydrothermal vents. Geobios 42:209–219

Lin Z, Sun X, Peckmann J et al (2016) How sulfate-driven anaerobic oxidation of methane affects the sulfur isotopic composition of pyrite: a SIMS study from the South China Sea. Chem Geol 440:26–41

Lin Z, Sun X, Strauss H et al (2017a) Multiple sulfur isotope constraints on sulfate-driven anaerobic oxidation of methane: evidence from authigenic pyrite in seepage areas of the South China Sea. Geochim Cosmochim Acta 211:153–173

Lin Z, Sun X, Lu Y et al (2017b) The enrichment of heavy iron isotopes in authigenic pyrite as a possible indicator of sulfate-driven anaerobic oxidation of methane: insights from the South China Sea. Chem Geol 449:15–29

Little CTS, Birgel D, Boyce AJ et al (2015) Late Cretaceous (Maastrichtian) shallow water hydrocarbon seeps from Snow Hill and Seymour Islands, James Ross Basin, Antarctica. Palaeogeogr Palaeoclimatol Palaeoecol 418:213–228

Loyd SJ, Sample J, Tripati RE et al (2016) Methane seep carbonates yield clumped isotope signatures out of equilibrium with formation temperatures. Nat Commun 7:12274

Luff R, Wallmann K (2003) Fluid flow, methane fluxes carbonate precipitation and biogeochemical turnover in gas hydrate-bearing sediments at Hydrate Ridge, Cascadia Margin: numerical modeling and mass balances. Geochim Cosmochim Acta 67(18):3404–3421

Luff R, Wallmann K, Aloisi G (2004) Numerical modeling of carbonate crust formation at cold vent sites: significance for fluid and methane budgets and chemosynthetic biological communities. Earth Planet Sci Lett 221:337–353

Machel HG (2000) Application of cathodoluminescence to carbonate diagenesis. In: Pagel M, Barbin V, Blanc P et al (eds) Cathodoluminescence in geosciences. Springer, New York, pp 271–301

MacRae ND, Nesbitt HW, Kronberg BI (1992) Development of a positive Eu anomaly during diagenesis. Earth Planet Sci Lett 109(3/4):585–591

Matsumoto R (2001) Methane hydrates. In: Steele JH, Thorpe SA, Turekian KK (eds) Encyclopedia of ocean sciences, 1st edn. Elsevier, New York, pp 1745–1757

Matveeva T, Savvichev AD, Semenova A et al (2015) Source, origin and spatial distribution of shallow sediment methane in the Chukchi Sea. Oceanography 28(3):202–217

Mazzini A, Ivanov MK, Parnell J et al (2004) Methane-related authigenic carbonates from the Black Sea: geochemical characterisation and relation to seeping fluids. Mar Geol 212:153–181

McArthur JM, Kennedy WJ, Chen M et al (1994) Strontium isotope stratigraphy for Late Cretaceous time: direct numerical calibration of the Sr isotope curve based on the US Western Interior. Palaeogeogr Palaeoclimatol Palaeoecol 108:95–119

McConnaughey TA (1989) ^{13}C and ^{18}O isotopic disequilibria in biological carbonates: I, patterns. Geochim Cosmochim Acta 53:151−162

McConnaughey TA, Gillikin DP (2008) Carbon isotopes in mollusk shell carbonates. Geo-Mar Lett 28:287–299
McLennan SM (1989) Rare-earth elements in sedimentary rocks—influence of provenance and sedimentary processes. Rev Mineral 21:169–200
Michaelis W, Seifert R, Nauhaus K et al (2002) Microbial reefs in the Black Sea fueled by anaerobic oxidation of methane. Science 297:1013–1015
Milucka J, Ferdelman TG, Polerecky L et al (2012) Zero-valent sulphur is a key intermediate in marine methane oxidation. Nature 491:541–546
Miyajima Y, Jenkins RG (this volume) Biomarkers in ancient hydrocarbon-seep carbonates. In: Kaim A, Cochran JK, Landman NH (eds) Ancient hydrocarbon seeps. Topics in geobiology, vol 50. Springer, New York
Miyajima Y, Watanabe Y, Jenkins RG et al (2018) Diffusive methane seepage in ancient deposits: examples from the Neogene Shin'etsu sedimentary basin, central Japan. J Sediment Res 88:449–466
Naehr TH, Eichhubl P, Orphan VJ et al (2007) Authigenic carbonate formation at hydrocarbon seeps in continental margin sediments: a comparative study. Deep-Sea Res II 54:1268–1291
Natalicchio M, Birgel D, Dela Pierre F et al (2012) Polyphasic carbonate precipitation in the shallow subsurface: insights from microbially-formed authigenic carbonate beds in the upper Miocene sediments of the Tertiary Piedmont (NW Italy). Palaeogeogr Palaeoclimatol Palaeoecol 329(330):158–172
Nothdurft LD, Webb GE, Kamber BS (2004) Rare earth element geochemistry of Late Devonian reefal carbonates, Canning Basin, Western Australia: confirmation of a seawater REE proxy in ancient limestones. Geochim Cosmochim Acta 68(2):263–283
Nöthen K, Kasten S (2011) Reconstructing changes in seep activity by means of pore water and solid phase Sr/Ca and Mg/Ca ratios in pockmark sediments of the Northern Congo Fan. Mar Geol 287(1−4):1–13
Paull CK, Ussler W III, Holbrook WS et al (2008) Origin of pockmarks and chimney structures on the flanks of the Storegga Slide, offshore Norway. Geo-Mar Lett 28:43–51
Peckmann J, Thiel V (2004) Carbon cycling at ancient methane-seeps. Chem Geol 205:443–467
Peckmann J, Thiel V, Michaelis W et al (1999) Cold seep deposits of Beauvoisin (Oxfordian, southeastern France) and Marmorito (Miocene, northern Italy): microbially induced authigenic carbonates. Int J Earth Sci 88:60–75
Peckmann J, Reimer A, Luth U et al (2001) Methane-derived carbonates and authigenic pyrite from the northwestern Black Sea. Mar Geol 177:129–150
Peckmann J, Goedert JL, Thiel V et al (2002) A comprehensive approach to the study of methane-seep deposits from the Lincoln Creek Formation, western Washington State, USA. Sedimentology 49:855–873
Peckmann J, Goedert JL, Heinrichs T et al (2003) The Late Eocene 'Whiskey Creek' methane-seep deposit (western Washington State) part II: petrology, stable isotopes, and biogeochemistry. Facies 48:241–254
Peckmann J, Thiel V, Reitner J et al (2004) A microbial mat of a large sulfur bacterium preserved in a Miocene methane-seep limestone. Geomicrobiol J 21:247–255. https://doi.org/10.1080/01490450490438757
Peckmann J, Campbell KA, Walliser OH et al (2007) A Late Devonian hydrocarbon-seep deposit dominated by dimerelloid brachiopods, Morocco. Palaios 22(2):114–122
Peketi A, Mazumdar A, Joshi RK et al (2012) Tracing the paleo sulfate-methane transition zones and H_2S seepage events in marine sediments: an application of C-S-Mo systematics. Geochem Geophys Geosyst 13(10):Q10007. https://doi.org/10.1029/2012GC004288
Pichler T, Veizer J (2004) The precipitation of aragonite from shallow-water hydrothermal fluids in a coral reef, Tutum Bay, Ambitle Island, Papua New Guinea. Chem Geol 207(1/2):31–45
Pierre C, Blanc-Valleron M-M, Caquineau S et al (2014) Mineralogical, geochemical and isotopic characterization of authigenic carbonates from the methane-bearing sediments of the Bering Sea continental margin (IODP Expedition 323, Sites U1343−U1345). Deep-Sea Res II 125(126):133–144

Planavsky NJ, Bekker A, Hofmann A et al (2012) Sulfur record of rising and falling marine oxygen and sulfate levels during the Lomagundi event. PNAS 109(45):18300–18305
Popp BN, Anderson TF, Sandberg PA (1986) Textural, elemental, and isotopic variations among constituents in Middle Devonian limestones, North America. J Sediment Petrol 56(5):715–727
Pourret O, Davranche M, Gruau G et al (2008) New insights into cerium anomalies in organic-rich alkaline waters. Chem Geol 251(1−4):120–127
Preisler A, de Beer D, Lichtschlag A et al (2007) Biological and chemical sulfide oxidation in a *Beggiatoa* inhabited marine sediment. ISME J 1:341–353. https://doi.org/10.1038/ismej.2007.50
Reeder RJ (1983) Crystal chemistry of the rhombohedral carbonates In: Reeder RJ (ed) Carbonates: mineralogy and chemistry. Reviews in Mineralogy vol 11. Mineralogical Society of America, Chantilly, pp 1−47
Reitner J, Peckmann J, Blumenberg M et al (2005) Concretionary methane-seep carbonates and associated microbial communities in Black Sea sediments. Palaeogeogr Palaeoclimatol Palaeoecol 227:18030
Ritger S, Carson B, Suess E (1987) Methane-derived authigenic carbonates formed by subduction-induced pore-water expulsion along the Oregon/Washington margin. Geol Soc Am Bull 98:147–156
Roberts HH, Feng D, Joye SB (2010) Cold-seep carbonates of the middle and lower continental slope, northern Gulf of Mexico. Deep-Sea Res II 57:2040–2054
Rongemaille E, Bayon G, Pierre C et al (2011) Rare earth elements in cold seep carbonates from the Niger Delta. Chem Geol 286:196–206
Rowe A, Landman NH, Cochran JK et al (2020) Late Cretaceous methane seeps as habitats for newly hatched ammonites. Palaios 35:1–13
Sample JC, Reid MR, Tobin HJ et al (1993) Carbonate cements indicate channeled fluid flow along a zone of vertical faults at the deformation front of the Cascadia accretionary wedge (northwest U.S. coast). Geology 21:507–510
Sansone FJ, Martens CS (1981) Methane production from acetate and associated methane fluxes from anoxic coastal sediments. Science 211:707–709
Savard MM, Beauchamp B, Veizer J (1996) Significance of aragonite cements around Cretaceous methane seeps. J Sediment Res 66(3):430–438
Sayama M (2001) Presence of nitrate-accumulating sulfur bacteria and their influence on nitrogen cycling in a shallow coastal marine sediment. Appl Environ Microbiol 67(8):3481–3487. https://doi.org/10.1128/AEM.67.8.3481-3487.2001
Schwedt A, Kreutzmann A-C, Polerecky L et al (2012) Sulfur respiration in a marine chemolithotrophic *Beggiatoa* strain. Front Microbiol 2:276. https://doi.org/10.3389/fmicb.2011.00276
Shackleton NJ, Kennett JP (1975) Paleotemperature history of the Cenozoic and initiation of Antarctic glaciation: oxygen and carbon isotope analyses in DSDP sites 277, 279 and 281. Deep Sea Drilling Project Initial Rep 29:743–755
Shields GA, Deynoux M, Strauss H et al (2007) Barite-bearing cap dolostones of the Taoudeni Basin, northwest Africa: sedimentary and isotopic evidence for methane seepage after a Neoproterozoic glaciation. Precambrian Res 153:209–235
Sholkovitz ER, Piepgras DJ, Jacobsen SB (1989) The pore water chemistry of rare earth elements in Buzzards Bay sediments. Geochim Cosmochim Acta 53:2847–2856
Smrzka D, Zwicker J, Klügel A et al (2016) Establishing criteria to distinguish oil-seep from methane-seep carbonates. Geology 44(8):667–670
Smrzka D, Zwicker J, Kolonic S et al (2017) Methane seepage in a Cretaceous greenhouse world recorded by an unusual carbonate deposit from the Tarfaya Basin, Morocco. Depositional Rec 3(1):4–37
Smrzka D, Zwicker J, Misch D et al (2019) Oil seepage and carbonate formation: a case study from the southern Gulf of Mexico. Sedimentology 66(6):2318–2353
Smrzka D, Feng D, Himmler T et al (2020) Trace elements in methane-seep carbonates: potentials, limitations, and perspectives. Earth Sci Rev 208:103263. https://doi.org/10.1016/j.earscirev.2020.103263

Soyol-Erdene T-O, Huh Y (2013) Rare earth element cycling in the pore waters of the Bering Sea Slope (IODP Exp. 323). Chem Geol 358:75–89

Stakes DS, Orange D, Paduan JB et al (1999) Cold-seeps and authigenic carbonate formation in Monterey Bay, California. Mar Geol 159:93–109

Stipp SLS, Lakshtanov LZ, Jensen JT et al (2003) Eu^{3+} uptake by calcite: preliminary results from coprecipitation experiments and observations with surface-sensitive techniques. J Contam Hydrol 61(1−4):33–43

Sverjensky DA (1984) Europium redox equilibria in aqueous solution. Earth Planet Sci Lett 67(1):70–78

Tachikawa K, Arsouze T, Bayon G et al (2017) The large-scale evolution of neodymium isotopic composition in the global modern and Holocene ocean revealed from seawater and archive data. Chem Geol 457:131–148

Teichert BAM, Bohrmann G, Suess E (2005) Chemoherms on Hydrate Ridge—unique microbially-mediated carbonate build-ups growing into to the water column. Palaeogeogr Palaeoclimatol Palaeoecol 227:67–85

Tong H, Feng D, Peckmann J et al (2019) Environments favoring dolomite formation at cold seeps: a case study from the Gulf of Mexico. Chem Geol 518:9–18

Torres ME, McManus JW, Huh C-A (2002) Fluid seepage along the San Clemente Fault scarp: basin-wide impact on barium cycling. Earth Planet Sci Lett 203:181–194

Tostevin R, Shields GA, Tarbuck GM et al (2016) Effective use of cerium anomalies as a redox proxy in carbonate-dominated marine settings. Chem Geol 438:146–162

Tribovillard N, Armynot du Châtelet E, Gay A et al (2013) Geochemistry of cold seepage-impacted sediments: per-ascensum or per-descensum trace metal enrichment? Chem Geol 340:1–12

Tucker ME, Wright VP (1990) Carbonate sedimentology. Blackwell Scientific, Oxford

Walker RJ, Hanson GN, Papike JJ et al (1986) Nd, O and Sr isotopic constraints on the origin of Precambrian rocks, southern Black Hills, South Dakota. Geochim Cosmochim Acta 50:2833–2846

Wang S, Yan W, Chen Z et al (2014) Rare earth elements in cold seep carbonates from the southwestern Dongsha area, northern South China Sea. Mar Pet Geol 57:482–493

Wang Q, Tong H, Huang C-Y et al (2018) Tracing fluid sources and formation conditions of Miocene hydrocarbon-seep carbonates in the central Western Foothills, central Taiwan. J Asian Earth Sci 168:186–196

Wang Q, Chen D, Peckmann J (2019) Iron shuttle controls on molybdenum, arsenic, and antimony enrichment in Pliocene methane-seep carbonates from the southern Western Foothills, southwestern Taiwan. Mar Pet Geol 100:263–269

Webb GE, Nothdurft LD, Kamber BS et al (2009) Rare earth element geochemistry of scleractinian coral skeleton during meteoric diagenesis: a sequence through neomorphism of aragonite to calcite. Sedimentology 56(5):1433–1463

Whiticar MJ (1999) Carbon and hydrogen isotope systematics of bacterial formation and oxidation of methane. Chem Geol 161:291–314

Wiese F, Kiel S, Pacvk A et al (2015) The beast burrowed, the fluid followed—crustacean burrows as methane conduits. Mar Pet Geol 66:631–640

Williscroft K, Grasby SE, Beauchamp B et al (2017) Extensive Early Cretaceous (Albian) methane seepage on Ellef Ringnes Island, Canadian High Arctic. Geol Soc Am Bull 129(7/8):788–805

Zhang N, Lin M, Snyder GT et al (2019) Clumped isotope signatures of methane-derived authigenic carbonate presenting equilibrium values of their formation temperatures. Earth Planet Sci Lett 512:207–213

Zwicker J, Smrzka D, Gier S et al (2015) Mineralized conduits are part of the uppermost plumbing system of Oligocene methane-seep deposits, Washington Stare (USA). Mar Pet Geol 66:616–630

Zwicker J, Smrzka D, Himmler T et al (2018) Rare earth elements as tracers for microbial activity and early diagenesis: a new perspective from carbonate cements of ancient methane-seep deposits. Chem Geol 501:77–85

Chapter 2
Biomarkers in Ancient Hydrocarbon Seep Carbonates

Yusuke Miyajima and Robert G. Jenkins

2.1 Introduction

2.1.1 What Are Biomarkers?

Biomarkers (biological markers) or "molecular fossils" are organic molecules preserved in geological samples (e.g., sediments and crude oils), which can be traced back to their source organism (Eglinton et al. 1964; Eglinton and Calvin 1967). Although organic molecules are prone to diagenetic alterations, their specific chemical structures can be preserved as biomarkers, and their precursor molecules can be identified in the geological record. One of the most stable and valuable biomarkers in sedimentary rocks are lipid biomarkers, which originate from cell membrane lipids of organisms. Biomarkers are taxonomically specific and can be assigned mostly to a higher phylogenic clade but sometimes to a distinct taxon, and they, therefore, tell us about life of the past (e.g., Brocks et al. 1999; Brocks and Pearson 2005; Birgel et al. 2008a). A great advantage of biomarker analysis is that we can obtain information on ancient microbial communities that are difficult to be preserved as body fossils. In addition to the detection of past life, biomarkers also give information on paleoenvironmental history because of their sensitivity to physicochemical parameters such as temperature and oxic/anoxic conditions (e.g., Prahl and Wakeham 1987; Schouten et al. 2002; Brocks et al. 2005). Furthermore, methodological developments in measuring the isotopic composition of each molecular

Y. Miyajima (✉)
Research Institute for Geo-Resources and Environment, Geological Survey of Japan, National Institute of Advanced Industrial Science and Technology (AIST), Tsukuba, Japan
e-mail: yusuke.miyajima@aist.go.jp

R. G. Jenkins
Faculty of Geosciences and Civil Engineering, Institute of Science and Engineering, Kanazawa University, Kanazawa, Japan
e-mail: robertgj@staff.kanazawa-u.ac.jp

A. Kaim et al. (eds.), *Ancient Hydrocarbon Seeps*, Topics in Geobiology 50,
https://doi.org/10.1007/978-3-031-05623-9_2

compound, i.e., compound-specific isotope analysis (CSIA, Hayes et al. 1990), have resulted in breakthroughs in understanding metabolic and biosynthetic processes through which biomarkers are produced. Readers can refer to Gaines et al. (2009) for a comprehensive history of biomarker research and for basic and key information on applications of biomarkers to studies on Earth history.

In methane-seep environments, biomarker analyses coupled with CSIA help us identify which organisms were related to methane consumption, as methane has a distinct isotopic composition strongly depleted in ^{13}C. This chapter first briefly reviews earlier studies on biomarkers in methane-seep environments. Then, standard methods to extract and analyze lipids from seep carbonates are introduced, with some notes on thermal maturity and biodegradation of samples. Subsequent sections overview the biomarkers for microorganisms related to anaerobic oxidation of methane (AOM) and aerobic methanotrophy known from modern and ancient seep environments, together with their stable carbon isotopic signatures. This chapter also shows some prospects and outlooks for biomarker applications to ancient seep environments, reviewing selected recent studies.

2.1.2 Pioneer Studies on Biomarkers at Cold Seeps

In methane-rich, reduced sedimentary environments, a unique microbial community plays a significant role in consuming methane. Under marine conditions, anaerobic oxidation of methane (AOM) is coupled with sulfate reduction:

$$CH_4 + SO_4^{2-} \rightarrow HCO_3^- + HS^- + H_2O$$

Although this reaction has been known from anoxic basins since the 1970s (Reeburgh 1976), the microbes performing the reaction remained unidentified until around 2000. Methanogenic archaea were thought to be candidates for the AOM-performing microbes in syntrophy with sulfate-reducing bacteria (e.g., Hoehler et al. 1994). Hinrichs et al. (1999) and Elvert et al. (1999) first broke through this assumption by identifying lipid biomarkers specific to cell membranes of archaea in cold-seep sediments off California and off the Cascadia margin. While the identified archaeal biomarkers were those known from cultivated methanogens, they were significantly depleted in the heavy stable carbon isotope (^{13}C), indicating that methane, generally depleted in ^{13}C, was consumed by the microbes to synthesize the lipids. By the application of fluorescence in situ hybridization (FISH) to anoxic cold-seep sediments of the Cascadia convergent margin, Boetius et al. (2000) visualized novel microbial consortia as cell aggregates composed of archaea surrounded by sulfate-reducing bacteria (SRB). Directly coupled FISH observation and isotope measurements using secondary ion mass spectrometry (SIMS) on similar consortia from anoxic sediments of the Californian seep sites by Orphan et al. (2001a) confirmed methane consumption by the archaea. The anaerobic methane-oxidizing archaea are now known to include at least three distinct phylogenetic clades,

ANME-1, ANME-2, and ANME-3, which are related to methanogens of the orders Methanosarcinales and Methanomicrobiales (Hinrichs et al. 1999; Boetius et al. 2000; Orphan et al. 2001b, 2002; Knittel et al. 2005; Niemann et al. 2006; Lösekann et al. 2007; Knittel and Boetius 2009). Bacterial partners of ANME-1 and ANME-2 archaea are SRB described as SEEP-SRB1 clades belonging to the *Desulfosarcina/Desulfococcus* (DSS) group and that of ANME-3 archaea are SRB closely related to *Desulfobulbus* spp. (DBB) (Boetius et al. 2000; Orphan et al. 2001b; Michaelis et al. 2002; Knittel et al. 2003; Niemann et al. 2006; Lösekann et al. 2007; Niemann and Elvert 2008). The ANME and SRB partners often form shell- or mat-type consortia, although single ANME cells, particularly those of ANME-1 archaea, have also been reported (Boetius et al. 2000; Michaelis et al. 2002; Knittel et al. 2005; Reitner et al. 2005; Niemann et al. 2006; Lösekann et al. 2007; Knittel and Boetius 2009) (Fig. 2.1; for a detailed review on microbes at cold seeps, see Shapiro this volume).

An alkalinity increase driven by AOM induces precipitation at methane seeps of carbonate minerals, which have a great potential to preserve organic compounds originating from the AOM consortia thriving in the sediments. At about the same time as the discovery of ANME biomarkers from modern seep sediments, V. Thiel and J. Peckmann with their co-workers first applied lipid biomarker analysis to

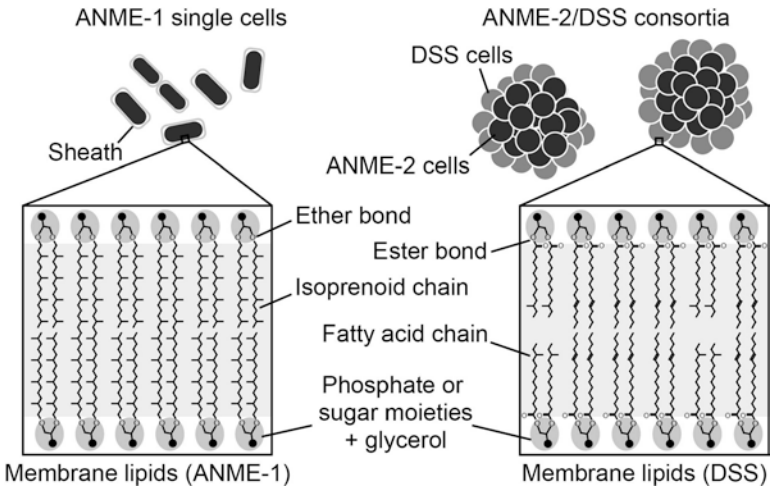

Fig. 2.1 Schematic illustrations of single cells and aggregates of anaerobic methane-oxidizing archaea (ANME) and sulfate-reducing bacteria (SRB). Single rectangular cells of ANME-1 with external sheaths and typical shell-type consortia of coccoid cells of ANME-2 and SRB of the clade *Desulfosarcina/Desulfococcus* (DSS) are shown. The diameter of the consortia is typically 3–5 µm on average (Knittel and Boetius 2009). Morphologies of the cells and aggregates are based on Boetius et al. (2000), Reitner et al. (2005), and Knittel and Boetius (2009). Lower insets show schemes of cell membranes of archaea (ANME-1) and bacteria (DSS) (structures based on De Rosa et al. 1991; Valentine 2007). Note that the composition of the membrane lipids of these organisms is estimated from biomarker inventories found in modern and ancient methane-seep environments (e.g., Niemann and Elvert 2008)

ancient methane-seep deposits (Peckmann et al. 1999a; Thiel et al. 1999). They extracted hydrocarbon biomarkers of anaerobic methane-oxidizing archaea and also aerobic methanotrophic bacteria, both highly depleted in ^{13}C, from Upper Jurassic (Oxfordian) and Miocene seep carbonates in France and Italy, respectively. Subsequent studies performed lipid biomarker analyses on ancient seep carbonates from all over the world, including the Miocene to Pleistocene of Italy (Peckmann et al. 2004; Blumenberg et al. 2015); the Upper Cretaceous, Miocene, and Pleistocene of Japan (Jenkins et al. 2008; Tsuboi et al. 2010; Miyajima et al. 2016), the Lower to Upper Cretaceous and Miocene of New Zealand (Pearson et al. 2010; Kiel et al. 2013); the Lower Jurassic to Upper Cretaceous, upper Eocene, and Oligocene of North America (Peckmann et al. 2002; Goedert et al. 2003; Birgel et al. 2006a, b); the lower Oligocene or upper Eocene of Peru (Kiel et al. 2020); the middle Eocene of Croatia (Natalicchio et al. 2015); the lower Eocene of Bulgaria (De Boever et al. 2009); the Paleocene of Svalbard (Hryniewicz et al. 2016); the Upper Cretaceous of Antarctica (Little et al. 2015); the Upper Cretaceous of Morocco (Smrzka et al. 2017); and the Lower Cretaceous of Ukraine (Peckmann et al. 2009), Romania (Sandy et al. 2012), Switzerland and France (Kiel et al. 2014), and Spain (Agirrezabala et al. 2013). A study in Namibia by Birgel et al. (2008a) showed that the biomarkers of AOM consortia can be preserved within seep carbonates even as old as upper Carboniferous (upper Pennsylvanian, ~300 Ma). Biomarkers of AOM-performing microbes are now potent tools to detect methane seepage and consumption in the past.

2.2 Basic Guide to Biomarker Studies of Ancient Seeps

2.2.1 Sample Preparation, Lipid Extraction, and Analysis

Methane-seep carbonates display a variety of petrographic fabrics (see Hryniewicz this volume). While this variability can be accompanied by fabric-specific differences in biomarker contents (see Sect. 2.6), such differences are usually unrecognizable due to generally large amounts of samples needed for the analysis (a few tens to hundreds of grams). One should recognize what kind of carbonate fabrics the sample mainly consists of and interpret their formation processes with complementary data such as petrographic observations and carbon and oxygen isotopic signatures of the carbonates.

Lipids are biomolecules insoluble in water but soluble in organic solvents and are the main components of oils, fats, and waxes (Peters et al. 2005). To efficiently extract lipids from consolidated sedimentary rocks, we cut, crush, and grind them into powders. To avoid organic contamination, weathered surfaces must be removed,

and samples should be pre-cleaned with distilled water, organic solvents (e.g., acetone, dichloromethane, and methanol), and/or acids (e.g., 10% HCl). Lipids can be extracted from the powdered samples by ultrasonication in organic solvents, often dichloromethane/methanol (e.g., Thiel et al. 1999; Peckmann et al. 2002; Birgel et al. 2006b; Miyajima et al. 2016) or *n*-hexane/dichloromethane mixtures (Jenkins et al. 2008). Lipid extraction in solvents is also possible via Soxhlet apparatus or automated extraction systems (e.g., Pancost et al. 2005; Stadnitskaia et al. 2005; Rossel et al. 2011). For carbonate samples, the powdered samples are in many cases dissolved in hydrochloric acid, and lipids are extracted from the acid-insoluble residues (e.g., Thiel et al. 1999; Peckmann et al. 2002; Birgel et al. 2006a, b), whereas in some cases, lipids are extracted from the powders without decalcification (e.g., Jenkins et al. 2008; Miyajima et al. 2016). According to Thiel et al. (1999), some lipid biomarkers were preferentially released after carbonate dissolution, most likely indicating intracrystalline preservation of the compounds within the mineral matrix. After centrifugation, the obtained lipid extracts in supernatants are separated by column chromatography into several fractions of increasing polarity, by sequential elution with nonpolar to polar solvent. For example, hydrocarbon and alcohol/ketone fractions can be separated from a lipid extract by elution with *n*-hexane and then dichloromethane in a silica gel-packed glass column (Thiel et al. 1999; Birgel et al. 2006b). Compounds in each fraction are analyzed using coupled gas chromatography-mass spectrometry (GC-MS), in which components are separated on a GC column and a mass fragmentation pattern (mass spectrum) of each component is obtained by scanning the mass-to-charge ratio (*m*/*z*) of ions filtered in a quadrupole mass analyzer in a mass spectrometer. Components can be identified based on comparison of their retention times in the chromatograms and/or mass spectra with those of published data or reference compounds. While hydrocarbon and aromatic fractions can be directly analyzed by GC-MS, some polar fractions such as alcohols and carboxyl acids have to be derivatized before analysis so as to lower their polarity for faster elution and better separation (e.g., Pancost et al. 2000; Elvert et al. 2003; Blumenberg et al. 2004; Tsuboi et al. 2010). Large molecules such as tetraethers are subjected to ether-bond cleavage and hydrogenation before GC-MS analyses (e.g., Thiel et al. 2001a; Blumenberg et al. 2004; Niemann et al. 2005; Tsuboi et al. 2010) or directly analyzed using high-performance liquid chromatography-mass spectrometry (HPLC-MS) (e.g., Hopmans et al. 2000; Stadnitskaia et al. 2005). Compound-specific isotope analysis providing the isotopic composition of each compound is performed using combined gas chromatography-combustion-isotope ratio mass spectrometry (GC-C-IRMS). In the case of stable carbon isotopes, each compound separated by GC is combusted to CO_2, whose isotope ratio ($^{13}C/^{12}C$) is obtained by integrating its peak areas in the ion chromatograms of *m*/*z* 44, 45, and 46. In measuring carbon isotopic compositions of derivatized molecules, isotope ratios have to be corrected for added carbon atoms.

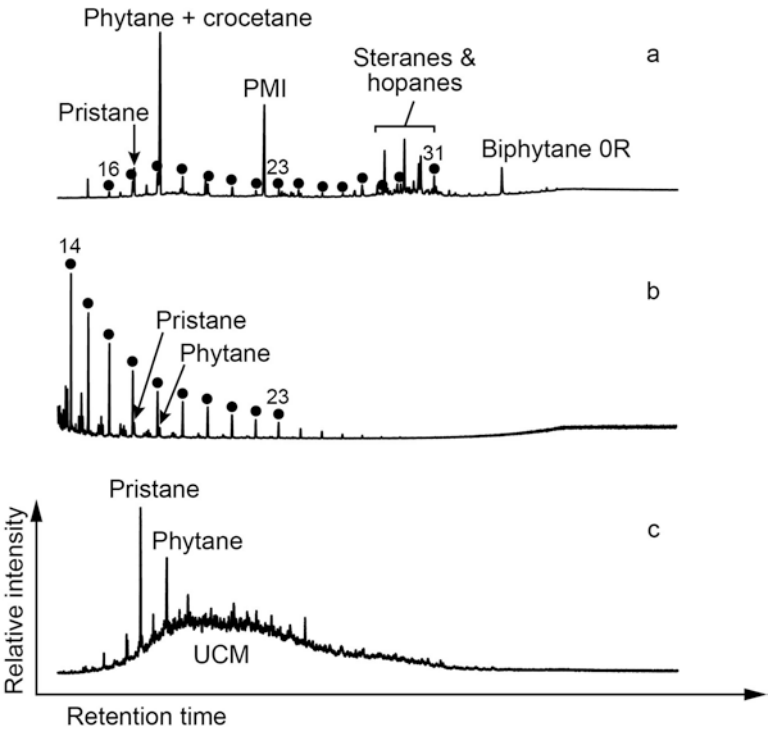

Fig. 2.2 Typical examples of total ion chromatograms of hydrocarbon fractions. (**a**) Hydrocarbon fraction including biomarkers of anaerobic methane-oxidizing archaea. (**b**) Hydrocarbons in a thermally mature sample. (**c**) Hydrocarbons affected heavily by biodegradation. Biphytane 0R, acyclic biphytane; filled circle with number, *n*-alkane of the respective carbon chain length; PMI, 2,6,10,15,19-pentamethylicosane; UCM, unresolved complex mixture

2.2.2 *Effects of Allochthonous Biomarkers, Thermal Maturity, and Biodegradation*

Lipids extracted from methane-seep carbonates or sediments often contain various compounds, including non-AOM-related allochthonous ones (Fig. 2.2a). For example, *n*-alkanes (straight-chained hydrocarbons) such as algae-derived *n*-C_{15}, *n*-C_{17}, and *n*-C_{19} alkanes and higher plant-derived *n*-C_{27}, *n*-C_{29}, and *n*-C_{31} alkanes are commonly found in marine and terrigenous sediments, respectively (Fig. 2.3; Peters et al. 2005 and references therein; subscript numbers indicate the total number of carbon atoms in the molecule). Head-to-tail linked isoprenoid hydrocarbons such as pristane (C_{19}) and phytane (C_{20}) are derived from phytol in phototroph pigments, although phytane is also derived from membrane lipids in archaea such as archaeol (e.g., Koga et al. 1993). C_{27} to C_{29}steroids originate mainly from eukaryotes such as phytoplankton, zooplankton, and higher plants. Hopanoids are common biomarkers for various types of bacteria and are known as the most widespread natural products

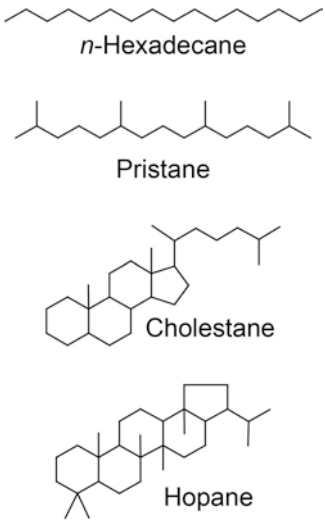

Fig. 2.3 Examples showing structures of common hydrocarbon biomarkers

preserved in sediments (e.g., Rohmer et al. 1984). Blumenberg et al. (2015) suggested that high abundances of allochthonous biomarkers in seep carbonates can obscure seep-related microbial signatures. Abundant allochthonous biomarkers indicate carbonate formation within sediments with high external organic matter input.

Allochthonous compounds are also known as indicators of thermal maturity of analyzed sediments. For example, in thermally mature samples, isoprenoid hydrocarbons are less abundant than *n*-alkanes, due to faster degradation of the former by thermal cracking (Tissot et al. 1971; Peters et al. 2005; Fig. 2.2b). *n*-Alkanes in thermally mature samples are characterized by nearly the same amounts of molecules having odd- and even-numbered carbon atoms (odd-to-even predominance near 1.0) and higher amounts of molecules with lower-numbered carbon atoms (Tissot and Welte 1984; Peters et al. 2005; Fig. 2.2b). Abundant *n*-alkanes can also originate from inputs of oil. Thermal maturity of samples can be further assessed by measuring isomer ratios of steranes and/or hopanes (Peters et al. 2005). Thermal maturity should also be examined based on other indices, such as carbonate oxygen isotopes or vitrinite reflectance of the surrounding sediments. AOM-related biomarkers such as isoprenoid hydrocarbons (see Sect. 2.3) could be detected in only small amounts or even unpreserved in thermally mature carbonate samples (Birgel et al. 2008a; Kiel et al. 2013, 2014).

Thermal maturitycan alter the isotopic composition of biomarkers (Sect. 2.5). Bjorøy et al. (1992) showed that the carbon isotopic compositions of *n*-alkanes and acyclic isoprenoids generally become slightly enriched in ^{13}C with increasing maturity (+1–4‰). This slight ^{13}C-enrichment is due to a preferential cleavage of the ^{12}C–^{12}C bonds in hydrocarbons during thermal cracking, the effect of which is compensated by a ^{12}C-enrichment through generation of additional hydrocarbons from kerogen (Bjorøy et al. 1992). Bjorøy et al. (1992) also showed that the isotopic

composition of terpenes, especially hopanes, can change drastically and the isotopic fingerprint of such biomarkers can disappear in mature samples. In addition, thermal maturity may result in elevated amounts of background peaks in the chromatograms, which may cause inaccuracy in isotopic analysis of biomarkers.

Heavily biodegraded oils are often characterized by prominent baseline humps in chromatograms, called the unresolved complex mixtures (UCM, Peters et al. 2005; Fig. 2.2c), which are also known from several modern and ancient methane-seep carbonates (Pancost et al. 2005; Peckmann et al. 2009; Kiel et al. 2013, 2014; Blumenberg et al. 2015). These humps, interpreted to have resulted from biodegradation of organic compounds or oil impregnation, can mask certain peaks in chromatograms or hamper precise compound-specific isotope analysis.

2.3 Biomarkers of AOM-Performing Microbes

The biomarker inventories from methane-seep environments have previously been reviewed in several papers (Peckmann and Thiel, 2004; Birgel and Peckmann 2008; Niemann and Elvert 2008; and a book chapter by Blumenberg 2010). Biomarkers of anaerobic methane-oxidizing archaea (ANME) and syntrophic sulfate-reducing bacteria (SRB) and their potential to be preserved as molecular fossils were reviewed by Peckmann and Thiel (2004) and Blumenberg (2010). This section fundamentally follows these papers and includes some more recent findings.

2.3.1 Biomarkers of ANME Archaea

In contrast to bacterial lipids having mostly ester-bond structures with fatty acid chains, archaeal membrane lipids have only ether-bond structures with isoprenoid chains (Fig. 2.1). The chemically stable ether bonds and the optimal cell membrane fluidity or compactness regulated by configuration of the isoprenoid chains enable archaea to thrive in extreme (e.g., hypersaline, high-temperature) environments (reviewed in De Rosa et al. 1991; Valentine 2007).

The most abundant hydrocarbon biomarker in hydrocarbon-seep environments is the tail-to-tail linked C_{25} isoprenoid PMI (2,6,10,15,19-pentamethylicosane) (Fig. 2.4 and Table 2.1, I). Its unsaturated homologues, PMIΔ1–5, are also reported from modern seeps (e.g., Chevalier et al. 2011, 2013, 2014). Another tail-to-tail linked C_{20} isoprenoid crocetane (2,6,11,15-tetramethylhexadecane, II) and its unsaturated homologues are also common, but not present in all seep environments (see below). Archaeol (III), a glycerol diether alcohol having two C_{20} isoprenoid (phytanyl) chains, is a typical membrane lipid of archaea. The *sn*-2,3-glycerol stereochemistry is specific to archaeal lipids, in contrast to *sn*-1,2-stereochemistry of bacterial glycerol lipids (De Rosa et al. 1991). From modern methane-seep environments, archaeol and *sn*-2- or *sn*-3-hydroxyarchaeol (IV) have been reported.

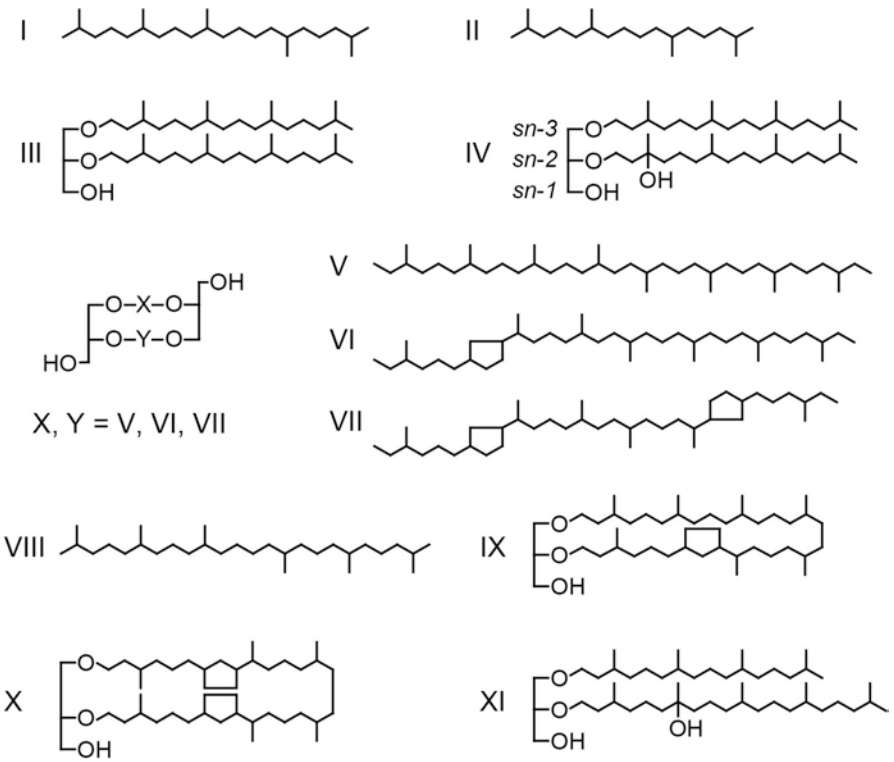

Fig. 2.4 Structures of biomarkers of anaerobic methane-oxidizing archaea

Table 2.1 Lipid biomarkers of anaerobic methane-oxidizing archaea

Component	Structure	Main source organisms at AOM sites
PMI (2,6,10,15,19-pentamethylicosane)	I	ANME-1, ANME-2, ANME-3
PMIΔ4, PMIΔ5		ANME-3
Crocetane (2,6,11,15-tetramethylhexadecane)	II	ANME-2
Archaeol	III	ANME-1, ANME-2, ANME-3
sn-2- or *sn*-3-Hydroxyarchaeol	IV	ANME-2 and ANME-3
Biphytanes with zero to two rings from GDGTs (glycerol dialkyl glycerol tetraethers)	V–VII	ANME-1
Squalane	VIII	AOM-related archaea
Macrocyclic glycerol diethers with one or two rings	IX, X	AOM-related archaea
Extended *sn*-2-hydroxyarchaeol	XI	AOM-related archaea

Glycerol dialkyl glycerol tetraethers (GDGTs) having two head-to-head linked C_{40}isoprenoid hydrocarbon (biphytanyl) chains with zero to two cyclopentane rings (V–VII) are also typical of archaeal lipids and known from methane seeps. While, except for crocetane, these compounds have been known as typical membrane lipids of methanogenic archaea (e.g., Koga et al. 1993, 1998), they have been attributed to ANME at methane seeps based on their strongly ^{13}C-depleted compound-specific isotope signatures (δ^{13}C values as low as around −140‰ vs. VPDB; Sect. 2.5).

The presence or relative abundance of specific biomarkers is proposed to be a useful tool to distinguish specific ANME clades at methane seeps. Compared with the ANME-1 community, the ANME-2 community contains more abundant PMIΔs (Blumenberg et al. 2004). Niemann et al. (2006) showed that the ANME-3 community exclusively contains PMIΔ4 and PMIΔ5. Although crocetane has so far been found only in a cultured methanogen (Jones and Holzer, 1991), its abundance and ^{13}C-depletion in ANME-2-rich mats at a methane seep in the Black Sea (Blumenberg et al. 2004) suggest that it can be regarded as a specific biomarker for ANME-2 archaea (Niemann and Elvert 2008). Blumenberg et al. (2004) also showed that ANME-1-dominated mats contain archaeol and GDGTs (biphytanes after ether cleavage), whereas ANME-2-dominated mats contain more *sn*-2-hydroxyarchaeol than archaeol and no GDGTs. A *sn*-2-hydroxyarchaeol-to-archaeol ratio of >1 is now considered to be a robust indicator for ANME-2 or ANME-3 archaea (Niemann and Elvert 2008 and references therein). The presence of ^{13}C-depleted GDGTs or biphytanes is generally indicative of ANME-1 archaea (Niemann et al. 2005; Stadnitskaia et al. 2005; Niemann and Elvert 2008), but these compounds have been detected also at some ANME-2-dominated methane seeps (e.g., Elvert et al. 2005).

In addition to the aforementioned ANME biomarkers, some other compounds are regarded as biomarkers for microbes participating in AOM or other methane-related biogeochemical processes. A tail-to-tail linked C_{30} isoprenoid squalene and its saturated derivative squalane (VIII), which are universally present in many archaea, are also known to show ^{13}C-depletion at methane seeps. The ^{13}C-depleted squalane and squalene have been suggested to originate from ANME-1 or an as yet undetected organism utilizing a ^{13}C-depleted carbon source (Elvert et al. 2000; Bertram et al. 2013; Wakeham 2020). Squalene is also known as a precursor molecule in biosynthesis of steroids and hopanoids (e.g., Summons et al. 1994; Elvert and Niemann 2008). Stadnitskaia et al. (2003, 2008) reported macrocyclic glycerol diethers containing one or two cyclopentane rings (IX and X) and an extended *sn*-2-hydroxyarchaeol with C_{20} and C_{25}isoprenoid chains (XI) as novel biomarkers for possibly AOM-performing archaea. In addition, ^{13}C-depleted phytanyl glycerol monoethers have also been detected at modern cold seeps (Hinrichs et al. 2000; Birgel et al. 2011; Chevalier et al. 2011).

Most of the AOM-related biomarkers have been ubiquitously reported from ancient methane-seep carbonates. Saturated isoprenoid hydrocarbon PMI and crocetane, as well as squalane, are biomarkers most resistant to diagenesis (Blumenberg 2010). The double bonds in unsaturated isoprenoids are less likely to be preserved in mature sediments. Although the glycerol diethers such as archaeol and

hydroxyarchaeols are less stable than hydrocarbon biomarkers, they have been detected in some Cenozoic seep carbonates (Peckmann and Thiel 2004; Birgel et al. 2008b; Pearson et al. 2010; Tsuboi et al. 2010). Highly ^{13}C-depleted phytane, phytanol, phytanic acid, and also other isoprenoid hydrocarbons in ancient seep carbonates are considered to be archaeol- or hydroxyarchaeol-derived products (Thiel et al. 1999; Peckmann and Thiel 2004; Peckmann et al. 2004; Birgel et al. 2006a, b, 2008a; Tsuboi et al. 2010). Birgel and Peckmann (2008) and Tsuboi et al. (2010) detected macrocyclic archaeols in Miocene and Pleistocene seep carbonates. The presence of GDGTs at ancient seeps is often inferred based on detection of ^{13}C-depleted acyclic or cyclic biphytanes in hydrocarbon fractions. Biphytanes are produced through ether cleavage of the GDGTs not only in the laboratory but also in diagenesis. Birgel et al. (2008b) and Smrzka et al. (2017) reported strongly ^{13}C-depleted biphytanic diacids with zero to two cyclopentane rings from Cenozoic and Cretaceous seep carbonates, suggesting that they are almost exclusively derived from methane-oxidizing archaea.

2.3.2 Biomarkers of SRB Partners

In contrast to archaea, bacterial membrane lipids are characterized by fatty acids esterified with glycerol (Fig. 2.1). Fatty acids having straight or terminally branched (2- and 3-methyl or *iso*- and *anteiso*-, respectively) skeletons of 14 to 18 carbon atoms are known as biomarkers of SRB and many other bacteria. Among various C_{14} to C_{18} fatty acid biomarkers of SRB from modern methane seeps, the most common compounds include saturated *iso*- and *anteiso*-C_{15} (Fig. 2.5 and Table 2.2, XII

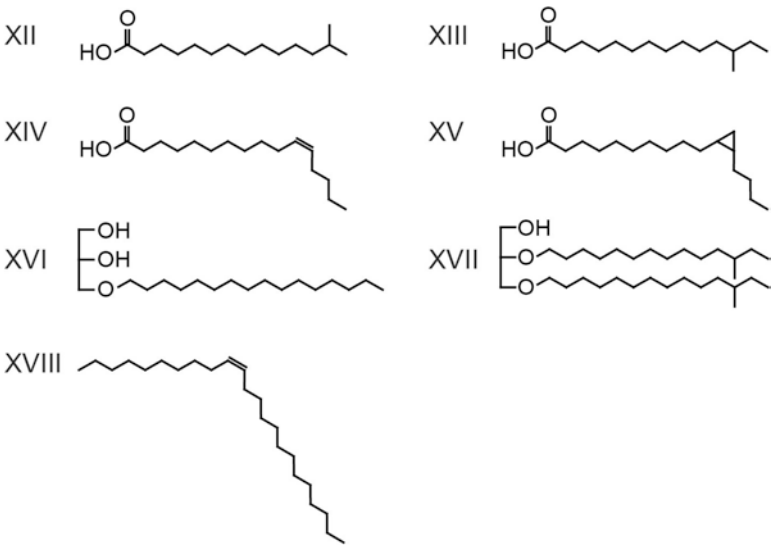

Fig. 2.5 Structures of biomarkers of sulfate-reducing bacteria involved in AOM

Table 2.2 Lipid biomarkers of sulfate-reducing bacteria involved in AOM

Component	Structure	Main source organisms at AOM sites
iso-C_{15} (13-Methyltetradecanoic) fatty acid	XII	ANME-2-related DSS group
anteiso-C_{15} (12-Methyltetradecanoic) fatty acid	XIII	ANME-1-related DSS group
n-$C_{16:1\omega5}$ (Hexadec-11-enoic) fatty acid	XIV	ANME-2-related DSS group
n-$C_{17:1\omega6}$ (Heptadec-11-enoic) fatty acid		ANME-3-related DBB group
Cyclopropyl $C_{17:0\omega5,6}$ (ω-5,6-cyclopropylhexadecanoic) fatty acid	XV	ANME-2-related DSS group
MAGEs (non-isoprenoidal monoalkyl glycerol ethers)	XVI (16-MAGE)	ANME-2-related DSS and ANME-3-related DBB groups
DAGES (non-isoprenoidal dialkyl glycerol diethers)	XVII (*anteiso*-15-DAGE)	ANME-1-related DSS group
n-$C_{23:1\omega10}$ (Tricos-10-ene)	XVIII	AOM-related SRB?

and XIII), mono-unsaturated *n*-C_{16} ($C_{16:1\omega5}$, XIV) and *n*-C_{17} ($C_{17:1\omega6}$), and monocyclic C_{17} (cyclopropyl $C_{17:0\omega5,6}$, XV) fatty acids (the subscript ":1" designates the number of double bonds, and "ω5" indicates the position of the double bonds or rings counted from the aliphatic end of the molecule). For the mono-unsaturated fatty acids, isomers with *cis* configuration of the double bond are more abundant than those with *trans* configuration (Elvert et al. 2003, 2005).

Besides glycerol esters with fatty acids, glycerol ethers with non-isoprenoidal alkyl chains occur in some thermophilic, ancestral bacteria and mesophilic SRB (e.g., Langworthy et al. 1983; Rütters et al. 2001). Indeed, non-isoprenoidal mono- and dialkyl glycerol ethers (MAGEs and DAGEs, respectively, e.g., XVI and XVII) are ubiquitous at modern methane seeps. Based on their somewhat ^{13}C-depleted signatures ($\delta^{13}C$ values as low as around −100‰), these bacterial biomarkers at seeps are attributed to SRB partners associated with ANME, which possibly utilize AOM-derived carbon sources for metabolism (see Sect. 2.5).

As in the ANME biomarkers, the presence or relative abundance of the bacterial biomarkers is helpful to distinguish SRB clades. According to Niemann and Elvert (2008), the ratios of *anteiso*-C_{15} to *iso*-C_{15}fatty acids tend to be higher in the ANME-1-associated *Desulfosarcina/Desulfococcus*(DSS) clade than in ANME-2-associated DSS, although they are not significantly different from a statistical point of view. They also proposed a $C_{16:1\omega5}$ to *iso*-C_{15} fatty acid ratio of <1.8 as a strong indicator for the ANME-1-associated DSS community. The cyclopropyl $C_{17:0\omega5,6}$ fatty acid is known to be restricted to the ANME-2-associated DSS (Elvert et al. 2003), and the $C_{17:1\omega6}$ fatty acid is present in a high amount in ANME-3-associated *Desulfobulbus* spp. (DBB) (Niemann et al. 2006). With regard to the non-isoprenoidal glycerol ethers, MAGEs seem to be more common in the ANME-2/DSS and ANME-3/DBB communities, whereas DAGEs are commonly more abundant in the ANME-1/DSS-dominated communities (Niemann and Elvert 2008).

In addition to the above, *n*-alkanes with ^{13}C-depletion have been regarded as biomarkers for bacteria participating in AOM or other methane-related processes. ^{13}C-depleted *n*-C_{23} alkene (*n*-tricosene, XVIII) and its saturated derivative (*n*-tricosane) at methane seeps are proposed as possible biomarkers of AOM-related bacteria (SRB), although their true source organism is still unknown (Thiel et al. 2001b; Peckmann and Thiel, 2004). An uncultivated bacterial group closely associated with AOM consortia, Candidate Division JS1, was proposed as a possible source of ^{13}C-depleted 7,14-tricosadiene at a cold seep in the Sea of Marmara (Chevalier et al. 2013). Stadnitskaia et al. (2005) also reported ^{13}C-depleted *n*-C_{24} alkene (*n*-tetracosene) from a methane-seep carbonate from the Black Sea.

Unsaturated carbon chains are prone to reduction and degradation during early diagenesis, and SRB biomarkers in ancient seep carbonates are mostly found as ^{13}C-depleted, saturated fatty acids or their alkanol and/or alkane derivatives (e.g., Goedert et al. 2003; Peckmann and Thiel 2004). Similar to modern seeps, straight-chained, terminally branched, or cyclic C_{14} to C_{17}fatty acids have been recognized as SRB biomarkers from ancient seeps (e.g., Peckmann et al. 2004; Birgel et al. 2006a, b, 2008a; Birgel and Peckmann 2008; Kiel et al. 2013). Even intact DAGEs have been found at some Cenozoic seeps (Peckmann and Thiel 2004; Peckmann et al. 2004; Blumenberg et al. 2015).

2.4 Biomarkers of Aerobic Methanotrophs

In addition to the AOM-related biomarkers, ^{13}C-depleted steroids and hopanoids have been reported from modern and ancient methane-seep environments. Some of these compounds are regarded as specific biomarkers of aerobic methanotrophic bacteria (reviewed by Birgel and Peckmann 2008). The presence of aerobic methanotrophs at seeps is important because it indicates intermittent oxic conditions caused by an increase in downward flux of oxic seawater or a decrease in upward flux of oxygen-depleted seeping fluid (Birgel et al. 2011; Natalicchio et al. 2015). It is also possible that a high methane flux at seeps causes aerobic consumption of methane that was not exhausted by AOM consortia at or above sediment-water interface.

Although steroids are lipids generally specific to eukaryotes, a family of aerobic methanotrophic bacteria (Methylococcaceae) can synthesize 4-methylated steroids ("4" indicates the position of the methyl group; e.g., Bouvier et al. 1976), which are known also from dinoflagellates (e.g., Peters et al. 2005). A series of lanostanes with significantly ^{13}C-depleted signatures, *nor*-lanostane (Fig. 2.6 and Table 2.3, XIX), lanostane (XX), and methyllanostane, are regarded as robust indicators for aerobic methanotrophs (Peckmann et al. 2004; Birgel and Peckmann 2008). They are most likely derived from lanosterols and other 4-methylated steroids, also regarded as biomarkers of aerobic methanotrophs at seeps (Peckmann et al. 1999a; Elvert and Niemann 2008; Birgel et al. 2011).

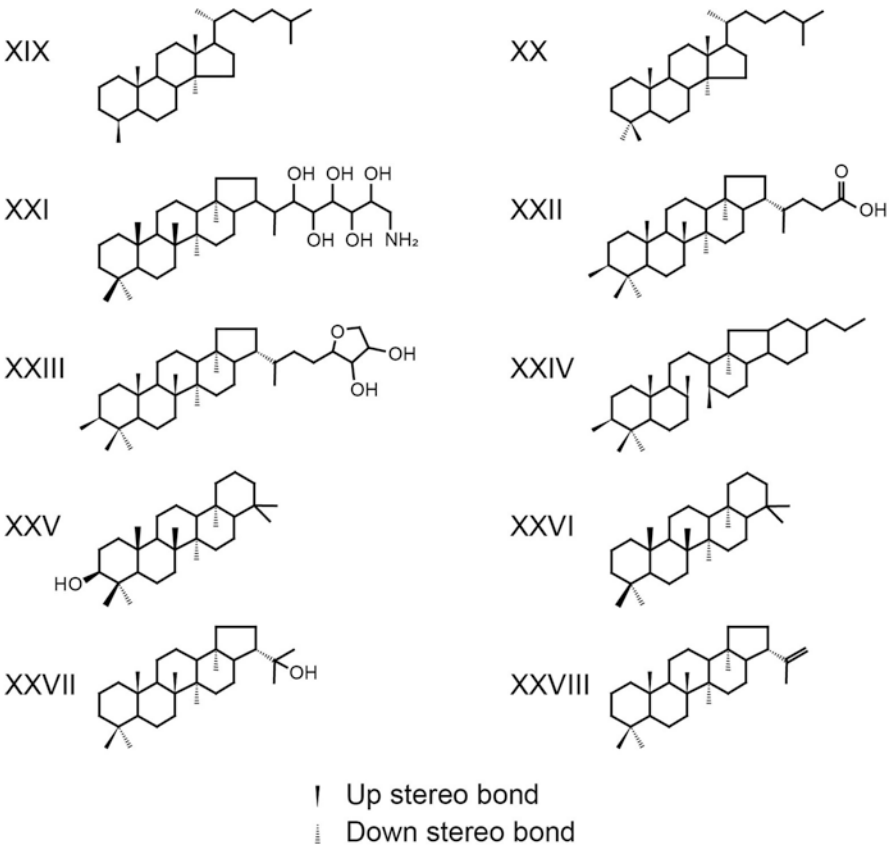

Fig. 2.6 Structures of biomarkers of aerobic methanotrophic bacteria

Hopanoids are produced by bacteria, and cultured aerobic methanotrophs are known to produce abundant bacteriohopanepolyols (BHPs) with three to five hydroxyl groups and a single amino group, aminobacteriohopanepentol (aminopentol, XXI), aminobacteriohopanetetrol (aminotetrol), and aminobacteriohopanetriol (aminotriol), and their 3β-methylated homologs (e.g., Summons et al. 1994; Cvejic et al. 2000; Talbot et al. 2001; Rush et al. 2016). These highly functionalized compounds are unamenable to GC analysis, and they are often analyzed using HPLC or subjected to periodic acid cleavage to produce GC-amenable terminal alcohols (e.g., Talbot et al. 2001). Intact amino-BHPs and their acid cleavage products are common in modern seep environments, but they have not been detected in ancient seep carbonates (Rush et al. 2016; Cordova-Gonzalez et al. 2020). Instead, Birgel and Peckmann (2008) proposed ^{13}C-depleted 3β-methylated hopanoids such as 17β(H),21β(H)-3β-methyl-32-hopanoic acid (XXII) and 32,35-3β-methyl-anhydrobacteriohopanetetrol (XXIII), which are thought to be degradation products of BHPs, as valuable biomarkers for aerobic methanotrophs (β(H) and α(H) refer to

Table 2.3 Lipid biomarkers of aerobic methanotrophic bacteria

Component	Structure	Main source organisms at AOM sites
nor-Lanostane	XIX	Type I/Type X aerobic methanotrophs
Lanostane	XX	Type I/Type X aerobic methanotrophs
Methyllanostane		Type I/Type X aerobic methanotrophs
Aminobacteriohopanepentol	XXI	Type I/Type X aerobic methanotrophs
Aminobacteriohopanetetrol		Type I/Type X and II aerobic methanotrophs
Aminobacteriohopanetriol		Type I/Type X and II aerobic methanotrophs
17β(H),21β(H)-3β-Methyl-32-hopanoic acid	XXII	Type I/Type X aerobic methanotrophs
32,35-3β-Methyl-anhydrobacteriohopanetetrol	XXIII	Type I/Type X aerobic methanotrophs
8α(H),14α(H)-34-Secohexahydrobenzohopane	XXIV	Type I/Type X aerobic methanotrophs
8β(H),14α(H)-34-Secohexahydrobenzohopane		Type I/Type X aerobic methanotrophs
17β(H),21β(H)-35-Hopanoic acid methyl ester		Type I/Type X aerobic methanotrophs
Tetrahymanol	XXV	Type I/Type X aerobic methanotrophs or other bacteria
Gammacerane	XXVI	Type I/Type X aerobic methanotrophs or other bacteria
Diplopterol	XXVII	Aerobic methanotrophs or SRB
Diploptene	XXVIII	Aerobic methanotrophs or SRB

up and down stereo C–H bonds, respectively). However, the 3-methylation was later found to be non-specific to methanotrophs (Welander and Summons 2012). Birgel et al. (2006a) and Birgel and Peckmann (2008) also interpreted 8α(H), 14α(H)-34-secohexahydrobenzohopane (XXIV), 8β(H),14α(H)-34-secohexahydrobenzohopane, and 17β(H),21β(H)-35-hopanoic acid methyl ester as possible biomarkers of aerobic methanotrophs based on their strongly ^{13}C-depleted signatures. Cultured aerobic methanotrophs and other bacteria can produce tetrahymanol (XXV, Banta et al. 2015; Cordova-Gonzalez et al. 2020), and thus strongly ^{13}C-depleted tetrahymanol and its diagenetic product gammacerane (XXVI) in seep deposits are also candidates for, though not specific, biomarkers of aerobic methanotrophs.

Aerobic methanotrophs can be classified into three groups: Type I including the family Methylococcaceae, Type II including *Methylosinus* and *Methylocystis*, and Type X including *Methylococcus capsulatus*, which belongs to Methylococcaceae but has a distinct metabolic pathway (Hanson and Hanson 1996). Type I and X methanotrophs are known to produce 4-methylated steroids and also 3-methylated BHPs (Summons et al. 1994). The presence or absence of 4-methylated steroids and 3-methylated hopanoids could thus be used to distinguish Type I/X- and Type

II-dominated methanotrophic communities (Birgel et al. 2011). The relative abundance of aminopentol, aminotetrol, and aminotriol can also be used to distinguish Type I/X from Type II (Birgel et al. 2011; Himmler et al. 2015; Rush et al. 2016).

Non-methylated C_{31} to C_{33} hopanoids, such as 17α(H),21β(H)-31-hopane, 17β(H),21β(H)-32-hopanol, and 17β(H),21β(H)-32-hopanoic acid, have been shown to have only slightly to highly ^{13}C-depleted signatures at seeps (Pancost et al. 2000; Birgel et al. 2006a, b, 2011; Birgel and Peckmann 2008; Himmler et al. 2015). Because these are ubiquitous compounds in various environments and are derived from various bacteria, possibly including aerobic methanotrophs, the slightly ^{13}C-depleted hopanoids (δ^{13}C values of −50‰ to −40‰) can represent mixed contributions from seep-endemic aerobic methanotrophs and other bacteria (Birgel and Peckmann 2008).

Sources of other ^{13}C-depleted hopanoids diplopterol (XXVII) and diploptene (XXVIII) at seeps are problematic. These compounds are known to be synthesized by aerobic bacteria including methanotrophs (e.g., Rohmer et al. 1984; Summons et al. 1994; Hinrichs et al. 2003; Elvert and Niemann 2008), while some strictly anaerobic bacteria, including SRB of the genus *Desulfovibrio*, were also found to produce them (e.g., Blumenberg et al. 2006). Therefore, diplopterol, diploptene, and their possible diagenetic products such as hop-17(21)-ene and 17α(H),21β(H)-30-hopane with intermediate δ^{13}C values (around −90‰ to −30‰) cannot be considered as reliable recorders of past aerobic methanotrophy at seeps (Birgel and Peckmann 2008).

2.5 Stable Carbon Isotope Signatures of Seep-Related Biomarkers

According to Pancost and Sinninghe Damsté (2003), "the carbon isotopic composition of an organism is dictated primarily by the isotopic composition of the carbon source and the mechanism by which that carbon is assimilated." The carbon isotopic composition of lipids is further controlled by isotope effects during biosynthesis (Hayes, 2001). Because most biomarkers originate from various sources, their compound-specific carbon isotope analyses are useful to recognize their true origins.

Carbon fixation by autotrophic organisms, such as photoautotrophs, is often accompanied by large isotopic fractionations. C_3 land plants use atmospheric carbon dioxide (δ^{13}C of ~−7‰) as a carbon source, and their bulk organic matter consequently has δ^{13}C values around −30‰. Marine algae have higher bulk δ^{13}C values. Lipids are more depleted in ^{13}C than bulk organic matter (e.g., *n*-alkanes from C_3 land plants have δ^{13}C values between −39‰ and −31‰: Collister et al. 1994). In the case of chemoautotrophs assimilating ^{13}C-depleted carbon sources, their lipids show significantly lower δ^{13}C values (e.g., Freeman et al. 1994). In contrast to the autotrophs, heterotrophic organisms consume organic matter for their carbon source with a very small isotope fractionation of ~1‰ (DeNiro and Epstein 1978).

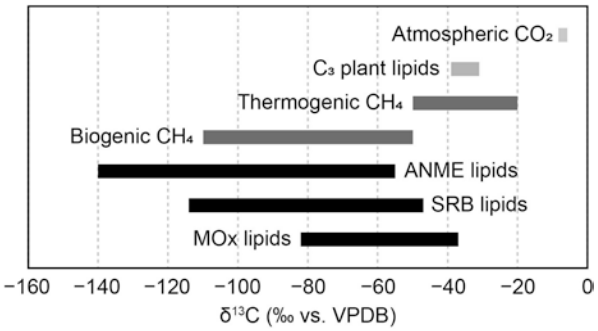

Fig. 2.7 Stable carbon isotopic compositions ($\delta^{13}C$ values) of carbon sources and lipids of phototrophic land plants and microorganisms living at modern methane seeps. MOx: aerobic methanotrophic bacteria. Values are after Collister et al. (1994), Whiticar (1999), Hinrichs et al. (2000), Elvert et al. (2003), Niemann et al. (2005), Londry et al. (2008), Niemann and Elvert (2008), Haas et al. (2010), and Cordova-Gonzalez et al. (2020). Readers can find a more comprehensive compilation of the $\delta^{13}C$ values of other carbon pools and organisms in Peters et al. (2005), Gaines et al. (2009), and Blumenberg (2010)

Carbon isotope signatures of methane-consuming organisms at methane seeps are different from those of photosynthesis-based ecosystems (Fig. 2.7). Methane is produced either abiotically or biotically from hydrogen and carbon dioxide or organic molecules. Abiotic methane generated from magmatic carbon dioxide at unsedimented hydrothermal environments has $\delta^{13}C$ values generally higher than −20‰ (e.g., McCollom and Seewald 2007). Methane produced from sedimentary organic matter has distinctly lower $\delta^{13}C$ values. Thermal degradation of organic matter generates thermogenic methane having $\delta^{13}C$ values between −50‰ and −20‰, whereas methanogenic archaea produce biogenic (microbial) methane with $\delta^{13}C$ values ranging from −110‰ to −50‰ either from carbon dioxide or simple organic molecules such as methanol and acetate (Whiticar 1999). Methane at cold seeps is generally either thermogenic, biogenic, or of mixed thermogenic/biogenic origin, and the distinct carbon isotope signatures of methane are reflected in biomass and lipids of AOM consortia (e.g., Orphan et al. 2001a) and other organisms exploiting the AOM-derived carbon.

2.5.1 Carbon Isotopic Composition of ANME Biomarkers

Archaeal lipids for ANME extracted from methane-seep deposits often show extremely low $\delta^{13}C$ values, ranging between −140‰ and −55‰ (mostly <−60‰) (Niemann et al. 2005; Londry et al. 2008; Niemann and Elvert 2008; Haas et al. 2010; Fig. 2.7). Although most lipid biomarkers of ANME are also present in methanogens or other archaeal groups (Summons et al. 1998; Londry et al. 2008; Alperin and Hoehler 2009; Nguyen et al. 2020), ANME biomarkers have been identified by

their low $\delta^{13}C$ values. Such extreme isotopic signatures have been attributed to the uptake of methane-derived carbon by the archaea. However, carbon assimilation pathways of these organisms remain not fully understood (Blumenberg et al. 2005; Nauhaus et al. 2007; Wegener et al. 2008; Kellermann et al. 2012).

The carbon isotope fractionation factor between methane and ANME lipids has not been determined based on culture experiments. However, carbon isotope offset ($\Delta\delta^{13}C_{lipid\ -\ methane}$) can be calculated based on the $\delta^{13}C$ values of methane and lipid biomarkers obtained from modern methane-seep environments (Niemann and Elvert 2008; Miyajima et al. 2020). Niemann and Elvert (2008) compiled the carbon isotope offsets between methane and archaeol or *sn*-2-hydroxyarchaeol and showed that the values are significantly different in ANME-1- and ANME-2-dominated systems. According to Niemann and Elvert (2008) and the updated compilation by Miyajima et al. (2020), the $\Delta\delta^{13}C$ values for archaeol and *sn*-2-hydroxyarchaeol are both on average −34‰ in the ANME-1-dominated systems, whereas they are −46‰ in the ANME-2-dominated systems. The isotope offset calculated at modern seeps can be useful to estimate the $\delta^{13}C$ values of the source methane contained in seep fluids and to reveal origins of methane at ancient methane seeps (Niemann and Elvert 2008; Birgel et al. 2011; Himmler et al. 2015; Miyajima et al. 2020). The $\Delta\delta^{13}C$ value for the isoprenoid PMI, which has a high potential for preservation in ancient samples (Blumenberg 2010), is specifically useful for estimation of $\delta^{13}C$ values of methane at ancient seeps. The $\Delta\delta^{13}C$ values for PMI range between −48‰ and −12‰ (average −33‰, $n = 6$) at ANME-1-dominated and between −68‰ and −12‰ (average −46‰, $n = 16$) at ANME-2-dominated seeps (Miyajima et al. 2020).

The $\Delta\delta^{13}C$ values have to be used with caution, however, because of the following uncertainties. First, if the archaeal lipids are not specific to ANME, the $\delta^{13}C$ values of the lipids could be mixed signatures from both ANME and other archaea such as methanogens. Although crocetane is a specific biomarker for ANME-2 (see Sect. 2.3.1), the use of $\delta^{13}C_{crocetane}$ values is problematic due to co-elution between crocetane and phytane in the chromatogram (Fig. 2.2a), which makes the measured $\delta^{13}C$ value a mixture from both compounds (this is why Miyajima et al. (2020) excluded crocetane from the calculation of the $\Delta\delta^{13}C$ values). Second, most of the reported $\Delta\delta^{13}C_{methane\ -\ lipid}$ values were calculated from $\delta^{13}C$ values of methane, which was not determined from the same samples on which biomarkers were analyzed (Niemann and Elvert 2008). The $\delta^{13}C$ values of methane can vary both spatially and temporally, due to several factors including mixing of methane from different sources or isotopic fractionation caused by methane oxidation (e.g., Holler et al. 2009). Third, as ANME have not been isolated, the mechanism for the incorporation of methane-derived carbon into ANME lipids, or the cause of such large carbon isotopic fractionations between methane and lipids, is still unknown (Pancost and Sinninghe Damsté 2003). In the case of methanogens, the magnitude of isotopic fractionation between substrate and product generally depends on many factors such as substrate limitation, temperature, growth phase, or a species involved (e.g., Londry et al. 2008; Nguyen et al. 2020). Methanogens grown with low hydrogen concentrations have been shown to exhibit large carbon isotopic fractionation between substrate (carbon dioxide) and lipids (Nguyen et al. 2020). This means that

at methane seeps where dissolved inorganic carbon is depleted in ^{13}C, the strongly ^{13}C-depleted lipids could be produced not only by ANME but also by methanogenic archaea (Alperin and Hoehler, 2009).

Several studies have attempted to determine the extent of methane-derived carbon uptake into lipids of AOM-performing microbes. Blumenberg et al. (2005) incubated an AOM-performing microbial mat from the Black Sea in vitro with ^{13}C-labeled methane. They found large isotopic shifts and net ^{13}C uptakes for polyunsaturated PMIΔs (PMIΔ4 and PMIΔ5), archaeol, and biphytanes, whereas isotopic shifts for PMI, crocetane, and *sn*-2-hydroxyarchaeol were only slight or showed no change. They suggested that PMIΔs represent early steps in the PMI biosynthesis and are subsequently reduced. The reason for the slight isotopic shifts for *sn*-2-hydroxyarchaeol and crocetane might be the low methane partial pressure in their experiment, which was not appropriate for biosynthetic activity of ANME-2 archaea (Blumenberg et al. 2004; Nauhaus et al. 2005; see Sect. 2.6.1). Nauhaus et al. (2007) and Wegener et al. (2008) showed that not only methane but also carbon dioxide, a significant proportion of which may be derived from methane oxidation, are incorporated into ANME biomarkers, with only 1% of methane directly channeled into biosynthesis. Kellermann et al. (2012) recently incubated ANME-1-dominated AOM communities from hydrothermally heated sediments of the Guaymas Basin, Gulf of California, with ^{13}C-labeled inorganic carbon or methane. They revealed that ANME-1 archaea assimilate inorganic carbon autotrophically, a process strictly coupled with dissimilatory methane oxidation. This suggests that the limited incorporation of methane-derived carbon into the archaeal lipids is due to indirect uptake of inorganic carbon from methane oxidation. Based on these studies, the strong ^{13}C-depletion of ANME lipids could not simply be a result of the direct transfer of the ^{13}C-depleted, methane-derived carbon into the lipid synthesis. Through the radiocarbon ($^{14}C/^{12}C$) analysis of ANME cells, Takano et al. (2018) revealed that ANME cell biomass has a $^{14}C/^{12}C$ ratio that is distinct from inorganic carbon dissolved in surface seawater. Their result indicates that ANME cell biomass uses ^{14}C-depleted carbon from seeping methane or probably from inorganic carbon produced by methane oxidation and dissolved in sediment pore water.

2.5.2 Carbon Isotopic Composition of SRB Biomarkers

Lipid biomarkers of SRB from seeps are also depleted in ^{13}C, with $\delta^{13}C$ values ranging between −114‰ and −47‰, which are generally higher than in the co-occurring ANME lipids (e.g., Hinrichs et al. 2000; Elvert et al. 2003; Niemann et al. 2005; Niemann and Elvert 2008; Fig. 2.7). The low $\delta^{13}C$ values of SRB lipids have been attributed to a direct or indirect methane-derived carbon transfer from ANME to the SRB partners, although the metabolic interaction between ANME and SRB partners remains enigmatic. According to Blumenberg et al. (2005), bacterial fatty acids of ANME-1- and ANME-2-associated SRB showed much larger $\delta^{13}C$ shifts than the archaeal lipids after incubation experiments with ^{13}C-labeled methane. The result of

Blumenberg et al. (2005) suggested an active biosynthesis by SRB using methane-derived carbon. On the other hand, Wegener et al. (2008) showed that SRB biomarkers from seep sediments incorporated ^{13}C-labeled carbon only after incubation with ^{13}C-labeled bicarbonate, which indicates an autotrophic growth of SRB. They suggested that direct methane uptake by SRB is not significant and electrons are transferred from ANME to SRB as an energy source for the autotrophic fixation of inorganic carbon. Wegener et al. (2015) recently found a dense nanowire network connecting ANME and SRB cells, which strongly supports the hypothesis of electron transfer between these organisms. Therefore, the low δ^{13}C values of SRB lipids may have resulted from their autotrophic growth (Londry et al. 2004; Alperin and Hoehler 2009) and could not directly reflect those of the source methane. The generally higher δ^{13}C values of the "SRB" lipids than the ANME lipids are also likely to reflect inputs from other bacteria not involved in AOM.

2.5.3 Carbon Isotopic Composition of Aerobic Methanotroph Biomarkers

Terpenoid lipids including hopanoids and some steroids in seep deposits showing a strong ^{13}C-depletion with respect to those of "normal" bacteria, such as cyanobacteria, can be assigned as biomarkers of aerobic methanotrophic bacteria. Terpenoids of aerobic methanotrophs from cultures and modern seeps (including symbionts of bathymodiolin mussels) have δ^{13}C values ranging between −82‰ and −37‰ (Cordova-Gonzalez et al. 2020 and references therein; Fig. 2.7), mostly lower than those of cyanobacterial hopanoids (~−32‰, Jahnke et al. 1999). From ancient seep deposits, hopanoids with δ^{13}C values as low as −110‰ were detected (Birgel et al. 2006a). It should be noted, however, that the ^{13}C-depletion in hopanoids is not a specific feature to methanotrophs. For example, the δ^{13}C value of hopanoids of ammonia-oxidizing chemoautotrophic bacteria is estimated to range down to −55‰ (Sakata et al. 2008).

Carbon isotope fractionation in lipids of aerobic methanotrophic bacteria has been studied based on culture experiments. The biomass of aerobic methanotrophs of *Methylococcus capsulatus* and *Methylomonas methanica* grown on methane has up to ~30‰ lower δ^{13}C values than methane, and their hopanoid and steroid lipids have δ^{13}C values up to 10‰ lower than those of the biomass (Summons et al. 1994). The extent of carbon isotope fractionation between carbon source and lipids is known to be different depending on the carbon assimilation pathways of methanotrophs. The ribulose monophosphate pathway used by Type I and X methanotrophs results in stronger carbon isotope fractionation than the serine pathway used by Type II methanotrophs (Summons et al. 1994; Hanson and Hanson 1996; Jahnke et al. 1999). The isotope offset ($\Delta\delta^{13}$C value) between methane and hopanoid lipids ranges between −31‰ and −16‰ (average −23‰) for *Methylococcus capsulatus* (Type X) and between −12‰ and +10‰ (average −1‰) for *Methylosinus trichosporium* (Type II) (Jahnke et al. 1999). Lipids of Type II methanotrophs are enriched

in ^{13}C with respect to methane in a methane-limited condition due to uptake of ^{13}C-enriched carbon dioxide for assimilation (Jahnke et al. 1999). Cordova-Gonzalez et al. (2020) also showed large $\Delta\delta^{13}C$ values for cultured Type I methanotrophs (averaging −16‰ and −25‰). Although Type II methanotrophs are not common in the marine environment (Hanson and Hanson 1996), terpenoid lipids of aerobic methanotrophs extracted from modern seep deposits exhibited small isotope offset from the source methane ($\Delta\delta^{13}C$ values averaging +1‰ or −9‰), indicating Type II methanotrophs as source organisms (Birgel et al. 2011; Himmler et al. 2015). For fossil seep deposits, Cordova-Gonzalez et al. (2020) estimated the $\Delta\delta^{13}C$ values for lipids of aerobic methanotrophs using the $\delta^{13}C_{methane}$ values back-calculated from the $\delta^{13}C$ values of ANME lipids. The resultant $\Delta\delta^{13}C$ values indicated the predominance of Type I/X methanotrophs at some ancient seeps, while higher and positive values were also shown at other sites.

The $\Delta\delta^{13}C$ values between methane and lipids of aerobic methanotrophs can be used as an additional tool to estimate the $\delta^{13}C$ values of the source methane at ancient seeps. Because the reported $\Delta\delta^{13}C$ values for cultured methanotrophs are smaller than the $\Delta\delta^{13}C$ values for ANME (see above), they might enable more certain estimations of the origins of methane at ancient seeps.

2.6 AOM Community and Seep Environment

The ANME-1-, ANME-2-, or ANME-3-dominated communities can be distinguished by distinct biomarker patterns such as the presence (abundance) or absence of crocetane and the *sn*-2-hydroxyarchaeol/archaeol ratio (Sect. 2.3). This section reviews distribution patterns of different ANME/SRB communities and their controlling factors in modern seep environments. Application of this knowledge to the biomarker inventory of ancient seep carbonates would enable characterization of the microenvironment in which the carbonates precipitated.

2.6.1 Factors Controlling the Distribution of AOM Communities

Methane-seep environments are mostly dominated by distinct ANME/SRB consortia. Differences in environmental preferences between different ANME groups have been studied based on both field observations and in vitro experiments. ANME-1/*Desulfosarcina/Desulfococcus* (DSS) consortia are known to dominate in subsurface sediments and interior parts of microbial reefs, while ANME-2/DSS consortia have been reported from surface sediments (Michaelis et al. 2002; Elvert et al. 2005; Knittel et al. 2005). Blumenberg et al. (2004) showed that ANME-2 archaea are dominant in microbial mats apparently exposed to higher methane partial pressure than those dominated by ANME-1 in the Black Sea. This observation was supported

by an in vitro experiment by Nauhaus et al. (2002, 2005); the ANME-2-dominated community showed significantly higher AOM rates at an elevated methane partial pressure than the ANME-1-dominated community. They also indicated that ANME-2 consortia are better adapted to cold temperatures than ANME-1 consortia. Small differences in other environmental preferences such as salinity and pH might also affect the development of either ANME-1 or ANME-2 communities, although the optima in these parameters are similar for both communities (Nauhaus et al. 2005). ANME-3/*Desulfobulbus* spp. (DBB) consortia have been reported mainly from microbial mats and sediments in mud volcanoes, and they seem to be adapted to a wide range of temperatures (Niemann et al. 2006, 2009; Brazelton et al. 2006; Omoregie et al. 2008; Rossel et al. 2011). Rossel et al. (2011) further examined the relationship between environmental characteristics and the distribution of intact polar membrane lipids in sediments and microbial mats from several hydrocarbon seeps. They proposed oxygen and sulfate concentrations as well as temperatures as the major factors controlling the distribution of different AOM consortia. According to Rossel et al. (2011), ANME-1/DSS consortia are associated with higher temperatures and lower oxygen contents in bottom waters, whereas ANME-2/DSS and ANME-3/DBB consortia are associated with lower temperatures and higher oxygen contents. This is consistent with the hypothesis in Knittel et al. (2005) that ANME-1 may be more sensitive to oxygen than ANME-2. In addition, ANME-2/DSS consortia are particularly prominent in environments with high sulfate concentrations.

The differences in environmental preferences between different AOM consortia can be used to infer seepage intensity at ancient methane seeps. Peckmann et al. (2009) indicated that an Early Cretaceous (Hauterivian) methane seep in the Crimean Peninsula was dominated by ANME-1 archaea based on the biomarker pattern of the seep limestone. The seep carbonate was characterized by a scarcity of void-filling cements that crosscut the carbonate matrix. It is generally believed that intense fluid seepage favors void-filling cement formation, such as fibrous rim cements, whereas diffusive, low-flux seepage results in carbonate rocks dominated by micrite with little cement (e.g., Peckmann et al. 2009; Kiel et al. 2014; Miyajima et al. 2016). Therefore, Peckmann et al.'s (2009) result is consistent with the fact that ANME-1 archaea are adapted to lower methane concentrations and thus lower seepage intensities and diffusive flows (Haas et al. 2010).

2.6.2 Micro-distribution of AOM Communities in Seep Carbonates

Authigenic carbonate rocks formed via AOM are recently regarded as important habitat substrates sustaining more diverse microbial communities than surrounding sediments (Case et al. 2015). AOM-performing microbes are known to form dense mats in cavities of seep carbonates (Michaelis et al. 2002; Reitner et al. 2005; Teichert et al. 2005; Mazzini et al. 2008; Bahr et al. 2010), and these endolithic AOM communities are possibly supported by fluid flow through open spaces

available within the carbonate bodies (Marlow et al. 2014, 2015). These observations from modern seep carbonates indicate that the abundance and composition of the lipid biomarkers of AOM-performing microbes differ between different carbonate phases of the given seep deposits, for example, between matrix and void-filling cement phases (for carbonate petrography, see Hryniewicz this volume).

Leefmann et al. (2008) examined the microscale distribution of biomarkers in a methane-seep carbonate at Hydrate Ridge, off Oregon, by microscale sampling of each carbonate phase. They showed that the biomarker distribution is highly localized; grey micrite constituting the rock matrix mainly contained biomarkers of ANME-1 archaea, whereas whitish aragonite filling the cavities contained more abundant biomarkers of ANME-2 archaea. The abundance of biomarkers and lack of allochthonous organic molecules in the whitish aragonite suggest that it represents fossilized biofilms of the ANME-2/*Desulfosarcina*/*Desulfococcus* (DSS) consortia. On the other hand, the lucent aragonite studied by Leefmann et al. (2008) contained only trace amounts of biomarkers, and this phase seems unlikely to be spatially associated with AOM-related microbes during its precipitation. Hagemann et al. (2013) applied the same method to an Oligocene methane-seep limestone from the Lincoln Creek Formation of Washington State and revealed that the relationships between the respective carbonate phases and their biomarker patterns are identical with the analogous modern seep carbonate of Hydrate Ridge. In the Oligocene carbonate, most abundant AOM-related biomarkers were found in yellow aragonite occurring in cavities. Due to small amounts of samples analyzed in these two studies, compound-specific carbon isotope analyses were not performed on biomarkers identified in each phase. The microscale distribution of biomarkers in seep carbonates highlights the caution required in analyzing biomarker contents in carbonates composed of various phases.

2.7 Future Outlook

Lipid biomarkers in ancient seep carbonates provide valuable information on the character and activity of seep-inhabiting microbial communities and also on paleoenvironmental conditions such as seepage intensity. However, there are still some uncertainties which have to be resolved.

One of these unresolved problems is the antiquity of the microbes living at cold seeps, such as ANME and their SRB partners. The oldest known examples of the ANME and SRB biomarkers so far are hydrocarbons reported in Birgel et al. (2008a) from upper Pennsylvanian seep limestones in the Ganigobis shales, southern Namibia (~300 Ma). Searches for much older records of biomarkers have been hindered by diagenetic alteration affecting ancient seep deposits. Earlier attempts to examine biomarker contents at Paleozoic seeps include those on the middle Devonian Hollard Mound (Peckmann et al. 1999b; see Jakubowicz et al. this volume), the upper Devonian *Dzieduszyckia* deposit (Peckmann et al. 2007), and the lower Carboniferous Iberg Reef (Peckmann et al. 2001). These attempts failed

because of the high maturity of the seep deposits (Birgel et al. 2008a). Smrzka et al. (2017) found ^{13}C-depleted biphytanic diacids in decalcified lipid extracts from an Upper Cretaceous seep deposit. Future exploration for older fossil records of AOM-related microbes may thus involve examination of polar fractions as well as hydrocarbons in total lipid extracts of decalcified samples.

The extent of carbon isotope fractionation between the source methane and the AOM-related lipids has been determined based on circumstantial evidence, and the controlling factors and mechanisms remain unclear. To determine the precise carbon isotope offset ($\Delta\delta^{13}C$ values), $\delta^{13}C$ values of methane and lipids should be measured on the same sample. The $\Delta\delta^{13}C$ values should also be determined through culture experiments. Improving our understanding of the carbon isotope fractionation between methane and the AOM-specific biomarkers would be helpful in estimating the isotopic composition of methane at ancient seeps based on the isotopic signatures of the biomarkers.

Understanding the microscale distribution of lipid biomarkers in sediments and carbonates would improve our interpretations on the conventional bulk biomarker analyses. High-resolution microscale imaging of lipids performed by Thiel et al. (2007) and Wörmer et al. (2014) is promising as a non-destructive analysis that can reveal biomarker distribution in relation to rock fabrics. At the same time, improvements in compound-specific isotope analyses on smaller amounts of samples could reveal carbon flows between microorganisms living in different microenvironments such as sediment matrix and cavities.

For modern seeps, coupling biomarker analysis with genetic analyses such as 16S rRNA would further improve the assignment of biomarkers to specific organisms. Such comprehensive research may also find novel biomarkers of microbes playing a role in biogeochemical processes at seeps (e.g., Stadnitskaia et al. 2005; Chevalier et al. 2013).

Aside from methane seeps, biomarker inventories and their compound-specific isotopic signatures characteristic of oil seeps, hydrothermal vents, and serpentinite-hosted hydrothermal environments await further exploration. Such information would be helpful to identify ancient examples of these extreme environments.

Acknowledgments We are sincerely grateful to Andrzej Kaim (Polish Academy of Sciences) for giving us the opportunity to write this chapter. We are very thankful to Russell Shapiro (California State University) and Michal Jakubowicz (Adam Mickiewicz University) for their constructive reviews. Susumu Sakata (AIST) kindly checked through the manuscript and helped improve the chapter.

References

Agirrezabala LM, Kiel S, Blumenberg M et al (2013) Outcrop analogues of pockmarks and associated methane-seep carbonates: a case study from the Lower Cretaceous (Albian) of the Basque-Cantabrian Basin, western Pyrenees. Palaeogeogr Palaeoclimatol Palaeoecol 390:94–115

Alperin MJ, Hoehler TM (2009) Anaerobic methane oxidation by Archaea/sulfate-reducing bacteria aggregates: 2, isotopic constraints. Am J Sci 309:958–984

Bahr A, Pape T, Abegg F et al (2010) Authigenic carbonates from the eastern Black Sea as an archive for shallow gas hydrate dynamics—results from the combination of CT imaging with mineralogical and stable isotope analyses. Mar Pet Geol 27:1819–1829

Banta AB, Wei JH, Welander PV (2015) A distinct pathway for tetrahymanol synthesis in bacteria. PNAS 112:13478–13483

Bertram S, Blumenberg M, Michaelis W et al (2013) Methanogenic capabilities of ANME-Archaea deduced from ^{13}C-labelling approaches. Environ Microbiol 15(8):2384–2393

Birgel D, Peckmann J (2008) Aerobic methanotrophy at ancient marine methane seeps: a synthesis. Org Geochem 39:1659–1667

Birgel D, Peckmann J, Klautzsch S et al (2006a) Anaerobic and aerobic oxidation of methane at Late Cretaceous seeps in the Western Interior Seaway, USA. Geomicrobiol J 23:565–577

Birgel D, Thiel V, Hinrichs K-U et al (2006b) Lipid biomarker patterns of methane-seep microbialites from the Mesozoic convergent margin of California. Org Geochem 37:1289–1302

Birgel D, Himmler T, Freiwald A et al (2008a) A new constraint on the antiquity of anaerobic oxidation of methane: Late Pennsylvanian seep limestones from southern Namibia. Geology 36(7):543–546

Birgel D, Elvert M, Han X et al (2008b) ^{13}C-depleted biphytanic diacids as tracers of past anaerobic oxidation of methane. Org Geochem 39:152–156

Birgel D, Feng D, Roberts HH et al (2011) Changing redox conditions at cold seeps as revealed by authigenic carbonates from Alaminos Canyon, northern Gulf of Mexico. Chem Geol 285:82–96

Bjorøy M, Hall PB, Hustad E et al (1992) Variation in stable carbon isotope ratios of individual hydrocarbons as a function of artificial maturity. Org Geochem 19:89–105

Blumenberg M (2010) Microbial chemofossils in specific marine hydrothermal and methane cold seep settings. In: Kiel S (ed) The vent and seep biota. Topics in Geobiology 33. Springer, Heidelberg, Germany, pp 73–106

Blumenberg M, Seifert R, Reitner J et al (2004) Membrane lipid patterns typify distinct anaerobic methanotrophic consortia. PNAS 101(30):11111–11116

Blumenberg M, Seifert R, Nauhaus K et al (2005) In vitro study of lipid biosynthesis in an anaerobically methane-oxidizing microbial mat. Appl Environ Microbiol 71(8):4345–4351

Blumenberg M, Krüger M, Nauhaus K et al (2006) Biosynthesis of hopanoids by sulfate-reducing bacteria (genus *Desulfovibrio*). Environ Microbiol 8(7):1220–1227

Blumenberg M, Walliser E-O, Taviani M et al (2015) Authigenic carbonate formation and its impact on the biomarker inventory at hydrocarbon seeps—a case study from the Holocene Black Sea and the Plio-Pleistocene northern Apennines (Italy). Mar Pet Geol 66:532–541

Boetius A, Ravenschlag K, Schubert CJ et al (2000) A marine microbial consortium apparently mediating anaerobic oxidation of methane. Nature 407:623–626

Bouvier P, Rohmer M, Benveniste P et al (1976) $\Delta^{8(14)}$-steroids in the bacterium *Methylococcus capsulatus*. Biochem J 159:267–271

Brazelton WJ, Schrenk MO, Kelley DS et al (2006) Methane- and sulfur-metabolizing microbial communities dominate the Lost City hydrothermal field ecosystem. Appl Environ Microbiol 72(9):6257–6270

Brocks JJ, Pearson A (2005) Building the biomarker tree of life. Rev Mineral Geochem 59:233–258

Brocks JJ, Logan GA, Buick R et al (1999) Archaean molecular fossils and the early rise of eukaryotes. Science 285:1033–1036

Brocks JJ, Love GD, Summons RE et al (2005) Biomarker evidence for green and purple sulphur bacteria in a stratified Palaeoproterozoic sea. Nature 437:866–870

Case DH, Pasulka AL, Marlow JJ et al (2015) Methane seep carbonates host distinct, diverse, and dynamic microbial assemblages. MBio 6(6):e01348–15

Chevalier N, Bouloubassi I, Birgel D et al (2011) Authigenic carbonates at cold seeps in the Marmara Sea (Turkey): a lipid biomarker and stable carbon and oxygen isotope investigation. Mar Geol 288:112–121

Chevalier N, Bouloubassi I, Birgel D et al (2013) Microbial methane turnover at Marmara Sea cold seeps: a combined 16S rRNA and lipid biomarker investigation. Geobiology 11:55–71

Chevalier N, Bouloubassi I, Stadnitskaia A et al (2014) Lipid biomarkers for anaerobic oxidation of methane and sulphate reduction in cold seep sediments of Nyegga pockmarks (Norwegian margin): discrepancies in contents and carbon isotope signatures. Geo-Mar Lett 34:280

Collister JW, Rieley G, Stern B et al (1994) Compound-specific $\delta^{13}C$ analyses of leaf lipids from plants with differing carbon dioxide metabolisms. Org Geochem 21:619–627

Cordova-Gonzalez A, Birgel D, Kappler A et al (2020) Carbon stable isotope patterns of cyclic terpenoids: a comparison of cultured alkaliphilic aerobic methanotrophic bacteria and methane-seep environments. Org Geochem 139:103940

Cvejic JH, Bodrossy L, Kovács KL et al (2000) Bacterial triterpenoids of the hopane series from the methanotrophic bacteria *Methylocaldum* spp.: phylogenetic implications and first evidence for an unsaturated aminobacteriohopanepolyol. FEMS Microbiol Lett 182:361–365

De Boever E, Birgel D, Thiel V et al (2009) The formation of giant tubular concretions triggered by anaerobic oxidation of methane as revealed by archaeal molecular fossils (lower Eocene, Varna, Bulgaria). Palaeogeogr Palaeoclimatol Palaeoecol 280:23–36

De Rosa M, Trincone A, Nicolaus B et al (1991) Archaebacteria: lipids, membrane structures, and adaptation to environmental stresses. In: di Prisco G (ed) Life under extreme conditions. Springer, Berlin, pp 61–87

DeNiro MJ, Epstein S (1978) Influence of diet on the distribution of carbon isotopes in animals. Geochim Cosmochim Acta 42:495–506

Eglinton G, Calvin M (1967) Chemical fossils. Sci Am 261:32–43

Eglinton G, Scott PM, Belsky T et al (1964) Hydrocarbons of biological origin from a one-billion-year-old sediment. Science 145:263–264

Elvert M, Niemann H (2008) Occurrence of unusual steroids and hopanoids derived from aerobic methanotrophs at an active marine mud volcano. Org Geochem 39:167–177

Elvert M, Suess E, Whiticar MJ (1999) Anaerobic methane oxidation associated with marine gas hydrates: superlight C-isotopes from saturated and unsaturated C_{20} and C_{25} irregular isoprenoids. Naturwissenschaften 86:295–300

Elvert M, Suess E, Greinert J et al (2000) Archaea mediating anaerobic methane oxidation in deep-sea sediments at cold seeps of the eastern Aleutian subduction zone. Org Geochem 31:1175–1187

Elvert M, Boetius A, Knittel K et al (2003) Characterization of specific membrane fatty acids as chemotaxonomic markers for sulfate-reducing bacteria involved in anaerobic oxidation of methane. Geomicrobiol J 20:403–419

Elvert M, Hopmans EC, Treude T et al (2005) Spatial variations of methanotrophic consortia at cold methane seeps: implications from a high-resolution molecular and isotopic approach. Geobiology 3:195–209

Freeman KH, Wakeham SG, Hayes JM (1994) Predictive isotopic biogeochemistry: hydrocarbons from anoxic marine basins. Org Geochem 21:629–644

Gaines SM, Eglinton G, Rullkötter J (2009) Echoes of life: what fossil molecules reveal about earth history. Oxford University Press, New York

Goedert JL, Thiel V, Schmale O et al (2003) The late Eocene 'Whiskey Creek' methane-seep deposit (western Washington State): part I, geology, palaeontology, and molecular geobiology. Facies 48:223–240

Haas A, Peckmann J, Elvert M et al (2010) Patterns of carbonate authigenesis at the Kouilou pockmarks on the Congo deep-sea fan. Mar Geol 268:129–136

Hagemann A, Leefmann T, Peckmann J et al (2013) Biomarkers from individual carbonate phases of an Oligocene cold-seep deposit, Washington State, USA. Lethaia 46:7–18

Hanson RS, Hanson TE (1996) Methanotrophic bacteria. Microbiol Rev 60(2):439–471

Hayes JM (2001) Fractionation of carbon and hydrogen isotopes in biosynthetic processes. In: Valley JW, Cole DR (eds) Reviews in mineralogy and geochemistry 43. Mineralogical Society of America, Chantilly, pp 225–277

Hayes JM, Freeman KH, Popp BN et al (1990) Compound-specific isotopic analyses: a novel tool for reconstruction of ancient biogeochemical processes. Org Geochem 16:1115–1128

Himmler T, Birgel D, Bayon G et al (2015) Formation of seep carbonates along the Makran convergent margin, northern Arabian Sea and a molecular and isotopic approach to constrain the carbon isotopic composition of parent methane. Chem Geol 415:102–117

Hinrichs K-U, Hayes JM, Sylva SP et al (1999) Methane-consuming archaebacteria in marine sediments. Nature 398:802–805

Hinrichs K-U, Summons RE, Orphan V et al (2000) Molecular and isotopic analysis of anaerobic methane-oxidizing communities in marine sediments. Org Geochem 31:1685–1701

Hinrichs K-U, Hmelo LR, Sylva SP (2003) Molecular fossil record of elevated methane levels in late Pleistocene coastal waters. Science 299:1214–1217

Hoehler TM, Alperin MJ, Albert DB et al (1994) Field and laboratory studies of methane oxidation in an anoxic marine sediment: evidence for a methanogen-sulfate reducer consortium. Glob Biogeochem Cycles 8:451–463

Holler T, Wegener G, Knittel K et al (2009) Substantial $^{13}C/^{12}C$ and D/H fractionation during anaerobic oxidation of methane by marine consortia enriched in vitro. Environ Microbiol Rep 1:370–376

Hopmans EC, Schouten S, Pancost RD et al (2000) Analysis of intact tetraether lipids in archaeal cell material and sediments by high performance liquid chromatography/atmospheric pressure chemical ionization mass spectrometry. Rapid Commun Mass Spectrom 14:585–589

Hryniewicz K, Bitner MA, Durska E et al (2016) Paleocene methane seep and wood-fall marine environments from Spitsbergen, Svalbard. Palaeogeogr Palaeoclimatol Palaeoecol 462:41–56

Hryniewicz K (this volume) Ancient Seep Carbonates: From Outcrop Appearance to Microscopic Petrography. In: Kaim A, Cochran JK, Landman NH (eds) Ancient methane seeps and cognate communities. Topics in Geobiology. Springer, Cham

Jahnke LL, Summons RE, Hope JM et al (1999) Carbon isotopic fractionation in lipids from methanotrophic bacteria II: the effects of physiology and environmental parameters on the biosynthesis and isotopic signatures of biomarkers. Geochim Cosmochim Acta 63(1):79–93

Jakubowicz M, Berkowski B, Hryniewicz K et al. (this volume) Middle Palaeozoic of Morocco: The Earliest-Known Methane Seep Metazoan Ecosystems. In: Kaim A, Cochran JK, Landman NH (eds) Ancient methane seeps and cognate communities. Topics in Geobiology. Springer, Cham

Jenkins RG, Hikida Y, Chikaraishi Y et al (2008) Microbially induced formation of ooid-like coated grains in the Late Cretaceous methane-seep deposits of the Nakagawa area, Hokkaido, northern Japan. Island Arc 17:261–269

Jones WJ, Holzer GU (1991) The polar and neutral lipid composition of *Methanosphaera stadtmanae*. Syst Appl Microbiol 14:130–134

Kellermann MY, Wegener G, Elvert M et al (2012) Autotrophy as a predominant mode of carbon fixation in anaerobic methane-oxidizing microbial communities. PNAS 109(47):19321–19326

Kiel S, Birgel D, Campbell KA et al (2013) Cretaceous methane-seep deposits from New Zealand and their fauna. Palaeogeogr Palaeoclimatol Palaeoecol 390:17–34

Kiel S, Glodny J, Birgel D et al (2014) The paleoecology, habitats, and stratigraphic range of the enigmatic Cretaceous brachiopod *Peregrinella*. PLoS One 9(10):e109260

Kiel S, Altamirano AJ, Birgel D et al (2020) Fossiliferous methane-seep deposits from the Cenozoic Talara Basin in northern Peru. Lethaia 53:166–182

Knittel K, Boetius A, Lemke A, Eilers H, Lochte K, Pfannkuche O, Linke P, Amann R (2003) Activity, distribution, and diversity of sulfate reducers and other bacteria in sediments above gas hydrate (Cascadia margin, Oregon). Geomicrobiol J 20:269–294

Knittel K, Boetius A (2009) Anaerobic oxidation of methane: progress with an unknown process. Annu Rev Microbiol 63:311–334

Knittel K, Lösekann T, Boetius A et al (2005) Diversity and distribution of methanotrophic archaea at cold seeps. Appl Environ Microbiol 71(1):467–479

Koga Y, Nishihara M, Morii H et al (1993) Ether polar lipids of methanogenic bacteria: structures, comparative aspects, and biosyntheses. Microbiol Rev 57(1):164–182

Koga Y, Morii H, Akagawa-Matsushita M et al (1998) Correlation of polar lipid composition with 16S rRNA phylogeny in methanogens: further analysis of lipid component parts. Biosci Biotechnol Biochem 62(2):230–236

Langworthy TA, Holzer G, Zeikus JG et al (1983) Iso- and anteiso-branched glycerol diethers of the thermophilic anaerobe *Thermodesulfotobacterium commune*. Syst Appl Microbiol 4(1):1–17

Leefmann T, Bauermeister J, Kronz A et al (2008) Miniaturized biosignature analysis reveals implications for the formation of cold seep carbonates at Hydrate Ridge (off Oregon, USA). Biogeosciences 5:731–738

Little CTS, Birgel D, Boyce AJ et al (2015) Late Cretaceous (Maastrichtian) shallow water hydrocarbon seeps from Snow Hill and Seymour Islands, James Ross Basin, Antarctica. Palaeogeogr Palaeoclimatol Palaeoecol 418:213–228

Londry KL, Jahnke LL, Des Marais DJ (2004) Stable carbon isotope ratios of lipid biomarkers of sulfate-reducing bacteria. Appl Environ Microbiol 70(2):745–751

Londry KL, Dawson KG, Grover HD et al (2008) Stable carbon isotope fractionation between substrates and products of *Methanosarcina barkeri*. Org Geochem 39:608–621

Lösekann T, Knittel K, Nadalig T et al (2007) Diversity and abundance of aerobic and anaerobic methane oxidizers at the Haakon Mosby Mud Volcano, Barents Sea. Appl Environ Microbiol 73(10):3348–3362

Marlow JJ, Steele JA, Ziebis W et al (2014) Carbonate-hosted methanotrophy represents an unrecognized methane sink in the deep sea. Nat Commun 5:5094

Marlow J, Peckmann J, Orphan V (2015) Autoendoliths: a distinct type of rock-hosted microbial life. Geobiology 13:303–307

Mazzini A, Ivanov MK, Nermoen A et al (2008) Complex plumbing systems in the near subsurface: geometries of authigenic carbonates from Dolgovskoy Mound (Black Sea) constrained by analogue experiments. Mar Pet Geol 25:457–472

McCollom TM, Seewald JS (2007) Abiotic synthesis of organic compounds in deep-sea hydrothermal environments. Chem Rev 107:382–401

Michaelis W, Seifert R, Nauhaus K et al (2002) Microbial reefs in the Black Sea fueled by anaerobic oxidation of methane. Science 297:1013–1015

Miyajima Y, Watanabe Y, Yanagisawa Y et al (2016) A late Miocene methane-seep deposit bearing methane-trapping silica minerals at Joetsu, central Japan. Palaeogeogr Palaeoclimatol Palaeoecol 455:1–15

Miyajima Y, Watanabe Y, Goto AS et al (2020) Archaeal lipid biomarker as a tool to constrain the origin of methane at ancient methane seeps: insight into subsurface fluid flow in the geological past. J Asian Earth Sci 189:104134

Natalicchio M, Peckmann J, Birgel D et al (2015) Seep deposits from northern Istria, Croatia: a first glimpse into the Eocene seep fauna of the Tethys region. Geol Mag 152:444–459

Nauhaus K, Boetius A, Krüger M et al (2002) In vitro demonstration of anaerobic oxidation of methane coupled to sulphate reduction in sediment from a marine gas hydrate area. Environ Microbiol 4(5):296–305

Nauhaus K, Treude T, Boetius A et al (2005) Environmental regulation of the anaerobic oxidation of methane: a comparison of ANME-I and ANME-II communities. Environ Microbiol 7(1):98–106

Nauhaus K, Albrecht M, Elvert M et al (2007) In vitro cell growth of marine archaeal-bacterial consortia during anaerobic oxidation of methane with sulfate. Environ Microbiol 9(1):187–196

Nguyen TB, Topçuoğlu BD, Holden JF et al (2020) Lower hydrogen flux leads to larger carbon isotopic fractionation of methane and biomarkers during hydrogenotrophic methanogenesis. Geochim Cosmochim Acta 271:212–226

Niemann H, Elvert M (2008) Diagnostic lipid biomarker and stable carbon isotope signatures of microbial communities mediating the anaerobic oxidation of methane with sulphate. Org Geochem 39:1668–1677

Niemann H, Elvert M, Hovland M et al (2005) Methane emission and consumption at a North Sea gas seep (Tommeliten area). Biogeosciences 2:335–351
Niemann H, Lösekann T, de Beer D et al (2006) Novel microbial communities of the Haakon Mosby mud volcano and their role as a methane sink. Nature 443:854–858
Niemann H, Fischer D, Graffe D et al (2009) Biogeochemistry of a low-activity cold seep in the Larsen B area, western Weddell Sea, Antarctica. Biogeosciences 6:2383–2395
Omoregie EO, Mastalerz V, de Lange G et al (2008) Biogeochemistry and community composition of iron- and sulfur-precipitating microbial mats at the Chefren mud volcano (Nile Deep Sea Fan, eastern Mediterranean). Appl Environ Microbiol 74(10):3198–3215
Orphan VJ, House CH, Hinrichs K-U et al (2001a) Methane-consuming Archaea revealed by directly coupled isotopic and phylogenetic analysis. Science 293:484–487
Orphan VJ, Hinrichs K-U, Ussler W III et al (2001b) Comparative analysis of methane-oxidizing archaea and sulfate-reducing bacteria in anoxic marine sediments. Appl Environ Microbiol 67(4):1922–1934
Orphan VJ, House CH, Hinrichs K-U et al (2002) Multiple archaeal groups mediate methane oxidation in anoxic cold seep sediments. PNAS 99(11):7663–7668
Pancost RD, Sinninghe Damsté JS (2003) Carbon isotopic compositions of prokaryotic lipids as tracers of carbon cycling in diverse settings. Chem Geol 195:29–58
Pancost RD, Sinninghe Damsté JS, De Lint S et al (2000) Biomarker evidence for widespread anaerobic methane oxidation in Mediterranean sediments by a consortium of methanogenic archaea and bacteria. Appl Environ Microbiol 66(3):1126–1132
Pancost RD, Zhang CL, Tavacoli J et al (2005) Lipid biomarkers preserved in hydrate-associated authigenic carbonate rocks of the Gulf of Mexico. Palaeogeogr Palaeoclimatol Palaeoecol 227:48–66
Pearson MJ, Grosjean E, Nelson CS et al (2010) Tubular concretions in New Zealand petroliferous basins: lipid biomarker evidence for mineralisation around proposed Miocene hydrocarbon seep conduits. J Pet Geol 33(3):205–220
Peckmann J, Thiel V (2004) Carbon cycling at ancient methane-seeps. Chem Geol 205:443–467
Peckmann J, Thiel V, Michaelis W et al (1999a) Cold seep deposits of Beauvoisin (Oxfordian; southeastern France) and Marmorito (Miocene; northern Italy): microbially induced authigenic carbonates. Int J Earth Sci 88:60–75
Peckmann J, Walliser OH, Riegel W et al (1999b) Signatures of hydrocarbon venting in a Middle Devonian carbonate mound (Hollard Mound) at the Hamar Laghdad (Antiatlas, Morocco). Facies 40:281–296
Peckmann J, Gischler E, Oschmann W et al (2001) An early Carboniferous seep community and hydrocarbon-derived carbonates from the Harz Mountains, Germany. Geology 29:271–274
Peckmann J, Goedert JL, Thiel V et al (2002) A comprehensive approach to the study of methane-seep deposits from the Lincoln Creek Formation, western Washington State, USA. Sedimentology 49:855–873
Peckmann J, Thiel V, Reitner J et al (2004) A microbial mat of a large sulfur bacterium preserved in a Miocene methane-seep limestone. Geomicrobiol J 21:247–255
Peckmann J, Campbell KA, Walliser OH et al (2007) A Late Devonian hydrocarbon-seep deposit dominated by dimerelloid brachiopods, Morocco. Palaios 22:114–122
Peckmann J, Birgel D, Kiel S (2009) Molecular fossils reveal fluid composition and flow intensity at a Cretaceous seep. Geology 37(9):847–850
Peters KE, Walters CC, Moldowan JM (2005) The biomarker guide, 2nd edn. Cambridge University Press, New York
Prahl FG, Wakeham SG (1987) Calibration of unsaturation patters in long-chain ketone compositions for paleotemperature assessment. Nature 330:367–369
Reeburgh WS (1976) Methane consumption in Cariaco Trench waters and sediments. Earth Planet Sci Lett 28:337–344
Reitner J, Peckmann J, Reimer A et al (2005) Methane-derived carbonate build-ups and associated microbial communities at cold seeps on the lower Crimean shelf (Black Sea). Facies 51:66–79

Rohmer M, Bouvier-Nave P, Ourisson G (1984) Distribution of hopanoid triterpenes in prokaryotes. J Gen Microbiol 130:1137–1150

Rossel PE, Elvert M, Ramette A et al (2011) Factors controlling the distribution of anaerobic methanotrophic communities in marine environments: evidence from intact polar membrane lipids. Geochim Cosmochim Acta 75:164–184

Rush D, Osborne KA, Birgel D et al (2016) The bacteriohopanepolyol inventory of novel aerobic methane oxidising bacteria reveals new biomarker signatures of aerobic methanotrophy in marine systems. PLoS One 11:e0165635

Rütters H, Sass H, Cypionka H et al (2001) Monoalkylether phospholipids in the sulfate-reducing bacteria *Desulfosarcina variabilis* and *Desulforhabdus amnigenus*. Arch Microbiol 176:435–442

Sakata S, Hayes JM, Rohmer M et al (2008) Stable carbon-isotopic compositions of lipids isolated from the ammonia-oxidizing chemoautotroph *Nitrosomonas europaea*. Org Geochem 39:1725–1734

Sandy MR, Lazăr I, Peckmann J et al (2012) Methane-seep brachiopod fauna within turbidites of the Sinaia Formation, eastern Carpathian Mountains, Romania. Palaeogeogr Palaeoclimatol Palaeoecol 323–325:42–59

Schouten S, Hopmans EC, Schefuß E et al (2002) Distributional variations in marine crenarchaeotal membrane lipids: a new tool for reconstructing ancient sea water temperatures? Earth Planet Sci Lett 204:265–274

Shapiro RS (this volume) Microbes in Modern and Ancient Hydrocarbon Seeps. In: Kaim A, Cochran JK, Landman NH (eds) Ancient methane seeps and cognate communities. Topics in Geobiology. Springer, Cham

Smrzka D, Zwicker J, Kolonic S et al (2017) Methane seepage in a Cretaceous greenhouse world recorded by an unusual carbonate deposit from the Tarfaya Basin, Morocco. Depositional Rec 3:4–37

Stadnitskaia A, Baas M, Ivanov MK et al (2003) Novel archaeal macrocyclic diether core membrane lipids in a methane-derived carbonate crust from a mud volcano in the Sorokin Trough, NE Black Sea. Archaea 1:165–173

Stadnitskaia A, Muyzer G, Abbas B et al (2005) Biomarker and 16S rDNA evidence for anaerobic oxidation of methane and related carbonate precipitation in deep-sea mud volcanoes of the Sorokin Trough, Black Sea. Mar Geol 217:67–96

Stadnitskaia A, Bouloubassi I, Elvert M et al (2008) Extended hydroxyarchaeol, a novel lipid biomarker for anaerobic methanotrophy in cold seepage habitats. Org Geochem 39:1007–1014

Summons RE, Jahnke LL, Roksandic Z (1994) Carbon isotopic fractionation in lipids from methanotrophic bacteria: relevance for interpretation of the geochemical record of biomarkers. Geochim Cosmochim Acta 58(13):2853–2863

Summons RE, Franzmann PD, Nichols PD (1998) Carbon isotopic fractionation associated with methylotrophic methanogenesis. Org Geochem 28(7/8):465–475

Takano Y, Chikaraishi Y, Imachi H et al (2018) Insight into anaerobic methanotrophy from $^{13}C/^{12}C$-amino acids and $^{14}C/^{12}C$-ANME cells in seafloor microbial ecology. Sci Rep 8:14070

Talbot HM, Watson DF, Murrell JC et al (2001) Analysis of intact bacteriohopanepolyols from methanotrophic bacteria by reversed-phase high-performance liquid chromatography-atmospheric pressure chemical ionisation mass spectrometry. J Chromatogr A 921:175–185

Teichert BMA, Bohrmann G, Suess E (2005) Chemoherms on Hydrate Ridge—unique microbially-mediated carbonate build-ups growing into the water column. Palaeogeogr Palaeoclimatol Palaeoecol 227:67–85

Thiel V, Peckmann J, Seifert R et al (1999) Highly isotopically depleted isoprenoids: molecular markers for ancient methane venting. Geochim Cosmochim Acta 63:3959–3966

Thiel V, Peckmann J, Richnow HH et al (2001a) Molecular signals for anaerobic methane oxidation in Black Sea seep carbonates and a microbial mat. Mar Chem 73:97–112

Thiel V, Peckmann J, Schmale O et al (2001b) A new straight-chain hydrocarbon biomarker associated with anaerobic methane cycling. Org Geochem 32:1019–1023

Thiel V, Heim C, Arp G et al (2007) Biomarkers at the microscopic range: ToF-SIMS molecular imaging of Archaea-derived lipids in a microbial mat. Geobiology 5:413–421
Tissot BP, Welte DH (1984) Petroleum formation and occurrence. Springer, New York
Tissot B, Califet-Debyser Y, Deroo G et al (1971) Origin and evolution of hydrocarbons in early Toarcian shales, Paris Basin, France. Am Assoc Pet Geol Bull 55:2177–2193
Tsuboi M, Nakamura E, Majima R et al (2010) (Reconstruction of ancient cold-seep activities based on biomarkers—a case study of lower Pleistocene Ofuna and Koshiba Formation, central Japan.) Fossils 87:5–21 (In Japanese with English abstract)
Valentine DL (2007) Adaptations to energy stress dictate the ecology and evolution of the Archaea. Nat Rev Microbiol 5:316–323
Wakeham SG (2020) Organic biogeochemistry in the oxygen-deficient ocean: a review. Org Geochem 149:104096
Wegener G, Niemann H, Elvert M et al (2008) Assimilation of methane and inorganic carbon by microbial communities mediating the anaerobic oxidation of methane. Environ Microbiol 10(9):2287–2298
Wegener G, Krukenberg V, Riedel D et al (2015) Intracellular wiring enables electron transfer between methanotrophic archaea and bacteria. Nature 526:587–590
Welander PV, Summons RE (2012) Discovery, taxonomic distribution, and phenotypic characterization of a gene required for 3-methylhopanoid production. PNAS 32:12905–12910
Whiticar MJ (1999) Carbon and hydrogen isotope systematics of bacterial formation and oxidation of methane. Chem Geol 161:291–314
Wörmer L, Elvert M, Fuchser J et al (2014) Ultra-high-resolution paleoenvironmental records via direct laser-based analysis of lipid biomarkers in sediment core samples. PNAS 111(44):15669–15674

Chapter 3
Ancient Seep Carbonates: From Outcrop Appearance to Microscopic Petrography

Krzysztof Hryniewicz

3.1 Introduction

Hydrocarbon seeps are localized submarine ecosystems where hydrocarbons discharge from the seabed into the water column. The majority of extant hydrocarbon seeps have been found on continental margins, where sediment degassing takes place above fluid-laden thick sedimentary columns (e.g., Sibuet and Olu 1998; Campbell 2006; Joye 2020). At seeps, hydrocarbon-bearing fluids migrate upward through various conduits toward the shallow subsurface, where they mix with the sulfate-bearing seawater infiltrating sedimentary pore space. Dissolved methane and sulfate enable the microbially mediated anaerobic oxidation of methane (AOM) according to the formula:

$$CH_4 + SO_4^{2-} \rightarrow HCO_3^- + HS^- + H_2O$$

This results in precipitation of methane-derived authigenic carbonates incorporating ^{12}C-enriched methanogenic carbon in the immediate (meter-scale) vicinity of the fluid outlets, usually within sediment or at the sediment-water interface (Ritger et al. 1987; Peckmann and Thiel 2004). In addition to carbonate cementation, seeping methane and dissolved sulfide formed during AOM provide metabolic energy for chemoautotrophic microbes and their chemosymbiotic invertebrate hosts, which frequently form mass accumulations at seeps (Levin 2005).

In line with their recent counterparts, ancient seep deposits typically (i) have restricted spatial and stratigraphic occurrence, often but not always (cf. Kauffman et al. 1996; Landman et al. 2012, this volume; Meehan and Landman 2016) within relatively deep-water facies, (ii) are characterized by extensive cementation by

K. Hryniewicz (✉)
Institute of Paleobiology, Polish Academy of Sciences, Warszawa, Poland
e-mail: krzyszth@twarda.pan.pl

A. Kaim et al. (eds.), *Ancient Hydrocarbon Seeps*, Topics in Geobiology 50,
https://doi.org/10.1007/978-3-031-05623-9_3

carbonate with low $\delta^{13}C$, and (iii) contain seep-endemic invertebrate macrofossils for which chemosymbiosis or close relations to a chemosynthetic food chain can be reliably inferred (e.g., Campbell and Bottjer 1993; Peckmann and Thiel 2004; Campbell 2006; Kiel et al. 2014a). These criteria have been commonly employed as part of a "seep search strategy," resulting in the identification of numerous ancient seep deposits worldwide (e.g., Kelly et al. 1995; Kauffman et al. 1996; Peckmann et al. 1999a, b, 2002, 2003, 2007, 2011; Kelly et al. 2000; Barbieri et al. 2005; Gill et al. 2005; Kiel and Peckmann 2007; Kiel and Peckmann 2008; Hammer et al. 2011; Agirrezabala et al. 2013; Kaim et al. 2013; Kiel et al. 2013; Zwicker et al. 2015; Hryniewicz et al. 2015a, 2016; Smrzka et al. 2017). In this contribution, the term "ancient seep carbonates" is applied to AOM-related carbonates which have been fossilized in marine rock formations and uplifted above sea level, although there are exceptions to this (e.g., Duranti and Mazzini 2005). Seep carbonates exposed on the seabed in localities where methane seepage has ceased, usually of Pleistocene to Holocene age, are not considered ancient seep carbonates in this review.

The base of this chapter relies on two separate data pools: literature describing extant seep carbonates studied on the seabed and that on ancient seep carbonates studied in outcrop. Both sources offer different, yet to a degree, complementary views of seep carbonate deposits. Extant seep carbonates are studied during or shortly after their formation on the seabed before they can be subjected to burial and diagenetic alteration. Consequently, (i) the most accessible fragments of extant seep deposits are either at the surface or shallow subsurface close to the seabed, while deeper parts are less accessible and less easy to study; (ii) they frequently preserve original mineralogies and textures formed due to AOM before the onset of diagenetic alteration. Ancient seep carbonates, on the other hand, (i) are studied mostly in outcrop, which, unless perfectly parallel to the bedding, allow relatively easy access to deeper horizons of the seep deposit while restricting the access to the surface of the deposit and (ii) have long and complex geological history and accumulate later diagenetic mineralogies and textures which have not yet formed in extant seep deposits. Burial diagenesis can alter mineralogy and textures to such an extent that establishing a straightforward relationship between some apparently congeneric textures in extant and ancient seep carbonates may not be possible.

This chapter is a review of the structure and petrography of ancient seep carbonates, from their size and external appearance in outcrop, to microscopic textures observed in thin section. A detailed discussion of geochemistry of seep carbonates is covered elsewhere in this volume (Cochran et al. this volume; Miyajima and Jenkins this volume). However, some consideration of stable carbon and oxygen isotope composition of particular carbonate phases and lipid biomarker contents of seep carbonates were unavoidable.

3.2 Size of Seep Deposits

3.2.1 Extant Seep Deposits

Seep carbonates incorporate part of the carbon released at methane seeps (e.g., Boetius and Suess 2004; Luff et al. 2004; Tsunogai et al. 2010; Römer et al. 2012); therefore, the size of a seep deposit is to a degree a function of the volume of methane that reached the sediment surface and was metabolized by AOM (Campbell 2006). The largest seep carbonates thus occur in areas where large volumes of methane are delivered to the seabed for prolonged periods of geological time. Some of the largest, single methane seep carbonates known today are up to 180-m-long and 90-m-high carbonate deposits above Hydrate Ridge off Oregon (e.g., Teichert et al. 2005), which started to form over 250 ka and are still growing today, albeit the carbonate accumulation rate was higher during the Pleistocene than afterward (Teichert et al. 2003). Larger seep carbonate deposits such as those at Hydrate Ridge are often supplied by substantial gas migration pathways including active faults (Carson and Screaton 1998) or blow-out pipes associated with mud volcanism (Perez-Garcia et al. 2009; Pape et al. 2014).

The majority of extant seep carbonates are much smaller than those from Hydrate Ridge. For example, at the Nyegga site in the Norwegian Sea where seep carbonates are associated with gas hydrates similar to those from Hydrate Ridge, the largest single carbonate deposit is about 4 m × 3 m × 2 m in size (Hovland and Svensen 2006). Seep carbonate pavements from Monterey Canyon off California are a few square meters in surface or less, and carbonate crusts and pavements measure around 5 cm in thickness (Stakes et al. 1999). Carbonate nodules are most commonly several centimeters in diameter, although larger structures of decimeter scale can form due to the amalgamation of many smaller nodules (Reitner et al. 2005a; Haas et al. 2010). Tubular carbonate conduits are usually either fragmented or partially buried when observed on the seabed; therefore their actual diameters are difficult to ascertain. Fragments of such conduits studied by underwater observation are usually less than 1 m high and up to 0.35 m in diameter (Takeuchi et al. 2007; Magalhães et al. 2012), although larger structures up to 4 m high and 0.5 m in diameter have also been observed (Magalhães et al. 2012). Tubular conduits studied on the seabed have mostly fallen over and are inactive, indicating that a substantial volume of sediment has been removed.

3.2.2 Ancient Seep Deposits

Comparing sizes of extant and ancient seep deposits is innately burdened by uncertainty. This results from the way both occur and are accessed; extant seep carbonates are exposed on the seabed, observed in plan view, and accessed from above using a submersible, with only limited access to deeper parts of the seep system

through gravity coring or drilling. Ancient seep carbonates, on the other hand, are mostly accessed on land in outcrop and are observed in cross section. It is relatively easy to measure the lateral extent of an extant seep carbonate, while measuring its vertical extent is possible only for the parts visible above the seabed or accessed via coring or drilling (e.g., Teichert et al. 2005). Conversely, it is possible to measure the thickness and cross-sectional length of an ancient seep deposit cropping out; however, it is very difficult to measure its lateral extent in all dimensions since these are partially hidden below the ground. An exception to this will be an outcrop surface parallel to the bedding (e.g., Allison et al. 2008), where an ancient seep carbonate can be studied on a plane just like its extant equivalent.

There are a few examples of particularly large ancient seep carbonates that are similar in size compared to the largest extant equivalents. One such example is the Middle Miocene Rocky Knob seep carbonate from East Coast Basin, New Zealand, which is roughly 175 m × 50 m in plan view (Campbell et al. 2008). The Late Triassic (Norian) Graylock Butte 1 (GB1) carbonate from Oregon, USA, measures roughly 70 m in exposed lateral extent and is approx. 4 m thick (Peckmann et al. 2011). A somewhat extreme example, and possibly the largest single seep carbonate preserved, could be a Late Cretaceous (Campanian) seep deposit from Oglala National Grassland, Nebraska, USA, which is ca. 400 m × 200 m in plan view (Fig. 3.1a; Landman et al. this volume, Fig. 14.3f). This deposit has not been studied in detail yet, and it is unknown whether it is a single carbonate body or several smaller ones in close proximity (Andrzej Kaim, personal communication). The Eocene Bear River seep deposit from Washington State, USA, is roughly 68 m long × 38 m wide × 15 m thick (Goedert and Benham 2003). On photographs of the seep deposit from 1954 (Danner 1966: fig. 231), there are fragments of outcrop which are sunken and covered with scree and could very well comprise non-carbonate deposits. The Bear River deposit can thus be several seep carbonate blocks stacked in close proximity, similar to other large ancient seep deposits. The Late Triassic (Norian) Graylock Butte 2 (GB2) deposit from Oregon, USA, represents numerous smaller (meter-scale) carbonate outcrops spread on a ridge along approx. 270 m of strike (Peckmann et al. 2011; own data). The Late Cretaceous Sada Limestone in Shikoku, Japan, comprises numerous meter-scale carbonate bodies dispersed on an area of approx. 250 m × 100 m (Nobuhara 2016). Carbonate stromatolites and boulders forming the Early Jurassic seep carbonate deposit from La Elina, Los Molles Formation, Neuquén Province, Argentina (Gómez-Pérez 2003), are spread in an area roughly 50 m × 45 m × 38 m (Fig. 3.1b, Krzysztof Hryniewicz, own data). Stacking of carbonate blocks forming these deposits implies that before compaction of the host sediment they could have been located much further apart vertically than they are now. Thus, they may be not ideally penecontemporaneous, and at each given time, the size of the seep may have been smaller than the area of the deposit cropping out today.

The great majority of known ancient seep deposits are relatively small carbonate bodies which are meter-scale or smaller and are either loosely scattered over a small

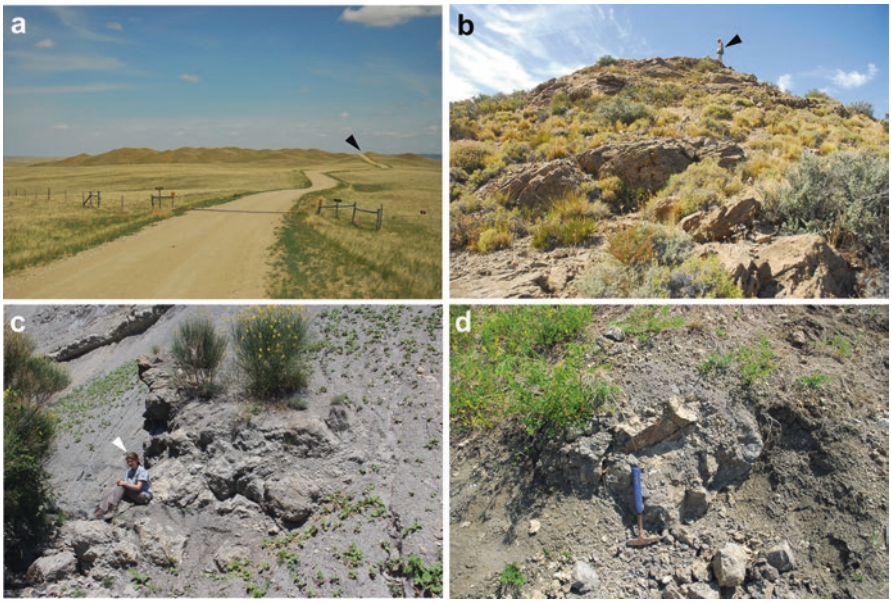

Fig. 3.1 Examples of ancient seep deposits of different sizes. (**a**) Oglala seep deposit (Upper Cretaceous, Campanian), Pierre Shale, Oglala National Grassland, Nebraska, USA. View toward the east. The deposit is ca. 400 m × 200 m in plan view. Montrose Road transecting the deposit in the southern part of the picture for scale (arrowhead). (**b**) La Elina seep deposit, La Elina (Lower Jurassic, Toarcian), Los Molles Formation, Neuquen Province, Argentina (Gómez-Pérez 2003). The deposit is ca. 50 m × 45 m × 38 m in plan view. The person standing on top of the deposit for scale (arrowhead). (**c**) One of the Beauvoisin seep deposits (Upper Jurassic, Oxfordian), Terres Noires Formation, Beauvoisin, Drome, France (Gaillard et al. 1992). Person for scale (arrowhead). (**d**) Small carbonate deposit, Indian Creek seep site (Upper Cretaceous, Campanian), Pierre Shale, Buffalo Gap National Grassland. Hammer for scale

area or isolated in siliciclastic host rock formations (Figs. 3.1c, d and 3.2). For example, the Late Cretaceous (Campanian) seep deposit from Yasukawa, Hokkaido, Japan, comprises four carbonate bodies larger than 0.5 m in diameter spread over an area of few dozen square meters, whereas the remainder of the deposit consists of small-, decimeter-, or centimeter-scale carbonate concretions loosely dispersed in the host sediments (e.g., Jenkins et al. 2007). Various Paleogene and Neogene seep carbonates in the Cascadia margin, Western USA, and Canada are preserved either as small-, decimeter-, or centimeter-sized nodules scattered in the host sediment or as carbonate-filled invertebrate fossils (Nesbitt et al. 2013). An example of a single, small ancient seep carbonate could be an Early Miocene seep carbonate from Tanohama, Tsushima, Japan, which is a lenticular carbonate ca. 3.7 m long and 1 m thick, surrounded by numerous decimeter- to centimeter-sized carbonate concretions scattered in the deep-water mudstone (Hryniewicz et al. 2021).

Fig. 3.2 Examples of smaller ancient seep deposits. (**a**) Yasukawa seep deposit (Upper Cretaceous, Campanian), Omagari Formation, Nakagawa District, Hokkaido, Japan (Jenkins et al. 2007). Two of four larger blocks (ca. 0.5 m in diameter) of seep carbonate (arrowheads) are visible. People in the right side of the picture for scale. (**b**) Tanohama seep deposit (Lower Miocene), Taishu Group, Tanohama, Tsushima, Japan (Hryniewicz et al. 2021). The deposit is ca. 3.7 m long and 1 m thick and is surrounded by numerous smaller, decimeter-sized carbonate nodules. People for scale. (**c**) Eagle Creek seep deposit (Lower Cretaceous, Barremian), Budden Canyon Formation, California, USA (Jenkins et al. 2013). One of the carbonate bodies (ca. 1 m in length) forming the carbonate deposit. Hammer for scale. (**d**) Tanami seep carbonate (upper Eocene–lower Oligocene), Tanamigawa Formation, Tanami, Wakayama Prefecture, Honshu, Japan. The deposit is ca. 3.5–4.5 m × 0.2–0.6 m × 0.2–0.6 m (Amano et al. 2013). Hammer for scale

3.3 Macroscopic Appearance

3.3.1 Extant Seep Carbonates

A characteristic feature of many extant seep carbonates is that their formation occurs at the sediment-water interface (e.g., Stakes et al. 1999; Peckmann et al. 2001; Greinert et al. 2001; Pierre and Fouquet 2007). The process behind this is the dependence of AOM on anaerobic conditions and the presence of dissolved seawater sulfate (Boetius et al. 2000), which results in carbonate formation in the shallow subsurface where the necessary conditions are met. Aerobic methane oxidation, on the other hand, will cause carbonate dissolution (Himmler et al. 2011). This means that most seep carbonates will form close to or at the sediment-water interface in a roughly horizontally oriented zone parallel to it and initially will not protrude significantly either above or below the seabed (Luff et al. 2004). The morphology that

seep carbonates exhibit during early stages of their formation is variable to some extent, but the most commonly reported examples are nodules, pavements, or small tubular concretions (e.g., Reitner et al. 2005a; Haas et al. 2009; Himmler et al. 2015). These precipitates are accessible to underwater observation only after they become exposed by bottom currents (e.g., Matsumoto 1990; Himmler et al. 2011; O'Reilly et al. 2014) or dislodged by other processes, such as gas hydrate growth underneath the carbonate (e.g., Greinert et al. 2001), mud volcano eruptions (e.g., Vanneste et al. 2012), explosive gas release (e.g., Mazzini et al. 2006), pockmark formation (e.g., Webb et al. 2009), or collapse of carbonate overhangs (Hovland and Judd 2007). Seep carbonates can also form at some depth under the sediment-water interface, but this is reported far less often than its shallower-formed counterparts as it is exposed only exceptionally when larger volumes of sediment are eroded away. Examples of such carbonates are various tubular conduits that form the deeper part of the plumbing system of submarine hydrocarbon seeps and were exposed by contourite or other strong eroding bottom currents (e.g., Takeuchi et al. 2007; Magalhães et al. 2012).

In exceptional cases, seep carbonates can also form above the sediment-water interface. Among such cases are marine anoxic basins with a water column depleted in oxygen, allowing AOM and carbonate formation to take place directly at or above the sediment-water interface. A typical example of seep deposits formed under such conditions are meter-scale columnar carbonates from the deeper waters of the Black Sea, which is totally anoxic below 150 m water depth (Peckmann et al. 2001; Reitner et al. 2005b). Similar mechanisms are responsible for the formation of columnar stromatolites in the Oxygen Minimum Zone off Pakistan in the Indian Ocean (e.g., Himmler et al. 2018).

It has been suggested by Teichert et al. (2005) that particularly strong and localized flux of reduced fluids can cause carbonate formation to build up into oxic bottom waters. An example of such a formation are seep carbonate mounds and pinnacles that project into the water column above the sediment, the so-called chemoherms, as observed on Hydrate Ridge off Oregon (e.g., Teichert et al. 2005). Carbonate authigenesis in such cases requires a thin veneer of an oxic/anoxic interface, provided by, for example, mats of sulfide-oxidizing bacteria (e.g., *Beggiatoa*) around active fluid outlets, such that all reduced and oxidized compounds necessary for AOM are simultaneously available (e.g., Boetius and Suess 2004). Methanogenic chemoherms may share some macroscopic features with carbonate buildups known from "classical" carbonate sedimentology (cf. Monty et al. 1995), such as slope aprons (e.g., Teichert et al. 2003).

3.3.2 Ancient Seep Carbonates

Most ancient seep deposits are more or less isolated carbonate bodies occurring within siliciclastic, deep marine host sediments (Campbell 2006 and references therein). Before extant seep deposits were discovered via submersibles on the

modern seafloor, and in the absence of stable isotopic criteria that identify their fossil counterparts, some carbonate deposits later identified as ancient seeps had been referred to as "reefs" (e.g., Danner 1966) and/or olistoliths (e.g., Ager 1965). The "reef" or other buildup-related origin was usually inferred based on textures superficially similar to these found in ancient reefs and mud mounds (cf. Peckmann et al. 1999a, 2002; Campbell et al. 2002; Hryniewicz et al. 2012; see also Monty et al. (1995) for a review of ancient mud mounds). Stromatactoid cavities and clotted micrites found at seep deposits are especially similar to those known from Paleozoic and Mesozoic deep-water mud mounds (e.g., Flajs et al. 1995) and on first glance could have been taken as circumstantial evidence for a buildup origin. An "olistolith" origin, on the other hand, was most probably proposed based on the assumption that a carbonate deposit with a mass accumulation of fossils could not have formed on an otherwise fossil-poor siliciclastic deep-sea bottom and must have been redeposited from shallow water settings (Ager 1965). In fact, several ancient seep deposits, although originating in a deep-water environment, have formed on a slope and subsequently slumped basinward before their final emplacement and burial (e.g., Berti et al. 1994; Sandy 2010; Kiel et al. 2014a, b), so an "olistolith" interpretation in such cases can be sedimentologically correct.

The relationship between seep deposits and the surrounding sediment is most easily observed on fresh outcrops devoid of vegetation. Such conditions are mostly met in arid deserts where the intensity of weathering and physical erosion is low and the vegetation is scant (e.g., Hryniewicz et al. 2017; Smrzka et al. 2017). In other areas, outcrops of seep deposits are restricted to cliffs, riverside scarps, and road cuts (Fig. 3.3a; Gaillard et al. 1992; Landman et al. 2012; Natalicchio et al. 2015; Zwicker et al. 2015; Meehan and Landman 2016; Hryniewicz et al. 2021; Landman et al. this volume), riverbeds (Fig. 3.3b; Jenkins et al. 2007; Kaim et al. 2013), or wave-cut platforms (Fig. 3.3c; Allison et al. 2008; Agirrezabala 2009; Agirrezabala et al. 2013), where weathered material is removed before it can cover up the seep deposit. Even in these settings, a large part of the seep deposit can be obscured by the accumulation of debris (Fig. 3.1a, b; cf. Hickman 2015) or be completely eroded away in a matter of years (e.g., Kiel 2010: fig. 14.5). Many ancient seep carbonate outcrops are partially covered with vegetation (Fig. 3.2a; Campbell et al. 2008), frequently on slopes where an "in situ" situation cannot be confirmed (Fig. 3.2b, c; Campbell and Bottjer 1993: fig. 9; Campbell et al. 2008) or that are partially flooded by a watercourse and covered by sediment (Fig. 3.1d; Kaim et al. 2009). Some seep deposits are known only from float (Fig. 3.3d) and have not been found "in situ" at all. This is particularly true for ancient seep deposits from Spitsbergen (Svalbard) where outcrops are heavily modified by periglacial processes such as frost wedging and solifluction. Out of 16 latest Jurassic–earliest Cretaceous seep deposits found on Spitsbergen, only two are "in situ," with the remainder having slumped to various degrees either en masse or as fragments (Hryniewicz et al. 2015b). A Paleocene seep deposit from Fossildalen, Spitsbergen, is known exclusively from float found in the riverbed (Fig. 3.3d; Hryniewicz et al. 2016).

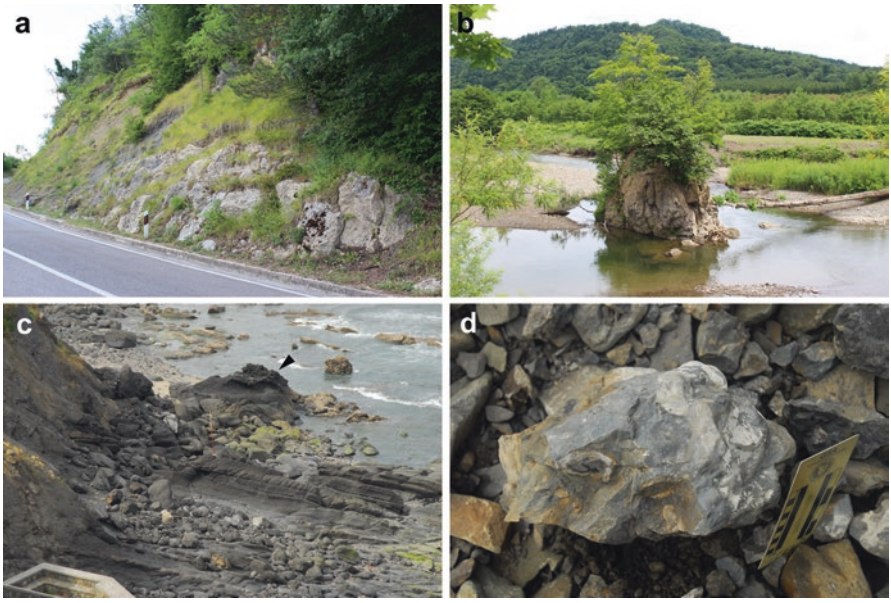

Fig. 3.3 Outcrops of ancient seep deposits. (**a**) Road cut, Buje seep deposit (Eocene), Flysch Units, Istria, Croatia (Natalicchio et al. 2015). The deposit (termed "Buje 1" in Natalicchio et al. 2015) is ca. 4 m thick and extends laterally for ca. 20 m. (**b**) A solitary carbonate islet exposed in a riverbed, Omagari (Upper Cretaceous, Campanian), Abeshinai River, Omagari Formation, Nakagawa District, Hokkaido, Japan. The islet is ca. 10 m in lateral extent. (**c**) Wave-cut platform, Kardala seep deposit (Lower Cretaceous, Albian), Black Flysch Group, Basque Country, Spain. The deposit (arrowhead) is ca. 20 m in lateral extent. (**d**) Float, Fossildalen seep deposit (Paleocene), Basilika Formation, Spitsbergen, Svalbard (Hryniewicz et al. 2016). This particular block is ca. 20 cm along the longer axis

When seep deposits are preserved "in situ," their observed shape can be very variable and can depend on numerous factors, such as the part of the seep deposit cropping out and the intensity and duration of seepage. Portions of the seep deposit formed close to the sediment-water interface frequently occur as lenticular bodies (Fig. 3.4a), which may be arranged parallel to the bedding plane, but not necessarily, and comprise either one larger carbonate body (Smrzka et al. 2017), accumulations of smaller carbonate nodules, or a combination of both (Gaillard et al. 1992; Landman et al. 2012; Meehan and Landman 2016; Hryniewicz et al. 2021). In some cases, only a few loose nodules of ^{13}C-depleted carbonate and associated fauna comprise a seep deposit and are evidence for past seepage activity at a given locality (e.g., Jenkins et al. 2007; Nesbitt et al. 2013). Extensive columnar bodies with the vertical dimension larger than the horizontal, either the so-called pseudobioherms (Fig. 3.4b; Gaillard et al. 1992) or pipe-like structures (e.g., de Beaver et al. 2011), can also form as a result of localized seepage; the latter are likely parts of the subsurface plumbing system of ancient hydrocarbon seeps, together with a variety of tubular concretions (Fig. 3.4c, d; e.g., Pearson et al. 2010; Wiese et al. 2015; Zwicker et al. 2015).

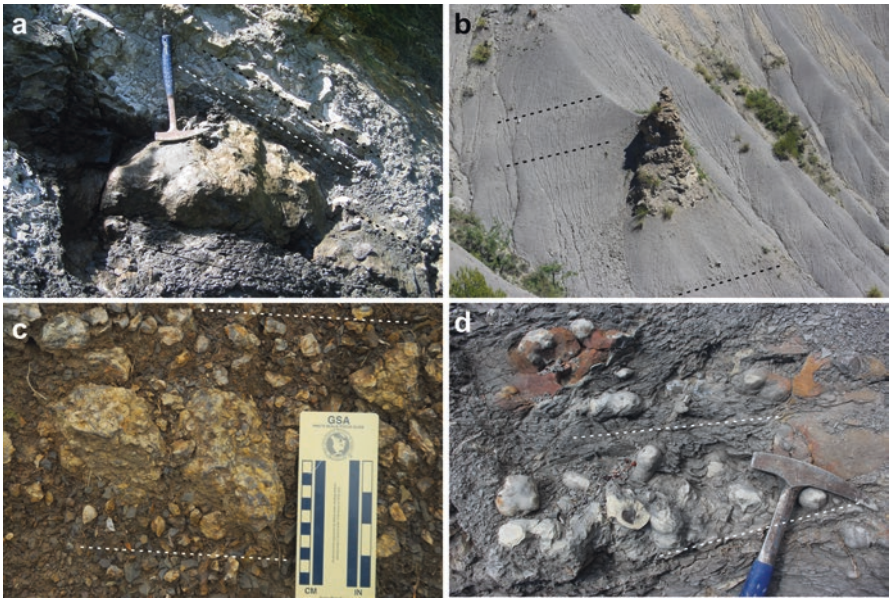

Fig. 3.4 Shapes of ancient seep deposits. (**a**) A lenticular carbonate arranged along the bedding plane (stippled line), Pombetsu seep deposit (Lower Cretaceous, Albian), Yezo Supergroup, Mikasa City, Hokkaido, Japan. (**b**) Pseudobioherm arranged perpendicular to the bedding plane (stippled line), Beauvoisin (Upper Jurassic, Oxfordian), Terres Noires Formation, Beauvoisin, Drome, France (Gaillard et al. 1992). (**c**) Accumulation of nodules and smaller carbonate blocks in the lateral zone of a lenticular seep deposit, stippled line marks the bedding surface, Tanohama seep deposit (Lower Miocene), Taishu Group, Tsushima, Japan. (**d**) Carbonate-filled burrows arranged along and perpendicular to the bedding surface (stippled line); base of one of the pseudobioherms (Upper Jurassic, Oxfordian), Terres Noires Formation, Beauvoisin, Drome, France

The main difficulty in comparing the morphology of ancient seep deposits with their extant counterparts is inferring the relationship of the seep carbonates to the sediment surface. The relationship between the sediment-water interface and the seep carbonates forming presently is verifiable. Conversely, the ancient sediment-water interface changed its position during geological time, and its position in outcrop has to be inferred for the given time based on observed depositional, biological, and diagenetic textures. This indicates that the relationship of the ancient sediment surface to the ancient seep deposit in the outcrop is not obvious or easy to infer, and there are very few diagnostic features indicating that ancient seep carbonates were at any given moment exposed above the seabed. One such feature is the presence of carbonate slope aprons, indicating that carbonate had a positive relief and provided a talus for its surroundings. Such structures are rarely reported from the fossil record; one such example could be cross-bedded slope facies from Miocene seep deposits from New Zealand (Campbell et al. 2008: fig. 13). A further rare case is the Cretaceous Amma Fatma seep deposit from Morocco, where a bed covering a large carbonate body pinches out, likely because the seep carbonate body protruded above the seafloor during the time of its formation (Smrzka et al. 2017). The

presence of fossil epifauna directly attached to the seep carbonate can also be a good proxy that the seep carbonate was exposed above the sediment-water interface. Among such examples are serpulid *Propomatoceros* sp. tubes (Vinn et al. 2014: fig. 5A) and unidentified cementing bivalves (Hryniewicz et al. 2014: fig. 10A, B) attached to fossil carbonate surfaces from the latest Jurassic to the earliest Cretaceous hydrocarbon seep carbonates from Spitsbergen. Many examples of attaching epifaunal fossils are, however, found either dispersed in the carbonate matrix or attached to other fossils (e.g., Vinn et al. 2013; Hryniewicz et al. 2015b); hence, their presence should not always be taken as unambiguous evidence of positive relief of ancient seep deposits.

3.4 Macroscopic Petrography

3.4.1 Extant Seep Carbonates

Macroscopic petrography of extant seep carbonates can be studied either directly on the seabed (e.g., Himmler et al. 2011: fig. 2a–d), on hand samples retrieved from the seabed by submersibles (e.g., Mazzini et al. 2004: fig. 4a, 5a, 6a, 7a, b; Himmler et al. 2011: fig. 2e–f; Smrzka et al. 2019: fig. 3b, d, 4b–d), or on polished slabs of retrieved hand samples (e.g., Mazzini et al. 2004: fig. 3; Teichert et al. 2005: fig. 5b–f; Haas et al. 2010: fig. 2c, 3b, 5b; Himmler et al. 2011: fig. 3). Since seep carbonates are frequently covered with biota or sediment which otherwise obscures the details visible on the surface (e.g., Van Dover et al. 2002: fig. 3a; Webb et al. 2009: fig. 3 b–d, e), observation of retrieved samples is a more unequivocal way to observe macroscopic petrography of extant seep deposits. This is with the proviso that the features targeted do not exceed the size of the sample extracted.

One of the most conspicuous features of the majority of extant seep carbonates is the abundance of cavities, which either show some preferential orientation (e.g., Himmler et al. 2016: fig. 2) or do not (e.g., Himmler et al. 2011: fig. 2, 3). A characteristic type of cavity at seep carbonates is represented by various tubular structures that acted as conduits for fluids and methane (e.g., Hovland 2002; Teichert et al. 2005; Haas et al. 2010; Malaghães et al. 2012). The cavities may remain unlined or be lined with cements to various degrees (e.g., Teichert et al. 2005; Himmler et al. 2011). There are multiple origins of cavities within the seep deposit, such as carbonate dissolution during periods of elevated acidity (Himmler et al. 2011), occlusion of cavities in between centers of carbonate precipitation (e.g., Haas et al. 2010), or dissolution of gas hydrate enclaves enclosed within carbonate precipitates (e.g., Greinert et al. 2001). Gas hydrates at seeps are frequently associated with breccias which formed from relatively brittle carbonate (Bohrmann et al. 1998); this is likely because formation of gas hydrate involves a significant volume increase and this has a potential for disrupting even strongly cemented layers of carbonate. Reasons for brecciation can be multiple and involve, for example, cementation of soft sediment brecciated due to mud and fluid expulsion (Vanneste et al.

2012) or slumping and collapse of positive carbonate relief (Greinert et al. 2001; Teichert et al. 2005). Different generations of breccias at extant seeps form at the surface or below it (cf. Greinert et al. 2001), and only the former are generally available for submersible-borne observation and sampling.

Laminated fabrics comparable to those known from other depositional environments also occur at seeps (e.g., Greinert et al. 2002; Himmler et al. 2018). The exact origin of the lamination in seep carbonates is difficult to ascertain as there are multiple causes for lamination in sedimentary rocks. At seeps, particular laminae grow toward the source of reducing compounds and generally into the sediment where the fluid flow originates, thus conforming to a general pattern of downward growth of seep deposits (e.g., Greinert et al. 2002). However, when bottom waters are oxygen-deficient and allow for an upward growth of seep carbonate, laminations can also form from the sediment surface upward into the water column similar to the cases known from more "classical" depositional settings (Himmler et al. 2016). Sediment baffling and trapping by chemosynthetic microbial mats can be one of the causes for laminated fabrics in seep carbonates (Himmler et al. 2016); microbial mats, in general, may become permineralized by Mg calcite and aragonite precipitates (Reitner et al. 2005b), and sediment baffling may even further contribute to the expression of particular laminae. Cementation of sedimentary laminations accentuated by gas hydrate can also result in layered carbonates (Mazzini et al. 2004). Fillings of tubular conduits (e.g., Greinert et al. 2002: fig. 4) and concretions forming at seeps are frequently layered in appearance (e.g., Reitner et al. 2005a; Haas et al. 2010).

One of the more peculiar fabrics of seep deposits are carbonate spheres formed due to calcification of microbial mats around fluid outlets (Reitner et al. 2005b). Amalgamation of such cemented microbial spheres results in thrombolitic fabric superficially similar to that known from non-seep fossil microbial carbonates (cf. Shapiro 2000). An important aspect of seep carbonate formation is biogeochemical feedback affecting rates of fluid flow, AOM, and carbonate precipitation (cf. Luff et al. 2005); thus, very complex patterns involving cavities, nodules, lamination, layering, and zonation will form at seeps due to self-regulatory processes even without any external cause.

3.4.2 Ancient Seep Carbonates

In addition to polished slabs used to study extant seep deposits recovered from the seabed, exposed surfaces are a very valuable source of information. This is largely due to subaerial weathering that accentuates even slight differences in mineralogy, crystal size, clay admixture, or fossil content that would otherwise be difficult to observe with the naked eye on unweathered surfaces. Some of the more spectacular examples of such features are, for example, carbonates with ankerite-filled vesicomyid bivalve shells (red-weathering) "floating" in a calcitic matrix (beige-weathering) from Early Miocene seep deposits from Tsushima, Japan (Fig. 3.5a; Hryniewicz et al. 2021: fig. 6), and tubeworm facies in Devonian (Peckmann et al. 2005: fig. 3),

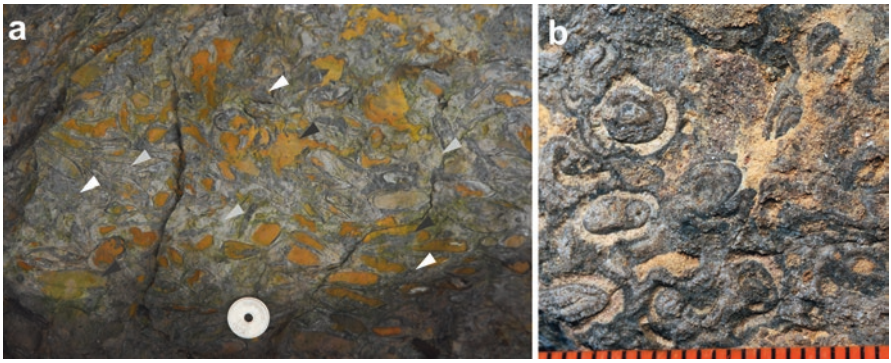

Fig. 3.5 Macroscopic petrography of ancient seep carbonates. (**a**) Weathering-accentuated differences in mineralogy; ankerite-filled vesicomyid bivalves and cavities (orange, indicated by black arrowheads) contrast with grey cements (indicated by white arrowheads) and beige microcrystalline carbonates (grey arrowheads). Kanoura seep deposit (Lower Miocene), Taishu Group, Tsushima, Japan (Hryniewicz et al. 2021). Coin for scale. (**b**) Weathering-accentuated agglutinated tubeworms within microcrystalline carbonate from La Elina seep deposit (Lower Jurassic, Toarcian), Los Molles Formation, Neuquen Province, Argentina (Gómez-Pérez 2003). Scale in mm

Jurassic (Fig. 5B; Gómez-Pérez 2003: fig. 8a), Cretaceous (Hikida et al. 2003: fig. 3), and Oligocene (Goedert et al. 2000: fig. 3) seep deposits. Various breccias, either polymictic or monomictic (e.g., Hikida et al. 2003: fig. 3.2, Bojanowski 2007; Conti and Fontana 2007; Conti et al. 2007), are also clearly visible on exposed surfaces, again due to differential weathering of clasts and matrix.

The macroscopic textures known from ancient seep deposits are roughly similar to those known from their extant counterparts (Figs. 3.6 and 3.7), with a few exceptions due to biological or geological causes. Breccias (Fig. 3.8) occur in both ancient and extant seeps, although perhaps not as commonly in ancient seep carbonates as in their *recent* counterparts. Reasons for ancient seep brecciation have been traditionally linked with gas hydrate buildup and dissociation (Bojanowski 2007; Conti and Fontana 2007) or dissipation of fluid overpressure (Hryniewicz et al. 2012). Hydrate-related brecciation may be evidenced by angular voids filled with cements "floating" within microcrystalline carbonate; this texture could represent a relic of hydrate clasts occluded with cements during or after hydrate dissociation (Bojanowski 2007).

Ancient seep textures different from those known from extant seeps may result, for example, from different faunas living at seeps during the geological past than are living in such environments today. Perhaps the most spectacular example of such biota are seep-dwelling brachiopods, which occur in Silurian–Cretaceous seeps in mass accumulations of numerous stacked individuals (e.g., Campbell and Bottjer 1995; Peckmann et al. 2001, 2007, 2011; Sandy 2010; Kiel et al. 2014a; Jakubowicz et al. 2017). The brachiopod carbonates (Fig. 3.9) from ancient seeps are unique due to (i) ecology of ancient seep-dwelling brachiopods, which were adapted to live epifaunally in low flux conditions, where no comparable shelly epifauna live today (cf. Sahling

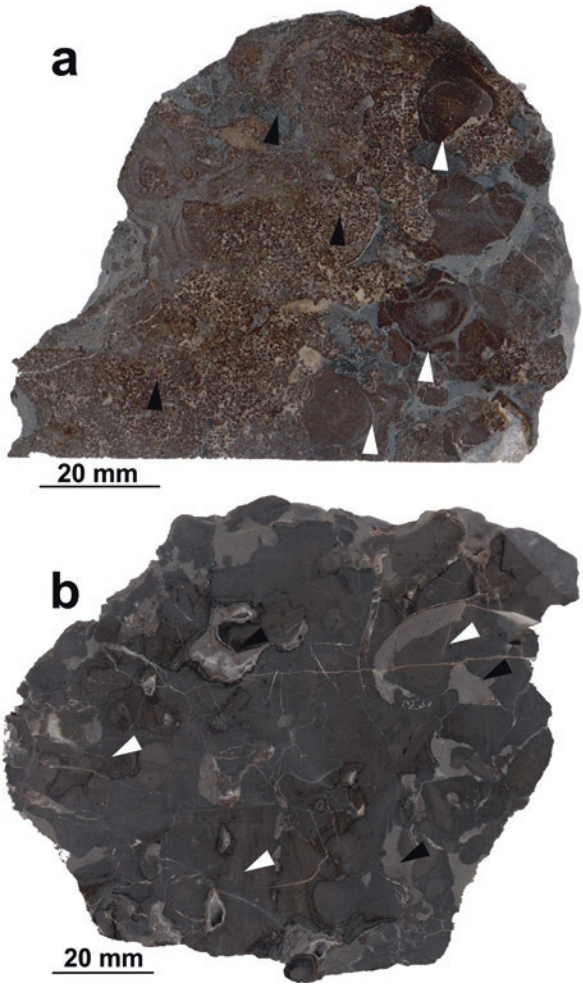

Fig. 3.6 Macroscopic petrography of ancient seep carbonates. (**a**) Microcrystalline carbonate nodules (white arrowheads) next to peloidal carbonate (black arrowheads). Baška seep deposit (Lower Cretaceous, Barremian), Hradiště Formation, Carpathians, Czech Republic (Kaim et al. 2013). (**b**) Coalesced microcrystalline carbonate nodules (white arrowheads) enclosing ambient deep-sea marly sediment (black arrowheads). Beauvoisin (Upper Jurassic, Oxfordian), Terres Noires Formation, Beauvoisin, Drome, France (Gaillard et al. 1992)

et al. 2002), and (ii) calcitic shells of brachiopods, which are much more chemically resistant than aragonitic or mixed aragonitic-calcitic shells of seep bivalves and much more frequently preserved in large numbers. Brachiopod shell frameworks filled with micritic carbonate are hallmarks of several ancient seep deposits and have no equivalent in extant seep carbonates. Rock-forming accumulations of ammonites in Late Cretaceous-aged seep deposits from Western Interior Seaway, USA, are also without equivalent at extant seeps (Landman et al. 2012, this volume).

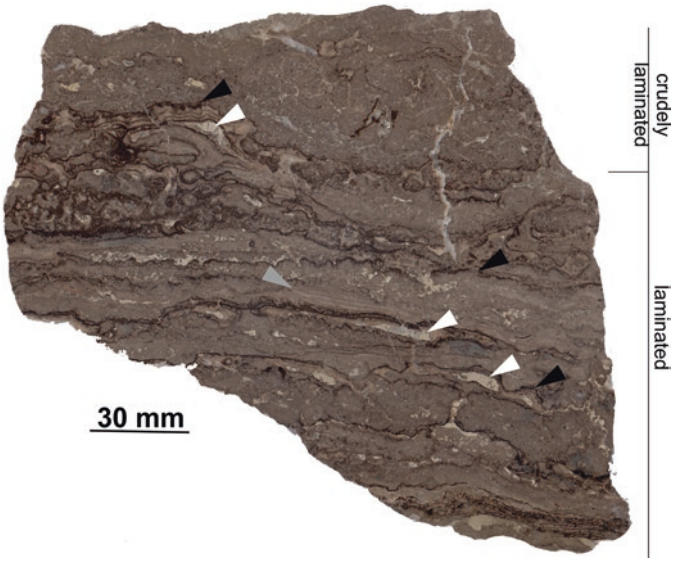

Fig. 3.7 Macroscopic petrography of ancient seep carbonates. A block of limestone showing juxtaposed laminated and crudely laminated facies; laminated facies is composed of layered sediment (sedimentary onlap indicated by grey arrowhead) and pyrite-covered corrosion surfaces (black arrowheads); white arrowheads indicate possible keystone vugs. Paskenta (Upper Jurassic, Tithonian), Great Valley Group, California, USA (Campbell et al. 2002)

Fig. 3.8 Microcrystalline carbonate and banded cements juxtaposed with pocket of breccia; note angular clasts with lithology similar to that of the surrounding carbonate, indicating little transport (arrowheads). Kami-Atsunai (Oligocene), Nuibetsu Formation, Tokachi District, Hokkaido, Japan

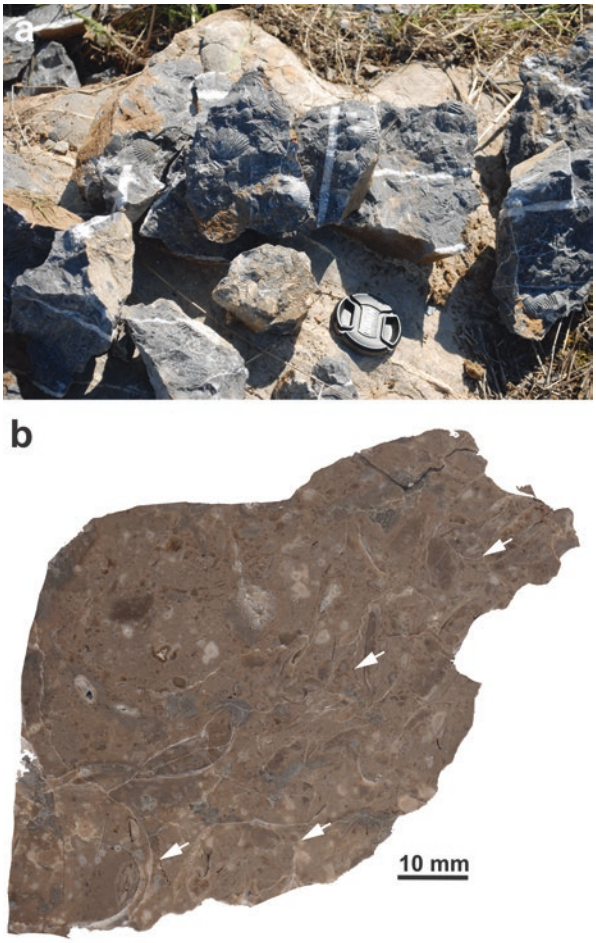

Fig. 3.9 Macroscopic petrography of ancient seep carbonates. (**a**) Rock-forming accumulation of dimerelloid brachiopod *Anarhynchia gabbi*, Bedford Canyon seep deposit (Middle Jurassic), Bedford Canyon Formation, California, USA. Lens cap for scale. (**b**) A polished slab of brachiopod carbonate with numerous thin brachiopod shells (arrows), Rice Valley (Lower Cretaceous, Hauterivian), Great Valley Group, California, USA

The long geological history of some ancient seep carbonates ensures that, in contrast to their extant counterparts, some ancient seep carbonates have been subjected to a much longer and more complex diagenesis in shallow and deep subsurface. Thus, during their diagenetic history, ancient seep carbonates accumulated textures which have not yet formed in extant seep carbonates (e.g., Campbell et al. 2002; Agirrezabala 2009). For example, cavities that are typical for extant seep carbonates are occluded in ancient seep deposits with one or several generations of fillings comprising clastics, carbonates, sulfate or quartz precipitates, or pyrobitumens (e.g., Campbell et al. 2002; Agirrezabala 2009; Hryniewicz et al. 2021). This is true for most ancient seep deposits, and only in some cases have the cavities so

typical of extant seep deposits escaped occlusion (e.g., Hryniewicz et al. 2015a: 234). Mineral phases and their spatial relationships can be observed rather easily on polished slabs and provide a first, approximate estimate of the geological history of a particular seep deposit. A more detailed study of petrography has to be undertaken using microscopic tools.

3.5 Microscopic Petrography

3.5.1 Extant Seep Carbonates

The phases formed at seeps due to AOM occur in close proximity or in superposition, often in mm or cm scale (e.g., Luff et al. 2004, 2005). It may be thus difficult to differentiate them without microscopic techniques, such as transmitted and reflected light and scanning electron microscope (SEM) imaging, aided by fluorescence microscopy for illustration of additional features (e.g., Aloisi et al. 2000; Pierre and Fouquet 2007; Feng et al. 2008, 2010; Himmler et al. 2018; Zwicker et al. 2020). Also, the broad range of chemical conditions found at seep environments causes different minerals to form in spatial or temporal succession, including not only aragonite, Mg calcite, and dolomite but also sulfates (barite), sulfides (pyrite), and phosphates. The identification of mineral (especially carbonate) phases may be equivocal using optical methods alone and requires other techniques, such as X-ray diffraction (e.g., Greinert et al. 2002; Mazzini et al. 2005). Even when phases can be differentiated using the above-mentioned methods, assigning them to a particular environment is very difficult using optical features alone. This is because the same mineral forming different phases can vary considerably with respect to environment-diagnostic stable $\delta^{13}C$ and $\delta^{18}O$ signatures; Sr, Mg, or REE elements; or lipid biomarker content (e.g., Leefmann et al. 2008; Feng et al. 2008, 2010; Zwicker et al. 2018). Hence, geochemical investigations are an inherent part of the microscopic petrographic studies of extant seep deposits.

To fully review all microscopic phases known from extant seep deposits is beyond the scope of this chapter. Given the amount of information presented in combined microscopic and geochemical studies of extant seep carbonates, it would perhaps require a separate volume. However, some phases are the most typical of seep carbonates. In this chapter, their appearance, origin, and significance are briefly discussed, with reference to the literature on the subject.

Two mineral phases are especially well documented in extant seep deposits: microcrystalline carbonates and banded carbonate cements. The proportion of both phases varies between different seep deposits, but together they are the volumetrically dominant mineral phases that comprise the bulk of most seep carbonates.

Microcrystalline carbonate at seeps can be composed of aragonite, Mg calcite, low-Mg calcite, or dolomite (e.g., Jørgensen 1989; Reitner et al. 2005a; Haas et al. 2010). Both micrite-sized (<4μm) and microspar-sized crystals (between 5μm and 30μm) occur. Aragonite and calcite mineralogies form close to the sediment-water

interface where carbonate anions (HCO_3^{2-}) provided by AOM and Ca^{2+} diffusing downward from seawater are available (Luff et al. 2005). Another control on seep carbonate mineralogy is the concentration of seawater sulfate anions (SO_4^{2-}), which inhibit magnesium partitioning into calcite, thus favoring aragonite formation when communication between seawater and pore space is maintained. Since aragonite forms much faster than calcite (Luff and Wallmann 2003), conditions in higher flux areas favor aragonite over calcite precipitation. Conversely, dissolved sulfide catalyzes Mg dehydration, thus enabling Mg calcite precipitation (Smrzka et al. 2021). As the alkalinity decreases due to decreasing flux, sediment deposition on the seabed, or clogging the pore space with carbonate, precipitation of aragonite slows down, and that of calcite "catches up," causing the latter to gain in importance. In addition, recrystallization of aragonite to calcite takes place, also resulting in the formation of calcitic microcrystalline carbonates.

The substrate for carbonate precipitation at seeps may be clasts or aragonite shells, which become covered with aragonite crusts (e.g., Aloisi et al. 2000: fig. 3a). Both aragonite and calcite also precipitate directly within the organic sheets as dumbbell-shaped aggregates and spherulites that nucleate on matrices of extracellular polymeric substances (e.g., Reitner et al. 2005a, b). At seeps, microbial substrates are extremely important for carbonate authigenesis; however substrates derived from, for example, sponges can also occur (cf. Dupraz et al. 2009). Organomineralization at seeps results in such fabrics as, for example, cemented microbial bundles or filaments, mineralized extracellular polymeric substances (e.g., Himmler et al. 2018: fig. 3), and peloids or clotted micrites of possible microbial origin (e.g., Teichert et al. 2005: Fig. 7c; Feng et al. 2010: fig. 4; cf. Flügel 2004 for a review of peloid origin). These fabrics are to a large degree similar to fabrics known from microbial carbonates forming elsewhere, for example, in cryptic habitats within reefs, hot springs, hypersaline ponds, or shallow water settings (e.g., Riding and Awramik 2000; Dupraz et al. 2009; Diaz and Eberli 2022). However, seep carbonates contain ^{13}C-depleted lipid biomarkers characteristic for AOM-mediating microbial consortia (methane-oxidizing archaea and sulfate-reducing bacteria; Boetius et al. 2000), and these are exclusive to such environments.

The formation of dolomite at seeps is somewhat less well constrained than that of aragonite and calcite. Previous studies suggested that sedimentary dolomite may form close to the area where sulfate is being consumed and the decomposition of an aqueous $MgSO_4^0$ complex takes place, followed by a rise in the Mg/Ca ratio (Baker and Kastner 1981). More recent studies somewhat corroborate this view (Lu et al. 2018). Sulfate reduction due to AOM and migration of released Mg ions to the parts of the seep system where little sulfate is available generally favors dolomite precipitation in the deeper subsurface (e.g., Takeuchi et al. 2007; Tong et al. 2019).

Botryoidal carbonate cements form due to rapid precipitation from supersaturated solutions. Either aragonite or calcite can precipitate and form botryoid crystal aggregates, depending on alkalinity, water temperature, and mineralogy of the substrate (cf. Aissaoui 1985, 1988; Savard et al. 1996). While this type of cementation is common at hydrocarbon seeps, it is not exclusive to them and occurs wherever supersaturated solutions are flushed through sedimentary pore space, for example,

on submerged reef slopes (Grammer et al. 1993). Aragonite and calcite forming botryoids are best distinguished with X-ray diffraction of powdered samples and staining with Feigl's solution. However, preliminary optical identification can be done under optical microscopy using normal and cross-polarized light; aragonite botryoids are composed of fine, flat-topped crystallites, while in calcite botryoids, each crystallite has a pyramid-shaped angular termination (Ross 1991).

Botryoidal cements form rather rapidly and require a large volume of fluids pumped through the pore space in a short time. Thus, at seeps they are associated with those parts of the seep system with a high flux of alkaline fluids. Such areas can be fluid conduits and outlets (e.g., Teichert et al. 2005), a matrix of carbonate breccia, often in the vicinity of dissociating methane hydrates (e.g., Greinert et al. 2001), and worm tubes (e.g., Haas et al. 2009). Botryoidal cements, either calcite or aragonite, can form several layers separated by pyrite crusts, indicating recurrent episodes of carbonate cementation and dissolution (own data).

Botryoidal aragonite is heavily depleted in ^{13}C, but it does not contain any meaningful concentrations of AOM-specific biomarkers (e.g., Himmler et al. 2015). This is likely because AOM took place elsewhere and alkalinity was not produced directly where the botryoidal aragonite precipitated (Hagemann et al. 2013). Instead, the carbonate phase which forms in direct proximity with AOM is termed "whitish aragonite." This phase contains the largest concentration of ^{13}C-depleted biomarkers such as archaeol, *sn*-2-hydroxyarchaeol, crocetane, PMI, and DAGE typical for AOM-mediating microbial consortia (Leefmann et al. 2008).

Among the non-carbonate minerals occurring at seeps, pyrite (FeS_2) is one of the more common ones. Mechanisms of pyrite precipitation at seeps are based on iron and organoclastic sulfate reduction taking place in organic-rich marine sediments, as well as AOM-related formation of sulfide (Peckmann and Thiel 2004; Cochran et al. this volume). These provide conditions for the formation of amorphous iron sulfides and greigite (Fe_2S_4), which transform into more stable pyrite. During seepage, excess sulfide is produced continuously through AOM, and pyrite precipitation at seeps is limited largely by the availability of sedimentary iron rather than sulfide. Thus, seeps developed in areas with little reactive iron are devoid of pyrite (e.g., Aloisi et al. 2000; Himmler et al. 2011). Pyrite at seeps can occur as framboidal aggregates dispersed in the carbonate matrix or filling pores (e.g., Feng et al. 2008) or as coatings on corrosion surfaces, which form during dissolution of authigenic carbonate by acidic solutions. The relation between pyrite formation and carbonate dissolution is not clear, however. Pyrite precipitation has been suggested (Peckmann and Thiel 2004) to take place when reduced iron and sulfide react, causing acidification of the environment according to the idealized reaction:

$$Fe^{2+} + 2H_2S \rightarrow FeS_2 + 4H^+$$

However, corrosion surfaces without any pyrite incrustation form in seeps as well due to sulfide oxidation and resulting formation of sulfuric acid (Himmler et al. 2011):

$$H_2S + 2O_2 \rightarrow SO_4^{2-} + 2H^+$$

Thus, pyrite incrustation of corrosion surfaces within seep carbonates can be either a phenomenon synchronous with corrosion or post-dating it.

3.5.2 Ancient Seep Carbonates

Techniques used to study extant and ancient seep carbonates are similar. Observations of carbonate thin sections under transmitted light and polished or etched surfaces under SEM are standard methods allowing observation and identification of phases (e.g., Peckmann et al. 2002; Peckmann and Thiel 2004; Barbieri and Cavalazzi 2005; Barbieri et al. 2005). In addition, techniques like epifluorescence microscopy and cathodoluminescence imaging are used (e.g., Buggisch and Krumm 2005; Hammer et al. 2011; Amano et al. 2013; Agirrezabala et al. 2013; Little et al. 2015; Natalicchio et al. 2015; Zwicker et al. 2015, 2018; Hryniewicz et al. 2021) as they can capture early authigenic phases which are otherwise modified because of later overprint.

One of the differences in studies of extant and ancient seep carbonates is that while the former are a mixture of aragonite and calcite, the latter are dominantly calcite and aragonite is rarely preserved. This is because aragonite is less stable during carbonate diagenesis than calcite (cf. Luff et al. 2005) and is preserved only under conditions of a relatively closed system with limited mobilization of elements (cf. Zwicker et al. 2018). This applies to all phases building ancient seep deposits.

Another difference lies in the paragenetic sequence of ancient seep carbonates, which are composed of two genetic components: the early diagenetic and late diagenetic (e.g., Campbell et al. 2002; Agirrezabala 2009; Blouet et al. 2017; Zwicker et al. 2018). The distinction between those two components is based on the environment of formation (at or close to the seabed for early diagenetic vs. in burial for late diagenetic), as well as thermal (ambient or near-ambient seawater temperature vs. elevated burial temperatures) and distribution criteria (broad vs. pore filing) (Agirrezabala 2009). The early diagenetic components of ancient seep deposits are a close equivalent to extant authigenic carbonates which form at present-day seeps, with a proviso that not all early diagenetic phases in ancient seep carbonates are recognized as authigenic phases in extant seep carbonates. This is because (i) some ancient early diagenetic phases apparently formed in shallow subsurface and thus are hardly accessible for sampling by submersibles at extant seeps and (ii) authigenic aragonite building the bulk of extant seep deposits is rarely preserved in the fossil record as outlined above; hence, its dissolution and recrystallization will result in a proportional increase in the significance of calcite in ancient seep carbonates. An example of the sampling bias may be siliceous cements, which formed after microcrystalline carbonate and banded cements, yet in the shallow subsurface when the fluid flux was still active (cf. Smrzka et al. 2015). The importance of aragonite

dissolution in terms of the appearance of some carbonate phases in ancient seep carbonates has been outlined elsewhere in this contribution.

The early diagenetic microcrystalline carbonates and banded cements at extant and ancient seep carbonates are similar. One to several generations of microcrystalline carbonates can be recognized based on their texture (Fig. 3.10a), $\delta^{13}C$ and $\delta^{18}O$ signatures, or elemental composition (e.g., Zwicker et al. 2015, 2018). Usually, the first generation of microcrystalline carbonate (Fig. 3.10a, b), termed micritic matrix, micrite 1, or otherwise, is volumetrically dominant and the most ^{13}C-depleted of all micrites, indicating formation influenced by AOM (Campbell et al. 2002; Agirrezabala 2009; Blouet et al. 2017). Later microcrystalline carbonates formed during early diagenesis, for example, pipe-filling micrites formed deeper in the sediment, tend to have much higher $\delta^{13}C$ signatures than the remainder of the conduits, indicating formation from a different carbon pool, for example, one affected by methanogenesis rather than by AOM (Zwicker et al. 2015). Such later phases, either micrite or microsparite, can be volumetrically important components of carbonate-cemented tubular conduits (e.g., Wiese et al. 2015; Zwicker et al. 2015; Blouet et al. 2017).

Banded cements (Fig. 3.10c–e) of ancient seep deposits are now largely recrystallized to calcite, but initial mineralogy may be indicated by crystal morphology, providing this was not modified during recrystallization. Initial aragonite can be identified by its flat-topped, needle-shaped crystals (Fig. 3.10c; Savard et al. 1996; Kiel et al. 2014a, b; Hryniewicz et al. 2016, 2021). In most cases, closer examination reveals that initial aragonite has been replaced by calcite pseudospar, which can be identified by randomly oriented optical crystal axes (Fig. 3.10d, e; cf. Ross 1991: fig. 5), and confirmed by X-ray diffraction (e.g., Hryniewicz et al. 2021). Original calcite mineralogy of banded cements can be identified due to pyramidal crystal tops and sweeping light extinction (e.g., Hammer et al. 2011: fig. 4f; cf. Ross 1991). Banded cements are one of the earliest phases of ancient seep deposits, forming after the first microcrystalline carbonate has cemented the pore space (e.g., Campbell et al. 2002; Hryniewicz et al. 2012). Ancient banded cements are frequently found in proximity to the so-called yellow cements (Fig. 3.10c–e). These cements are equivalent to the "whitish aragonite" of Leefmann et al. (2008), but they preserve aragonitic microcrystalline texture only in exceptional cases (Zwicker et al. 2018 and references therein) and otherwise are recrystallized to calcitic, yellow coarse spar (e.g., Hammer et al. 2011; Hryniewicz et al. 2021). Strong fluorescence of yellow cements (Zwicker et al. 2018) and very high contents of biomarkers typical for AOM-mediating microbial consortia (Hagemann et al. 2013) indicate that the phase originated through permineralization of microbial communities mediating AOM and causing the rise of alkalinity at seeps. Banded and yellow cement associations sometimes form "cake"-like textures, with several layers of yellow and banded cements superimposed, indicating recurrent growth and cementation of AOM-mediating microbial consortia.

Because ancient seep carbonates formed close to or at the sediment-water interface, they may have become exposed and modified by bottom currents just as "regular" marine carbonates do. Textures formed during these processes indicate that the

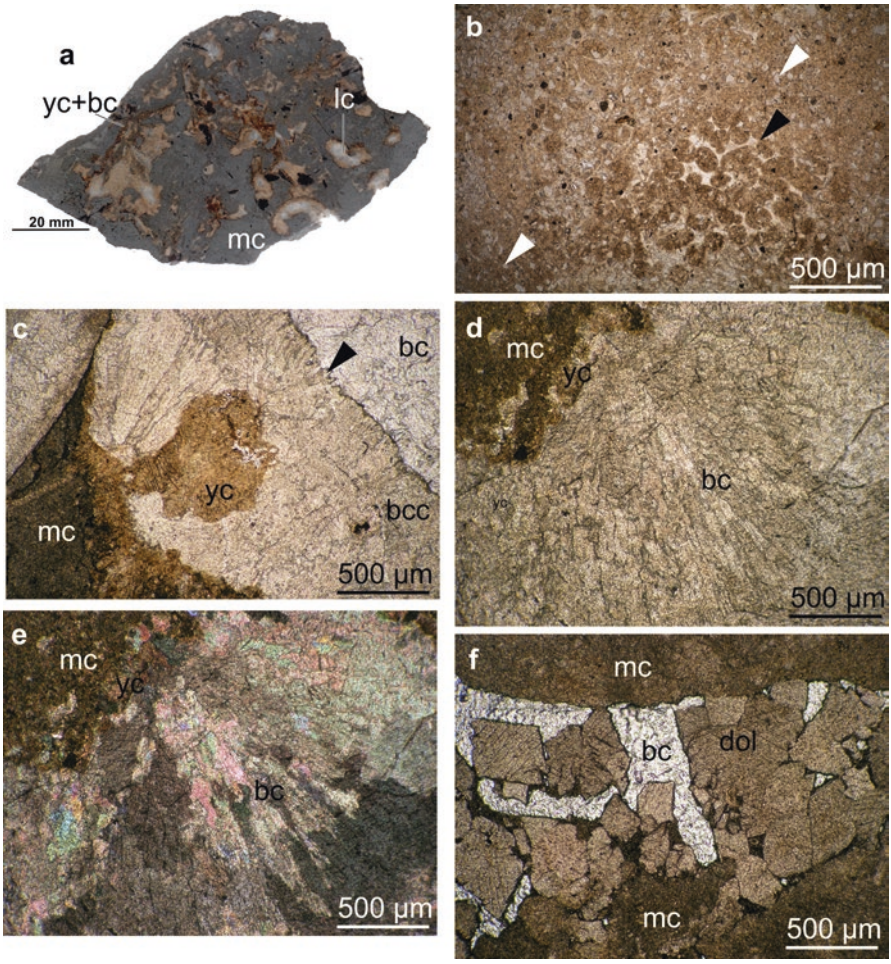

Fig. 3.10 Microscopic petrography of ancient seep carbonates. (**a**) An example of spatial distribution of main textures in ancient seep carbonate polished slab. bc, banded cement; lc, late cements; mc, microcrystalline carbonate; yc, yellow cements. Shikorozawa seep deposit (Lower Cretaceous, Albian), Yezo Supergroup, Hokkaido, Japan. (**b**) An example of microcrystalline carbonate cementing quartz grains (white arrowheads) and fecal pellets (black arrowhead). Fossildalen seep deposit (Paleocene), Basilika Formation, Spitsbergen, Svalbard (Hryniewicz et al. 2016). Plane-polarized light. (**c**) An example of an association of microcrystalline carbonate and cavity-filling yellow and banded cements, with flat-topped crystal termination (arrowhead). The remainder of the cavity is filled with blocky calcite. bc, blocky calcite; bcc, banded cements; yc, yellow cements; mc, microcrystalline carbonate. Tanohama seep deposit (Lower Miocene), Taishu Group, Tsushima, Japan (Hryniewicz et al. 2021). Plane-polarized light. (**d**) An example of cavity-filling yellow-banded cement association. (**e**) The same sample, with cross-polarized light. Note randomly oriented crystal optic axes. Both D and E from Tanohama seep deposit (Lower Miocene), Taishu Group, Tsushima, Japan (Hryniewicz et al. 2021). (**e**) An example of late diagenetic filling of cavity within early microcrystalline carbonate. The late diagenetic filling is composed of blocky calcite and dolomite crystals. bc, blocky calcite; dol, dolomite; mc, microcrystalline carbonate. Tanohama seep deposit (Lower Miocene), Taishu Group, Tsushima, Japan (Hryniewicz et al. 2021). Plane-polarized light

carbonate was exposed at a certain time and are good proxies of ambient conditions at the site of seepage. For example, sediment transported by submarine currents over the seep carbonate may have entered the cavity where a particular banded cement precipitated and formed a pocket incorporated into the cement crust, as illustrated for Paleocene seep carbonates from Spitsbergen (e.g., Hryniewicz et al. 2016: fig. 6E). Bottom currents may also have remodeled shell debris of seep-dwelling biota. In one of the earliest Cretaceous seeps from Spitsbergen, concentration and local imbrication of shells (i.e., orientation of elongated clasts so that they overlap each other) were caused by submarine currents removing finer particles from the surface of the seep deposit. Early diagenetic carbonates can bear signs of erosion, transport, and subsequent redeposition. For example, some seep carbonate-filled thyasirid bivalves from the Paleocene shallow water succession of Spitsbergen are found within the "normal" marine siltstone. Yellow and banded authigenic cements filling cavities within these fossils have been displaced from their original position, fragmented, and incorporated into classic filling of the remaining cavity (Hryniewicz et al. 2016: fig. 6A–D). This has been interpreted as an effect of redeposition at the seep where carbonate authigenesis took place through mass movement down the shallow marine delta slope. The crusts were fragmented during transport, and the remainder of the cavity was filled after the redeposited shell had been covered with sediment.

Silicification is an important early diagenetic process which has shaped several ancient seep carbonates. It was especially important in those environments where radiolarian and diatom tests were common as sources of biogenic silica (Kuechler et al. 2012; Smrzka et al. 2015; Miyajima et al. 2016). The mobilization of silica at seeps is possible due to AOM-related rise of alkalinity, with CO_2 degassing due to seepage amplifying the effect on pH increase and dissolution of siliceous tests (Smrzka et al. 2015). Migrating silica is re-precipitated at the periphery of a seep deposit where the alkalinity and rate of AOM are lower than near the center of the seep or after a decrease in pH (e.g., due to sulfide oxidation or due to cessation of AOM) causing supersaturation with respect to silica. The latter is of special importance for paleontologists because it will cause preferential dissolution of aragonitic shells that are simultaneously replaced by silica precipitation, resulting in silicified fossils (chiefly of mollusks) and preserving the finest sculptural details (e.g., Kaim et al. 2008, 2009; Hybertsen and Kiel 2018; Hryniewicz et al. 2019).

These later diagenetic components are unique to ancient seep deposits and are unknown from their extant counterparts. Burial diagenetic pore fluids feature a chemistry different from that of seawater, and the seep deposit can be progressively isolated from marine and hydrocarbon-rich solutions (Campbell et al. 2002). Under these burial conditions, new phases and modification of existing ones can result in the dissolution of metastable minerals and their replacement with low-Mg calcite (cf. Bathurst 1975). Depending on the geological history of the area where a given ancient seep is located, the late diagenetic components differ in each deposit. For example, there are ancient seep carbonates which show very little (if any) late diagenetic carbonate. One such case is the latest Jurassic limestone boulders from Novaya Zemlya (Hryniewicz et al. 2015a), which are composed of microcrystalline

carbonate cementing fecal pellets, corrosion surfaces with or without associated pyrite, and banded cements lining the cavities. The remainder of the cavities is void, with no late diagenetic cements having been precipitated. Values of $\delta^{18}O$ in these seep carbonates range from −1.3‰ to 0.0‰ VPDB (with one outlier of −3.1‰ VPDB), which indeed indicates little diagenetic overprint. The geological area where the Novaya Zemlya boulders formed (this is unknown since all the boulders studied are erratics) has likely experienced little burial since the latest Jurassic. On the other end of the spectrum are seep deposits with complex late diagenetic histories and components (Fig. 3.10f). For example, Albian (Early Cretaceous) seeps from the Basque-Cantabrian Basin are filled with successive generations of calcite and dolomite cements, as well as pyrobitumen formed during burial involving rifting, emplacement of magmatic intrusions, petroleum generation and migration, and folding (Agirrezabala 2009; Jakubowicz et al. 2021). Deep burial and loading may also lead to pressure dissolution of seep carbonates, leaving characteristic pressure-solution seams reminiscent of those known from "normal" marine carbonates (e.g., Hryniewicz et al. 2021; cf. Łuczyński 2001). Epigenetic weathering during unroofing may result in oxidation of reduced compounds, such as pyrite, and formation of gypsum (Blouet et al. 2017).

3.6 Concluding Remarks and Future Directions

Recognition of ancient seep deposits is based on geochemical, faunal, geological, and petrographic criteria (Campbell 2006). Geochemical criteria, specifically low $\delta^{13}C$ and presence of ^{13}C-depleted lipid biomarkers typical of AOM-mediating microbial consortia, are undoubtedly most decisive for recognition of seep-related carbonates in the fossil record. Faunal criteria, i.e., the identification of fossil seep-obligate fauna, such as vesicomyid bivalves or abyssochryssoid gastropods, are also important for identification of a given ancient carbonate as seep-related. However, there are cases when the most straightforward criteria (geochemical and faunal) are unavailable and a seep origin of the carbonate has to be ascertained mostly on petrographic grounds. For example, carbonates from the latest Silurian El-Borj seep deposit in Morocco have relatively high $\delta^{13}C$ signatures (not lower than −6‰ VPDB) and thus are not low enough to be easily classified as seep-related purely on geochemical grounds. Faunal criteria are also not decisive, since the only fossil known from this deposit is the atrypid gastropod *Septatrypa lantenoisi*, which does not belong to a group associated with ancient seep deposits. Yet, the presence of banded cements typical for seep deposits led Jakubowicz et al. (2017) to tie the origin of the El-Borj deposit to methane seepage and to explain the anomalously heavy carbon isotope composition of the carbonates to the positive $\delta^{13}C$ Ludfordian excursion, which shifted seawater and seep carbonate $\delta^{13}C$ toward higher values (Jakubowicz et al. 2017). This interpretation was further strengthened by the discovery of a species of the seep-restricted modiomorphid bivalve *Ataviaconcha* at El-Borj, which was previously known only from a Middle Devonian Hollard Mound

seep deposit (Hryniewicz et al. 2017). Hence, in spite of the multitude of geochemical approaches available in the twenty-first century, petrographic methods are still an important part of the diagnosis of ancient seep deposits.

Most seep carbonates are known from the Cenozoic and Cretaceous, with Jurassic and especially older deposits much less common. For example, there are only nine Jurassic, three Triassic, two Carboniferous, one Devonian, and one Silurian unequivocal seep deposit known. It is currently unknown whether this pattern is an expression of the "pull of the *recent*" phenomenon (Raup 1979) or if there are other explanations. It has been suggested that substrate bio-irrigation by marine fauna (e.g., chemosymbiotic bivalves and vestimentiferan tube worms) can enhance AOM and carbonate authigenesis at seeps (Luff et al. 2004). A consistent increase in the number of known seep carbonates from the Late Jurassic/Early Cretaceous-age interval onward does indeed coincide with the colonization of seeps by infaunal lucinid and thyasirid bivalves, which are efficient bio-irrigators. Bio-irrigation takes place through burrows, and these (when preserved) are easily observed in macro- and microscopic samples of seep carbonates. Thus, establishing petrographic and geochemical criteria for bio-irrigation at ancient seeps is a step toward testing the hypothesis on faunal forcing of increased carbonate mineralization at seeps during the Meso- and Cenozoic.

There are no unequivocal seep deposits of Proterozoic, Cambrian or Ordovician age known. Further exploration and collecting may help discover such deposits and move the geological age of carbonate mineralization at seeps further back in time.

Acknowledgments I am very thankful to editors Andrzej Kaim (Institute of Paleobiology PAS, Poland), J. Kirk Cochran (Stony Brook University, New York, USA), and Neil H. Landman (American Museum of Natural History, New York, USA) for an opportunity to contribute to this book. I would like also to thank Andrzej Kaim for donating whole rock specimens and photos from various seep deposits around the world, which I used during the preparation of this chapter. Many fruitful discussions in the office and in the field with Kazutaka Amano (Joetsu University of Education, Joetsu, Japan), Michał Jakubowicz (Adam Mickiewicz University, Poznań, Poland), Robert G. Jenkins (Kanazawa University, Kanazawa, Japan), Andrzej Kaim, Steffen Kiel (Swedish Museum of Natural History, Stockholm, Sweden), and Crispin T.S. Little (University of Leeds, Leeds, UK) are sincerely acknowledged. Special thanks goes to referees J. Kirk Cochran and Jennifer Zwicker (University of Vienna, Vienna, Austria) for their thorough reviews which helped substantially improve this contribution.

References

Ager DV (1965) The adaptations of Mesozoic brachiopods to different environments. Palaeogeog Palaeoclimat Palaeoecol 1:143–172

Agirrezabala LM (2009) Mid-Cretaceous hydrothermal vents and authigenic carbonates in a transform margin, Basque-Cantabrian Basin (western Pyrenees): a multidisciplinary study. Sedimentology 56:969–996

Agirrezabala LM, Kiel S, Blumenberg M et al (2013) Outcrop analogues of pockmarks and associated methane-seep carbonates: a case study from the Lower Cretaceous (Albian) of the Basque-Cantabrian Basin, western Pyrenees. Palaeogeog Palaeoclimat Palaeoecol 390:94–115

Aissaoui DM (1985) Botryoidal aragonite and its diagenesis. Sedimentology 32:345–361
Aissaoui DM (1988) Magnesian calcite cements and their diagenesis: dissolution and dolomitization, Mururoa Atoll. Sedimentology 35:821–841
Allison PA, Hasselbo SP, Brett CE (2008) Methane seeps on Early Jurassic dysoxic seafloor. Palaeogeog Palaeoclimat Palaeoecol 270:230–238
Aloisi G, Pierre C, Rouchy J-M et al (2000) Methane-related authigenic carbonates of eastern Mediterranean Sea mud volcanoes and their possible relation to gas hydrate destabilization. Earth Planet Sci Lett 184:321–338
Amano K, Jenkins RG, Sako Y et al (2013) A Paleogene deep-sea methane-seep community from Honshu, Japan. Palaeogeog Palaeoclimat Palaeoecol 387:126–133
Baker PA, Kastner M (1981) Constraints on the formation of sedimentary dolomite. Science 213:214–216
Barbieri R, Cavalazzi B (2005) Microbial fabrics from Neogene cold-seep carbonates, northern Apennine, Italy. Palaeogeog Palaeoclimat Palaeoecol 227:143–155
Barbieri R, Ori GG, Cavalazzi B (2005) A Silurian cold-seep ecosystem from the Middle Atlas, Morocco. Palaios 19:527–542
Bathurst RCG (1975) Carbonate sediments and their diagenesis. Elsevier, Amsterdam
Berti M, Cuzzani MG, Landuzzi A et al (1994) Hydrocarbon-derived imprints in olistostromes of the Early Sarrevallian Marnoso-arenacea Formation, Romagna Appenines (northern Italy). Geo-Mar Lett 14:192–200
Blouet J-P, Imbert P, Fourbet A (2017) Mechanisms of biogenic gas formation revealed by seep carbonate paragenesis, Panoche Hills, California. Am Assoc Pet Geol Bull 101:1309–1340
Boetius A, Suess E (2004) Hydrate Ridge: a natural laboratory for the study of microbial life fueled by methane from near-surface gas hydrates. Chem Geol 205:291–310
Boetius A, Ravenschlag K, Schubert CJ et al (2000) A marine microbial consortium apparently mediating anaerobic oxidation of methane. Nature 407:623–626
Bohrmann G, Greinert J, Suess E et al (1998) Authigenic carbonates from the Cascadia subduction zone and their relation to gas hydrate stability. Geology 26:647–650
Bojanowski MJ (2007) Oligocene cold-seep carbonates from the Carpathians and their inferred relation to gas hydrates. Facies 53:347–360
Buggisch W, Krumm S (2005) Palaeozoic cold seep carbonates from Europe and North Africa—an integrated isotopic and geochemical approach. Facies 51:566–583
Campbell KA (2006) Hydrocarbon seep and hydrothermal vent palaeoenvironments and paleontology: past developments and future research directions. Palaeogeog Palaeoclimat Palaeoecol 232:362–407
Campbell KA, Bottjer D (1993) Fossil cold seeps. Natl Geogr Res Explor 9:326–343
Campbell KA, Bottjer D (1995) Brachiopods and chemosymbiotic bivalves in Phanerozoic hydrothermal vent and cold seep environments. Geology 23:321–324
Campbell KA, Farmer JD, Des Marais D (2002) Ancient hydrocarbon seeps from Mesozoic convergent margin of California: carbonate geochemistry, fluids and palaeonenvironments. Geofluids 2:63–94
Campbell KA, Francis DA, Collins M et al (2008) Hydrocarbon seep carbonates of a Miocene forearc (East Coast Basin), North Island, New Zealand. Sediment Geol 204:83–105
Carson B, Screaton EJ (1998) Fluid flow in accretionary prism: evidence for focused, time-variable discharge. Rev Geophys 36:329–351
Cochran JK, Landman NH, Jakubowicz M et al (this volume) Geochemistry of Cold Hydrocarbon Seeps: An Overview. In: Kaim A, Cochran JK, Landman NH (eds) Ancient hydrocarbon seeps, Topics in geobiology, vol 50. Springer, Cham
Conti S, Fontana D (2007) Anatomy of seep carbonates: ancient examples from the Miocene of northern Apennines (Italy). Palaeogeog Palaeoclimat Palaeoecol 227:156–175
Conti S, Artoni A, Piola G (2007) Seep-carbonates in a thrust-related anticline at the leading edge of an orogenic wedge: the case of the middle–late Miocene Salsomaggiore Ridge (northern Apennines, Italy). Sediment Geol 199:233–251

Danner WR (1966) Limestone resources of western Washington. State Wash Div Mines Geol Bull 52:1–474

De Beaver E, Birgel D, Muchez P et al (2011) Fabric and formation of grapestone concretions within an unusual ancient methane seep system. Terra Nova 23:56–61

Diaz M, Eberli GP (2022) Microbial contribution to early marine cementation. Sedimentology 9:798 –822

Dupraz C, Reid PR, Braissant O et al (2009) Process of carbonate cementation in modern microbial mats. Earth Sci Rev 96:141–162

Duranti D, Mazzini A (2005) Large-scale hydrocarbon-driven sand injection in the Paleogene of the North Sea. Earth Planet Sci Lett 239:327–335

Feng D, Chen D, Roberts HH (2008) Sedimentary fabrics in the authigenic carbonates from Bush Hill: implications for the seabed fluid flow and its dynamic signature. Geofluids 8:301–310

Feng D, Chen D, Peckmann J et al (2010) Authigenic carbonates from methane seeps of the northern Congo fan: microbial formation mechanism. Mar Pet Geol 27:748–756

Flajs G, Vigener M, Keupp H et al (1995) Mud mounds: a polygenetic spectrum of fine-grained carbonate buildups. Facies 32:1–70

Flügel E (2004) Microfacies of carbonate rocks: analysis, interpretation and application. Springer, Berlin

Gaillard C, Rio M, Rolin Y et al (1992) Fossil chemosynthetic communities related to vents or seeps in sedimentary basins: the pseudobioherms of southeastern France compared to other world examples. Palaios 7:451–465

Gill FL, Harding IC, Little CTS et al (2005) Palaeogene and Neogene cold-seep communities in Barbados, Trinidad and Venezuela: an overview. Palaeogeog Palaeoclimat Palaeoecol 227:191–209

Goedert JL, Benham SR (2003) Biogeochemical processes at ancient methane seeps: the Bear River site in southwestern Washington. In: Swanson TW (ed) Western Cordillera and adjacent areas, vol 4. Geological Society of America Field Guide, Boulder, pp 201–208

Goedert JL, Peckmann J, Reitner J (2000) Worm tubes in an allochtonous cold-seep carbonate from lower Oligocene rocks in western Washington. J Paleontol 74:992–999

Gómez-Pérez I (2003) An early Jurassic deep-water stromatolitic bioherm related to possible methane seepage (Los Molles Formation, Neuquén, Argentina). Palaeogeog Palaeoclimat Palaeoecol 201:21–49

Grammer GM, Ginsburg RN, Swart PK et al (1993) Rapid growth rates of syndepositional marine aragonite cements in steep marginal slope deposits, Bahamas and Belize. J Sediment Petrol 63:983–989

Greinert J, Bohrmann G, Suess E (2001) Gas hydrate-associated carbonates and methane-venting at Hydrate Ridge: classification, distribution, and origin of authigenic lithologies. In: Paull CK, Dillon PW (eds) Natural gas hydrates: occurrence, distribution, and detection, Geophysical Monograph, vol 124, pp 99–113

Greinert J, Bohrmann G, Elvert M (2002) Stromatolitic fabric of authigenic carbonate crust: results of anaerobic methane oxidation at cold seeps in 4,850 m water depth. Int J Earth Sci 91:698–711

Haas A, Little CTS, Sahling H et al (2009) Mineralization of vestimentiferan tubes at methane seeps on the Congo deep-sea fan. Deep-Sea Res I 56:283–293

Haas A, Peckmann J, Elvert M et al (2010) Patterns of carbonate authigenesis at the Kouilou pockmarks on the Congo deep-sea fan. Mar Geol 268:129–136

Hagemann A, Leefmann T, Peckmann J et al (2013) Biomarkers from individual carbonate phases of an Oligocene cold-seep deposit, Washington State, USA. Lethaia 46:7–18

Hammer Ø, Nakrem HA, Little CTS et al (2011) Hydrocarbon seeps from close to the Jurassic–Cretaceous boundary. Palaeogeog Palaeoclimat Palaeoecol 306:15–26

Hickman CS (2015) Paleogene marine bivalves of the deep-water Keasey Formation in Oregon, part III: the heteroconchs. PaleoBios 32:1–44

Hikida Y, Suzuki S, Togo Y et al (2003) An exceptionally well-preserved fossil seep community from the Cretaceous Yezo Group in the Nakagawa area, Hokkaido, northern Japan. Paleontol Res 7:329–342
Himmler T, Brinkmann T, Bohrmann G et al (2011) Corrosion patterns of seep carbonates from the eastern Mediterranean Sea. Terra Nova 23:206–212
Himmler T, Birgel D, Bayon G et al (2015) Formation of seep carbonates along the Makran convergent margin, northern Arabian Sea and a molecular and isotopic approach to constrain the carbon isotopic composition of parent methane. Chem Geol 415:102–117
Himmler T, Bayon G, Wangner D et al (2016) Seep-carbonate lamination controlled by cyclic particle flux. Sci Rep 6:37439
Himmler T, Smrzka D, Zwicker J et al (2018) Stromatolites below the photic zone in the northern Arabian Sea formed by calcifying microbial mats. Geology 46:339–342
Hovland M (2002) On the self-sealing nature of marine seeps. Cont Shelf Res 22:2387–2394
Hovland M, Judd A (2007) Seabed fluid flow: the impact on biology, geology and the marine environment. Cambridge University Press, Cambridge
Hovland M, Svensen H (2006) Submarine pingoes: indicators of shallow gas hydrates in a pockmark at Nyegga, Norwegian Sea. Mar Geol 228:15–23
Hryniewicz K, Hammer Ø, Nakrem HA et al (2012) Microfacies of the Volgian–Ryazanian (Jurassic–Cretaceous) hydrocarbon seep carbonates from Sassenfjorden, central Spitsbergen, Svalbard. Norw J Geol 92:113–131
Hryniewicz K, Little CTS, Nakrem HA (2014) Bivalves from the latest Jurassic–earliest Cretaceous hydrocarbon seep carbonates from central Spitsbergen, Svalbard. Zootaxa 3859:1–66
Hryniewicz K, Hagström J, Hammer Ø et al (2015a) Late Jurassic–Early Cretaceous hydrocarbon seep boulders from Novaya Zemlya and their faunas. Palaeogeog Palaeoclimat Palaeoecol 436:231–244
Hryniewicz K, Nakrem HA, Hammer Ø et al (2015b) Palaeoecology of latest Jurassic–earliest Cretaceous hydrocarbon seep carbonates from Spitsbergen, Svalbard. Lethaia 48:353–374
Hryniewicz K, Bitner MA, Durska E et al (2016) Paleocene methane seep and wood-fall marine environments from Spitsbergen, Svalbard. Palaeogeog Palaeoclimat Palaeoecol 462:41–56
Hryniewicz K, Jakubowicz M, Belka Z et al (2017) New bivalves from the Middle Devonian methane seep in Morocco: the oldest record of repetitive shell morphologies among some seep bivalve molluscs. J Syst Palaeontol 15:19–41
Hryniewicz K, Amano K, Bitner MA et al (2019) A late Paleocene fauna from shallow-water chemosynthesis-based ecosystems, Spitsbergen, Svalbard. Acta Palaeontol Pol 64:101–141
Hryniewicz K, Miyajima Y, Amano K et al (2021) Formation, diagenesis and fauna from the Miocene Taishu Group of Tsushima (Japan). Geol Mag 158:964–984
Hybertsen F, Kiel S (2018) A middle Eocene seep deposit with silicified fauna from the Humptulips Formation in western Washington State, USA. Acta Palaeontol Pol 63:751–758
Jakubowicz M, Hryniewicz K, Belka Z (2017) Mass occurrence of seep-specific bivalves in the oldest-known cold seep metazoan community. Sci Rep 7:14292
Jakubowicz M, Agirrezabala L, Dopieralska J et al (2021) The role of magmatism in hydrocarbon generation in sedimented rifts: a Nd isotope perspective from mid-Cretaceous methane-seep deposits of the Basque-Cantabrian Basin, Spain. Geochim Cosmochim Acta 303:223–248
Jenkins RG, Kaim A, Hikida Y (2007) Methane-flux-dependent lateral faunal changes in the Late Cretaceous chemosymbiotic assemblage from the Nakagawa area of Hokkaido, Japan. Geobiology 5:127–139
Jenkins RG, Kaim A, Little CTS et al (2013) Worldwide distribution of the modiomorphid bivalve genus *Caspiconcha* in late Mesozoic hydrocarbon seeps. Acta Palaeontol Pol 58:357–382
Jørgensen NO (1989) Holocene methane-derived, dolomite-cemented sandstone pillars from the Kattegat, Denmark. Mar Geol 88:71–81
Joye SB (2020) The geology and biogeochemistry of hydrocarbon seeps. Ann Rev Earth Planet Sci 48:205–231

Kaim A, Jenkins RG, Warén A (2008) Provannid and provannid-like gastropods from Late Cretaceous cold seeps of Hokkaido (Japan) and the fossil record of Provannidae. Zool J Linn Soc 154:421–436

Kaim A, Jenkins RG, Hikida Y (2009) Gastropods from Late Cretaceous Omagari and Yasukawa hydrocarbon seep deposits in the Nakagawa area, Hokkaido, Japan. Acta Palaeontol Pol 54:463–490

Kaim A, Skupien P, Jenkins RG (2013) A new Lower Cretaceous hydrocarbon seep locality from the Czech Carpathians and its fauna. Palaeogeog Palaeoclimat Palaeoecol 390:42–51

Kauffman EG, Arthur MA, Howe B et al (1996) Widespread venting of methane-rich fluids in Late Cretaceous (Campanian) submarine springs (Tepee Buttes), Western Interior Seaway, U.S.A. Geology 24:799–802

Kelly SRA, Ditchfield PW, Doubleday PA et al (1995) An Upper Jurassic methane-seep limestone from the Fossil Bluff Group Forearc Basin of Alexander Island, Antarctica. J Sediment Res A 65:274–282

Kelly SRA, Blanc E, Price SP et al (2000) Early Cretaceous giant bivalves from seep-relate limestone mounds, Wollaston Forland, northeast Greenland. In: Harper EM, Taylor JD, Crame JA (eds) The evolutionary biology of the Bivalvia. Geological Society of London, London, pp 227–246

Kiel S (2010) An Eldorado for palaeontologists: the Cenozoic seeps of western Washington State, USA. In: Kiel S (ed) The vent and seep biota. Springer, Heidelberg, pp 433–448

Kiel S, Peckmann J (2007) Chemosymbiotic bivalves and stable carbon isotopes indicate hydrocarbon seepage and four unusual Cenozoic fossil localities. Lethaia 40:345–357

Kiel S, Peckmann J (2008) Paleoecology and evolutionary significance of an Early Cretaceous *Peregrinella*-dominated hydrocarbon-seep deposit on the Crimean Peninsula. Palaios 23:751–759

Kiel S, Birgel D, Campbell KA et al (2013) Cretaceous methane-seep deposits from New Zealand and their fauna. Palaeogeog Palaeoclimat Palaeoecol 390:17–34

Kiel S, Glodny J, Birgel D et al (2014a) The paleoecology, habitats, and stratigraphic range of the enigmatic Cretaceous brachiopod *Peregrinella*. PLoS One 9(10):e109260

Kiel S, Hansen C, Nitzsche KN et al (2014b) Using $^{87}Sr/^{86}Sr$ to date fossil methane seep deposits: methodological requirements and an example for the Great Valley Group, California. J Geol 122:353–366

Kuechler RR, Birgel D, Kiel S et al (2012) Miocene methane-derived authigenic carbonates from southwestern Washington, USA and a model for silification at seeps. Lethaia 45:259–273

Landman NH, Cochran JK, Larson NL et al (2012) Methane seeps as ammonite habitats in the U.S. Western Interior Seaway revealed by isotopic analyses of well-preserved shell material. Geology 40:507–510

Landman NH, Cochran KJ, Brezina J et al (this volume) Methane seeps in the Late Cretaceous Western Interior Seaway. In: Kaim A, Cochran JK, Landman NH (eds) Ancient hydrocarbon seeps, Topics in geobiology, vol 50. Springer, Cham

Leefmann T, Bauermeister J, Kronz A et al (2008) Miniaturized biosignature analysis reveals implications for the formation of cold seep carbonates at Hydrate Ridge (off Oregon, USA). Biogeosciences 5:731–738

Levin LA (2005) Ecology of cold seep sediments: interactions of fauna with flow, chemistry and microbes. Oceanogr Mar Biol Annu Rev 43:1–46

Little CTS, Birgel D, Boyce AJ et al (2015) Late Cretaceous (Maastrichtian) shallow water hydrocarbon seeps from Snow Hill and Seymour Islands, James Ross Basin, Antarctica. Palaeogeog Palaeoclimat Palaeoecol 418:213–228

Lu Y, Xiaming S, Xu H et al (2018) Formation of dolomite catalyzed by sulfate-driven anaerobic oxidation of methane: mineralogical and geochemical evidence from the northern South China Sea. Am Mineral 103:720–734

Łuczyński P (2001) Pressure-solution and chemical compaction of condensed Middle Jurassic deposits, High-Tatric Series, Tatra Mountains. Geol Carpathica 52:91–102

Luff R, Wallmann K (2003) Fluid flow, methane fluxes, carbonate precipitation and biogeochemical turnover in gas hydrate-bearing sediments at Hydrate Ridge, Cascadia Margin: numerical modeling and mass balance. Geochim Cosmochim Acta 67:3403–3421

Luff R, Wallmann K, Aloisi G (2004) Numerical modelling of carbonate crust formation at cold vent sites: significance for fluid and methane budgets and chemosynthetic biological communities. Earth Planet Sci Lett 221:337–357

Luff R, Greinert J, Wallmann K et al (2005) Simulation of long-term feedbacks from authigenic carbonate crust formation at cold vent sites. Chem Geol 216:157–174

Magalhães V, Pinheiro LM, Ivanov MK et al (2012) Formation process of methane-derived authigenic carbonates from the Gulf of Cadiz. Sediment Geol 243(244):155–168

Matsumoto R (1990) Vuggy carbonate crust formed by hydrocarbon seepage on the continental shelf of Baffin Island, northeast Canada. Geochem J 24:143–158

Mazzini A, Ivanov MK, Parnell J et al (2004) Methane-related authigenic carbonates from the Black Sea: geochemical characterization and relation to seeping fluids. Mar Geol 212:153–181

Mazzini A, Aloisi G, Akhmanov GG et al (2005) Integrated petrographic and geochemical record of hydrocarbon seepage on Vøring Plateau. J Geol Soc London 162:815–827

Mazzini A, Svensen H, Hovland M et al (2006) Comparisons and implications from strikingly different authigenic carbonates in a Nyegga complex pockmark, G11, Norwegian Sea. Mar Geol 231:89–102

Meehan KC, Landman NH (2016) Faunal associations in cold-methane seep deposit from the Upper Cretaceous Pierre Shale, South Dakota. Palaios 31:291–301

Miyajima Y, Jenkins JG (this volume) Biomarkers in Ancient Hydrocarbon-Seep Carbonates. In: Kaim A, Cochran JK, Landman NH (eds) Ancient hydrocarbon seeps, Topics in geobiology, vol 50. Springer, Cham

Miyajima Y, Watanabe Y, Yanagisawa Y et al (2016) A late Miocene methane seep deposit bearing methane-trapping silica minerals at Joetsu, central Japan. Palaeogeog Palaeoclimat Palaeoecol 455:1–15

Monty CLV, Bosence DWJ, Bridges PH et al (1995) Carbonate mud-mounds: their origin and evolution. Int Assoc Sedimentologists Spec Publ 23:11–48

Natalicchio M, Peckmann J, Birgel D et al (2015) Seep deposits from northern Istria, Croatia: a first glimpse into the Eocene seep fauna of the Tethys region. Geol Mag 152:444–459

Nesbitt EA, Martin RA, Campbell KA (2013) New records of Oligocene diffuse hydrocarbon seeps, northern Cascadia margin. Palaeogeog Palaeoclimat Palaeoecol 390:116–129

Nobuhara T (2016) Mass occurrence of the enigmatic gastropod *Elmira* in the Late Cretaceous Sada Limestone seep deposit in southwestern Shikoku, Japan. PalZ 90:701–722

O'Reilly SS, Hryniewicz K, Little CTS et al (2014) Shallow water methane-derived authigenic carbonate at the Codling Fault Zone, western Irish Sea. Mar Geol 357:139–150

Pape T, Geprägs P, Hammerschmidt S et al (2014) Hydrocarbon seepage and its sources at mud volcanoes of the Kumano Forearc Basin, Nankai Trough subduction zone. Geochem Geophys Geosyst 15:2180–2194

Pearson MJ, Grosjean E, Nelson CS et al (2010) Tubular concretions in New Zealand petroliferous basins: lipid biomarker evidence for mineralization around proposed Miocene hydrocarbon seep conduits. J Pet Geol 33:205–220

Peckmann J, Thiel V (2004) Carbon cycling and ancient methane seeps. Chem Geol 205:443–467

Peckmann J, Little CTS, Gill F et al (2005) Worm tube fossils from the Hollard Mound hydrocarbon-seep deposit, Middle Devonian, Morocco: Palaeozoic seep-related vestimentiferans? Palaeogeogr Palaeoclimatol Palaeoecol 227:242–257

Peckmann J, Thiel V, Michaelis W et al (1999a) Cold seep deposits of Beauvoisin (Oxfordian; southeastern France) and Marmorito (Miocene, northern Italy): microbially induced authigenic carbonates. Int J Earth Sci 88:60–75

Peckmann J, Walliser O, Riegel W et al (1999b) Signatures of hydrocarbon venting in the Middle Devonian carbonate mound (Hollard Mound) at the Hamar Laghdad (Morocco). Facies 40:281–296

Peckmann J, Reimer A, Luth U et al (2001) Methane-derived carbonates and authigenic pyrite from the northwestern Black Sea. Mar Geol 177:129–150
Peckmann J, Goedert JL, Thiel V et al (2002) A comprehensive approach to the study of methane-seep deposits from the Lincoln Creek Formation, western Washington State, USA. Sedimentology 49:855–873
Peckmann J, Goedert JL, Heinrichs T et al (2003) A late Eocene 'Whiskey Creek' methane seep deposit (western Washington State): part II, petrology, stable isotopes, and biogeochemistry. Facies 48:241–254
Peckmann J, Campbell KA, Walliser OH et al (2007) A Late Devonian hydrocarbon-seep deposit dominated by dimerelloid brachiopods, Morocco. Palaios 22:114–122
Peckmann J, Kiel S, Sandy MR et al (2011) Mass occurrence of the brachiopod *Halorella* in Late Triassic methane-seep deposits, eastern Oregon. J Geol 119:207–220
Perez-Garcia C, Feseker T, Mienert J et al (2009) The Håkon Mosby mud volcano: 330000 years of focused fluid flow activity at the SW Barents Sea slope. Mar Geol 262:105–115
Pierre C, Fouquet Y (2007) Authigenic carbonates from methane seeps of the Congo deep-sea fan. Geo-Mar Lett 27:249–257
Raup DM (1979) Biases in the fossil record of species and genera. Bull Carnegie Mus Nat His 13:85–91
Reitner J, Peckmann J, Blumenberg M et al (2005a) Concretionary methane-seep carbonates and associated microbial communities in Black Sea sediments. Palaeogeog Palaeoclimat Palaeoecol 227:18–30
Reitner J, Peckmann J, Reimer A et al (2005b) Methane-derived carbonate buildups and associated microbial communities at cold seeps on the lower Crimean shelf (Black Sea). Facies 51:66–79
Ritger S, Carson B, Suess E (1987) Methane-derived authigenic carbonates formed by subduction-induced pore-water expulsion along the Oregon/Washington margin. Geol Soc Am Bull 98:147–156
Riding RE, Awramik SM (2000) Microbial sediments. Springer, Heidelberg
Römer M, Sahling H, Pape T et al (2012) Quantification of gas bubble emissions from submarine hydrocarbon seeps at the Makran continental margin (offshore Pakistan). J Geophys Res 117:C10015
Ross DJ (1991) Botryoidal high-magnesium calcite marine cements from the Upper Cretaceous of the Mediterranean Region. J Sediment Petrol 61:349–353
Sahling H, Rickert D, Lee RW et al (2002) Macrofaunal community structure and sulfide flux at gas hydrate deposits from the Cascadia convergent margin, NE Pacific. Mar Ecol Prog Ser 231:121–138
Sandy MR (2010) Brachiopods from ancient hydrocarbon seeps and hydrothermal vents. In: Kiel S (ed) The vent and seep biota. Springer, Heidelberg, pp 279–314
Savard MM, Beauchamp B, Veizer J (1996) Significance of aragonite cements around Cretaceous marine methane seeps. J Sediment Res 66:430–438
Shapiro RS (2000) A comment on the systematic confusion of thrombolites. Palaios 15:166–169
Sibuet M, Olu K (1998) Biogeography, biodiversity and fluid dependence of deep-sea cold-seep communities at active and passive margins. Deep-Sea Res Part II 45:517–567
Smrzka D, Kraemer SM, Zwicker J et al (2015) Constraining silica diagenesis in methane-seep deposits. Palaeogeog Palaeoclimat Palaeoecol 420:13–26
Smrzka D, Zwicker J, Kolonic S et al (2017) Methane seepage in a Cretaceous greenhouse world recorded by an unusual carbonate deposit from the Tarfaya Basin, Morocco. Depositional Rec 3:4–37
Smrzka D, Zwicker J, Misch D et al (2019) Oil seepage and carbonate formation: a case study from the southern Gulf of Mexico. Sedimentology 66:2318–2353
Smrzka D, Zwicker J, Lu Y et al (2021) Trace element distribution in methane-seep carbonates: the role of mineralogy and dissolved sulfide. Chem Geol 580:120357
Stakes DS, Orange D, Paduan JB et al (1999) Cold seeps and authigenic carbonate formation in Monterey Bay, California. Mar Geol 159:93–109

Takeuchi R, Matsumoto R, Ogihara S et al (2007) Methane-induced dolomite 'chimneys' on the Kuroshima Knoll, Ryukyu Islands, Japan. J Geochem Explor 95:16–28

Teichert B, Eisenhauer A, Bohrmann G et al (2003) U/Th systematics and ages of authigenic carbonates from Hydrate Ridge, Cascadia Margin: records of fluid flow variations. Geochim Cosmochim Acta 67:3845–3857

Teichert B, Bohrmann G, Suess E (2005) Chemocherms on Hydrate Ridge—unique microbially-mediated carbonate build-ups growing into the water column. Palaeogeog Palaeoclimat Palaeoecol 227:67–85

Tong H, Feng D, Peckman J et al (2019) Environments favoring dolomite formation at cold seeps: a case study from the Gulf of Mexico. Chem Geol 518:9–18

Tsunogai U, Kosaka A, Nakayama N et al (2010) Origin and fate of deep-sea seeping methane bubbles at Kuroshima Knoll, Ryukyu forearc region, Japan. Geochem J 44:461–476

Van Dover CL, Aharon P, Bernhard JM et al (2002) Blake Ridge methane seeps: characterization of a soft-sediment, chemosynthetically based ecosystem. Deep-Sea Res I 50:281–300

Vanneste H, Kastner M, James RH et al (2012) Authigenic carbonates from the Darwin Mud Volcano, Gulf of Cadiz: a record of palaeo-seepage of hydrocarbon-bearing fluids. Chem Geol 300(301):24–39

Vinn O, Kupriyanova E, Kiel S (2013) Serpulids (Annelida, Polychaeta) at Cretaceous to modern hydrocarbon seeps: ecological and evolutionary patters. Palaeogeog Palaeoclimat Palaeoecol 390:35–41

Vinn O, Hryniewicz K, Little CTS et al (2014) A boreal seprulid fauna from Volgian–Ryazanian (latest Jurassic–earliest Cretaceous) shelf sediments and hydrocarbon seeps from Svalbard. Geodiversitas 36:527–540

Webb KE, Barnes DKA, Planke S (2009) Pockmarks: refugees for marine benthic biodiversity. Limnol Oceanogr 54:1776–1788

Wiese F, Kiel S, Pack A et al (2015) The beast burrowed, the fluid followed—crustacean burrows as methane conduits. Mar Pet Geol 66:631–640

Zwicker J, Smrzka D, Gier S et al (2015) Mineralized conduits are part of the uppermost plumbing system of Oligocene methane-seep deposits, Washington State (USA). Mar Pet Geol 66:616–630

Zwicker J, Smrzka D, Himmler T et al (2018) Rare earth elements as tracers for microbial activity and early diagenesis: a new perspective for carbonate cements of ancient methane-seep deposits. Chem Geol 501:77–85

Zwicker J, Smrzka D, Steindl FR et al (2020) Mineral authigenesis within chemosynthetic microbial mats: coated grain formation and phosphogenesis at Cretaceous hydrocarbon seep, New Zealand. Depositional Rec 7:294–310

Part II
Seep Biota

Chapter 4
Microbes in Modern and Ancient Hydrocarbon Seeps

Russell S. Shapiro

4.1 Introduction

Microbial ecosystems, chiefly consortia of methane-oxidizing archaea and sulfate-reducing bacteria, drive the metabolic factory at methane seeps. The higher trophic levels of these nutrient oases include brachiopods, mollusks, and vestimentiferans that feed off of the energy supplied by the microbes. The geological record of seeps as anomalous deposits of carbonate is also a byproduct of redox changes around localized microbial ecosystems. Paradoxically, the fossil record of the microbes themselves is very sparse and difficult to ascertain even though modern systems host up to hundreds of microbial aggregates per mg wet weight (Marlow et al. 2014; Knittel et al. 2018).

The difficulty in recognizing a fossil record of microbes at ancient methane seeps is related to several factors connected to fossilization. As body fossils, bacteria and archaea are rarely preserved in any environment due primarily to degradation by other organisms. Should a cell escape predation, the lack of a robust cell wall relative to diagenetic processes means that most organic material is altered to unrecognizable carbon deposits. If a cell happens to be permineralized or molded by carbonate or other minerals prior to structural destruction, its small size (~1–5 μm typical) makes it challenging to recognize. Further complicating recognition is the near lack of distinct morphological features associated with simple cocci and filaments. Of the known extant groups, all form simple spheres, rods, or spherical aggregates (Boetius et al. 2000; Orphan et al. 2002; Reitner et al. 2005). Trace fossils, such as stromatolites or thrombolites (Shapiro 2007), provide a better target, but the record of well-established microbialites at methane seeps is still poorly developed.

R. S. Shapiro (✉)
Department of Earth and Environmental Sciences, California State University Chico, Chico, CA, USA
e-mail: rsshapiro@csuchico.edu

A. Kaim et al. (eds.), *Ancient Hydrocarbon Seeps*, Topics in Geobiology 50,
https://doi.org/10.1007/978-3-031-05623-9_4

In this chapter, the current state of knowledge of modern seep microbial ecosystems is briefly reviewed, then there is a discussion of taphonomy, followed by a review of the known fossil record. The final section provides suggestions for a search strategy in future studies.

4.2 Current Knowledge on Extant Systems

The composition and metabolic pathways at modern seeps are well characterized at higher taxonomic levels and are driven by the primary fuel sources of methane and sulfate (Orphan et al. 2004). Consortia of anaerobic methane-oxidizing archaea (ANME-1, ANME-2, and ANME-3) and sulfate-reducing bacteria (SRB) belonging to the *Desulfocsarcina/Desulfococcus* group dominate (Hinrichs et al. 1999; Boetius et al. 2000; Lanoil et al. 2001; Orphan et al. 2001; Michaelis et al. 2002; Knittel and Boetius 2009; Niemann et al. 2006) (Fig. 4.1a). Specifically, pore water sulfate is reduced as a consequence of organic matter oxidation. Additional organic matter is consumed by methanogens (Martens and Berner 1974) producing methane in shallow sediments and defining a sulfate-methane transition zone (SMTZ). Methane in

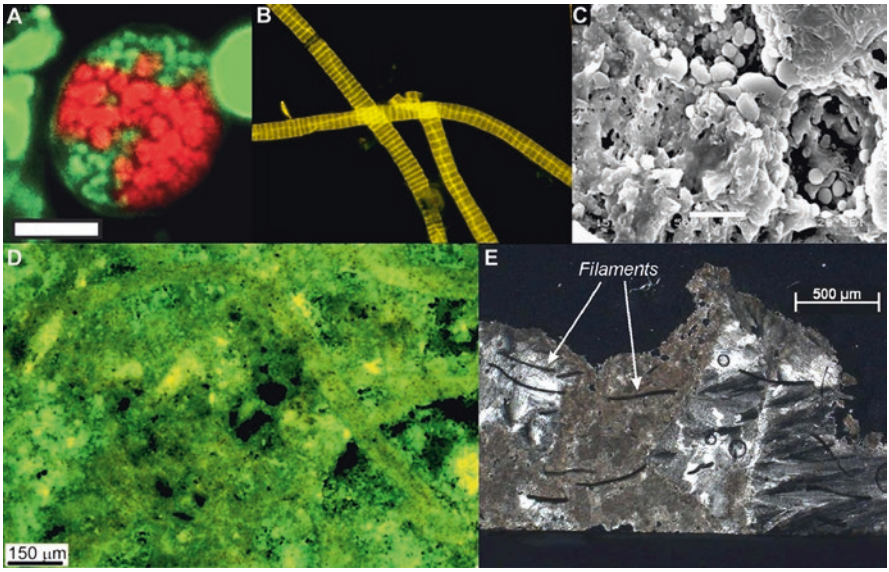

Fig. 4.1 Microbes in extant and fossil seeps. (**a**) Fluorescence imagery of an aggregate of an inner core of archaeal cells of ANME-1 surrounded by an outer shell of sulfate-reducing bacteria. (**b**) View of large sulfur-oxidizing bacteria typical of an active seep courtesy of Dr. Karen Lloyd. (**c**) SEM image of purported fossilized cells preserved within extracellular polymeric substance at a Cretaceous seep (Shapiro 2004). (**d**) Fluorescence image of fossilized filaments attributed to large bacteria from the Miocene of Italy (Dela Pierre et al. 2012). (**e**) Photomicrograph of sulfur oxidizers preserved in the carbonates at Hydrate Ridge (Teichert et al. 2005)

the SMTZ may also be supplied by older sources, either biological or thermogenic, migrating along faults and fractures or released by destabilizing frozen clathrates. In modern oceans, the sulfate reduction zone is generally 1–10 m thick, while the methane source zone may extend for 100 s of meters (Pohlman et al. 2013). In addition to the sulfate-driven-anaerobic oxidation of methane (SD-AOM) community, relatively large filamentous sulfide-oxidizing microbes such as *Beggiatoa*, *Thioploca*, *Thiothrix*, and *Arcobacter* are typically found at the sediment surface feeding off the sulfide byproduct (Jannasch et al. 1989) (Fig. 4.1b).

With regard to linking extant localized ecosystems to the fossil record, there are several potentials. First, because the process of SR-AOM raises alkalinity and draws down CO_2, there is the potential to preserve microbes in authigenic carbonates (Melim et al. 2016). Secondly, there are geochemical signatures, either as biomarkers or isotopic shifts, that might be preserved in the early cements showing sulfate reduction, methane oxidation, or a combination of the two processes. Finally, there is the rock record itself of anomalous deposits, primarily carbonates, that may show a linkage to a microbial origin.

4.3 Paths to Fossilization (Taphonomy)

As noted above, the fossil record of microbes at seeps is scanty, which is non-intuitive, as the microbial ecosystem fosters rapid precipitation of calcium carbonate (as well as barite, locally) and should favor entombment and preservation. However, the cells themselves are a rich source of organic carbon and thus are rapidly degraded in the natural setting.

Cells may fossilize through permineralization and more rarely secondary silicification. As in other, non-seep carbonate settings, most of the microbes are not obligate calcifiers, but their cell walls serve as a source for the nucleation of crystals. Rapid permineralization is required to preserve the cells in three dimensions. Once entombed, cells may be preserved as carbonaceous structures and recognized as such via Raman spectroscopy or similar analysis. In addition to carbonate, barite ($BaSO_4$) and sulfides are other potential primary precipitates that could persist in the rock record. Following entombment and burial, it is possible that subsurface fluids could foster replacement of the carbonate with silica, though evidence for this in the literature is not clear. Though not the focus of this chapter, it should be noted that a more likely path to fossilization is the preservation of more diagenesis-resistant biosignatures such as lipids and other chain hydrocarbons (see Miyajima and Jenkins this volume).

4.4 Microbial Fossil Record at Seeps

Microbial body fossils have only been recorded from a few seep locations in the rock record. This is not surprising as the most well-known microbe repository—stromatolites and similar structures—are only known to host fossil microbes in less than 1% of all reported cases. Very few papers purport to find microfossils in seeps—even in modern settings (e.g., Cavagna et al. 1999; Chen et al. 2005; Bojanowski 2007; Martire et al. 2010) (Fig. 4.1c–f).

In an early paper, Shapiro (2004) presented morphological evidence for microbes in the Cretaceous Tepee Buttes seep carbonates of Colorado. He noted that micropeloids (also known as "structure grumeleuse" in the literature; Bathurst 1976) potentially represent degraded microbial mats or extracellular polymeric substances (Fig. 4.2). The interpretation is based on the dominance of dark organic matter, indistinct margins compared to larger fecal pellets, and the variable sizes. Thus, micropeloid is a descriptive feature and is unrelated to fecal pellets. Other authors have used similar arguments to justify a biological origin for micropeloids (Chafetz 1986; Buczynski and Chafetz 1993; Peckmann et al. 2002). Though rare, morphological evidence for several different potential microfossil types is presented with caution and also acknowledging the context within the microfabrics. Coccoids, 0.5–1 μm in diameter, are found within micropeloids, specifically at the margins where cements initiate off of micropeloids. Though sheaths are also discussed, there is more caution in assessing a biological origin.

In a critical study of the offshore Eel River seep carbonates (Pleistocene), Bailey et al. (2010) employed multiple techniques toward morphologically distinctive clusters in the carbonates. The clusters resembled ANME colonies but lacked organic carbon. They concluded that the clusters are not biological but rather a diagenetic feature after framboidal pyrite. Similar features were also noted in Shapiro (2004). Framboidal pyrite is common in seep carbonates as well as in fossil whale falls (e.g., Shapiro and Spangler 2009) and other reducing environments and is not a

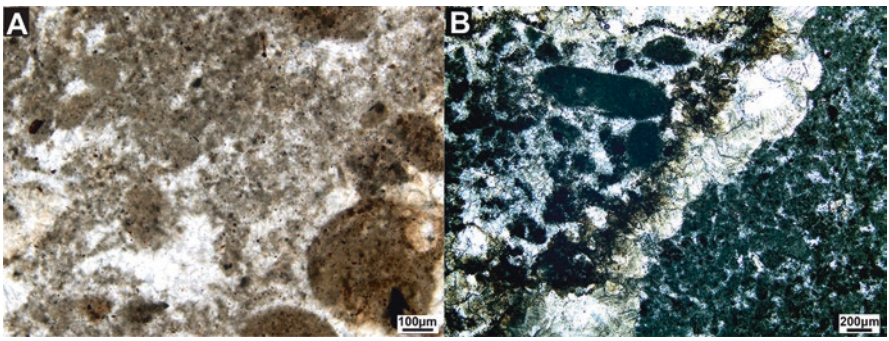

Fig. 4.2 Micropeloids. Two different images showing contrast of sub-micrometer micropeloids with diffuse boundaries associated with fecal pellets. (**a**) Cretaceous Tepee Buttes, Colorado, USA. (**b**) Jurassic Bedford Canyon, California, USA. Both views, plane-polarized light

robust biogenic feature. Interestingly, other authors have used the presence of framboidal pyrite as evidence of biological activity in seeps (Cavalazzi et al. 2012), burrows (Gong et al. 2008), and other environments. The argument is that while framboids may be created by abiotic processes, such as volcanism (e.g., England and Ostwald 1993), the temperatures are much higher than recorded in carbonate environments. In other words, at near standard surface temperature and pressure conditions, biological processes favor framboid formation (e.g., Ohfuji and Rickard 2005). Clearly, this is an exciting area, but more research needs to be carried out.

While the focus thus far has been on looking for fossil evidence of ANME colonies, there have also been reports of large fossilized filaments, suggestive of sulfide-oxidizing bacteria, similar to modern *Beggiatoa*. Teichert and others (2005) described such filaments from the sub-fossil Hydrate Ridge chemoherms. The thread-like, unbranched filaments are 7–25 μm in diameter and 120–715 μm long within the carbonate. The authors drew the similarity to the *Beggiatoa* filaments found at the surface. Similar structures were also noted by Barbieri and Cavalazzi (2005) in the Miocene of Italy who linked the preservation to the early extracellular production of aragonite, as described by Peckmann and others (2004). Putative filaments were also figured from the Miocene (Messinian) carbonates of northwest Italy by Dela Pierre and others (2012) and linked to coupled sulfate reduction-anaerobic oxidation of methane.

It should also be noted that an earlier paper on barite beds within the Devonian Slaven Chert of Nevada noted large fossil filaments (Graber and Chafetz 1990). Since that publication, the barite beds have been re-interpreted—at least in part—to be connected with methane seeps. This is based on the presence of limestone with ^{13}C-depleted isotope signatures and the presence of the dimerelloid brachiopod *Dzieduszyckia*. Subsequent studies have not identified the filaments for an updated context.

Larger, macroscale microbialites are more difficult to assess at seep localities. Structures that could be defined as stromatolites by displaying a laminated structure accreting off of a hard surface are rare, though described from modern seeps (e.g., Greinert et al. 2002; Himmler et al. 2018). They have also been described from the oldest known seeps, the Silurian El Borj limestone lenses of Morocco (Barbieri et al. 2004); Jurassic seeps of Antarctica (Kelly et al. 1995); Cretaceous Tepee Buttes of Colorado, USA (Shapiro 2004); and other locales (Fig. 4.3). A greater potential lies in deciphering the complex micrite and cement fabrics that are nearly ubiquitous at all seep sites throughout the geological column (e.g., Peckmann et al. 1999; Barbieri and Cavalazzi 2005). This alternation of euhedral-subhedral cements (aragonite or calcite), often with micrite, forming bands from millimeters to centimeters in thickness that "dome" across the deposits has typically been linked to redox changes in the venting fluid. Petrography and biomarker analysis were used in a study of Devonian Kess-Kess seep limestones from Morocco to suggest a clear microbial origin for laminated texture (Guido et al. 2013). Recently, Hryniewicz and others (2020) published descriptions of stromatolitic crusts dominated by crystalline calcite as opposed to micrite.

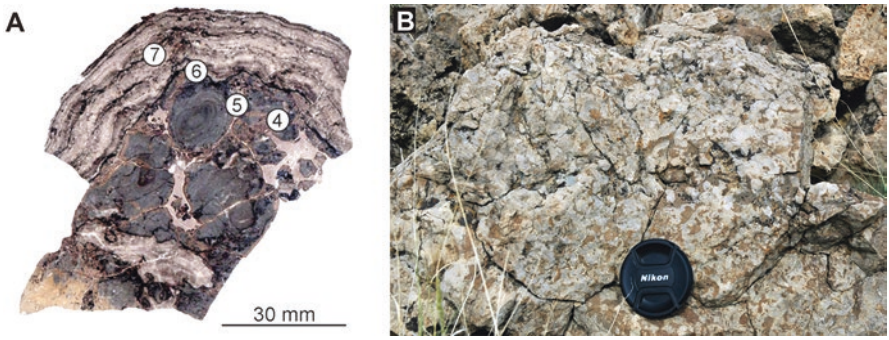

Fig. 4.3 Microbialitic textures. (**a**) Stromatolitic crust developing off of intraclasts, Miocene Tanohama Limestone, Japan (From Hryniewicz et al. 2020). (**b**) Field photo of thrombolItic textures, Cretaceous Tepee Buttes, Colorado, USA

4.5 Search Strategy for Future Studies

As demonstrated by this review, the microbial consortia, so ubiquitous in active seeps and responsible for the raising of alkalinity and production of carbonate, have largely eluded detection in the rock record. Future efforts are recommended to focus on the following strategies: target specific petrofabrics and fabric boundaries, incorporate new technologies as they develop, and connect potential morphological features to clearer geochemical proxies.

4.5.1 Targeting Particular Petrofabrics

Seep carbonates throughout the geological record share similar petrofabrics, specifically botryoidal cements, yellow calcite, micrite, and micropeloids. While none of these are unique to seeps, the mosaic of complex fabrics as well as dissolution boundaries typifies seep carbonates. Active microbial communities are often found at the interface of micrite and botryoidal cements (Fig. 4.4). Examining this boundary should be a primary target option. As noted in this review as well as previous papers, "micropeloids" on the order of 10s to 100s of micrometers in diameter and with diffuse margins may be directly related to microbial consortia or extracellular polymeric substances. This fabric in particular may yield preserved cells with proper preparation and study of extremely well-preserved deposits.

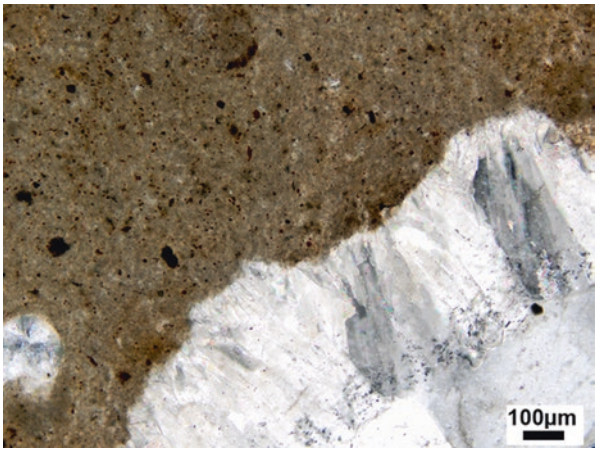

Fig. 4.4 Potential microfabric targets for future research. Interface of primary cements and underlying sediments

4.5.2 Utilization of More Focused Technologies

Twenty years ago, the major tools employed in the search of microbial fossils were high-resolution transmitted light and scanning electron microscopes. The ability to focus analyses such as cathodoluminescence, X-ray diffraction, and secondary ion mass spectrometry at the sub-micrometer scale will help target potential microfossils. These techniques, as well as others such as X-ray absorption and Raman spectroscopy, have already been applied to studies of ancient stromatolites (e.g., Brotton et al. 2007).

4.5.3 Connection with Clearer Geochemical Proxies

For many years now, paleontologists have relied on robust biomarkers such as isoprenoids and hopanoids to record preservation of the SD-AOM ecosystem (Peckmann and Thiel 2004; Birgel and Peckmann 2008). With increasing resolution requiring less material, specific petrofabrics can be targeted for biomarkers and then evaluated for microfossils. Additionally, there has been a recent drive to apply other techniques such as rare earth elements (Zwicker et al. 2018; Bayon et al. 2020; Smrzka et al. 2020), sulfur and other isotopes (Feng et al. 2016), and clumped isotopes (Thiagarajan et al. 2020) to pinpointing both evidence of microbial activity and specific metabolisms or vital effects (See Cochran et al. this volume).

4.6 Conclusions

The microbial fossil record at methane seeps is exceedingly poor compared with the density of cells at active seeps. This parallels the known record from other microbialites such as stromatolites and wrinkled sedimentary structures. Furthermore, reliance on morphological evidence is often dubious as the archaea and bacteria known from seeps have simple morphology and there are well-established pseudofossils developed from mineralogical precursors. While a few microbial trace fossils (e.g., stromatolitic or thrombolytic crusts) have been documented, other presumed, abiotic petrographic features such as crystalline bands, sulfides, and micropeloids need to be further explored. Finally, there needs to be stronger correlative evidence from biomarkers and other geochemical proxies to substantiate claims of recognizing fossilized microbial activity. These corroborating proxies are going to be most critical as evidence for past seeps are being pushed further back into the geological past beyond the macrofossil record.

Acknowledgments The author appreciates discussions over the years with Kathy Campbell, Jörn Peckmann, Andrzej Kaim, Robert Jenkins, Michal Jakubowicz, Victoria Orphan, and Shana Goffredi. Yusuke Miyajima and Jennifer Zwicker provided careful and valuable reviews that greatly improved this contribution.

References

Bailey JV, Raub TD, Meckler AN, Harrison BK, Raub TMD, Green AM, and Orphan VJ (2010) Pseudofossils in relict methane seep carbonates resemble endemic microbial consortia. Palaeogeog Palaeoclimat Palaeoecol 285:131–142

Barbieri R, Cavalazzi B (2005) Microbial fabrics from Neogene cold seep carbonates, Northern Apennine, Italy. Palaeogeog Palaeoclimat Palaeoecol 227:143–155

Barbieri R, Ori GG, Cavalazzi B (2004) A Silurian cold-seep ecosystem from Middle Atlas, Morocco. PALAIOS 19:527–542

Bathurst RGC (1976) Carbonate sediments and their diagenesis. Developments in sedimentology 12. Elsevier, Amsterdam

Bayon G, Lemaitre N, Barrat J-A et al (2020) Microbial utilization of rare earth elements at cold seeps related to aerobic methane oxidation. Chem Geol 555:119832

Birgel D, Peckmann J (2008) Aerobic methanotrophy at ancient marine methane seeps: a synthesis. Org Geochem 39(12):1659–1667

Boetius A, Ravenschlag K, Schubert CJ et al (2000) A marine microbial consortium apparently mediating anaerobic oxidation of methane. Nature 407:623–626

Bojanowski MJ (2007) Oligocene cold-seep carbonates from the Carpathians and their inferred relation to gas hydrates. Facies 53:347–360

Brotton SJ, Shapiro R, Van der Laan G et al (2007) Valence state fossils in Proterozoic stromatolites by L-edge X-ray absorption spectroscopy. J Geophys Res 112:G03004. https://doi.org/10.1029/2006JG000185

Buczynski C, Chafetz HS (1993) Habit of bacterially induced precipitates of calcium carbonate: examples from laboratory experiments and recent sediments. In: Rezak R, Lavoie DL (eds) Carbonate microfabrics. Springer, New York, pp 105–116

Cavagna S, Clari P, Martire L (1999) The role of bacteria in the formation of cold seep carbonates: geological evidence from Monferrato (Tertiary, NW Italy). Sediment Geol 126:253–270

Cavalazzi B, Barbieri R, Cady SL et al (2012) Iron-framboids in the hydrocarbon-related Middle Devonian Hollard Mound of the Anti-Atlas mountain range in Morocco: evidence of potential microbial biosignatures. Sediment Geol 263(264):183–193

Chafetz HS (1986) Marine peloids: a product of bacterially induced precipitation of calcite. J Sediment Petrol 56:812–817

Chen DF, Huang YY, Yuan XL et al (2005) Seep carbonates and preserved methane oxidizing Archaea and sulfate reducing bacteria fossils suggest recent gas venting on the seafloor in the northeastern South China Sea. Mar Pet Geol 22:613–621

Cochran JK, Landman NH, Jakubowicz M et al (this volume) Geochemistry of Cold Hydrocarbon Seeps: An Overview. In: Kaim A, Cochran JK, Landman NH (eds) Ancient hydrocarbon seeps, Topics in geobiology, vol 50. Springer, Cham

Dela Pierre F, Clari P, Bernardi E et al (2012) Messinian carbonate-rich beds of the Tertiary Piedmont Basin (NW Italy): microbially-mediated products straddling the onset of the salinity crisis. Palaeogeog Palaeoclimat Palaeoecol 344(345):78–93

England BM, Ostwald J (1993) Framboid-derived structures in some Tasman fold belt base metal sulphide deposits, New-South Wales, Australia. Ore Geol Rev 7:381–412

Feng D, Peng Y, Bao H et al (2016) A carbonate-based proxy for sulfate-driven anaerobic oxidation of methane. Geology 44(12):999–1002

Gong Y-M, Shi GR, Weldon EA et al (2008) Pyrite framboids interpreted as microbial colonies within the Permian Zoophycos spreiten from southeastern Australia. Geol Mag 145:95–103

Graber KK, Chafetz HS (1990) Petrography and origin of bedded barite and phosphate in the Devonian Slaven Chert of Central Nevada. J Sediment Petrol 60(6):897–911

Greinert J, Bohrmann G, Elvert M (2002) Stromatolitic fabric of authigenic carbonate crusts: result of anaerobic methane oxidation at cold seeps in 4,850 m water depth. Int J Earth Sci 91:698–711

Guido A, Mastandrea A, Demasi F et al (2013) Preliminary biogeochemical data on microbial carbonatogenesis in ancient extreme environments (Kess-Kess Mounds, Morocco). Riv Ital Paleontol Stratigr 119(1):19–29

Himmler T, Smrzka D, Zwicker J et al (2018) Stromatolites below the photic zone in the northern Arabian Sea formed by calcifying chemotrophic microbial mats. Geology 46:339–342

Hinrichs KU, Hayes JM, Sylva SP et al (1999) Methane-consuming Archaeobacteria in marine sediments. Nature 398:802–805

Hryniewicz K, Miyajima Y, Amano K et al (2020) Formation, diagenesis and fauna of cold seep carbonates from the Miocene Taishu Group of Tsushima (Japan). Geol Mag 158(6):964–984. https://doi.org/10.1017/S001675682000103X

Jannasch HW, Nelson DC, Wirsen CO (1989) Massive natural occurrence of unusually large bacteria (*Beggiatoa* spp.) at a hydrothermal deep-sea vent site. Nature 342:834–836

Kelly SRA, Ditchfield PW, Doubleday PA et al (1995) An Upper Jurassic methane-seep limestone from the Fossil Bluff Group forearc basin of Alexander Island, Antarctica. J Sediment Res 65:274–282

Knittel K, Boetius A (2009) Anaerobic oxidation of methane: progress with an unknown process. Ann Rev Microbiol 63:311–334

Knittel K, Wegener G, Boetius A (2018) Anaerobic methane oxidizers. In: McGenity TJ (ed) Microbial communities utilizing hydrocarbons and lipids: members, metagenomics and ecophysiology. Springer, New York, pp 1–21. https://doi.org/10.1007/978-3-319-60063-5_7-1

Lanoil BD, Sassen R, La Duc MT et al (2001) Bacteria and Archaea physically associated with Gulf of Mexico gas hydrates. Appl Environ Microbiol 67:5143–5153

Marlow JJ, Steele JA, Ziebis W et al (2014) Carbonate-hosted methanotrophy represents an unrecognized methane sink in the deep sea. Nat Commun 5:5094. https://doi.org/10.1038/ncomms6094

Martens CS, Berner RA (1974) Methane production in the interstitial waters of sulfate-depleted marine sediments. Science 185:1167–1169

Martire L, Natalicchio M, Petriea CC et al (2010) Petrographic evidence of the past occurrence of gas hydrates in the Tertiary Piedmont Basin (NW Italy). Geo-Mar Lett 30:461–476

Melim LA, Northup DE, Boston PJ et al (2016) Preservation of fossil microbes and biofilms in cave pool carbonates and comparison to other microbial carbonate environments. PALAIOS 31:177–189
Michaelis W, Seifert R, Nauhaus K et al (2002) Microbial reefs in the Black Sea fueled by anaerobic oxidation of methane. Science 297(5583):1013–1015
Miyajima Y, Jenkins JG (this volume) Biomarkers in Ancient Hydrocarbon-Seep Carbonates. In: Kaim A, Cochran JK, Landman NH (eds) Ancient hydrocarbon seeps, Topics in geobiology, vol 50. Springer, Cham
Niemann H, Loesekann T, de Beer D et al (2006) Novel microbial communities of the Haakon Mosby mud volcano and their role as a methane sink. Nature 443:854–858
Ohfuji H, Rickard D (2005) Experimental syntheses of framboids – a review. Earth Sci Rev 71:147–170
Orphan VJ, Hinrichs KU, Ussler W III et al (2001) Comparative analysis of methane-oxidizing Archaea and sulfate-reducing bacteria in anoxic marine sediments. Appl Environ Microbiol 67:1922–1934
Orphan VJ, House CH, Hinrichs KU et al (2002) Multiple archaeal groups mediate methane oxidation in anoxic cold seep sediments. PNAS 99:7663–7668
Orphan VJ, Ussler W III, Naehr TH et al (2004) Geological, geochemical, and microbiological heterogeneity of the seafloor around methane vents in the Eel River Basin, offshore California. Chem Geol 205(3/4):265–289
Peckmann J, Thiel V (2004) Carbon cycling at ancient methane-seeps. Chem Geol 205:443–467
Peckmann J, Walliser OH, Riegel W et al (1999) Signatures of hydrocarbon venting in a Middle Devonian carbonate mound (Hollard Mound) at the Hamar Laghdad (Anti-Atlas Morocco). Facies 40:281–296
Peckmann J, Goedert JL, Thiel V et al (2002) A comprehensive approach to the study of methane-seep deposits from the Lincoln Creek Formation, Western Washington State, USA. Sedimentology 49:855–873
Peckmann J, Thiel V, Reitner J et al (2004) A microbial mat of a large sulfur bacterium preserved in a Miocene methane-seep limestone. Geomicrobiol J 21:247–255
Pohlman JW, Riedel M, Bauer JE, Canuel EA, Paull CK, Lapham L, Grabowski KS, Coffin RB, Spence GD (2013) Anaerobic methane oxidation in low-organic content methane seep sediments. Geochim Cosmochim Acta 108:184–201
Reitner J, Peckmann J, Blumenberg M et al (2005) Concretionary methane-seep carbonates and associated microbial communities in Black Sea sediments. Palaeogeog Palaeoclimat Palaeoecol 227:18–30
Shapiro RS (2004) Recognition of fossil prokaryotes in Cretaceous methane seep carbonates: relevance to astrobiology. Astrobiology 4:438–449
Shapiro RS (2007) Stromatolites: a 3.5 billion year ichnologic record. In: Miller W III (ed) Trace fossils: concepts, problems, prospects. Elsevier, pp 382–290
Shapiro RS, Spangler E (2009) Bacterial fossil record in whale-falls: petrographic evidence of microbial sulfate reduction. Palaeogeog Palaeoclimat Palaeoecol 274(3/4):196–206
Smrzka D, Feng D, Himmler T et al (2020) Trace elements in methane-seep carbonates: potentials, limitations, and perspectives. Earth-Sci Rev 208:103263
Teichert BMA, Bohrmann G, Suess E (2005) Chemoherms on Hydrate Ridge – unique microbially mediated carbonate build-ups growing into the water column. Palaeogeog Palaeoclimat Palaeoecol 227:67–85
Thiagarajan N, Crémière A, Blättler C et al (2020) Stable and clumped isotope characterization of authigenic carbonates in methane cold seep environments. Geochim Cosmochim Acta 279:204–219. https://doi.org/10.1016/j.gca.2020.03.015
Zwicker J, Smrzka D, Himmler T et al (2018) Rare earth elements as tracers for microbial activity and early diagenesis: a new perspective from carbonate cements of ancient methane-seep deposits. Chem Geol 501:77–85

Chapter 5
Crustaceans in Cold Seep Ecosystems: Fossil Record, Geographic Distribution, Taxonomic Composition, and Biology

Adiël A. Klompmaker, Torrey Nyborg, Jamie Brezina, and Yusuke Ando

5.1 Introduction

Cold seep fluids provide an additional source of energy for various sulfide- and hydrocarbon-harvesting bacteria, often in symbiosis with invertebrates, attracting a variety of other organisms including crustaceans (e.g., Levin 2005; Vanreusel et al. 2009; Vrijenhoek 2013) (Fig. 5.1). These arthropods are abundant inhabitants of today's cold seep environments (Chevaldonné and Olu 1996; Martin and Haney 2005; Karanovic and Brandão 2015) and could play an important role in structuring seep ecosystems. The percentage of crustaceans of all macrofaunal specimens is highly variable locally in modern seeps, from 0% to >50% (Dando et al. 1991; Levin et al. 2000; Fujikura et al. 2002; Bergquist et al. 2003; Cordes et al. 2006, 2007, 2010a; Ritt et al. 2010, 2011; Lessard-Pilon et al. 2010; Levin et al. 2015; Grupe et al. 2015). Crustacean density is suggested to be higher in/around seeps than in surrounding areas (e.g., Senowbari-Daryan et al. 2007) because there is ample food available and many crustaceans can cope with relatively low oxygen

A. A. Klompmaker (✉)
Department of Museum Research and Collections & Alabama Museum of Natural History, University of Alabama, Tuscaloosa, AL, USA

Department of Integrative Biology & Museum of Paleontology, University of California, Berkeley, CA, USA
e-mail: adielklompmaker@gmail.com

T. Nyborg
Department of Earth and Biological Sciences, Loma Linda University, Loma Linda, CA, USA
e-mail: tnyborg06g@llu.edu

J. Brezina
South Dakota School of Mines and Technology, Rapid City, SD, USA

Y. Ando
Mizunami Fossil Museum, Mizunami, Japan

A. Kaim et al. (eds.), *Ancient Hydrocarbon Seeps*, Topics in Geobiology 50,
https://doi.org/10.1007/978-3-031-05623-9_5

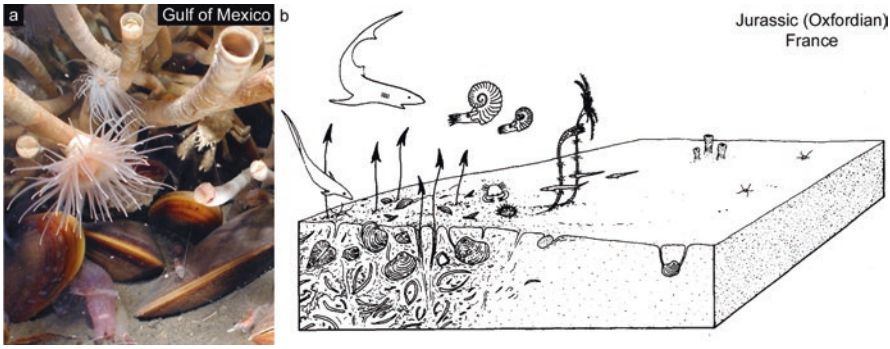

Fig. 5.1 An example of part of a modern seep community in the Gulf of Mexico (**a**) and a reconstruction of the macrofauna inhabiting a fossil hydrocarbon seep from the Late Jurassic (Oxfordian) of Beauvoisin, SE France (**b**). Decapod crustaceans are interpreted to be part of the seep community. Arrows in b indicate the escape of hydrocarbon gas such as methane into the water column. (Modified after Cordes et al. (2010b, Fig. 10.4a) and Rolin et al. (1990, Fig. 20))

levels at seeps. Some decapod crustaceans have adapted their respiratory system by developing larger appendages (scaphognathites) resulting in increased water flow over the gills per stroke to enhance oxygen uptake (Decelle et al. 2010, for caridean shrimps), and a number of ostracods may increase the water flow over their respiratory surface (Whatley 1991). The composition of decapods from modern cold seeps is dominated by members of the caridean shrimp family Alvinocarididae, squat lobsters (Galatheoidea and Chirostyloidea), and true crabs (Brachyura) (Chevaldonné and Olu 1996; Martin and Haney 2005). Ostracod species commonly found at cold seeps are members of the Podocopida and Platycopida clades (Russo et al. 2012). Other crustaceans such as copepods, amphipods, cumaceans, tanaidaceans, and isopods are also commonly found at seeps (e.g., Humes 1988; Levin et al. 2000, 2015; Ritt et al. 2010, 2011; Degen et al. 2012).

A limited number of studies are dedicated to fossil seep crustaceans or their inferred traces (Bishop and Williams 2000; Senowbari-Daryan et al. 2007; Peckmann et al. 2007b; Schweitzer and Feldmann 2008; Karasawa 2011; Russo et al. 2012; Wiese et al. 2015; Kiel et al. 2016; Yamaguchi et al. 2016). Consequently, their importance in structuring faunas at these biodiversity hotspots on the sea floor is poorly known, including to what extent seeps acted as refuges from extinction (Campbell 2006), the timing of invasion of cold seeps, the degree of endemism, depth preferences, and the longevity of crustacean lineages. Although many of these aspects cannot be answered yet, a first step in addressing these questions is to synthesize the present data. The goal of this paper is to review the global fossil record of crustaceans from cold seeps based on an extensive literature search and quantitative analysis of occurrences. We first discuss general trends regarding the study of fossil seep crustaceans per decade, their geography, and the number occurrences and crustacean-bearing seep localities through time. Subsequently, we focus on individual crustacean clades with an existing fossil record in seeps while also

providing information on modern occurrences, composition, and biology of these clades for a better framework to understand their ecological and evolutionary role in ancient seep ecosystems.

Institutional Abbreviations

AMNH	American Museum of Natural History, New York, USA
GPIBo	Goldfuß-Museum, Steinmann-Institut für Geologie, Mineralogie und Paläontologie, Universität Bonn, Bonn, Germany
GSUB	Geosciences Collection of the University of Bremen at the Faculty 5, Bremen, Germany
LACMIP	Invertebrate Paleontology Department, Natural History Museum of Los Angeles, Los Angeles, California, USA
MFM	Mizunami Fossil Museum, Mizunami, Japan
NHMUK	Natural History Museum, London, England
NIWA	National Institute of Water and Atmospheric Research, Wellington, New Zealand
NMB G	Naturhistorisches Museum Basel, Basel, Switzerland
PRI	Paleontological Research Institution, Ithaca, New York, USA
SDSM	Museum of Geology, South Dakota School of Mines and Technology, Rapid City, South Dakota, USA
UCMP	University of California Museum of Paleontology, Berkeley, California, USA
USNM	US National Museum of Natural History, Smithsonian Institution, Washington, D.C., USA
UWBM	Burke Museum, University of Washington, Seattle, Washington State, USA
ZPAL	Institute of Paleobiology, Polish Academy of Sciences, Warsaw, Poland

5.2 Crustaceans in Fossil Cold Seeps: A Quantitative Analysis

Crustaceans are more commonly present in fossil cold seeps than previously known, as suggested by our extensive search into the literature and new records reported herein, yielding 331 taxon occurrences (Table 5.1). While the percentage of crustaceans among macrofossils (thus excluding ostracods) is variable from 0% to >50% in modern seeps (see above), this percentage is typically low in fossil assemblages, with 0.05% for the latest Jurassic–earliest Cretaceous seeps of Spitsbergen (Hryniewicz et al. 2015a), 5.3% in a Late Cretaceous seep from Japan (Jenkins et al. 2007b), 0–0.9% for Late Cretaceous cold seeps from South Dakota (Meehan and Landman 2016), and 0 – <2.7% for Eocene seeps from Washington State (Goedert and Squires 1990). This result may be in part a reflection of the low preservation potential of crustaceans relative to mollusks (Kidwell and Flessa 1995; Stempien

Table 5.1 Occurrences of crustaceans in fossil cold seeps arranged by class, then stratigraphically from old to young. Specimens in Handle (2014) and Meehan and Landman (2016) have been included as Decapoda herein because they are being restudied

Type of evidence	Repair scar in	Class	Lowest possible rank/ name	Number of specimens	Age	Locality	Stratigraphic unit	Paleobathymetry	Reference(s)
Repair scar	Brachiopod *Sulcirostra paronai*	? Malacostraca	? Decapoda		Sinemurian	N of Seneca, Oregon, USA			Sandy et al. (2005), Sandy (2010), and Peckmann et al. (2013, for locality)
Coprolite		Malacostraca	*Favreina fontana*		early Oxfordian	Beauvoisin, France	Terres Noires Formation		Peckmann et al. (1999) and Senowbari-Daryan et al. (2007)
Coprolite		Malacostraca	*Favreina* cf. *F. martellensis*	1	early Oxfordian	Beauvoisin, France	Terres Noires Formation		Peckmann et al. (1999) and Senowbari-Daryan et al. (2007)
Coprolite		Malacostraca	*Palaxius salataensis*		early Oxfordian	Beauvoisin, France	Terres Noires Formation		Senowbari-Daryan et al. (2007)
Coprolite		Malacostraca	*Palaxius* isp.	3	early Oxfordian	Beauvoisin, France	Terres Noires Formation		Senowbari-Daryan et al. (2007)
Body fossil		Malacostraca	decapod crustacean carapace fragments, appendages, and pincers		early-middle Oxfordian	Beauvoisin, France	Terres Noires Formation		Gaillard et al. (1985, 1992), Rolin et al. (1990), and Peckmann et al. (1999)
Body fossil		Malacostraca	? galatheoid appendage	1	Tithonian–Berriasian	Seep 4, Sassenfjorden area, Spitsbergen, Norway	Uppermost Slottsmøya Member, upper Agardhfjellet Formation	Shallow	Hammer et al. (2011) and Hryniewicz et al. (2015a)
Body fossil		Malacostraca	Decapoda		late Barremian	Eagle Creek, California, USA	Lower Chickabally Mudstone Member, Budden Canyon Formation		Jenkins et al. (2013)
Burrow		Malacostraca	*Thalassinoides*		late Barremian	Locality B2335, Northeast Greenland	Kuhnpasset Beds		Kelly et al. (2000)

Body fossil		Malacostraca	*Goniodromites* sp.	1	middle Cenomanian	Kanajirisawa Creek, Obira-cho, Hokkaido, Japan	Tenkaritoge Formation		Karasawa and Kano (2021)
Body fossil		Malacostraca	*Callianassa* s.l. *hayanoi*	2	early late Albian	Loc. IK2031, Ponbetsu, MikasaCity, central Hokkaido, Japan	Middle Yezo Group	Subneritic	Karasawa (2011)
Body fossil		Malacostraca	*Callianassa* sp.		late Albian	East of Ea, Spain	Ubidepea mudstone of Ogella unit	Middle bathypelagic	Agirrezabala et al. (2013)
Coprolite		Malacostraca	crustacean fecal pellet		late Albian	East of Ea, Spain	Ubidepea mudstone of Ogella unit	Middle bathypelagic	Agirrezabala et al. (2013)
Burrow		Malacostraca	*Thalassinoides paradoxicus*		late Albian	East of Ea, Spain	Ubidepea mudstone of Ogella unit	Middle bathypelagic	Wiese et al. (2015)
Burrow		Malacostraca	*Thalassinoides suevicus*		late Albian	East of Ea, Spain	Ubidepea mudstone of Ogella unit	Middle bathypelagic	Wiese et al. (2015)
Body fossil		Malacostraca	*Callianassa*		late Albian to mid-Cenomanian	Awanui II, Raukumara Peninsula, North Island, New Zealand			Kiel et al. (2013)
Repair scar	Bivalve *Nucinella gigantea*	? Malacostraca	? Decapoda		Cenomanian	Kanajirisawa, Obira town, Hokkaido, Japan			Kiel et al. (2008)
Coprolite		Malacostraca	Decapoda		late Cenomanian	Alton Sink/ Cottonwood Canyon, Utah, USA	Lower part Tropic Shale	Shallow	Kiel et al. (2012)
Coprolite		Malacostraca	*Palaxius decemlunulatus*		Turonian–Cenomanian	Amma Fatma, Tarfaya Basin, Morocco		Shallow	Smrzka et al. (2017)
Body fossil		Malacostraca	Decapoda	5	early Campanian	Yasukawa site, Nakagawa area, Hokkaido, Japan	Upper Omagari Formation	Interface continental-shelf and continental slope	Jenkins et al. (2007a, b)

(continued)

Table 5.1 (continued)

Type of evidence	Repair scar in	Class	Lowest possible rank/ name	Number of specimens	Age	Locality	Stratigraphic unit	Paleobathymetry	Reference(s)
Body fossil		Malacostraca	*Callianassa*		mid-Campanian	Waipiro III, Raukumara Peninsula, North Island, New Zealand			Kiel et al. (2013)
Body fossil		Malacostraca	Decapoda	10	late Campanian	MoG 15, Forster Butte, Ranch Road Tepee, Lindsey Ranch, South Dakota, USA	*Baculites scotti* Zone, Pierre Shale	100–250 m or < 100 m	Laird and Belanger (2019, suppl. Table 1)
Body fossil		Malacostraca	Decapoda	2	late Campanian	MoG 13, Forster Butte, Ranch Road Tepee, Lindsey Ranch, South Dakota, USA	*Baculites scotti* Zone, Pierre Shale	100–250 m or < 100 m	Laird and Belanger (2019, suppl. Table 1)
Body fossil		Malacostraca	Decapoda	1	late Campanian	MoG 12, Forster Butte, Ranch Road Tepee, Lindsey Ranch, South Dakota, USA	*Baculites scotti* Zone, Pierre Shale	100–250 m or < 100 m	Laird and Belanger (2019, suppl. Table 1)
Body fossil		Malacostraca	"Raninidae" (probably Lyreididae)	1	late Campanian	MoG 2, Breidenbach Ranch (GAB 70), South Dakota, USA	*Baculites scotti* Zone, Pierre Shale	100–250 m or < 100 m	Laird and Belanger (2019, suppl. Table 1)
Body fossil		Malacostraca	Decapoda	1	late Campanian	MoG 2, Breidenbach Ranch (GAB 70), South Dakota, USA	*Baculites scotti* Zone, Pierre Shale	100–250 m or < 100 m	Laird and Belanger (2019, suppl. Table 1)
Body fossil		Malacostraca	Decapoda	4	late Campanian	AMNH 3440, South Dakota, USA	*Baculites scotti–Didymoceras nebrascense* zones, Pierre Shale	100–250 m or < 100 m	Handle (2014) and Meehan and Landman (2016)
Body fossil		Malacostraca	*Heus foersteri*	2	late Campanian	Pat Gilkey Ranch, Oelrichs Tepee Butte field, South Dakota, USA	*Didymoceras nebrascense* zone, Pierre Shale	100–250 m or < 100 m	Bishop and Williams (2000), Laird and Belanger (2019), and pers. comm. Neal Larson

Body fossil		Malacostraca	*Heus manningi*	3	late Campanian	Discovery Tepee, Lindsey Ranch, Newell Tepee Butte field, South Dakota, USA	*Didymoceras nebrascense* zone, Pierre Shale	100–250 m or < 100 m	Bishop and Williams (2000), Laird and Belanger (2019), and pers. comm. Neal Larson
Body fossil		Malacostraca	*Konidromites bjorki*	3	late Campanian	Discovery Tepee, Lindsey Ranch, Newell Tepee Butte field, South Dakota, USA	*Didymoceras nebrascense* zone, Pierre Shale	100–250 m or < 100 m	Bishop and Williams (2000), Laird and Belanger (2019), and pers. comm. Neal Larson
Body fossil		Malacostraca	Decapoda	1	late Campanian	Discovery Tepee, Lindsey Ranch, Newell Tepee Butte field, South Dakota, USA	*Didymoceras nebrascense* zone, Pierre Shale	100–250 m or < 100 m	Laird and Belanger (2019, suppl. Table 1)
Body fossil		Malacostraca	Decapoda	1	late Campanian	Richards Ranch Tepee Butte 12, South Dakota, USA	*Didymoceras nebrascense* Zone, Pierre Shale	100–250 m or < 100 m	Laird and Belanger (2019, suppl. Table 1)
Body fossil		Malacostraca	Decapoda	1	late Campanian	MoG 4, Breidenbach Ranch Small Tepee near 2nd Lake, South Dakota, USA	*Didymoceras nebrascense* Zone, Pierre Shale	100–250 m or < 100 m	Laird and Belanger (2019, suppl. Table 1)
Body fossil		Malacostraca	Decapoda	1	late Campanian	MoG 3, Austin's Butte, Gilkey Ranch, South Dakota, USA	*Didymoceras nebrascense* Zone, Pierre Shale	100–250 m or < 100 m	Laird and Belanger (2019, suppl. Table 1)
Body fossil		Malacostraca		1	late Campanian	MoG 1, Reinhard Butte (GAB 69), South Dakota, USA	*Didymoceras nebrascense* Zone, Pierre Shale	100–250 m or < 100 m	Laird and Belanger (2019, suppl. Table 1)
Body fossil		Malacostraca	*Latheticocarcinus punctatus*	1	late Campanian	Four miles SSE Fountain, El Paso County, Colorado, USA	*Baculites scotti–Exiteloceras jenneyi* zones, Pierre Shale	100–250 m or < 100 m	Bishop and Williams (2000), pers. comm. Neal Larson, pers. obs. AAK
Body fossil		Malacostraca	*Secretanella spinosa*	1	late Campanian	AMNH 3529 (WPT 140), Pennington County, South Dakota, USA	*Didymoceras cheyennense* Zone, Pierre Shale	100–250 m or < 100 m	Jamie Brezina collection, pers. obs. AAK

(continued)

Table 5.1 (continued)

Type of evidence	Repair scar in	Class	Lowest possible rank/ name	Number of specimens	Age	Locality	Stratigraphic unit	Paleobathymetry	Reference(s)
Body fossil		Malacostraca	*Secretanella* sp.	1	late Campanian	AMNH 3529 (WPT 140), Pennington County, South Dakota, USA	*Didymoceras cheyennense* Zone, Pierre Shale	100–250 m or < 100 m	Jamie Brezina collection, pers. obs. TN and AAK
Body fossil		Malacostraca	*Elektrocarcinus pierrensis*	2	late Campanian	WPT 123, South Dakota, USA	*Didymoceras cheyennense* Zone, Pierre Shale	100–250 m or < 100 m	Jamie Brezina collection, pers. obs. TN and AAK
Body fossil		Malacostraca	Decapoda	2	late Campanian	AMNH 3418, South Dakota, USA	*Didymoceras cheyennense* Zone, Pierre Shale	100–250 m or < 100 m	Handle (2014) and Meehan and Landman (2016)
Body fossil		Malacostraca	Decapoda	1	late Campanian	AMNH 3464, South Dakota, USA	*Didymoceras cheyennense* Zone, Pierre Shale	100–250 m or < 100 m	Handle (2014) and Meehan and Landman (2016)
Body fossil		Malacostraca	"crabs"		late Campanian	AMNH 3418, South Dakota, USA	*Didymoceras cheyennense* Zone, Pierre Shale	100–250 m or < 100 m	Larson et al. (2013)
Body fossil		Malacostraca	"crabs"		late Campanian	AMNH 3495 (WPT 130a and b), Pennington County, South Dakota, USA	*Didymoceras cheyennense* Zone, Pierre Shale	100–250 m or < 100 m	Larson et al. (2013)
Body fossil		Malacostraca	*Callianassa*		late Campanian	AMNH 3495 (WPT 130a and b), Pennington County, South Dakota, USA	*Didymoceras cheyennense* Zone, Pierre Shale	100–250 m or < 100 m	Larson et al. (2013)
Body fossil		Malacostraca	unknown crabs		late Campanian	AMNH 3529 (WPT 140), Pennington County, South Dakota, USA	*Didymoceras cheyennense* Zone, Pierre Shale	100–250 m or < 100 m	Larson et al. (2013)
Body fossil		Malacostraca	? *Protocallianassa cheyennensis*	57	late Campanian	AMNH 3529 (WPT 140), Pennington County, South Dakota, USA	*Didymoceras cheyennense* Zone, Pierre Shale	100–250 m or < 100 m	Jamie Brezina collection, pers. obs. AAK and TN

Body fossil		Malacostraca	? *Protocallianassa cheyennensis*	5	late Campanian	AMNH 3495 (WPT 130a and b), Pennington County, South Dakota, USA	*Didymoceras cheyennense* Zone, Pierre Shale	100–250 m or < 100 m	Jamie Brezina collection, pers. obs. AAK
Body fossil		Malacostraca	*Latheticocarcinus punctatus*	3	late Campanian	AMNH 3529 (WPT 140), Pennington County, South Dakota, USA	*Didymoceras cheyennense* Zone, Pierre Shale	100–250 m or < 100 m	Jamie Brezina collection, pers. obs. TN and AAK
Body fossil		Malacostraca	*Latheticocarcinus punctatus*	3	late Campanian	AMNH 3495 (WPT 130a and b), Pennington County, South Dakota, USA	*Didymoceras cheyennense* Zone, Pierre Shale	100–250 m or < 100 m	Jamie Brezina collection, pers. obs. TN
Body fossil		Malacostraca	*Latheticocarcinus punctatus*	1	late Campanian	WPT 137, South Dakota, USA	*Didymoceras cheyennense* Zone, Pierre Shale	100–250 m or < 100 m	Jamie Brezina collection, pers. obs. TN
Body fossil		Malacostraca	*Heus* sp.	7	late Campanian	AMNH 3529 (WPT 140), Pennington County, South Dakota, USA	*Didymoceras cheyennense* Zone, Pierre Shale	100–250 m or < 100 m	Jamie Brezina collection, pers. obs. AAK
Body fossil		Malacostraca	*Latheticocarcinus punctatus*	15	late Campanian	AMNH 3529 (WPT 140), Pennington County, South Dakota, USA	*Didymoceras cheyennense* Zone, Pierre Shale	100–250 m or < 100 m	Jamie Brezina collection, pers. obs. TN and AAK
Body fossil		Malacostraca	*Latheticocarcinus punctatus*	2	late Campanian	AMNH 3495 (WPT 130a and b), Pennington County, South Dakota, USA	*Didymoceras cheyennense* Zone, Pierre Shale	100–250 m or < 100 m	Jamie Brezina collection, pers. obs. TN and AAK
Body fossil		Malacostraca	*Latheticocarcinus punctatus*	1	late Campanian	WPT 144, South Dakota, USA	*Didymoceras cheyennense* Zone, Pierre Shale	100–250 m or < 100 m	Jamie Brezina collection, pers. obs. TN
Body fossil		Malacostraca	Decapoda	11	late Campanian	AMNH 3529 (WPT 140), Pennington County, South Dakota, USA	*Didymoceras cheyennense* Zone, Pierre Shale	100–250 m or < 100 m	Jamie Brezina collection, pers. obs. AAK

(continued)

Table 5.1 (continued)

Type of evidence	Repair scar in	Class	Lowest possible rank/ name	Number of specimens	Age	Locality	Stratigraphic unit	Paleobathymetry	Reference(s)
Body fossil		Malacostraca	*Dakoticancer overanus*	1	late Campanian	AMNH 3529 (WPT 140), Pennington County, South Dakota, USA	*Didymoceras cheyennense* Zone, Pierre Shale	100–250 m or < 100 m	Jamie Brezina collection, pers. obs. TN
Body fossil		Malacostraca	*Dakoticancer overanus*	1	late Campanian	WPT 128, South Dakota, USA	*Didymoceras cheyennense* Zone, Pierre Shale	100–250 m or < 100 m	Jamie Brezina collection, pers. obs. TN
Body fossil		Malacostraca	*Latheticocarcinus punctatus*	2	late Campanian	AMNH 3529 (WPT 140), Pennington County, South Dakota, USA	*Didymoceras cheyennense* Zone, Pierre Shale	100–250 m or < 100 m	Jamie Brezina collection, pers. obs. TN
Body fossil		Malacostraca	*Latheticocarcinus punctatus*	1	late Campanian	AMNH 3495 (WPT 130a and b), Pennington County, South Dakota, USA	*Didymoceras cheyennense* Zone, Pierre Shale	100–250 m or < 100 m	Jamie Brezina collection, pers. obs. TN
Body fossil		Malacostraca	*Elektrocarcinus pierrensis*	1	late Campanian	AMNH 3495 (WPT 130a and b), Pennington County, South Dakota, USA	*Didymoceras cheyennense* Zone, Pierre Shale	100–250 m or < 100 m	Jamie Brezina collection, pers. obs. AAK
Body fossil		Malacostraca	Decapoda	5	late Campanian	AMNH 3419, South Dakota, USA	*Baculites compressus* Zone, Pierre Shale	100–250 m or < 100 m	Handle (2014) and Meehan and Landman (2016)
Body fossil		Malacostraca	Decapoda	1	late Campanian	AMNH 3456, South Dakota, USA	*Baculites compressus* Zone, Pierre Shale	100–250 m or < 100 m	Handle (2014) and Meehan and Landman (2016)
Body fossil		Malacostraca	Decapoda	3	late Campanian	AMNH 3488, South Dakota, USA	*Baculites compressus* Zone, Pierre Shale	100–250 m or < 100 m	Handle (2014) and Meehan and Landman (2016)
Body fossil		Malacostraca	Decapoda	1	late Campanian	AMNH 3490, South Dakota, USA	*Baculites compressus* Zone, Pierre Shale	100–250 m or < 100 m	Handle (2014) and Meehan and Landman (2016)

Body fossil		Malacostraca	Decapoda	3	late Campanian	AMNH 3420, South Dakota, USA	*Baculites compressus* Zone, Pierre Shale	100–250 m or < 100 m	Handle (2014) and Meehan and Landman (2016)
Body fossil		Malacostraca	Decapoda		late Campanian	AMNH 3419, South Dakota, USA	*Baculites compressus* Zone, Pierre Shale	100–250 m or < 100 m	Larson et al. (2013)
Body fossil		Malacostraca	unidentified crabs		late Campanian	AMNH 3420, South Dakota, USA	*Baculites compressus* Zone, Pierre Shale	100–250 m or < 100 m	Larson et al. (2013)
Body fossil		Malacostraca	*Callianassa* sp.		late Campanian	AMNH 3420, South Dakota, USA	*Baculites compressus* Zone, Pierre Shale	100–250 m or < 100 m	Larson et al. (2013)
Body fossil		Malacostraca	Miscellaneous crabs		late Campanian	AMNH 3456, South Dakota, USA	*Baculites compressus* Zone, Pierre Shale	100–250 m or < 100 m	Larson et al. (2013)
Body fossil		Malacostraca	*Latheticocarcinus punctatus*	1	late Campanian	AMNH 3420, South Dakota, USA	*Baculites compressus* Zone, Pierre Shale	100–250 m or < 100 m	Jamie Brezina collection, pers. obs. TN
Body fossil		Malacostraca	*Dakoticancer overanus*	1	late Campanian	AMNH 3420, South Dakota, USA	*Baculites compressus* Zone, Pierre Shale	100–250 m or < 100 m	Jamie Brezina collection, pers. obs. TN
Body fossil		Malacostraca	Decapoda		late Campanian	Locality 1, South Dakota, USA	*Baculites compressus* zone, Pierre Shale	100–250 m or < 100 m	Kato et al. (2017)
Body fossil		Malacostraca	Decapoda		late Campanian	Locality 3, South Dakota, USA	*Baculites compressus* zone, Pierre Shale	100–250 m or < 100 m	Kato et al. (2017)
Body fossil		Malacostraca	Decapoda		late Campanian	Locality 5, South Dakota, USA	*Baculites compressus* zone, Pierre Shale	100–250 m or < 100 m	Kato et al. (2017)
Body fossil		Malacostraca	Decapoda		late Campanian	Locality 14, South Dakota, USA	*Baculites compressus* zone, Pierre Shale	100–250 m or < 100 m	Kato et al. (2017)

(continued)

Table 5.1 (continued)

Type of evidence	Repair scar in	Class	Lowest possible rank/ name	Number of specimens	Age	Locality	Stratigraphic unit	Paleobathymetry	Reference(s)
Burrow		Malacostraca	Decapoda		Maastrichtian	Locality D5.345.2, Seymour Island, Antarctica	Lopez de Bertodano Formation	Shallow	Little et al. (2015)
Burrow		Malacostraca	*Thalassinoides*		Danian	Outcrop A, Panoche Hills, California, USA	Dos Palos Shale Member, Moreno Formation		Blouet et al. (2017)
Burrow		Malacostraca	*Thalassinoides*		Danian	Outcrop B, Panoche Hills, California, USA	Cima Sandstone Lentil, Moreno Formation		Blouet et al. (2017)
Body fossil		Malacostraca	*Valamunida haeggi*	8	late Paleocene	Zachariassendalen, Spitsbergen, Norway	Basilika Formation	Offshore shelf-prodelta	Hryniewicz et al. (2019)
Body fossil		Malacostraca	*Valamunida haeggi*	6	late Paleocene	Hollendarbukta, Spitsbergen, Norway	Basilika Formation	Offshore shelf-prodelta	Vonderbank (1970) and Hryniewicz et al. (2019)
Body fossil		Malacostraca	*Protomunida spitzbergica*	1	late Paleocene	Fossildalen, Spitsbergen, Norway	Basilika Formation	Offshore shelf-prodelta	Gripp (1927)
Body fossil		Malacostraca	*Protomunida spitzbergica*	1	late Paleocene	Hollendarbukta, Spitsbergen, Norway	Basilika Formation	Offshore shelf-prodelta	Vonderbank (1970) and Hryniewicz et al. (2016, 2019)
Body fossil		Malacostraca	*Valamunida haeggi*	1	late Paleocene	Fossildalen, Spitsbergen, Norway	Basilika Formation	Offshore shelf-prodelta	Hägg (1925)
Body fossil		Malacostraca	*Shinkaia katapsyxis*	115	earliest middle Eocene	LACM 12385, Grays Harbor County, Washington, USA	Humptulips Formation	500–2000 m	Goedert and Squires (1990), Squires and Goedert (1995), Schweitzer and Feldmann (2008), Kiel (2010), herein
Body fossil		Malacostraca	*Callianassa* sp.		earliest middle Eocene	CSUN 1583, Grays Harbor County, Washington, USA	Humptulips Formation	? 1500–2000 m	Goedert and Kaler (1996)
Body fossil		Malacostraca	Callianassidae (callianassid claws)		middle Eocene	Buje, Istria, Croatia		700–1200 m	Natalicchio et al. (2015)

Body fossil		Malacostraca	Crustacean fragments		middle Eocene	Buje, Istria, Croatia		700–1200 m	Natalicchio et al. (2015)
Coprolite		Malacostraca	*Palaxius habanensis*		late middle Eocene	? UWBM B7083, Grays Harbor County, Washington, USA	Humptulips Formation	"Shallower water"	Peckmann et al. (2007a, p. 278)
Body fossil		Malacostraca	Callianassidae	2	late middle Eocene	UWBM B7083, Grays Harbor County, Washington, USA	Humptulips Formation	"Shallower water"	Peckmann et al. (2007a, p. 278)
Coprolite		Malacostraca	*Palaxius* isp.		late Eocene	Willapa Bay, Washington, USA	Siltstone of Shoalwater Bay Formation		Smrzka (2013)
Coprolite		Malacostraca	*Favreina* isp.		late Eocene	Vernonia-Timber site, Oregon, USA	Keasey Formation	Bathyal	Campbell (1995)
Body fossil		Malacostraca	*Callianassa* sp.		early Oligocene	LACMIP loc. 15911/8233, Shipwreck Point, Olympic Peninsula, Washington, USA	Makah Formation		Goedert and Campbell (1995)
Body fossil		Malacostraca	*Eucalliax capsulasetaea*	21	early Oligocene	Cerro La Salina, Talara Basin, Peru	Heath Shales		Kiel et al. (2019, 2020)
Burrow		Malacostraca	callianassid decapods (or bivalves)		early Oligocene	Satsop River site 5, Washington, USA	Lincoln Creek Formation	400–800 m	Zwicker et al. (2015)
Coprolite		Malacostraca	*Palaxius* isp.		early Oligocene	Satsop River site 5, Washington, USA	Lincoln Creek Formation	400–800 m	Zwicker et al. (2015)
Burrow		Malacostraca	callianassid decapods (or bivalves)		early Oligocene	Canyon River (CRB), Washington, USA	Lincoln Creek Formation	400–800 m	Zwicker et al. (2015)
Repair scar	Bivalve *Conchocele bisecta*	Malacostraca	crab	54	early Oligocene	1.5 km east of Kami-Atsunai railway station in Urahoro-cho, Hokkaido, Japan	Nuibetsu Formation		Kiel et al. (2016)
Repair scar	Bivalve *Bathymodiolus inouei*	Malacostraca	crab	21	early Oligocene	1.5 km east of Kami-Atsunai railway station in Urahoro-cho, Hokkaido, Japan	Nuibetsu Formation		Kiel et al. (2016)

(continued)

Table 5.1 (continued)

Type of evidence	Repair scar in	Class	Lowest possible rank/ name	Number of specimens	Age	Locality	Stratigraphic unit	Paleobathymetry	Reference(s)
Repair scar	Bivalve *Hubertschenckia ezoensis*	Malacostraca	crab	4	early Oligocene	1.5 km east of Kami-Atsunai railway station in Urahoro-cho, Hokkaido, Japan	Nuibetsu Formation		Kiel et al. (2016)
Body fossil		Malacostraca	? goneplacoid/xanthoid carapace	1	early Oligocene	Mata Cana, Department Córdoba, Colombia			Kiel and Hansen (2015)
Body fossil		Malacostraca	? *Callianassa*	6	early Oligocene	Mata Cana, Department Córdoba, Colombia			Kiel and Hansen (2015)
Body fossil		Malacostraca	*Neocallichirus* aff. *N. porterensis*		Oligocene	USGS loc. M1755, Sitkalidak Island, Alaska, USA	Sitkalidak Formation		Moore (1969), Amano and Kiel (2007), and Peckmann et al. (2007b)
Repair scar	Gastropod *Provanna antiqua*	? Malacostraca			earliest late Oligocene	LACMIP 16504, Grays Harbor County, Washington, USA	Lincoln Creek Formation	400–800 m	Kiel (2006), AAK reinterpretation
Repair scar	Gastropod *Turrinosyrinx hickmanae*	? Malacostraca	? Decapoda		late Oligocene	UMBM B8301 (= LACMIP 17746), Grays Harbor County, Washington, USA	Lincoln Creek Formation	400–800 m	Kiel (2006), AAK reinterpretation
Body fossil		Malacostraca	*Callianassa knapptonensis*		late Oligocene	UWBM B6781 (= LACMIP 17426 and Satsop River site 4), Mason County, Washington, USA	Lincoln Creek Formation	400–800 m	Peckmann et al. (2002)
Body fossil		Malacostraca	*Neocallichirus porterensis*		late Oligocene	UWBM B6781 (= LACMIP 17426 and Satsop River site 4), Mason County, Washington, USA	Lincoln Creek Formation	400–800 m	Peckmann et al. (2002)

Burrow		Malacostraca	callianassid decapods (or bivalves)		late Oligocene	UWBM B6781 (= LACMIP 17426 and Satsop River site 4), Mason County, Washington, USA	Lincoln Creek Formation	400–800 m	Zwicker et al. (2015)
Body fossil		Malacostraca	*Callianopsis clallamensis*	194	late Oligocene	Twin Rivers Quarry, Clallam County, Washington, USA	Pysht Formation		East (2006) and Nesbitt et al. (2013)
Body fossil		Malacostraca	*Callianopsis clallamensis*	10	late Oligocene	Clallam Bay, Clallam County, Washington, USA	Pysht Formation		Withers (1924), East (2006), and Nesbitt et al. (2013)
Body fossil		Malacostraca	*Glypturus* sp.	2	Aquitanian–Burdigalian	Corro Colorado, Venezuela	Husite member, Pozón Formation	100–170 m	Kiel and Hansen (2015)
Burrow		Malacostraca	*Thalassinoides*		Early Miocene	Haunui, North Island, New Zealand	Ihungia Formation	Inner shelf to mid bathyal	Troup (2010)
Burrow		Malacostraca	*Thalassinoides*		Early Miocene	Ugly Hill, North Island, New Zealand	Ihungia Formation	Inner shelf to mid bathyal	Troup (2010)
Body fossil		Malacostraca	crab carapace		Early Miocene	North Mathesons Bay, New Zealand	N4, Kawau Subgroup	Upper bathyal (100–1000 m)	Eagle et al. (1999)
Coprolite		Malacostraca	*Palaxius decemlunulatus*	3	Early to Middle Miocene	LACMIP loc. 6132 (Frankfort), Pacific County, Washington, USA	Bald Ridge unit, Astoria Formation	15–600 m	Kuechler et al. (2012)
Coprolite		Malacostraca	*Palaxius habanensis*	1	Early to Middle Miocene	LACMIP loc. 6132 (Frankfort), Pacific County, Washington, USA	Bald Ridge unit, Astoria Formation	15–600 m	Kiel (2010)
Body fossil		Malacostraca	claw fragments of crab		Middle Miocene	Miura-Boso area, Japan	Hayama Formation	1200–1600 m	Kanie et al. (1992), Kanie (1996), pers. comm. AAK August 2017
Body fossil		Malacostraca	Decapoda	3	Middle Miocene	Caldecott Tunnel excavation, Oakland, California, USA	Sobrante Formation	350–400 m	Powell et al. (2019)

(continued)

Table 5.1 (continued)

Type of evidence	Repair scar in	Class	Lowest possible rank/ name	Number of specimens	Age	Locality	Stratigraphic unit	Paleobathymetry	Reference(s)
Body fossil		Malacostraca	Decapoda		Miocene	Northern East Coast Basin, North Island, New Zealand	Moonlight Limestone	? Bathyal	Campbell (2006)
Body fossil		Malacostraca	decapod fragments		Miocene	Bexhaven, North Island, New Zealand	Bexhaven Limestone Formation	Slope and bathyal	Campbell et al. (2008)
Burrow		Malacostraca	? *Thalassinoides*		Miocene	Bexhaven, North Island, New Zealand	Bexhaven Limestone Formation	Slope and bathyal	Campbell et al. (2008)
Burrow		Malacostraca	? *Thalassinoides*		Miocene	Karikarihuata, North Island, New Zealand	Bexhaven Limestone Formation	Slope and bathyal	Campbell et al. (2008)
Burrow		Malacostraca	? *Thalassinoides*		Miocene	Moonlight North, North Island, New Zealand	Bexhaven Limestone Formation	Slope and bathyal	Campbell et al. (2008)
Burrow		Malacostraca	*Ophiomorpha nodosa*		Middle Miocene	Subiya area, northern Kuwait	Ghar Formation	Intertidal to subtidal	Hyžný et al. (2018): mud volcanoes
Body fossil		Malacostraca	*Neocallichirus* sp.		Middle Miocene	Subiya area, northern Kuwait	Ghar Formation	Intertidal to subtidal	Hyžný et al. (2018): mud volcanoes
Coprolite		Malacostraca	? Brine shrimp *Artemia*		early Messinian	Around Cornigliasca, Italy	Valle Versa Chaotic Complex		Natalicchio et al. (2013)
Repair scar	Gastropod *Mohnia vernalis*	Malacostraca	Decapoda	1	Late Pleistocene	3297C off Joetsu, Japan		894 m	Amano et al. (2013)
Body fossil		Malacostraca	*Calliax* sp.		Late Pleistocene–Early Holocene	MEDCOR-78, offshore Sicily, Italy		813 m	Taviani et al. (2013)
Body fossil		Maxillopoda	? *Capitulum lailae*		late Paleocene	Fossildalen, Spitsbergen	Basilika Formation	Offshore shelf-prodelta	Gripp (1927), Withers (1953), and Hryniewicz et al. (2019)

Body fossil		Maxillopoda	barnacle		Early Miocene	North Mathesons Bay, New Zealand	N4, Kawau Subgroup	Upper bathyal (100–1000 m)	Eagle et al. (1999)
Body fossil		Maxillopoda	Balanidae	1	Middle Miocene	Caldecott Tunnel excavation, Oakland, California, USA	Sobrante Formation	350–400 m	Powell et al. (2019)
Body fossil		Maxillopoda	*Ashinkailepas indica*	> 100 plates and scales	Late Pleistocene	Krishna-Godavari Basin, offshore India		Continental margin	Gale et al. (2020)
Body fossil		Maxillopoda	*Verruca stroemia*	1	Late Pleistocene	Core JM10-335GC, Vestnesa Ridge, west of Svalbard		Continental margin	Thomsen et al. (2019)
Body fossil		Maxillopoda	Cirripedia	fragments	Late Pleistocene	Core HH12-929GC, Vestnesa Ridge, west of Svalbard		Continental margin	Thomsen et al. (2019)
Body fossil		Ostracoda	Ostracoda		late Silurian	Middle Atlas, Morocco	Serie a facies flysch		Barbieri et al. (2004) and Buggisch and Krumm (2005)
Body fossil		Ostracoda	Ostracoda		early Eifelian	Hollard Mound, eastern Anti-Atlas, Morocco			Hryniewicz et al. (2017)
Body fossil		Ostracoda	Ostracoda		early Fammenian	1.7 km ENE of Sidi Amar, Morocco		Below photic zone	Peckmann et al. (2007b)
Body fossil		Ostracoda	*Ogmoconcha amalthei*		late Pliensbachian	NE of Cremlingen, Germany	*spinatum* Zone	Shallow	Teichert and Luppold (2013)
Body fossil		Ostracoda	Ostracoda		Toarcian–mid-Bajocian	SW of Zapala, Neuquén Basin, Argentina	Lower part Los Molles Formation	> 50 m	Gómez-Pérez (2001, 2003)
Body fossil		Ostracoda	Ostracoda		early middle Oxfordian	Beauvoisin, France	Terres Noires Formation		Rolin et al. (1990), Gaillard et al. (1992), and Peckmann et al. (1999)
Body fossil		Ostracoda	Ostracoda		Tithonian	Offset Ridge, Antarctica	Gateway Pass Limestone Bed, Atoll Nunataks Formation		Kelly et al. (1995)

(continued)

Table 5.1 (continued)

Type of evidence	Repair scar in	Class	Lowest possible rank/ name	Number of specimens	Age	Locality	Stratigraphic unit	Paleobathymetry	Reference(s)
Body fossil		Ostracoda	Ostracoda		late Tithonian	? Bakan Bay, Nova Zembla, Russia			Hryniewicz et al. (2015b)
Body fossil		Ostracoda	*Neonesidea* ? sp.	1	late middle Eocene	UWBM B7083, Grays Harbor County, Washington, USA	Humptulips Formation	Shallower water	Yamaguchi et al. (2016)
Body fossil		Ostracoda	Krithidae gen. et sp. indet 2	1	late Eocene–early Oligocene	UMBM B8302, Mason County, Washington, USA	Lincoln Creek Formation	400–800 m	Yamaguchi et al. (2016)
Body fossil		Ostracoda	*Krithe* cf. *adelspergi*	1	early Oligocene	LACMIP loc. 15911/8233, Shipwreck Point, Olympic Peninsula, Washington, USA	Makah Formation		Yamaguchi et al. (2016)
Body fossil		Ostracoda	*Cytherella* sp.	1	early Oligocene	LACMIP loc. 15911/8233, Shipwreck Point, Olympic Peninsula, Washington, USA	Makah Formation		Yamaguchi et al. (2016)
Body fossil		Ostracoda	*Palmoconcha* sp.2	1	early Oligocene	UMBM B7897, Mason County, Washington, USA	Lincoln Creek Formation	400–800 m	Yamaguchi et al. (2016)
Body fossil		Ostracoda	*Acanthocythereis acroreticulata*	4	early Oligocene	UMBM B7897, Mason County, Washington, USA	Lincoln Creek Formation	400–800 m	Yamaguchi et al. (2016)
Body fossil		Ostracoda	*Bosquetina* sp.	5	early Oligocene	UMBM B7897, Mason County, Washington, USA	Lincoln Creek Formation	400–800 m	Yamaguchi et al. (2016)
Body fossil		Ostracoda	*Cytherella* spp.	1	early Oligocene	UMBM B7897, Mason County, Washington, USA	Lincoln Creek Formation	400–800 m	Yamaguchi et al. (2016)
Body fossil		Ostracoda	*Propontocypris* sp.2	1	earliest late Oligocene	LACMIP 16504, Grays Harbor County, Washington, USA	Lincoln Creek Formation	400–800 m	Yamaguchi et al. (2016)

Body fossil		Ostracoda	*Loxoconcha*? sp.	9	late Oligocene	UWBM B6781 (= LACMIP 17426 and Satsop River site 4), Mason County, Washington, USA	Lincoln Creek Formation	400–800 m	Yamaguchi et al. (2016)
Body fossil		Ostracoda	*Cytheropteron* cf. *C. demenocali*	5	late Oligocene	UWBM B6781 (= LACMIP 17426 and Satsop River site 4), Mason County, Washington, USA	Lincoln Creek Formation	400–800 m	Yamaguchi et al. (2016)
Body fossil		Ostracoda	*Propontocypris* sp.1	6	late Oligocene	UWBM B6781 (= LACMIP 17426 and Satsop River site 4), Mason County, Washington, USA	Lincoln Creek Formation	400–800 m	Yamaguchi et al. (2016)
Body fossil		Ostracoda	*Propontocypris* sp.2	1	late Oligocene	UWBM B6781 (= LACMIP 17426 and Satsop River site 4), Mason County, Washington, USA	Lincoln Creek Formation	400–800 m	Yamaguchi et al. (2016)
Body fossil		Ostracoda	*Palmoconcha* sp.1	5	late Oligocene	UWBM B6781 (= LACMIP 17426 and Satsop River site 4), Mason County, Washington, USA	Lincoln Creek Formation	400–800 m	Yamaguchi et al. (2016)
Body fossil		Ostracoda	*Krithe* cf. *K. adelspergi*	1	late Oligocene	UWBM B6781 (= LACMIP 17426 and Satsop River site 4), Mason County, Washington, USA	Lincoln Creek Formation	400–800 m	Yamaguchi et al. (2016)
Body fossil		Ostracoda	*Pontocythere*? sp.	6	late Oligocene	UWBM B6781 (= LACMIP 17426 and Satsop River site 4), Mason County, Washington, USA	Lincoln Creek Formation	400–800 m	Yamaguchi et al. (2016)
Body fossil		Ostracoda	*Macropyxis*? sp.	1	late Oligocene	UMBM B8292, Clallam County, Washington, USA	Pysht Formation, upper part		Yamaguchi et al. (2016)

(continued)

Table 5.1 (continued)

Type of evidence	Repair scar in	Class	Lowest possible rank/ name	Number of specimens	Age	Locality	Stratigraphic unit	Paleobathymetry	Reference(s)
Body fossil		Ostracoda	Krithidae gen. et sp. indet 1	1	late Oligocene	UMBM B8301 (= LACMIP 17746), Grays Harbor County, Washington, USA	Lincoln Creek Formation	400–800 m	Yamaguchi et al. (2016)
Body fossil		Ostracoda	Ostracoda		Aquitanian	Buenavista de Maicillal, Venezuela	Husite member, Pozón Formation	100–170 m	Kiel and Hansen (2015)
Body fossil		Ostracoda	Ostracoda		Neogene	Northern Apennines, Italy			Barbieri and Cavalazzi (2005)
Body fossil		Ostracoda	*Neonesidea* cf. *N. conformis*	10	Serravallian	SC561/Cals1 W/ Cals2 W 15–24, Sarsetta, northern Apennines, Italy	Termina Formation		Russo et al. (2012)
Body fossil		Ostracoda	*Cytherella vulgata*	3	Serravallian	SC561, Sarsetta, northern Apennines, Italy	Termina Formation		Russo et al. (2012)
Body fossil		Ostracoda	*Krithe oertlii*	21	Serravallian	SC561/Cals1 W/ Cals2 W 15–24, Sarsetta, northern Apennines, Italy	Termina Formation		Russo et al. (2012)
Body fossil		Ostracoda	*Xestoleberis communis*	2	Serravallian	SC561, Sarsetta, northern Apennines, Italy	Termina Formation		Russo et al. (2012)
Body fossil		Ostracoda	*Xestoleberis* sp.2	1	Serravallian	SC561, Sarsetta, northern Apennines, Italy	Termina Formation		Russo et al. (2012)
Body fossil		Ostracoda	*Abyssocypris* sp.	6	Serravallian	Cals1 W, Sarsetta, northern Apennines, Italy	Termina Formation		Russo et al. (2012)
Body fossil		Ostracoda	*Argilloecia* gr. *acuminata*	10	Serravallian	Cals1 W, Sarsetta, northern Apennines, Italy	Termina Formation		Russo et al. (2012)

Body fossil		Ostracoda	*Buntonia multicostata*	2	Serravallian	Cals1 W, Sarsetta, northern Apennines, Italy	Termina Formation		Russo et al. (2012)
Body fossil		Ostracoda	*Cardobairdia glabra*	4	Serravallian	Cals1 W/Cals2 W 15–24, Sarsetta, northern Apennines, Italy	Termina Formation		Russo et al. (2012)
Body fossil		Ostracoda	*Cytherella* gr. *russoi*	26	Serravallian	Cals1 W/Cals2 W 15–24, Sarsetta, northern Apennines, Italy	Termina Formation		Russo et al. (2012)
Body fossil		Ostracoda	*Henryhowella asperrima*	22	Serravallian	Cals1 W/Cals2 W 15–24, Sarsetta, northern Apennines, Italy	Termina Formation		Russo et al. (2012)
Body fossil		Ostracoda	*Krithe compressa*	24	Serravallian	Cals1 W/Cals2 W 15–24, Sarsetta, northern Apennines, Italy	Termina Formation		Russo et al. (2012)
Body fossil		Ostracoda	*Parakrithe* gr. *dactylomorpha*	10	Serravallian	Cals1 W/Cals2 W 15–24, Sarsetta, northern Apennines, Italy	Termina Formation		Russo et al. (2012)
Body fossil		Ostracoda	*Xestoleberis* gr. *prognata*	8	Serravallian	Cals1 W/Cals2 W 15–24, Sarsetta, northern Apennines, Italy	Termina Formation		Russo et al. (2012)
Body fossil		Ostracoda	*Argilloecia* sp.	3	Serravallian	Cals2 W 15–24, Sarsetta, northern Apennines, Italy	Termina Formation		Russo et al. (2012)
Body fossil		Ostracoda	*Paleoblitacythereis bossioi*	1	Serravallian	Cals2 W 15–24, Sarsetta, northern Apennines, Italy	Termina Formation		Russo et al. (2012)
Body fossil		Ostracoda	*Quasibuntonia radiatopora*	1	Serravallian	Cals2 W 15–24, Sarsetta, northern Apennines, Italy	Termina Formation		Russo et al. (2012)

(continued)

Table 5.1 (continued)

Type of evidence	Repair scar in	Class	Lowest possible rank/ name	Number of specimens	Age	Locality	Stratigraphic unit	Paleobathymetry	Reference(s)
Body fossil		Ostracoda	*Cytherella* gr. *russoi*	1	Serravallian	B6, Sasso delle Streghe, northern Apennines, Italy	Termina Formation		Russo et al. (2012)
Body fossil		Ostracoda	*Krithe oertlii*	1	Serravallian	B6, Sasso delle Streghe, northern Apennines, Italy	Termina Formation		Russo et al. (2012)
Body fossil		Ostracoda	*Argilloecia conoidea*	34	Late Pleistocene–Holocene	Mound B (site 18), Porcupine Basin, offshore west of Ireland		650–1000 m	Coles et al. (1996)
Body fossil		Ostracoda	*Argilloecia cylindrica*	1	Late Pleistocene–Holocene	Mound B (site 18), Porcupine Basin, offshore west of Ireland		650–1000 m	Coles et al. (1996)
Body fossil		Ostracoda	*Argilloecia* spp.	1	Late Pleistocene–Holocene	Mound B (site 18), Porcupine Basin, offshore west of Ireland		650–1000 m	Coles et al. (1996)
Body fossil		Ostracoda	*Buntonia textilis*	5	Late Pleistocene–Holocene	Mound B (site 18), Porcupine Basin, offshore west of Ireland		650–1000 m	Coles et al. (1996)
Body fossil		Ostracoda	*Bythocypris affinis*	19	Late Pleistocene–Holocene	Mound B (site 18), Porcupine Basin, offshore west of Ireland		650–1000 m	Coles et al. (1996)
Body fossil		Ostracoda	*Bythocypris bosquetiana*	13	Late Pleistocene–Holocene	Mound B (site 18), Porcupine Basin, offshore west of Ireland		650–1000 m	Coles et al. (1996)
Body fossil		Ostracoda	*Bythocypris tenera*	1	Late Pleistocene–Holocene	Mound B (site 18), Porcupine Basin, offshore west of Ireland		650–1000 m	Coles et al. (1996)

Body fossil		Ostracoda	*Cytherella serratula*	13	Late Pleistocene–Holocene	Mound B (site 18), Porcupine Basin, offshore west of Ireland		650–1000 m	Coles et al. (1996)
Body fossil		Ostracoda	*Cytheropteron garganicum*	1	Late Pleistocene–Holocene	Mound B (site 18), Porcupine Basin, offshore west of Ireland		650–1000 m	Coles et al. (1996)
Body fossil		Ostracoda	*Cytheropteron inflatum*	37	Late Pleistocene–Holocene	Mound B (site 18), Porcupine Basin, offshore west of Ireland		650–1000 m	Coles et al. (1996)
Body fossil		Ostracoda	*Cytheropteron porterae*	1	Late Pleistocene–Holocene	Mound B (site 18), Porcupine Basin, offshore west of Ireland		650–1000 m	Coles et al. (1996)
Body fossil		Ostracoda	*Cytheropteron testudo*	1	Late Pleistocene–Holocene	Mound B (site 18), Porcupine Basin, offshore west of Ireland		650–1000 m	Coles et al. (1996)
Body fossil		Ostracoda	*Cytheropteron tenuialatum*	2	Late Pleistocene–Holocene	Mound B (site 18), Porcupine Basin, offshore west of Ireland		650–1000 m	Coles et al. (1996)
Body fossil		Ostracoda	*Cytheropteron* spp.	1	Late Pleistocene–Holocene	Mound B (site 18), Porcupine Basin, offshore west of Ireland		650–1000 m	Coles et al. (1996)
Body fossil		Ostracoda	*Echinocythereis echinata*	9	Late Pleistocene–Holocene	Mound B (site 18), Porcupine Basin, offshore west of Ireland		650–1000 m	Coles et al. (1996)
Body fossil		Ostracoda	*Echinocythereis laticarinata*	128	Late Pleistocene–Holocene	Mound B (site 18), Porcupine Basin, offshore west of Ireland		650–1000 m	Coles et al. (1996)

(continued)

Table 5.1 (continued)

Type of evidence	Repair scar in	Class	Lowest possible rank/ name	Number of specimens	Age	Locality	Stratigraphic unit	Paleobathymetry	Reference(s)
Body fossil		Ostracoda	*Hemiparacytheridea variabile*	2	Late Pleistocene–Holocene	Mound B (site 18), Porcupine Basin, offshore west of Ireland		650–1000 m	Coles et al. (1996)
Body fossil		Ostracoda	*Henryhowella* gr. *asperrima*	17	Late Pleistocene–Holocene	Mound B (site 18), Porcupine Basin, offshore west of Ireland		650–1000 m	Coles et al. (1996)
Body fossil		Ostracoda	*Hermanites* cf. *haidingeri*	6	Late Pleistocene–Holocene	Mound B (site 18), Porcupine Basin, offshore west of Ireland		650–1000 m	Coles et al. (1996)
Body fossil		Ostracoda	*Kangarina abyssicola*	6	Late Pleistocene–Holocene	Mound B (site 18), Porcupine Basin, offshore west of Ireland		650–1000 m	Coles et al. (1996)
Body fossil		Ostracoda	*Krithe aquilonia*	105	Late Pleistocene–Holocene	Mound B (site 18), Porcupine Basin, offshore west of Ireland		650–1000 m	Coles et al. (1996)
Body fossil		Ostracoda	*Krithe keijii*	1	Late Pleistocene–Holocene	Mound B (site 18), Porcupine Basin, offshore west of Ireland		650–1000 m	Coles et al. (1996)
Body fossil		Ostracoda	*Krithe* juveniles	182	Late Pleistocene–Holocene	Mound B (site 18), Porcupine Basin, offshore west of Ireland		650–1000 m	Coles et al. (1996)
Body fossil		Ostracoda	*Macrocyprissa arcuata*	1	Late Pleistocene–Holocene	Mound B (site 18), Porcupine Basin, offshore west of Ireland		650–1000 m	Coles et al. (1996)

Body fossil		Ostracoda	*Microceratina poligonia*	3	Late Pleistocene–Holocene	Mound B (site 18), Porcupine Basin, offshore west of Ireland		650–1000 m	Coles et al. (1996)
Body fossil		Ostracoda	*Macrocythere* cf. *M. depressa*	3	Late Pleistocene–Holocene	Mound B (site 18), Porcupine Basin, offshore west of Ireland		650–1000 m	Coles et al. (1996)
Body fossil		Ostracoda	*Monoceratina* n. sp.	3	Late Pleistocene–Holocene	Mound B (site 18), Porcupine Basin, offshore west of Ireland		650–1000 m	Coles et al. (1996)
Body fossil		Ostracoda	*Muellerina abyssicola*	84	Late Pleistocene–Holocene	Mound B (site 18), Porcupine Basin, offshore west of Ireland		650–1000 m	Coles et al. (1996)
Body fossil		Ostracoda	*Neonesidea inflata*	10	Late Pleistocene–Holocene	Mound B (site 18), Porcupine Basin, offshore west of Ireland		650–1000 m	Coles et al. (1996)
Body fossil		Ostracoda	*Paracytherois flexuosa*	33	Late Pleistocene–Holocene	Mound B (site 18), Porcupine Basin, offshore west of Ireland		650–1000 m	Coles et al. (1996)
Body fossil		Ostracoda	*Paracytherois* spp.	6	Late Pleistocene–Holocene	Mound B (site 18), Porcupine Basin, offshore west of Ireland		650–1000 m	Coles et al. (1996)
Body fossil		Ostracoda	*Paradoxostoma normani*	5	Late Pleistocene–Holocene	Mound B (site 18), Porcupine Basin, offshore west of Ireland		650–1000 m	Coles et al. (1996)
Body fossil		Ostracoda	*Paradoxostoma* gr. *variabile*	4	Late Pleistocene–Holocene	Mound B (site 18), Porcupine Basin, offshore west of Ireland		650–1000 m	Coles et al. (1996)

(continued)

Table 5.1 (continued)

Type of evidence	Repair scar in	Class	Lowest possible rank/ name	Number of specimens	Age	Locality	Stratigraphic unit	Paleobathymetry	Reference(s)
Body fossil		Ostracoda	*Paradoxostoma* spp.	9	Late Pleistocene–Holocene	Mound B (site 18), Porcupine Basin, offshore west of Ireland		650–1000 m	Coles et al. (1996)
Body fossil		Ostracoda	*Parakrithe angusta*	1	Late Pleistocene–Holocene	Mound B (site 18), Porcupine Basin, offshore west of Ireland		650–1000 m	Coles et al. (1996)
Body fossil		Ostracoda	*Pseudocythere* gr. *caudata*	3	Late Pleistocene–Holocene	Mound B (site 18), Porcupine Basin, offshore west of Ireland		650–1000 m	Coles et al. (1996)
Body fossil		Ostracoda	*Sclerochilus* gr. *contortus*	36	Late Pleistocene–Holocene	Mound B (site 18), Porcupine Basin, offshore west of Ireland		650–1000 m	Coles et al. (1996)
Body fossil		Ostracoda	*Semicytherura coeca*	1	Late Pleistocene–Holocene	Mound B (site 18), Porcupine Basin, offshore west of Ireland		650–1000 m	Coles et al. (1996)
Body fossil		Ostracoda	*Thaerocythere crenulata*	2	Late Pleistocene–Holocene	Mound B (site 18), Porcupine Basin, offshore west of Ireland		650–1000 m	Coles et al. (1996)
Body fossil		Ostracoda	Ostracod indet.	2	Late Pleistocene–Holocene	Mound B (site 18), Porcupine Basin, offshore west of Ireland		650–1000 m	Coles et al. (1996)
Body fossil		Ostracoda	*Argilloecia acuminata*	4	Late Pleistocene–Holocene	Mound C (site 25), Porcupine Basin, offshore west of Ireland		650–1000 m	Coles et al. (1996)

Body fossil		Ostracoda	*Argilloecia conoidea*	39	Late Pleistocene–Holocene	Mound C (site 25), Porcupine Basin, offshore west of Ireland		650–1000 m	Coles et al. (1996)
Body fossil		Ostracoda	*Argilloecia cylindrica*	8	Late Pleistocene–Holocene	Mound C (site 25), Porcupine Basin, offshore west of Ireland		650–1000 m	Coles et al. (1996)
Body fossil		Ostracoda	*Buntonia textilis*	1	Late Pleistocene–Holocene	Mound C (site 25), Porcupine Basin, offshore west of Ireland		650–1000 m	Coles et al. (1996)
Body fossil		Ostracoda	*Bythocypris affinis*	43	Late Pleistocene–Holocene	Mound C (site 25), Porcupine Basin, offshore west of Ireland		650–1000 m	Coles et al. (1996)
Body fossil		Ostracoda	*Bythocypris bosquetiana*	7	Late Pleistocene–Holocene	Mound C (site 25), Porcupine Basin, offshore west of Ireland		650–1000 m	Coles et al. (1996)
Body fossil		Ostracoda	*Cluthia keiji*	2	Late Pleistocene–Holocene	Mound C (site 25), Porcupine Basin, offshore west of Ireland		650–1000 m	Coles et al. (1996)
Body fossil		Ostracoda	*Cytherella serratula*	61	Late Pleistocene–Holocene	Mound C (site 25), Porcupine Basin, offshore west of Ireland		650–1000 m	Coles et al. (1996)
Body fossil		Ostracoda	*Cytheropteron garganicum*	1	Late Pleistocene–Holocene	Mound C (site 25), Porcupine Basin, offshore west of Ireland		650–1000 m	Coles et al. (1996)
Body fossil		Ostracoda	*Cytheropteron inflatum*	43	Late Pleistocene–Holocene	Mound C (site 25), Porcupine Basin, offshore west of Ireland		650–1000 m	Coles et al. (1996)

(continued)

Table 5.1 (continued)

Type of evidence	Repair scar in	Class	Lowest possible rank/ name	Number of specimens	Age	Locality	Stratigraphic unit	Paleobathymetry	Reference(s)
Body fossil		Ostracoda	*Cytheropteron tenuialatum*	1	Late Pleistocene–Holocene	Mound C (site 25), Porcupine Basin, offshore west of Ireland		650–1000 m	Coles et al. (1996)
Body fossil		Ostracoda	*Cytheropteron* spp.	4	Late Pleistocene–Holocene	Mound C (site 25), Porcupine Basin, offshore west of Ireland		650–1000 m	Coles et al. (1996)
Body fossil		Ostracoda	*Echinocythereis laticarinata*	230	Late Pleistocene–Holocene	Mound C (site 25), Porcupine Basin, offshore west of Ireland		650–1000 m	Coles et al. (1996)
Body fossil		Ostracoda	*Hemiparacytheridea variabile*	4	Late Pleistocene–Holocene	Mound C (site 25), Porcupine Basin, offshore west of Ireland		650–1000 m	Coles et al. (1996)
Body fossil		Ostracoda	*Henryhowella* gr. *asperrima*	60	Late Pleistocene–Holocene	Mound C (site 25), Porcupine Basin, offshore west of Ireland		650–1000 m	Coles et al. (1996)
Body fossil		Ostracoda	*Hermanites* cf. *H. haidingeri*	1	Late Pleistocene–Holocene	Mound C (site 25), Porcupine Basin, offshore west of Ireland		650–1000 m	Coles et al. (1996)
Body fossil		Ostracoda	*Kangarina abyssicola*	2	Late Pleistocene–Holocene	Mound C (site 25), Porcupine Basin, offshore west of Ireland		650–1000 m	Coles et al. (1996)
Body fossil		Ostracoda	*Krithe aquilonia*	124	Late Pleistocene–Holocene	Mound C (site 25), Porcupine Basin, offshore west of Ireland		650–1000 m	Coles et al. (1996)

Body fossil		Ostracoda	*Krithe keijii*	8	Late Pleistocene–Holocene	Mound C (site 25), Porcupine Basin, offshore west of Ireland		650–1000 m	Coles et al. (1996)
Body fossil		Ostracoda	*Krithe morkhoveni*	12	Late Pleistocene–Holocene	Mound C (site 25), Porcupine Basin, offshore west of Ireland		650–1000 m	Coles et al. (1996)
Body fossil		Ostracoda	*Krithe praetexta*	10	Late Pleistocene–Holocene	Mound C (site 25), Porcupine Basin, offshore west of Ireland		650–1000 m	Coles et al. (1996)
Body fossil		Ostracoda	*Krithe* juveniles	203	Late Pleistocene–Holocene	Mound C (site 25), Porcupine Basin, offshore west of Ireland		650–1000 m	Coles et al. (1996)
Body fossil		Ostracoda	*Loxocauda* cf. *L. decipiens*	2	Late Pleistocene–Holocene	Mound C (site 25), Porcupine Basin, offshore west of Ireland		650–1000 m	Coles et al. (1996)
Body fossil		Ostracoda	*Macrocypris* spp.	1	Late Pleistocene–Holocene	Mound C (site 25), Porcupine Basin, offshore west of Ireland		650–1000 m	Coles et al. (1996)
Body fossil		Ostracoda	*Macrocythere* cf. *M. depressa*	1	Late Pleistocene–Holocene	Mound C (site 25), Porcupine Basin, offshore west of Ireland		650–1000 m	Coles et al. (1996)
Body fossil		Ostracoda	*Monoceratina* n. sp.	69	Late Pleistocene–Holocene	Mound C (site 25), Porcupine Basin, offshore west of Ireland		650–1000 m	Coles et al. (1996)
Body fossil		Ostracoda	*Muellerina abyssicola*	4	Late Pleistocene–Holocene	Mound C (site 25), Porcupine Basin, offshore west of Ireland		650–1000 m	Coles et al. (1996)

(continued)

Table 5.1 (continued)

Type of evidence	Repair scar in	Class	Lowest possible rank/ name	Number of specimens	Age	Locality	Stratigraphic unit	Paleobathymetry	Reference(s)
Body fossil		Ostracoda	*Neonesidea inflata*	51	Late Pleistocene–Holocene	Mound C (site 25), Porcupine Basin, offshore west of Ireland		650–1000 m	Coles et al. (1996)
Body fossil		Ostracoda	*Paracytherois flexuosa*	16	Late Pleistocene–Holocene	Mound C (site 25), Porcupine Basin, offshore west of Ireland		650–1000 m	Coles et al. (1996)
Body fossil		Ostracoda	*Paracytherois* spp.	12	Late Pleistocene–Holocene	Mound C (site 25), Porcupine Basin, offshore west of Ireland		650–1000 m	Coles et al. (1996)
Body fossil		Ostracoda	*Paradoxostoma normani*	3	Late Pleistocene–Holocene	Mound C (site 25), Porcupine Basin, offshore west of Ireland		650–1000 m	Coles et al. (1996)
Body fossil		Ostracoda	*Paradoxostoma* gr. *variabile*	3	Late Pleistocene–Holocene	Mound C (site 25), Porcupine Basin, offshore west of Ireland		650–1000 m	Coles et al. (1996)
Body fossil		Ostracoda	*Propontocypris trigonella*	10	Late Pleistocene–Holocene	Mound C (site 25), Porcupine Basin, offshore west of Ireland		650–1000 m	Coles et al. (1996)
Body fossil		Ostracoda	*Pseudocythere* gr. *caudata*	22	Late Pleistocene–Holocene	Mound C (site 25), Porcupine Basin, offshore west of Ireland		650–1000 m	Coles et al. (1996)
Body fossil		Ostracoda	*Sclerochilus* gr. *contortus*	46	Late Pleistocene–Holocene	Mound C (site 25), Porcupine Basin, offshore west of Ireland		650–1000 m	Coles et al. (1996)

Body fossil		Ostracoda	*Semicytherura* sp.	1	Late Pleistocene–Holocene	Mound C (site 25), Porcupine Basin, offshore west of Ireland		650–1000 m	Coles et al. (1996)
Body fossil		Ostracoda	*Thaerocythere crenulata*	13	Late Pleistocene–Holocene	Mound C (site 25), Porcupine Basin, offshore west of Ireland		650–1000 m	Coles et al. (1996)
Body fossil		Ostracoda	*Typhlocythere ruggieri*	1	Late Pleistocene–Holocene	Mound C (site 25), Porcupine Basin, offshore west of Ireland		650–1000 m	Coles et al. (1996)
Body fossil		Ostracoda	ostracod indet.	1	Late Pleistocene–Holocene	Mound C (site 25), Porcupine Basin, offshore west of Ireland		650–1000 m	Coles et al. (1996)
Body fossil		Ostracoda	*Argilloecia conoidea*	2	Late Pleistocene–Holocene	Mound D (site 81), Porcupine Basin, offshore west of Ireland		650–1000 m	Coles et al. (1996)
Body fossil		Ostracoda	*Argilloecia cylindrica*	2	Late Pleistocene–Holocene	Mound D (site 81), Porcupine Basin, offshore west of Ireland		650–1000 m	Coles et al. (1996)
Body fossil		Ostracoda	*Argilloecia* spp.	1	Late Pleistocene–Holocene	Mound D (site 81), Porcupine Basin, offshore west of Ireland		650–1000 m	Coles et al. (1996)
Body fossil		Ostracoda	*Buntonia textilis*	1	Late Pleistocene–Holocene	Mound D (site 81), Porcupine Basin, offshore west of Ireland		650–1000 m	Coles et al. (1996)
Body fossil		Ostracoda	*Bythocypris affinis*	22	Late Pleistocene–Holocene	Mound D (site 81), Porcupine Basin, offshore west of Ireland		650–1000 m	Coles et al. (1996)

(continued)

Table 5.1 (continued)

Type of evidence	Repair scar in	Class	Lowest possible rank/ name	Number of specimens	Age	Locality	Stratigraphic unit	Paleobathymetry	Reference(s)
Body fossil		Ostracoda	*Bythocypris tenera*	10	Late Pleistocene–Holocene	Mound D (site 81), Porcupine Basin, offshore west of Ireland		650–1000 m	Coles et al. (1996)
Body fossil		Ostracoda	*Cytherella serratula*	9	Late Pleistocene–Holocene	Mound D (site 81), Porcupine Basin, offshore west of Ireland		650–1000 m	Coles et al. (1996)
Body fossil		Ostracoda	*Cytheropteron inflatum*	44	Late Pleistocene–Holocene	Mound D (site 81), Porcupine Basin, offshore west of Ireland		650–1000 m	Coles et al. (1996)
Body fossil		Ostracoda	*Cytheropteron* gr. *punctatum*	3	Late Pleistocene–Holocene	Mound D (site 81), Porcupine Basin, offshore west of Ireland		650–1000 m	Coles et al. (1996)
Body fossil		Ostracoda	*Cytheropteron* cf. *C. abyssorum*	5	Late Pleistocene–Holocene	Mound D (site 81), Porcupine Basin, offshore west of Ireland		650–1000 m	Coles et al. (1996)
Body fossil		Ostracoda	*Cytheropteron* spp.	9	Late Pleistocene–Holocene	Mound D (site 81), Porcupine Basin, offshore west of Ireland		650–1000 m	Coles et al. (1996)
Body fossil		Ostracoda	*Echinocythereis echinata*	3	Late Pleistocene–Holocene	Mound D (site 81), Porcupine Basin, offshore west of Ireland		650–1000 m	Coles et al. (1996)
Body fossil		Ostracoda	*Henryhowella* gr. *asperrima*	3	Late Pleistocene–Holocene	Mound D (site 81), Porcupine Basin, offshore west of Ireland		650–1000 m	Coles et al. (1996)

Body fossil		Ostracoda	*Kangarina abyssicola*	5	Late Pleistocene–Holocene	Mound D (site 81), Porcupine Basin, offshore west of Ireland		650–1000 m	Coles et al. (1996)
Body fossil		Ostracoda	*Krithe aquilonia*	41	Late Pleistocene–Holocene	Mound D (site 81), Porcupine Basin, offshore west of Ireland		650–1000 m	Coles et al. (1996)
Body fossil		Ostracoda	*Krithe dohchodeira*	31	Late Pleistocene–Holocene	Mound D (site 81), Porcupine Basin, offshore west of Ireland		650–1000 m	Coles et al. (1996)
Body fossil		Ostracoda	*Krithe morkhoveni*	1	Late Pleistocene–Holocene	Mound D (site 81), Porcupine Basin, offshore west of Ireland		650–1000 m	Coles et al. (1996)
Body fossil		Ostracoda	*Krithe* spp.	4	Late Pleistocene–Holocene	Mound D (site 81), Porcupine Basin, offshore west of Ireland		650–1000 m	Coles et al. (1996)
Body fossil		Ostracoda	*Krithe* juveniles	143	Late Pleistocene–Holocene	Mound D (site 81), Porcupine Basin, offshore west of Ireland		650–1000 m	Coles et al. (1996)
Body fossil		Ostracoda	*Monoceratina* n. sp.	3	Late Pleistocene–Holocene	Mound D (site 81), Porcupine Basin, offshore west of Ireland		650–1000 m	Coles et al. (1996)
Body fossil		Ostracoda	*Muellerina abyssicola*	242	Late Pleistocene–Holocene	Mound D (site 81), Porcupine Basin, offshore west of Ireland		650–1000 m	Coles et al. (1996)
Body fossil		Ostracoda	*Paracytherois flexuosa*	5	Late Pleistocene–Holocene	Mound D (site 81), Porcupine Basin, offshore west of Ireland		650–1000 m	Coles et al. (1996)

(continued)

Table 5.1 (continued)

Type of evidence	Repair scar in	Class	Lowest possible rank/ name	Number of specimens	Age	Locality	Stratigraphic unit	Paleobathymetry	Reference(s)
Body fossil		Ostracoda	*Paradoxostoma* gr. *variabile*	1	Late Pleistocene–Holocene	Mound D (site 81), Porcupine Basin, offshore west of Ireland		650–1000 m	Coles et al. (1996)
Body fossil		Ostracoda	*Propontocypris trigonella*	2	Late Pleistocene–Holocene	Mound D (site 81), Porcupine Basin, offshore west of Ireland		650–1000 m	Coles et al. (1996)
Body fossil		Ostracoda	*Pseudocythere* gr. *caudata*	1	Late Pleistocene–Holocene	Mound D (site 81), Porcupine Basin, offshore west of Ireland		650–1000 m	Coles et al. (1996)
Body fossil		Ostracoda	*Sclerochilus* gr. *contortus*	11	Late Pleistocene–Holocene	Mound D (site 81), Porcupine Basin, offshore west of Ireland		650–1000 m	Coles et al. (1996)
Body fossil		Ostracoda	*Sclerochilus* sp.	2	Late Pleistocene–Holocene	Mound D (site 81), Porcupine Basin, offshore west of Ireland		650–1000 m	Coles et al. (1996)
Body fossil		Ostracoda	*Thaerocythere crenulata*	55	Late Pleistocene–Holocene	Mound D (site 81), Porcupine Basin, offshore west of Ireland		650–1000 m	Coles et al. (1996)
Body fossil		Ostracoda	*Typhlocythere ruggieri*	3	Late Pleistocene–Holocene	Mound D (site 81), Porcupine Basin, offshore west of Ireland		650–1000 m	Coles et al. (1996)
Body fossil		Ostracoda	*Argilloecia acuminata*	5	Late Pleistocene–Holocene	Mound A (sites 40–41), Porcupine Basin, offshore west of Ireland		650–1000 m	Coles et al. (1996)

Body fossil		Ostracoda	*Argilloecia conoidea*	11	Late Pleistocene–Holocene	Mound A (sites 40–41), Porcupine Basin, offshore west of Ireland		650–1000 m	Coles et al. (1996)
Body fossil		Ostracoda	*Argilloecia cylindrica*	4	Late Pleistocene–Holocene	Mound A (sites 40–41), Porcupine Basin, offshore west of Ireland		650–1000 m	Coles et al. (1996)
Body fossil		Ostracoda	*Argilloecia* spp.	10	Late Pleistocene–Holocene	Mound A (sites 40–41), Porcupine Basin, offshore west of Ireland		650–1000 m	Coles et al. (1996)
Body fossil		Ostracoda	*Buntonia* sp.	1	Late Pleistocene–Holocene	Mound A (sites 40–41), Porcupine Basin, offshore west of Ireland		650–1000 m	Coles et al. (1996)
Body fossil		Ostracoda	*Bythocypris affinis*	10	Late Pleistocene–Holocene	Mound A (sites 40–41), Porcupine Basin, offshore west of Ireland		650–1000 m	Coles et al. (1996)
Body fossil		Ostracoda	*Bythocypris tenera*	12	Late Pleistocene–Holocene	Mound A (sites 40–41), Porcupine Basin, offshore west of Ireland		650–1000 m	Coles et al. (1996)
Body fossil		Ostracoda	*Bythocythere dromedaria*	1	Late Pleistocene–Holocene	Mound A (sites 40–41), Porcupine Basin, offshore west of Ireland		650–1000 m	Coles et al. (1996)
Body fossil		Ostracoda	*Cytherella serratula*	1	Late Pleistocene–Holocene	Mound A (sites 40–41), Porcupine Basin, offshore west of Ireland		650–1000 m	Coles et al. (1996)
Body fossil		Ostracoda	*Cytheropteron carolinae*	1	Late Pleistocene–Holocene	Mound A (sites 40–41), Porcupine Basin, offshore west of Ireland		650–1000 m	Coles et al. (1996)

(continued)

Table 5.1 (continued)

Type of evidence	Repair scar in	Class	Lowest possible rank/ name	Number of specimens	Age	Locality	Stratigraphic unit	Paleobathymetry	Reference(s)
Body fossil		Ostracoda	*Cytheropteron inflatum*	25	Late Pleistocene–Holocene	Mound A (sites 40–41), Porcupine Basin, offshore west of Ireland		650–1000 m	Coles et al. (1996)
Body fossil		Ostracoda	*Cytheropteron inornatum*	1	Late Pleistocene–Holocene	Mound A (sites 40–41), Porcupine Basin, offshore west of Ireland		650–1000 m	Coles et al. (1996)
Body fossil		Ostracoda	*Cytheropteron* gr. *punctatum*	9	Late Pleistocene–Holocene	Mound A (sites 40–41), Porcupine Basin, offshore west of Ireland		650–1000 m	Coles et al. (1996)
Body fossil		Ostracoda	*Cytheropteron testudo*	5	Late Pleistocene–Holocene	Mound A (sites 40–41), Porcupine Basin, offshore west of Ireland		650–1000 m	Coles et al. (1996)
Body fossil		Ostracoda	*Cytheropteron vespertilio*	1	Late Pleistocene–Holocene	Mound A (sites 40–41), Porcupine Basin, offshore west of Ireland		650–1000 m	Coles et al. (1996)
Body fossil		Ostracoda	*Cytheropteron tenuialatum*	11	Late Pleistocene–Holocene	Mound A (sites 40–41), Porcupine Basin, offshore west of Ireland		650–1000 m	Coles et al. (1996)
Body fossil		Ostracoda	*Cytheropteron* spp.	4	Late Pleistocene–Holocene	Mound A (sites 40–41), Porcupine Basin, offshore west of Ireland		650–1000 m	Coles et al. (1996)
Body fossil		Ostracoda	*Echinocythereis laticarinata*	13	Late Pleistocene–Holocene	Mound A (sites 40–41), Porcupine Basin, offshore west of Ireland		650–1000 m	Coles et al. (1996)

Body fossil		Ostracoda	*Eucythere* sp.	1	Late Pleistocene–Holocene	Mound A (sites 40–41), Porcupine Basin, offshore west of Ireland		650–1000 m	Coles et al. (1996)
Body fossil		Ostracoda	*Eucytherura calabra*	1	Late Pleistocene–Holocene	Mound A (sites 40–41), Porcupine Basin, offshore west of Ireland		650–1000 m	Coles et al. (1996)
Body fossil		Ostracoda	*Henryhowella* gr. *asperrima*	14	Late Pleistocene–Holocene	Mound A (sites 40–41), Porcupine Basin, offshore west of Ireland		650–1000 m	Coles et al. (1996)
Body fossil		Ostracoda	*Henryhowella* gr. *asperrima*	2	Late Pleistocene–Holocene	Mound A (sites 40–41), Porcupine Basin, offshore west of Ireland		650–1000 m	Coles et al. (1996)
Body fossil		Ostracoda	*Kangarina abyssicola*	1	Late Pleistocene–Holocene	Mound A (sites 40–41), Porcupine Basin, offshore west of Ireland		650–1000 m	Coles et al. (1996)
Body fossil		Ostracoda	*Krithe aquilonia*	40	Late Pleistocene–Holocene	Mound A (sites 40–41), Porcupine Basin, offshore west of Ireland		650–1000 m	Coles et al. (1996)
Body fossil		Ostracoda	*Krithe dohchodeira*	4	Late Pleistocene–Holocene	Mound A (sites 40–41), Porcupine Basin, offshore west of Ireland		650–1000 m	Coles et al. (1996)
Body fossil		Ostracoda	*Krithe* juveniles	89	Late Pleistocene–Holocene	Mound A (sites 40–41), Porcupine Basin, offshore west of Ireland		650–1000 m	Coles et al. (1996)
Body fossil		Ostracoda	*Macrocypris* spp.	1	Late Pleistocene–Holocene	Mound A (sites 40–41), Porcupine Basin, offshore west of Ireland		650–1000 m	Coles et al. (1996)

(continued)

Table 5.1 (continued)

Type of evidence	Repair scar in	Class	Lowest possible rank/ name	Number of specimens	Age	Locality	Stratigraphic unit	Paleobathymetry	Reference(s)
Body fossil		Ostracoda	*Microceratina poligonia*	1	Late Pleistocene–Holocene	Mound A (sites 40–41), Porcupine Basin, offshore west of Ireland		650–1000 m	Coles et al. (1996)
Body fossil		Ostracoda	*Monoceratina insignis*	2	Late Pleistocene–Holocene	Mound A (sites 40–41), Porcupine Basin, offshore west of Ireland		650–1000 m	Coles et al. (1996)
Body fossil		Ostracoda	*Monoceratina* n. sp.	26	Late Pleistocene–Holocene	Mound A (sites 40–41), Porcupine Basin, offshore west of Ireland		650–1000 m	Coles et al. (1996)
Body fossil		Ostracoda	*Muellerina abyssicola*	1	Late Pleistocene–Holocene	Mound A (sites 40–41), Porcupine Basin, offshore west of Ireland		650–1000 m	Coles et al. (1996)
Body fossil		Ostracoda	*Neonesidea inflata*	5	Late Pleistocene–Holocene	Mound A (sites 40–41), Porcupine Basin, offshore west of Ireland		650–1000 m	Coles et al. (1996)
Body fossil		Ostracoda	*Paracytherois flexuosa*	5	Late Pleistocene–Holocene	Mound A (sites 40–41), Porcupine Basin, offshore west of Ireland		650–1000 m	Coles et al. (1996)
Body fossil		Ostracoda	*Paradoxostoma normani*	262	Late Pleistocene–Holocene	Mound A (sites 40–41), Porcupine Basin, offshore west of Ireland		650–1000 m	Coles et al. (1996)
Body fossil		Ostracoda	*Paradoxostoma* gr. *variabile*	3	Late Pleistocene–Holocene	Mound A (sites 40–41), Porcupine Basin, offshore west of Ireland		650–1000 m	Coles et al. (1996)

Body fossil		Ostracoda	*Paradoxostoma* spp.	3	Late Pleistocene–Holocene	Mound A (sites 40–41), Porcupine Basin, offshore west of Ireland		650–1000 m	Coles et al. (1996)
Body fossil		Ostracoda	*Polycope orbicularis*	1	Late Pleistocene–Holocene	Mound A (sites 40–41), Porcupine Basin, offshore west of Ireland		650–1000 m	Coles et al. (1996)
Body fossil		Ostracoda	*Propontocypris trigonella*	2	Late Pleistocene–Holocene	Mound A (sites 40–41), Porcupine Basin, offshore west of Ireland		650–1000 m	Coles et al. (1996)
Body fossil		Ostracoda	*Pseudocythere* gr. *caudata*	15	Late Pleistocene–Holocene	Mound A (sites 40–41), Porcupine Basin, offshore west of Ireland		650–1000 m	Coles et al. (1996)
Body fossil		Ostracoda	*Sclerochilus* gr. *contortus*	9	Late Pleistocene–Holocene	Mound A (sites 40–41), Porcupine Basin, offshore west of Ireland		650–1000 m	Coles et al. (1996)
Body fossil		Ostracoda	*Sclerochilus* sp.	3	Late Pleistocene–Holocene	Mound A (sites 40–41), Porcupine Basin, offshore west of Ireland		650–1000 m	Coles et al. (1996)
Body fossil		Ostracoda	*Thaerocythere crenulata*	7	Late Pleistocene–Holocene	Mound A (sites 40–41), Porcupine Basin, offshore west of Ireland		650–1000 m	Coles et al. (1996)
Body fossil		Ostracoda	ostracod indet.	1	Late Pleistocene–Holocene	Mound A (sites 40–41), Porcupine Basin, offshore west of Ireland		650–1000 m	Coles et al. (1996)

2005) and varying preservation potentials within marine arthropods (Klompmaker et al. 2017). One of us (JB) found that only 12/168 (7%) of Late Cretaceous seeps in South Dakota, USA, contained brachyuran decapods, but not all seeps were sampled exhaustively nor were decapods targeted. Amphipoda, Cumacea, and Copepoda have not been in the found fossil seeps because many are comparatively soft-bodied, small, and fragile (e.g., Selden et al. 2010). Isopods, found in concretions, appear to have been living close to seeps during the early Oligocene in Washington State, USA (Wieder and Feldmann 1989; Goedert and Campbell 1995), but confirmed occurrences from within seep limestone bodies are unknown to us.

Research on crustaceans from cold seep deposits has increased markedly; few papers are known to us from before the 1990s, but since then the number of papers per decade has been increasing steadily with a record of 39 papers in the previous decade (Fig. 5.2). This trend exemplifies the increasing interest in and recognition of fossil cold seeps in general.

Crustaceans in fossil seeps are mainly reported from Europe and the United States thus far (89% of occurrences, Fig. 5.3), which is at least in part a reporting bias as is known for marine invertebrates in general (e.g., Wall et al. 2009). Other occurrences are known from New Zealand, Japan, Morocco, South America, Antarctica, Spitsbergen, Greenland, and Nova Zembla (Fig. 5.3). Most occurrences are found close to current or former convergent plate boundaries or fault zones.

Stratigraphically, most occurrences are found in Cretaceous–Quaternary carbonate rocks (Fig. 5.4). Occurrences are primarily based on body fossils (89%), although coprolites, burrows, and repair scars can be common in certain periods (Fig. 5.4a). Focusing on localities rather than occurrences shows that the Cretaceous–Neogene yields the most crustacean-bearing localities thus far (Fig. 5.4c). Once again, body fossils are the dominant type of crustacean evidence reported (75%). Occurrences are dominated by podocopid ostracods, while decapod crustaceans make up the most records in localities (Figs. 5.4b and 5.5d). The difference is due to data in Coles et al. (1996), who reported many Quaternary ostracod occurrences from four localities west of Ireland. Numerically, ostracod specimens are the dominant crustaceans reported in fossil cold seeps, with 3411 ostracod specimens compared to the 631 specimens of decapod malacostracans.

The degree to which identification of crustaceans in fossil seeps to lower taxonomic ranks is possible varies per clade. For ostracods, the taxonomy has been well-resolved for occurrences in three major studies (Coles et al. 1996; Russo et al. 2012; Yamaguchi et al. 2016). Ninety-four percent of ostracod body fossil occurrences are identified to at least the genus level and 73% to the species level. Conversely, identifications to the genus and species level of 53% and 38%, respectively, are found for decapod body fossils. The fact that ostracods are generally more complete in seep limestones may explain this difference.

The rate at which decapods can be found at fossil cold seeps has only been quantified for the so-called Late Cretaceous tepee buttes in South Dakota and Colorado, USA. Bishop and Williams (2000) found 21 brachyuran specimens in 73 working days. Assuming a work day of 8 h, this results in an average rate of 0.04 crab specimens per hour. This low number is not representative for decapods in all seeps, in part because ghost shrimps are not included and because some seeps are much

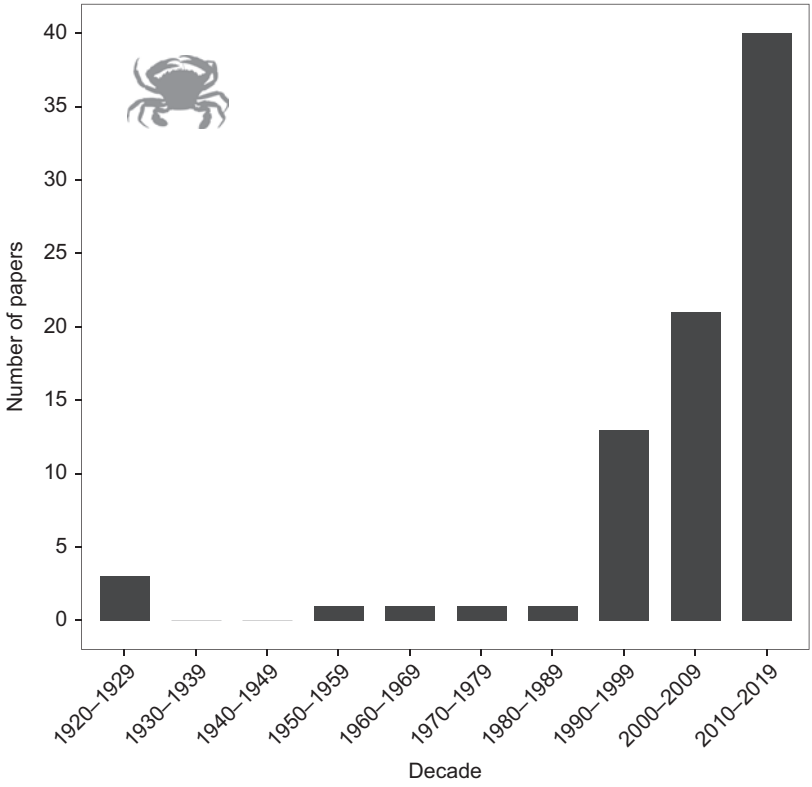

Fig. 5.2 The number of papers including fossil crustaceans in cold seeps over the last 100 years

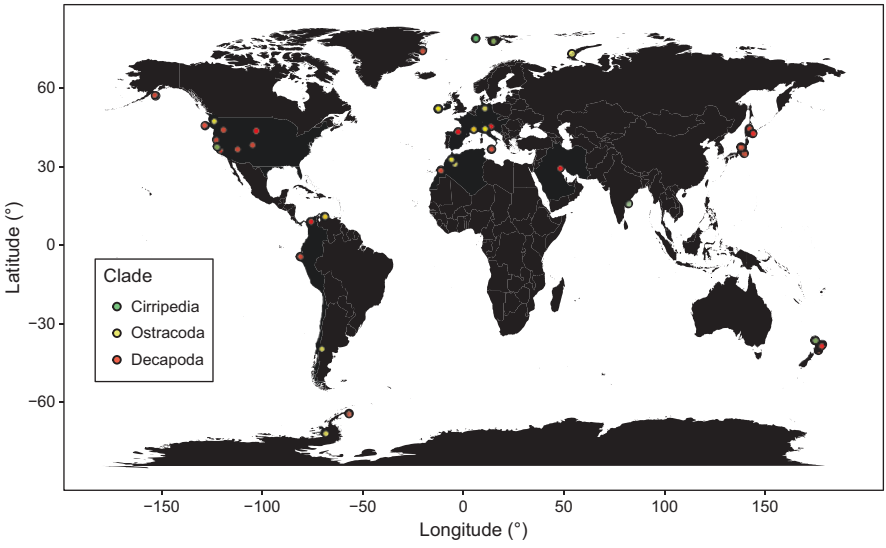

Fig. 5.3 Fossil cold seep localities containing crustaceans per taxonomic class around the world. A color transparency of 0.8 is used for each dot to highlight areas in which more occurrences have been found

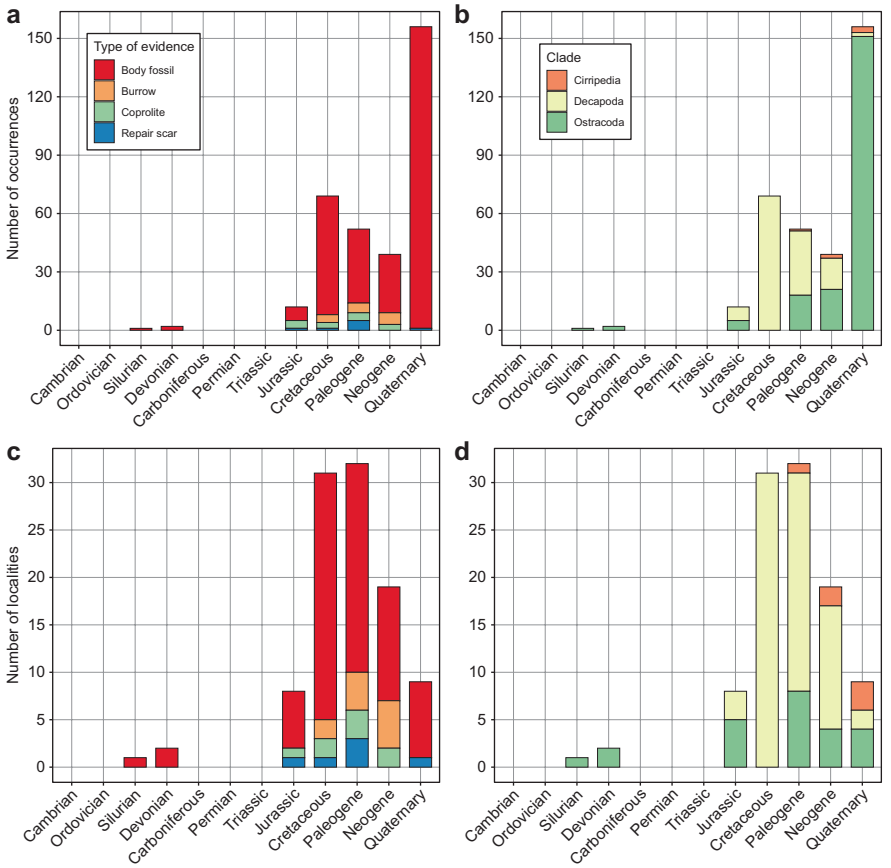

Fig. 5.4 The number of occurrences and localities of crustaceans in cold seeps for each Phanerozoic period per type of evidence and per clade. (**a**) Number of occurrences per type of evidence. (**b**) Number of occurrences per clade. (**c**) Number of localities per type of evidence. (**d**) Number of localities per clade

richer in decapods than others (pers. obs. AAK). The other extreme is the very high abundance of *Shinkaia katapsyxis* in an Eocene cold seep in Washington State, which may not be surprising because congenerics can be very abundant at modern seeps (see Fig. 5.5 for comparison). Schweitzer and Feldmann (2008) reported 112 carapaces, 107 claw pairs, and tens of pereiopods remains in just 22 kg of carbonate rock, although admittedly these rocks were probably selected for decapod remains. For comparison, the decapod-rich mid-Cretaceous coral-algal reef deposits from Koskobilo in Spain yielded 235 decapods in 36 h or 6.5 specimens per hour (Klompmaker et al. 2013a), while Danian coral-bryozoan limestones in Denmark yielded 209 specimens (Klompmaker et al. 2016) in 27 h or 7.7 specimens per hour (2014 field notes AAK).

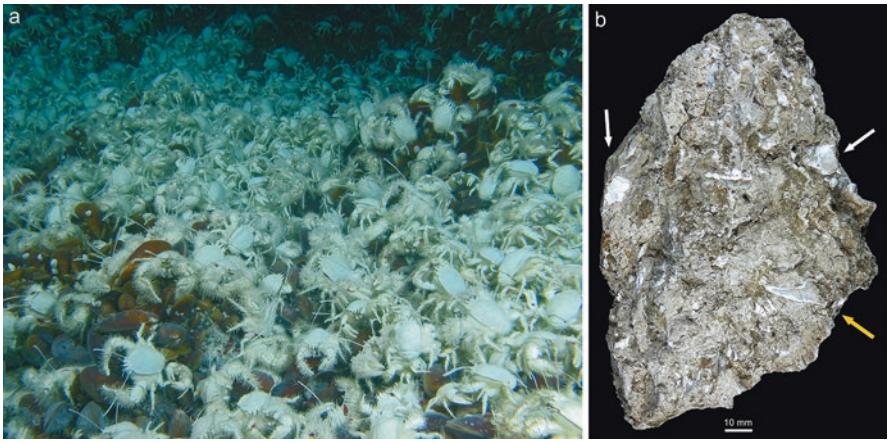

Fig. 5.5 The munidopsid squat lobster *Shinkaia* from modern and fossil cold seeps. (**a**) Mass occurrence of the extant *Shinkaia crosnieri* at the Formosa Ridge in the South China Sea at a depth of 1126 m. Image is taken by the JAMSTEC ROV during a cold seep cruise in 2007 (credit: JAMSTEC and TORI). (**b**) A carbonate rock sample (UCMP 220896) of the Eocene Humptulips Formation of Washington, USA, exemplifying the abundance of the squat lobster *Shinkaia katapsyxis*. White arrows point to carapaces, while the orange arrow is directed toward a fixed finger. Other white parts on the rock surface without an arrow represent appendage fragments

5.3 Decapod Crustaceans

5.3.1 Modern Occurrences and Composition

Extant decapod crustaceans are found in seeps worldwide. The review articles by Chevaldonné and Olu (1996) and Martin and Haney (2005) that include decapod crustaceans in cold seeps and subsequent studies on cold seep faunas show that seeps with decapods are primarily found in the Gulf of Mexico (Komai and Segonzac 2005; Cordes et al. 2010a; Coykendall et al. 2017), along the west coast of North America (Sakai and Türkay 1999; Levin et al. 2000, 2015; Levin and Michener 2002; Niemann et al. 2013), in the northwestern Pacific (Chevaldonné and Olu 1996; Fujikura et al. 2002; Sahling et al. 2003; Dong and Li 2015), and New Zealand (Ahyong 2008; Baco et al. 2010). Other occurrences, for example, include Congo (Macpherson and Segonzac 2005), Chile (Sellanes et al. 2008), Turkey (Olu-Le Roy et al. 2004), Brazil (Fujikura et al. 2017), the east coast of North America (Van Dover et al. 2003), Barbados (Olu et al. 1996), Spain (Dworschak and Cunha 2007; Hyžný and Gašparič 2014), in the North Sea (Dando et al. 1991), and Denmark (Jensen et al. 1992).

Martin and Haney (2005) reported 125 species found in vent and seep environments, of which over 30 are known from cold seeps. Decapods in cold seeps are represented mainly by squat lobsters (Galatheoidea and some Chirostyloidea), king or stone crabs (Lithodidae), true crabs (Brachyura), and shrimps (Caridea, mostly

Alvinocaris spp., and some Dendrobranchiata) (Chevaldonné and Olu 1996; Martin and Haney 2005). Less commonly reported are burrowing shrimps (Axiidea), hermit crabs (Paguroidea), and lobsters (Astacidea and Polychelida) (Chevaldonné and Olu 1996; Martin and Haney 2005; Sellanes et al. 2008). Endemicity is low among seep decapods (Macpherson and Segonzac 2005; Martin and Haney 2005; Sellanes et al. 2008).

5.3.2 Biology

Squat lobsters (Galatheoidea and some Chirostyloidea) are predominantly epifaunal benthics with a varied diet. They are suspension and deposit feeders, predators including some cannibals, and scavengers, while others consume algae (Lovrich and Thiel 2011). Taxa that live in cold seeps have a varied diet as well. Some seep galatheoids appear to be predators on small heterotrophs and scavengers (Chevaldonné and Olu 1996; MacAvoy et al. 2008), while others may be deposit feeders based on stomach content (Macpherson and Segonzac 2005) or feed on bacteria (Barry et al. 1996). *Munidopsis* sp. from the Gulf of Mexico probably eats hydroids (Becker et al. 2009; Cordes et al. 2010c) and/or a barnacle and a caridean shrimp (Cordes et al. 2010c). Another species of *Munidopsis* may consume other decapods and worms (Cordes et al. 2010c). Isotopic evidence suggests that *Munidopsis* sp. from Alaska relies on chemosynthetically fixed carbon from tropic levels above the primary producers (Levin and Michener 2002). Some have a diet tied to the most abundant primary producers. *Shinkaia crosnieri* scrapes off epibiontic bacteria from their setae as a source of nutrition (Tsuchida et al. 2011), and the same applies for *Kiwa puravida* (Thurber et al. 2011). As for squat lobsters in general (Schweitzer and Feldmann 2010), seep squat lobsters probably did not break molluscan shells given their fairly small claws and their claw morphology.

The other group of anomurans often found in cold seeps, the king crabs (Lithodidae), are epifaunal taxa that prey on vesicomyid and mytilid bivalves and are also deposit-feeders (Hashimoto et al. 1989; Chevaldonné and Olu 1996; Barry et al. 1996). Hashimoto et al. (1989, Fig. 10) even showed king crabs fighting over a clam held by the chelipeds of one crab, and we here show a king crab holding a broken shell (Fig. 5.6). Although king crabs have a generalized diet, non-seep confamilials are suggested to be durophagous predators (Aronson et al. 2015); stomach content does frequently contain mollusks (Abelló 1995; Comoglio and Amin 1999), and experiments show that king crabs can crush mollusk shells (Jørgensen and Primicerio 2007). Lithodids prefer deep and cold waters; only a few taxa live in waters <200 m, and shallow-water occurrences are restricted to high latitudes (Hall and Thatje 2009a), both of which are related to a low tolerance of high temperatures (Hall and Thatje 2009a; Thatje and Hall 2016).

The true crabs (Brachyura) are represented by a variety of clades at cold seeps including members of Goneplacidae, Atelecyclidae, Cancridae, Homolodromiidae, Trichopeltariidae, Polybiidae, Mathildellidae, Geryonidae, and Majoidea (Dando

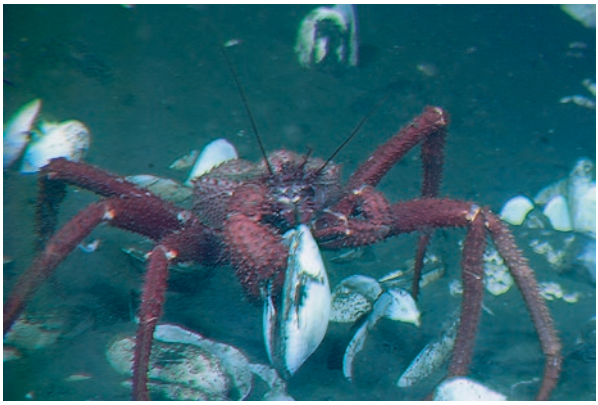

Fig. 5.6 The anomuran king crab *Paralomis multispina* feeding on a bivalve of which the left valve is already broken. Sagami Bay, Japan, 13 March 2006. (Credit: JAMSTEC)

et al. 1991; Jensen et al. 1992; Olu-Le Roy et al. 2004; Martin and Haney 2005; Ahyong 2008; Quattrini et al. 2015). These groups tend to be benthic crabs generally not capable of swimming (Hartnoll 1971) and burying/burrowing (Warner 1977; Bellwood 2002). A number of studies have shed light on the diet of crabs in seeps. One study from Monterey Bay seeps off California (Barry et al. 1996) suggested that the spider crab *Chionoecetes bairdi* preys on vesicomyid clams, while the other spider crab, *Chorilia longipes*, grazes on bacteria and clam siphons. Another study suggested that a congeneric from Oregon, *Chionoecetes tanneri*, is a carnivore on macrofauna (Levin and Michener 2002), but this taxon also directly feeds on seep bacteria and Archaea off the coast of British Columbia, Canada (Seabrook et al. 2019). Similarly, *Chionoecetes opilio* was observed to be grazing on cold seep bacterial mats in the Barents Sea in the Arctic (Sen et al. 2018). In the Gulf of Mexico, an atelecylid crab is heavily dependent on carbon from seeps (MacAvoy et al. 2002), while another study suggested a diet consisting of hydroids and a polychaete for this taxon (Cordes et al. 2010c). The spider crab *Rochinia crassa* was interpreted not to be a major shell-crusher, but would feed on thin-shelled mussels, gastropods, crustaceans, and hydroids instead (MacAvoy et al. 2002). Members of Goneplacidae, Cancridae, Mathildellidae, Geryonidae, and Majoidea are inferred to be durophagous (Schweitzer and Feldmann 2010) so it is likely that some crabs crushed bivalve shells at seeps. Most crab species (7) associated with seeps are described from New Zealand (Ahyong 2008), and the figured large claws of the males of *Trichopeltarion janetae*, *Neopilumnoplax nieli*, and *Pycnoplax victoriensis* appear suitable for crushing shells (his Figs. 8c, 15b, and 23c).

Shrimp occurrences in modern seep are dominated by members of Alvinocarididae from the genus *Alvinocaris*. These organisms live on the ocean floor as adults and are variously capable of swimming (Pond et al. 1997; Aguzzi et al. 2007). They are often found in high densities on bivalve beds in seeps (Olu et al. 1996; Van Dover

et al. 2003; Komai and Segonzac 2005; Ramirez-Llodra and Segonzac 2006). Substantial progress has been made to unravel the diet of *Alvinocaris*. The diet is best known for *Alvinocaris muricola*; analysis of stomach contents has revealed diatoms and Foraminifera (Komai and Segonzac 2005), but the same species is also a scavenger observed feeding on the tissue of mussels after their shells were broken by a submersible (Ramirez-Llodra and Segonzac 2006). Isotopic analyses of the same species and *A. stactophila* suggest a generalist feeding strategy for both, with low $\delta^{15}N$ values of *A. muricola* being attributed to a bacterial diet, while higher values for the same species may indicate feeding at higher trophic levels (meiofauna) or organic matter originating from surface waters (Becker et al. 2013). Previous isotopic analyses and subsequent modeling of food webs suggested that *Alvinocaris stactophila* most likely consumed hydroids and sabellid polychaetes and a number of other potential prey, indeed suggesting a generalist-type diet. Even more seems known about alvinocaridids from hydrothermal vents, whose feeding strategies differ from capturing bacteria, scavenging, and preying on confamilials (Pond et al. 1997; Polz et al. 1998; Gebruk et al. 2000; Stevens et al. 2008). Their small chelipeds do not seem suitable to break mollusk shells.

The Axiidea shrimps including ghost shrimps are known to burrow (Dworschak et al. 2012; Kornienko 2013; Hyžný and Klompmaker 2015). They have rarely been reported from modern seeps because they are difficult to observe and catch (Martin and Haney 2005) but are very commonly associated with fossil seeps (see below). Burrowing must be only possible in loose sediments away from the carbonate deposits. Very little is known about the diet of extant axiideans associated with seeps. The only remark we are aware of is by Felder and Kensley (2004), who hypothesized that *Calaxius carneyi* could feed on bacteria. Burrowing shrimps living elsewhere are primarily deposit and suspension feeders consuming detrital material, seaweed, algae, seagrass, and phytoplankton (Dworschak 1987; Stapleton et al. 2001; Shimoda et al. 2007; Kneer et al. 2008; Dworschak et al. 2012), with callianassids being predominantly deposit feeders. For now, we can only assume that the diet of seep axiids is similar to representatives living elsewhere in that small particles caught in suspension or in the substrate are the main source of nutrition. The rare presence of astacidean and polychelid lobsters and hermit crabs in seeps does not allow for meaningful generalizations about their diet in seeps.

5.3.3 Fossil Record and Evolution

5.3.3.1 Body Fossils

Squat lobsters (Galatheoidea and Chirostyloidea) are common in seeps today but are only reported from three fossil seep localities consisting of four occurrences so far (Figs. 5.7 and 5.8). *Shinkaia katapsyxis* is described from the Eocene of Washington State (Schweitzer and Feldmann 2008; Kiel 2010a), *Protomunida spitzbergica* and *Valamunida haeggi* were found in the late Paleocene of Spitsbergen

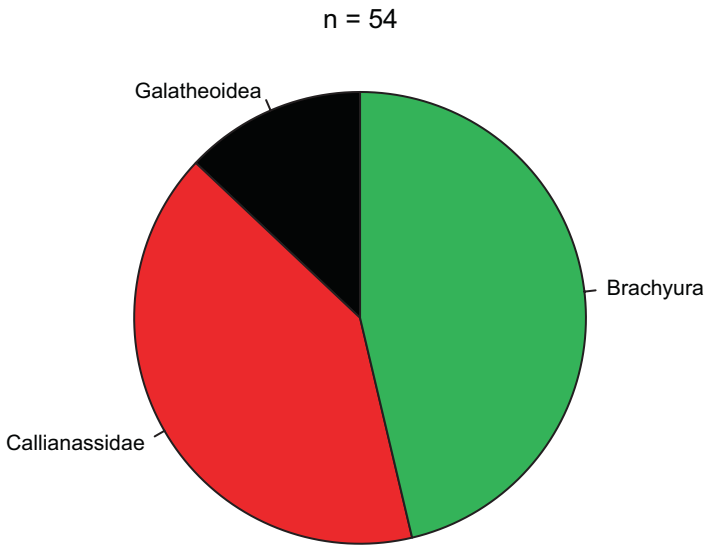

Fig. 5.7 Occurrence-based pie diagram of decapod body fossils in cold seeps

(Hägg 1925; Gripp 1927; Vonderbank 1970; Hryniewicz et al. 2016, 2019), and a likely galatheoid appendage was reported from the latest Jurassic–earliest Cretaceous (Tithonian-Berriasian) of again Spitsbergen (Hammer et al. 2011; Hryniewicz et al. 2015a). Galatheoids have a fossil record dating back to the Middle Jurassic (Bathonian) (Van Straelen 1925), with a major diversification in Late Jurassic shallow-water reefs in Europe (Robins et al. 2013, 2016; Robins and Klompmaker, 2019). Other diverse reef assemblages originate from the mid-Cretaceous of Spain (Klompmaker et al. 2012a) and the Eocene-Oligocene of Italy (De Angeli and Garassino 2002). Conversely, only two fossil species of Chirostyloidea have been confirmed: the Late Cretaceous *Pristinaspina gelasina* (Schweitzer and Feldmann 2000; Ahyong and Roterman 2014) from siliciclastic rocks of Alaska and the Eocene *Eouroptychus montemagrensis* from a coral limestone of Italy (De Angeli and Ceccon 2012). If the Tithonian–Berriasian seep decapod is indeed a galatheoid appendage, this diverse group inhabited cold seeps early on in their evolutionary history. Given their fossil record and fairly calcified cuticle, more fossil squat lobsters are expected from fossil cold seep deposits.

Among the other anomuran groups commonly present in modern seeps are king crabs (Lithodidae, phylogenetically nested within the Paguroidea (Noever and Glenner 2018; Hall and Thatje 2018)), but no fossil occurrences from seeps are known thus far. The total number of extant lithodid species known is more than 100, and they occur in predominantly deep water (Hall and Thatje 2009a, b). Only a limited number of fossil occurrences are known: *Paralomis debodeorum* from Middle to Late? Miocene in New Zealand (Feldmann 1998), *Paralithodes bishuensis* and *Paralomis* sp. from the Early Miocene of Japan (Takeda et al. 1986; Mizuno and Takeda 1993; Karasawa et al. 2017), and undetermined lithodid chelae from the

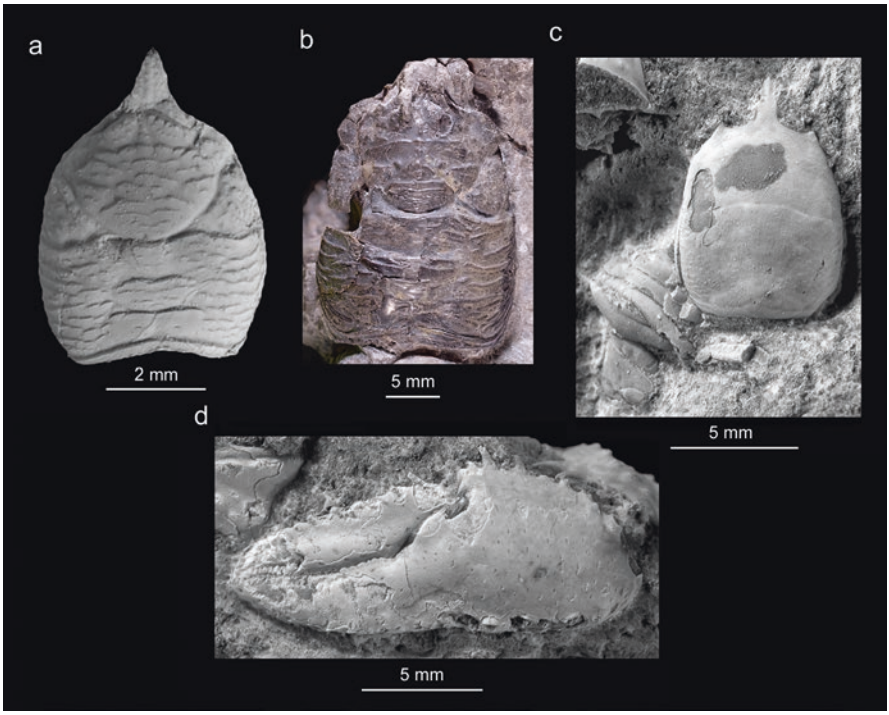

Fig. 5.8 Examples of Anomura including squat lobsters (Galatheoidea). (**a**) Dorsal carapace of the neotype of *Protomunida spitzbergica* (GPIBo 85) from the late Paleocene of Spitsbergen (from Hryniewicz et al. 2016, Fig. 12k). (**b**) Dorsal carapace of the holotype of *Valamunida haeggi* from the late Paleocene of Spitsbergen (from Hryniewicz et al. 2019, Fig. 21a$_1$). (**c**) Dorsal carapace and partial abdomen of *Shinkaia katapsyxis* (holotype, USNM 536286) from the earliest middle Eocene of Washington State, USA (from Schweitzer and Feldmann 2008, Fig. 2.1). (**d**) Outer surface of propodus and dactylus of *Shinkaia katapsyxis* (USNM 536298) from the earliest middle Eocene from Washington State, USA (from Schweitzer and Feldmann 2008, Fig. 3.7). Figure 5.8a, c, and d whitened prior to photography. For localities, see Table 5.1

Early? Miocene of southern Argentina (Feldmann et al. 2011). The age of these occurrences is consistent with estimates from molecular and morphological analyses suggesting an Early Miocene origin (Cunningham et al. 1992; Bracken-Grissom et al. 2013). Most fossil occurrences are from the Pacific, which may be consistent with their suggested divergence from shallow-water anomurans in the northern Pacific (Hall and Thatje 2009a; Noever and Glenner 2018). Thus, lithodids are also expected from late Cenozoic cold seeps around the Pacific, particularly given their relatively well-calcified cuticle. Hermit crabs (Paguroidea) have not been found in fossil cold seeps thus far.

A fair number of true crabs (Brachyura) have been found in fossil seeps so far (Figs. 5.7 and 5.9). One record, referred to a ?goneplacoid or a ?xanthoid (Kiel and Hansen 2015; Luque et al. 2017) is from the early Oligocene of Colombia, whereas four Late Cretaceous (Campanian–Maastrichtian) species from the so-called tepee

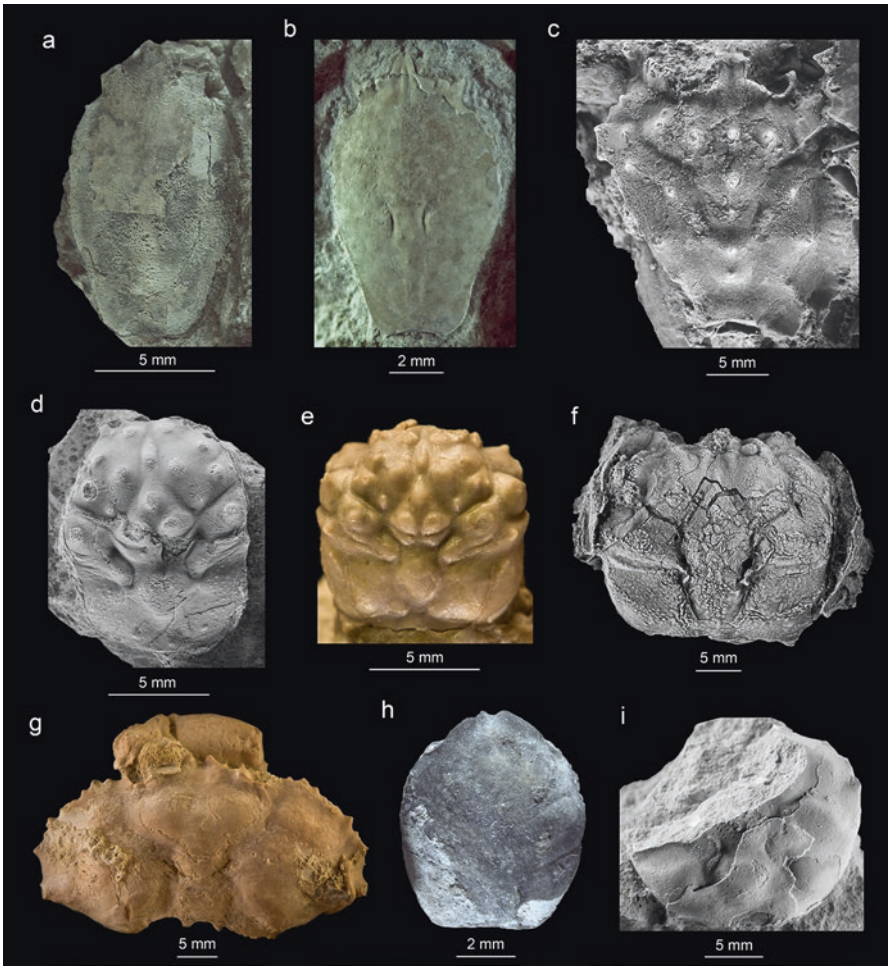

Fig. 5.9 Examples of true crabs (Brachyura) from fossil cold seeps. (**a**–**h**) New photos of specimens from South Dakota, USA. (**a**) Dorsal carapace of *Heus manningi* (holotype, SDSM 11018) from the Late Cretaceous (Campanian–Maastrichtian). (**b**) Dorsal carapace of *Heus foersteri* (paratype, SDSM 11017) from the Late Cretaceous (Campanian–Maastrichtian). (**c**) Partial dorsal carapace of *Elektrocarcinus pierrensis* (AMNH 82676) from the Late Cretaceous (late Campanian). (**d**) Dorsal carapace of *Latheticocarcinus punctatus* (AMNH 82677) from the Late Cretaceous (late Campanian). (**e**) Dorsal carapace of *Latheticocarcinus punctatus* with well-preserved sides (AMNH 82678) from the Late Cretaceous (late Campanian). (**f**) Dorsal carapace of *Dakoticancer overanus* (AMNH 82679) from the Late Cretaceous (late Campanian). (**g**) Dorsal carapace and associated appendage of *Secretanella spinosa* (AMNH 82680) from the Late Cretaceous (late Campanian). (**h**) Dorsal carapace of *Konidromites bjorki* (holotype, SDSM 11021) from the Late Cretaceous (Campanian–Maastrichtian). (**i**) Partial dorsal carapace of a possible goneplacoid or xanthoid crab (PRI 68650) from the early Oligocene of Colombia (from Kiel and Hansen 2015, Fig. 5g). Figures 5.9c, d, f, and i whitened prior to photography. For localities, see Table 5.1

buttes in South Dakota and Colorado have been reported (Bishop and Williams 2000; Meehan and Landman 2016). The latter include lyreidid frog crabs (*Heus foersteri* and *Heus manningi*), the homolid *Latheticocarcinus punctatus*, and the konidromitid *Konidromites bjorki*. New discoveries in seeps from South Dakota include the dakoticancrid *Dakoticancer overanus*, the etyid *Secretanella spinosa*, and the necrocarcinid *Elektrocarcinus pierrensis*. Lyreididae and Homolidae are extant, but do not occur in modern cold seeps (Martin and Haney 2005), whereas konidromitids, necrocarcinids, dakoticancrids, and etyids are extinct. The inferred depth from the Late Cretaceous seeps in South Dakota is 100–250 m (Meehan and Landman 2016) or <100 m (Meehan et al. 2018), an environment in which not many deep-sea decapods are to be expected. The lyreidid frog crabs have a morphology consistent with a burying behavior, implying that these decapods lived in soft sediments at or near the seep. Extant homolids are reported predominantly from waters between 200 and 500 m (Guinot and Richer de Forges 1995, Fig. 74), but they did occur frequently in shallower waters early in their evolutionary history in the Mesozoic (Schweitzer et al. 2004; Feldmann and Schweitzer 2009), probably including the seep record herein. The flat and wide carapace of *Secretanella spinosa* strongly suggests that it was a swimming crab and may have been an occasional inhabitant of seeps. Most recently, the epifaunal crab *Goniodromites* sp. was recorded from an early Late Cretaceous (Cenomanian) seep in Japan (Karasawa and Kano, 2021). Many more Brachyura are expected from fossil seeps because they are a common occurrence in modern seeps, have an extensive fossil record starting in the Jurassic (Klompmaker et al. 2013b; Schweitzer and Feldmann 2015), and have a relatively high preservation potential within the Arthropoda (Klompmaker et al. 2017).

No representatives of caridean shrimps assigned to Alvinocarididae have been found in fossil seeps, but some alvinocaridids (*Harthofia* spp.) have been reported from Late Jurassic thin-bedded limestones from Germany (Polz 2007; Schweigert 2011). The assignment of *Harthofia* to Alvinocarididae was, however, provisional (Polz 2007). Indeed, phylogenetic analyses suggest that Alvinocarididae is a derived rather than a basal clade (Bracken et al. 2009; Sudarsky 2016) and the group containing *Alvinocaris* would have radiated as late as the Miocene (Shank et al. 1999). Despite their abundance in modern seeps, it is unlikely that many if any remains will be found due to the low preservation potential of swimming shrimps (Plotnick 1986; Klompmaker et al. 2017).

While modern occurrences of burrowing shrimps (Axiidae and Gebiidea) from seeps are rare, they represent the most commonly found decapod body fossil in fossil seeps (Figs. 5.7 and 5.10). Claws of burrowing shrimps attributed to Axiidae are particularly found in the Cretaceous and Cenozoic, including (?*Proto)callianassa*, *Callianopsis*, *Calliax, Eucalliax*, *Glypturus*, and *Neocallichirus* (Peckmann et al. 2002, 2007b; Karasawa 2011; Larson et al. 2013; Agirrezabala et al. 2013; Kiel et al. 2013, 2020; Nesbitt et al. 2013; Natalicchio et al. 2015; Kiel and Hansen 2015) (Table 5.1). This difference is caused by the fact that burrowing shrimps are difficult to observe and collect in the ocean bottom today, requiring special extracting methods (Dworschak 2015). As for frog crabs, it is likely that they did not live within the

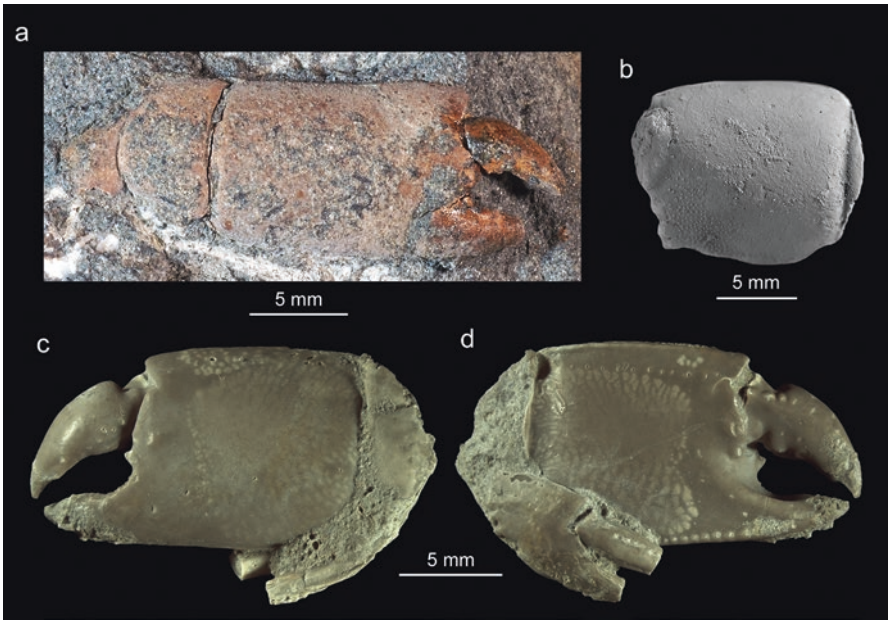

Fig. 5.10 Examples of Axiidea, here ghost shrimps (Callianassidae), from fossil cold seeps. (**a**) Outer surface of cheliped of *Callianassa* s.l. *hayanoi* (holotype, MFM247023) from the mid-Cretaceous (early late Albian) of Japan (new photo). (**b**) Outer surface of propodus (manus) of *Glypturus* sp. (NMB G17968) from the Early Miocene (Aquitanian–Burdigalian) of Venezuela (from Kiel and Hansen 2015, Fig. 16f). (**c**, **d**) Outer and inner surfaces of propodus and dactylus of a major cheliped and outer surface of a minor cheliped of ?*Protocallianassa cheyennensis* (AMNH 82681) from the Late Cretaceous (late Campanian) of South Dakota, USA (new photos). Note the opener and closer muscle scars for *P. cheyennensis* (see Klompmaker et al. 2019a). Figure 5.10b whitened prior to photography. For localities, see Table 5.1

hard carbonate rock, but in the soft sediments at or near the cold seep. Alternatively, their extensive burrows in initially soft sediments may have served as conduits for seep fluids after which carbonate formation commenced (Wiese et al. 2015; Zwicker et al. 2015). Ghost shrimp claws are found in association with tube structures/burrows in seeps from the mid-Cretaceous (Albian) of Spain (Agirrezabala et al. 2013), from Middle Miocene mud volcanoes from Kuwait (Hyžný et al. 2018), and from other fossil deposits (Hyžný and Klompmaker 2015). Much more taxonomic work can be done on ghost shrimps given their common occurrence in fossil seeps.

5.3.3.2 Burrows

In addition to the axiids associated with a burrow mentioned above (Agirrezabala et al. 2013), several burrows attributed to the trace fossil *Thalassinoides* have been reported from fossil seeps (Fig. 5.11). They include burrows from the

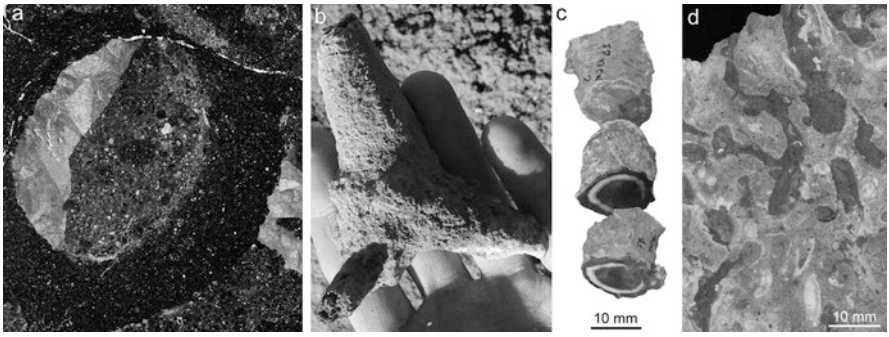

Fig. 5.11 Examples of burrows attributed to decapod crustaceans associated with fossil cold seeps. (**a**) Thin section across a burrow (*Thalassinoides paradoxicus*) from the mid-Cretaceous (late Albian) of Spain, repository and scale unknown (from Wiese et al. 2015, Fig. 5a). (**b**) *Thalassinoides* from the Paleocene (Danian) of California, USA, repository and precise scale unknown (from Blouet et al. 2017, Fig. 5d). (**c**) An early Oligocene burrow from Washington State, USA, repository unknown (from Zwicker et al. 2015, Fig. 3f). (**d**) ?*Thalassinoides* from the Miocene of New Zealand, GNS Science paleontology collections, Avalon, or University of Auckland field collections (from Campbell et al. 2008, Fig. 7c). For localities, see Table 5.1

mid-Cretaceous (Albian) of Spain (Wiese et al. 2015), the latest Cretaceous (Maastrichtian) of the James Ross Basin in Antarctica (Little et al. 2015), the earliest Paleocene (Danian) of California (Blouet et al. 2017), the early Oligocene of Washington State (Zwicker et al. 2015), and the Miocene of New Zealand (Campbell et al. 2008; Troup 2010). Burrows attributed to crustaceans, including shrimps, have recently been reported from Late Cretaceous seeps in the Western Interior Seaway, USA (Landman et al. this volume). In South Dakota, higher concentrations of ghost shrimp claws are found around burrow-like carbonates, but only one claw was found in what appeared to be a burrow (JB, pers. obs.). *Thalassinoides* burrows in general contain a variety of decapods including a crab, several lobsters, and ghost shrimps (Neto de Carvalho et al. 2007), but the majority appear to be associated with Axiidae (Neto de Carvalho et al. 2007; Hyžný and Klompmaker 2015). Lobsters are not known from fossil seeps thus far and are very rare in modern seeps. Axiidae have been found in association with seep burrows and/or are known from the same general area and age. Other than the mid-Cretaceous (Albian) seeps from Spain (Agirrezabala et al. 2013; Wiese et al. 2015), Axiidae were also reported from the early Oligocene seeps of Washington State (Goedert and Campbell 1995) and from the Late Cretaceous of the James Ross Basin in Antarctica (Ball 1960; Feldmann et al. 1993). Thus, most burrows in fossil seeps are probably caused by Axiidae, a clade that appeared in the Early Cretaceous (Hyžný and Klompmaker 2015).

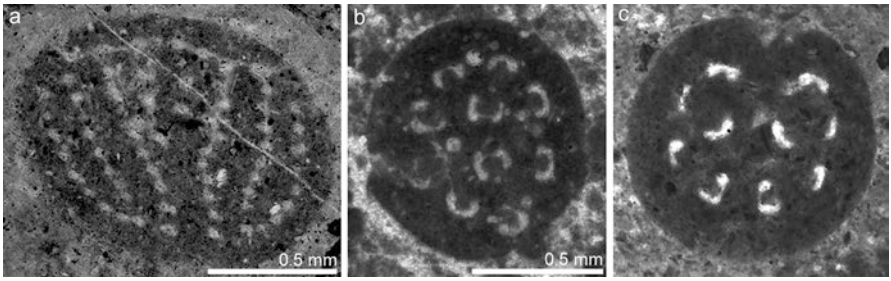

Fig. 5.12 Examples of coprolites attributed to crustaceans from fossil cold seeps. (**a**) The holotype of *Favreina fontana* (GSUB I20–I29: thin section Bea2.2b.1) from the Late Jurassic (Oxfordian) of France (from Senowbari-Daryan et al. 2007, Fig. 2b). (**b**) *Palaxius decemlunulatus* (? Oxford University Museum) from the Late Cretaceous (Cenomanian–Turonian) of Morocco (from Smrzka et al. 2017, Fig. 10b). (**c**) *Palaxius habanensis* from the Early to Middle Miocene of Washington State, USA, repository and scale unknown (from Kiel 2010a, Fig. 14.3). For localities, see Table 5.1

5.3.3.3 Fecal Pellets

Microcoprolites or fecal pellets provide an important additional source of information about the occurrence of crustaceans in fossil cold seeps. Compared to body fossils, they are very abundant and fossilize in seep limestones (Fig. 5.12). *Palaxius* spp. and *Favreina* spp. are known from fossil seeps. *Palaxius* has been reported from the Late Jurassic (Oxfordian) of France (Senowbari-Daryan et al. 2007), the Late Cretaceous (Cenomanian–Turonian) of Morocco (Smrzka et al. 2017), and the Eocene, Oligocene, and Miocene of Washington State (Peckmann et al. 2007b; Kiel 2010a; Kuechler et al. 2012; Smrzka 2013; Zwicker et al. 2015). *Favreina* is known from the Oxfordian of France (Peckmann et al. 1999; Senowbari-Daryan et al. 2007) and the Eocene of Oregon (Campbell 1995). Crustacean coprolites not assigned to an ichnotaxon originate from the mid-Cretaceous (Albian) of Spain (Agirrezabala et al. 2013), the Cenomanian of Utah (Kiel et al. 2012), and the latest Miocene (Messinian) of Italy (Natalicchio et al. 2013).

Microcoprolites referable to crustaceans are produced *at least* by true crabs, glypheoid lobsters, galatheoids anomurans, and (callianassid) axiideans (Brönnimann 1972; Förster and Hillebrandt 1984; Schweigert et al. 1997). Although the size and general internal structure of coprolites can point to a decapod crustacean producer (e.g., Moore 1933), attribution of coprolites to a particular species of crustacean is challenging because multiple species can produce coprolites referable to the same ichnospecies (e.g., Senowbari-Daryan et al. 2017). The stratigraphic ranges of some coprolite ichnospecies span multiple geological periods (Blau et al. 1993; Senowbari-Daryan and Kube 2003; Kietzmann et al. 2010). From fossil seeps, *Palaxius decemlunulatus* is known from the Late Cretaceous to the Miocene, a duration of ~80 my (Kuechler et al. 2012; Smrzka et al. 2017). Crustacean species' longevity tends to be shorter, although some exceptions with stratigraphic ranges of up to tens of millions of years are reported (summarized in Klompmaker

et al. 2012b). Nevertheless, it is possible to link certain coprolites to crustacean species where they co-occur locally (e.g., Förster and Hillebrandt 1984; Becker and Chamberlain 2006; Feldmann et al. 2013, 2015), including in seep deposits (Peckmann et al. 2007b). A search for microcoprolites in seeps older than the Oxfordian has the potential to uncover the timing of macrocrustaceans invading seeps. Inferring the producer of coprolites without accompanying body fossils remains difficult, but the stratigraphic range of decapod clades may be used to narrow down the possible producers.

5.3.3.4 Repair Scars

A final piece of evidence for the presence of crustaceans in cold seeps are repair scars in mollusks (Fig. 5.13). However, repair scars cannot be attributed unambiguously to crustaceans. Shell damage can also be caused by durophagous gastropods, birds, and fishes in the Meso–Cenozoic (Alexander and Dietl 2003). The depth of cold seeps precludes birds as viable predators, and predatory gastropods that can break shells such as *Murex*, *Busycon*, *Sinistrofulgur*, and *Busycotypus* (Nielsen 1975; Dietl 2003a, b) are absent to rare in modern cold seeps (e.g., Sasaki et al. 2010). This leaves predatory fishes as alternatives to crustaceans. Fishes are present in modern cold seeps (Kulm et al. 1986; Juniper and Sibuet 1987; Sellanes et al. 2008; Cordes et al. 2010c), but to what extent they are able to break shells is unknown. Furthermore, damage to infaunal bivalves can be caused by burrowing (Checa 1993; Alexander and Dietl 2005). Specifically, burrowing in an attempt to avoid predators and sediment overburden or erosion resulting in trapped particles and collision with hard objects within the sediments may cause damage commencing at the commissure (Checa 1993; Alexander and Dietl 2005). Burrowing/burying bivalves are present in seep faunas including solemyids, thyasirids, nucinellids, and lucinids (Amano et al. this volume).

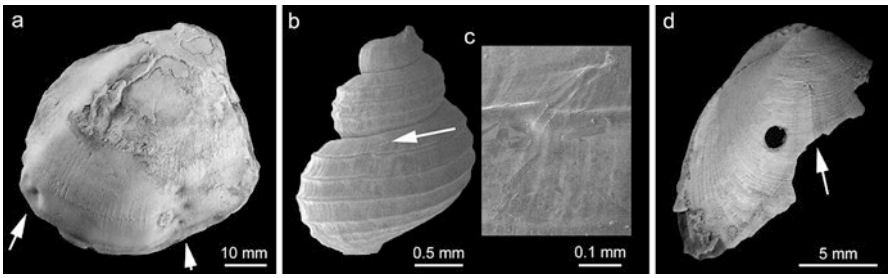

Fig. 5.13 Examples of repair scars in fossil cold seep mollusks that may be produced by decapod crustaceans. (**a**) Divots in the bivalve *Conchocele bisecta* (collection Joetsu University of Education) from the early Oligocene of Japan (from Kiel et al. 2016, Fig. 1a). (**b**, **c**) A repair scar in the gastropod *Provanna antiqua* (LACMIP 13249) from the late Oligocene of Washington State, USA (from Kiel 2006, Figs. 5.7 and 5.8). (**d**) An elongated repair scar in the bivalve *Nucinella gigantea* (UMUT MM 29527) from the mid-Cretaceous (Cenomanian) of Japan, with a predatory drill hole left of the scar (from Kiel et al. 2008, Fig. 3a). For localities, see Table 5.1

Repair scars reported from fossil cold seeps include those in the brachiopod *Sulcirostra paronai* from the Early Jurassic (Sinemurian) of Oregon, USA (Sandy et al. 2005; Sandy 2010); the bivalve *Nucinella gigantea* from the mid-Cretaceous (Cenomanian) of Japan (Kiel et al. 2008); the bivalves *Hubertschenckia ezoensis*, *Bathymodiolus inouei*, and *Conchocele bisecta* from the early Oligocene of Japan (Kiel et al. 2016); the gastropods *Provanna antiqua* and *Turrinosyrinx hickmanae* from the late Oligocene of Washington State, USA (Kiel 2006); and the gastropod *Mohnia vernalis* from the Late Pleistocene of Japan (Amano et al. 2013). Scars were also briefly mentioned from Devonian seep brachiopods (Kiel 2010b, p. 255), but these records would benefit from further study. In the most extensive study of repair scars in fossil cold seeps thus far, Kiel et al. (2016) showed substantially higher repair scar frequency (and drilling frequency) in the infaunal thyasirid *C. bisecta* relative to the epifaunal mytilid *B. inouei* and the semi-infaunal vesicomyid *H. ezoensis*. The last two species are interpreted to have lived closer to the sulfide-rich seepage. Consequently, predatory crabs would have preferentially attacked specimens of *C. bisecta* away from the toxic fluids despite the fact that this infaunal species is least accessible to predators. Most damage to *C. bisecta* was found at the ventral margin, which is the deepest point of the shell in life position (Kiel et al. 2016). Although the predation hypothesis remains viable, some of the repaired damages could also have resulted from burrowing, notably divot-shaped scars (Checa 1993; Klompmaker et al. 2019b). Regardless, studying repair scar frequencies in mollusks can be used to infer the presence and potentially the importance of shell-breaking predators in structuring seep communities.

5.4 Ostracods

5.4.1 Modern Occurrences and Composition

The presence of ostracods in modern cold seeps was most recently summarized by Karanovic and Brandão (2015). Seep ostracods identified to the genus level are known from the Black Sea near Turkey and the northern part of the Gulf of Mexico, while additional occurrences not identified to low taxonomic levels have been reported off the coast of Norway including Spitsbergen, again in the Gulf of Mexico, off the west coast of North America, and possibly off Antarctica (Montagna et al. 1987; Sommer et al. 2007; Van Gaever et al. 2009; Ritt et al. 2010; Bright et al. 2010; Hauquier et al. 2011; Decker et al. 2012; Degen et al. 2012; Portnova et al. 2014; Yasuhara et al. 2018).

Ostracods in cold seeps are dominated in terms of diversity and abundance by representatives of Podocopida and to a lesser extent Platycopida (Coles et al. 1996; Ritt et al. 2010; Degen et al. 2012; Table 5.1). Ostracod faunas at cold seeps are usually not endemic at the species level and consist of a mixture of shallow and deep-water taxa in addition to widely distributed taxa (Karanovic and Brandão

2015). Quaternary seep carbonate mounds west of Ireland contain predominantly upper bathyal ostracods and some shallow-water taxa due to contamination (Coles et al. 1996). These Irish ostracods are much more abundant in cold seeps than at a control site. Ostracod density is higher away from the direct center of the seep site for Norwegian seeps (Decker et al. 2012).

5.4.2 Biology

Most Podocopida are epifaunal, but *Krithe*, commonly present in cold seeps, is infaunal. *Cytherella*, the platycopid taxon commonly present in cold seeps, has an infaunal life habit (Russo et al. 2012). Feeding modes differ between the orders: while podocopids are detritus feeders, filter feeding is employed by platycopids (Smith and Horne 2002; Russo et al. 2012).

Considerable debate has revolved around the use of ostracods to infer oxygen concentrations, which is also of interest here due to relatively low oxygen levels at seep sites. Two proxies have been used: (1) the percentage of platycopids and (2) the size of the anterior vestibulum of *Krithe/Parakrithe*.

The "Platycopid Signal Hypothesis" (Whatley 1991) proposes that as oxygen levels decrease, the percentage of platycopids of all ostracods increases because these filter-feeding ostracods would be able to move sufficient water along their respiratory surface on the ventral side (Whatley 1990, 1991; Whatley et al. 2003); this is further supported by experimental evidence on *Cytherella* (Corbari et al. 2005). Whatley et al. (2003, p. 360) also presented a table for percentages of platycopids and inferred oxygen levels, with medium oxygen concentrations for assemblages consisting of 40–60% platycopid specimens and low oxygen levels for assemblages with >60% platycopid specimens. This method was used to infer oxygen levels in deep time (Whatley 1991, 1995; Boomer and Whatley 1992; Lethiers and Whatley 1994). However, the Platycopid Signal Hypothesis was not supported by renewed analyses because platycopids are not consistently dominant in oxygen minimum zones today (Brandão 2008; Brandão and Horne 2009) and *Cytherella* was found throughout a Miocene outcrop on the Caribbean island of Trinidad with varying inferred oxygen levels rather than only in the oxygen minimum zone (Wilson et al. 2014). The fossil record of seep ostracods is not consistent either with the Platycopid Signal Hypothesis because percentages are low and vary from 0% to 18.8% (Table 5.2). Podocopids adapted to low oxygen conditions were also abundant in Miocene seep ostracod assemblages (Russo et al. 2012). Rather than a proxy for oxygen levels, Horne et al. (2011) proposed that high percentages of platycopids would indicate oligotrophic nutrient levels because modern platycopids feed on nanno- and picoplankton, groups that are dominant in oligotrophic waters.

The size and shape of the anterior vestibulum of the podocopids *Krithe/Parakrithe* have been hypothesized to negatively correlate with oxygen concentrations (Peypouquet 1975, 1979) in the North Atlantic, and preliminary support was claimed based on one species from Sweden (McKenzie et al. 1989). If correct, this proxy

Table 5.2 Percentages of platycopid specimens of all ostracods collected from subfossil to fossil cold seeps. Only assemblages of ≥10 specimens are incorporated

Locality	Age	Number of platycopids	Total number of ostracods	% platycopids
Mound A (sites 40–41), west of Ireland (Coles et al. 1996)	Late Pleistocene–Holocene	1	624	0.2
Mound B (site 18), west of Ireland (Coles et al. 1996)	Late Pleistocene–Holocene	13	792	1.6
Mound C (site 25), west of Ireland (Coles et al. 1996)	Late Pleistocene–Holocene	61	1124	5.4
Mound D (site 81), west of Ireland (Coles et al. 1996)	Late Pleistocene–Holocene	9	664	1.4
SC561/Cals1 W/Cals2 W 15–24, Sarsetta, Italy (Russo et al. 2012)	Middle Miocene (Serravallian)	29	154	18.8
UWBM B6781, Washington, USA (Yamaguchi et al. 2016)	late Oligocene	0	33	0.0
UMBM B7897, Washington, USA (Yamaguchi et al. 2016)	early Oligocene	1	11	9.1

could be used to evaluate oxygen levels in deep time (references in Whatley and Zhao 1993). For fossil seeps, Russo et al. (2012) implied that *Krithe* with large vestibulums were present in Miocene seeps from Italy. However, when re-evaluating this relationship using 12 *Krithe* and four *Parakrithe* species over a 150–4000 m depth range including five water masses varying in oxygen content in the South China Sea, the pattern did not hold up (Whatley and Zhao 1993). Species with four different vestibulum sizes co-occurred in 57% of the samples, and the vestibulum of one species reported from a depth range of 2775 m was said not to differ in size. Similar conclusions were reached using fossil and modern North Atlantic species (Coles et al. 1996; Van Harten 1996). Furthermore, considerable variation of anterior vestibulum size in a small range of oxygen concentrations was shown within one Holocene species from Brazil (Do Carmo et al. 2009).

Dispersal mechanisms of seep ostracods are poorly known, but Karanovic and Brandão (2015) proposed that they could either hitchhike on other animals such as fishes or survive through the digestive tract of predators.

5.4.3 Fossil Record and Evolution

Ostracods are the most abundant and diverse crustaceans found in fossil seep deposits, with 86% of specimens and 65% of taxon occurrences. The oldest seep ostracods are reported from a hematite facies in an early phase of a Late Silurian seep (Barbieri et al. 2004; Buggisch and Krumm 2005), followed by ostracods outside/

above the central zone of a Middle Devonian seep (Hryniewicz et al. 2017) and ostracods in a brachiopod seep limestone from the Late Devonian (Peckmann et al. 2007a) (Fig. 5.14). All occurrences are from Morocco and not identified further. The only seep ostracod occurrences from the Mesozoic are Jurassic in age and originate from a variety of countries: Russia (Nova Zembla) (Hryniewicz et al. 2015b), France (Rolin et al. 1990; Gaillard et al. 1992; Peckmann et al. 1999), Germany (Teichert and Luppold 2013), Antarctica (Kelly et al. 1995), and Argentina (Gómez-Pérez 2001, 2003). None of them is identified further, except for the monospecific German occurrence (*Ogmoconcha amalthei*). More localities and occurrences are known from the Cenozoic (Fig. 5.4). Although ostracods from the Mio- to Pliocene of Italy (Barbieri and Cavalazzi 2005) and the Early Miocene of Venezuela (Kiel and Hansen 2015) have not been identified further, three papers have done so in great detail (Table 5.1) for Oligocene ostracods from Washington State (Yamaguchi et al. 2016), Middle Miocene ostracods from Italy (Russo et al. 2012), and Late Pleistocene–Holocene ostracods west of Ireland (Coles et al. 1996). The fact that only three articles have focused on fossil ostracods from fossil cold seeps thus far, and only from the Cenozoic, implies that much more research can be done such as depth estimates (Yamaguchi et al. 2016); taphonomic aspects (e.g., Boomer et al. 2003; Yamaguchi et al. 2016); faunal composition changes through time; degree of endemism in deep time; and diversity, body size, predation, and abundance trends across seeps.

5.5 Barnacles

5.5.1 Modern Occurrences and Composition

A limited number of barnacles are known from modern cold seeps, with most reported taxa being restricted to the Pacific Ocean. Non-parasitic taxa from the Pacific are dominated by stalked barnacles from the scalpelliform Neolepadidae family and include *Ashinkailepas kermadecensis* from New Zealand (Buckeridge, 2009) (Fig. 5.15a), *Ashinkailepas seepiophila* from Japan (Fujikura et al. 2002; Yamaguchi et al. 2004), *Leucolepas longa* from Papua New Guinea (Southward et al. 2002; Southward and Jones 2003; Stecher et al. 2003), *Neolepas* sp. from offshore India (Mazumdar et al. 2019), *Vulcanolepas parensis* from the Pacific–Antarctic Ridge (Southward 2005), and possibly *Vulcanolepas osheai* found near New Zealand (Buckeridge 2000; Southward 2005). Other Pacific records include rare occurrences of the scalpelliforms *Arcoscalpellum* sp., *Scalpellum projectum*, *Scalpellum* sp., and an unidentified scalpellid from Chile (Sellanes et al. 2008; Báez and Sellanes 2009; Zapata-Hernández et al. 2014). The latter authors also noted the presence of the lepadiform *Lepas* sp. and three other unidentified species of Cirripedia. Other records from the Pacific include unidentified Cirripedia from the Sea of Okhotsk west of Russia (Sahling et al. 2003) and some other Cirripedia from

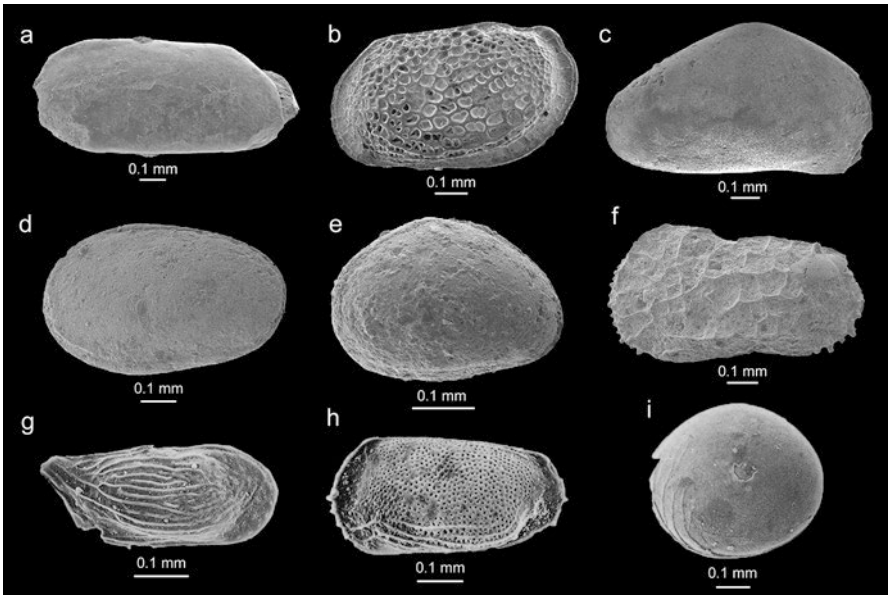

Fig. 5.14. Examples of ostracods found in association with (sub)fossil cold seeps from the Oligocene of Washington State, USA (**a**–**c**), the Middle Miocene (Serravallian) of Italy (**d**–**f**), and the Late Pleistocene–Holocene west of Ireland (**g**–**i**). (**a**) The podocopid *Krithe* cf. *adelspergi* (UMBM 101157) (from Yamaguchi et al. 2016, Fig. 3.13). (**b**) The podocopid *Palmoconcha* sp. (UMBM 101160) (from Yamaguchi et al. 2016, Fig. 4.4). (**c**) The podocopid *Propontocypris* sp. (UMBM 101162) (from Yamaguchi et al. 2016, Fig. 4.11). (**d**) The platycopid *Cytherella* gr. *russo*, repository unknown (from Russo et al. 2012, pl. 1.2). (**e**) The podocopid *Xestoleberis communis*, repository unknown (from Russo et al. 2012, pl. 1.4). (**f**) The podocopid *Paleoblitacythereis ruggierii*, repository unknown (from Russo et al. 2012, pl. 1.6). (**g**) The podocopid *Loxocauda* cf. *decipiens* (core 25, ERA-Maptec Ltd.) (from Coles et al. 1996, pl. 1.18). (**h**) The podocopid *Microceratina poligonia* (core 18, ERA-Maptec Ltd.) (from Coles et al. 1996, pl. 5.4). (**i**) The halocyprid *Polycope orbicularis* (core 41, ERA-Maptec Ltd.) (from Coles et al. 1996, pl. 6.17)

inactive parts of seeps west of Costa Rica (Levin et al. 2015, Table S1), the latter of which are not included in our analyses. The parasitic rhizocephalan barnacle *Parthenopea australis* infesting the callianopsid shrimp host *Vulcanocalliax* sp. was found near active cold seeps off west New Zealand (Lörz et al. 2008; Lützen et al. 2009). Other rhizocephalans were encountered on the crabs *Trichopeltarion janetae*, *Neopilumnoplax nieli*, and *Pycnoplax victoriensis* off west New Zealand (Ahyong 2008). The only barnacles associated with seeps outside the Pacific that we are aware of are the verrucomorph *Costatoverruca floridana* (Carney 1994; Bergquist et al. 2003; Cordes et al. 2006, 2010c; Becker et al. 2009) and an unidentified cirriped on the carapace of the spider crab *Rochinia crassa* (MacAvoy et al. 2002), both from the Gulf of Mexico, in addition to the aforementioned *Neolepas* sp. from offshore India (Mazumdar et al. 2019).

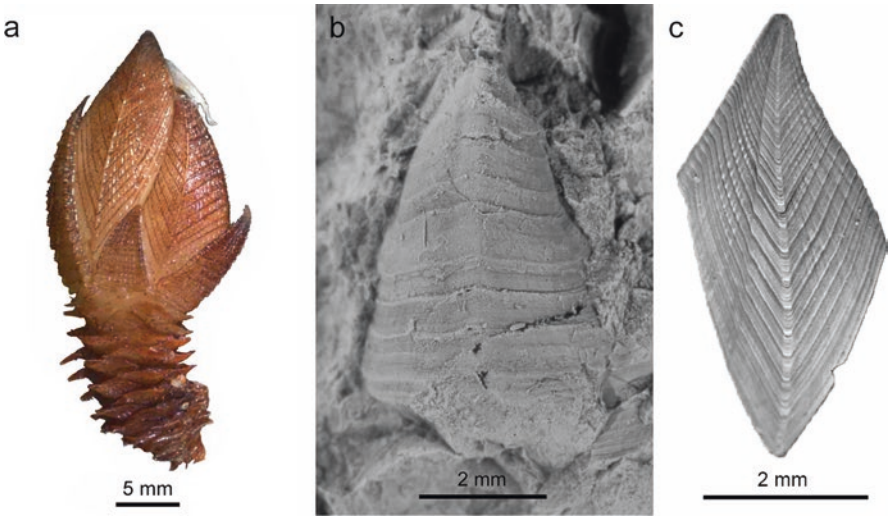

Fig. 5.15 Modern and fossil barnacles associated with seeps. (**a**) Holotype (NIWA-44722) of the extant stalked barnacle *Ashinkailepas kermadecensis* from a cold seep at the Kermadec Ridge, NE of New Zealand (from Buckeridge 2009, pl. 1.5, *Zootaxa*, reused with permission from Magnolia Press). (**b**) Rostral plate of the barnacle ?*Capitulum lailae* (ZPAL V.48/22) from the late Paleocene of Spitsbergen. (**c**) External view of the holotype of *Ashinkailepas indica* (a tergum, NHMUK IC 1409) from the Late Pleistocene, offshore India (from Gale et al. 2020, Fig. 4b)

5.5.2 Biology

Barnacles are filter or suspension feeders, including modern stalked barnacles living in cold seep environments (e.g., Tunnicliffe and Southward 2004). The biology of *Ashinkailepas seepiophila* and *Leucolepas longa* is best known. The nauplius larvae of *A. seepiophila* have large nutrient reservoirs, nauplius appendages are equipped with long plumose setae for flotation, and larval development of this species is completed within 65 days in the lab (Yorisue et al. 2013). Most specimens of the sulfide-adapted stalked barnacle *L. longa* grow on bivalves, but rocks and worm tubes are also used, while their larvae are suitable for long-distance dispersal (Tunnicliffe and Southward 2004). The parasitic barnacles rely on nutrients from their host rather than from a seep directly.

5.5.3 Fossil Record and Evolution

To our knowledge, barnacles were only mentioned five times in association with fossil cold seeps. First, Eagle et al. (1999) reported an unidentified barnacle from a bathyal Lower Miocene concretionary siltstone that may represent a hydrocarbon seep based on the bivalves and unusual foraminifera. None of the three bivalve taxa

(*Linucula*, *Jupiteria*, and *Notocallista*) are chemosymbiotic taxa known to inhabit cold seeps (e.g., Kiel 2010b; Amano et al., 2022), but the first two genera are nuculids, members of which are found at modern seeps and vents (Kiel 2010c). Subsequent stable isotope analyses on foraminifera and a bivalve resulted in highly negative $\delta^{13}C$ values consistent with methane seepage and the presence of the possibly endemic, highly abundant benthic foraminifer *Amphimorphinella butonensis* (Hayward et al. 2011). Second, a well-known seep-wood fall community from the late Paleocene of Spitsbergen contained a single species of barnacle, the scalpelliform pollicipedid ?*Capitulum lailae* in a seep limestone (Gripp 1927; Withers 1953; Hryniewicz et al. 2019) (Fig. 5.15b). Generic placement of this taxon remains uncertain, and *Scillaelepas* or *Pycnolepas* as the genus name may also be possibilities (pers. comm. William Newman to AAK, May 2019). The third record is an undetermined balanid from the Middle Miocene of central California, USA (Powell et al. 2019). The final records include the neolepadid *Ashinkailepas indica* from the Late Pleistocene from offshore India (Gale et al. 2020) and Late Pleistocene occurrences of *Verruca stroemia* and other cirriped fragments west of Svalbard (Thomsen et al. 2019).

Neolepadidae (previously known as the subfamily Neolepadinae prior to Gale et al. 2020) appears to be a clade that originated fairly late in the evolutionary history of cirripeds, with the stem and crown node estimated to occur within the Cretaceous (Pérez-Losada et al. 2008). However, in addition to reporting on an Eocene neolepadid, Carriol et al. (2016) also ascribed a Jurassic taxon to this family, both non-seep barnacles. A previous phylogenetic analysis including most of the extant seep barnacles suggests a Cenozoic origin of Neolepadidae (Herrera et al. 2015, Fig. 3). Today, members of this clade also inhabit hydrothermal vents (Newman et al. 2006; Buckeridge et al. 2013; Herrera et al. 2015; Watanabe et al. 2021). Representatives of a related but extinct clade, Eolepadinae, are not known from fossil seeps (e.g., Buckeridge and Grant-Mackie 1985). Pollicipedidae have a confirmed fossil record from the Jurassic onward (Gale 2014), with the earliest known record of *Capitulum* dating from the Late Cretaceous (Kočová Veselská et al. 2015).

Balanomorph barnacles, very common in the fossil record of shallow marine deposits (e.g., Foster and Buckeridge 1987; Gale and Sørensen 2015), are rarely present in modern and fossil cold seeps like in modern hydrothermal vents (Yamaguchi and Newman 1990, 1997).

5.6 Conclusions

- Crustaceans are much more common in fossil seeps than previously known and are found on each continent.
- Decapod crustaceans are represented by body fossils and traces (coprolites, repair scars in mollusks, and burrows); ostracods and barnacles are known from body fossils.

- Trace fossils can be used to detect the presence of decapods when their body fossils are lacking.
- In terms of stratigraphic range, ostracods have the longest stratigraphic record of crustaceans in fossil seeps starting in the Silurian. Barnacles associated with seeps have been found only in the Cenozoic thus far. Decapod crustaceans are present in seeps from the Jurassic onward.
- While modern seep decapods are dominated by alvinocaridid shrimps, galatheoid squat lobsters, king crabs, and true crabs, the fossil record consists primarily of axiidaen ghost shrimps and true crabs thus far. Preservation and recognition are likely to have influenced this discrepancy.
- The relatively unexplored fossil record of seep crustaceans provides many opportunities for systematic and paleoecological research.

Acknowledgments We thank Andrzej Kaim for the invitation to work on this exciting topic, for the items of literature, and for the useful comments. We thank reviewers Matus Hyžný and Denis Audo for their useful input as well as William Newman for his comments on the preprint. Neil Landman also provided useful comments. JB thanks the research crews from the AMNH, Stony Brook University, and Brooklyn College for their hard work collecting at seeps in the Western Interior Seaway, ranchers for allowing access to private property, and the USDA Forest Service for granting access to forest service and BLM land. For various reasons, we express our gratitude to (in alphabetical order by family name) Christina Belanger, Gale Bishop, Simone Brandão, Tim-Yam Chan, Erica Clites, Rodney Feldmann, Katsunori Fujikura, Krzysztof Hryniewicz, Azusa Ikuta, Yasumitsu Kanie, Hiroaki Karasawa, Steffen Kiel, Neal Larson, Ryuichi Majima, William Newman, Michael Sandy, Carrie Schweitzer, Sally Shelton, and Chau-Chang Wang and to all publishers/organizations for permissions to reuse images. The National Science Foundation grant #1802718 helped present this research at the 9th International Crustacean Congress in Washington, DC, May 2018. An American Museum of Natural History Lerner-Gray grant was used to study fossil seep decapods from South Dakota in their collection in 2018, of which the detailed results will be forthcoming in a future paper.

References

Abelló P (1995) Note on the diet of *Lithodes ferox* (Anomura: Lithodidae) off Namibia. S Afr J Mar Sci 15:273–277. https://doi.org/10.2989/025776195784156304

Agirrezabala LM, Kiel S, Blumenberg M et al (2013) Outcrop analogues of pockmarks and associated methane-seep carbonates: a case study from the Lower Cretaceous (Albian) of the Basque-Cantabrian Basin, western Pyrenees. Palaeogeogr Palaeoclimatol Palaeoecol 390:94–115. https://doi.org/10.1016/j.palaeo.2012.11.020

Aguzzi J, Ramirez-Llodra E, Telesnicki G et al (2007) Day-night activity rhythm of the cold seep shrimp *Alvinocaris stactophila* (Caridea: Alvinocarididae) from the Gulf of Mexico. J Mar Biol Assoc UK 87:1175–1180. https://doi.org/10.1017/S0025315407057311

Ahyong ST (2008) Deepwater crabs from seamounts and chemosynthetic habitats off eastern New Zealand (Crustacea: Decapoda: Brachyura). Zootaxa 1708:1–72

Ahyong ST, Roterman CN (2014) Pristinaspinidae, a new family of Cretaceous kiwaiform stem-lineage squat lobster (Anomura, Chirostyloidea). Scr Geol 147:125–133

Alexander RR, Dietl GP (2003) The fossil record of shell-breaking predation on marine bivalves and gastropods. In: Kelley PH, Kowalewski M, Hansen TA (eds) Predator-prey interactions in the fossil record. Kluwer Academic/Plenum Publishers, New York, pp 141–176

Alexander RR, Dietl GP (2005) Non-predatory shell damage in Neogene western Atlantic deep-burrowing bivalves. Palaios 20:280–295. https://doi.org/10.2110/palo.2004.p04-29

Amano K, Kiel S (2007) Fossil vesicomyid bivalves from the North Pacific region. Veliger 49:270–293

Amano K, Hasegawa S, Ishihama S (2013) Molluscan fossils from core samples collected from off Joetsu during MD179 cruise. J Jpn Assoc Pet Technol 78:92–96

Amano K, Hryniewicz K, Jenkins RG et al (this volume) Bivalvia. In: Kaim A, Cochran JK, Landman NH (eds) Ancient methane seeps and cognate communities. Topics in geobiology. Springer, Cham

Aronson RB, Smith KE, Vos SC et al (2015) No barrier to emergence of bathyal king crabs on the Antarctic shelf. PNAS 112:12997–13002. https://doi.org/10.1073/pnas.1513962112

Baco AR, Rowden AA, Levin LA et al (2010) Initial characterization of cold seep faunal communities on the New Zealand Hikurangi margin. Mar Geol 272:251–259. https://doi.org/10.1016/j.margeo.2009.06.015

Báez P, Sellanes J (2009) Nuevo registro de *Scalpellum projectum* (Crustacea: Cirripedia: Thoracica: Scalpellidae) para el talud continental de Chile. Lat Am J Aquat Res 37:247–251. https://doi.org/10.3856/vol37-issue2-fulltext-11

Ball HW (1960) Upper Cretaceous Decapoda and Serpulidae from James Ross Island, Graham Land. Falkland Isl Dependencies Surv Sci Rep 24(1–30):pls 1–7

Barbieri R, Cavalazzi B (2005) Microbial fabrics from Neogene cold seep carbonates, northern Apennine, Italy. Palaeogeogr Palaeoclimatol Palaeoecol 227:143–155. https://doi.org/10.1016/j.palaeo.2005.04.026

Barbieri R, Ori GG, Cavalazzi B (2004) A Silurian cold-seep ecosystem from the Middle Atlas, Morocco. Palaios 19:527–542. https://doi.org/10.1669/0883-1351(2004)019<0527:ASCEFT>2.0.CO;2

Barry JP, Gary Greene H, Orange DL et al (1996) Biologic and geologic characteristics of cold seeps in Monterey Bay, California. Deep-Sea Res I 43:1739–1762. https://doi.org/10.1016/S0967-0637(96)00075-1

Becker MA, Chamberlain JA (2006) Anomuran microcoprolites from the lowermost Navesink Formation (Maastrichtian), Monmouth County, New Jersey. Ichnos 13:1–9. https://doi.org/10.1080/10420940500511645

Becker EL, Cordes EE, Macko SA et al (2009) Importance of seep primary production to *Lophelia pertusa* and associated fauna in the Gulf of Mexico. Deep-Sea Res I 56:786–800. https://doi.org/10.1016/j.dsr.2008.12.006

Becker EL, Cordes EE, Macko SA et al (2013) Using stable isotope compositions of animal tissues to infer trophic interactions in Gulf of Mexico lower slope seep communities. PLoS One 8:e74459. https://doi.org/10.1371/journal.pone.0074459

Bellwood O (2002) The occurrence, mechanics and significance of burying behaviour in crabs (Crustacea: Brachyura). J Nat Hist 36:1223–1238. https://doi.org/10.1080/00222930110048891

Bergquist DC, Ward T, Cordes EE et al (2003) Community structure of vestimentiferan-generated habitat islands from Gulf of Mexico cold seeps. J Exp Mar Biol Ecol 289:197–222. https://doi.org/10.1016/S0022-0981(03)00046-7

Bishop GA, Williams AB (2000) Fossil crabs from tepee buttes, submarine seeps of the Late Cretaceous Pierre Shale, South Dakota and Colorado, U.S.A. J Crustac Biol 20:286–300. https://doi.org/10.1163/1937240X-90000031

Blau J, Grün B, Gießen MS (1993) Crustaceen-Koprolithen aus der Trias der westlichen Tethys (Lienzer Dolomiten, Österreich; Pragser Dolomiten, Italien) und vom Gondwana-Westrand (oberes Magdalenatal, Kolumbien, Südamerika). Paläontol Z 67:193–214. https://doi.org/10.1007/BF02985878

Blouet J-P, Imbert P, Foubert A (2017) Mechanisms of biogenic gas migration revealed by seep carbonate paragenesis, Panoche Hills, California. AAPG Bull 101:1309–1340. https://doi.org/10.1306/10171616021

Boomer I, Whatley R (1992) Ostracoda and dysaerobia in the Lower Jurassic of Wales: the reconstruction of past oxygen levels. Palaeogeogr Palaeoclimatol Palaeoecol 99:373–379. https://doi.org/10.1016/0031-0182(92)90024-Y

Boomer I, Horne DJ, Slipper IJ (2003) The use of ostracods in palaeoenvironmental studies, or what can you do with an ostracod shell? Paleontol Soc Pap 9:153–180

Bracken HD, De Grave S, Felder DL (2009) Phylogeny of the infraorder Caridea based on mitochondrial and nuclear genes (Crustacea: Decapoda). Decapod Crustac Phylogenetics 28:281–305

Bracken-Grissom HD, Cannon ME, Cabezas P et al (2013) A comprehensive and integrative reconstruction of evolutionary history for Anomura (Crustacea: Decapoda). BMC Evol Biol 13:128. https://doi.org/10.1186/1471-2148-13-128

Brandão SN (2008) First record of a living Platycopida (Crustacea, Ostracoda) from Antarctic waters and a discussion on *Cytherella serratula* (Brady, 1880). Zootaxa 1866:349–372

Brandão SN, Horne DJ (2009) The Platycopid Signal of oxygen depletion in the ocean: a critical evaluation of the evidence from modern ostracod biology, ecology and depth distribution. Palaeogeogr Palaeoclimatol Palaeoecol 283:126–133. https://doi.org/10.1016/j.palaeo.2009.09.007

Bright M, Plum C, Riavitz LA et al (2010) Epizooic metazoan meiobenthos associated with tubeworm and mussel aggregations from cold seeps of the northern Gulf of Mexico. Deep-Sea Res II 57:1982–1989. https://doi.org/10.1016/j.dsr2.2010.05.003

Brönnimann P (1972) Remarks on the classification of fossil anomuran coprolites. Paläontol Z 46:99–103. https://doi.org/10.1007/BF02989556

Buckeridge JS (2000) *Neolepas osheai* sp. nov., a new deep-sea vent barnacle (Cirripedia: Pedunculata) from the Brothers Caldera, south-west Pacific Ocean. N Z J Mar Freshw Res 34:409–418. https://doi.org/10.1080/00288330.2000.9516944

Buckeridge JS (2009) *Ashinkailepas kermadecensis*, a new species of deep-sea scalpelliform barnacle (Thoracica: Eolepadidae) from the Kermadec Islands, southwest Pacific. Zootaxa 2021:57–65

Buckeridge JS, Grant-Mackie JA (1985) A new scalpellid barnacle (Cirripedia: Thoracica) from the Lower Jurassic of New Caledonia. Géologie Fr 1:15–18

Buckeridge JS, Linse K, Jackson JA (2013) *Vulcanolepas scotiaensis* sp. nov., a new deep-sea scalpelliform barnacle (Eolepadidae: Neolepadinae) from hydrothermal vents in the Scotia Sea, Antarctica. Zootaxa 3745(551). https://doi.org/10.11646/zootaxa.3745.5.4

Buggisch W, Krumm S (2005) Palaeozoic cold seep carbonates from Europe and North Africa—an integrated isotopic and geochemical approach. Facies 51:566–583. https://doi.org/10.1007/s10347-005-0005-5

Campbell KA (1995) Dynamic development of Jurassic-Pliocene cold-seeps, convergent margin of western North America. Dissertation, University of Southern California

Campbell KA (2006) Hydrocarbon seep and hydrothermal vent paleoenvironments and paleontology: past developments and future research directions. Palaeogeogr Palaeoclimatol Palaeoecol 232:362–407. https://doi.org/10.1016/j.palaeo.2005.06.018

Campbell KA, Francis DA, Collins M et al (2008) Hydrocarbon seep-carbonates of a Miocene forearc (East Coast Basin), North Island, New Zealand. Sediment Geol 204:83–105. https://doi.org/10.1016/j.sedgeo.2008.01.002

Carney RS (1994) Consideration of the oasis analogy for chemosynthetic communities at Gulf of Mexico hydrocarbon vents. Geo-Mar Lett 14:149–159. https://doi.org/10.1007/BF01203726

Carriol R-P, Bonde N, Jakobsen SL, Høeg JT (2016) New stalked and sessile cirripedes from the Eocene Mo Clay, northwest Jutland (Denmark). Geodiversitas 38:21–32. https://doi.org/10.5252/g2016n1a2

Checa A (1993) Non-predatory shell damage in Recent deep-endobenthic bivalves from Spain. Palaeogeogr Palaeoclimatol Palaeoecol 100:309–331. https://doi.org/10.1016/0031-0182(93)90061-M

Chevaldonné P, Olu K (1996) Occurrence of anomuran crabs (Crustacea: Decapoda) in hydrothermal vent and cold-seep communities: a review. Proc Biol Soc Wash 109:286–298

Coles GP, Ainsworth NR, Whaley RC et al (1996) Foraminifera and Ostracoda from Quaternary carbonate mounds associated with gas seepage in the Porcupine Basin, offshore Western Ireland. Rev Esp Micropaleontol 28:113–151

Comoglio LI, Amin OA (1999) Feeding habits of the false southern king crab *Paralomis granulosa* (Lithodidae) in the Beagle Channel, Tierra del Fuego, Argentina. Sci Mar 63:361–366. https://doi.org/10.3989/scimar.1999.63s1361

Corbari L, Mesmer-Dudons N, Carbonel P et al (2005) *Cytherella* as a tool to reconstruct deep-sea paleo-oxygen levels: the respiratory physiology of the platycopid ostracod *Cytherella* cf. *abyssorum*. Mar Biol 147:1377–1386. https://doi.org/10.1007/s00227-005-0040-3

Cordes EE, Bergquist DC, Predmore BL et al (2006) Alternate unstable states: convergent paths of succession in hydrocarbon-seep tubeworm-associated communities. J Exp Mar Biol Ecol 339:159–176. https://doi.org/10.1016/j.jembe.2006.07.017

Cordes EE, Carney SL, Hourdez S et al (2007) Cold seeps of the deep Gulf of Mexico: community structure and biogeographic comparisons to Atlantic equatorial belt seep communities. Deep-Sea Res I 54:637–653. https://doi.org/10.1016/j.dsr.2007.01.001

Cordes EE, Becker EL, Hourdez S et al (2010a) Influence of foundation species, depth, and location on diversity and community composition at Gulf of Mexico lower-slope cold seeps. Deep-Sea Res II 57:1870–1881. https://doi.org/10.1016/j.dsr2.2010.05.010

Cordes EE, Hourdez S, Roberts HH (2010b) Unusual habitats and organisms associated with the cold seeps of the Gulf of Mexico. In: Kiel S (ed) The vent and seep biota. Springer, Dordrecht, Netherlands, pp 315–331

Cordes EE, Becker EL, Fisherb CR (2010c) Temporal shift in nutrient input to cold-seep food webs revealed by stable-isotope signatures of associated communities. Limnol Oceanogr 55:2537–2548. https://doi.org/10.4319/lo.2010.55.6.2537

Coykendall DK, Nizinski MS, Morrison CL (2017) A phylogenetic perspective on diversity of Galatheoidea (*Munida*, *Munidopsis*) from cold-water coral and cold seep communities in the western North Atlantic Ocean. Deep-Sea Res II 137:258–272. https://doi.org/10.1016/j.dsr2.2016.08.014

Cunningham CW, Blackstone NW, Buss LW (1992) Evolution of king crabs from hermit crab ancestors. Nature 355:539–542. https://doi.org/10.1038/355539a0

Dando PR, Austen MC, Burke RA et al (1991) Ecology of a North Sea pockmark with an active methane seep. Mar Ecol Prog Ser 70:49–63. https://doi.org/10.3354/meps070049

De Angeli A, Ceccon L (2012) *Eouroptychus montemagrensis* n. gen., n. sp., (Crustacea, Decapoda, Anomura, Chirostylidae) dell'Eocene inferiore (Ypresiano) di Monte Magrè (Vicenza, Italia settentrionale). Lav Soc Veneziana Sci Nat 37:19–24

De Angeli A, Garassino A (2002) Galatheid, chirostylid and porcellanid decapods (Crustacea, Decapoda, Anomura) from the Eocene and Oligocene of Vicenza (N Italy). Mem Della Soc Ital Sci Nat E Mus Civ Storia Nat Milano 30:1–40

Decelle J, Andersen AC, Hourdez S (2010) Morphological adaptations to chronic hypoxia in deep-sea decapod crustaceans from hydrothermal vents and cold seeps. Mar Biol 157:1259–1269. https://doi.org/10.1007/s00227-010-1406-8

Decker C, Morineaux M, Van Gaever S et al (2012) Habitat heterogeneity influences cold-seep macrofaunal communities within and among seeps along the Norwegian margin: part 1, macrofaunal community structure: macrofaunal communities at Norwegian cold seeps. Mar Ecol 33:205–230. https://doi.org/10.1111/j.1439-0485.2011.00503.x

Degen R, Riavitz L, Gollner S et al (2012) Community study of tubeworm-associated epizooic meiobenthos from deep-sea cold seeps and hot vents. Mar Ecol Prog Ser 468:135–148. https://doi.org/10.3354/meps09889

Dietl GP (2003a) Interaction strength between a predator and dangerous prey: *Sinistrofulgur* predation on *Mercenaria*. J Exp Mar Biol Ecol 289:287–301. https://doi.org/10.1016/S0022-0981(03)00047-9

Dietl GP (2003b) Coevolution of a marine gastropod predator and its dangerous bivalve prey. Biol J Linn Soc 80:409–436. https://doi.org/10.1046/j.1095-8312.2003.00255.x

Do Carmo DA, Meireles RP, Suarez PAZ et al (2009) Size variations of the vestibula of *Krithe gnoma* Do Carmo & Sanguinetti, 1999 (Ostracoda): a new procedure for their analysis. Carnets Géol 9:1–9

Dong D, Li X (2015) Galatheid and chirostylid crustaceans (Decapoda: Anomura) from a cold seep environment in the northeastern South China Sea. Zootaxa 4057:91–105. https://doi.org/10.11646/zootaxa.4057.1.5

Dworschak PC (1987) Feeding behaviour of *Upogebia pusilla* and *Callianassa tyrrhena* (Crustacea, Decapoda, Thalassinidea). Investig Pesq 51:421–429

Dworschak PC (2015) Methods collecting Axiidea and Gebiidea (Decapoda): a review. Ann Naturhistorischen Mus Wien B 117:5–21

Dworschak PC, Cunha MR (2007) A new subfamily, Vulcanocalliacinae n. subfam., for *Vulcanocalliax arutyunovi* n. gen., n. sp. from a mud volcano in the Gulf of Cádiz (Crustacea, Decapoda, Callianassidae). Zootaxa 1460:35–46

Dworschak PC, Felder DA, Tudge CC (2012) Infraorders Axiidea de Saint Laurent, 1979 and Gebiidea de Saint Laurent, 1979 (formerly known collectively as Thalassinidea). In: Charmantier-Daures Schram M, Vaupel Klein Forest C (eds) Treatise on zoology—anatomy, taxonomy, biology, The Crustacea vol. 9B. Brill, Leiden, pp 109–219

Eagle MK, Hayward BW, Grant-Mackie JA et al (1999) Fossil communities in an early Miocene transgressive sequence, Mathesons Bay, Leigh, Auckland. Tane 37:43–67

East EH (2006) Reconstruction of the fossil mud shrimp *Callianopsis clallamensis*. J Crustac Biol 26:168–175. https://doi.org/10.1651/C-2562.1

Felder DL, Kensley BF (2004) A new species of axiid shrimp from chemosynthetic communities of the Louisiana continental slope, Gulf of Mexico (Crustacea: Decapoda: Thalassinidea). Proc Biol Soc Wash 117:68–75

Feldmann RM (1998) *Paralomis debodeorum*, a new species of decapod crustacean from the Miocene of New Zealand: first notice of the Lithodidae in the fossil record. N Z J Geol Geophys 41:35–38. https://doi.org/10.1080/00288306.1998.9514788

Feldmann RM, Schweitzer CE (2009) Revision of Jurassic Homoloidea De Haan, 1839, from the Ernstbrunn and Štramberk limestones, Austria and the Czech Republic. Ann Naturhistorischen Mus Wien A 111:183–205

Feldmann RM, Tshudy DM, Thomson MRA (1993) Late Cretaceous and Paleocene decapod crustaceans from James Ross Basin, Antarctic Peninsula. Paleontol Soc Mem 28:1–41

Feldmann RM, Schweitzer CE, Casadío S et al (2011) New Miocene Decapoda (Thalassinidea; Brachyura) from Tierra Del Fuego, Argentina: paleobiogeographic implications. Ann Carnegie Mus 79:91–123. https://doi.org/10.2992/007.079.0202

Feldmann RM, Schweitzer CE, Baltzly LM et al (2013) New and previously known decapod crustaceans from the Late Cretaceous of New Jersey and Delaware, USA. Bull Mizunami Fossil Mus 39:7–37

Feldmann RM, Schweitzer CE, Boessenecker RW (2015) A new squat lobster (Decapoda: Anomura: Galatheoidea) from the Pliocene Purisima Formation, California. Ann Carnegie Mus 83:85–93. https://doi.org/10.2992/007.083.0202

Förster R, Hillebrandt AV (1984) Das Kimmeridge des Profeta-Jura in Nordchile mit einer *Mecochirus-Favreina*-Vergesellschaftung (Crustacea, Decapoda-Ichnogenus). Mitteilungen Bayrischen Staatssamml Paläontol Hist Geol 24:67–84

Foster BA, Buckeridge JS (1987) Barnacle palaeontology. Crustac Issues 5:43–62

Fujikura K, Hashimoto J, Okutani T (2002) Estimated population densities of megafauna in two chemosynthesis-based communities: a cold seep in Sagami Bay and a hydrothermal vent in the Okinawa Trough. Benthos Res 57:21–30. https://doi.org/10.5179/benthos1996.57.1_21

Fujikura K, Yamanaka T, Sumida PYG et al (2017) Discovery of asphalt seeps in the deep southwest Atlantic off Brazil. Deep-Sea Res II 146:35–44. https://doi.org/10.1016/j.dsr2.2017.04.002

Gaillard C, Bourseau J-P, Boudeulle M et al (1985) Les pseudo-biohermes de Beauvoisin (Drôme): un site hydrothermal sur la marge tethysienne à l'Oxfordien? Bull Soc Géol Fr 1:69–78

Gaillard C, Rio M, Rolin Y et al (1992) Fossil chemosynthetic communities related to vents or seeps in sedimentary basins: the pseudobioherms of southeastern France compared to other world examples. Palaios 7:451–465. https://doi.org/10.2307/3514829

Gale AS (2014) New cirripedes (Crustacea, Thoracica) from the Jurassic and Cretaceous of the United Kingdom. Proc Geol Assoc 125:406–418. https://doi.org/10.1016/j.pgeola.2014.07.003

Gale AS, Sørensen AM (2015) Origin of the balanomorph barnacles (Crustacea, Cirripedia, Thoracica): new evidence from the Late Cretaceous (Campanian) of Sweden. J Syst Palaeontol 13:791–824. https://doi.org/10.1080/14772019.2014.954824

Gale AS, Little CTS, Johnson JE et al (2020) A new neolepadid cirripede from a Pleistocene cold seep, Krishna-Godavari Basin, offshore India. Acta Palaeontol Pol 65(2):351–362. https://doi.org/10.4202/app.00705.2019

Gebruk AV, Southward EC, Kennedy H et al (2000) Food sources, behaviour, and distribution of hydrothermal vent shrimps at the Mid-Atlantic Ridge. J Mar Biol Assoc U K 80:485–499

Goedert JL, Campbell KA (1995) An early Oligocene chemosynthetic community from the Makah Formation, northwestern Olympic Peninsula, Washington. Veliger 38:22–29

Goedert JL, Kaler KL (1996) A new species of *Abyssochrysos* (Gastropoda: Loxonematoidea) from a middle Eocene cold-seep carbonate in the Humptulips Formation, western Washington. Veliger 39:65–70

Goedert JL, Squires RL (1990) Eocene deep-sea communities in localized limestones formed by subduction-related methane seeps, southwestern Washington. Geology 18:1182–1185. https://doi.org/10.1130/0091-7613(1990)018<1182:EDSCIL>2.3.CO;2

Gómez-Pérez I (2001) Estromatolitos de aguas profundas en la Formación Los Molles (Neuquén, Argentina): ?chimeneas de metano en el fondo marino jurásico? Rev Asoc Argent Sedimentol 8:1–14

Gómez-Pérez I (2003) An Early Jurassic deep-water stromatolitic bioherm related to possible methane seepage (Los Molles Formation, Neuquén, Argentina). Palaeogeogr Palaeoclimatol Palaeoecol 201:21–49. https://doi.org/10.1016/S0031-0182(03)00508-X

Gripp K (1927) Beiträge zur Geologie von Spitzbergen. Abh Naturwiss Ver Hamburg 21:3–38, pls 1–7

Grupe BM, Krach ML, Pasulka AL et al (2015) Methane seep ecosystem functions and services from a recently discovered southern California seep. Mar Ecol 36:91–108. https://doi.org/10.1111/maec.12243

Guinot D, Richer de Forges B (1995) Crustacea Decapoda Brachyura: révision de la famille des Homolidae de Haan, 1839. Résultats Camp MUSORSTOM 13:283–517

Hägg R (1925) A new Tertiary fauna from Spitsbergen. Bull Geol Inst Univ Upps 20:39–55

Hall S, Thatje S (2009a) Global bottlenecks in the distribution of marine Crustacea: temperature constraints in the family Lithodidae. J Biogeogr 36:2125–2135. https://doi.org/10.1111/j.1365-2699.2009.02153.x

Hall S, Thatje S (2009b) Four new species of the family Lithodidae (Crustacea: Decapoda) from the collections of the National Museum of Natural History, Smithsonian Institution. Zootaxa 2302:31–47

Hall S, Thatje S (2018) Evolution through cold and deep waters: the molecular phylogeny of the Lithodidae (Crustacea: Decapoda). Sci Nat 105:19. https://doi.org/10.1007/s00114-018-1544-2

Hammer Ø, Nakrem HA, Little CTS et al (2011) Hydrocarbon seeps from close to the Jurassic–Cretaceous boundary, Svalbard. Palaeogeogr Palaeoclimatol Palaeoecol 306:15–26. https://doi.org/10.1016/j.palaeo.2011.03.019

Handle KC (2014) Paleoecology of Late Cretaceous methane cold-seeps of the Pierre Shale, South Dakota. Dissertation, City University of New York

Hartnoll RG (1971) The occurrence, methods and significance of swimming in the Brachyura. Anim Behav 19:34–50. https://doi.org/10.1016/S0003-3472(71)80132-X

Hashimoto J, Ohta S, Tanaka T et al (1989) Deep-sea communities dominated by the giant clam, *Calyptogena soyoae*, along the slope foot of Hatsushima Island, Sagami Bay, Central Japan. Palaeogeogr Palaeoclimatol Palaeoecol 71:179–192. https://doi.org/10.1016/0031-0182(89)90037-0

Hauquier F, Ingels J, Gutt J et al (2011) Characterisation of the nematode community of a low-activity cold seep in the recently ice-shelf free Larsen B Area, eastern Antarctic Peninsula. PLoS One 6:e22240. https://doi.org/10.1371/journal.pone.0022240

Hayward BW, Gregory MR, Kennett JP (2011) An extinct foraminifer endemic to hydrocarbon seeps? Geology 39:603–605. https://doi.org/10.1130/G31974.1

Herrera S, Watanabe H, Shank TM (2015) Evolutionary and biogeographical patterns of barnacles from deep-sea hydrothermal vents. Mol Ecol 24:673–689. https://doi.org/10.1111/mec.13054

Horne DJ, Brandão SN, Slipper IJ (2011) The Platycopid Signal deciphered: responses of ostracod taxa to environmental change during the Cenomanian-Turonian Boundary Event (Late Cretaceous) in SE England. Palaeogeogr Palaeoclimatol Palaeoecol 308:304–312. https://doi.org/10.1016/j.palaeo.2011.05.034

Hryniewicz K, Nakrem HA, Hammer Ø et al (2015a) The palaeoecology of the latest Jurassic−earliest Cretaceous hydrocarbon seep carbonates from Spitsbergen, Svalbard. Lethaia 48:353–374. https://doi.org/10.1111/let.12112

Hryniewicz K, Hagström J, Hammer Ø et al (2015b) Late Jurassic–Early Cretaceous hydrocarbon seep boulders from Novaya Zemlya and their faunas. Palaeogeogr Palaeoclimatol Palaeoecol 436:231–244. https://doi.org/10.1016/j.palaeo.2015.06.036

Hryniewicz K, Bitner MA, Durska E et al (2016) Paleocene methane seep and wood-fall marine environments from Spitsbergen, Svalbard. Palaeogeogr Palaeoclimatol Palaeoecol 462:41–56. https://doi.org/10.1016/j.palaeo.2016.08.037

Hryniewicz K, Jakubowicz M, Belka Z et al (2017) New bivalves from a Middle Devonian methane seep in Morocco: the oldest record of repetitive shell morphologies among some seep bivalve molluscs. J Syst Palaeontol 15:19–41. https://doi.org/10.1080/14772019.2015.1136900

Hryniewicz K, Amano K, Bitner MA et al (2019) A late Paleocene fauna from shallow-water chemosynthesis-based ecosystems, Spitsbergen, Svalbard. Acta Palaeontol Pol 64:101–141. https://doi.org/10.4202/app.00554.2018

Humes AG (1988) Copepoda from deep-sea hydrothermal vents and cold seeps. Hydrobiologia 167(168):549–554. https://doi.org/10.1007/BF00026351

Hyžný M, Gašparič R (2014) Ghost shrimp *Calliax* de Saint Laurent, 1973 (Decapoda: Axiidea: Callianassidae) in the fossil record: systematics, palaeoecology and palaeobiogeography. Zootaxa 3821:37–57. https://doi.org/10.11646/zootaxa.3821.1.3

Hyžný M, Klompmaker AA (2015) Systematics, phylogeny, and taphonomy of ghost shrimps (Decapoda): a perspective from the fossil record. Arthropod Syst Phylogeny 73:401–437

Hyžný M, Duane MJ, Reinink-Smith LM et al (2018) Taphonomy of ghost shrimps (Decapoda: Axiidea: Callianassidae) associated with their burrows within a middle Miocene mud volcano complex of Persian (Arabian) Gulf, Kuwait. Palaeogeogr Palaeoclimatol Palaeoecol 511:218–231. https://doi.org/10.1016/j.palaeo.2018.08.006

Jenkins RG, Kaim A, Hikida Y (2007a) Antiquity of the substrate choice among acmaeid limpets from Late Cretaceous chemosynthesis-based communities. Acta Palaeontol Pol 52:369–373

Jenkins RG, Kaim A, Hikida Y et al (2007b) Methane-flux-dependent lateral faunal changes in a Late Cretaceous chemosymbiotic assemblage from the Nakagawa area of Hokkaido, Japan. Geobiology 5:127–139. https://doi.org/10.1111/j.1472-4669.2007.00106.x

Jenkins RG, Kaim A, Little CTS et al (2013) Worldwide distribution of the modiomorphid bivalve genus *Caspiconcha* in late Mesozoic hydrocarbon seeps. Acta Palaeontol Pol 58:357–382

Jensen P, Aagaard I, Burke RA Jr et al (1992) 'Bubbling reefs' in the Kattegat: submarine landscapes of carbonate-cemented rocks support a diverse ecosystem at methane seeps. Mar Ecol Prog Ser 83:103–112

Jørgensen LL, Primicerio R (2007) Impact scenario for the invasive red king crab *Paralithodes camtschaticus* (Tilesius, 1815) (Reptantia, Lithodidae) on Norwegian, native, epibenthic prey. Hydrobiologia 590:47–54. https://doi.org/10.1007/s10750-007-0756-9

Juniper S, Sibuet M (1987) Cold seep benthic communities in the Japan subduction zones: spatial organization, trophic strategies and evidence for temporal evolution. Mar Ecol Prog Ser 40:115–126. https://doi.org/10.3354/meps040115

Kanie Y (1996) Paleoenvironmental study on the chemosynthethic fossil assemblages of the Hayama Formation and the related late Cenozoic assemblages from the Miura-Boso area, south-central Japan. Fossils 60:53–58

Kanie Y, Asami S, Okada H et al (1992) White clam community discovered from fractured claystone of the Miocene Hayama Group, Miura Peninsula, south-central Japan. Sci Rep Yokosuka City Mus 40:31–35

Karanovic I, Brandão SN (2015) Biogeography of deep-sea wood fall, cold seep and hydrothermal vent Ostracoda (Crustacea), with the description of a new family and a taxonomic key to living Cytheroidea. Deep-Sea Res II 111:76–94. https://doi.org/10.1016/j.dsr2.2014.09.008

Karasawa H (2011) New axiidean Decapoda from the Albian (Lower Cretaceous) chemosynthetic community of Hokkaido, Japan. Bull Mizunami Fossil Mus 37:27–29

Karasawa H, Kano M (2021) A first notice of the goniodromitid crab from the Cenomanian (Upper Cretaceous) cold seep deposit of Hokkaido, Japan, with the redescription of *Sabellidromites inflata* (Collins and Karasawa, 1993) (Decapoda: Goniodromitidae). Boletín de la Sociedad Geológica Mexicana 73:A020121. https://doi.org/10.18268/BSGM2021v73n3a020121

Karasawa H, Mizuno Y, Hachiya K et al (2017) Reappraisal of anomuran and brachyuran decapods from the lower Miocene Morozaki Group, Japan, collected by the Tokai Fossil Society. Bull Mizunami Fossil Mus 43:47–69

Kato M, Oji T, Shirai K (2017) Paleoecology of echinoderms in cold seep environments revealed by isotope analysis in the Late Cretaceous Western Interior Seaway. Palauis 32:218–230. https://doi.org/10.2110/palo.2016.079

Kelly SRA, Ditchfield PW, Doubleday PA et al (1995) An Upper Jurassic methane-seep limestone from the Fossil Bluff Group forearc basin of Alexander Island, Antarctica. J Sediment Res 65A:274–282. https://doi.org/10.1306/D426809A-2B26-11D7-8648000102C1865D

Kelly SRA, Blanc E, Price SP et al (2000) Early Cretaceous giant bivalves from seep-related limestone mounds, Wollaston Forland, northeast Greenland. Geol Soc Lond Spec Publ 177:227–246. https://doi.org/10.1144/GSL.SP.2000.177.01.13

Kidwell SM, Flessa KW (1995) The quality of the fossil record: populations, species, and communities. Ann Rev Ecol Syst 24:433–464. https://doi.org/10.1146/annurev.earth.24.1.433

Kiel S (2006) New records and species of molluscs from Tertiary cold-seep carbonates in Washington State, USA. J Paleontol 80:121–137. https://doi.org/10.1666/0022-3360(2006)080[0121:NRASOM]2.0.CO;2

Kiel S (2010a) An Eldorado for paleontologists: the Cenozoic seeps of western Washington State, USA. In: Kiel S (ed) The vent and seep biota. Springer, Dordrecht, pp 433–448

Kiel S (2010b) On the potential generality of depth-related ecologic structure in cold-seep communities: evidence from Cenozoic and Mesozoic examples. Palaeogeogr Palaeoclimatol Palaeoecol 295:245–257. https://doi.org/10.1016/j.palaeo.2010.05.042

Kiel S (2010c) The fossil record of vent and seep mollusks. In: Kiel S (ed) The vent and seep biota. Springer, Dordrecht, pp 255–277

Kiel S, Hansen BT (2015) Cenozoic methane-seep faunas of the Caribbean region. PLoS One 10:e0140788. https://doi.org/10.1371/journal.pone.0140788

Kiel S, Amano K, Jenkins RG (2008) Bivalves from Cretaceous cold-seep deposits on Hokkaido, Japan. Acta Palaeontol Pol 53:525–537. https://doi.org/10.4202/app.2008.0310

Kiel S, Wiese F, Titus AL (2012) Shallow-water methane-seep faunas in the Cenomanian Western Interior Seaway: no evidence for onshore-offshore adaptations to deep-sea vents. Geology 40:839–842. https://doi.org/10.1130/G33300.1

Kiel S, Birgel D, Campbell KA et al (2013) Cretaceous methane-seep deposits from New Zealand and their fauna. Palaeogeogr Palaeoclimatol Palaeoecol 390:17–34. https://doi.org/10.1016/j.palaeo.2012.10.033

Kiel S, Amano K, Jenkins RG (2016) Predation scar frequencies in chemosymbiotic bivalves at an Oligocene seep deposit and their potential relation to inferred sulfide tolerances. Palaeogeogr Palaeoclimatol Palaeoecol 453:139–145. https://doi.org/10.1016/j.palaeo.2016.04.026

Kiel S, Altamirano AJ, Birgel D et al (2019) Fossiliferous methane-seep deposits from the Cenozoic Talara Basin in northern Peru. Lethaia 53:166–182. https://doi.org/10.1111/let.12349

Kiel S, Hybertsen F, Hyžný M et al (2020) Mollusks and a crustacean from early Oligocene methane-seep deposits in the Talara Basin, northern Peru. Acta Palaeontol Pol 65:109–138. https://doi.org/10.4202/app.00631.2019

Kietzmann DA, Blau J, Fernández DE et al (2010) Crustacean microcoprolites from the Upper Jurassic–Lower Cretaceous of the Neuquén Basin, Argentina: systematics and biostratigraphic implications. Acta Palaeontol Pol 55:277–284. https://doi.org/10.4202/app.2009.0094

Klompmaker AA, Feldmann RM, Robins CM et al (2012a) Peak diversity of Cretaceous galatheoids (Crustacea, Decapoda) from northern Spain. Cretac Res 36:125–145. https://doi.org/10.1016/j.cretres.2012.03.003

Klompmaker AA, Feldmann RM, Schweitzer CE (2012b) A hotspot for Cretaceous goniodromitids (Decapoda: Brachyura) from reef associated strata in Spain. J Crustac Biol 32:780–801. https://doi.org/10.1163/193724012X635340

Klompmaker AA, Ortiz JD, Wells NA (2013a) How to explain a decapod crustacean diversity hotspot in a mid-Cretaceous coral reef. Palaeogeogr Palaeoclimatol Palaeoecol 374:256–273. https://doi.org/10.1016/j.palaeo.2013.01.024

Klompmaker AA, Schweitzer CE, Feldmann RM et al (2013b) The influence of reefs on the rise of Mesozoic marine crustaceans. Geology 41:1179–1182. https://doi.org/10.1130/G34768.1

Klompmaker AA, Jakobsen SL, Lauridsen BW (2016) Evolution of body size, vision, and biodiversity of coral-associated organisms: evidence from fossil crustaceans in cold-water coral and tropical coral ecosystems. BMC Evol Biol 16:132. https://doi.org/10.1186/s12862-016-0694-0

Klompmaker AA, Portell RW, Frick MG (2017) Comparative experimental taphonomy of eight marine arthropods indicates distinct differences in preservation potential. Palaeontology 60:773–794. https://doi.org/10.1111/pala.12314

Klompmaker AA, Hyžný M, Portell RW et al (2019a) Muscles and muscle scars in fossil malacostracan crustaceans. Earth-Sci Rev 194:306–326. https://doi.org/10.1016/j.earscirev.2019.04.012

Klompmaker AA, Kelley PH, Chattopadhyay D et al (2019b) Predation in the marine fossil record: studies, data, recognition, environmental factors, and behavior. Earth-Sci Rev 194:472–520. https://doi.org/10.1016/j.earscirev.2019.02.020

Kneer D, Asmus H, Vonk JA (2008) Seagrass as the main food source of *Neaxius acanthus* (Thalassinidea: Strahlaxiidae), its burrow associates, and of *Corallianassa coutierei* (Thalassinidea: Callianassidae). Est Coast Shelf Sci 79:620–630. https://doi.org/10.1016/j.ecss.2008.05.013

Kočová Veselská M, Kočí T, Collins JSH et al (2015) A new species of scalpelliform cirripede (Crustacea, Cirripedia) from the upper Cenomanian–lower Turonian shallow-water facies at Velim (Bohemian Cretaceous Basin) and its palaeoecological implications. Neues Jahrb Geol Paläontol Abh 278:201–211. https://doi.org/10.1127/njgpa/2015/0525

Komai T, Segonzac M (2005) A revision of the genus *Alvinocaris* Williams and Chace (Crustacea: Decapoda: Caridea: Alvinocarididae), with descriptions of a new genus and a new species of *Alvinocaris*. J Nat Hist 39:1111–1175. https://doi.org/10.1080/00222930400002499

Kornienko ES (2013) Burrowing shrimp of the infraorders Gebiidea and Axiidea (Crustacea: Decapoda). Russ J Mar Biol 39:1–14. https://doi.org/10.1134/S1063074013010033

Kuechler RR, Birgel D, Kiel S et al (2012) Miocene methane-derived carbonates from southwestern Washington, USA and a model for silicification at seeps: Miocene seep carbonates. Lethaia 45:259–273. https://doi.org/10.1111/j.1502-3931.2011.00280.x

Kulm LD, Suess E, Moore JC et al (1986) Oregon subduction zone: venting, fauna, and carbonates. Science 231:561–566. https://doi.org/10.1126/science.231.4738.561

Laird JD, Belanger CL (2019) Quantifying successional change and ecological similarity among Cretaceous and modern cold-seep faunas. Paleobiology 45:114–135. https://doi.org/10.1017/pab.2018.41

Landman NH, Cochran JK, Brezina J et al (this volume) Methane seeps in the Late Cretaceous Western Interior Seaway. In: Kaim A, Cochran JK, Landman NH (eds) Ancient methane seeps and cognate communities. Topics in Geobiology. Springer, Cham

Larson NL, Brezina J, Landman NH et al (2013) Hydrocarbon seeps: unique habitats that preserved the diversity of fauna in the Late Cretaceous Western Interior Seaway. Geological Society of Wyoming Field Guide 2013. Geological Society of Wyoming, Caspar, pp 1–20

Lessard-Pilon S, Porter MD, Cordes EE et al (2010) Community composition and temporal change at deep Gulf of Mexico cold seeps. Deep-Sea Res II 57:1891–1903. https://doi.org/10.1016/j.dsr2.2010.05.012

Lethiers F, Whatley R (1994) The use of Ostracoda to reconstruct the oxygen levels of late Palaeozoic oceans. Mar Micropaleontol 24:57–69. https://doi.org/10.1016/0377-8398(94)90011-6

Levin LA (2005) Ecology of cold seep sediments: interactions of fauna with flow, chemistry and microbes. Oceanogr Mar Biol Ann Rev 43:1–46

Levin LA, Michener RH (2002) Isotopic evidence for chemosynthesis-based nutrition of macrobenthos: the lightness of being at Pacific methane seeps. Limnol Oceanogr 47:1336–1345. https://doi.org/10.4319/lo.2002.47.5.1336

Levin LA, James DW, Martin CM et al (2000) Do methane seeps support distinct macrofaunal assemblages? Observations on community structure and nutrition from the northern California slope and shelf. Mar Ecol Prog Ser 208:21–39. https://doi.org/10.3354/meps208021

Levin LA, Mendoza GF, Grupe BM et al (2015) Biodiversity on the rocks: macrofauna inhabiting authigenic carbonate at Costa Rica methane seeps. PLoS One 10:e0131080. https://doi.org/10.1371/journal.pone.0131080

Little CTS, Birgel D, Boyce AJ et al (2015) Late Cretaceous (Maastrichtian) shallow water hydrocarbon seeps from Snow Hill and Seymour Islands, James Ross Basin, Antarctica. Palaeogeogr Palaeoclimatol Palaeoecol 418:213–228. https://doi.org/10.1016/j.palaeo.2014.11.020

Lörz A-N, Glenner H, Lützen J (2008) New records of Rhizocephala (Cirripedia) from New Zealand, including the first rhizocephalan records from hot vents and cold seeps. Crustaceana 81:1013–1019. https://doi.org/10.1163/156854008X354911

Lovrich GA, Thiel M (2011) Ecology, physiology, feeding and trophic role of squat lobsters. In: Poore G, Ahyong ST, Taylor J (eds) The biology of squat lobsters. CRC Press, Boca Raton, pp 183–222

Luque J, Schweitzer CE, Santana W et al (2017) Checklist of fossil decapod crustaceans from tropical America: part I, Anomura and Brachyura. Nauplius 25:e2017025. https://doi.org/10.1590/2358-2936e2017025

Lützen J, Glenner H, Lörz A (2009) Parasitic barnacles (Cirripedia: Rhizocephala) from New Zealand off-shore waters. N Z J Mar Freshw Res 43:613–621. https://doi.org/10.1080/00288330909510027

MacAvoy SE, Carney RS, Fisher CR et al (2002) Use of chemosynthetic biomass by large, mobile, benthic predators in the Gulf of Mexico. Mar Ecol Prog Ser 225:65–78. https://doi.org/10.3354/meps225065

MacAvoy SE, Carney RS, Morgan E et al (2008) Stable isotope variation among the mussel *Bathymodiolus childressi* and associated heterotrophic fauna at four cold-seep communities in the Gulf of Mexico. J Shellfish Res 27:147–151. https://doi.org/10.2983/0730-8000(2008)27[147:SIVATM]2.0.CO;2

Macpherson E, Segonzac M (2005) Species of the genus *Munidopsis* (Crustacea, Decapoda, Galatheidae) from the deep Atlantic Ocean, including cold-seep and hydrothermal vent areas. Zootaxa 1095:1–60

Martin JW, Haney TA (2005) Decapod crustaceans from hydrothermal vents and cold seeps: a review through 2005. Zool J Linn Soc 145:445–522. https://doi.org/10.1111/j.1096-3642.2005.00178.x

Mazumdar A, Dewangan P, Peketi A et al (2019) The first record of active methane (cold) seep ecosystem associated with shallow methane hydrate from the Indian EEZ. J Earth Syst Sci 128:18. https://doi.org/10.1007/s12040-018-1044-y

McKenzie KG, Majoran S, Emami V et al (1989) The *Krithe* problem—first test of Peypouquet's hypothesis, with a redescription of *Krithe praetexta praetexta* (Crustacea, Ostracoda). Palaeogeogr Palaeoclimatol Palaeoecol 74:343–354. https://doi.org/10.1016/0031-0182(89)90069-2

Meehan KC, Landman NH (2016) Faunal associations in cold-methane seep deposits from the Upper Cretaceous Pierre Shale, South Dakota. Palaios 31:291–301. https://doi.org/10.2110/palo.2015.055

Meehan KC, Mego Vela M, Gilles NV et al (2018) Foraminifera from the upper Campanian Pierre Shale methane cold-seeps, South Dakota. Cretac Res 89:235–247. https://doi.org/10.1016/j.cretres.2018.03.023

Mizuno Y, Takeda M (1993) Crustacea. In: Tokaikaseki-morozaki-sougun-kankou-kai (ed) Fossils from the Miocene Morozaki Group—fossils of Aichi Prefecture. Tokai Fossil Society, Nagoya, pp 77–90

Montagna PA, Bauer JE, Toal J et al (1987) Temporal variability and the relationship between benthic meiofaunal and microbial populations of a natural coastal petroleum seep. J Mar Res 45:761–789. https://doi.org/10.1357/002224087788326894

Moore HB (1933) The fæcal pellets of the Anomura. Proc R Soc Edinb 52:296–308. https://doi.org/10.1017/S0370164600019544

Moore GW (1969) New formations on Kodiak and adjacent islands, Alaska. US Geol Surv Bull 1274:A27–A35

Natalicchio M, Dela Pierre F, Clari P et al (2013) Hydrocarbon seepage during the Messinian salinity crisis in the Tertiary Piedmont Basin (NW Italy). Palaeogeogr Palaeoclimatol Palaeoecol 390:68–80. https://doi.org/10.1016/j.palaeo.2012.11.015

Natalicchio M, Peckmann J, Birgel D et al (2015) Seep deposits from northern Istria, Croatia: a first glimpse into the Eocene seep fauna of the Tethys region. Geol Mag 152:444–459. https://doi.org/10.1017/S0016756814000466

Nesbitt EA, Martin RA, Campbell KA (2013) New records of Oligocene diffuse hydrocarbon seeps, northern Cascadia margin. Palaeogeogr Palaeoclimatol Palaeoecol 390:116–129. https://doi.org/10.1016/j.palaeo.2013.05.001

Neto de Carvalho C, Viegas PA, Cachao M (2007) *Thalassinoides* and its producer: populations of *Mecochirus* buried within their burrow systems, Boca do Chapim Formation (Lower Cretaceous), Portugal. Palaios 22:104–109. https://doi.org/10.2110/palo.2006.p06-011r

Newman WA, Yamaguchi T, Southward AJ et al (2006) Cirripedia. In: Desbruyères D, Segonzac M, Bright M (eds) Handbook of deep-sea hydrothermal vent fauna. Biologiezentrum, Linz, pp 356–368

Nielsen C (1975) Observations on *Buccinum undatum* L. attacking bivalves and on prey responses, with a short review on attack methods of other prosobranchs. Ophelia 13:87–108. https://doi.org/10.1080/00785326.1974.10430593

Niemann H, Linke P, Knittel K et al (2013) Methane-carbon flow into the benthic food web at cold seeps—a case study from the Costa Rica subduction zone. PLoS One 8:e74894. https://doi.org/10.1371/journal.pone.0074894

Noever C, Glenner H (2018) The origin of king crabs: hermit crab ancestry under the magnifying glass. Zool J Linn Soc 182:300–318. https://doi.org/10.1093/zoolinnean/zlx033

Olu K, Sibuet M, Harmegnies F et al (1996) Spatial distribution of diverse cold seep communities living on various diapiric structures of the southern Barbados prism. Prog Oceanogr 38:347–376. https://doi.org/10.1016/S0079-6611(97)00006-2

Olu-Le Roy K, Sibuet M, Fiala-Médioni A et al (2004) Cold seep communities in the deep eastern Mediterranean Sea: composition, symbiosis and spatial distribution on mud volcanoes. Deep-Sea Res I 51:1915–1936. https://doi.org/10.1016/j.dsr.2004.07.004

Peckmann J, Thiel V, Michaelis W et al (1999) Cold seep deposits of Beauvoisin (Oxfordian; southeastern France) and Marmorito (Miocene; northern Italy): microbially induced authigenic carbonates. Int J Earth Sci 88:60–75. https://doi.org/10.1007/s005310050246

Peckmann J, Goedert JL, Thiel V et al (2002) A comprehensive approach to the study of methane-seep deposits from the Lincoln Creek Formation, western Washington State, USA. Sedimentology 49:855–873. https://doi.org/10.1046/j.1365-3091.2002.00474.x

Peckmann J, Campbell KA, Walliser OH et al (2007a) A Late Devonian hydrocarbon-seep deposit dominated by dimerelloid brachiopods, Morocco. Palaios 22:114–122. https://doi.org/10.2110/palo.2005.p05-115r

Peckmann J, Senowbari-Daryan B, Birgel D et al (2007b) The crustacean ichnofossil *Palaxius* associated with callianassid body fossils in an Eocene methane-seep limestone, Humptulips Formation, Olympic Peninsula, Washington: seep-associated crustacean fossils. Lethaia 40:273–280. https://doi.org/10.1111/j.1502-3931.2007.00026.x

Peckmann J, Sandy MR, Taylor DG et al (2013) An Early Jurassic brachiopod-dominated seep deposit enclosed by serpentinite, eastern Oregon, USA. Palaeogeogr Palaeoclimatol Palaeoecol 390:4–16. https://doi.org/10.1016/j.palaeo.2013.01.003

Pérez-Losada M, Harp M, Høeg JT et al (2008) The tempo and mode of barnacle evolution. Mol Phylogenet Evol 46:328–346. https://doi.org/10.1016/j.ympev.2007.10.004

Peypouquet JP (1975) Les variations des caractères morphologiques internes chez les ostracodes des genres *Krithe* et *Parakrithe*: relation possible avec le teneur en O_2 dissous dans l'eau. Bull Inst Géol Bassin Aquitaine 17:81–88

Peypouquet J-P (1979) Ostracodes et paléo-environnements: méthodologie et application aux domaines profonds du Cénozoïque. Bull Bur Rech Géol Minières 4:3–79

Plotnick RE (1986) Taphonomy of a modern shrimp: implications for the arthropod fossil record. Palaios 1:286–293

Polz H (2007) Die Garnelengattung *Harthofia* g. nov. (Crustacea: Decapoda: Pleocyemata: Caridea) mit zwei neuen Arten aus den Solnhofener Plattenkalken von Eichstätt. Archaeopteryx 25:1–13

Polz MF, Robinson JJ, Cavanaugh CM et al (1998) Trophic ecology of massive shrimp aggregations at a Mid-Atlantic Ridge hydrothermal vent site. Limnol Oceanogr 43:1631–1638. https://doi.org/10.4319/lo.1998.43.7.1631

Pond DW, Dixon DR, Bell MV et al (1997) Occurrence of 16:2(n-4) and 18:2(n-4) fatty acids in the lipids of the hydrothermal vent shrimps *Rimicaris exoculata* and *Alvinocaris markensis*: nutritional and trophic implications. Mar Ecol Prog Ser 156:167–174

Portnova DA, Mokievsky VO, Haflidason H et al (2014) Metazoan meiobenthos and nematode assemblages in the Nyegga Region of methane seepage (Norwegian Sea). Russ J Mar Biol 40:255–265. https://doi.org/10.1134/S1063074014040075

Powell CL II, Clites EC, Poust AW (2019) Miocene marine macropaleontology of the fourth bore Caldecott Tunnel excavation, Berkeley Hills, Oakland, California, USA. PaleoBios 36:1–34. https://escholarship.org/uc/item/1gm970pg

Quattrini AM, Nizinski MS, Chaytor JD et al (2015) Exploration of the canyon-incised continental margin of the northeastern United States reveals dynamic habitats and diverse communities. PLoS One 10:e0139904. https://doi.org/10.1371/journal.pone.0139904

Ramirez-Llodra E, Segonzac M (2006) Reproductive biology of *Alvinocaris muricola* (Decapoda: Caridea: Alvinocarididae) from cold seeps in the Congo Basin. J Mar Biol Assoc U K 86:1347–1356. https://doi.org/10.1017/S0025315406014378

Ritt B, Sarrazin J, Caprais J-C et al (2010) First insights into the structure and environmental setting of cold-seep communities in the Marmara Sea. Deep-Sea Res I 57:1120–1136. https://doi.org/10.1016/j.dsr.2010.05.011

Ritt B, Pierre C, Gauthier O et al (2011) Diversity and distribution of cold-seep fauna associated with different geological and environmental settings at mud volcanoes and pockmarks of the Nile Deep-Sea Fan. Mar Biol 158:1187–1210. https://doi.org/10.1007/s00227-011-1679-6

Robins CM, Klompmaker AA (2019) Extreme diversity and parasitism of Late Jurassic squat lobsters (Decapoda: Galatheoidea) and the oldest records of porcellanids and galatheids. Zool J Linn Soc 187:1131–1154. https://doi.org/10.1093/zoolinnean/zlz067

Robins CM, Feldmann RM, Schweitzer CE (2013) Nine new genera and 24 new species of the Munidopsidae (Decapoda: Anomura: Galatheoidea) from the Jurassic Ernstbrunn Limestone of Austria, and notes on fossil munidopsid classification. Ann Naturhistorischen Mus Wien A 115:167–251

Robins CM, Feldmann RM, Schweitzer CE et al (2016) New families Paragalatheidae and Catillogalatheidae (Decapoda: Anomura: Galatheoidea) from the Mesozoic, restriction of the genus *Paragalathea*, and establishment of 6 new genera and 20 new species. Ann Naturhistorischen Mus Wien A 118:65–131

Rolin Y, Gaillard C, Roux M (1990) Ecologie des pseudobiohermes des Terres Noires jurassiques liés à paléo-sources sous-marines: le site oxfordien de Beauvoisin (Drôme, Bassin du Sud-Est, France). Palaeogeogr Palaeoclimatol Palaeoecol 80:79–105. https://doi.org/10.1016/0031-0182(90)90123-O

Russo A, Pugliese N, Serventi P (2012) Miocene ostracodes of cold seep settings from northern Apennines (Italy). Rev Micropaléontologie 55:29–38. https://doi.org/10.1016/j.revmic.2011.09.001

Sahling H, Galkin SV, Salyuk A et al (2003) Depth-related structure and ecological significance of cold-seep communities—a case study from the Sea of Okhotsk. Deep-Sea Res I 50:1391–1409. https://doi.org/10.1016/j.dsr.2003.08.004

Sakai K, Türkay M (1999) A new subfamily, Bathycalliacinae n. subfam., for *Bathycalliax geomar* n. gen., n. sp. from the deep water cold steps off Oregon, USA (Crustacea, Decapoda, Callianassidae). Senckenberg Biol 79:203–210

Sandy MR (2010) Brachiopods from ancient hydrocarbon seeps and hydrothermal vents. In: Kiel S (ed) The vent and seep biota. Springer, Dordrecht, pp 279–314

Sandy MR, Goedert JL, Peckmann J et al (2005) Brachiopods under attack—evidence of predation on a mass-occurrence of the rhynchonellid brachiopod *Sulcirostra* from an autochtonous cold-seep limestone—Early Jurassic of Oregon, U.S.A. Abstracts, 5th National Symposium of Paleontology, University of Bucharest, Romania

Sasaki T, Warén A, Kano Y et al (2010) Gastropods from Recent hot vents and cold seeps: systematics, diversity and life strategies. In: Kiel S (ed) The vent and seep biota. Springer, Dordrecht, pp 169–254

Schweigert G (2011) The decapod crustaceans of the Upper Jurassic Solnhofen Limestones: a historical review and some recent discoveries. Neues Jahrb Geol Paläontol Abh 260:131–140. https://doi.org/10.1127/0077-7749/2011/0162

Schweigert G, Seegis DB, Fels A et al (1997) New internally structured decapod microcoprolites from Germany (late Triassic/early Miocene), southern Spain (Early/Middle Jurassic) and Portugal (Late Jurassic): taxonomy, palaeoecology and evolutionary implications. Paläontol Z 71:51–69. https://doi.org/10.1007/BF03022546

Schweitzer CE, Feldmann RM (2000) First notice of the Chirostylidae (Decapoda) in the fossil record and new Tertiary Galatheidae (Decapoda) from the Americas. Bull Mizunami Fossil Mus 27:147–165

Schweitzer CE, Feldmann RM (2008) New Eocene hydrocarbon seep decapod crustacean (Anomura: Galatheidae: Shinkaiinae) and its paleobiology. J Paleontol 82:1021–1029. https://doi.org/10.1666/08-007.1

Schweitzer CE, Feldmann RM (2010) The Decapoda (Crustacea) as predators on Mollusca through geologic time. Palaios 25:167–182. https://doi.org/10.2110/palo.2009.p09-054r

Schweitzer CE, Feldmann RM (2015) Faunal turnover and niche stability in marine Decapoda in the Phanerozoic. J Crustac Biol 35:633–649. https://doi.org/10.1163/1937240X-00002359

Schweitzer CE, Nyborg TG, Feldmann RM et al (2004) Homolidae De Haan, 1839 and Homolodromiidae Alcock, 1900 (Crustacea: Decapoda: Brachyura) from the Pacific Northwest of North America and a reassessment of their fossil records. J Paleontol 78:133–149. https://doi.org/10.1666/0022-3360(2004)078<0133:HDHAHA>2.0.CO;2

Seabrook S, De Leo FC, Thurber AR (2019) Flipping for food: the use of a methane seep by tanner crabs (*Chionoecetes tanneri*). Front Mar Sci 6:43. https://doi.org/10.3389/fmars.2019.00043

Selden PA, Huys R, Stephenson MH et al (2010) Crustaceans from bitumen clast in Carboniferous glacial diamictite extend fossil record of copepods. Nat Commun 1:1–6. https://doi.org/10.1038/ncomms1049

Sellanes J, Quiroga E, Neira C (2008) Megafauna community structure and trophic relationships at the recently discovered Concepcion Methane Seep Area, Chile, 36°S. ICES J Mar Sci 65:1102–1111. https://doi.org/10.1093/icesjms/fsn099

Sen A, Åström EKL, Hong W-L et al (2018) Geophysical and geochemical controls on the megafaunal community of a high Arctic cold seep. Biogeosciences 15:4533–4559. https://doi.org/10.5194/bg-15-4533-2018

Senowbari-Daryan B, Kube B (2003) The ichnogenous *Palaxius* (crustacean coprolite) and description of *P. hydranensis* n. sp. from the upper Triassic (Norian part of 'Pantokrator' limestone) of Hydra (Greece). Paläontol Z 77:115–122. https://doi.org/10.1007/BF03004563

Senowbari-Daryan B, Gaillard C, Peckmann J (2007) Crustacean microcoprolites from Jurassic (Oxfordian) hydrocarbon-seep deposits of Beauvoisin, southeastern France. Facies 53:229–238. https://doi.org/10.1007/s10347-006-0096-7

Senowbari-Daryan B, El Rab AG, Heindel K et al (2017) *Palaxius salataensis* Brönnimann, Cros and Zaninetti, 1972, the oldest crustacean microcoprolite from the early Carboniferous of Guangxi, South China. Palaontologische Z 91:299–305. https://doi.org/10.1007/s12542-017-0355-7

Shank TM, Black MB, Halanych KM et al (1999) Miocene radiation of deep-sea hydrothermal vent shrimp (Caridea: Bresiliidae): evidence from mitochondrial cytochrome oxidase subunit I. Mol Phylogenet Evol 13:244–254. https://doi.org/10.1006/mpev.1999.0642

Shimoda K, Aramaki Y, Nasuda J et al (2007) Food sources for three species of *Nihonotrypaea* (Decapoda: Thalassinidea: Callianassidae) from western Kyushu, Japan, as determined by carbon and nitrogen stable isotope analysis. J Exp Mar Biol Ecol 342:292–312. https://doi.org/10.1016/j.jembe.2006.11.003

Smith AJ, Horne DJ (2002) Ecology of marine, marginal marine and nonmarine ostracodes. In: Holmes JA, Chivas AR (eds) The Ostracoda: applications in quaternary research, Geophysical Monograph Series vol. 131. American Geophysical Union, Washington, DC, pp 37–64

Smrzka D (2013) Petrography and geochemistry of Eocene cold-seep carbonates from Washington State, USA. Thesis, University of Vienna

Smrzka D, Zwicker J, Kolonic S et al (2017) Methane seepage in a Cretaceous greenhouse world recorded by an unusual carbonate deposit from the Tarfaya Basin, Morocco. Depositional Rec 3:4–37. https://doi.org/10.1002/dep2.24

Sommer S, Gutzmann E, Pfannkuche O (2007) Sediments hosting gas hydrate: oases for metazoan meiofauna. Mar Ecol Prog Ser 337:27–37. https://doi.org/10.3354/meps337027

Southward AJ (2005) Systematics and ecology of a new species of stalked barnacle (Cirripedia: Thoracica: Scalpellomorpha: Eolepadidae: Neolepadini) from the Pacific-Antarctic Ridge at 38° S. Senckenb Marit 35:147–156. https://doi.org/10.1007/BF03043683

Southward AJ, Jones DS (2003) A revision of stalked barnacles (Cirripedia: Thoracica: Scalpellomorpha: Eolepadidae: Neolepadinae) associated with hydrothermalism, including a description of a new genus and species from a volcanic seamount off Papua New Guinea. Senckenb Marit 32:77–93. https://doi.org/10.1007/BF03043086

Southward EC, Schulze A, Tunnicliffe V (2002) Vestimentiferans (Pogonophora) in the Pacific and Indian oceans: a new genus from Lihir Island (Papua New Guinea) and the Java Trench, with the first report of *Arcovestia ivanovi* from the North Fiji Basin. J Nat Hist 36:1179–1197. https://doi.org/10.1080/00222930110040402

Squires RL, Goedert JL (1995) An extant species of *Leptochiton* (Mollusca: Polyplacophora) in Eocene and Oligocene cold-seep limestones, Olympic Peninsula, Washington. Veliger 38:47–53

Stapleton KL, Long M, Bird FL (2001) Comparative feeding ecology of two spatially coexisting species of ghost shrimp, *Biffarius arenosus* and *Trypaea australiensis* (Decapoda: Callianassidae). Ophelia 55:141–150. https://doi.org/10.1080/00785236.2001.10409481

Stecher J, Tunnicliffe V, Türkay M (2003) Population characteristics of abundant bivalves (Mollusca, Vesicomyidae) at a sulphide-rich seafloor site near Lihir Island, Papua New Guinea. Can J Zool 81:1815–1824. https://doi.org/10.1139/z03-180

Stempien JA (2005) Brachyuran taphonomy in a modern tidal-flat environment: preservation potential and anatomical bias. Palaios 20:400–410

Stevens CJ, Limén H, Pond DW et al (2008) Ontogenetic shifts in the trophic ecology of two alvinocaridid shrimp species at hydrothermal vents on the Mariana Arc, western Pacific Ocean. Mar Ecol Prog Ser 356:225–237. https://doi.org/10.3354/meps07270

Sudarsky S (2016) A phylogenetic analysis of fossil and extant shrimp-like decapods (Dendrobranchiata and Caridea). Thesis, Kent State University

Takeda M, Mizuno Y, Yamaoka M (1986) Some fossil crustaceans from the Miocene Morozaki Group in the Chita Peninsula, central Japan. Kaseki-No-Tomo Publ Tokai Fossil Soc 28:12–22

Taviani M, Angeletti L, Ceregato A et al (2013) The Gela Basin pockmark field in the strait of Sicily (Mediterranean Sea): chemosymbiotic faunal and carbonate signatures of postglacial to modern cold seepage. Biogeosciences 10:4653–4671. https://doi.org/10.5194/bg-10-4653-2013

Teichert BMA, Luppold FW (2013) Glendonites from an Early Jurassic methane seep—climate or methane indicators? Palaeogeogr Palaeoclimatol Palaeoecol 390:81–93. https://doi.org/10.1016/j.palaeo.2013.03.001

Thatje S, Hall S (2016) The effect of temperature on the evolution of per offspring investment in a globally distributed family of marine invertebrates (Crustacea: Decapoda: Lithodidae). Mar Biol 163:48. https://doi.org/10.1007/s00227-015-2776-8

Thomsen E, Rasmussen TL, Sztybor K et al (2019) Cold-seep fossil macrofaunal assemblages from Vestnesa Ridge, eastern Fram Strait, during the past 45000 years. Polar Research 38:3310. https://doi.org/10.33265/polar.v38.3310

Thurber AR, Jones WJ, Schnabel K (2011) Dancing for food in the deep sea: bacterial farming by a new species of Yeti crab. PLoS One 6:e26243. https://doi.org/10.1371/journal.pone.0026243

Troup MJ (2010) Sedimentology and petrology of Miocene cold-seep carbonates in southern Hawke's Bay: geological evidence for past seabed hydrocarbon seepage. Dissertation, University of Waikato

Tsuchida S, Suzuki Y, Fujiwara Y et al (2011) Epibiotic association between filamentous bacteria and the vent-associated galatheid crab, *Shinkaia crosnieri* (Decapoda: Anomura). J Mar Biol Assoc U K 91:23–32. https://doi.org/10.1017/S0025315410001827

Tunnicliffe V, Southward AJ (2004) Growth and breeding of a primitive stalked barnacle *Leucolepas longa* (Cirripedia: Scalpellomorpha: Eolepadidae: Neolepadinae) inhabiting a volcanic seamount off Papua New Guinea. J Mar Biol Assoc U K 84:121–132. https://doi.org/10.1017/S0025315404008987h

Van Dover CL, Aharon P, Bernhard JM et al (2003) Blake Ridge methane seeps: characterization of a soft-sediment, chemosynthetically based ecosystem. Deep-Sea Res I 50:281–300. https://doi.org/10.1016/S0967-0637(02)00162-0

Van Gaever S, Olu K, Derycke S et al (2009) Metazoan meiofaunal communities at cold seeps along the Norwegian margin: influence of habitat heterogeneity and evidence for connection with shallow-water habitats. Deep-Sea Res I 56:772–785. https://doi.org/10.1016/j.dsr.2008.12.015

Van Harten D (1996) The case against *Krithe* as a tool to estimate the depth and oxygenation of ancient oceans. In: Moguilevsky A, Whatley R (eds) Microfossils and oceanic environments. University of Wales Press, Aberystwyth, pp 297–304

Van Straelen V (1925) Contribution à l'étude des Crustacés Décapodes de la période jurassique. Mém Acad R Belg Sci 7:1–462, pls 1–10

Vanreusel A, Andersen A, Boetius A et al (2009) Biodiversity of cold seep ecosystems along the European margins. Oceanography 22:110–127. https://doi.org/10.5670/oceanog.2009.12
Vonderbank K (1970) Geologie und Fauna der Tertiären ablagerungen Zentral-Spitsbergens. Norsk Polarinst Skr 153:5–119, pls 1–21
Vrijenhoek RC (2013) On the instability and evolutionary age of deep-sea chemosynthetic communities. Deep-Sea Res II 92:189–200. https://doi.org/10.1016/j.dsr2.2012.12.004
Wall PD, Ivany LC, Wilkinson BH (2009) Revisiting Raup: exploring the influence of outcrop area on diversity in light of modern sample-standardization techniques. Paleobiology 35:146–167. https://doi.org/10.1666/07069.1
Warner GF (1977) The biology of crabs. Van Nostrand Reinhold, New York
Watanabe HK, Chen C, Chan BKK (2021) A new deep-sea hot vent stalked barnacle from the Mariana Trough with notes on the feeding ecology of *Vulcanolepas*. Mar Biodivers 51:9. https://doi.org/10.1007/s12526-020-01144-x
Whatley RC (1990) Ostracoda and global events. In: Whaley RC, Maybury C (eds) Ostracoda and global events. Chapman and Hall, London, pp 3–24
Whatley R (1991) The platycopid signal: a means of detecting kenoxic events using Ostracoda. J Micropalaeontol 10:181–185. https://doi.org/10.1144/jm.10.2.181
Whatley RC (1995) Ostracoda and oceanic palaeoxygen levels. Mitt Hamburg Zool Mus Inst 92:337–353
Whatley R, Zhao Q (1993) The *Krithe* problem: a case history of the distribution of *Krithe* and *Parakrithe* (Crustacea, Ostracoda) in the South China Sea. Palaeogeogr Palaeoclimatol Palaeoecol 103:281–297. https://doi.org/10.1016/0031-0182(93)90146-A
Whatley RC, Pyne RS, Wilkinson IP (2003) Ostracoda and palaeo-oxygen levels, with particular reference to the Upper Cretaceous of East Anglia. Palaeogeogr Palaeoclimatol Palaeoecol 194:355–386. https://doi.org/10.1016/S0031-0182(03)00333-X
Wieder RW, Feldmann RM (1989) *Palaega goedertorum*, a fossil isopod (Crustacea) from late Eocene to early Miocene rocks of Washington State. J Paleontol 63:73–80. https://doi.org/10.1017/S0022336000040981
Wiese F, Kiel S, Pack A et al (2015) The beast burrowed, the fluid followed—crustacean burrows as methane conduits. Mar Pet Geol 66:631–640. https://doi.org/10.1016/j.marpetgeo.2015.03.004
Wilson B, Coimbra JC, Hayek L-AC (2014) Ostracoda (Arthropoda, Crustacea) in a Miocene oxygen minimum zone, Trinidad, West Indies: a test of the Platycopid Signal Hypothesis. J S Am Earth Sci 54:210–216. https://doi.org/10.1016/j.jsames.2014.06.003
Withers TH (1924) Some decapod crustaceans (*Callianassa* and *Ranina*) from the Oligocene of Washington State, U.S.A. Ann Mag Nat Hist 14:121–127. https://doi.org/10.1080/00222932408633095
Withers TH (1953) British Museum (natural history) catalogue of the fossil Cirripedia in the Department of Geology: vol. 3, Tertiary. Bartholomew Press, Dorking
Yamaguchi T, Newman WA (1990) A new and primitive barnacle (Cirripedia: Balanomorpha) from the North Fiji Basin abyssal hydrothermal field, and its evolutionary implications. Pac Sci 44:135–155
Yamaguchi T, Newman WA (1997) *Eochionelasmus paquensis*, new species (Cirripedia: Balanomorpha), from 17°25'S, north of Easter Island: first record of a sessile hydrothermal barnacle from the East Pacific Rise. J Crustac Biol 17:488–496. https://doi.org/10.2307/1549443
Yamaguchi T, Newman WA, Hashimoto J (2004) A cold seep barnacle (Cirripedia: Neolepadinae) from Japan and the age of the vent/seep fauna. J Mar Biol Assoc U K 84:111–120. https://doi.org/10.1017/S0025315404008975h
Yamaguchi T, Goedert JL, Kiel S (2016) Marine ostracodes from Paleogene hydrocarbon seep deposits in Washington State, USA and their ecological structure. Geobios 49:407–422. https://doi.org/10.1016/j.geobios.2016.06.003
Yasuhara M, Sztybor K, Rasmussen TL et al (2018) Cold-seep ostracods from the western Svalbard margin: direct palaeo-indicator for methane seepage? J Micropalaeontol 37:139–148. https://doi.org/10.5194/jm-37-139-2018

Yorisue T, Kado R, Watanabe H et al (2013) Influence of water temperature on the larval development of *Neoverruca* sp. and *Ashinkailepas seepiophila*—implications for larval dispersal and settlement in the vent and seep environments. Deep-Sea Res I 71:33–37. https://doi.org/10.1016/j.dsr.2012.10.007

Zapata-Hernández G, Sellanes J, Thurber AR et al (2014) New insights on the trophic ecology of bathyal communities from the methane seep area off Concepción, Chile (~36° S). Mar Ecol 35:1–21. https://doi.org/10.1111/maec.12051

Zwicker J, Smrzka D, Gier S et al (2015) Mineralized conduits are part of the uppermost plumbing system of Oligocene methane-seep deposits, Washington State (USA). Mar Pet Geol 66:616–630. https://doi.org/10.1016/j.marpetgeo.2015.05.035

Chapter 6
Non-calcareous Tubeworms in Ancient Hydrocarbon Seeps

Magdalena N. Georgieva and Crispin T. S. Little

6.1 Introduction

Tubeworms are among the most abundant and conspicuous inhabitants of both present-day (Bergquist et al. 2003) and ancient seep environments (Fig. 6.1) (Campbell 2006). The term tubeworm most commonly refers to tube-forming members of the phylum Annelida, which build tubular structures that serve as protection for their inhabitants from predators and environmental stressors (Merz 2015). When present in large aggregations, as is often the case within chemosynthetic environments, tubeworms have an important ecological role in influencing habitat heterogeneity, as tubeworm 'bushes' can alter local physical conditions and serve as primary habitat for a diversity of marine taxa (e.g. Tsurumi and Tunnicliffe (2003)). Annelids can construct their tubes from a variety of materials, but robust, non-mucus annelid tubes generally fall into three broad types: calcareous tubes which are mostly observed within the family Serpulidae (Vinn and Mutvei 2009; see Vinn this volume), agglutinated tubes in which organic secretions are used to adhere sediment particles onto the tube wall, and tubes comprised predominantly of organic secretions.

The most prominent tube dwellers within modern seeps are annelids belonging to the family Siboglinidae (Fig. 6.1a, e). Species of this taxon construct organic chitin-protein tubes (Blackwell et al. 1965; Gaill et al. 1989; Shillito et al. 1995) and are specialists within reducing environments (Hilário et al. 2011). In addition to seeps, siboglinids can be found in large numbers occupying hydrothermal vents, reduced sediments and on and around organic falls such as sunken vertebrate bones

M. N. Georgieva (✉)
Department of Life Sciences, Natural History Museum, London, UK
e-mail: m.georgieva@nhm.ac.uk

C. T. S. Little
School of Earth and Environment, University of Leeds, Leeds, UK
e-mail: earctsl@leeds.ac.uk

A. Kaim et al. (eds.), *Ancient Hydrocarbon Seeps*, Topics in Geobiology 50,
https://doi.org/10.1007/978-3-031-05623-9_6

Fig. 6.1 Tubes of the main organic tube-building annelid families occurring at seeps and examples of tube fossils from seeps. (**a**) Tube of the vestimentiferan siboglinid *Escarpia* sp., Mid-Cayman Rise, scale bar is 10 mm. (**b**) Tube of the chaetopterid *Spiochaetopterus typicus*, NHMUK 1900.5.1.354-355, scale bar is 5 mm. (**c**) Fossil seep tubes from Rocky Knob, Miocene, New Zealand, scale bar is 10 mm. (**d**) Fossil seep tubes from Ellef Ringnes Island, Cretaceous, Canada, scale bar is 10 mm. (**e**) Tube of the vestimentiferan siboglinid *Lamellibrachia anaximandri* in cross section, scale bar is 200 μm. (**f**) Fossil seep tube from Rocky Knob in cross section, Miocene, New Zealand, scale bar is 200 μm. (**g**) Fossil seep tubes from Ellef Ringnes Island in cross section, Cretaceous, Canada, scale bar is 1 mm

and plant material. In addition to the siboglinids, tubeworms belonging to a variety of other annelid families can occur within modern seep environments, including the calcareous-tube-building Serpulidae (Olu et al. 1996a, b; Levin et al. 2012; Amon et al. 2017; Goffredi et al. 2020), Chaetopteridae (Fig. 6.1b) (Olu et al. 1997; Sibuet and Olu 1998; Nishi et al. 1999; Levin et al. 2000; Van Dover et al. 2003), Maldanidae, Ampharetidae, Terebellidae, Sabellidae and Trichobranchidae (Levin et al. 2003; Turnipseed et al. 2004; Levin and Mendoza 2007). While non-tubicolous (errant) annelids also inhabit seeps to take advantage of the increased productivity within these sites, those that form tubes have a much greater likelihood of fossilising, as tubes are generally more robust structures with greater resistance to decay. Currently, tubes are the only trace of annelids in the fossil record of seeps.

Tubular fossils are common in many ancient seep deposits (Fig. 6.1c–d, f–g), demonstrating that tube-dwelling animals have been important members of seep environments throughout evolutionary history (Campbell 2006; Georgieva et al. 2017) and have inhabited these environments since at least the Devonian (Peckmann et al. 2005) and perhaps even the Silurian (Barbieri et al. 2004). As annelids are the main tube dwellers within modern seep environments, and based on their similarity on a variety of scales to annelid tubes, fossil tubes from seeps are generally also considered to have been made by annelids. The majority of fossil tubes from ancient seep environments that have formally or tentatively been assigned to modern annelid lineages have been ascribed either to the siboglinids or the serpulids (Vinn et al. 2012; Georgieva et al. 2017). However, while designations of the latter family are generally uncontroversial, those assigned to siboglinids have received more debate due to inconsistencies with molecular age estimates for this lineage, as well as the use of tube identifying characters that are not unique to this group (Kiel and Dando 2009; Vrijenhoek 2013).

This review summarizes current understanding of tube-dwelling annelids within seep environments, both in the present deep ocean and throughout geological history, structured according to tube composition.

6.2 Non-calcareous Tubeworms

6.2.1 Family Siboglinidae

6.2.1.1 Overview

The family Siboglinidae (Caullery, 1914) contains four monophyletic lineages – vestimentiferans, frenulates, moniliferans (the genus *Sclerolinum* Southward 1961) and *Osedax* (Rouse et al. 2004), which are all tube-building and specialists within a variety of reducing environments. With the exception of the genus *Osedax*, which relies exclusively on sunken vertebrate bones for nutrition (Rouse et al. 2011) and can sometimes have only a thin mucus tube (Amon et al. 2014), members of all other siboglinid lineages construct more robust chitin-protein tubes and can inhabit seep environments, often in abundance. Vestimentiferan worms and their tubes are often large (Fig. 6.1a), up to 50 mm in diameter (e.g. the tubes of the hydrothermal vent-dwelling giant tubeworm *Riftia pachyptila*), while frenulates and *Sclerolinum* generally construct tubes less than 3 mm in diameter, but which are of considerable length in comparison to their diameter.

6.2.1.2 Biology

The seep-inhabiting lineages of siboglinids (vestimentiferans, frenulates and *Sclerolinum*) are exceptionally well-adapted to chemosynthetic environments as they lack a functional digestive system and instead rely on chemoautotrophic symbiotic bacteria stored internally within a specialised organ, known as the trophosome, for their nutrition (Cavanaugh et al. 1981; Southward et al. 2005; Hilário et al. 2011). Some siboglinid species appear to have affinities for particular chemosynthetic environment types, such as the vestimentiferans *Riftia pachyptila*, *Tevnia jerichonana* and *Ridgeia piscesae* which are only known from hydrothermal vents; many frenulates (e.g. *Siboglinum ekmani*, *Spirobrachia orkneyensis*) which are currently only known from reducing sediments (Webb 1964a; Smirnov 2000a) and *Sclerolinum* species (e.g. *Sclerolinum brattstromi*) known only from organic falls (Webb 1964b). However, many genera of these three linages can dwell on more than one type of reducing environment and are also commonly found in seeps. These include the vestimentiferan genera *Lamellibrachia*, *Escarpia* and *Seepiophila* (e.g. Cordes et al. 2007); the *Sclerolinum* species *S. contortum* (Smirnov 2000b; Eichinger et al. 2013) and members of the frenulate genera *Oligobrachia*, *Spirobrachia*, *Lamellisabella* and *Bobmarleya* (Smirnov 2000b; Hilário and Cunha 2008). Based on molecular phylogenetic studies, it has been suggested that as frenulates are found mostly in sedimented environments and basal vestimentiferans occupy seeps, siboglinids have undergone evolutionary transitions from sediments into seeps (and onto organic falls) and finally into vents (Black et al. 1997; Schulze and Halanych 2003).

The tubes (and bodies) of seep-inhabiting siboglinids are characteristically long in comparison to their diameter (Fig. 6.1a). Indeed, the posterior ends of some vestimentiferan tubes can be very extensive and heavily entangled in the tubes of conspecifics, and thus resemble plant roots. The posterior part is often buried deep within sulphidic sediments, while the anterior extends into the water column, thus bridging the oxic/anoxic sediment interface to allow simultaneous uptake of reduced compounds and oxygen (Dando et al. 2008). This also increases habitat availability for endosymbiotic bacteria (Southward 1986). At present, mainly sulphur-oxidising symbionts belonging to the Gammaproteobacteria have been found within vestimentiferans and *Sclerolinum*, whereas frenulates harbour phylogenetically distinct gammaproteobacterial endosymbionts (Lösekann et al. 2008; Thornhill et al. 2008) and some frenulate species also possess methanotrophic symbionts (Schmaljohann et al. 1990; Schmaljohann 1991).

6.2.1.3 Fossil Record and Evolution

The evolutionary history of Siboglinidae has received much attention to date, as well as debate. Many tube fossils that have been found within ancient seep (and also hydrothermal vent) environments have formally or tentatively been ascribed to the siboglinids, extending into the Carboniferous at seeps (Peckmann et al. 2005) and

the Silurian-early Ordovician at hydrothermal vents (Little et al. 1997, 1999a; Georgieva et al. 2021). In addition to considerations of the similarity of environment between fossil vent and seep tubes to that of recent siboglinids, fossil siboglinid identifications are based on analogies of tube morphology between fossil tubes and those of siboglinids, as well as studies of fossilisation. Fossil seep tubes ascribed to siboglinids generally occur at high densities, have a similar diameter, are long and exhibit some tapering along their length (Goedert et al. 2000), may have a tangled appearance that resembles vestimentiferan roots (e.g. Hikida et al., 2003) and have a tube wall that appears to originally have been organic in composition (Peckmann et al. 2005). Fossil tubes from seeps rarely demonstrate tube wall ornamental features such as collars and fine wrinkles, but these can be preserved at hydrothermal vents and have thus been compared to similar ornamentation on modern siboglinid tubes (Little et al. 1999b; Shpanskaya et al. 1999). Studies of the fossilisation of modern siboglinid tubes are rare; however, existing research from seeps demonstrates that as vestimentiferan tubes are replaced by carbonate minerals, fine relict textures from the originally organic tube wall remain (Haas et al. 2009).

Despite the above considerations, identifications of siboglinids in the fossil record of vents and seeps are difficult as organic tubes from other annelid families, notably the chaetopterids (Fig. 6.1b), can also possess similar morphological features to those of siboglinids (Kiel and Dando 2009). Chaetopterids can also occur at high densities within chemosynthetic environments; their tubes are of a similar range in diameter to those of vestimentiferans and can possess similar ornamental details such as wrinkles and collars on their outer tube surfaces. Aside from tube morphology, several attempts to estimate a molecular age for siboglinids have derived figures between 50 and 126 Ma for the divergence between vestimentiferans and frenulates (Black et al. 1997; Hurtado 2002; Vrijenhoek 2013; Li et al. 2019), and therefore are generally inconsistent with Palaeozoic vestimentiferan fossil identifications. However, recent findings on the evolutionary history of *Osedax*, which forms the sister group to vestimentiferans and moniliferans, extend the fossil record and molecular origination of this group to the mid-Cretaceous (Danise and Higgs 2015; Taboada et al. 2015), demonstrating that fossil evidence for siboglinids generally predates molecular age estimates. As the above molecular age estimates for vestimentiferan origins have large ranges, direct fossil evidence is required to confirm when seep-inhabiting siboglinids originated and evolved to a chemosynthetic mode of life.

6.2.1.4 Classification and Tube Characters

The inability to distinguish fossil tubes of siboglinids from ancient chemosynthetic environments from those of other annelids (such as chaetopterids and potentially also those of non-annelids; Kiel and Dando, 2009) calls for a more thorough approach to the identification of fossil seep and vent tubes that includes a detailed survey of the tube characters that siboglinid tubes possess, which of these are likely to be retained during fossilisation and which are homoplastic. Such a comparison of

a range of modern annelid tubes with fossil tubes from vents and seeps was performed using a cladistic framework, whereby 48 tube characters were identified and scored for a range of both modern annelid and fossil vent and seep tubes. This analysis revealed that of the 14 fossil seep tubes included, none could definitively be ascribed to siboglinids (Georgieva et al. 2017), which was largely a result of fossil seep tubes lacking outer tube wall ornamental features that can aid identification, and being fragmentary, thus making it difficult to assess for characters such as tapering and variation in the preservation of the tube wall. The above analysis did however result in some fossil hydrothermal vent tubes being identified as those of vestimentiferans, due to a combination of unique shared characters such as large flaring tube collars and the occurrence of both fine longitudinal and transverse wrinkles on the outer tube wall. The oldest vent tube fossils ascribed to the vestimentiferans from this cladistic analysis date to the early Jurassic and thus provide another intriguing perspective on the question of when these remarkable annelids evolved. The above study generally lends support to a Mesozoic origin of the siboglinids, as well as urging greater caution in the designation of fossil tubes from chemosynthetic environments to the siboglinids without thorough analysis of all available tube characters. For a fossil seep tube to be identified as having been made by a siboglinid with greater certainty, such a tube would need to possess a combination of characters that are more often encountered in the tubes of siboglinids such as contortion, tapering, tube roots, collar structures, remnants of a thick originally-organic tube wall and well-preserved organic compounds that correspond to the chitin-protein composition of siboglinid tubes.

6.2.2 Family Chaetopteridae

6.2.2.1 Overview

The family Chaetopteridae Audouin and Milne Edwards, 1833, currently includes four genera: *Chaetopterus* Cuvier, 1830; *Mesochaetopterus* Potts, 1914; *Phyllochaetopterus* Grube, 1863; and *Spiochaetopterus* Sars, 1856 (Fig. 6.1b), the former two forming distinct monophyletic clades in phylogenetic analyses, while the latter two genera do not (Moore et al. 2017). With the exception of one seemingly non-tubicolous pelagic species, *Chaetopterus pugaporcinus*, all chaetopterids are benthic tube-builders. Members of this family can construct tubes that are either comprised solely of organic secretions or that are agglutinated, with organic tubes mainly occurring in the genera *Phyllochaetopterus* and *Spiochetopterus*, while agglutinated tubes are more commonly formed by *Mesochaetopterus* and occasionally also by *Chaetopterus* species.

6.2.2.2 Biology

Chaetopterids are well known from shallow waters and shelf depths; however, members of this family are increasingly reported from the deep sea at up to near hadal depths (e.g. Okumura et al. 2016). They occur within a range of marine habitats, occasionally also being found within seeps (Nishi et al. 1999) as well as other reducing environments such as hydrothermal vents (Morineaux et al. 2010) and on whalefalls (Nishi and Rouse 2007). Chaetopterids from chemosynthetic environments have been reported from cold seeps in Sagami Bay of Japan (Nishi et al. 1999), from mud volcanoes on the Barbados Accretionary Prism (Olu et al. 1997), from cold seeps along Blake Ridge (Van Dover et al. 2003) and the Wagner Fault in the northern Gulf of California (Canet et al. 2010). A species of *Phyllochaetopterus*, *P. gigas*, has been described from a whalefall in Monterey Bay (Nishi and Rouse 2014), while the species *P. polus* is known from the hydrothermal vent site Ashadze-1 (Morineaux et al. 2010; Fabri et al. 2011) on the Mid-Atlantic Ridge and *P. lauensis* from near vents in the Lau Basin (Nishi and Rouse 2007). Intriguingly, a chaetopterid species was recently reported from a serpentinite-hosted hydrothermal vent system known as the Shinkai Seep Field, where brucite-carbonate chimneys are covered by colonies of *Phyllochaetopterus*, the tubes of which may in some cases also be embedded within the chimneys (Okumura et al. 2016).

Chaetopterids are either filter-feeding via a mucous bag or deposit feeders (Jumars et al. 2015), and those that occur within seeps and other reduced environments are not yet known to possess chemosynthetic symbionts on which they are reliant for nutrition. Instead, their abundance within some chemosynthetic environments has been attributed to filter- and deposit-feeding on the greater bacterial biomass within these environments (Kiel and Dando 2009; Nishi and Rouse 2014).

6.2.2.3 Fossil Record and Evolution

Recent phylogenetic analyses for the annelid phylum have revealed chaetopterids to be a basal radiation with respect to most other annelid families (Weigert et al. 2014; Andrade et al. 2015). Despite their potentially early origination among annelids, no definitive fossil chaetopterids are currently known. The Cambrian fossil *Hyolithellus* has been suggested to resemble chaetopterid tubes and to have had a similar mode of life, but tube ultrastructure is very different between the two, making it unlikely that *Hyolithellus* is closely related to modern chaetopterids (Skovsted and Peel 2011). Wrinkly *Sinotubulites* tubes from the Late Ediacaran-Early Cambrian also resemble tubes of the chaetopterid genus *Phyllochaetopterus*, but generally have not been ascribed to this family (Chen et al. 2008; Cai et al. 2015). As outlined above, there are however suggestions that some of the vent and seep tube fossils considered to originally have been organic-walled and ascribed to siboglinids may instead have been made by chaetopterids (Kiel and Dando 2009).

6.2.2.4 Classification and Tube Characters

The tubes of chaetopterid genera *Chaetopterus* and *Mesochaetopterus* are generally parchment or paper like and incorporate sediment fragments such as sand, mud and shells (Britayev and Martin 2019). The tubes of genera *Phyllochaetopterus* and *Spiochaetopterus* are composed mostly of organic secretions, with few adhered sediment grains, if any. *Phyllochaetopterus* and *Spiochaetopterus* tubes can also possess tube wall ornamental details such as annulations, wrinkles and small collars (Fig. 6.1b) and occasionally also bear internal, perforated partitions (Barnes 1965). The organic component of chaetopterid tubes constitutes many layered organic sheets, comprised of a fibrous protein within a carbohydrate matrix (Gaill and Hunt 1988). Chitin is also regularly reported to be present in chaetopterid tubes (Britayev and Martin 2019), but was not detected in recent chemical analyses of tubes from all four genera (Georgieva et al. 2017). In some species, tube fibres between successive tube layers are oriented in 0°, 45° and 65° angles, which are deemed to give the tubes high mechanical strength (Shah et al. 2014, 2015) and have not been observed in siboglinid tubes (Georgieva et al. 2017). An in-depth comparison of fossil vent and seep tubes with those of modern siboglinids and chaetopterids reveals one Devonian fossil vent tube, *Tevidestus serriformis*, is perhaps most likely to have been made by a chaetopterid (Georgieva et al. 2017), as this fossil also exhibits fibres crossed at near 90° angles. For the majority of fossil seep tubes, however, the fragmentary nature of known fossils and their lack of outer wall ornamentation make it very difficult to evaluate the identity of the tube dweller.

6.3 Other Organic Tube Dwellers at Seeps

While siboglinids and chaetopterids are the main organic tube dwellers within present-day seep environments, some species of the annelid family Ampharetidae Malmgren, 1866, may also construct tubes of mainly organic secretions, such as the genus *Glyphanostomum*, as well as members of the closely related family Alvinellidae. However, species of ampharetids with purely organic, non-agglutinated tubes are not well documented from seeps, and alvinellids are currently only known from hydrothermal vent environments. Nevertheless, the potential exists for annelids that were neither chaetopterids nor siboglinids to have constructed fossil seep tubes deemed to have originally been organic-walled.

6.4 Agglutinated Tube Dwellers at Seeps

Several annelid families that dwell mainly within agglutinated tubes have been reported from cold seeps, such as Maldanidae Malmgren, 1867; Ampharetidae Malmgren, 1866; and Terebellidae Johnston, 1846. Maldanids have been reported

from seeps at Blake Ridge (Van Dover et al. 2003) as well as from seeps in the southern part of the Barbados Accretionary Prism. The latter belong to the genus *Nicomache* (Olu et al. 1996b), which has also been reported from hydrothermal vents in polar regions (Eilertsen et al. 2018). Ampharetids are among the most common polychaetes found at seeps and can at times be incredibly abundant, dominating faunal assemblages (Reuscher and Fiege 2016). There are currently 12 species known from seeps, reported from seeps of the Makran accretionary prism off Pakistan (Reuscher and Fiege 2016), the Cascadia Margin off Oregon (Reuscher et al. 2012) and off Costa Rica (Stiller et al. 2013), in the Lihir Basin (Bismarck Archipelago), and along the Aleutian Trench (Reuscher et al. 2009). Terebellid polychaetes are also reported from seeps off Oregon and in the Lihir Basin (Reuscher et al. 2012). In addition to the above families, annelids in the families Sabellidae and Trichobranchidae have also been observed at a number of modern seeps (Cordes et al. 2005; Reuscher et al. 2012).

Agglutinated tube fossils are poorly known from the seep fossil record. However, there are a few instances of these, for example, Jurassic tube fossils from the Les Molles Formation in Argentina (Gómez-Pérez 2003). Tube fossils from this locality have ~1-mm-thick walls comprised of micrite. Tube fossils from the Miocene Fukuzaki locality of Tsushima Island, Japan, also appear to have originally been agglutinated (Hryniewicz et al. 2021). However, with these tube fossils as well as those from Argentina, it is difficult to rule out that the tubes could have been made by other marine organisms, such as crustaceans, which can also construct agglutinated tubes.

6.5 Conclusions

Probable annelids living within organic-walled tubes have occupied seeps since at least the Devonian (Georgieva et al. 2017), and these tubeworms, along with tubeworms living within agglutinated tubes, are among the dominant inhabitants of seep environments today. At ancient seeps, non-calcareous tubeworms are often very abundant within the deposits in which they occur and must therefore have made effective use of seep chemosynthetic production and must also have been key components of these ancient ecosystems, providing habitat structure as well as mediating carbon flow to higher trophic levels. Progress in understanding the evolutionary timings of when different annelid lineages moved into seeps is, however, largely hindered by the lack of morphological details observable on many seep tube fossils, as well as the more limited utility of tubes for identification, in which homoplasies can often exist (Merz and Woodin 2006; Kiel and Dando 2009). The situation is also not helped by a poor fossil record for non-calcareous tubicolous annelids in general. For the siboglinids, more detailed fossils from hydrothermal vents demonstrate that this family may have colonised vents during the Mesozoic, while the seep fossil record contains tube fossils likely to be siboglinids that date to the Cretaceous (Georgieva et al. 2017). For other annelid families such as chaetopterids and

ampharetids, the picture is even less clear. However, this knowledge gap provides much opportunity for the development of new techniques for fossil identification, such as through the characterisation of organic compounds preserved within tube fossils.

Acknowledgements MNG is grateful for the support from Natural Environment Research Council's (UK) research grants NE/K500847/1 and NE/C000714/1. We are very grateful to donors of both fossil and modern material for analysis, Adrian Glover for material from the Mid-Cayman Rise (Fig. 6.1a), Kathy Campbell for material from Rocky Knob (Fig. 6.1c, f), Steve Grasby and Benoit Beauchamps for material from Ellef Ringnes (Fig. 6.1d, g) and Ann Andersen for material from the Mediterranean Sea (Fig. 6.1e).

References

Amon DJ, Wiklund H, Dahlgren TG et al (2014) Molecular taxonomy of *Osedax* (Annelida: Siboglinidae) in the Southern Ocean. Zool Scr 43:405–417

Amon DJ, Gobin J, Van Dover CL et al (2017) Characterization of methane-seep communities in a deep-sea area designated for oil and natural gas exploitation off Trinidad and Tobago. Front Mar Sci 4:342

Andrade SCS, Novo M, Kawauchi GY et al (2015) Articulating 'archiannelids': phylogenomics and annelid relationships, with emphasis on meiofaunal taxa. Mol Biol Evol 32(11):2860–2875

Audouin JV, Milne Edwards H (1833) Classification des Annélides et description de celles qui habitent les côtes de la France. Ann Sci Nat 1(30):411–425

Barbieri R, Ori GG, Cavalazzi B (2004) A Silurian cold-seep ecosystem from the Middle Atlas, Morocco. Palaios 19(6):527–542

Barnes R (1965) Tube-building and feeding in chaetopterid polychaetes. Biol Bull 129(2):217–233

Bergquist DC, Ward T, Cordes EE et al (2003) Community structure of vestimentiferan-generated habitat islands from Gulf of Mexico cold seeps. J Exp Mar Biol Ecol 289(2):197–222

Black MB, Halanych KM, Maas PAY et al (1997) Molecular systematics of vestimentiferan tube-worms from hydrothermal vents and cold-water seeps. Mar Biol 130(2):141–149

Blackwell J, Parker K, Rudall K (1965) Chitin in pogonophore tubes. J Mar Biol Ass UK 45:51–54

Britayev TA, Martin D (2019) Chaetopteridae Aodouin & Milne Edwards, 1833. In: Purschke G, Böggemann M, Westheide W (eds) Annelida, vol 1, basal groups and Pleistoannelida, Sedentaria I. De Gruyter, Berlin, pp 156–176

Cai Y, Xiao S, Hua H et al (2015) New material of the biomineralizing tubular fossil *Sinotubulites* from the late Ediacaran Dengying Formation, South China. Precambrian Res 261:12–24

Campbell KA (2006) Hydrocarbon seep and hydrothermal vent paleoenvironments and paleontology: past developments and future research directions. Palaeogeog Palaeoclimat Palaeoecol 232(2–4):362–407

Canet C, Prol-Ledesma RM, Dando PR et al (2010) Discovery of massive seafloor gas seepage along the Wagner Fault, northern Gulf of California. Sediment Geol 228(3/4):292–303

Caullery M (1914) Sur les Siboglinidae, type nouveau d'invertébrés receuillis par l'expédition du Siboga. C R Hebdomadaires Séances Acad Sci 158:2014–2017

Cavanaugh CM, Gardiner SL, Jones ML et al (1981) Prokaryotic cells in the hydrothermal vent tube worm *Riftia pachyptila* Jones: possible chemoautotrophic symbionts. Science 213:340–342

Chen Z, Bengtson S, Zhou CM et al (2008) Tube structure and original composition of *Sinotubulites*: shelly fossils from the late Neoproterozoic in southern Shaanxi, China. Lethaia 41:37–45

Cordes E, Hourdez S, Predmore B et al (2005) Succession of hydrocarbon seep communities associated with the long-lived foundation species *Lamellibrachia luymesi*. Mar Ecol Prog Ser 305:17–29

Cordes E, Carney S, Hourdez S et al (2007) Cold seeps of the deep Gulf of Mexico: community structure and biogeographic comparisons to Atlantic equatorial belt seep communities. Deep-Sea Res Part I 54:637–653

Cuvier G (1830) Le règne animal distribué d'après son organisation, pour servir de base à l'histoire naturelle des animaux et d'introduction à l'anatomie comparée. Déterville & Crochard, Paris

Dando PR, Southward AJ, Southward EC et al (2008) Interactions between sediment chemistry and frenulate pogonophores (Annelida) in the north-east Atlantic. Deep-Sea Res Part I 55(8):966–996

Danise S, Higgs ND (2015) Bone-eating *Osedax* worms lived on Mesozoic marine reptile deadfalls. Biol Lett 11(4):20150072

Eichinger I, Hourdez S, Bright M (2013) Morphology, microanatomy and sequence data of *Sclerolinum contortum* (Siboglinidae, Annelida) of the Gulf of Mexico. Org Divers Evol 13:311–329

Eilertsen MH, Georgieva MN, Kongsrud JA et al (2018) Genetic connectivity from the Arctic to the Antarctic: *Sclerolinum contortum* and *Nicomache lokii* (Annelida) are both widespread in reducing environments. Sci Rep 8(1):4810

Fabri M-C, Bargain A, Briand P et al (2011) The hydrothermal vent community of a new deep-sea field, Ashadze-1, 12°58′N on the Mid-Atlantic Ridge. J Mar Biol Ass UK 91(1):1–13

Gaill F, Hunt S (1988) Tubes. In: Westheide W, Hermans CO (eds) The ultrastructure of Polychaeta, 494. Fischer, New York

Gaill F, Chanzy H, Vuong R (1989) Structural organisation and localisation of the β chitin secreted by deep sea hydrothermal vent worms. Biol Cellulaire 66:8a

Georgieva MN, Little CTS, Watson JS et al (2017) Identification of fossil worm tubes from Phanerozoic hydrothermal vents and cold seeps. J Syst Palaeontol 17(4):1–43

Georgieva MN, Little CTS, Maslennikov V V., Glover AG, Ayupova NR, Herrington RJ (2021) The history of life at hydrothermal vents. Earth Sci Rev 217:103602. https://doi.org/10.1016/j.earscirev.2021.103602

Goedert J, Peckmann J, Reitner J (2000) Worm tubes in an allochthonous cold-seep carbonate from lower Oligocene rocks of western Washington. J Paleontol 74(6):992–999

Goffredi SK, Tilic E, Mullin SW et al (2020) Methanotrophic bacterial symbionts fuel dense populations of deep-sea feather duster worms (Sabellida, Annelida) and extend the spatial influence of methane seepage. Sci Adv 6(14):eaay8562

Gómez-Pérez I (2003) An Early Jurassic deep-water stromatolitic bioherm related to possible methane seepage (Los Molles Formation, Neuquén, Argentina). Palaeogeog Palaeoclimat Palaeoecol 201(1/2):21–49

Grube AE (1863) Beschreibung neuer oder wenig bekannter Anneliden, Sechster Beitrag. Arch Naturgeschichte 29:37–69

Haas A, Little CTS, Sahling H et al (2009) Mineralization of vestimentiferan tubes at methane seeps on the Congo deep-sea fan. Deep-Sea Res Part I Oceanogr Res Pap 56(2):283–293

Hikida Y, Suzuki S, Togo Y et al (2003) An exceptionally well-preserved fossil seep community from the Cretaceous Yezo Group in the Nakagawa area, Hokkaido, northern Japan. Paleontol Res 7:329–342

Hilário A, Cunha MR (2008) On some frenulate species (Annelida: Polychaeta: Siboglinidae) from mud volcanoes in the Gulf of Cadiz (NE Atlantic). Sci Mar 72(2):361–371

Hilário A, Capa M, Dahlgren TG et al (2011) New perspectives on the ecology and evolution of siboglinid tubeworms. PloS One 6(2):e16309

Hryniewicz K, Miyajima Y, Amano K et al (2021) Formation and diagenesis of cold seep carbonates from Miocene Taishu Group at Tsushima (Japan). Geol Mag 158:964–984

Hurtado LA (2002) Evolution and biogeography of hydrothermal vent organisms in the eastern Pacific Ocean. Dissertation, Rutgers University

Johnston G (1846) An index to the British Annelides. Ann Mag Nat Hist 1(16):433–462
Jumars PA, Dorgan KM, Lindsay SM (2015) Diet of worms emended: an update of polychaete feeding guilds. Ann Rev Mar Sci 7(1):497–520
Kiel S, Dando PR (2009) Chaetopterid tubes from vent and seep sites: implications for fossil record and evolutionary history of vent and seep annelids. Acta Palaeontol Pol 54(3):443–448
Levin LA, Mendoza GF (2007) Community structure and nutrition of deep methane-seep macrobenthos from the North Pacific (Aleutian) Margin and the Gulf of Mexico (Florida Escarpment). Mar Ecol 28(1):131–151
Levin LA, James DW, Martin CM et al (2000) Do methane seeps support distinct macrofaunal assemblages? Observations on community structure and nutrition from the northern California slope and shelf. Mar Ecol Prog Ser 208:21–39
Levin L, Ziebis W, Mendoza G et al (2003) Spatial heterogeneity of macrofauna at northern California methane seeps: influence of sulfide concentration and fluid flow. Mar Ecol Prog Ser 265:123–139
Levin LA, Orphan VJ, Rouse GW et al (2012) A hydrothermal seep on the Costa Rica margin: middle ground in a continuum of reducing ecosystems. Proc R Soc Ser B Biol Sci 279(1738):2580–2588
Li Y, Tassia MG, Waits DS et al (2019) Genomic adaptations to chemosymbiosis in the deep-sea seep-dwelling tubeworm *Lamellibrachia luymesi*. BMC Biol 17(1):91
Little CTS, Herrington RJ, Maslennikov VV et al (1997) Silurian hydrothermal-vent community from the southern Urals, Russia. Nature 385(6612):146–148
Little CTS, Maslennikov VV, Morris NJ et al (1999a) Two Palaeozoic hydrothermal vent communities from the southern Ural mountains, Russia. Palaeontology 42(6):1043–1078
Little CTS, Herrington RJ, Haymon RM et al (1999b) Early Jurassic hydrothermal vent community from the Franciscan Complex, San Rafael Mountains, California. Geology 27:167–170
Lösekann T, Robador A, Niemann H et al (2008) Endosymbioses between bacteria and deep-sea siboglinid tubeworms from an Arctic cold seep (Haakon Mosby Mud Volcano, Barents Sea). Environ Microbiol 10:3237–3254
Malmgren AJ (1866) Nordiska hafs-annulater. Öfversigt af Königlich Vetenskapsakademiens Förhandlingar, Stockholm 22(5):355–410
Malmgren AJ (1867) Annulata Polychaeta Spetsbergiæ, Grœnlandiæ, Islandiæ et Scandinaviæ. Hactenus Cognita, Helsingforslæ
Merz RA (2015) Textures and traction: how tube-dwelling polychaetes get a leg up. Invertebr Biol 134(1):61–77
Merz RA, Woodin SA (2006) Polychaete chaetae: function, fossils, and phylogeny. Integr Comp Biol 46(4):481–496
Moore JM, Nishi E, Rouse GW (2017) Phylogenetic analyses of Chaetopteridae (Annelida). Zool Scr 46(5):596–610
Morineaux M, Nishi E, Ormos A et al (2010) A new species of *Phyllochaetopterus* (Annelida: Chaetopteridae) from deep-sea hydrothermal Ashadze-1 vent field, Mid-Atlantic Ridge: taxonomical description and partial COI DNA sequence. Cah Biol Mar 51:239–248
Nishi E, Rouse G (2007) A new species of *Phyllochaetopterus* (Chaetopteridae: Annelida) from near hydrothermal vents in the Lau Basin, western Pacific Ocean. Zootaxa 1621:55–64
Nishi E, Rouse GW (2014) First whale fall chaetopterid: a gigantic new species of *Phyllochaetopterus* (Chaetopteridae: Annelida) from the deep sea off California. Proc Biol Soc Wash 126(4):287–298
Nishi E, Miura T, Bhaud M (1999) A new species of *Spiochaetopterus* (Chaetopteridae: Polychaeta) from a cold-seep site off Hatsushima in Sagami Bay, central Japan. Proc Biol Soc Wash 112(1):210–215
Okumura T, Ohara Y, Stern RJ et al (2016) Brucite chimney formation and carbonate alteration at the Shinkai Seep Field, a serpentinite-hosted vent system in the southern Mariana forearc. Geochem Geophys Geosyst 17(9):3775–3796

Olu K, Duperret A, Sibuet M et al (1996a) Structure and distribution of cold seep communities along the Peruvian active margin: relationship to geological and fluid patterns. Mar Ecol Prog Ser 132:109–125

Olu K, Sibuet M, Harmegnies F et al (1996b) Spatial distribution of diverse cold seep communities living on various diapiric structures of the southern Barbados prism. Prog Oceanogr 38:347–376

Olu K, Lance S, Sibuet M et al (1997) Cold seep communities as indicators of fluid expulsion patterns through mud volcanoes seaward of the Barbados accretionary prism. Deep-Sea Res Part I 44(5):811–841

Peckmann J, Little CTS, Gill F et al (2005) Worm tube fossils from the Hollard Mound hydrocarbon-seep deposit, Middle Devonian, Morocco: palaeozoic seep-related vestimentiferans? Palaeogeog Palaeoclimat Palaeoecol 227(1–3):242–257

Potts FA (1914) Polychaeta from the N.E. Pacific: the Chaetopteridae, with an account of the phenomenon of asexual reproduction in *Phyllochaetopterus* and the description of two new species of Chaetopteridae from the Atlantic. Proc Zool Soc Lond 67:955–994

Reuscher MG, Fiege D (2016) Ampharetidae (Annelida: Polychaeta) from cold seeps off Pakistan and hydrothermal vents off Taiwan, with the description of three new species. Zootaxa 4139(2):197–208

Reuscher M, Fiege D, Wehe T (2009) Four new species of Ampharetidae (Annelida: Polychaeta) from Pacific hot vents and cold seeps, with a key and synoptic table of characters for all genera. Zootaxa 2191:1–40

Reuscher M, Fiege D, Wehe T (2012) Terebellomorph polychaetes from hydrothermal vents and cold seeps with the description of two new species of Terebellidae (Annelida: Polychaeta) representing the first records of the family from deep-sea vents. J Mar Biol Assoc UK 92(05):997–1012

Rouse GW, Goffredi SK, Vrijenhoek RC (2004) *Osedax*: bone-eating marine worms with dwarf males. Science 305(5684):668–671

Rouse GW, Goffredi SK, Johnson SB et al (2011) Not whale-fall specialists, *Osedax* worms also consume fishbones. Biol Lett 7(5):736–739

Sars M (1856) Nye Annelider. In: Beyer FD (ed) Fauna Littoralis Norvegiae, 24. Bergen

Schmaljohann R (1991) Oxidation of various potential-energy sources by methanotrophic endosymbionts of *Siboglinum poseidoni* (Pogonophora). Mar Ecol Prog Ser 76:143–148

Schmaljohann R, Faber E, Whiticar M et al (1990) Coexistence of methane-based and sulphur-based endosymbioses between bacteria and invertebrates at a site in the Skagerrak. Mar Ecol Prog Ser 61:119–124

Schulze A, Halanych K (2003) Siboglinid evolution shaped by habitat preference and sulfide tolerance. Hydrobiologia 496:199–205

Shah DU, Vollrath F, Porter D et al (2014) Housing tubes from the marine worm *Chaetopterus* sp.: biomaterials with exceptionally broad thermomechanical properties. J R Soc Interface 11(98):20140525

Shah DU, Vollrath F, Stires J et al (2015) The biocomposite tube of a chaetopterid marine worm constructed with highly-controlled orientation of nanofilaments. Mater Sci Eng C 48:408–415

Shillito B, Lechaire J-P, Goffinet G et al (1995) Composition and morphogenesis of the tubes of vestimentiferan worms. Geol Soc Lond Spec Publ 87(1):295–302

Shpanskaya AY, Maslennikov VV, Little CTS (1999) Vestimentiferan tubes from the early Silurian and Middle Devonian hydrothermal biota of the Uralian palaeobasin. Paleontolog Zhur 33:222–228

Sibuet M, Olu K (1998) Biogeography, biodiversity and fluid dependence of deep-sea cold-seep communities at active and passive margins. Deep-Sea Res Part II 45:517–567

Skovsted CB, Peel JS (2011) *Hyolithellus* in life position from the lower Cambrian of North Greenland. J Paleontol 85(1):37–47

Smirnov RV (2000a) A new species of *Spirobrachia* (Pogonophora) from the Orkney Trench (Antarctica). Polar Biol 23(8):567–570

Smirnov RV (2000b) Two new species of Pogonophora from the Arctic mud volcano off northwestern Norway. Sarsia 85(2):141–150
Southward EC (1961) Pogonophora. In: Weber M (ed) Siboga—Expeditie. Brill, Leiden
Southward EC (1986) Gill symbionts in thyasirids and other bivalve molluscs. J Mar Biol Ass UK 66:889–914
Southward E, Schulze A, Gardiner S (2005) Pogonophora (Annelida): form and function. Hydrobiologia 535:227–251
Stiller J, Rousset V, Pleijel F et al (2013) Phylogeny, biogeography and systematics of hydrothermal vent and methane seep *Amphisamytha* (Ampharetidae, Annelida), with descriptions of three new species. Syst Biodivers 11(1):35–65
Taboada S, Riesgo A, Bas M et al (2015) Bone-eating worms spread: insights into shallow-water *Osedax* (Annelida, Siboglinidae) from Antarctic, subantarctic, and Mediterranean waters. PLoS One 10(11):e0140341
Thornhill DJ, Wiley AA, Campbell AL et al (2008) Endosymbionts of *Siboglinum fiordicum* and the phylogeny of bacterial endosymbionts in Siboglinidae (Annelida). Biol Bull 214(2):135–144
Tsurumi M, Tunnicliffe V (2003) Tubeworm-associated communities at hydrothermal vents on the Juan de Fuca Ridge, northeast Pacific. Deep-Sea Res Part I Oceanogr Res Pap 50(5):611–629
Turnipseed M, Jenkins CD, Van Dover CL (2004) Community structure in Florida Escarpment seep and Snake Pit (Mid-Atlantic Ridge) vent mussel beds. Mar Biol 145(1):121–132
Van Dover CL, Aharon P, Bernhard JM et al (2003) Blake Ridge methane seeps: characterization of a soft-sediment, chemosynthetically based ecosystem. Deep-Sea Res Part I 50:281–300
Vinn O (this volume) Calcareous Tubeworms in Ancient Hydrocarbon Seeps. In: Kaim A, Cochran JK, Landman NH (eds) Ancient methane seeps and cognate communities. Topics in Geobiology. Springer, Cham
Vinn O, Mutvei H (2009) Calcareous tubeworms of the Phanerozoic. Estonian J Earth Sci 58(4):286–296
Vinn O, Kupriyanova EK, Kiel S (2012) Systematics of serpulid tubeworms (Annelida, Polychaeta) from Cretaceous and Cenozoic hydrocarbon-seep deposits in North America and Europe. Neues Jahrb Geol Palaeontol Abh 265(3):315–325
Vrijenhoek RC (2013) On the instability and evolutionary age of deep-sea chemosynthetic communities. Deep-Sea Res Part II 92:189–200
Webb M (1964a) A redescription of *Siboglinum ekmani* Jagersten (Pogonophora). Sarsia 15:37–47
Webb M (1964b) Additional notes on *Sclerolinum brattstromi* (Pogonophora) and the establishment of a new family, Sclerolinidae. Sarsia 16:47–58
Weigert A, Helm C, Meyer M et al (2014) Illuminating the base of the annelid tree using transcriptomics. Molec Biol Evol 31(6):1391–1401

Chapter 7
Calcareous Tubeworms in Ancient Hydrocarbon Seeps

Olev Vinn

7.1 Introduction

Among the poorly studied groups in chemosynthetic communities are calcareous tubeworms of the family Serpulidae (Polychaeta, Annelida) (Vinn et al. 2013). As few as four serpulid species belonging to the genera *Protis*, *Laminatubus*, and *Hyalopomatus* are known from hydrothermal vents in the Pacific Ocean (ten Hove and Zibrowius 1986; Lenihan et al. 2008; Kupriyanova et al. 2010). In addition, a species of *Neovermilia* is known from hydrothermal seeps of Jaco Scarp in Costa Rica (Kupriyanova, E.K., personal observations). There are also large beds of *Neovermilia* sp. reported from seeps off of northern Peru (Olu et al. 1996a). *Neovermilia* occurs abundantly around mussel beds and bacterial mats at seeps on the Barbados prism in the Atlantic Ocean (Olu et al. 1996b; Segonzac et al. 1997; Amon et al. 2017). Other unidentified serpulids have often been mentioned in extant communities associated with hydrothermal vents and cold seeps (e.g., Hessler and Smithey 1983; Juniper and Sibuet 1987; Bergquist et al. 2003; López-González et al. 2003).

Phanerozoic vent and seep deposits commonly contain tubular fossils often considered to have been made by annelids, but their taxonomy has remained elusive; many tubular fossils are referred to simply as "worm tubes," rather than being assigned to specific modern or fossil lineages or have received controversial assignments (Campbell 2006). Carboniferous and other ancient calcareous tubeworm records were recently found not to be serpulids (see Georgieva et al. 2019). Serpulids do not show any specific adaptations to seep environments. They are probably simply taking advantage of the abundant hard carbonate substrate available for colonization (Vinn et al. 2013). Other deep-water habitats where chemosynthesis plays an important role in the food chain are sunken carcasses of large vertebrates and sunken

O. Vinn (✉)
Institute of Ecology and Earth Sciences, University of Tartu, Tartu, Estonia
e-mail: olev.vinn@ut.ee

A. Kaim et al. (eds.), *Ancient Hydrocarbon Seeps*, Topics in Geobiology 50,
https://doi.org/10.1007/978-3-031-05623-9_7

wood (Smith et al. 1989; Kiel and Goedert 2006). Serpulids have been reported at present-day sunken whale carcasses (Smith and Baco 2003; Fujiwara et al. 2007) and plant remains (Wolff 1979; Pailleret et al. 2007), but nothing is known about fossil examples except for abundant serpulid tube fragments at a Late Jurassic wood-mollusk association (Kaim 2011). Serpulids mostly occur at seeps in low abundance, but, more rarely, serpulids can occur in large abundance at seeps. For example, serpulids are abundant in the Sada Limestone, Japan (Nobuhara et al. 2008), and in the Miocene seeps of Italy (Kiel et al. 2018).

7.2 Calcareous Tubeworms

7.2.1 Family Serpulidae

7.2.1.1 Overview

The family Serpulidae is a discrete group of sedentary calcareous tubeworms within the clade Sabellida (ten Hove and Kupriyanova 2009). Serpulids are a large and highly successful group that has attained a cosmopolitan geographic and wide bathymetric distribution, from the intertidal to hadal zones (e.g., ten Hove and Kupriyanova 2009; Kupriyanova and Nishi 2011; Kupriyanova et al. 2014). They form two major clades, serpulins and filogranins, based on morphological and molecular data (Kupriyanova et al. 2006).

7.2.1.2 Biology

Serpulids are not exclusive to seeps and vents and are common on hard substrata in all marine habitats at all depths, being an important element of the encrusting biota in the geological past as well as in recent seas (Ippolitov et al. 2014). Few serpulid species, such as *Ditrupa arietina*, are not attached to the substrate during their growth. They are partially excavated into the soft bottom instead (ten Hove and Smith 1990). Some symbiotic serpulids can grow partially embedded within corals and sponges (ten Hove and Kupriyanova 2009). Others intergrow with microbial communities to form biostalactites in marine caves (Guido et al. 2012, 2017; Sanfilippo et al. 2015). All serpulids are suspension feeders. Their branchial crown is used for feeding and respiration (ten Hove and Kupriyanova 2009). Chemosymbiosis has not been suggested for any species of Serpulidae. An operculum, serving as a tube plug when a worm withdraws into its tube, is generally present in serpulids (ten Hove and Kupriyanova 2009). Serpulids are important fouling organisms, and many species can also form reefs (ten Hove and van den Hurk 1993). Serpulids are most common in normal marine environments, but an exceptional species *Marifugia cavatica* dwells in fresh water (ten Hove and Kupriyanova 2009).

7.2.1.3 Fossil Record and Evolution

Serpulids have a rich fossil record as their calcareous tubes have relatively good preservation potential, especially when compared to soft-bodied annelids and tubeworms with organic tubes. The earliest serpulids appeared in the Permian of Sicily (Sanfilippo et al. 2017, 2018), where they are known from shallow marine sediments. Fossils of calcareous tubeworms reported from older rocks do not belong to serpulids but to an extinct group of lophophorate tubeworms (Vinn and Mutvei 2009). Serpulids diversified greatly during the Jurassic (Jäger 1983, 2005; Ippolitov 2007a, b, 2010). The serpulid faunas of the Mesozoic and Cenozoic are relatively well described, though mostly based on European material (for reviews see Lommerzheim 1979; Jäger 1983, 2005). Seven serpulid genera are known from fossil hydrocarbon seeps (Vinn et al. 2012, 2014; Georgieva et al. 2019). Serpulids colonized seep environments sometime during the Late Jurassic or Early Cretaceous (Vinn et al. 2014). The earliest representatives occur in fossil seeps of Svalbard (Vinn et al. 2014). Serpulid tube fossils are also known from seeps of the Sada Limestone, Japan (Nobuhara et al. 2008); the Ca' Fornace site, Italy (Kiel et al. 2018); and from Bexhaven, New Zealand (Georgieva et al. 2019, and references therein). From an evolutionary perspective, three of seven serpulid genera (*Propomatoceros*, *Nogrobs*, *Protis*) colonized the seep environment soon after (in geological terms) their first appearance in the fossil record, a pattern seen also among other taxonomic groups inhabiting seeps (Vinn et al. 2013).

7.2.1.4 Classification and Tube Characters

Seep serpulids do not form a monophyletic clade; instead, they contain species from both major clades of the family Serpulidae (Vinn et al. 2013, 2014). Tube characters of seep serpulids are shared with the rest of the serpulid fauna. Attached serpulids usually have a widened tube base. Serpulid tubes have circular to multiangular cross sections (Ippolitov et al. 2014); however, the tube lumen always has a circular cross section. Tubes often show a longitudinal keel or keels and perpendicular peristomes (Ippolitov et al. 2014). Serpulid tubes have a characteristic microstructure (Vinn et al. 2008). Their growth lamellae are chevron shaped in longitudinal section. Chevron-shaped growth lamellae are the best character to distinguish serpulid tubes from similar Palaeozoic to Jurassic tentaculitoid tubeworms and other tubicolous invertebrates. Serpulids of the serpulin clade can have calcitic tubes with an external prismatic layer or complex-oriented microstructure (Vinn et al. 2008). Serpulids of the filogranin clade usually have aragonitic tubes with unoriented microstructure (Vinn et al. 2008).

Clade A (Serpulin Serpulids)
Hyalopomatus Marenzeller, 1878 – A single species is known from the Middle Eocene Humptulips seep of Washington State (Vinn et al. 2012). The tube comprises two layers in the seep serpulid *Hyalopomatus* aff. *biformis* (Vinn et al. 2012).

A thin outer layer is composed of a spherulitic prismatic structure with the thicker ends of the spherulitic fans oriented toward the tube exterior. The microstructure of the thick inner layer varies from homogeneous to fine, irregularly oriented prismatic (Vinn et al. 2012).

Nogrobs de Montfort, 1808 – Two species occur in Mesozoic seeps (Fig. 7.1a, b) (Vinn et al. 2012, 2014). There are three microstructurally distinct layers in the tube wall of the seep serpulid *Nogrobs hydrocarbonicus*: a thick outer prismatic layer, a thin middle layer of fine granular homogeneous structure, and a thick inner prismatic layer.

Propomatoceros Ware, 1975 – *Propomatoceros* is used as a "dustbin genus" for all single-keeled serpulid tubes with a more or less circular cross section (M. Jäger, pers. comm. 2011). Two species occur in Mesozoic seeps (Vinn et al. 2012, 2014). Two types of tube microstructure are present in the tube wall of the seep serpulid *Propomatoceros* sp.: an outer layer composed of spherulitic prismatic structure and an inner layer composed of fine homogenous granular structure (Vinn et al. 2012) (Fig. 7.1c).

Pyrgopolon de Montfort, 1808 – Two species occur in latest Jurassic-Early Cretaceous seeps of Svalbard (Vinn et al. 2014). The tube wall is moderately thick

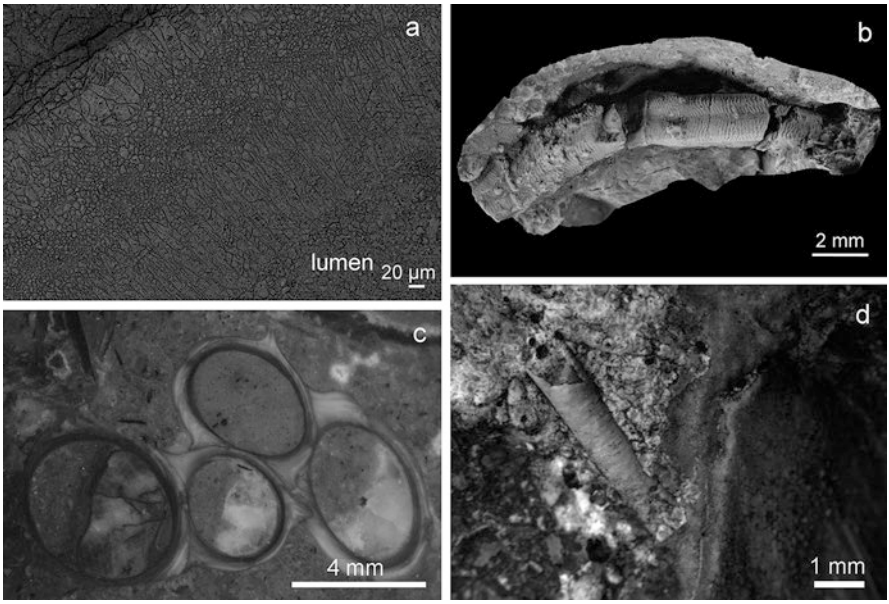

Fig. 7.1 Serpulidae: (**a**) Tube cross section of *Nogrobs hydrocarbonicus* (Vinn et al. 2012), showing outer and inner spherulitic prismatic layers and thin, middle, fine-grained homogeneous layer. (**b**) *Nogrobs* aff. *quadricarinata* (Münster in Goldfuss, 1831), specimen showing shape and external ornament of the tube, Myklegardfjellet seep, Volgian of Svalbard. (**c**) *Propomatoceros* sp., two cross sections of tubes from the Late Cretaceous (Campanian-Maastrichtian) Sada Limestone in Shikoku, Japan. (**d**) *Protis* sp., Late Miocene, from Case Rovereti near Santa Sofia, Italy

and has two layers, an inner granular layer and outer prismatic layer (Vinn et al. 2014).

Serpula Linnaeus, 1758 – Description of the species *Serpulidae* sp. (Georgieva et al. 2019) from the Middle Miocene of New Zealand is tentatively assigned here to the genus *Serpula*. The tube of this species is quite different from that of *Hyalopomatus*, *Nogrobs*, *Propomatoceros*, and *Pyrgopolon*.

Clade B (filogranin serpulids) Protis Ehlers, 1887 – A single species is known from the Late Miocene Case Rovereti seep deposit near Santa Sofia, northern Italy (Fig. 7.1d) (Vinn et al. 2012). The tubes are small and single layered. The tube microstructure is variable, consisting mostly of massive calcite crystals alternating with layered calcite (Vinn et al. 2012).

Spirorbis – A single species of an unidentified spirorbid is known from the Late Eocene Bear River seep in Washington State (Vinn et al. 2012).

7.3 Conclusions

Some serpulids colonized seeps soon after (geologically speaking) their first appearance in the fossil record, similar to many mollusks from vents and seeps (Warén and Bouchet 2001; Kiel 2010a, b). In contrast, gastropods and bivalves at vents and seeps are usually restricted to these environments, while serpulids are generally considered "colonists" (Olu et al. 1996a). Serpulids at Cretaceous and Cenozoic methane seep deposits are characterized by low diversity and mostly low abundance. They belong to several genera and both serpulid clades, but in most fossil seeps, they are represented by a single species only. The lack of common morphologic traits among seep serpulids indicates that life in the seep environment was not associated with any specific selective pressure on the morphology of the tubes.

Acknowledgments Financial support was provided by the Estonian Research Council project IUT20-34 "The Phanerozoic journey of Baltica: sedimentary, geochemical and biotic signatures of changing environment – PalaeoBaltica." I am grateful to reviewers Magdalena Georgieva and Rossana Sanfilippo for constructive comments on the manuscript.

References

Amon DJ, Gobin J, Van Dover CL et al (2017) Characterization of methane-seep communities in a deep-sea area designated for oil and natural gas exploitation off Trinidad and Tobago. Front Mar Sci 4:342. https://doi.org/10.3389/fmars.2017.00342

Bergquist DC, Ward T, Cordes EE et al (2003) Community structure of vestimentiferan generated habitat islands from Gulf of Mexico cold seeps. J Exp Mar Biol Ecol 289:197–222

Campbell KA (2006) Hydrocarbon seep and hydrothermal vent paleoenvironments and paleontology: past developments and future research directions. Palaeogeogr Palaeoclimatol Palaeoecol 232:362–407

Fujiwara Y, Kawato M, Yamamoto T et al (2007) Three-year investigations into sperm whale-fall ecosystems in Japan. Mar Ecol 28:219–232
Georgieva MN, Little CTS, Watson JS et al (2019) Identification of fossil worm tubes from Phanerozoic hydrothermal vents and cold seeps. J Syst Palaeontol 17:287–329
Guido A, Mastandrea A, Rosso A et al (2012) Micrite precipitation induced by sulphate reducing bacteria in serpulid bioconstructions from submarine caves (Syracuse, Sicily). Rend Online Soc Geol Ital 21:933–934
Guido A, Jimenez CK, Rosso A et al (2017) Cryptic serpulid-microbialite bioconstructions in the Kakoskali submarine cave (Cyprus, eastern Mediterranean). Facies 63:21
Hessler RR, Smithey WM (1983) The distribution and community structure of megafauna at the Galapagos Rift hydrothermal vents. In: Rona PA, Boström K, Laubier L et al (eds) Hydrothermal processes at seafloor spreading centers, NATO conference series (IV Marine Sciences), vol 12. Springer, Boston, pp 735–770
Ippolitov AP (2007a) Contribution to the revision of some late Callovian serpulids (Annelida, Polychaeta) of central Russia: Part 1. Paleontol J 41:260–267
Ippolitov AP (2007b) Contribution to the revision of some late Callovian serpulids (Annelida, Polychaeta) of central Russia: part 2. Paleontol J 41:429–436
Ippolitov AP (2010) Serpulid (Annelida, Polychaeta) evolution and ecological diversification patterns during Middle–Late Jurassic. Earth Sci Front 17:207–208
Ippolitov AP, Vinn O, Kupriyanova EK et al (2014) Written in stone: history of serpulid polychaetes through time. Mem Mus Victoria 71:123–159
Jäger M (1983) Serpulidae (Polychaeta Sedentaria) aus der norddeutschen höheren Oberkreide—Systematik, Stratigraphie, Ökologie. Geol Jahrb (Reihe A) 68:3–219
Jäger M (2005) Serpulidae und Spirorbidae (Polychaeta Sedentaria) aus Campan und Maastricht von Norddeutschland, den Niederlanden, Belgien und angrenzenden Gebieten. Geol Jahrb (Reihe A) 157(2004):121–249
Juniper SK, Sibuet M (1987) Cold seep benthic communities in Japan subduction zones: spatial organization, trophic strategies and evidence for temporal evolution. Mar Ecol Prog Ser 40:115–126
Kaim A (2011) Non-actualistic wood-fall associations from Middle Jurassic of Poland. Lethaia 34:109–124
Kiel S (2010a) On the potential generality of depth-related ecologic structure in cold-seep communities: Cenozoic and Mesozoic examples. Palaeogeogr Palaeoclimatol Palaeoecol 295:245–257
Kiel S (2010b) The fossil record of vent and seep mollusks. In: Kiel S (ed) The Vent and Seep Biota. Topics in Geobiology. Springer, Heidelberg, pp. 255–278
Kiel S, Goedert JL (2006) A wood-fall association from late Eocene deep-water sediments of Washington State, USA. Palaios 21:548–556
Kiel S, Sami M, Taviani M (2018) A serpulid-*Anodontia*-dominated methane-seep deposit from the Miocene of northern Italy. Acta Palaeontol Pol 63:569–577
Kupriyanova EK, Nishi E (2011) New records of the deep-sea *Nogrobs grimaldii* (Annelida, Serpulidae). Mar Biodivers Rec 4:e74
Kupriyanova EK, Macdonald T, Rouse GW (2006) Phylogenetic relationships within Serpulidae (Annelida: Polychaeta) inferred from molecular and morphological data. Zool Scr 35:421–439
Kupriyanova EK, Nishi E, Kawato M et al (2010) New records of Serpulidae (Annelida, Polychaeta) from hydrothermal vents of North Fiji, Pacific Ocean. Zootaxa 2389:57–68
Kupriyanova EK, Vinn O, Taylor PD et al (2014) Serpulids living deep: calcareous tubeworms beyond the abyss. Deep-Sea Res Part I 90:91–104
Lenihan HS, Mills SW, Mullineaux LS et al (2008) Biotic interactions at hydrothermal vents: recruitment inhibition by the mussel *Bathymodiolus thermophilus*. Deep-Sea Res Part I 55:1707–1717
Lommerzheim A (1979) Monographische Bearbeitung der Serpulidae (Polychaeta sedentaria) aus dem Cenoman (Oberkreide) am Südwestrand des Münsterländer Beckens. Decheniana 132:110–195

López-González PJ, Rodríguez E, Gili J-M et al (2003) New records on sea anemones (Anthozoa: Actiniaria) from hydrothermal vents and cold seeps. Zool Verh 345:215–243

Nobuhara T, Onda D, Kikuchi N et al (2008) (Lithofacies and fossil assemblages of the Upper Cretaceous Sada Limestone, Shimanto City, Kochi Prefecture, Shikoku, Japan.) Fossils [Palaeontol Soc Jpn] 84:47–60 (In Japanese with English abstract)

Olu K, Duperret A, Sibuet M et al (1996a) Structure and distribution of cold seep communities along the Peruvian active margin: relationship to geological and fluid patterns. Mar Ecol Prog Ser 132:109–125

Olu K, Sibuet M, Harmegnies F et al (1996b) Spatial distribution of diverse cold seep communities living on various diapiric structures of the southern Barbados prism. Prog Oceanogr 38:347–376

Pailleret M, Haga T, Petit P et al (2007) Sunken wood from the Vanuatu Islands: identification of wood substrates and preliminary description of associated fauna. Mar Ecol 28:233–241

Sanfilippo R, Rosso A, Guido A et al (2015) Metazoan/microbial biostalactites from present-day submarine caves in the Mediterranean Sea. Mar Ecol 36:1277–1293

Sanfilippo R, Rosso A, Reitano A et al (2017) First record of sabellid and serpulid polychaetes from the Permian of Sicily. Acta Palaeontol Pol 62:25–38

Sanfilippo R, Rosso A, Reitano A et al (2018) New serpulid polychaetes from the Permian of western Sicily. Acta Palaeontol Pol 63:579–584

Segonzac M, Hekinian R, Auzende J-M et al (1997) Recently discovered animal communities on the South East Pacific Rise (17–19°S and the Eastern Microplaque Region). Cah Biol Mar 38:140–141

Smith CR, Baco AR (2003) Ecology of whale falls at the deep-sea floor. Oceanogr Mar Biol Annu Rev 41:311–354

Smith CR, Kukert H, Wheatcroft RA et al (1989) Vent fauna on whale remains. Nature 341:27–28

ten Hove HA, Kupriyanova EK (2009) Taxonomy of Serpulidae: the state of affairs. Zootaxa 2036:1–126

ten Hove HA, Smith RS (1990) A re-description of *Ditrupa gracillima* Grube, 1878 (Polychaeta, Serpulidae) from the Indo-Pacific, with a discussion of the genus. Rec Aust Mus 42:101–118

ten Hove HA, van den Hurk P (1993) A review of Recent and fossil serpulid 'reefs': actuopaleontology and the 'Upper Malm' serpulid limestones in NW Germany. Geol Mijnb 72:23–67

ten Hove HA, Zibrowius H (1986) *Laminatubus alvini* gen. et sp. n. and *Protis hydrothermica* sp. n. (Polychaeta, Serpulidae) from the bathyal hydrothermal vent communities in the eastern Pacific. Zool Scr 15:21–31

Vinn O, Mutvei H (2009) Calcareous tubeworms of the Phanerozoic. Estonian J Earth Sci 58:286–296

Vinn O, ten Hove HA, Mutvei H et al (2008) Ultrastructure and mineral composition of serpulid tubes (Polychaeta, Annelida). Zool J Linnean Soc 154:633–650

Vinn O, Kupriyanova EK, Kiel S (2012) Systematics of serpulid tubeworms (Annelida, Polychaeta) from Cretaceous and Cenozoic hydrocarbon-seep deposits in North America and Europe. Neues Jahrb Geol Palaontol Abh 256:315–325

Vinn O, Kupriyanova EK, Kiel S (2013) Serpulids (Annelida, Polychaeta) at Cretaceous to modern hydrocarbon seeps: ecologic and evolutionary patterns. Palaeogeogr Palaeoclimatol Palaeoecol 390:35–41

Vinn O, Hryniewicz K, Little CTS et al (2014) A Boreal serpulid fauna from Volgian-Ryazanian (latest Jurassic-earliest Cretaceous) shelf sediments and hydrocarbon seeps from Svalbard. Geodiversitas 36:527–540

Warén A, Bouchet P (2001) Gastropoda and Monoplacophora from hydrothermal vents and seeps; new taxa and records. Veliger 44(2):116–231

Wolff T (1979) Macrofaunal utilization of plant-remains in the deep sea. Sarsia 64:117–136

Chapter 8
Brachiopods at Hydrocarbon Seeps

Andrzej Baliński, Maria Aleksandra Bitner, and Michał Jakubowicz

8.1 Introduction

Brachiopods are exclusively marine, sessile, ciliary suspension filter-feeding invertebrates with a soft body enclosed in a shell consisting of two unequal valves (ventral and dorsal). The brachiopod shell is composed of calcium carbonate or calcium phosphate impregnated with organic substance and externally covered by a thin organic layer, the periostracum. The majority of brachiopods have a calcitic shell with valves hinged along the posterior edge by sockets and teeth. They constitute a major group of articulated brachiopods or rhynchonelliformeans. Another smaller group, craniiformeans, also have a calcitic (or possibly aragonitic) shell, but it is not articulated as they do not have special hinge structures. The third group of brachiopods, linguliformeans, have organophosphatic and inarticulated shells.

Brachiopods appeared first in the Lower Cambrian, being dominant members of Palaeozoic benthic communities until the Permian-Triassic mass extinctions (Curry and Brunton 2007). Since the Mesozoic, their diversity and abundance have been dramatically reduced, and today they are represented by about 115 genera and 400 species; brachiopods are considered a minor, although a widely distributed phylum (Emig et al. 2013). The majority of extant brachiopods live on continental shelves and bathyal slopes, but they can also be found in the intertidal zone and at abyssal depths (Richardson 1997; Logan 2007).

The majority of brachiopods, both extant and fossil, represent an epifaunal mode of life being attached to the substrate by a pedicle. Some, such as the living craniiformeans, are firmly cemented to hard substrates and several others rested freely

A. Baliński (✉) · M. A. Bitner
Institute of Paleobiology, Polish Academy of Sciences, Warszawa, Poland
e-mail: balinski@twarda.pan.pl; bitner@twarda.pan.pl

M. Jakubowicz
Isotope Research Unit, Adam Mickiewicz University, Poznań, Poland
e-mail: mjakub@amu.edu.pl

A. Kaim et al. (eds.), *Ancient Hydrocarbon Seeps*, Topics in Geobiology 50,
https://doi.org/10.1007/978-3-031-05623-9_8

unattached on the sea bottom or anchored their shell in the sediment by long spines. One group of extant inarticulated brachiopods, the lingulids, lives infaunally in deep, U-shaped vertical burrows excavated in soft sediment (Emig 1997). There is evidence that the infaunal mode of life in lingulids appeared as early in their phylogenetic pathway as the Early Ordovician (Baliński and Sun 2013).

All extant brachiopods are suspension feeders. They pump water through the tentacle-bearing respiratory and feeding apparatus, known as the lophophore, from which they extract particulate nutrients such as phytoplankton, bacteria and organic detritus. Brachiopods also appear to be able to absorb dissolved organic matter directly from seawater (James et al. 1992).

Carbon and oxygen isotope ratios of fossil brachiopod shells have been used for decades to investigate environmental conditions in ancient oceans. The low-magnesium calcite of articulated brachiopod shells is considered exceptionally suitable for isotopic studies (Brand 1989; Parkinson and Cusack 2007; Brand et al. 2015), but vital effects may sometimes be important (Brand et al. 2003; Romanin et al. 2018).

No extant brachiopods are known to be associated with vent/seep environments; however, some species are found in the vicinities of hydrothermal vents, associated with mid-ocean spreading ridges, but there is no evidence that they are members of chemosynthesis-based communities (Zezina 2003, 2008; Lee et al. 2008). On the other hand, many Palaeozoic and Mesozoic seep faunas are dominated by brachiopods. The oldest brachiopods known from chemosynthesis-based associations are Silurian in age. Two subphyla, Linguliformea and Rhynchonelliformea, have fossil representatives associated with ancient chemosynthesis-based communities (Sandy 2010). Usually they are characterized by monospecific assemblages with numerous individuals. However, their ability for possible chemosymbiosis remains doubtful (see discussion below).

8.2 Overview of Brachiopod Occurrences at Palaeozoic Hydrocarbon Seeps

8.2.1 Order: Lingulida Waagen, 1885

Superfamily: Discinoidea Gray, 1840
Family: Uncertain

The oldest occurrence of brachiopods in a hydrothermal vent deposit was that of the lingulide *Pyrodiscus* Little, Maslennikov, Morris and Gubanov, 1999, described from the Yaman-Kasy sulphide deposits of the Ural Mountains, Russia (Little et al. 1997, 1999). The stratigraphic dating of this finding is uncertain, but Little et al. (1999) suggested the Upper Silurian (Ludlow). This oldest known hydrothermal vent community comprises, beside the aforementioned lingulide, tubes of the probable polychaete *Eoalvinellodes annulatus*, the vestimentiferan *Yamankasia rifeia*,

the kirengellid tergomyan *Thermoconus shadlunae*, an indeterminate vetigastropod, and the ambonychiid bivalve *Mytilarca* sp. (Little et al. 1999). The lingulide *Pyrodiscus* is a poorly known genus probably belonging to Discinoidea (Holmer and Popov 2007) and distinguished by a suboval, very large shell, attaining up to 93 mm in width. During life, it possessed a functional pedicle and followed a sessile epifaunal mode of life. According to Little et al. (1999), the Yaman-Kasy community lived during active hydrothermal venting in deep water and was dependent on the vent fluid as the main energy source through chemosynthetic primary bacterial production.

8.2.2 Order: Rhynchonellida Kuhn, 1949

Superfamily: Dimerelloidea Buckman, 1918

All rhynchonellide brachiopods known to date that are associated with vent/seep environments belong to superfamily Dimerelloidea ranging from the Upper Devonian (Famennian) until today. Several members of this superfamily are distinguished by costate, large to very large shell dimensions. Although the extant dimerelloideans (Cryptoporidae) are not known from vent/seep settings, it has been suggested by several authors that Devonian to Cretaceous representatives of this lineage were possibly exclusively associated with chemosynthesis-dominated environments (e.g., Sandy and Campbell 1994; Manceñido and Owen 2001; Gischler et al. 2003; Peckmann et al. 2007; Kiel and Peckmann 2008; Sandy 2010).

Family: Peregrinellidae Ager, 1965
Dzieduszyckia Siemiradzki, 1909

This is one of the largest Palaeozoic rhynchonellides characterized by a strongly costate shell with opposite sulci on each valve (Fig. 8.1a–c, g–i, m–o). Although it can be frequently found in great shell accumulations, its distribution is patchy and scattered on distant palaeocontinents, suggesting long-distance dispersal capabilities and high reproductive capacities (Van Dover et al. 2002; Baliński and Biernat 2003). The genus has been described from Laurussia, Kazakhstania, northern Gondwana and South China. It was first described from the Famennian of the Holy Cross Mountains, Poland (Siemiradzki 1909), and subsequently from a borehole situated in the same region (Fig. 8.1a–c) (Biernat 1967). *Dzieduszyckia* is known to occur in the Famennian of the South Urals (Nalivkin 1947; Rozman 1962), Kazakhstan (Rozman 1962), and Tajikistan (Menakova 1991) (Fig. 8.1g–i). Recently, Nie et al. (2016) summarized the occurrences of the genus in southern China. From eastern Laurussia, the genus was reported in present-day Nevada (Cloud Jr. and Boucot 1971) and Mexico (Noll et al. 1984). Both latter occurrences are characterized by accumulations of *Dzieduszyckia* shells in bedded barite deposits that were once interpreted as low-temperature hydrothermal vent settings (Poole et al. 1983). More recently, however, these settings have been reinterpreted as

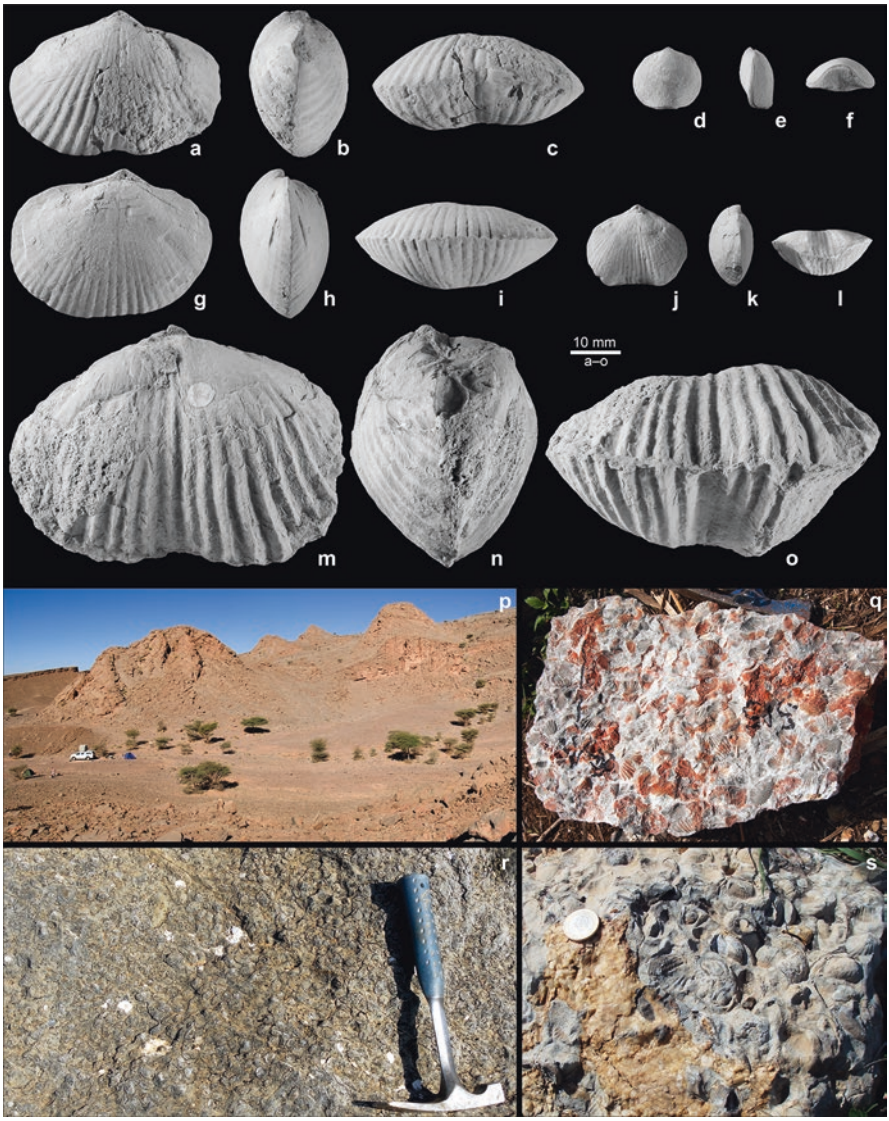

Fig. 8.1 Palaeozoic brachiopods from hydrocarbon seep deposits. (**a**–**c**) *Dzieduszyckia kielcensis* (Roemer, 1866) from the Famennian of Ruda Strawczyńska borehole, Poland. (**d**–**f**) *Septatrypa tumulorum* Baliński and Halamski, 2018, (in Halamski and Baliński 2018) from the Kess-Kess Formation (late Emsian) of Hamar Laghdad, Morocco. (**g**–**i**) *Dzieduszyckia bashkirica* (Tschernyschew, 1887) from the western slopes of the South Urals. (**j**–**l**) *Ibergirhynchia contraria* (Roemer, 1850) from the Early Carboniferous of the Iberg Reef, Harz Mountains, Germany. (**m**–**o**) *Dzieduszyckia crassicostata* (Termier and Termier, 1948) from the Famennian of Morocco. (**p**) Late Emsian Kess-Kess mud mounds related to submarine hydrothermal venting at the Hamar Laghdad area of southern Morocco, the site of atrypide *Septatrypa tumulorum* Baliński and Halamski, 2018 (in Halamski and Baliński 2018). (**q**) Fragment of a limestone layer with a mass occurrence of *Dzieduszyckia* sp. in the Famennian of southern Guangxi, China. (**r**) Monospecific assemblage of *Septatrypa lantenoisi* (Termier, 1936) in micritic carbonates from the Upper Silurian El Borj seep deposit, Moroccan Meseta; Unit B (*sensu* Barbieri et al. 2004). (**s**) Typical field appearance of the carbonate blocks hosting mass concentrations of *Dzieduszyckia* sp. at the Sidi Amar site (Moroccan Meseta; for locality details see Jakubowicz et al. this volume)

hydrocarbon seeps (Torres et al. 2003; Campbell 2006; Johnson et al. 2004; Canet et al. 2014).

The stratigraphic distribution of *Dzieduszyckia* is inadequately known but can generally be summarized as Famennian. For the Moroccan *Dzieduszyckia*, an early Famennian age was suggested (Hollard and Morin 1973; Ager et al. 1976) and subsequently confirmed by conodont dating (Peckmann et al. 2007). Recently, Nie et al. (2016) reported *Dzieduszyckia* from several exposures scattered in Guangxi and Guizhou provinces in southern China (Fig. 8.1q) and provided conodont dating for these findings spanning from the Upper *Palmatolepis triangularis* Zone to the Upper *Palmatolepis rhomboidea* Zone (Early to Middle Famennian).

In Morocco, *Dzieduszyckia* is especially diverse being represented by a few species found at several outcrops of the Moroccan Meseta (e.g., Termier and Termier 1950; Ager et al. 1976; see review in Baliński and Biernat 2003; Jakubowicz et al. this volume) (Fig. 8.1s). The analyses of the Polish and Moroccan shell material of *Dzieduszyckia* and associated sediment provided by Baliński and Biernat (2003) did not show any signature of unusual environmental conditions. However, Peckmann et al. (2007) resampled and analysed the carbon isotope signatures of the *Dzieduszyckia*-bearing limestone from Morocco, finding strong evidence that they formed at a hydrocarbon seep in a dysphotic or aphothic environment. The differing isotopic records of Baliński and Biernat (2003) and Peckmann et al. (2007), as well as the occurrences of *Dzieduszyckia* in well-bedded limestones in China (Nie et al. 2016), suggest that this brachiopod might have occurred at both hydrocarbon seeps as well as other environmental settings. The degree of ecological plasticity suggested for *Dzieduszyckia* may have thus been greater than that observed in most benthic invertebrates inhabiting modern seeps (Peckmann et al. 2007, p. 121).

Ibergirhynchia Gischler, Sandy and Peckmann, 2003

Gischler et al. (2003) described the seep-related rhynchonellide *Ibergirhynchia contraria* (Roemer, 1850) from the uppermost Viséan (Lower Carboniferous) of the Harz Mountains (Germany) (Fig. 8.1j–l). This brachiopod was found in a low-diversity accumulation in microbial limestone that covered the drowned Middle-Late Devonian Iberg Reef. The seep deposits on top of the Iberg Reef formed a seamount during the Famennian and Early Carboniferous, which was permeated by methane. The source of the methane may have been thermogenic from the volcanic base of the reef or derived from a petroleum reservoir (Peckmann et al. 2001; Gischler et al. 2003).

The shell of *Ibergirhynchia contraria* is medium-sized, reaching up to about 20 mm in length, slightly transverse in outline, and has a weakly sulcate dorsal valve and a corresponding fold on the ventral valve. The distinct radial costation of the shell, reminiscent of that in some species of the Famennian genus *Dzieduszyckia*, is noteworthy. Although it is difficult to be certain as to the type of crura, because their detailed structure is not known, it is highly probable that *Ibergirhynchia* is a descendant from the Famennian *Dzieduszyckia*, as suggested by Gischler et al. (2003). These authors suggested that both *Dzieduszyckia* and *Ibergirhynchia* represent a long lineage of seep-dwelling genera of the Dimerelloidea ranging from the

Devonian to the Cretaceous that were protected in this kind of environment, acting as a refuge from the effects of mass extinctions. Lower Cretaceous *Peregrinella* may be regarded as a Mesozoic relic of this seep-associated rhynchonellide lineage (Campbell et al. 1993; Campbell and Bottjer 1995a).

8.2.3 Order: Atrypida Rzhonsnitskaia, 1960

Superfamily: Lissatrypoidea Twenhofel, 1914
Family: Septatrypidae Kozłowski, 1929
Septatrypa Kozłowski, 1929

This genus is the only representative of the atrypide brachiopods whose occurrence is interpreted as related to chemosynthetic-based communities. Species belonging to this genus are characterized by a medium-sized, dorsibiconvex, smooth shell with distinct ventral sulcus and dorsal fold. Its stratigraphic range spans the Silurian (Aeronian) until the Lower Devonian (Pragian).

A characteristic monospecific shell accumulation of *Dubaria lantenoisi* (*Septatrypa lantenoisi*; synonymy of *Dubaria* and *Septatrypa* was postulated by Copper (2002, 2004)) has been described by Ager et al. (1976) from an Upper Silurian (Ludfordian; Jakubowicz et al. 2017) limestone lens in central Morocco ('El Borj deposit'; for a detailed locality description, see Jakubowicz et al. this volume) (Fig. 8.1r). Originally interpreted as representative of isolated shoals (Ager et al. 1976), the *Dubaria* (=*Septatrypa*)-rich carbonates were first suggested to be an ancient seep deposit by Campbell and Bottjer (1995a). Subsequently, this view has been supported with petrographic, palaeontological and carbon isotope evidence (Barbieri et al. 2004; Buggisch and Krumm 2005; Jakubowicz et al. 2017). *Septatrypa* is most characteristic of the basal part of the El Borj deposit, where they form mass accumulations and represent the only invertebrates collected (Barbieri et al. 2004). This facies, dominated by micritic carbonates, has been interpreted as representing diffuse fluid flow (Jakubowicz et al. 2017). In the upper part of the deposit, comprised by an isopachous-cement-rich limestone indicative of increased, focused fluid flow, the atrypids are less common and co-occur with large, seep-specialised modiomorphid bivalves (Jakubowicz et al. 2017).

It is worth noting that recently Halamski and Baliński (2018) reported nearly monospecific occurrence of *Septatrypa* within the hydrothermal-related Emsian Kess-Kess mud mounds (Belka 1998) in the Hamar Laghdad mountain range (Fig. 8.1d–f, p). This may suggest that *Septatrypa* was adapted during the Silurian and Lower Devonian to live at hydrocarbon seeps and hydrothermal vents, although this brachiopod occurred in other environmental settings more frequently. Similar to the case of the Famennian rhynchonellide *Dzieduszyckia*, such a distribution suggests a certain ecological plasticity.

8.3 Overview of Brachiopod Occurrences at Mesozoic and Cenozoic Hydrocarbon Seeps

8.3.1 Lingulida Waagen, 1885

Superfamily: Linguloidea Menke, 1828
Family: Lingulidae Menke, 1828

The only representatives of the family Lingulidae, found in the Lower Cretaceous cold seep carbonate body in the Sassenfjorden area, central Spitsbergen, are common, variably fragmented shells that belong to the genus *Lingularia* Biernat and Emig, 1993, clearly resembling the Late Jurassic species *L. similis* Biernat and Emig, 1993 (Holmer and Nakrem 2012; Sandy et al. 2014). Their occurrence at the seep site is most likely fortuitous.

8.3.2 Rhynchonellida Kuhn, 1949

Superfamily: Dimerelloidea Buckman, 1918

This rhynchonellide superfamily comprises three families (Dimerellidae, Halorellidae and Peregrinellidae) with the majority of its representatives related to chemosynthesis-based communities (Manceñido and Owen 2001; Manceñido et al. 2002).

Family: Dimerellidae Buckman, 1918

Sulcirostra Cooper and Muir-Wood, 1951 (Fig. 8.2a–c), is a dimerelloid genus known from the Lower Jurassic of Germany, Switzerland, Italy, Croatia, Morocco and the USA (Sulser and Furrer 2008; Kiel et al. 2021). A nearly monospecific mass occurrence of *Sulcirostra paronai* (Böse, 1894) at Seneca (Oregon, USA) is associated with a serpentinite-enclosed seep carbonate (Peckmann et al. 2013). The *Sulcirostra* shell is of medium-size, rectimarginate to gently sulcate, and covered with numerous fine ribs (see also Manceñido and Dagys 1992).

Cooperrhynchia Sandy and Campbell, 1994 (Fig. 8.2d–f), is recorded only from the Upper Jurassic site of Paskenta in California where it is moderately abundant (Sandy and Campbell 1994; Andrzej Kaim *pers. comm.* 2020) and represented by the monotypic *Cooperrhynchia schucherti* (Stanton, 1895). The species is medium-sized with a thin, smooth shell; the anterior commissure is narrowly sulcate, but a median shallow sulcus can be present on the ventral valve (Sandy and Campbell 1994).

Family: Peregrinellidae Ager, 1965

Anarhynchia Ager, 1968 (Fig. 8.3), is known from the Lower to Middle Jurassic, and it is the only dimerelloidean genus yet known from both seeps and vents (Sandy 2001, 2010; Kiel and Peckmann 2019). It was reported from the hydrothermal vent

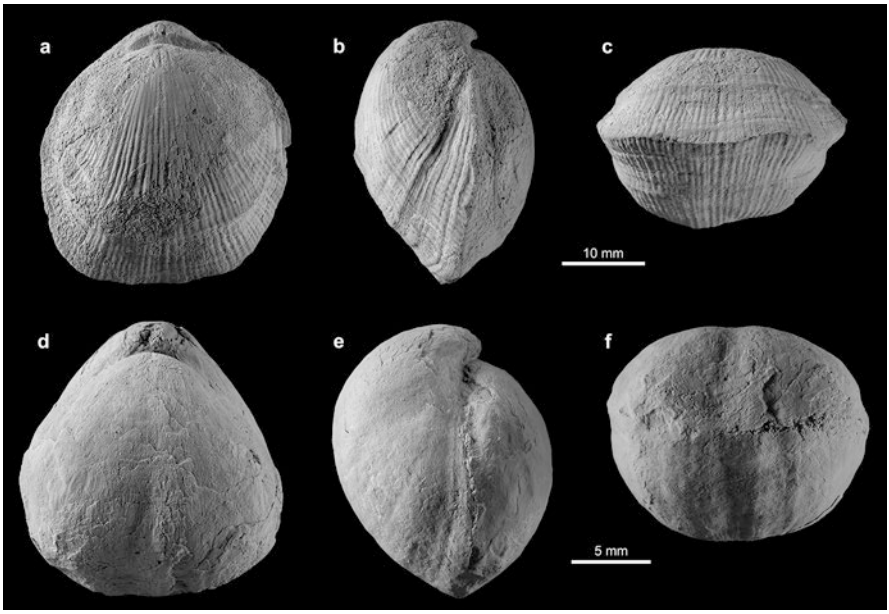

Fig. 8.2 (**a**–**c**) *Sulcirostra paronai* (Böse, 1894) from Lower Jurassic hydrocarbon seep deposits at Seneca (Oregon, USA); dorsal, lateral and anterior views of articulated specimen. (**d**–**f**) *Cooperrhynchia schucherti* (Stanton 1895) from Upper Jurassic hydrocarbon seep deposits at Paskenta (California, USA); dorsal, lateral and anterior views of articulated specimen. Photos by Andrzej Baliński

deposits in Figueroa (California) by Little et al. (1999, 2004). *Anarhynchia* is also known from alleged seep deposits of Argentina, California and Oregon (Ager 1968; Manceñido and Dagys 1992; Sandy 1995, 2001, 2010; Stefanoff and Sandy 1998; Sandy and Campbell 2003). More recently, this genus was reported from the Lower Jurassic seep deposits in northern British Columbia with the dominant species being *Anarhynchia smithi* (Pálfy et al. 2017). *Anarhynchia* is a large, coarsely ribbed brachiopod with a rectimarginate anterior commissure.

The Early Cretaceous genus *Peregrinella* Oehlert, 1887 (Fig. 8.4d–f), is one of the best known genera associated with chemosynthesis-based communities. It is also the most speciose genus with over ten species described. *Peregrinella* is the largest Mesozoic brachiopod genus reaching a length of up to 100 mm, with a strongly costate surface. It is widely distributed, being known throughout Europe from France to the Crimea, North America, Tibet and China (Biernat 1957; Hou and Wang 1984; Sun 1986; Campbell and Bottjer 1995a, b; Sandy et al. 1995; Sandy and Blodgett 1996; Posenato and Morsilli 1999; Lazăr et al. 2005; Kiel and Peckmann 2008; Sandy et al. 2012; Kiel et al. 2014; Sandy and Peckmann 2016). *Peregrinella* seems to be the last element in this seep-associated dimerelloidean evolutionary lineage from the Paleozoic (Sandy 2010).

Family: Halorellidae Ager, 1965

Fig. 8.3 Mass accumulation of *Anarhynchia gabbi* Ager, 1968, in Middle Jurassic hydrocarbon seep deposits in Bedford Canyon (California, USA); age constraints of this locality follow the interpretation of Imlay (1980). Photo by Andrzej Kaim

Halorella Bittner, 1884 (Fig. 8.4a–c), is a genus with large-sized (reaching nearly 60 mm in width), strongly costate shells with characteristic transverse outline and opposite median sulci on both valves. It is known from the Late Triassic and has a wide geographic distribution, being recognized in Europe, Asia, New Zealand and North America (Ager 1968; Milne and Campbell 1969; Sandy 1995; Manceñido et al. 2002; Peckmann et al. 2011; Kiel et al. 2017, 2021). Mass occurrences of this brachiopod are known from Norian seep sites in Oregon, USA (Peckmann et al. 2011), and Norian-Carnian seeps in Turkey (Kiel et al. 2017).

Family: Uncertain

The Early Jurassic dimerelloidean *Carapezzia* Tolmin, 1930, could also have been adapted to hydrothermal vent and cold seep environments. This genus contains three species, reported from Austria, Italy and Switzerland (Sulser and Furrer 2008). *Carapezzia* is characterized by a large, smooth, strongly biconvex, rectimarginate shell with a high, incurved beak that is regarded as a generic character for this brachiopod.

8.3.3 Order: Terebratulida Waagen, 1883

Terebratulides are rare in Mesozoic and Cenozoic seep deposits, and they do not form mass occurrences.

Superfamily: Terebratuloidea Gray, 1840

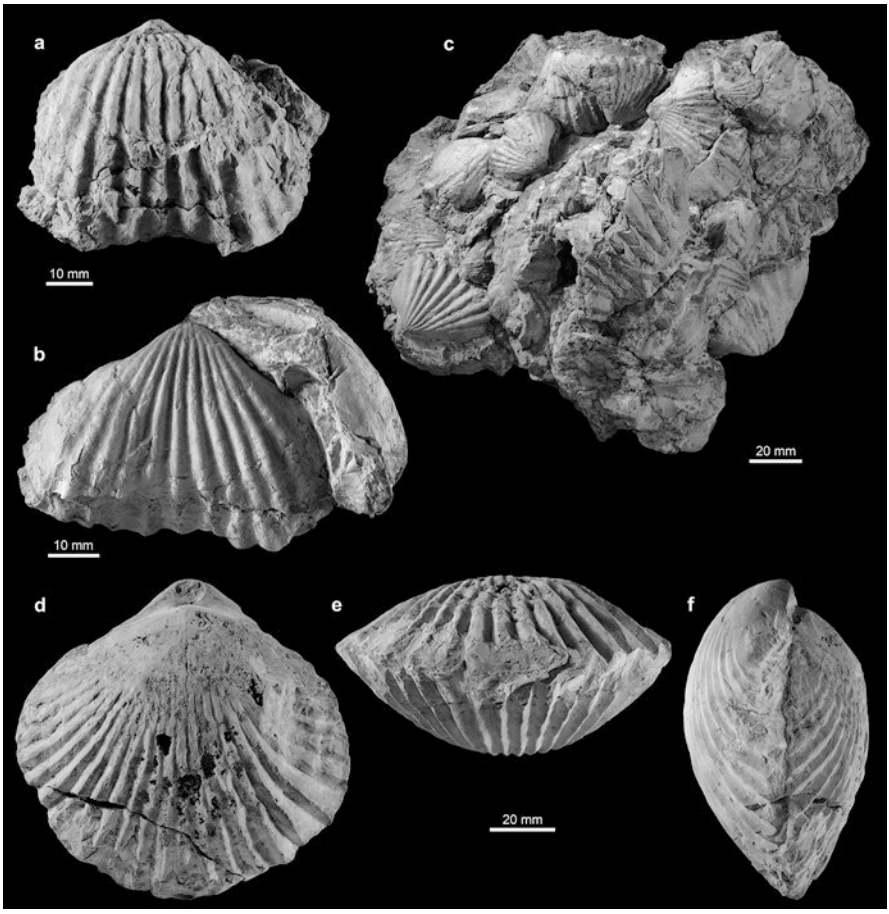

Fig. 8.4 (**a**–**c**) *Halorella* sp. from Upper Triassic hydrocarbon seep deposits on Graylock Butte (Oregon, USA); (**a**) Dorsal view of articulated specimen. (**b**) Ventral view of articulated specimen. (**c**) In situ accumulation of *Halorella* sp. (**d**–**f**) *Peregrinella multicarinata* (Lamarck, 1819) from Lower Cretaceous seep deposits at Raciborsko in southern Poland: dorsal, anterior and lateral views of articulated specimen. Photos by Andrzej Baliński

Family: Sellithyrididae Muir-Wood, 1965

Late Paleocene shallow-water chemosynthesis-based assemblage from the Basilika Formation, Spitsbergen, contains one species of short-looped brachiopod, *Neoliothyrina nakremi* Bitner, 2019 (Hryniewicz et al. 2019). The genus *Neoliothyrina* Sahni, 1925, was previously only known from the Upper Cretaceous of Great Britain, Denmark, Germany and Poland (Cooper 1983). Nevertheless, none of the Cretaceous *Neoliothyrina* species was associated with chemosynthesis-based ecosystems; all species come from the white chalk, opoka and marl facies (Steinich 1965; Popiel-Barczyk 1968).

Superfamily: Cancellothyridoidea Thomson, 1926
Family: Chlidonophoridae Muir-Wood, 1959

The Upper Cretaceous hydrocarbon seep deposits at Omagari (Hokkaido, Japan) yield a monospecific association of the chlidonophorid brachiopod *Eucalathis methanophila* Bitner, 2010 (Kaim et al. 2010). This species represents the oldest and only Mesozoic record of the genus *Eucalathis* Fischer and Oehlert 1890. This locality constitutes the only specimen-rich occurrence of terebratulide brachiopods at hydrocarbon seeps to date.

Family: Zeilleriidae Allan, 1940

Among the species of the genus *Modestella* Owen in Casey 1961, only the Early Cretaceous *Modestella jeletzkyi* Sandy, 1990, seems to be seep-related. It was recognised in cold seep deposits of Arctic Canada (Sandy 1990, 1995; Beauchamp and Savard 1992).

Family: Megathyrididae Dall, 1870

A single valve of the genus *Argyrotheca* Dall, 1900, has been recently found in the middle Eocene hydrocarbon seep deposits in western Washington State, USA (Goedert et al. 2021). This is the first record of a megathyridid brachiopod in seep deposits; however, because of the very limited material, it is impossible to tell whether the *Argyrotheca* specimen was a member of the seep community (see also discussion in Goedert et al. 2021).

Apart from above-discussed brachiopod genera associated with chemosynthesis-based associations, numerous brachiopods, some of them only tentatively determined, have been reported by Sandy et al. (2014) from the Late Jurassic-Early Cretaceous shallow-water hydrocarbon seep deposits from central Spitsbergen, Svalbard. Rhynchonellides are represented by two genera, *Pseudomonticlarella* Smirnova, 1987, and *Ptilorhynchia* Crickmay, 1933, (with two species) belonging to the families Norellidae Ager, 1959, and Rhynchonellidae d'Orbigny, 1847, respectively. Among Terebratulida, representatives of the family Sellithyrididae Muir-Wood, 1965 (genera *Cyrtothyris* Middlemiss, 1959; *Praelongithyris* Middlemiss, 1959); family Lissajousithyrididae Cooper, 1983 (genera *Rouillieria* Makridin, 1960 – with two species, and *Uralella* Makridin in Licharew, Makridin and Rzhonsnitskaya, 1960); family Loboidothyrididae Makridin, 1964 (genera *Seductorithyris* Sandy, Hryniewicz, Hammer, Nakrem and Little, 2014; *Pinaxiothyris* Dagys, 1968; and *Placothyris* Westphal, 1970); and family Kingenidae Elliott, 1948 (genus *Zittelina* Rollier, 1919) have been recognised. The Spitsbergen seep brachiopods are rich in species but of low abundance, which is in contrast with typical brachiopod seep assemblages. However, none of the genera and species recognised at the Spitsbergen seeps are seep-restricted. Single brachiopods found at Paleogene and Neogene seeps, mostly in Japan, represented both by rhynchonellides and terebratulides (Bitner et al. 2019), are not interpreted as members of seep associations but considered as fortuitous occurrences of background taxa.

8.4 Palaeoecological and Evolutionary Patterns: The Elusive Case of Brachiopod-Dominated Seep Communities

While the fossil record of cold seep ecosystems remains fragmentary, the past decade has seen substantial progress in our understanding of the palaeoecology of pre-Cenozoic chemosynthesis-based communities. In particular, the descriptions of brachiopod-containing, but bivalve-dominated seep assemblages from the Upper Silurian and Middle Devonian of Morocco (Hryniewicz et al. 2017; Jakubowicz et al. 2017, this volume) and the Upper Triassic of Turkey (Kiel et al. 2017; Kiel 2018) altered the long-held perception of Palaeozoic to mid-Cretaceous seeps as being dominated by brachiopods (Campbell and Bottjer 1995a; Campbell 2006; Jenkins et al. 2013). This revised picture has reinvigorated the discussion on the factors responsible for the changing fate of brachiopods and bivalves at seeps (Jakubowicz et al. 2017; Jenkins et al. 2018; Kiel and Peckmann 2019). The causes of, and possible relationship between, the apparent temporal disappearance of 'modern-type' bivalve-dominated seep ecosystems after the Middle Devonian and subsequent 250-M-yr-long brachiopod proliferation at seeps, remain, however, enigmatic. This question is particularly pertinent when the morphological 'inferiority' commonly suggested for brachiopods (James et al. 1992; Sandy 2010) is confronted with the seep-specialised, probably chemosymbiosis-related characters found in mid-Palaeozoic seep bivalves (the modiomorphid genus *Ataviaconcha*; Hryniewicz et al. 2017; Jakubowicz et al. 2017; Jakubowicz et al. this volume).

8.4.1 Ecological Constraints

A key difficulty in studies of the early evolution of the seep shelly faunas is the limited utility of an actualistic approach. None of the lineages of brachiopods (Atrypida, Devonian-Cretaceous Dimerelloidea) and semi-infaunal bivalves (Silurian-Devonian Modiomorphidae, Triassic-Oligocene Kalenteridae) that formed

Fig. 8.5 (continued) The brachiopod superfamily Dimerelloidea is depicted as including the three rhynchonellide families with abundant representatives at ancient seeps: Halorellidae, Peregrinellidae and Dimerellidae (Baliński and Biernat 2003; Kaim et al. 2010; Sandy 2010). The interpretation of terebratulides as specialized or opportunistic seep dwellers remains uncertain (Kaim et al. 2010; Sandy 2010). For the atrypids, their record in chemosynthesis-based communities may be possibly extended to the Lower Devonian (Emsian), if their mass occurrence around a putative low-temperature hydrothermal vent (Halamski and Baliński 2018) is included. (**b**) Supercontinents present during the geological history of cold-seep metazoan communities (see Torsvik et al. (2012) and references therein; palaeogeographic configurations after Torsvik et al. (2012)). (**c**) Selected reconstructions of temporal changes in seawater sulphate concentrations ($[SO_4^{2-}]_{sw}$; Berner 2004; Halevy et al. 2012; Wortmann and Paytan 2012; Algeo et al. 2015; adapted from Algeo et al. 2015). For the curve of Algeo et al. (2015), the ±1σ uncertainty range is indicated. The reconstructions illustrate secular trends and likely do not capture some short-term (<2 M yr) excursions (some possibly including $[SO_4^{2-}]_{sw}$ decreases to even <1 mM; see Stebbins et al. (2019) and references therein)

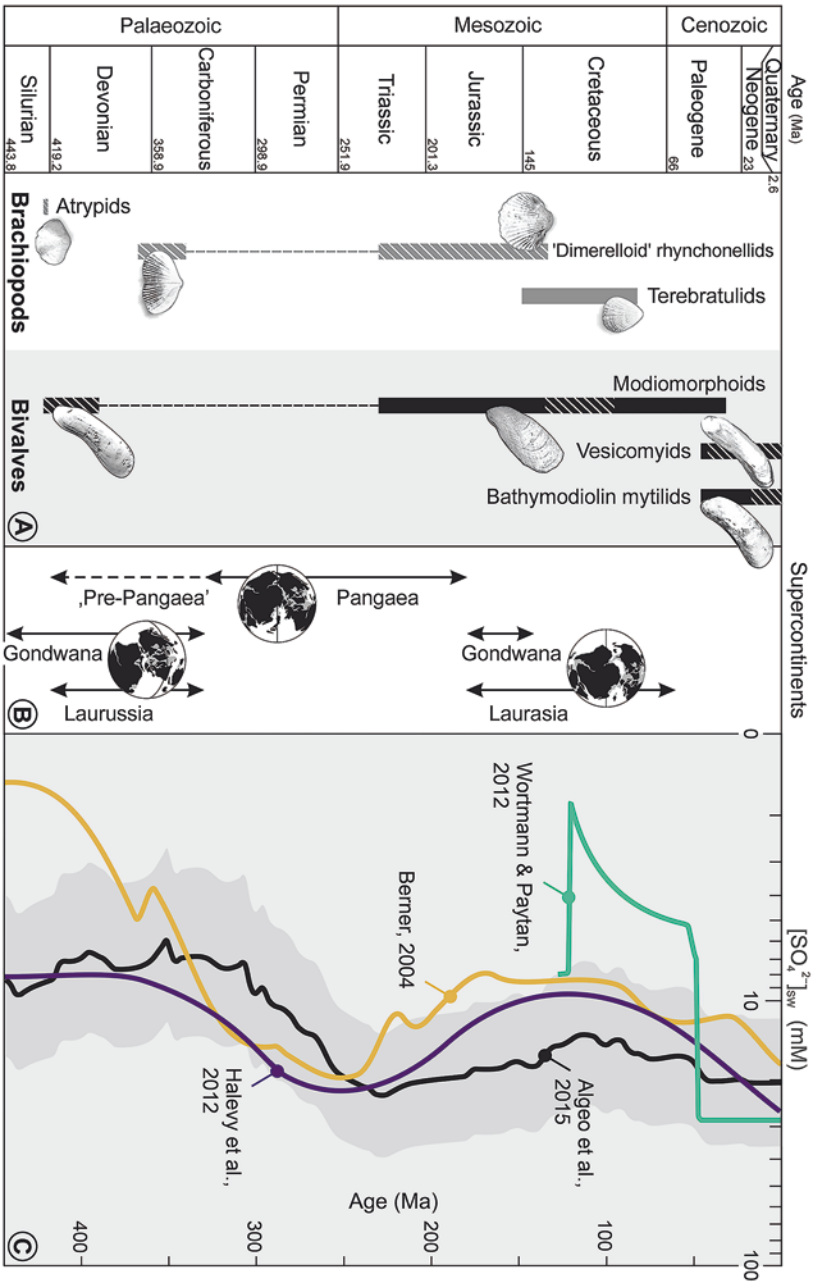

Fig. 8.5 (**a**) The fossil record of articulated brachiopods and epifaunal to semi-infaunal bivalves known from methane seep deposits (modified and updated after Jakubowicz et al. 2017). Intervals for which representatives of different lineages are known to have formed mass accumulations at seeps are cross-hatched. The bivalve clade Modiomorphoida is perceived here as including Palaeozoic Modiomorphidae and Mesozoic to mid-Cenozoic Kalenteridae, detailed taxonomic relationships between which remain unclear (Jenkins et al. 2013, 2018; Hryniewicz et al. 2017; Kiel 2018; Kiel et al. 2020).

mass accumulations at Palaeozoic and Mesozoic seeps survived in these environments until recently (Fig. 8.5). Because most groups of sessile macroinvertebrates forming dense clusters at modern seeps have developed close cooperation with chemosynthetic microbes, the possibility of chemosymbiosis in seep brachiopods has been commonly considered (Campbell and Bottjer 1995b; Sandy 1995, 2010; Kaim et al. 2010). Nevertheless, the general morphology and metabolic characteristics of brachiopods have also been invoked to question their potential to develop close chemosymbioses (Hryniewicz et al. 2017; Kiel and Peckmann 2019). For the Silurian atrypid *Septatrypa lantenoisi*, its relatively small, smooth, uniplicate shell represents a common adaptation to a deep-water habitat (Fürsich and Hurst 1974) and does not provide any indication of an unusual life strategy. For the dimerelloideans, unequivocal morphological traits attributable to seep-related habitats also appear lacking, although many taxa were typified by a notably large size (Baliński and Biernat 2003; Sandy 2010; Kiel et al. 2014). The significance of this feature in the context of possible chemosymbiosis remains dubious. In contrast to bivalves, brachiopods are typified by low tissue density, the lack of gills and a cardiovascular system and limited ability to increase metabolic rates (James et al. 1992; Ballanti et al. 2012), which may be unfavourable for the development of advanced (especially endo-) chemosymbioses (Hryniewicz et al. 2017; Kiel and Peckmann 2019; but see Angiolini et al. 2019). Given the variety of seep- and vent-related animals that developed less specialised ectosymbioses, some type of brachiopod cooperation with chemosymbionts cannot, however, be excluded. Interestingly, no modern chemosymbiotic brachiopods are known, even though many species inhabit oxygen-depleted and sulphide-enriched habitats (Tunnicliffe and Wilson 1988; James et al. 1992), in which chemosymbioses might be advantageous. Furthermore, unlike many epifaunal to semi-infaunal bivalves, which are relatively motile (Thayer 1985; Luff et al. 2004; Duperron 2010), brachiopods are essentially immobile and only capable of some shell reorientation (Thayer 1985), which limits their ability to adjust to temporal variations in fluid flow and migration pathways. In general terms, brachiopods do not seem, therefore, well suited to compete with strongly specialised molluscs at seeps.

Recently, Kiel and Peckmann (2019) provided a reappraisal of previous studies on the palaeoecology of seep dimerelloideans, putting forward a concept of different feeding strategies employed by pre-Cenozoic seep brachiopods and bivalves. This recent contribution reflects a growing consensus that the seep brachiopods were most likely non-endosymbiotic, and, in some cases, perhaps opportunistic, suspension feeders taking advantage of increased water column nutrient availability associated with fluid seepage (cf., Campbell and Bottjer 1995a; Sandy 2010; Kiel et al. 2014; Hryniewicz et al. 2017; Jakubowicz et al. 2017), rather than directly competing with bivalves for reduced chemical compounds. The most important source of the brachiopod nutrition comes from the finest fraction of suspended organic matter, including bacterioplankton (Rhodes and Thompson 1993). Notably, the low metabolic rates and oxygen requirements of brachiopods, with their ability to sustain periods of sulphide exposure by switching to anaerobic metabolism and to feed on irregularly available food resources, make them successful ecological

generalists able to thrive in a variety of marginal habitats (Tunnicliffe and Wilson 1988; James et al. 1992; Rhodes and Thompson 1993; Boyer and Droser 2007; Peck 2008; Ballanti et al. 2012). In addition, both rhynchonellides and atrypides, the two brachiopod orders forming mass concentrations at seeps possessed advanced, spirolophous lophophores considered particularly effective in utilising limited oxygen content (Rhodes and Thompson 1993; Boyer and Droser 2007; Manceñido and Gourvennec 2008).

The generalist strategy seems also in line with the perception of several episodes of seep colonisation by different dimerelloidean taxa recruited from background deep-water faunas (Kaim et al. 2010; Sandy 2010; Peckmann et al. 2011). While a considerable degree of specialisation to seeps was proposed for large-sized, Jurassic *Anarhynchia* (Pálfy et al. 2017) and Cretaceous *Peregrinella* (Campbell and Bottjer 1995b; Kiel et al. 2014), latest Devonian *Dzieduszyckia* occurred in both seep-related and non-seep, deep-water habitats (Baliński and Biernat 2003; Peckmann et al. 2007; Nie et al. 2016). The same applies probably to some seep-associated terebratulides (Kaim et al. 2010; Sandy 2010) and different species of *Septatrypa*, known also from non-seep, both deep- and shallow-water settings (Copper 2004; Baliński 2012; Racki et al. 2012; Halamski and Baliński 2018). For other dimerelloideans known from seeps, evidence appears, in turn, more equivocal. Although some genera are known only from seeps (Carboniferous *Ibergirhynchia*, Jurassic *Cooperrhynchia*), they otherwise lack morphological features that could be defined as clearly distinctive from those of other deep-water rhynchonellides (cf., Gischler et al. 2003; Sandy 2010). In addition, no evidence of methane seepage has been found for *Halorella* and *Sulcirostra* occurrences associated with Upper Triassic and Jurassic neptunian dykes (Lazăr et al. 2020; Kiel et al. 2021), although such a setting may also have sustained other types of fluid expulsion (e.g., low-temperature hydrothermal vents; cf., Lazăr et al. 2017; Matyszkiewicz et al. 2016). The 'non-seep' accumulations of Jurassic *Sulcirostra* and *Carapezzia* documented from Switzerland are, in turn, allochthonous, and thus their original habitat is uncertain (Sulser and Furrer 2008).

Finally, multiple lines of palaeoecological, sedimentological and geochemical evidence point to the brachiopods preferentially colonizing seeps with relatively low flow rates, and thus lower concentrations of metabolic toxins, most importantly hydrogen sulphide (Peckmann et al. 2009, 2011; Kiel et al. 2014; Jakubowicz et al. 2017; Kiel and Peckmann 2019). Notably, where both brachiopods and bivalves are found within the same seep deposits, brachiopods are most typical of micritic, moderately ^{13}C-depleted carbonates indicative of diffuse seepage. The sparry cement-dominated facies implying advective flow are, in turn, more commonly host to large, presumably chemosymbiotic bivalves (Jakubowicz et al. 2017; Lower Cretaceous of California: M. Jakubowicz, *pers. obs.*). To date, detailed comparative studies of habitats of brachiopods and bivalves occurring at the same seeps have, however, been rare and represent an important future research direction. For further discussion of advective vs. diffusive flow at seeps, see Cochran et al. this volume).

8.4.2 *Possible Controls on the Brachiopod Versus Bivalve Dominance at Seeps Over Time*

The realization that assemblages of large, seep-specialised bivalves not only coexisted with brachiopods at Mesozoic seeps but were already present during the mid-Palaeozoic underscores the need to understand factors responsible for, first, the remarkable success and, second, the demise of the brachiopod-dominated seep ecosystems. Two general explanations, referred here to as the 'palaeogeographic' (Jakubowicz et al. 2017) and 'feeding strategy' (Kiel and Peckmann 2019) hypotheses, have been considered to date in this context. Both ideas have, however, been presented as crude outlines only, and more detailed models are yet to be proposed and tested.

8.4.2.1 Palaeogeographic Hypothesis and the Role of the Frasnian-Famennian Crisis

Jakubowicz et al. (2017) invoked a possible role of the special global tectonic configuration present between the late Palaeozoic and mid-Mesozoic due to the formation of Pangaea. This palaeogeography, associated with a restricted area of continental margins and low level of tectonic activity, has previously been suggested to account for the general scarcity of late Palaeozoic to early Mesozoic seeps (Campbell and Bottjer 1995a; Peckmann and Goedert 2005; Peckmann et al. 2011). Indeed, there seems to be a crude coincidence between the supercontinent amalgamation and the proliferation of the Dimerelloidea, whereas the gradual decrease in their role corresponds approximately to the progressive Pangaea disintegration (Fig. 8.5). By the time of its final, Early Cretaceous breakup, only species of a single dimerelloidean genus, the large, widely-distributed *Peregrinella*, remained present at seeps (Campbell and Bottjer 1995a, b; Kiel and Peckmann 2008; Sandy 2010; Kiel et al. 2014). This was accompanied by the gradual restoration of bivalve-dominated seep ecosystems (Kaim et al. 2010; Jenkins et al. 2013, 2018). Distribution and spacing of seep sites is an important control on the success of seep-specialised biota, because a key challenge in adapting to these habitats is the necessity of dispersal between remote seeps (Van Dover et al. 2002; Arellano et al. 2014). While many modern seep mussels display remarkably broad geographical distribution, an important factor in their long-distance dispersal is their ability to feed at a larval stage (i.e., planktotrophy; Arellano et al. 2014). As implied by their larval development patterns, most Palaeozoic bivalves, among them the Anomalodesmata (Valentine and Jablonski 2010; including the modiomorphids), as well as the Mesozoic Kalenteridae (Kaim and Schneider 2012), were probably non-planktotrophic, in which case they had no advantage over most brachiopods (Freeman and Lundelius 2005). In terms of their dispersal strategy, the modiomorphoids may have, therefore, resembled the extant seep-dwelling vesicomyids, largely dependent in their dispersal on a high number of geographically close seeps

(Olu et al. 2010; Krylova and Sahling 2011). In an ocean with rare, geographically distant seeps, a net result of this might have been the limited advantage of advanced specialisation to seep-related habitats, creating favourable conditions for taxa applying more opportunistic strategies, such as brachiopods.

The crucial question in the 'palaeogeographic' scenario is whether in any geotectonic configuration, the seeps could have been so sparse that the dispersal difficulties significantly limited the value of strong specialisation. At present, this question remains unanswered. Although active plate margins apparently host the majority of modern seeps (Suess 2014), a substantial proportion of extant seeps occur at passive margins. Seeps at the latter setting can be expected to be less sensitive to changes in palaeoceanographic configuration. This question is also key to the model suggesting that the sparse fossil record of the late Carboniferous to Jurassic seep deposits reflects an actual scarcity of seeps during this time (cf., Campbell and Bottjer 1995a; Peckmann and Goedert 2005; Peckmann et al. 2011). The documented fossil record of pre-Jurassic seeps is indeed very fragmentary, with only six localities known from the 170-M-yr-long interval ranging from the Late Devonian to the Late Triassic (two of which host no brachiopods; Buggisch and Krumm 2005; Himmler et al. 2008).

Pertinent to any model exploring Phanerozoic trends in the composition of seep ecosystems is the possible involvement of the Late Devonian (Frasnian-Famennian: F-F) mass extinction. This crisis, involving major dysoxic ('Kellwasser') events (e.g., Wendt and Belka 1991; Bond et al. 2004), took place between the development of the younger of the mid-Palaeozoic modiomorphid-dominated seeps (Eifelian Hollard Mound; Hryniewicz et al. 2017) and the oldest dimerelloidean-dominated seep (upper Famennian Khenifra deposits; Peckmann et al. 2007). Indeed, if we accept the sedimentological evidence that the Palaeozoic seep-obligate communities were limited to relatively deep-water environments, as are their modern counterparts, they could have been vulnerable to such oxygenation perturbations. However, the potential of anoxic events to globally reset seep ecosystems has repeatedly been questioned. There seems to be no close correspondence between such events and major shifts in the evolution of seep ecosystems (Jacobs and Lindberg 1998; Kiel and Little 2006; Vrijenhoek 2013; Hryniewicz et al. 2019; but see Roterman et al. 2018). One explanation for this apparently limited effect is that many anoxic episodes were not strictly synchronous on a global scale. Most importantly, this has specifically been documented for the F-F events, which show some diachronism and were not universally recorded in different areas (e.g., Wendt and Belka 1991; Bond et al. 2004). The potential of the F–F turnover to erase the bivalve-dominated seep communities depends, therefore, on their distribution; it could have been more significant if they were indeed limited to the south-eastern Rheic Ocean, as their presently known fossil record might suggest. Even the original distance between the Anti-Atlas and Meseta segments of the north-western Gondwana margin, host to the Hollard Mound and El Borj-Meseta deposits, respectively, remains, however, a matter of contention (*see* Jakubowicz et al. this volume).

While the atrypide brachiopods, common at Silurian seeps, became extinct during the F-F crisis, the fossil record of the seep-related modiomorphids is more

difficult to interpret in this context. The fossil record of modiomorphid-like bivalves, including both seep-related and non-seep taxa, extends through the Mesozoic, until the Paleogene (Damborenea 2004; Griffin and Pastorino 2006; Kiel et al. 2020). Following the F-F crisis, clusters of unidentified large bivalves were also present at a mid-Carboniferous seep in France (Tantes Mound, S. Kiel, *pers. comm.*; M. Jakubowicz, *pers. obs.*). Subsequently, an important component of many Mesozoic seep ecosystems were kalenterid bivalves, whose affinity to, and possibly direct descent from, Palaeozoic seep modiomorphids has been proposed (Fig. 8.5) (Modiomorphidae and Kalenteridae are currently placed together within the clade Modiomorphoida; Jenkins et al. 2013, 2018; Hryniewicz et al. 2017; Kiel 2018). At present, a possible role of the F-F extinction in facilitating seep colonisation by dimerelloideans remains, therefore, insufficiently understood. Given the apparently broad ecological range of *Dzieduszyckia* and its association with non-seep, pelagic environments (Peckmann et al. 2007; Nie et al. 2016), it remains possible that its appearance after the F-F dysoxic events reflects its recruitment from a background fauna adapted to oxygen-deficient habitats. The Devonian was generally a time of elevated diversity of brachiopods typical of low-oxygen environments (Boyer and Droser 2007).

8.4.2.2 Feeding Strategy Hypothesis, with Constraints from Habitat Preferences and Background Seawater Sulphate Chemistry

Kiel and Peckmann (2019) recently hypothesised that the resource partitioning between the seep brachiopods and bivalves may provide an explanation for the Phanerozoic patterns in dominance between these two groups of seep benthos. This view stems from a critical review of the fossil record of the seep shelly assemblages, based on which Kiel and Peckmann (2019) suggested generally that the 'presence, absence, or relative abundance of each clade at a given site was largely controlled by the chemical composition of the seep fluids (the proportions of sulfide, methane, and/or oil)'. Nevertheless, palaeoenvironmental interpretation of given ancient seeps in terms of fluid composition and flow regimes remains a major challenge (see below). Furthermore, Kiel and Peckmann (2019) did not propose a specific mechanism by which the suggested habitat and feeding behaviour differences would translate into the temporal shifts in bivalve vs. brachiopod dominance. Thus, the 'palaeogeographic' and 'feeding strategy' explanations cannot be, at the moment, regarded as mutually exclusive. The different types of specialisation to seep habitats may, in fact, provide a mechanism by which the changes in the global paleogeography would translate into the composition of the seep assemblages (Jakubowicz et al. 2017).

Among factors other than the geotectonic context, Kiel and Peckmann (2019) considered a possible role of changing fluid flow rates, although the mechanism by which the proportion of diffuse and advective seeps would have shown secular changes in time was not explored. Additionally, Kiel and Peckmann (2019) invoked a possible role of temporal changes in background seawater sulphate concentrations

($[SO_4^{2-}]_{SW}$; cf., Bristow and Grotzinger 2013; Kiel 2015). In such a model, brachiopod success would be favoured during times of low $[SO_4^{2-}]_{SW}$ and associated, limited amounts of toxic sulphide produced during the sulphate-limited anaerobic oxidation of methane (AOM). Periods of bivalve dominance would, in turn, correspond to intervals of high $[SO_4^{2-}]_{SW}$. The potential of seawater sulphate content to control major palaeoecological changes in seep communities remains, however, unclear. There are significant discrepancies among the various proposed Phanerozoic $[SO_4^{2-}]_{SW}$ curves (Fig. 8.5). For example, the Early Jurassic, specifically invoked by Kiel and Peckmann (2019) as an interval of 'particularly low seawater sulphate concentration' (shifted to 1–5 mM during the Toarcian, according to Newton et al. (2011)) to explain the proliferation of the dimerelloidean *Anarhynchia smithi* at an apparently advective seep (Pálfy et al. 2017), in the new reconstruction of Algeo et al. (2015), is shown as a time of high, essentially modern-level $[SO_4^{2-}]_{SW}$ (Fig. 8.5). The relevant, lower Pliensbachian occurrence of *A. smithi* predates, in fact, the Toarcian $[SO_4^{2-}]_{SW}$ excursion (Newton et al. 2011). Similarly, the Early Cretaceous disappearance of seep dimerelloideans falls within a time of low $[SO_4^{2-}]_{SW}$. Conversely, the reconstruction of Algeo et al. (2015) places the acme of the seep-specialised modiomorphoid bivalves (Early Cretaceous, middle Palaeozoic; Jenkins et al. 2013; Jakubowicz et al. 2017) within intervals of decreased, rather than increased $[SO_4^{2-}]_{SW}$. Furthermore, the presence of seep carbonate bodies embedding all mass occurrences of seep dimerelloideans provides evidence for relatively intense sulphate-driven AOM (cf., Luff et al. 2004; Karaca et al. 2010). It remains to be verified whether the lowest feasible Phanerozoic $[SO_4^{2-}]_{SW}$ levels (~2–5 mM, perhaps with short-term <1 mM excursions; Newton et al. 2011; Wortmann and Paytan 2012; Witts et al. 2018; Stebbins et al. 2019) can be an effective AOM-limiting factor (for discussions see Wegener and Boetius 2009; Beal et al. 2011; Bristow and Grotzinger 2013; Timmers et al. 2015). Based on experimental evidence, it has been postulated that the rate of AOM does not substantially decrease until $[SO_4^{2-}]_{SW}$ are below 2 mM (Meulepas et al. 2009; Beal et al. 2011; Timmers et al. 2015). A crucial constraint is likely the efficiency of seawater recharge. At present-day $[SO_4^{2-}]_{SW}$, sulphate-limited AOM is most characteristic of advective seeps, whereas diffuse seeps, a habitat proposed for dimerelloideans, are typically methane-limited (Luff and Wallmann 2003; Wegener and Boetius 2009).

Kiel and Peckmann (2019) suggested that the seep dimerelloideans relied specifically on bacterioplankton performing aerobic oxidation of methane and/or higher hydrocarbons. Accordingly, they interpreted the affinity of the dimerelloideans to diffuse seeps as the result of more methane that would pass the sediment-water interface in places of low seepage rates. Increased concentrations of bottom-water methane are, however, typically associated with sites of vigorous fluid seepage, at which methane supply exceeds the metabolic capacity of anaerobic microbes, resulting in sulphate-limited AOM (cf., Luff et al. 2004; Wegener and Boetius 2009; Karaca et al. 2010). Diffuse seeps are, in turn, typically associated with a deep sulphate-methane transition zone and near-entire anaerobic methane consumption (Luff and Wallmann 2003; Wegener and Boetius 2009; Steeb et al. 2015). If, on the other hand, diffuse methane seepage reaches the bottom seawater because methane concentrations are very low, and thus AOM is very limited (as

typical of background sediments, rather than active seeps; references in Kiel and Peckmann 2019), then this could not explain the precipitation of the extensive, dimerelloidean-hosting seep-carbonate bodies. The alkalinity buildup necessary for precipitation of seep carbonates requires relatively intense AOM, sustained by moderately high flow rates (Luff et al. 2004; Karaca et al. 2010; Bristow and Grotzinger 2013). Consequently, the suggested link between the diffuse seepage and higher bottom-water methane concentrations may introduce an unnecessary complication to the model of brachiopods as non-endosymbiotic suspension feeders inhabiting places of low-intensity fluid flow.

At the moment, a contentious issue is also the suggested relationship between some dimerelloidean occurrences and seepage of non-methane, heavy hydrocarbons ('oil seeps'; Kiel and Peckmann 2019). Despite much recent effort to establish criteria for identification of ancient oil seeps, none of the proposed petrological and geochemical methods provides unequivocal evidence in this context (cf., Peckmann et al. 2007; Smrzka et al. 2016, 2019; Sun et al. 2020). A further complication is that longer-chain hydrocarbons typically accompany thermogenic methane (e.g., Simoneit et al. 1988; Sturz et al. 1996; Whiticar 1999), and even at classical 'oil seeps', methane may be volumetrically dominant (e.g., MacDonald et al. 2004). Among non-methane hydrocarbons, best-documented electron donors for chemosynthetic microbes, including chemosymbionts of macroinvertebrates (Rubin-Blum et al. 2017), are, in turn, other gaseous alkanes (ethane-butane), rather than oil (Kniemeyer et al. 2007; Singh et al. 2017; Chen et al. 2019). For these reasons, it may not be practical to distinguish between 'methane' and 'oil' seeps in palaeoecological studies. The metabolic toxicity of liquid hydrocarbons is substantially higher than that of methane, especially for metazoan life (Smith et al. 2000; Sassen et al. 2004; Bergquist et al. 2004; Orcutt et al. 2010; Joye 2020). Hence, any hypothesis suggesting an association between brachiopods and oil seepage requires particularly firm support, especially for earliest seep-dwelling dimerelloideans (*Dzieduszyckia*, *Ibergirhynchia*; cf., Peckmann et al. 2001, 2007). Rather than being attracted to diffuse seeps by particularly high bottom-water hydrocarbon concentrations, it appears reasonable that the brachiopods were excluded from the vigorous, high-toxicity seeps by their lack of advanced specialisation to such habitats. In general, while brachiopods could have plausibly fed on hydrocarbon-oxidizing bacterioplankton, their nutrition could have also included other planktic microorganisms, zooplankton and particulate organic matter, increased concentrations of which are all common above seeps (Levin et al. 2016).

8.5 Conclusions

Palaeozoic brachiopods associated with ancient seep settings are represented by members of three orders: Lingulida, Rhynchonellida and Atrypida. The oldest known hydrothermal vent community, dated as Upper Silurian, includes lingulide *Pyrodiscus* distinguished by a very large shell. Palaeozoic representatives of the two

other brachiopod orders have to date been documented at ancient seeps from the Silurian to the Carboniferous. For the Atrypida, the species *Septatrypa lantenoisi* is known from a single, Upper Silurian seep locality, where it forms dense clusters co-occurring with dense assemblages of large, seep-specialised bivalves. In addition, another species of the genus, *S. tumulorum*, has been reported from putative low-temperature hydrothermal vent communities of Lower Devonian mud mounds. *Septatrypa* lacks, however, clear morphological traits that would suggest its advanced adaptation to seep- or vent-related habitats, including a symbiosis with chemosynthetic microbes. The same applies to members of the rhynchonellide superfamily Dimerelloidea, known from dense, monospecific clusters in Upper Devonian to Lower Cretaceous seep deposits. One member of this group, Famennian *Dzieduszyckia*, which was described from Laurussia, Kazakhstania, northern Gondwana and South China, is one of the largest Palaeozoic rhynchonellides. This genus, together with other lower Carboniferous (*Ibergirhynchia*) and Mesozoic dimerelloideans, represents a long lineage of seep-dwelling genera ranging from the Devonian to the Lower Cretaceous. In the Mesozoic, mass occurrences of seep-dwelling dimerelloideans are known from the Upper Triassic (*Halorella*), Jurassic (*Sulcirostra*, *Cooperrhynchia*, *Anarhynchia*) and, in particular, Lower Cretaceous (large, globally distributed *Peregrinella*).

The extent of adaptation of the Dimerelloidea to seep habitats remains disputable. Some genera are known also from non-seep settings; for some dimerelloidean taxa, a degree of specialization to seeps seems, nevertheless, suggested by their exceptionally large size (up to 100 mm), strongly costate ornament and an apparent limitation to seep-related palaeoenvironments. Petrological and geochemical characteristics of their host seep carbonates imply that the brachiopod clusters were most typical of areas of diffuse fluid flow, and thus relatively low concentrations of toxic chemical compounds. Where dimerelloideans are found together with semi-infaunal, seep-obligate bivalves, the bivalves apparently occupied, in turn, areas of increased flow rates.

In comparison with Mesozoic rhynchonellides, terebratulide brachiopods are much less common in seep deposits. So far the best-known association is that reported from the Upper Cretaceous Omagari site in Japan with terebratulide *Eucalathis* occurring in significant quantities. No extant brachiopods are known to be associated with vent/seep environments. Although some species are found in the vicinity of hydrothermal vents, associated with mid-ocean spreading ridges, there is no evidence that they are members of chemosynthesis-based communities.

The controls on the relative success of seep-dwelling brachiopods and bivalves remain arguably the most enigmatic aspect of the pre-Cenozoic record of chemosynthesis-based ecosystems. The Late Devonian appearance of the dimerelloidean-dominated seep faunas appears particularly intriguing given that, in contrast to the brachiopods, the mid-Palaeozoic seep bivalves apparently showed advanced adaptations to seepage-affected habitats, most likely including chemosymbiosis. An involvement of the Late Devonian mass extinction is a possibility; however, its verification may require better resolution of the fossil record, including taxonomic recognition of putative Carboniferous seep-inhabiting modiomorphids. Equally

unclear are constraints on the Early Cretaceous disappearance of the brachiopod-rich seep communities. Preliminary ideas for the origin of the temporal patterns in the brachiopod vs. bivalve dominance at seeps consider a role of palaeogeographic factors or distinct feeding strategies, but comprehensive models remain lacking.

Acknowledgments Special thanks are due to Andrzej Kaim (Institute of Paleobiology), for his encouragement and support during the project and the opportunity to use the photograph of the mass accumulation of *Anarhynchia gabbi*. We are deeply indebted to the referees, Elisabeth M. Harper (University of Cambridge) and Miguel Manceñido (Universidad Nacional de La Plata), for critical and valuable comments. Sincere thanks are expressed to Krzysztof Hryniewicz and Andrzej Kaim (Institute of Paleobiology), Russell Shapiro (California State University in Chico) and Steffen Kiel (Swedish Museum of Natural History) for discussions on various aspects of the palaeoecology of fossil seep-related brachiopods and bivalves.

References

Ager DV (1968) The supposedly ubiquitous Tethyan brachiopod *Halorella* and its relations. J Palaeontol Soc India 5–9:54–70

Ager DV, Cossey SPJ, Mullin PR et al (1976) Brachiopod ecology in mid-Palaeozoic sediments near Khenifra, Morocco. Palaeogeog Palaeoclimat Palaeoecol 20:171–185

Algeo TJ, Luo GM, Song HY et al (2015) Reconstruction of secular variation in seawater sulfate concentrations. Biogeosciences 12:2131–2151

Angiolini L, Crippa G, Azmy K et al (2019) The giants of the phylum Brachiopoda: a matter of diet? Palaeontology 62(6):889–917

Arellano SM, Van Gaest AL, Johnson SB et al (2014) Larvae from deep-sea methane seeps disperse in surface waters. Proc Biol Sci 281(1786):20133276

Baliński A (2012) The brachiopod succession through the Silurian-Devonian boundary beds at Dnistrove, Podolia, Ukraine. Acta Palaeontol Pol 57(4):897–924

Baliński A, Biernat G (2003) New observations on rhynchonelloid brachiopod *Dzieduszyckia* from the Famennian of Morocco. Acta Palaeontol Pol 48(3):463–474

Baliński A, Sun Y (2013) Preservation of soft tissues in an Ordovician linguloid brachiopod from China. Acta Palaeontol Pol 58:115–120

Ballanti LA, Tullis A, Ward PD (2012) Comparison of oxygen consumption by *Terebratalia transversa* (Brachiopoda) and two species of pteriomorph bivalve molluscs: implications for surviving mass extinctions. Paleobiology 38(4):525–537

Barbieri R, Ori GG, Cavalazzi B (2004) A Silurian cold-seep ecosystem from the Middle Atlas, Morocco. Palaios 19:527–542

Beal EJ, Claire MW, House CH (2011) High rates of anaerobic methanotrophy at low sulfate concentrations with implications for past and present methane levels. Geobiology 9(2):131–139

Beauchamp B, Savard M (1992) Cretaceous chemosynthetic carbonate mounds in the Canadian Arctic. Palaios 7:434–450

Belka Z (1998) Early Devonian Kess-Kess carbonate mud mounds of the eastern Anti-Atlas (Morocco), and their relation to submarine hydrothermal venting. J Sediment Res 68:368–377

Bergquist DC, Fleckenstein C, Szalai EB et al (2004) Environment drives physiological variability in the cold seep mussel *Bathymodiolus childressi*. Limnol Oceanogr 49(3):706–715

Berner RA (2004) A model for calcium, magnesium and sulfate in seawater over Phanerozoic time. Am J Sci 304:438–453

Biernat G (1957) On *Peregrinella multicarinata* (Lamarck) (Brachiopoda). Acta Palaeontol Pol 2:19–50

Biernat G (1967) New data on the genus *Dzieduszyckia* Siemiradzki, 1909 (Brachiopoda). Acta Palaeontol Pol 12:133–155
Bitner MA, Hryniewicz K, Amano K et al (2019) New data on non-dimerelloid brachiopods from chemosynthesis-based communities. In: Abstract volume, 2nd international workshop on ancient hydrocarbon seep and cognate communities, 13–15 June 2019, Sapporo, Japan, p 24
Bond D, Wignall PB, Racki G (2004) Extent and duration of marine anoxia during the Frasnian–Famennian (Late Devonian) mass extinction in Poland, Germany, Austria and France. Geol Mag 141:173–193
Boyer DL, Droser ML (2007) Devonian monospecific assemblages: new insights into the ecology of reduced-oxygen depositional settings. Lethaia 40(4):321–333
Brand U (1989) Biogeochemistry of late Paleozoic North American brachiopods and secular variation of seawater composition. Biogeochemistry 7:159–193
Brand U, Logan A, Hiller N et al (2003) Geochemistry of modern brachiopods: applications and implications for oceanography and paleoceanography. Chem Geol 198:305–334
Brand U, Azmy K, Griesshaber E et al (2015) Carbon isotope composition in modern brachiopod calcite: a case of equilibrium with seawater? Chem Geol 411:81–96
Bristow TF, Grotzinger JP (2013) Sulfate availability and the geological record of cold-seep deposits. Geology 41(7):811–814
Buggisch W, Krumm S (2005) Palaeozoic cold seep carbonates from Europe and North Africa—an integrated isotopic and geochemical approach. Facies 51(1–4):566–583
Campbell KA (2006) Hydrocarbon seep and hydrothermal vent paleoenvironments and paleontology: past developments and future research directions. Palaeogeog Palaeoclimat Palaeoecol 232:362–407
Campbell KA, Bottjer DJ (1995a) Brachiopods and chemosymbiotic bivalves in Phanerozoic hydrothermal vent and cold seep environments. Geology 23(4):321–324
Campbell KA, Bottjer DJ (1995b) *Peregrinella*: an early Cretaceous cold-seep-restricted brachiopod. Paleobiology 21(4):461–478
Campbell KA, Carlson C, Bottjer DJ (1993) Fossil cold seep limestones and associated chemosymbiotic macroinvertebrate faunas, Jurassic–Cretaceous Great Valley Group, California. In: Graham S, Lowe D (eds) Advances in the sedimentary geology of the Great Valley Group, Pacific section, vol 73. Society of Economic Paleontologists and Mineralogists, Los Angeles, pp 37–50
Canet C, Anadón P, González-Partida E et al (2014) Paleozoic bedded barite deposits from Sonora (NW Mexico): evidence for a hydrocarbon seep environment of formation. Ore Geol Rev 56:292–300
Chen SC, Musat N, Lechtenfeld OJ et al (2019) Anaerobic oxidation of ethane by Archaea from a marine hydrocarbon seep. Nature 568(7750):108–111
Cloud PE Jr, Boucot AJ (1971) *Dzieduszyckia* in Nevada. Smithson Contrib Paleobiol 3:175–180
Cooper GA (1983) The Terebratulacea (Brachiopoda) Triassic to recent: a study of the brachidia (loops). Smithson Contrib Paleobiol 50:1–290
Copper P (2002) Atrypida. In: Kaesler RL (ed) Brachiopoda 4 (rev), Rhynchonelliformea. Treatise on invertebrate paleontology, part H. Geological Society of America and University of Kansas, Boulder, pp H1377–H1474
Copper P (2004) Silurian (late Llandovery–Ludlow) atrypid brachiopods from Gotland, Sweden, and the Welsh Borderlands, Great Britain. NRC Research Press, Ottawa
Cochran JK, Landman NH, Jakubowicz M et al (this volume) Geochemistry of cold hydrocarbon seeps: an overview. In: Kaim A, Cochran JK, Landman NH (eds) Ancient hydrocarbon seeps, Topics in Geobiology, vol. 50. Springer, Cham
Curry GB, Brunton CHC (2007) Stratigraphic distribution of brachiopods. In: Selden PA (ed) Brachiopoda 6 (rev), supplement. Treatise on invertebrate paleontology, part H. Geological Society of America and University of Kansas, Boulder, pp 2901–2965
Damborenea SE (2004) Early Jurassic *Kalentera* (Bivalvia) from Argentina and its palaeobiogeographical significance. Ameghiniana 41(2):145–198

Duperron S (2010) The diversity of deep-sea mussels and their bacterial symbioses. In: Kiel S (ed) The vent and seep biota: aspects from microbes to ecosystems, Topics in geobiology, vol 33. Springer, Dordrecht, pp 137–167

Emig CC (1997) Ecology of inarticulated brachiopods. In: Kaesler RL (ed) Brachiopoda 1 (rev). Treatise on invertebrate paleontology, part H. Geological Society of America and University of Kansas, Boulder, pp 473–495

Emig CC, Bitner MA, Álvarez F (2013) Phylum Brachiopoda. In: Zhang Z-Q (ed) Animal biodiversity: an outline of higher-level classification and survey of taxonomic richness (addenda 2013), Zootaxa, vol 3703, pp 75–78

Freeman G, Lundelius J (2005) The transition from planktotrophy to lecithotrophy in larvae of lower Palaeozoic rhynchonelliform brachiopods. Lethaia 38(3):219–254

Fürsich FT, Hurst JM (1974) Environmental factors determining the distributions of brachiopods. Palaeontology 17:879–900

Gischler E, Sandy MR, Peckmann J (2003) *Ibergirhynchia contraria* (F.A. Roemer, 1850) an early Carboniferous seep-related rhynchonellide brachiopod from the Harz Mountains, Germany—a possible successor to *Dzieduszyckia*? J Paleontol 77:293–303

Goedert JL, Sandy MR, Peckmann J (2021) First report of the megathyridid (Terebratullidina) brachiopod *Argyrotheca* from a hydrocarbon seep deposit, middle Eocene Humptulips Formation, Washington State, USA. PalZ 95(1):97–103

Griffin M, Pastorino G (2006) *Madrynomya bruneti* n. gen. and sp. (Bivalvia: ?Modiomorphidae): a Mesozoic survivor in the Tertiary of Patagonia? J Paleontol 80:272–282

Halamski AT, Baliński A (2018) Early Dalejan (Emsian) brachiopods from Hamar Laghdad (eastern Anti-Atlas, Morocco). Neues Jahrb Geol Palaontol Abh 290:127–152

Halevy I, Peters SE, Fischer WW (2012) Sulfate burial constraints on the Phanerozoic sulfur cycle. Science 337:331–334

Himmler T, Freiwald A, Stollhofen H et al (2008) Late Carboniferous hydrocarbon-seep carbonates from the glaciomarine Dwyka Group, southern Namibia. Palaeogeog Palaeoclimat Palaeoecol 257(1/2):185–197

Hollard H, Morin P (1973) Les gisements de *Dzieduszyckia* (Rhynchonellida) du Famennien inférieur du massif Hercynien central du Maroc. Serv Géol Maroc Notes Mém 249:7–14

Holmer LE, Nakrem HA (2012) The lingulid brachiopod *Lingularia* from lowermost Cretaceous hydrocarbon seep bodies, Sassenfjorden area, central Spitsbergen, Svalbard. Norw J Geol 92:167–174

Holmer L, Popov LE (2007) Linguliformea. In: Selden PA (ed) Brachiopoda 6 (rev), supplement. Treatise on invertebrate paleontology, part H. Geological Society of America and University of Kansas, Boulder, pp 2532–2574

Hou H, Wang J (1984) The discovery of Early Cretaceous *Peregrinella* (Brachiopoda) in Xizang (Tibet). Bull Chin Acad Geol Sci 10:207–217

Hryniewicz K, Jakubowicz M, Belka Z et al (2017) New bivalves from a Middle Devonian methane seep in Morocco: the oldest record of repetitive shell morphologies among some seep bivalve molluscs. J Syst Palaeontol 15(1):19–41

Hryniewicz K, Amano A, Bitner MA et al (2019) A late Paleocene fauna from shallow-water chemosynthesis-based ecosystems, Spitsbergen, Svalbard. Acta Palaeontol Pol 64(1):101–141

Imlay RW (1980) Jurassic paleobiogeography of the conterminous United States in its continental setting. Geol Surv Prof Pap 1062:1–134

Jacobs DK, Lindberg DR (1998) Oxygen and evolutionary patterns in the sea: onshore/offshore trends and recent recruitment of deep-sea faunas. PNAS 95:9396–9401

Jakubowicz M, Hryniewicz K, Belka Z (2017) Mass occurrence of seep-specific bivalves in the oldest-known cold seep metazoan community. Sci Rep 7:14292

Jakubowicz M, Berkowski B, Hryniewicz K et al (this volume) Middle Palaeozoic of Morocco: the earliest-known methane seep metazoan ecosystems. In: Kaim A, Cochran JK, Landman NH (eds) Ancient hydrocarbon seeps, Topics in geobiology, vol 50. Springer, Cham

James MA, Ansell AD, Collins MJ et al (1992) Biology of living brachiopods. In: Blaxter JHS, Southward AJ (eds) Advances in marine biology, vol 28. Academic, London, pp 175–387

Jenkins RG, Kaim A, Little CTS et al (2013) Worldwide distribution of the modiomorphid bivalve genus *Caspiconcha* in late Mesozoic hydrocarbon seeps. Acta Palaeontol Pol 58(2):357–382
Jenkins RG, Kaim A, Hikida Y et al (2018) Four new species of the Jurassic to Cretaceous seep-restricted bivalve *Caspiconcha* and implications for the history of chemosynthetic communities. J Paleontol 92(4):596–610
Johnson CA, Kelley KD, Leach DL (2004) Sulfur and oxygen isotopes in barite deposits of the western Brooks Range, Alaska and its implications for the origin of the Red Dog massive sulfide deposits. Econ Geol 99:1435–1448
Joye S (2020) The geology and biogeochemistry of hydrocarbon seeps. Ann Rev Earth Planet Sci 48:205–231
Kaim A, Schneider S (2012) A conch with a collar: early ontogeny of the enigmatic fossil bivalve *Myoconcha*. J Paleontol 86(4):652–658
Kaim A, Bitner MA, Jenkins RG et al (2010) A monospecific assemblage of terebratulide brachiopods in the Upper Cretaceous seep deposits of Omagari, Hokkaido, Japan. Acta Palaeontol Pol 55(1):73–84
Karaca D, Hensen C, Wallmann K (2010) Controls on authigenic carbonate precipitation at cold seeps along the convergent margin off Costa Rica. Geochem Geophys Geosyst 11(8):Q08S27
Kiel S (2015) Did shifting seawater sulfate concentrations drive the evolution of deep-sea methane-seep ecosystems? Proc Biol Sci 282(1804):20142908
Kiel S (2018) Three new bivalve genera from Triassic hydrocarbon-seep deposits in southern Turkey. Acta Palaeontol Pol 63:221–234
Kiel S, Little CT (2006) Cold-seep mollusks are older than the general marine mollusk fauna. Science 313(5792):1429–1431
Kiel S, Peckmann J (2008) Paleoecology and evolutionary significance of an early Cretaceous *Peregrinella*-dominated hydrocarbon-seep deposit on the Crimean Peninsula. Palaios 23(11):751–759
Kiel S, Peckmann J (2019) Resource partitioning among brachiopods and bivalves at ancient hydrocarbon seeps: a hypothesis. PLoS One 14(9):e0221887
Kiel S, Glodny J, Birgel D et al (2014) The paleoecology, habitats, and stratigraphic range of the enigmatic Cretaceous brachiopod *Peregrinella*. PLoS One 9(10):e109260
Kiel S, Krystyn L, Demirtaş F et al (2017) Late Triassic mollusk-dominated hydrocarbon-seep deposits from Turkey. Geology 45(8):751–754
Kiel S, Hybertsen F, Hyžný M et al (2020) Mollusks and a crustacean from early Oligocene methane-seep deposits in the Talara Basin, northern Peru. Acta Palaeontol Pol 65:109–138
Kiel S, Huemer J, Gussone N et al (2021) Brachiopods in early Mesozoic cryptic habitats: Continuous colonization, rapid adaptation, and wide geographic distribution. Palaeogeog Palaeoclimat Palaeoecol 583:110668
Kniemeyer O, Musat F, Sievert S et al (2007) Anaerobic oxidation of short-chain hydrocarbons by marine sulphate-reducing bacteria. Nature 449(7164):898–901
Krylova EM, Sahling H (2011) Vesicomyidae (Bivalvia): current taxonomy and distribution. PLoS One 5:e9957
Lazăr I, Sandy MR, Campbell KA (2005) The paleoecologic, paleobiogeographic, and biostratigraphic significance of the Early Cretaceous rhynchonellid brachiopod *Peregrinella* from the southern Carpathian Mountains, Romania. Abstracts with Programs, Geological Society of America 37–14
Lazăr I, Sandy MR, Forel M-B et al (2017) Late Triassic brachiopod *Halorella* assemblages from paleokarst cavities near Vaşcău, Apuseni Mountains, Romania. In: Lazăr I, Grădinaru M, Vasile S (eds) Abstract Book, The 11th Romanian Symposium of Palaeontology, 25–30 September 2017. University of Bucharest, Bucharest, pp 71–72
Lazăr I, Schlagintweit F, Grădinaru E (2020) *Halorina cryptica* nov. ichnogen., nov. ichnosp., mass-occurrence of Upper Triassic crustacean microcoprolites from neptunian dikes and sills cutting the Dachstein-type carbonate platform and their paleoenvironmental significance (northern Apuseni Mountains, Romania). Geobios 61:31–39

Lee DE, Gregory MR, Lüter C et al (2008) *Melvicalathis*, a new brachiopod genus (Terebratulida: Chlidonophoridae) from deep sea volcanic substrates, and the biogeographic significance of the mid-ocean ridge system. Zootaxa 1866:136–150

Levin LA, Baco AR, Bowden DA et al (2016) Hydrothermal vents and methane seeps: rethinking the sphere of influence. Front Mar Sci 3. https://www.frontiersin.org/articles/10.3389/fmars.2016.00072/full

Little CTS, Herrington RJ, Maslennikov VV et al (1997) Silurian hydrothermal-vent community from the southern Urals, Russia. Nature 385:146–148

Little CTS, Maslennikov VV, Morris NJ et al (1999) Two Palaeozoic hydrothermal vent communities from the southern Ural Mountains, Russia. Palaeontology 42:1043–1078

Little CTS, Danelian T, Herrington RJ et al (2004) Early Jurassic hydrothermal vent community from the Franciscan complex. California. J Paleontol 78(3):542–559

Logan A (2007) Geographic distribution of extant articulated brachiopods. In: Selden PA (ed) Brachiopoda 6 (rev), supplement. Treatise on invertebrate paleontology, part H. Geological Society of America and University of Kansas, Boulder, pp 3082–3115

Luff R, Wallmann K (2003) Fluid flow, methane fluxes, carbonate precipitation and biogeochemical turnover in gas hydrate-bearing sediments at Hydrate Ridge, Cascadia Margin: numerical modeling and mass balances. Geochim Cosmochim Acta 67(18):3403–3421

Luff R, Wallmann K, Aloisi G (2004) Numerical modeling of carbonate crust formation at cold vent sites: significance for fluid and methane budgets and chemosynthetic biological communities. Earth Planet Sci Lett 221(1–4):337–353

MacDonald IR, Bohrmann G, Escobar E et al (2004) Asphalt volcanism and chemosynthetic life in the Campeche Knolls, Gulf of Mexico. Science 304(5673):999–1002

Manceñido MO, Dagys AS (1992) Brachiopods of the circum-Pacific region. In: Westerman GEG (ed) The Jurassic of the circum-Pacific, International Geological Correlation Programme Project 171. Cambridge University Press, New York, pp 328–333

Manceñido MO, Gourvennec R (2008) A reappraisal of feeding current systems inferred for spire-bearing brachiopods. Earth Environ Sci Trans R Soc Edinburgh 98(3/4):345–356

Manceñido MO, Owen EF (2001) Post-Palaeozoic Rhynchonellida (Brachiopoda): classification and evolutionary background. In: Brunton CHC, Cocks LRM, Long SL (eds) Brachiopods past and present, Systematics association special volume, vol 63. Taylor & Francis, London, pp 189–200

Manceñido MO, Owen EF, Savage NM et al (2002) Dimerelloidea. In: Kaesler RL (ed) Brachiopoda 4 (rev), Rhynchonelliformea. Treatise on invertebrate paleontology, part H. Geological Society of America and University of Kansas, Boulder, pp 1236–1245

Matyszkiewicz J, Krajewski M, Kochman A et al (2016) Oxfordian neptunian dykes with brachiopods from the southern part of the Kraków-Częstochowa Upland (southern Poland) and their links to hydrothermal vents. Facies 62:12

Menakova GN (1991) (Brachiopods). In: Dzhalilov MR (ed) (Atlas of the fossil fauna and flora of Tadzhikistan, Ordovician, Silurian, Devonian.) Donish, Dushanbe, pp 177–200 (In Russian)

Meulepas RJW, Jagersma CG, Khadem AF et al (2009) Effect of environmental conditions on sulfate reduction with methane as electron donor by an Eckernförde Bay enrichment. Environ Sci Technol 43:6553–6559

Milne JDG, Campbell JD (1969) Upper Triassic fossils from Oroua Valley, Ruahine Range, New Zealand. Trans R Soc N Z Geol 6(18):247–250

Nalivkin DV (1947) (Class Brachiopoda.) In: Nalivkin DV, Verber VN (eds) (Alas rukovodâŝih form iskopaemyh faun SSSR, tom 3, Devonskaâ Sistema.). VSEGEI–Gosgeoltehizdat, Leningrad, pp 63–134 (In Russian)

Newton RJ, Reeves EP, Kafousia N et al (2011) Low marine sulfate concentrations and the isolation of the European epicontinental sea during the Early Jurassic. Geology 39(1):7–10

Nie T, Guo W, Sun Y-L et al (2016) Age and distribution of the Late Devonian brachiopod genus *Dzieduszyckia* Siemiradzki, 1909 in southern China. Palaeoworld 25(4):600–615

Noll JH, Dutro JT Jr, Beus SS (1984) A new species of the Late Devonian (Famennian) brachiopod *Dzieduszyckia* from Sonora, Mexico. J Paleontol 58:1412–1421

Olu K, Cordes EE, Fisher CR et al (2010) Biogeography and potential exchanges among the Atlantic equatorial belt cold-seep faunas. PLoS One 5:e11967

Orcutt BN, Joye SB, Kleindienst S et al (2010) Impact of natural oil and higher hydrocarbons on microbial diversity, distribution, and activity in Gulf of Mexico cold-seep sediments. Deep-Sea Res Part II 57(21–23):2008–2021

Pálfy J, Kovács Z, Price GD et al (2017) A new occurrence of the Early Jurassic brachiopod *Anarhynchia* from the Canadian Cordillera confirms its membership in chemosynthesis-based ecosystems. Can J Earth Sci 54(12):1179–1193

Parkinson D, Cusack M (2007) Stable oxygen and carbon isotopes in extant brachiopod shells: keys to deciphering ancient ocean environments. In: Selden PA (ed) Brachiopoda 6 (rev), supplement. Treatise on invertebrate paleontology, part H. Geological Society of America and University of Kansas, Boulder, pp 2522–2531

Peck LS (2008) Brachiopods and climate change. Earth Environ Sci Trans R Soc Edinburgh 98(3/4):451–456

Peckmann J, Goedert JL (2005) Geobiology of ancient and modern methane-seeps. Palaeogeog Palaeoclimat Palaeoecol 227(1–3):1–5

Peckmann J, Gischler E, Oschmann W et al (2001) An early Carboniferous seep community and hydrocarbon-derived carbonates from the Harz Mountains, Germany. Geology 29(3):271–274

Peckmann J, Campbell KA, Walliser OH et al (2007) A Late Devonian hydrocarbon-seep deposit dominated by dimerelloid brachiopods, Morocco. Palaios 22(2):114–122

Peckmann J, Birgel D, Kiel S (2009) Molecular fossils reveal fluid composition and flow intensity at a Cretaceous seep. Geology 37(9):847–850

Peckmann J, Kiel S, Sandy MR et al (2011) Mass occurrences of the brachiopod *Halorella* in Late Triassic methane-seep deposits, eastern Oregon. J Geol 119(2):207–220

Peckmann J, Sandy MR, Taylor DG et al (2013) An Early Jurassic brachiopod-dominated seep deposit enclosed by serpentinite, eastern Oregon, USA. Palaeogeog Palaeoclimat Palaeoecol 390:4–16

Poole FG, Murchey B, Stewart JH (1983) Bedded barite deposits of middle and late Paleozoic age in central Sonora, Mexico. Abstracts with programs, Geological Society of America 15–299

Popiel-Barczyk E (1968) Upper Cretaceous terebratulids (Brachiopoda) from the Middle Vistula Gorge. Prace Muzeum Ziemi 12:3–86

Posenato R, Morsilli M (1999) New species of *Peregrinella* (Brachiopoda) from the Lower Cretaceous of the Gargano Promontory (southern Italy). Cretaceous Res 20:641–654

Racki G, Baliński A, Wrona R et al (2012) Faunal dynamics across the Silurian–Devonian positive isotope excursions ($\delta^{13}C$, $\delta^{18}O$) in Podolia, Ukraine: comparative analysis of the Ireviken and Klonk events. Acta Palaeontol Pol 57(4):795–832

Rhodes MC, Thompson RJ (1993) Comparative physiology of suspension-feeding in living brachiopods and bivalves—evolutionary implications. Paleobiology 19(3):322–334

Richardson JR (1997) Ecology of articulated brachiopods. In: Kaesler RL (ed) Brachiopoda 1 (rev). Treatise on invertebrate paleontology, part H. Geological Society of America and University of Kansas, Boulder, pp 441–460

Roemer FA (1850) Beiträge zur Kenntnis des nordwestlichen Harzgebirges. Palaeontographica 3:1–67

Romanin M, Crippa G, Ye F et al (2018) A sampling strategy for Recent and fossil brachiopods: selecting the optimal shell segment for geochemical analyses. Riv Ital Paleontol Stratigr 124(2):369–359

Roterman CN, Lee WK, Liu X et al (2018) A new yeti crab phylogeny: Vent origins with indications of regional extinction in the East Pacific. PLoS One 13:e0194696

Rozman HS (1962) Stratigraphy and brachiopods of the Famennian stage of the Mugodzhary and adjacent areas. Tr Geologičeskogo Inst Akad Nauk SSSR 50:1–195. (In Russian)

Rubin-Blum M, Antony CP, Borowski C et al (2017) Short-chain alkanes fuel mussel and sponge *Cycloclasticus* symbionts from deep-sea gas and oil seeps. Nat Microbiol 2:17093

Sandy MR (1990) A new early Cretaceous articulate brachiopod from the Northwest Territories, Canada, and its paleobiogeographic significance. J Paleontol 64:367–372

Sandy MR (1995) A review of some Palaeozoic and Mesozoic brachiopods as members of cold seep chemosynthetic communities: 'unusual' palaeoecology and anomalous palaeobiogeographic patterns explained. Földtani Közlöny 125(3/4):241–258

Sandy MR (2001) Mesozoic articulated brachiopods from the Western Cordillera of North America: their significance for palaeogeographic and tectonic reconstruction, palaeobiogeography and palaeoecology. In: Brunton CHC, Cocks LRM, Long SL (eds) Brachiopods past and present, Systematics association special volume, vol 63. Taylor & Francis, London, pp 394–410

Sandy MR (2010) Brachiopods from ancient hydrocarbon seeps and hydrothermal vents. In: Kiel S (ed) The vent and seep biota: aspects from microbes to ecosystems, Topics in geobiology, vol 33. Springer, Dordrecht, pp 279–314

Sandy MR, Blodgett RB (1996) *Peregrinella* (Brachiopoda: Rhynchonellida) from the Early Cretaceous, Wrangellia Terrane, Alaska. In: Copper P, Jin J (eds) Brachiopods. Balkema, Rotterdam, pp 239–242

Sandy MR, Campbell KA (1994) New rhynchonellid brachiopod genus from Tithonian (Upper Jurassic) cold seep deposits of California and its paleoenvironmental setting. J Paleontol 68:1243–1252

Sandy MR, Campbell KA (2003) *Anarhynchia* (Jurassic Brachiopoda) in a possible seep deposit from Bedford Canyon, California, USA. Abstracts with Programs, Geological Society of America 35(6):381

Sandy MR, Peckmann J (2016) The Early Cretaceous brachiopod *Peregrinella* from Tibet: a confirmed hydrocarbon-seep occurrence for a seep-restricted genus. PalZ 90:691–699

Sandy MR, Owen EF, Blodgett RB (1995) Peregrinellid brachiopod (Brachiopoda, Rhynchonellida) from the Early Cretaceous of the Wrangellia Terrane, southern Alaska, U.S.A.—first record of a 'Tethyan' *Peregrinella*-ally from high paleolatitudes and its paleobiogeographic and paleoecologic significance. Abstracts, 3rd International Brachiopod Congress, Sudbury, Ontario, Canada, 2–5 September 1995, p 67

Sandy MR, Lazăr I, Peckmann J et al (2012) Methane-seep brachiopod fauna within turbidites of the Sinaia Formation, eastern Carpathian Mountains, Romania. Palaeogeog Palaeoclimat Palaeoecol 323–325:42–59

Sandy MR, Hryniewicz K, Hammer Ø et al (2014) Brachiopods from Late Jurassic–Early Cretaceous hydrocarbon seep deposits, central Spitsbergen, Svalbard. Zootaxa 3884(6):501–532

Sassen R, Roberts HH, Carney R et al (2004) Free hydrocarbon gas, gas hydrate, and authigenic minerals in chemosynthetic communities of the northern Gulf of Mexico continental slope: relation to microbial processes. Chem Geol 205(3/4):195–217

Siemiradzki J (1909) Zbiory L. Zejsznera z kieleckiego dewonu. Sprawozdania Komisji Fizyograficznej 43:62–94

Simoneit BRT, Kawka OE, Brault M (1988) Origin of gases and condensates in the Guaymas Basin hydrothermal system (Gulf of California). Chem Geol 71(1–3):169–182

Singh R, Guzman MS, Bose A (2017) Anaerobic oxidation of ethane, propane, and butane by marine microbes: a mini review. Front Microbiol 8:2056

Smith EB, Scott KM, Nix ER et al (2000) Growth and condition of seep mussels (*Bathymodiolus childressi*) at a Gulf of Mexico brine pool. Ecology 81(9):2392–2403

Smrzka D, Zwicker J, Klügel A et al (2016) Establishing criteria to distinguish oil-seep from methane-seep carbonates. Geology 44(8):667–670

Smrzka D, Zwicker J, Misch D et al (2019) Oil seepage and carbonate formation: a case study from the southern Gulf of Mexico. Sedimentology 66(6):2318–2353

Stebbins A, Algeo TJ, Olsen C et al (2019) Sulfur-isotope evidence for recovery of seawater sulfate concentrations from a PTB minimum by the Smithian-Spathian transition. Earth-Sci Rev 195:83–95

Steeb P, Krause S, Linke P et al (2015) Efficiency and adaptability of the benthic methane filter at Quepos Slide cold seeps, offshore of Costa Rica. Biogeosciences 12(22):6687–6706

Stefanoff M, Sandy MR (1998) Evolutionary relationships of *Anarhynchia*, a possible chemosynthetic Jurassic brachiopod from North America. Abstracts with Programs, Geological Society of America 30A-72–73

Steinich G (1965) Die artikulaten Brachiopoden der Rügener Schreibkreide (Unter-Maastricht). Paläont Abh 2(1):1–220
Sturz AA, Sturdivant AE, Leif RN et al (1996) Evidence for retrograde hydrothermal reactions in near surface sediments of Guaymas Basin, Gulf of California. Appl Geochem 11:645–665
Suess E (2014) Marine cold seeps and their manifestations: geological control, biogeochemical criteria and environmental conditions. Int J Earth Sci 103(7):1889–1916
Sulser H, Furrer H (2008) Dimerelloid rhynchonellide brachiopods in the Lower Jurassic of the Engadine (Canton Graubünden, National Park, Switzerland). Swiss J Geosci 101:203–222
Sun DL (1986) Discovery of Early Cretaceous *Peregrinella* (Brachiopoda) in Xizang (Tibet) and its significance. Palaeontol Catayana 2:211–227
Sun Y, Gong S, Li N et al (2020) A new approach to discern the hydrocarbon sources (oil vs. methane) of authigenic carbonates forming at marine seeps. Mar Pet Geol 114:104230
Termier G, Termier H (1950) Paléontologie marocaine, II: Invertébrés de l'ere primaire, II: Bryozoaires et brachiopodes. Serv Géol Maroc Notes Mém 77:21–252
Thayer CW (1985) Brachiopods versus mussels—competition, predation, and palatability. Science 228(4707):1527–1528
Timmers PH, Widjaja-Greefkes HC, Ramiro-Garcia J et al (2015) Growth and activity of ANME clades with different sulfate and sulfide concentrations in the presence of methane. Front Microbiol 6:988
Torres ME, Bohrmann G, Dubé TE et al (2003) Formation of modern and Paleozoic stratiform barite at cold methane seeps on continental margins. Geology 31:897–900
Torsvik TH, Van der Voo R, Preeden U et al (2012) Phanerozoic polar wander, palaeogeography and dynamics. Earth-Sci Rev 114(3/4):325–368
Tunnicliffe A, Wilson K (1988) Brachiopod populations: distribution in fjords of British Columbia (Canada) and tolerance of low oxygen concentrations. Mar Ecol Prog Ser 47:117–128
Valentine JW, Jablonski D (2010) Origins of marine patterns of biodiversity: some correlates and applications. Palaeontology 53(6):1203–1210
Van Dover CL, German CR, Speer KG et al (2002) Evolution and biogeography of deep-sea vent and seep invertebrates. Science 295(5558):1253–1257
Vrijenhoek RC (2013) On the instability and evolutionary age of deep-sea chemosynthetic communities. Deep-Sea Res Part II 92:189–200
Wegener G, Boetius A (2009) An experimental study on short-term changes in the anaerobic oxidation of methane in response to varying methane and sulfate fluxes. Biogeosciences 6:867–876
Wendt J, Belka Z (1991) Age and depositional environment of Upper Devonian (early Frasnian to early Famennian) black shales and limestones (Kellwasser facies) in the eastern Anti-Atlas, Morocco. Facies 25:51–90
Whiticar MJ (1999) Carbon and hydrogen isotope systematics of bacterial formation and oxidation of methane. Chem Geol 161(1–3):291–314
Witts JD, Newton RJ, Mills BJW et al (2018) The impact of the Cretaceous-Paleogene (K-Pg) mass extinction event on the global sulfur cycle: evidence from Seymour Island, Antarctica. Geochim Cosmochim Acta 230:17–45
Wortmann UG, Paytan A (2012) Rapid variability of seawater chemistry over the past 130 million years. Science 337:334–336
Zezina ON (2003) On the ecological, morphological, and evolutionary features of brachiopods living in marginal and extreme environments. Paleontol J 37(3):263–269
Zezina ON (2008) Biogeography of the Recent brachiopods. Paleontol J 42(8):830–858

Chapter 9
Extant and Fossil Sponges Associated with Hydrothermal Vent and Cold Seep Communities

Andrzej Pisera, Krzysztof Hryniewicz, Maria Aleksandra Bitner, and Andrzej Kaim

9.1 Introduction

Sponges are well known from present-day hydrothermal communities and cold seeps, and most of them are background organisms that may occur elsewhere. Only a few are proven to be dependent on chemosynthesis. On the other hand, sponges are only rarely reported and very poorly known from fossil hydrothermal vent and cold seep deposits. Here we present, based on published data, an overview of present-day sponges reported from such communities, as well as a review of all supposedly vent- and seep-associated fossil sponges reported so far. We also present new occurrences of sponges in ancient seep sites. Because the sponge taxonomy as presented in most textbooks, especially paleontological, involves rather old taxonomic concepts, we review here the current taxonomy of sponges (based generally on the World Porifera Database) with a review of the most important characters, to facilitate further understanding of descriptions and discussions.

9.2 Porifera Grant, 1836

Sponges appear to be the oldest living Metazoa. They are exclusively aquatic sedentary animals feeding by filtration of fine particles and dissolved organic matter. Very few taxa also developed carnivory. Sponges possess several specialized cell types that are not organized into tissue or organs or are syncytial. Most sponges have an internal skeleton that may be mineralized—siliceous or calcareous, in the form of discrete elements called spicules, more rarely as solid basal calcareous—or organic

A. Pisera (✉) · K. Hryniewicz · M. A. Bitner · A. Kaim
Institute of Paleobiology, Polish Academy of Science, Warszawa, Poland
e-mail: apis@twarda.pan.pl; krzyszth@twarda.pan.pl; bitner@twarda.pan.pl; kaim@twarda.pan.pl

A. Kaim et al. (eds.), *Ancient Hydrocarbon Seeps*, Topics in Geobiology 50,
https://doi.org/10.1007/978-3-031-05623-9_9

collagenous (spongin forming fibers in the Demospongiae) (see Van Soest et al. 2012).

9.2.1 *Homoscleromorpha Bergquist, 1978*

These are usually encrusting sponges with small loose siliceous spicules in one size category. They are reported neither from recent chemosynthesis-based communities nor from the fossil ones.

9.2.2 *Demospongiae Sollas, 1885*

These sponges have siliceous megascleres that are tetraxons and monaxons, mostly free, but sometimes may be articulated. Spicules are differentiated into megascleres and microscleres, of which especially the latter are useful for taxonomy but, unfortunately, rarely preserved as fossils. Most sponges possess rather simple megascleres, but, e.g., many Poecilosclerida and especially Astrophorida have numerous characteristic megascleres that may help in their recognition in the fossil state. This is also true for the so-called Sclerosponges (demosponges with massive basal calcareous skeletons) and Lithistida (articulated skeleton of siliceous desma spicules) both morphofunctional (polyphyletic) groupings of sponges, especially well known among paleontologists because of their high fossilization potential due to their articulated skeletons. The majority of demosponges are marine, but one group, i.e., the Spongillina, is widely distributed in terrestrial freshwater water bodies worldwide.

9.2.3 *Hexactinellida Schmidt, 1870*

These sponges are characterized by triaxon (hexactine) siliceous spicules and/or their derivatives. Spicules may be free or fused; they are differentiated into micro- and megascleres. Hexactinellids are exclusively marine.

9.2.4 *Calcarea Bowerbank, 1862*

These sponges are characterized by exclusively calcareous spicules and are exclusively marine.

9.3 Extant Sponges Associated with Vent and Seep Communities

There are several hexactinellid sponges known from modern hydrothermal vents. Boury-Esnault and De Vos (1988) reported the hexactinellid genus *Caulophacus* from the East Pacific Ridge zone of "strong hydrothermal" influence, but Tabachnick et al. (2017) questioned this report, pointing out that dense aggregations of hexactinellid sponges are unknown in the close vicinity of hydrothermal vents. At the same time, he reports the occurrence of another hexactinellid, *Hyalonema*, from a cold seep area in the North Atlantic (citing unpublished data from Norwegian expeditions). Another hexactinellid (family Euplectellidae, order Lyssacinosida) was reported by Desbruyères and Alayse-Danet (1994) as growing on old submarine lava flows in the North Fiji Basin.

Specialized deep-sea demosponges of the family Cladorhizidae Dendy, 1922, characterized by carnivorous habit and/or lack of an aquiferous system (Hajdu and Vacelet 2002) and often with feather-like branching morphology, are frequently the most common sponges in areas of deep-water hydrothermal venting today. These belong to genera *Cladorhiza* Sars, 1872, reported from the NE Atlantic that may form even sponge fields associated with mud volcanoes and methane flows (Vacelet et al. 1995; Vacelet and Boury-Esnault 2002); *Eucheliplum*a Topsent, 1909, from the Atlantic, aggregations at hydrothermal fields of Ascension Island (Koschinsky et al. 2006); *Abyssocladia* Lévi, 1964, from the Fiji Basin (Vacelet and Segonzac 2006), Solomon Islands (Vacelet and Kelly 2014), American and Samoa (Staudigel et al. 2006); and *Asbestopluma* Topsent, 1901 and *Chondrocladia* Thomson, 1873, from the East Pacific Rise (Vacelet and Segonzac 2006). Some of the cladorhizid spicules (Fig. 9.1c, d, microscleres) are of very characteristic shape that could be recognized in the fossil state, even if disassociated after the death of the sponge. However, they are of very small size and thus very rarely preserved and/or very difficult to find using standard paleontological procedures. Because some Cladorhizidae may occur in other deep-sea environments, and some even in shallow water (e.g., Chevaldonné et al. 2014), they should be treated as associated rather than obligate hydrothermal vent fauna.

Quite different demosponges occur in more shallow-water vents and seeps. They usually display more typical morphologies and rather simple spiculation. The demosponges *Haliclona* Grant, 1841; *Pseudosuberites* Topsent, 1896; and *Protosuberites* Swartschewsky, 1905, are reported by Kelly and Rowden (2019, with references) from the Callypso hydrothermal vent off New Zealand. All of them have very simple spicules (oxeas and tylostyles) that would be difficult to interpret, even if preserved in the fossil record. Bowden et al. (2013) reported several other, tentatively identified demosponges from the same area. The only report of lithistid sponges associated with hydrothermal sites is that by Kelly (2007) from the area around hydrothermal sites in the Bay of Plenty and southern Kermadec Arc (New Zealand). Demosponges of the genera *Thenea* (especially common), *Stylocordyla*, and *Phakellia* and five other undetermined (seemingly) demosponges are reported by

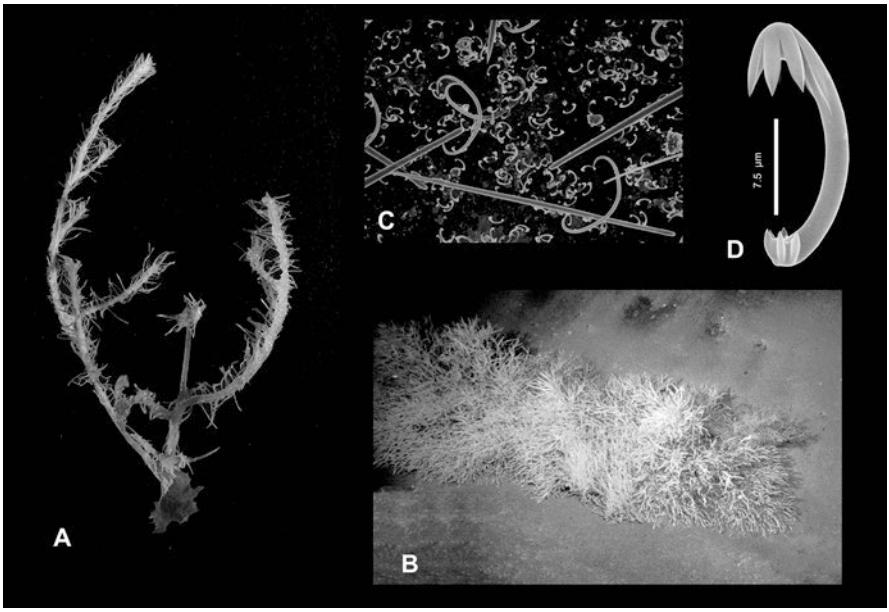

Fig. 9.1 *Cladorhiza methanophila* Vacelet and Boury-Esnault. (**a**) Habitus of sponge (holotype). (**b**) Submarine photo of the sponge group (approximately 40 cm high), Barbados Trench, 4943 deep. (**c**) Assemblage of spicules; styles, sigmancistra, and anisochel. (**d**) Anisochelae microsclere of this species. (All photos courtesy J. Vacelet, and N. Boury-Esnault, Marseille). **c** and **d** SEM

Sen et al. (2018) from the cold seeps around gas hydrate mounds in High Arctic (Barents Sea), while Bertolino et al. (2017) described a diverse assemblage (nine species) of demosponges from shallow-water hydrothermal vents off Sulawesi (Indonesia). None of these sponges are "vent-obligate" species because they occur in nearby coral reefs as well. Bertolino et al. (2017) suggested that the sponges near hydrothermal vents take advantage of higher (relative to normal sea water) silica contents. Similarly explained is the occurrence of astrophorid demosponge *Geodia* in the vent community of Milos Island (Aegean Sea) by Pansini et al. (2000). Large accumulation of spicules in the sediments of Matupi Harbour (Papua New Guinea) is characterized by diffuse hydrothermalism and is interpreted by Tarasov et al. (1999) as caused by stimulated sponge growth due to increased silicon in water resulting from volcanic activity.

Probably the richest and the most diversified seep-associated fauna of sponges (79 demosponge species and 3 hexactinellid species) was described from the Gulf of Cadiz (Atlantic) by Sitja et al. (2019). This fauna is associated with mud volcano methane seeps.

There are very few cases where the nutrition of sponges has been proven to be based on chemosynthesis. Notably, it was first demonstrated for a demosponge *Cladorhiza methanophila* Vacelet and Boury-Esnault (Fig. 9.1) from the Barbados Trench (Vacelet et al. 1995; Vacelet and Boury-Esnault 2002). It was proven that,

apart from being carnivorous, this sponge relies on chemosynthesis, due to the fact that it hosts symbiotic methanotrophic bacteria, its tissue displays very negative $\delta^{13}C$ values, and methanol dehydrogenase activity was observed. Another example is demosponge *Protosuberites thurberi* Kelly and Rowden, 2019 (Fig. 9.2) that had been reported from cold seeps off New Zealand (Baco et al. 2010; Thurber et al. 2010) where it forms extensive encrusting to digitate mats. Two sponge species, *Hymedesmia* (*Stylopus*) *methanophila* Cardenas, 2019, and *Iophon methanophila* Cardenas, 2019, reported from hydrocarbon (asphalt) seeps at Campeche Knolls in the southern Gulf of Mexico (Rubin-Blum et al. 2019), are also considered to benefit from chemosynthesis as they host methanotrophic (methane-oxidizing) bacteria in their tissue. Again, their spicules, even if preserved in the fossil record, because of the simple morphology that appears in many sponge groups, are not diagnostic, and it would be difficult to assign them to these taxa based on spicules alone.

There is only one report of a calcareous sponge species of the genus S*ycon* (associated with demosponge *Tethya*) from the hydrothermal vent community at the shallow section of subpolar Mid-Atlantic Ridge (Fricke et al. 1989).

There are also reports of freshwater demosponges (Spongillina) associated with hydrothermal vents and seeps in terrestrial lakes. Such sponges of the endemic family Lubomirskiidae are reported from the Baikal hydrothermal vents and methane

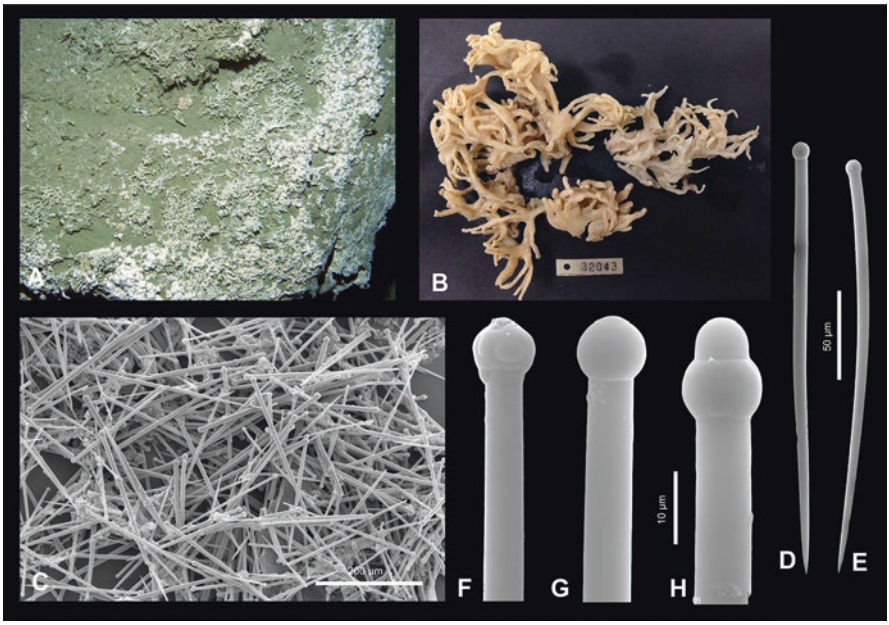

Fig. 9.2 *Pseudosuberites thurberi* Kelly and Rowden, 2019. (**a**) Submarine photo showing finger-like sponge masses growing on the rock surface NIWA Stn TAN0616/85: image 100; 41.781° S, 175.401° E, 1049 m. (**b**) Habitus of sponge; paratype NIWA 32043. (**c**) Assemblage of loose spicules (tylostyles). (**d**, **e**) Exemplary tylostyles from the paratype NIWA 32043. (**f**–**h**) Tylostyle head from the paratype NIWA 32043. (**a**, **b** courtesy of M. Kelly, NIWA, Auckland). **c**–**h** SEM

seeps (Crane et al. 1991; Gebruk et al. 1993), but no details are available. The genus *Heterorotula* occurs in Lake Taupo deep hydrothermal vents in New Zealand (Pronzato and Manconi 2019). These genera have rather characteristic spicules that may allow their recognition in the fossil record, if preserved (see e.g., Pronzato et al. 2017; Weinberg et al. 2004).

9.4 Fossil Sponges Associated with Vent and Seep Communities

9.4.1 Cambrian of China

There are very few records of fossil sponges from hydrothermal vents or cold seeps. The oldest (but uncertain) record of sponges comes from the Lower Cambrian of China that are identified as putative hexactinellids and astrophorid demosponges (Steiner et al. 2002). It is not clear if the sponges lived under hydrothermal conditions or if deposits containing sponges were modified later by hydrothermal activity. Another early Cambrian hexactinellid sponge, displaying aberrant morphology, was interpreted as a potentially chemosynthetic organism reliant on endosymbiotic bacteria (Botting et al. 2012), but the sponge nature of the described specimen itself is highly disputable.

9.4.2 Jurassic of France and Spitsbergen

The Mesozoic record of sponges from cold seeps is relatively scarce, but it is better than in the Paleozoic. Diversified assemblage of sponges (lyssacinosid hexactinellids, lychnicosid hexactinellids, lithistid, and other demosponges) occurs in carbonate deposits of Oxfordian age in Beauvoisin (France) interpreted as cold seep deposits (Gaillard et al. 1992; Peckmann et al. 1999). Accordingly, it was suggested (unfortunately without proof) that sponges in this association depended on chemosynthesis. In our opinion, as in other cases, more probably they just represent background fauna, as all these types of sponges are also known from "normal" marine Jurassic facies. The hexasterophoran sponge *Laocoetis*, which is characterized by a regularly fused skeleton (better known as *Craticularia*, which is very common in late Jurassic deposits of Europe) (Fig. 9.3), was reported by Hammer et al. (2011) and Hryniewicz et al. (2012, 2015) from seep deposits close to Jurassic/Cretaceous boundary beds in Svalbard.

Fig. 9.3 Hexactinellid sponge *Laocoetis* sp. from cold seep at Jurassic/Cretaceous boundary at Svalbard

9.4.3 Cretaceous (Campanian) of Hokkaido, Japan

We present herein the first report of sponges in cold seep deposits in Japan from localities Gakkonosawa and Yasukawa in northern Hokkaido (Kaim et al. 2009). In Gakkonosawa only hexactinosan sponges have been found. They form irregular folded and tubular masses visible in the seep carbonate (Fig. 9.4a, b). Dissolution in acid provided fragments of the fused skeletons (Fig. 9.4c), apparently different from those in Yasukawa; in both cases, they may belong to the family Euretidae.

In Yasukawa, one species of hexactinosan sponge (hexactinellids with fused skeleton) is observed as fragments of the skeleton (Fig. 9.5d, f). There are also some rare demosponge spicules represented by oxeas (broken) (Fig. 9.5a, b) and one triaene (Fig. 9.5c); the latter indicates astrophorid sponges. This sponge fauna requires more collecting effort and further studies.

Fig. 9.4 Gakkonosawa seep (Campanian, Hokkaido, Japan). (**a**, **b**) Tubular-folded sponge walls as seen in the seep rock. (**c**) Dictyonal skeleton, SEM

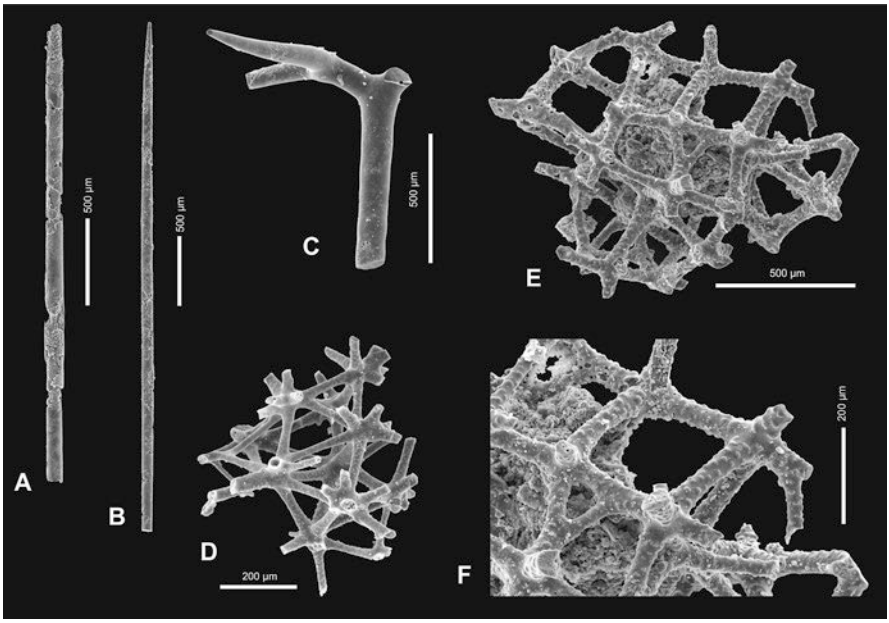

Fig. 9.5 Yasukawa seep (Campanian, Hokkaido, Japan) sponge spicules. (**a**, **b**) Demosponge oxeas. (**c**) Demoponge triaen (Astrophorida). (**d**–**f**) Hexactinellid (Hexactinosa) skeleton fragment (**f** details of **e**, showing strong sculpture of rays). All SEM

9.4.4 Paleogene and Neogene of Oregon and Washington, USA

Probably the richest fossil fauna of sponges associated with seeps occurs in the Eocene to Miocene rocks of Washington and Oregon, USA. This region is generally rich in fossiliferous seep deposits and is even described as "Eldorado for a palaeontologist" (Kiel 2010). Bodily preserved sponges are common (Rigby and Jenkins 1983; Rigby and Goedert 1996) and are exclusively hexactinellids. The very characteristic hexactinellid *Aphrocallistes polytretos* Rigby and Jenkins (Fig. 9.6e, f)

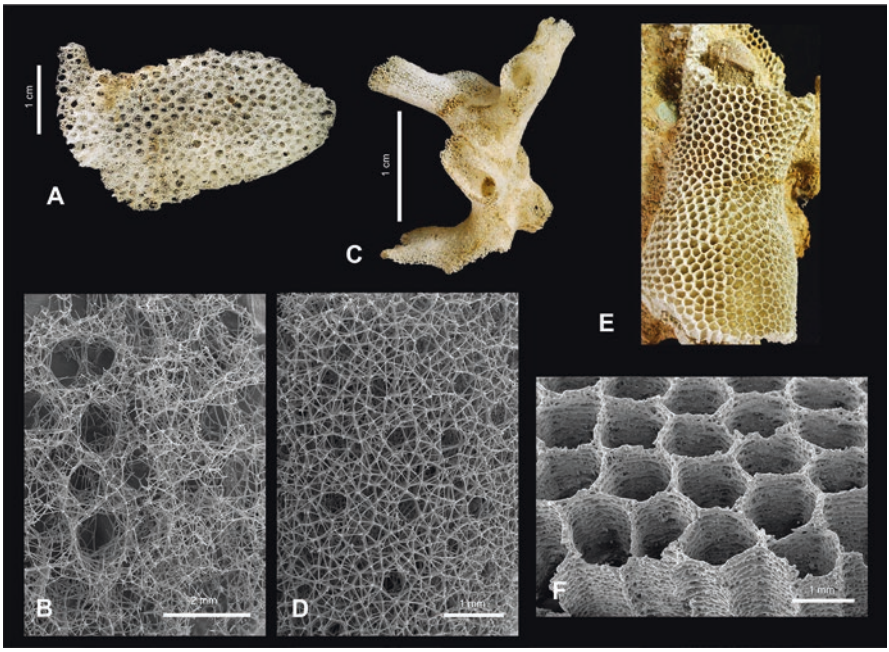

Fig. 9.6 Hexactinellid sponges from seeps. (**a**, **b**) *Hexactinella conica* Rigby and Goedert. (**c**, **d**) *H. tubula* Rigby and Goedert, Oligocene of Olympic Peninsula, Washington. (**e**, **f**) *Aphrocallistes polytretos* Rigby and Jenkins. **b**, **d**, and **f** SEM

occurs in various seeps of Eocene to Miocene age in Southwest Washington and Oligocene to Miocene seeps of NW Oregon, while *Eurete geoderti* Rigby and Jenkins occurs in the Oligocene of Southwest Washington. Four species, *Hexactinella conica* Rigby and Goedert (Fig. 9.6a, b), *H. tubula* Rigby and Goedert (Fig. 9.6c, d), *Eurete goederti* Rigby and Jenkins, and *Farrea* sp., were described by Rigby and Goedert (1996) from the Oligocene seeps of the Olympic Pennisula (Washington State, USA).

New material of seep rocks from the Middle Eocene cold seep of Northern Dotty Hills, Washington State (CSUN loc. 1570), representing a transition zone between the Crescent/McIntosh formations dissolved in acid yielded spicules of euretid hexactinellid (different from those reported above) and diverse demosponge triaenes, plus oxeas (Fig. 9.7). They clearly belong to several different species (and probably genera) of astrophorid demosponges.

In contrast, the new material from Wynoochee seep carbonates of Eocene-Oligocene age from Washington State yielded only demosponge spicules: Various oxeas, triaenes, and sterrasters (Fig. 9.8) also belong to astrophorid demosponges.

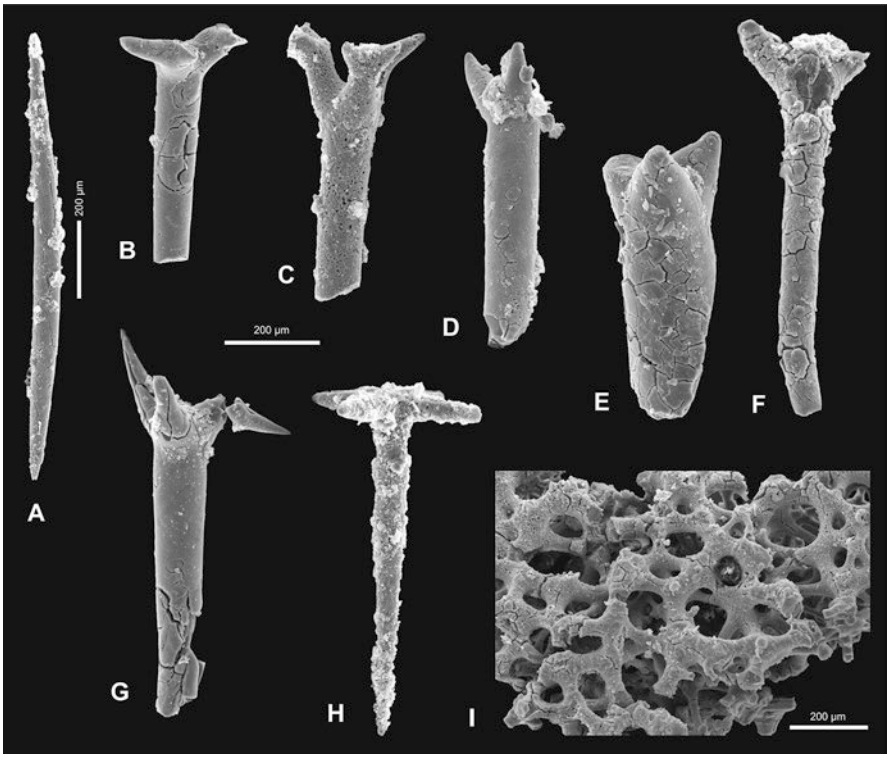

Fig. 9.7 Northern Doty Hills seep (Middle Eocene, Washington State, USA), sponge spicules. (**a**) Demosponge oxea. (**b**–**h**) Various demosponge triaenes (Astrophorida). (**i**) Hexactinellid (Hexactinosa) skeleton. All SEM

9.5 Discussion and Summary

The most common sponges in the present-day seep and vent communities are Demospongiae, while Hexactinellida are rare (*Farrea* sp., and maybe also *Aphrocallistes* sp., is seen commonly on videos from hydrothermal vents of Recent Atlantic mid-oceanic ridge environments during RV Meteor expeditions; D. Janussen, personal information, 2020), especially those with fused skeletons, and Calcarea are only exceptionally reported. The majority of extant sponges known from such environments belong to groups with loose (not fused or articulated) spicules that fall apart after the death of the sponge; thus, their fossilization potential is low. Most of these sponges are considered "background" fauna because they do not depend directly on chemosynthesis and can occur in other environments as well. Those few taxa that are proved to be chemosynthesis-based have no skeletal characters that would allow one to easily differentiate them in the fossil state. In more general terms, demosponges from the family Cladorhizidae may dominate nowadays deep-water hydrothermal vents, but sponges of this family occur in other

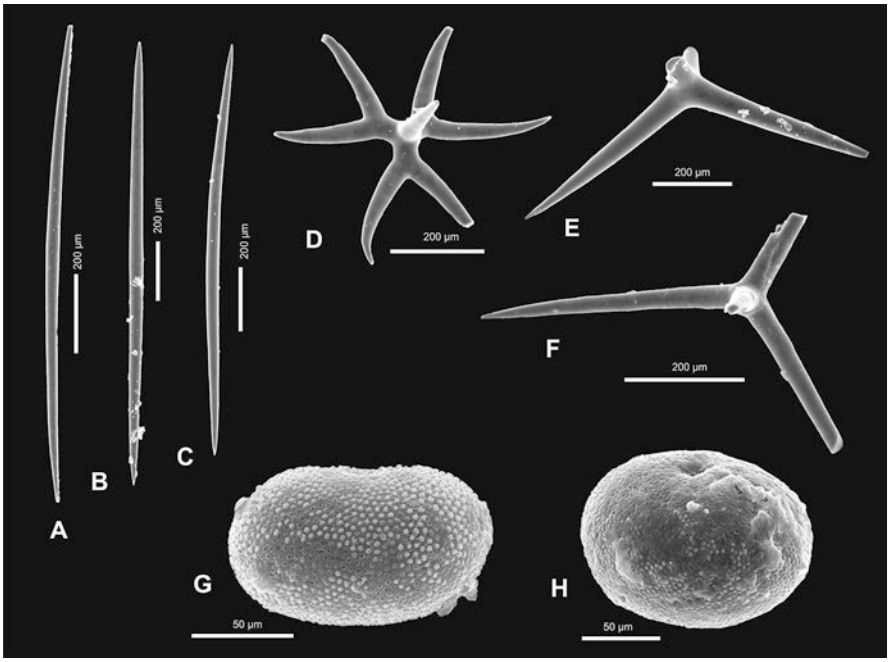

Fig. 9.8 Wynoochee seep, (Eocene-Oligocene, Washington State, USA), sponge spicules. (**a**–**c**) Demosponge oxea. (**d**–**f**) Demosponge triaenes ((**d**) Dichotriaen, (**e**, **f**) Simple triaenes) (Astrophorida)). (**g**, **h**) Demosponge sterrasters (Astrophorida, Geodiidae). All SEM

environments as well, including also some shallow-water settings (Hestetun et al. 2017; Chevaldonné et al. 2014). In more shallow seeps and vents, various other demosponges (including astrophorids) are common.

The oldest (but questionable) fossil record of sponges associated with hydrothermally influenced deposits comes from the Lower Cambrian of China. These forms are identified as putative hexactinellids and astrophorid demosponges (Steiner et al. 2002). The oldest Mesozoic seep-associated sponges (both hexactinellids and demosponges) are reported from the Late Jurassic of France (Gaillard et al. 1992; Peckmann et al. 1999), and hexactinellids and probably demosponges are reported from Jurassic/Cretaceous boundary beds in Svalbard (Hammer et al. 2011; Hryniewicz et al. 2012, 2015).

The presence of sponges in seep deposits of Late Cretaceous age (Campanian) in Japanese localities of Gakkonosawa and Yasukawa is reported here for the first time. This fauna consists of hexactinelids with fused skeleton (Hexactinosa), but loose spicules of astrophorid demosponges have also been found.

The Paleogene and Neogene records of seep and vent sponges are more common but mostly limited to northwest USA (Washington and Oregon) and consist of hexactinellid sponges with fused rigid skeletons. New findings of hexactinellids with rigid skeletons, accompanied by astrophorid demosponge spicules, are reported here also from the Eocene Crescent Formation of Washington State, USA.

This report clearly shows that Hexactinosa (Hexactinellida with fused skeletons) are the most common sponges occurring at ancient seeps though they are rare in their modern counterparts. Those in turn are inhabited mostly by demosponges with skeletons composed of loose spicules. Such sponges are very rarely reported from the ancient communities—what we interpret as a taphonomic effect—most of all due to the lack of preservation of complete sponges. The dominance of hexactinellids with fused skeletons in the fossil communities over demosponges cannot, however, be exclusively an artifact (taphonomic effect due to their higher preservation potential or because they are bodily preserved and thus easily spotted in rock) because they have not been reported so far from present-day communities (those hexactinellids observed in modern seeps and vents have loose spicules). No calcareous sponges have been reported so far from any ancient vent and seep communities.

Our review and study of new sponge occurrences in fossil seep and vent communities reveal that sponges are rarely reported from fossil vent and cold seep communities, not because they were rare but rather overlooked, as shown by dissolving some seep rocks in acid. It also suggests that, at least in the case of hydrothermal vents, the occurrence of sponges may be due to the fact that such localities are characterized by increased silica concentrations in sea water.

Acknowledgments We would like to thank J. Vacelet and N. Boury-Esnault (Marseille) for allowing the use of their photos of *Cladorhiza methanophila* and M. Kelly (Auckland) for supplying the material of *P. thurberi* and some macrophotos of this sponge. An anonymous reviewer and D. Janussen are acknowledged for their help to improve this manuscript.

References

Baco AR, Rowden AA, Levin LA et al (2010) Initial characterisation of cold seep faunal communities on the New Zealand Hikurangi margin. Mar Geol 272(1):251–259

Bertolino M, Oprandi A, Santini C et al (2017) Hydrothermal waters enriched in silica promote the development of a sponge community in North Sulawesi (Indonesia). Eur Zool J 84(1):128–135. https://doi.org/10.1080/11250003.2016.1278475

Botting JP, Muir LA, Li X-F et al (2012) An enigmatic, possibly chemosymbiotic, hexactinellid sponge from the early Cambrian of South China. Acta Palaeontol Pol 58(3):641–649. https://doi.org/10.4202/app.2011.0140

Boury-Esnault N, De Vos L (1988) *Caulophacus cyanae* n. sp., a new hexactinellid sponge from hydrothermal vents. Biogeography of the genus *Caulophacus Schulze*, 1887. Oceanologica Acta volume spécial 8:51–60

Bowden DA, Rowden AA, Thurber AR et al (2013) Cold seep epifaunal communities on the Hikurangi Margin, New Zealand: composition, succession, and vulnerability to human activities. PLoS One 8(10):e76869. https://doi.org/10.1371/journal.pone.0076869

Chevaldonné P, Pérez T, Crouzet J-M et al (2014) Unexpected records of 'deep-sea' carnivorous sponges *Asbestopluma hypogea* in the shallow NE Atlantic shed light on new conservation issues. Mar Ecol 36(3):475–484. https://doi.org/10.1111/maec.12155

Crane K, Hecker B, Golubev V (1991) Hydrothermal vents in Lake Baikal. Nature 350:281

Desbruyères D, Alayse-Danet A-M (1994) Deep-sea hydrothermal communities in southwestern Pacific back-arc basins (the North Fiji and Lau basins): composition, microdistribution and food web. Mar Geol 116:227–242

Fricke H, Giere O, Stetter K et al (1989) Hydrothermal vent communities at the shallow subpolar Mid-Atlantic ridge. Marine Biol 102:425–429

Gaillard C, Rio M, Rolin Y et al (1992) Fossil chemosynthetic communities related to vents or seeps in sedimentary basins: the pseudobioherms of southeastern France compared to other world examples. Palaios 7:451–465

Gebruk AV, Kuznetsov AI, Namsarev BB et al (1993) The role of bacterial organics in the feeding of deepwater benthic animals in Frolikha Bay (Lake Baikal) under conditions of elevated heat flow. Izvestiya RAN, Seriya Biologicheskaya 6:903–908

Hammer Ø, Nakrem HA, Little CTS et al (2011) Hydrocarbon seeps from close to the Jurassic-Cretaceous boundary. Palaeogeog Palaeoclimat Palaeoecol 306:15–26

Hajdu E, Vacelet J (2002) Family Cladorhizidae Dendy, 1922. In: Hooper JNA, Van Soest RWM (eds) Systema Porifera. A guide to the classification of sponges. Kluwer Academic/Plenum, NY, pp 636–641

Hestetun JT, Tompkins-Macdonald G, Rapp HT (2017) A review of carnivorous sponges (Porifera: Cladorhizidae) from the Boreal North Atlantic and Arctic. Zool J Linn Soc 181:1–69

Hryniewicz K, Hammer Ø, Nakrem HA et al (2012) Microfacies of the Volgian–Ryazanian (Jurassic–Cretaceous) hydrocarbon seep carbonates from Sassenfjorden, central Spitsbergen, Svalbard. Norw J Geol 92:113–131

Hryniewicz K, Nakrem HA, Hammer Ø et al (2015) The palaeoecology of the latest Jurassic–earliest Cretaceous hydrocarbon seep carbonates from Spitsbergen, Svalbard. Lethaia 48(3):353–374

Kaim A, Jenkins RG, Hikida Y (2009) Gastropods from Late Cretaceous Omagari and Yasukawa hydrocarbon seep deposits in the Nakagawa area, Hokkaido, Japan. Acta Palaeontol Pol 54(3):463–490

Kelly M, Rowden AA (2019) New sponge species from hydrothermal vent and cold seep sites off New Zealand. Zootaxa 4576(3):401–438

Kiel S (2010) An Eldorado for paleontologists: the Cenozoic seeps of western Washington State, USA. In: Kiel S (ed) The vent and seep biota: aspects from microbes to ecosystems, Topics in geobiology, vol 33. Springer, Cham, Switzerland, pp 433–448

Koschinsky A, Billings A, Devey C et al (2006) Discovery of new hydrothermal vents on the southern Mid-Atlantic Ridge (4 S–10 S) during Cruise M68/1. InterRidge News 15:9–15

Pansini M, Morri C, Bianchi CN (2000) The sponge community of a subtidal area with hydrothermal vents: Milos Island Aegean Sea. Est Coast Mar Sci 51:627–635. https://doi.org/10.1006/ecss.2000.0674

Peckmann J, Thiel V, Michaelis W et al (1999) Cold seep deposits of Beauvoisin (Oxfordian; southeastern France) and Marmorito (Miocene; northern Italy): microbially induced authigenic carbonates. Int J Earth Sci 88:60–75

Pronzato R, Manconi R (2019) An overview on the freshwater sponge fauna (Demospongiae: Spongillida) of New Zealand and New Caledonia with new insights into *Heterorotula* from deep thermal vents of the Lake Taupo. J Nat Hist 53(35/36):2207–2229

Pronzato R, Pisera A, Manconi R (2017) Fossil freshwater sponges: taxonomy, geographic distribution, and critical review. Acta Palaeontol Pol 62:467–495

Rigby JK, Goedert JL (1996) Fossil sponges from a localized cold-seep limestone in Oligocene rocks of the Olympic Peninsula, Washington. J Paleontol 70:900–908

Rigby JK, Jenkins DE (1983) The Tertiary sponges *Aphrocallistes* and *Eurete* from western Washington and Oregon. Nat Hist Mus LA County Contrib Sci 344:1–13

Rubin-Blum M, Chakkiath P, Antony L et al (2019) Fueled by methane: deep-sea sponges from asphalt seeps gain their nutrition from methane-oxidizing symbionts. ISME J 13:1209–1225

Sen A, Åström EK, Hong W-L et al (2018) Geophysical and geochemical controls on the megafaunal community of a high Arctic cold seep. Biogeosciences 15:4533–4559. https://doi.org/10.5194/bg-15-4533-2018

Sitjà C, Maldonado FMC, Rueda JL (2019) Deep-water sponge fauna from the mud volcanoes of the Gulf of Cadiz (North Atlantic, Spain). J Mar Biol Ass UK 99:807–831. https://doi.org/10.1017/S0025315418000589

Staudigel H, Hart SR, Pile A et al (2006) Vailulu'u Seamount, Samoa: life and death on an active submarine volcano. Proc Natl Acad Sci 103(17):6448–6453. https://doi.org/10.1073/pnas.0600830103

Steiner M, Bernd E, Erdtmann D et al (2002) Submarine-hydrothermal exhalative ore layers in black shales from South China and associated fossils—insights into a Lower Cambrian facies and bio-evolution. Palaeogeog Palaeoclimat Palaeoecol 169(3/4):165–191

Tabachnick K, Janussen D, Menshenina L (2017) Cold biosilicification in Metazoan psychrophilic glass sponges. In: Ehrlich H (ed) Extreme biomimetics. Springer, Cham, pp 53–80

Tarasov VG, Gebruk AV, Shulkin VM et al (1999) Effect of shallow-water hydrothermal venting on the biota of Matupi Harbour (Rabaul Caldera, New Britain Island, Papua New Guinea). Cont Shelf Res 19:79–116. https://doi.org/10.1016/S0278-4343(98)00073-9

Thurber AR, Kröger K, Neira C et al (2010) Stable isotope signatures and methane use by New Zealand cold seep benthos. Mar Geol 272:260–269. https://doi.org/10.1016/j.margeo.2009.06.001

Vacelet J, Boury-Esnault N (2002) A new species of carnivorous deep-sea sponge (Demospongiae: Cladorhizidae) associated with methanotrophic bacteria. Cah Biol Mar 43:141–148

Vacelet J, Kelly MA (2014) New species of Abyssocladia (Porifera, Demospongiae, Poecilosclerida, Cladorhizidae) and other carnivorous sponges from the Far Eastern Solomon Islands. Zootaxa 3815(3):11. https://doi.org/10.11646/zootaxa.3815.3.4

Vacelet J, Segonzac M (2006) Porifera. In: Desbruyères D, Segonzac M, Bright M (eds) Handbook of deep-sea hydrothermal vent fauna. Land Oberösterreich, Biologiezentrum der Oberösterreichische Landesmuseen, Linz, pp 35–47

Vacelet J, Boury-Esnault N, Fiala-Médoni A et al (1995) A methanotrophic carnivorous sponge. Nature 377:296

Van Soest RWM, Boury-Esnault N, Vacelet J et al (2012) Global diversity of sponges (Porifera). PLoS One 7(4):e35105. https://doi.org/10.1371/journal.pone.0035105

Weinberg I, Glyzina O, Weinberg E et al (2004) Types of interactions in consortia of Baikalian sponges. In: Pansini M, Pronzato R, Bavestrello G et al (eds) Sponge science in the new millennium. Officine Grafiche Canessa Rapallo, Genova, pp 655–663

Chapter 10
Bivalvia in Ancient Hydrocarbon Seeps

Kazutaka Amano, Steffen Kiel, Krzysztof Hryniewicz, and Robert G. Jenkins

10.1 Introduction

Kazutaka AmanoSteffen Kiel, and Krzysztof Hryniewicz

Bivalves are one of the major animal classes inhabiting hydrothermal vents, hydrocarbon seeps, and whale-fall and wood-fall sites, because several bivalve clades developed symbiotic associations with chemotrophic bacteria that provide them with the bulk of their nutrition. Bivalves house the symbionts in their enlarged gills, either intra- or extracellularly. The symbionts are thiotrophic or methanotrophic gammaproteobacteria and are obtained either by environmental acquisition (also called horizontal transmission), or they are passed on from the parent to the offspring (called vertical transmission) (e.g., Duperron 2010; Taylor and Glover 2010) (Table 10.1).

In extant bivalves, chemosymbiosis has been documented in nine families or subfamilies. These are widely dispersed among the bivalve tree of life, showing that chemosymbiosis was repeatedly and independently acquired by several bivalve groups through Earth history (Figs. 10.1 and 10.2). The degree to which their

K. Amano (✉)
Department of Geoscience, Joetsu University of Education, Joetsu, Japan
e-mail: amano@juen.ac.jp

S. Kiel
Department of Palaeobiology, Swedish Museum of Natural History, Stockholm, Sweden
e-mail: steffen.kiel@nrm.se

K. Hryniewicz
Institute of Paleobiology, Polish Academy of Sciences, Warszawa, Poland
e-mail: krzyszth@twarda.pan.pl

R. G. Jenkins
College of Science and Engineering, Kanazawa University, Kanazawa, Japan
e-mail: robertgj@staff.kanazawa-u.ac.jp

A. Kaim et al. (eds.), *Ancient Hydrocarbon Seeps*, Topics in Geobiology 50,
https://doi.org/10.1007/978-3-031-05623-9_10

Table 10.1 Chemosymbiotic type and symbiotic acquisition methods in six extant bivalve families. References are in the text

Family	Symbiont type	Symbiont acquisition
Solemyidae	Thiotrophic	Mostly maternal
Nucinellidae	Potentially chemoautotrophic	?
Mytilidae	Thiotrophic, methanotrophic	Environmental
Lucinidae	Thiotrophic	Environmental
Thyasiridae	Thiotrophic	Environmental
Vesicomyidae	Thiotrophic	Mostly maternal

members depend on chemosymbiosis for nutrition varies considerably. Some have reduced their gut and rely largely or exclusively on their symbionts (Solemyidae, Nucinellidae, Bathymodiolinae, Pliocardiinae among Vesicomyidae), while others retain a functional gut and can derive a significant part of their nutrition from other sources (Lucinidae, Thyasiridae). Whereas all investigated lucinids have symbionts, most smaller species of Thyasiridae and Vesicomyinae do not harbor symbionts at all (Taylor and Glover 2010; Krylova and Sahling 2010). Among the Montacutidae, Basterotiidae, and Teredinidae, chemosymbiosis is rare and only documented in a single species of each family: *Syssitomya pourtalesiana* among the Montacutidae, *Atopomya dolobrata* among the Basterotiidae, and *Kuphus polythalamia* among the Teredinidae (Oliver et al. 2012; Oliver 2013; Distel et al. 2017, respectively).

Bivalves have a remarkable fossil history at seeps, with about 150 named species and many more reported in open nomenclature. In addition to the main groups of modern chemosymbiotic bivalves, all of which occur at fossil seeps, a few others have been abundant at seeps in the older geologic past, suggesting even further instances of the acquisition of chemosymbiosis in Earth history. These groups include the families Kalenteridae and Modiomorphidae among the Archiheterodonta (Hryniewicz et al. 2017b; Jenkins et al. 2018b) and a genus of the Anomalodesmata not assigned to any family (Kiel et al. 2017; Kiel 2018). Furthermore, chemosymbiosis was inferred for the large Permian bivalve *Shikamaia* of the family Alatoconchidae, which, however, does not occur in an ancient seep environment (Asato and Kase 2019). Some authors suggested or stressed that large Cretaceous inoceramids might have depended on the chemosymbiosis, based on their size, their mode of occurrence, and stable carbon isotope data (MacLeod and Hoppe 1992; Kauffman et al. 2007; Walliser et al. 2018, 2019). However, the isotope data are inconclusive (Grossman 1993), and the structure of well-preserved, phosphatized gills of *Inoceramus sutherlandi* and *Platyceramus* sp. is very different from that

rences of chemosymbiosis, ? chemosymbiosis suggested but questionable, (*)extinct family with assumed chemosymbiotic members. Chemosymbiosis is inferred for the Triassic anomalodesmatan species *Aksumya krystyni*, but it has not been assigned to any anomalodesmatan family; hence, a + sign is placed at the base of the anomalodesmatans. Note that among Mytilidae only members of the subfamily Bathymodilinae are chemosymbiotic, not the entire family. Kalenteridae are here placed basal to all other archiheterodonts except Modiomorphidae solely. Tree compiled from Bieler et al. (2014), Combosch et al. (2017), and Sato et al. (2020)

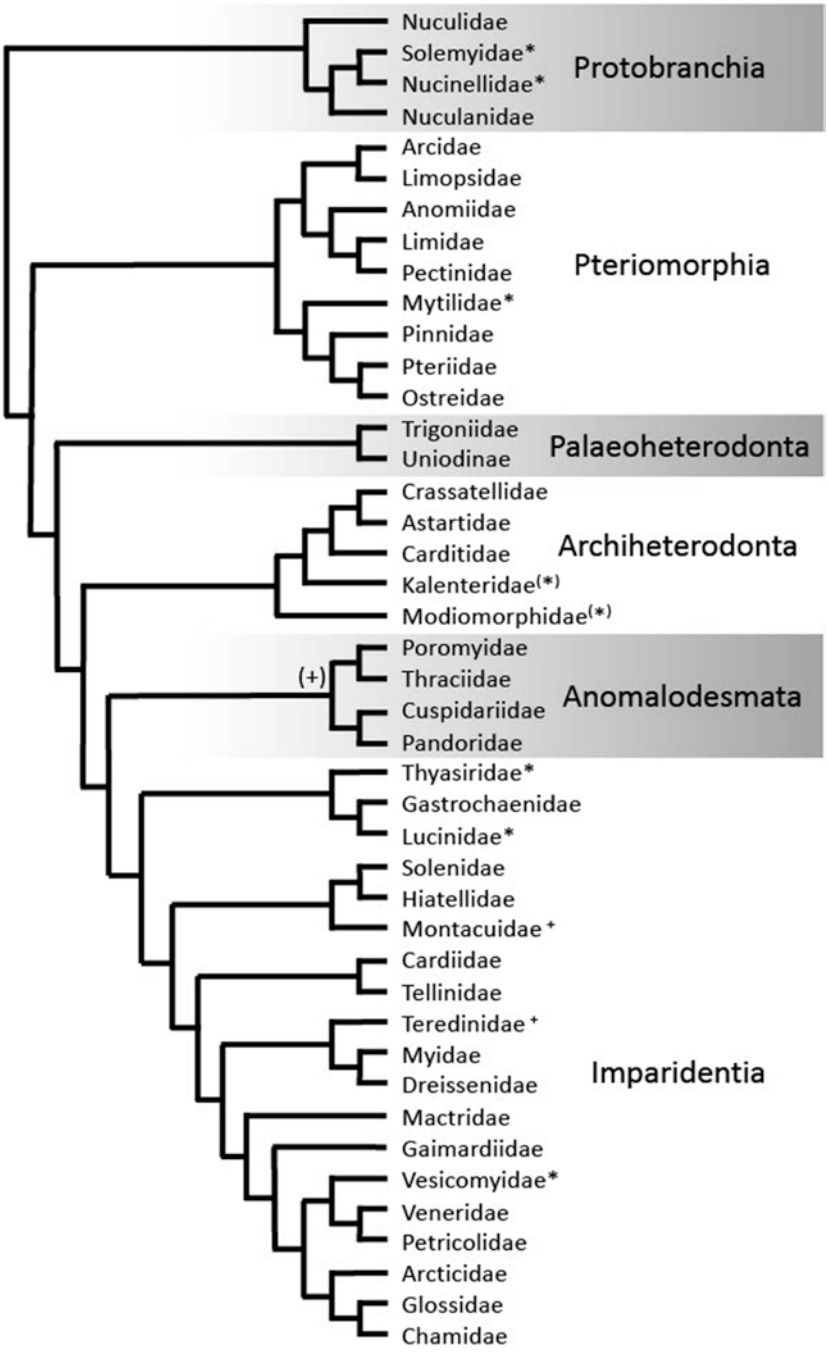

Fig. 10.1 Simplified phylogenetic tree of the Bivalvia showing the distribution of chemosymbiotic clades. *Families with chemosymbiosis as dominant feeding mode, + families with rare occur-

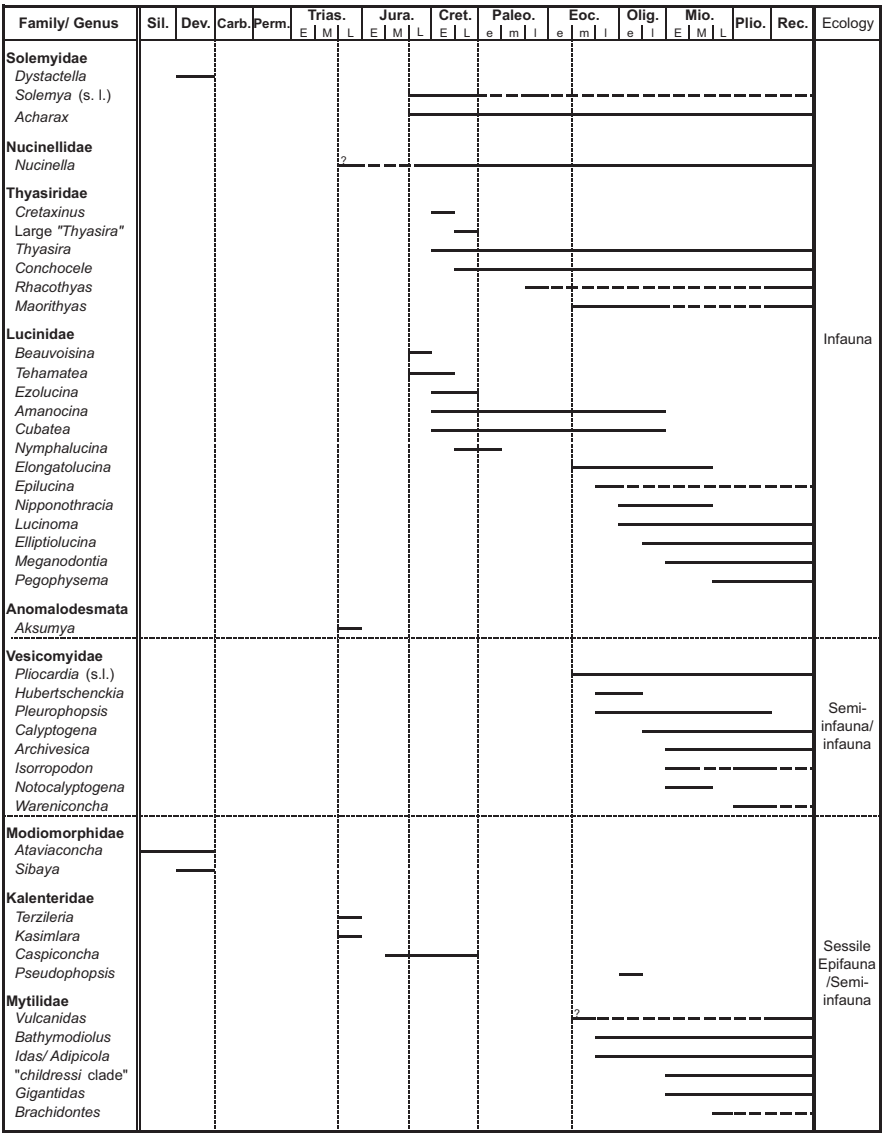

Fig. 10.2 Chronostratigraphic range chart of chemosymbiotic bivalve genera; solid lines show the confirmed fossil record, while dashed lines show the inferred occurrences

observed in the commonest extant chemosymbiotic bivalves (Knight et al. 2014). Hence it seems more plausible that inoceramids were filter-feeder (e.g., Kiel 2010a).

The recent findings of modiomorphid and kalenterid bivalves at Paleozoic and Mesozoic seeps have shed considerable doubt on an earlier hypothesis that brachiopods dominated the seeps in the Paleozoic and Mesozoic and were outcompeted by chemosymbiotic bivalves only from the Late Cretaceous onward (Campbell and

Bottjer 2006). Many of the modiomorphids and kalenterids co-occur with brachiopods at individual seep deposits: the Silurian-Devonian modiomorphid *Ataviaconcha* with the atrypid brachiopod *Septatrypa*, the Triassic kalenterids *Terzileria* and *Kasimlara* with the dimerelloid brachiopod *Halorella*, and the Cretaceous kalenterid *Caspiconcha* with the dimerelloid brachiopod *Peregrinella*. By reviewing the ecology and geochemical settings of these occurrences, Kiel and Peckmann (2019) put forward the new hypothesis that brachiopods and bivalve were partitioning resources: brachiopods relied on methane for nutrition via free-living methanotrophic bacteria, whereas the bivalves relied on sulfide via their sulfide-oxidizing symbionts.

10.2 Family Solemyidae

Krzysztof Hryniewicz

Members of family Solemyidae Gray, 1840, are one of the most basal bivalve clades (Fig. 10.1) with a fossil record going back to the Early Paleozoic. They have a global distribution and are known from the tropics to high latitudes from shallow waters down to ca. 5350 m water depth (Fujiwara 2003; Taylor and Glover 2010; Hansen et al. 2019). All representatives of the two recognized extant genera of *Solemya* and *Acharax* live in obligate symbiosis with sulfur-oxidizing gammaproteobacteria (Coan et al. 2000; Imhoff et al. 2003; Stewart and Cavanaugh 2006; Taylor and Glover 2010). The symbionts are stored intracellulary in bacteriocytes located at the abfrontal zones of ctenidial filaments (Dubilier et al. 2008; Taylor and Glover 2010). Symbiont transmission in solemyid varies depending on the species. For example, symbionts of *Solemya reidi* and *S. velum* are likely transmitted from parent to offspring (vertical transmission; Gustafson and Reid 1988; Cary 1994; Krueger et al. 1996; Russell et al. 2018), while symbionts of *S. pervernicosa* are more alike those of lucinid and thyasirid bivalves than to those of *S. reidi* and *S. velum*, suggesting environmental acquisition (horizontal transmission; Fujiwara et al. 2009).

Solemyids disperse via short-living, actively swimming pericalymma larvae similar to that of other protobranch bivalves (Gustafson and Reid 1986). They occur in a range of habitats, from seeps, vents, and oxygen-minimum zones to other reduced sediments at seagrass beds, sewage outfalls, and around whale carrions (Reid 1980; Métivier and Cosel 1993; Coan et al. 2000; Neulinger et al. 2006; Kamenev 2009; Fujiwara et al. 2009; Taylor and Glover 2010; Oliver et al. 2011; Sato et al. 2013; Walton 2015). *Solemya* commonly inhabits the shelf and slope depths (e.g., Taylor et al. 2008; Kamenev 2009; Rodrigues et al. 2011; cf. Sato et al. 2013), whereas *Acharax* is commonly associated with deeper settings (e.g., Neulinger et al. 2006). Solemyids are burrowers, often building a U- to Y-shaped burrow extending as deep as 30 cm below the sediment-water interface (Owen 1961; Stanley 1970; Reid 1980; Stewart and Cavanaugh 2006; Seike et al. 2012),

and can be occasionally trapped and killed in their burrows by rapidly deposited sediment cover (Hryniewicz et al. 2020). The species of *Solemya* living in settings with high organic matter content are often gutless (e.g., Reid 1980; Coan et al. 2000), while others have retained their gut and are capable of suspension feeding (e.g., Krueger et al. 1992; Taylor et al. 2008; Simone et al. 2015). Relatively little is known about the biology of *Acharax*, but the available data suggest that at least some species are gutless (Métivier and Cosel 1993). Solemyids are able to thrive at relatively low sulfide levels (Anderson et al. 1987; Conway et al. 1992), and at seeps, they have been recorded from the marginal zones (Sahling et al. 2002; Jenkins et al. 2007). Some species of *Solemya* are able to swim if disturbed (Reid 1980; Taylor et al. 2008).

10.2.1 Fossil Record and Evolution

The oldest known solemyids are *Dystactella ordovicicus* (Pojeta and Runnegar 1985) and *Dystactella aedilis* (Isakar and Sinitsyna 1985) from the Middle Ordovician of Estonia. They belong to the branch of anteroventrally expanded solemyids that has gone extinct in the Paleozoic. The extant genera *Solemya* and *Acharax* belong to the branch of elongated solemyids, known at least since the Devonian (Meek 1873). A possible ancestor of this branch is the anteriorly elongated genus *Psiloconcha* Ulrich, 1894, of Ordovician age. The oldest solemyid from a seep deposit is *Dystactella*? *eisenmanni* Hryniewicz, Jakubowicz, Belka, Dopieralska, and Kaim, 2017, from a Middle Devonian seep carbonate in Morocco (Aitken et al. 2002; Hryniewicz et al. 2017b). *Solemya* and *Acharax* first appeared at seeps in the Jurassic (Hryniewicz et al. 2014; Kaim et al. 2014). An alleged solemyid species has been found in an early Carboniferous (Viséan) seep in Germany (Peckmann et al. 2001). The oldest undoubted *Solemya* species at seep deposits include *Solemya* (*Petrasma*) cf. *woodwardiana* from the latest Jurassic-earliest Cretaceous shallow-water seeps in Svalbard (Fig. 10.3a–d[1]; Hryniewicz et al. 2014, 2015a), and *Solemya rossiana* has been reported from latest Maastrichtian (Late Cretaceous) shallow-water seeps in Snow Hill Island, Antarctica (Little et al. 2015).

1 **Institutional Abbreviations in the Figure Captions**

GZG = Geowissenschaftliches Zentrum, University of Göttingen, Germany
JUE = Joetsu University of Education, Japan; collection now at the University Museum of University of Tokyo, Japan
PMO = Natural History Museum, University of Oslo, Norway
PRI = Paleontological Research Institution, Ithaca, USA
UMUT = University Museum of Tokyo University, Japan
UOA = University of Auckland, New Zealand
USNM = Smithsonian Natural History Museum, Washington DC, USA
UWBM = University of Washington, Burke Museum, Seattle, USA

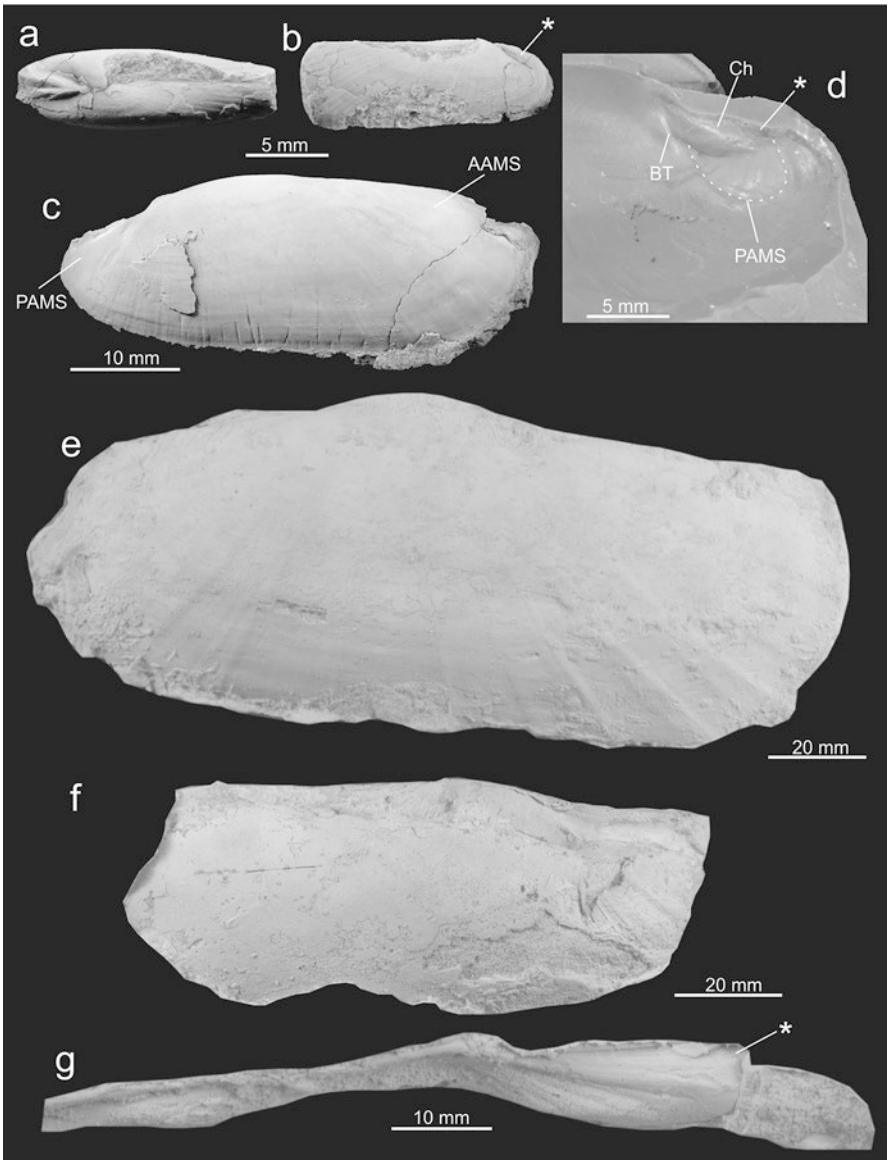

Fig. 10.3 Solemyidae. (**a**–**d**) *Solemya* (*Petrasma*) cf. *woodwardiana* (Leckenby 1859) from a latest Jurassic-earliest Cretaceous seep site on Spitsbergen, Svalbard. (**a**, **b**) PMO 224.956: the asterisk indicates the position of the posterior adductor muscle scar (PAMS) extending into the shell dorsally of the chondrophore (Ch). (**c**, **d**) PMO 217.249: (c) specimen displaying both the anterior and posterior adductor muscle scars (AAMS and PAMS); (**d**) rubber cast of an internal mold showing PAMS supported on buttress (BT). (**e**–**g**) *Acharax yokosukaensis* (Kanie and Kuramochi, 1995) from Early Miocene seep sites in Ibaraki Prefecture, Honshu, Japan. (**e**) JUE no. 15887-2; (**f**) JUE no. 15887-4; (**g**) JUE no. 15887-2; the asterisk indicates the protruding external ligament attachment. (**a**–**d**: Hryniewicz et al. 2014; **e**–**g**: Amano and Ando 2011)

Solemya sp. was described from Paleocene wood-fall communities in Spitsbergen Island (Hryniewicz et al. 2019). The oldest species described as *Acharax* is *Acharax stantoni* from the Late Jurassic-Early Cretaceous (Tithonian-Albian) seeps of California (Kaim et al. 2014). Further Cretaceous species of *Acharax* found at seeps are Early Cretaceous (Albian) *Acharax mikasaensis* from the Ponbetsu seep site and the Campanian *Acharax cretacea* from the Yasukawa seep site, both in Hokkaido (Kanie and Nishida 2000; Kiel et al. 2008). Various species of *Acharax* are known also for seeps in the Paleogene (e.g., Amano et al. 2013a, b), the Neogene (e.g. Amano and Ando 2011; Kiel and Taviani 2018), and the late Pleistocene off of Svalbard (Hansen et al. 2019). The largest specimen of *Acharax* at a seep deposit reached at least 296 mm in length and is of the latest Early Miocene age (Fig. 10.3e–g; Amano and Ando 2011). In addition to the seep occurrences listed above, ancient *Solemya* is reported from shelfal siliciclastics, especially those organic-rich (e.g., Roemer 1839; Duff 1978; Kiel 2010a), while *Acharax* is more typical of deep-water environments (e.g., Vokes 1955; Taviani et al. 2011; Kaim et al. 2014).

10.2.2 Classification and Shell Characters

Two extant genera are recognized among Solemyidae, *Solemya* Lamarck, 1818, and *Acharax* Dall, 1908, and are well supported by molecular data (Sharma et al. 2013; Fukasawa et al. 2017). Distinguishing *Solemya* and *Acharax* based on shells requires information on the ligament and the internal radial rib in front of the posterior adductor muscle scar (Taylor et al. 2008; Kamenev 2009; Oliver et al. 2011). Most shell characters, i.e., the elongated shell shape, a thick periostracum, and broad but shallow radial ribs are present in both genera; thus, the easiest way to distinguish *Solemya* from *Acharax* is by the ligament; *Solemya* has an internal ligament set in a chondrophore (Fig. 10.3a–d), whereas *Acharax* has an external ligament supported by a thickened shell margin (Fig. 10.3e–g). Although the difference is noticeable on well-preserved shells, fossils are usually incomplete or partial internal molds lacking the ligament margin (Hryniewicz et al. 2014), rendering a generic identification of the specimens problematic. The internal features of both genera are similar and should not be used for generic distinction (e.g., Vokes 1955; Kamenev 2009; Oliver et al. 2011).

The genus *Solemy*a is subdivided into the subgenera *Solemya* s.s.; *Solemyarina* Iredale, 1931; *Petrasma* Dall, 1908a; *Zesolemya* Iredale, 1939; *Austrosolemya* Taylor, Glover, and Williams, 2008; and *Pseudacharax* Huber, 2010, based on the difference in length and character of the anterior ligament extension, relation of the chondrophore to posterior adductor muscle scar, and presence of a buttress, supporting the anterior margin of posterior adductor muscle scar. A detailed discussion and table of the differences between particular subgenera of *Solemya* were presented by Taylor et al. (2008), Kamenev (2009), Oliver and Taylor (2012), and Hryniewicz et al. (2014). The Paleozoic genera *Dystactella* Hall and Whitfield, 1872, and

Clinopistha Meek and Worthen, 1870, have commarginal ornament and an external ligament. They differ by the rate of anterioventral expansion: weak in *Dystactella* and strong in *Clinopistha* (Pojeta 1988).

10.3 Family Nucinellidae

Kazutaka Amano and Krzysztof Hryniewicz

The family Nucinellidae Vokes, 1956, is considered either as the sister taxon to Solemyidae (Fig. 10.4) or at least closely related to it (Sharma et al. 2013). The species of *Nucinella* are shallow burrowers and are not obligate vent and seep inhabitants but also occur in "normal" marine sediments of 6 m to 3500 m in depth (e.g., Matsukuma et al. 1982; La Perna 2005; McLeod et al. 2010; Oliver and Taylor, 2012). Chemosymbiosis has been suggested for some species of *Nucinella* based on their reduced or absent digestive tract (e.g., Kuznetsov and Shileyko 1984; Reid 1998). These suggestions were partially confirmed by the accumulation of light carbon in the tissues of *Nucinella maoriana*, similar in magnitude to that of species of Thyasiridae and Solemyidae with confirmed chemosymbiosis found in their immediate surroundings (McLeod et al. 2010). Oliver and Taylor (2012) found potentially chemoautotrophic bacteria in the gills of the modern species *Nucinella owenensis* and *Huxleyia habooba*, which were recovered from the oxygen-minimum zone in the Arabian Sea off of southern Oman. Thus, *Nucinella* potentially is a member of chemosynthetic communities in seep sites.

10.3.1 Fossil Record and Evolution

The oldest fossil *Nucinella* species are *N. taylori* and *N. nakremi* from earliest Triassic marine sediments in Spitsbergen (Foster et al. 2017). A very small (~2 mm long) *Nucinella*? sp. has been reported from the early Carnian (earliest Late Triassic)

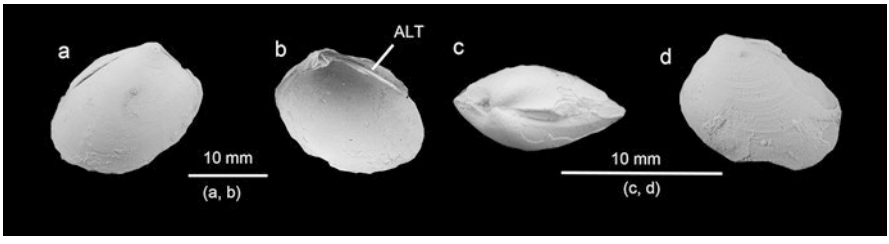

Fig. 10.4 Nucinellidae. (**a**–**d**) *Nucinella gigantea* Amano, Jenkins, and Hikida, 2007, from a Campanian seep site in Nakagawa Town, Hokkaido, Japan. (**a**, **b**) UMUT MM29245; Holotype; *ALT* anterior lateral tooth. (**c**, **d**) UMUT MM29248; Paratype. (**a**–**d**: Amano et al. 2007)

"normal" marine Cassian Formation from Northern Italy (Nützel and Kaim 2014), but the generic assignment of this species is uncertain. Later Mesozoic and Cenozoic non-seep species of *Nucinella* are associated with a variety of shallow to deep marine sediments (e.g., Vokes 1956; Clausen and Wignall 1990; Wignall et al. 2005). Seep species of *Nucinella* are generally larger than their non-seep relatives and are known since the Jurassic and possibly the Triassic. Peckmann et al. (2011) illustrated "a possible *Nucinella*" from a Late Triassic (Norian) seep site in Oregon. However, as the hinge of this species is unknown, it is difficult to judge whether this is the oldest record of this genus from seep deposits. Hammer et al. (2011) illustrated *Nucinella* sp. from uppermost Jurassic-lowermost Cretaceous seep carbonates in Svalbard. This oldest confirmed species of *Nucinella* has been described as *N. svalbardensis* (maximum length = 23 mm) by Hryniewicz et al. (2014). Coeval but smaller species of *Nucinella* have recently been reported from the latest Jurassic seep deposits from Novaya Zemlya in Arctic Russia (Hryniewicz et al. 2015b). As-yet undescribed species of *Nucinella* have been reported from a Barremian (Early Cretaceous) seep site in California (Kaim et al. 2014) and from the mid-Cretaceous Awanui II deposit on the North Island of New Zealand (Kiel et al. 2013). The Late Cretaceous *Nucinella gigantea* (maximum length = 18 mm) was described from Cenomanian and Campanian seep deposits on Hokkaido by Amano et al. (2007a) and Kiel et al. (2008) (Fig. 10.4). Amano et al. (2013b) found one large specimen of *Nucinella* sp. (23 mm in length) in the upper Eocene to lower Oligocene Tanamigawa Formation in Honshu. Moreover, one fossil specimen (14 mm in length) of *Nucinella* sp. was described along with other chemosymbiotic species from the Lower Miocene Kurosedani Formation in Toyama Prefecture, Honshu (Amano et al. 2019b). These records indicate that large *Nucinella* species were common in the latest Jurassic-earliest Cretaceous boreal shallow-water seeps (Hryniewicz et al. 2014, 2015a, b) and the Late Cretaceous Hokkaido seeps (Amano et al. 2007a, b; Kiel et al. 2008) but rather rare in Cenozoic fossil chemosynthetic communities.

10.3.2 Classification and Shell Characters

The genus *Nucinella* Wood, 1851, is characterized by usually small (a few mm in length) nuculiform shell with a smooth surface except for growth lines, a continuous row of taxodont teeth in the cardinal area, a long anterior lateral tooth, and one adductor muscle scar (Fig. 10.4). The largest living species, *N. boucheti* La Perna, 2005, reaches 25 mm in length. *Huxleyia* A. Adams, 1860, differs from *Nucinella* by having cardinal taxodont teeth only anterior to the umbo, posteriorly bound by a deeply sunken resilium. *Nucinella* is easily discriminated from smooth-shelled nuculids such as *Leionucula* by having a long anterior lateral tooth and one adductor scar only and by lacking a nacreous inner layer.

10.4 Family Mytilidae

Steffen Kiel and Kazutaka Amano

Chemosymbiotic species among the Mytilidae occur only in a single subfamily, the Bathymodiolinae. Bathymodiolins range in size from a few mm to approximately 360 mm in length and have colonized a broad range of chemosynthetic environments including vents, seeps, whale fall, and wood fall (Duperron 2010; Lorion et al. 2013). Most bathymodiolins are epifaunal, although some large species live half-buried in the sediment. Typically, methane seeps and hydrothermal vents are inhabited by large species, while wood and bones are colonized by small species. Bathymodiolins disperse via planktotrophic larvae, some of which are able to stay as long as 17 months in surface waters and feed on phytoplankton (Arellano and Young 2009; Arellano et al. 2014; Laming et al. 2015, 2018). After settling on the seafloor and metamorphosis, juveniles undergo a transformation from heterotrophy to chemosymbiosis, via mixotrophy, associated with increasing body size and gill proliferation (Laming et al. 2018). Although juveniles need to attach themselves to hard substrates with byssus threads, larger individuals can cut the byssus and actively move around to find the optimal position for the uptake of reduced compounds (Duperron 2010).

In contrast to all other groups of chemosymbiotic bivalves, bathymodiolins take up the sulfides and other reduced compounds via their inhalant current (Duperron 2010). Also unique among chemosymbiotic bivalves is that the bathymodiolins can harbor methanotrophic symbionts, either exclusively or in addition to the sulfur oxidizers (Childress et al. 1986). All other chemosymbiotic bivalve families rely solely on sulfur-oxidizing symbionts (Dubilier et al. 2008). While the acquisition of sulfur-oxidizing symbionts is considered an apomorphy of the group and is linked to its origin, methanotrophic symbionts were apparently acquired only much later in the evolutionary history of bathymodiolins (Lorion et al. 2013). Bathymodiolins have a wide range of symbiotic associations, with most symbionts being either sulfur or methane oxidizers, although some species are known to host as many as six different symbionts, including methyl and hydrogen oxidizers (Duperron et al. 2008; Duperron 2010; Petersen et al. 2011). The symbionts are housed in the gills, where they are located either extra- or intracellular. The phylogeny of the group suggests that extracellular symbiont location is the ancestral condition, whereas the more integrated, intracellular symbiont location is the derived condition (Lorion et al. 2013). Methanotrophic symbionts are only known from species with intracellular symbiont location, suggesting that the ability to house symbionts intracellularly is an evolutionary prerequisite for the acquisition of methanotrophic symbionts (Lorion et al. 2013). The symbionts are environmentally acquired after metamorphosis (Laming et al. 2018), and both the sulfur oxidizers and the methane oxidizers are gammaproteobacteria (Duperron et al. 2006). The small wood-inhabiting species *Idas argenteus* apparently lost its symbionts and turned to preying on larvae of

xylophagain (wood-feeding) bivalves (Ockelmann and Dinesen 2011; Rodrigues et al. 2015), indicating that chemosymbiosis is not an evolutionary one-way street.

A few non-chemosymbiotic mytilid species have been reported from fossil chemosynthesis-based habitats, including *Musculus*? sp. from Paleocene wood-fall communities in Spitsbergen (Hryniewicz et al. 2019), *Brachidontes* sp. from Miocene seep deposits in Cuba and Venezuela (Kiel and Hansen 2015), and *Samiolus iohannesbaptistae* from a Late Miocene "Calcari a *Lucina*" seep deposit in northern Italy (Kiel and Taviani 2017).

10.4.1 Fossil Record and Evolution

Bathymodiolins first appear in the fossil record in the middle Eocene (Kiel and Amano 2013). A time-calibrated molecular phylogenetic tree indicated a latest Cretaceous or early Cenozoic origin followed by a major radiation during the late Eocene-early Oligocene, possibly because the increased global circulation of cold deep water after the initial glaciation of Antarctica slowed larval metabolic rates, thereby increasing their longevity and dispersal capabilities (Lorion et al. 2013). Based on the phylogenetically basal position of various wood- and bone-inhabiting species, the "wooden steps" hypothesis was proposed, which claims that bathymodiolins first adapted to the low sulfide concentrations at sunken wood and bones on the seafloor and subsequently adapted to the higher sulfide concentrations at methane seeps and hydrothermal vents (Distel et al. 2000; Smith and Baco 2003). The general pattern of wood- and bone-inhabiting species in basal positions and the vent- and seep-inhabiting species in more derived positions has been confirmed by most subsequent molecular phylogenetic studies (Samadi et al. 2007; Lorion et al. 2008; Miyazaki et al. 2010; Thubaut et al. 2013). However, from the paleontological point of view, the role of whale carcasses as evolutionary stepping stones is less clear. The oldest records of bathymodiolins are from middle Eocene seep deposits, while examples from whale falls (and wood falls) are so far only known from the late Eocene onward (Kiel and Goedert 2006a, b; Kiel 2008). Large marine reptile bones in the late Mesozoic supported a similar suit of taxa as early Cenozoic whale falls, but lack bathymodiolins or other epifaunal chemosymbiotic bivalves (Kaim et al. 2008; Jenkins et al. 2017). Also, wood-fall communities are known from late Mesozoic deep-water deposits, but again, bathymodiolins or other epifaunal chemosymbiotic bivalves are missing from these communities (Kiel et al. 2009; Kaim 2011).

10.4.2 Classification and Shell Characters

Based on molecular phylogenetic work, it is now well established that all chemosymbiotic mytilids inhabiting vents, seeps, bones, and wood form a single monophyletic clade, the bathymodiolins (Distel et al. 2000; Samadi et al. 2007; Miyazaki

et al. 2010; Lorion et al. 2013; Thubaut et al. 2013; Liu et al. 2018). Their closest relative among the Mytilidae is *Modiolus modiolus* (although the sample size is limited), with which bathymodiolins share similarly shaped shells including the morphology of the prodissoconch, as well as a similar shell microstructure (Génio et al. 2012). Within the bathymodiolins, genera are difficult to distinguish based on shell characters, especially among the small taxa. The larger genera may be distinguished using the morphology of muscle attachment scars, although these are typically very weak and are rarely found in fossils older than Miocene.

1. *Bathymodiolus* Kenk and Wilson, 1985: Large mussels with the general shape of the horse mussel *Modiolus* found at hydrothermal vents and methane seeps have initially been assigned to the genus *Bathymodiolus*, based on *B. thermophilus* from the first known vent communities on the Galapagos Ridge (Kenk and Wilson 1985). With increasing numbers of species being discovered at vents and seeps worldwide, molecular work indicated that these large-sized *Bathymodiolus* species belong to at least two distinct clades: *Bathymodiolus* (sensu stricto) and the so-called *childressi* clade, a group of species closely related to *Bathymodiolus childressi* from the Gulf of Mexico. A distinction of the two clades on conchological ground may be possible because they differ by the structure of the posterior retractor muscle scars (see discussion of the "*childressi* clade"). *Bathymodiolus* may be distinguished from *Modiolus* based on its very early juvenile shell, which is triangular in *Bathymodiolus* and more modioliform (more elongate) in *Modiolus*. Based on this character, the Oligocene *Modiolus willapaensis* Squires and Goedert, 1991, was the first fossil species to be identified as belonging to *Bathymodiolus* (Kiel 2006). With the distinction between *Bathymodiolus* (s.s.) and the *childressi* clade being difficult to make in the absence of well-preserved muscle scars, many fossil mussels from methane seep deposits of the Cenozoic age are simply referred to as *Bathymodiolus* (sensu lato). These include several species from the Eocene to Oligocene of Washington State, USA (Kiel and Amano 2013); *Bathymodiolus* (s.l.) *inouei* Amano and Jenkins, 2011, from the late Eocene to Oligocene of Japan (Fig. 10.5c, e, g; Amano et al. 2013b); and *B.* (s.l.) *palmarensis* from the Oligocene of Colombia, as well as several Miocene species from the Caribbean region, Italy, Japan, and New Zealand (Gill et al. 2005; Amano et al. 2010; Kiel et al. 2010; Kiel and Hansen 2015; Kiel and Taviani 2017).
2. *Gigantidas* Cosel and Marshall, 2003: Based on *Gigantidas gladius* Cosel and Marshall, 2003, from extant vents on the Kermadec Ridge north of New Zealand, this genus includes large and very elongate shells and can be separated from *Bathymodiolus* (s.l.) by its elongated shell and strongly concave ventral margin. A single fossil species, *Gigantidas coseli* Saether, Little, Campbell, Marshall, Collins and Alfaro, 2010, has been described from Early to Middle Miocene seep deposits on North Island, New Zealand (Fig. 10.5i; Saether et al. 2010).
3. The "*childressi* clade": *Bathymodiolus childressi* Gustafson, Turner, Lutz and Vrijenhoek, 1998, from methane seeps in the Gulf of Mexico was only hesitantly assigned to *Bathymodiolus* because molecular phylogenetic data indicated that it

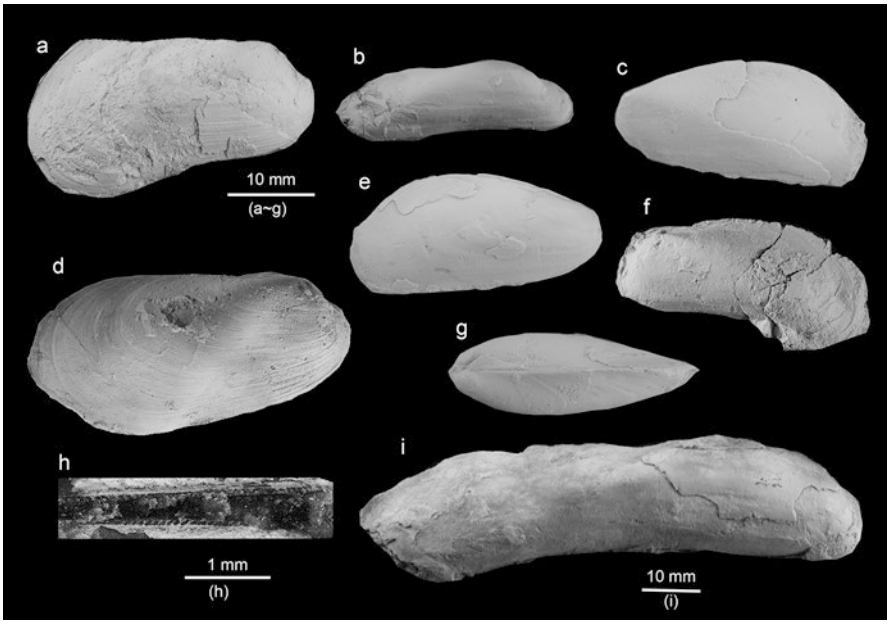

Fig. 10.5 Mytilidae (Bathymodiolinae). (**a**) *Bathymodiolus* (s.l.) *heretaunga* Saether, Little, Campbell, Marshall, Collins, and Alfaro, 2010, from the Middle Miocene Moonlight North seep site in North Island, New Zealand. (**b**) *Adipicola chikubetsuensis* Amano, 1984, from an early Middle Miocene whale-fall site in Shosanbetsu village, Hokkaido, Japan; JUE no. 15002; Holotype. (**c**, **e**, **g**) *Bathymodiolus* (s.l.) *inouei* Amano and Jenkins, 2011, from an early Oligocene seep site in Urahoro Town, Hokkaido, Japan; JUE no. 15873; Holotype. (**d**) *Vulcanidas*? *goederti* Kiel and Amano, 2013, from a middle Eocene seep site in Washington State, USA; UWBM 98890; Holotype. (**f**) *Adipicola* sp. from a Middle Miocene whale-fall site in Nupinai, Hokkaido, Japan. (**h**) *Idas*? *olympicus* Kiel and Goedert 2007, from an early Oligocene seep site in Washington State, USA; UWBM 98918. (**i**) *Gigantidas coseli* Saether, Little, Campbell, Marshall, Collins, and Alfaro, 2010, from the Middle Miocene Moonlight North seep site in North Island, New Zealand. (**b**: Amano 1984; **c**, **e**, **g**: Amano and Jenkins 2011; **d**, **h**: Kiel and Amano 2013; **f**: Amano et al. 2007; **a**, **i**: collection by Amano)

belonged to a different clade within the Bathymodiolinae than *B. thermophilus* (Gustafson et al. 1998). Among members of the "*childressi* clade," the posterior byssal retractors form a continuous scar united with the posterior adductor muscles, reflecting the multibundle posterior byssal retractor complex diagnostic of modern species of this clade (Cosel 2002; Saether et al. 2010). This feature distinguishes the "*childressi* clade" from *Bathymodiolus* (s.s.), in which the anterior and posterior portions of the posterior byssal retractor scars, are well separated. Although several authors suggested establishing a new genus for the "*childressi* clade" (Gustafson et al. 1998; Jones and Vrijenhoek 2006), others suggested including this clade in *Gigantidas* (Thubaut et al. 2013; Xu et al. 2019; Jang et al. 2020). A single fossil species, *Bathymodiolus* (s.l.) *heretaunga* Saether, Little, Campbell, Marshall, Collins and Alfaro, 2010 (Fig. 10.5a), from the

Miocene of New Zealand, has been assigned to the "*childressi* clade" (Saether et al. 2010).

4. *Vulcanidas* Cosel and Marshall, 2010: This phylogenetically basal genus is based on *Vulcanidas insolatus* Cosel and Marshall, 2010, from vents north of New Zealand. Its shell is similar in shape to that of *Bathymodiolus* (s.l.), and it may be distinguished from other bathymodiolins by its distinct ridge running from the beak to the posterior ventral margin, with a concave margin anterior to it and expanding posterior shell portion behind this ridge. The only fossil record so far is *Vulcanidas*? *goederti* Kiel and Amano, 2013 (Fig. 10.5d), from seep carbonates of the middle Eocene Humptulips Formation in Washington State, which is also the oldest fossil record of the bathymodiolins.
5. *Idas* Jeffreys, 1876/*Adipicola* Dautzenberg, 1927: Numerous small (<20 mm) mussels living on wood, bone, and other organic substrates in deep water have been variously assigned to *Adipicola* and *Idas* (Dell 1987). Molecular phylogenetic work has shown that these species are found within various clades among the bathymodiolins and, furthermore, that they show a wide range of morphologic diversity. This makes it currently very difficult to assign small, fossil bathymodiolins to either of these genera. Two generic names (*Lignomodiolus* and *Nypamodiolus*) have prematurely been applied to these taxa by Thubaut et al. (2013) and have since been used in other publications (Génio et al. 2015; Samadi et al. 2015; Liu et al. 2018; Xu et al. 2019). However, the two genera have not been formally described, and no type species have been designated; hence, the names are *nomen nuda* and are presently not available. Morphologically, *Idas* may be separated from *Adipicola* by small crenulations on its hinge, which are absent in *Adipicola* (Fig. 10.5h). A few fossil records of these taxa are known, the oldest being *Idas*? *olympicus* Kiel and Goedert, 2007, from late Eocene to Oligocene deep-water whale-fall and wood-fall communities in Washington State, USA (Goedert et al. 1995; Kiel and Goedert 2007). Further records are *Adipicola chikubetsuensis* (Amano, 1984) from an early Middle Miocene whale fall in northern Hokkaido, Japan (Fig. 10.5b; Amano and Little 2005); *Adipicola* sp. from a Middle Miocene whale fall in eastern Hokkaido, Japan (Fig. 10.5f; Amano et al. 2007a, b); and *Adipicola* sp. from a late Middle to early Late Miocene whale fall in central Hokkaido (Jenkins et al. 2018a). *Adipicola apenninica* occurs at a Middle Miocene whale fall (Danise et al. 2016), and *Idas* sp. was reported from Pliocene whale and wood falls in northern Italy (Bertolaso and Palazzi 1994). *Idas* sp. was also illustrated from a Pliocene shallow-water whale fall in northern Italy (Danise et al. 2010). Under certain circumstances, possibly the absence of large bathymodiolins, extant *Idas* colonizes methane seeps, for example, in the Mediterranean Sea (Olu et al. 2004). Fossil seep carbonates with *Idas*? *olympicus* have been reported from the Oligocene of western Washington State (Kiel and Amano 2013); *Idas* aff. *tauroparva* is known from the Late Miocene "Calcari a *Lucina*" in northern Italy (Kiel et al. 2018); and a single specimen of *Idas* sp. was found in early Oligocene seep carbonate in northern Peru (Kiel et al. 2020a, b).

10.5 Families Modiomorphidae and Kalenteridae

Robert G. JenkinsKrzysztof Hryniewicz, and Steffen Kiel

The Modiomorphida is a heterogeneous clade of bivalves ranging from the Ordovician to the Miocene, and both its internal and external phylogenetic relationships are controversial. For the sake of this review of Modiomorphida from fossil vents and seeps, we consider the clade related to Carditida (cf. Kaim and Schneider 2012; Jenkins et al. 2013) rather than to Anomalodesmata (Morris et al. 1991) or to Cardiida (Carter et al. 2011). Among the traditionally defined families of Modiomorphida, only the Modiomorphidae Miller, 1877, and Kalenteridae Marwick, 1953, include taxa at fossil vents and seeps.

Although Modiomorphida are extinct and there is no direct proof for chemosymbiosis in the fossil record, the vent- and seep-inhabiting taxa are generally assumed to have been chemosymbiotic based on the actualistic principle. Modiomorphida at fossils vents and seeps are often large or abundant, and all bivalves with these traits at modern vents and seeps are chemosymbiotic. Hence it seems a fair assumption that also the vent- and seep-inhabiting Modiomorphida were chemosymbiotic (Kelly et al. 2000; Hryniewicz et al. 2017b; Jakubowicz et al. 2017; Jenkins et al. 2013, 2018b; Kiel et al. 2017; Kiel and Peckmann 2019).

Modiomorphida have modioliform shells (hence the name), some species exceed 300 mm in length, and several of the seep-inhabiting taxa are quite elongated, showing a striking resemblance to elongate extant bathymodiolins and vesicomyids (Hryniewicz et al. 2017b). Furthermore, some species of the kalenterid *Caspiconcha* were found in densely packed clusters and positioned at an angle of ~30° relative to bedding plane (Kelly et al. 2000; Kiel and Peckmann 2008) and possess a gape at the anterior ventral shell margin (Jenkins et al. 2013). These traits indicate that seep-inhabiting Modiomorphida had a semi-infaunal lifestyle to ensure access to both sulfide from within the sediment and oxygen from the water column, as in extant vesicomyids and some bathymodiolins (Jenkins et al. 2013; Hryniewicz et al. 2017b; Krylova et al. 2010).

10.5.1 Fossil Record and Evolution

Vent- and seep-inhabiting members of the Modiomorphidae are known from the Silurian and Devonian, with the Silurian *Ataviaconcha* sp. from the El-Borj seep deposit in Morocco being the as-yet earliest record of bivalves from chemosynthesis-based ecosystems (Jakubowicz et al. 2017). The Kalenteridae include four genera occurring at fossil seeps, *Terzileria* and *Kasimlara* from the Late Triassic, *Caspiconcha* from the Late Jurassic to Late Cretaceous, and *Pseudophopsis* from the Eocene to the early Oligocene. This stratigraphically patchy distribution of different kalenterid genera inhabiting seeps raised the question if these genera are repeated

radiations of various kalenterid lineages that convergently developed similar morphological adaptations to this habitat (the "repeated colonization hypothesis"), or if they are members of a single phylogenetic lineage that continuously inhabited deep-sea hydrocarbon seeps (the "single lineage hypothesis") (cf. Kiel 2018). In favor of the first hypothesis, Hryniewicz et al. (2017b) argued that the elongate modioliform shell shape is a necessary adaptation to reach sulfide deep in the sediment while staying in contact with oxygenated bottom waters, possibly enhanced by competition with infaunal chemosymbiotic species. A possible counter-argument is that the repeated development of elongate shells occurs also among vesicomyids (with very elongate specimens among the genera *Pleurophopsis*, *Archivesica*, and *Abyssogena*) and bathymodiolins (i.e., *Gigantidas* and *Bathymodiolus boomerang*), both of which are largely restricted to chemosynthesis-based ecosystems. However, especially the early Mesozoic, fossil record of seeps is still very patchy, and more data and phylogenetic analyses are needed to solve this issue.

The kalenterid genus *Caspiconcha* has a prominent place in the history of research on the vent and seep fauna. Two Cretaceous members of *Caspiconcha* have been misidentified as vesicomyids or mytilids in the earlier literature, resulting in considerable misinterpretations of the fossil ranges of these modern chemosynthetic bivalve clades (e.g., Little and Vrijenhoek 2003; Kiel and Little 2006). These cases are the alleged mytilid *Modiola major* from seep deposits in California, USA (Fig. 10.6c, d), and the alleged vesicomyid "*Calyptogena* sp." from Hokkaido, Japan. These two species are now recognized as *Caspiconcha major* and *Caspiconcha lastsamurai*, respectively (Amano and Kiel 2007b; Kiel and Peckmann 2008; Jenkins et al. 2013, 2018b).

10.5.2 Classification and Shell Characters

Family Modiomorphidae

1. *Ataviaconcha* Hryniewicz, Jakubowicz, Belka, Dopieralska, and Kaim, 2017, is based on *A. wendti* (Hryniewicz et al. 2017b) from the Middle Devonian Hollard Mound seep deposit in Morocco. Its shell is elongated and modioliform with enlarged anterior and posterior lobes and reaches >100 mm in length. Larger specimens have a boomerang-like shape with a deep ventral sinus. Both anterior and posterior adductor muscle scars are present, and it lacks the "caspiconchid process" close to the anterior shell margin (see *Caspiconcha*). A weak socket is present in the cardinal area of the right valve; the shell is otherwise edentulous. At least some of these morphological features, such as large, elongated modioliform shell with enlarged anterior and posterior lobes, are also seen in the Silurian *Ataviaconcha* sp. from El-Borj (Jakubowicz et al. 2017). The genus hence ranges from the late Silurian to the Middle Devonian.
2. *Sibaya* Little, Maslenikov, Morris, and Gubanov, 1999, is based on the sole species *Sibaya ivanovi*, which is known exclusively from the Devonian Sibay vent

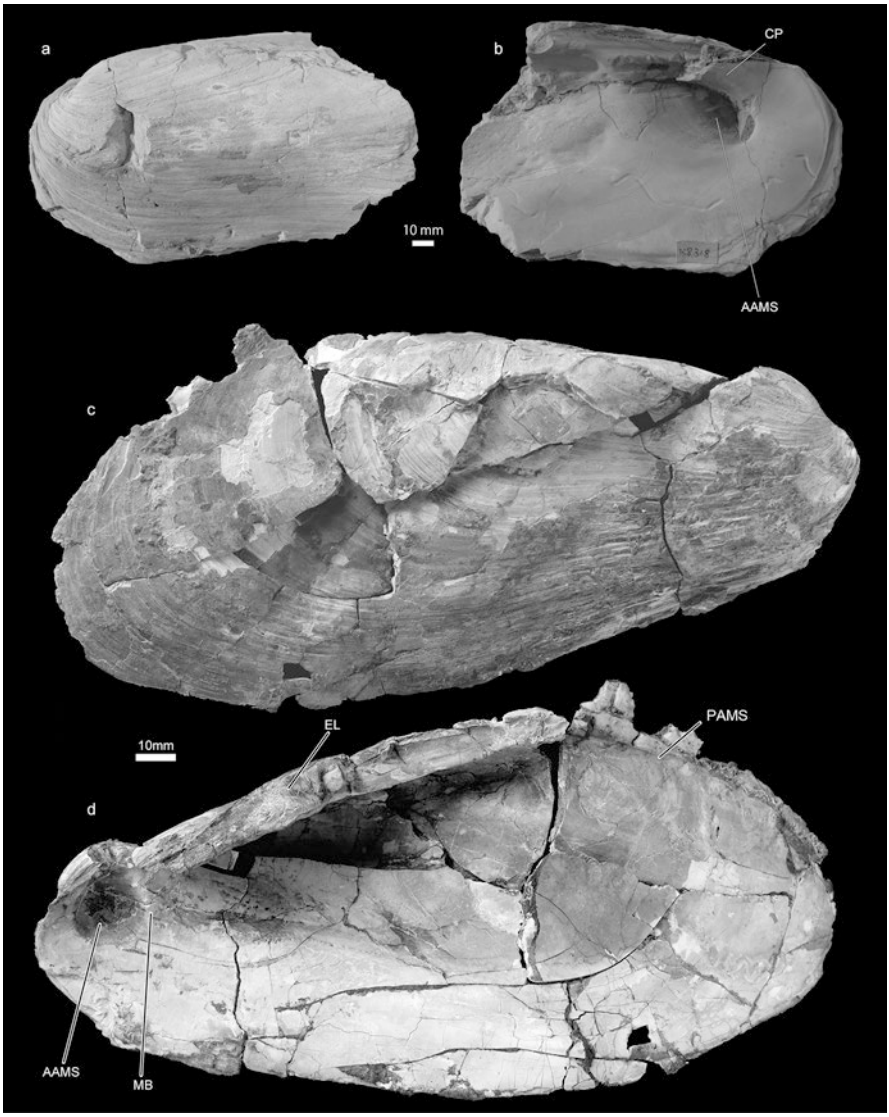

Fig. 10.6 Kalenteridae. (**a**, **b**) *Caspiconcha whithami* Kelly, 2000, from an Early Cretaceous seep site in Greenland; K8318 stored at the Sedgwick Museum, the University of Cambridge; Holotype. *AAMS* anterior adductor muscle scar, *CP* caspiconchid process. (**c**, **d**) *Caspiconcha major* (Gabb, 1869) from the Early Cretaceous Eagle Creek seep site in California, USA; CAS 72527-9 stored at California Academy of Science. *AAMS* anterior adductor muscle scar, *PAMS* posterior adductor scar, *MB* myophoric buttress, *EL* external ligament. (**a**, **b**: Kelly et al. 2000; **c**, **d**: Gabb 1869)

site in the Ural Mountains, where it co-occurs with worm tubes (Little et al. 1999). Two specimens of *S. ivanovi* have so far been discovered, one of them incomplete, which in addition to its restricted occurrence, further limits the knowledge on *Sibaya*. A study of limited materials available indicates that *Sibaya* had an ovoid shell reaching 70 mm in length and lacked a ventral sinus. Its external ornament was composed of a series of commarginal growth lines. Ligament was external, the dorsal margin of both valves connected with periostracum. Internal structures, like pallial line and muscle scar impressions, are as yet unknown. The genus is known so far only from the Middle Devonian.

Family Kalenteridae

3. *Kasimlara* Kiel, 2018, includes the Upper Triassic type species, *K. kosuni*, and an as-yet undescribed species from the same seep deposits, and can be separated from *Caspiconcha* and *Terzileria* by having a small pallial sinus and a much smaller anterior adductor muscle scar (Kiel 2018).
4. *Terzileria* Kiel, 2018, is known only from its Upper Triassic type species, *T. gregaria* Kiel, 2018, and differs from *Caspiconcha* by having an anterior adductor muscle scar separated from a pedal retractor scar and located at a more ventral position and the pallial line being closer to the shell margin (Kiel 2018).
5. *Caspiconcha* was introduced for *Caspiconcha whithami*, Kelly, in Kelly et al. (2000) (Fig. 10.6a, b) from Early Cretaceous seep deposits in Greenland. It is characterized by a cuneiform to mytiliform shell with a smooth shell surface apart from growth lines, an anterior adductor muscle scar deeply set within the myophoric buttress, which is partially covered by the so-called caspiconchiid process, and an edentulous hinge; the shell has a crossed lamellar shell structure and lacks nacre (Kelly et al. 2000; Jenkins et al. 2013). *Caspiconcha* differs from *Myoconcha* by its caspiconchid process and its edentulous hinge plate. It presently includes seven named species, the oldest being *Caspiconcha major* from a Upper Jurassic (Tithonian) seep deposit in California, USA. The genus reached its highest diversity and a nearly worldwide geographic distribution in the Albian (Kiel and Peckmann 2008; Jenkins et al. 2013), followed by a rather sudden demise after the end of the Early Cretaceous. One further Late Cretaceous species of *Caspiconcha* is known from the Santonian of Amakusa in southern Japan (Jenkins et al. 2018b) and is awaiting formal description.
6. *Pseudophopsis* Kiel, Hybertsen, Hyžný, and Klompmaker, 2020, is based on *Pleurophopsis peruviana* Olsson, 1931, from the Oligocene of Peru and includes *Unio bitumen* Cooke, 1919, from the Eocene of Cuba (Kiel et al. 2020b). The elongate-oval shells are well inflated, reach 100 mm in length, and are sculptured by rough growth lines only; the hinge plate is either edentulous or bears weak teeth subparallel to the shell margin. *Pseudophopsis* differs from *Caspiconcha* by having a round rather than elongate anterior adductor muscle scar without posterodorsal projection, and the Miocene kalenterid *Madrynomya* Griffin and Pastorino, 2006, has more coiled and more pointed umbones and a much broader but shorter hinge plate.

10.6 Family Lucinidae

Steffen Kiel

Lucinids are the most species-rich group of chemosymbiotic bivalves (Taylor and Glover 2006). The highest diversity is found in shallow water, particularly in sea grass environments, but they are also recorded from the depth of 2500 m, especially from the tropics (Glover and Taylor 2016; Taylor et al. 2014). Lucinids live buried in the sediment, with the umbones orientated upward and the inhalant and exhalant siphons reaching upward in mucus-lined tubes (Allen 1958). Sulfide is taken up by the foot from the sediment pore water and transported to the symbiont-hosting gills. The symbionts are typically gammaproteobacteria, which are environmentally acquired after metamorphosis and are housed intracellularly in the gills (Duperron et al. 2007). The main shell features of lucinids are a roundish to oval shell often with a posterior ridge, an elongate anterior adductor muscle scar that is detached from the pallial line, and the lack of a pallial sinus, and some taxa show an impression of the pallial blood vessel. The hinge often has cardinal and lateral teeth, although groups with reduced dentition or even edentulous forms exist, especially among seep-inhabiting clades (Taylor and Glover 2009; Kiel 2013). Lucinids have a prodissoconch (early ontogenetic shell) with a large initial shell (prodissoconch I) that reflects lecithotrophic development, although some species show indications of a short planktonic larval phase (Glover and Taylor 2007). Shallow-water lucinids have a wide range of shell shapes and ornamentations (Taylor and Glover 2006), whereas seep-inhabiting taxa tend to be smooth, elongate-oval, and flat (Taylor and Glover 2009; Kiel 2013). Exceptions to this are *Nymphalucina* and *Lucinoma* with their strong and sharp ribs, and the very inflated *Meganodontia*.

10.6.1 Fossil Record and Evolution

Lucinidae seem to have originated in the Silurian. *Iliona prisca* from the Silurian of Gotland (Sweden) shares characteristic features with modern lucinids, such as the elongate, detached anterior adductor muscle scar and the scar of the pallial blood vessel. These two characters are thought to be associated with the chemosymbiotic mode of life (Taylor and Glover 2006). Furthermore, *Iliona prisca* was found in a similar life position as Recent lucinids (Liljedahl 1991; Taylor and Glover 2006). Thus, lucinids are considered to have acquired their chemosymbiotic mode of life in the early Paleozoic time.

Diversity among lucinids remained low for most of the Paleozoic and Mesozoic. The rapid and large radiation of the modern groups started in the mid-Cretaceous and was considered related to the rise of sea grasses and mangroves (Stanley 2014). Deep-water groups are known since the Jurassic (Taylor et al. 2014), and the first occurrences at methane seeps are from the Upper Jurassic (Gaillard et al. 1992; Kiel

2013). This late appearance at seeps is peculiar given that lucinids are considered to have acquired their chemosymbiotic mode of life in the Silurian. This may be a sampling artifact because pre-Jurassic seep deposits are scarce (Kiel 2010a) or might reflect the overall diversification of the Lucinidae, which were rare during the Paleozoic and most of the Mesozoic and only started diversifying in the Cretaceous (Stanley 2014; Kiel and Peckmann, 2019).

10.6.2 Classification and Shell Characters

Molecular phylogenetic work conducted during the last decade showed that contrary to previous classifications, neither the Thyasiridae nor the Ungulinidae belong to the lucinids (Williams et al. 2004; Taylor et al. 2007a, b). Seven subfamilies of the Lucinidae are currently recognized based on molecular data – these being the Codakiinae, Leucosphaerinae, Lucininae, Monitilorinae, Myrteinae, and Pegophyseminae; the status of Milthinae is presently equivocal due to the lack of material available for molecular work (Taylor et al. 2011). Members of the Myrteinae have colonized deep-sea methane seeps since the Jurassic and were the most diverse group in this environment during the remainder of the Mesozoic (Kiel 2013). The Codakiinae started colonizing seeps in the Late Cretaceous with the genus *Nymphalucina*, and the most common codakiin at Recent seeps, *Lucinoma*, first appeared in this environment in the Oligocene (Kiel 2013). Among the Pegophyseminae, *Meganodontia* and *Pegophysema* are known from vent/seep environments (Bouchet and Cosel 2004; Kiel and Hansen 2015) and were reported from Miocene seep deposits in both Italy and the Caribbean region (Kiel and Hansen 2015; Kiel and Taviani 2017). Many lucinid genera found in Mesozoic and Cenozoic deep-water seep deposits are restricted to this type of habitat and show morphologies that are unknown from shallow-water environments, with the notable exception of the widespread genus *Lucinoma*. Two species of Lucininae, *Megaxinus ellipticus* (Borson) and *Megaxinus stironensis*, were found at a Pliocene seep site in northern Italy (Kiel and Taviani 2018).

As more fossil seeps are being described, the number of genera living in, and possibly being restricted to, this environment is likely to increase. In the following, the main shell features of the seep-inhabiting lucinid genera are outlined.

Subfamily Myrteinae

The genera *Amanocina*, *Elliptiolucina*, *Elongatolucina*, and *Nipponothracia* are all characterized by an elongate-oval, smooth shell with an edentulous hinge and are considered as a single seep-inhabiting lineage among the Myrteinae (Kiel 2013).

1. *Myrtea* Turton, 1822: The extant *Myrtea amorpha* (Sturany, 1896) occurs at seeps in the Mediterranean Sea (Olu et al. 2004), but in the fossil record, this genus tends to be used as a "trash bin taxon" for various Myrteinae of uncertain affinity and should be treated carefully. In eastern Hokkaido, *Myrtea ezoensis* (Nagao) survived from the Cretaceous to the Paleocene (Amano et al. 2018a).

2. *Beauvoisina* Kiel, Campbell, and Gaillard, 2010: This monotypic genus occurs only in Oxfordian (Late Jurassic) seep deposits at Beauvoisin in southeastern France. Shells are elongate-oval, reach 140 mm in length, are smooth except for rough growth increments, and have two cardinal teeth in each valve and a short ligament nymph. The pallial line and muscle attachment scars are very indistinct to almost indiscernible; the anterior adductor muscle scar is broad and elongated and reaches about half the shell height. A peculiar feature of this genus, which distinguishes it from the otherwise very similar *Tehamatea* and *Cubatea*, is a ridge inside the lunule (Kiel et al. 2010; Kiel 2013).
3. *Cubatea* Kiel, Campbell, and Gaillard, 2010: Based on an Eocene species from Cuba, *Cubatea asphaltica* (Fig. 10.7b) (Cooke, 1919), the genus is now recognized from the Upper Cretaceous of New Zealand to the Neogene of the Caribbean region (Kiel 2013; Kiel and Hansen 2015). Shells are of moderate size (50–100 mm), elongate-oval, with regular rib-like growth increments on the juvenile shell, and a mostly smooth adult shell. The hinge plate is broad, with one strong and often bifid cardinal tooth in the right valve, and two cardinals in the left valve; the lateral teeth are very strong and bifid. The anterior adductor muscle scar is distinctive, relatively short and broad, almost rectangular, is ventrally detached from the pallial line for about 2/3 of its length, and is diverging from the pallial line for about half its own width. The genus *Tehamatea* is very similar and differs mainly in having indistinct (but similarly shaped) muscle attachment scars and weaker lateral teeth. *Ezolucina* differs by having an elongate lunule (Amano et al. 2008; Kiel et al. 2010; Kiel 2013).
4. *Tehamatea* Kiel, 2013: The genus is based on an Early Cretaceous species, *Tehamatea ovalis* (Stanton, 1895), from Tehama County in California, USA (Fig. 10.7a), and reached a worldwide distribution during Late Jurassic to Late Cretaceous time (Agirrezabala et al. 2013; Kiel 2013; Hryniewicz et al. 2014). Its shell characters are essentially those of *Cubatea*; the differences between *Cubatea* and *Ezolucina* are outlined in the discussion of *Cubatea*.
5. *Ezolucina* Amano, Jenkins, Kurihara, and Kiel, 2008: The genus is based on *Vesicomya inflata* Kanie and Nishida, 2000, from the Cenomanian (Upper Cretaceous) of Japan, a large, moderately inflated, veneriform shell with a very elongate lunule. In large specimens, the posterior side has a strong ridge resulting in a somewhat pointed posterior shell margin. The hinge has one strong cardinal tooth in the right valve and two in the left valve. The anterior adductor muscle scar is broad with a rectangular ventral end and reaches just below the midline of the shell (Amano et al. 2008). The type of locality of *Ezolucina inflata* is not a seep deposit, but *Ezolucina* has subsequently been reported from Cretaceous seep deposits in New Zealand (Amano et al. 2008; Kiel et al. 2013).
6. *Cryptolucina* Saul, Squires, and Goedert, 1996: The type species, *Cryptolucina megadyseides* Saul, Squires, and Goedert, 1996, has an elongate-oval shell with a nearly smooth surface; an edentulous hinge; an anterior adductor muscle scar similar to that of *Cubatea*, *Tehamatea*, and *Ezolucina*; and a strongly prosogyrate umbo (Saul et al. 1996). This morphology of the umbo distinguishes *Cryptolucina* from *Beauvosina*, *Cubatea*, *Ezolucina*, and *Tehamatea*. The type

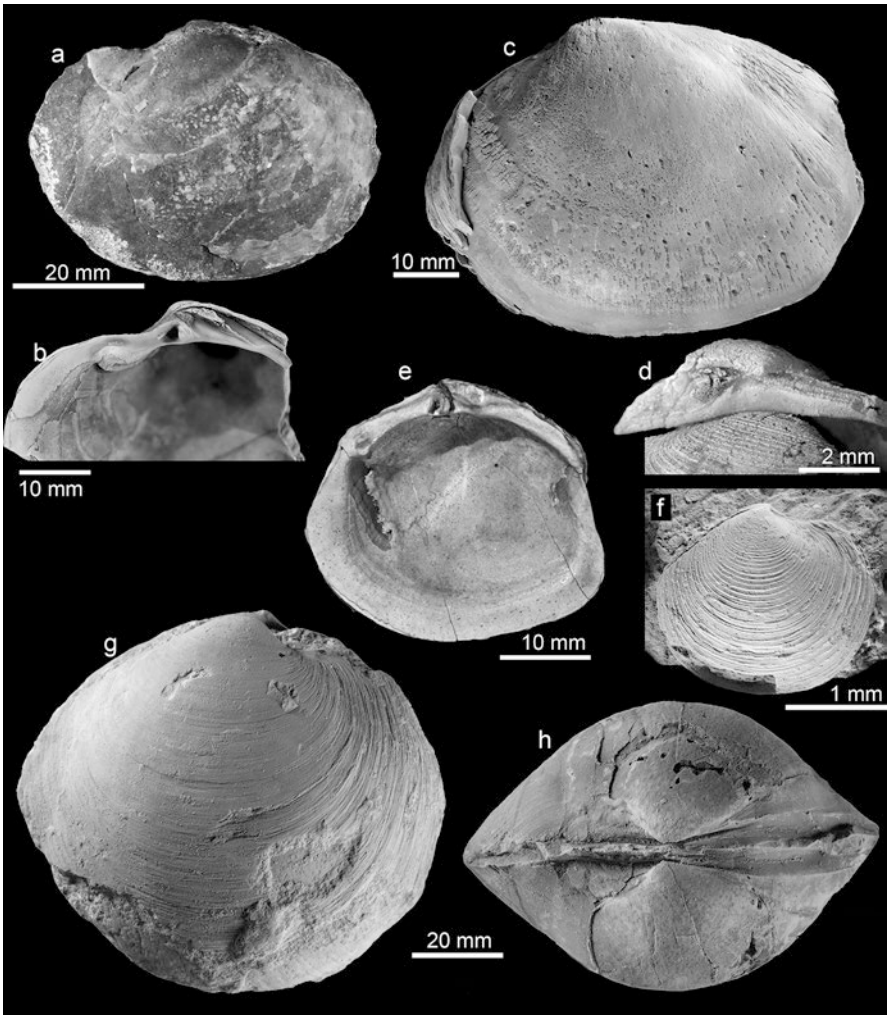

Fig. 10.7 Lucinidae. (**a**) *Tehamatea ovalis* (Stanton, 1895) from an Early Cretaceous seep site in California, USA; USNM 23056; Holotype. (**b**) *Cubatea asphaltica* (Cooke, 1919) from an Eocene seep site in Cuba; USNM 533988. (**c**) *Elliptiolucina washingtonia* Kiel, 2013, from an Oligocene seep site in Washington State, USA; GZG.INV.88327; Holotype. (**d**) *Amanocina ezoensis* (Kanie and Kuramochi, 1996) from a Late Cretaceous seep site in Hokkaido, Japan; UMUT MM 29541. (**e**) *Nymphalucina cleburni* (White, 1882) from the Late Cretaceous of Colorado, USA; USNM 9971. (**f**) *Lucinoma* sp. from the Pliocene Stirone River seep site in northern Italy. (**g**, **h**) *Meganodontia* sp. from a Miocene seep site in Cuba. (**a**–**c**: Kiel 2013; **d**: Kiel et al. 2008; **e**: Kiel and Peckmann 2007; **f**: collection by Steffen Kiel and Marco Taviani; **g**, **h**: PRI collection)

species was described from middle Eocene mudstone of the Humptulips Formation in Washington State, USA, and the assignments of all other species considered as belonging to this genus have been questioned (e.g., Kiel 2013), which may leave *Cryptolucina* as a monotypic genus that is probably not seep-related.

7. *Amanocina* Kiel, 2013: This genus differs from the other three edentulous seep lucinids by lacking the triangular depression in the hinge plate below the umbo and by having a narrower and longer anterior adductor muscle scar. It is based on the Cenomanian (Upper Cretaceous) *Amanocina yezoensis* (Fig. 10.7d) (Kanie and Kuramouchi 1996) and is currently known from the Barremian (Lower Cretaceous) of Greenland, the Albian (Lower Cretaceous) of New Zealand, the Cenomanian (Upper Cretaceous) of Hokkaido, and the Oligocene of Colombia (Kiel 2013).
8. *Nipponothracia* Kanie and Sakai, 1997: The shells of this genus are oval and have the umbo in a subcentral position, in contrast to many species of *Elliptiolucina* and *Elongatolucina* with their umbo displaced toward the anterior. *Nipponothracia* is based on *Thracidora gigantea* Shikama, 1968, and is currently known from the Oligocene of the northern Peru and the Middle Miocene of central Japan and Trinidad (Kase et al. 2007; Kiel 2013; Kiel and Hansen, 2015).
9. *Elongatolucina* Gill and Little, 2013: Shells are large, reaching a length of 180 mm or more, very elongate, and have the umbo in a very anterior position. The anterior adductor muscle scar is detached from the pallial line for most of its length and may reach slightly below the midline of the shell. A character that may distinguish this genus from *Elliptiolucina* is the flattened lateral side of the shell of *Elongatolucina*. The genus is based on *Cryptolucina elassodyseides* Saul, Squires, and Goedert, 1996, and is currently known from the middle Eocene of the Washington State, the Oligocene of Colombia, and the Middle Miocene Venezuela (Gill and Little 2013; Kiel 2013; Kiel and Hansen 2015).
10. *Elliptiolucina* Cosel and Bouchet, 2008: This is the only extant genus of the "edentulous seep lucinids"; shells are elongate-oval and rarely reach beyond 130 mm in length – differences between *Nipponothracia* and *Elongatolucina* are outlined above. Molecular data clearly support its position within the Myrteinae (Kuhara et al. 2014). The currently oldest record is from the late Oligocene of the North American Pacific coast, with further records from the Neogene of the central Indo-West Pacific and New Zealand (Fig. 10.7c; Kiel 2013; Amano et al. 2018b).

Subfamily Codakiinae

11. *Nymphalucina* Speden, 1970: This genus was widespread in the Late Cretaceous Western Interior Seaway, a broad epicontinental sea stretching from the Gulf of Mexico to the Arctic Ocean, where it occured in seep and non-seep environments (Speden 1970; Kauffman et al. 1996; Kiel et al. 2012). *Lucina scotti*, likely belonging to *Nymphalucina*, has recently been reported from shallow-water seeps in Campanian-Maastrichtian (Late Cretaceous) sediments on Snow

Hill and Seymour islands on the eastern side of the Antarctic Peninsula (Little et al. 2015). The genus thus appears to be widespread. Shells are oval to pentagonal with a distinctive posterior ridge, sharp commarginal ribs and a very elongated lunule. There are two to three cardinal teeth in each valve, which radiate and diverge away from the umbo. The anterior lateral teeth are very strong; the one in the left valve is bifid (Fig. 10.5e). The anterior adductor muscle scar is narrow, detached from the pallial line for most of its length, and reaches just below the midline of the shell (Speden 1970; Kiel 2013). *Lucinoma* differs by having less distinctive anterior lateral teeth, a heart-shaped lunule, and often a slightly longer anterior adductor muscle scar.

12. *Epilucina* Dall, 1901: *Epilucina washingtoniana* (Clark, 1925) occurs in two upper Eocene seep deposits in the Wagonwheel Formation in central California (Squires and Gring 1996), but these are so far the only records of this genus at seeps. The genus is characterized by roundish shells with coarse commarginal ribs; a small, heart-shaped, strongly asymmetrical lunule; a long external ligament; and a weak posterior ridge and/or groove. The hinge plate is moderately broad and bears two cardinal teeth in each valve; anterior and posterior lateral teeth are well developed (Kurihara 2007). The genus differs from *Lucinoma* by its strong lateral teeth, and the anterior adductor muscle scar is further detached from the pallial line in *Lucinoma*.
13. *Lucinoma* Dall, 1901: The origin of this genus might go back to the Paleocene (Petersen and Vedelsby 2000; Taylor et al. 2011), and since the Oligocene time, it can be found at seep deposits worldwide (Goedert and Campbell 1995; Majima et al. 2005; Kiel et al. 2020b). There are at least 24 extant species (Taylor and Glover 2010), and 11 species have been reported from fossil seep deposits alone; most of these records need revision. In contrast to most Mesozoic deep-water lucinids, the genus is not restricted to seeps but is widespread in muddy sediments. Shells are roundish to oval, often with a somewhat pointed anterior margin, a truncate and angular posterior margin, and a posterior ridge. The sculpture consists of distinctive and often sharp-crested commarginal ribs (Fig. 10.7f). The hinge plate is narrow and has two cardinals in each valve, one of which may be bifid; the anterior lateral teeth are not well developed (Salas and Woodside 2002; Holmes et al. 2005; Taylor and Glover 2010). *Nymphalucina* builds similar shells; *see Nymphalucina* section for characters distinguishing the two genera.

Subfamily Pegophyseminae

14. *Meganodontia* Bouchet and Cosel, 2004: The genus is based on the extant species *M. acetabulum* Bouchet and Cosel, 2004, from a possible venting area off of Taiwan. Members of the genus have recently been recognized in Miocene seep deposits in Italy (Kiel and Taviani 2017), New Zealand (Amano et al. 2018b) ,and the Caribbean region (Fig. 10.7g, h; Kiel and Hansen, 2015). The main shell features include very large (typically > 100 mm) and very inflated shells lacking sculpture except for rough growth increments, a narrow and edentulous hinge plate, a long and thin ligament nymph, and a broad, more-or-

less straight anterior adductor muscle scar that is widely detached from the pallial line and extends for about 2/3 of the shell height toward the ventral shell margin (Bouchet and Cosel 2004). Members of the *Anodontia* clade differ by being smaller and by having a shorter and/or narrower anterior adductor muscle scar (Taylor and Glover 2005).

15. *Pegophysema* Stewart, 1930/*Anodontia* Link, 1807: When Taylor et al. (2011) established a new subfamily Pegophyseminae based on the genus *Pegophysema*, they put *Anodontia* into the subfamily Leucoshaerinae. However, it is very difficult to separate these genera on morphological grounds. Compared to *Meganodontia*, *Pegophysema* and *Anodontia* have a smaller and narrower anterior adductor muscle scar, a more swollen umbo, and a straight hinge (see Amano et al. 2018b). A fossil *Pegophysema* was reported from the Lower Pliocene of the Dominican Republic (Kiel and Hansen 2015); *Anodontia mioinflata* was described from a Late Miocene seep, and *Anodontia* sp. was recorded from a Late Pliocene seep, both in northern Italy (Kiel and Taviani 2018; Kiel et al. 2018).

Subfamily Lucininae

16. *Megaxinus* Brugnone, 1880: The genus is based on *Lucina transversa* Bronn, 1831, from the Italian Pliocene, and its occurrence at seeps is presently restricted to the Upper Pliocene Stirone River seep complex in northern Italy (Kiel and Taviani 2018). Shells reach about 50 mm in length, are roundish to rounded-quadrate in outline, lack sculpture, and have an only weakly developed posterior ridge and a distinct lunule. Internally, they have a mostly edentulous hinge plate, and the long and tapering anterior adductor muscle scar runs very close to the pallial line but is detached from it for about ¾ of its length.

10.7 Family Thyasiridae

Kazutaka Amano and Krzysztof Hryniewicz

The family Thyasiridae was traditionally classified among Lucinoidea (e.g., Dall 1901; Chavan 1969) until molecular studies have shown that both lucinoids and thyasirids are distinct clades (Taylor et al. 2007a, b). Members of the family Thyasiridae inhabit reduced environments from intertidal mudflats to the deep sea, and many of them harbor sulfur-oxidizing bacteria in or on their gill (Dufour 2005; Oliver and Levin 2006; Oliver and Holmes 2006; Taylor and Glover 2010). In the last decade, six new genera have been proposed from Recent and fossil chemosynthetic communities: *Channelaxinus* Valentich-Scott and Coan, 2012; *Cretaxinus* Hryniewicz, Little, and Nakrem, 2014; *Ochetoctena* Oliver, 2014; *Ascetoaxinus* Oliver and Frey, 2014; *Wallerconcha* Valentich-Scott and Powell, 2014; and *Rhacothyas* Åström and Oliver, 2017.

Thyasirids have a global distribution but are most common in colder waters (Dufour 2018). They include both symbiotic and asymbiotic species;

symbiont-bearing species almost exclusively have gills with two demibranchs, and have by far the highest diversity of symbiont location and integration of symbionts among the bivalves (Dufour 2005). Six gill types have so far been recognized among thyasirids, reflecting progressive integration of symbionts and increasing reliance on chemosymbiosis (Oliver 2014). Symbionts are hosted either on the surface of the gills among the microvilli of the bacteriocytes (Dufour 2005) or in deep invaginations of bacteriocytes, the so-called bacterial chambers (Kharlameko et al. 2016). As far as they have been studied, all symbionts are thiotrophic gammaproteobacteria and are hosted extracellularly (e.g., Imhoff et al. 2003); only symbionts of *Maorithyas hadalis* have been said to be stored intracellulary (Fujiwara et al. 2001). The symbionts are likely acquired from the surrounding environment, at least in the case of *Thyasira* cf. *gouldi* (Batsone et al. 2014).

Most thyasirids are infaunal and burrow in the sediment with the aid of their vermiform foot (Dando and Southward 1986; Oliver and Killeen 2002; Dufour and Felbeck 2003; Dufour 2018), which can be extended up to 30 times the length of the shell (Dufour and Felbeck 2003). Regardless of being symbiotic or asymbiotic, thyasirids construct extensive burrows, likely resulting from pedal feeding combined with the farming of chemosynthetic bacteria along the burrow walls (Zanzer and Dufour 2017). Larger thyasirids have been observed on the sea floor, for example, *Conchocele bisecta* (Conrad 1849) in the Sea of Okhotsk (Sahling et al. 2002; Kharlameko et al. 2016) and *Conchocele novaeguinensis* Okutani, 2002, at a water depth of approximately 470 m off of Papua New Guinea (Okutani 2002). A fragmentary specimen of *C. bisecta*, possibly crushed by a crustacean predator, was obtained from a core sample from the Sea of Japan. These observations were used by Amano et al. (2013a) to infer that *C. bisecta* is a shallow burrower. Earlier works (e.g., Kamenev et al. 2001) claimed that *C. bisecta* uses suspension feeding in addition to chemosymbiosis for nutrition. However, this claim was largely refuted by further studies, which have shown that *C. bisecta* relies almost exclusively on chemosynthetic food source (Kharlameko et al. 2016).

10.7.1 Fossil Record and Evolution

Fossil representatives of the family have been recorded from seep sites and whale-fall and wood-fall sites (e.g., Amano et al. 2007b; Kiel et al. 2009; Kiel 2010a). The oldest thyasirid, *Cretaxinus* Hryniewicz, Little, and Nakrem, 2014, is known from the earliest Cretaceous seep site on Spitsbergen. Then, the following thyasirid genera have been reported from hydrocarbon seep deposits since the Late Cretaceous: *Thyasira* Lamarck, 1818, the large Late Cretaceous *"Thyasira" hataii* from the Sada Limestone seep deposit in Japan, which belongs to a new genus; *Conchocele* Gabb, 1866; *Maorithyas* Fleming, 1950; and *Rhacothyas* Åström and Oliver in Åström et al. (2017). *Lucina sculpta* Phillips, 1829, from the Albian Gault Clay in England was illustrated as the "oldest thyasirid" by Taylor et al. (2007a, b); its systematic affiliation is uncertain because its internal morphology is unknown.

As noted by Kiel et al. (2008) and Kaim et al. (2013), *Lucina rouyana* (d'Orbigny, 1844) from Lower Cretaceous (Valanginian-Hauterivian) rocks in Europe could be the oldest species of *Thyasira* (s.s.). The second oldest species is *T.* (s.s.) *tanabei* Kiel, Amano, and Jenkins, 2008 (Fig. 10.8a, b, d, e), from Albian to Campanian

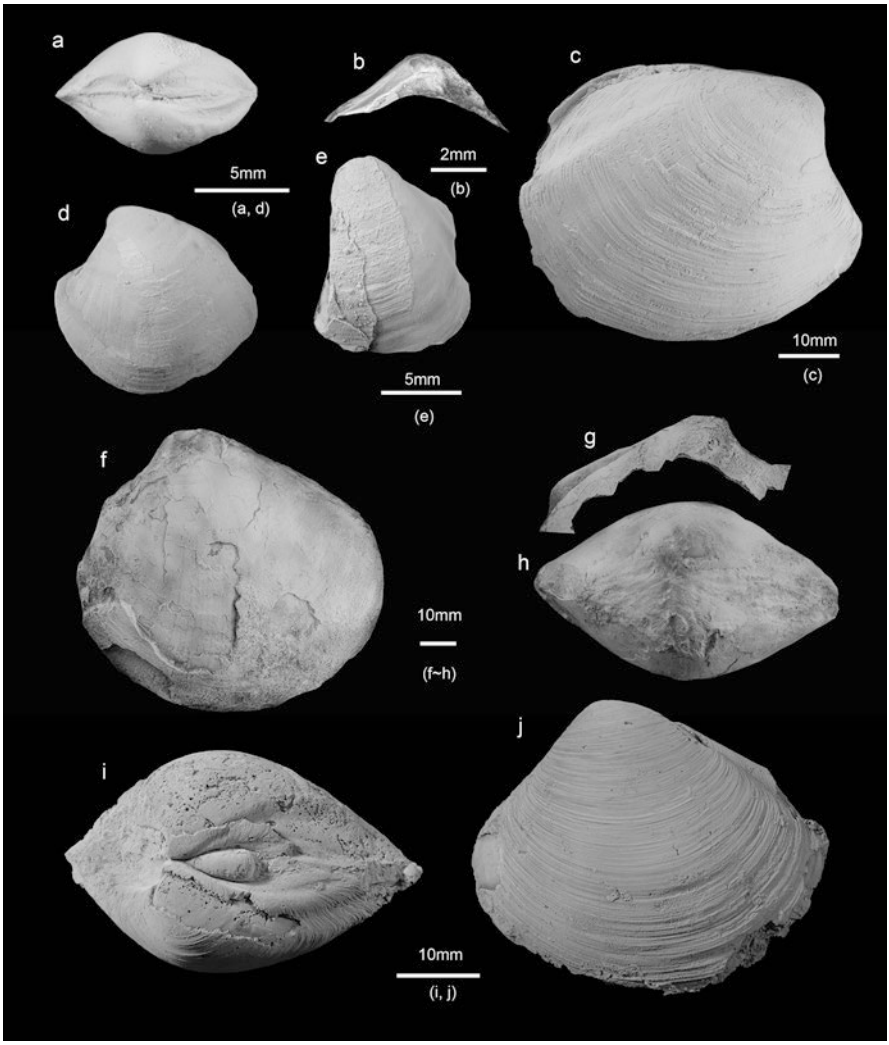

Fig. 10.8 Thyasiridae. *Thyasira* (s.s.) *tanabei* Kiel, Amano, and Jenkins, 2008, from a Late Cretaceous seep site in northern Hokkaido, Japan; (**a**, **b**) UMUT MM29533, holotype; (**d**) UMUT MM 29537, paratype; (**e**) UMUT MM 29536, paratype. (**c**) *Conchocele bisecta* (Conrad, 1849) from an early Miocene seep site in Ibaraki Pref., Honshu, Japan. (**f**, **g**, **h**) *Thyasira* sp. from a Late Cretaceous seep site in Kochi Pref., Shikoku, Japan. (**i**, **j**) *Cretaxinus hurumi* Hryniewicz, Little, and Nakrem, 2014, from an earliest Cretaceous seep site in Spitsbergen, Svalbard; PMO 217.277, holotype. (**a**, **b**, **d**, **e**: Kiel et al. 2008; **c**, **f**, **g**, **h**: collection by Amano; **i**, **j**: Hryniewicz et al. 2014)

seep deposits on Hokkaido. In the northern Pacific area, *Thyasira* species are also known from Paleocene deep-water deposits (Kalishevich et al. 1981; Amano et al. 2015). After the late Eocene, *Thyasira* became much less common at hydrocarbon seeps; rare examples include *Thyasira* (s.s.) sp. from Miocene seep sites in New Zealand (Campbell et al. 2008; Amano et al. 2015), *T.* (s.s.) *nakazawai* Matsumoto, 1971, from an Early Miocene seep from the Wappazawa Formation in central Honshu, Japan, and *T.* (s.s.) *montanita* at a seep deposit from the Oligocene-Miocene boundary in Ecuador (Kiel et al. 2021).

The oldest species of *Conchocele*, *Conchocele townsendi* (White, 1890), is known from Maastrichtian seep deposits on Snow Hill Island, Antarctica (Kiel et al. 2008; Little et al. 2015; Hryniewicz et al. 2017a). The next oldest species are *C.* aff. *conradi* (Rosenkranz 1970) from the Danian Kangilia Formation in western Greenland (Rosenkranz 1970) and *C. conradii* from the Thanetian Basilika Formation in Spitsbergen (Hryniewicz et al. 2016, 2017b). *Conchocele* was also reported from Paleocene sediments in New Zealand (Beu and Maxwell 1990). In the northern Pacific, *Conchocele* flourished since late Eocene, and *Thyasira* (s.s.) contemporaneously declined (Amano et al. 2015, 2018a; Hryniewicz et al. 2017a). In the Early Miocene, *Conchocele* invaded the deep-water basin of the Sea of Japan at latest 1 million years after the basin formed (Amano et al. 2019b).

Two species of *Maorithyas* have been found at fossil seep sites, these being *Maorithyas humptulipsensis* Hryniewicz, Amano, Jenkins, and Kiel, 2017a), from the middle Eocene Humptulips Formation (Hryniewicz et al. 2017) and *Maorithyas folgeri* (Wagner and Schilling 1923) from the Eocene Wagonwheel Formation and the Oligocene San Emigdio Formation in Southern California, USA. A single fossil species of *Rhacothyas*, *R. spitzbergensis*, has been described from Paleocene seep and wood-fall communities in Spitsbergen Island (Hryniewicz et al. 2019).

10.7.2 Classification and Shell Characteristics

The size of thyasirids ranges from a few mm to about 200 mm in length (senior author's observation). Most thyasirids are characterized by an edentulous hinge and a sulcated posterodorsal shell area. Molecular phylogenetic work on 13 species of thyasirids divided them into two well-defined clades (Taylor et al. 2007a, b) – *T. flexuosa*/*T. gouldi*/*T. polygonata* from "normal" marine-reduced environments and *T. sarsii*/*T. methanophila* from seeps – and a third clade which lacks strong support and is composed of asymbiotic species including *Mendicula ferruginosa*, *Leptaxinus indusarium*, *Anodontorhina cyclia*, and *Axinulus*.

Several fossil seep thyasirid genera are known, yet due to lack of data and difficulty of identifying thyasirids based on the shell features alone, their taxonomy is only partially resolved. Several taxa are problematic, and more material for further studies is needed. Below we list the main morphological features of ancient seep-inhabiting thyasirids as currently understood.

1. *Cretaxinus* Hryniewicz, Little, and Nakrem, 2014: This genus was proposed for *C. hurumi* from lowermost Cretaceous (uppermost Berriasian) seep carbonates from the Slottsmøya Member in central Spitsbergen, Svalbard. The genus is characterized by a rather large shell reaching 57 mm in length, posterodorsally flattened and poorly pronounced sulci without auricle, and by a thick external ligament (Fig. 10.8i, j). In contrast to other large thyasirids, *Cretaxinus* has a rather weak and short anterior adductor muscle scar and a strong and deep posterior adductor muscle scar. The inner shell surface is covered by dense radial striae, probably resulting from descending mantle muscle scars. The species occurs in small clusters of up to ten specimens, associated with the lucinid *Tehamatea rasmusseni*, the solemyid *Solemya* (*Petrasma*) cf. *woodwardiana*, and *Nucinella svalbardensis* (Hryniewicz et al. 2014, 2015a).
2. *Thyasira* Lamarck, 1818: This genus includes two subgenera: *Thyasira* (s.s.) and *Philis* Fisher, 1924. *Philis* can be separated from *Thyasira* (s.s.) by having a small tooth-like projection below the umbo. Both subgenera have small shells (up to 30 mm among the Recent species) with two folds and an auricle. Of the two symbiotic clades, the *T. flexuosa*/*T. gouldi*/*T. polygonata* clade differs from the *T. sarsii*/*T. methanophila* clade by having less inflated shells with a medial flattened area (Amano et al. 2015). Huber (2015) splits *Thyasira* into *T.* (s.s.) and eight undescribed groups including the *T. sarsii*/*T. methanophila* clade, for which a new genus may be warranted.
3. Large Cretaceous *Thyasira*: A large species from the Upper Cretaceous Sada Limestone in Shikoku, Japan, was described as *Aphrodina* (*Aphrodina*) *hataii* (Fig. 10.8f, g, h) by Katto and Hattori (1964). Tashiro (1992) allocated this species to *Thyasira* (s.l.), but the species differs from the genus *Thyasira* by lacking a distinct auricle and by reaching up to 80 mm in length. Although the size of this species is similar to that of *Conchocele*, its well-rounded posterior margin separates it from *Conchocele* (Nobuhara et al. 2008). Taxonomic work on this species is ongoing.
4. *Conchocele* Gabb, 1866: This genus is characterized by a large shell (up to 200 mm in length) with a long, deeply sunken ligament, a beak situated near the anterior end, a subtruncated anterior margin, and an elongated anterior adductor muscle scar (Fig. 10.8c). The sulci developed in the posterodorsal shell area are strong and deep.
5. *Maorithyas* Fleming, 1950: This genus was proposed on the Recent species, *M. marama* Fleming, 1950, from New Zealand and is characterized by its moderate size (up to 62 mm in length), thin, globose shell with a well-defined lunule.
6. *Rhacothyas* Åström and Oliver in Åström et al., 2017: The genus was introduced for the Recent species *R. kolgae* Åström and Oliver, 2017, from methane seeps off Svalbard. The genus is characterized by a small (up to 25 mm), thin, and luciniform shell with edentulous hinge, a small sunken lunule, and a weak posterior sulcus. Its external surface is sculptured by raised and narrowly spaced commarginal lamellae and weak posterior sulcus. The only fossil record so far is the Paleocene *R. spitzbergensis*, from shallow marine deposits on Svalbard.

10.8 Family Vesicomyidae

Kazutaka Amano and Steffen Kiel

The Vesicomyidae is the second most species-rich family of chemosymbiotic bivalves after the Lucinidae, and they are arguably the most successful radiation into chemosynthetic environments. More than 100 extant species have been described, and there are approximately 30 named fossil species and even more reported in open nomenclature. Vesicomyidae inhabit hydrothermal vents, methane seeps, and whale- and wood-fall sites and are also found in organic-rich deep-sea environments. Geographically they are found worldwide from the Arctic via the tropics to Antarctic waters and in depths from 100 to 9500 m (Krylova and Sahling 2010).

Vesicomyids have a broad size range, ranging from a few mm to more than 300 mm in length. Only the smallest species (belonging to the genus *Vesicomya*) apparently lack symbionts, whereas the larger species host symbionts on which they rely for nutrition. The symbionts are exclusively sulfur-oxidizing gammaproteobacteria that are transmitted mostly from parent to offspring (vertical transmission), resulting in coevolution between host and symbiont lineages (Peek et al. 1998). Sulfide is taken up from the sediment (or in the case of hydrothermal vents, from fluids seeping through crevices between pillow lavas) via the bivalves' extensile foot and is transported to the intracellular symbionts in the gills. Most vesicomyids are semi-infaunal except for species smaller than approximately 20 mm long, which tend to live completely buried in the sediment. The larger species frequently move around at the sediment surface, probably to search for optimal sulfide flux (Krylova and Sahling 2010).

Vesicomyids disperse via lecithotrophic larvae, yet at least some species have wide transoceanic distributions (Kojima et al. 2004; Audzijonyte et al. 2012). The small-scale distribution of vesicomyid species at individual seep sites appears to relate to their sulfide-binding and storage capacity. Species with a high binding and storage capacity (such as *Calyptogena pacifica*) are able to live in areas with lower sulfide flux than species with lower binding and storage capacity (such as *Archivesica kilmeri*), which can only survive in areas with a steady and high supply of sulfide (Barry et al. 1997).

10.8.1 Fossil Record and Evolution

Vesicomyids first appeared in the North Pacific in the middle Eocene, with the earliest record being from the Humptulips Formation in western Washington State, USA (Amano and Kiel 2007b; Hybertsen and Kiel 2018). Another potential middle Eocene record comes from deep-water deposits of the Murotohanto Group in Tokushima Prefecture, Japan (as "*Crassatellites* nov. sp."; Hatae 1960; Suyari and

Yamazaki 1987) but this still needs confirmation. The few middle Eocene seep deposits from the eastern Atlantic and Tethyan region lack vesicomyids (Natalicchio et al. 2015; SK, unpublished). From the late Eocene to Oligocene, vesicomyids occur throughout the Pacific and Caribbean regions (Olsson 1931; Amano and Kiel 2007b; Kiel and Amano 2010; Amano et al. 2013b; Kiel and Hansen 2015; Kiel et al. 2020a, 2020b), but seep deposits are unknown from outside this region, preventing a comprehensive assessment of the biogeography of vesicomyids. From the Miocene onward, seep deposits with vesicomyid bivalves are known from virtually all ocean basins (Beets 1942, 1953; Gill et al. 2005; Majima et al. 2005; Kiel 2007; Amano and Kiel 2007b; Kiel 2010b; Kiel and Amano 2010; Amano and Kiel 2011; Amano and Kiel 2012; Amano et al. 2014a, b; Kiel and Hansen 2015; Kiel and Taviani 2017, 2018; Kase et al. 2019; Amano et al. 2019a, b).

Also, molecular age estimates for the vesicomyids suggest a middle Eocene origin (Baco et al. 1999; Vrijenhoek 2013). Based on the roughly coeval appearance of large whales and vesicomyid bivalves, it was hypothesized that the (geologically) sudden appearance of sulfide-emitting whale carcasses on the seafloor expanded the dispersal capacities of vent and seep-inhabiting species to such an extent that it triggered the radiation of new groups into these habitats (Baco et al. 1999; Smith and Baco 2003).

Other investigations using time-calibrated molecular phylogenetic trees (chronograms) of the vesicomyids indicated that lineages of pliocardiine vesicomyids have accumulated at a regular pace since the Eocene, with no signs of diversification pulses (Valdés et al. 2013; Johnson et al. 2017). The fossil record also provides insights into this issue, but the diversification pattern seen in the fossil record should not be overemphasized because although the genus-level classification of fossil vesicomyids is improving, there are still many uncertainties. Our current understanding of the fossil record of vesicomyid genera is shown in Table 10.2. However, ongoing taxonomic revisions and further discoveries of new taxa and new seep deposits are likely to change this picture. For example, species currently assigned to *Pliocardia* and pre-Miocene species assigned to *Archivesica* are likely to be placed

Table 10.2 Characteristics of the vesicomyid genera having fossil records. + present; – absent; ± basically absent, but sometimes present; ? unknown

Genus	Maximum size (mm)	Elongate shell	Lunular incision	Subumbonal pit	pallial sinus	3a tooth	lined 3a & 3b	nymphal ridge
Isorropodon	47	–	–	+	–	+	+	–
Pliocardia	47	–	+	+	+	+	–	–
Wareniconcha	120	–	–	+	–	+	–	–
Pleurophopsis	180	+	–	–	–	–	–	–
Ectenagena	70	+	–	+	–	–	–	–
Archivesica	250	±	–	+	+	+	–	–
Hubertschenckia	75	-	–	+	+	+	–	+
Calyptogena	90	±	–	–	–	+	–	+
Notocalyptogena	52	+	–	–	–	+	–	–

in new genera as mentioned later. There are many poorly preserved specimens in the fossil record, which may also belong to new genera or may extend the fossil record of described genera further back in time. New genera will continue to be named also for extant species, exemplified by the recent introduction of *Turneroconcha* Krylova and Sahling, 2020, for the iconic giant white clam *Calyptogena magnifica* from the East Pacific Rise hydrothermal vents. Once established, fossil species may be assigned to these new genera. Furthermore, especially the small, thin-shelled genera (e.g., Cosel and Salas 2002) are less likely to be found in the fossil record than large, thick-shelled genera (Valentine et al. 2006).

There is limited fossil evidence for an onshore-offshore pattern, a gradual adaptation to deeper water, in the evolution of the Vesicomyidae. *Hubertschenckia* appears to have lived in lower sublittoral to upper bathyal depths (Amano and Jenkins 2007). Its probable descendant *Archivesica* now lives in bathyal depth (Kojima 2008). Moreover, extensive work on vesicomyids in Japan indicates that *Archivesica* and *Calyptogena*, which today live in bathyal depths, took over this ecological niche from the genus *Pleurophopsis* during the Late Miocene (Amano and Kiel 2011; Amano et al. 2019a). A similar onshore-offshore pattern was recognized in molecular phylogenies of the bathymodiolins (Distel et al. 2000; Lorion et al. 2013) with the additional point of an adaptation from low-sulfide environments (wood-falls) to high-sulfide environments (vents/seeps), but this had not been seen in the molecular study of vesicomyids (Decker et al. 2012).

10.8.2 Classification and Shell Characters

The generic classification of both fossil and recent vesicomyid bivalves is an active, though difficult, field of research suffering from the frequent convergence of many shell characters, resulting in inconsistencies between morphological and molecular data. Krylova and Sahling (2010) distinguish two subfamilies: Vesicomyinae consists of only the small and asymbiotic type genus *Vesicomya*; Pliocardiinae includes all other genera. Shell characters used to distinguish species and genera include shell size and shape, presence or absence of a lunule or lunular incision, the point of contact between pallial line and the adductor muscle scars, the presence and shape of a pallial sinus, and the morphology of the right valve hinge area (number and arrangement of teeth, subumbonal pit, posterior nymphal ridge) (Fig. 10.9, Table 10.2). A comprehensive overview of the vesicomyid genera, their characters, and species compositions (although some assignments remain controversial) was provided by Krylova and Sahling (2010); here we discuss only genera with a fossil record.

1. *Pliocardia* Woodring, 1925: The Pliocene type species, *Anomalocardia bowdeniana* Dall, 1903, has a small (~10 mm), oval shell (Fig.10.9g) with a strong posterior ridge and sulcus, and a lunular incision. It has three cardinal teeth in the right valve, of which 3a is typically thin, while 3b is broad (Fig. 10.9f) and points

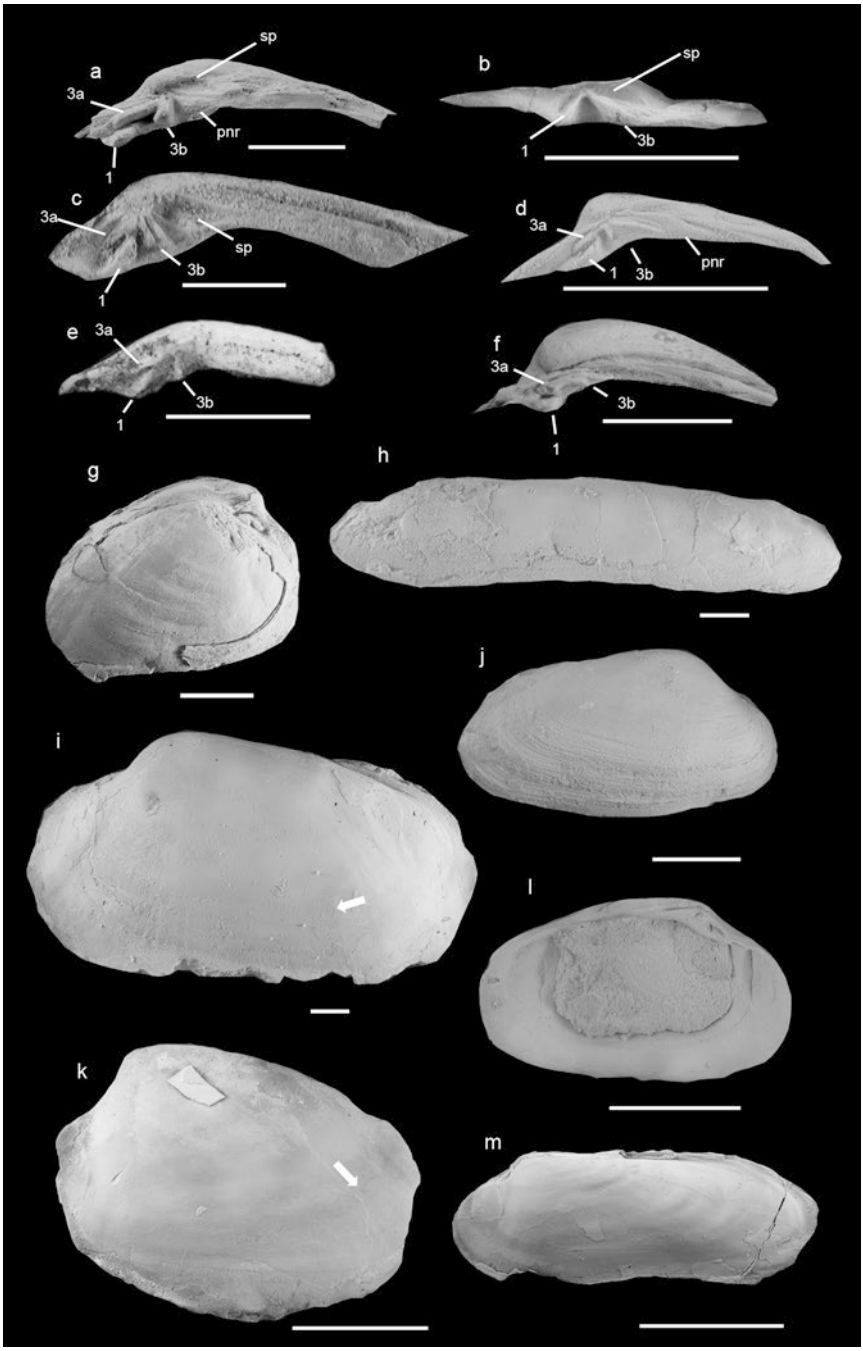

Fig. 10.9 Vesicomyidae. All scale bars are 10 mm. (**a**, **k**) *Hubertschenckia ezoensis* (Yokoyama 1890) from a late Eocene seep site in Hokkaido, Japan: (**a**) hinge of right valve with subumbonal

in a posteroventral direction (Woodring 1925; Krylova and Janssen 2006; Amano and Kiel 2007b). In molecular phylogenies, extant species with this type of morphology fall within at least two distinct clusters: one with *Vesicomya crenulomarginata* and *V. kuroshimana* and the other with *Calyptogena ponderosa* and *C. cordata* (Kojima et al. 2004; Martin and Goffredi 2011; Audzijonyte et al. 2012; Valdés et al. 2013; Johnson et al. 2017). *Pliocardia* is used for the former group, whereas the latter is typically referred to as '*cordata* group' (Johnson et al. 2017). Apart from their general similarity to *Pliocardia*, these extant species vary greatly in size and also in the presence and shape of the pallial sinus. The same applies to the fossil species currently considered as belonging to *Pliocardia*, including the oldest species of the Vesicomyidae, *Pliocardia* aff. *tschudi* from the middle Eocene of Washington State (Amano and Kiel 2007b; Amano et al. 2014a), *Vesicomya tsuchudi* from the lower Oligocene of Peru (Kiel et al. 2020b), and *Pliocardia*? *tanakai* from the Middle Miocene Bessho Formation in central Honshu (Miyajima et al., 2017). Clearly, the species currently assigned to *Pliocardia* are in need of taxonomic revision, and the introduction of one or more new genera may be necessary (Amano et al. 2014a; Martin and Goffredi 2011; Kiel et al. 2020b).

2. *Wareniconcha* Cosel and Olu, 2009: This genus is based on the Recent species *Wareniconcha guineensis* (Thiele and Jaeckel 1931) living in the Gulf of Guinea. It is characterized by having a veneriform, medium-sized shell, a narrow hinge plate with a strong middle cardinal tooth (1) in the right valve and a subumbonal pit, and the lack of a pallial sinus. One large fossil species, *Wareniconcha mercenarioides*, occurs at a Pliocene methane-seep deposit at Liog-Liog Point on Leyte Island, Philippines (Kase et al. 2019).
3. *Pleurophopsis* Van Winkle, 1919: This is an exclusively fossil genus based on *P. unioides* Van Winkle, 1919, from Miocene seep deposits in Trinidad. It is characterized by an elongate shell with two cardinal teeth in the right valve

pit (sp) and posterior nymphal ridge (pnr); JUE no.15837-12; (**k**) inner surface of left valve with pallial sinus (indicated by white arrow), JUE no. 15837-10. (**b**, **m**) *Pleurophopsis hokkaidoensis* (Amano and Kiel 2007b) from the early Middle Miocene whale-fall site in Shosanbetsu Village, Hokkaido, Japan; (**b**) rubber cast of right valve hinge with subumbonal pit (sp), JUE no. 15851, paratype; (**m**) JUE no. 15848, holotype. (**c**, **i**) *Archivesica kawamurai* (Kuroda, 1943) from Pliocene seep sites in Kanagawa Pref. (c) and Chiba Prefecture (**i**), Honshu, Japan; (**c**) right valve hinge with subumbonal pit (sp); JUE no. 15877-2; (**i**) inner surface of left valve with pallial sinus (indicated by white arrow); JUE no. NSM no. 4409. (**d**, **l**) *Calyptogena pacifica* Dall, 1891, from a Late Miocene seep site in Aomori Prefecture, Honshu, Japan; (**d**) right valve hinge with subumbonal pit (sp) and posterior nymphal ridge (pnr), JUE no. 15884-5; (**l**) JUE no. 15884-1. (**e**, **j**) *Notocalyptogena neozelandica* Amano, Saether, Little, and Campbell, 2014, from the Early Miocene Ugly Hill seep site, North Island, New Zealand; (**e**) UOA L4593, paratype; (**j**) UOA L4591, holotype. (**f**, **g**) *Pliocardia kawadai* (Aoki, 1954) from an Early Miocene seep site in Fukushima Pref., Honshu, Japan; (**f**) JUE no. 15895-2; (**g**) JUE no. 15895-3. (**h**) *Pleurophopsis uchimuraensis* (Kuroda 1931) from a Middle Miocene seep site in Nagano Prefecture, Honshu, Japan; JUE no. 15865-1. (**a**, **b**, **k**, **m**: Amano and Kiel 2007b; **c**, **i**: Amano and Kiel, 2010; **d**, **l**: Amano and Jenkins 2011b; **e**, **j**: Amano et al. 2014b; **f**, **g**: Amano and Kiel 2012; **h**: Amano and Kiel 2011)

(a strong cardinal 1 and a short 3b, cardinal 3a is reduced; Fig. 10.9b). The anterior adductor muscle scar and pedal retractor muscle scar are separate, and the pallial line starts at the posteroventral margin of the anterior adductor muscle scar. A synonym is *Adulomya* Kuroda, 1931, with the Miocene type species *A. uchimuraensis* Kuroda, 1931 (see also Amano et al. 2019a; Fig. 10.9h). *Pleurophopsis* shares its elongated shell and two cardinal teeth in the right valve with the Recent genus *Ectenagena* Woodring, 1938, but differs by the absence of a deep umbonal pit. The oldest fossil record of *Pleurophopsis* may be *P. chinookensis* (Squires and Goedert 1991) from upper Eocene seep deposits of western Washington State, USA (Amano and Kiel 2007b).

4. *Calyptogena* Dall, 1891: Based on the extant *Calyptogena pacifica* (Fig. 10.9d, l), this genus includes species with moderately sized shells, characterized by having a posterior nymphal ridge on the hinge plate, three cardinal teeth in the right valve of which cardinal 3b typically points in an antero-ventral direction, and the absence of a pallial sinus, subumbonal pit, and lunular incision (Krylova and Sahling 2006). In particular, the posterior nymphal ridge is unusual among vesicomyids and clearly distinguishes this genus from all others. The oldest fossil record is *Calyptogena katallaensis* from the Oligocene of Alaska (Kiel and Amano 2010); the oldest record of an extant species is *Calyptogena pacifica* from the Upper Miocene of Japan (Amano and Jenkins 2011b).
5. *Notocalyptogena* Amano, Saether, Little, and Campbell, 2014: This is so far a monospecific genus based on *N. neozelandica* (Fig. 10.9e, j), from the Early and Middle Miocene of New Zealand (Amano et al. 2014b). *Notocalyptogena* and *Calyptogena* share elongate ovate shells (maximum length = 90 mm; Krylova and Sahling 2006), three cardinal teeth in the right valve, and the lack of a subumbonal pit and a pallial sinus. *Notocalyptogena* differs from *Calyptogena* by lacking a stout posterior cardinal tooth (3b) and a posterior nymphal ridge.
6. *Hubertschenckia* Takeda, 1953: This is an exclusively fossil genus based on *Tapes ezoensis* Yokoyama, 1890, from the late Eocene to Oligocene of northern and central Japan (Amano et al. 2013b; Amano and Kiel 2007b; Takeda 1953). Its shell is elongate ovate, has three cardinal teeth in the right valve, a subumbonal pit, and a shallow pallial sinus (Fig. 10.9a, k). *Hubertschenckia* differs from *Archivesica* by having a smaller shell (about 75 mm versus up to 300 mm in *Archivesica*; Krylova and Sahling, 2010), a long anterior cardinal tooth (3a), a middle tooth (1) that runs parallel to the hinge margin, and a vertical posterior cardinal tooth (3b) (Amano and Kiel 2007b).
7. *Archivesica* Dall, 1908b: The extant type species *A. gigas* (Dall, 1896) is characterized by an elongate, broad, ovate shell with three cardinal teeth in the right valve; a subumbonal pit; and a shallow pallial sinus. The cardinals are thin; cardinal 1 starts below the umbo, is curved, and points to the anterior; 3a runs roughly parallel to the posterior shell margin and is fused with 3b, which points to the posterior. The oldest record of the genus is *Archivesica sakoi* Amano, Jenkins, Ohara, and Kiel, 2014, from the Lower Miocene Shikiya Formation in Wakayama Prefecture, southern Honshu, followed by several species in the Middle to Late Miocene species of Italy (Kiel and Taviani 2017), the Late Miocene of Japan (Amano and Kiel, 2010; Amano and Suzuki 2010), and the

Pliocene-Pleistocene of California (Squires 1991). Problematics are the relationships to, or synonymies with, the three genera *Phreagena*, *Laubiericoncha*, and *Akebiconcha*. *Phreagena* Woodring, 1938, is based on the Pliocene species *Phreagena lasia* Woodring and may be distinguishable from *Archivesica* by having a thicker shell with narrower subumbonal pit, a longer ligament, and a deeper anterior pedal retractor scar (Krylova and Janssen 2006). *Laubiericoncha* Cosel and Olu, 2008, based on the extant *L. myriamae* Cosel and Olu was separated from *Archivesica* by having a tapering posterior part of shell, a short and broad pallial sinus, and a deep anterior pedal retractor scar. *Akebiconcha* Kuroda, 1943, based on the extant *A. kawamurai* Kuroda (Fig. 10.9c, i) was not compared with *Archivesica* at its proposal. The concept of the generic composition of the pliocardiins as outlined by Krylova and Sahling (2010) was not entirely supported by recent molecular phylogenetic work (Audzijonyte et al. 2012; Johnson et al. 2017); thus, *Phreagena* and *Akebiconcha* are regarded as a synonym of *Archivesica* (Amano and Kiel 2007b). Moreover, *Laubiericoncha* Cosel and Olu, 2008, based on *L. myriamae* Cosel and Olu, 2008 falls within a large cluster including the type species of *Archivesica* (Audzyonite et al. 2012; Decker et al. 2012; Johnson et al. 2017), and also based on shell characters, it is difficult to distinguish from *Archivesica* (Amano and Kiel 2007b; Amano and Suzuki 2010). Although Johnson et al. (2017) referred to a large clade including all these taxa as "*gigas* group," it has to be referred to as *Archivesica* because *A. gigas* is the type species of *Archivesica*.

8. *Isorropodon* Sturany, 1896: The type species, *Isorropodon perplexum*, is extant in the Mediterranean Sea. This genus comprises species with small, thin, ovate shells that may or may not have a posterior ridge, lack a lunular incision, and have a *Vesicomya*-like dentition with the cardinals in the right valve all arranged roughly in one line and undulating sub-parallel to the dorsal shell margin. *Pliocardia* differs by having a lunular incision and a more *Archivesica*-like hinge dentition with a thick posterior cardinal tooth (3b) in the right valve that points postero-ventrally. *Vesicomya* has a more globular, roundish shell with a lunular incision (Cosel and Salas 2001). Fossil species includes *Isorropodon frankfortensis* Amano and Kiel, 2007b, from the Lower Miocene in southwestern Washington State, USA (Amano and Kiel 2007b), and *Isorropodon* sp. from the Pliocene Stirone River deposit in Italy (Kiel and Taviani 2018).

10.9 The Anomalodesmata

Steffen Kiel

Anomalodesmatan bivalves have not been reported from modern seeps, and only a few are known from the older fossil record. A single cuspidariid species, *Thermomya sulcata* Chen, Okutani, Watanabe, and Kojima, 2018, was reported from a back-arc vent site in the Southern Mariana Trough (Chen et al. 2018), but although the

anatomy of the available specimens are too poorly preserved to assess the potential of chemosymbiosis, this seems unlikely as all other cuspidariids are carnivore (e.g., Morton and Machado 2019).

A definitive anomalodesmatan, *Aksumya* Kiel, 2018, occurs in Upper Triassic seep deposits in Turkey and is restricted to seeps (Kiel et al. 2017). Its shells reach up to 82 mm in length, are oval-elongate with a drawn-out and somewhat pointed posterior margin, are apparently edentulous, sculptured by irregular growth lines, and have microscopic spines, which clearly identify them as members of the Anomalodesmata (Sartori and Harper 2009). The feeding habits of *Aksumya* is unknown, and chemosymbiosis can only be inferred from its relatively large size, its abundance at seeps, and its restriction to the seep environment.

Several taxa previously reported as anomalodesmatans from Paleozoic seeps (i.e., from the Hollard Mound; Aitken et al. 2002) are now considered as belonging to the modiomorphids (see above; Hryniewicz et al. 2017a). From the Permian of Brazil, members of three genera of presumed anomalodesmatans (*Anhembia*, *Tambaquyra*, and *Maackia*) were reported from concretionary limestone deposits, interpreted as cold seep deposits (Matos et al. 2017). If this interpretation is correct, anomalodesmatans would have reached a remarkable diversity at late Paleozoic-early Mesozoic seeps. However, the figured outcrops and rock samples look unlike those of other, confirmed, seep deposits, and lack the typical "seep cements" such as banded and botryoidal rim cements (cf. Peckmann and Thiel 2004). In addition, the reported carbon isotope values are only as low as −7.6‰ and thus well within the range of septarians and other concretions resulting from the oxidation of organic matter (Irwin et al. 1977). Furthermore, the interpretation of Matos et al. (2017) of these bivalves as chemosymbiotic relies partly on a questionable comparison of shell characters of non-chemosymbiotic bivalves and partly on the negative isotope signature of the shells themselves. However, studies on extant and fossil bivalves have shown that metabolic carbon (which would carry a signal for chemosymbiosis) is not incorporated into the shell (Paull et al. 1989; Kiel and Peckmann 2007). Moreover, the Permian shells from Brazil are recrystallized and hence do not carry the original isotopic signature of the shell but rather of the dissolved carbon incorporated during their recrystallization. A single specimen of *Pleuromya*? has been collected from the Paleocene seep fauna of the Basilika Formation on Spitsbergen Island (Hryniewicz et al. 2019).

10.10 Conclusions

Kazutaka Amano

The chronostratigraphic ranges of all genera of mainly seep-inhabiting chemosymbiotic bivalves are shown in Fig. 10.2; records from hydrothermal vent, whale fall and wood fall are also included. This shows an overall increase in bivalve diversity at seeps since the Paleozoic, a pattern that was linked earlier to the general increase of bivalve biodiversity through the Phanerozoic (Kiel and Peckmann 2019). Forsey

(2013) emphasized a large increase in seep bivalve diversity starting in the Jurassic and considered this increase as being part of the "Mesozoic Marine Revolution" (Vermeij 1977, 1987). Remarkably, apart from the Devonian solemyid *Dystactella*, many infaunal chemosymbiotic bivalve taxa such as the solemyids, thyasirids, and lucinids appeared in the Late Jurassic and diversified in the Cretaceous. This timing is synchronous with the increasing infaunality of bivalves as an antipredatory strategy, known as one of the effects of the "Mesozoic Marine Revolution." However, these patterns and their potential causes should be treated cautiously because the fossil record of seeps and seep communities beyond the Cretaceous is still very sparse (Campbell 2006; Kiel 2009, 2015; Hryniewicz et al. 2017b; Kiel and Peckmann 2019).

Drill holes made by predatory gastropods have been reported from chemosymbiotic bivalves soon after the first appearance of these gastropods in the mid-Cretaceous (Taylor et al. 1983): in Cenomanian nucinellids; Eocene thyasirids and vesicomyids; Oligocene thyasirids and bathymodiolins; and Miocene thyasirids, vesicomyids, and bathymodiolins (Amano 2003; Amano and Jenkins 2007; Amano and Kiel 2007a; Kiel et al. 2008, 2016). The fossil record of these drill holes thus suggests increasing predation pressure since the Late Cretaceous. Remarkably, this coincides roughly with a "mid-Cretaceous faunal turnover" from pre- to post-Albian seep faunas (Kiel et al. 2012; Jenkins et al. 2013, 2018b; Kiel 2015). Although this faunal change is not readily apparent in terms of genus richness or extinction and origination pattern (Fig. 10.2), the lifestyle of the dominant bivalves at seeps changed from epifaunal to infaunal. Kiel (2015) suggested that this "mid-Cretaceous faunal turnover" resulted from a decrease in seawater sulfate concentrations but did not consider drilling predation in this context. However, drill holes in the main epifaunal bivalve at seeps at that time, *Caspiconcha*, have never been reported. Disentangling the biological, chemical, and physical environmental changes leading to the described changes in seep bivalve diversity and life habits in the late Mesozoic requires further research.

Many clades of the modern vent and seep fauna, including the dominant bathymodiolins and vesicomyids with their semi-infaunal or epifaunal lifestyles, appeared in the Eocene (Fig. 10.2). Jacobs and Lindberg (1998) and Vrijenhoek (2013) claimed that deep-water anoxia during the Paleocene-Eocene Thermal Maximum (PETM) caused the extinction of the deep-sea fauna, including that at vents and seeps. Furthermore, also molecular age estimates indicate an early Cenozoic origin of many of the major groups at vents and seeps, and the PETM extinction is considered to have played a major role in this pulse of origination, by extinguishing old groups and making room for new ones (Chelvadonné et al. 2002; Jones et al. 2006; Vrijenhoek. 2013). However, the (admittedly patchy) fossil record during this time interval (Fig. 10.2) does not show any extinctions (Hryniewicz et al. 2017a, 2019). Kiel (2015) argued that the mid-Eocene appearance of semi-infaunal and epifaunal bivalves such as bathymodiolins and vesicomyids was linked to a dramatic rise in seawater sulfate concentrations (Wortmann and Paytan 2012), which resulted in increased sulfide availability at vents and seeps, and organic substrates. New and more detailed fossil records across the end-Cretaceous and PETM extinction events are needed to test these competing hypotheses.

Acknowledgments We thank Andrzej Kaim for his invitation to contribute to this chapter. We also thank Simon Schneider and Elizabeth M. Harper for their review and useful comments. This work was partly supported by a Grant-in-aid for Scientific Research from the Japan Society for Promotion of Science (C, 26400500, 2014–2016; C, 17K05691, 2017–2019) to KA and RGJ and a National Science Foundation grant (No. 2014/B/ST10/04886) to KH.

References

Adams A (1860) On some new genera and species of Mollusca from Japan. Ann Mag Nat Hist (ser 3) 5:299–303

Agirrezabala LM, Kiel S, Blumenberg M et al (2013) Outcrop analogues of pockmarks and associated methane-seep carbonates: a case study from Lower Cretaceous (Albian) of the Basque-Cantabrian Basin, western Pyrenees. Palaeogeogr Palaeoclimatol Palaeoecol 390:94–115

Aitken SA, Henderson CM, Collom CJ et al (2002) Stratigraphy, paleoecology and origin of Lower Devonian (Emsian) carbonate mud buildups, Hamar Laghdad, eastern Anti-Atlas, Morocco. Bull Can Petrol Geol 50:217–243

Allen JA (1958) On the basic form and adaptations to habitat in the Lucinacea (Eulamellibranchia). Philos Trans R Soc Lond B 241:421–484

Amano K (1984) Two species of Mytilidae (Bivalvia) from the Miocene deposits in Hokkaido, Japan. Venus 43:183–189

Amano K (2003) Predatory gastropod drill holes in Upper Miocene cold seep Bivalves, Hokkaido, Japan. Veliger 46:90–96

Amano K, Ando H (2011) Giant fossil *Acharax* (Bivalvia: Solemyidae) from the Miocene of Japan. Nautilus 125:207–212

Amano K, Jenkins RG (2007) Eocene drill holes in cold-seep bivalves of Hokkaido, northern Japan. Mar Ecol 28:108–114

Amano K, Jenkins RG (2011a) New fossil *Bathymodiolus* (*sensu lato*) (Bivalvia: Mytilidae) from Oligocene seep-carbonates in eastern Hokkaido, Japan, with remarks on the evolution of the genus. Nautilus 125:29–35

Amano K, Jenkins RG (2011b) Fossil record of extant vesicomyid species from Japan. Venus 69:163–176

Amano K, Kiel S (2007a) Drill holes in bathymodiolin mussels from a Miocene whale-fall community in Hokkaido, Japan. Veliger 49:265–269

Amano K, Kiel S (2007b) Fossil vesicomyid bivalves from the North Pacific region. Veliger 49:270–293

Amano K, Kiel S (2010) Taxonomy and distribution of fossil *Archivesica* (Bivalvia: Vesicomyidae) in Japan. Nautilus 124:155–165

Amano K, Kiel S (2011) Fossil *Adulomya* (Vesicomyidae, Bivalvia) from Japan. Veliger 51:76–90

Amano K, Kiel S (2012) Two fossil vesicomyid species (Bivalvia) from Japan and their biogeographic implications. Nautilus 126:79–85

Amano K, Little CTS (2005) Miocene whale-fall community from Hokkaido, northern Japan. Palaeogeogr Palaeoclimatol Palaeoecol 215:345–356

Amano K, Suzuki A (2010) Redescription of '*Calyptogena' shiretokensis Uozumi* (Bivalvia: Vesicomyidae) from the Miocene Rusha Formation on the Shiretoko Peninsula, eastern Hokkaido, Japan. Venus 68:165–171

Amano K, Jenkins RG, Hikida Y (2007a) A new gigantic *Nucinella* (Bivalvia: Solemyoida) from the Cretaceous cold-seep deposit in Hokkaido, northern Japan. Veliger 49:84–90

Amano K, Little CTS, Inoue K (2007b) A new Miocene whale-fall community from Japan. Palaeogeogr Palaeoclimatol Palaeoecol 247:236–242

Amano K, Jenkins RG, Kurihara Y et al (2008) A new genus for *Vesicomya inflata* Kanie and Nishida, a lucinid shell convergent with that of vesicomyids, from Cretaceous strata of Hokkaido, Japan. Veliger 50:255–262

Amano K, Jenkins RG, Aikawa M et al (2010) A Miocene chemosynthetic community from the Ogaya Formation in Joetsu: evidence for depth-related ecologic control among fossil seep communities in the Japan Sea back-arc basin. Palaeogeogr Palaeoclimatol Palaeoecol 286:164–170

Amano K, Hasegwa S, Ishihama S (2013a) (Molluscan fossils from core sample collected from off Joetsu during MD 179 cruise.) J Jpn Ass Petrol Technol 78:92–96 (In Japanese)

Amano K, Jenkins RG, Sako Y et al (2013b) A Paleogene deep-sea methane-seep community from Honshu, Japan. Palaeogeogr Palaeoclimatol Palaeoecol 387:126–133

Amano K, Jenkins RG, Ohara M et al (2014a) Miocene vesicomyid species (Bivalvia) from Wakayama in southern Honshu, Japan. Nautilus 128:9–17

Amano K, Saether KP, Little CTS et al (2014b) Fossil vesicomyid bivalves from Miocene hydrocarbon seep sites, North Island, New Zealand. Acta Palaeontol Pol 59:421–428

Amano K, Little CTS, Campbell KA et al (2015) Paleocene and Miocene *Thyasira sensu stricto* (Bivalvia: Thyasiridae) from chemosynthetic communities from Japan and New Zealand. Nautilus 129:43–53

Amano K, Jenkins RG, Kurita H (2018a) New and Mesozoic-relict mollusks from Paleocene wood-fall communities in Urahoro Town, eastern Hokkaido, northern Japan. J Paleontol 92:634–647

Amano K, Little CTS, Campbell KA (2018b) Lucinid bivalves from Miocene hydrocarbon seep sites of eastern North Island, New Zealand, with comments on Miocene New Zealand seep faunas. Acta Palaeontol Pol 63:371–382

Amano K, Miyajima Y, Jenkins RG et al (2019a) Miocene to Recent biogeographic history of vesicomyid bivalves in Japan, with two new records of the family. Nautilus 133:48–56

Amano K, Miyajima Y, Nakagawa K et al (2019b) Chemosymbiotic bivalves from the lower Miocene Kurosedani Formation in Toyama Prefecture, central Honshu, Japan. Paleontol Res 23:208–219

Anderson AE, Childress JJ, Favuzzi JA (1987) Net uptake of CO_2 driven by sulfide and thiosulphate oxidation in the bacterial symbiont-containing bivalve *Solemya reidi*. J Exp Biol 133:1–31

Aoki S (1954) Mollusca from the Miocene Kabeya Formation, Joban coal-field, Fukushima Prefecture, Japan. Sci Rep Tokyo Kyoiku Daigaku (Sec C) 3:23–41

Arellano SM, Young CR (2009) Spawning, development, and the duration of larval life in a deep-sea cold-seep mussel. Biol Bull 216:149–162

Arellano SM, Van Gaest AL, Johnson SB et al (2014) Larvae from deep-sea methane seeps disperse in surface waters. Proc R Soc B 281:20133276

Asato K, Kase T (2019) (Paleoecology of *Shikamaia*, the Permian giant bivalves (Alatoconchidae: Ambonychioidea) from Japan.) Abstracts of the annual meeting of the Malacological Society of Japan 2019:20 (In Japanese)

Åström EKL, Oliver PG, Carroll ML (2017) A new genus and two new species of Thyasiridae associated with methane seeps off Svalbard. Arctic Ocean Mar Biol Res 13(4):402–416

Audzijonyte A, Krylova EM, Sahling H et al (2012) Molecular taxonomy reveals broad trans-oceanic distributions and high species diversity of deep-sea clams (Bivalvia: Vesicomyidae: Pliocardiinae) in chemosynthetic environments. Syst Biodivers 10:403–415

Baco AR, Smith CR, Peek AS et al (1999) The phylogenetic relationships of whale-fall vesicomyid clams based on mitochondrial COI DNA sequences. Mar Ecol Prog Ser 182:137–147

Barry JP, Kochevar RE, Baxter CH (1997) The influence of pore-water chemistry and physiology on the distribution of vesicomyid clams at cold seeps in Monterey Bay: implications for patterns of chemosynthetic community organization. Limnol Oceanogr 42:318–328

Batstone RT, Laurich JR, Salvo F et al (2014) Divergent chemosymbiosis-related characters in Thyasira cf. gouldi (Bivalvia, Thyasiridae). PLoS One 9(3):e92856

Beets C (1942) Beiträge zur Kenntnis der angeblich oberoligocänen Mollusken-Fauna der Insel Buton, Niederländisch-Ostindien. Leidse Geol Meded 13:255–328

Beets C (1953) Reconsideration of the so-called Oligocene fauna in the asphaltic deposits of Buton (Malay Archipelago). Leidse Geol Meded 17:237–258
Bertolaso L, Palazzi S (1994) La posizione sistematica di *Delphinula bellardii* Michelotti, 1847. Boll Malacol 29:291–302
Beu AG, Maxwell PA (1990) Cenozoic Mollusca of New Zealand. New Zealand Geological Survey Palaeontogical Bulletin 58. New Zealand Department of Scientific and Industrial Research, Lower Hutt
Bieler R, Mikkelsen PM, Collins TM et al (2014) Investigating the bivalve tree of life—an exemplar-based approach combining molecular and novel morphological characters. Invertebr Syst 28:32–115
Bouchet P, Cosel RV (2004) The world's largest lucinid is an undescribed species from Taiwan (Mollusca: Bivalvia). Zool Stud 43:704–711
Bron HG (1831) Italiens Tertiar-gebide und deren organische Einschlüsse. Heidelburg.
Brugnone G (1880) Le conchiglie plioceniche selle vicinanze di Caltasetta. Boll Soc Malacol Ital 6:85–158
Campbell KA (2006) Hydrocarbon seep and hydrothermal vent paleoenvironments and paleontology: past developments and future research directions. Palaeogeogr Palaeoclimatol Palaeoecol 232:362–407
Campbell KA, Bottjer DJ (2006) Brachiopods and chemosymbiotic bivalves in Phanerozoic hydrothermal vent and cold-seep paleoenvironments. Geology 23:321–324
Campbell KA, Francis DA, Collins M et al (2008) Hydrocarbon seep carbonates of a Miocene forearc (East Coast Basin), North Island, New Zealand. Sediment Geol 204:83–105
Carter JG, Altaba CR, Anderson LC et al (2011) A synoptical classification of the Bivalvia (Mollusca). Paleontol Contrib 4:1–47
Cary SC (1994) Vertical transmission of a chemoautotrophic symbiont in the protobranch bivalve, *Solemya reidi*. Mol Mar Biol Biotechnol 3:121–130
Chavan A (1969) Superfamily Lucinacea Fleming, 1828. In: Moore RC (ed) Mollusca 6, Bivalvia 2. Treatise on invertebrate paleontology, part N. Geological Society of America and University of Kansas, Boulder, pp N491–N518
Chen C, Okutani T, Watanabe HK et al (2018) The first cuspidariid bivalve associated with a hydrothermal vent discovered from the southern Mariana Trough. Venus 76:39–44
Chevaldonné P, Jollivet D, Desbruyères D et al (2002) Sister-species of eastern Pacific hydrothermal-vent worms (Ampharetidae, Alvinelidae, Vestimentifera) provide new mitochondrial clock calibration. Cah Biol Mar 43:367–370
Childress JJ, Fisher CR, Brooks JM et al (1986) A methanotrophic marine molluscan (Bivalvia Mytilidae) symbiosis: mussels fueled by gas. Science 233:1306–1308
Clark BL (1925) Pelecypoda from the marine Oligocene of western North America. Univ Calif Publ Geol Sci 15:69–136
Clausen CK, Wignall PB (1990) Early Kimmeridgian bivalves of southern England. Meso Res 2:97–149
Coan EV, Scott PV, Bernard FR (2000) Bivalve seashells of western North America: marine bivalve molluscs from Arctic Alaska to Baja California. Santa Barbara Museum of Natural History monograph 2. Santa Barbara Museum of Natural History, Santa Barbara
Combosch JD, Collins TM, Glover EM et al (2017) A family-level tree of life for bivalves based on a Sanger-sequencing approach. Mol Phylogenet Evol 107:191–208
Conrad TA (1849) Fossils from northwestern America. In: Dana JD (ed) United States exploring expedition during the years 1838, 1839, 1840, 1841, 1842 under the command of Charles Wilkes, U.S.N., atlas, geology, vol 10. Sherman, Philadelphia, pp 722–728
Conway NM, Howes BL, McDowell Capuzzo JE et al (1992) Characterization and site description of *Solemya borealis* (Bivalvia; Solemyidae), another bivalve-bacteria symbiosis. Mar Biol 112:601–613
Cooke CW (1919) Contributions to the geology and paleontology of the West Indies IV: Tertiary mollusks from the Leeward Islands and Cuba. Carnegie Inst Wash Publ 291:103–156

Cosel RV (2002) A new species of bathymodioline mussel (Mollusca, Bivalvia, Mytilidae) from Mauritania (West Africa), with comments of the genus *Bathymodiolus* Kenk and Wilson, 1985. Zoosystema 24:259–271

Cosel RV, Bouchet P (2008) Tropical deep-water lucinids (Mollusca: Bivalvia) from the Indo-Pacific: essentially unknown, but diverse and occasionally gigantic. In: Héros V, Cowie R, Bouchet P (eds) Tropical deep sea benthos, vol 25. Mém Mus Natl Hist Nat, Paris 196:115–213

Cosel RV, Marshall BA (2003) Two new species of large mussels (Bivalvia Mytilidae) from active submarine volcanoes and a cold seep off the eastern North Island of New Zealand, with descriptions of a new genus. Nautilus 117:31–46

Cosel RV, Marshall BA (2010) A new genus and species of large mussel (Mollusca: Bivalvia: Mytilidae) from the Kermadec Ridge. Tuhinga 21:59–73

Cosel RV, Olu K (2008) A new genus and new species of Vesicomyidae (Mollusca, Bivalvia) from cold seeps on the Barbados accretionary prism, with comments on other species. Zoosystema 30:929–944

Cosel RV, Olu K (2009) Large Vesicomyidae (Mollusca: Bivalvia) from cold seeps in the Gulf of Guinea off the coasts of Gabon, Congo and northern Angola. Deep-Sea Res Part II 56:2350–2379

Cosel RV, Salas C (2001) Vesicomyidae (Mollusca: Bivalvia) of the genera *Vesicomya*, *Waisiuconcha*, *Isorropodon* and *Callogonia* in the eastern Atlantic and the Mediterranean. Sarsia 86:333–366

d'Orbigny AD (1844) Paléontologie Francaise, terrains Crétacés, vol 3. Mollusques. G. Masson, Paris

Dall WH (1891) Scientific results of explorations by the U.S. Fish Commission Steamer Albatross XX: on some new or interesting West American shells obtained from dredgings of the U.S. Fish Commission steamer Albatross in 1888. Proc US Natl Mus 14:174–191

Dall WH (1896) Diagnoses of new species of mollusks from the west coast of America. Proc US Natl Mus Nat Hist 18:7–20

Dall WH (1901) Synopsis of the Lucinacea and of the American species. Proc US Natl Mus Nat Hist 23:779–833

Dall, WH (1903) Contributions to the Tertiary of Florida with especial reference to the Silex-bed of Tampa and the Pliocene beds of the Caloosahatchee River, including in many cases a complete revision of the generic groups treated of and their American Tertiary species, Part VI: concluding the work. Trans Wagner Free Inst Sci Phila 3:1219–1654

Dall WH (1908a) A revision of the Solenomyacidae. Nautilus 22:1–2

Dall WH (1908b) Reports on the dredging operations off the west coast of Central America to the Galapagos, to the west coast of Mexico, and in the Gulf of California, in charge of Alexander Agassiz, carried on by the US Fish Commission Steamer 'Albatross,' during 1891, Lieut. Commander Z. L. Tanner, USN, commanding, XXXVII: reports on the scientific results of the expedition to the eastern tropical Pacific, in charge of Alexander Agassiz, by the U. S. Fish Commission Steamer 'Albatross,' from October, 1904, to March, 1905, Lieut. Commander L. M. Garrett, USN, commanding, XIV: the Mollusca and the Brachiopoda. Bull Mus Comp Zool Harvard Univ 43:205–487

Dando PR, Southward AJ (1986) Chemoautotrophy in bivalve molluscs of the genus *Thyasira*. J Mar Biol Assoc UK 66:915–929

Danise S, Dominici S, Bertolaso L (2010) Mollusk species at a Pliocene shelf whale fall (Orciano Pisano, Tuscany). Plaios 25:449–456

Danise S, Bertolaso L, Dominici S (2016) Bathymodioline mussel dominated Miocene whale fall from Italy. Boll Soc Paleontol Ital 55:47–53

Dautzenberg PH (1927) Mollusques provenant des campagnes scientifiques du Prince Albert Ier de Monaco dans l'Océan Atlantique et dans le Golfe de Gascogne. Résultats des Campagnes Scientifiques Accomplies sur son Yacht par Albert Ier Prince Souverain de Monaco LVVII. Impri Monaco, Monaco

Decker C, Olu K, Cunha RL et al (2012) Phylogeny and diversification patterns among vesicomyid bivalves. PLoS One 7:1–8
Dell RK (1987) Mollusca of the family Mytilidae (Bivalvia) associated with organic remains from deep water off New Zealand, with revisions of the genera *Adipicola* Dautzenberg, 1927 and *Idasola* Iredale, 1915. Natl Mus NZ Rec 3:17–36
Distel DL, Baco AR, Chuang E et al (2000) Do mussels take wooden steps to deep-sea vents? Nature 403:725–726
Distel DL, Altamia MA, Lin Z et al (2017) Discovery of chemoautotrophic symbiosis in the giant shipworm *Kuphus polythalamia* (Bivalvia: Teredinidae) extends wooden-steps theory. Proc Natl Acad Sci USA 114(18):E3652–E3658
Dubilier N, Bergin C, Lott C (2008) Symbiotic diversity in marine animals: the art of harnessing chemosynthesis. Nat Rev Microbiol 6:725–740
Duff KL (1978) Bivalvia from the English lower Oxford Clay (Middle Jurassic). Palaeontol Soc Monogr 132(1–137):pls 1–13
Dufour SC (2005) Gill anatomy and evolution of symbiosis in the bivalve family Thyasiridae. Biol Bull 208:200–212
Dufour SC (2018) Bivalve chemosymbioses on mudflats. In: Beninger PG (ed) Mudflat ecology. Springer, Heidelberg, pp 169–184
Dufour SC, Felbeck H (2003) Sulphide mining by the superextensile foot of symbiotic thyasirid bivalves. Nature 426:65–67
Duperron S (2010) The diversity of deep-sea mussels and their bacterial symbioses. In: Kiel S (ed) The vent and seep biota, Topics in geobiology 33. Springer, Heidelberg, pp 137–167
Duperron S, Bergin C, Zielinski F et al (2006) A dual symbiosis shared by two mussel species, *Bathymodiolus azoricus* and *Bathymodiolus puteoserpentis* (Bivalvia: Mytilidae), from hydrothermal vents along the northern Mid-Atlantic Ridge. Environ Microbiol 8:1141–1447
Duperron S, Fiala-Médoni A, Caprais JC et al (2007) Evidence for chemoautotrophic symbiosis in a Mediterranean cold seep clam (Bivalvia: Lucinidae): comparative sequence analysis of bacterial 16S rRNA, APS reductase and RubisCO genes. FEMS Microbiol Ecol 59:64–74
Duperron S, Halary S, Lorion J et al (2008) Unexpected co-occurrence of six bacterial symbionts in the gills of the cold seep mussel *Idas* sp. (Bivalvia: Mytilidae). Environ Microbiol 10:433–445
Fischer P (1861) Decription d'une genre nouveau. J Conchyliol 9:345–347
Fleming CA (1950) New Zealand Recent Thyasiridae (Mollusca). Trans R Soc NZ 78:251–254
Forsey GF (2013) Fossil evidence for the escalation and origin of marine mutualisms. J Nat Hist 47:1833–1864
Foster WJ, Danise S, Twitchett R (2017) A silicified early Triassic marine assemblage from Svalbard. J Syst Palaeontol 15:851–877
Fujiwara Y (2003) Endosymbioses between invertebrates and chemosymbiotic bacteria. Jpn J Benthol 58:26–33
Fujiwara Y, Kato C, Masui N et al (2001) Dual symbiosis in a cold seep thyasirid clam *Maorithyas hadalis* from the hadal zone in the Japan Trench, western Pacific. Mar Ecol Prog Ser 214:151–159
Fujiwara Y, Okutani T, Yamanaka T et al (2009) *Solemya pervernicosa* lives in sediment underneath submerged whale carcasses: its biological significance. Venus 68:27–37
Fukasawa Y, Matsumoto H, Beppu S et al (2017) Molecular phylogenetic analysis of chemosymbiotic Solemyidae and Thyasiridae. Open J Mar Sci 7:124–141
Gabb WM (1866) Description of the Tertiary invertebrate fossils. Calif Geol Surv Palaeontol 2:1–38
Gaillard C, Rio M, Rolin Y (1992) Fossil chemosynthetic communities related to vents or seeps in sedimentary basins: the pseudobioherms of southeastern France compared to other world examples. Palaios 7:451–465
Génio L, Kiel S, Cunha MR et al (2012) Shell microstructures of mussels (Bivalvia: Mytilidae: Bathymodiolinae) from deep-sea chemosynthetic sites: do they have a phylogenetic significance? Deep-Sea Res Part I 64:86–103

Génio L, Rodrigues CF, Guedes IF et al (2015) Mammal carcasses attract a swarm of mussels in the deep Atlantic: insights into colonization and biogeography of a chemosymbiotic species. Mar Ecol 36:71–81
Gill FL, Little CTS (2013) A new genus of lucinid bivalve from hydrocarbon seeps. Acta Palaeontol Pol 58:573–578
Gill FL, Harding IC, Little CTS et al (2005) Palaeogene and Neogene cold seep communities in Barbados, Trinidad and Venezuela: an overview. Palaeogeogr Palaeoclimatol Palaeoecol 227:191–209
Glover EA, Taylor JD (2007) Diversity of chemosymbiotic bivalves on coral reefs: Lucinidae (Mollusca, Bivalvia) of New Caledonia and Lifou. Zoosystema 29:109–181
Glover EA, Taylor JD (2016) Lucinidae of the Philippines: highest known diversity and ubiquity of chemosymbiotic bivalves from intertidal to bathyal depths (Mollusca: Bivalvia: Lucinidae). Mém Mus Natl Hist Nat 208:65–234
Goedert JL, Campbell KA (1995) An early Oligocene chemosynthetic community from Makah Formation, northeast Olympic Peninsula, Washington. Veliger 38:22–129
Goedert JL, Squires RL, Barnes LG (1995) Paleoecology of whale-fall habitats from deep-water Oligocene rocks, Olympic Peninsula, Washington State. Palaeogeogr Palaeoclimatol Palaeoecol 118:151–158
Gray JE (1840) Shells of molluscan animals. In: Synopsis of the contents of the British Museum, ed. 42. Woodfall & Son, London, pp 105–152
Griffin M, Pastorino G (2006) *Madrynomya bruneti* n. gen. and sp. (Bivalvia: ?Modiomorphidae): a Mesozoic survivor in the Tertiary of Patagonia? J Paleontol 80:272–282
Grossman EL (1993) Evidence that inoceramid bivalves were benthic and harbored chemosynthetic symbionts: comment and reply. Geology 21:94–96
Gustafson RG, Reid RGB (1986) Development of the pericalymma larva of *Solemya reidi* (Bivalvia: Cryptodonta: Solemyidae) as revealed by light and electron microscopy. Mar Biol 93:411–427
Gustafson RG, Reid RGB (1988) Association of bacteria with larvae of gutless protobranch bivalve *Solemya reidi* (Cryptodonta: Solemyidae). Mar Biol 97:389–401
Gustafson RG, Turner RD, Lutz RA et al (1998) A new genus and five new species of mussels (Bivalvia: Mytilidae) from deep-sea sulfide/hydrocarbon seeps in the Gulf of Mexico. Malacologia 40:63–112
Hall J, Whitfield RP (1872) Descriptions of new species of fossils from the vicinity of Louisville, Kentucky, and the falls of the Ohio; from the collection of Dr. James Knapp, of Louisville (continued). Preprint, Published in advance of the Report of the New York State Museum, Albany
Hammer Ø, Nakrem HA, Little CTS et al (2011) Hydrocarbon seeps from close to the Jurassic-Cretaceous boundary, Svalbard. Palaeogeogr Palaeoclimatol Palaeoecol 306:15–26
Hansen J, Ezat MM, Åström EKL et al (2019) New late Pleistocene species of *Acharax* from Arctic methane seeps off Svalbard. J Syst Palaeontol 18(2):197–212
Hatae N (1960) (The geology and the geological structure of Amakusa-Shimo-shima, Kumamoto Prefecture.) Sci Rep Kagoshima Univ 9:61–107 (In Japanese)
Holmes AM, Oliver PG, Sellanes J (2005) A new species of *Lucinoma* (Bivalvia: Lucinoidea) from a methane gas seep off the southwest coast of Chile. J Conchol 38:673–681
Hryniewicz K, Little CTS, Nakrem HA (2014) Bivalves from the latest Jurassic–earliest Cretaceous hydrocarbon seep carbonates from central Spitsbergen, Svalbard. Zootaxa 3859:1–66
Hryniewicz K, Nakrem HA, Hammer Ø et al (2015a) Palaeoecology of the latest Jurassic–earliest Cretaceous hydrocarbon seep carbonates from central Spitsbergen, Svalbard. Lethaia 48:353–374
Hryniewicz K, Hagström J, Hammer Ø et al (2015b) Late Jurassic–Early Cretaceous hydrocarbon seep boulders from Novaya Zemlya and their faunas. Palaeogeogr Palaeoclimatol Palaeoecol 436:231–244
Hryniewicz K, Bitner MA, Durska E et al (2016) Paleocene methane seep and wood-fall marine environments from Spitsbergen, Svalbard. Palaeogeogr Palaeoclimatol Palaeoecol 462:41–56

Hryniewicz K, Amano K, Jenkins RG et al (2017a) Thyasirid bivalves from Cretaceous and Paleogene cold seeps. Acta Palaeontol Pol 62:705–728
Hryniewicz K, Jakubowicz M, Belka Z et al (2017b) New bivalves from a Middle Devonian methane seep in Morocco: the oldest record of repetitive shell morphologies among some seep bivalve molluscs. J Syst Palaeontol 15:19–41
Hryniewicz K, Amano K, Bitner MA et al (2019) A late Paleocene fauna from shallow-water chemosynthesis-based ecosystems, Spitsbergen, Svalbard. Acta Palaeontol Pol 64:101–141
Hryniewicz K, Bakayeva S, Heneralova L et al (2020) Taphonomy and palaeoecology of deep-water chemosymbiotic bivalves from the Eocene of Outer Eastern Carpathians, Ukraine. Palaeogeogr Palaeoclimatol Palaeoecol 553:109782
Huber M (2010) Compendium of bivalves. ConchBooks, Hackenheim
Huber M (2015) Compendium of bivalves 2. ConchBooks, Harxheim
Hybertsen F, Kiel S (2018) A middle Eocene seep deposit with silicified fauna from the Humptulips Formation in western Washington State, USA. Acta Palaeontol Pol 63:751–768
Imhoff JF, Sahling H, Süling J et al (2003) 16s rDNA-based phylogeny of sulphur-oxidising bacterial endosymbionts in marine bivalves from cold-seep habitats. Mar Ecol Prog Ser 249:39–51
Iredale T (1931) Australian Molluscan notes, no. 1. Rec Aust Mus 18:201–235
Iredale T (1939) Mollusca, part I. Scientific Reports of the Great Barrier Reef Expedition 1928–1929, 5. British Museum (Natural History), London, pp 209–245
Irwin H, Curtis C, Coleman M (1977) Isotopic evidence for source of diagenetic carbonates formed during burial of organic-rich sediments. Nature 269:209–213
Isakar M, Sinitsyna I (1985) (Redescription of E. Eichwald's Ordovician bivalve species.) Proc Acad Sci Estonian SSR Geol 34:46–54 (In Russian)
Jacobs DK, Lindberg DR (1998) Oxygen and evolutionary patterns in the sea: onshore/offshore trends and recent recruitment of deep-sea faunas. Proc Natl Acad Sci USA 95:9396–9401
Jakubowicz M, Hryniewicz K, Belka Z (2017) Mass occurrence of seep-specific bivalves in the oldest-known cold seep metazoan community. Sci Rep 7:14292
Jang S-J, Ho P-T, Jun S-Y et al (2020) A newly discovered *Gigantidas* bivalve mussel from the Onnuri Vent Field on the northern Central Indian Ridge. Deep-Sea Res Part I 161:103299
Jeffreys JG (1876) New and peculiar Mollusca of the Pecten, Mytilus and Arca families, procured in the Valorous expedition. Ann Mag Nat Hist 18:424–436
Jenkins RG, Kaim A, Hikida Y et al (2007) Methane-flux-dependent lateral faunal changes in a Late Cretaceous chemosymbiotic assemblage from the Nakagawa area of Hokkaido, Japan. Geobiology 5:127–139
Jenkins RG, Kaim A, Little CTS et al (2013) Worldwide distribution of the modiomorphid bivalve genus *Caspiconcha* in late Mesozoic hydrocarbon seeps. Acta Palaeontol Pol 58:357–382
Jenkins RG, Kaim A, Sato K et al (2017) Discovery of chemosynthesis-based association on the Cretaceous basal leatherback sea turtle from Japan. Acta Palaeontol Pol 62:683–690
Jenkins RG, Kaim A, Amano K et al (2018a) A new Miocene whale-fall community dominated by the bathymodiolin mussel *Adipicola* from the Hobetsu area, Hokkaido, Japan. Paleontol Res 22:105–111
Jenkins RG, Kaim A, Hikida Y et al (2018b) Four new species of the Jurassic to Cretaceous seep-restricted bivalve *Caspiconcha* and implications for the history of chemosynthetic communities. J Paleontol 92:596–610
Johnson SB, Krylova EM, Audzijonyte A et al (2017) Phylogeny and origins of chemosynthetic vesicomyid clams. Syst Biodivers 15:346–360
Jones WJ, Vrijenhoek RC (2006) Evolutionary relationships within the *'Bathymodiolus' childressi* group. Cah Biol Mar 47:403–407
Jones WJ, Won YJ, Maas PAY et al (2006) Evolution of habitat use by deep-sea mussels. Mar Biol 148:841–851
Kaim A (2011) Non-actualistic wood-fall associations from Middle Jurassic of Poland. Lethaia 44:109–124

Kaim A, Schneider S (2012) A conch with a collar: early ontogeny of the enigmatic fossil bivalve *Myoconcha*. J Paleontol 86:652–658
Kaim A, Kobayashi Y, Echizenya H et al (2008) Chemosynthesis-based associations on Cretaceous plesiosaurid carcasses. Acta Paleontol Pol 53:97–104
Kaim A, Skupien P, Jenkins RG (2013) A new Lower Cretaceous hydrocarbon seep locality from the Czech Carpathians and its fauna. Palaeogeogr Palaeoclimatol Palaeoecol 390:42–51
Kaim A, Jenkins RG, Tanabe K et al (2014) Mollusks from late Mesozoic seep deposits, chiefly in California. Zootaxa 3861:401–440
Kalishevich TG, Zalinskaja ED, Serova MY (1981) (Development of organic world of the Pacific Belt on the Mesozoic and Cenozoic boundary: foraminifers, molluscs and palynoflora of the Northwestern Sector) Nauka Publishing House, Moscow (In Russian)
Kamenev GM (2009) North Pacific species of the genus *Solemya* Lamarck, 1818 (Bivalvia: Solemyidae) with notes on *Acharax johnsoni* (Dall, 1891). Malacologia 51:233–261
Kamenev GM, Nadtochy VA, Kuznetsov AP (2001) *Conchocele bisecta* (Conrad, 1849) (Bivalvia: Thyasirisae) from cold-water methane-rich areas of the sea of Okhotsk. Veliger 44:84–94
Kanie Y, Kuramouchi T (1996) Description on possibly chemosynthetic bivalves from the Cretaceous deposits of Obira-cho, northwestern Hokkaido. Sci Rep Yokosuka City Mus 44:63–68
Kanie Y, Nishida T (2000) New species of chemosynthetic bivalves, *Vesicomya* and *Acharax*, from the Cretaceous deposits of northwestern Hokkaido. Sci Rep Yokosuka City Mus 47:79–84
Kanie Y, Sakai T (1997) Chemosynthetic bivalve *Nipponothracia*, gen. nov. from the Lower Cretaceous and middle Miocene mudstones in Japan. Venus 56:205–220
Kase T, Kurihara Y, Hagino K (2007) Middle Miocene chemosynthetic thraciid *Nipponothracia gigantea* (Shikama, 1968) from central Japan is a large lucinid bivalve (Lucinoidea; Mollusca). Veliger 49:294–302
Kase T, Isaji S, Aguilar YM et al (2019) A large new *Wareniconcha* (Bivalvia: Vesicomyidae) from a Pliocene methane seep deposit in Leyte, Philippines. Nautilus 133:26–30
Katto J, Hattori M (1964) Some Veneridae from the Shimantogawa Group in the Outer Zone of Shikoku, Japan. Res Rep Kochi Univ Nat Sci I 13:7–10
Kauffman EG, Arthur MA, Howe B et al (1996) Widespread venting of methane-rich fluids in Late Cretaceous (Campanian) submarine springs (Tepee Buttes), Western Interior Seaway, U.S.A. Geology 24:799–802
Kauffman EG, Harries PJ, Meyer C et al (2007) Paleoecology of giant Inoceramidae (*Platyceramus*) on a Santonian (Cretaceous) seafloor in Colorado. J Paleontol 81:64–81
Kelly SRA, Blanc E, Price SP et al (2000) Early Cretaceous giant bivalves from seep-related limestone mounds, Wollaston Foreland, northeast Greenland. In: Harper EM, Taylor JD, Crame JA (eds) The evolutionary biology of the Bivalvia. Geological Society of London Special Publication 177. Geological Society, London, pp 227–246
Kenk VC, Wilson BR (1985) A new mussel (Bivalvia, Mytilidae) from hydrothermal vents in the Galapagos Rift Zone. Malacologia 26:253–271
Kharlameko VI, Kamenev GM, Kalachev AV et al (2016) Thyasirid bivalves from the methane seep community off Paramushir Island (Sea of Okhotsk) and their nutrition. J Molluscan Stud 82:391–402
Kiel S (2006) New records and species of mollusks from Tertiary cold-seep carbonates in Washington State, USA. J Paleontol 80:121–137
Kiel S (2007) Status of the enigmatic fossil vesicomyid bivalve *Pleurophopsis*. Acta Palaeontol Pol 52:639–642
Kiel S (2008) Fossil evidence for micro- and macrofaunal utilization of large nekton-falls: examples from early Cenozoic deep-water sediments in Washington State, USA. Palaeogeogr Palaeoclimatol Palaeoecol 267:161–174
Kiel S (2009) Global hydrocarbon seep-carbonate precipitation correlates with deep-water temperatures and eustatic sea-level fluctuations since the Late Jurassic. Terra Nova 21:279–284

Kiel S (2010a) The fossil record of vent and seep mollusks. In: Kiel S (ed) The vent and seep biota. Topics in Geobiology 33. Springer, Heidelberg, pp 255–278
Kiel S (2010b) On the potential generality of depth-related ecologic structure in cold-seep communities: Cenozoic and Mesozoic examples. Palaeogeogr Palaeoclimatol Palaeoecol 295:245–257
Kiel S (2013) Lucinid bivalves from ancient methane seeps. J Molluscan Stud 79:346–363
Kiel S (2015) Did shifting seawater sulfate concentrations drive the evolution of deep-sea vent and seep ecosystems? Proc R Soc B 282:20142908
Kiel S (2018) Three new bivalve genera from Triassic hydrocarbon seep deposits in southern Turkey. Acta Palaeontol Pol 63:221–234
Kiel S, Amano K (2010) Oligocene and Miocene vesicomyid bivalves from the Katalla district in southern Alaska, USA. Veliger 51:76–84
Kiel S, Amano K (2013) The earliest bathymodiolin mussels: evaluation of Eocene and Oligocene taxa from deep-sea methane seep deposits in western Washington State, USA. J Paleontol 87:589–602
Kiel S, Goedert JL (2006a) Deep-sea food bonanzas: early Cenozoic whale-fall communities resemble wood-fall rather than seep communities. Proc R Soc B 273:2625–2631
Kiel S, Goedert JL (2006b) A wood-fall association from late Eocene deep-water sediments of Washington State, USA. Palaios 21:548–556
Kiel S, Goedert JL (2007) Six new mollusk species associated with biogenic substrates in Cenozoic deep-water sediments in Washington State, USA. Acta Palaeontol Pol 52:41–52
Kiel S, Hansen BT (2015) Cenozoic methane-seep faunas of the Caribbean region. PLoS One 10:e0140788
Kiel S, Little TCS (2006) Cold-seep mollusks are older than the general marine mollusk fauna. Science 313:1429–1431
Kiel S, Peckmann J (2007) Chemosymbiotic bivalves and stable carbon isotopes indicate hydrocarbon seepage at four unusual Cenozoic fossil localities. Lethaia 40:345–357
Kiel S, Peckmann J (2008) Paleoecology and evolutionary significance of an Early Cretaceous *Peregrinella*-dominated hydrocarbon-seep deposit on the Crimean Peninsula. Palaios 23:751–759
Kiel S, Peckmann J (2019) Resource partitioning among brachiopods and bivalves at ancient hydrocarbon seeps: a hypothesis. PLoS One 14:e0221887
Kiel S, Taviani M (2017) Chemosymbiotic bivalves from Miocene methane-seep carbonates in Italy. J Paleontol 91:444–466
Kiel S, Taviani M (2018) Chemosymbiotic bivalves from the late Pliocene Stirone River hydrocarbon seep complex in northern Italy. Acta Palaeontol Pol 63:557–568
Kiel S, Amano K, Jenkins RG (2008) Bivalves from Cretaceous cold seep deposits on Hokkaido, Japan. Acta Palaeontol Pol 53:525–537
Kiel S, Amano K, Hikida Y et al (2009) Wood-fall associations from Late Cretaceous deep-water sediments of Hokkaido, Japan. Lethaia 42:74–82
Kiel S, Campbell KA, Gaillard C (2010) New and little known mollusks from ancient chemosynthetic environments. Zootaxa 2390:26–48
Kiel S, Wiese F, Titus AL (2012) Shallow-water methane-seep faunas in the Cenomanian Western Interior Seaway: no evidence for onshore-offshore adaptations to deep-sea vents. Geology 40:839–842
Kiel S, Birgel D, Campbell KA et al (2013) Cretaceous methane-seep deposits from New Zealand and their fauna. Palaeogeogr Palaeoclimatol Palaeoecol 390:17–34
Kiel S, Birgel D, Lu Y et al (2021) A thyasirid-dominated methane-seep deposit from Montañita, Ecuador, from the Oligocene-Miocene boundary. Palaeogeogr Palaeoclimatol Palaeoecol 247: 110477
Kiel S, Amano K, Jenkins RG (2016) Predation scar frequencies in chemosymbiotic bivalves at an Oligocene seep deposit and their potential relation to inferred sulfide tolerances. Palaeogeogr Palaeoclimatol Palaeoecol 453:139–145

Kiel S, Krystyn L, Demirtaş F et al (2017) Late Triassic mollusk-dominated hydrocarbon-seep deposits from Turkey. Geology 45:751–754
Kiel S, Sami M, Taviani M (2018) A serpulid-*Anodontia*-dominated methane-seep deposit from the Miocene of northern Italy. Acta Palaeontol Pol 63:569–577
Kiel S, Altamirano AJ, Birgel D et al (2020a) Fossiliferous methane-seep deposits from the Cenozoic Talara Basin in northern Peru. Lethaia 53:166–182
Kiel S, Hybertsen F, Hyžný M et al (2020b) Mollusks and a crustacean from early Oligocene methane-seep deposits in the Talara Basin, northern Peru. Acta Palaeontol Pol 65:109–138
Knight RI, Morris NJ, Todd JA et al (2014) Exceptional preservation of a novel gill grade in large Cretaceous inoceramids: systematic and palaeobiological implications. Palaeontology 57:37–54
Kojima S (2008) (Evolution and phylogeny of vesicomyids.) In: Fujikura K, Okutani T, Maruyama T (eds) Deep-sea life-Biological observations using research submersibles. Tokai University Press, Hatano, pp 143–145 (In Japanese)
Kojima S, Fujikura K, Okutani T (2004) Multiple trans-Pacific migrations of deep-sea vent/seep-endemic bivalves in the family Vesicomyidae. Mol Phylogenet Evol 32:396–406
Krueger DM, Dubilier N, Cavanaugh CM (1992) Chemoautotrophic symbiosis in the tropical clam *Solemya occidentalis* (Bivalvia: Protobranchia): ultrastructural and phylogenetic analysis. Mar Biol 126:55–64
Krueger DM, Gustafson RG, Cavanaugh CM (1996) Vertical transmission of chemoautotrophic symbionts in the bivalve *Solemya velum* (Bivalvia: Protobranchia). Biol Bull 190:195–202
Krylova EM, Janssen R (2006) Vesicomyidae from Edison Seamount (south west Pacific: Papua New Guinea: New Ireland fore-arc basin). Arch Molluskenkd 135:231–261
Krylova EM, Sahling H (2006) Recent bivalve molluscs of the genus *Calyptogena* (Vesicomyidae). J Mollusan Stud 72:359–395
Krylova EM, Sahling H (2010) Vesicomyidae (Bivalvia): current taxonomy and distribution. PLoS One 5:e9957
Krylova EM, Sahling H (2020) A new genus *Turneroconcha* (Bivalvia: Pliocardiinae) for the giant hydrothermal vent clam *'Calyptogena' magnifica*. Zootaxa 4808(1):79–100
Kuhara T, Kano Y, Yoshikoshi K et al (2014) Shell morphology, anatomy and gill histology of the deep-sea bivalve *Elliptiolucina ingens* and molecular phylogenetic reconstruction of the chemosynthetic family Lucinidae. Venus 72:13–27
Kurihara Y (2007) Occurrence of *Epilucina californica* (Conrad) (Bivalvia: Lucinidae) from the Neogene of Japan, with notes on the biogeographic history of *Epilucina*. Paleontol Res 11:29–39
Kuroda T (1931) (Fossil Mollusca.) In: Homma F (ed) Geology of the central part of Shinano, part 4. Kokin Shoin, Tokyo, pp 1–90 (In Japanese)
Kuroda T (1943) (*Akebiconcha*, a new pelecypod genus.) Venus 13:14–18 (In Japanese)
Kuznetsov AP, Shileyko AA (1984) (On gutless Protobranchia (Bivalvia).) Biol Nauki 1984: 39–40 (In Russian)
La Perna R (2005) A gigantic deep-sea Nucinellidae from the tropical West Pacific (Bivalvia: Protobranchia). Zootaxa 881:1–10
Lamarck JB (1818) Histoire naturelle des animaux sans vertèbres, vol 5. Deterville, Paris
Laming SR, Duperron S, Gaudron SM et al (2015) Adapted to change: the rapid development of symbiosis in newly settled, fast-maturing chemosymbiotic mussels in the deep sea. Mar Environ Res 112(B):100–112
Laming SR, Gaudron SM, Duperron S (2018) Lifecycle ecology of deep-sea chemosymbiotic mussels: a review. Front Mar Sci 5(282):1–15
Leanza A (1940) *Myoconcha neuquena* n. sp. Del Lias de Piedra Pintada en El Neuquén. Paleontologia 22:123–131
Leckenby J (1859) On the Kelloway Rock of Yorkshire coast. Q J Geol Soc 15:4–15
Liljedahl L (1991) Contrasting feeding strategies in bivalves from the Silurian of Gotland. Palaeontology 34:219–235

Link HF (1807) Beschreibung der Naturalien-Sammlung der Universität Rostock. Universität Rostock, Rostock
Little CTS, Vrijenhoek RC (2003) Are hydrothermal vent animals living fossils? Trends Ecol Evol 18:582–588
Little CTS, Maslenikov VV, Morris NJ et al (1999) Two Paleozoic hydrothermal vent communities from the southern Ural Mountains, Russia. Palaeontology 42:1043–1078
Little CTS, Birgel D, Boyce AJ et al (2015) Late Cretaceous (Maastrichtian) shallow water hydrocarbon seeps from Snow Hill and Seymour Islands James Ross Basin, Antarctica. Palaeogeogr Palaeoclimatol Palaeoecol 418:213–228
Liu J, Liu H, Zhang H (2018) Phylogeny and evolutionary radiation of the marine mussels (Bivalvia: Mytilidae) based on mitochondrial and nuclear genes. Mol Phylogenet Evol 126:233–240
Lorion J, Duperron S, Gros O et al (2008) Several deep-sea mussels and their associated symbionts are able to live both on wood and on whale falls. Proc R Soc B 276:177–185
Lorion J, Kiel S, Faure B et al (2013) Adaptive radiation of chemosymbiotic deep-sea mussels. Proc R Soc B 280:20131243
MacLeod KG, Hoppe KA (1992) Evidence that inoceramid bivalves were benthic and harbored chemosynthetic symbionts. Geology 20:117–120
Majima R, Nobuhara T, Kitazaki T (2005) Review of fossil chemosynthetic assemblages in Japan. Palaeogeogr Palaeoclimatol Palaeoecol 227:86–123
Martin AM, Goffredi SK (2011) *'Pliocardia' krylovata*, a new species of vesicomyid clam from cold seeps along the Costa Rica margin. J Mar Biol Assoc UK 92:1127–1137
Marwick J (1953) Divisions and faunas of the Hokonui System (Triassic and Jurassic). Paleontol Bull 21:1–141
Matos SA, Warren LV, Fürsich FT et al (2017) Paleoecology and paleoenvironments of Permian bivalves of the Serra Alta Formation, Brazil: ordinary suspension feeders or late Paleozoic Gondwana seep organisms? J S Am Earth Sci 77:21–41
Matsukuma A, Okutani T, Tsuchi R (1982) Three new species of the Nucinellidae (Bivalvia: Protobranchia) from Pacific coast of Japan. Venus 40:177–186
Matsumoto E (1971) Oligocene mollusks from the Setogawa Group in central Japan. Bull Natl Sci Mus (Jpn) 14:661–669
McLeod RJ, Wing SR, Skilton JE (2010) High incidence of invertebrate-chemoautotroph symbioses in benthic communities of the New Zealand fjords. Limnol Oceanogr 55:2097–2106
Meek FB (1873) Descriptions of invertebrate fossils of the Silurian and Devonian systems. Geol Surv Ohio Rep 1:1–243
Meek FB, Worthen AH (1870) Description of new species and genera of fossils from the Palaeozoic rocks of the western states. Proc Acad Natl Sci Phila 1870:22–45
Métivier B, Cosel RV (1993) *Acharax alinae* n. sp., Solemyidae (Mollusca: Bivalvia) géante du Bassin de Lau. CR Acad Sci Ser III Sci Vie 316:229–237
Miller SA (1877) The American Palaeozoic fossils, a catalogue of the genera and species. Cincinnati, Ohio
Miyajima Y, Nobuhara T, Koike H (2017) Taxonomic reexamination of three vesicomyid species (Bivalvia) from the middle Miocene Bessho Formation in Nagano Prefecture, central Japan, with notes on vesicomyid diversity. Nautilus 131:51–66
Miyazaki JI, Martins LDO, Fujita Y et al (2010) Evolutionary process of deep-sea *Bathymodiolus* mussels. PLoS One 5:e10363
Morris NJ, Dickins JM, Astafieva-Urbaitis K (1991) Upper Palaeozoic anomalodesmatan Bivalvia. Bull Br Mus (Nat Hist) Geol 47:51–100
Morton B, Machado FM (2019) Predatory marine bivalves: a review. In: Sheppard C (ed) Advances in marine biology 84. Academic/Elsevier, London
Natalicchio M, Peckmann J, Birgel D et al (2015) Seep deposits from northern Istria, Croatia: a first glimpse into the Eocene seep fauna of the Tethys region. Geol Mag 152:444–459

Neulinger SC, Sahling H, Süling J et al (2006) Presence of two phylogenetically distinct groups in the deep-sea mussel *Acharax* (Mollusca: Bivalvia: Solemyidae). Mar Ecol Prog Ser 312:161–168

Nobuhara T, Onda D, Kikuchi N et al (2008) (Lithofacies and fossil assemblages of the Upper Cretaceous Sada Limestone, Shimanto City, Kochi Prefecture, Shikoku, Japan.) Fossils 84:47–60 (In Japanese)

Nützel A, Kaim A (2014) Diversity, palaeoecology and systematics of a marine fossil assemblage from the late Triassic fossil Cassian Formation at Settsass Scharte, N Italy. Palaeontol Z 88:405–431

Ockelmann KW, Dinesen GE (2011) Life on wood—the carnivorous deep-sea mussel *Idas argenteus* (Bathymodiolinae, Mytilidae, Bivalvia). Mar Biol Res 7:71–84

Okutani T (2002) A new thyasirid *Conchocele novaqguinensis* n. sp. from thanatocoenosis associated with a possible cold seep activity off New Guinea. Venus 61(3/4):141–145

Oliver PG (2013) Description of *Atopomya dolobrata* gen. et sp. nov.: first record of bacterial symbiosis in the Saxicavellinae (Bivalvia). J Conchol 41:359–367

Oliver PG (2014) 'Tubular gills': extreme gill modification in the Thyasiroidea with the description of *Ochetoctena tomasi* gen. et sp. nov. (Bivalvia: Thyasiroidea). Zoosyst Evol 90:121–132

Oliver PG, Frey MA (2014) *Ascetoaxinus quatsinoensis* sp. et gen. nov. (Bivalvia: Thyasiroidea) from Vancouver Island, with notes on *Conchocele* Gabb, 1866, and *Channelaxinus* Valentich-Scott & Coan, 2012. Zootaxa 3869:452–468

Oliver PG, Holmes AM (2006) A new species of Thyasiridae (Bivalvia) from chemosynthetic communities in the Atlantic Ocean. J Conchol 39:175–183

Oliver PG, Killeen IJ (2002) The Thyasiridae (Mollusca: Bivalvia) of the British continental shelf and North Sea oilfields: an identification manual. Studies of Marine Biodiversity and Systematics from the National Museum of Wales, BIOMÔR Reports 3. National Museum of Wales, Cardiff

Oliver PG, Levin L (2006) A new species of the family Thyasiridae (Mollusca: Bivalvia) from the oxygen minimum zone of the Pakistan Margin. J Mar Biol Assoc UK 86:411–416

Oliver PG, Taylor JD (2012) Bacterial symbiosis in the Nucinellidae (Bivalvia: Solemyida) with descriptions of two new species. J Molluscan Stud 78:81–91

Oliver PG, Rodrigues CF, Cunha MR (2011) Chemosymbiotic bivalves from the mud volcanoes of the Gulf of Cadiz, NE Atlantic, with descriptions of new species of Solemyidae, Lucinidae and Vesicomyidae. ZooKeys 113:1–38

Oliver PG, Southward EC, Dando PR (2012) Bacterial symbiosis in *Syssitomya pourtalesiana* Oliver, 2012 [Galeommatoidea, Montacutidae]: a bivalve commensal with the deep-sea echinoid *Pourtalesia*. J Molluscan Stud 79:30–41

Olsson AA (1931) Contributions to the Tertiary paleontology of northern Peru, Part 4: the Peruvian Oligocene. Bull Am Paleontol 17:97–264

Olu-Le Roy K, Sibuet M, Fiala-Médioni A et al (2004) Cold seep communities in the deep eastern Mediterranean Sea: composition, symbiosis and spatial distribution on mud volcanoes. Deep-Sea Res Part I 51:1915–1936

Owen G (1961) A note on the habits and nutrition of *Solemya parkinsoni* (Protobranchia: Bivalvia). Q J Microsc Sci 102:15–21

Paull CK, Martens CS, Chanton JP et al (1989) Old carbon in living organisms and young $CaCO_3$ cements from abyssal brine seeps. Nature 342:166–168

Peckmann J, Thiel V (2004) Carbon cycling at ancient methane-seeps. Chem Geol 205:443–467

Peckmann J, Gischler E, Oschmann W et al (2001) An Early Carboniferous seep community and hydrocarbon-derived carbonates from the Harz Mountains, Germany. Geology 29:271–274

Peckmann J, Kiel S, Sandy MR et al (2011) Mass occurrences of the brachiopod *Halorella* in late Triassic methane-seep deposits, eastern Oregon. J Geol 119:207–220

Peek AS, Feldman RA, Lutz RA et al (1998) Cospeciation of chemoautotrophic bacteria and deep sea clams. Proc Natl Acad Sci USA 95:9962–9966

Petersen GH, Vedelsby A (2000) An illustrated catalogue of the Paleocene Bivalvia from Nuussuaq, northwest Greenland: their paleoenvironments and the paleoclimate. Steenstrupia 25:25–120
Petersen JM, Zielinski FU, Pape T et al (2011) Hydrogen is an energy source for hydrothermal vent symbioses. Nature 476:176–180
Phillips J (1829) Illustrations of the geology of Yorkshire, 1st edn. John Murray, York
Pojeta J (1988) The origin and Paleozoic diversification of solemyoid pelecypods. NM Bur Mines Mineral Resour Mem 44:201–271
Pojeta J, Runnegar B (1985) The early evolution of diasome molluscs. In: Trueman ER, Clarke MR (eds) Evolution. The mollusca, vol 10. Academic, Orlando, pp 295–336
Reid RGB (1980) Aspects of biology of a gutless species of *Solemya* (Bivalvia: Protobranchia). Can J Zool 58:386–393
Reid RGB (1998) Order Solemyoida. In: Beesley PL, Ross GJB, Wells A (eds) Mollusca Southern Synthesis, Fauna of Australia, part A, vol 5. CSIRO Publishing, Melbourne, pp 241–247
Rodrigues CF, Duperron S, Gaudron SM (2011) First documented record of a living solemyid bivalve in a pockmark of the Nile Deep-Sea Fan (eastern Mediterranean Sea). Mar Biodivers Rec 4:e10. https://doi.org/10.1017/s175526721100008x
Rodrigues CF, Laming SR, Gaudroni SR et al (2015) A sad tale: has the small mussel *Idas argenteus* lost its symbionts? Biol J Linn Soc 114:398–405
Roemer FJ (1839) Die Versteinerungen des norddeutschen Oolithen-Gebirges: ein Nachtrag. Hahn, Hannover
Rosenkranz A (1970) Marine Upper Cretaceous and lowermost Tertiary deposits in west Greenland. Bull Geol Soc Den 19:406–453
Russell SL, McCartney E, Cavanaugh CM (2018) Transmission strategies in a chemosynthetic symbiosis: detection and quantification of symbionts in host tissues and their environment. Proc Biol Sci 285:20182157
Saether KP, Little CTS, Campbell KA et al (2010) New fossil mussels (Bivalvia: Mytilidae) from Miocene hydrocarbon seep deposits, North Island, New Zealand, with general remarks on vent and seep mussels. Zootaxa 2577:1–45
Sahling H, Rickert D, Lee RW et al (2002) Macrofaunal community structure and sulfide flux at gas hydrate deposits from the Cascadia convergent margin, NE Pacific. Mar Ecol Prog Ser 231:121–138
Salas C, Woodside J (2002) *Lucinoma kazani* n. sp (Mollusca: Bivalvia): evidence of a living benthic community associated with a cold seep in the Eastern Mediterranean Sea. Deep-Sea Res Part I 49:991–1005
Samadi S, Quéméré E, Lorion J et al (2007) Molecular phylogeny in mytilids supports the wooden steps to deep-sea vents hypothesis. C R Biol 330:446–456
Samadi S, Puillandre N, Pante E et al (2015) Patchiness of deep-sea communities in Papua New Guinea and potential susceptibility to anthropogenic disturbances illustrated by seep organisms. Mar Ecol 36(Suppl 1):109–132
Sartori AF, Harper EM (2009) Sticky bivalves from the Mesozoic: clues to the origin of the anomalodesmatan arenophilic system. Lethaia 42:486–494
Sato K, Watanabe H, Sasaki T (2013) A new species of *Solemya* (Bivalvia: Protobranchia: Solemyidae) from a hydrothermal vent in the Iheya Ridge in the mid-Okinawa Trough, Japan. Nautilus 123(3):93–100
Sato K, Kano Y, Setiamarga DHE et al (2020) Molecular phylogeny of protobranch bivalves and systematic implications of their shell microstructure. Zool Scr 49(4):458–472
Saul LR, Squires RL, Goedert JL (1996) A new genus of cryptic lucinid? bivalve from Eocene cold seeps and turbidite-influenced mudstone, western Washington. J Paleontol 70:788–794
Seike K, Jenkins RG, Watanabe H et al (2012) Novel use of burrow casting as a research tool in deep-sea ecology. Biol Lett 8:648–651
Sharma PP, Zardus JD, Boyle EE et al (2013) Into the deep: a phylogenetic approach to the bivalve subclass Protobranchia. Mol Phylogenet Evol 69:188–204

Shikama T (1968) On a giant *Thracidora* from the Hayama Group, Miura Peninsula. Sci Rep Yokohama Natl Univ (sec 2) 14:13–16, pl 2
Simone LRL, Mikkelsen PM, Bieler R (2015) Comparative anatomy of selected marine bivalves from the Florida Keys, with notes on Brazilian congeners (Mollusca: Bivalvia). Malacologia 58:1–127
Smith CR, Baco AR (2003) Ecology of whale falls at the deep-sea floor. Oceanogr Mar Biol Annu Rev 41:311–354
Speden IG (1970) The type Fox Hills Formation, Cretaceous (Maestrichtian), South Dakota, part 2, systematics of the Bivalvia. Peabody Mus Nat Hist Yale Univ Bull 33:1–222
Squires RL (1991) New morphologic and stratigraphic information on *Calyptogena (Calyptogena) gibbera* Crickmay, 1929, (Bivalvia: Vesicomyidae), from the Pliocene and Pleistocene of southern California. Veliger 34:73–77
Squires RL, Goedert JL (1991) New late Eocene mollusks from localized limestone deposits formed by subduction-related methane seeps, southwestern Washington. J Paleontol 65:412–416
Squires RL, Gring MP (1996) Late Eocene chemosynthetic? bivalves from suspect cold seeps, Wagonwheel Mountain, central California. J Paleontol 70:63–73
Stanley SM (1970) Relation of shell form to life habits of the Bivalvia (Mollusca). Geological Society of America Memoir 125. Geological Society of America, Boulder
Stanley SM (2014) Evolutionary radiation of shallow-water Lucinidae (Bivalvia with endosymbionts) as a result of the rise of seagrasses and mangroves. Geology 42:803–806
Stanton TW (1895) Contributions to the Cretaceous paleontology of the Pacific coast: the fauna of the Knoxville beds. US Geol Surv Bull 133:1–132
Stewart RB (1930) Gabb's California Cretaceous and Tertiary type lamellibranchs. Acad Nat Sci Phila Spec Pub 3(3):1–314
Stewart FJ, Cavanaugh CM (2006) Bacterial endosymbioses in *Solemya* (Mollusca: Bivalvia)-Model systems for studies of symbiont-host adaptation. Antonie Van Leeuwenhoek 90:343–360
Sturany R (1896) Zoologische Ergebnisse VII, Mollusken I (Prosobranchier und Opisthobranchier; Scaphopoden; Lamellibranchier) gesammelt von S.M. Schiff 'Pola' 1890–1894. Denkschr Kaiserl Akad Wiss Math-Naturwiss Cl 63:1–36
Suyari K, Yamazaki T (1987) (Boundary between the north and south Shimanto subbelts in Tokushima Prefecture.) J Sci Univ Tokushima 20:37–46 (In Japanese)
Takeda H (1953) The Poronai Formation (Oligocene Tertiary) of Hokkaido and South Sakhalin and its fossil fauna. Stud Coal Geol 3:1–103
Tashiro M (1992) (Fossil monograph—Japanese Cretaceous bivalves). Jono Printing, Japan (In Japanese)
Taviani M, Angeletti L, Ceregato A (2011) Chemosymbiotic bivalves of the family Solemyidae (Bivalvia, Protobranchia) in the Neogene of the Mediterranean Basin. J Paleontol 85:1067–1076
Taylor JD, Glover EA (2005) Cryptic diversity of chemosymbiotic bivalves: a systematic revision of worldwide Anodontia (Mollusca: Bivalvia: Lucinidae). Syst Biodivers 3:281–338
Taylor JD, Glover EA (2006) Lucinidae (Bivalvia) – the most diverse group of chemosymbiotic molluscs. Zool J Linnean Soc 148:421–438
Taylor JD, Glover EA (2009) New lucinid bivalves from hydrocarbon seeps of the western Atlantic (Mollusca: Bivalvia: Lucinidae). Steenstrupia 30:111–124
Taylor JD, Glover EA (2010) Chemosymbiotic bivalves. In: Kiel S (ed) The vent and seep biota. Springer, Heidelberg, pp 107–133
Taylor JD, Cleevely RJ, Morris NJ (1983) Predatory gastropods and their activities in the Blackdown Greensand (Albian) of England. Palaeontology 26:521–553
Taylor JD, Williams ST, Glover EA (2007a) Evolutionary relationships of the bivalve family Thyasiridae (Mollusca: Bivalvia), monophyly and superfamily status. J Mar Biol Assoc UK 87:565–574
Taylor JD, Williams ST, Glover EA et al (2007b) A molecular phylogeny of heterodont bivalves (Mollusca: Bivalvia: Heterodonta): new analyses of 18S and 28S rRNA genes. Zool Scr 36:587–606

Taylor JD, Glover EA, Williams ST (2008) Ancient chemosynthetic bivalves: systematics of Solemyidae from eastern and southern Australia. In: Davie PJF, Phillips JA (eds) Proceedings of the 13th international marine biological workshop: the marine fauna and flora of Moreton Bay, Queensland. Mem Qld Mus – Nature 54:75–104

Taylor JD, Glover EA, Smith L et al (2011) Molecular phylogeny and classification of the chemosymbiotic bivalve family Lucinidae (Mollusca: Bivalvia). Zool J Linnean Soc 163:15–49

Taylor JD, Glover EA, Williams ST (2014) Diversification of chemosymbiotic bivalves: origins and relationships of deeper water Lucinidae. Biol J Linn Soc 11:401–420

Thiele J, Jaeckel S (1931) Muscheln der Deutschen Tiefsee-Expedition, II Teil. Deutsche Tiefsee-Expedition 1898−1899 21. G. Fischer, Jena, pp 159–268

Thubaut J, Puillandre N, Faure BM et al (2013) The contrasted evolutionary fates of deep-sea chemosynthetic mussels (Bivalvia, Bathymodiolinae). Ecol Evol 3:4748–4766

Turton W (1822) *Conchylia dithyra Insularum britannicarum*: the bivalve shells of the British Islands. Natali, London

Ulrich EO (1894) The Lower Silurian Lamellibranchiata of Minnesota. Minnesota Geol Nat Hist Surv Final Rep 3:475–628

Valdés F, Sellanes J, D'Elía G (2013) Phylogenetic position of vesicomyid clams from a methane seep off central Chile (~36°S) with a molecular timescale for the diversification of the Vesicomyidae. Zool Stud 51:1154–1164

Valentich-Scott P, Coan EV (2012) Thyasiroidea. In: Coan EV, Valentich-Scott P (eds) Bivalve seashells of tropical West America: marine bivalve mollusks from Baja California to northern Peru, part 1. Santa Barbara Museum of Natural History, Santa Barbara, pp 362–372

Valentich-Scott P, Powell CL II, Lorenson TD et al (2014) A new genus and species of Thyasiridae (Mollusca, Bivalvia) from deep-water, Beaufort Sea, northern Alaska. ZooKeys 462:11–26

Valentine JW, Jablonski D, Kidwell SM et al (2006) Assessing the fidelity of the fossil record by using marine bivalves. Proc Natl Acad Sci USA 103:6599–6604

Van Winkle K (1919) Remarks on some new species from Trinidad. Bull Am Paleontol 8:19–27

Vermeij GJ (1977) The Mesozoic marine revolution: evidence of snails, predators and grazers. Paleobiology 3:245–258

Vermeij GJ (1987) Evolution and escalation: an ecological history of life. Princeton University Press, Princeton, New Jersey

Vokes HE (1955) Notes on Tertiary and Recent Solemyacidae. J Paleontol 29:534–545

Vokes HE (1956) Notes on Nucinellidae (Pelecypoda) with description of a new species from the Eocene of Oregon. J Paleontol 30:652–671

Vrijenhoek RC (2013) On the instability and evolutionary age of deep-sea chemosynthetic communities. Deep-Sea Res Part II 92:189–200

Wagner CM, Schilling KH (1923) The San Lorenzo Group of the San Emigdio region, California. Univ Calif Publ Bull Dep Geol Sci 14:235–276

Walliser EO, Mertz-Kraus R, Schöne BR (2018) The giant inoceramid *Platyceramus platinus* as a high-resolution paleoclimate archive for the Late Cretaceous of the Western Interior Seaway. Cretac Res 86:73–90

Walliser EO, Tanabe K, Hikida Y et al (2019) Sclerochronological study of the gigantic inoceramids *Sphenoceramus schmidti* and *S. sachalinensis* from Hokkaido, northern Japan. Lethaia 52:410–428

Walton K (2015) New Zealand living Solemyidae (Bivalvia: Protobranchia). Molluscan Res 35:246–261

White CA (1882) On certain Cretaceous fossils from Arkansas and Colorado. Proc US Natl Mus 4:136–138

White CA (1890) On certain Mesozoic fossils from the islands of St. Paul's and St. Peter's in the Straits of Magellan. Proc US Natl Mus 13:13–14

Wignall PB, Newton RJ, Little CTS (2005) The timing of paleoenvironmental change and cause-and effect relationships during the early Jurassic mass extinction in Europe. Am J Sci 305:1014–1032

Williams ST, Taylor JD, Glover EA (2004) Molecular phylogeny of the Lucinoidea (Bivalvia): non-monophyly and separate acquisition of bacterial chemosymbionts. J Molluscan Stud 70:187–202

Wood SV (1851) Monograph of the Crag Mollusca with descriptions of shells from the upper Tertiaries of the British Isles, part 2, bivalves. Palaeontogr Soc Monogr 4:1–150

Woodring WP (1925) Miocene Mollusca from Bowden Jamaica: pelecypods and scaphopods. Carnegie Inst Wash Publ 336:1–564

Woodring WP (1938) Lower Pliocene mollusks and echinoids from the Los Angeles Basin, California, and their inferred environment. US Geol Surv Prof Pap 190:1–67

Wortmann UG, Paytan A (2012) Rapid variability of seawater chemistry over the past 130 million years. Science 337:334–336

Xu T, Feng D, Tao J et al (2019) A new species of deep-sea mussel (Bivalvia: Mytilidae: *Gigantidas*) from the South China Sea: morphology, phylogenetic position, and gill-associated microbes. Deep-Sea Res Part I 146:79–90

Yokoyama M (1890) Versteinerungen aus der japanischen Kreide. Palaeontographica 36:159–202

Zanzerl H, Dufour SC (2017) The burrowing behavior of symbiotic and asymbiotic thyasirid bivalves. J Conchol 42:299–308

Chapter 11
A Review of Gastropods at Ancient Hydrocarbon Seeps

Andrzej Kaim

11.1 Introduction

Gastropods are one of the major animal classes inhabiting hydrothermal vents, hydrocarbon seeps, and organic falls. Although only a few seep/vent gastropods host bacterial symbionts, many taxa on specific and generic (or even higher) levels are seep/vent obligates or seep/vent favored taxa (i.e., occurring in much larger densities in chemosynthesis-based environments). Sasaki et al. (2010) presented an exhaustive review of Recent gastropods occurring in chemosynthesis-based communities. This seminal work along with the *Handbook on Deep-sea Hydrothermal Fauna* (Desbruyères et al. 2006) is used here as a source of basic information on living seep and vent gastropods. A brief summary of the fossil record of gastropods in chemosynthesis-based environments has been presented by Kiel (2010), but the knowledge on fossil seep/vent gastropods has expanded significantly since that publication rendering a new more comprehensive review necessary (Table 11.1). The gastropods from shallow-water seep sites from the Western Interior Seaway (Kiel et al. 2012; Landman et al. 2012; Meehan and Landman 2016) are intentionally left aside and not discussed here as none of the reported taxa so far is seep obligate or even seep favored but rather taxa typical of ambient environments (see also Landman et al. this volume). Some reports of seep faunas provide only very rough identifications pending more comprehensive taxonomic work; good examples of that are gastropods from Miocene seeps in New Zealand mentioned in Campbell et al. (2008a). Since there are no illustrations of these gastropods (except for Saether et al. 2010), it is difficult to treat them with any confidence, especially because taxonomic concepts of ancient seep gastropods have changed dramatically over the last decade.

A. Kaim (✉)
Institute of Paleobiology, Polish Academy of Sciences, Warszawa, Poland
e-mail: kaim@twarda.pan.pl

A. Kaim et al. (eds.), *Ancient Hydrocarbon Seeps*, Topics in Geobiology 50,
https://doi.org/10.1007/978-3-031-05623-9_11

The systematics in this chapter are basically those from the nomenclator of Bouchet et al. (2017) with additions from newer literature, and the *World Register of Marine Taxa* (http://www.marinespecies.org/) kept up to date by their editors. Two new families (Desbruyeresidae and Rubyspiridae) and one subfamily (Alviniconchinae) of abyssochrysoids are diagnosed as it is known already since over a decade that they cluster separately from the family Provannidae (where they are traditionally included) in all molecular studies (Johnson et al. 2010; Chen et al. 2016, 2019b; Linse et al. 2019; Souza et al. 2020). For general information on the biology of Recent gastropods, the reader is referred to the milestone works of Beesley et al. (1998) and Ponder et al. (2020). The organization of the sections follows the relative importance of particular groups in ancient hydrocarbon seeps rather than systematics.

11.2 Abyssochrysoidea

The superfamily Abyssochrysoidea Tomlin, 1927, is a group of deep-water gastropods, and all but species of the eponymous genus *Abyssochrysos* Tomlin, 1927, are intimately associated with chemosynthesizing communities. According to morphological features (Warén and Ponder 1991) and molecular data (Colgan et al. 2007), the abyssochrysoids are caenogastropods most closely related to Littorinidae. The group possesses also a long and robust fossil record (Fig. 11.1), perhaps the richest among gastropods obligate to chemosynthesis-based environments. All molecular phylogenies produced so far (Johnson et al. 2010; Chen et al. 2016, 2019a, b; Linse et al. 2019; Souza et al. 2020) recover five main clades. The clades are as follows: Abyssochrysidae (contains non-chemosynthetic *Abyssochrysos* and species of *Cordesia* in Souza et al. 2020), Provannidae (contains all species of *Provanna*), a clade named Alviniconchinae here (contains species of *Alviniconcha* and monospecific *Ifremeria*; Souza et al. (2020) recovered *Ifremeria* as a separate clade sister to Alviniconchinae and all other abyssochrysoids but Provannidae), a clade named Desbruyeresidae here (contains all species of *Desbruyeresia*), and a clade named Rubyspiridae here (contains all species of *Rubyspira*). The divergence time of *Provanna* and *Desbruyeresia* ranges down to at least Cenomanian (approx. 97 Mya) (Kaim et al. 2008a, 2021) rendering their separate familial status feasible. All analyses recover Provannidae as the most basal living group of abyssochrysoids. The extinct family Hokkaidoconchidae (Kaim et al. 2008a), most likely a stem group of Abyssochrysoidea, is rooted in Triassic zygopleuroids (early Ptenoglossa). Abyssochrysoids display a number of different shell morphologies ranging from very elongated ptenoglossan-like shells in *Abyssochrysos* and *Hokkaidoconcha*, tiny cerithioid shells of *Desbruyeresia* and *Provanna*, and robust, expanded shells of *Paskentana*, *Alviniconcha*, and *Ifremeria*. This variety of shell morphologies resulted in difficulties in identification of the group in the fossil record. Fortunately, if planktotrophic, all taxa display characteristic high-spired reticulate protoconchs, typically decollated in *Desbruyeresia*, *Cordesia*, and *Provanna* (if planktotrophic). Several species of *Provanna* and *Abyssochrysos*, in particular modern ones, possess

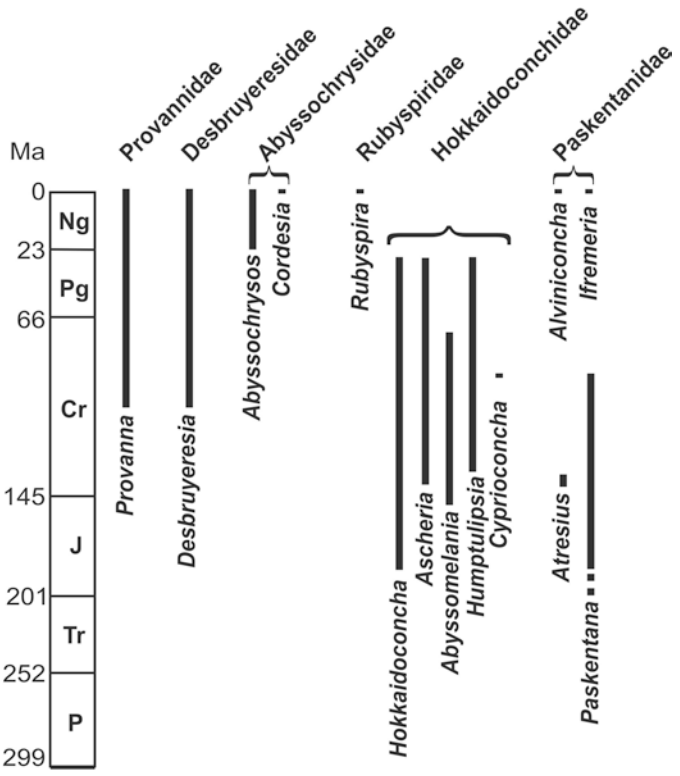

Fig. 11.1 Geological ranges of abyssochrysoid gastropods

lecithotrophic larval shells. The family Paskentanidae (Kaim et al. 2014), which is based on the extinct genus *Paskentana*, is proposed herein to be a parent taxon of Recent Alviniconchinae.

11.2.1 Hokkaidoconchidae

Hokkaidoconchidae (Kaim et al. 2008a) are known only from the fossil record and range from the Early Jurassic seep deposits of Argentina (Kaim et al. 2015, 2016) to the early Miocene seeps of Barbados ("zygopleurid sp. A" of Gill et al. (2005), reinterpreted as Hokkaidoconchidae by Kaim et al. 2008a). Both earliest and latest occurrences await formal descriptions (see also Gill and Little this volume). Currently, the family consists of *Abyssomelania* Kaim et al., 2014; *Ascheria* Kaim et al., 2014; *Cyprioconcha* Kaim et al., 2021; *Hokkaidoconcha* Kaim et al., 2008a; and *Humptulipsia* Kiel, 2008. The acme of hokkaidoconchid occurrences (both in diversity and number of individuals) is in the Cretaceous. Although hokkaidoconchids are yet to be found in the Triassic, the presence of *Paskentana*-like shells in the Upper Triassic seep deposits in Turkey (Kiel et al. 2017) suggests that both

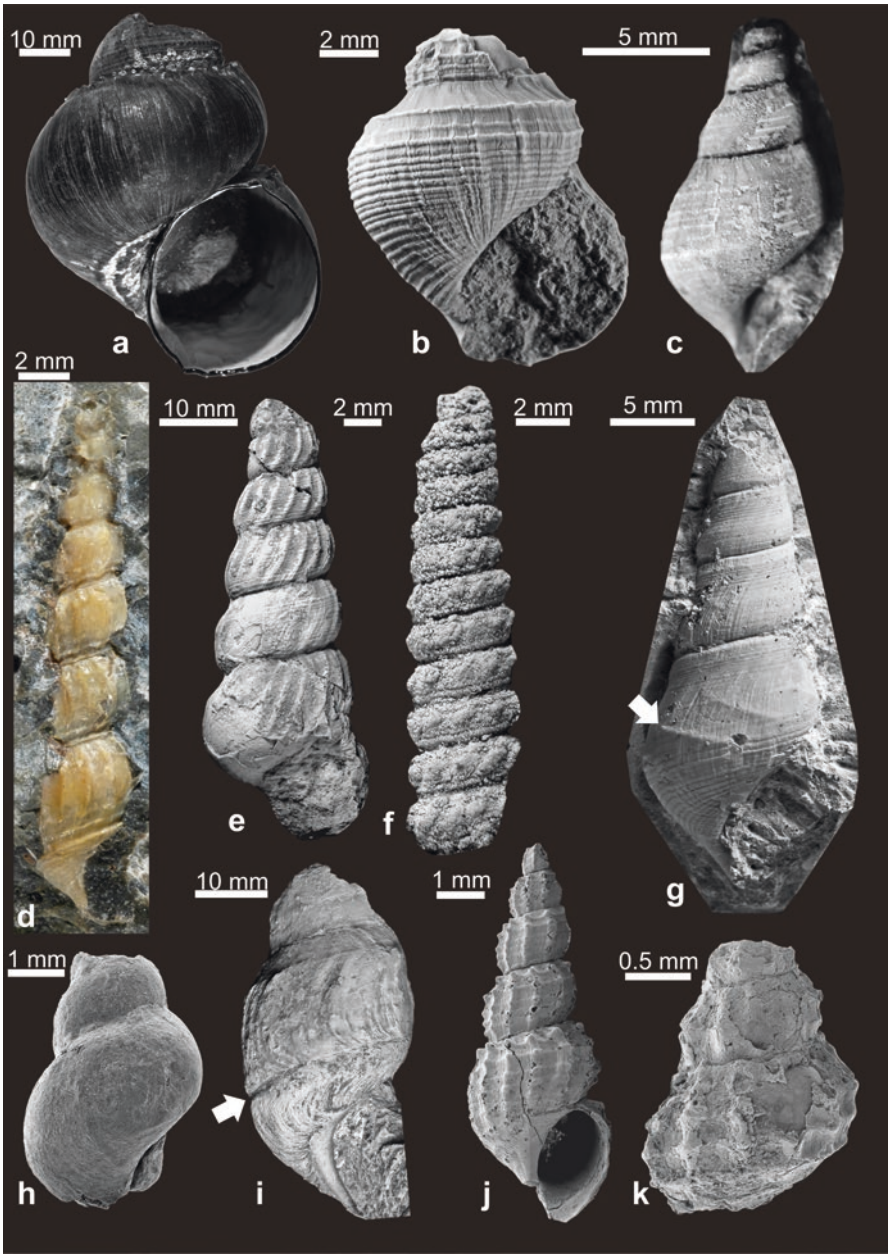

Fig. 11.2 Abyssochrysoid gastropods. (**a**) Recent shell of *Ifremeria nautilei* Bouchet and Warén, 1991, from the Manus Basin (see Kaim et al. 2012). (**b**) *Paskentana humerosa* (Stanton, 1895) from Valanginian (Early Cretaceous) seep carbonates at Bear Creek, California, USA (see Kaim et al. 2014). (**c**) *Atresius liratus* Gabb, 1869, from Valanginian (Early Cretaceous) seep carbonates at Rocky Creek, California, USA (see Johnson et al. 2010). (**d**) *Hokkaidoconcha hikidai*

lineages had already diverged at that time. The gross ptenoglossan morphology of hokkaidoconchids suggests that they most likely diverged from *Zygopleura*-like ptenoglossans after the Permian–Triassic extinction events, perhaps in the Early or Middle Triassic.

Species of *Hokkaidoconcha* are characterized by a very tall and multispiral teleoconch (Fig. 11.2d) reminiscent of some coeval ptenoglossans (e.g., *Confusiscala* or *Gibboscala*) and abyssochrysoid multispiral (non-decollate) protoconch (Kaim et al. 2008a). The oldest formally described species of *Hokkaidoconcha* is *H. novacula* from the Oxfordian seep of Beauvoisin, Southeastern France (Kiel et al. 2010), and the youngest is *H. hikidai* from the Campanian Yasukawa seep site in Hokkaido, Japan (Kaim et al. 2008a). Another two species described from the Oligocene asphalt mine in Cuba by Cooke (1919) such as *Hemisinus bituminifer* Cooke, 1919, and *Hemisinus costatus* Cooke, 1919, may also belong to *Hokkaidoconcha*, but their revision is pending. The Toarcian (Early Jurassic) hokkaidonchid from La Elina seep in Argentina mentioned by Kaim et al. (2015, 2016) is most likely also a species of *Hokkaidoconcha*, and the early Miocene "zygopleurid sp. A" of Gill et al. (2005) from a seep in Barbados most likely belongs here. All known species of *Hokkaidoconcha* were found at ancient seep sites with the sole exception of *H. morisseaui* described from hydrothermal vent deposits in Cyprus (Kaim et al. 2021). *Hokkaidoconcha* displays cosmopolitan distribution and is known from the Americas, Asia, Australasia, Europe, and, with some doubt, Antarctica.

Humptulipsia is a genus of middle-sized abyssochrysoids (Fig. 11.2i) included in the Hokkaidoconchidae by Kaim et al. (2014) due to the hokkaidoconchid-like ornamentation of the juvenile shell in its type species, *H. raui* (see Fig. 1.9 in Kiel 2008 and Fig. 7H in Kaim et al. 2014). All species of *Humptulipsia* are characterized by a slit located in the abapical portion of the whorl. There are just three species of *Humptulipsia* described so far. The oldest species is *H. macsotayi* Kiel et al., 2010, from the Hauterivian (Early Cretaceous) seep deposits in Rottier, Southeastern France (Kiel et al. 2010); another is *H. nobuharai* known from the Sada Limestone in Shikoku, Japan (Kaim et al. 2014); while the youngest is the type species *H. raui* from the Eocene of Washington State (Goedert and Kaler 1996; Kiel 2008; Kaim et al. 2014). All occurrences are at ancient hydrocarbon seeps.

Fig. 11.2 (continued) Kaim et al., 2009, from a Campanian (Late Cretaceous) Yasukawa seep site in Hokkaido, Japan (see Kaim et al. 2009). (**e**) *Ascheria gigantea* (Kiel et al., 2008) from Early Cretaceous seep carbonates at East Berryessa, California, USA (see Kaim et al. 2014). (**f**) *Cyprioconcha robertsoni* Kaim et al., 2021, from Cenomanian–Turonian (Late Cretaceous) hydrothermal vent sulfide deposits at Kambia, Cyprus (see Kaim et al. 2021). (**g**) *Abyssomelania cramptoni* Kaim et al., 2014, from Campanian (Late Cretaceous) seep carbonates at Waipiro III, New Zealand (see Kaim et al. 2014), the arrow indicates an abyssomelanid riblet. (**h**) *Provanna*? sp. from Miocene seep carbonates at Tanohama, Tsushima Island, Japan (see Hryniewicz et al. 2021). (**i**) *Humptulipsia raui* (Goedert and Kaler, 1996) from seep carbonates in Western Washington State (see Kaim et al. 2014), the arrow indicates a humptulipsid slit. (**j**) *Desbruyeresia kanajirisawensis* Kaim et al., 2008a, from Cenomanian (Late Cretaceous) seep carbonates at Kanajirisawa, Hokkaido, Japan (see Kaim et al. 2008a). (**k**) *Provanna nakagawensis* Kaim et al., 2009, from a Campanian (Late Cretaceous) Yasukawa seep site in Hokkaido, Japan (see Kaim et al. 2009)

Ascheria is a genus of hokkaidoconchids having tall and relatively high shells (Fig. 11.2e) with characteristic subsutural constriction. *Ascheria* is known from Lower Cretaceous seeps of California and the Czech Republic (Kaim et al. 2013, 2014) and ranges temporally to Oligocene seeps in Peru (Kiel et al. 2020b). All species of *Ascheria* are known from ancient hydrocarbon seeps except for *Ascheria canni* Kaim et al., 2021, described from hydrothermal vent deposits in Cyprus.

Abyssomelania unites big abyssochrysoids (Fig. 11.2g) bearing characteristically widely spaced prosocline riblets (named abyssomelanid riblets by Kaim et al. 2014) on their shells. The type species *A. cramptoni* Kaim et al., 2014, has been described from the Campanian (Upper Cretaceous) seep carbonates at Waipiro Bay, New Zealand. Another species, *Abyssomelania campbellae* Kaim et al., 2014, is known from the Albian (Early Cretaceous) seep carbonates of Cold Fork of Cottonwood Creek in California (Kaim et al. 2014). The oldest occurrence is that of *Abyssomelania* sp. in the Tithonian (Late Jurassic) seep carbonates at Sassenfjorden, Svalbard (Kaim et al. 2017).

Monospecific genus *Cyprioconcha* (type species, *Cyprioconcha robertsoni*) has been recently described by Kaim et al. (2021) from the Turonian (Late Cretaceous) hydrothermal vent deposits in Cyprus. *Cyprioconcha* differs from the other genera in Hokkaidoconchidae in lacking axial ornamentation on the early whorls, in having exceptionally narrow whorls (Fig. 11.2f) with a nearly flat-topped profile, and its continuous bend toward the sutures.

11.2.2 Abyssochrysidae

Abyssochrysidae Tomlin, 1927, consists of non-chemosynthetic *Abyssochrysos* and *Cordesia* Warén and Bouchet, 2009, dwelling on organic falls and at hydrocarbon seeps (Souza et al. 2020). Modern species of *Abyssochrysos* constitute a small and very uniform group of six species (see Houbrick 1979; Bouchet 1991; Killeen and Oliver 2000), which are known from Brazil, West and South Africa, Oman, and Indonesia. All described species display a smooth, lecithotrophic larval shell, while one undescribed species from deep water off New Caledonia reported by Kaim et al. (2008a) has an unusual lecithotrophic protoconch of two whorls, similar to that of *Provanna*. None of the Recent species of *Abyssochrysos* is reported to be a member of a chemoautotrophic-based community so far. Apparently, they are regular deep-water taxa, and it remains disputable whether it is a primary condition or secondary adaptation. The fossil record of *Abyssochrysos* is very poor. The Miocene counterpart of *Abyssochrysos melvilli* (Schepman, 1909) was reported from Fiji (Ladd 1977; Houbrick 1979) from non-seep deep-sea deposits. It has been suggested by Kaim et al. (2008a) that the Middle Jurassic *Acanthostrophia acanthica* Conti and Fischer, 1984, from Italy could be an abyssochrysoid, but the detailed study of Kaim and Conti (2010) has shown that it is a member of Protorculidae, according to an earlier suggestion by Nützel (1998). All other species of *Abyssochrysos* reported previously from ancient seep deposits have been reinterpreted as hokkaidoconchids (see Table 11.1 in Kaim et al. 2008a).

Table 11.1 A list of gastropods from ancient seep and vent localities (and some more important organic falls)

Higher taxon	Family	Species name	References	Type horizon	Locality/region	Substrate	Comments
Abyssochrysoidea	Hokkaidoconchidae	*?Hokkaidoconcha* sp.	Gill et al., 2005	Miocene	Belleplaine, Barbados	Seep	As zygopleurid
		Hokkaidoconcha bituminifer	Cooke, 1919	Eocene	Bejucal, Cuba	Seep	As *Hemisinus*
		Hokkaidoconcha costata	Cooke, 1919	Eocene	Bejucal, Cuba	Seep	As *Hemisinus*
		Hokkaidoconcha hikidai	Kaim et al., 2008a	Campanian	Yasukawa, Japan	Seep	
		Hokkaidoconcha morenoensis	Kiel et al., 2008	Santonian	Moreno Gulch, CA, USA	Seep	
		Hokkaidoconcha morisseaui	Kaim et al., 2021	Turonian	Troodos, Cyprus	Vent	
		Hokkaidoconcha sp. 2	Kiel et al., 2013	Cenomanian	Port Awanui, New Zealand	Seep	
		Hokkaidoconcha tanabei	Kaim et al., 2008a, b	Cenomanian	Kanajirisawa, Japan	Seep	Type species
		Hokkaidoconcha sp.	Agirrezabala et al., 2013	Albian	Ispaster, Spain	Seep	
		Hokkaidoconcha sp. 1	Kiel et al., 2013	Albian	Port Awanui, New Zealand	Seep	
		Hokkaidoconcha sp.	Kaim et al., 2013	Barremian	Baška, Czechia	Seep	
		Hokkaidoconcha bilirata	Kiel et al., 2008	Hauterivian	Wilbur Springs, CA, USA	Seep	
		Hokkaidoconcha sp.	Kaim et al., 2017	Berriassian	Sassenfjorden, Svalbard	Seep	

(continued)

Table 11.1 (continued)

Higher taxon	Family	Species name	References	Type horizon	Locality/region	Substrate	Comments
		Hokkaidoconcha occidentalis	Kiel et al., 2008	Tithonian	Paskenta, CA, USA	Seep	Also NW Berryessa and Wilbur Springs
		Hokkaidoconcha tehamaensis	Kiel et al., 2008	Tithonian	Paskenta, CA, USA	Seep	
		Hokkaidoconcha sp.	Kiel et al., 2008	Tithonian	NW Berryessa, CA, USA	Seep	Might be *Atresius* or *Paskentana*
		Hokkaidoconcha hignalli	Kaim and Kelly, 2009	Tithonian	Alexander Island, Antarctica	Seep	Might be *Boreomica*
		?*Hokkaidoconcha* sp.	Kaim et al., 2017	Tithonian	Sassenfjorden, Svalbard	Seep	
		Hokkaidoconcha novacula	Kiel et al., 2010	Oxfordian	Beauvoisin, France	Seep	
		Humptulipsia raui	Goedert and Kaler, 1996	Eocene	Humptulips, WA, USA	Seep	Type species
		Humptulipsia nobuharai	Kaim et al., 2014	Campanian–Maastrichtian	Sada Limestone, Japan	Seep	
		Humptulipsia macsotayi	Kiel et al., 2008	Hauterivian	Rottier, France	Seep	
		Ascheria elenensis	Olsson, 1931, Kiel et al., 2020b	Eocene	Ecuador	Seep	Described by Olsson (1931) as *Anconia*
		Ascheria salina	Kiel et al., 2020b	Oligocene	Talara Basin, Peru	Seep	
		Ascheria sp.	Kaim et al., 2014	Eocene	Joes River, Barbados	Seep	
		Ascheria canni	Kaim et al., 2021	Turonian	Troodos, Cyprus	Vent	

Higher taxon	Family	Species name	References	Type horizon	Locality/region	Substrate	Comments
		Ascheria gigantea	Kiel et al., 2008	Early Cretaceous	East Berryessa, CA, USA	Seep	Type species
		Ascheria euscosmeta	Kaim et al., 2013	Early Cretaceous	Hradiště and Koňákov, Czechia	Seep	
		Abyssomelania cramptoni	Kaim et al., 2014	Campanian	Waipiro Bay, New Zealand	Seep	Type species
		Abyssomelania campbellae	Kaim et al., 2014	Albian	Cold Fork of Cottonwood Creek, CA, USA	Seep	
		Abyssomelania sp.	Kaim et al., 2017	Tithonian	Sassenfjorden, Svalbard	Seep	
		Cyprioconcha robertsoni	Kaim et al., 2021	Cenomanian–Turonian	Troodos, Cyprus	Vent	Type species
	Pakentanidae	*Paskentana dixoni*	Kaim et al., 2021	Turonian	Troodos, Cyprus	Vent	
		Paskentana xenophontosi	Kaim et al., 2021	Turonian	Troodos, Cyprus	Vent	
		Paskentana wilburensis	Stanton, 1895; Kiel et al., 2008	Hauterivian	Wilbur Springs, CA, USA	Seep	
		Paskentana hamiltonensis	Kaim et al., 2014	Valanginian	Bear Creek, CA, USA	Seep	
		Paskentana humerosa	Stanton, 1895; Kiel et al., 2008	Valanginian	Bear Creek, CA, USA	Seep	
		Paskentana anistratenkorum	Kiel et al., 2010	Berriassian	Planerskoje, Crimea	Seep	

(continued)

Table 11.1 (continued)

Higher taxon	Family	Species name	References	Type horizon	Locality/region	Substrate	Comments
		Paskentana globosa	Kiel et al., 2008	Late Jurassic–Early Cretaceous	Knoxville, CA, USA	Seep	
		Paskentana paskentaensis	Stanton, 1895; Kiel et al., 2008	Tithonian	Paskenta, CA, USA	Seep	Type species
		Paskentana berryessaensis	Kiel et al., 2008	Tithonian	Berryessa Lake, CA, USA	Seep	
		Paskentana umbilicata	Kiel et al., 2010	Oxfordian	Beauvoisin, France	Seep	
		Paskentana-like	Kiel et al., 2017	Late Triassic	Terziler, Turkey	Seep	
		Atresius liratus	Gabb, 1869; Kiel et al., 2008, Kaim et al., 2014	Hauterivian	Wilbur Springs, CA, USA	Seep	Type species
	Desbruyeresidae	*Desbruyeresia*? sp.	Kiel et al., 2020a	Pliocene	Leyte, Philippines	Seep	
		Desbruyeresia belliata	Hybertsen and Kiel, 2018	Eocene	Washington State, USA	Seep	
		Desbruyeresia kanajirisawensis	Kaim et al., 2008a	Cenomanian	Kanajirisawa, Japan	Seep	
		Desbruyeresia kinousensis	Kaim et al., 2021	Turonian	Troodos, Cyprus	Vent	
		Desbruyeresia memiensis	Kaim et al., 2021	Turonian	Troodos, Cyprus	Vent	
		Desbruyeresia kambiaensis	Kaim et al., 2021	Turonian	Troodos, Cyprus	Vent	

Higher taxon	Family	Species name	References	Type horizon	Locality/region	Substrate	Comments
	Provannidae	*Provanna azurini*	Kiel et al., 2020a	Pliocene	Leyte, Philippines	Seep	
		Provanna marshalli	Saether et al., 2010	Miocene	Rocky Knob, New Zealand	Seep	
		Provanna sp.	Gill et al., 2005; Kiel and Hansen, 2015	Miocene	Trinidad/Venezuela	Seep	
		Provanna hirokoae	Amano and Little, 2014	Miocene	Kita–Kuroiwa, Japan	Seep	
		Provanna alexi	Amano and Little, 2014	Miocene	Shosanbetsu, Japan	Whale fall	
		Provanna fortis	Hybertsen and Kiel, 2018	Eocene	Washington State, USA	Seep	
		Provanna antiqua	Squires, 1995	Oligocene	Washington State, USA	Seep	Also wood, also in Peru
		Provanna urahoroensis	Amano and Jenkins, 2013	Oligocene	Kami-Atsunai, Japan	Seep	
		Provanna pelada	Kiel et al., 2020b	Oligocene	Talara Basin, Peru	Seep	
		Provanna tappuensis	Kaim et al., 2008a	Cenomanian	Kanajirisawa, Japan	Seep	
		Provanna? sp.	Kaim et al., 2008b; Saether et al., 2010	Coniacian	Shirochiunezawa, Japan	Plesiosaurid carcasses	*Desbruyeresia*?
		Provanna nakagawensis	Kaim et al., 2009	Campanian	Omagari, Japan	Seep	

(continued)

Table 11.1 (continued)

Higher taxon	Family	Species name	References	Type horizon	Locality/region	Substrate	Comments
Neomphalida	Neomphalidae	*Retiskenea*? sp.	Kiel et al., 2020a	Pliocene	Leyte, Philippines	Seep	
		Retiskenea? sp.	Kiel et al., 2020b	Oligocene	Talara Basin, Peru	Seep	
		Retiskenea statura	Goedert and Benham, 1999	Eocene–Oligocene	Washington State, USA	Seep	
		Retiskenea? sp.	Kiel et al., 2012	Albian–Cenomanian	Awanui, New Zealand	Seep	
		Retiskenea tuberculata	Campbell et al., 2008b	Hauterivian	Wilbur Springs, CA, USA	Seep	
		Retiskenea kieli	Campbell et al., 2008b	Albian	Cold Fork of Cottonwood Creek, CA, USA	Seep	
		Planorbidella? sp.	Kiel et al., 2020a	Pliocene	Leyte, Philippines	Seep	
		Leptogyra squiresi	Kiel and Goedert, 2007	Eocene	Washington State, USA	Seep	
	Peltospiridae	*Depressigyra* sp.	Hybertsen and Kiel, 2018	Eocene	Washington State, USA	Seep	Peltospirid identity uncertain
	Melanodrymiidae	*Lithomphalus enderlini*	Kiel and Campbell, 2005	Valanginian	Rocky Creek, CA, USA	Seep	Neomphalid identity uncertain
	uncertain	*Elmira cornuarietis*	Cooke, 1919; Kiel and Hansen, 2015	Eocene	Elmira, Cuba	Seep	Type species, spelled *E. cornuatietis* by Kiel and Hansen, 2015
		Elmira shimantoensis	Nobuhara et al., 2016	Campanian–Maastrichtian	Sada Limestone, Japan	Seep	

Higher taxon	Family	Species name	References	Type horizon	Locality/region	Substrate	Comments
Cocculinida	Cocculinidae	*Coccopigya* sp.	Kiel et al., 2020b	Oligocene	Talara Basin, Peru	Seep	
		Gastropod limpet 1	Hybertsen and Kiel, 2018	Eocene	Washington State, USA	Seep	
Lepetellida	Pyropeltidae	*Pyropelta seca*	Kiel et al., 2020b	Oligocene	Talara Basin, Peru	Seep	
		Pyropelta sp.	Kiel, 2006	Oligocene	Washington State, USA	Seep	
		Gastropod limpet 2	Hybertsen and Kiel, 2018	Eocene	Washington State, USA	Seep	Or pseudococculinid
	Fissurellidae	Fissurellid? limpet	Goedert and Squires, 1990	Eocene	Washington State, USA	Seep	
		Fissurellid	Gill et al., 2005	Eocene–Miocene	Windy Hill, Barbados	Seep	
		Fissurella bipunctata	Kiel et al., 2010	Albian	Cold Fork of Cottonwood Creek, CA, USA	Seep	
		Puncturella mcleani	Kiel et al., 2010	Valanginian	Bear Creek, CA, USA	Seep	
	Sutilizonidae	*Triassurella goederti*	Kiel et al., 2010	Valanginian	Bear Creek, CA, USA	Seep	
Patellida	Pectinodontidae	Limpet gastropod sp. 1	Saether et al., 2012	Miocene	Hawke's Bay, New Zealand	Seep	Originally as *Serradonta*
		Bathyacmaea kimberleyae	Kiel et al., 2020a	Pliocene	Leyte, Philippines	Seep	Probably *Bathyacmaea*
		Bathyacmaea omagariensis	Kaim et al., 2009	Campanian	Omagari and Yasukawa, Japan	Seep	Two morphotypes
		Bathyacmaea sp.	Kiel et al. 2013	Campanian	Waipiro Bay, New Zealand	Seep	Originally as *Serradonta*
		?*Pectinodonta borealis*	Kaim et al., 2017	Berriassian	Sassenfjorden, Svalbard	Seep	

(continued)

Table 11.1 (continued)

Higher taxon	Family	Species name	References	Type horizon	Locality/region	Substrate	Comments
Seguenziida	Chilodontaidae	*Chilodonta*? *reticulata*	Kaim et al., 2014	Valanginian	Bear Creek, CA, USA	Seep	
	Cataegidae	*Cataegis ramosi*	Kiel et al., 2020a	Pliocene	Leyte, Philippines	Seep	
		Cataegis godineauensis	Kiel and Hansen, 2015	Miocene	Freeman's Bay and Jordan Hill, Trinidad	Seep	
		Cataegis godineauensis	Kiel and Hansen, 2015	Oligocene	Sta. Clara, Colombia	Seep	
		Cataegis nakagawensis	Kaim et al., 2009	Campanian	Omagari, Japan	Seep	
		Cataegis? sp.	Kaim et al., 2014	Valanginian	Bear Creek, CA, USA	Seep	
	Eucyclidae	*Bathybembix aeola*	Nobuhara and Tanaka, 1993	Pliocene	Kakegawa, Japan	Seep	
		Bathybembix sp.	Kiel and Goedert, 2006	Eocene	Washington State, USA	Wood	
		Ambercyclus morganensis	Kiel et al., 2008; Kaim et al., 2017	Valanginian	Rocky Creek, CA, USA	Seep	
		Ambercyclus dilleri	Kiel et al., 2008; Kaim et al., 2017	Tithonian	Paskenta, CA, USA	Seep	
		Ambercyclus cf. *dilleri*	Kiel et al., 2008; Kaim et al., 2017	Tithonian–Valanginian	NW Berryessa, CA, USA	Seep	
		Eucycloidea bitnerae	Kaim et al., 2017	Tithonian	Sassenfjorden, Svalbard	Seep	
		Eucyclid sp.	Hryniewicz et al., 2015	Oxfordian–Kimmeridgian	Novaya Zemlya, Russia	Seep	
	Seguenziidae	*Vetulonia philippinensis*	Kiel et al., 2020a	Pliocene	Leyte, Philippines	Seep	Familial status of *Vetulonia* uncertain

Higher taxon	Family	Species name	References	Type horizon	Locality/region	Substrate	Comments
Trochida	Colloniidae	*Cantrainea* sp.	Kiel and Hansen, 2015	Miocene	Freeman's Bay and Jordan Hill, Trinidad	Seep	
		Cantrainea sp.	Kiel et al., 2020a, b	Oligocene	Talara Basin, Peru	Seep	
		Hikidea yasukawensis	Kaim et al., 2009	Campanian	Yasukawa, Japan	Seep	
		Hikidea omagariensis	Kaim et al., 2009	Campanian	Omagari, Japan	Seep	
		Hikidea osoensis	Kaim et al., 2014	Valanginian	Bear Creek, CA, USA	Seep	Type species
		Hikidea svalbardensis	Kaim et al., 2017	Berriasian	Sassenfjorden, Svalbard	Seep	
		Hikidea-like	Kiel et al., 2017	Late Triassic	Terziler, Turkey	Seep	
		Homalopoma? sp. B	Goedert and Squires, 1990; Kiel 2006	Eocene–Oligocene	Washington State, USA	Seep	
		Homalopoma? sp.	Amano et al., 2018	Miocene	Hawke's Bay, New Zealand	Seep	Not illustrated
		Homalopoma domeniconii	Moroni, 1966	Miocene	Calcare a Lucine, Italy	Seep	
		Homalopoma abeshinaiensis	Kaim et al., 2009	Campanian	Omagari, Japan	Seep	
		Phanerolepida onoensis	Kaim et al., 2014	Barremian	Eagle Creek, CA, USA	Seep	
		Margarita naticoides	Cooke, 1919	Eocene	Elmira, Cuba	Seep	*Hikidea*?
	Trochidae	Trochoid incertae sedis	Kiel et al., 2020b	Oligocene	Talara Basin, Peru	Seep	
		Margarites hayashii	Kiel et al., 2020a	Pliocene	Leyte, Philippines	Seep	

(continued)

Table 11.1 (continued)

Higher taxon	Family	Species name	References	Type horizon	Locality/region	Substrate	Comments
		Margarites sp.	Tanaka, 1959	Miocene	Akanuda, Japan	Seep	*Hikidea*?
		Margarites (*Pupillaria*) *columbiana*	Squires and Goedert, 1991; Kiel 2006	Eocene–Oligocene	Washington State, USA	Seep	
		Margarites sasakii	Kaim et al., 2009	Campanian	Omagari, Japan	Seep	
		Francisciconcha maslennikovi	Little et al., 2004	Pliensbachian	Figueroa, CA, USA	Vent	Trochid identity uncertain
	Solariellidae	Solariellinid incertae sedis	Kiel, 2006	Oligocene	Washington State, USA	Seep	
		Solariella sp.	Kiel et al., 2020a	Pleistocene	Leyte, Philippines	Seep	
	Skeneidae	*Dillwynella* sp.	Kiel et al., 2020a	Pliocene	Leyte, Philippines	Seep	
		Lopheliella? sp.	Kiel et al., 2020a	Pliocene	Leyte, Philippines	Seep	
	Uncertain	*"Pseudoliotia? sp."*	Miyajima et al., 2018	Pliocene	Matsunoyama, Japan	Seep	
Neritimorpha	Phenacolepadidae	*Thalassonerita megastoma*	Moroni, 1966	Miocene	Calcare a Lucine, Italy	Seep	Type species
		Thalassonerita eocenica	Squires and Goedert, 1996	Eocene	Washington State, USA	Seep	
		Neritimorpha indet.	Kiel et al., 2020b	Oligocene	Talara Basin, Peru	Seep	
	Neritidae	Neritid gastropod	Kiel et al., 2010	Berriassian	Planerskoje, Crimea	Seep	
		Neritid	Kiel et al., 2010	Oxfordian	Beauvoisin, France	Seep	

Higher taxon	Family	Species name	References	Type horizon	Locality/region	Substrate	Comments
Neogastropoda	Buccinidae	*Eosipho*? sp.	Miyajima et al., 2018	Pliocene	Matsunoyama, Japan	Seep	
		Eosipho hoernesi	Moroni, 1966	Miocene	Calcare a Lucine, Italy	Seep	Described as *Neptunea hoernesi*
		Mitrella sp.	Amano et al., 2018	Miocene	Hawke's Bay, New Zealand	Seep	
		Ancistrolepis koyamai	Kiel and Amano, 2010	Miocene	Morai, Japan	Seep	Not illustrated
		Ancistrolepis koyamai	Tanaka, 1959; Amano and Oleinik, 2016	Miocene	Akanuda, Japan	Seep	
		Ancistrolepis teglandae	Kiel and Amano, 2010	Oligocene	Chilkat, AK, USA	Seep	
		Ancistrolepis modestoideus	Amano and Oleinik, 2016	Eocene	Poronai, Japan	Seep	
		Ancistrolepis sp.	Amano and Oleinik, 2016	Eocene	Kiritachi, Japan	Seep	
		Bathyancistrolepis mikasaensis	Amano and Oleinik, 2016	Eocene	Poronai, Japan	Seep	
		Trominina japonica	Amano and Jenkins, 2013	Oligocene	Kami-Atsunai, Japan	Seep	
	Nassariidae	*Tritia ruggierii*	Moroni, 1966	Miocene	Calcare a Lucine, Italy	Seep	Described as *Hinia ruggierii*
	Conoidea	*Benthomangelia*? sp.	Kiel, 2006	Oligocene	Washington State, USA	Seep	
		Xanthodaphne campbellae	Kiel, 2006	Oligocene	Washington State, USA	Seep	
		Turrinosyrinx hickmanae	Kiel, 2006	Oligocene	Washington State, USA	Seep	

(continued)

Table 11.1 (continued)

Higher taxon	Family	Species name	References	Type horizon	Locality/region	Substrate	Comments
	Muricoidea	*Abyssotrophon*? sp.	Amano et al., 2013	Eocene–Oligocene	Tanami, Japan	Seep	
	uncertain	Turrid, Buccinid, Mitrid	Campbell et al., 2008a	Miocene	East Coast Basin, New Zealand	Seep	Not illustrated
		"*Neadmete* sp."	Miyajima et al., 2018	Pliocene	Matsunoyama, Japan	Seep	*Ancistrolepis*?
		"*Riuguhdrillia* sp."	Miyajima et al., 2018	Pliocene	Matsunoyama, Japan	Seep	
		"*Propebela* sp. A"	Miyajima et al., 2018	Pliocene	Matsunoyama, Japan	Seep	
		"*Propebela* sp. B"	Miyajima et al., 2018	Pliocene	Matsunoyama, Japan	Seep	
		Tall neogastropod	Kiel and Hansen, 2015	Oligocene	Mata Cana, Colombia	Seep	
		Neogastropod	Kiel and Hansen, 2015	Oligocene	Sta. Clara, Colombia	Seep	
		Neogastropoda indet.	Kaim et al., 2009	Campanian	Yasukawa, Japan	Seep	
	Pseudotritonidae	Maturifusid sp.	Hryniewicz et al., 2015	Berriasian–Valanginian	Novaya Zemlya, Russia	Seep	
	Purpurinidae	*Bathypurpurinopsis stantoni*	Kiel et al., 2008	Albian	Cold Fork of Cottonwood Creek, CA, USA	Seep	Purpurinid identity uncertain
		Cretadmete sp.	Kaim et al., 2017	Tithonian	Sassenfjorden, Svalbard	Seep	

Higher taxon	Family	Species name	References	Type horizon	Locality/region	Substrate	Comments
Heterobranchia	Cephalaspidea	"*Acteon*" sp.	Kiel et al., 2020b	Oligocene	Talara Basin, Peru	Seep	
		Acteon sp.	Kiel, 2006	Eocene to Oligocene	Washington State, USA	Seep	
		?*Sulcoactaeon* sp.	Kaim et al., 2009	Campanian	Yasukawa, Japan	Seep	
		Acteon exsculptus	Hryniewicz et al., 2015	Berriasian–Valanginian	Novaya Zemlya, Russia	Seep	As Bullinid sp.
		Acteon frearsianus	Hryniewicz et al., 2015	Berriasian–Valanginian	Novaya Zemlya, Russia	Seep	As Bullinid sp.
		Cylichna cf. *kozukensis*	Tanaka, 1959	Miocene	Akanuda, Japan	Seep	
		Cylichna sp.	Kiel et al., 2020b	Oligocene	Talara Basin, Peru	Seep	
		Cylichna sp.	Kiel, 2006	Oligocene	Washington State, USA	Seep	
		Ellipsoscapha sp.	Hryniewicz et al., 2019	Paleocene	Basilika Formation, Svalbard	Seep	
		Diaphana sp.	Kaim et al., 2014	Valanginian	West Berryessa, CA, USA	Seep	
		Opisthobranch	Kiel et al., 2017	Late Triassic	Terziler, Turkey	Seep	
	Orbitestellidae	*Lurifax goederti*	Kiel, 2006	Eocene-Oligocene	Washington State, USA	Seep	
	Hyalogyrinidae	*Hyalogyrina knorringfjelletensis*	Kaim et al., 2017	Berriassian	Sassenfjorden, Svalbard	Seep	
		Hyalogyrina? sp.	Kiel, 2006	Oligocene	Washington State, USA	Seep	
		Hyalogyrina sp.	Hybertsen and Kiel, 2018	Eocene	Washington State, USA	Seep	
	Xylodisculidae	*Xylodiscula okutanii*	Kiel and Goedert, 2007	Oligocene-Miocene	Washington State, USA	Wood	

(continued)

Table 11.1 (continued)

Higher taxon	Family	Species name	References	Type horizon	Locality/region	Substrate	Comments
Rissooidea	Rissoidae	*Boreomica hammeri*	Kaim et al., 2017	Berriassian	Sassenfjorden, Svalbard	Seep	
		Boreomica pusilla	Hryniewicz et al., 2015	Berriasian–Early Valanginian	Novaya Zemlya, Russia	Seep	
		Boreomica undulata	Hryniewicz et al., 2015	Tithonian	Novaya Zemlya, Russia	Seep	
		Hokkaidoconcha? hignalli	Kaim and Kelly, 2009	Tithonian	Alexander Island, Antarctica	Seep	Familial status uncertain
Stromboidea	Aporrhaidae	*Aporrhais* cf. *gracilis*	Hryniewicz et al., 2019	Paleocene	Basilika Formation, Svalbard	Seep	
		Aporrhaidae indet.	Schwartz et al., 2003	Paleocene	Panoche Hills, CA, USA	Seep	Originally as provannids
		Aporrhaid gastropod from Awanui	Kiel et al., 2013	Cenomanian	Awanui, New Zealand	Seep	
		Pseudanchura biangulata	Kaim et al., 2014	Barremian	Eagle Creek, CA, USA	Seep	
	Xenophoridae	*Xenophora borsoni*	Moroni, 1966	Miocene	Calcare a Lucine, Italy	Seep	

Higher taxon	Family	Species name	References	Type horizon	Locality/region	Substrate	Comments
Naticoidea	Naticidae	*Euspira pallida*	Miyajima et al., 2018	Pliocene	Matsunoyama, Japan	Seep	
		Euspira pallida	Amano, 2003	Miocene	Morai, Japan	Seep	
		Naticidae gen. et sp. indet.	Amano et al., 2018	Miocene	Hawke's Bay, New Zealand	Seep	
		Tectonatica janthostomoides	Tanaka, 1959	Miocene	Akanuda, Japan	Seep	
		Cryptonatica sp.	Amano et al., 2013	Eocene–Oligocene	Tanami, Japan	Seep	
		Euspira meisensis	Amano et al., 2013	Oligocene	Kami-Atsunai, Japan	Seep	
		Sassenfjordia sassenfjordensis	Kaim et al., 2017	Berriassian	Sassenfjorden, Svalbard	Seep	Naticid identity uncertain; type species
Campaniloidea	Ampullinidae	*Globularia isfjordensis*	Hryniewicz et al., 2019	Paleocene	Basilika Formation, Svalbard	Seep	
		Ampullinid gastropod	Kiel and Peckmann, 2008	Berriassian	Planerskoje, Crimea	Seep	
Triphoroidea	Cerithiopsidae	Cerithiopsid incertae sedis	Kiel, 2006	Oligocene	Washington State, USA	Seep	
Vanikoroidea	Eulimidae	*Niso littlei*	Kiel, 2006	Oligocene	Washington State, USA	Seep	
		Eulimid sp. 1	Kiel, 2006	Oligocene	Washington State, USA	Seep	
		Eulimid sp. 2	Kiel, 2006	Oligocene	Washington State, USA	Seep	
Cypraeoidea	Cypraeoidea	*Cypraea semen*	Cooke, 1919; Kiel and Peckmann, 2007	Eocene	Elmira, Cuba	Seep	

(continued)

Table 11.1 (continued)

Higher taxon	Family	Species name	References	Type horizon	Locality/region	Substrate	Comments
Cerithioidea	Turritellidae	*Orectospira wadana*	Amano and Jenkins, 2013	Oligocene	Kami-Atsunai, Japan	Seep	
		Orectospira wadana	Amano et al., 2013	Eocene–Oligocene	Tanami, Japan	Seep	
Pyramidelloidea	Amathinidae	*Carinorbis clathrata*	Moroni, 1966	Miocene	Calcare a Lucine, Italy	Seep	Described as *Phasianema taurocrassum*
Tonnoidea	Cassidae	*Galeodea delibrata*	Moroni, 1966	Miocene	Calcare a Lucine, Italy	Seep	

Paleozoic taxa and species from the Western Interior Seaway shallow-water seeps are not included

Additionally, it has been recently suggested by Souza et al. (2020) that *Cordesia* Warén and Bouchet, 2009, with two described species, one dwelling on organic falls (*C. atlantica*) and one at hydrocarbon seeps (*C. provannoides*), in the Atlantic Ocean might be another genus belonging to the Abyssochrysidae according to their molecular data. The shells of *Cordesia* are relatively small (the holotype of *C. atlantica* is 7.05 mm high and 4.90 mm wide) and quite broad with weak spiral and axial sculpture and a large aperture with a distinct, short siphonal canal (Warén and Bouchet 2009; Souza et al. 2020).

11.2.3 Paskentanidae

The family Paskentanidae Kaim et al., 2014, which comprises the genera *Paskentana* Kiel et al., 2008, and *Atresius* Gabb, 1869, are moderately sized gastropods with a littoriniform to high-spired teleoconch and a subsutural ramp on the early whorls. According to Kiel et al. (2008), *Paskentana* possesses a protoconch resembling that of provannids. Both *Paskentana* and monospecific *Atresius* have similar early ontogenetic shells that inclined Kaim et al. (2014) to unite them into a single family.

The species of *Paskentana* are characterized by a littoriniform shell of moderate size (Fig. 11.2b) with very thin shell wall, similar in several aspects to Recent *Alviniconcha*. In some localities, *Paskentana* occurs in great numbers (e.g., the Valanginian seep site at Bear Creek, California). The oldest *Paskentana*-like gastropod is reported by Kiel et al. (2017) from the Carnian (Late Triassic) seep deposit of Turkey. An undescribed species of *Paskentana* is also known from the Toarcian (Early Jurassic) site in Argentina (Kaim et al. 2015, 2016). The oldest formally described species is *P. umbilicata* from the Oxfordian (Late Jurassic) seep site at Beauvoisin, southeastern France (Kiel et al. 2010). The youngest known *Paskentana* from a seep site is from the Hauterivian in California (Kiel et al. 2008), but two younger species are known from Turonian hydrothermal vent deposits in Cyprus (Kaim et al. 2021). One may hypothesize that *Paskentana* moved from hydrocarbon seeps to hydrothermal vents in the mid-Cretaceous.

Although Kaim et al. (2014) placed *Atresius liratus* Gabb, 1869, in Paskentanidae (Fig. 11.2c) due to the similarity of its early whorls to the corresponding whorls in *Paskentana*, its taxonomic position remains somewhat controversial (see Kiel et al. 2008 for a review). The extraordinarily similar shell morphology of this species to the Recent bone eating abyssochrysoid *Rubyspira osteovora* Johnson et al., 2010, led to a suggestion that they may be related (Johnson et al. 2010). Even the juvenile shells are somewhat similar but less so that of the coeval *Paskentana humerosa* (compare Fig. 8D, I and 8E, J in Kaim et al. 2014). Clarifying the relation between *Atresius* and *Rubyspira* requires further research and collection effort.

11.2.4 Alviniconchinae New Subfamily

Type genus: *Alviniconcha* Okutani and Ohta, 1988
Genera included: Type genus and *Ifremeria* Bouchet and Warén, 1991
Diagnosis: Shell large and globose and shell wall thin with thick periostracum. Aperture with a shallow anterior sinus or notch.
Remarks: Alviniconchinae differ markedly from all other abyssochrysoids in having globose shells (Fig. 11.2a) expanded for sheltering hypertrophied symbiont-bearing gills. In the majority of molecular phylogenies, they are recovered as a separate clade that diverged not later than in the Cretaceous (e.g., Johnson et al. 2010). In the most recent molecular study, *Ifremeria* is placed as a sister taxon to all other abyssochrysoids but Provannidae. The only similar group is Paskentanidae, also having globose to littorinimorph shells with thin shells and with shallow anterior sinus. They are slightly smaller and less globose as one might have expected for a more ancient stage in the evolution of Alviniconchinae. It is worth noting that Alviniconchinae inhabit exclusively hydrothermal vents while Paskentanidae first appeared at hydrocarbon seeps and then moved to hydrothermal vents in the middle Cretaceous (compare Kaim et al. 2021). One may therefore suggest that Alviniconchinae is a crown group of Paskentanidae. It is suggested herein that Paskentanidae consists of two subfamilies: Mesozoic Paskentaninae (*Paskentana* and *Atresius*) and Cenozoic Alviniconchinae (*Alviniconcha* and *Ifremeria*). The link between both groups is missing so far due to the lack of a fossil record of Cenozoic hydrothermal vent deposits with preserved mollusk fauna.

11.2.5 Desbruyeresidae New Family

Type genus: *Desbruyeresia* Warén and Bouchet, 1993
Genera included: Type genus only.
Diagnosis: Shell small and slender with high spire (Fig. 11.2j) and small rounded aperture. Suture usually moderately to deeply incised. Sculpture composed of axial ribs and spiral cords with intersections occasionally equipped with knobs or spines. Protoconchs multispiral with finely cancellate ornamentation indicating planktotrophic development. Central teeth of radula divided into large central cusp and several lateral cusps.
Remarks: Desbruyeresidae are similar in many respects to Provannidae sensu stricto (i.e., genus *Provanna*), differing mainly in central radular teeth, multispiral larval shells indicative of planktotrophic development, and usually more slender and higher-spired shells. They also are invariantly recovered in different positions in molecular trees (Johnson et al. 2010; Chen et al. 2016, 2019a, b; Souza et al. 2020). Today, species of *Desbruyeresia* occur at the West Pacific vent sites and serpentinization-related seeps, and there is a single species on record from Indian Ocean vents (Sasaki et al. 2010; Chen et al. 2016). *Desbruyeresia* is rela-

tively rare in the fossil record. In addition to the newly described three species from the Turonian (Late Cretaceous) hydrothermal vents in Cyprus, the genus is known from Cenomanian seep deposits in Japan (Kaim et al. 2008a) and Eocene seeps in Washington State, USA (Hybertsen and Kiel 2018). Possible species of *Desbruyeresia* have been reported from Pliocene seeps in Leyte Island, Philippines (Kiel et al. 2020a). Another species of *Desbruyeresia* has been reported (as Provannidae gen. et spp. indet.) from the Coniacian plesiosaur fall in Hokkaido, Japan, by Kaim et al. (2008b). The divergence time between Desbruyeresidae and Provannidae is therefore estimated to be at least mid-Cretaceous. It is worth noting that all Cretaceous occurrences of *Desbruyeresia* and *Provanna* are known from Western Pacific and Tethys while there are none in the numerous Early Cretaceous seep sites of California, though other abyssochrysoids are fairly common there. This may suggest that both groups originated in the Western Pacific; this is, however, hard to confirm since the oldest in this region is of Albian age (e.g., Shimazu and Jenkins 2019).

11.2.6 Provannidae

As understood herein, Provannidae are composed exclusively of species of the nominative genus *Provanna* Dall, 1918, as they are recovered separately in all available molecular phylogenies (Johnson et al. 2010; Chen et al. 2016, 2019a, b; Souza et al. 2020). The genus *Provanna* is very rich in species (Fig. 11.2h, k) and distributed worldwide in all types of chemosynthesis-based communities. The fossil record is also relatively rich starting with the Cenomanian (Upper Cretaceous) seep site of Kanajirisawa, Hokkaido, Japan (Kaim et al. 2008a), and being particularly common in Cenozoic seeps (e.g., Squires 1995; Gill et al. 2005; Saether et al. 2010; Amano and Jenkins 2013; Amano and Little 2014; Kiel and Hansen 2015; Hybertsen and Kiel 2018; Kiel et al. 2020a, b; Hryniewicz et al. 2021).

Another genus that has been included in Provannidae by Bouchet et al. (2005) is *Pseudonina* Sacco, 1896, with a single Miocene–Pliocene species of *Pseudonina bellardii* (Michelotti, 1847) reported from sunken wood in Italy (Bertolaso and Palazzi 1994). The protoconch of this species is, however, more similar to protoconchs of epitoniids as already observed by Bertolaso and Palazzi (1994).

11.2.7 Rubyspiridae New Family

Type genus: *Rubyspira* Johnson et al., 2010
Genera included: Type genus only.
Diagnosis: Adult shell tall, whorls sculptured spirally covered by a periostracum forming small bristles, no siphonal canal, protoconch multispiral, and two pallial tentacles present.

Remarks: All species of Rubyspiridae predominantly thrive on whale carcasses (Johnson et al. 2010; Hasegawa et al. 2019; Souza et al. 2020) with some additional occurrences on sunken wood (Souza et al. 2020). Molecular phylogenies invariantly recover Rubyspiridae as a sister clade of Abyssochrysidae. The only fossil abyssochrysoid reminiscent of *Rubyspira* is *Atresius liratus* Gabb, 1869, and according to Kaim et al. (2014), *Atresius* belongs to Paskentanidae. The relation between *Atresius* (and Paskentanidae) and *Rubyspira* requires further research and collection effort.

11.3 Neomphalida

Neomphalida McLean, 1990, is a clade of order rank, which together with Cocculinida comprise the subclass Neomphaliones in the class Gastropoda (Bouchet et al. 2017). Anatomical characters suggest inclusion of neomphalids in Vetigastropoda (Aktipis et al. 2008), but molecular studies recover them as basal to Vetigastropoda (Geiger and Thacker 2006). The exact position of Neomphalina on the gastropod tree of life is still controversial. Neomphalids were originally considered to be endemic to hydrothermal vents, but now, they are known also from hydrocarbon seeps and organic falls (Kano 2008; Warén and Bouchet 2009; Sasaki et al. 2010), although they are much less common there than at the vents. The living neomphalids are divided into three families (Melanodrymiidae, Neomphalidae, and Peltospiridae), which display a very wide range of shell morphologies from limpets (e.g., *Neomphalus*, *Echinopelta*) through small and simple skeneiforms (e.g., *Retiskenea*, *Depressigyra*) to trochoid-like forms (e.g., *Melanodrymia*). Therefore, the fossil record of neomphaline gastropods is a difficult matter since there are only a few characters that could be used to recognize them from shells alone. Seemingly, the best character is the protoconch morphology, which in neomphalids occurs in two types: either with a fine net sculpture, especially on the initial part (Melanodrymiidae and Neomphalidae), or a strongly bent type with prominent spiral ridges in the Peltospiridae (Sasaki et al. 2010). Auxiliary characters helpful in recognition of neomphalids in the fossil record are the presence of shell pores in some taxa, for example, in *Leptogyra squiresi* from the Eocene sunken wood of Washington State (Kiel and Goedert 2006, 2007), and crossed-lamellar shell structure in trochiform neomphalids (Kiel and Campbell 2005) in contrast to similar trochoids and turbinids, which usually have a nacreous shell layer.

Nearly all Mesozoic reports of neomphalids concern *Retiskenea*- or *Retiskenea*-like gastropods. The genus *Retiskenea* (Fig. 11.3b), with type species *R. diploura* Warén and Bouchet, 2001, from the Aleutian Trench is the only neomphaline restricted to hydrocarbon seeps today. No wonder then that it is also the most common neomphaline in the fossil record. Possibly, the oldest occurrence to date is the *Retiskenea*-like gastropod reported by Kaim et al. (2015, 2016) from the Toarcian (Early Jurassic) La Elina seep in Argentina. The oldest formally described species is *Retiskenea*? *kieli* Campbell et al., 2008b, from the Tithonian (Late Jurassic) seep

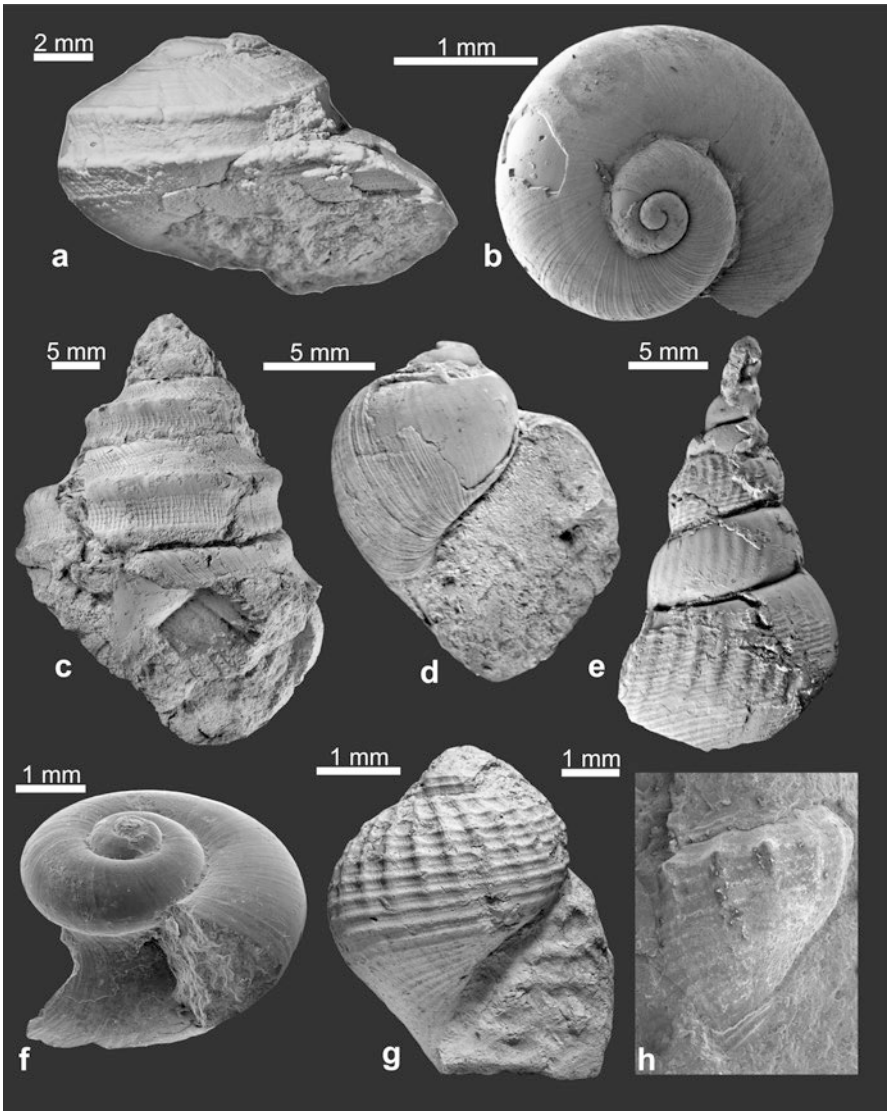

Fig. 11.3 Neomphalid and other gastropods. (**a**) Neomphalid *Lithomphalus enderlini* Kiel and Campbell, 2005, from Valanginian (Early Cretaceous) seep carbonates at Bear Creek, California, USA (see Kaim et al. 2014). (**b**) Neomphalid *Retiskenea*? *tuberculata* Campbell et al., 2008a, b, from Valanginian (Early Cretaceous) seep carbonates at Bear Creek, California, USA (see Kaim et al. 2014). (**c**) Eucyclid *Eucycloidea bitnerae* Kaim et al. 2017, from Tithonian (Late Jurassic) seep carbonates in Sassenfjorden, Svalbard (see Kaim et al. 2017). (**d**) Ampullinid *Globularia isfjordensis* (Vonderbank, 1970) from Paleocene seep carbonates in Hollendarbukta, Svalbard (see Hryniewicz et al. 2019). (**e**) Aporrhaid *Aporrhais* cf. *gracilis* Koenen, 1885, from Paleocene seep carbonates in Hollendarbukta, Svalbard (see Hryniewicz et al. 2019). (**f**) Hyalogyrinid *Hyalogyrina knorringfjelletensis* sp. nov. from the Berriasian (Early Cretaceous) seep carbonates at Sassenfjorden, Svalbard (see Kaim et al. 2017). (**g**) Purpurinid *Cretadmete* sp. from Tithonian (Late Jurassic) seep carbonates at Sassenfjorden, Svalbard (see Kaim et al. 2017). (**h**) Neogastropoda indet. From the Campanian (Late Cretaceous) Yasukawa seep site in Hokkaido, Japan (see Kaim et al. 2009)

site at Paskenta, California (Kaim et al. 2014). Other species of *Retiskenea* are known from the Cretaceous of California (Campbell et al. 2008a, b; Kaim et al. 2014) and New Zealand (Kiel et al. 2013) as well as from the Cenozoic seeps of Washington State (Goedert and Benham 1999; Kiel 2006), the Philippines (Kiel et al. 2020a), and Peru (Kiel et al. 2020b).

More problematic is alleged Cretaceous melanodrymiid *Lithomphalus enderlini* Kiel and Campbell, 2005 (Fig. 11.3a). Kiel and Campbell (2005) considered it possible that *L. enderlini* represented a Cretaceous neomphaline gastropod based on its shell shape and its crossed-lamellar shell structure. The general gross morphology is reminiscent of several vetigastropods and in particular cataegins (e.g., Kaim et al. 2014), which, however, possess nacreous rather than crossed-lamellar shell structure. Nevertheless, the neomphaline and melanodrymiid identity of *L. enderlini* proposed by Kiel and Campbell (2005) requires further research and collecting effort. *Lithomphalus enderlini* has been found in two Valanginian (Lower Cretaceous) seep sites of Rocky Creek and Bear Creek in California (Kiel and Campbell 2005; Kaim et al. 2014).

Two additional neomphaline gastropods are known from the Eocene sunken wood and seeps of Washington State. The neomphalid *Leptogyra squiresi* is known from sunken wood (Kiel and Goedert 2006, 2007) while the peltospirid *Depressigyra* sp. is known from hydrocarbon seeps (Kiel 2006; Hybertsen and Kiel 2018). Another possible neomphalid gastropod genus is *Elmira* Cooke, 1919, with two described species *E. cornuarietis* Cooke, 1919, from Eocene seeps in Cuba, and *E. shimantoensis* Kiel and Nobuhara in Nobuhara et al., 2016, from a Maastrichtian (Late Cretaceous) seep in Shikoku, Japan (Kiel and Hansen 2015; Nobuhara et al. 2016). Nobuhara et al. (2016) suggest that *Elmira* might be related to peltospirids based on general shell morphology and microstructure. *Elmira shimantoensis* occurs in mass aggregations in a way similar to Recent neomphalids but also alviniconchins. The shells of alviniconchins and paskentanids, in general, however, are very thin in contrast to *Elmira*, which is rather thick shelled. The exact taxonomic position of *Elmira* requires further work.

Surprising is the absence of any neomphaline gastropods in the Turonian (Upper Cretaceous) hydrothermal vent deposits in Cyprus, the richest and most diverse ancient vent site (Kaim et al. 2021). The only potential ancient vent neomphaline gastropod is *Francisciconcha maslennikovi* Little et al., 2004, a trochomorph gastropod from an Early Jurassic hydrothermal vent community in the Franciscan complex, San Rafael Mountains, California. Neither the shell structure nor protoconch of *F. maslennikovi* is known (Little et al. 2004). In general, it remains largely unknown when the radiation of neomphaline gastropods in vent communities took place since the fossil data are so scarce. The only certain point is that the neomphalids appeared in chemosynthesis-based communities (seeps) already in early Mesozoic times and are represented most of all by *Retiskenea*-like species.

11.4 Limpets

Limpet gastropods do not constitute a monophyletic group, and limpet-shaped taxa have evolved repeatedly in nearly all major gastropod clades. Since they have few diagnostic shell characters and in many cases their identity in fossil material is poorly constrained (see, for example, Kiel et al. 2020a), they are treated jointly here. Gastropod limpets are very common at Recent vents and seeps while they are less so in their ancient counterparts.

11.4.1 Cocculinida

Cocculinida Haszprunar, 1987, is a small group of deep-water limpet-shaped gastropods living on organic substrates (e.g., Haszprunar 1998). Currently, they are treated as a clade of order rank, sister to Neomphalida, with which they form the subclass Neomphaliones (Bouchet et al. 2017). The family Pyropeltidae McLean and Haszprunar, 1987, is known to occur at hydrothermal vents (McLean and Haszprunar 1987; Warén and Bouchet 2001; Sasaki et al. 2003) and is currently placed in Lepetellida and order Vetigastropoda (Bouchet et al. 2017) in contrast to previous classifications (e.g., Desbruyères et al. 2006; Kiel 2010).

Possible fossil cocculinides are known from Mesozoic (Kiel et al. 2009; Kaim 2011), Eocene (Kiel and Goedert 2006), Miocene, and Pliocene (Marshall 1986) wood falls, and *Coccopigya* sp. is reported from an Oligocene seep in Peru (Kiel et al. 2020b). Another limpet reported by Hybertsen and Kiel (2018) from the Eocene of Washington State as "gastropod limpet 1" might be a cocculinide while "gastropod limpet 2" might be a lepetellide (pseudocculinid or pyropeltid) (Hybertsen and Kiel 2018).

11.4.2 Lepetellida

Superfamily Lepetelloidea Dall, 1882, is a small group of deep-water limpets which are currently placed in Lepetellida, Vetigastropoda (Bouchet et al. 2017). One of its families, Pyropeltidae McLean and Haszprunar, 1987, is known to occur abundantly at hydrothermal vents (McLean and Haszprunar 1987; Warén and Bouchet 2001; Sasaki et al. 2003) but occurs also at seeps and organic falls (McLean 1992; Sasaki et al. 2010). Fossil pyropeltids are known from ancient seeps in the Eocene of Washington State (Kiel 2006; Hybertsen and Kiel 2018) and Oligocene of Peru (Kiel et al. 2020b).

Another superfamily of Lepetellida, the keyhole and slit limpets of Fissurelloidea Fleming, 1822, are also known to occur at vents and seeps though they are not particularly common in such environments (Sasaki et al. 2010). Nevertheless, they

occur also in ancient seeps including two species from Early Cretaceous seeps in California (Kiel et al. 2010). *Fissurella bipunctata* Stanton, 1895, is known from the Albian Cold Fork of Cottonwood Creek site, while *Puncturella mcleani* Kiel et al., 2010, is known from the Valanginian Bear Creek site. Additional fissurellids are known from Eocene seeps in Washington State (Goedert and Squires 1990) and from Eocene–Miocene seep deposits on Barbados (Gill et al. 2005).

One more group of lepetellides known from chemosynthesis-based communities are Sutilizonidae McLean, 1989, characterized by a long and wide slit (McLean 1989). Fossil sulitizonid *Triassurella goederti* Kiel et al., 2010, have been identified at the Valanginian seep site of Bear Creek in California (Kiel et al. 2010).

11.4.3 Patellida

Patellida Ihering, 1876, is the only order of the subclass Patellogastropoda Lindberg, 1986, and it consists of three superfamilies: Eoacmaeoidea Nakano and Ozawa, 2007; Patelloidea Rafinesque, 1815; and Lottioidea Gray, 1840 (Bouchet et al. 2017). Patellogastropods are arguably the most primitive group of living gastropods (e.g., Lindberg 1998), inhabiting a wide variety of marine environments. Members of two lottioid families (Neolepetopsidae McLean, 1990, and Pectinodontidae Pilsbry, 1891) occur in chemosynthesis-based communities. Neolepetopsids are unknown from the fossil record while pectinodontids are relatively common, particularly in Late Cretaceous seeps in Japan. The seep pectinodontids in Japan were previously classified into two distinct genera: *Bathyacmaea* Okutani et al., 1992, and *Serradonta* Okutani et al., 1992. The same genera were identified at modern (Okutani et al. 1992; Sasaki et al. 2003) and ancient seep sites (Hikida et al. 2003; Jenkins et al. 2007a, b; Kaim et al. 2009; Saether et al. 2012). Subsequently, it turned out that both genera should be merged into one (with the name *Bathyacmaea* having priority) and the differences in morphology and radula are of ecophenotypic nature (Chen et al. 2019a; Sato et al., 2020). *Bathyacmaea* with a low and wide shell (Fig. 11.4a, b) predominantly attaches to bivalve shells while laterally compressed *Serradonta* (Fig. 11.4c, d) thrives on worm tubes and at localities where worm tubes occur in large quantities, for example, the Campanian Omagari site in Hokkaido, Japan (Hikida et al. 2003; Jenkins et al. 2007a, b; Kaim et al. 2009). Additionally, some species of genus *Pectinodonta* live on Recent and ancient sunken wood ranging back to the Oligocene of Washington State (Lindberg and Hedegaard 1996) and Miocene of New Zealand (Marshall 1985). Another possible species of the genus has been described by Kaim et al. (2017) as *Pectinodonta borealis* from the Berriasian (Early Cretaceous) seep in Svalbard.

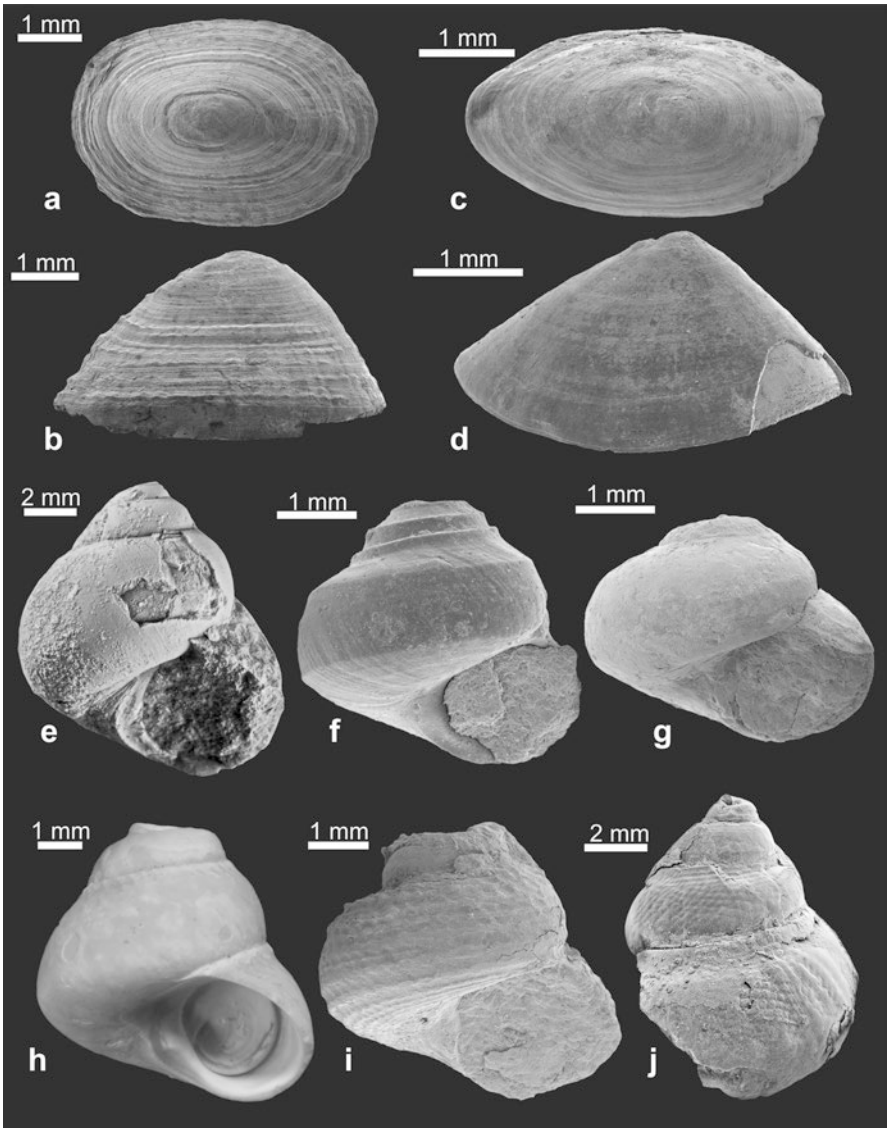

Fig. 11.4 Patellid and trochomorph gastropods. The flattened (**a**, **b**) and compressed (**c**, **d**) morphotypes of the pectinodontid patellid *Bathyacmaea omagariensis* (Kaim et al., 2009) from the Campanian (Late Cretaceous) Omagari seep site in Hokkaido, Japan (see Kaim et al. 2009). (**e**) Colloniid *Hikidea osoensis* Kaim et al., 2014, from Valanginian (Early Cretaceous) seep carbonates at Bear Creek, California, USA. (**f**) Colloniid *Hikidea yasukawensis* (Kaim et al., 2009) from the Campanian (Late Cretaceous) Yasukawa seep site in Hokkaido, Japan (see Kaim et al. 2009). (**g**) Colloniid *Hikidea omagariensis* (Kaim et al., 2009) from the Campanian (Late Cretaceous) Omagari seep site in Hokkaido, Japan (see Kaim et al. 2009). (**h**) Recent shell of *Cantrainea nuda* Okutani, 2001, from "depression B" of the Minami-Ensei Knoll, Okinawa Trough, Japan (see Kaim et al. 2009), note the similarity to the species of *Hikidea*. (**i**) Colloniid *Homalopoma abeshinaiensis* Kaim et al., 2009, from the Campanian (Upper Cretaceous) Omagari seep site in Hokkaido, Japan (see Kaim et al. 2009). (**j**) Colloniid *Phanerolepida onoensis* Kaim et al., 2014, from the Barremian (Early Cretaceous) seep site at Eagle Creek, California, USA (see Kaim et al. 2014)

11.5 Trochomorph Vetigastropods

Trochomorphs (or trochoideans) are the most diverse group among vetigastropods and are known worldwide from the tropics to the polar regions and from the shallowest intertidal zone to bathyal depths (Hickman and McLean 1990; Hickman 1996). Hickman and McLean (1990) suggested that they have an extensive fossil record ranging back to the Middle Triassic, though gastropods similar to trochoideans are reported from as early as the Ordovician (Hynda 1986; Dzik 1994). However, trochoideans as they were understood in the twentieth century are a polyphyletic group with at least two major groups of similar morphology known since the Mesozoic: Seguenziida and Trochida. Representatives of both orders occur at chemosynthesis-based communities at least since the early Mesozoic times. The oldest trochomorphs are known already from Paleozoic seeps and vents (see Little 2002 and Georgieva et al. 2021 for a review), but their preservation precludes any meaningful identification. The oldest Mesozoic trochoideans, though lacking identifications, are illustrated by Kiel et al. (2017) from Carnian–Norian (Late Triassic) seeps in Turkey (i.e., "gastropod with three keels," "gastropod with one strong keel," "*Hikidea*-like gastropod"). Of special interest is trochomorph *Francisciconcha maslennikovi* Little et al., 2004, from the Pliensbachian (Early Jurassic) hydrothermal vent deposit at Figueroa, California (Little et al. 2004), but its attribution to trochoideans remains disputable due to diagenetic distortion of pyrite-replaced shell; *F. maslennikovi* could be even a neomphalid.

11.5.1 Seguenziida

The molecular analyses of Kano (2008) and Kano et al. (2009) showed that the clade of deep-sea gastropods forming the order Seguenziida Verrill, 1884, is a monophyletic clade in Vetigastropoda consisting not only of the family Seguenziidae but also the trochoid-like families traditionally included in Trochida: Calliotropidae (=Eucyclidae), Chilodontaidae, and Cataegidae. Species of all the abovementioned groups occur at chemosynthesis-based communities, though Chilodontaidae is only known from the fossil record. Apart from that, there are four genera of Seguenziida, which were encountered at seeps or vents but not yet assigned to families (Sasaki et al. 2010). Those are *Adeuomphalus* Seguenza, 1876; *Moelleriopsis* Bush, 1897; *Akritogyra* Warén, 1992; and *Ventsia* Warén and Bouchet, 1993. Of these four, only *Adeuomphalus* occurs in the fossil record, but only as a regular deep-water dweller (Kaim 2004). One genus and species of Seguenziidae Verrill, 1884, is known exclusively from vents. *Bathymargarites symplector* Warén and Bouchet, 1989, is relatively common from the vents at the East Pacific Rise. No taxa of Seguenziidae have been found so far in the fossil record of seeps and vents though *Vetulonia philippinensis* (a genus of uncertain position among Seguenziida) from Pliocene seeps in Leyte Island, Philippines, has been classified in this family by Kiel et al. (2020a).

Cataegidae McLean and Quinn, 1987, are present both in Recent and fossil seeps. *Cataegis meroglypta* McLean and Quinn, 1987, is known from Recent seeps in the Caribbean (Sasaki et al. 2010). The fossil record of possible seep cataegids ranges back to the Valanginian (Early Cretaceous). Kaim et al. (2014) described *Cataegis*? sp. from Bear Creek seep site in California. Another species, *Cataegis nakagawensis*, has been described from a Campanian (Late Cretaceous) seep at Omagari, Hokkaido, Japan, by Kaim et al. (2009). *Cataegis godineauensis* (Van Winkle, 1919) occurs in Oligocene–Miocene seeps in the Caribbean (Colombia and Trinidad; Kiel and Hansen 2015), and *Cataegis ramosa* has been described from Pliocene seeps in Leyte Island, Philippines (Kiel et al. 2020a).

Two Recent species occasionally found at seeps, *Bathybembix macdonaldi* (Dall, 1890) and *Putzeysia wiseri* (Calcara, 1842), were previously attributed to the family Chilodontaidae Wenz, 1938, but currently, they are included in Eucyclidae (MolluscaBase eds. 2021a, b). Both are rather uncommon at seeps and vents, and both also occur on the regular deep-sea bottom (Sasaki et al. 2010). A possible seep chilodontaid has been described by Kaim et al. (2014) as *Chilodonta*? *reticulata* from the Valanginian (Early Cretaceous) Bear Creek seep site in California. In contrast, the extinct species of Eucyclidae Koken, 1896, are relatively common in Mesozoic seep sites. The oldest occurrence is the "Eucyclid sp." from Oxfordian–Kimmeridgian seeps in Novaya Zemlya, Arctic Russia (Hryniewicz et al. 2015). *Ambercyclus dilleri* (Stanton, 1895) from Paskenta, California, is of Tithonian age (Kiel et al. 2008), and *Eucycloidea bitnerae* Kaim et al., 2017, from Sassenfjorden, Svalbard (Fig. 11.3c), ranges from Tithonian to Berriasian (Kaim et al. 2017). Another species of *Ambercyclus*, *A. morganensis* (Stanton, 1895), is known from a Valanginian seep site at Rocky Creek in California (Kiel et al. 2008, see also Kaim et al. 2017). Additionally, *Bathybembix* sp. has been reported by Kiel and Goedert (2006) from an Eocene sunken wood community in Washington State.

11.5.2 Trochida

The order Trochida Cox and Knight, 1960, is represented by several families in Recent chemosynthesis-based communities, including Calliostomatidae, Trochidae, Turbinidae, Colloniidae, Margaritidae, and Solariellidae (Sasaki et al. 2010). However, only Colloniidae have abundant representation in ancient seeps while Margaritidae and Solariellidae have only single reports. It might be related to relative difficulty in interpretation of trochomorph shells when they are poorly preserved, and for that reason, many specimens are treated in the open nomenclature.

11.5.2.1 Colloniidae Cossmann in Cossmann and Peyrot, 1917

Colloniid trochomorphs are represented in the fossil record by species of *Cantrainea*, *Hikidea*, *Phanerolepida*, and *Homalopoma*. Particularly common are the Campanian *Hikidea yasukawensis* (Kaim et al., 2009) and *Hikidea omagariensis* (Kaim et al.,

2009) in the Campanian (Late Cretaceous) seeps of Yasukawa and Omagari in Hokkaido, Japan (Fig. 11.4f, g; Kaim et al. 2009). Besides that, *Hikidea svalbardensis* occurs in a Berriasian seep in Sassenfjorden, Svalbard (Kaim et al. 2017), and the type species of *Hikidea osoensis* has been described from a Valanginian seep at Bear Creek, California (Fig. 11.4e; Kaim et al. 2014). Other possible species are a *Hikidea*-like gastropod from a Triassic seep in Turkey (Kiel et al. 2017) and "*Margarita naticoides* Cooke, 1919," from an Oligocene seep in Cuba (Cooke 1919). The closest Recent relative of *Hikidea* is seemingly *Cantrainea nuda* Okutani, 2001, the species that possesses totally smooth shells apart from a finely pleated subsutural cord (Fig. 11.4h; see also Kaim et al. 2009: Fig. 7G). This species is known from a single specimen, its diagnosis is based solely on shell characters, and it actually may belong to the genus *Hikidea*. The single occurrence of *C. nuda* is known from a vent in Okinawa Trough (Okutani 2001) while other species of *Cantrainea* occur both at seeps and vents and also on regular deep-sea bottoms (Sasaki et al. 2010). Occurrences of *Cantrainea* at ancient seeps include *Cantrainea* sp. at the Miocene seep in Trinidad (Kiel and Hansen 2015) and another *Cantrainea* sp. at the Oligocene seep in Peru (Kiel et al. 2020b). Another species of *Hikidea* has been reported (as vetigastropod gen. et sp. indet.) by Kaim et al. (2008b) from the Coniacian plesiosaur fall in Hokkaido, Japan. A species of *Homalopoma*, *H. abeshinaiensis* (Fig. 11.4i), has been described from the Campanian Omagari seep in Hokkaido, Japan (Kaim et al. 2009). Two additional species have been reported in open nomenclature from Oligocene seeps in Washington State (Goedert and Squires 1990; Kiel 2006). Another species *Homalopoma domeniconii* has been described by Moroni (1966) from Miocene seep in Italy. It seems that *Cantrainea*, *Hikidea*, and *Homalopoma* are closely related, but a molecular study, including *C. nuda*, is required to clarify the nature of this relation.

Phanerolepida Dall, 1907, is a colloniid genus based on the Recent deep-water species *Turbo transenna* Watson, 1879, from Japan (Okutani and Iwahori 1992) with a bathymetric range that overlaps with the bathymetric range of hydrocarbon seep sites occurring in the same area. Some additional fossil species are described from upper Eocene deep-water sediments on the Pacific coast of North America and from the Miocene of Kamchatka and Miocene/Pliocene deposits of Japan (see Hickman 1972; Amano 2005). The only seep occurrence so far is *Phanerolepida onoensis* (Fig. 11.4j) from the Barremian Eagle Creek seep deposit in California (Kaim et al. 2014), which is also the oldest occurrence of this genus.

Margaritidae Thiele, 1924, are represented by three species (*Margarites ryukyuensis*, *M. huloti*, and *M. shinkai*) in seeps and vents off Japan (Sasaki et al. 2010). Three fossil species of *Margarites* are known to date. *Margarites sasakii* has been described from a Campanian Omagari seep in Hokkaido, Japan (Kaim et al. 2009); *M. columbianus* Squires and Goedert, 1991, has been reported from Eocene–Oligocene seeps in Washington State (Goedert and Squires 1990; Squires and Goedert 1991; Kiel 2006); and *Margarites hayashii* has been reported from Pliocene seeps in Leyte Island, Philippines (Kiel et al. 2020a). The occurrences of Solariellidae Powell, 1951, at fossil seeps are reported by Kiel (2006) from an Oligocene seep in Washington State and by Kiel et al. (2020a) from Pleistocene seeps in Leyte Island, Philippines.

11.6 Neritimorpha

Neritimorpha Koken, 1896, is a distinct clade of gastropods of uncertain relationship to other gastropods. Most recent molecular studies (Cunha and Giribet 2019) suggest that it forms a sister clade to a clade comprising Caenogastropoda and Heterobranchia. Neritimorphs are typically shallow-water, but there are also a few taxa adapted to deep water including seeps and vents (Sasaki et al. 2010). The family Phenacolepadidae Pilsbry, 1895, is clearly divided into two distinct subfamilies: shallow-water Phenacolepadinae Pilsbry, 1895, and deep-water Shinkailepadinae Okutani et al., 1989. Species of the genus *Shinkailepas* are known from vents worldwide (Sasaki et al. 2010), while the monotypic genus *Olgasolaris* Beck, 1992, with the type species *O. tollmanni* from the Manus back-arc basin has been recently synonymized with *Shinkailepas* (Fukumori et al. 2019). Another monotypic genus *Bathynerita* Clarke, 1989, with the type species *Bathynerita naticoidea*, which is distributed at hydrocarbon seep sites in the Louisiana Slope of the Gulf of Mexico and the Caribbean (Warén and Bouchet 2001), has been recently synonymized with *Thalassonerita* Moroni, 1966, and relocated from Neritidae to Shinkailepadinae (Fukumori et al. 2019). The type species of *Thalassonerita*, *T. megastoma* Moroni, 1966, has been described from a Miocene seep in Italy (Moroni 1966). Another species, *Thalassonerita eocenica* Squires and Goedert, 1996, has been described from middle Eocene seep deposits in Washington State, USA (Squires and Goedert 1996; Hybertsen and Kiel 2018). Another neritid from an Oligocene cold-seep deposit of the Lomitos cherts, Peru, has been mentioned by Olsson (1931) but never illustrated (Kiel et al. 2020b). The only available specimen from that locality is badly preserved and left by Kiel et al. (2020a, b) in open nomenclature as Neritimorpha indet.

Two poorly preserved neritids have been also found in the Oxfordian (Late Jurassic) seep carbonates at Beauvoisin, France (Kiel et al. 2010), and an Early Cretaceous seep in the Crimea (Kiel and Peckmann 2008), but they are most likely not related to *Thalassonerita* (Kiel, 2010), being more conchologically similar to other Mesozoic neritoids (Fukumori et al. 2019). Molecular age estimates suggest that shinkailepadids diverged from neritids in the Late Cretaceous (Kano et al. 2002).

11.7 Neogastropoda

The order Neogastropoda Wenz, 1938, is one of the most extremely diversified and abundant groups of benthic predators and scavengers. Nearly all are marine forms and they constitute about one-third of all living gastropod species. No wonder then that they also adapted to vent and seep environments. The most common in such environments are Buccinidae and Turridae while the other groups are rare (Sasaki et al. 2010). Almost all modern families of neogastropods emerged in the Cretaceous

and starting with the Late Cretaceous neogastropods are common fossils in marine sediments, while older findings are rare and all need a critical review. Based on shell morphology, it seems that the first true neogastropods appeared in the Early Cretaceous (Kollmann 1982; Taylor and Morris 1988; Kaim 2004) with the oldest known record from the Valanginian (early Early Cretaceous) of Poland (Kaim 2004). The earliest known occurrence of a true neogastropod at ancient seeps is "Neogastropoda indet." (Fig. 11.3h) reported by Kaim et al. (2009) from the Campanian (Late Cretaceous) seep at Yasukawa, Hokkaido, Japan. Some neogastropods are also recorded from Miocene and Pliocene seeps in Japan, but their preservation is rather poor and their taxonomy is not fully resolved (see, for example, Tanaka 1959; Miyajima et al. 2018).

Two extinct groups of Mesozoic caenogastropods are repetitively discussed as possible stem and/or sister groups of Neogastropoda, Purpurinidae and Pseudotritonidae (= Maturifusidae), with a fossil record reaching back to the Triassic. Both groups are reported from ancient seeps.

11.7.1 Purpurinidae and Pseudotritonidae

The family Purpurinidae Zittel, 1895, was proposed to be a sister (Taylor et al. 1980) or ancestral group of neogastropods (Kaim 2004) and may represent ancestors of Tonnoidea (Bandel 1993). The purpurinid *Cretadmete* sp. (Fig. 11.3g) has been reported by Kaim et al. (2017) from the Tithonian (Late Jurassic) seep in Sassenfjorden, Svalbard. According to Kiel et al. (2008), another possible purpurinid is *Bathypurpurinopsis stantoni* Kiel et al., 2008, from the Albian (Early Cretaceous) seep of Cold Fork of Cottonwood Creek in California.

The Pseudotritonidae Golikov and Starobogatov, 1987 (= Maturifusidae Gründel, 2001), is commonly regarded as a stem group of the Neogastropoda (e.g., Taylor et al. 1980; Szabó 1983; Riedel 2000; Kaim 2004). A possible pseudotritonid has been reported as "Maturifusid sp." by Hryniewicz et al. (2015) from a Berriasian–Early Valanginian seep in Novaya Zemlya, Arctic Russia.

11.7.2 Buccinoidea

Buccinidae Rafinesque, 1815, are relatively common and diversified at Recent seeps and vents and include the genera *Neptunea*, *Buccinum*, *Eosipho*, *Bayerius*, and *Callioncha* (Sasaki et al. 2010). Buccinids have also been encountered in Cenozoic seeps. *Colus sekiuensis* Kiel and Goedert, 2007, has been found both at an Oligocene seep in Peru (Kiel et al. 2020b) and organic falls in Washington State (Kiel and Goedert 2007). Additionally, *Colus*? sp. has been reported by Hybertsen and Kiel (2018) from an Eocene seep in Washington State. Another species, *Colus* cf. *fujimotoi* Hirayama, 1955, is known from Eocene and Oligocene seeps in Hokkaido, Japan

(Amano and Kiel 2011). Furthermore, *Trominina japonica* (Takeda, 1953) has been identified in the Oligocene seep carbonate at Kami-Atsunai in Hokkaido (Amano et al. 2013). *Eosipho hoernesi* and nassarid *Tritia ruggierii* have been reported by Moroni (1966) from Miocene seep in Italy.

Another bunch of buccinid species encountered at seeps represent the family Parancistrolepidinae Habe, 1972. Amano and Oleinik (2016) reported *Ancistrolepis modestoideus* (Takeda, 1953) and *Bathyancistrolepis mikasaensis* Amano and Oleinik, 2016, from an Eocene seep at Mikasa in Hokkaido, *Ancistrolepis* sp. from an Eocene Kiritachi seep in Hokkaido, and *Ancistrolepis koyamai* (Kuroda, 1931) from a Miocene Akanuda seep in Nagano Prefecture, Central Honshu. The latter species is also known from non-seep deposits (Amano et al., 1996). *Clinopegma* aff. *borealis* Tiba, 1969, is known from a Miocene seep at Morai in Hokkaido (Amano, 2003). Another occurrence might be *Ancistrolepis teglandae* (Weaver, 1942) where this species is associated with Oligocene vesicomyids but seep carbonates were not found (Kiel and Amano 2010). One other possible buccinid is also *Levifusus*? *angelicus* Cooke, 1919, from an Eocene seep of Cuba (Kiel and Peckmann 2007). Questionable buccinid *Urahorosphaera kanekoi* were described from the sunken wood community of the Paleocene Katsuhira Formation (Amano and Oleinik 2014).

11.7.3 Conoidea

Species of Conoidea Fleming, 1822, are generally common predators in deep-sea environments, and they are also abundant at Recent seeps and vents (Sasaki et al. 2010). Species of three different conoidean families (Mangeliidae, Raphitomidae, and Turridae) are known from Oligocene seeps in Washington State (Kiel 2006), namely, *Benthomangelia*? sp.; *Xanthodaphne campbellae* Kiel, 2006; and *Turrinosyrinx hickmanae* Kiel, 2006; respectively.

11.7.4 Muricoidea

Muricoidea Rafinesque, 1815, are rather uncommon at Recent seeps, basically restricted to three species of *Trophon* Montfort, 1810, which also occur on the regular deep-sea bottom (Sasaki et al. 2010). Two species of Muricoidea are known from Cenozoic seeps in Japan: *Abyssotrophon*? sp. is reported from a late Eocene to early Oligocene seep at Tanami, Southern Honshu (Amano et al. 2013), and *Trophonopsis* sp. is recorded from a Miocene Akanuda seep in Nagano Prefecture, Central Honshu (Miyajima et al. 2017).

11.8 Heterobranchia

Heterobranchia Burmeister, 1837, is a clade of subclass rank comprising highly diversified taxa in marine, freshwater, and continental environments. In contrast, the diversity of heterobranchs is relatively low in Recent vent and seep communities (Sasaki et al. 2010). Five major groups of heterobranchs are reported so far from Recent seeps and vents, Pyramidellidae, Cephalaspidea, Orbitestellidae, Hyalogyrinidae, and Xylodisculidae (Sasaki et al. 2010), with the latter being more characteristic to wood falls. All but Pyramidellidae are known from ancient chemosynthesis-based communities.

11.8.1 Cephalaspidea

Cephalaspids are unknown from Recent hydrothermal vents and rare at seeps. Also in the fossil record, they are uncommon and may constitute fortuitous occurrences. Most common in ancient seeps are acteonoids. *Acteon exsculptus* Tullberg, 1881, and *Acteon frearsianus* Tullberg, 1881, are known from a Berriasian–Early Valanginian seep in Novaya Zemlya (Tullberg 1881; Hryniewicz et al. 2015), both species awaiting revision (Hryniewicz et al. 2015). Moreover, ?*Sulcoactaeon* sp. (Fig. 11.5b) has been reported from a Campanian Yasukawa seep in Hokkaido, Japan (Kaim et al. 2009), and two species of *Acteon* in open nomenclature have been reported from Eocene to Oligocene seeps in Washington State (Kiel 2006) and an Oligocene seep in Peru (Kiel et al. 2020a, b). Besides acteonoids, the diaphanid *Diaphana* sp. has been recorded by Kaim et al. (2014) from the Valanginian seeps of West Berryessa, California, scaphandrid *Ellipsoscapha* sp. (Fig. 11.5c) from Paleocene seeps in Svalbard (Hryniewicz et al. 2019), and two species of *Cylichna* in open nomenclature from Oligocene seeps in Washington State and Peru by Kiel (2006) and Kiel et al. (2020a, b), respectively. *Eocylichna multistriata* (Takeda, 1953) has been reported from the Oligocene Kami-Atsunai seep in Hokkaido (Amano and Jenkins 2013). An unidentified cephalaspid has also been reported by Kiel et al. (2017) from a Late Triassic seep in Turkey.

11.8.2 Orbitestellidae

The orbitestellid genus *Lurifax* unites vent and seep taxa in the Mediterranean, New Zealand, Japan, and the Mid-Atlantic Ridge (Sasaki et al. 2010). A single fossil species, *Lurifax goederti* Kiel, 2006, is known from the Eocene to Oligocene seeps in Washington State (Kiel 2006).

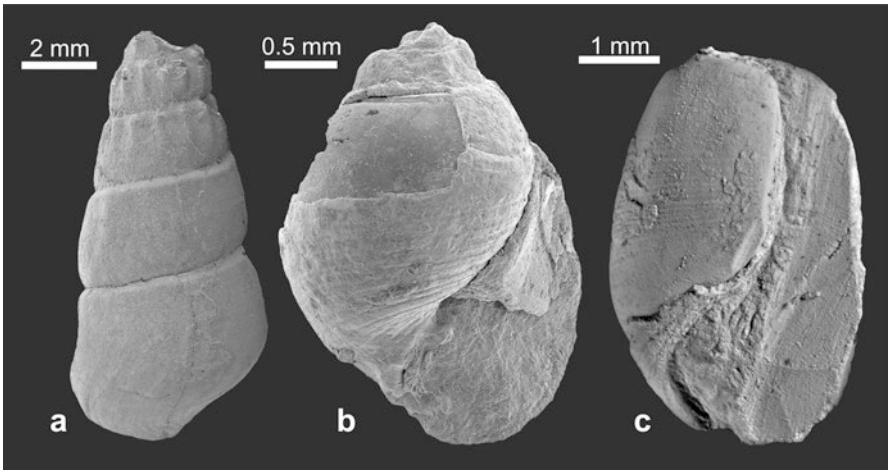

Fig. 11.5 Rissoid? (or hokkaidoconchid) and heterobranch gastropods. (**a**) Rissoid (or hokkaidoconchid) *Hokkaidoconcha*? *hignalli* Kaim and Kelly, 2009, from Tithonian (Late Jurassic) Gateway Pass seep carbonates in Alexander Island, Antarctica (see Kaim and Kelly 2009). (**b**) Cephalaspid ?*Sulcoactaeon* sp. from the Campanian (Late Cretaceous) Yasukawa seep site in Hokkaido, Japan (see Kaim et al. 2009). (**c**) Scaphandrid *Ellipsoscapha* sp. from the Paleocene seep carbonates in Hollendarbukta, Svalbard (see Hryniewicz et al. 2019)

11.8.3 Hyalogyrinidae

Hyalogyrinids occur abundantly on bacterial mats in sulfide-rich areas at seeps and whale falls as well as at vents (Braby et al. 2007; Sasaki et al. 2010). Their simple small shells are difficult to tell apart from other similar forms of skeneids, trochids, and neomphalids, in particular in fossil material when shells are poorly preserved (see, e.g., "skeneiform gastropod" in Kaim et al. 2009: p. 483, which highlights this problem). Therefore, only two species of *Hyalogyrina* have been identified so far: *Hyalogyrina knorringfjelletensis* Kaim et al., 2017 (Fig. 11.3f), from the Berriasian seep in Sassenfjorden, Svalbard (Kaim et al. 2017), and *Hyalogyrina* sp. from the Eocene to Oligocene seeps in Washington State (Kiel 2006; Hybertsen and Kiel 2018).

11.8.4 Xylodisculidae

Though some xylodisculids have been found at seeps and vents, they are most common at wood falls (Sasaki et al. 2010). A single fossil species, *Xylodiscula okutanii* Kiel and Goedert, 2007, is known from an Oligocene–Miocene wood fall in Washington State (Kiel and Goedert 2007).

11.9 Other Groups

Several other groups of gastropods have some representatives in Recent and ancient seeps, but they most commonly constitute fortuitous occurrences or possess only a few taxa typical of chemosynthesis-based communities. Such singular occurrences can be highlighted by the presence of *Cypraea semen* Cooke, 1919, at an Eocene seep in Cuba (Kiel and Peckmann 2007), "Cerithiopsid incertae sedis" of Kiel (2006) at an Oligocene seep in Washington State, and the turritellid *Orectospira wadana* (Yokoyama, 1890) at a late Eocene–early Oligocene seep at Tanami, Southern Honshu, Japan (Amano et al. 2013), and at an early Oligocene seep at Kami-Atsunai, Hokkaido, Japan (Amano and Jenkins 2013). Amathinid *Carinorbis clathrata* (described as *Phasianema taurocrassum*) and cassid *Galeodea delibrata* have been reported by Moroni (1966) from Miocene seep in Italy. Occurrences of other groups are listed below.

11.9.1 Rissoidae

Rissoids are not typical gastropods of chemosynthesis-based communities. Although some rissoids (*Alvania*, *Benthonella*, *Pseudosetia*, and *Rissoa*) do occur at seeps and vents, especially in the North Atlantic (e.g., Gebruk et al. 2003; Sasaki et al. 2010; Schander et al. 2010; Génio et al. 2013), it seems that it is a relatively recent colonization event rather than ancient adaptation (Kaim et al. 2017). One possible genus with ancient history in seeps is the extinct *Boreomica* Guzhov, 2017, which was established for taxa thus far classified as *Hudlestoniella* Cossmann, 1909. Guzhov (2017) argued that these taxa differ from the type species of *Hudlestoniella*, warranting description of a new genus. Kaim et al. (2004) and, subsequently, Guzhov (2017) classified *Hudlestoniella* (and thus *Boreomica*) in the Rissoidae based on protoconch morphology.

Boreomica undulata (Tullberg 1881) and *Boreomica pusilla* (Tullberg 1881) are known from Tithonian and Berriasian–Early Valanginian seeps in Novaya Zemlya, respectively (Hryniewicz et al. 2015), while *Boreomica hammeri* (Kaim et al., 2017) is known from a Berriasian seep in Sassenfjorden, Svalbard (Kaim et al. 2017). Another species of *Boreomica* might be *Hokkaidoconcha hignalli* Kaim and Kelly, 2009 (Fig. 11.5a), known from a mass occurrence in the Tithonian (Late Jurassic) Gateway Pass seep from Alexander Island in Antarctica (Kaim and Kelly 2009), since it is similar to *Boreomica hammeri* from Svalbard (Kaim et al. 2017). The protoconch of *H. hignalli* is unknown; therefore, its hokkaidoconchid or rissoid identity cannot be confirmed (Kaim et al. 2017).

11.9.2 Aporrhaidae

Aporrhaids are gastropods that live on muddy and sandy bottoms, sometimes in very large populations, but in Recent seas they are restricted to two genera only (*Aporrhais* and *Arrhoges*). In the past, this group was much more diversified, especially in the Jurassic and Cretaceous (see, for example, Kaim 2004), and depleted in diversity in Cenozoic times. Seep occurrences of aporrhaids should be considered fortuitous and include *Pseudanchura biangulata* (Anderson, 1938) from a Barremian seep at Eagle Creek, California (Kaim et al. 2014); *Aporrhais* cf. *gracilis* Koenen, 1885 (Fig. 11.3e), from a Paleocene seep in Svalbard (Hryniewicz et al. 2019); Aporrhaidae indet. (originally as a provannid) from a Paleocene seep in Panoche Hills, California (Schwartz et al. 2003); and "aporrhaid gastropod" from a Cenomanian seep at Awanui, New Zealand (Kiel et al. 2013). Xenophorid *Xenophora borsoni* has been reported by Moroni (1966) from Miocene seep in Italy.

11.9.3 Ampullinidae and Naticidae

The Ampullinidae vs. Naticidae conundrum is another highlight of a problem in identification of morphologically simple shells in the fossil record. Naticids are predatory littorinimorphs while ampullinids are campaniloid grazers with similarly smooth and globular shells (for more information, see, for example, Kase and Ishikawa 2003). Representatives of both groups have been identified in ancient seeps. "Ampullinid gastropod" has been reported by Kiel and Peckman (2008) from a Berriasian seep in the Crimea (Kiel and Peckmann 2008), while *Globularia isfjordensis* (Vonderbank, 1970) is common from a Paleocene seep in Svalbard (Fig. 11.3d; Hryniewicz et al. 2019).

Naticids at ancient seeps are represented by *Cryptonatica* sp. from a late Eocene to early Oligocene Tanami seep in Southern Honshu, Japan (Amano et al. 2013), and from a Miocene Morai seep in Hokkaido, Japan (Amano 2003); *Euspira meisensis* (Makiyama, 1926) from an Oligocene seep at Kami-Atsunai, Hokkaido, Japan (Amano and Jenkins 2013); *E. pallida* (Broderip and Sowerby, 1829) from a Miocene Morai seep, Hokkaido, Japan (Amano 2003), and Pliocene Matsunoyama seep, Central Japan (Miyajima et al. 2018); *Euspira*? sp. from an Eocene Poronai seep, Hokkaido, Japan (Amano and Jenkins 2007); and possibly *Sassenfjordia sassenfjordensis* Kaim et al., 2017, from a Berriasian seep in Sassenfjorden, Svalbard (Kaim et al. 2017). Occurrences of naticid-like shells are commonly associated with predatory drill holes, which may suggest that they are indeed naticids. Such drill holes have been noted previously in fossil cold-seep mollusks by Amano (2003), Amano and Jenkins (2007), Amano and Kiel (2007), Kiel et al. (2008, 2016), and Hryniewicz et al. (2019).

11.9.4 Eulimidae

Eulimids are parasitic snails common in Recent oceans but not yet reported from seeps and vents (Sasaki et al. 2010). Three species of eulimids (*Niso littlei* Kiel, 2006, Eulimid sp. 1, and Eulimid sp. 2) were reported by Kiel (2006) from Oligocene seeps in Washington State.

11.10 Conclusions and Future Directions

Gastropods are one of the most important groups of organisms adapted to thrive in chemosynthesis-based communities. Trochomorph gastropods are known already from Paleozoic seeps and vents (Peckmann et al. 2001; Little 2002) though their taxonomy remains poorly explored due to poor preservation.

The Carnian–Norian (Late Triassic) seep fauna from Turkey (Kiel et al. 2017) display a high diversity of gastropods including possible abyssochrysoid *Paskentana*, possible trochoidean *Hikidea*, and an unidentified cephalaspid (Fig. 11.6). The Jurassic and Cretaceous were times of abyssochrysoid dominance in seep and vent gastropod communities. *Abyssomelania*, *Hokkaidoconcha*, and *Paskentana* are known already in the Jurassic. *Ascheria*, *Atresius*, and *Humptulipsia* appear in the Early Cretaceous, while *Cyprioconcha*, *Desbruyeresia*, and *Provanna* are reported from the Late Cretaceous (the latter two are most likely present already in the latest Early Cretaceous). In several ancient seeps, abyssochrysoids occur in mass accumulations (e.g., *Paskentana* in the Valanginian Bear Creek seep and *Desbruyeresia* in the Cenomanian Kanajirisawa seep). Also from the Jurassic is the oldest report of neomphalid gastropods in seeps, though their diversity is much restricted in comparison to present diversity. Most common are species of *Retiskenea*, which also today occur in seeps. Noteworthy is the absence of neomphalids in Late Cretaceous vents in Cyprus, while abyssochrysoids are common and well diversified there. This may suggest that the neomphalid radiation in vents came much later. The time of this radiation is unknown due to the absence of fossiliferous vent deposits from Cenozoic times. Limpet-shaped gastropods occur occasionally at seeps already in the Jurassic but are really common only in Campanian (Late Cretaceous) seeps in Japan where a compressed morphotype of *Bathyacmaea* thriving on worm tubes is very abundant. Similarly, colloniid vetigastropods appear in large quantities only in Late Cretaceous seeps although they were present already in the Early Cretaceous. Eucyclid seguenziids are extremely common in Jurassic seas (e.g., Ferrari et al. 2014) and they apparently migrated to Jurassic seeps while cataegids appeared in the Cretaceous and still occur at seeps today. Stem and/or sister groups of neogastropods (Purpurinidae and Pseudotritonidae) first appeared at seeps in the Jurassic, while true neogastropods are nearly absent in Mesozoic seeps, apart from a single poorly preserved specimen in a Campanian (Late Cretaceous) seep in Japan. Otherwise, neogastropods appear in larger numbers in Oligocene seeps. Cephalaspids

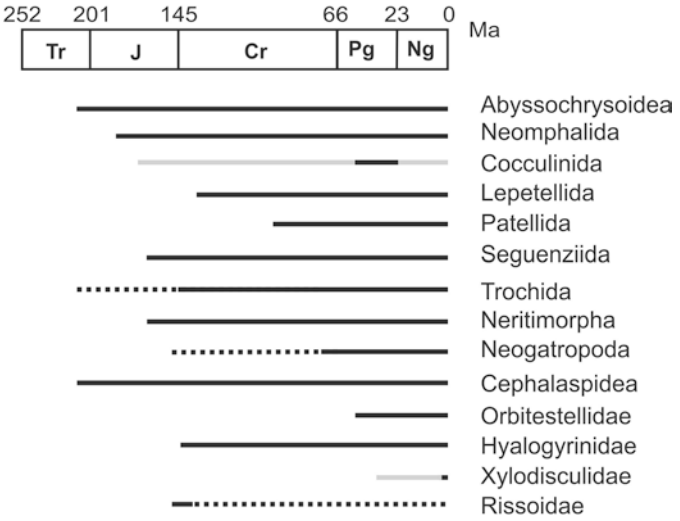

Fig. 11.6 Geological ranges of major gastropod clades at seep/vents (black lines) and organic falls (gray lines). Paleozoic occurrences (as taxonomically uncertain) not included

are recorded at seeps from the Triassic but never occur in larger numbers, being apparently only opportunistic in these environments.

Nearly nothing is known about gastropods from Paleozoic seeps, and still too little is known about gastropods from the Triassic and Early Jurassic seeps. A Toarcian seep fauna from Argentina (currently under study) may partially fill this gap. Another poorly known period in the evolution of chemosynthesis-based communities is the latest Cretaceous–Paleocene interval. This paucity of information causes a major problem in evaluating the influence of the Cretaceous–Paleogene extinction event on the evolution of seep and vent faunas. Another major problem in interpreting the evolution of chemosynthesis-based communities is the paucity of ancient vent communities in general and Cenozoic ones in particular.

Acknowledgments First of all, I would like to thank Anders Warén for "infecting" me with the interest in gastropods from chemosynthesis-based communities and continuous support ever since my scholarship of the Swedish Institute at Naturhistoriska Riksmuseet, Stockholm, during snowy winter 2001/2002. Kazushige Tanabe and Takenori Sasaki are thanked for hosting me as a JSPS fellow at the University of Tokyo. During the tenure of this fellowship, I was able to visit my first ancient seep sites and to write my first seep papers. Also there I met Robert G. Jenkins (then a PhD student and now a researcher at the University of Kanazawa), and this encounter has resulted in a long-lasting and fruitful cooperation. Robert is also thanked for countless hours spent together on discussions, fieldwork, and collections. Neil H. Landman is thanked for hosting me as a Fulbright fellow at the AMNH in New York City when the idea of this book originated. I would also like to thank all colleagues and friends who assisted me in the field (or in any other way) and/or provided materials for my studies. Last, but not least, I thank my family, Ewa, Kosma, and Izabella, for the support and understanding (and long detours to seep sites during our vacations). Finally, I'm grateful to Kazutaka Amano and Kristian P. Saether for comprehensive reviews of this chapter and Krzysztof Hryniewicz, Neil H. Landman, and J. Kirk Cochran for the help, comments, and corrections.

References

Agirrezabala LM, Kiel S, Blumenberg M et al (2013) Outcrop analogues of pockmarks and associated methane-seep carbonates: a case study from the Lower Cretaceous (Albian) of the Basque-Cantabrian Basin, western Pyrenees. Palaeogeogr Palaeoclimatol Palaeoecol 390:94–115

Aktipis SW, Giribet G, Lindberg DR et al (2008) Gastropoda: an overview and analysis. In: Ponder WF, Lindberg DR (eds) Phylogeny and evolution of the Mollusca. University of California Press, Berkeley, pp 201–237

Amano K (2003) Predatory gastropod drill holes in upper Miocene cold seep bivalves, Hokkaido, Japan. Veliger 46:90–96

Amano K (2005) Migration and adaptation of late Cenozoic cold-water molluscs in the North Pacific. In: Elewa AM (ed) Migration of organisms: climate, geography, ecology. Springer, Berlin, pp 127–150

Amano K, Jenkins RG (2007) Eocene drill holes in cold-seep bivalves of Hokkaido, northern Japan. Mar Ecol 28:108–114

Amano K, Jenkins RG (2013) A new species of *Provanna* (Gastropoda: Provannidae) from an Oligocene seep deposit in eastern Hokkaido, Japan. Paleontol Res 17:325–329

Amano K, Kiel S (2007) Fossil vesicomyid bivalves from the North Pacific region. Veliger 49:270–293

Amano K, Kiel S (2011) Fossil *Adulomya* (Vesicomyidae, Bivalvia) from Japan. Veliger 51:76–90

Amano K, Little CTS (2014) Miocene abyssochrysoid gastropod *Provanna* from Japanese seep and whale-fall sites. Acta Palaeontol Pol 59:163–172

Amano K, Little CTS, Campbell KA (2018) Lucinid bivalves from Miocene hydrocarbon seep sites of eastern North Island New Zealand with comments on Miocene New Zealand seep faunas. Acta Palaeontol Pol 63:371–382

Amano K, Oleinik A (2014) A new genus of Buccinoidea (Gastropoda) from Paleocene deposits in eastern Hokkaido, Japan. Nautilus 128:122–128

Amano K, Oleinik A (2016) Ancistrolepidine gastropods (Buccinidae) from the upper Eocene hydrocarbon seep deposits in Hokkaido, northern Japan. Nautilus 130:158–163

Amano K, Ukita M, Sato S (1996) Taxonomy and distribution of the subfamily Ancistrolepidinae (Gastropoda: Buccinidae) from the Plio-Pleistocene of Japan. Trans Proc Palaeontol Soc Jpn 176:467–477

Amano K, Jenkins RG, Sako Y et al (2013) A Paleogene deep-sea methane-seep community from Honshu, Japan. Palaeogeogr Palaeoclimatol Palaeoecol 387:126–133

Anderson FM (1938) Lower Cretaceous deposits in California and Oregon. Geol Soc Am Spec Pap 16:1–339

Bandel K (1993) Caenogastropoda during Mesozoic times. Scr Geol Spec Issue 2:7–56

Beck LA (1992) Two new neritacean limpets (Gastropoda: Prosobranchia: Neritacea: Phenacolepadidae) from active hydrothermal vents at Hydrothermal Field 1 'Wienerwald' in the Manus Back-Arc Basin (Bismarck Sea, Papua New Guinea). Ann Naturhist Mus Wien B 92:277–286

Beesley PL, Ross GJB, Wells A (1998) Mollusca: the southern synthesis, Fauna of Australia, vol 5. CSIRO Publishing, Melbourne

Bertolaso L, Palazzi S (1994) La posizione sistematica di *Delphinula bellardii* Michelotti, 1847. Appunti di Malacologia Neogenica vol. 2. Boll Malacol 29:291–302

Bouchet P (1991) New records and new species of *Abyssochrysos* (Mollusca, Caenogastropoda). J Nat Hist 25:305–313

Bouchet P, Warén A (1991) *Ifremeria nautilei*, nouveau gastéropode d'évents hydrothermaux, probablement associé à des bactéries symbiotiques. C R Acad Sci Paris 312:495–501

Bouchet P, Rocroi J-P, Frýda J et al (2005) Classification and nomenclator of gastropod families. Malacologia 47:1–368

Bouchet P, Rocroi J-P, Hausdorf B et al (2017) Revised classification, nomenclator and typification of gastropod and monoplacophoran families. Malacologia 61:1–526

Braby CE, Rouse GW, Johnson SB et al (2007) Temporal variation among *Osedax* boneworms and related megafauna on whale-falls in Monterey Bay, California. Deep-Sea Res I 54:1773–1791
Broderip WJ, Sowerby GBI (1829) Observations on new or interesting Mollusca contained, for the most part, in the Museum of the Zoological Society. Zool J 4:359–379
Burmeister H (1837) Handbuch der Naturgeschichte, vol 2. Zoologie, Enslin, Berlin
Bush K (1897) Revision of the marine gastropods referred to *Cyclostrema*, *Adeorbis*, *Vitrinella* and related genera with descriptions of some new genera and species belonging to the Atlantic fauna of America. Trans Connecticut Acad Arts Sci 10:97–144
Calcara P (1842) Nuove ricerche ed osservazioni sopra vari molluschi Siciliani: nuove specie di *Calyptrea*. Il Maurolico [Gabinetto Letterario Messina] 13:1–14
Campbell KA, Francis DA, Collins M et al (2008a) Hydrocarbon seep-carbonates of a Miocene forearc (East Coast Basin), North Island, New Zealand. Sediment Geol 204:83–105
Campbell KA, Peterson D, Alfaro AC (2008b) Two new species of *Retiskenea*? (Gastropoda: Neomphalidae) from Lower Cretaceous hydrocarbon seep-carbonates of northern California. J Paleontol 82:140–153
Chen C, Ogura T, Hirayama H et al (2016) First seep-dwelling *Desbruyeresia* (Gastropoda: Abyssochrysoidea) species discovered from a serpentinite-hosted seep in the Southeastern Mariana Forearc. Molluscan Res 36:277–284
Chen C, Watanabe HK, Nagai Y et al (2019a) Complex factors shape phenotypic variation in deep-sea limpets. Biol Lett 15:20190504
Chen C, Watanabe HK, Sasaki T (2019b) Four new deep-sea provannid snails (Gastropoda: Abyssochrysoidea) discovered from hydrocarbon seep and hydrothermal vents in Japan. R Soc Open Sci 6:190393
Clarke AH (1989) New mollusks from under-sea oil seep sites off Louisiana. Malacol Data Net 2:122–134
Colgan DJ, Ponder WF, Beacham E et al (2007) Molecular phylogenetics of Caenogastropoda (Gastropoda: Mollusca). Mol Phyloget Evol 42:717–737
Conti MA, Fischer J-C (1984) La faune à gastropodes du Jurassique moyen de Case Capenine (Umbria, Italie), systématique, paléobiogéographie, paléoécologie. Geol Romana 21(for 1982):125–183
Cooke CW (1919) Contributions to the geology and paleontology of the West Indies IV: Tertiary mollusks from the Leeward Islands and Cuba. Carnegie Inst Wash Publ 291:103–156
Cossmann M (1909) Essais de paléoconchologie compare, 8th edn. Cossmann & Rudeval, Paris
Cossmann M, Peyrot A (1917) Conchologie néogénique de l'Aquitaine: scaphopodes et gastropodes. Actes Soc Linn Bordeaux 69:157–365
Cox LR, Knight JB (1960) Suborders of Archaeogastropoda. Proc Malacol Soc Lond 33:262–264
Cunha TJ, Giribet G (2019) A congruent topology for deep gastropod relationships. Proc R Soc B 286:20182776
Dall WH (1882) On certain limpets and chitons from the deep waters off the eastern coast of the United States. Proc U S Natl Mus 4:400–414
Dall WH (1890) Contributions to the Tertiary fauna of Florida, with especial reference to the Miocene Silex-beds of Tampa, and the Pliocene beds of the Caloosahatchee River: part I. Trans Wagner Free Inst Sci Phila 3:1–178
Dall WH (1907) Descriptions of new species of shells, chiefly Buccinidae, from the dredgings of the U.S.S. 'Albatross' during 1906, in the northwestern Pacific, Bering, Okhotsk, and Japanese Seas. Smithson Misc Collect 50:139–173
Dall WH (1918) Description of new species of shells, chiefly from Magdalena Bay, Lower California. Proc Biol Soc Wash 31:5–8
Desbruyères D, Segonzac M, Bright M (2006) Handbook of deep-sea hydrothermal vent fauna. Biologiecentrum der Oberösterreichische Landesmuseum, Linz
Dzik J (1994) Evolution of 'small shelly fossils' assemblages. Acta Palaeontol Pol 39:247–313

Ferrari SM, Kaim A, Damborenea SE (2014) The genera *Calliotropis* Seguenza and *Ambercyclus* n. gen. (Vetigastropoda, Eucyclidae) from the Early Jurassic of Argentina. J Paleontol 88:1174–1188

Fleming J (1822) The philosophy of zoology, a general view of the structure, functions and classification of animals, vol 2. Constable, Edinburgh

Fukumori H, Yahagi T, Warén A et al (2019) Amended generic classification of the marine gastropod family Phenacolepadidae: transitions from snails to limpets and shallow-water to deep-sea hydrothermal vents and cold seeps. Zool J Linnean Soc 185:636–655

Gabb WM (1869) Cretaceous and Tertiary fossils. Calif Geol Surv Paleontol 2:1–299

Gebruk AV, Krylova EM, Lein AY et al (2003) Methane seep community of the Håkon Mosby mud volcano (the Norwegian Sea): composition and trophic aspects. Sarsia 88:394–403

Geiger DL, Thacker CE (2006) Molecular phylogeny of basal gastropods (Vetigastropoda) show stochastic colonization of chemosynthetic habitats at least from the mid Triassic. Cah Biol Mar 47:343–346

Génio L, Warén A, Matos FL et al (2013) The snails' tale in deep-sea habitats in the Gulf of Cadiz (NE Atlantic). Biogeosciences 10:5159–5170

Georgieva MN, Little CTS, Maslennikov VV et al (2021) The history of life at hydrothermal vents. Earth Sci Rev 217:103602

Gill FL, Little CTS (this volume) Chapter 16: Caribbean ancient seep communities. In: Kaim A, Cochran JK, Landman NH (eds) Ancient hydrocarbon seeps. Topics in geobiology. Springer, Cham

Gill FL, Harding IC, Little CTS et al (2005) Palaeogene and Neogene cold seep communities in Barbados, Trinidad and Venezuela: an overview. Palaeogeogr Palaeoclimatol Palaeoecol 227:191–209

Goedert JL, Benham SR (1999) A new species of *Depressigyra*? (Gastropoda: Peltospiridae) from cold-seep carbonates in Eocene and Oligocene rocks of western Washington. Veliger 24:112–116

Goedert JL, Kaler KL (1996) A new species of *Abyssochrysos* (Gastropoda: Loxonematoidea) from a middle Eocene cold-seep carbonate in the Humptulips Formation, western Washington. Veliger 39:65–70

Goedert JL, Squires RL (1990) Eocene deep-sea communities in localized limestones formed by subduction-related methane seeps, southwestern Washington. Geology 18:1182–1185

Golikov AN, Starobogatov YI (1987) Sistema otriada Cerithiiformes I ego polozhenie v podklasse Pectinibranchia. Vsesoiuznoe Soveshchanie po Izucheniiu Molliuskov 8:23–28

Gray JE (1840) Shells of molluscous animals. In: Synopsis of the contents of the British Museum, 42nd edn. Woodfall & Son, London, pp 86–89, 105–152

Gründel J (2001) Nerithimorpha und weitere Caenogastropoda (Gastropoda) aus dem Dogger Norddeutschlands und des nordwestlischen Polens. Berl Geowiss Abh E 36:45–99

Guzhov AV (2017) On new Jurassic Rissooidea and Zygopleuroidea convergently similar to them (Gastropoda: Pectinibranchia). Paleontol J 51:1375–1394

Habe T (1972) Notes on the genus *Parancistrolepis* Azuma (Buccinidae). Nautilus 86:51–52

Hasegawa K, Fujiwara Y, Okutani T et al (2019) A new gastropod associated with a deep-sea whale carcass from São Paulo Ridge, southwest Atlantic. Zootaxa 4568:347–356

Haszprunar G (1987) Anatomy and affinities of cocculinid limpets (Mollusca, Archeogastropoda). Zool Scr 16:305–324

Haszprunar G (1998) Superorder Cocculiniformia. In: Beesley PL, Ross GJB, Wells A (eds) Mollusca: the southern synthesis. Fauna of Australia, vol 5. CSIRO Publishing, Melbourne, pp 653–664

Hickman CS (1972) Review of the bathyal gastropod genus *Phanerolepida* (Homalopomatinae) and description of a new species from the Oregon Oligocene. Veliger 15:107–112

Hickman CS (1996) Phylogeny and patterns of evolutionary radiation in trochoidean gastropods. In: Taylor J (ed) Origin and evolutionary radiation of the Mollusca. Oxford University Press, Oxford

Hickman CS, McLean JH (1990) Systematic revision and suprageneric classification of trochacean gastropods. Nat Hist Mus Los Angeles Co Sci Ser 35:1–169
Hikida Y, Suzuki S, Togo Y et al (2003) An exceptionally well-preserved seep community from the Cretaceous Yezo forearc basin in Hokkaido, northern Japan. Paleontol Res 7:329–342
Hirayama K (1955) The Asagai Formation and its molluscan fossils in the Northern Region, Joban Coal-field, Fukushima Prefecture, Japan. Tokyo Kyoiku Daigaku Sci Rep Sec C 4:23–130
Houbrick RS (1979) Classification and systematic relationship of the Abyssochrysidae, a relict family of bathyal snails (Prosobranchia: Gastropoda). Smithson Contrib Zool 290:1–21
Hryniewicz K, Hagström J, Hammer Ø et al (2015) Late Jurassic–Early Cretaceous hydrocarbon seep boulders from Novaya Zemlya and their faunas. Palaeogeogr Palaeoclimatol Palaeoecol 436:231–244
Hryniewicz K, Amano K, Bitner MA et al (2019) A late Paleocene fauna from shallow-water chemosynthesis-based ecosystems, Spitsbergen, Svalbard. Acta Palaeontol Pol 64:101–141
Hryniewicz K, Miyajima Y, Amano K et al (2021) Formation, diagenesis and fauna of cold seep carbonates from the Miocene Taishu Group of Tsushima (Japan). Geol Mag 158:964–984
Hybertsen F, Kiel S (2018) A middle Eocene seep deposit with silicified fauna from the Humptulips Formation in western Washington State, USA. Acta Palaeontol Pol 63:751–768
Hynda VA (1986) Mielkaja bentosnaja fauna ordovika jugo-zapada Vostochno-Evropejskoj platformy. Naukova Dumka, Kiev
Ihering HV (1876) Versuch eines natürlichen Systemes der Mollusken. Jahrb Dtsch Malakozoolog Gesell 3:97–148
Jenkins RG, Kaim A, Hikida Y (2007a) Antiquity of the substrate choice among acmaeid limpets from the Late Cretaceous chemosynthesis-based communities. Acta Palaeontol Pol 52:369–373
Jenkins RG, Kaim A, Hikida Y et al (2007b) Methane-flux-dependent lateral faunal changes in a Late Cretaceous chemosymbiotic assemblage from the Nakagawa area of Hokkaido, Japan. Geobiology 5:127–139
Johnson SB, Warén A, Lee RW et al (2010) *Rubyspira*, new genus and two new species of bone-eating deep-sea snails with ancient habits. Biol Bull 219:166–177
Kaim A (2004) The evolution of conch ontogeny in Mesozoic open sea gastropods. Palaeontol Pol 62:3–183
Kaim A (2011) Non-actualistic wood-fall associations from Middle Jurassic of Poland. Lethaia 44:109–124
Kaim A, Conti MA (2010) A problematic zygopleuroid gastropod *Acanthostrophia* revisited. Zitteliana A 50:21–24
Kaim A, Kelly SRA (2009) Mass occurrence of hokkaidoconchid gastropods in the Upper Jurassic methane seep carbonate from Alexander Island, Antarctica. Antarct Sci 21:279–284
Kaim A, Beisel AL, Kurushin NI (2004) Mesozoic gastropods from Siberia and Timan (Russia). Part 1: Vetigastropoda and Caenogastropoda (exclusive of Neogastropoda). Pol Polar Res 24:241–266
Kaim A, Jenkins RG, Warén A (2008a) Provannid and provannid-like gastropods from the Late Cretaceous cold seeps of Hokkaido (Japan) and the fossil record of the Provannidae (Gastropoda: Abyssochrysoidea). Zool J Linnean Soc 154:421–436
Kaim A, Kobayashi Y, Echizenya H et al (2008b) Chemosynthesis-based associations on Cretaceous plesiosaurid carcasses. Acta Palaeontol Pol 53:97–104
Kaim A, Jenkins RG, Hikida Y (2009) Gastropods from Late Cretaceous hydrocarbon seep deposits in Omagari and Yasukawa, Nakagawa area, Hokkaido, Japan. Acta Palaeontol Pol 54:463–690
Kaim A, Tucholke BE, Warén A (2012) A new Late Pliocene large provannid gastropod associated with hydrothermal venting at Kane Megamullion Mid-Atlantic Ridge. J Syst Palaeontol 10:423–433
Kaim A, Skupien P, Jenkins RG (2013) A new Lower Cretaceous hydrocarbon seep locality from the Czech Carpathians and its fauna. Palaeogeogr Palaeoclimatol Palaeoecol 390:42–51
Kaim A, Jenkins RG, Tanabe K et al (2014) Mollusks from late Mesozoic seep deposits, chiefly in California. Zootaxa 3861:401–440

Kaim A, Jenkins RG, Parent H et al (2015) Early Jurassic seep from Argentina displays faunal composition of modern aspect. In: Abstract volume, Jahrestagung der Paläontologischen Gesellschaft, 14–16 September 2015, Schiffweiler-Reden, Germany

Kaim A, Jenkins RG, Hryniewicz K et al (2016) Early Mesozoic seeps and the advent of modern seep faunas. In: Abstract volume, 1st international workshop on ancient hydrocarbon seep and cognate communities, 13–17 June 2016, Warsaw, Poland

Kaim A, Hryniewicz K, Little CTS et al (2017) Gastropods from the Late Jurassic–Early Cretaceous seep deposits in Spitsbergen, Svalbard. Zootaxa 4329:351–374

Kaim A, Little CTS, Kennedy WJ et al (2021) Late Cretaceous hydrothermal vent communities from the Troodos Ophiolite, Cyprus: systematics and evolutionary significance. Pap Palaeontol 7:1927–1947

Kano Y (2008) Vetigastropod phylogeny and a new concept of Seguenzioidea: independent evolution of copulatory organs in the deep-sea habitats. Zool Scr 37:1–21

Kano Y, Chiba S, Kase T (2002) Major adaptive radiation in neritopsine gastropods estimated from 28S rRNA sequences and fossil records. Proc R Soc Lond B 269:2457–2465

Kano Y, Chikyu E, Warén A (2009) Morphological, ecological and molecular characterization of the enigmatic planispiral snail genus Adeuomphalus (Vetigastropoda: Seguenzioidea). J Molluscan Stud 75:397–418

Kase T, Ishikawa M (2003) Mystery of naticid predation history solved: evidence from a 'living fossil' species. Geology 31:403–406

Kiel S (2006) New records and species of mollusks from Tertiary cold-seep carbonates in Washington State, USA. J Paleontol 80:121–137

Kiel S (2008) An unusual new gastropod from an Eocene hydrocarbon seep in Washington State. J Paleontol 82:188–191

Kiel S (2010) The fossil record of vent and seep mollusks. In: Kiel S (ed) The vent and seep biota. Springer, Heidelberg, pp 255–277

Kiel S, Amano K (2010) Oligocene and Miocene vesicomyid bivalves from the Katalla district in southern Alaska, USA. Veliger 51:76–84

Kiel S, Amano K, Jenkins RG (2016) Predation scar frequencies in chemosymbiotic bivalves at an Oligocene seep deposit and their potential relation to inferred sulfide tolerances. Palaeogeogr Palaeoclimatol Palaeoecol 453:139–145

Kiel S, Campbell KA (2005) *Lithomphalus enderlini* gen. et sp. nov. from cold-seep carbonates in California – a Cretaceous neomphalid gastropod? Palaeogeogr Palaeoclimatol Palaeoecol 227:232–241

Kiel S, Goedert JL (2006) A wood-fall association from Late Eocene deep-water sediments of Washington State, USA. PALAIOS 21:548–556

Kiel S, Goedert JL (2007) Six new mollusk species associated with biogenic substrates in Cenozoic deep-water sediments in Washington State, USA. Acta Palaeontol Pol 52:41–52

Kiel S, Hansen BT (2015) Cenozoic methane-seep faunas of the Caribbean region. PLoS One 10(10):e0140788

Kiel S, Peckmann J (2007) Chemosymbiotic bivalves and stable carbon isotopes indicate hydrocarbon seepage at four unusual Cenozoic fossil localities. Lethaia 40:345–357

Kiel S, Peckmann J (2008) Paleoecology and evolutionary significance of an Early Cretaceous *Peregrinella*-dominated hydrocarbon-seep deposit on the Crimean Peninsula. PALAIOS 23:751–759

Kiel S, Campbell KA, Elder WP et al (2008) Jurassic and Cretaceous gastropods from hydrocarbon-seeps in forearc basin and accretionary prism settings, California. Acta Palaeontol Pol 53:679–703

Kiel S, Amano K, Hikida Y et al (2009) Wood-fall associations from Late Cretaceous deep-water sediments of Hokkaido, Japan. Lethaia 42:74–82

Kiel S, Campbell KA, Gaillard C (2010) New and little known mollusks from ancient chemosynthetic environments. Zootaxa 2390:26–48

Kiel S, Wiese F, Titus AL (2012) Shallow-water methane-seep faunas in the Cenomanian Western Interior Seaway: no evidence for onshore-offshore adaptations to deep-sea vents. Geology 40:839–842
Kiel S, Birgel D, Campbell KA et al (2013) Cretaceous methane-seep deposits from New Zealand and their fauna. Palaeogeogr Palaeoclimatol Palaeoecol 390:17–34
Kiel S, Krystyn L, Demirtaş F et al (2017) Late Triassic mollusk-dominated hydrocarbon-seep deposits from Turkey. Geology 45:751–754
Kiel S, Aguilar YM, Kase T (2020a) Mollusks from Pliocene and Pleistocene seep deposits in Leyte, Philippines. Acta Palaeontol Pol 65:589–627
Kiel S, Hybertsen F, Hyžný M et al (2020b) Mollusks and a crustacean from early Oligocene methane-seep deposits in the Talara Basin, northern Peru. Acta Palaeontol Pol 65:109–138
Killeen IJ, Oliver PG (2000) A new species of *Abyssochrysos* (Gastropoda: Loxonematoidea) from the Oman margin. J Molluscan Stud 66:95–98
Koenen AV (1885) Über eine Paleocäne Fauna von Kopenhagen. Abh Königl Ges Wiss Göttingen 32:1–128
Koken E (1896) Die Gastropoden der Trias um Hallstatt. Jahrb K-K Geol Reichsanst Wien 46:37–126
Kollmann HA (1982) Gastropoden-Faunen aus der höheren Unterkreide Nordwestdeutschlands. Geol Jahrb A 65:517–551
Kuroda T (1931) Fossil Mollusca. In: Homma F (ed) Geology of the central part of Shinano, part 4. Kokon Shoin, Tokyo, pp 1–90
Ladd HS (1977) Cenozoic fossil mollusks from eastern Pacific Islands: gastropods (Eratoidea through Harpidae). Geol Surv Prof Pap 533:1–84
Landman NH, Cochran JK, Larson NL et al (2012) Methane seeps as ammonite habitats in the U.S. Western Interior Seaway revealed by isotopic analyses of well-preserved shell material. Geology 40:507–510
Landman NH, Cochran JK, Brezina J et al (this volume) Chapter 14: methane seeps in the Late Cretaceous Western Interior Seaway. In: Kaim A, Cochran JK, Landman NH (eds) Ancient hydrocarbon seeps. Topics in geobiology. Springer, Cham
Lindberg DR (1986) Radular evolution in the Patellogastropoda. Am Malacol Bull 4:115
Lindberg DR (1998) Order Patellogastropoda. In: Beesley PL, Ross GJB, Wells A (eds) Mollusca: the southern synthesis. Fauna of Australia, vol 5. CSIRO Publishing, Melbourne, pp 639–652
Lindberg DR, Hedegaard C (1996) A deep water patellogastropod from Oligocene water-logged wood of Washington State, USA (Acmaeoidea: Pectinodonta). J Molluscan Stud 62:299–314
Linse K, Nye V, Copley JT et al (2019) On the systematics and ecology of two new species of Provanna (Gastropoda: Provannidae) from deep-sea hydrothermal vents in the Caribbean Sea and Southern Ocean. J Molluscan Stud 85:426–439
Little CTS (2002) The fossil record of hydrothermal vent communities. Cah Biol Mar 43:313–316
Little CTS, Danelian T, Herrington RJ et al (2004) Early Jurassic hydrothermal vent community from the Franciscan Complex, California. J Paleontol 78:542–559
Makiyama J (1926) Tertiary Fossils from North Kankyô-dô, Korea. Mem Coll Sci Kyoto Univ B 2:143–160
Marshall BA (1985) Recent and Tertiary deep-sea limpets of the genus *Pectinodonta* Dall (Mollusca: Gastropoda) from New Zealand and New South Wales. N Z J Zool 12:273–282
Marshall BA (1986) Recent and Tertiary Cocculinidae and Pseudococculinidae (Mollusca: Gastropoda) from New Zealand and New South Wales. N Z J Zool 12:505–546
McLean JH (1989) New slit-limpets (Scissurellacea and Fissurellacea) from hydrothermal vents: part 1, systematic descriptions and comparisons based on shell and radular characters. Nat Hist Mus Los Angeles Co Contrib Sci 407:1–29
McLean JH (1990) A new genus and species of neomphalid limpet from the Mariana vents with a review of current understanding of relationships among Neomphalacea and Peltospiracea. Nautilus 104:77–86

McLean JH (1992) Cocculiniform limpets (Cocculinidae and Pyropeltidae) living on whale bone in the deep sea off California. J Molluscan Stud 58:401–414
McLean JH, Haszprunar G (1987) Pyropeltidae, a new family of cocculiniform limpets from hydrothermal vents. Veliger 30:196–205
McLean JH, Quinn JF Jr (1987) *Cataegis*, a new genus of three new species from the continental slope (Trochidae: Cataeginae new subfamily). Nautilus 101:111–116
Meehan KC, Landman NH (2016) Faunal associations in cold-methane seep deposits from the Upper Cretaceous Pierre Shale, South Dakota. PALAIOS 31:291–301
Michelotti G (1847) Description des fossiles des terrains Miocènes de l'Italie septentrionale. Natuurkundige Verhandelingen van de Hollandsche Maatschappij der Wetenschappen te Haarlem 2 3(2):1–408
Miyajima Y, Nobuhara T, Koike H (2017) Taxonomic reexamination of three vesicomyid species (Bivalvia) from the middle Miocene Bessho Formation in Nagano Prefecture, central Japan, with notes on vesicomyid diversity. Nautilus 131:51–66
Miyajima Y, Watanabe Y, Jenkins RG et al (2018) Diffusive methane seepage in ancient deposits: examples from the Neogene Shin'etsu sedimentary basin, central Japan. J Sediment Res 88:449–466
MolluscaBase eds (2021a) MolluscaBase: *Putzeysia wiseri* (Calcara, 1842). http://marinespecies.org/aphia.php?p=taxdetails&id=141832. Accessed 20 Oct 2021
MolluscaBase eds (2021b) MolluscaBase: *Bathybembix macdonaldi* (Dall, 1890). http://www.marinespecies.org/aphia.php?p=taxdetails&id=512109. Accessed 20 Oct 2021
Moroni MA (1966) Malacofauna del 'Calcare a Lucine' di S. Sofia. Forlì Palaeontogr Ital 60:69–87
Nakano T, Ozawa T (2007) Worldwide phylogeography of limpets of the older Patellogastropoda: molecular, morphological and palaeontological evidence. J Molluscan Stud 73:79–99
Nobuhara T, Tanaka T (1993) Palaeoecology of *Akebiconcha kawamurai* (Bivalvia: Vesicomyidae) from the Pliocene Tamari Silt Formation in the Kakegawa area, central Japan. Palaeogeogr Palaeoclimatol Palaeoecol 102:27–40
Nobuhara T, Onda D, Sato T et al (2016) Mass occurrence of the enigmatic gastropod *Elmira* in the Late Cretaceous Sada Limestone seep deposit in southwestern Shikoku, Japan. Palaontol Z 90:701–722
Nützel A (1998) Über die Stammesgeschichte der Ptenoglossa (Gastropoda). Berl Geowiss Abh E 26:1–229
Okutani T (2001) Six new bathyal and shelf trochoidean species in Japan. Venus 60:121–127
Okutani T, Iwahori A (1992) Noteworthy gastropods collected from bathyal zone in Tosa Bay by the R/V Kotaka-Maru in 1987 and 1988. Venus 51:235–268
Okutani T, Ohta S (1988) A new gastropod mollusk associated with hydrothermal vents in the Mariana Back-arc Basin, western Pacific. Venus 47:1–10
Okutani T, Saito H, Hashimoto J (1989) A new neritacean limpet from a hydrothermal vent site near Ogasawara Islands, Japan. Venus 48:223–230
Okutani T, Tsuchida E, Fujikura K (1992) Five bathyal gastropods living within or near the *Calyptogena* community of the Hatsushima Islet, Sagami Bay. Venus 51:137–148
Olsson AA (1931) Contributions to the Tertiary paleontology of northern Peru: part 4, the Peruvian Oligocene. Bull Am Paleontol 17:97–264
Peckmann J, Gischler E, Oschmann W et al (2001) An early Carboniferous seep community and hydrocarbon-derived carbonates from the Harz Mountains, Germany. Geology 29:271–274
Pilsbry HA (1891–1892) Manual of conchology, structural and systematic, with illustrations of the species, ser. 1, vol. 13: Acmaeidae, Lepetidae, Patellidae, Titiscaniidae. Conchological Section, Academy of Natural Sciences, Philadelphia
Pilsbry HA (1895) Catalogue of the marine mollusks of Japan with descriptions of a new species and notes on others collected by Frederik Stearns. Stearns, Detroit
Ponder WF, Lindberg DR, Ponder JM (2020) Biology of the Mollusca. CRC Press, Boca Raton
Powell AWB (1951) Antarctic and Subantarctic Mollusca: Pelecypoda and Gastropoda. Discovery Rep 26:47–196

Rafinesque CS (1815) Analyse de nature, ou tableau de l'univers et des corps organismes. Jean Barravecchia, Palerme
Riedel F (2000) Ursprung und Evolution der 'höheren' Caenogastropoda. Berl Geowiss Abh E 32:1–240
Sacco F (1896) I molluschi dei terreni terziarii del Piemonte e della Liguria: parte XXI, Naricidae, Modulidae, Phasianellidae, Turbinidae, Delphinulidae, Cyclostrematidae, Tornidae. Carlo Clausen, Torino
Saether K, Little CTS, Campbell KA (2010) A new fossil provannid gastropod from Miocene hydrocarbon seep deposits, East Coast Basin, North Island, New Zealand. Acta Palaeontol Pol 55:507–517
Saether KP, Little CTS, Marshall BA et al (2012) Systematics and palaeoecology of a new fossil limpet (Patellogastropoda: Pectinodontidae) from Miocene hydrocarbon seep deposits, East Coast Basin, North Island, New Zealand with an overview of known fossil seep pectinodontids. Molluscan Res 32:1–15
Sasaki T, Okutani T, Fujikura K (2003) New taxa and new records of patelliform gastropods associated with chemoautosynthesis-based communities in Japanese waters (Mollusca: Gastropoda). Veliger 46:189–210
Sasaki T, Warén A, Kano Y et al (2010) Gastropods from Recent hot vents and cold seeps: systematics, diversity and life strategies. In: Kiel S (ed) The vent and seep biota. Springer, Heidelberg, pp 169–254
Sato K, Watanabe HK, Jenkins RG et al (2020) Phylogenetic constraint and phenotypic plasticity in the shell microstructure of vent and seep pectinodontid limpets. Mar Biol 167:79
Schander C, Rapp HT, Kongsrud JA et al (2010) The fauna of hydrothermal vents on the Mohn Ridge (North Atlantic). Mar Biol Res 6:155–171
Schepman MM (1909) The Prosobranchia of the Siboga Expedition, 2: Taenioglossa and Ptenoglossa. Siboga Exped 49:100–231
Schwartz H, Sample J, Weberling KD et al (2003) An ancient linked fluid migration system: cold-seep deposits and sandstone intrusions in the Panoche Hills California, USA. Geo-Mar Lett 23:340–350
Seguenza G (1876) Studii stratigrafici sulla formazione pliocenica dell'Italia Meridionale. Boll R Com Geol Ital 7:7–15
Shimazu N, Jenkins RG (2019) Early Cretaceous Utagoesawa seep community from Yubari City, Hokkaido, Japan. Abstract volume. 2nd international workshop on ancient hydrocarbon seep and cognate communities, 13–15 June 2019, Sapporo, Japan
Souza BHM, Passos FD, Shimabukuro M et al (2020) An integrative approach distinguishes three new species of Abyssochrysoidea (Mollusca: Caenogastropoda) associated with organic falls of the deep south-west Atlantic. Zool J Linnean Soc 191:748–771
Squires RL (1995) First fossil species of the chemosynthetic-community gastropod *Provanna*: localized cold-seep limestones in upper Eocene and Oligocene rocks, Washington. Veliger 38:30–36
Squires RL, Goedert JL (1991) New late Eocene mollusks from localized limestone deposits formed by subduction-related methane seeps, southwestern Washington. J Paleontol 65:412–416
Squires RL, Goedert JL (1996) A new species of *Thalassonerita*? (Gastropoda: Neritidae?) from a middle Eocene cold-seep carbonate in the Humptulips Formation, western Washington. Veliger 39:270–272
Stanton TW (1895) Contributions to the Cretaceous paleontology of the Pacific coast: the fauna of the Knoxville beds. US Geol Surv Bull 133:1–132
Szabó J (1983) Lower and Middle Jurassic gastropods from the Bakony Mountains (Hungary): part V, supplement to Archaeogastropoda; Caenogastropoda. Ann Hist Nat Mus Natl Hung 75:27–46
Takeda H (1953) The Poronai Formation (Oligocene Tertiary) of Hokkaido and South Sakhalin and its fossil fauna. Stud Coal Geol [Hokkaido Assoc Coal Mining Technologists] 3:1–103

Tanaka K (1959) Molluscan fossils from central Shinano, Nagano Prefecture, Japan: part 1, fossils from Akanuda Limestone. J Shinshu Univ, Fac Educ 8:115–133
Taylor JD, Morris NJ (1988) Relationship of neogastropods. Malacol Rev Suppl 4:167–179
Taylor JD, Morris N, Taylor C (1980) Food specialization and the evolution of predatory prosobranch gastropods. Palaeontology 23:375–409
Thiele J (1924) Revision des Systems der Trochacea. Mitt Zool Mus Berlin 11:47–74
Tiba R (1969) New species of the genus *Clinopegma*, *C. borealis* n. sp. (Buccinidae). Venus 28:135–136
Tomlin JRLB (1927) Reports on marine Mollusca in the collections of the South African Museum, II: families Abyssochrysidae, Oocorythidae, Haliotidae, Tonnidae. Ann S Afr Mus 25:77–83
Tullberg SA (1881) Ueber Versteinerungen aus den Aulacellen-Schichten Novaja-Semljas. Bihang Till Kunlige Svenska Vetenskap Akademie Handlingar 6:1–25
Van Winkle K (1919) Remarks on some new species from Trinidad. Bull Am Paleontol 8:19–33
Verrill AE (1884) Second catalogue of Mollusca recently added to the fauna of the New England coast and the adjacent part of the Atlantic, consisting mostly of deep-sea species, with notes on others previously recorded. Trans Connecticut Acad Arts Sci 6:139–194
Vonderbank K (1970) Geologie und Fauna der tertiären Ablagerungen Zentral-Spitsbergens. Nor Polarinst Skr 153:5–119
Warén A (1992) New and little known ‘skeneimorph’ gastropods from the Mediterranean Sea and the adjacent Atlantic Ocean. Boll Malacol 27:149–248
Warén A, Bouchet P (1989) New gastropods from East Pacific hydrothermal vents. Zool Scr 18:67–102
Warén A, Bouchet P (1993) New records, species, genera, and a new family of gastropods from hydrothermal vents and hydrocarbon seeps. Zool Scr 22:1–90
Warén A, Bouchet P (2001) Gastropoda and Monoplacophora from hydrothermal vents and seeps: new taxa and records. Veliger 44:116–231
Warén A, Bouchet P (2009) New gastropods from deep-sea hydrocarbon seeps off West Africa. Deep-Sea Res II 57:2326–2349
Warén A, Ponder WF (1991) New species, anatomy and systematic position of the hydrothermal vent and hydrocarbon seep gastropod family Provannidae fam. n. (Caenogastropoda). Zool Scr 20:27–56
Watson RB (1879) Mollusca of the H.M.S. ‘Challenger’ Expedition: IV, Trochidae continued viz. the genera *Basilissa* and *Trochus*, and the Turbinidae, viz. the genus *Turbo*. J Linn Soc 14:692–716
Weaver CE (1942) Paleontology of the marine Tertiary formations of Oregon and Washington. Wash Univ Pubs Geol 5:1–789
Wenz W (1938) Gastropoda, teil 2: Prosobranchia. In: Schindewolf OH (ed) Handbuch der Paläozoologie, Band 6. Gebrüder Borntraeger, Berlin
Yokoyama M (1890) Versteinerungen aus der japanischen Kreide. Palaeontographica 36:159–202

Chapter 12
Ammonites as Inhabitants of Ancient Hydrocarbon Seeps

Neil H. Landman, Neal L. Larson, J. Kirk Cochran, Jamie Brezina, and Matthew P. Garb

12.1 Introduction

Ammonites are present in fossil methane seep deposits but are not ubiquitous. They occur in deposits that span the Devonian to Cretaceous. New evidence at several of these sites reveals that the ammonites probably lived at these seeps all their lives and did not float in after death. Because of their post-hatching planktonic phase, ammonites were able to disperse widely and were probably attracted to seeps because of the availability of food, becoming an integral part of the seep ecosystem. Thus, the study of the species composition and distribution of ammonites at seeps provides new insights into the mode of life of these animals.

The presence of ammonites at seep deposits also provides insights into the nature of the seeps as well. Like modern nautilus, ammonites were constrained by depth limitations (Westermann 1996). Thus, the depth of the methane seeps where

N. H. Landman (✉)
Department of Invertebrate Paleontology, American Museum of Natural History, New York, NY, USA
e-mail: landman@amnh.org

N. L. Larson
Larson Paleontology Unlimited, Keystone, SD, USA

J. K. Cochran
School of Marine and Atmospheric Sciences, Stony Brook University, Stony Brook, NY, USA

Department of Invertebrate Paleontology, American Museum of Natural History, New York, NY, USA

J. Brezina
Department of Mining Engineering, South Dakota School of Mines and Technology, Rapid City, SD, USA

M. P. Garb
Department of Earth and Environmental Sciences, Brooklyn College, Brooklyn, NY, USA

A. Kaim et al. (eds.), *Ancient Hydrocarbon Seeps*, Topics in Geobiology 50,
https://doi.org/10.1007/978-3-031-05623-9_12

ammonites lived could not have exceeded the depth limits of the ammonites themselves. In addition, the physical and chemical properties at the sites could not have exceeded the tolerance limits of ammonites with respect to temperature, salinity, and concentrations of hydrogen sulfide and oxygen.

12.2 Ammonite Paleobiology

Ammonites belong to the class Cephalopoda, one of the main classes of the Mollusca. They are closely related to squids, cuttlefish, and octopus. Studies of comparative morphology reveal that they are phylogenetically more closely related to the Coleoidea than to the Nautiloidea (Jacobs and Landman 1993). Nevertheless, because ammonites retain an external shell, many aspects of their growth and mode of life can be investigated in analogy with modern nautilus.

Ammonites were exclusively marine and lived in the water column. Depending on the species and ontogenetic stage, they may have lived near the bottom (demersal or nektobenthic) or higher up in the water column. Although the exact temperature and salinity requirements of ammonites are unknown, modern cephalopods cannot tolerate salinities below approximately 20 psu nor temperatures above 35 °C (Vidal et al. 2016). Most coleoids prefer fully oxygenated water, and this is consistent with facies and faunal associations for many ammonites. However, studies of modern nautilus indicate that it is tolerant of low-oxygen conditions (Wells and Wells 1985).

The external shell of both nautilus and ammonites is divided into two parts, the body chamber that contained the soft fleshy parts of the animal and the phragmocone, which is subdivided into a series of buoyancy chambers (Fig. 12.1a, b). The

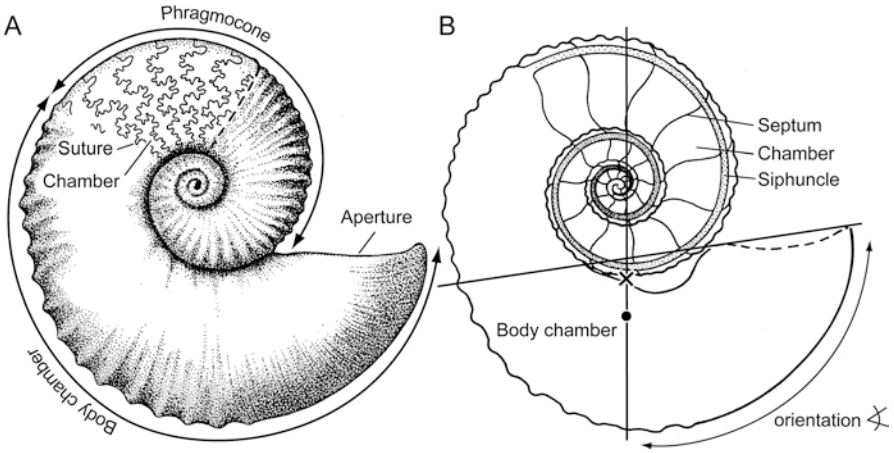

Fig. 12.1 Morphologic terms applied to ammonites, showing the external (**a**) and internal parts of the shell (**b**). The ammonite is oriented in its life position based on the centers of mass (•) and buoyancy (x)

chambers are separated by partitions called septa. The contact where the septum meets the inside surface of the outer shell wall is known as the suture.

During life, the shell functioned as a buoyancy apparatus that permitted the animal to maintain near neutral buoyancy as it grew. The mode of growth in nautilus has been well documented by Ward (1987). If we assume that ammonites followed the same mode of growth, a new chamber was secreted at the back of the body chamber as the animal grew at the aperture. The newly created chamber was initially filled with liquid, but as the animal grew larger, the liquid was removed through a thin tube called the siphuncle and replaced by a combination of gasses. The gasses in the newly formed chamber compensated for the additional weight of the soft tissue and shell as the animal grew. As a result, the animal would have maintained near neutral buoyancy in the water column, allowing it to swim and maneuver nearly weightlessly in the water column.

In nautilus, after the liquid is removed from the most recently formed chamber, the gas in the chamber attains a maximum pressure of 1 atm. Thus, the shell of nautilus, and by inference ammonites, is a pressure vessel that must withstand the compressive forces of the surrounding water. Nautilus is limited to a depth of 700 m, beyond which the shell implodes (Saunders and Ward 1987). Studies of the shape of the nautilus shell and septa, as well as the size and structure of the siphuncle, have yielded theoretical estimates in agreement with actual values (Hewitt and Westermann 1987). Similar studies on ammonites have also yielded depth estimates of the depth at which these animals probably lived (Hewitt 1996: Table 2), which are consistent with inferences based on the facies distributions and faunal associations of the ammonites. Thus, it is likely that ancyloceratids (e.g., *Baculites* and *Hoploscaphites*) lived at depths of less than 100 m whereas phylloceratids and lytoceratids (e.g., *Hypophylloceras* and *Anagaudryceras*, respectively) lived at depths of 200–300 m.

Ammonites, like other cephalopods, were probably capable of locomotion, although the exact propulsive mechanism is unknown (Cherns et al. 2021). In some ammonites, large muscle scars appear on the sides of the body chamber and have been interpreted as the scars of cephalic retractor muscles (Doguzhaeva and Mapes 2015). Many of these ammonites also exhibit a ventral sinus at the aperture, which may have accommodated the funnel or hyponome. Such ammonites could have used their retractor muscles to pull the body back into the shell while compressing the water in the mantle to produce a pulse-like jet, as described in nautilus by Chamberlain (1987). In ammonites with small dorsal and ventral muscle scars but no evidence of retractor muscle scars, two other propulsive mechanisms have been suggested. Some ammonites may have employed the same mechanism used by nautilus at low swimming speeds or at rest. The animal uses the mantle musculature to produce a respiratory stream that serves to aerate the gills, which generates a weak jet (Wells and Wells 1985). Jacobs and Landman (1993) have also suggested that some ammonites may have used a coleoid-like contractible mantle during swimming. Whatever the particular mechanism, it is unlikely that ammonites were capable of swimming as fast as squid or fish, simply because an external shell produces large drag forces. Nevertheless, some streamlined ammonites such as *Placenticeras*

were better adapted to reduce drag and the acceleration forces that resist movement, especially at larger sizes and higher velocities (Jacobs and Chamberlain 1996; Naglik et al. 2015).

The orientation of the ammonite in the water column is a clue to the mode of life of the ammonite (Westermann 1996; Ritterbush and Bottjer 2012). For example, if the aperture faces downward, the animal can access food on the seafloor. The orientation of the aperture can be estimated by determining the centers of mass and buoyancy (Fig. 12.1b). This can be accomplished either experimentally or using computer models combined with CT scanning (Hoffmann et al. 2015). The results are expressed as the orientation angle of the aperture with respect to the vertical (Saunders and Shapiro 1986). In both ammonites and fossil nautilids, such methods involve a number of simplifying assumptions (Landman et al. 2010). For example, it is assumed that the phragmocone was entirely filled with air without any liquid present. If the last few chambers were filled with liquid, the angle of orientation increases (pointing upward). In addition, it is assumed that the soft body was uniformly distributed throughout the body chamber. If the soft body protruded beyond the aperture, the angle of orientation decreased (pointing downward). In adults of many heteromorph ammonites such as *Hoploscaphites* and *Didymoceras*, for example, the orientation of the aperture is 90 °, that is, the aperture faces upward (Landman et al. 2012a; Peterman et al. 2020). In contrast, in modern nautilus, the orientation of the aperture (at resting position) is approximately 30 °, that is, the aperture faces downward (Saunders and Shapiro 1986).

The diet of ammonites is difficult to reconstruct but is based on studies of the morphology of the buccal apparatus (Fig. 12.2) and gut contents in exceptionally well-preserved fossils. The buccal apparatus consists of a pair of upper and lower jaws and a tongue-like ribbon with tiny teeth (the radula) that lies between them. Tanabe et al. (2015) classified ammonite jaws into five morphotypes, each of which can be interpreted in terms of its function. For example, the rhynchaptychus-type jaw, which occurs in phylloceratids and lytoceratids, is equipped with calcareous tips on the apical end. Similar jaws are present in modern nautilus and may have been adapted to scavenging lobster carapaces on the seafloor. In contrast, the aptychus-type jaw, which occurs in ancyloceratids, features a lower jaw that ends in a blunt margin and may have been better adapted for passively feeding on small organisms in the water column, such as zooplankton (Kruta et al. 2011; Tanabe et al. 2015). This jaw is characteristic of the group of ammonites called the Aptychophora, which includes the Ancyloceratina and most of the Ammonitina (Engeser and Keupp 2002).

12.3 Methane Seep Deposits

The discussion below is organized geographically and alphabetically by country and only focuses on methane seep deposits that contain ammonites. Many of the descriptions in the literature only treat ammonites in passing. The list is not

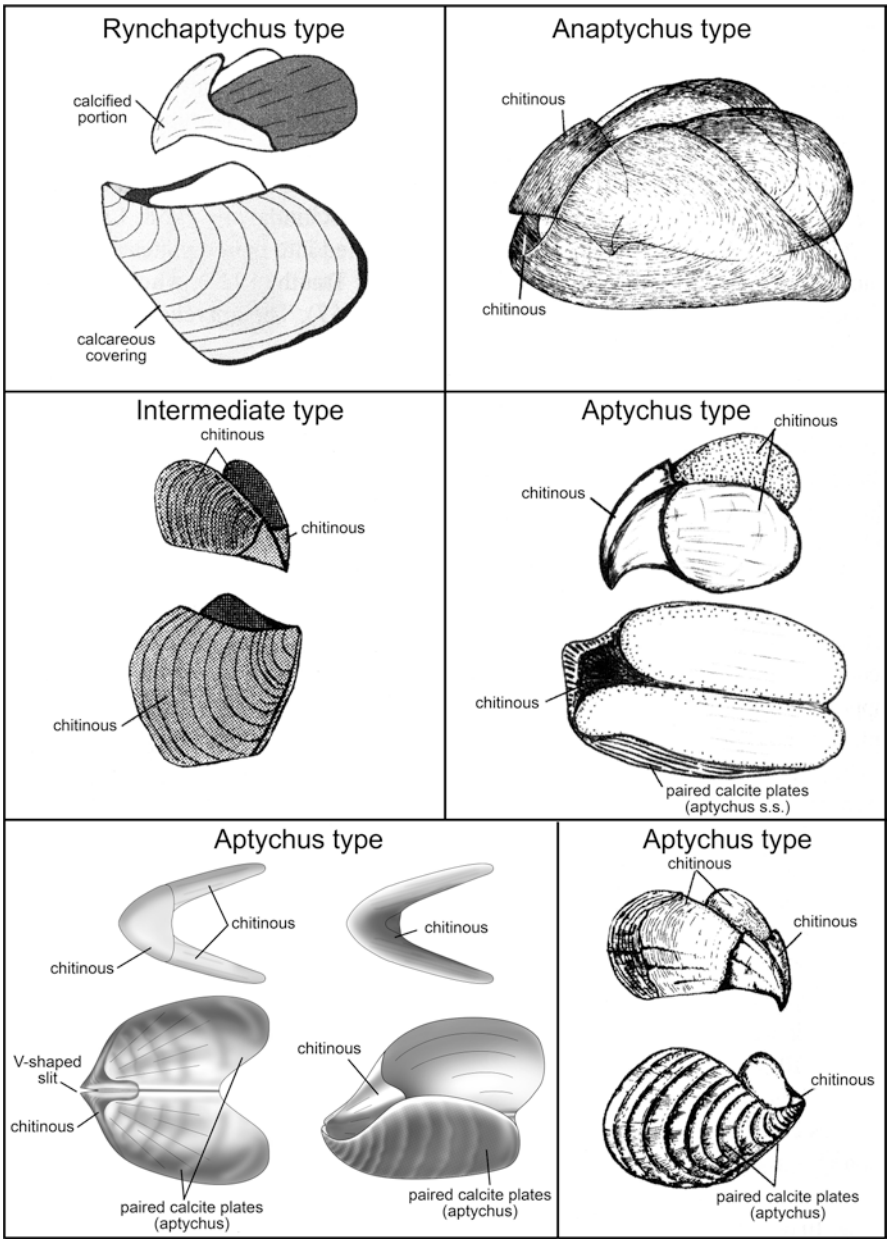

Fig. 12.2 Variety of jaws in Mesozoic ammonites. (Modified from Tanabe et al. 2015)

exhaustive but attempts to cover the best-known Paleozoic and Mesozoic seep deposits throughout the world. The list of ammonite species in seep deposits is presented in Appendix Table 12.1 with an estimated depth at which the ammonites

lived (<100 m, 100–200 m, and 200–300 m), mostly based on the conclusions in Hewitt (1996) and Westermann (1996).

12.3.1 Antarctica

Little et al. (2015) reported the presence of ammonites in methane seep deposits in Antarctica (Fig. 12.3f, g). These deposits occur in the lower Maastrichtian Snow Hill Formation on Snow Hill Island and in the lower-upper Maastrichtian Lopez de Bertodano Formation on Seymour Island (Witts and Little this volume). The fauna at the seeps is not very diverse and is dominated by an infaunal bivalve. In addition, the seep fauna is not restricted to the seeps (non-seep obligates) but also occurs in the surrounding shelf area.

In the Snow Hill Island Formation on Snow Hill Island, seep deposits consist of large cement-rich carbonate bodies filled with the bivalve *Thyasira townsendi*, many in life position, with a concentration of more than 120/m^2 forming a coquina. They are associated with numerous small ammonites and ammonite fragments, many of which appear to be juveniles (Fig. 12.3f, g). The ammonites belong to the genera *Gunnarites* and *Anagaudryceras*. Little et al. (2015) suggested that these ammonites "could have been current swept into the '*Thyasira*' layers" and doubted that the ammonites lived at the site. While we agree that the ammonite deposit unquestionably represents a hydrodynamic accumulation (after all, ammonites lived in the water column, not in the sediment), the abundance of specimens, the presence of two species, and the fact that many of the specimens are juveniles suggest that the source of the ammonites was local, that is, from the seep. This conclusion is reinforced by the presence of additional ammonites including *Jacobites anderssoni* and *Gunnarites bhavaniformis* associated with *T. townsendi* in the interbeds between the cemented layers. Higher up in the section in the Lopez de Bertodano Formation on Seymour Island, similar carbonate bodies filled with *T. townsendi* are associated with several specimens of *Maorites seymouriensis*. Nearby sites at the same stratigraphic horizon have yielded additional ammonite species.

The seep deposits in the Lopez de Bertodano Formation on Seymour Island also contain concentrations of micrite-cemented carbonate burrow systems. The matrix of these concretions exhibits very low values of $\delta^{13}C$ ranging from −40% to −50%. Such values are indicative of C derived from methane, which is enriched in ^{12}C. Similar burrow-like systems have been observed in both ancient and modern seep deposits (Campbell 2006). Little et al. (2015) did not report any associated ammonites. However, Ivany and Artruc (2016) analyzed the carbon isotopic composition of the outer shell wall of a specimen of *Diplomoceras maximum* from this formation. They observed $\delta^{13}C$ values of as low as −30% and suggested that this ammonite was probably living in association with methane seeps. Furthermore, Tobin and Ward (2015) observed overall offsets of $\delta^{13}C$ between ammonites and

benthic mollusks in this formation. They suggested that this difference may reflect the incorporation of metabolic CO_2 in the secretion of the ammonite shells or possibly that the ammonites lived in close proximity to methane seeps.

The ammonites associated with the Antarctic seep deposits are mostly lytoceratids, phylloceratids, and desmoceratids. These groups prefer relatively deep water of 100–200 m. This depth is consistent with inferences about the environment of deposition by Little et al. (2015). *Diplomoceras maximum*, an ancyloceratid, is unrestricted in its depth preferences, ranging from relatively shallow to relatively deep.

12.3.2 Argentina

Kaim et al. (2016) reported a seep deposit (called "La Elina") from the Neuquén-Mendoza Basin, Patagonia, west-central Argentina. The deposit occurs in the middle Toarcian (Lower Jurassic) Los Molles Formation and crops out over an area of approximately 2000 m^2. It is dominated by worm tubes and mollusks, most of which are gastropods and bivalves. Four species of ammonites are also present.

H. Parent (pers. comm. 2017) documented the abundance and size of the ammonites in the seep deposit and in the surrounding shale. *Calliphylloceras* sp. is abundant in the seep deposit and consists of juveniles (≈20 mm diameter) but is absent in the surrounding shale. *Phylloceras* sp. is rare in the seep deposit and also consists of juveniles (≈20 mm diameter); it is rare in the surrounding shale and occurs as fragmentary adults (≤400 mm diameter). *Hildaitoides retrocostatus* is abundant in the seep deposit and in the surrounding shale and consists of both juveniles and adults at both sites. *Phymatoceras* sp. is rare in the seep deposit and consists of fragments of adults; it is abundant in the surrounding shale where it also consists of fragments of adults. These ammonites indicate a relatively deep-water environment 100–200 m deep.

12.3.3 Canadian Arctic

Beauchamp and Savard (1992) and Williscroft et al. (2017) described cold seep deposits in the Canadian Arctic that are associated with ammonites. The seep deposits occur on Prince Patrick and Ellef Ringnes Islands in the Lower Cretaceous (Aptian-Albian) Christopher Formation. This formation consists of shales and siltstones that were deposited in relatively deep water (<400 m) on the outer shelf to upper slope of the Sverdrup Basin and adjoining Eglinton Graben. The seep deposits appear as resistant carbonate mounds, beds, and crusts.

The fossil assemblage is dominated by bivalves followed by tube worms, gastropods, ammonites, scaphopods, and brachiopods. Fossils are scarce or absent in the surrounding shale. Two ammonite species were identified by Beauchamp and Savard (1992): *Arcthoplites* sp. and *Callizoniceras* (*Colvillia*) ex. aff. *crassicostata*. Williscroft et al. (2017) documented five additional ammonite species in their subsequent study of Ellef Ringnes Island: *Arcthroplites* (?) cf. *belli*, *Cleoniceras* sp., *Beudanticeras* sp., *Puzosia* aff. *sigmoidalis*, and *Freboldiceras* aff. *irenense*.

12.3.4 England

A cold methane seep-ammonite association has been reported from the Sinemurian (Lower Jurassic) of England (Allison et al. 2008). The seep deposits occur in the rhythmically bedded limestone-marl-shale succession of the Blue Lias Formation. The deposits consist of conical mounds composed of micritic limestone as much 4 m in diameter and 1.5 m in height. One of the mounds contains foraminifera, crinoid ossicles, rare bivalves, and abundant ammonites. The ammonites, although not identified, are small (<1 cm in diameter), but complete.

12.3.5 France

One of the most ammonite-rich seep deposits occurs near Beauvoisin, Southeastern France (Rolin et al. 1990). The deposits occur at several horizons in lower-middle Oxfordian (Jurassic) black marls of the Terres Noires Formation. The deposits consist of massive micrite-cemented carbonate masses 1–15 m high and 1–20 m wide forming lenses or columns interbedded with calcareous shales. They are bordered by small concretions that rapidly disappear toward the margins. The carbonate masses and concretions are very fossiliferous compared to the much less fossiliferous black shales.

The carbonate masses are dominated by large infaunal lucinid bivalves, the largest of which is 18 cm long (bivalves comprise up to 30% of the rock). The bivalves are articulated, but not in life position. The deposits also contain a rich fauna of ammonites, most of which occur in the small irregular concretions on the margins of the masses (Fig. 12.3e, h, i). The ammonites include perispinctids and phylloceratids, including numerous *Sowerbyceras*, followed by oppeliids, cardioceratids, and pachyceratids. In contrast, haploceratids, lytoceratids, and oecoptychiids are rare. Bourseau (1977) noted a difference in the preservation of ammonites based on their size, which he ascribed to a taphonomic bias. Small specimens and microconchs with peristomal modifications are well preserved whereas larger specimens and macroconchs are incomplete. He noted that the fauna includes a large number

of juveniles (approximately 30% of the individuals), a fact that was also noted by Landman et al. (2019). The deposits contain abundant aptychi (parts of the jaws of ammonites) and rhyncolites (parts of the jaws of nautilids). In addition, two genera of belemnites are present: *Hibolites* and *Duvalia*.

The fauna in the seeps is much richer than that in the surrounding shale. Rolin et al. (1990) did a comparative study of the fauna in the seeps and at nearby stratigraphically equivalent non-seep sites. Taking into account taphonomic differences (preservation in cemented carbonate concretions versus preservation in black shales), they noted that the fauna at the seeps is much more abundant with respect to bivalves, gastropods, ammonites, crustaceans, echinoderms, and fish. They concluded that all these animals were living at the seeps. Some of them such as the bivalves were restricted to the seeps, whereas the ammonites may have been "electifs" opting to remain at the seeps feasting on the abundant food source but equally at home elsewhere. Based on the abundance of ammonite juveniles, Bourseau (1977) also speculated that the ammonites may have preferentially laid their eggs at these sites.

Rolin et al. (1990) referred to the environment as bathyal or mesobathyal. The ammonites are dominated by phylloceratids and perispinctids (approximately 30% of the fauna). This assemblage suggests relatively deep water (80–150 m deep, according to one estimate cited in Bourseau (1977)). Evidently, these seeps occurred below the photic zone but served as a focus for ammonites and other fauna.

12.3.6 Greenland

Kelly et al. (2000) described limestone mounds (the Kuhnpasset Beds) in the Wollaston Foreland, Northeast Greenland, which contain ammonites. The mounds occur in upper Barremian (Lower Cretaceous) mudstones and are subcircular to subovoid in plan view and 1–3 m in diameter and up to 1.8 m in height. They are dominated by large lucinid and modiomorphid bivalves. In contrast, in the surrounding mudstone, bivalves are uncommon and consist of small nuculaceans and arcaceans, with larger inoceramids.

The mounds also contain several species of ammonites including lytoceratids, *Sanmartinoceras*, *Audouliceras*, and *Epicheloniceras*. In addition to the ammonites, the nautilid *Cymatoceras* is also present. Kelly et al. (2000) stated that "these cephalopods may represent active predators and scavengers, presumably attracted to the rich fauna of the mounds."

12.3.7 Japan

Hikida et al. (2003) described a methane seep deposit from Omagari in the Nakagawa area, Hokkaido, Northern Japan, which contains ammonites. The deposit occurs in the Campanian (Upper Cretaceous) Omagari Formation and consists of an ellipsoidal calcareous mudstone 6 × 10 m in diameter and 5 m in thickness. It comprises two facies, a lower breccia facies and an upper worm tube boundstone facies. Jenkins et al. (2007) described additional deposits in the same area, which are better exposed. The environment of deposition is interpreted as "the interface between a continental-shelf margin and a continental slope" (Jenkins et al. 2007).

According to Hikida et al. (2003), the breccia facies contains abundant bivalves, gastropods, worm tubes, brachiopods, foraminifera, and a few ammonites (*Gaudryceras tenuiliratum*). All of the ammonite specimens are broken, and many of them are missing the body chamber. The same ammonite species was reported by Jenkins et al. (2007: Table 3) from their nearby site. In fact, this species is a common inhabitant in deeper-water environments (Westermann 1996).

12.3.8 Morocco

Many seep deposits associated with ammonites occur in Morocco. Some of the most spectacular are Devonian in age and are known as Kess Kess, which refers to the resemblance between the deposits and the dishes used to cook the famous Moroccan couscous (Belka 1998). The deposits appear as giant carbonate mud mounds that are conical to pinnacle in shape and up to 50 m in height, with circular to subcircular bases more than 100 m in diameter (Aitken et al. 2002; Cavalazzi et al. 2007; Berkowski and Klug 2011; Jakubowicz et al. this volume). The mounds are located on the Hamar Laghdad elevation 18 km east-southeast of Erfoud in the Anti-Atlas Mountains. Most of the mounds are Emsian (Early Devonian) in age, but the Hollard Mound in the eastern part of the elevation is Eifelian (Middle Devonian) in age (Peckmann et al. 1999, 2005).

The mounds have been interpreted as the sites of hydrocarbon seepage although the source of the methane is unclear and may have been thermogenic flowing along faults. The mounds formed on the continental shelf in relatively shallow water below wave base (Belka and Berkowski 2005; Cavalazzi et al. 2007). The mounds are composed of skeletal wackestones and mudstones. The fauna in the mounds is rich in invertebrates especially corals, arthropods, and crinoids and also includes ammonoids and orthoconic nautiloids. Klug (2002) noted *Agoniatites fecundus* in the uppermost layers of some of the mud mounds. However, the distribution and abundance of ammonoid species in the mud mounds and in the surrounding sediments have not yet been worked out in detail.

Smrzka et al. (2017) described a carbonate deposit in lower Turonian (Upper Cretaceous) black shales from the Amma Fatma Plage, southwest of Essaouira. The

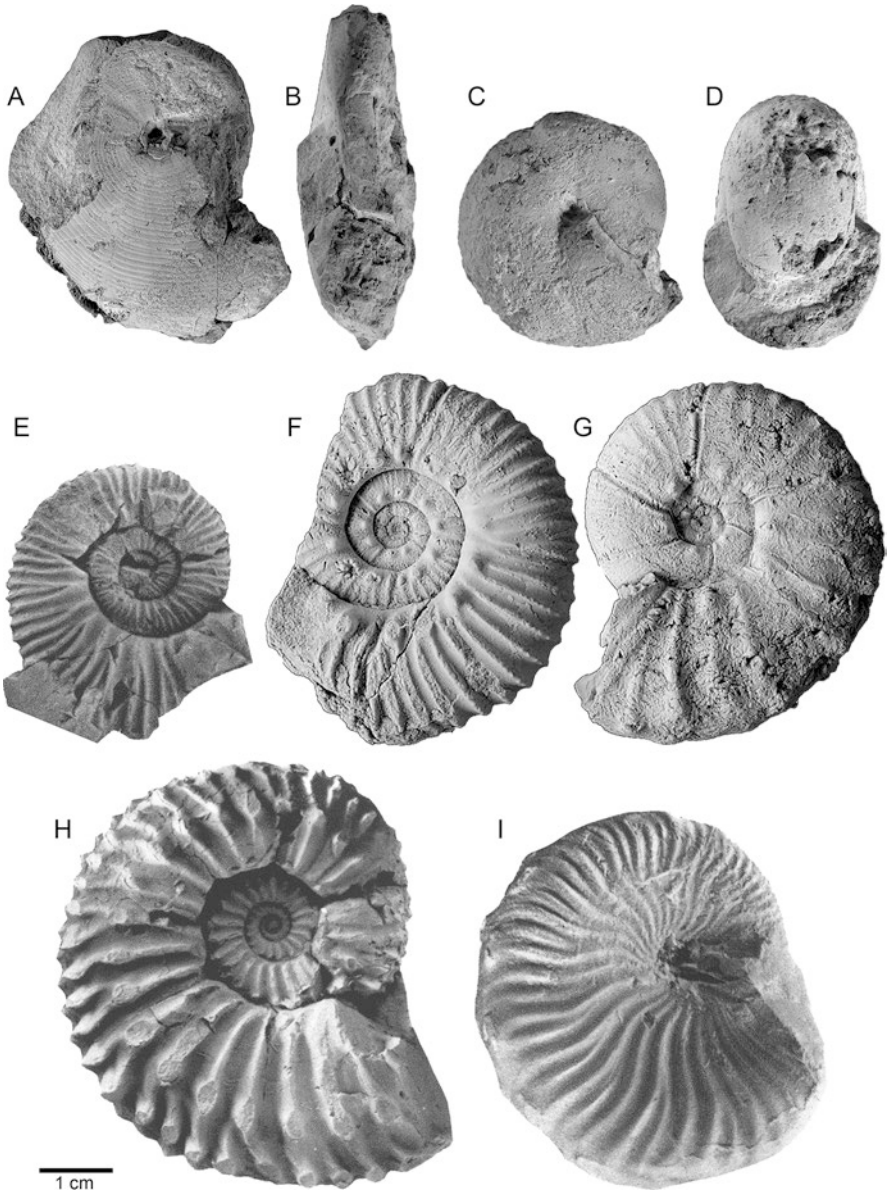

Fig. 12.3 Ammonites associated with methane seep deposits. (**a**, **b**) *Sagenites* sp., Norian (Upper Triassic), Oregon. (**c**, **d**) *Arcestes* sp., Norian (Upper Triassic), Oregon. (**e**) *Peltoceras* (*Parawedekindia*) sp. gr. *arduennense*, Oxfordian (Upper Jurassic), France (from Bourseau 1977). (**f**) *Gunnarites* sp., Maastrichtian (Upper Cretaceous), Antarctica (from Little et al. 2015). (**g**) *Jacobites anderssoni*, Maastrichtian (Upper Cretaceous), Antarctica (from Little et al. 2015). (**h**) *Cardioceras* (*C.*). sp. A, Oxfordian (Upper Jurassic), France (from Bourseau 1977). (**i**) *Taramelliceras* (*T.*) *obumbrans*, Oxfordian (Upper Jurassic), France (from Bourseau 1977). All figures are X 1

seep deposit formed in the Tarfaya Basin in relatively shallow water. It contains a low-diversity molluscan fauna consisting of bivalves, gastropods, and ammonites, but none of them represent seep-obligate species. The ammonites include juveniles and adults of *Benueites* sp. and *B*. cf. *benueensis*.

12.3.9 New Zealand

Kiel et al. (2012b) described methane seep deposits from New Zealand that contain ammonites. The deposits occur at Port Awanui on the Raukumara Peninsula, eastern North Island, New Zealand, and outcrop as reworked boulders along the shore. They are composed of calcareous mudstone and date from the late Albian-mid Cenomanian.

The fauna is dominated by lucinid and modiomorphid bivalves. Kiel et al. (2012b: Fig. 4) illustrated four ammonite specimens that occur in the deposits: *Scaphites equalis coverhamensis*, Kossmaticeratidae gen. et sp. indet., *Neograhamites* cf. *transitorius*, and a smooth, undescribed species. Based on the degree of endemism of the bivalves and gastropods, Kiel et al. (2012b) estimated that the environment of deposition was relatively deep on the outer shelf to upper slope. However, the presence of a species of *Scaphites* suggests a shallower depth of 100–200 m (Hewitt 1996).

12.3.10 Novaya Zemlya

Ammonites have been reported from seep deposits from the Arctic island of Novaya Zemlya (Hryniewicz et al. 2015). The deposits occur as isolated carbonate boulders that range from Late Jurassic to Early Cretaceous in age and are similar in age to the deposits in Svalbard (see below). The fauna is dominated by mollusks with fewer numbers of echinoderms, brachiopods, foraminifera, serpulids, and ostracods. In general, the fauna is not restricted to the seeps and resembles that of the surrounding non-seep shelf environments.

Ammonites occur in two kinds of boulders. They occur in calcareous sandstone boulders that contain 11 macro-invertebrate species, 9 of which are mollusks. The ammonites are mostly uncrushed with original shell structure including nacre. The most numerous specimens in these concretions are *Amoeboceras* sp., which occur as both mature and juvenile specimens. They are late Oxfordian to early Kimmeridgian in age. Because the venter is generally incomplete, they cannot be identified to species level. They are perisphinctids and according to Westermann (1996) probably lived at depths of 100–200 m.

Black limestone boulders contain 13 macro-invertebrate species that are well preserved. They include two specimens of *Craspedites okensis* of late Volgian (=

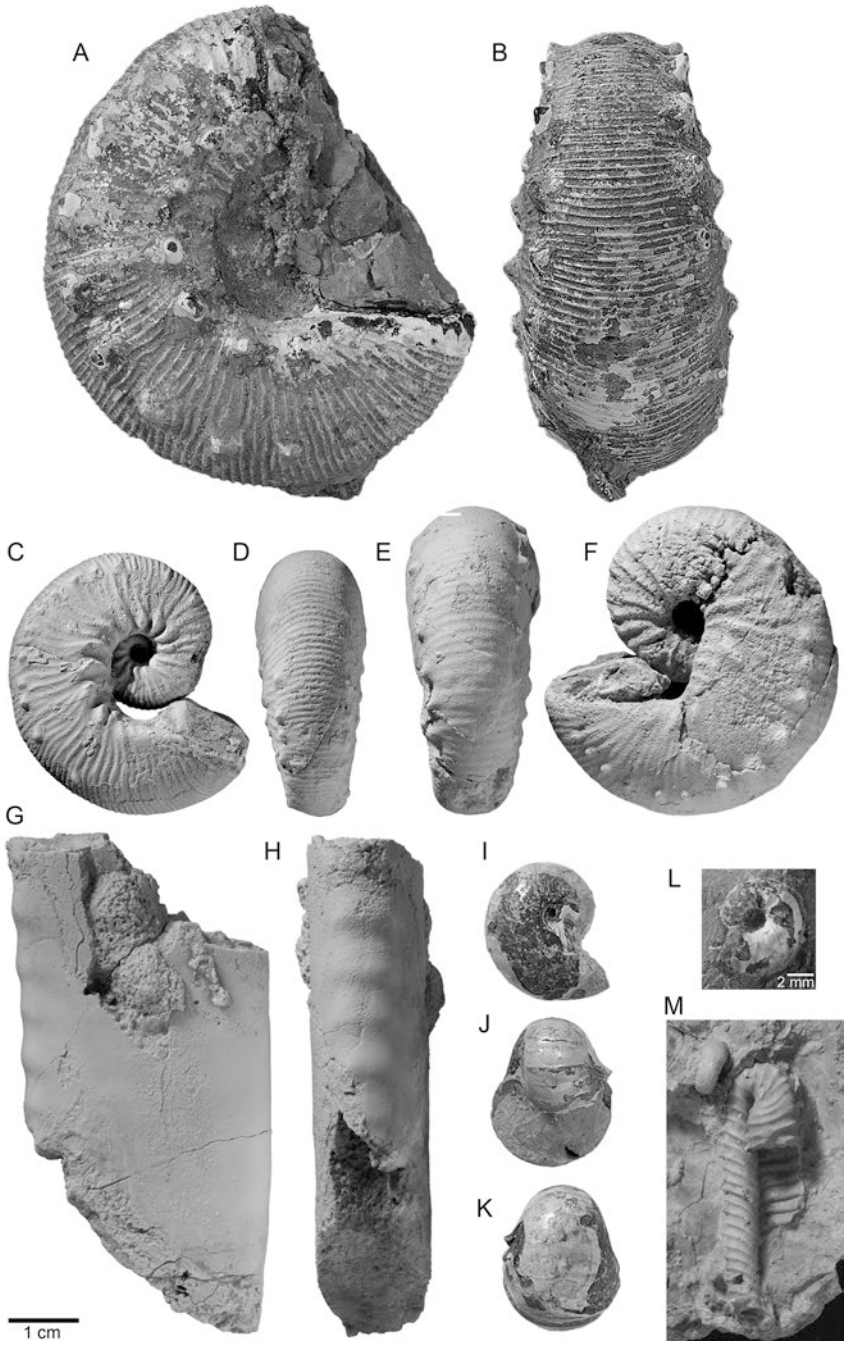

Fig. 12.4 Ammonites and nautilids associated with methane seep deposits, Upper Cretaceous (Campanian) Pierre Shale, South Dakota and Wyoming. (**a**) *Hoploscaphites nodosus*, microconch, AMNH 90781. (**c**, **d**) *Hoploscaphites gilberti*, microconch, USNM 547324. (**e**, **f**) *Hoploscaphites gilberti*, macroconch, USNM 83717. (**g**, **h**) *Baculites corrugatus*, AMNH 58544. (**i–k**) *Eutrephoceras dekayi*, AMNH 64529. (**l**) Juvenile of *Hoploscaphites*, AMNH 66244. (**m**) *Solenoceras bearpawense*, AMNH 108454. All figures are x 1 except (**l**). Abbreviations: *AMNH* American Museum of Natural History, *USNM* United States National Museum

late Tithonian) age. This is a stephanoceratid and, according to Hewitt (1996), would have lived at a depth of 100–200 m (Appendix Table 12.1).

12.3.11 Oregon, USA

Peckmann et al. (2011) described a seep deposit from the Norian (Upper Triassic) of Grant County, eastern Oregon. The deposit consists of two limestone bodies in the Rail Cabin Member of the Vesper Formation. The dominant fossil is the rhynchonellide brachiopod *Halorella*. Other fossils are rare, but two ammonites have since been discovered at the site (A. Kaim, pers. comm., 2016) and are tentatively identified as *Sagenites* sp. and *Arcestes* sp. (Fig. 12.3a–d). It is likely that the same ammonites occur in other parts of the Rail Cabin Member, as documented in Taylor and Guex (2002).

12.3.12 Spitsbergen (Svalbard)

Ammonites have been reported from seep deposits ("carbonate bodies") as much as 5 m in diameter in the uppermost Jurassic-lowermost Cretaceous of Spitsbergen (Hammer et al. 2011; Wierzbowski et al. 2011). The seep deposits occur in the Slottsmøya Member of the Agardhfjellet Formation in the Saaenfjordenniana area, which was deposited in a shallow epicontinental sea. The ammonites co-occur with abundant bivalves, gastropods, brachiopods, worm tubes, and a few belemnoids. None of these species is restricted to the seeps, that is, they are non-seep obligate but rather background fauna (Hryniewicz et al. 2014). The fact that obligate taxa are rare or absent appears to be a common feature of shallow-water vent and seep deposits (Dando, 2010).

A total of 153 ammonite specimens and 1 aptychus are present in 11 "carbonate bodies." The ammonites consist of ten species belonging to six genera of the Ammonitina (*Craspedites*, *Kachpurites*, *Hectoroceras*, *Borealites*, *Surites*, and *Tollia*) and range in age from the late Volgian to latest Ryazanian. These are all perisphinctids and, according to Westermann (1996), would have probably lived at depths of approximately 100 m. All of the species are known from other regions outside of the seeps, although fragmentary specimens cannot be compared with other material.

12.3.13 Turkey

Kiel et al. (2017) reported methane seep deposits from the Upper Triassic (upper Carnian-lower Norian) of Turkey. The sites are located in the Kasımlar Basin in the Anamas Akseki autochthon in the Taurus Mountains. According to the authors,

"this basin is interpreted as a small ocean basin separating large carbonate platforms to the east and west, interspersed with several rifted continental fragments capped by Mesozoic carbonate platforms." The seep deposits contain fragments of the ammonoid *Arcestes* sp.; it is unclear if they were living at the site.

12.3.14 Western Interior, USA

Ammonites are common in methane seep deposits in the US Western Interior (Colorado, Kansas, South Dakota, Montana, Wyoming, and Nebraska) (see Landman et al. this volume). Such deposits were first described by Gilbert and Gulliver (1895) along the Front Range of the Rocky Mountains in Colorado and were called "Tepee buttes." These are geomorphic features that represent erosional remnants of the seep deposits. They appear as conical hills or mounds, usually in clusters, and are composed of limestone, up to 60 m in diameter and 10 m in height. They occur in the Upper Cretaceous Pierre Shale and Bearpaw Shale from central Montana to south-central Colorado and from the Front Range of the Rocky Mountains to western Kansas (Kauffman et al. 1996: Bishop and Williams 2000; Shapiro and Fricke 2002; Metz 2010; Larson et al. 2014; Ryan et al. 2020; Landman et al. this volume). They range in age from the middle Campanian to the early Maastrichtian. Kiel et al. (2012a) have also reported similar deposits from the upper Cenomanian Tropic Shale of Utah.

The seep deposits from the US Western Interior contain a diverse assemblage of organisms including ammonites, nautilids, bivalves, notably inoceramids, and aggregations of chemosymbiotic-harboring lucinids, gastropods, scaphopods, crinoids, asteroids, ophiuroids, crabs, echinoids, sponges, bryozoans, corals, tube worms, dinoflagellates, radiolaria, foraminifera, fish, and reptiles (Bishop and Williams 2000; Landman et al. 2012b; Larson et al. 2014; Meehan and Landman 2016; Hunter et al. 2016). A total of 30 molluscan species were reported at single sites from Campanian seep deposits in Colorado (Howe 1987). The diversity of organisms is higher at seeps with extensive carbonate deposits opposed to those without them, presumably because such deposits provided additional habitats for organisms that required hard substrates for attachment (Meehan and Landman 2016). In contrast, the shale surrounding the seep deposits is usually more depauperate and may have been characterized by more dysoxic water conditions.

Ammonites have been reported in the seep deposits of the Pierre Shale ranging from the top of the middle Campanian to the lower part of the lower Maastrichtian (Figs. 12.4 and 12.5). They span the *Baculites scotti/Didymoceras nebrascense* Zones, *D. stevensoni* Zone, *Exiteloceras jennyi* Zone, *D. cheyennense* Zone, *B. compressus/B. cuneatus* Zones, *B. reesidei* Zone, *B. jenseni* Zone, and *B. baculus* Zones (see Cobban et al. (2006) for a zonal chart of the area). Five to eight ammonite species occur in each of these zones and represent the genera *Baculites*, *Didymoceras*, *Exiteloceras*, *Hoploscaphites*, *Menuites*, *Nostoceras*, *Pachydiscus*, *Placenticeras*, *Solenoceras*, and *Spiroxybeloceras*. With one possible exception

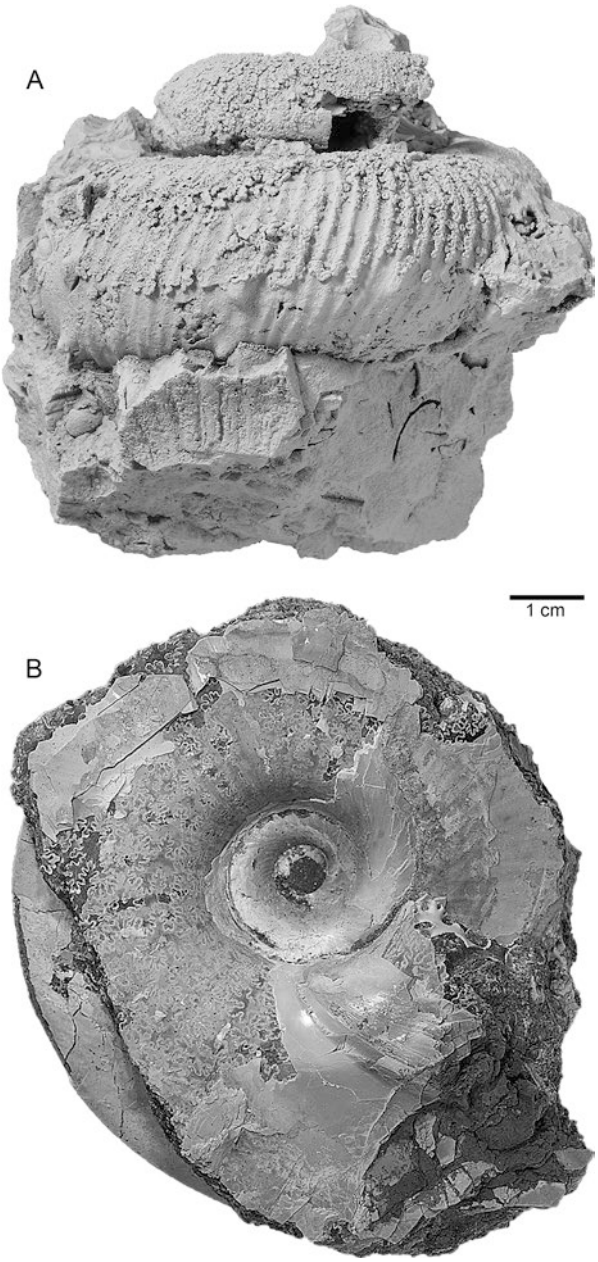

Fig. 12.5 Ammonites associated with methane seep deposits, Upper Cretaceous (Campanian) Pierre Shale, South Dakota and Nebraska. (**a**) *Didymoceras nebrascense*, AMNH 102288. (**b**) *Placenticeras intercalare*, AMNH 64499. All figures are x 1. Abbreviation: *AMNH* American Museum of Natural History

(*H. gilberti*), the species are not restricted to the seeps but also occur elsewhere in the basin (Landman et al. 2013).

The abundance of ammonites varies depending on the site. For example, in the same area with multiple seeps from the *Didymoceras nebrascense*/*Baculites scotti* Zones near Newell, Butte County, South Dakota, some seep deposits are more ammonite rich than others; still other seep deposits consist of nothing but carbonates and lucinids. In addition, the species composition varies depending on the seep deposit. For example, baculitid ammonites are generally more abundant than scaphitid ammonites, but the reverse is true in the *Baculites baculus* Zone in Niobrara County, Wyoming. Such variation may reflect differences in the abundance of food or concentration of oxygen, methane, or hydrogen sulfide.

Several lines of evidence have been marshalled to argue that ammonites lived at the seeps (Landman et al. 2012b, 2018):

1. Ammonites are much more abundant at the seep deposits than in the surrounding shale. Meehan and Landman (2016) reported a total of 17 specimens of *Hoploscaphites nodosus* from a seep deposit in the *Didymoceras cheyennense* Zone, Custer County, South Dakota. Landman et al. (2013) reported a total of 19 specimens of *H. gilberti* in a seep deposit from the *D. nebrascense* Zone, Weston County, Wyoming. In addition, one of us (N.L.L.), in association with S. Jorgensen, collected nearly 30 complete specimens of *H. gilberti* in a seep deposit from the *D. nebrascense* Zone, Fall River County, South Dakota. In contrast, the same ammonites are rare or absent in the surrounding shale.
2. In ammonites in which sexual dimorphs can be recognized, both dimorphs occur in the same seep deposit. For example, Landman et al. (2013) reported 12 macroconchs and 16 microconchs of *H. gilberti* in a seep deposit from the *D. nebrascense* Zone, Weston County, Wyoming.
3. Ammonite jaws and hooklike structures are present in seep deposits (Fig. 12.6). Because these structures are very delicate and easily lost after death, their presence suggests that the ammonites did not float into the sites after the animals died, but rather that they lived there.
4. Ammonites at seeps exhibit sublethal and lethal injuries (Fig. 12.7). Sublethal injuries are recognizable as scars on the shell and reflect attacks that occurred during the lifetime of the animal but did not result in death. Lethal injuries are indicated by missing pieces of shell, which tend to occur in the same position on the ammonite (Larson 2003; Takeda et al. 2016). Many of these injuries may have been inflicted at or near the seep sites, suggesting that the ammonites formed an integral part of an integrated community.
5. Many seep deposits contain both juveniles and adults of the same species (Rowe et al. 2020). For example, juveniles of *Hoploscaphites* and *Baculites* are common in seep deposits from the *Didymoceras cheyennense* Zone of southwestern South Dakota (Fig. 12.4l).
6. In several of the seep deposits in South Dakota, the ammonites are well preserved and retain their original aragonitic shells. As a result, the isotope composition of the shells records, in principle, the original conditions in the water

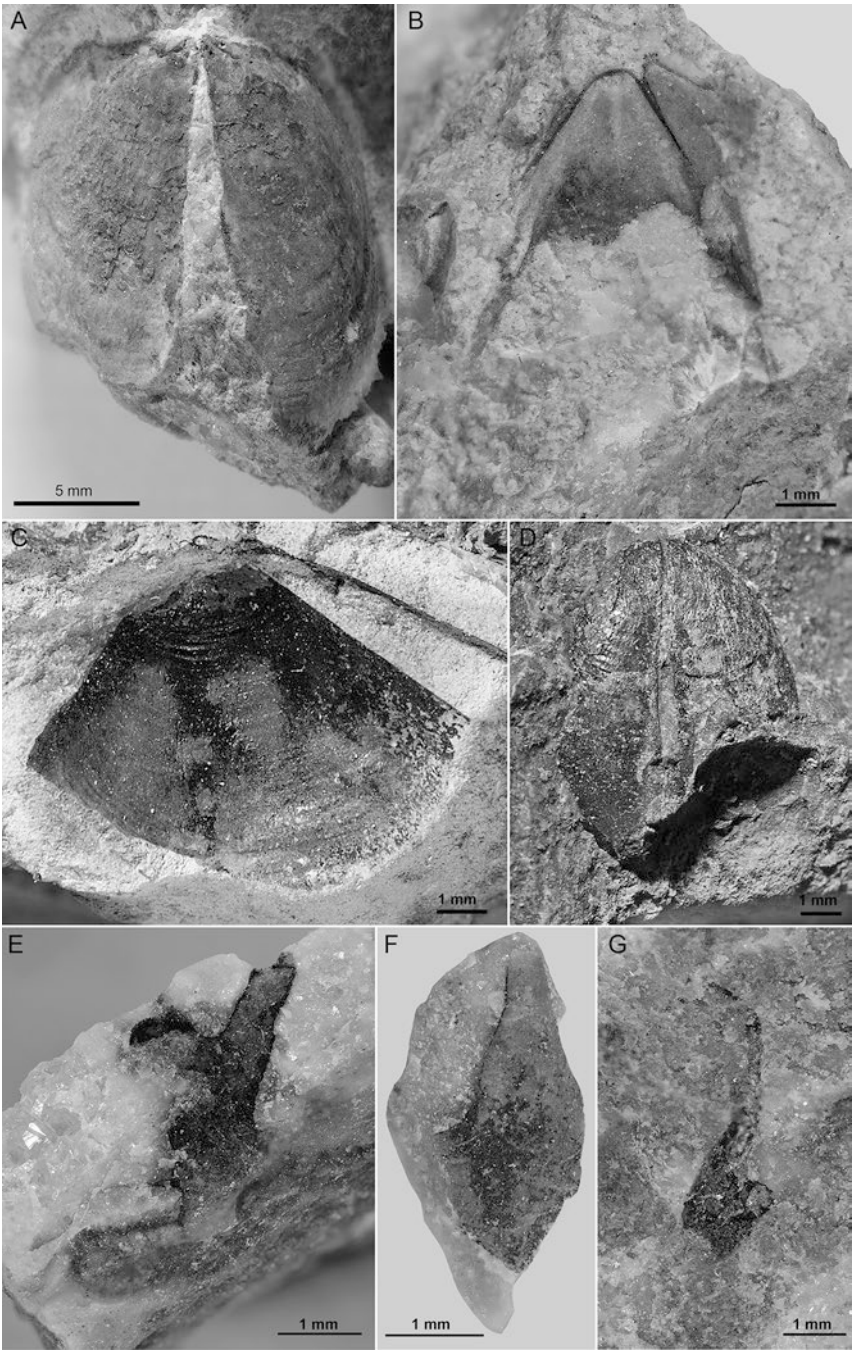

Fig. 12.6 Jaws and hooklike structures attributed to *Hoploscaphites* from seep deposits in the Upper Cretaceous (Campanian) Pierre Shale, South Dakota. (**a**) Lower jaw showing the midline slit, ventral view, apex on the top, AMNH 64532. (**b**) Upper jaw, apex on the top, AMNH 64547. (**c**) Impression of the left side of the lower jaw, midline slit on the right, AMNH 63423. (**d**) Lower jaw showing the midline slit, ventral view, apex on the top, AMNH 99198. (**e**) Hooklike structure showing one of the points projecting to the upper right, AMNH 63530. (**f**) Hooklike structure with the basal portion exposed on the bottom, AMNH 63531. (**g**) Hooklike structure with one point complete and one point broken, AMNH 64533. Abbreviation: *AMNH* American Museum of Natural History

Fig. 12.7 Healed injury on the outer flanks of *Placenticeras meeki*, AMNH 108168, methane seep deposit, Upper Cretaceous (Campanian) Pierre Shale, South Dakota. The injury was severe enough to affect the mantle. The adoral direction is toward the bottom of the photo. Figure is x 1. Abbreviation: *AMNH* American Museum of Natural History

column where the ammonites lived. A comparison of the carbon isotopic composition of the specimens at seeps with specimens of the same species from age-equivalent non-seep sites reveals a significant difference (Landman et al. 2012b; Cochran et al. 2015; Landman et al. 2018). The values of $\delta^{13}C$ are significantly lower in seep specimens than in age-equivalent non-seep specimens (Fig. 12.8). Anaerobic oxidation of ^{12}C-enriched methane at seeps produces a dissolved inorganic carbon reservoir with a low $\delta^{13}C$ signature that can be imprinted on seep carbonates as well as on the shells of mollusks living at the seeps. The low $\delta^{13}C$ of the well-preserved shells of ammonites from seeps compared with those of non-seep ammonites suggests that the seep ammonites were living in close proximity to the seep ecosystem.

In addition to methane seep deposits, ammonites have also been reported in association with reptile carcasses, which could represent relatively small, localized chemosynthetic communities. A mosasaur skeleton-ammonite association was discovered in the Campanian (Upper Cretaceous) Sharon Springs Member of the Pierre Shale, Niobrara County, Wyoming (D. Burnham, R. DePalma, pers. comm. 2016). It consists of a large, fairly complete, partially articulated skeleton of *Clidastes* associated with a 1-cm-thick ammonite layer that occurs just above and around the mosasaur

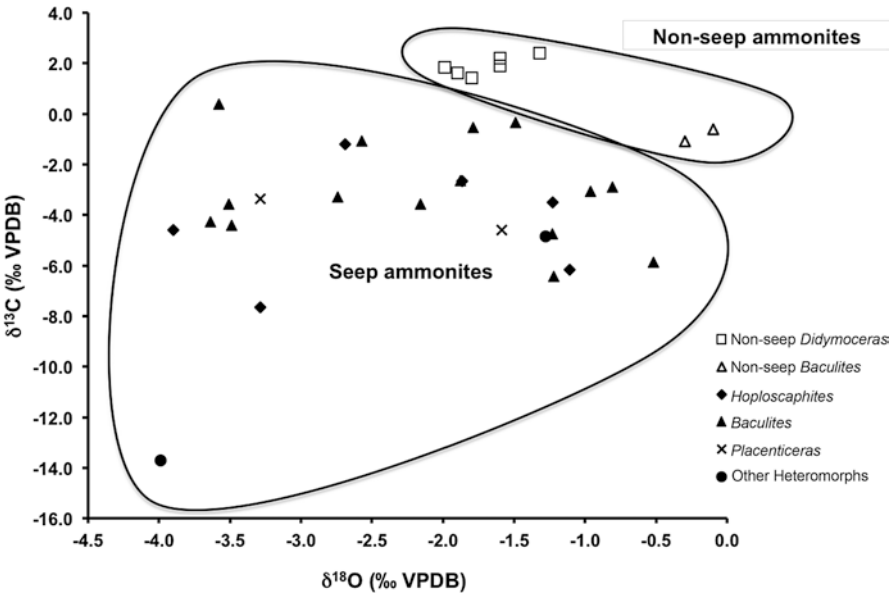

Fig. 12.8 Comparison of the carbon isotopic composition ($\delta^{13}C$ ‰VPDB) of well-preserved specimens of *Baculites compressus* collected at seep sites with specimens of the same species from age-equivalent non-seep sites. As a consequence of the impact of anaerobic methane oxidation on the $\delta^{13}C$ of the DIC reservoir from which the shells formed, the values of $\delta^{13}C$ are consistently lower in the specimens at the seeps, suggesting that they were living at the site. (Data from Landman et al. 2018)

(Fig. 12.9). The accumulation comprises thousands of small specimens of *Baculites haresi*, along with a few *Hoploscaphites*, all of which are juveniles with intact body chambers. The specimens of *B. haresi* are approximately 1–2 cm long and are oriented northwest-southeast with the apical ends pointing toward the southeast, implying a current from that direction (Fig. 12.10).

The Sharon Springs Member has been interpreted as having been deposited on an anoxic bottom (Gill and Cobban 1966; Byers 1979). The most common fossils are nektonic: mosasaurs, fish, squid (enchoteuthids), and ammonites (*Baculites haresi*). The only benthic organisms are large, flat-sided inoceramids, but these animals may have contained chemosymbiotic bacteria that helped them tolerate a low-oxygen environment (MacLeod and Hoppe 1992). Landman (1988) reported small juveniles of *Baculites* 5 mm in length sparsely preserved in small gray limestone

Fig. 12.9 Mass occurrence of juvenile specimens of *Baculites* and *Hoploscaphites*, PBMNH.10.115, associated with a mosasaur carcass in the Upper Cretaceous (Campanian) Sharon Springs Member of the Pierre Shale, Wyoming. North is toward the upper left. Figure is x 1. Abbreviation: *PBMNH* Palm Beach Museum of Natural History

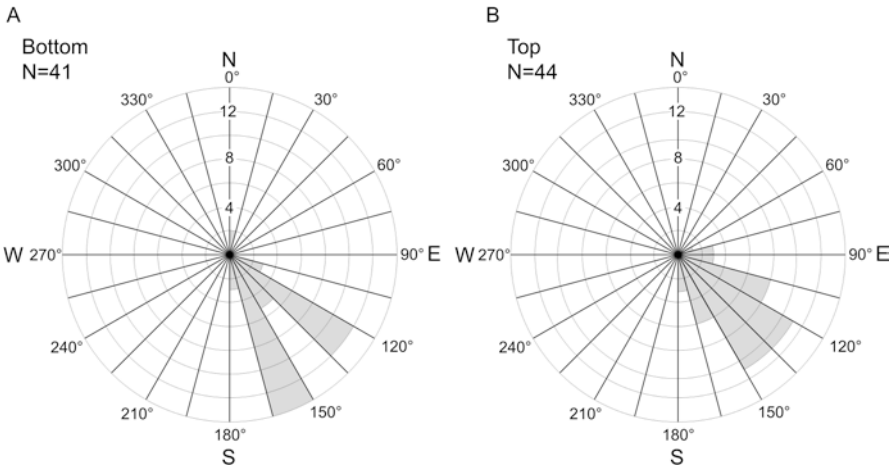

Fig. 12.10 Rose diagrams showing the orientation of the juvenile specimens of *Baculites* associated with the mosasaur carcass. The layer is 1 cm thick; the current direction is from the southeast

concretions in this stratigraphic interval. He interpreted the presence of such small juveniles as evidence that the ammonites lived well above the seafloor at this stage of their lives.

The mass occurrence of ammonite juveniles in association with the mosasaur skeleton is the first report of such an occurrence and could represent remains of a chemosynthetic-based community. Such systems have previously been reported in association with plesiosaurid skeletons in the Upper Cretaceous of Japan (Kaim et al. 2008). These communities depend on the anaerobic microbial decomposition of the organic compounds (lipids) in the bones of the reptile skeleton. In the Sharon Springs Member, more research is required to document the presence of other organisms living on and around the skeleton such as gastropods and bivalves as well as microborings in the bones. If this association represents the remains of a chemosynthetic-based community, the ammonites would have been attracted to the small organisms surrounding the rotting carcass as well as the rotting carcass itself.

The death and burial of the ammonites may have been due to rising anoxia. At the same time, a current must have resuspended fine sediment on the bottom and buried the ammonites. The southeast current parallels the shoreline to the west (Gill and Cobban 1966: Fig. 16, *Baculites obtusus* Zone) and would account for the preferred orientation of the ammonite specimens.

12.4 Conclusions

In many of the seep deposits described, ammonites are more abundant at the seeps than in the surrounding sedimentary rocks. The deposits in the US Western Interior and Southeastern France also contain ammonite jaws and hooklike structures, which are attributed to ammonites. Both kinds of structures are very delicate and could not have been transported into the sites after the ammonites died. In addition, the isotopic composition of well-preserved ammonites from the US Western Interior and Antarctica exhibits unusually low (light) values of $\delta^{13}C$ compared to those of ammonites from age-equivalent non-seep sites. All of this evidence suggests that the ammonites lived at these seeps.

However, ammonites were not restricted to seeps. Because they were able to disperse widely during the post-hatching phase, ammonites inhabited many other environments. Thus, they represent background taxa and are not seep obligate. Nevertheless, if an individual was lucky enough to stumble on a seep site, perhaps through olfactory cues, it may have stayed there for the rest of its life. The seep undoubtedly provided a nutrient-rich environment. Therefore, even though ammonites were mobile animals, they may have spent part or most of their lives at seeps. In addition, because many seeps occur in clusters (seep fields), ammonites may have drifted or migrated from one seep to another.

In seep deposits where the evidence suggests that ammonites lived at the seep, the ammonites can serve as a means of determining the paleodepth of the site (Appendix Table 12.1). In contrast, ammonites are rare or absent in deep-water hydrothermal vent deposits and probably did not live at these sites. For example, Kaim et al. (2021) reported a single gaudryceratid ammonite from a hydrothermal vent deposit in the Upper Cretaceous (upper Cenomanian-lower Turonian) Troodos Ophiolite in Cyprus. The depth at this site is estimated to have been 2500–5000 m, far exceeding the implosion depth of any ammonite.

Acknowledgments We thank J. D. Witts (University of Bristol, UK) and A. Kaim (Institute of Paleobiology, Warsaw, Poland) for photographs of ammonites as well as stimulating discussions about methane seeps, H. Parent (National University of Rosario Pellegrini, Rosario, Argentina) for information about seeps and ammonites in Argentina, C. Klug (University of Zurich) for references about seeps in Morocco, J. Slattery (University of South Florida) and Robert DePalma (Palm Beach Museum of Natural History) for information about the mosasaur-ammonite association in the Sharon Springs Member of the Pierre Shale, S. Thurston (AMNH) for help in preparing the figures, and M. Slovacek (AMNH) for help in preparing Fig. 12.10. We thank Royal H. Mapes (AMNH) and James D. Witts for reviewing this manuscript and making many helpful suggestions. This research was supported by the N. D. Newell Fund (AMNH).

Appendix

Table 12.1 Ammonite species from methane seep deposits

Species	Source	Locality	Age	Water depth (m)
Agoniatites fecundus	Klug (2002)	Erfoud, Morocco	Emsian (Lower Devonian)	<100
Sagenites sp.	A. Kaim (pers. comm. 2016)	Oregon, USA	Norian (Upper Triassic)	100–200
Arcestes sp.	A. Kaim (pers. comm. 2016)	Oregon, USA	Norian (Upper Triassic)	100–200
Arcestes sp.	Kiel et al. (2016)	Turkey	Upper Carnian-lower Norian (Upper Triassic)	100–200
Phylloceras sp.	H. Parent (pers. comm. 2017)	Patagonia, Argentina	Toarcian (Lower Jurassic)	100–200
Calliphylloceras sp.	H. Parent (pers. comm. 2017)	Patagonia, Argentina	Toarcian (Lower Jurassic)	100–200
Hildaitoides retrocostatus	H. Parent (pers. comm. 2017)	Patagonia, Argentina	Toarcian (Lower Jurassic)	100–200
Phymatoceras sp.	H. Parent (pers. comm. 2017)	Patagonia, Argentina	Toarcian (Lower Jurassic)	100–200
Perisphinctes (*Otosphinctes*) *montfalconensis*	Bourseau (1977)	SE France	Oxfordian (Upper Jurassic)	100–200
Perisphinctes (*Otosphinctes*) *paturattensis*	Bourseau (1977)	SE France	Oxfordian (Upper Jurassic)	100–200
Perisphinctes (*Dichotomosphinctes*) *antecedens*	Bourseau (1977)	SE France	Oxfordian (Upper Jurassic)	100–200
Perisphinctes rotöides	Bourseau (1977)	SE France	Oxfordian (Upper Jurassic)	100–200
Pseudogregoryceras iteni	Bourseau (1977)	SE France	Oxfordian (Upper Jurassic)	100–200
Euaspidoceras (*E.*) *catena*	Bourseau (1977)	SE France	Oxfordian (Upper Jurassic)	100–200
Euaspidoceras (*E.*) *ovale*	Bourseau (1977)	SE France	Oxfordian (Upper Jurassic)	100–200
Protophites christoli	Bourseau (1977)	SE France	Oxfordian (Upper Jurassic)	100–200
Subcardioceras excavatum	Bourseau (1977)	SE France	Oxfordian (Upper Jurassic)	100–200
Pachyceras (*Tornquistes*) *kobyi*	Bourseau (1977)	SE France	Oxfordian (Upper Jurassic)	100–200
Cardioceras (*Subvertebriceras*) *densiplicatum*	Bourseau (1977)	SE France	Oxfordian (Upper Jurassic)	100–200

(continued)

Table 12.1 (continued)

Species	Source	Locality	Age	Water depth (m)
Campylites (*C.*) *delmontanus delmontanus*	Bourseau (1977)	SE France	Oxfordian (Upper Jurassic)	100–200
Campylites (*Neoprionoceras*) *henrici henrici*	Bourseau (1977)	SE France	Oxfordian (Upper Jurassic)	100–200
Taramelliceras (*T.*) *obumbrans*	Bourseau (1977)	SE France	Oxfordian (Upper Jurassic)	100–200
Taramelliceras (*T.*) *dentostriatum*	Bourseau (1977)	SE France	Oxfordian (Upper Jurassic)	100–200
Taramelliceras (*T.*) *callicerum*	Bourseau (1977)	SE France	Oxfordian (Upper Jurassic)	100–200
Amoeboceras sp.	Hryniewicz et al. (2015)	Novaya Zemlya	Oxfordian-Kimmeridgian (Upper Jurassic)	100–200
Craspedites (*C.*) *okensis*	Hryniewicz et al. (2015)	Novaya Zemlya	Volgian (Upper Jurassic-Lower Cretaceous)	100–200
Craspedites (*C.*) *okensis*	Wierzbowski et al. (2011)	Spitsbergen	Volgian (Upper Jurassic-Lower Cretaceous)	<100
Craspedites (*Taimyroceras*) *originalis*	Wierzbowski et al. (2011)	Spitsbergen	Volgian (Upper Jurassic-Lower Cretaceous)	<100
Kachpurites sp.	Wierzbowski et al. (2011)	Spitsbergen	Volgian (Upper Jurassic-Lower Cretaceous)	<100
Hectoroceras (?*Shulginites*) sp.	Wierzbowski et al. (2011)	Spitsbergen	Volgian-Ryazanian (Upper Jurassic-Lower Cretaceous)	<100
Borealites (*Ronkinites*) *rossicus*	Wierzbowski et al. (2011)	Spitsbergen	Ryazanian (Lower Cretaceous)	<100
Borealites (*Pseudocraspedites*) sp.	Wierzbowski et al. (2011)	Spitsbergen	Ryazanian (Lower Cretaceous)	<100
Surites (*S.*) *spasskensis*	Wierzbowski et al. (2011)	Spitsbergen	Ryazanian (Lower Cretaceous)	<100
Surites (*S.*) *spasskensoides*	Wierzbowski et al. (2011)	Spitsbergen	Ryazanian (Lower Cretaceous)	<100
Surites (*Bojarkia*) *tzikwinianus*	Wierzbowski et al. (2011)	Spitsbergen	Ryazanian (Lower Cretaceous)	<100
Tollia (*T.*) *tolli*	Wierzbowski et al. (2011)	Spitsbergen	Ryazanian (Lower Cretaceous)	<100
Sanmartinoceras sp.	Kelly et al. (2000)	NE Greenland	Barremian (Lower Cretaceous)	100–200
Audouliceras sp.	Kelly et al. (2000)	NE Greenland	Barremian (Lower Cretaceous)	100–200
Epicheloniceras sp.	Kelly et al. (2000)	NE Greenland	Barremian (Lower Cretaceous)	100–200

Species	Source	Locality	Age	Water depth (m)
Arcthroplites sp.	Beauchamp and Savard (1992)	Canadian Arctic	Aptian-Albian (Lower Cretaceous)	200–300
Callizoniceras (*Colvillia*) ex. aff. *crassicostata*	Beauchamp and Savard (1992)	Canadian Arctic	Aptian-Albian (Lower Cretaceous)	200–300
Arcthroplites (?) cf. *belli*	Williscroft et al. (2017)	Canadian Arctic	Albian (Lower Cretaceous)	200–300
Cleoniceras sp.	Williscroft et al. (2017)	Canadian Arctic	Albian (Lower Cretaceous)	200–300
Beudanticeras sp.	Williscroft et al. (2017)	Canadian Arctic	Albian (Lower Cretaceous)	200–300
Puzosia aff. *sigmoidalis*	Williscroft et al. (2017)	Canadian Arctic	Albian (Lower Cretaceous)	200–300
Freboldiceras aff. *irenense*	Williscroft et al. (2017)	Canadian Arctic	Albian (Lower Cretaceous)	200–300
Scaphites equalis coverhamensis	Kiel et al. (2012b)	Raukumara Peninsula, New Zealand	Albian-Cenomanian (Middle Cretaceous)	100–200
Kossmaticeratidae gen. et sp. indet.	Kiel et al. (2012b)	Raukumara Peninsula, New Zealand	Albian-Cenomanian (Middle Cretaceous)	100–200
Neograhamites cf. *transitorius*	Kiel et al. (2012b)	Raukumara Peninsula, New Zealand	Albian-Cenomanian (Middle Cretaceous)	100–200
Benueites sp.	Smrzka et al. (2017)	Essaouira, Morocco	Turonian (Upper Cretaceous)	<100
B. cf. *benueensis*	Smrzka et al. (2017)	Essaouira, Morocco	Turonian (Upper Cretaceous)	<100
Gaudryceras tenuiliratum	Hikida et al. (2003) and Jenkins et al. (2007)	Hokkaido, Japan	Campanian (Upper Cretaceous)	200–300
Baculites compressus	Larson et al. (2014)	WI	Campanian (Upper Cretaceous)	<100
Baculites corrugatus	Larson et al. (2014)	WI	Campanian (Upper Cretaceous)	<100
Baculites cuneatus	Larson et al. (2014)	WI	Campanian (Upper Cretaceous)	<100
Baculites eliasi	Larson et al. (2014)	WI	Campanian (Upper Cretaceous)	<100
Baculites pseudovatus	Larson et al. (2014)	WI	Campanian (Upper Cretaceous)	<100
Baculites scotti	Larson et al. (2014)	WI	Campanian (Upper Cretaceous)	<100
Baculites undatus	Larson et al. (2014)	WI	Campanian (Upper Cretaceous)	<100

Species	Source	Locality	Age	Water depth (m)
Didymoceras cheyennense	Larson et al. (2014)	WI	Campanian (Upper Cretaceous)	<100
Didymoceras nebrascense	Larson et al. (2014)	WI	Campanian (Upper Cretaceous)	<100
Exiteloceras jenneyi	This study	WI	Campanian (Upper Cretaceous)	<100
Hoploscaphites brevis	Larson et al. (2014)	WI	Campanian (Upper Cretaceous)	<100
Hoploscaphites gilberti	Larson et al. (2014)	WI	Campanian (Upper Cretaceous)	<100
Hoploscaphites nodosus	Larson et al. (2014)	WI	Campanian (Upper Cretaceous)	<100
Hoploscaphites gilli	Larson et al. (2014)	WI	Campanian (Upper Cretaceous)	<100
Hoploscaphites plenus	This study	WI	Maastrichtian (Upper Cretaceous)	<100
Menuites oralensis	This study	WI	Campanian (Upper Cretaceous)	<100
Nostoceras monotuberculatum	Larson et al. (2014)	WI	Campanian (Upper Cretaceous)	<100
Pachydiscus sp.	This study	WI	Campanian (Upper Cretaceous)	<100
Placenticeras intercalare	Larson et al. (2014)	WI	Campanian (Upper Cretaceous)	<100
Placenticeras meeki	Larson et al. (2014)	WI	Campanian (Upper Cretaceous)	<100
Solenoceras bearpawense	Larson et al. (2014)	WI	Campanian (Upper Cretaceous)	<100
Spiroxybeloceras meekanum	Larson et al. (2014)	WI	Campanian (Upper Cretaceous)	<100
Hoploscaphites sp.	This study	WI	Maastrichtian (Upper Cretaceous)	<100
Diplomoceras maximum	Ivany and Artruc (2016)	Seymour Island, Antarctica	Maastrichtian (Upper Cretaceous)	100–200
Anagaudryceras sp.	Little et al. (2015)	Snow Hills Island, Antarctica	Maastrichtian (Upper Cretaceous)	100–200
Jacobites anderssoni	Little et al. (2015)	Snow Hills Island, Antarctica	Maastrichtian (Upper Cretaceous)	100–200
Gunnarites sp.	Little et al. (2015)	Snow Hills Island, Antarctica	Maastrichtian (Upper Cretaceous)	100–200

Species	Source	Locality	Age	Water depth (m)
Gunnarites bhavaniformis	Little et al. (2015)	Snow Hills Island, Antarctica	Maastrichtian (Upper Cretaceous)	100–200
Gunnarites antarcticus	Little et al. (2015)	Snow Hills Island, Antarctica	Maastrichtian (Upper Creataceous)	100–200
Maorites seymouriensis	Little et al. (2015)	Seymour Island, Antarctica	Maastrichtian (Upper Cretaceous)	100–200

The species are arranged in the table from geologically oldest on the top to geologically youngest at the bottom. The authors' names associated with each species are given in the "source" references. In Bourseau (1977), because of the large number of taxa, we did not include the species listed in open nomenclature. The "water depth (m)" refers to the maximum depth at which the ammonites lived based on the conclusions of Hewitt (1996) and Westermann (1996). Ryazanian, "Boreal" Berriasian; Volgian, "Boreal" Tithonian-Berriasian; WI, Kansas, Colorado, Wyoming, South Dakota, Montana, and Nebraska

References

Aitken S, Collom CJ, Henderson CM et al (2002) Stratigraphy, paleoecology, and origin of Lower Devonian (Emsian) carbonate mud buildups, Hamar Laghdad, eastern Anti-Atlas, Morocco, Africa. Bull Can Petrol Geol 50:217–243

Allison PA, Hesselbo SP, Brett CE (2008) Methane seeps on an early Jurassic dysoxic seafloor. Palaeogeog Palaeoclimat Palaeoecol 270:230–238

Beauchamp B, Savard M (1992) Cretaceous chemosynthetic carbonate mounds in the Canadian Arctic. PALAIOS 7:434–450

Belka Z (1998) Early Devonian Kess-Kess carbonate mud mound of the eastern Anti-Atlas (Morocco), and their relation to submarine hydrothermal venting. J Sediment Res 68:368–377

Belka Z, Berkowski B (2005) Discovery of thermophyllic corals in an ancient hydrothermal vent community, Devonian. Acta Geol Pol 55:1–7

Berkowski B, Klug C (2011) Lucky rugose corals on crinoid stems: unusual examples of subepidermal epizoans from the Devonian of Morocco. Lethaia 45:24–33

Bishop GA, Williams AB (2000) Fossil crabs from tepee buttes, submarine seeps of the Late Cretaceous Pierre Shale, South Dakota and Colorado, USA. J Crustac Biol 20(2):286–300

Bourseau J-P (1977) L'Oxfordien moyen à nodules des 'Terres Noires' de Beauvoisin (Drôme). Nouv Arch Mus Hist Natl Lyon 15:1–116

Byers CW (1979) Biogenic structures of black shale paleoenvironments. Postilla 174:1–43

Campbell KA (2006) Hydrocarbon seep and hydrothermal vent paleoenvironments and paleontology: past development and future research directions. Palaeogeog Palaeoclimat Palaeoecol 232:362–407

Cavalazzi B, Barbieri R, Ori GG (2007) Chemosynthetic microbialites in the Devonian carbonate mounds of Hamar Laghdad (Anti-Atlas, Morocco). Sediment Geol 200:73–88

Chamberlain JA Jr (1987) Locomotion of *Nautilus*. In: Saunders WB, Landman NH (eds) *Nautilus*: the biology and paleobiology of a living fossil. Plenum Press, New York, pp 489–525

Cherns L, Spencer ART, Rahman IA, Garwood RJ, Reedman C, Burca G, Turner MJ, Hollingworth NTJ, Hilton J (2021) Correlative tomography of an exceptionally preserved Jurassic ammonite implies hyponome-propelled swimming. Geology. https://doi.org/10.1130/G49551.1

Cobban WA, Walaszczyk I, Obradovich JD et al (2006) A USGS zonal table for the Upper Cretaceous middle Cenomanian–Maastrichtian of the Western Interior of the United States based on ammonites, inoceramids, and radiometric ages. US Geological Survey Open-File Report 2006-1250, pp 1–46

Cochran JK, Landman NH, Larson NL et al (2015) Geochemical evidence (C and Sr isotopes) for methane seeps as ammonite habitats in the Late Cretaceous (Campanian) Western Interior Seaway. Swiss J Palaeontol 134(2):153–165

Dando PR (2010) Biological communities at marine shallow-water vent and seep sites. In: Kiel S (ed) The vent and seep biota: aspects from microbes to ecosystems, Topics in geobiology, vol. 33. Springer, Cham, pp 333–378

Doguzhaeva L, Mapes RA (2015) The body chamber length variations and muscle and mantle attachments in ammonoids. In: Klug C, Korn D, DeBaets K et al (eds) Ammonoid paleobiology. Springer, Cham, pp 545–584

Engeser T, Keupp H (2002) Phylogeny of aptychi-possessing *Neoammonoidea* (Aptychophora nov., Cephalopoda). Lethaia 24:79–96

Gilbert GK, Gulliver FR (1895) Tepee Buttes. Geol Soc Am Bull 6:333–342

Gill JR, Cobban WA (1966) The Red Bird section of the Upper Cretaceous Pierre Shale in Wyoming. US Geol Surv Prof Pap 393A:1–73

Hammer Ø, Nakrem HA, Little CTS et al (2011) Hydrocarbon seeps from close to the Jurassic-Cretaceous boundary, Svalbard. Palaeogeog Palaeoclimat Palaeoecol 306:15–26

Hewitt RA (1996) Architecture and strength of the ammonoid shell. In: Landman NH, Tanabe K, Davis RA (eds) Ammonoid paleobiology. Plenum, New York, pp 297–339

Hewitt RA, Westermann GEG (1987) *Nautilus* shell architecture. In: Saunders WB, Landman NH (eds) *Nautilus*: the biology and paleobiology of a living fossil. Plenum, New York, pp 435–162

Hikida Y, Suzuki S, Togo Y et al (2003) An exceptionally well-preserved fossil seep community from the Cretaceous Yezo Group in the Nakagawa area, Hokkaido, Japan. Paleontolog Res 7(4):329–342

Hoffmann R, Lemanis R, Naglik C, Klug C (2015) Ammonoid buoyancy. In: Klug C, Korn D, De Baets K, Kruta I, Mapes RH (eds) Ammonoid paleobiology: from anatomy to ecology, Topics in geobiology, vol. 43. Springer, New York, pp 613–648

Howe B (1987) Tepee buttes: a petrological, paleontological, and paleoenvironmental study of Cretaceous submarine spring deposits. Thesis, University of Colorado

Hryniewicz K, Nakrem HA, Hammer Ø et al (2014) The palaeoecology of the latest Jurassic-earliest Cretaceous hydrocarbon seep carbonates from Spitsbergen, Svalbard. Lethaia 48:353–374

Hryniewicz K, Hagström J, Hammer Ø et al (2015) Late Jurassic-Early Cretaceous hydrocarbon seep boulders from Novaya Zemlya and their faunas. Palaeogeog Palaeoclimat Palaeoecol 436:231–244

Hunter A, Larson NL, Landman NH et al (2016) A new crinoid from cold methane seep deposits in the Upper Cretaceous Pierre Shale. J Paleontol 90(3):506–524

Ivany LC, Artruc EG (2016) Isotope ecology of a giant heteromorph ammonite from Antarctica. In: Abstracts with programs. Geological Society of America, pp 145–144

Jacobs DK, Chamberlain JA Jr (1996) Buoyancy and hydrodynamics in ammonoids. In: Landman NH, Tanabe K, Davis RA (eds) Ammonoid paleobiology. Plenum, New York, pp 169–224

Jacobs DK, Landman NH (1993) Is nautilus a good model for the function and behavior of ammonoids? Lethaia 26:1–12

Jakubowicz M, Berkowski B, Hryniewicz K, Belka Z (this volume) Middle Palaeozoic of Morocco: the earliest-known methane seep metazoan ecosystems. In: Kaim A, Cochran JK, Landman NH (eds) Ancient hydrocarbon seeps, Topics in geobiology. Springer, New York

Jenkins RG, Kaim A, Hikida Y et al (2007) Methane-flux-dependent lateral faunal changes in a Late Cretaceous chemosymbiotic assemblage from Nakagawa area of Hokkaido, Japan. Geobiology 5:127–139

Kaim A, Kobayashi Y, Echizenya H et al (2008) Chemosynthesis-based associations on Cretaceous plesiosaurid carcasses. Acta Palaeontol Pol 54(1):97–104

Kaim A, Jenkins R, Hryniewicz K et al (2016) Early Mesozoic seeps and the advent of modern seep faunas. In: Abstracts, 1st international workshop on ancient hydrocarbon seep and cognate communities, Warsaw, Poland, June 2016

Kaim A, Little CTS, Kennedy WJ et al (2021) Late Cretaceous hydrothermal vent communities from the Troodos Ophiolite, Cyprus: systematics and evolutionary significance. Pap Palaeontol 7(4):1927–1947

Kauffman EG, Arthur MA, Howe B et al (1996) Widespread venting of methane-rich fluids in Late Cretaceous (Campanian) submarine seeps (Tepee Buttes), Western Interior Seaway, U.S.A. Geology 24:799–802

Kelly SRA, Blanc E, Price SP et al (2000) Early cretaceous giant bivalves from seep-related limestone mounds, Wollaston Forland, Northeast Greenland. In: Harper EM, Taylor JD, Crame JA (eds) The evolutionary biology of the Bivalvia, Geological society special publication, no. 177. Geological Society of London, London, pp 227–246

Kiel S, Weiser F, Titus AL (2012a) Shallow-water methane-seep faunas in the Cenomanian Western Interior Seaway: no evidence for onshore-offshore adaptations to deep-sea vents. Geology 40(9):839–842

Kiel S, Birgel D, Campbell KA, Crampton JS, Schiøler P, Peckmann J (2012b) Cretaceous methane-seep deposits from New Zealand and their fauna. Palaeogeog Palaeoclimat Palaeoecol 390:17–34

Kiel S, Krystyn L, Demirtas F et al (2017) Late Triassic mollusk-dominated hydrocarbon-seep deposits from Turkey. Geology 45(8):751–754

Klug C (2002) Quantitative stratigraphy and taxonomy of late Emsian and Eifelian ammonoids of the eastern Anti-Atlas (Morocco). Cour Forschunginst Senckenb 238:1–109

Kruta I, Landman NH, Rouget I et al (2011) The role of ammonites in the Mesozoic marine food web revealed by jaw preservation. Science 331:70–72

Landman NH (1988) Early ontogeny of Mesozoic ammonites and nautilids. In: Wiedmann J, Kullmann J (eds) Cephalopods present and past. Schweizerbart'sche Verlagsbuchhandlung, Stuttgart, pp 215–228

Landman NH, Kennedy WJ, Cobban WA et al (2010) Scaphites of the '*nodosus* group' from the Upper Cretaceous (Campanian) of the Western Interior of North America. Am Mus Natl Hist Bull 342:1–242

Landman NH, Cobban WA, Larson NL (2012a) Mode of life and habitat of scaphitid ammonites. In: Neige P, Rouget I (eds) Cephalopods present and past, 8th international symposium, Dijon, 30 August 30−2 September 2010, vol 45. Geobios, pp 87–98

Landman NH, Cochran JK, Larson NL et al (2012b) Methane seeps as ammonite habitats in the U.S. Western Interior Seaway revealed by isotopic analyses of well-preserved shell material. Geology 40:507–510

Landman NH, Kennedy WJ, Cobban WA et al (2013) A new species of *Hoploscaphites* (Ammonoidea: Ancyloceratina) from cold methane seeps in the Upper Cretaceous of the U.S. Western Interior. Am Mus Novit 3781:1–39

Landman NH, Cochran JK, Slovacek M et al (2018) Isotope sclerochronology of ammonites (*Baculites compressus*) from methane seep and non-seep sites in the Late Cretaceous Western Interior Seaway, USA: implications for ammonite habitat and mode of life. Am J Sci 318:603–639

Landman NH, Witts JD, Garb MP et al (2019) Ammonites as an integral part of cold methane seep faunas: comparison of sites from the Upper Jurassic of France and the Upper Cretaceous of North America. In: Abstracts with programs. Geological Society of America, pp 197–195

Landman NH, Cochran JK, Brezina J et al (this volume) Methane seeps in the Late Cretaceous Western Interior Seaway, USA. In: Kaim A, Cochran JK, Landman NH (eds) Ancient hydrocarbon seeps, Topics in geobiology. Springer, New York

Larson NL (2003) Predation and pathologies in the Late Cretaceous ammonite family Scaphitidae. Mid-Am Paleontol Soc (MAPS) Digest 26(3):1–30

Larson NL, Brezina J, Landman NH et al (2014) Hydrocarbon seeps: unique habitats that preserved the diversity of fauna in the Late Cretaceous Western Interior Seaway. https://www.academia.edu/4641897/Hydrocarbon_seeps_unique_habitats. Accessed 4 Nov 2021

Little CTS, Birgel D, Boyce AJ et al (2015) Late Cretaceous (Maastrichtian) shallow water hydrocarbon seeps from Snow Hill and Seymour Islands, James Ross Basin, Antarctica. Palaeogeog Palaeoclimat Palaeoecol 418:213–228

MacLeod KG, Hoppe KA (1992) Evidence that inoceramid bivalves were benthic and harbored chemosynthetic symbionts. Geology 20:117–120. https://doi.org/10.1130/0091-7613(1992)020<0117:ETIBWB>2.3.CO;2

Meehan K, Landman NH (2016) Faunal associations in cold-methane seep deposits from the Upper Cretaceous Pierre Shale, South Dakota. PALAIOS 31(6):291–301

Metz CL (2010) Tectonic controls on the genesis distribution of Late Cretaceous, Western Interior Basin hydrocarbon seep mounds (Tepee Buttes) of North America. J Geol 118:201–221

Naglik C, Tajika A, Chamberlain J, Klug C (2015) Ammonoid locomotion. In: Klug C, Korn D, De Baets K, Kruta I, Mapes RH (eds) Ammonoid paleobiology: from anatomy to ecology, Topics in geobiology, vol. 43. Springer, New York, pp 649–688

Peckmann J, Walliser OH, Riegel W et al (1999) Signatures of hydrocarbon venting in a Middle Devonian carbonate mound (Hollard Mound) at the Hamar Laghdad (Antiatlas, Morocco). Facies 40:281–296

Peckmann J, Little CTS, Gill F et al (2005) Worm tube fossils from the Hollard Mound hydrocarbon-seep deposit, Middle Devonian, Morocco: Paleozoic seep-related vestimentiferans? Palaeogeog Palaeoclimat Palaeoecol 227:242–257

Peckmann J, Kiel S, Sandy MR et al (2011) Mass occurrences of the brachiopod *Halorella* in Late Triassic methane-seep deposits, eastern Oregon. J Geol 119:207–220

Peterman DJ, Yacobucci MM, Larson NL, Ciampaglio C, Linn T (2020) A method to the madness: ontogenetic changes in the hydrostatic properties of *Didymoceras* (Nostoceratidae: Ammonoidea). Paleobiology 46(2):237–258

Ritterbush KA, Bottjer DJ (2012) Westermann Morphospace displays ammonoid shell shape and hypothetical paleoecology. Paleobiology 38(3):424–446

Rolin Y, Gaillard C, Roux M (1990) Ecologie des pseudobiohermes des Terres Noires jurassiques liés à des paléo-sources sous-marine: le site Oxfordien de Beauvoisin (Drôme, Bassin du Sud-Est, France). Palaeogeog Palaeoclimat Palaeoecol 80:79–105

Rowe A, Landman NH, Witts J et al (2020) Late Cretaceous methane seeps as habitats for newly hatched ammonites. PALAIOS 35:1–13

Ryan D, Witts JD, Landman NH (2020) Paleoecological analysis of a methane seep in the Late Cretaceous (Maastrichtian) Western Interior, USA. Lethaia 54:185–203

Saunders WB, Shapiro EA (1986) Calculation and simulation of ammonoid hydrostatics. Paleobiology 12:64–79

Saunders WB, Ward PD (1987) Ecology, distribution, and population characteristics of *Nautilus*. In: Saunders WB, Landman NH (eds) *Nautilus*: the biology and paleobiology of a living fossil. Plenum, New York, pp 137–162

Shapiro RS, Fricke H (2002) Tepee buttes: fossilized methane-seep ecosystems. In: Leonard EM et al (eds) High Plains to Rio Grande rift: Late Cenozoic evolution of Central Colorado, vol 3. Geological Society of America Field Guide, pp 94–101

Smrzka D, Zwicker J, Kolonic S et al (2017) Methane seepage in a Cretaceous greenhouse world recorded by an unusual carbonate deposit from the Tarfaya Basin, Morocco. Depositional Rec 3(1):4–37

Takeda Y, Tanabe K, Sasaki T et al (2016) Durophagous predation on scaphitid ammonoids in the Late Cretaceous Western Interior Seaway of North America. Lethaia 49(1):28–42
Tanabe K, Kruta I, Landman NH (2015) Ammonoid buccal mass and jaw apparatus. In: Klug C, Korn D, DeBaets K et al (eds) Ammonoid paleobiology. Springer, Cham, pp 429–484
Taylor DG, Guex J (2002) The Triassic/Jurassic system boundary in the John Day Inlier, east-central Oregon. Geology 64:3–28
Tobin TS, Ward PD (2015) Carbon isotope ($\delta^{13}C$) differences between Late Cretaceous ammonites and benthic mollusks from Antarctica. Palaeogeog Palaeoclimat Palaeoecol 428:50–57
Vidal EAG et al (2016) Cephalopod culture: current status of main biological models and research priorities. In: Vidal EAG (ed) Advances in cephalopod science: biology, ecology, cultivation and fisheries, Advances in marine biology. Elsevier, New York, pp 1–98
Ward PD (1987) The natural history of *nautilus*. Allen and Unwin, Boston
Wells MJ, Wells J (1985) Ventilation and oxygen uptake by *Nautilus*. J Exp Biol 118:297–312
Westermann GEG (1996) Ammonoid life and habitat. In: Landman NH, Tanabe K, Davis RA (eds) Ammonoid paleobiology. Plenum, New York, pp 607–707
Wierzbowski A, Hryniewicz K, Hammer Ø et al (2011) Ammonites from hydrocarbon seep carbonate bodies from the uppermost Jurassic-lowermost Cretaceous of Spitsbergen and their biostratigraphical importance. Neues Jahrb Geol Palaontol Abh 262(3):267–288
Williscroft K, Grasby SE, Beauchamp B et al (2017) Extensive Early Cretaceous (Albian) methane seepage on Elleff Ringnes Island, Canadian High Arctic. Geol Soc Am Bull 129(7/8):788–805
Witts JD, Little CTS (this volume) Fossil methane-seep deposits and communities from the Mesozoic of Antarctica. In: Kaim A, Cochran JK, Landman NH (eds) Ancient hydrocarbon seeps, Topics in geobiology. Springer, New York

Chapter 13
Echinoderms at Ancient Hydrocarbon Seeps and Cognate Communities

Jamie Brezina, Neal L. Larson, and Neil H. Landman

13.1 Introduction

Today, echinoderms are found in every corner of the seas and oceans, even on the seafloor below the ice in the Arctic and Antarctica. They are relatively common at modern hydrocarbon seeps, including, for example, the Gulf of Mexico (Pawson et al. 2015), the Mediterranean Sea (Zeppilli et al. 2011) and off the coast of California and Oregon (Torres et al. 2009). Echinoderms and other animals are attracted to these sites because they furnish a source of nutrients, both on the seafloor and in the overlying water column. Indeed, in a recent video, a brittlestar was observed preying upon a swimming squid (NOAA ship Okeanos Explorer expedition in 2017). Most echinoderms are mobile, allowing them to search for food at seep sites. In addition, echinoderms are attracted to hydrocarbon seeps due to the presence of carbonate crusts and structures that provide a hard substrate.

In contrast to their modern counterparts, echinoderms are rare at ancient hydrocarbon seeps, with only a few reported occurrences. Their rarity may be related to environmental parameters including water chemistry, oxygen levels, food availability and presence or absence of a hard substrate. In addition, echinoderms may not have been preserved as fossils due to their low preservation potential. In general, after death, echinoderms rapidly decay, and their skeletons become disarticulated

J. Brezina (✉)
Department of Mining Engineering, South Dakota School of Mines and Technology, Rapid City, SD, USA

N. L. Larson
Larson Paleontology Unlimited, Keystone, SD, USA

N. H. Landman
Department of Invertebrate Paleontology, American Museum of Natural History, New York, NY, USA
e-mail: landman@amnh.org

A. Kaim et al. (eds.), *Ancient Hydrocarbon Seeps*, Topics in Geobiology 50,
https://doi.org/10.1007/978-3-031-05623-9_13

(Hess et al. 2011; T. Oji, pers. comm., 2020). However, it is possible that the high rate of calcium carbonate precipitation at many seeps promoted their fossilization. Collecting bias might also be a factor in the low number of reported occurrences, as specimens may not be visible on the surface of the outcrop. Many new species of echinoderms have been discovered by screening and washing sediments and then examining the washed sediments for small fragments known as ossicles (spines, arms, plates and columnals). This chapter provides a brief overview of reported occurrences of echinoderms at ancient hydrocarbon seeps and cognate communities (e.g. wood falls). The list is organized alphabetically by region and will be more fully expanded upon in the future.

13.2 Occurrences

13.2.1 Antarctica

Occasional crinoid ossicles have been reported by Kelly et al. (1995) from the Late Jurassic (Tithonian) seep deposit in Alexander Island, Antarctica, which otherwise is dominated by gastropods and lucinid bivalves (Kaim and Kelly 2009).

13.2.2 England

An ichthyosaur fall was discovered in the Upper Jurassic (Oxfordian) Ringstead Clay Member in Dorset, England, by Danise et al. (2014). The ichthyosaur has been identified as a species of *Ophthalmosaurus*. Prior to burial, the skeleton was colonized by a benthic community—including echinoids. However, it is unlikely to have represented a fully formed chemosynthetic community because the sulfophilic stage was lacking and the scavenger stage was followed directly by the reef stage—this is rarely observed in modern examples of vertebrate falls (compare Smith and Baco (2003)). Simms (1999) also described several occurrences of crinoids associated with wood falls in Jurassic sediments of England. Most likely, as already suggested by Buckland (1837), these crinoids could have been pseudoplanktonic, living on driftwood for many years before it sank to the seafloor.

13.2.3 France

Upper Jurassic (Oxfordian) seep deposits have been documented from the Terres Noires Formation near Beauvoisin in Southeast France (Rolin et al. 1990). The seep deposits occur in grey to black marly shale similar to the Pierre Shale in North

America. The deposits contain concentrations of the irregular echinoid *Tithonia oxfordiana* Gaillard et al. 2011. According to Gaillard et al. (2011), the seeps may have acted as a refuge for this species.

13.2.4 Germany

The Jurassic (Toarcian) Posidonia Shale in Germany contains several examples of crinoids in close association with wood logs (e.g. Hess (1999)). The crinoids were apparently attached to the logs while they were still floating or after they sunk to the seafloor (Seilacher and Hauff 2004), thus forming a pseudoplanktic rather than a chemosynthetic community (Hunter et al. 2020).

13.2.5 Greenland

Lower Cretaceous seep deposits are present in Wollaston Foreland, Northeast Greenland, as described by Kelly et al. (2000) and Nakrem et al. (2020). Large echinoid spines have been observed at some of these sites (C.T.S. Little, pers. comm., 2019).

13.2.6 Italy

Numerous echinoid ossicles have been reported by Peckmann et al. (1999) from Miocene lucinid-dominated methane seep deposits in Marmorito, Northern Italy.

13.2.7 Japan

A number of ancient seep deposits are exposed in Japan but not all of them are fully explored. Crinoids have been documented from Cretaceous seep deposits in the Yezo Group in Hokkaido (Kato and Oji 2015; Kato 2019). The crinoids belong to the Isocrinidae (see Hess (2011)). They are not endemic to the seeps but occur elsewhere in the basin. In addition, *Isselicrinus* sp. has been discovered by Kazutaka Amano near or at a wood fall in the Katsuhira Formation in Urahoro Town, Eastern Hokkaido (Amano et al. 2018; A. Hunter, pers. comm. 2020).

13.2.8 Morocco

Several seep deposits are present in the Silurian and Devonian of Morocco (Jakubowicz et al. this volume). However, the origin of these deposits is unclear and they may reflect a mixture of cold and hydrothermal seepage. Stalked crinoids have been reported from some of these sites, although it is unknown if they were seep-obligate or opportunistic.

13.2.9 Namibia

Some crinoid ossicles have been reported from Upper Carboniferous seep carbonates in Southern Namibia (Himmler et al. 2008).

13.2.10 New Zealand

Some echinoid spines have been reported by Saether (2011) from Miocene seep deposits at Wanstead and Rocky Knob in New Zealand. The specimens from Rocky Knob have been identified as cidaroids (Saether 2011).

13.2.11 Novaya Zemlya

Hryniewicz et al. (2015) researched seep deposits from the Arctic Island of Novaya Zemlya. The deposits appear to date from the Late Jurassic/Early Cretaceous. Skeletal plates of echinoderms were identified in thin sections. Further research is needed at these localities to understand the paleoenvironment and composition of the seep communities.

13.2.11.1 Poland

The Bathonian (Middle Jurassic) clays in Poland contain several logs of wood supporting rich benthic communities (Kaim 2011). These communities include crinoids, echinoids, asteroids and ophiuroids. Kaim (2011) argued that the crinoids (*Balanocrinus* and *Chariocrinus*) settled on the wood when it was already on the sea bottom. Therefore, the crinoids were benthic rather than pseudoplanktonic. These associations represent Jurassic wood-fall communities, which, in contrast to their modern counterparts, do not contain chemosymbiotic animals. This disparity results from the absence of xylophagain wood-boring bivalves. These bivalves

produce significant numbers of faecal pellets, the decomposition of which increases the amount of sulphide around sunken driftwood.

13.2.12 Svalbard

Numerous fossil seep deposits are present in Spitsbergen in the Svalbard Archipelago (Hammer et al. 2011; Hryniewicz et al. 2014). The deposits occur in the uppermost Volgian-Ryazanian (Jurassic-Cretaceous) Slottsmøya Member of the Agardhfjellet Formation. The carbonate bodies occur in a dark shale, similar to sites in France and the USA. Crinoid ossicles belonging to the Isocrinidae and echinoid test plates are present but rare, in these deposits.

13.2.13 Turkey

Kiel et al. (2017) reported echinoderm fragments in methane seep deposits from the Upper Triassic (upper Carnian-lower Norian). The sites are located within the Kasımlar Basin from the Anamas Akseki autochthon in the Taurus Mountains in Southern Turkey.

13.2.14 Washington State, USA

Hybersten and Kiel (2018) described a middle Eocene cold seep deposit at the Weatherwax site in the basal Humptulips Formation along the West Fork of Satsop River in Washington State. The deposit contains silicified fossils including echinoid spines. Goedert and Squires (1993) noted spatangoid echinoids and crinoid ossicles (*Isocrinus*?) in an Oligocene seep deposit at Murdock Creek, and Goedert and Peckmann (2005) also reported echinoderms from an Eocene seep deposit near Knappton, both in Washington State. In addition, Goedert and Campbell (1995) documented seep deposits containing echinoid spines in the Lower Oligocene Makah Formation in the northwestern Olympic Peninsula of Washington State near Shipwreck Point.

13.2.15 Western Interior, USA

Methane seep deposits are very abundant in the Northern Great Plains of North America (Larson et al. 2013; Landman et al. this volume). The seeps developed in the Late Cretaceous Western Interior Seaway (WIS). Hundreds of metres of

organic-rich sediments extending from the Middle to Upper Jurassic Sundance Formation up through the Upper Cretaceous Pierre Shale and Bearpaw Shale are the likely sources of hydrocarbons. Due to plate tectonics, the western and central regions of the USA were slowly uplifted, creating fractures and faults during the Laramide orogeny. These fractures and faults probably provided pathways for pore waters, hydrocarbons, minerals and gases to escape towards the surface. These underlying mechanisms are the key to understanding seep development in the WIS.

In general, echinoderms are rare in the Upper Cretaceous of the Western Interior of North America. However, the rapid rate of carbonate precipitation at the sediment-water interface at some methane seeps probably increased the chances of echinoderm preservation. Indeed, many of the fossils from these sites are preserved in exquisite detail. Exploration, mapping and research are ongoing in this region as new species and new localities are discovered (Brezina et al. in preparation). Future exploration will also yield additional clues to understanding the formation of these seep deposits.

Gill and Cobban (1966) documented fragments of asteroids (starfish) near seep deposits in the Pierre Shale on the Old Woman Anticline in eastern Wyoming. Subsequently, several species of echinoderms have been reported from seep deposits in the upper Campanian *Didymoceras cheyennense* Zone of the Pierre Shale in South Dakota (Figs. 13.1 and 13.2). These include a regular echinoid (*Gauthieria* sp.), an irregular echinoid (*Hemiaster* sp.) a feather star comatulid crinoid (*Glenotremites brezinai* (in press)), a brittlestar (ophiuroid) (*Brezinacantha tolis* Thuy et al., 2018), a starfish (asteroid) (*Betelgeusia brezinai* Blake et al., 2018), and a stalked crinoid (*Lakotacrinus brezinai* Hunter et al., 2016). Many of these same species also occur in seep deposits in the overlying upper Campanian *Baculites compressus* and *B. cuneatus* Zones of the Pierre Shale in South Dakota (Larson et al. 2013; Landman et al. 2010; Larson et al. 1997; Hunter et al. 2016; Kato et al. 2017). A few additional specimens of echinoids (*Hemiaster humpreysanus* and *Eurysalenia minima*) have also been discovered near or at seep deposits in the lower Maastrichtian *B. eliasi* and *B. baculus* Zones of the Pierre Shale on the Cedar Creek Anticline in Montana (Ryan et al. 2020).

The brittlestar (ophiuroid) *Brezinacantha tolis* is present in a methane seep deposit in the Pierre Shale of western South Dakota (Fig. 13.2a–c). The specimens are concentrated at the edge of the seep deposit. They appear as a mass occurrence, all cemented together. The individuals at the top of the mass are articulated whereas those at the bottom are disarticulated, consisting of fragments and ossicles. Thuy et al. (2018) suggested that these brittlestars may have inhabited the same area for an extended period of time and, following death, were cemented together by seep carbonates.

The stalked crinoid *Lakotacrinus brezinai* is present in upper Campanian seep deposits in the Pierre Shale of Nebraska, South Dakota, Montana, and Colorado (Fig. 13.2f–h). It has, so far, not been reported from elsewhere in the basin and may have been restricted to the seeps. Because it lacks a holdfast, it may have drifted from one area of a seep to another or even to an adjacent seep in the same seep field. It is preserved in small concretions (SACs) or loose in the shale. It also occurs in

Fig. 13.1 Echinoderms from hydrocarbon seep deposits, Upper Cretaceous (upper Campanian) Pierre Shale, western South Dakota, USA. (**a**) Irregular echinoid *Hemiaster* sp., AMNH 82711, AMNH loc. 3420. (**b**) Irregular echinoid *Hemiaster* sp., AMNH 82710, AMNH loc. 3419. (**c**) Irregular echinoid *Hemiaster* sp., AMNH 82713, AMNH loc. 3419. (**d**) Regular phymosomatoid echinoid, AMNH 82705, AMNH loc. 3509. (**e**) Regular phymosomatoid echinoid, AMNH 82706, AMNH loc. 3509. (**f**) Regular phymosomatoid echinoid, AMNH 82707, AMNH loc. 3509. (**g**) Regular phymosomatoid echinoids, AMNH 82716, AMNH loc. 3654. (**h**) Comatulid crinoid (feather star) *Glenotremites brezinai*, calyx, AMNH 164729, AMNH loc. 3529. See Appendix Table 13.1 for locality details

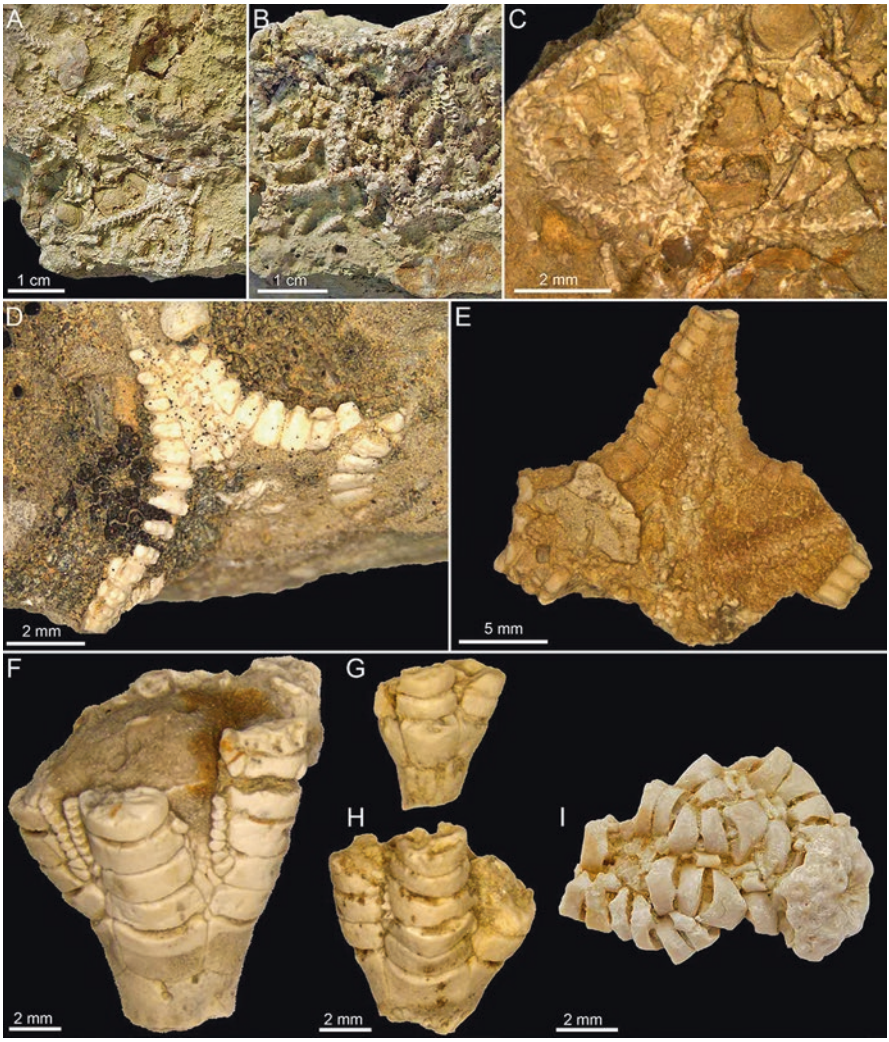

Fig. 13.2 Echinoderms from methane seep deposits, Upper Cretaceous (upper Campanian) Pierre Shale, western South Dakota, USA. (**a**) Brittlestar (ophiuroid) *Brezinacantha tolis* Thuy et al., 2018, AMNH 164730, AMNH loc. 3509a. (**b**) Brittlestar (ophiuroid) *Brezinacantha tolis* Thuy et al., 2018, AMNH 113585, AMNH loc. 3509a. (**c**) Brittlestar (ophiuroid) *Brezinacantha tolis* Thuy et al., 2018, AMNH 164731, AMNH loc. 3509a. (**d**) Asteroid (starfish) *Betelgeusia brezinai* Blake et al., 2018, AMNH 164732, AMNH loc. 3529. (**e**) Asteroid (starfish) *Betelgeusia brezinai* Blake et al., 2018, AMNH 111823, AMNH loc. 352. (**f**) Stalked crinoid *Lakotacrinus brezinai* Hunter et al., 2016, juvenile partial crown, AMNH 84500, AMNH loc. 3509b. (**g**) Stalked crinoid *Lakotacrinus brezinai* Hunter et al., 2016, juvenile partial crown, AMNH 84495, AMNH loc. 3509b. (**h**) *Lakotacrinus brezinai* Hunter et al., 2016, juvenile partial crown, AMNH 84499, AMNH loc. 3509b. (**i**) Comatulid crinoid (feather star) *Glenotremites brezinai*, partial crown, AMNH 161016, AMNH loc. 3529. See Appendix Table 13.1 for locality details

association with large tabular plates consisting of whole or broken inoceramid shells. These plates probably formed a carbonate crust that was rapidly cemented together at the time, producing a hard substrate. *Lakotacrinus brezinai* persisted for at least 3 Myr of the 6–7 Myr of recorded seepage around the Black Hills and eastern Rocky Mountain Region.

Kato et al. (2017) analysed the carbon isotopic composition of *Lakotacrinus brezinai* for clues to its mode of life. The values of $\delta^{13}C$ of the skeletal material are very low and range from −32‰ to −11‰. Given the highly specialized morphology of *L. brezinai*, in combination with its low $\delta^{13}C$ values, Kato et al. (2017) argued that it was adapted to cold seep environments, in agreement with the earlier suggestion of Hunter et al. (2016) that this species was probably an obligate member of the chemosynthetic community. In contrast, the morphology and carbon isotopic composition of the echinoids at the same seep sites are not significantly different from those at non-seep sites, suggesting that the echinoids were opportunistic rather than obligate members of the chemosynthetic community (Kato et al. 2017). It is worth noting, however, that the isotopic composition of echinoderms as well as other fossil materials from the Upper Cretaceous Western Interior is sometimes subject to alteration due to post-depositional processes (Hunter et al. 2018; Kato et al. 2018).

13.3 Conclusions

Echinoderms are rare in ancient hydrocarbon seep deposits and other unique environments, possibly due to several factors like low preservation potential. Most of them represent background fauna that colonized the seep from elsewhere in the seaway or oceanic basin. Modern hydrocarbon seeps, hydrothermal vents and cognate communities host a wide range of echinoderms including starfish, brittlestars, feather stars, holothuroids and echinoids. New species are regularly being described from these sites. Future exploration of ancient methane seep deposits will also lead to new discoveries and a better understanding of the paleoenvironments in which these communities developed.

Acknowledgments The authors would like to thank the private landowners, ranchers and farmers for allowing access to seep sites, the USDA Forest Service for allowing research permits, the private collectors for allowing access to collections and their donations and the countless fellow worldwide researchers that made this collaboration and research possible. We would also like to thank all of the teachers, professors and students involved in this ongoing project. Special thanks to ranchers in western South Dakota, Wyoming and Montana, granting J. Brezina access to private property. The authors thank J. Kirk Cochran (Stony Brook University) and Andrzej Kaim (Institute of Paleobiology, Polish Academy of Science) for help in editing the manuscript and organizing the bibliography. We also thank Selina R. Cole (US National Museum of Natural History) for reviewing the manuscript and making many helpful suggestions.

Appendix

Table 13.1 AMNH localities, Pierre Shale. Abbreviations: *B. comp.= Baculites compressus; D. chey. = Didymoceras cheyennense;* study number is a way point number (WPT) assigned by J. Brezina

Loc.	Study no. (WPT)	Zone	State	County	TRS	Latitude (N)	Longitude (W)
3419	61	*B. comp.*	SD	Custer	SEC 30 T3S, R11E	43° 45′ 41″	102° 51′ 9″
3420	61	*D. comp.*	SD	Custer	SEC 19, T3S, R11E	43° 46′ 15″	102° 51′ 26″
3509	130A, B	*D. chey.*	SD	Pennington	SEC 15, T2S, R10E	43° 52′ 39″	102° 54′ 40″
3529	140	*D. chey.*	SD	Pennington	SEC 3, T2S, R10E	43° 54′ 22″	102° 54′ 27″
3654	136	*D. chey.*	SD	Custer	SEC10, T5S, R9E	43° 37′ 50″	103° 2′ 26″

References

Amano K, Jenkins RG, Kurita H (2018) New and Mesozoic-relict mollusks from Paleocene wood-fall communities in Urahoro Town, eastern Hokkaido, northern Japan. J Paleontol 92:634–647

Blake DB, Halligan WK, Larson NL (2018) A new species of the asteroid genus *Betelgeusia* (Echinodermata) from methane seep settings, Late Cretaceous of South Dakota. J Paleontol 92(2):196–206

Brezina et al (in preparation) Fossil echinoderms in methane seep deposits from the Upper Cretaceous Pierre Shale in the Western Interior of North America

Buckland W (1837) Geology and mineralogy, considered with respect to natural theology: v. 6, The Bridgewater treatises: pt. 1: 1–618; pt. 2: 1–129, 69 pl., London, Wm. Pickering

Danise S, Twitchett RJ, Matts K (2014) Ecological succession of a Jurassic shallow-water ichthyosaur fall. Nature Commun 5:4789

Gaillard C, Neraudeau D, Thierry J (2011) *Tithonia oxfordiana*, a new irregular echinoid associated with Jurassic seep deposits in south-east France. Palaeontology 54:735–752

Gill JR, Cobban WA (1966) The Red Bird section of the Upper Cretaceous Pierre Shale in Wyoming. USGS Prof Pap 393-A:1–73

Goedert J, Campbell KA (1995) An early Oligocene chemosynthetic community from the Makah Formation, northwestern Olympic Peninsula, Washington. Veliger 38:22–29

Goedert JL, Peckmann J (2005) Corals from deep-water methane-seep deposits in Paleogene strata of Western Oregon and Washington, U.S.A. In: Freiwald A, Roberts JM (eds) Cold-water corals and ecosystems. Springer, Berlin, pp 27–40

Goedert JL, Squires RL (1993) First Oligocene records of *Calyptogena* (Bivalvia: Vesicomyidae). Veliger 36:72–77

Hammer O, Nakrem HA, Little CTS, Hryniewicz K et al (2011) Hydrocarbon seeps from close to the Jurassic–Cretaceous boundary, Svalbard. Palaeogeogr Palaeoclimatol Palaeoecol 396:15–26

Hess H (1999) Lower Jurassic Posidonia Shale of Southern Germany. Fossil Crinoids:183–196

Hess H (2011) Isocrinida. In: Hess H, Messing CG, Ausich WI (eds) Treatise on invertebrate paleontology, Part T, Echinodermata 2 revised, Crinoidea, vol 3. University of Kansas Press, Lawrence, pp 42–69

Hess H, Ausich WI, Brett CE, Simms MJ (2011) Fossil Crinoids. Palaeontology 54:735–752

Himmler T, Freiwald A, Stollhofen H, Peckmann J (2008) Late Carboniferous hydrocarbon-seep carbonates from the glaciomarine Dwyka Group, southern Namibia. Palaeogeogr Palaeoclimatol Palaeoecol 257:185–197

Hryniewicz K, Nakrem HA, Hammer Ø et al (2014) The palaeoecology of the latest Jurassic-earliest Cretaceous hydrocarbon seep carbonates from Spitsbergen, Svalbard. Lethaia 48:353–374

Hryniewicz K, Hagström J, Hammer Ø et al (2015) Late Jurassic–Early Cretaceous hydrocarbon seep boulders from Novaya Zemlya and their faunas. Palaeogeogr Palaeoclimatol Palaeoecol 436:231–244

Hunter AW, Larson NL, Landman NH et al (2016) A new crinoid from cold methane seep deposits in the Upper Cretaceous Pierre Shale. J Paleontol 90(3):506–524

Hunter AW, Larson NL, Brezina J (2018) Comment to Kato et al. (2017), "Paleoecology of echinoderms in cold seep environments revealed by isotope analysis in the Late Cretaceous Western Interior Seaway". Palaios 33:282–283

Hunter AW, Casenove D, Mayers C, Mitchell EG (2020) Reconstructing the ecology of a Jurassic pseudoplanktonic raft colony. R Soc Open Sci 7(7):200142

Hybertsen F, Kiel S (2018) A middle Eocene seep deposit with silicified fauna from the Humptulips Formation in western Washington State, USA. Acta Palaeontol Pol 63:751–768

Jakubowicz M, Berkowski B, Hryniewicz K, Bełka Z (this volume) Middle Paleozoic of Morocco: the earliest-known Methane Seep Metazoan Ecosystems. In: Kaim A, Cochran JK, Landman NH (eds) Ancient Hydrocarbon Seeps. Topics in Geobiology, vol 50. Springer, New York

Kaim A (2011) Non-actualistic wood-fall associations from Middle Jurassic of Poland. Lethaia 44:109–124

Kaim A, Kelly SRA (2009) Mass occurrence of hokkaidoconchid gastropods in the Upper Jurassic methane seep carbonate from Alexander Island, Antarctica. Antarct Sci 21:279–284

Kato M (2019) Crinoids lived around the Cretaceous seeps: the second example from cold-seep deposit in the Yezo Group in Hokkaido, Japan. Zoosymposia 15:88–97

Kato M, Oji T (2015) Comparison of fossil echinoderms from Upper Cretaceous cold seep environments between Japan and central United States. Paper presented at Japan Geoscience Union Meeting, Makuhari, Chiba, Japan, 24–28 May 2015

Kato M, Oji T, Shirai K (2017) Paleoecology of echinoderms in cold seep environments revealed by isotope analysis in the Late Cretaceous Western Interior Seaway. Palaios 32:218–230

Kato M, Oji T, Shirai K (2018) Reply to comment on Kato et al. (2017) "Paleoecology of echinoderms in cold seep environments revealed by isotope analysis in the Late Cretaceous Western Interior Seaway". Palaios 33:284–285

Kelly SRA, Ditchfield PW, Doubleday PA, Marshall JD (1995) A late Jurassic methane-seep limestone from the Fossil Bluff Group forearc basin of Alexander Island, Antarctica. J Sediment Res A65:274–282

Kelly SRA, Blanc E, Price SP, Whitham AG (2000) Early Cretaceous giant bivalves from seep-related limestone mounds, Wollaston Forland, Northeast Greenland. Geol Soc London Spec Publ 177:227–246

Kiel S, Krystyn L, Demirtas F et al (2017) Late Triassic mollusk-dominated hydrocarbon-seep deposits from Turkey. Geology 45(8):751–754

Landman NH, Kennedy WJ, Cobban WA et al (2010) Scaphites of the '*nodosus* group' from the Upper Cretaceous (Campanian) of the Western Interior of North America. Bull Am Mus Nat Hist 342:1–242

Landman NH, Cochran JK, Brezina J et al (this volume) Methane Seeps in the Late Cretaceous Western Interior Seaway, USA. In: Kaim A, Cochran JK, Landman NH (eds) Ancient hydrocarbon seeps. Topics in geobiology, vol 50. Springer, New York

Larson NL, Jorgensen SD, Farrar RA et al (1997) Ammonites and the other cephalopods of the Pierre Seaway. Geoscience Press, Tucson

Larson et al (2013) Hydrocarbon Seeps: Unique habitats that preserved the diversity of fauna in the Late Cretaceous Western Interior Seaway

Nakrem HA, Little CTS, Kelly SRA (2020) Early Cretaceous hydrocarbon seep carbonates from Wollaston Forland, Northeast Greenland. NGF Abstr Proc Geol Soc Norw 1:149

Pawson DL, Nizinski MS, Ames CL, Pawson DJ (2015) Deep-sea echinoids and holothurians (Echinodermata) near cold seeps and coral communities in the northern Gulf of Mexico. Bull Mar Sci 91:167–204

Peckmann J, Thiel V, Michaelis W, Clari P, Gaillard C, Martire L, Reitner J (1999) Cold seep deposits of Beauvoisin (Oxfordian; southeastern France) and Marmorito (Miocene; northern Italy): microbially induced authigenic carbonates. Int J Earth Sci 88:60–75

Rolin Y, Gaillard C, Roux M (1990) Ecologie des pseudobiohermes des Terres Noires jurassiques liés à des paléo-sources sous-marine: le site oxfordien de Beauvoisin (Drôme, Bassin du sud-Est, France). Palaeogeogr Palaeoclimatol Palaeoecol 80:79–105

Ryan DR, Witts JD, Landman NH (2020) Palaeoecological analysis of a methane seep deposit from the Upper Cretaceous (Maastrichtian) of the U.S. Western Interior. Lethaia 54:185–203

Saether KP (2011) A taxonomic and palaeobiogeographic study of the fossil fauna of Miocene hydrocarbon seep deposits, North Island, New Zealand. PhD thesis archived at ResearchSpace@Auckland 7. https://researchspace.auckland.ac.nz/handle/2292/6676

Seilacher A, Hauff RB (2004) Constructional morphology of pelagic crinoids. Palaios 19(1):3–16

Simms MJ (1999) *Pentacrinites* from the Lower Jurassic of the Dorset coast of southern England. In: Hess H, Ausich WI, Brett CE, Simms MJ (eds) Fossil Crinoids. Cambridge University Press, Cambridge, pp 177–182

Smith C, Baco A (2003) Ecology of whale falls at the deep-sea floor. Oceanogr Mar Biol 41:311–354

Thuy B, Landman NH, Larson NL, Numberger-Thuy LD (2018) Brittle-star mass occurrence on a Late Cretaceous methane seep from South Dakota, USA. Sci Rep 8:9617

Torres ME, Embley RW, Merle SG et al (2009) Methane sources feeding cold seeps on the shelf and upper continental slope off central Oregon, USA. Geochem Geophys Geosyst 10:Q11003

Zeppilli D, Mea M, Corinaldesi C, Danovaro R (2011) Mud volcanoes in the Mediterranean Sea are hot spots of exclusive meiobenthic species. Progr Ocean 91(3):260–272

Chapter 14
Vertebrates: Skate and Shark Egg Capsules at Ancient Hydrocarbon Seeps

Tina Treude

14.1 Overview and Examples

Cold seeps have been recognized not only as exotic ecosystems but also as important places to provide nutrition, habitat, and shelter for non-seep organisms on continental margins around the world (Levin et al. 2016; Thurber et al. 2014). This ecological linkage emphasizes that seeps play an important role in maintaining deep-sea biodiversity. Today, studies suggest that such relationships existed over geological timescales. One example is the discovery of fossilized cat shark egg capsules, identified as *Scyliorhinotheca goederti*, at a late Eocene-aged Bear River methane-seep deposit in Western Washington, USA (Kiel et al. 2013; Treude et al. 2011). The capsules were preserved three-dimensionally and were enclosed in carbonates with $\delta^{13}C$ values as low as −36.5‰ VPDB, suggesting that carbonate formation was induced by the microbial anaerobic oxidation of methane (AOM) (Kiel et al. 2013). The presence of AOM-derived carbonates indicates that the originally collagenous capsules experienced a sudden shift from oxic to anoxic conditions, favoring AOM activity concomitant with an increase in alkalinity and the precipitation of aragonite. Together, these processes likely facilitated the preservation and mineralization of the capsules. In a final step, aragonitic parts of the capsule wall recrystallized to calcite.

The egg capsules (30 in total) that were recovered from the Bear River seep deposit have an inflated fusiform shape and a slightly constricted waist with maximum dimensions of 50 × 15 × 11 mm (length × width × thickness) (Kiel et al. 2013) (Fig. 14.1). Their anterior border is slightly concave, with two well-developed

T. Treude (✉)
Department of Earth, Planetary, and Space Sciences, University of California, Los Angeles, CA, USA

Department of Atmospheric and Oceanic Sciences, University of California, Los Angeles, CA, USA
e-mail: ttreude@g.ucla.edu

A. Kaim et al. (eds.), *Ancient Hydrocarbon Seeps*, Topics in Geobiology 50,
https://doi.org/10.1007/978-3-031-05623-9_14

Fig. 14.1 *Scyliorhinotheca goederti* (Kiel et al. 2013) egg capsules in 35 Ma cold seep carbonates from the Bear River Seep Deposit, Washington State, USA. (**a**) Internal mold of egg capsule embedded in cold seep carbonate (scale bar: 5 mm). (**b**) External and internal molds of egg capsules (scale bar: 4 mm). The ribbed capsule wall (white arrows) is visible, and fossilized worm tubes (black arrows) surround the capsules. (Figure from Treude et al. (2011), used with permission from Inter Research)

respiratory fissures but no horns. The posterior end has horns, which are short and pointing at, or twisting around, each other. The capsule wall thickness is approximately 100 μm. Individual capsule ribs are up to 700 μm high and between 100 and 150 μm wide. Several of the egg capsules show indentations that potentially formed after hatching of the young shark. Many capsules are only preserved as internal molds, while some are external molds. All capsules are found closely associated with abundant remains of bathymodiolin mussels, hexactinellid sponges, and tube worms (Treude et al. 2011), which provide good clinging objects, suggesting that the structured habitat was selected to avoid the eggs being dragged away by currents (Vazquez et al. 2018).

To the best of my knowledge, there are currently only a few other occurrences of elasmobranch egg capsules in the fossil record of seeps, from the Miocene of New Zealand (Rocky Knob), the Cretaceous of Canada (Prince Patrick Island), and California (Cold Fork Cottonwood Creek) (C. Little, pers. comm.). While such discoveries could be viewed as odd coincidences, findings of elasmobranch capsules at modern seeps suggest a more common ecological relationship (Treude et al. 2011). Similar to their fossil relatives, modern elasmobranchs such as the cat shark *Galeus melastomus* and the skate *Bathyraja* spp. appear to take advantage of the structured seep habitat by placing their egg capsules between sheltering tube worms and carbonate boulders. Seeps likely provide some of the few three-dimensional structures on the otherwise rather plain areas of the deep-sea floor.

Structured seep habitats have also been found to be used as egg nurseries by bony fish (blob sculpin *Psychrolutes phrictus*) and octopuses (*Graneledone* sp.) (Drazen et al. 2003). Recently, the release of pore fluids warmer than ambient sub-zero water temperatures at a Norwegian seep site has been postulated to aid egg incubation and prevent embryo mortality for the Arctic skate *Amblyraja hyperborea* (Sen et al. 2019). A conceptual summary of habitat structures offered by seeps is illustrated in Fig. 14.2. Future studies should pay attention to additional fossil evidence that could

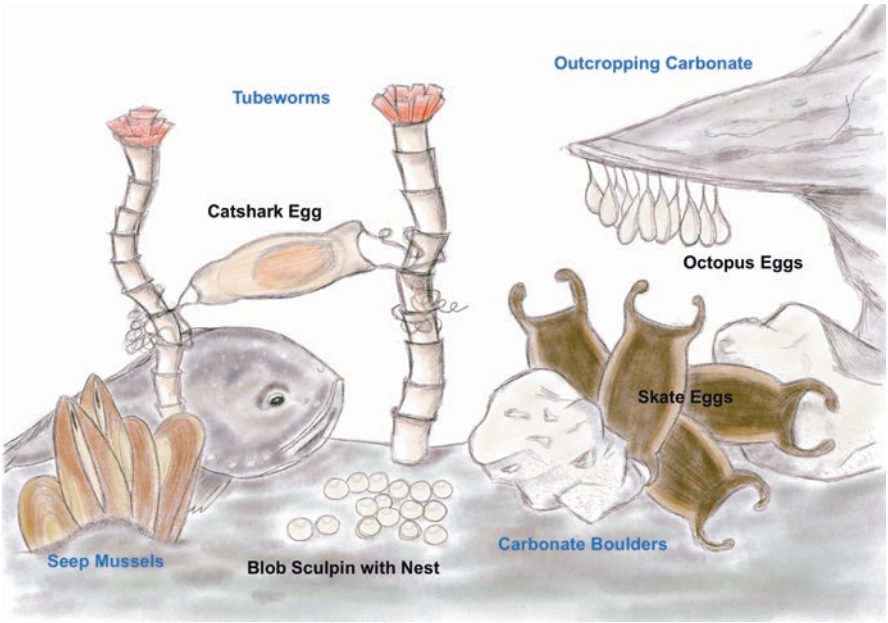

Fig. 14.2 Conceptual drawing of cold seep nursery. Habitat-forming seep organisms and structures in blue letters; organisms that take advantage of the seep habitat to lay their eggs in black letters: cat shark eggs are clinging to tube worms; octopus eggs are attached to outcropping carbonate; skate eggs are placed between carbonate boulders; and blob sculpin eggs are sheltered by different seep structures. Note that the sizes of animals and structures are not always to scale

confirm relationships between seep and non-seep ecosystems in the past. Some evidence, however, might be harder to detect depending on the preservational potential of the organisms and their eggs.

References

Drazen JC, Goffredi SK, Schlining B et al (2003) Aggregations of egg-brooding deep-sea fish and cephalopods on the Gorda Escarpment: a reproductive hot spot. Biol Bull 205(1):1–7

Kiel S, Peckmann J, Simon K (2013) Catshark egg capsules from a late Eocene deep-water methane-seep deposit in western Washington State, USA. Acta Palaeontol Pol 58(1):77–84

Levin LA, Baco AR, Bowden DA et al (2016) Hydrothermal vents and methane seeps: rethinking the sphere of influence. Front Mar Sci 3(72):1–23

Sen A, Himmler T, Hong WL et al (2019) Atypical biological features of a new cold seep site on the Lofoten-Vesterålen continental margin (northern Norway). Sci Repts 9(1):1–14

Thurber AR, Sweetman AK, Narayanaswamy BE et al (2014) Ecosystem function and services provided by the deep sea. Biogeosci 11(14):3941–3963

Treude T, Kiel S, Link P et al (2011) Elasmobranch egg capsules associated with modern and ancient cold seeps: a nursery for marine deep-water predators. Mar Ecol Prog Ser 437:175–181

Vazquez DM, Belleggia M, Schejter L et al (2018) Avoiding being dragged away: finding egg cases of *Schroederichthys bivius* (Chondrichthyes: Scyliorhinidae) associated with benthic invertebrates. J Fish Biol 92(1):248–253

Part III
Fossil Seep Ecosystems

Chapter 15
Methane Seeps in the Late Cretaceous Western Interior Seaway, USA

Neil H. Landman, J. Kirk Cochran, Jamie Brezina, Neal L. Larson, Matthew P. Garb, Kimberly C. Meehan, and Corinne Myers

15.1 Introduction

Hydrocarbon seep deposits, in one form or another, have been studied in the Upper Cretaceous Western Interior of North America since the end of the nineteenth century (Gilbert and Gulliver 1895). The broad geographic and stratigraphic distribution of these deposits suggests that they comprised one of the largest and most long-lived seep fields on the planet (Metz 2010). These seeps formed in the Western Interior Seaway (WIS) in relatively shallow water and attracted a wide variety of

N. H. Landman (✉)
Department of Invertebrate Paleontology, American Museum of Natural History, New York, NY, USA
e-mail: landman@amnh.org

J. K. Cochran
Department of Invertebrate Paleontology, American Museum of Natural History, New York, NY, USA

School of Marine and Atmospheric Sciences, Stony Brook University, Stony Brook, NY, USA

J. Brezina
Department of Mining Engineering, South Dakota School of Mines and Technology, Rapid City, SD, USA

N. L. Larson
Larson Paleontology Unlimited, Keystone, SD, USA

M. P. Garb
Department of Earth and Environmental Sciences, Brooklyn College, Brooklyn, NY, USA

K. C. Meehan
Department of Geology, University at Buffalo (SUNY, Buffalo), Buffalo, USA

C. Myers
Department of Earth and Planetary Sciences, University of New Mexico, Albuquerque, NM, USA

A. Kaim et al. (eds.), *Ancient Hydrocarbon Seeps*, Topics in Geobiology 50,
https://doi.org/10.1007/978-3-031-05623-9_15

organisms, including ammonites, inoceramids, gastropods, crabs, tube worms, echinoderms, and chemosymbiotic lucinids (Fig. 15.1). Most of the fauna comprised the same taxa as in the rest of the WIS, but it also included species that were unique to these sites.

The nature of these deposits has been debated since their discovery. Gilbert and Gulliver (1895) suggested, among other hypotheses, that these structures formed as the result of favorable conditions on the sea floor over long periods of time promoting the colonization of lucinid bivalves. Dane et al. (1937) speculated that the deposits formed as the result of precipitation due to submarine springs of low volume, but relatively high concentrations of calcium carbonate, producing hospitable sites for the growth of many kinds of organisms. Petta and Gerhard (1977) suggested that the deposits formed due to sediment baffling around grass beds in shallow marine lagoons, producing large mounds of carbonate mud. According to this hypothesis, the calcium carbonate in the deposits accumulated from the breakdown of calcareous chlorophytes and calcareous epibionts that were attached to the grasses. Not until the seminal studies of Kauffman et al. (1996), which utilized detailed isotopic, stratigraphic, and paleontologic data, did the methane seep origin of these deposits become apparent.

The specimens illustrated in this chapter are reposited in the Department of Invertebrate Paleontology at the American Museum of Natural History (AMNH), New York, New York. The sites in South Dakota, Wyoming, Montana, and Nebraska are referred to by AMNH locality numbers and study numbers (WPT) and are listed in Appendix Table 15.1.

15.2 Geologic Setting

During the Late Cretaceous, the Western Interior Foreland Basin was occupied by a broad seaway that extended from the proto-Gulf of Mexico to the western Canadian Arctic (Cobban and Reeside 1952; Gill and Cobban 1966; Kauffman and Caldwell 1993) (Fig. 15.2). The western shore of the WIS was bordered by a north-south trending unstable cordillera, and the eastern margin was formed by the low-lying stable platform of the eastern part of the conterminous USA and Canada (Cobban et al. 1994; Larson et al. 1997; Landman et al. 2010).

The geologic record of the Late Cretaceous WIS is rich in cephalopods and inoceramid bivalves, which has permitted a refined biostratigraphic zonation of this region. The ammonite zonation of the Upper Cretaceous Western Interior was first summarized by Cobban and Reeside (1952). Since then, it has undergone many revisions and presently consists of 66 zones, several of which are further subdivided into two, three, or four inoceramid zones. The presence of bentonites in the stratigraphic section has permitted determination of absolute ages based on $^{40}Ar/^{39}Ar$ analyses of the sanidines in the bentonites. We follow the standard biostratigraphic zonation of Cobban et al. (2006) in which the Campanian Stage is divided into three substages and the Maastrichtian Stage is divided into two substages (Fig. 15.2).

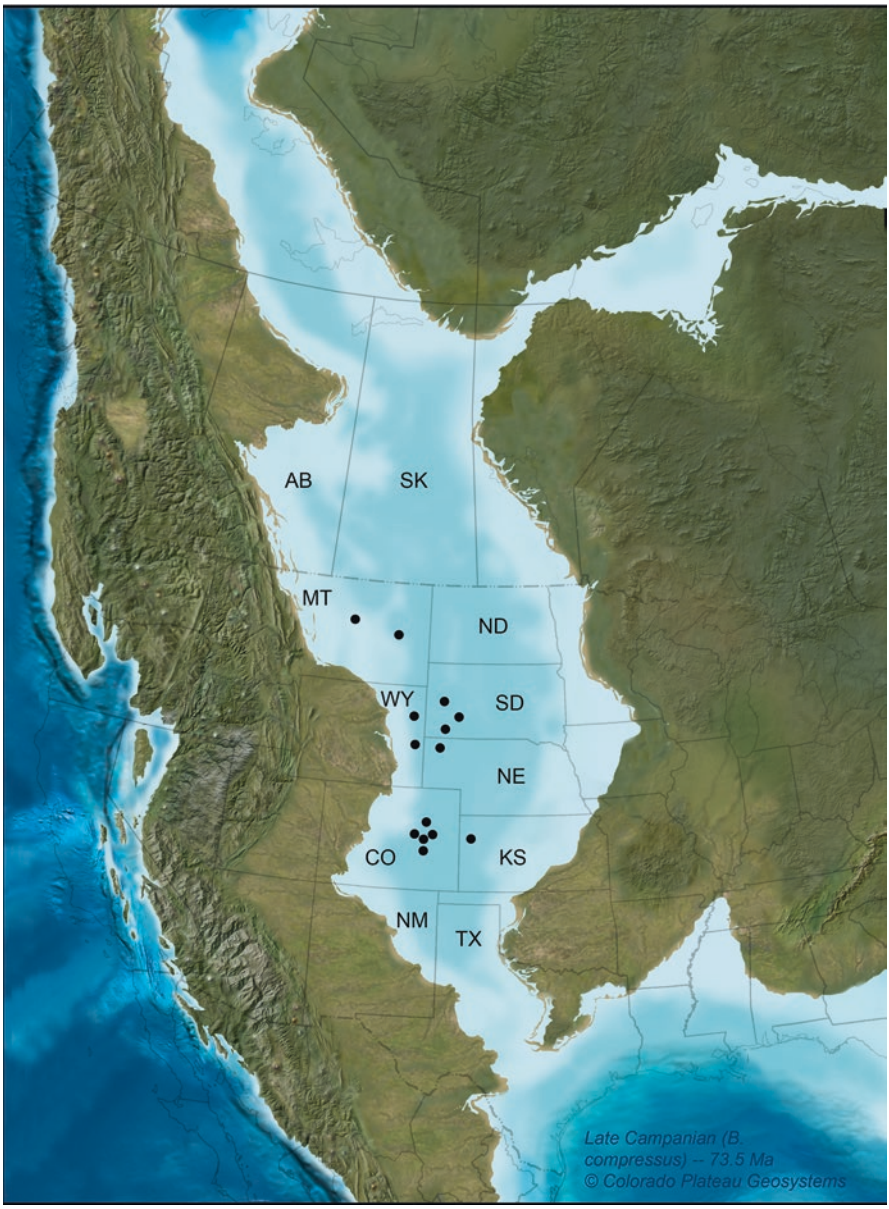

Fig. 15.1 Map of the Western Interior Seaway during the Late Cretaceous (late Campanian) showing main areas of methane seeps (dots) in Montana, Wyoming, South Dakota, Nebraska, Colorado, Utah, Kansas, and Texas (Blakey 2014, source map used with permission © 2021 Colorado Plateau Geosystems, Inc.). A single dot may represent multiple localities

SERIES	Stages	Substages	Ammonite zones	Inoceramid zones	Age (Ma)	Seeps
					66.0	
		Upper	*Hoploscaphites nebrascensis*			
			Hoploscaphites nicolleti			
			Hoploscaphites birkelundae			
	Maastrichtian	Lower	*Baculites clinolobatus*	*"Inoceramus" balchii*	69.59±0.36	
			Baculites grandis	*Trochoceramus radiosus*	70.00±0.45	*
			Baculites baculus	*"Inoceramus" incurvus*	71.96±0.08	
				Endocostea typica	71.98±0.31 72.50±0.31	*
UPPER CRETACEOUS (part)		Upper	*Baculites eliasi*	*"Inoceramus" redbirdensis*		*
			Baculites jenseni	*"Inoceramus" oblongus*		*
			Baculites reesidei		73.41±0.46	*
			Baculites cuneatus	*"Inoceramus" altus*		*
			Baculites compressus		73.79±0.36	**
			Didymoceras cheyennense		74.67±0.15	**
			Exiteloceras jenneyi	*Sphaeroceramus pertenuiformis*	75.08±0.11	*
			Didymoceras stevensoni		75.16±0.12	*
			Didymoceras nebrascense	*"Inoceramus" tenuilineatus*	75.19±0.28	***
	Campanian	Middle	*Baculites scotti*		75.56±0.11 75.84±0.26	***
			Baculites reduncus			
			Baculites gregoryensis			*
			Baculites perplexus	*Cataceramus subcompressus*		*
			Baculites sp. (smooth)			
			Baculites asperiformis			
			Baculites maclearni	*"Inoceramus" azerbaydjanensis*		
			Baculites obtusus		80.58±0.55	
		Lower	*Baculites* sp. (weak flank ribs)			
			Baculites sp. (smooth)	*Cataceramus balticus*		
			Scaphites hippocrepis III			
			Scaphites hippocrepis II		81.86±0.36	
			Scaphites hippocrepis I			
			Scaphites leei III	*Sphenoceramus lundbreckensis*	83.6±0.2	

Fig. 15.2 Biostratigraphic zonation of the Upper Cretaceous Western Interior (Cobban et al. 2006) showing intervals with methane seep deposits (asterisks). The number of asterisks indicates the relative abundance of seep deposits. Absolute ages are updated from Lynds and Slattery (2017) and Landman et al. (2018a, b)

During the Late Cretaceous, the WIS formed an episodically restricted, shallow epicontinental sea. The climate was warm during a "greenhouse" interval of Earth history, with little to no permanent polar ice and a latitudinal temperature gradient reduced by up to 50%, as compared with today (Barron 1983; Covey et al. 1996; Huber et al. 2002; Spicer and Corfield 1992; Jenkyns et al. 2004; Hay 2008). Eustatic as well as regional sea level oscillations significantly impacted water chemistry and mixing during the approximately 35 Myr in which the WIS was "open" to both the proto-Gulf of Mexico and Arctic Oceans. This has made detailed oceanography of the WIS challenging to reconstruct, but some aspects are clear. The WIS was generally shallow (≤100 m), with substantial input of freshwater from surface runoff and groundwater leaching from the cordillera (Kauffman 1984; Fricke et al. 2010; Cochran et al. 2003). Mixing of warmer, saltier waters from the south with colder, fresher waters from the north may have led to some degree of periodic water stratification and even at times a brackish water cap (Wright 1987; Corbett and Watkins 2013; Fisher and Arthur 2002; Schröder-Adams 2014; He et al. 2005). Periods of higher sea level (e.g., middle Campanian) likely reflected more "normal marine" environments in the WIS with better vertical mixing and an oxygenated bottom. In contrast, during periods of lower sea level (e.g., late Campanian-Maastrichtian), the WIS experienced significant restriction to open ocean circulation (especially to the north), and bottom waters became substantially less oxygenated (Kauffman 1984; Tsujita and Westermann 1998; Fisher and Arthur 2002; Schröder-Adams 2014).

15.3 Geomorphology of Seep Deposits

Seep deposits in the Upper Cretaceous Western Interior in the area around Pueblo, Boone, and Colorado Springs, Colorado, were called "tepee buttes" by Gilbert and Gulliver (1895) (Fig. 15.3a). They were so called because of their superficial resemblance to the tepees or lodges of the Shoshone and other American Plains Indians. These stony outcroppings are conical in shape and up to 20 m in height with circular bases up to 60 m in diameter and flat to pointed summits 3–8 m in diameter (Fenneman 1931). The top of each butte is held up by fossiliferous limestone blocks, which often tumble down the slopes, creating a layer of colluvium that protects the slopes from erosion. In classic tepee buttes, the surrounding soft shale has partially eroded away leaving the hard, resistant limestone projecting at the top, with soft sedimentary deformation features occasionally appearing underneath the limestone.

Seep deposits elsewhere in the Upper Cretaceous Western Interior can assume many other forms, however, depending on the size, shape, and lithology of the carbonates that make up the deposits (Figs. 15.3, 15.4 and 15.5). The abundance and distribution of fossils are also important factors in determining how the deposits appear. In some instances, for example, massive accumulations of indurated lucinids produce hard, resistant blocks that cover the surface of the deposits, making them resistant to erosion (Fig. 15.5b). The appearance of the deposits ultimately depends on how much weathering has taken place and how much of the surrounding

Fig. 15.3 Close-ups of methane seep deposits in the Pierre Shale of Colorado, Wyoming, South Dakota, and Nebraska. (**a**) Classic "tepee butte" along the Front Range of Colorado, as illustrated by Gilbert (1896: pl. 67). (**b**) Overview of seep deposits at AMNH loc. 3494, *Baculites scotti-Didymoceras nebrascense* Zones, Pierre Shale, Weston County, Wyoming. Photo by S. Klofak. (**c**) Overview of seep deposit at AMNH loc. 3812, Pierre Shale, Custer County, South Dakota. The seep deposit forms a long ridge approximately 100 m in length with a lower mound at one end and a higher mound on the other end, so that the total difference in height is approximately 10 m. The fossils at the bottom belong to the *D. cheyennense* Zone, and the fossils at the top belong to the *B. compressus* Zone. (**d**) Close-up of seep deposit at AMNH loc. 3344, *B. scotti-D. nebrascense* Zones, Pierre Shale, Butte County, South Dakota. Photo by B. Brown. E. Seep deposit near AMNH loc. 3344, *B. scotti-D. nebrascense* Zones, Pierre Shale, Butte County, South Dakota. Photo by B. Brown. (**f**) Overview of seep deposits, AMNH loc. 3666, *B. scotti-D. nebrascense* Zones, Pierre Shale, Sioux County, Nebraska. These are among some of the largest fossil seep deposits on the planet

Fig. 15.4 Methane seep deposits in the Pierre Shale, South Dakota. Photos by S.M. Klofak and M.P. Garb. (**a**) Exposure of seep deposit in cross section revealing the main carbonate body (arrow), AMNH loc. 3528, *Baculites compressus* Zone, Pierre Shale, Meade County, South Dakota. (**b**) Exposure of seep deposit in cross section, AMNH loc. 3504, *B. compressus* Zone, Pierre Shale, Custer County, South Dakota. The main carbonate body (arrow) is approximately 2.5 m wide. (**c**) Exposure of seep deposit in cross section, AMNH 3418, *Didymoceras cheyennense* Zone, Pierre Shale, Custer County, South Dakota. (**d**) Close-up of pipes (arrow) at AMNH loc. 3418, *D. cheyennense* Zone, Pierre Shale, Custer County, South Dakota. E. Specimen of *Placenticeras* sp. embedded in shale at AMNH loc. 3528, *B. compressus-B. cuneatus* Zones, Pierre Shale, Meade County, South Dakota. (**f**) Close-up of pipes and subspherical SACs at AMNH loc. 3528, *B. compressus* Zone, Pierre Shale, Meade County, South Dakota

host rock still remains. It is important to emphasize that the shape of the deposits in the present-day landscape may bear little resemblance to their shape as topographic features on the ancient sea floor.

Seep deposits in the Upper Cretaceous Western Interior also appear as steep chimneys or pinnacles informally known as “rock haystacks” 5–10 m in height and

Fig. 15.5 Methane seep deposits in the Pierre Shale, South Dakota. Photos by M.P. Garb. (**a**) Exposure of seep deposit in cross section, AMNH loc. 3440, *Didymoceras nebrascense* Zone, Pierre Shale, Butte County, South Dakota. (**b**) Close-up of specimens of *Nymphalucina occidentalis*, AMNH loc. 3440, *D. nebrascense* Zone, Pierre Shale, Butte County, South Dakota. (**c**) Seep deposit, AMNH loc. 3529, *D. cheyennense* Zone, Pierre Shale, Pennington County, South Dakota. (**d**) Seep deposit, AMNH loc. 3419, *Baculites compressus* Zone, Pierre Shale, Custer County, South Dakota. (**e**) Micritic mass, AMNH loc. 3545, *B. compressus-B. cuneatus* Zones, Pierre Shale, Meade County, South Dakota. (**f**) Close-up of micritic mass with burrow markings, AMNH loc. 3545, *B. compressus-B. cuneatus* Zones, Pierre Shale, Meade County, South Dakota

2–3 m in diameter with all of the surrounding shale eroded away, as exposed in the area around Newell, Butte County, South Dakota (Fig. 15.3f). Seep deposits can form large grass-covered mounds informally known as "ant hills" as much as 20 m in height with circular bases 10–20 m in diameter, for example, in Weston County, Wyoming (Fig. 15.3b). Like tepee buttes, the ant hills are capped by limestone blocks, but the sides of the deposits are more gently inclined. Occasionally, multiple ant hills coalesce together forming elongate ridges several 100 m in length, with a series of small peaks along the tops of the ridges, for example, in Sioux County, Nebraska, which may represent some of the largest seep deposits on the planet (Fig. 15.3f).

Seep deposits can also appear as low-lying, hard limestone mounds free of grass cover, roughly elliptical in outline with dimensions of 30 m × 15 m and as much as 5 m high, bearing an uncanny resemblance to Paleozoic reefs, as in the deposits in the Ojinaga Formation, Texas, and those in the Pierre Shale in Custer County, South Dakota (Fig. 15.5c, d). They can also appear as small broken-up masses of carbonate rubble with dimensions of 2 m × 2 m and 0.5 m high, which can usually be spotted from a distance by a break in the vegetation (Fig. 15.3d). Indeed, changes in the vegetation are a clue to the existence of a seep deposit because of the presence of the carbonates themselves and iron and sulfur minerals in the shale. Finally, the deposits can appear in cross section in stream and river cuts (Fig. 15.4a–c). In these exposures, the light-gray-weathering, massive carbonate bodies stand out in sharp contrast to the surrounding gray- to black-weathering shales (Fig. 15.5e, f).

15.4 Geographic Distribution

Methane seep deposits are geographically widespread throughout the Upper Cretaceous Western Interior (Fig. 15.6). From west to east, they stretch from south-central Colorado along the Front Range of the Rockies (Kauffman et al. 1996) to western Kansas (Elias 1933). They occur as far south as Presidio County, West Texas (Metz 2002), and southern Utah (Kiel et al. 2012). In the area around the Black Hills, they occur in northeastern Wyoming (Landman et al. 2013), northwestern South Dakota (Landman et al. 2013), southwestern South Dakota (Larson et al. 2014; Cochran et al. 2015; Hunter et al. 2016), and northwestern Nebraska. In Montana, they are present on the Miles City Arch in Carter County, on the Porcupine Dome in Garfield and Rosebud counties, on the Cedar Creek Anticline in Dawson County (Landman et al. 2020; Ryan et al. 2020), in the Cat Creek and Devils Basin oilfields in Petroleum and Musselshell counties, and in the Fort Peck area in McCone and Valley counties. They occur as far north as Alberta, Canada (Collom and Johnston 2000). Based on the distribution of seep deposits in Colorado, South Dakota, Montana, Wyoming, and Kansas, Landman et al. (2012) estimated that they cover an area of 13,350 km^2. However, this figure is undoubtedly an underestimate, as it is biased by the limited availability of outcrops. In fact, pieces of seep carbonates are occasionally found on gravel bars along the streams and rivers draining the

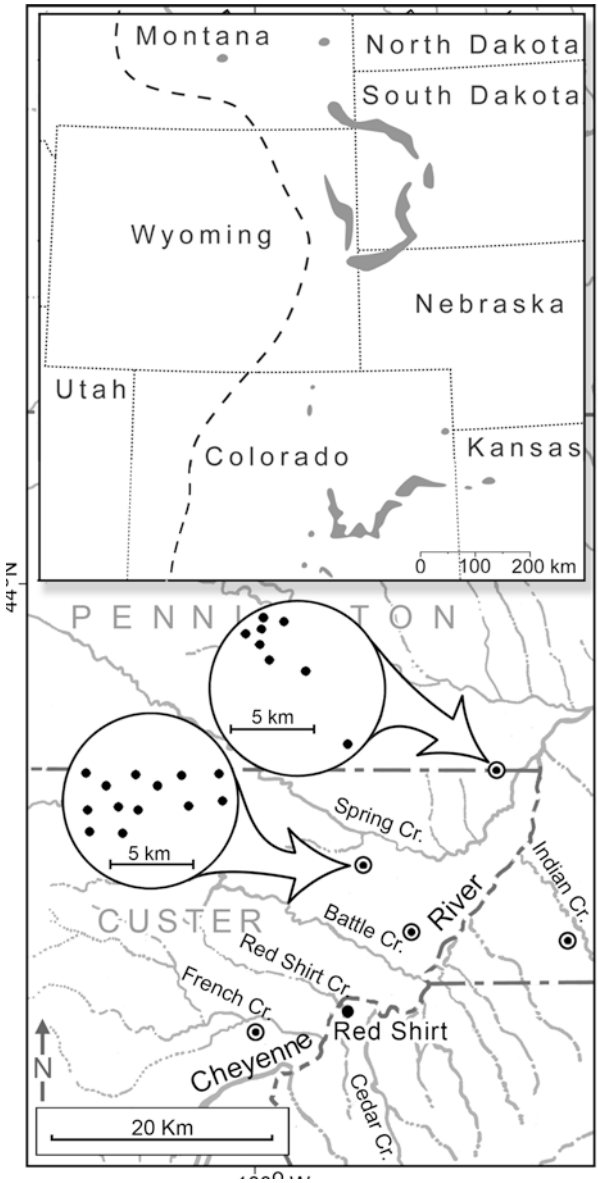

Fig. 15.6 Overview: Distribution of seep deposits in the Upper Cretaceous Western Interior Seaway (shaded locations of seeps in the top panel from Metz (2010)). The dashed line represents the western shoreline of the WIS during the deposition of the *Didymoceras cheyennense* Zone. Close-up: Distribution of methane seeps in the *D. cheyennense* and *Baculites compressus* Zones of the Pierre Shale in southwestern South Dakota

Black Hills, especially in western South Dakota, suggesting the existence of additional seep deposits, now eroded away.

The distribution of seep deposits has been mapped in minute detail in certain areas. In the region around the Black Hills in South Dakota and Wyoming, seep deposits have been mapped by Darton (1902, 1904, 1905, 1919), Darton and O'Hara (1909), Darton and Paige (1925), and Mapel and Pillmore (1963); in Colorado, they have been mapped by Fisher (1906), Finlay (1916), Lavington (1933), and Sharps (1976, 1980); and in Kansas by Elias (1931). These maps reveal the ubiquity of the deposits. For example, in 1 mi^2 section just east of Oelrichs, Fall River County, South Dakota, Darton (1902) mapped 45 seep deposits (Fig. 15.7). In 1 mi^2 section north of Newell, Butte County, South Dakota, Darton (1919) mapped 65 deposits (Fig. 15.8). Altogether, Metz (2010) counted 1350 seep deposits based on an examination of the geologic maps of Colorado and South Dakota prepared by the US Geological Survey between 1895 and 1936.

In addition to their abundance, two other patterns emerge in examining the geographic distribution of these deposits. First, they usually occur in clusters. For example, in the map by Darton (1919) of Fall River County, South Dakota, as many as six deposits occur in tight clusters (Fig. 15.7). Second, the seep deposits usually occur in linear arrangements. For example, in the map cited above, as many as 12 deposits occur in a straight line over a distance of approximately 1 km. These patterns may reflect the original distribution of seeps on the sea floor. They may further reflect fault lines that existed in the basin during the Late Cretaceous and facilitated upward fluxes of methane toward the sediment-water interface. Indeed, Gilbert (1897) noted that seep deposits in the area near Pueblo, Colorado, are oriented in a north-south belt paralleling the Rocky Mountains Front, possibly reflecting faults associated with the Laramide orogeny (Metz 2010). Larson et al. (2014) also suggested that seeps around the Black Hills formed from fluids and gasses migrating along faults and fractures in the Late Cretaceous prior to the uplift of the Black Hills (see below).

It is important to emphasize, however, that the present-day distribution of seep deposits is limited by the available outcrop. The availability of outcrop depends on such features as anticlines that bring rocks of the appropriate age to the surface. It also depends on the pattern of streams and rivers that erode the landscape to expose these rocks. Therefore, the abundance of seep deposits today is an underestimate of the original number of seeps on the sea floor. It is likely that they formed extensive seep fields covering broad stretches of the basin.

15.5 Stratigraphic Distribution

Methane seep deposits formed in the Western Interior of North America from the late Cenomanian to the early Maastrichtian (Fig. 15.2). The oldest methane seep deposits occur in the upper Cenomanian *Metoicoceras geslinianum* and *Neocardioceras juddi* Zones in the Tropic Shale of Utah (Kiel et al. 2012). The next younger deposits occur in the upper Coniacian *Scaphites* (*S.*) *depressus* Zone in the

Fig. 15.7 Map of tepee buttes near Newell, Butte County, South Dakota (Darton 1919). The dots represent seep deposits

oolitic limestones of the Bad Heart Formation of Alberta (Collom and Johnston 2000). The next younger deposits occur in the lower Campanian *Submortoniceras tequequitense* Zone in the upper Ojinaga Formation of the Sierra Vieja region, Presidio County, West Texas (Metz, 2002).

The rest of the seep deposits in the Upper Cretaceous Western Interior occur in the Pierre Shale in Colorado, Kansas, Wyoming, South Dakota, Nebraska, and

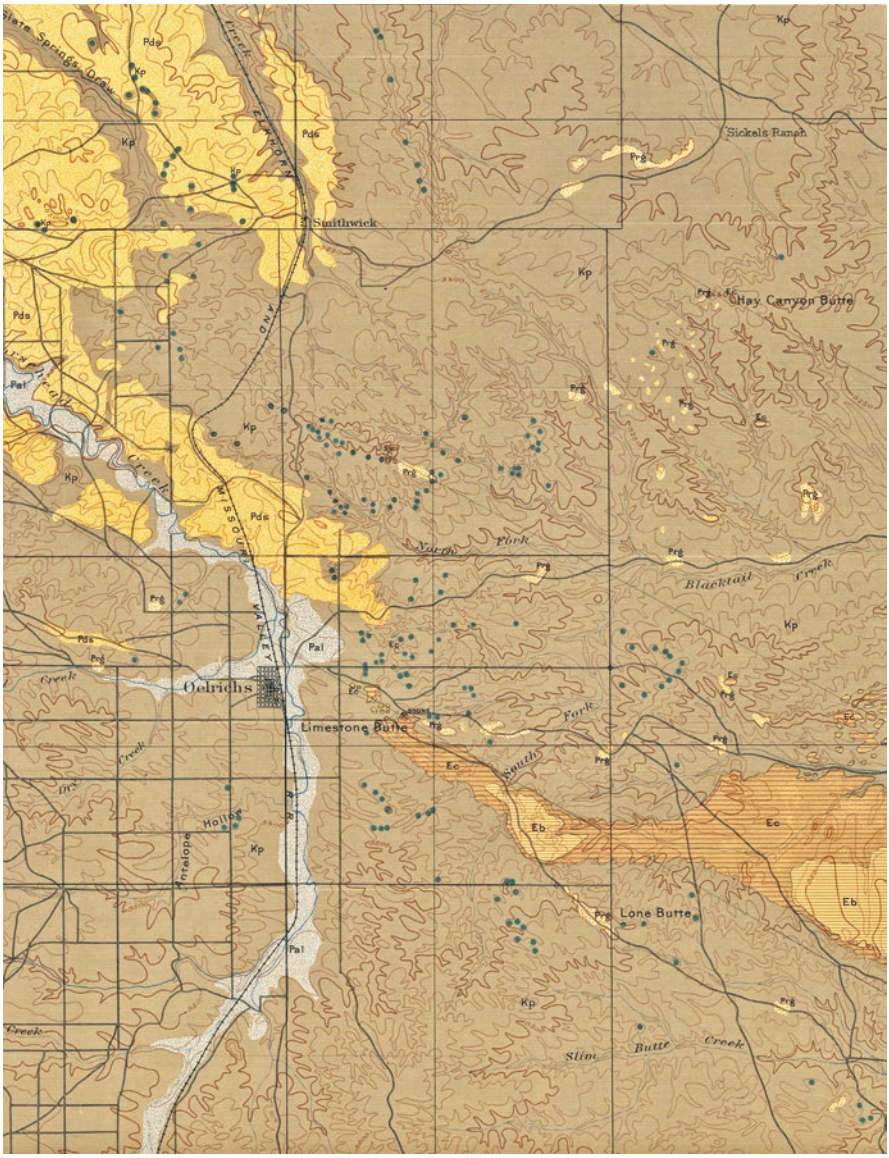

Fig. 15.8 Map of tepee buttes near Oelrichs, Custer County, South Dakota (Darton 1902). The dots represent seep deposits

Montana and the Bearpaw Shale in Montana and Canada (time equivalent to the upper Pierre Shale). The Pierre Shale is approximately 1000 m thick at its informal reference section at Red Bird, Wyoming, and consists of organic-rich dark- to light-gray-weathering clayey to silty shale (Gill and Cobban 1966). The seep deposits in the Pierre Shale extend from the middle Campanian to the lower Maastrichtian,

spanning 6–7 Myr (Fig. 15.2). However, the abundance and geographic extent of the seep deposits in the Pierre Shale vary throughout this time interval.

The oldest seep deposits in the Pierre Shale occur in the middle Campanian *Baculites perplexus* and *B. gregoryensis*Zones, but these deposits have only been reported from two sites. Gill and Cobban (1966) reported tepee butte deposits of this age from the upper part of the Mitten Shale Member and lower part of the Red Bird Silty Member of the Pierre Shale in Niobrara County, east-central Wyoming. Scott and Cobban (1986b) reported tepee butte deposits from the *B. gregoryensis* Zone in the uppermost beds of the Mitten Shale Member near Round Butte, Colorado.

The most widespread and abundant seep deposits in the Pierre Shale occur in the upper middle Campanian *Baculites scotti* and lower upper Campanian *Didymoceras nebrascense* Zones. These are the deposits that were originally described as tepee buttes from Colorado (Fig. 15.3a) by Gilbert and Gulliver (1895). They occupy what is called "the tepee butte zone" of the Pierre Shale near Fountain, Pueblo, and Boone in east-central Colorado (Gilbert 1897; Lavington 1933; Scott 1969; Scott and Cobban 1986a; Kauffman et al. 1996, Bishop and Williams 2000). These deposits are also present in other areas of Colorado including the Cañon City-Florence area, north of Walsenburg, west of Gardner at Huerfano Park (Scott and Cobban 1975; Howe and Kauffman 1986), west of Colorado Springs between Hugo and Kit Carson (Lavington 1933), west of Berthoud (Lavington 1933; Scott and Cobban 1965), and near Round Butte (Scott and Cobban 1986b).

Seep deposits of this age are also common in parts of South Dakota, Wyoming, and Nebraska. They are present in Weston and Crook counties in northeastern Wyoming (Landman et al. 2013); Butte County in northwestern South Dakota (Darton 1919; Bishop and Williams 2000; Landman et al. 2013); Pennington, Meade, Custer, and Fall River counties in southwestern South Dakota (Darton 1902; Bishop and Williams 2000; Landman et al. 2012; Larson et al. 2014; Hunter et al. 2016; Kato et al. 2017); and Sioux County in northwestern Nebraska. Seep deposits have also been identified from the two overlying zones (*Didymoceras stevensoni* and *Exiteloceras jennyi* Zones) in Carter County, Montana.

The second most widespread and abundant seep deposits in the Pierre Shale occur in the upper Campanian *Didymoceras cheyennense*, *Baculites compressus*, and *B. cuneatus* Zones. These deposits are locally common in Meade, Pennington, and Custer counties, southwestern South Dakota (Darton 1902, 1919; Landman et al. 2012, 2018a, b; Larson et al. 2014; Hunter et al. 2016; Kato et al. 2017). Elias (1933) also reported seep deposits of this age in the upper part of the Weskan Shale Member of the Pierre Shale in Wallace County, western Kansas.

In the upper part of the upper Campanian, seep deposits are present, but they have not yet been well documented. They occur in the *B. reesidei* and possibly *B. jenseni* Zones in the Bearpaw Shale on the Porcupine Dome and Cat Creek Anticline, Montana, and in the *B. reesidei-B. eliasi* Zones in the Salt Grass Member of the Pierre Shale in Wallace County, western Kansas (Elias 1933). They also occur in the *B. eliasi* Zone in the upper part of the Pierre Shale southwest of Longmont, Colorado (Scott and Cobban 1965), and in the same zone in the Kara Bentonitic

Member and overlying part of the Pierre Shale in Crook and Weston Counties, Wyoming (Robinson et al. 1959, 1964).

In the lower Maastrichtian, seep deposits occur in the *Baculites baculus* Zone in the lower part of the upper unnamed shale member of the Pierre Shale in Niobrara County, Wyoming (Gill and Cobban 1966). They occur at the base of this zone in the Pierre Shale on the Cedar Creek Anticline in Dawson County, Montana (Landman et al. 2019, 2020; Ryan et al. 2020). Finally, seep deposits have been reported from the *B. grandis* and *B. clinolobatus* Zones in the Beecher Island Shale Member of the Pierre Shale in Wallace County, western Kansas (Elias 1933).

15.6 Methods of Study

The seep deposits in the Upper Cretaceous US Western Interior have been extensively studied over the last 25 years. Over the course of these studies, samples of limestone and well-preserved shell material have been analyzed for carbon, oxygen, and strontium isotopes (Kauffman et al. 1996; Krauss et al. 2009; Landman et al. 2012, 2018a, b; Cochran et al. 2015). Shell material has been screened to determine the quality of preservation according to the *Preservation Index (PI)* published by Cochran et al. (2010), utilizing only material with PI $\geq$3 for isotopic analyses. The mineralogy of the limestones has been studied in bulk and thin section using scanning electron microscopy (SEM), X-ray diffraction analysis (XRD), and electron microprobe (EMP). The limestone has also been analyzed for biomarkers to detect the former presence of sulfate-reducing bacteria (Birgel et al. 2006).

The structural framework and faunal composition of the seep deposits have been examined in detail. The seep deposits from the *Baculites scotti-Didymoceras nebrascense* Zones of the Pierre Shale of Colorado have been investigated by Howe (1987) and Kauffman et al. (1996) by taking blocks of limestone along the long and short axes of deposits as well as from the surrounding shale. The blocks were 30 cm × 30 cm and were extracted at 1 m intervals, labeled, and brought back to the laboratory for polishing and dissection. In contrast, the seep deposits from the *B. scotti-B. baculus* Zones of the Pierre Shale of South Dakota, Wyoming, Nebraska, and Montana, were sampled by intensive surface collecting and breaking off fresh chunks of limestone. Wherever feasible, fossils were collected in situ. However, it is always possible to confound variation in spatial distribution with variation in stratigraphic distribution due to downward slide of material. Samples were brought back to the laboratory for identification, preparation, and isotopic analysis (Landman et al. 2012; Meehan and Landman 2016; Hunter et al. 2016; Rowe et al. 2020; Ryan et al. 2020).

Some seep deposits were fortuitously exposed in cross section along stream and river cuts allowing for a detailed analysis of the seep structure and faunal distribution. Fossils and seep-associated concretions (SACs) were mapped with respect to their distance from the main carbonate body. At AMNH loc. 3418 from the *Didymoceras cheyennense* Zone of the Pierre Shale, Custer County, South Dakota,

the face of the exposure was mapped using a grid work of ropes attached to the outcrop to subdivide the deposit into 1 m^2 sections, allowing us to record the location of fossils and SACs (Fig. 15.4c, d). In these instances, it was theoretically possible to tease out spatial from stratigraphic variation, but even here, it is not always easy to trace the same event bed throughout the stratigraphic section.

15.7 Oxygen and Carbon Isotopic Composition

The oxygen and carbon isotopic composition of seep carbonates and associated shells of well-preserved fossils provides important clues about the seep environment. Values of $\delta^{13}C$ of seep carbonates are commonly much lower than those in age-equivalent non-seep deposits elsewhere in the basin (Fig. 15.9). For example, in seep deposits from the upper Cenomanian *Metoicoceras geslinianum* and *Neocardioceras juddi* Zones in the Tropic Shale of Utah, the values of $\delta^{13}C$ range from −25‰ to −21‰ at one site and −37‰ to −33‰ at another site (Kiel et al. 2012). In seep deposits from the lower Campanian *Submortoniceras tequequitense* Zone in the upper Ojinaga Formation of the Sierra Vieja region, Presidio County, West Texas, the values of $\delta^{13}C$ range from −35‰ to −26‰ at one site and −36‰ to −28‰ at another site (Metz 2002). In seep deposits from the middle Campanian *Baculites scotti*-upper Campanian *Didymoceras nebrascense* Zones of the Pierre Shale in Colorado, the values of $\delta^{13}C$ range from −45‰ to −40‰ (Kauffman et al. 1996). In seep deposits from the upper Campanian *D. cheyennense* Zone of the Pierre Shale in South Dakota, the values of $\delta^{13}C$ range from −47‰ to −12‰ (Landman et al. 2012). In seep deposits from the upper Campanian *B. compressus*-*B. cuneatus* Zones of the Pierre Shale in South Dakota, the values of $\delta^{13}C$ range from −51‰ to −37‰ (Landman et al. 2018). Finally, in seep deposits from the lower Maastrichtian *B. baculus* Zone of the Pierre Shale in Montana, the values of $\delta^{13}C$ range from −51.5‰ to −49.5‰ (Ryan et al. 2020).

In comparison, the values of $\delta^{13}C$ of concretionary matrix ($CaCO_3$) at age-equivalent non-seep sites are higher. For example, in the concretionary matrix at non-seep sites in the upper Campanian *Baculites compressus*-*B. cuneatus* Zones of the Pierre Shale in South Dakota, the value of $\delta^{13}C$ equals −22‰ (Landman and Klofak 2012). In the concretionary matrix at non-seep sites in the lower Maastrichtian *B. baculus* Zone of the Pierre Shale in Montana, the values of $\delta^{13}C$ range from −13‰ to −10‰ (Landman et al. 2015). The lower values of $\delta^{13}C$ of the carbonates in seep deposits compared with those in age-equivalent non-seep deposits are the result of the influence of anaerobic oxidation of methane (AOM) on the isotopic composition of the dissolved inorganic carbon (DIC) reservoir from which the seep carbonates precipitated (Boetius et al. 2000) (Fig. 15.9). (See Cochran et al. this volume, for further discussion of seep geochemistry; see the section on Faunal Composition for a comparison between the carbon isotopic compositions of well-preserved shell material at seep and age-equivalent non-seep sites.)

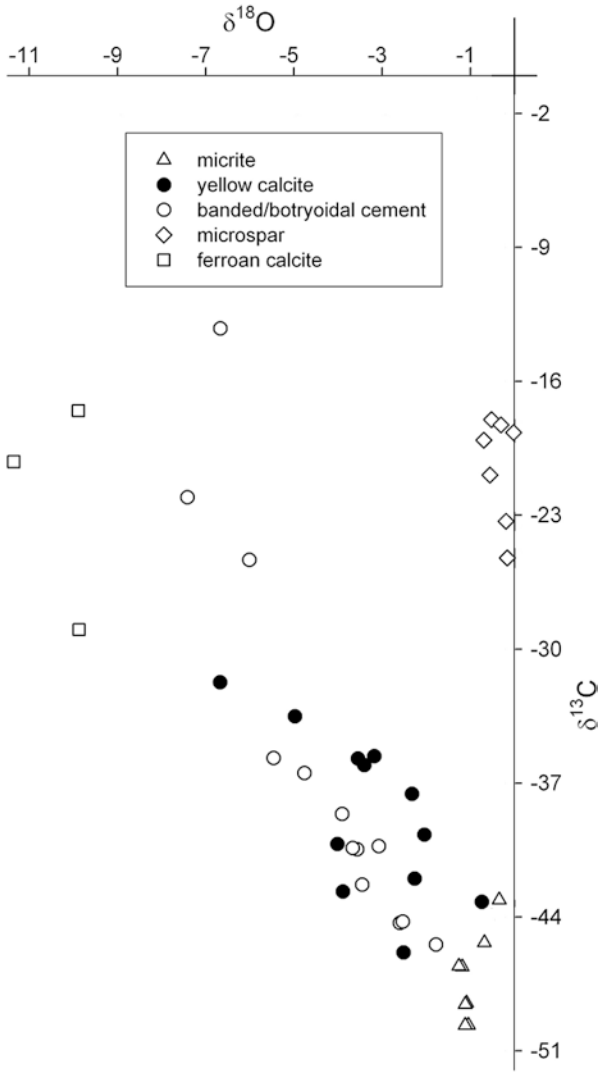

Fig. 15.9 Values of $\delta^{13}C$ and $\delta^{18}O$ of the seep carbonates from the *Baculites scotti-Didymoceras nebrascense* Zones of the Pierre Shale of Colorado (data replotted from Krause et al. (2009)). The low values of $\delta^{13}C$ of the seep carbonates (triangles) are due to the anaerobic oxidation of methane

In contrast, the values of $\delta^{18}O$ of the carbonates and well-preserved shell material (e.g., *Baculites*) at seep sites are similar to those of carbonates and well-preserved shell material at age-equivalent non-seep sites in other parts of the basin. For example, in seep carbonates from the upper Campanian *B. compressus-B. cuneatus* Zones of the Pierre Shale in South Dakota, the values of $\delta^{18}O$ range from −1‰ to 0‰ (Landman et al. 2018a, b). Similarly, in samples of well-preserved shell material

from the same site, the average values of δ ^{18}O range from −2.5‰ to −0.3‰. In comparison, the value of δ^{18}O in the concretionary matrix from non-seep sites from the same time interval equals −2‰ (Landman and Klofak 2012). As well, in samples of well-preserved shell material from the same non-seep site, the average values of δ ^{18}O range from −2‰ to −1‰ (Cochran et al. 2010).

The values of δ^{18}O in the carbonates and well-preserved molluscan shell material at seep sites translate into water temperatures of 15–25 ° C, using the equation of Grossman and Ku (1986) modified by Hudson and Anderson (1989) and assuming a value of −1‰ for the oxygen isotopic composition of the WIS (Shackleton and Kennett 1975; Dennis et al. 2013). This temperature range overlaps with that derived from analysis of carbonates and well-preserved shell material (e.g., *Baculites*) at age-equivalent non-seep sites elsewhere in the basin (e.g., He et al. (2005), Landman and Klofak (2012), Landman et al. (2015, 2018a, b). This similarity implies that the seep deposits were not hydrothermally driven but formed at the same temperature as the ambient water and thus are "cold" seeps (for more on modern cold seeps, see Kiel (2010)).

The isotopic values of the late burial cements in seep deposits exhibit a trend toward lower values of δ^{18}O and higher values of δ^{13}C (Kauffman et al. 1996). Krause et al. (2009) performed a series of analyses on the micritic limestone, ferroan calcite, yellow calcite, and botryoidal cement in seep deposits from the middle Campanian *Baculites scotti* and upper Campanian *Didymoceras nebrascense* Zones of the Pierre Shale in Colorado (Fig. 15.9). The values of δ^{13}C in the micritic limestone range from −50‰ to −43‰, and the values of δ^{18}O range from −1‰ to 0‰. On the other end of the spectrum, the values of δ^{13}C of the ferroan calcite range from −29‰ to −18‰, and the values of δ^{18}O range from −11‰ to −10‰. These trends indicate a series of late-stage diagenetic alterations, likely influenced by meteoric water.

15.8 Origin of Methane

The likely source of most of the methane in the Upper Cretaceous Western Interior is biogenic, produced by the decomposition of sedimentary organic matter. The methane probably originated from the organic-rich Pierre Shale and underlying Niobrara Formation, Carlile Shale, Greenhorn Limestone, Belle Fourche Shale, and Mowry Shale, representing a thickness of as much as 1500 m. The low values of δ^{13}C of the carbonates in the seep deposits are consistent with the anaerobic oxidation of methane (AOM) (Boetius 2000). Birgel et al. (2006) also analyzed the hydrocarbon and fatty acid fraction from samples of limestone in seep deposits from the middle Campanian *Baculites scotti* and upper Campanian *Didymoceras nebrascense* Zones of the Pierre Shale in Colorado. These samples preserve strongly ^{13}C-depleted biomarkers reflecting AOM produced by the consortium of methanotrophic Archaea and sulfate-reducing Bacteria (see Cochran et al. this volume).

In the WIS, the methane likely migrated to the sediment-water interface through a system of faults and fractures acting as a plumbing network. These features probably developed in association with increased tectonic activity during the initiation of the Laramide orogeny starting in the late Campanian. Indeed, Kaufmann et al. (1996) noted that the seep deposits in Colorado trend south-southeast to north-northwest parallel to the Colorado Front Range and Wet Mountains on the west side and southwest-northeast parallel to the Los Animas Arch on the east side. In addition, normal faults may have developed on the sea floor during the early stages of the Laramide orogeny (Tweto 1980). Landman et al. (2012) and Cochran et al. (2015) hypothesized that the seep deposits in the area of eastern Wyoming and western South Dakota originated due to the incipient uplift of the Black Hills during the late Campanian based on the values of $^{87}Sr/^{86}Sr$ in the seep deposits, relative to those in open marine systems at the time. In fact, seep deposits disappear toward the east of the Black Hills even though there is plenty of Pierre Shale, possibly due to the absence of an underlying fault system.

Metz (2010) suggested that the presence of methane seeps in the WIS was related to the position of the broad forebulge depozone in the basin. According to her hypothesis, an increase in the degree of flexure of the forebulge produced a topographic high, causing faults and fractures that promoted the migration of methane. During transgressions, for example, in the middle to late Campanian, the amount of sediment loading would have increased near the orogenic belt, resulting in an increase in the degree of flexure of the forebulge and elevated rates of methane release. In contrast, during regressions, the amount of sediment loading would have decreased near the orogenic belt resulting in a concomitant decrease in the degree of flexure and reduced levels of methane release. However, the idealized model of the foreland basin used by Metz (2010) in her arguments may not be applicable to the late Campanian-early Maastrichtian (see Larson et al. (2014)). Instead, the basin may have been subdivided into multiple fault blocks at this time in association with a change in the angle of subduction of the Farallon Plate (Cross 1986).

15.9 Seep Duration

During the deposition of the Pierre Shale, seep activity persisted from the middle Campanian *Baculites perplexus* Zone to the lower Maastrichtian *B. baculus* Zone, and possibly up to the *B. clinolobatus* Zone, spanning at least 6 Myr (Fig. 15.2). This may represent one of the longest known intervals of seep activity within a single basin in Earth history (see Hryniewicz this volume, for a compilation of fossil seeps of the world).

The temporal duration of a single seep in the WIS is difficult to determine. The most reliable way is to examine the ammonites (and inoceramids) at the bottom and top of a seep deposit to evaluate if they belong to the same or different biozone. The absolute ages of biozones are reasonably well constrained by radiometric dating of

bentonite beds (e.g., Cobban et al. (2006), Merewether and McKinney (2015), Landman et al. (2018a, b, 2020)).

AMNH loc. 3342 in Fall River County, South Dakota, is a grass-covered seep deposit 30 m high that exposes carbonates on the bottom and top. The fossils at the bottom belong to the *Baculites scotti* Zone, and the fossils at the top belong to the *Didymoceras nebrascense* Zone. The difference in age between these two zones equals 0.51 ± 0.34 Myr based on the radiometric ages published in Cobban et al. (2006). AMNH loc. 3812 in Custer County, South Dakota, is a seep deposit that forms a long ridge approximately 100 m in length with a lower mound at one end and a higher mound on the other end, so that the total difference in height between them is approximately 10 m (Fig. 15.3c). The fossils at the bottom belong to the *D. cheyennense* Zone, and the fossils on the top belong to the *B. compressus* Zone, corresponding to an age difference of 0.88 ± 0.39 Myr, based on the radiometric ages published in Cobban et al. (2006). Thus, the seep deposits at both sites span part or all of two ammonite zones, implying that seep activity may have lasted for as long as 0.5–0.9 million years.

15.10 Seep Structure and Faunal Distribution

Studies of the seep deposits in the Upper Cretaceous Western Interior reveal broad variation in seep structure and faunal composition. The structure of the seep deposits from the *Baculites scotti-Didymoceras nebrascense* Zones of the Pierre Shale in Colorado has been extensively studied by Howe (1987) and Kauffman et al. (1996) (see also Arthur et al. (1982), Howe and Kauffman (1986), Kauffman et al. (1990), Bishop and Williams (2000), Bash et al. (2005), Dahl et al. (2005), Anderson et al. (2005), and Larson et al. (2014)). Based on samples of in situ limestone blocks extracted from the seep deposits, they assembled a hypothetical model of seep structure featuring five faunal rings surrounding a central core (Fig. 15.10). The central part of the seep ("spring core facies") consists of a micritic, vuggy, peloidal limestone containing few fossils, mostly reworked lucinids, and a network of anastomosing burrows. Howe (1987) illustrated this facies in cross section as a continuous vertical deposit that interfingers with the surrounding shale.

The "spring core facies" is surrounded by a vuggy, peloidal limestone facies that Howe (1987) called the "*Nymphalucina* coquina." It contains a monospecific assemblage of lucinids in life position, many of which are hollow. The fact that the lucinids are preserved in life position suggests that they lived at the site and were buried in place (Fig. 15.10). The aragonitic shells of the lucinids have been replaced by clear blocky calcite and patches of fibrous chert (Krause et al. 2009). The interiors of the valves have been filled with geopetal structures consisting of peloidal grainstone and fibrous, botryoidal, magnesium (Mg)-rich calcite and clear, blocky, ferroan calcite spar (Fig. 15.11). The lucinids are encased in peloidal grainstone and fibrous, botryoidal, magnesium-rich calcite.

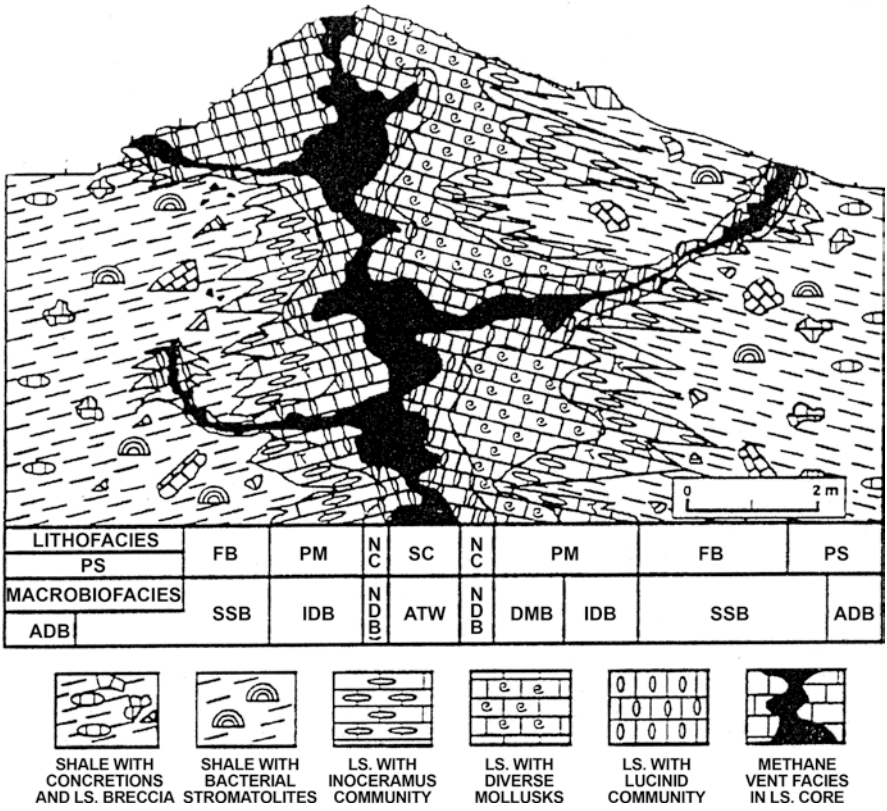

Fig. 15.10 Idealized cross section of a methane seep deposit in Colorado. Abbreviations: Lithofacies: *SC* spring core facies, *NC Nymphalucina* coquina, *PM* peloidal micrite facies, *FB* flank breccias in shale, *PS* concretionary Pierre Shale surrounding mound. Macrobiofacies (bottom): *ATW* agglutinated tube worm biofacies in vents, *NDB Nymphalucina*-dominated biofacies, *DMB* diverse molluscan biofacies, *IDB Inoceramus*-dominated biofacies, *SSB* bacterial (?) stromatolite-serpulid worm biofacies in proximal shales, *ADB* ammonite-dominated biofacies, with small bivalves and gastropods in concretions surrounding deposit (modified from Kauffman et al. (1996), used by permission of the Geological Society of America)

The "*Nymphalucina* coquina" is surrounded by the "brecciated facies," which is surrounded, in turn, by the "middle flank facies," both of which comprise most of the rest of the deposits and contain extensively recrystallized shell material (Fig. 15.10). At some sites, the middle flank facies borders the brecciated facies on the outside, but at other sites, the reverse is true. Both facies are vuggy with peloidal micrite. They contain lucinids, generally not in life position, and a diverse assemblage of other mollusks including ammonites, inoceramids, and gastropods. Some of the lucinids are fragmentary and occur in horizontal beds.

Both of these facies, and especially the brecciated facies, are characterized by fractures and micritic clasts. According to Shapiro and Fricke (2002), authigenic carbonates in seep deposits consist of a variety of fabrics that must have developed

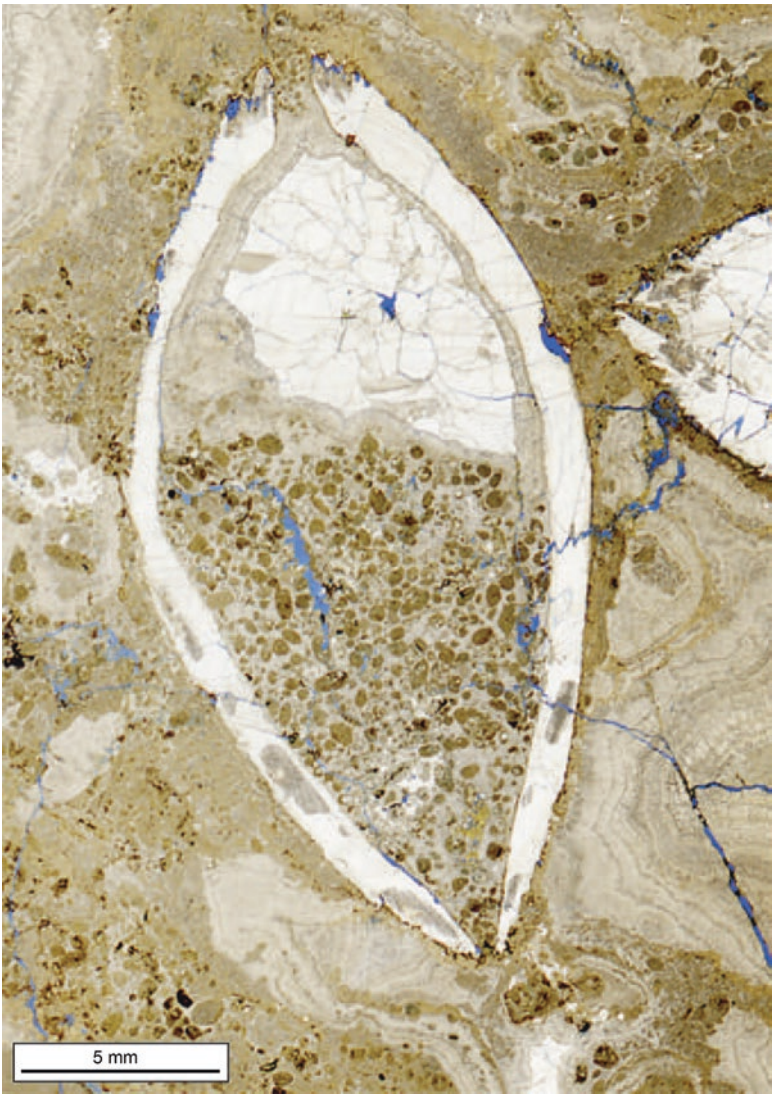

Fig. 15.11 Thin section of a lucinid from a seep deposit in the *Baculites scotti-Didymoceras nebrascense* Zones of the Pierre Shale, Colorado. (Modified from Krause et al. (2009))

at different times during diagenesis (see Hryniewicz et al. this volume). Several generations of early diagenetic cements reflect multiple episodes of dissolution (corrosion) and brecciation. The pelloids are the products of microbial activity or, more likely, fecal activity (Kiel, pers. comm., 2020). They are uncompacted and enclosed by fibrous to bladed calcite cements. The vugs are also lined with multiple generations of cements. Cracks in the micrite are filled with cements or intraclasts derived from the micrite.

Finally, Howe (1987) documented an "oncolite-mud" facies at the margins of the limestone (Fig. 15.10). It consists of abundant, small, irregular masses that Kauffman et al. (1996) identified as stromatolites. The masses are associated with large patchy areas of micrite with irregular, ragged edges. Howe (1987) also documented small pipes, tubes, and irregular limestone structures in the surrounding shale that Cochran et al. (2015) subsequently called "seep-associated concretions" (SACs). In addition, Howe (1987) noted what she called "slump blocks of limestone core and flank facies" in the surrounding shale and remarked that "the bedding of these slump blocks was disjunct with that of the surrounding shale." The faunal community in the surrounding shale is depauperate, dominated by inoceramids, but also contains lucinids and gastropods.

The structure of the seep deposits in Colorado has not been studied in detail since Howe (1987) and Kauffman et al. (1996). Seep deposits of approximately the same age (*Baculites scotti-Didymoceras nebrascense* Zones) are present around the Black Hills (South Dakota, Montana, Nebraska, and Wyoming). These deposits share many of the same structural features documented by Howe (1987). The most conspicuous among them are large masses of vuggy limestone consisting of peloidal micrite. The limestone contains whole and broken fossils, small clasts, and early diagenetic cements forming a porous, clotted texture. However, the concentric pattern of zonation of the facies observed in Colorado is not apparent.

For example, at AMNH loc. 3440, near Newell, Butte County, South Dakota, a large carbonate mass (the main carbonate body or "spring core facies") holds up the top of the deposit (Fig. 15.5a, b). The sides of the mound are covered with irregular pieces of vuggy, peloidal limestone containing abundant and diverse fossils. Numerous articulated lucinids are present, many of which are hollow. Similarly, at AMNH loc. 3386 in Butte County, South Dakota, the limestone is a biomicrite with large vugs up to 1.5 cm long. Lucinids are abundant and articulated, although not in life position, and are accompanied by a variety of other fossils including inoceramids and ammonites (Meehan and Landman 2016). Many lucinids as well as the phragmocones of ammonites are hollow, suggesting rapid burial and cementation before compaction. In addition, ammonite jaws are present, suggesting little transport after the death of the animals, followed by rapid burial (Landman et al. 2013).

The seep deposits from the *Baculites baculus* Zone of the Pierre Shale in Dawson County, Montana (AMNH loc. 3911), also feature large masses of vuggy limestone (Ryan et al. 2020). These deposits are of limited extent (2 m in diameter by 3 m in height) and consist of fossiliferous, peloidal limestone with few SACs. The fauna is dominated by lucinids, most of which are hollow, but also includes a wide variety of other species such as scaphites, nostoceratids, scaphopods, and echinoids. No concentric pattern of faunal distribution is apparent.

Studies of other seep deposits in the Pierre Shale reveal additional variation in seep structure and faunal distribution, which undoubtedly reflects variation in the concentration of methane in seep fluids and the rate and duration of methane emissions. In deposits from the *Didymoceras cheyennense* to *Baculites cuneatus* Zones in South Dakota, the main carbonate bodies are massive, with few vugs. They appear as globular, billowing, micritic limestones ranging up to 3 m in diameter and

up to 3 m in height. They widen and narrow up section and contain few fossils but are usually surrounded by a large number of fossiliferous SACs that vary in shape and composition (Figs. 15.12, 15.13 and 15.14).

An example of such a deposit is AMNH loc. 3529 from the *Didymoceras cheyennense* Zone of the Pierre Shale, Custer County, South Dakota (Fig. 15.5c). It features a massive, bulbous, micritic limestone body that holds up the top of the mound. The limestone contains a few fossils of inoceramids, lucinids, and baculites. It is surrounded by brown-weathering (oxidized) shale with orange partings that contains hundreds of tabular SACs forming platy, pavement-like coquinites. Most of the fossils occur in the SACs or loose in the weathered shale and consist of fragmentary and whole inoceramid shells as well as lucinids, gastropods, ammonites, crinoids, crustaceans, and asteroids. The SACs are not connected physically to the bulbous carbonate mass nor do they represent detached pieces of it but instead are embedded in the shale. Similar crusts are present at AMNH locs. 3419 and 3420 from the *Baculites compressus* Zone of the Pierre Shale, Custer County, South Dakota (Fig. 15.5d). The accompanying SACs are very fossiliferous and contain inoceramids, scaphites, and many species that require a hard substrate for attachment, such as sponges and crinoids.

The details of seep structure are visible in several deposits that are fortuitously exposed in cross section along river cuts. Study of these exposures further reveals the variation in seep structure among deposits and departures from the model described by Howe et al. (1987) and Kauffman et al. (1996). At AMNH loc. 3418 from the *Didymoceras cheyennense* Zone of the Pierre Shale, Custer County, South Dakota, the light gray bulbous mass is surrounded by dark gray shale (Fig. 15.4c, d). The mass is 2 m in diameter and 2.5 m in height. It is irregular in shape, with a few fossils, and interfingers with the surrounding shale. The sediments immediately surrounding the main body consist of brownish-gray calcareous shale with yellow and orange partings as well as the mineral melanterite, which is a product of pyrite weathering. The shale contains abundant SACs that are elongate and subspherical rather than angular or tabular in shape (Figs. 15.12 and 15.13). They range in size from 1 to 20 cm long, with smooth surfaces.

Landman et al. (2012) carefully documented the distribution of fossils at this site by gridding the outcrop into 1 m^2 quadrants and recording the fossils in each quadrant (Fig. 15.13). The fossil distribution does not conform to the concentric zonation model proposed by Howe (1987) and Kauffman et al. (1996). Lucinids, inoceramids, scaphites, and baculites are more abundant on the north side of the carbonate body at lower horizons and more abundant on the south side of the carbonate body at higher horizons, coinciding with the abundance of SACs in each area. This asymmetric distribution may reflect the fact that the locus of methane emission changed from the north to the south side of the site over time. Gastropods, although limited in number, are more abundant on the north side, and didymoceratids and spiroxybeloceratids are more abundant in the middle of the exposure. In areas of shale devoid of SACs, the only shelled organisms are inoceramids.

Fossils at this site extend up to a distance of 5 m on either side of the large carbonate mass and are usually preserved in three dimensions with their original

Fig. 15.12 SACs (seep-associated concretions) from seep deposits in the Pierre Shale of South Dakota (reprinted from Cochran et al. (2015); http://creativecommons.org/licenses/by/4.0/). (**a**) Portion of a large pipe 30 cm long x 10 cm diameter composed of Mg-rich calcite with apatite and pyrite (AMNH 64594, AMNH loc. 3545, Meade County). (**b**) Irregular SAC (AMNH 80770, AMNH loc. 3419, Custer County). (**c**) Subspherical SAC (AMNH 645611, AMNH loc. 3528, Meade County). (**d**) Platy SAC (top view) containing inoceramids and lucinids (AMNH 108407, AMNH loc. 3529, Pennington County)

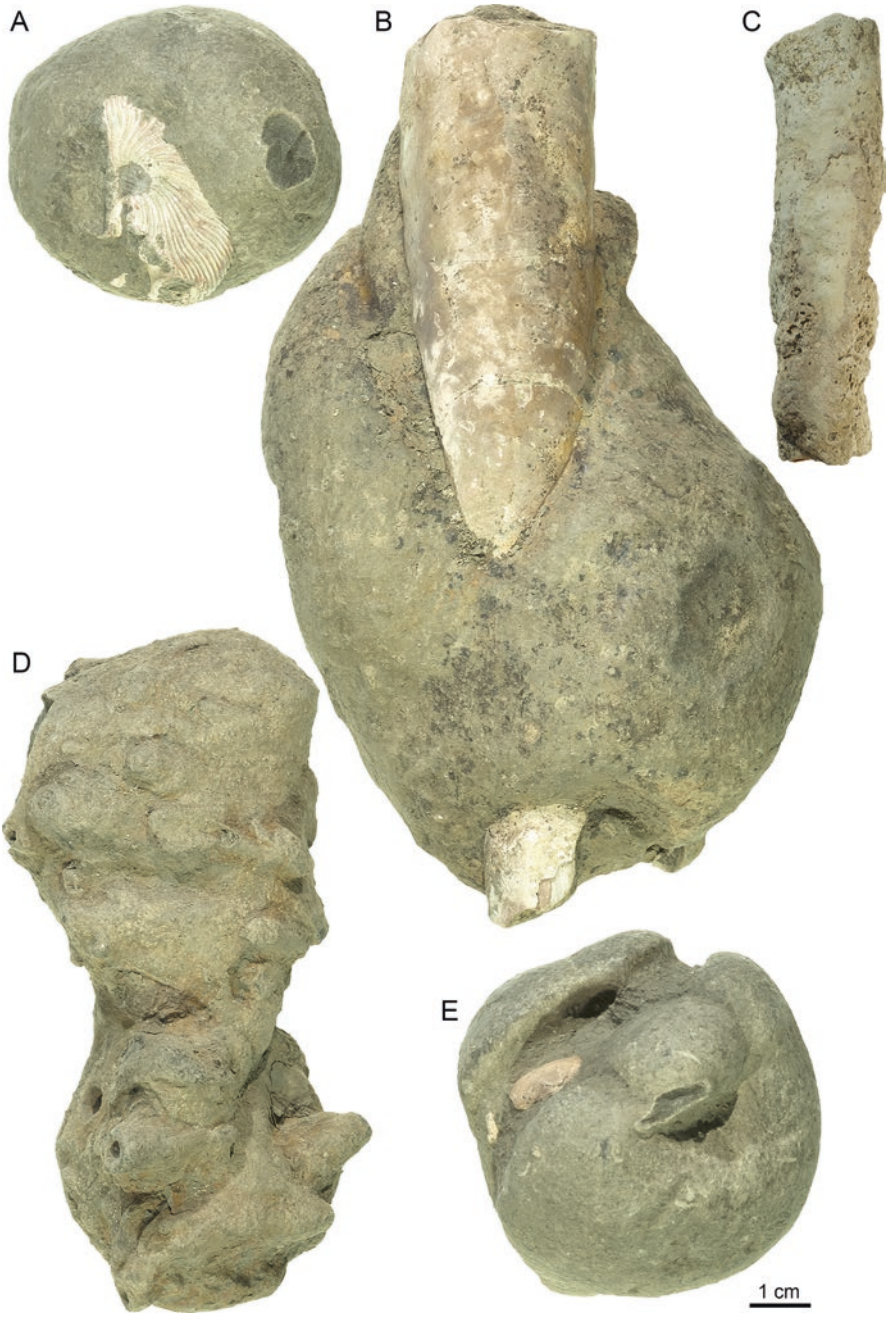

Fig. 15.13 SACs (seep-associated concretions) and tubes from seep deposits in the Pierre Shale, South Dakota. (**a**, **b**, **e**) Subspherical SACs from AMNH loc. 3528, Meade County, composed of Mg-rich calcite with minor amounts of apatite and pyrite containing well-preserved specimens of scaphites (**a**: AMNH 64625), baculites (**b**: AMNH 64595), and lucinids (**e**: AMNH 64623). (**c**) Small pipe-like SAC (AMNH 64608, AMNH loc. 3528, Meade County). (**d**) Tube (AMNH 79109, AMNH loc. 3418, Custer County). (Reprinted from Cochran et al. (2015); http://creativecommons.org/licenses/by/4.0/)

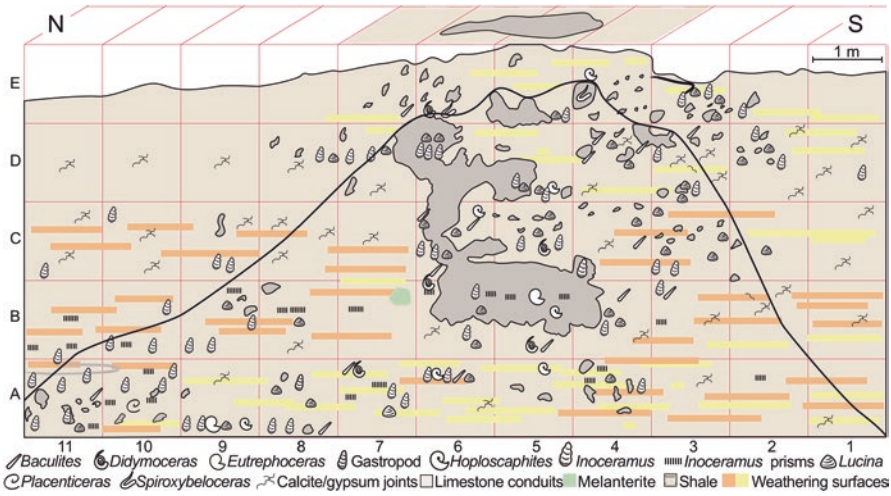

Fig. 15.14 Cross section of a seep deposit in the Pierre Shale, *Didymoceras cheyennense* Zone, AMNH loc. 3418, Custer County, South Dakota. The thin black outline indicates the probable shape of the seep deposit if it were eroded back, with the resistant carbonate masses holding up the top of the mound, forming a tepee butte. (Modified from Landman et al. (2012), used by permission of the Geological Society of America)

mineralogy. They occur throughout the section but are more common at some horizons than others. The most abundant fossils are lucinids and inoceramids that occasionally form crushed, flattened accumulations. All of the lucinids are articulated indicating little transport after death. The shale on the outer margins of the seep deposit, up to 20 m away, is much darker gray, with fewer or no fossils, more typical of the Pierre Shale at non-seep sites. The thin black outline shown in Fig. 15.14 indicates the likely shape of this seep deposit if the surrounding shales were weathered back, leaving the resistant carbonate masses holding up the top of the mound and forming a tepee butte-like seep deposit.

AMNH loc. 3545 from the *Baculites compressus-B. cuneatus* Zones of the Pierre Shale, Meade County, South Dakota, is also exposed in cross section. It features a large carbonate body consisting of several globular masses, which are sparsely fossiliferous. The shale immediately surrounding the carbonate body (up to a distance of approximately 2 m) preserves a rich assemblage of crushed and non-crushed molluscan shells, which retain their original mineralogy. The shale also contains large, massive pipe-like SACs ranging from 10 cm in length and 1 cm in diameter to 40 cm in length and 10 cm in diameter (Fig. 15.12), as well as smaller, hollow tubes with granular outer surfaces, which may have originally formed as crustacean burrows but were subsequently utilized as conduits for methane flow (see below). As shown in thin section, these pipe-like SACs are composed of carbonate-cemented shale filled with pelloids. They also exhibit brecciated features, indicating breakage and re-cementation of the material in the pipes. Subspherical- or dumbbell-shaped SACs are also present in the shale and occasionally bear one or two fossils such as

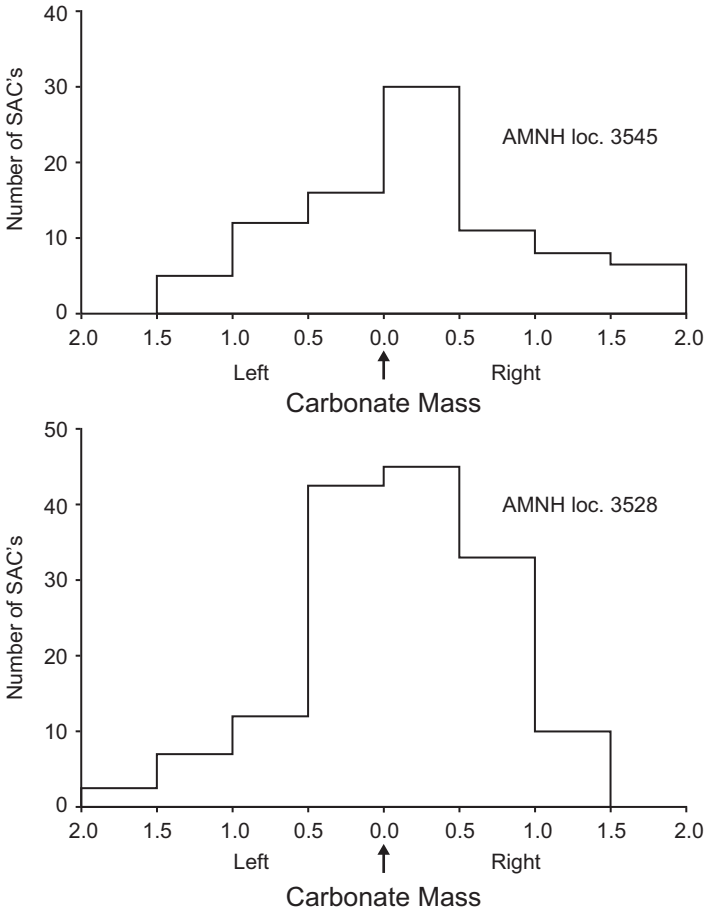

Fig. 15.15 Distribution of seep-associated concretions (SACs) relative to the main carbonate body (centered at 0) at two seep deposits in the Pierre Shale of South Dakota (measurements by M. Garb and A. Rashkova)

baculites and scaphites. The SACs abruptly disappear within a distance of approximately 1–2 m of the main carbonate body (Fig. 15.15).

15.11 Faunal Composition

15.11.1 Abundance and Diversity

The most striking feature of the seep deposits in the Western Interior of North America is the abundance of organisms at these sites relative to their paucity in the surrounding shale. This is not simply a taphonomic artifact due to preferential

preservation in carbonate concretions. In fact, many of the fossils in seep deposits are preserved in the shale itself, immediately adjacent to the carbonate masses, rather than in concretions. The shale surrounding the seep deposits (10s of meters away) yields few or no fossils. As noted above, at AMNH loc. 3418, the shale on the outer margins of the seep deposit (10–20 m away) is much darker and contains few or no fossils (Fig. 15.14).

The fauna in the seep deposits from the Cenomanian Tropic Shale in Utah has been described by Kiel et al. (2012) and includes a variety of bivalves (inoceramids, lucinids, solemyids, and arcoids), opisthobranch gastropods, serpulid worm tubes, and ammonites. The fauna in the seep deposits from the lower Campanian Ojinaga Formation in Texas has been described by Metz (2002) and includes bivalves (inoceramids, *Exogyra*, and *Cyprimeria*), ammonites (*Placenticeras*), gastropods, and small solitary corals. The fauna in the seep deposits from the Campanian-Maastrichtian Pierre Shale in Colorado, Wyoming, South Dakota, Nebraska, and Montana includes inoceramids, lucinids, gastropods, crinoids, nautilids (*Eutrephoceras*), ammonites (*Solenoceras*, *Menuites*, *Baculites*, *Hoploscaphites*, *Placenticeras*, *Didymoceras*, and *Spiroxybeloceras*), irregular and regular echinoids, asteroids, crabs, ophiuroids, shrimp, sponges, corals, serpulid worm tubes, algae, foraminifera (both planktonic and benthic species comprising calcareous, agglutinated, and arenaceous forms), radiolaria, bryozoa, fish, sharks, and reptiles (Figs. 15.16, 15.17, 15.18, 15.19 and 15.20; Howe 1987; Kauffman et al. 1996; Bishop and Williams 2000; Landman et al. 2012, 2013; Larson et al. 2014; Meehan and Landman 2016; Hunter et al. 2016; Blake et al. 2018; Thuy et al. 2018; Laird and Belanger 2018; Meehan et al. 2018; Ryan et al. 2020). In addition, the seep system must have contained abundant organic matter in the form of phytoplankton and zooplankton, which are not preserved as fossils and which must have afforded an abundant source of food for other animals.

The seeps also hosted a large microbial community. Shapiro and Fricke (2002: Fig. 6) examined the seep deposits from the Campanian of Colorado and identified possible microbial filaments consisting of agglomerations of cocci and straight and curved rods 0.5–1 μm in diameter. They occur in the pelloids and are associated with framboidal pyrite (Shapiro 2004; Shapiro and Gale 2001). Thus, the entire framework of the seep limestones may have represented a thrombolytic microbialite, reflecting the original microbial ecosystem (for further details, see Shapiro this volume). Indeed, Birgel et al. (2006) reported biomarkers in these deposits indicative of sulfate-reducing bacteria that mediated the anaerobic oxidation of methane. In addition, bacterial mats are present, which reveal fine laminations in cross section (Fig. 15.19r, v).

It is important to note, however, that many seep deposits in the WIS are devoid of macrofossils. For example, in the area near Oelrichs, Fall River County, South Dakota, in which Darton (1902) mapped hundreds of seep deposits, we estimate that 7–10% of them lack macrofossils (Fig. 15.8). The presence of large masses of limestone indicates the precipitation of authigenic calcium carbonate. However, it is possible that the methane in these seeps did not reach the sediment-water interface and, therefore, did not support a seep ecosystem. In addition, the levels of oxygen

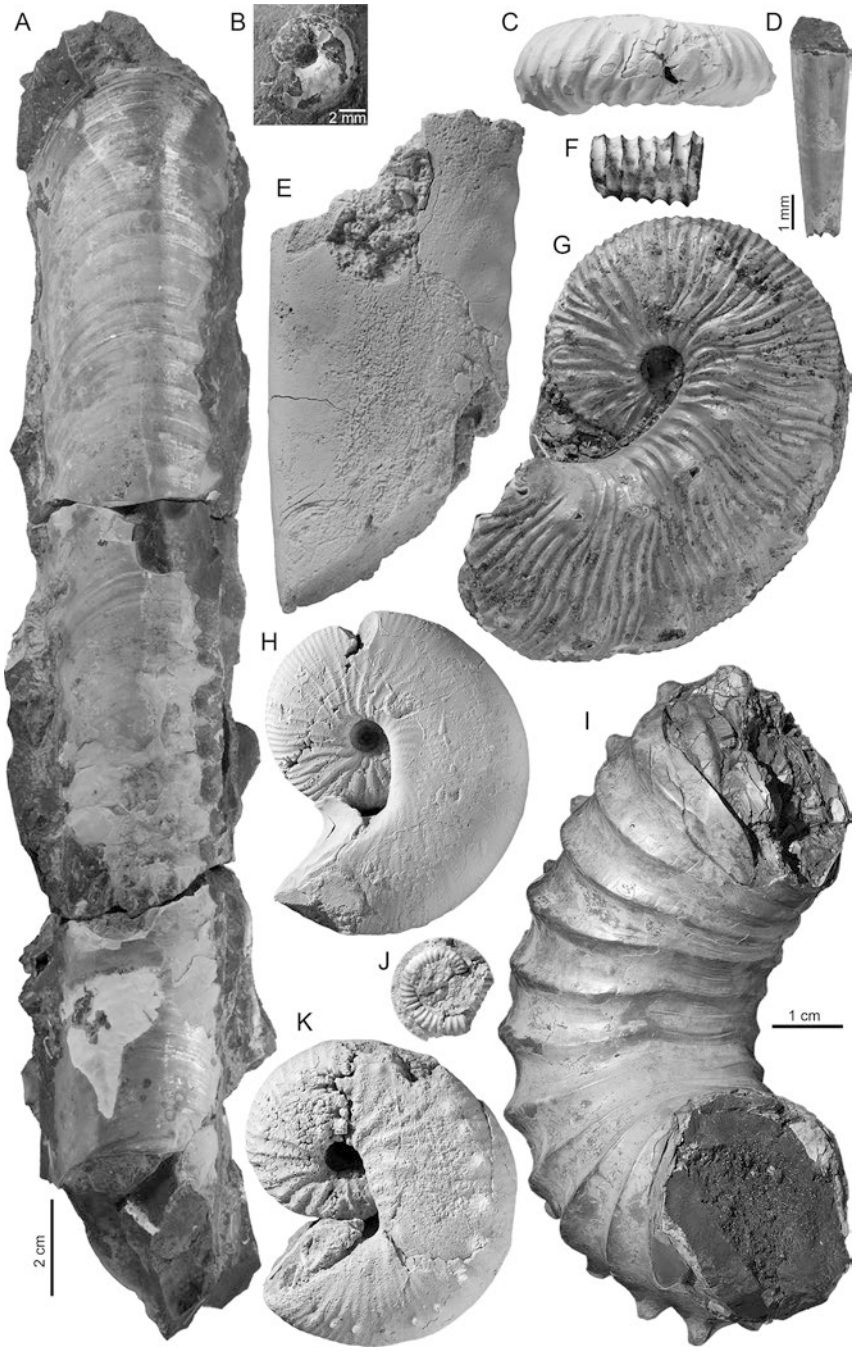

Fig. 15.16 Ammonite fauna in methane seep deposits in the Campanian Pierre Shale, South Dakota and Wyoming. (**a**) *Baculites corrugatus* Elias, 1933, mature macroconch, ventral view,

(continued)

may have been too low, and/or the concentrations of hydrogen sulfide may have been too high to sustain life.

15.11.2 Background Taxa

Most species in the seep deposits in the WIS reflect the background fauna and are not seep-obligate (Kiel et al. 2012; Meehan and Landman 2016). In general, the fauna is abundant but not diverse, with a few species usually being dominant. In the seep deposits from the Campanian-Maastrichtian Pierre Shale, the dominant macroinvertebrates are lucinids (sometimes almost exclusively), tube worms, baculites, and inoceramids (Kauffman et al. 1996; Laird and Belanger 2018). For example, at AMNH loc. 3489 from the *Didymoceras cheyennense* Zone of the Pierre Shale in Custer County, South Dakota, Meehan and Landman (2016) documented that baculites, inoceramids, and lucinids comprise 90.9% of the total number of organisms sampled (n = 197), suggesting that these organisms formed the "foundation" of the seep ecosystem. For a counter example, a seep deposit from the *Baculites jenseni* Zone of Musselshell County, Montana (WPT 69), is dominated by lucinids and baculites, but no inoceramids.

Because all of the seeps in the WIS developed in relatively shallow water (see below), any differences in faunal abundance among them are not due to variation in water depth. This contrasts with observations of modern seeps in which variation in water depth is an important factor in explaining differences in faunal abundance. For example, Sahling et al. (2003) documented that faunal diversity decreases with increasing depth in seep communities in the Sea of Okhotsk in the western Pacific Ocean. In the WIS, in contrast, differences in faunal abundance among seeps are more likely due to variations in the chemical gradients on the sea floor and in the overlying water column, reflecting the persistence and rate of methane flow and the concentrations of oxygen and hydrogen sulfide. The other important factor

with aperture on the top, AMNH 58552, AMNH loc. 3418. (**b**) *Hoploscaphites brevis* (Meek 1876), juvenile, left lateral view, AMNH 66244, AMNH loc. 3418. (**c**) *Didymoceras cheyennense* (Meek and Hayden 1856), fragment, AMNH 63440, AMNH loc. 3418. (**d**) *Baculites* sp., juvenile, lateral view, AMNH 112942, AMNH loc. 3545. (**e**) *Baculites compressus* Say, 1820, right lateral view, AMNH 58544, AMNH loc. 3419. (**f**) *Spiroxybeloceras meekanum* (Whitfield 1877), fragment, AMNH 66289, AMNH loc. 3418. (**g**) *Hoploscaphites brevis* (Meek 1876), mature microconch, left lateral view, AMNH 66275, AMNH loc. 3418. (**h**) *Hoploscaphites gilli* Cobban and Jeletzky 1965, mature macroconch, left lateral view, USNM 547334, USGS Mesozoic loc. D1900, *B. scotti-D. nebrascense* Zones, Niobrara County, Wyoming (non-seep site, but species is also present at age-equivalent seep sites). (**i**) *Didymoceras cheyennense* (Meek and Hayden 1856), AMNH 102504, AMNH loc. 3489, *D. cheyennense* Zone, Pennington County, South Dakota (non-seep site, but species is also present at age-equivalent seep sites). (**j**) *Didymoceras cheyennense* (Meek and Hayden 1856), early whorls, AMNH 82739, AMNH loc. 3529. (**k**) *Hoploscaphites gilberti* Landman et al. 2014, mature macroconch, left lateral view, AMNH 83717, AMNH loc. 3386. The 1 cm scale bar on the bottom applies to all specimens except **a**, **b**, and **d**

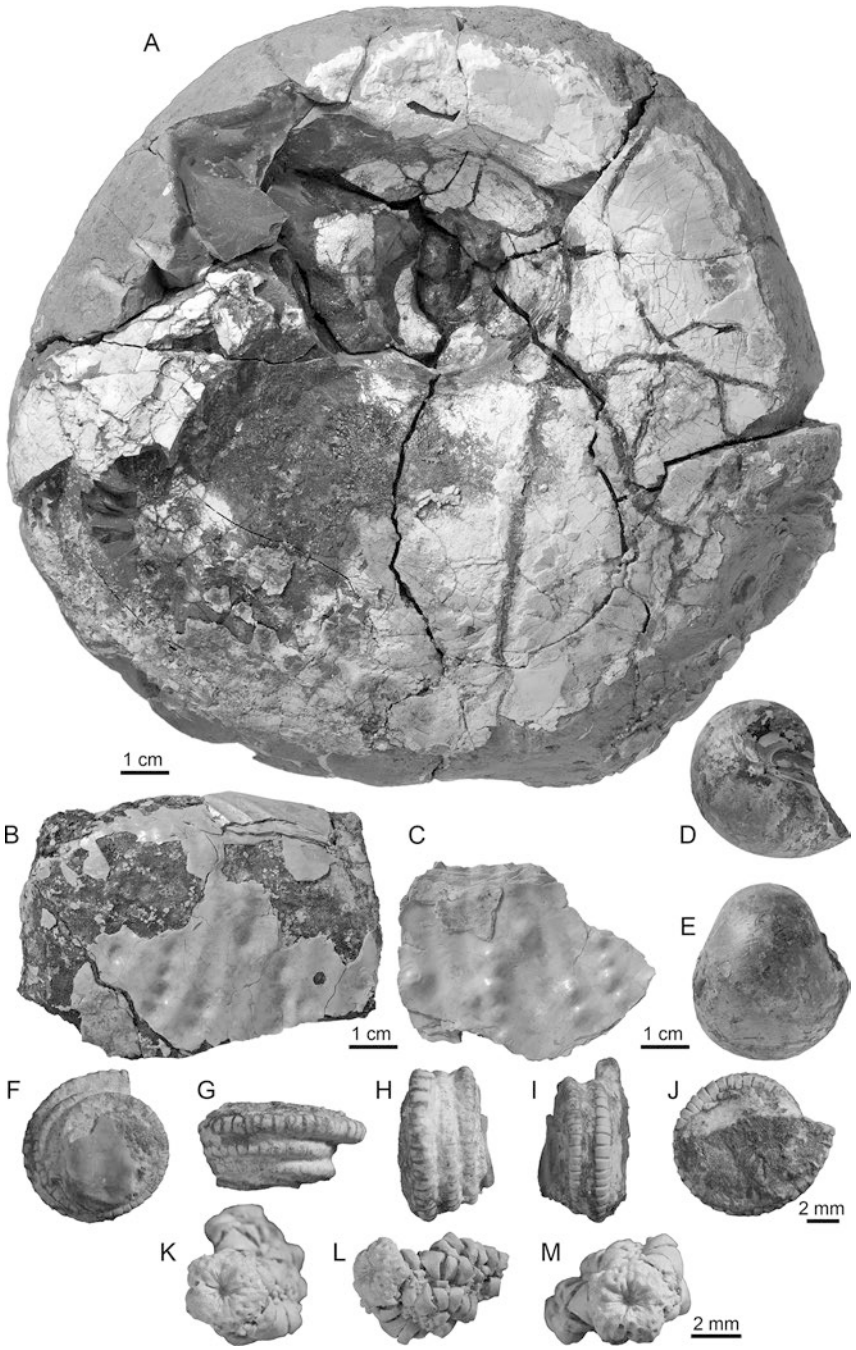

Fig. 15.17 Fauna in methane seep deposits in the Campanian Pierre Shale, South Dakota. (**a**) *Pachydiscus* sp., left lateral view, AMNH 105841, AMNH loc. 3528. (**b**, **c**) Fragment of *Inoceramus* sp., with an infestation of blister pearls, AMNH 108328, AMNH loc. 3528. (**d**, **e**) Right lateral and ventral views of *Eutrephoceras dekayi* (Morton 1834), AMNH 63647, AMNH loc. 3545. (**f–j**) Curled arm of a crinoid, probably *Lakotacrinus brezinai* Hunter et al. 2016, five views, AMNH 161015, AMNH loc. 3507. (**k**–**m**). Crown of a comatulid (feather star), possibly *Glenotremites*, three views, AMNH 161016, AMNH loc. 3529

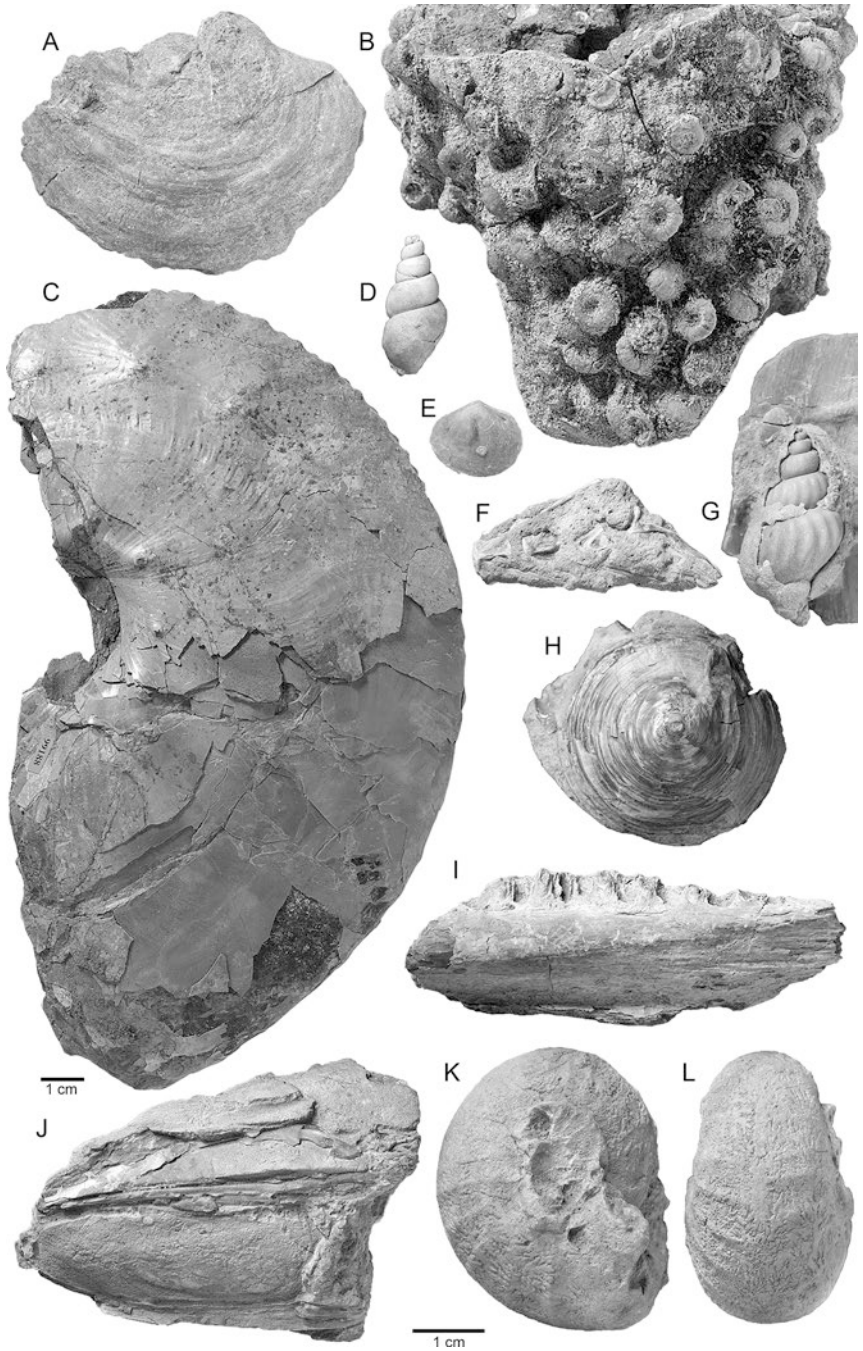

Fig. 15.18 Fauna in methane seep deposits in the Campanian Pierre Shale, South Dakota, and Nebraska. (**a)** *Ostrea* sp., AMNH 82749, AMNH loc. 3529. (**b)** Echinoids, AMNH 82716, AMNH loc. 3654. (**c)** *Placenticeras costatum* Hyatt 1903, left lateral view, AMNH 99188, AMNH loc. 3545. (**d)** *Drepanochilus* sp., AMNH 82750, AMNH loc. 3529. (**e)** Bivalve, AMNH 82748, AMNH loc. 3529. (**f)** Articulated fish vertebra, AMNH 82743, AMNH loc. 3529. (**g)** *Bellifusis* sp., AMNH 82741, AMNH loc. 3529. (**h**) Fish vertebra, AMNH 82747, AMNH loc. 3686. (**i)** Fish jaw, AMNH 82740, AMNH loc. 3529. (**j**) Fish, unidentified head bones, AMNH 82746, AMNH loc. 3529. (**k**, **l**) *Menuites* sp., AMNH 82737, right and ventral views, AMNH loc. 3666. The 1 cm scale bar on the bottom applies to all specimens except (**c)**

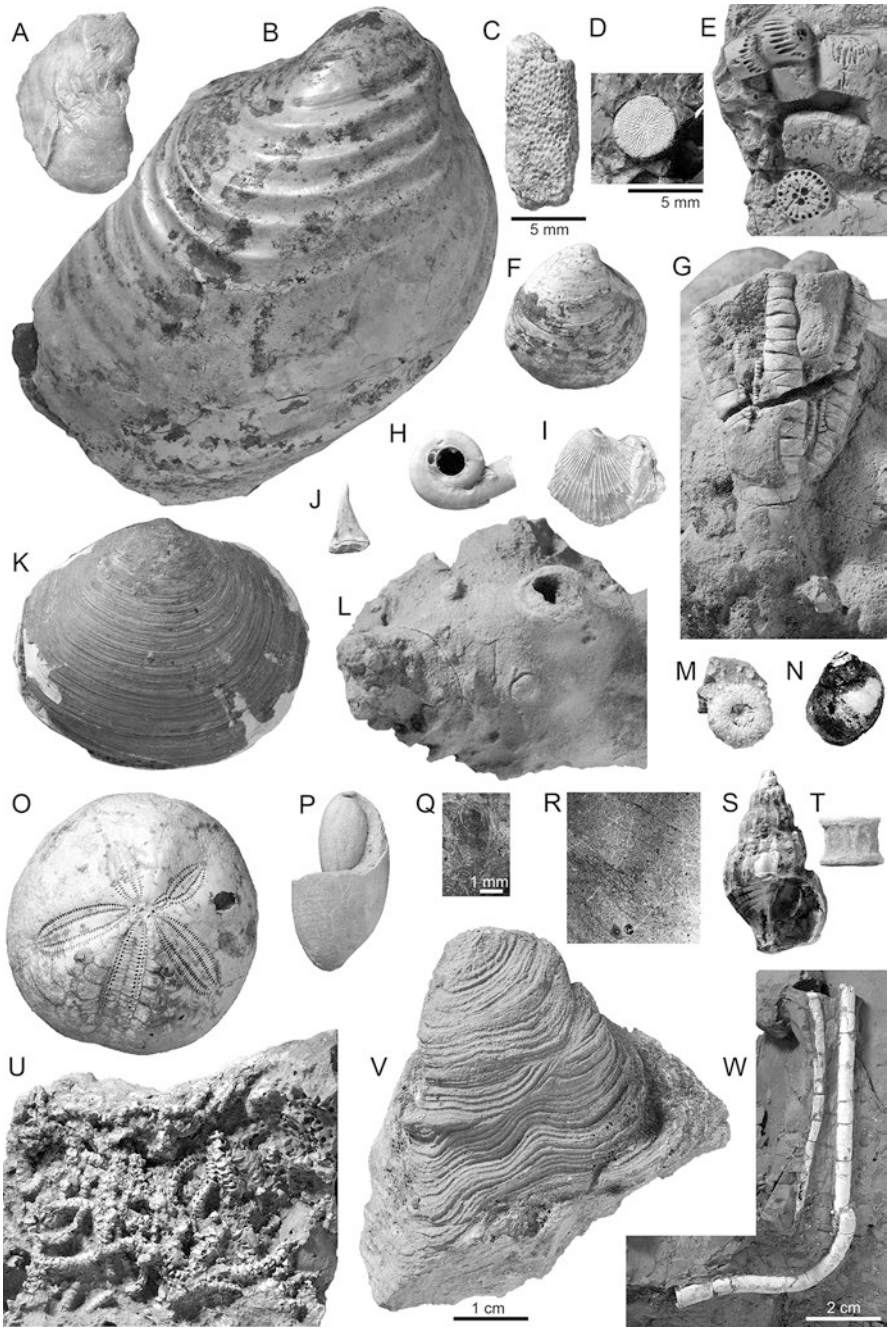

Fig. 15.19 Fauna in methane seep deposits in the Campanian Pierre Shale, South Dakota, and Montana. (**a**) *Ostrea* sp., AMNH 82729, AMNH loc. 3529. (**b**) "*Inoceramus*" *sagensis* Owen 1852, AMNH 66248, AMNH loc. 3418. (**c**) Bryozoan, AMNH 82730, AMNH loc. 3529. (**d**) *Microbacia*

(continued)

controlling faunal abundance and diversity is the nature of the substrate, that is, whether it is a soft, clayey mud or a hard carbonate crust (for a description of a hard ground substrate, see Hunter et al. (2016); for an example of a soft, muddy bottom, see Ryan et al. (2020)). Currents on the sea floor may also have contributed to the development of the seep community, for example, by periodically exposing the carbonate crust, permitting the settlement of oysters and inoceramids (see below).

15.11.3 Hard Ground Taxa

The development of a hard crust at a seep is the result of the authigenic precipitation of calcium carbonate at the sediment-water interface. Such hard grounds provide suitable substrates for animals to colonize, which, in turn, promote further development of the hard substrate. For example, accumulations of large inoceramid shells form broad tabular pavements (1–3 m across) that provide additional surfaces to which animals can attach. This is an example of positive feedback.

The presence of a hard substrate permits the colonization of many species, some of which are unique to these habitats. Such species include stalked articulate crinoids, feather stars, sponges, regular and irregular echinoids, ophiuroids, asteroids, tube worms, crabs, bryozoa, and corals. However, even in seep deposits in which these organisms appear, the background taxa are still dominant (Meehan and Landman 2018). In addition, it is possible that some of these species actually occur elsewhere but are preferentially preserved in the seep deposits. For example, echinoids are, in fact, present in age-equivalent non-seep sites, but they are more difficult to recognize because their tests are commonly broken up due to predation and/or are fused into the fine-grained concretionary matrix (Landman and Klofak 2012).

The distribution of hard ground fauna has been extensively studied at AMNH loc. 3529 from the *Didymoceras cheyennense* Zone of the Pierre Shale, Custer County, South Dakota. Crinoids occur in patches associated with tabular SACs composed of inoceramid valves. If this pattern reflects their original distribution, it suggests that the crinoids were gregarious in life and formed clusters of tens to

sp., AMNH 82731, AMNH loc. 3529. (**e**) Columnals of *Lakotacrinus brezinai* Hunter et al. 2016, AMNH 66260, AMNH loc. 3419. (**f**) *Crassatella evansi* Hall and Meek 1856, AMNH 108491, AMNH loc. 3418. (**g**) Crown of *Lakotacrinus brezinai* Hunter et al. 2016, AMNH 69618, AMNH loc. 3456. (**h**) Serpulid worm tube, AMNH 82732, AMNH loc. 3529. (**i**) *Pecten* sp., AMNH 82733, AMNH loc. 3529. (**j**) Fish tooth, AMNH 82734, AMNH loc. 3529. (**k**) *Nymphalucina occidentalis* (Morton 1842), AMNH 66246, AMNH loc. 3418. (**l**) Sponge, AMNH 66249, AMNH loc. 3419. (**M**) Echinoid, AMNH 82706, AMNH loc. 3509. (**n**) *Euspira obliquata* (Hall and Meek 1856), AMNH 80369, AMNH loc. 3418. (**o**) Echinoid, AMNH 82710, AMNH loc. 3456. (**P**) Gastropod, AMNH 82735, AMNH loc. 3529. (**q**) Lingulid brachiopod, AMNH 116218i, AMNH loc. 3911. (**r**, **v**) Algal mat (stromatolite?), AMNH 82727, surface and cross section, AMNH loc. 3420. (**s**) *Drepanochilus triliratus* Stephenson 1941, AMNH 108492, AMNH loc. 3418. (**t**) Fish vertebra, AMNH 82736, AMNH loc. 3529. (**u**) *Brezinacantha tolis* Thuy et al. 2018, AMNH 113585, AMNH loc. 3509. (**w**) Tube worm, AMNH 82738, AMNH loc. 3528. The 1 cm scale bar on the bottom applies to all specimens except **c**, **d**, **q**, and **w**

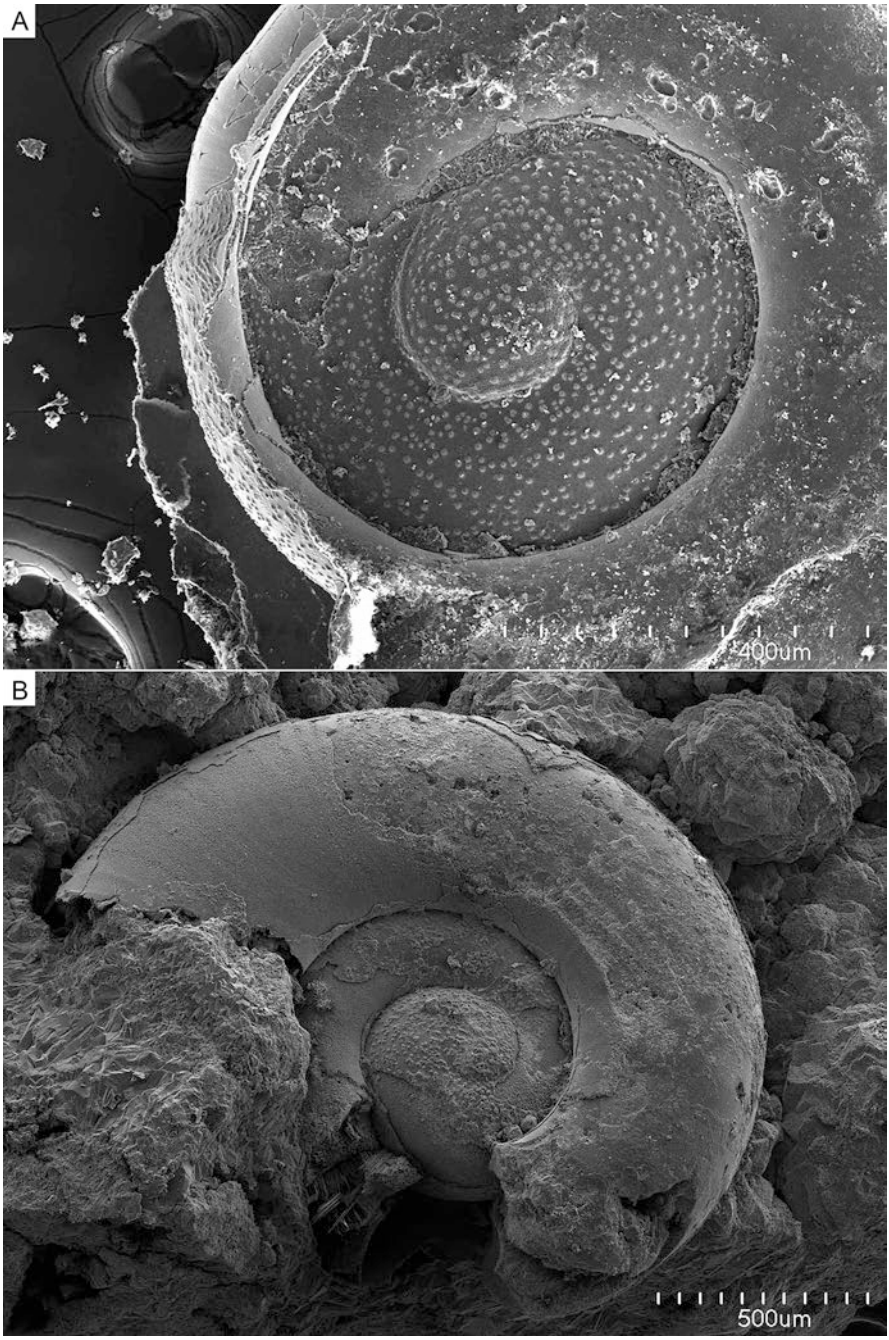

Fig. 15.20 Small juveniles of *Hoploscaphites* preserved in seep deposits, AMNH loc. 3440. A. AMNH 112950. B. AMNH 112949. The tuberculate micro-ornamentation on the embryonic shell is visible. (Photos by A. Rowe)

hundreds of individuals (Hunter et al. 2016). Because these crinoids lack attachment discs or cirri, they probably anchored themselves in the irregular crevices of the substrate. Alternatively, they may have used their long arms for anchoring on the bottom (Hunter et al. 2016). They are preserved either articulated or slightly disarticulated, without any signs of abrasion, indicating that they were buried soon after death, perhaps trapped in bacterial mats. Their preservation was also facilitated by the rapid rate of authigenic precipitation of carbonate at the sediment-water interface.

Asteroids, ophiuroids, and gastropods at this seep site also seem to occur in patches (Blake et al. 2018; Thuy et al. 2018). The hard, crustal substrate probably promoted an increase in habitat complexity, providing small niche-like spaces for such animals as gastropods and echinoids (Meehan and Landman 2016). The remains (claws) of ghost shrimp are also clustered together, associated with concentrations of burrow-shaped SACs. Most intriguingly, certain ammonites such as didymoceratids and spiroxybeloceratids also appear to be more abundant in some areas of this seep deposit than others. If this pattern reflects their original distribution, it suggests that the ammonites homed in on food-rich resources, with important implications for the mode of life of these animals. In contrast, baculites, scaphites, and placenticeratids do not show a preferred distribution but occur everywhere in the deposit. Ultimately, of course, the distribution of organisms at this seep site probably reflects the distribution of food resources, as well as the concentration of O_2 and H_2S in the area.

15.11.4 Ammonites as Seep Inhabitants

Landman et al. (2012, 2018a, b) advanced the hypothesis that ammonites formed an integral part of the seep community, rather than simply representing empty shells that floated in after the death of the animals. They based this hypothesis on both isotopic and paleontologic evidence. Several seep deposits in South Dakota contain exceptionally well-preserved shell material, permitting geochemical analyses of the ammonite shells themselves. The ammonites from seep sites exhibit lower values of $\delta^{13}C$ (as low as −14‰) than ammonites from age-equivalent non-seep sites (as high as 3‰) (see Landman et al. this volume, for further discussion).

The relatively low values of $\delta^{13}C$ of the ammonites from seep sites suggest that they were impacted by a methane-derived ^{12}C-enriched signal in the DIC reservoir above the seep. Indeed, Landman et al. (2018a, b) compared estimates of $\delta^{13}C$ of the DIC reservoir above two seeps in the *Baculites compressus* Zone (−0.7‰) with an age-equivalent non-seep site in the same basin (+2.3‰). The $\delta^{13}C$ of the ammonites may also reflect incorporation of metabolic carbon from the prey that the ammonites ate at the seep. For example, ammonites may have fed on small microorganisms in the water column, such as floating larvae, as documented by Kruta et al. (2011). Such "vital" effects can produce non-equilibrium fractionation in the shell relative to the $\delta^{13}C$ of the DIC reservoir (He et al. 2005; Lukeneder et al. 2010; Tobin and

Ward 2015; Landman et al. 2018a, b). The isotope measurements of Landman et al. (2018) were performed on specimens of the same species (*B. compressus*) from seep and non-seep environments, suggesting that if the fraction of metabolic carbon incorporated into the shell was equivalent at both sites, then the lower values of $\delta^{13}C$ in the seep ammonites were the result of the animals living at the seep.

This hypothesis is reinforced by the $^{87}Sr/^{86}Sr$ isotope ratios of the shells of seep ammonites, which are elevated relative to the coeval sea water values (Landman et al. 2012; Cochran et al. 2015; Cochran et al. this volume). The data suggest that (1) seep fluids likely acquired the elevated values of $^{87}Sr/^{86}Sr$ through reaction with a radiogenic Sr source (the nascent Black Hills granite) at depth in the deposit and (2) these anomalous values of $^{87}Sr/^{86}Sr$ were imprinted on the dissolved Sr in the water above the seep and thus were incorporated into the shells of ammonites living there. The Sr isotope results suggest that seep fluids must have migrated from depth through the overlying muddy sediments via fractures and faults and likely accumulated biogenic methane en route.

In addition to isotopic data, Landman et al. (2010, 2012) documented paleontological evidence that the ammonites preserved in seep deposits in the basin actually lived there and did not float in as empty shells after death. One piece of evidence in support of this interpretation is that the ammonites preserved in seep deposits occur as both adults and juveniles, including newly hatched individuals (Fig. 15.20). In fact, the abundance of small juveniles in some deposits suggests that these sites acted as ammonite nurseries (Rowe et al. 2020). In addition, in ammonites in which sexual dimorphism can be recognized, both dimorphs (presumably the males and females) occur in the same seep deposit. Because ammonites, like modern cephalopods, probably congregated en masse for reproductive purposes, the presence of both sexes implies the existence of a breeding population (Landman et al. 2010). Furthermore, ammonite jaws, comprising upper and lower mandibles, are also present in seep deposits. Jaws are very delicate structures, and their preservation implies that the ammonites did not float into the site after death. Finally, many ammonites at seep sites exhibit lethal injuries, as indicated by missing portions of shell material from the adapical end of the body chamber. These injuries probably occurred at the seep sites, suggesting that ammonites formed an integral part of the seep food web.

The isotopic composition of echinoderms has also been investigated for clues about their mode of life. Kato et al. (2017) analyzed the carbon isotopic composition of crinoids from seep deposits in the upper Campanian Pierre Shale. The skeletons of these specimens are well preserved with little or no diagenetic alteration. The microstructure is intact, and the concentration of Mg is similar to that in modern echinoderms and much higher than that in the surrounding shale matrix. The values of $\delta^{13}C$ of the skeletal material are very low and range from −32‰ to −11‰. Therefore, as with the ammonites, these low values suggest that the crinoids lived at the seep and incorporated a light carbon isotopic signature in their skeletons (for counter arguments, see Hunter et al. (2018) and Kato et al. (2018)).

15.11.5 Cognate Community

As documented by Brezina et al. (2019), a large log was discovered in the upper Campanian Pierre Shale in Custer County, South Dakota, near AMNH loc. 3504 (Fig. 15.21). The whole region is peppered with seep deposits and probably comprised a seep field. The log is 2.8 m long and preserved in a concretion 3.4 m long. The concretion also contains scaphites and baculites. The surface of the log is covered with a thin crust of bivalves, which represents a wood fall association. The log is oriented east-west, possibly reflecting the prevailing currents, and may have come to rest in a depression on the sea floor. Although wood is not uncommon in the Pierre Shale, most of it consists of small fragments, which are not associated with a wood fall fauna.

15.12 Paleoenvironment at the Seep

15.12.1 Migration of Methane

As noted above, the low values of $\delta^{13}C$ of the limestones in the Upper Cretaceous US Western Interior seep deposits indicate that methane was the primary source of carbon. In addition, Birgel et al. (2006) studied the molecular fossils preserved in the limestones from the Campanian seep deposits in Colorado. They documented ^{13}C-depleted archaeal lipids that were derived from anaerobic oxidation of methane (AOM). They also reported a suite of ^{13}C-depleted biomarkers indicating the former presence of sulfate-reducing bacteria. These bacteria are part of the consortium of Archaea and Bacteria that account for one of the principal pathways of AOM.

Methane may have migrated to the sediment-water interface through diffusion and advection along fractures in the fine, unconsolidated sediments. Methane may also have reached the overlying water column via preexisting, relic burrow networks that were exapted for methane conduits (Krause et al. 2009; Wiese et al. 2015; Cochran et al. 2015; Cochran et al. this volume). The tubes in the seep deposits in the Campanian Pierre Shale of Colorado were initially attributed to vestimentiferan and pogonophoran tube worms, but it is more likely that they were crustacean burrows. For example, at AMNH loc. 3344 near Newell, Butte County, South Dakota (Fig. 15.3d), the main carbonate body contains anastomosing hollow tubes, which probably represent the burrows of ghost shrimp, similar to those reported by Howe (1987). The burrows may have originally been lined with bacteria that promoted methane oxidation and carbonate precipitation within the burrows. Variation in the material filling the burrows (e.g., siliciclastic sediments, calcitic spar, and cements) and the carbon isotopic composition of the infill indicate how long and how often the burrows acted as methane conduits. In the seep deposits from the Campanian Pierre Shale of Colorado, Krause et al. (2009) argued that the presence of meniscate and vesiculate fabrics attests to the former presence of bubbles. The

Fig. 15.21 Wood fall near AMNH loc. 3504, Custer County, South Dakota. A. Overview of the log (AMNH 135076). It is 2.8 m long and preserved inside a concretion. B. Close-up of a bivalve on the surface of the log. C, D. Cross sections through the black crusty outer layer of the log showing the thin white lenses of crushed shell debris. E, F. *Baculites compressus*, AMNH 161727, in the same concretion as the log, lateral and adapical views, respectively

bubbles would have entrained siliciclastic grains and at the same time promoted authigenic precipitation of carbonate, followed by precipitation of blocky calcite spar inside the tubes.

15.12.2 Water Depth

All the seeps in the US Western Interior, ranging from the Cenomanian to the early Maastrichtian, formed in relatively shallow water. The depth of the WIS during the deposition of the upper Campanian and lower Maastrichtian Pierre Shale was ≤100 m (Gill and Cobban 1966; Kauffman et al. 1996). This is consistent with interpretations based on foraminiferal assemblages (Bergstresser 1981; Howe 1987; Laird and Belanger 2018; Meehan et al. 2018). In addition, Kiel et al. (2012) cited the presence of cyanobacteria in concretions from the Cenomanian Tropic Shale of Utah as evidence that these seeps formed in the photic zone. In this respect, the seeps in the US Western Interior are similar to those in Spitsbergen, Svalbard, which also developed in an epicontinental sea setting (Hryniewicz et al. 2014).

15.12.3 Distance from the Shore

The seeps in the WIS formed in offshore settings, perhaps coincident with the forebulge depozone as suggested by Metz (2010) (however, see the earlier discussion on the origin of methane). According to reconstructions of the shoreline by Cobban et al. (1994), the seeps from the *Baculites scotti-Didymoceras nebrascense* Zones in Colorado formed 550 km east of the shoreline. The seeps of the same age in Wyoming, South Dakota, and Nebraska formed 225–325 km east of the shoreline (Cobban et al. 1994). The seeps from the *Baculites compressus* Zone in southwestern South Dakota developed 275 km east of the shoreline, although the position of the shoreline at that time is not well constrained (Landman and Klofak 2012).

Seeps may also have developed closer to shore, but no record of them exists. The higher permeability of coarser-grained sediments characteristic of nearshore sediments in the WIS would have facilitated the flow of methane but would not have promoted the development of a complex plumbing network. In addition, such sediments are typically organic poor and, thus, unlikely to have generated much methane by methanotrophic bacteria. Indeed, no seep deposits are known in the *Baculites compressus-B. reesidei* Zones of the Pierre Shale near Kremmling, Colorado, which represents a setting nearer the paleo-shoreline (Izett et al. 1971; Cobban et al. 1992).

15.12.4 Seeps as Refuges

Seeps may have represented semipermanent, self-sustaining habitats in the WIS even in times of environmental catastrophe. For example, volcanic ashfalls occasionally blanketed the WIS leading to widespread extermination of benthic and nektic fauna (Landman et al. 2018a, b). However, at seep sites, life may have persisted uninterruptedly because the local ecosystem was unimpaired (Brophy et al. 2018, 2022). Similarly, episodes of sea floor anoxia may have wrought havoc on broad swatches of the basin. However, if the seep deposits extended above the layer of low oxygenation, some animals may have survived (Landman et al. 2013). Larvae of these animals could then have repopulated other parts of the basin following the return of more hospitable conditions.

15.12.5 Expression of Seeps on the Sea Floor

In their study of the seep deposits from the *Baculites scotti-Didymoceras nebrascense* Zones of the Pierre Shale in Colorado, Kauffman et al. (1996) envisioned the seeps as having formed elevated carbonate chimneys up to 5 m above the sea floor, resulting from the concentrated movement of methane along a single channel. The chimney interfingered with the muddy sediments as it grew, reflecting starts and stops in methane emission. Kauffman et al. (1996) interpreted the concentric zonation of fossil assemblages around a central core as reflecting "a strong environmental gradient from chemically restrictive conditions around methane vents, across elevated, more-oxygenated mound flanks, and onto the dysoxic sea floor." They argued that the breakage of shells and their distribution on the flanks may have been due to slumping from higher slopes surrounding the central chimney. Kauffman et al. (1996) and Howe (1987) also identified slump blocks in the surrounding shale that were disjunct with the shale and suggested that these blocks fell down the slopes of the seep deposit onto the sea floor at the time the seeps were active.

The hypothesis of a chimney-like structure is complicated by the fact that the formation of seep carbonate involves AOM, which requires anoxic conditions and typically proceeds in the sulfate-methane transition zone 10s to perhaps 100s of centimeters below the sediment-water interface (Cochran et al. this volume). Formation of a chimney-like structure by AOM above the sediment-water interface requires anoxic conditions in the water column, as observed today, for example, on the northwestern shelf of the Black Sea and on the Nile deep-sea fan in the Mediterranean (Michaelis et al. 2002; Bayon et al. 2013). However, if the carbonate chimneys envisioned by Kauffman et al. (1996) developed in an anoxic water column, the faunal community associated with the chimneys would not have survived.

Carbonate chimneys can develop in an oxic water column under special circumstances. For example, Teichert et al. (2005) observed carbonate chimneys 10s of meters high at Hydrate Ridge on the Cascadia margin off the coast of Oregon. They

hypothesized that formation of these chimneys was due to mats of sulfide-oxidizing bacteria (*Beggiatoa*) that effectively coated the carbonate and provided an interface between the oxic water column and the underlying anoxic environment containing the archaean-bacterial consortium in which AOM and carbonate formation occurs. The formation of chimneys, as envisioned by Kauffman et al. (1996), would have required a similar, microbially mediated scenario.

In contrast, we argue that the seeps in the WIS did not form chimneys on the sea floor but were expressed instead as features with little or no relief. Authigenic precipitation of carbonate occurred below the sediment-water interface in the sulfate-methane transition zone. Seep deposits with an abundance of irregular, platy SACs would have appeared as crusts on the sea floor (Fig. 15.22). These crusts were periodically exhumed by bottom currents, exposing the hard rocky substrate (see Kiel (2010) for a description of modern seeps with a similar appearance, for example, in the Gulf of Mexico). This is consistent with the presence of organisms such as sponges, crinoids, and bryozoa that required a hard surface for attachment.

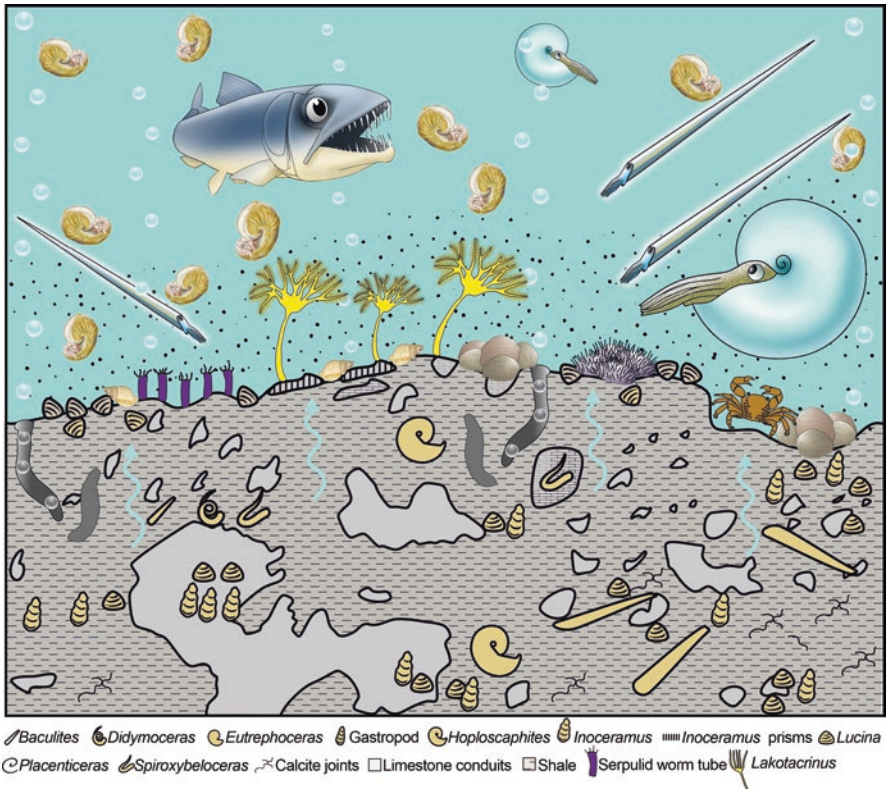

Fig. 15.22 Hypothetical reconstruction in cross section of a methane seep deposit in South Dakota during the late Campanian. The ammonites are species of *Hoploscaphites*, *Didymoceras*, *Spiroxybeloceras*, *Baculites*, and *Placenticeras*. (Reprinted from Landman et al. (2018a, b), used by permission of the *American Journal of Science*)

Colonization by inoceramids and oysters would have further stabilized this substrate, producing a platy, tabular pavement.

Seep deposits with large masses of vuggy, peloidal limestone containing numerous articulated lucinids would also have appeared as limestone crusts on the sea floor. The rapid authigenic precipitation of carbonate would have preserved the infauna living in the sediment (e.g., lucinids) as well as the epifauna living on the surface (e.g., inoceramids) and the nekton that settled to the bottom (e.g., ammonites, fish, mosasaurs). Differences in the abundance and size of vugs in the limestone are probably related to variation in the rate of flow and concentration of methane. The bubbles would have fragmented the authigenic deposits producing fractures and micritic clasts. Such brecciation and corrosion may have permitted occasional flushing of the bottom with more oxygen-rich waters. The broken-up micritic clasts were rapidly cemented together by syndepositional lithification, which probably occurred at the same rate as sediment aggradation.

Seep deposits that feature large, massive, micritic carbonates surrounded by shale containing subspherical SACs and pipes would not have been expressed on the sea floor except for the emission of seep fluids into the overlying water column (see Cochran et al. this volume). Advective transport of methane along fractures and preexisting burrow systems likely resulted in the formation of the large limestone masses at or below the sediment-water interface. Diffusion of methane in the sediments led to the formation of the subspherical SACs, which occasionally preserved organisms inside them (Figs. 15.12, 15.13 and 15.14). The presence of horizontal lenses of crushed inoceramid shells in some of these deposits indicates that these seeps occasionally developed accumulations of shelly debris on the sea floor. However, these accumulations were not extensive enough to attract animals that required hard substrates such as crinoids, sponges, and bryozoa.

15.13 Conclusions

Seep deposits in the Upper Cretaceous Western Interior of North America appear today as prominent geomorphic features in the landscape. They vary in shape depending on the size and lithology of the carbonate bodies that make up the deposits. They are geographically widespread; the bulk of them range from the upper middle Campanian to the early Maastrichtian, lasting for a duration of approximately 7 Myr. The presence of methane has been confirmed by isotopic analyses of the seep carbonates, which exhibit values of $\delta^{13}C$ as low as −50‰ VPDB. These low values of $\delta^{13}C$ indicate that the carbon was derived from bacterially mediated methane oxidation, thereby increasing the concentration of dissolved inorganic carbon and promoting the authigenic precipitation of carbonate minerals. The likely source of the methane was biogenic, produced by the decomposition of sedimentary organic matter, originating from the Pierre Shale and underlying formations.

Differences in the structure, lithofacies, and fossil composition of seep deposits may reflect differences in the duration and rate of methane emission. It is possible that the vugginess and low number of SACs (seep-associated concretions) observed

in deposits from the *Baculites scotti-Didymoceras nebrascense* Zones of the Pierre Shale in Colorado are due to high concentrations of methane emerging as bubbles into the overlying water via a central conduit. As a result, these deposits may have appeared as low-relief features on the sea floor. In contrast, the seep deposits from the *D. cheyennense-B. compressus* Zones of the Pierre Shale in South Dakota with massive, micritic carbonates and abundant SACs in the surrounding shale probably formed via diffuse methane flow at or below the sediment-water interface in the sulfate-methane transition zone. In some of these deposits, authigenic precipitation of carbonates resulted in the development of hard, irregular limestone crusts that were periodically exhumed by sediment dispersal.

Seeps formed unique habitats on the sea floor of the WIS in an otherwise homogenous environment. The most striking feature of these seeps is the abundance of organisms relative to the paucity in the surrounding shale. Most seep species reflect the background fauna of the WIS and are not seep-obligate. In general, the fauna is abundant but not diverse, with only a few species being dominant. Because all of these seeps developed at nearly the same water depth, any variation in faunal abundance among them is not due to variation in water depth but rather to variation in the chemical gradients on the sea floor and in the overlying water column reflecting the persistence and rate of methane flow and the concentrations of dissolved oxygen and hydrogen sulfide. Low values of $\delta^{13}C$ and elevated values of $^{87}Sr/^{86}Sr$ in the shells of well-preserved ammonites collected at seeps suggest that the chemistry of the overlying water column was affected by the seep fluids.

One of the most important factors controlling faunal abundance and diversity at the seeps was the nature of the substrate, consisting of either soft clayey mud or hard carbonate crusts. The development of hard crusts provided suitable substrates for animals to settle on and attach to, allowing for the formation of unique communities. These communities included stalked articulate crinoids, feather stars, sponges, ophiuroids, asteroids, regular and irregular echinoids, tube worms, crabs, bryozoa, and corals. In turn, these communities attracted a diverse suite of other organisms including gastropods, scaphites, baculites, nautilids, fish, and mosasaurs.

Acknowledgments At the American Museum of Natural History, we thank Ana Rashkova, Bushra Hussaini, Mary Conway, Kathleen Sarg, and Marion Savas for accessioning material and assigning AMNH numbers, Mariah Slovacek and Ana Raskhova for collecting fossils in the field and preparing specimens, and Stephen Thurston for photographing specimens and preparing figures. We thank Barbara A. Beasley for arranging permits to collect on the Buffalo Gap National Grassland, South Dakota. We thank Cheryl L. Metz for calling our attention to the maps of the Black Hills produced by N. H. Darton. Many students, colleagues, and family members have helped us collect in the field and interpret the results, and we wish to express our thanks to the ranchers, farmers, and private landowners who granted us permission to collect on their property: Malcolm Bedell, Gale Bishop, Shannon Brophy, Jim and Joyce Grier, William Halligan, Kayla Irizarry, Steve Jorgensen, the late Susan Klofak, Ekaterina Larina, Luke Larson, Tom Linn, Jone Naujokaityte, Dustin Perriguey, Remy Rovelli, James Witts, Adiel Klompmaker, Joshua Slattery, Joshua Laird, Christina Robins, Ben Thuy, Aaron Hunter, Tatsuo Oji, Paul Taylor, Ted Hubbard, Daniel Blake, Mary Haas, Andrzek Kaim, George Philips, Robert Jenkins, and all the doctors who treated us after our field injuries. This research was supported, in part, by the N.D. Newell Fund (AMNH). We are grateful for incisive reviews by William Halligan, Stephen Kiel, Russell Shapiro, and Andrzej Kaim whose comments substantially improved this manuscript.

Appendix

Table 15.1 AMNH localities, Pierre Shale. Abbreviations: *B. bac.*, *Baculites baculus*; *B. comp.*, *Baculites compressus*; *B. cun.*, *Baculites cuneatus*; *B. scotti*, *Baculites scotti*; *D. chey.*, *Didymoceras cheyennense*; *D. neb.*, *Didymoceras nebrascense.* Study number is a waypoint number (WPT) assigned by J. Brezina

Loc.	Study no. (WPT)	Zone	State	County	TRS	Latitude (N)	Longitude (W)
3342	–	*B. scotti-D. neb.*	SD	Fall River	SW 1/4 SEC 2, T8S, R7E	43° 22′ 48″	103° 15′ 19″
3344	–	*B. scotti-D. neb.*	SD	Butte	SE 1/4 SEC 9, T9N, R7E	44° 45′ 20″	103° 16′ 29″
3386	–	*B. scotti-D. neb.*	SD	Butte	NW 1/4 SEC 17, T9N, R7E	44° 44′ 47″	103° 17′ 47″
3418	59	*D. chey.*	SD	Custer	SEC 14, T3S, R10E	43° 47′ 18″	102° 53′ 20″
3419	61	*B. comp.*	SD	Custer	SEC 30 T3S, R11E	43° 45′ 41″	102° 51′ 9″
3420	61	*D. chey.*	SD	Custer	SEC 19, T3S, R11E	43° 46′ 15″	102° 51′ 26″
3440	36	*B. scotti-D. neb.*	SD	Butte	NW 1/4 SEC 10, T10N, R6E	44° 50′ 23″	103° 22′ 33″
3456	75	*B. comp.*	SD	Pennington	SEC5, T4S, R11E	43° 44′ 8″	102° 49′ 30″
3489	90	*D. chey.*	SD	Pennington	W 1/2 SEC 35, T3S, R12E	43° 45′ 11″	102° 39′ 36″
3494	–	*D. neb.*	WY	Weston	SE 1/4 SEC 18, T43N, R61W	43° 42′ 3″	104° 13′ 55″
3504	98	*B. comp.*	SD	Custer	SEC 19, T4S, R10E	43° 41′ 36″	102° 58′ 36″
3507	60	*B. comp*.	SD	Pennington	SEC 14, T2S, R10E	43° 52′ 42”	102° 53′ 30”
3509	130A, B	*D. chey.*	SD	Pennington	SEC 15, T2S, R10E	43° 52′ 39″	102° 54′ 40″
3528	174	*B. comp.-B. cun.*	SD	Meade	SEC 35, T3N, R14E	44° 10′ 22″	102° 24′ 6″
3529	140	*D. chey.*	SD	Pennington	SEC 3, T2S, R10E	43° 54′ 22″	102° 54′ 27″
3545	63	*B. comp.-B. cun.*	SD	Meade	SEC 18, T4N, R15E	44° 18′ 35″	102° 21′ 2″
3654	136	*D. chey.*	SD	Custer	SEC10, T5S, R9E	43° 37′ 50″	103° 2′ 26′
3666/3531	150	*B. scotti*	NB	Sioux	SEC 19, T34N, R55W	42° 54′ 54″	103° 51′ 19″

(continued)

Table 15.1 (continued)

Loc.	Study no. (WPT)	Zone	State	County	TRS	Latitude (N)	Longitude (W)
3686	67	*B. comp.*	SD	Custer	–	43° 53′ 33”	102° 43′ 41”
3812	79	*D. chey-B. comp.*	SD	Dawson	SEC2, T2S, R11E	43° 54′ 11″	102° 45′ 34″
3911	173	*B. bac.*	MT	Dawson	SEC15, T13N, R56E	46° 52′ 48″	104° 37′ 17″
–	69	*B. jenseni*	MT	Musselshell	–	47° 47′ 34”	107° 48′ 26”

References

Anderson J, Shapiro R, Lyons T (2005) Petrology and petrography of the Tepee Buttes (Cretaceous) methane-deep carbonates. In: Abstracts with programs, Geological Society of America 37:138

Arthur MA, Kauffman EG, Scholle PA et al (1982) Chemical and paleobiological evidence for the submarine spring origin of carbonate mounds in the Pierre Shale (Cretaceous of Colorado). In: Abstracts with programs, Geological Society of America 14:435

Barron EJ (1983) A warm, equable Cretaceous: the nature of the problem. Earth Sci Rev 19:305–338

Bash E, Shapiro R, Anderson J et al (2005) Distribution and mapping of the Cretaceous Tepee Buttes of the Western Interior Seaway. In: Abstracts with programs, Geological Society of America 37:138

Bayon G, Dupré S, Ponzevera E et al (2013) Formation of carbonate chimneys in the Mediterranean Sea linked to deep-water oxygen depletion. Nat Geosci 6:755–760

Bergstresser TJ (1981) Foraminiferal biostratigraphy and paleobathymetry of the Pierre Shale, Colorado, Kansas, and Wyoming. University of Wyoming, Dissertation

Birgel D, Peckman J, Klautzch S et al (2006) Anaerobic and aerobic oxidation of methane at Late Cretaceous seeps in the Western Interior Seaway, USA. Geomicrobiol J 23:565–577

Bishop GA, Williams AB (2000) Fossil crabs from tepee buttes, submarine seeps of the Late Cretaceous Pierre Shale, South Dakota and Colorado, USA. J Crustac Biol 20(2):286–300

Blake DB, Halligan WK, Larson NL (2018) A new species of the asteroid (Echinodermata) genus *Betelgeusia* from methane seep settings, Late Cretaceous of South Dakota. J Paleontol 92(2):196–206

Blakey R (2014) Paleogeography of the Western Interior Seaway of North America. Western Interior Seaway (NAM) series. Late Campanian (*B. compressus*). Used by permission: Colorado Plateau Geosystems https://deeptimemaps.com/map-room/. Accessed 21 Nov 2021

Boetius A, Ravenschlag K, Schubert CJ et al (2000) A marine microbial consortium apparently mediating anaerobic oxidation of methane. Nature 407:623–626

Brezina JA, Larson NL, Landman NH (2019) Fossil wood fall and associated fauna from the Late Cretaceous Western Interior Seaway in South Dakota. Paper presented at second international workshop on ancient hydrocarbon seep and cognate communities, Sapporo, Hokkaido, Japan, 13–15 June 2019

Brophy SK, Garb MP, Landman NH et al (2018) Biotic response to a Late Cretaceous ash fall: comparative faunal analyses from a methane seep and non-seep ecosystem within the Western Interior Seaway. Abstracts with programs, Geological Society of America 50(6):257–214

Brophy SK, Garb MP, Naujokaityte J et al (2022) Methane seeps as possible refugia during ash falls in the Late Cretaceous Western Interior Seaway. Geology 50(4):442–447

Cobban WA, Jeletzky JA (1965) A new scaphite from the Campanian rocks of the Western Interior of North America. J Paleontol 39(5):794–801

Cobban WA, Reeside JB Jr (1952) Correlation of the Cretaceous formations of the Western Interior of the United States. Geol Soc Am Bull 63:1011–1044

Cobban WA, Kennedy WJ, Scott GR (1992) Upper Cretaceous heteromorph ammonites from the *Baculites compressus* Zone of the Pierre Shale in north-central Colorado. US Geol Surv Bull 2024:A1–A11

Cobban WA, Mereweather EA, Fouch TD et al (1994) Some Cretaceous shorelines in the Western Interior of the United States. In: Caputo MV, Peterson JA, Franczyk KJ (eds) Mesozoic systems of the Rocky Mountain region, USA. Rocky Mountain Section Society for Sedimentary Geology, Denver, Colorado, pp 393–413

Cobban WA, Walaszczyk I, Obradovich JD et al (2006) A USGS zonal table for the Upper Cretaceous Middle Cenomanian-Maastrichtian of the Western Interior of the United States based on ammonites, inoceramids, and radiometric ages. US Geol Surv Open-File Rep 2006-1250:1–46

Cochran JK, Landman NH, Turekian KK et al (2003) Paleoceanography of the Late Cretaceous (Maastrichtian) Western Interior Seaway of North America: evidence from Sr and O isotopes. Palaeogeog Palaeoclimat Palaeoecol 191:45–64

Cochran JK, Kallenberg K, Landman NH et al (2010) Effect of diagenesis on the Sr, O, and C isotope composition of Late Cretaceous mollusks from the Western Interior Seaway of North America. Am J Sci 310:69–88

Cochran JK, Landman NH, Larson NL et al (2015) Geochemical evidence (C and Sr isotopes) for methane seeps as ammonite habitats in the Late Cretaceous (Campanian) Western Interior Seaway. Swiss J Paleontol 134(2):153–165

Cochran, JK, Landman NH, Jakubowicz M et al (this volume) Chapter 1: Geochemistry of cold hydrocarbon seeps: an overview. In: Kaim A, Cochran JK, Landman NH (eds) Ancient hydrocarbon seeps. Topics in Geobiology, vol. 50. Springer, Cham

Collom CJ, Johnston PA (2000) Late Cretaceous seep facies in the Western Interior of Canada and the United States: iron ooids, carbonate mounds, and associated tectonism. In: Program with extended abstracts (CD), GeoCanada 2000 Millenium Geoscience Summit, University of Calgary, Alberta, 29 May–2 June 2000

Corbett MJ, Watkins DK (2013) Calcareous nannofossil paleoecology of the mid-Cretaceous Western Interior Seaway and evidence of oligotrophic surface waters during OAE2. Palaeogeog Palaeoclimat Palaeoecol 392:510–523

Covey C, Sloan LC, Hoffert MI (1996) Paleoclimate data constraints on climate sensitivity: the paleocalibration method. Clim Chang 32:165–184

Cross TA (1986) Tectonic controls of foreland basin subsidence and Laramide style deformation, western United States. In: Allen PA, Homewood P (eds) Foreland basins. International Association of Sedimentology Special Publications, vol 8, Blackwell Scientific, Oxford, pp 15–39

Dahl RM, Close HG, Parsons-Hubbard K et al (2005) Paleoecology and topographic expression of a Cretaceous cold-seep: a taphonomic analysis of the Tepee Butte limestone. In: Abstracts with programs, Geological Society of America 37(7):138

Dane CH, Pierce WG, Reeside JB Jr (1937) The stratigraphy of the Upper Cretaceous rocks north of the Arkansas River in eastern Colorado. US Geol Surv Prof Pap 186-K:207–232

Darton NH (1902) Oelrichs folio: South Dakota–Nebraska. United States Geologic Survey Geologic Atlas of the United States 85. United States Geological Survey, Reston, Virginia

Darton NH (1904) Newcastle folio: Wyoming–South Dakota. United States Geological Survey Geologic Atlas of the United States 107. United States Geological Survey, Reston, Virginia

Darton NH (1905) Preliminary report on the geology and underground water resources of the central Great Plains. US Geol Surv Prof Pap 32:1–108

Darton NH (1919) Newell folio: South Dakota. United States Geological Survey Geologic Atlas of the United States 209. United States Geological Survey, Reston, Virginia

Darton NH, O'Harra CC (1909) Belle Fourche folio: South Dakota. United States Geological Survey Geologic Atlas of the United States 164. United States Geological Survey, Reston, Virginia

Darton NH, Paige S (1925) Central Black Hills folio: South Dakota. United States Geological Survey Geologic Atlas of the United States 219. United States Geological Survey, Reston, Virginia

Dennis KJ, Cochran JK, Landman NH et al (2013) The climate of the Late Cretaceous: new insights from the application of the carbonate clumped isotope thermometer to Western Interior Seaway macrofossils. Earth Planet Sci Lett 362:51–65

Elias MK (1931) The geology of Wallace County, Kansas. Kansas Geol Surv Bull 18:1–254

Elias MK (1933) Cephalopods of the Pierre Formation of Wallace County, Kansas, and adjacent area. Univ Kansas Sci Bull 21(9):289–363

Fenneman NM (1931) Physiography of western United States. McGraw-Hill, New York

Finlay GJ (1916) Colorado Springs folio: Colorado. United States Geological Survey Geologic Atlas of the United States 203. United States Geological Survey, Reston, Virginia

Fisher CA (1906) Nepesta folio: Colorado. United States Geological Survey Geologic Atlas of the United States 135. United States Geological Survey, Reston, Virginia

Fisher CG, Arthur MA (2002) Water mass characteristics in the Cenomanian Western Interior Seaway as indicated by stable isotopes of calcareous organisms. Palaeogeog Palaeoclimat Palaeoecol 188:189–213

Fricke HC, Foreman BZ, Sewall JO (2010) Integrated climate model-oxygen isotope evidence for a North American monsoon during the Late Cretaceous. Earth Planet Sci Lett 289:11–21

Gilbert GK (1896) The underground water of the Arkansas Valley in eastern Colorado. US Geol Surv Ann Rept 17(2):551–601

Gilbert GK (1897) Pueblo folio: Colorado. United States Geological Survey Geologic Atlas of the United States 36. United States Geologic Survey, Reston, Virginia

Gilbert GK, Gulliver FR (1895) Tepee buttes. Geol Soc Am Bull 6:333–342

Gill JR, Cobban WA (1966) The Red Bird section of the Upper Cretaceous Pierre Shale in Wyoming. US Geol Surv Prof Pap 393-A:1–73

Hall J, Meek FB (1856) Description of new species of fossils, from the Cretaceous formations of Nebraska, with observations upon *Baculites ovatus* and *B. compressus*, and the progressive development of the septa in *Baculites*, *Ammonites*, and *Scaphites*. Mem Am Acad Arts Sci 5:379–411

Hay WW (2008) Evolving ideas about the Cretaceous climate and ocean circulation. Cret Res 29:725–753

He S, Kyser TK, Caldwell WGE (2005) Paleoenvironment of the Western Interior Seaway inferred from $\delta^{18}O$ and $\delta^{13}C$ values of molluscs from the Cretaceous Bearpaw marine cyclothem. Palaeogeog Palaeoclim Palaeoecol 217:67–85

Howe B (1987) Tepee Buttes: a petrological, paleontological, paleoenvironmental study of Cretaceous submarine spring deposits. Thesis, University of Colorado

Howe B, Kauffman EG (1986) Tepee Buttes, late Campanian submarine springs and the biofacies, between Colorado Springs and Boone, Colorado. In: Kauffman EG (ed), Cretaceous biofacies of the central part of the Western Interior Seaway: a field guidebook. 4th North American Paleontological Convention, University of Colorado, Boulder, pp 155–175

Hryniewicz K (this volume) Appendix: Fossil seeps of the world. In: Kaim A, Cochran JK, Landman NH (eds) Ancient hydrocarbon seeps. Topics in Geobiology, vol 50. Springer, Cham. (Appendix)

Huber BT, Norris RD, MacLeod KG (2002) Deep-sea paleotemperature record of extreme warmth during the Cretaceous. Geology 30:123–126

Hudson JD, Anderson TF (1989) Ocean temperatures and isotopic compositions through time. Earth Environ Sci Trans R Soc Edinburgh: Earth Sci 80(3/4):183–192

Hunter AW, Larson NL, Landman NH et al (2016) A new crinoid from cold methane seep deposits in the Upper Cretaceous Pierre Shale. J Paleontol 90(3):506–524

Hunter AW, Brezina J, Larson NL (2018) Comment to Kato et al. (2017), Paleoecology of echinoderms in cold seep environments revealed by isotope analysis in the Late Cretaceous Western Interior Seaway. PALAIOS 33(6):282–283

Hyatt A (1903) Pseudoceratites of the Cretaceous. US Geol Surv Monogr 44:1–351

Izett GA, Cobban WA, Gill JR (1971) The Pierre Shale near Kremmling, Colorado, and its correlation to the east and the west. US Geol Surv Prof Pap 684-A:1–19

Jenkyns HC, Forster A, Schouten S et al (2004) High temperatures in the Late Cretaceous Arctic Ocean. Nature 432:888–892

Kato M, Oji T, Shirai K (2017) Paleoecology of echinoderms in cold seep environments revealed by isotope analysis in the Late Cretaceous Western Interior Seaway. PALAIOS 32:218–230

Kato M, Oji T, Shirai K (2018) Reply to comment on Kato et al. (2017) Paleoecology of echinoderms in cold seep environments revealed by isotope analysis in the Late Cretaceous Western Interior Seaway. PALAIOS 33(6):284–285

Kauffman EG (1984) Paleobiogeography and evolutionary response dynamic in the Cretaceous Western Interior Seaway of North America. In: Westermann GEG (ed), Jurassic–Cretaceous biochronology and paleogeography of North America. Geol Ass Canada Spec Pap 27:273–306

Kauffman EG, Caldwell WGE (1993) The Western Interior Basin in space and time. In: Caldwell WGE, Kauffman EG (eds), Evolution of the Western Interior Basin. Geol Ass Can Spec Pap 39:1–30

Kauffman EG, Arthur MA, Scholle P et al (1990) Lithofacies, biofacies, and geochemistry of the Tepee Buttes, Late Campanian (Cretaceous) submarine springs, Pueblo-Boone area, southern Colorado: Cretaceous rhythms, events and resources field trip. University of Colorado, Boulder

Kauffman EG, Arthur MA, Howe B et al (1996) Widespread venting of methane-rich fluids in Late Cretaceous (Campanian) submarine springs (Tepee Buttes), Western Interior Seaway, U.S.A. Geology 24:799–802

Kiel S (ed) (2010) The vent and seep biota: aspects from microbes to ecosystems. Topics in Geobiology, vol 33. Springer, Cham

Kiel S, Weise F, Titus AL (2012) Shallow-water methane-seep faunas in the Cenomanian Western Interior Seaway: no evidence for onshore-offshore adaptations to deep-sea vents. Geology 40(9):839–842

Krause FF, Clark J, Sayegh SG et al (2009) Tube worm fossils or relic methane expulsing conduits? PALAIOS 24:41–50

Kruta I, Landman NH, Rouget I et al (2011) The role of ammonites in the Mesozoic marine food web revealed by jaw preservation. Science 331:70–72

Laird JD, Belanger CL (2018) Quantifying successional change and ecological similarity among Cretaceous and modern cold-seep faunas. Paleobiology 45(1):114–135

Landman NH, Klofak SM (2012) Anatomy of a concretion: life, death, and burial in the Western Interior Seaway. PALAIOS 27:672–693

Landman NH, Kennedy WJ, Cobban WA et al (2010) Scaphites of the '*nodosus* group' from the Upper Cretaceous (Campanian) of the Western Interior of North America. Bull Am Mus Natl Hist 342:1–242

Landman NH, Cochran JK, Larson NL et al (2012) Methane seeps as ammonite habitats in the U.S. Western Interior Seaway revealed by isotopic analyses of well-preserved shell material. Geology 40(6):507–510

Landman NH, Kennedy WJ, Cobban WA et al (2013) A new species of *Hoploscaphites* (Ammonoidea: Ancyloceratina) from cold methane seeps in the Upper Cretaceous of the U.S. Western Interior. Am Mus Novit 3881:1–39

Landman NH, Grier JC, Grier JW et al (2015) 3-D orientation and distribution of ammonites in a concretion from the Upper Cretaceous Pierre Shale of Montana. Swiss J Paleontol 134(2):257–279

Landman NH, Cochran JK, Slovacek M et al (2018a) Isotope sclerochronology of ammonites (*Baculites compressus*) from methane seep and non-seep sites in the Late Cretaceous

Western Interior Seaway, USA: implications for ammonite habitat and mode of life. Am J Sci 318:603–639

Landman NH, Jicha BR, Cochran JK et al (2018b) $^{40}Ar/^{39}Ar$ date of a bentonite associated with a methane seep deposit in the upper Campanian *Baculites compressus* Zone, Pierre Shale, South Dakota. Cret Res 90:90–96

Landman NH, Kennedy WJ, Larson NL et al (2019) Description of two species of *Hoploscaphites* (Ammonoidea: Ancyloceratina) from the Upper Cretaceous (lower Maastrichtian) of the U.S. Western Interior. Bull Am Mus Natl Hist 427:1–72

Landman NH, Kennedy WJ, Grier J et al (2020) Large scaphitid ammonites (*Hoploscaphites*) from the Upper Cretaceous (upper Campanian–lower Maastrichtian) of North America: endless variation on a single theme. Bull Am Mus Natl Hist 441:1–131

Larson NL, Jorgensen SD, Farrar RA et al (1997) Ammonites and the other cephalopods of the Pierre Seaway. Geoscience Press, Tucson, Arizona

Larson NL, Brezina J, Landman NH et al (2014) Hydrocarbon seeps: unique habitats that preserved the diversity of fauna in the Late Cretaceous Western Interior Seaway. Wyoming Geological Society Guidebook, Caspar, Wyoming. https://www.academia.edu/4641897/Hydrocarbon_seeps_unique_habitats. Accessed 4 Nov 2021

Lavington CS (1933) Montana Group in eastern Colorado. Am Assoc Pet Geol Bull 17:397–410

Lukeneder A, Harzhauser M, Müllegger S et al (2010) Ontogeny and habitat change in Mesozoic cephalopods revealed by stable isotopes ($\delta^{18}O$, $\delta^{13}C$). Earth Planet Sci Lett 296:103–114

Lynds RM, Slattery JS (2017) Correlation of the Upper Cretaceous stratigraphy of Wyoming. Wyoming State Geol Surv Open File Rept:2017–2013

Mapel WJ, Pillmore CL (1963) Geology of the Newcastle area, Weston County, Wyoming. US Geol Surv Bull 1141-N:1–85

Meehan K, Landman NH (2016) Faunal associations in cold-methane seep deposits from the Upper Cretaceous Pierre Shale, South Dakota. Palaios 31(6):291–301

Meehan KC, Mego Vela M, Gilles NV et al (2018) Foraminifera from the upper Campanian Pierre Shale methane cold-seeps. South Dakota Cret Res. https://doi.org/10.1016/j.cretres.2018.03.023

Meek FB (1876) A report on the invertebrate Cretaceous and Tertiary fossils of the upper Missouri country. US Geol Surv Terr Rept 9:1–629, pls 1–45

Meek FB, Hayden FV (1856) Descriptions of new species of Gasteropoda from the Cretaceous formations of Nebraska Territory. Proc Acad Natl Sci Phila 8:63–69

Merewether EA, McKinney KC (2015) Chronostratigraphic cross section of Cretaceous formations in western Montana, western Wyoming, eastern Utah, northeastern Arizona, and northwestern New Mexico, U.S.A. US Geol Surv Open-File Rept 2015–1087. https://doi.org/10.3133/ofr20151087

Metz CL (2002) Upper Cretaceous (Campanian) sequence and biostratigraphy, west Texas to east-central Utah and development of cold-seep mounds in the Western Interior Cretaceous basin. Texas A&M University, Dissertation

Metz CL (2010) Tectonic controls on the genesis and distribution of Late Cretaceous, Western Interior Basin hydrocarbon seep mounds (tepee buttes) of North America. J Geol 118:201–213

Michaelis W, Seifert R, Nauhaus K et al (2002) Microbial reefs in the Black Sea fueled by anaerobic oxidation of methane. Science 297:1013–1015

Morton SG (1834) Synopsis of the organic remains of the Cretaceous group of the United States illustrated by nineteen plates, to which is added an Appendix containing a tabular view of the Tertiary fossils hitherto discovered in North America. Biddle, Philadelphia

Morton SG (1842) Description of some new species of organic remains of the Cretaceous group of the United States: with a tabular view of the fossils hitherto discovered in this formation. J Acad Natl Sci Phila 8(2):207–227

Owen DD (1852) Report of a geological survey of Wisconsin, Iowa, and Minnesota; and incidentally of a portion of Nebraska Territory made under instructions from the United States Treasury Department, 2 vols. Lippincott, Grambo, Philadelphia

Petta TJ, Gerhard LC (1977) Marine grass banks, a possible explanation for carbonate lenses, Tepee Zone, Pierre Shale (Cretaceous), Colorado. J Sediment Res 47(3):1018–1026
Robinson CS, Mapel WJ, Cobban WA (1959) Pierre Shale along western and northern flanks of Black Hills, Wyoming and Montana. Am Ass Pet Geol Bull 43:101–123
Robinson CS, Mapel WJ, Bergendahl MH (1964) Stratigraphy and structure of the northern and western flanks of the Black Hills Uplift, Wyoming, Montana, and South Dakota. US Geol Surv Prof Pap 404:1–134
Rowe A, Landman NH, Witts JW et al (2020) Late Cretaceous methane seeps as habitats for newly hatched ammonites. PALAIOS 35:1–13
Ryan D, Witts JD, Landman NH (2020) Paleoecological analysis of a methane seep in the Late Cretaceous (Maastrichtian) Western Interior, USA. Lethaia 54:185–203
Sahling H, Galkin SV, Salyuk A et al (2003) Depth-related structure and ecological significance of cold-seep communities—a case study from the Sea of Okhotsk. Deep-Sea Res Part I 50:1391–1409
Say T (1820) Observations on some species of zoophytes, shells, &c. principally fossil. Am J Sci Arts 2(2):34–45
Schröder-Adams C (2014) The Cretaceous Polar and Western Interior seas: paleoenvironmental history and paleoceanographic linkages. Sediment Geol 301:26–40
Scott GR (1969) General and engineering geology of the northern part of Pueblo, Colorado. US Geol Surv Bull 1262:1–131
Scott GR, Cobban WA (1965) Geologic and biostratigraphic map of the Pierre Shale between Jarre Creek and Loveland. Colorado US Geol Surv Misc Geol Invest Map Ser I-439. scale 1:48,000
Scott GR, Cobban WA (1975) Geology and biostratigraphic map of the Pierre Shale in the Canon City-Florence Basin and the Twelvemile Park area, south-central Colorado. US Geol Surv Misc Geol Invest Map Ser I-937. scale 1:48,000
Scott GR, Cobban WA (1986a) Geologic and biostratigraphic map of the Pierre Shale in the Colorado Springs-Pueblo area. Colorado. US Geol Surv Misc Geol Invest Map Ser I-1627. scale 1:100,000
Scott GR, Cobban WA (1986b) Geology, biostratigraphic, and structure map of the Pierre Shale between Loveland and Round Butte. Colorado. US Geol Surv Misc Geol Invest Map Ser I-1700. scale 1:50,000
Shackleton NJ, Kennett JP (1975) Paleotemperature history of the Cenozoic and initiation of Antarctic glaciation: oxygen and carbon isotope analyses in DSDP sites 277, 279 and 281. Init Rep Deep Sea Drilling Prog 29:743–755
Shapiro RS (2004) Recognition of fossil prokaryotes in Cretaceous methane seep carbonates: relevance to astrobiology. Astrobiology 4:438–449
Shapiro RS, Fricke H (2002) Tepee buttes: fossilized methane-seep ecosystems. In: Leonard EM et al (eds), High Plains to Rio Grande Rift: Late Cenozoic evolution of central Colorado. Geol Soc Am Field Guide 3:94–101
Shapiro RS, Gale CM (2001) Bacterial fossils from Cretaceous methane-seep carbonates. In: Abstracts with programs, Geological Society of America 33(6):A453
Sharps JA (1976) Geologic map of the Lamar Quadrangle. Colorado and Kansas US Geol Surv Misc Geol Invest Map Ser I-944. scale 1:250,000
Sharps JA (1980) Geologic map of the Limon 1″ X 2″ quadrangle, Colorado and Kansas. US Geol Surv Misc Geol Invest Map Ser I-1250., scale 1:250,000
Spicer RA, Corfield RM (1992) A review of terrestrial and marine climates in the Cretaceous with implications for modeling the 'Greenhouse Earth.' Geol Mag 129:169–180
Stephenson LW (1941) The larger invertebrates of the Navarro Group of Texas (exclusive of corals and crustaceans and exclusive of the fauna of the Escondido Formation). Univ Texas Bull 4101:1–641
Teichert BMA, Bohrmann G, Suess E (2005) Chemoherms on Hydrate Ridge—unique microbially-mediated carbonate build-ups growing into the water column. Palaeogeog Palaeoclimat Palaeoecol 227:67–85

Thuy B, Landman NH, Larson NL et al (2018) Brittle star mass occurrence on a Late Cretaceous methane seep from South Dakota, USA. Sci Rep 8-9617:1–9

Tobin TS, Ward PD (2015) Carbon isotope ($\delta^{13}C$) differences between Late Cretaceous ammonites and benthic mollusks from Antarctica. Palaeogeog Palaeoclimat Palaeoecol 428:50–57

Tsujita CJ, Westermann GEG (1998) Ammonoid habitats and habits in the Western Interior Seaway: a case study from the Upper Cretaceous Bearpaw Formation of southern Alberta, Canada. Palaeogeog Palaeoclimat Palaeoecol 144:135–160

Tweto O (1980) Summary of Laramide orogeny in Colorado. In: Kent HC, Porter KW (eds), Colorado geology. Proceedings, Symposium on Colorado geology, Denver, pp 129–134

Weise F, Kiel S, Pack A et al (2015) The beast burrowed, the fluid followed—crustacean burrows as methane conduits. Mar Pet Geol 66(3):631–640

Whitfield RP (1877) Preliminary report on the paleontology of the Black Hills, containing descriptions of new species of fossils from the Potsdam, Jurassic, and Cretaceous formations of the Black Hills of Dakota. US Geographical and Geological Survey of the Rocky Mountain Region, Washington, DC

Wright EK (1987) Stratification and paleocirculation of the Late Cretaceous Western Interior Seaway of North America. Geol Soc Am Bull 99:480–490

Chapter 16
Middle Palaeozoic of Morocco: The Earliest-Known Methane Seep Metazoan Ecosystems

Michał Jakubowicz, Błażej Berkowski, Krzysztof Hryniewicz, and Zdzisław Belka

16.1 Overview

Of the six Palaeozoic hydrocarbon seep carbonate occurrences documented to date (Campbell 2006; Himmler et al. 2008; Jakubowicz et al. 2017), the three oldest ones are known from the middle Palaeozoic of Morocco. Studies of the Moroccan seep deposits are, therefore, central to our understanding of the early evolution of chemosynthesis-based communities. Indeed, the mid-Palaeozoic seeps of northwestern Africa played important roles in formulating general models of the evolutionary patterns in the development of seep-related ecosystems over time (Campbell and Bottjer 1995a, b; Baliński and Biernat 2003; Peckmann et al. 2005; Hryniewicz et al. 2017; Jakubowicz et al. 2017) and also served as objectives of some pioneering geochemical investigations (Feng et al. 2009; Jakubowicz et al. 2015). Likewise, even including the Upper Devonian barite-dominated seep deposits of Western North America (Torres et al. 2003; Canet et al. 2014), the number of studies devoted to the three Moroccan seep sites remains considerably higher than those of the remaining Palaeozoic seeps combined, and further work is in progress.

Rather than a single fossil hydrocarbon seep province, the three middle Palaeozoic seeps of northwestern Africa represent a spatially and stratigraphically disjunct record of changes in palaeoecology of early seep communities spanning a total time of over 50 Myr (Figs. 16.1 and 16.2). Notably, the two oldest seep metazoan

M. Jakubowicz (✉) · Z. Belka
Isotope Research Unit, Adam Mickiewicz University, Poznań, Poland
e-mail: mjakub@amu.edu.pl; zbelka@amu.edu.pl

B. Berkowski
Institute of Geology, Adam Mickiewicz University, Poznań, Poland
e-mail: bbrk@amu.edu.pl

K. Hryniewicz
Institute of Paleobiology, Polish Academy of Sciences, Warszawa, Poland
e-mail: krzyszth@twarda.pan.pl

A. Kaim et al. (eds.), *Ancient Hydrocarbon Seeps*, Topics in Geobiology 50,
https://doi.org/10.1007/978-3-031-05623-9_16

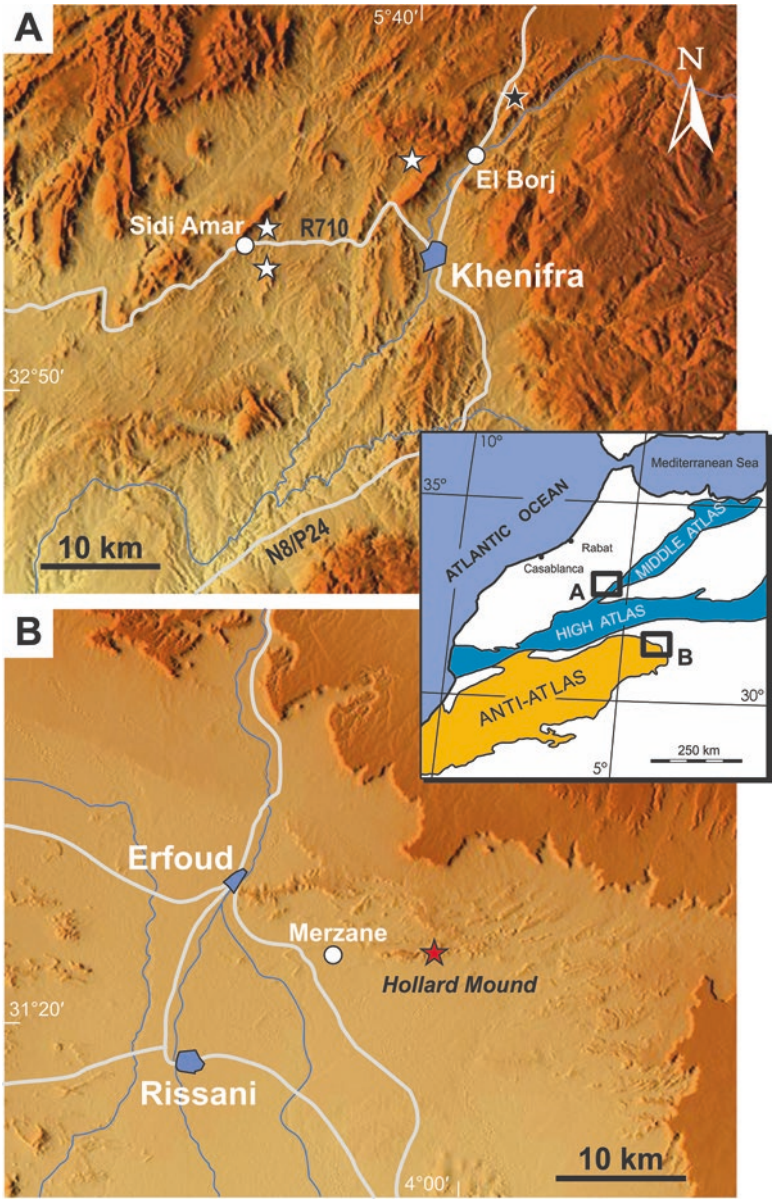

Fig. 16.1 Relief maps of the eastern Moroccan Meseta around Khenifra (**a**) and the eastern Anti-Atlas (**b**) with indicated locations of the Silurian (black star) and Devonian (white stars) seep deposits. The maps are constructed by using public domain data. Inset shows regional geology and location of the study area

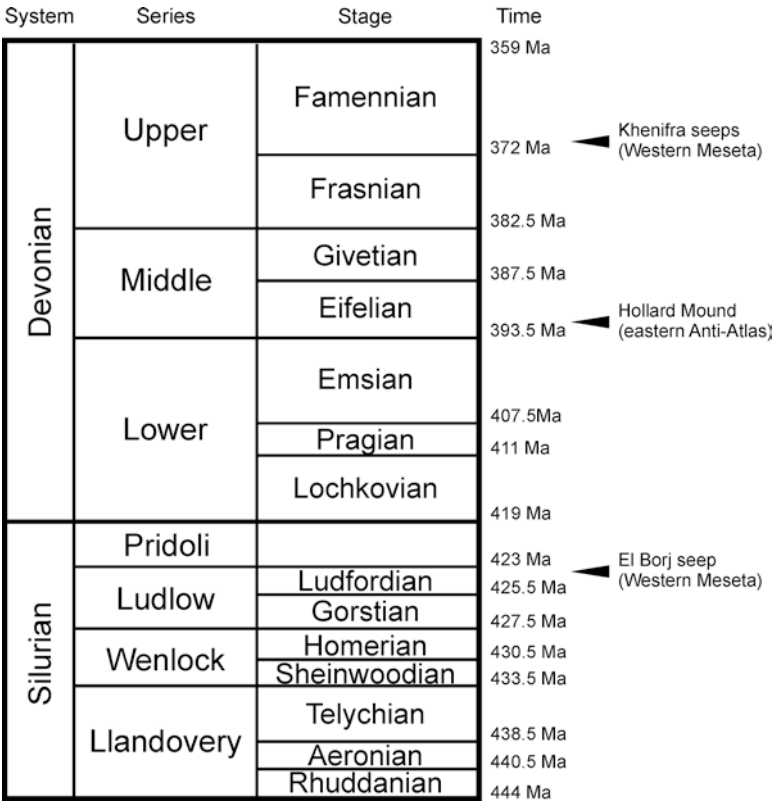

Fig. 16.2 Middle Palaeozoic chronostratigraphic chart (After Cohen et al. 2013) with indicated stratigraphic positions of the Moroccan seep deposits

communities are at the same time the only two Palaeozoic seeps dominated by monospecific bivalve accumulations (Peckmann et al. 1999; Hryniewicz et al. 2017; Jakubowicz et al. 2017), whereas the youngest of the Moroccan seeps provides the first record of clusters of dimerelloid brachiopods (Peckmann et al. 2007), a lineage that recurred in seep assemblages over the next 240 Myr. The investigations of Moroccan seeps offer, therefore, a unique insight into the period of a remarkable success of Palaeozoic bivalve-dominated seep communities, particularly intriguing given the dominance of modern seeps by evolutionarily distant, yet morphologically convergent, bivalve taxa. These studies provide a new look at the concept of modern chemosynthesis-based communities as representing a 'glimpse of antiquity' (Newman 1985), showing that while this view is largely not true taxonomically, it is clearly in terms of recurring morphological themes.

16.2 The El Borj Seep, Upper Silurian, Moroccan Meseta

16.2.1 General Description

The oldest seep deposit of northwestern Africa, and the oldest unambiguous metazoan seep palaeoecosystem, in general, is found 6 km north of the village of El Borj, ~17 km north of Khenifra in the Moroccan Meseta (33°03′57″N, 5°36′16″W; Fig. 16.1a). This seep has usually been referred to as the 'El Borj body/deposit' (Barbieri et al. 2004; Campbell 2006) or 'El Borj seep' (Jakubowicz et al. 2017). Buggisch and Krumm (2005) introduced the term '*Septatrypa*Mound', which is, however, not favoured by us given no evidence for the originally mound-type morphology of the limestone body. The easiest access to the seep locality is to the east of the road N8/P24 (section Khenifra-Azrou), near the primary school house. The seep site is surrounded by agricultural fields, but the access is unconstrained.

The first description of the El Borj limestones was given by Ager et al. (1976) as part of their comparative investigations of several brachiopod occurrences of the Moroccan Meseta. Since the study was published prior to the first discoveries of modern chemosynthesis-based assemblages in the late 1970s, the authors did not recognise the cold seep-related origin of the carbonates. Instead, they interpreted the brachiopod associations as having inhabited 'shoals within shallow, muddy basins' and described the abundant isopachous sparry cements as 'algal lamellae'. Subsequently, the seep-related character of the El Borj palaeoecosystem was speculated upon by Campbell and Bottjer (1995a). The first palaeoecological and petrographic indications of the involvement of methane oxidation in the formation of the El Borj carbonates were documented by Barbieri et al. (2004), nearly 30 years after the initial description by Ager et al. (1976). A following article of Buggisch and Krumm (2005) provided additional petrographic and geochemical data. However, none of these studies presented decisive evidence for the former hydrocarbon seepage in the form of light carbon isotope signatures, which remained a source of some controversy regarding the origin of El Borj carbonate deposit (see Sect. 16.2.3). It was not until very recently when the unexpectedly high $\delta^{13}C$ values typifying the El Borj carbonates were accounted for by Jakubowicz et al. (2017) as a result of their precipitation during a period of a pronounced positive excursion in the carbon isotope composition of seawater. The study also revised previous perceptions of the seep palaeoecology, documenting a previously unrecognised, abundant presence of seep-specialised bivalves.

16.2.2 Stratigraphy and Facies Context

The El Borj deposit comprises a carbonate body ~70 m in width and ~15 m in thickness (Fig. 16.3a), emplaced within a sequence of predominantly argillaceous, shale sediments. For a long time, the stratigraphy of the seep remained poorly constrained.

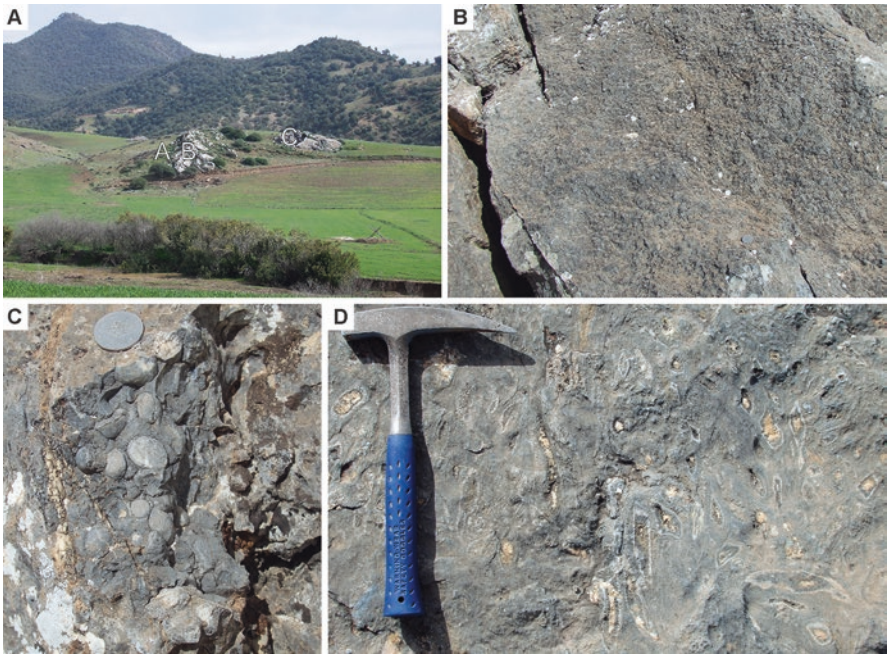

Fig. 16.3 Upper Silurian seep carbonates of El Borj. (**a**) General view of the El Borj deposit seen from the west, with indicated three constituent facies (Units A–C; see text). (**b** and **c**) Mass concentrations of the atrypid brachiopod *Septatrypa lantenoisi* found in Unit B. (**d**) Typical appearance of Unit C. Note the presence of numerous elongated, cement-filled cavities, the majority of which represent interiors of deformed, partially dissolved bivalve shells

The age of the deposit was tentatively assigned to the upper Silurian/lowermost Devonian by Ager et al. (1976) based on the occurrence of the crinoid *Scyphocrinus elegans* in the surrounding strata. Subsequently, the latest Silurian age was suggested by Buggisch and Krumm (2005) based on a single sample containing the conodont *Ozarkodina remscheidensis eosteinhornensis*. Nonetheless, while previous workers assumed an in situ position of the seep limestones within the shales, combined facies and conodont analyses performed by Jakubowicz et al. (2017) showed that the adjacent strata represent a mélange of rocks, ranging from the upper Silurian to the Carboniferous. The facies context of the El Borj body is, therefore, similar to that of the other, Upper Devonian seep carbonates of the Moroccan Meseta (see Sect. 16.4), found 25 km to the southwest. The conodont data collected by Jakubowicz et al. (2017), including the record of *Ozarkodina crispa* in crinoid-rich limestones found as pockets within the seep carbonates, constrain the upper age limit of the El Borj body to the late Ludfordian.

The El Borj deposit comprises a succession of three petrographically distinct facies, referred to as Units A–C by Barbieri et al. (2004; Fig. 16.3a). Petrographic descriptions of these facies were given by Barbieri et al. (2004), Buggisch and Krumm (2005) and Jakubowicz et al. (2017). Unit A consists of alterations of

limestones and marls, with many beds enriched in iron oxides, in places forming haematitic crusts. Although Unit A contains rare atrypid brachiopods, the abundance of seep-related macroinvertebrates is limited to Units B and C. Unit B, most distinct in the field due to the presence of dense accumulations of atrypids, is composed predominantly of homogeneous, brownish micritic matrix, with few cavities other than the shell interiors (Figs. 16.3b, c, and 16.4a). The first generation of

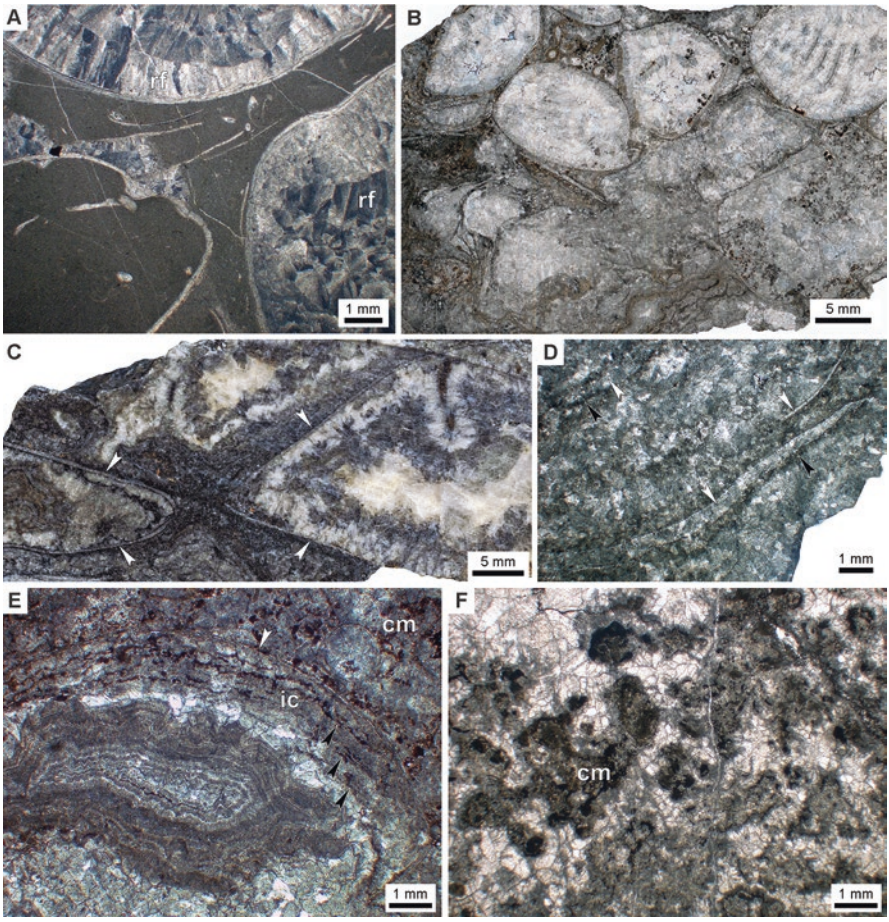

Fig. 16.4 El Borj carbonates observed in thin section (**a**, **b**, and **d**–**f**) and polished slab (**c**) views. (**a**) The brachiopod-rich carbonates of Unit B. Note the simple paragenetic sequence; the bulk of the limestone is made up of a microsparitic carbonate, with the shell interiors infilled with an early radiaxial-fibrous cement (rf) and late blocky spar. (**b**–**f**) Concentrations of atrypid brachiopods (**b**) and modiomorphid bivalves (**c** – **e**; the shells indicated with white arrows) observed in Unit C. Compared to Unit B, the paragenetic sequence is here much more complex and includes multiple generations of early isopachous cements (**e**; ic), clotted, microbial-derived fabrics (**e**, **f**; cm) and corrosion surfaces (**d**, **e**; black arrows). Note strong recrystallisation of the bivalve shells (arrow in **d**), resulting in total obliteration of their original structure. Abbreviations: rf, radiaxial-fibrous cement; cm, clotted micrite

sparry cements is usually developed as radiaxial-fibrous calcite, devoid of distinct banding, major growth discontinuities or coatings of non-carbonate minerals (Fig. 16.4a). The remaining parts of the pores were occluded with banded-to-blocky cements. The simple paragenetic sequence likely reflects a relatively low-emission, diffuse character of the flow at the time of the brachiopod community development (Jakubowicz et al. 2017).

The most complex paragenetic sequence is observed in Unit C, inferred to record a period of increased, spatially and temporarily variable fluid flow rate (Jakubowicz et al. 2017). In field view, this facies is conspicuously different from the remaining, stratigraphically older units owing to its cementstone-type fabric ('stromatolitic facies' of Barbieri et al. (2004)) and distinct faunal assemblage, comprised by dense clusters of both brachiopods and bivalves (Figs. 16.3d and 16.5). The bulk of the limestone embedding the fossils is composed of multiple generations of laminated early cements (Fig. 16.4b–f). The early cements are mainly of isopachous, fibrous fabric, largely recrystallised to a fine spar mosaic. The intricate appearance of the early cements reflects a combination of their small-scale banding, frequent inclusions, micritic coatings, numerous corrosion surfaces, dissolution cavities as well as clotted, microbial-derived fabrics. Centres of the largest cavities were ultimately infilled with blocky calcite spar.

Except for the brachiopod-rich carbonates described here, several cement-rich carbonate lenses devoid of brachiopods were reported from within 1 km^2 from the El Borj occurrence by Ager et al. (1976). These lenses have not been, to our knowledge, studied in detail, and further work is needed to verify their potential relation to hydrocarbon seepage.

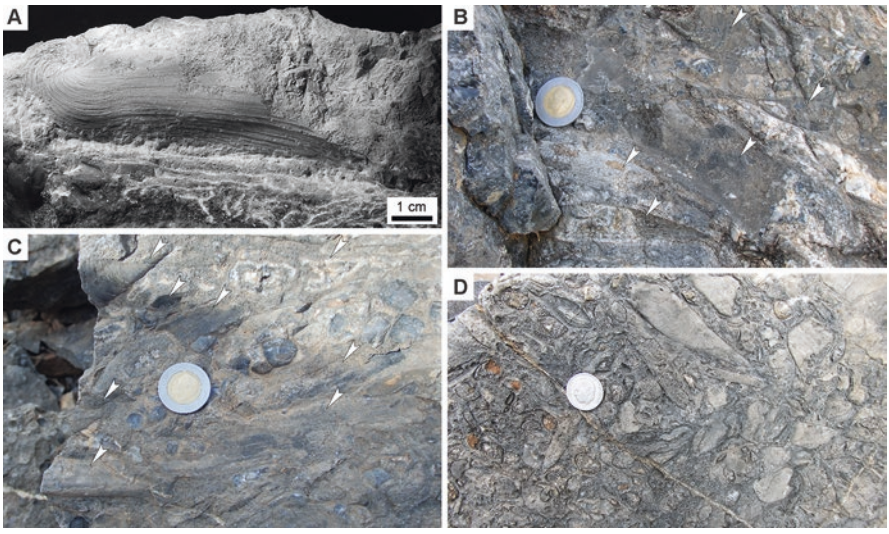

Fig. 16.5 The modiomorphid bivalve *Ataviaconcha* sp. from the El Borj seep. (**a**) *Ataviaconcha* specimen showing an arcuate shape typical of the genus. Reprinted from Jakubowicz et al. (2017) under the Creative Commons Attribution 4.0 International Licence, http://creativecommons.org/licenses/by/4.0/. (**b**–**d**) Field appearance of the clusters of the modiomorphids (arrowed in **b** and **c**) and atrypid brachiopods found in Unit **c**

16.2.3 Geochemistry

Unlike typical cold seep limestones, characterised by strongly negative $\delta^{13}C$ signals, the El Borj carbonates display $\delta^{13}C$ values ranging from −3 to +7‰ V-PDB (Barbieri et al. 2004; Buggisch and Krumm 2005; Jakubowicz et al. 2017). For over a decade that passed since the study of Barbieri et al. (2004), these apparently anomalous, largely positive signatures were variously explained. Barbieri et al. (2004) interpreted them as a result of diagenetic alteration, which resulted in overprinting the primarily more ^{13}C-depleted signals. Buggisch and Krumm (2005) and Himmler et al. (2008) attempted, in turn, to explain the ^{13}C-enrichment by carbonate precipitation due to methane generation (i.e. methanogenesis), rather than methane oxidation. Both these interpretations encountered problems in accounting for the combination of palaeoecological, petrological and geochemical features of the El Borj deposit (see supplementary discussion in Jakubowicz et al. (2017)). Only once the refined stratigraphic framework was established, have the high isotopic signatures been explained by the formation of the seep limestones during the late Ludfordian positive excursion in the carbon isotope composition of ambient seawater (Jakubowicz et al. 2017). Since the excursion, arguably the largest throughout the Phanerozoic, saw $\delta^{13}C_{seawater}$ values ranging from +6 up to even +12‰ V-PDB (see Calner (2005), Loydell and Frýda (2011), Jarochowska and Kozłowski (2014) and references therein), the seep carbonates were, in fact, typified by signals down to 10–16‰ lower than the signature of background seawater. Indeed, this scale of the ^{13}C-depletion makes the El Borj deposit similar to other Palaeozoic to late Mesozoic seep limestones (for references, see Campbell (2006) and Jakubowicz et al. (2017)).

Besides the carbon isotope measurements, geochemical studies of the El Borj seep included oxygen (Barbieri et al. 2004; Buggisch and Krumm 2005; Jakubowicz et al. 2017) and strontium (Jakubowicz et al. 2017) isotope measurements, as well as some elemental analyses (Buggisch and Krumm 2005). The low $\delta^{18}O$ values, reaching down to −12‰ V-PDB for the early diagenetic phases, have been interpreted as reflecting various levels of oxygen isotope exchange during diagenetic alteration (Jakubowicz et al. 2017) and are generally similar to values reported for analogous phases in different mid-Palaeozoic carbonate build-ups of Morocco (cf. Aitken et al. 2002; Jakubowicz et al. 2013). The isotopic ratios of strontium, another geochemical proxy susceptible to diagenetic overprinting, were affected by diagenesis to a lesser degree, as implied by marine or near-marine signals recorded in the early isopachous cements (Jakubowicz et al. 2017).

16.2.4 Fauna

The most conspicuous faunal elements of the El Borj palaeoecosystem are mass concentrations of atrypid brachiopods (Units B and C; Ager et al. 1976; Barbieri et al. 2004) and modiomorphid bivalves (Unit C; Jakubowicz et al. 2017). Other

possibly seep-related biota are represented by rare, small (~0.5–1 mm wide and several mm long) tube-shaped fossils possibly attributable to tube worms, described from the upper part of Unit C by Buggisch and Krumm (2005). Other faunal elements embedded within the seep limestones include rare, small gastropods (Jakubowicz et al. 2017), orthocone nautiloids (Barbieri et al. 2004) and crinoid fragments.

The abundant atrypids are represented by a single species, *Septatrypa* (=*Dubaria*) *lentenoisi* (Ager et al. 1976; Fig. 16.6; see also Baliński et al. this volume). The thin-walled shells are typically 18–25 mm in width, although specimens attaining up to 32 mm have occasionally been observed. The shells show some morphological variability but typically became progressively more elongated during growth. The ventral valve shows a well-defined sulcus; a corresponding fold of the dorsal valve is poorly developed and more pronounced only in the anterior part of the shell. The pedicle foramen is rarely distinct and it is not clear whether it was functional in adult specimens. Barbieri et al. (2004) suggested that *S. lantenoisi* lived unattached, attaining an umbo-down position due to their partial burial within the soft sediment. A similar growth position has been proposed for some atrypid (see Barbieri et al. (2004)) and many pentamerid taxa (e.g. Anderson and Makurath (1973), Jin (2008)). The brachiopod clusters of Unit B reach in places over 60 specimens/100 cm^2 and in many areas constitute the only visible macrofossils (Fig. 16.3b, c).

The brachiopods remain common in Unit C, where they are accompanied by mass concentrations of the bivalves (Figs. 16.3d and 16.5b–d). Most of the bivalve shells were strongly affected by diagenesis, which commonly resulted in their entire dissolution and replacement with diagenetic carbonate phases (Jakubowicz et al. 2017; Fig. 16.4d). As a result, the original outlines of many shells were strongly

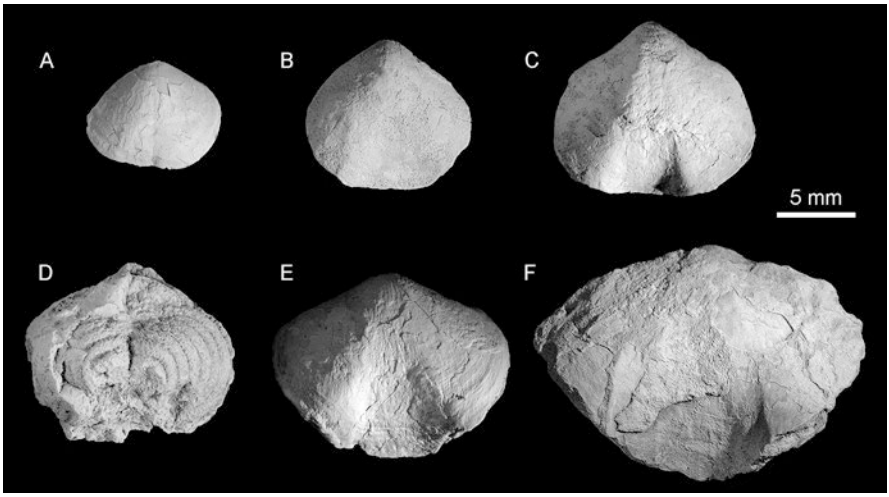

Fig. 16.6 Growth series of the atrypid brachiopod *Septatrypa lantenoisi* from the El Borj seep. A specimen illustrated in D exhibits well-preserved spiralia

Fig. 16.7 Reconstruction of the benthic community that inhabited the Silurian methane seep of El Borj. Through much of its activity, the El Borj seep hosted clusters of the small, epifaunal atrypid brachiopod *Septatrypa lantenoisi*. During the stage of the most intense fluid flow, these brachiopods were accompanied by mass concentrations of the apparently seep-specialised, large, semi-infaunal modiomorphoid bivalve *Ataviaconcha* sp. Reprinted from Jakubowicz et al. (2017) under the Creative Commons Attribution 4.0 International Licence, http://creativecommons.org/licenses/by/4.0/

deformed and thus may be difficult to recognise, a feature presumably responsible for the bivalves being unnoticed in previous studies (Ager et al. 1976; Barbieri et al. 2004; Buggisch and Krumm 2005). A thin section view of a bivalve specimen can be seen in the study of Barbieri et al. (2004; their fig. 9B). Jakubowicz et al. (2017) identified the bivalves as members of the genus *Ataviaconcha*, belonging to the extinct family Modiomorphidae. The systematic position of the Modiomorphidae remains disputable; most current workers place the taxon within the Anomalodesmata (Cope 2000; Griffin and Pastorino 2006) or Carditida (Hryniewicz et al. 2017). The shells attained large sizes (up to 160 mm in length) and are typified by the ventral margin with a broad sinus, thus producing a conspicuously incurved shape (Fig. 16.5a). The bivalves formed aggregates of up to 250 individuals/m^2 (Fig. 16.7), with many individuals showing consistent orientation directions.

16.3 The Hollard Mound, Middle Devonian, Eastern Anti-Atlas

16.3.1 General Description

When measured by the sheer number of publications, no single pre-Cenozoic seep has attracted to date as much scientific attention as the Middle Devonian Hollard Mound. The name was coined by Walliser (1991) to commemorate Henri Hollard,

a French geologist who laid the foundations for much of the present knowledge of the Palaeozoic of the eastern Anti-Atlas area (e.g. Hollard (1967, 1974, 1981)). The terminology may be here somewhat confusing, since the actual seep carbonate bodies are found in the lower portion of the considerably more extensive elevation referred to as the 'mound', in total some 30 m high and 300 m wide (see Jakubowicz et al. (2015), Hryniewicz et al. (2017)). The seep is located in the easternmost part of the Hamar Laghdad ridge, ~20 km southeast of the city of Erfoud (31°22′48″N, 4°01′49″W; Fig. 15.1b). The easiest access to the seep site is from the village of Merzane, located 8 km to the west of the Hollard Mound; the mound can be accessed directly by car using dirt roads running along the southern rim of the Hamar Laghdad ridge. Geological work in the area is, at the moment, unconstrained, although there are plans to propose Hamar Laghdad as a UNESCO World Heritage site (Henriet et al. 2014).

The first general description of the faunal assemblage present in the Hollard Mound was given by Töneböhn (1991). The deposit was identified as a fossil methane seep by Peckmann et al. (1999) based on the peculiar faunal association and negative carbon isotope signatures observed in bedded carbonates found at the base of the build-up. This was followed by numerous studies addressing various aspects of palaeoecology (Aitken et al. 2002; Peckmann et al. 2005; Berkowski 2006; Berkowski and Weyer 2012; Jakubowicz et al. 2013; Hryniewicz et al. 2017) and sedimentary environment (Mounji et al. 1999; Buggisch and Krumm 2005; Cavalazzi 2007; Cavalazzi et al. 2007, 2012; Feng et al. 2009; Jakubowicz et al. 2015) of the seep. This burst of publications reflects a combination of the unique, well-preserved faunal assemblage, good exposure, relatively easy accessibility and, perhaps most importantly, location of the Hollard Mound in the area known worldwide for spectacular outcrops of Lower Devonian mud mounds (Brachert et al. 1992; Belka 1998). For a long time, the Hollard Mound was not only the oldest-known unequivocal hydrocarbon seep (cf. Jakubowicz et al. 2017) but also the sole example of the 'modern-type', that is, bivalve-dominated seep community documented from the Palaeozoic, generally regarded as a time of brachiopod dominance at seeps (e.g. Campbell and Bottjer (1995a), Peckmann et al. (2005), Campbell (2006), Kiel (2010), Jenkins et al. (2013)). Nevertheless, the evolutionary significance of the Devonian bivalve-dominated seep long remained disregarded (for discussions, see Hryniewicz et al. (2017) and Jakubowicz et al. (2017)).

16.3.2 Stratigraphy and Facies Context

The Hollard Mound constitutes one of few Middle Devonian carbonate build-ups of the Hamar Laghdad area, generally dominated by upper Lower Devonian (Emsian) carbonate mud mounds, locally called 'Kess-Kess' (Brachert et al. 1992; Aitken et al. 2002). The mounds grew on a former seafloor elevation provided by a Lochkovian eruption of basaltic volcaniclastics. The inferred activity of submarine fluid discharges in the area lasted from the Early until the early Late Devonian and

included, except the episode of hydrocarbon seepage, emissions of low-temperature hydrothermal fluids. Belka (1998) and Mounji et al. (1998) attributed the formation of the Kess-Kess mounds to expulsions of hydrothermal solutions that originated from interactions between circulating seawater and the underlying volcaniclastics and carbonate sedimentary pile. This perception was supported by following sedimentological, geochemical and palaeontological investigations (Aitken et al. 2002; Berkowski 2004; Belka and Berkowski 2005; Cavalazzi et al. 2007; Franchi et al. 2015a, b; Belka et al. 2015).

In the eastern part of Hamar Laghdad, activity of submarine fluid emissions persisted locally until the end of the Middle Devonian (Berkowski 2006; Jakubowicz et al. 2014a, b), resulting in the formation of a single Givetian mud mound and the Eifelian seep carbonates of the Hollard Mound. As a whole, the elevation traditionally referred to as the Hollard Mound is formed by a continuous succession of Emsian to Givetian strata, well exposed due to the presence of a near-vertical fault cross-cutting the mound along the N-S direction (Fig. 16.8a). Peckmann et al. (1999) described the mound as ranging in age from the lowermost Eifelian (*partitus* conodont Zone) to the uppermost Givetian (*disparilis* conodont Zone). Nonetheless, the Givetian is represented only by haemipelagic strata onlapping the mound from the south (Töneböhn 1991; Berkowski and Weyer 2012). The carbonates hosting the characteristic, bivalve-dominated faunal associations occur only in the lower portion of the succession (Fig. 16.8a), mostly dated to the *partitus* Zone, but partially ranging into the *costatus* Zone. Most previous investigations focused on a large, well-exposed occurrence of the seep carbonates exposed in the northern part of the mound, which hosts rich concentrations of bivalves and, locally, putative tube worms. In addition, another, smaller seep carbonate body, also bearing a bivalve fauna, was recently described by Jakubowicz et al. (2015) from the eastern slope of the build-up (Fig. 15.8a).

The seep carbonates of the Hollard Mound are typically crudely bedded, although in some parts of the build-up, the bedding is obscured by large amounts of rock debris and a dense network of thick, dark-coloured veins (Fig. 16.8b). The veins are infilled with a complex paragenetic sequence comprising multiple generations of laminated isopachous cements (Peckmann et al. 1999; Buggisch and Krumm 2005; Cavalazzi et al. 2007, 2012; Cavalazzi 2007) and likely represent rejuvenations of pre-existing fluid flow pathways (Jakubowicz et al. 2015). In the lower part of the larger of the two seep carbonate bodies, two distinct facies can be distinguished: (1) predominantly microcrystalline carbonates hosting the dense bivalve accumulation, referred to as a 'bivalve limestone' by Peckmann et al. (2005; Fig. 16.8c–e), and (2) sparry cement-dominated carbonates containing concentrations of tube-shaped fossils, found adjacent to a large, near-vertical vein and termed a 'worm tube limestone' by Peckmann and co-workers (2005; Fig. 16.8f; for a detailed facies map, see fig. 2D in Hryniewicz et al. (2017)). The bivalve-bearing limestone is mostly composed of microsparitic matrix, in places riddled with dissolution cavities, pyrite crystals (Peckmann et al. 1999) and irregular dissolution zones composed of small-scale intercalations of the microspar and laminated cements, referred to as 'diffuse corrosion areas' by Jakubowicz et al. (2015; Fig. 16.9b–e). The former open spaces

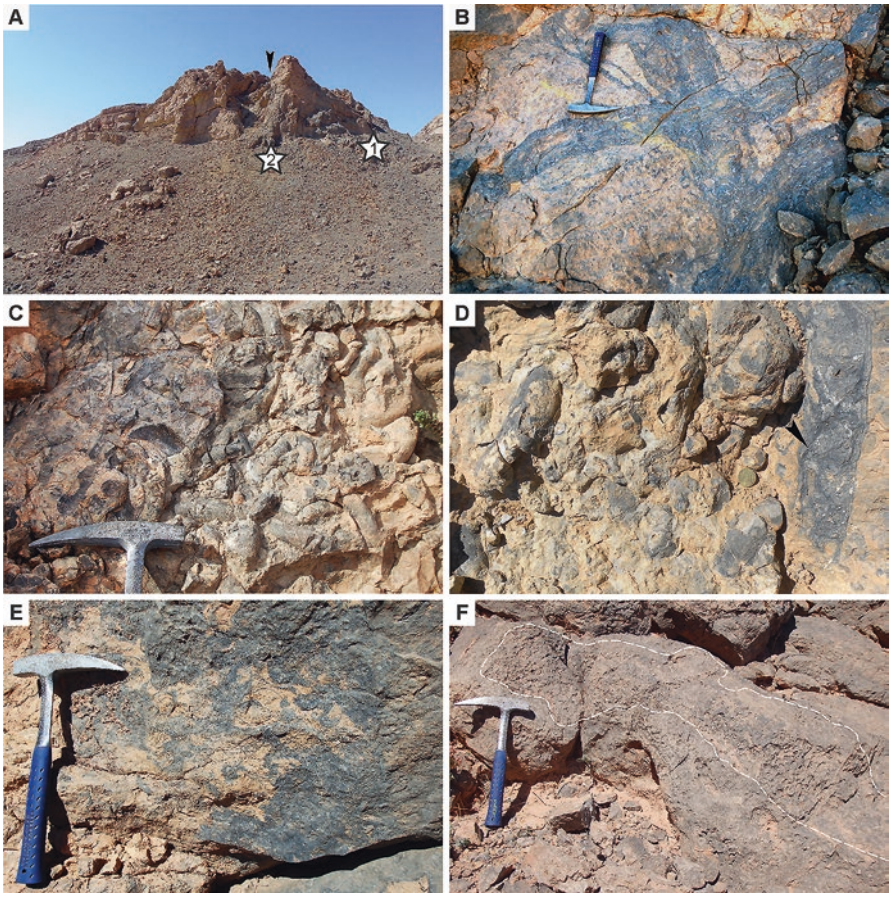

Fig. 16.8 Middle Devonian seep carbonates of the Hollard Mound. (**a**) General view of the mound seen from the east, with indicated positions of the two bivalve-rich seep carbonate bodies (stars). Note the presence of a near-vertical fault cross-cutting the build-up (arrow). (**b**) Typical appearance of cement-filled veins that cut across the seep carbonates. Note the intersection relationships implying that the veins represent several different generations. (**c**–**e**) Seep carbonates hosting dense bivalve clusters. Note the presence of cement-filled veins (**d**) and corrosion areas (**e**) truncating the bivalve limestone. (**f**) Dark-coloured, isopachous cement-dominated carbonates containing abundant fossils of tube-shaped organisms (the facies indicated with a dashed line border) found adjacent to a large, near-vertical vein in the central portion of the larger of the two seep carbonate bodies (No. 1 in **a**)

are lined with laminated, early diagenetic cements, showing clear traces of a formerly fibrous fabric. An even more complex paragenetic sequence is observed in the worm tube-rich facies, nearly devoid of microcrystalline matrix and composed of several generations of laminated cements, corrosion surfaces, dissolution cavities, microbial-derived clots and microstromatolites (Peckmann et al. 2005; Jakubowicz et al. 2015; Figs. 16.9f and 16.10). The remaining parts of the cavities were ultimately occluded with bladed to blocky calcite and, in places, dolomite crystals.

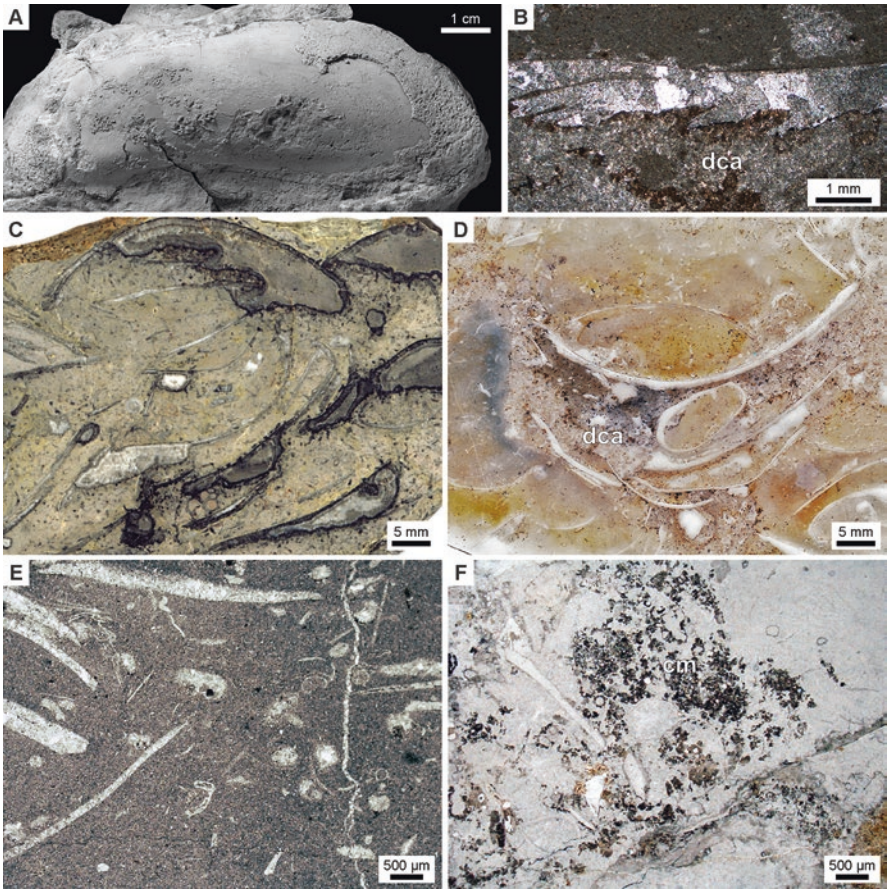

Fig. 16.9 Fossils and microfacies of the Hollard Mound seep carbonates. (**a**) Specimen of the modiomorphid *Ataviaconcha wendti*. Note the conspicuous incurved shape of the shell. (**b**) Photomicrograph of the modiomorphid shell showing strong diagenetic alteration of its original material. Note the corrosion surface, lined with micritic clots and pyrite, present at the contact of the shell with a diffuse corrosion area (dca). The diffuse corrosion areas are interpreted as a result of diffuse flow of H_2S-enriched fluids seeping through the micritic sediment, resulting in partial corrosion of the carbonate matrix and its subsequent cementation with early cements. The shells commonly served as barriers limiting the upward fluid migration, thus limiting corrosion of the overlying sediment (see Jakubowicz et al. 2015). (**c** and **d**) Polished slab (**c**) and entire thin section (**d**) views of the bivalve-rich carbonates showing their typical patchy appearance, largely reflecting the abundance of dissolution cavities and diffuse corrosion areas (dca). (**e**) Photomicrograph of the homogeneous, microsparitic matrix engulfing the bivalve shells in the central part of the seep carbonate body. (**f**) Photomicrograph (transmitted light with a white card background) showing clotted, micropeloidal fabrics (cm) found in abundance in the worm tube limestone

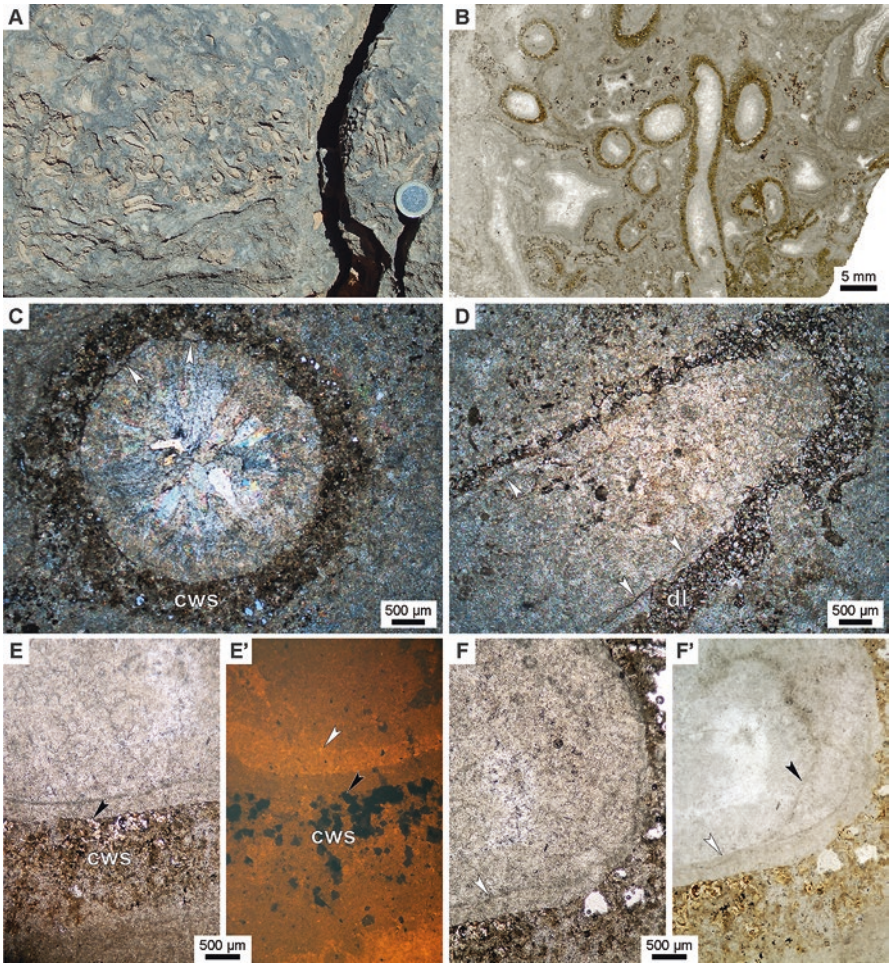

Fig. 16.10 Inferred tube worm fossils found in the seep carbonates of the Hollard Mound. (**a** and **b**) Field (**a**) and thin section (**b**) views of the tube clusters. Note the presence of characteristic, brownish carbonate collars ('carbonate with spheres' sensu Peckmann et al. 2005) engulfing the tubes and their embedding by multiple generations of isopachous sparry cements. (**c** and **d**) Photomicrographs of the tubes observed in transverse (**c**) and diagonal (**d**) sections. The original carbonate with spheres (cws in **c**) has been replaced in places with dolomite (dl in **d**). Note local preservation of the calcite-indurated original tube laminae (arrows). (**e** and **e′**) Transmitted light and corresponding cathodoluminescence views (black arrows for reference) of a tube wall. Cathodoluminescence observation reveals the former presence of the tube wall delamination (white arrow), currently indistinguishable in the transmitted light view (note infilling of the resulting pore with orange luminescent cement). The continuity of luminescence characteristics of the carbonate-replaced tube wall, carbonate with spheres (cws) and first cement generation rimming the carbonate collars attests early diagenetic replacement of the original tube wall, in agreement with the observations made on modern siboglinid tubes (Haas et al. 2009). (**f** and **f′**) Transmitted light views of a portion of a tube wall with (**f′**) and without (**f**) a white card background. Note delamination of the tube wall laminae (arrows), best defined in the white card background view

16.3.3 Geochemistry

A suite of geochemical techniques have been applied in studies of the Hollard Mound carbonates. These include not only standard, stable isotope measurements (Peckmann et al. 1999, 2005; Cavalazzi et al. 2007; Jakubowicz et al. 2013, 2015) but also elemental analyses (Buggisch and Krumm 2005; Feng et al. 2009; Cavalazzi et al. 2012; Jakubowicz et al. 2015) and Nd isotope investigations (Jakubowicz et al. 2015). Biomarker studies, while attempted, proved unsuccessful because of the advanced thermal maturity of the analysed deposit (Belka 1991; Birgel et al. 2008; L. Marynowski, personal communication).

The $\delta^{13}C$ values measured in the early diagenetic phases mostly range from −8 to −23‰ V-PDB (Peckmann et al. 1999, 2005; Cavalazzi et al. 2007; Jakubowicz et al. 2013, 2015). Except for the cement-filled veins, the lowest of the carbon isotope ratios were invariably measured in the worm tube-rich carbonates. As a general trend, the carbon isotope composition becomes progressively heavier up the section (Jakubowicz et al. 2013). Jakubowicz et al. (2015) measured carbonate contents in coeval haemipelagic strata as 86% and thus noted that the signals observed in the microspar-dominated samples must be modified to some degree by incorporation of the local seafloor sediment, with its $\delta^{13}C = 0$ to −2‰ V-PDB. According to Peckmann et al. (2005) and Jakubowicz et al. (2015), the $\delta^{13}C_{carbonate}$ values, as combined with the geotectonic setting of the Hollard Mound, can be most likely attributed to a thermogenic origin of the emitted methane. Speculations as to the considerable involvement of higher hydrocarbons into the development of the seep palaeoecosystem (Peckmann et al. 2005; Cavalazzi et al. 2007) were, in turn, questioned (for a discussion, see Jakubowicz et al. (2015)).

The measured oxygen isotope composition, reaching down to −12‰ V-PDB for the microcrystalline phases (Peckmann et al. 1999, 2005; Cavalazzi et al. 2007; Jakubowicz et al. 2013, 2015), is generally depleted in ^{18}O relative to contemporaneous marine calcites. As in the case of the El Borj seep carbonates, these signals fall within the range typical of mid-Palaeozoic carbonate build-ups of Morocco and presumably reflect diagenetic elemental exchange under the conditions of increased temperatures (cf., Jakubowicz et al. 2013). This is probably the case also for the strontium isotope system, with the measured $^{87}Sr/^{86}Sr_{carbonate}$ ratios ranging from 0.7093 to 0.7097 for the microspars and 0.7084 to 0.7088 for the laminated cements (M. Jakubowicz, unpublished data), that is, being considerably more radiogenic than the signals of coeval marine carbonates (0.7078–0.7079; Denison et al. 1997; van Geldern et al. 2006).

The Hollard Mound remains one of a few fossil seeps for which rare earth element (REE) concentrations (Feng et al. 2009; Jakubowicz et al. 2015) and Nd isotope composition (Jakubowicz et al. 2015) were determined. The features observed in the REE inventory, with overall high REE concentrations and MREE-enriched to flattish shale-normalised REE patterns, are generally similar to those known from others, both modern and fossil seep precipitates (Feng et al. 2009; Himmler et al. 2010; Rongemaille et al. 2011; Wang et al. 2018). In general, they reflect seep

carbonate formation at a shallow depth below the sediment-water interface and hence contemporaneously with release of large quantities of REE derived from reduction of Fe-Mn oxides (cf. Himmler et al. 2010; Rongemaille et al. 2011). Similarly, the measured Y/Ho ratios (Jakubowicz et al. 2015) fall between those of seawater and chondrite, reflecting mixing between the signals of ambient seawater and seeping fluids typical of both cold seeps and hydrothermal vents (Bau and Dulski 1999; Himmler et al. 2010; Wang et al. 2018). The seep carbonates lack phases showing positive Ce anomalies, indicative of precipitation under anoxic conditions and common in some other seep deposits (e.g. Rongemaille et al. (2011), Wang et al. (2014)). While Feng et al. (2009) and Jakubowicz et al. (2015) offered somewhat different explanations of this feature, both studies pointed to the critical role of an inflow of oxic, Ce-depleted seawater to the sites of authigenic carbonate precipitation.

A distinctive characteristic of many of the seep carbonate samples is the presence of positive Eu anomalies in the shale-normalised REE patterns. Jakubowicz et al. (2015) considered different scenarios that could have resulted in both primary and diagenetic Eu-enrichment and attributed it to former interactions between the seeping fluids and the underlying volcaniclastic rocks, the latter typified by a conspicuously Eu-enriched REE inventory. The interactions between the methane-charged solutions and the volcaniclastic strata are consistent with neodymium isotope ratios recorded in the Hollard Mound carbonates, with most of the measured εNd values being significantly higher than the ratios reconstructed for coeval local seawater and shifted towards the isotopic composition of the volcaniclastics (Jakubowicz et al. 2015). The study of Jakubowicz et al. (2015) served to demonstrate that Nd isotopes provide a generally useful tool of tracking former fluid-rock interactions at cold seeps, particularly those for which isotopically distinct Nd reservoirs can be expected to occur in the local basement.

16.3.4 Fauna

The most distinctive biotic components of the Hollard Mound palaeoecosystem are tight aggregates of bivalves found throughout the two seep carbonate bodies and most common in the lower part of the seep carbonate succession (Peckmann et al. 1999; Hryniewicz et al. 2017). Hryniewicz et al. (2017) identified the bivalves as belonging to a single, previously unknown genus and species of modiomorphid bivalves, *Ataviaconcha wendti*. A species of *Ataviaconcha* has subsequently been described also from the late Silurian seep community of El Borj (Jakubowicz et al. 2017; see Sect. 16.2). The adult *A. wendti* specimens are large (up to 120 mm long) and distinctly arcuate due to the presence of a deep, well-developed sinus (Fig. 16.9a). The bivalves formed clusters of up to 150 specimens/m^2; many of the shells display consistent orientations.

Except the abundant modiomorphids, the bivalve limestone of the Hollard Mound hosts also much less numerous, smaller shells of solemyid bivalves (Aitken

et al. 2002; Hryniewicz et al. 2017). The solemyids were recognised by Hryniewicz et al. (2017) as a new species of the Ordovician to Devonian genus *Dystactella*, *D. eisenmanni*. The shells of *D. eisenmanni* are found in carbonates rich in branching burrows notably similar to those produced by the modern Solemyidae (Hryniewicz et al. 2017). In addition, the modiomorphid assemblages are accompanied by infrequent, large (over 10 mm long), unidentified discinoid brachiopods (Fig. 16.11a), which occur in close proximity or directly attached to the *Ataviaconcha* shells. The brachiopod fauna is currently under study.

Other than the bivalves, the most characteristic faunal elements of the Middle Devonian seep community are tube-shaped fossils of possibly annelid origin, found in beds overlying the initial, bivalve-dominated horizons, within a sparry cement-dominated facies adjacent to a large vein (Fig. 16.8f). The tubes show mostly subparallel orientation and form concentrations of up to 500 individuals/100 cm^2 (Fig. 16.10a, b). The original tubes are rarely fossilised; their morphology was examined in detail by Peckmann et al. (2005), who interpreted them as a calcitic replacement after an originally chitinous precursor (see also Haas et al. (2009)). The tubes are approximately circular in the transverse section, with diameters of several mm and the wall thickness of up to ~0.5 mm (Fig. 16.10c–f′). In some cases, growth of isopachous cements caused delamination of laminae making up the wall (Fig. 16.10e–f′). The former tubes are recognisable in the field mostly due to their embedding within irregular, porous, micritic carbonate cements, up to 5 mm thick, referred to as the 'carbonate with spheres' by Peckmann et al. (1999, 2005; Fig. 16.10a–d). As shown by Haas et al. (2009), at modern seeps, very similar carbonate collars form around posterior parts ('roots') of vestimentiferan worms. Taxonomic classification of the tube-shaped fossils is troublesome because the tubes alone yield little clues of taxonomic value (cf. Kiel and Dando 2009; Georgieva et al. 2017). Peckmann and co-workers (2005) concluded that the features of the Hollard Mound tubes make them similar to those of modern seep-dwelling members of the polychaete family Siboglinidae and directly suggested that they may represent 'the oldest known seep-related vestimentiferans'. While acknowledging the discrepancy between such a view and the molecular clock-based divergence estimates for the siboglinid clade Vestimentifera, calculated at no less than ~125 Myr (see Hilário et al. (2011) and Vrijenhoek (2013) and references therein), the authors proposed that the Palaeozoic tubes 'could represent earlier stem-group lineages that are not ancestral to the crown-group taxa'. Although the latter interpretation is feasible, it needs to be stressed, however, that it precludes assigning the putative Palaeozoic stem groups to the Vestimentifera, which, by definition, represent a crown group that separated from the frenulatan siboglinids (Pleijel et al. 2009; Li et al. 2017) not earlier than in the Cretaceous. Hence, the lowest taxonomic level that the putative Hollard Mound polychaetes can be assigned to remains the family Siboglinidae.

Besides the tube worms and very rare, strongly corroded, usually unidentifiable fragments of other organisms, the only fossils observed in the worm tube limestone are small gastropods (Fig. 16.11b–d). Some of the specimens exhibit regular projections of the external shell surface (Fig. 16.11c, d), which resemble remains of

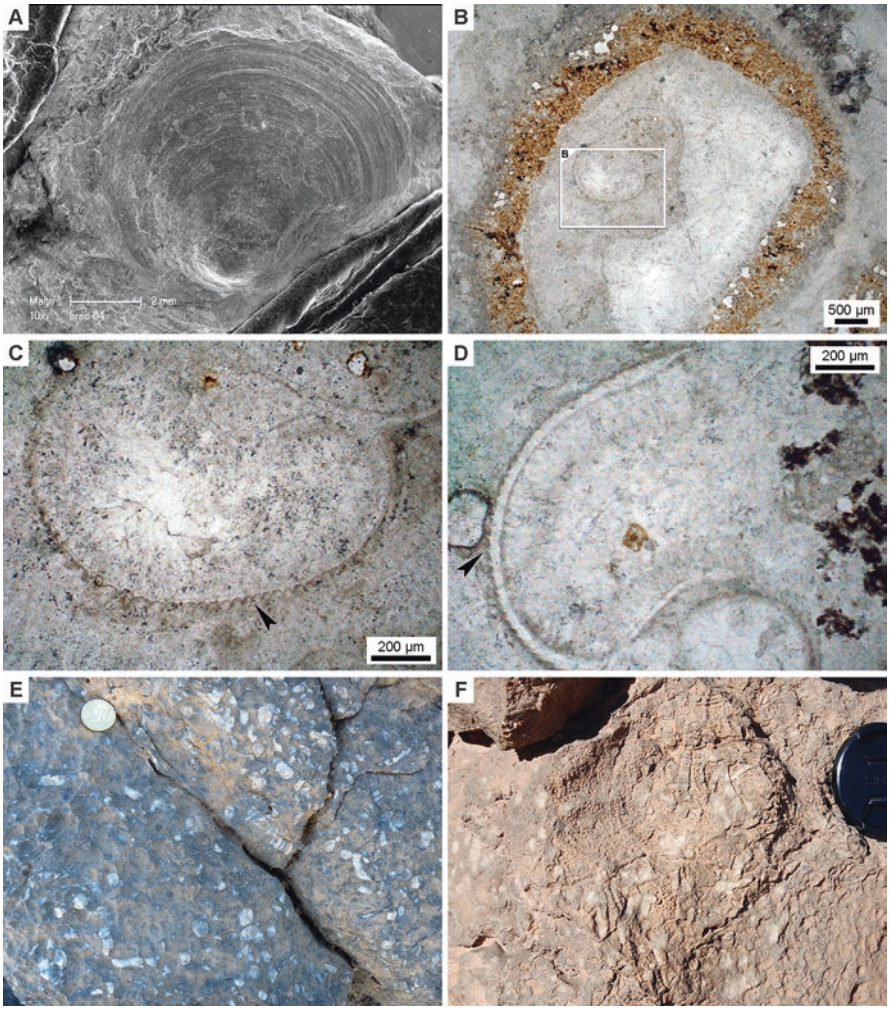

Fig. 16.11 Fossils of the Hollard Mound seep carbonates. (**a**) Scanning electron micrograph of an unidentified discinoid brachiopod species found among the modiomorphid shells. (**b–d**) Thin section views of small gastropods found in the worm tube limestone (one of the tubes illustrated in **b**). Note the presence of characteristic projections of the external shell surface (arrows), reminiscent of periostracal hairs found in some Cenozoic vent-related provannids (Kaim et al. 2012; Johnston et al. 2015; A. Kaim, personal communication). (**e** and **f**) Mass concentrations of the rugose coral '*Amplexus*' *florescens* found in the upper portion of the seep carbonate deposit

periostracal hairs known from the Cenozoic vent-related, provannid genus *Alviniconcha* (Kaim et al. 2012; Johnson et al. 2015; A. Kaim, personal communication). The protective role of the hairy periostracum may be implied by the exceptional preservation of the formerly aragonitic gastropods, which, unlike most other bioclasts, escaped severe dissolution. Unfortunately, the shells were to date observed exclusively in thin sections, and thus their taxonomic identification is not possible.

A peculiar feature of the palaeoecosystem of the Hollard Mound is the presence of dense, monospecific assemblages of solitary rugose corals, which co-occur with sparse modiomorphid bivalves in the upper part of the seep carbonate body (Berkowski 2006; Jakubowicz et al. 2013; Fig. 16.11e–f). The assemblages, found in the form of nest-like accumulations a few tens of centimetres – to few metres – across, were composed of the species *'Amplexus' florescens*, a non-dissepimented, morphologically strongly simplified coral most typical of Palaeozoic deep-water environments. In many places, the corals followed a very unusual, 'calice-in-calice' growth pattern, in which most individuals grew in empty calices of dead corals still projecting above the seafloor (Berkowski 2006; Jakubowicz et al. 2013).

Compared to other fossil hydrocarbon seeps, the seep carbonates of the Hollard Mound contain locally relatively frequent remains of background, non-seep-obligate taxa. These include fragments of crinoids, brachiopods, phacopid trilobites, tabulate corals, tentaculitids and ostracods; fragments of non-seep biota are, however, common only in the marginal parts of the seep carbonate bodies. Their abundance seems to reflect a comparatively high diversity of background deep-water fauna, which was typical of the Hamar Laghdad area from the Pragian until the Givetian (Brachert et al. 1992; Berkowski 2008; Jakubowicz et al. 2013, 2014a; Król et al. 2016). Generally, this can be attributed to a high content of carbonate grains available for attachment in the background sediments, predominantly composed of haemipelagic carbonates, rather than argillaceous siliciclastics that host most seep deposits known from elsewhere.

16.4 The Khenifra Seeps, Late Devonian, Moroccan Meseta

16.4.1 Overview

The stratigraphically youngest of the Moroccan seep deposits are found at several occurrences located north and west of Khenifra in the Moroccan Meseta (Ager et al. 1976; Fig. 16.1a). The best studied of these localities is situated ~1 km east of the village of Sidi Amar, 14 km west of Khenifra (32°57′09″N, 5°49′15″W; Ager et al. 1976; Peckmann et al. 2007). These seep carbonates were referred to as the '*Dzieduszyckia* deposit' (Peckmann et al. 2007; Birgel et al. 2008) or 'Sidi Amar location' (Naehr et al. 2009). Since Devonian occurrences of the genus *Dzieduszyckia* are known also from several different localities around the world, some very distant from the Moroccan shelf of Gondwana (e.g. in western Laurussia; see Baliński and Biernat (2003) and their fig. 1), we prefer using the latter, geographic term as more specific. To refer to the various *Dzieduszyckia*-rich seep deposits located around Khenifra in general, we suggest, in turn, applying the name 'Khenifra seeps'. The Sidi Amar site can be easily accessed from the road R710 (Kaf Ennessoure-Khenifra). The limestone blocks are irregularly distributed on agricultural fields along a distance of some 2 km to the north and south of the road (Fig. 16.1); the access is unrestricted.

First descriptions of the *Dzieduszyckia* occurrences near Khenifra were given by Termier (1936, 1938) and Termier and Termier (1948, 1949), who assigned the brachiopods to *Halorella*, another genus of the superfamily Dimerelloidea, currently known to be restricted to the Triassic (Ager 1968; Sandy 2010). The brachiopod-rich limestones were referred to in several following studies devoted to geology of the Western Meseta (e.g. Roulleau (1956), Hollard and Morin (1973)). The first detailed description of both the brachiopods and their host carbonates was given by Ager et al. (1976), who studied several occurrences of *Dzieduszyckia* (identified by him as *Eoperegrinella*; for a taxonomic discussion, see Baliński and Biernat (2003)) near Khenifra. Given the lack of modern chemosynthesis-based ecosystems known at that time, none of these early studies recognised the relationship between the presence of very rich, low-diversity epibenthic fauna and former methane seepage. As in the case of the El Borj seep palaeoecosystem (see Sect. 16.2), Ager et al. (1976) suggested that the brachiopod communities inhabited local shoals surrounded by relatively deep-water environments and interpreted the abundant isopachous seep cements as algal layers.

The seep-related origin of various *Dzieduszyckia* occurrences known from Gondwana and Laurussia was first proposed by Campbell and Bottjer (1995a) in their general paper on trends in the composition of seep-related shelly faunas throughout the Phanerozoic. This view was supported by Gischler et al. (2003) based on their analysis of morphological similarities among different members of the Dimerelloidea known from Carboniferous and Mesozoic seep deposits. The question of the possible seep-related habitat of *Dzieduszyckia* was subsequently addressed by Baliński and Biernat (2003) but found unsupported based on their stable isotope analyses of the brachiopod shells. It was only the study of Peckmann and co-workers (2007) that provided combined petrological and stable isotope evidence for the seep-related origin of the *Dzieduszyckia*-bearing carbonates.

16.4.2 Stratigraphy and Facies Context

The *Dzieduszyckia* occurrences of Moroccan Meseta are found in the form of numerous, isolated blocks (Fig. 16.12) disseminated at several localities within a shale-dominated succession and thus interpreted as a biostrome (Ager et al. 1976). The succession itself is Carboniferous in age, not older than the late Visean (Ager et al. 1976) and represents a mélange of blocks transported basinwards from tectonically uplifted areas (Walliser et al. 2000). This tectonic setting reflects a complex geological history of the Meseta Domain of the Variscan orogen during the Late Devonian-Late Carboniferous, associated with progressive accretion of this area, once composed of several distinct blocks, to north-western Gondwana (Hoepffner et al. 2005; Michard et al. 2010). Only in rare places do *Dzieduszyckia*-rich limestones seem to be preserved in situ, within continuous successions of Upper Devonian to Carboniferous strata (Ager et al. 1976; Peckmann et al. 2007). The brachiopod-bearing carbonates were dated to the early Famennian based on

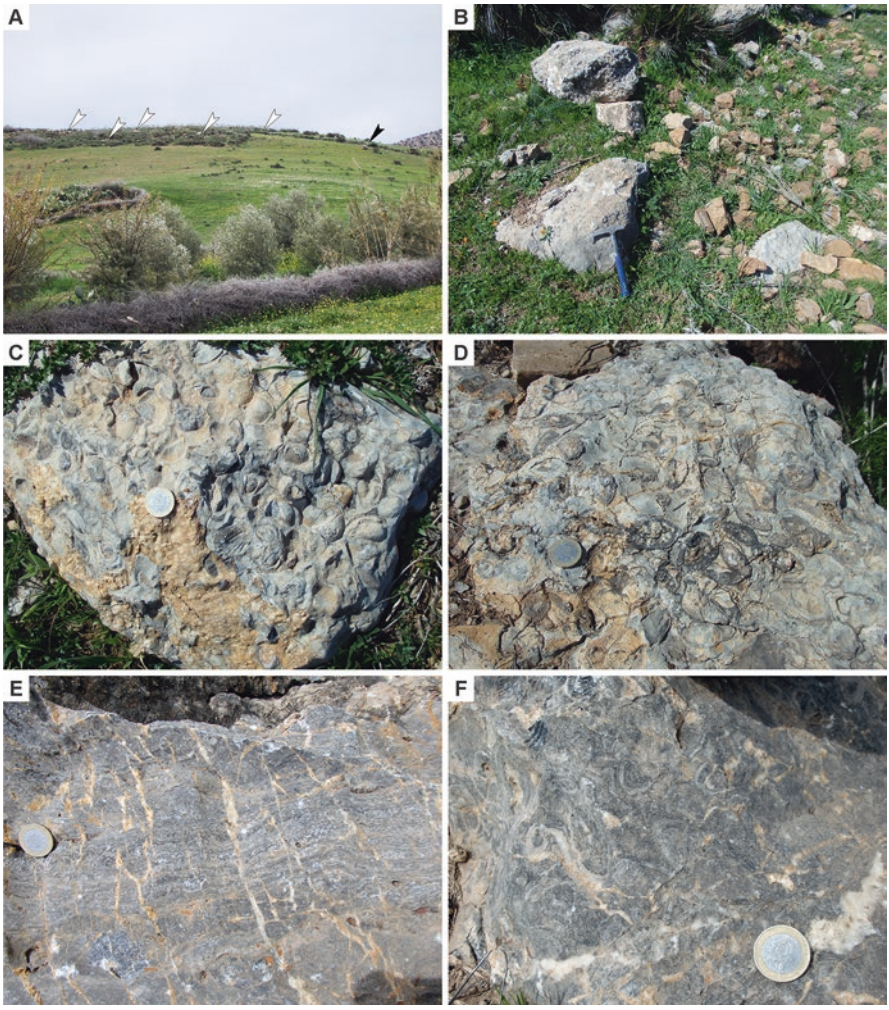

Fig. 16.12 Upper Devonian Khenifra seep carbonates exposed at the Sidi Amar site. (**a**) General view of a small hill north of the road R710 (seen from the east; see Fig. 16.1) with indicated positions of some of the largest blocks of the seep limestones (white arrows, brachiopod limestone facies; black arrow, microbial limestone facies). (**b–d**) Blocks of microcrystalline carbonates hosting mass concentrations of the dimerelloid brachiopod *Dzieduszyckia*. (**e** and **f**) Field views of the isopachous cement-dominated (microbial limestone sensu Peckmann et al. 2007) seep carbonates. Note the presence of *Dzieduszyckia* shells in some portions of the carbonate blocks (**f**)

goniatite and conodont faunas (Hollard and Morin 1973; Ager et al. 1976; not younger than *P. marginifera* to late *P. trachytera* Zones according to Peckmann et al. (2007)).

Peckmann et al. (2007) distinguished two main facies of the seep carbonates, which they referred to as (1) the brachiopod limestone (Fig. 16.12b–d) and (2) the microbial limestone (Fig. 16.12e, f). The brachiopod-rich carbonates are

predominantly microsparitic (Fig. 16.13a, b); the microspar is mostly homogeneous in appearance and only locally riddled with pyrite crystals or microbial-derived clots. The former open spaces present in the interiors of the shells and, in places, among the densely packed brachiopods were locally infilled by early laminated cements, consisting of a fine sparry mosaic with clear ghosts of an originally fibrous fabric (Peckmann et al. 2007). Nevertheless, in many areas, the isopachous fibrous cement generation is lacking, and all the open spaces were occluded by bladed to blocky calcite spar (Fig. 16.13b). Corrosion surfaces are observed locally but are relatively uncommon. In addition, centres of some cavities were occluded with pyrobitumen (Peckmann et al. 2007).

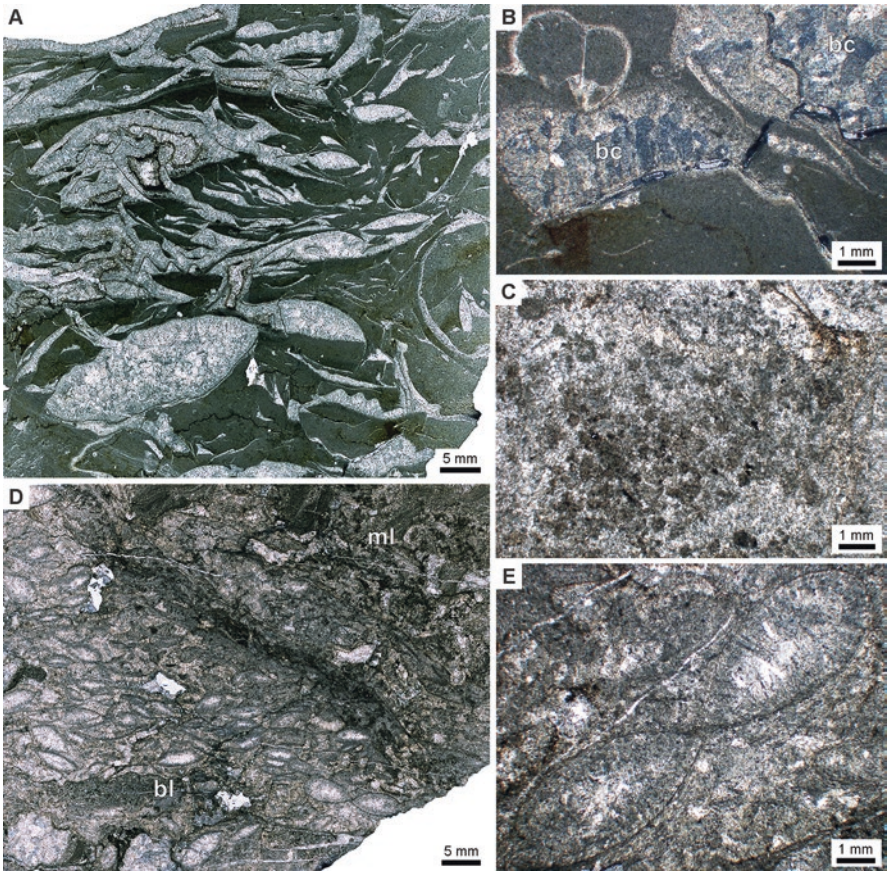

Fig. 16.13 Khenifra seep carbonates, the Sidi Amar site, observed in thin sections. (**a** and **b**) Brachiopod limestone facies. Note the simple paragenetic sequence, with the dominance of homogeneous brownish, microsparitic matrix. The brachiopod shells are commonly infilled exclusively with bladed to blocky calcite spar (bc). (**c**–**e**) Microbial limestone facies. Note the presence of clotted, microbial-derived textures (**c**; cm). While the bulk of the microbial limestone (ml in **d**) is devoid of macrofossils, concentrations of small brachiopods can be observed in places (bl in **d**; **e**)

The ‘microbial limestone’ facies is composed mostly of several generations of isopachous laminated cements (Fig. 16.13d, e). Despite their recrystallisation, the original fibrous texture is still well visible; in places, botryoidal lumps can be observed. Central portions of cavities were infilled with blocky calcite crystals and, occasionally, pyrobitumen (Peckmann et al. 2007). This facies contains few fossils but in places hosts concentrations of brachiopods, typically dominated by small forms (Fig. 16.13d, e). In addition, a variety of inferred microbial-derived fabrics are present in the form of peloidal clots (Fig. 16.13c) or subparallel filamentous structures interpreted as putative remains of former microbial filaments (Peckmann et al. 2007).

16.4.3 Geochemistry

To date, only two studies included geochemical analyses of the Khenifra seep deposits. The first stable isotope data of the *Dzieduszyckia*-rich limestones were given by Baliński and Biernat (2003). These investigations were carried out on archived palaeontological material and thus included mostly the brachiopod shells, and a few samples of the sediment directly attached to them. The analyses gave essentially marine carbon isotope signals for the brachiopods and only slightly ^{13}C-depleted (down to −3.5‰ V-PDB) signatures for the surrounding carbonates, which Baliński and Biernat (2003) interpreted as no evidence of the former hydrocarbon seepage. Nonetheless, the implications of the signals measured in the shells remain unclear, since brachiopods are lacking from modern chemosynthesis-based communities, and thus possible isotope fractionation mechanisms of fossil seep-specialised brachiopods are not known. Modern chemosymbiotic bivalves typically show, in turn, only moderate, if any, deviation from carbon isotope signals expected for marine carbonates (Lietard and Pierre 2009; Nedoncelle et al. 2014), by no means matching the pronounced ^{13}C-depletion recorded in authigenic seep limestones.

A considerably larger set of carbon isotope data was provided by Peckmann et al. (2007) for the seep carbonates of the Sidi Amar site. The δ^{13}C values measured by them fall between +1.5 and −3‰ V-PDB for the microspars and −2 to less than −12‰ V-PDB for early isopachous cements, pointing to the involvement of hydrocarbon oxidation in the formation of the latter. Peckmann et al. (2007) related the generally moderate level of the ^{13}C-depletion observed in the early diagenetic phases to the dominance of liquid hydrocarbons (i.e. oil), rather than methane in the fluids discharged at the Sidi Amar site. The perception of the important role of oil in the development of the Sidi Amar seep remains, however, controversial, since the presence of pyrobitumen (thermally altered petroleum) is limited to the late stage of the paragenetic sequence. Likewise, the significant contribution of oil oxidation to sustaining Palaeozoic seep ecosystems was generally questioned (Jakubowicz et al. 2015). Instead, the moderately negative δ^{13}C values found at the Sidi Amar seep can be accounted for by a diffuse flow of methane-rich fluids, in agreement with the

general perception of palaeoecology of seep-related brachiopods (cf. Peckmann et al. 2009; Kiel et al. 2014; Jakubowicz et al. 2017; see Sect. 16.4.4).

As in the case of the other hydrocarbon seeps of Morocco, the oxygen isotope signatures of the carbonates are depleted in ^{18}O relative to the composition of contemporaneous seawater (Baliński and Biernat 2003; Peckmann et al. 2007), which most likely reflects diagenetic alteration of the original signals. Besides the results of the stable isotope measurements, Peckmann et al. (2007) reported also some elemental data of the seep carbonates and interpreted high Sr contents measured in one of the botryoidal cement samples as indicative of its originally aragonitic mineralogy. Additionally, biomarker investigations were attempted but were unsuccessful due to high maturity of the studied limestones (Birgel et al. 2008).

16.4.4 Fauna

The only abundant metazoan fossils found in the Khenifra seeps are those of members of the brachiopod genus *Dzieduszyckia* (Rhynchonellida: Dimerelloidea; Fig. 16.14). The shells show considerable variability in their external morphological characteristics, which is partially reflected in their taxonomic classification. At least three different species have been distinguished: *D. crassicostata* (Termier and Termier 1948), *D. intermedia* (Termier 1936) and *D. tenuicostata* (Termier 1936; all originally described under the generic name *Halorella* and later attributed to the genus *Eoperegrinella* by Ager et al. (1976)). In addition, several different species were erected in the studies of Termier, but their distinguishing features can be likely

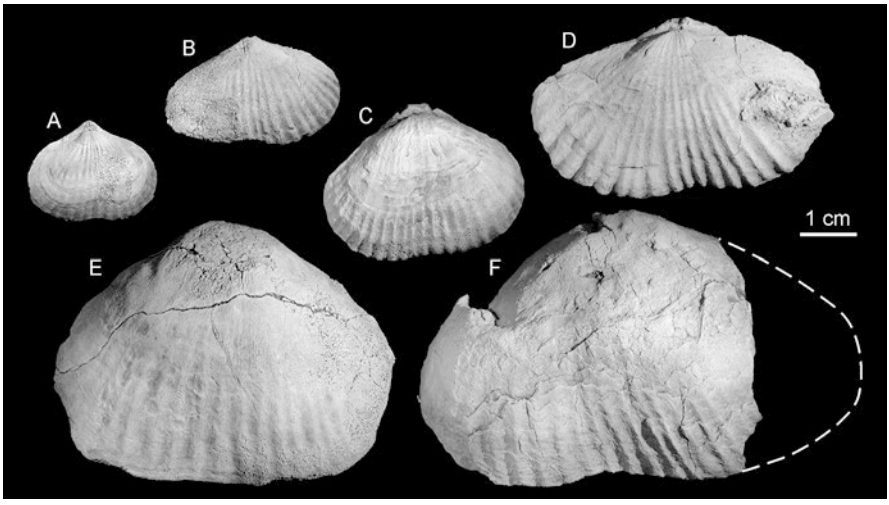

Fig. 16.14 Different growth stages of *Dzieduszyckia*brachiopods found in the Khenifra seep carbonates, the Sidi Amar site. Note that the effect of growth allometry is imposed on the high intraspecific morphological variability

attributed to the high intraspecific variability (for a discussion on the taxonomy of Moroccan *Dzieduszyckia*, see Baliński and Biernat (2003)). Reaching up to 80 mm in width for its Moroccan representatives, *Dzieduszyckia* was among the largest Palaeozoic rhynchonellids. The shells are typically elongated, roughly heart-shaped, bisulcate and most often distinctly costate, although smoother forms have been reported from one of the localities near Sidi Amar (Ager et al. 1976). Many of the shells show pronounced asymmetry. Systematic position of the genus *Dzieduszyckia* within the superfamily Dimerelloidea has been a matter of debate; of the three families comprising the Dimerelloidea (Halorellidae, Peregrinellidae, Dimerellidae), Halorellidae was interpreted as a parent taxon of the subfamily Dzieduszyckiinae by Baliński and Biernat (2003).

Other than the *Dzieduszyckia* shells, the Khenifra seeps contain some fragments of gastropods, ostracods, trilobites, sponges (Peckmann et al. 2007) and terebratulid brachiopods (Ager et al. 1976). Interestingly, structures described as 'worm tubes' were reported by Ager et al. (1976); unfortunately, however, the tubes have not been observed in the following studies, including our brief inspection of the Sidi Amar site, and await detailed description. In addition to the benthic fossils, the seep carbonates contain also rare remains of goniatites and nautiloids (Ager et al. 1976).

16.5 Seep-Related, But Whether Seep-Obligate? Remarks on the Degree of Seep Specialisation and Some Patterns in the Early Evolution of Seep Communities

16.5.1 Overview

When studying the oldest-known cold seep metazoan assemblages, developed 425–370 Ma at the northwestern margin of Gondwana, it would perhaps be sensible to expect them to contain a high proportion of organisms characterised by low levels of specialisation to reducing habitats. Indeed, this appears true for some groups, such as atrypid brachiopods or amplexoid corals, and may be implied by some petrological and stable isotope characteristics of the three Moroccan seep deposits. Nevertheless, other groups, most notably the modiomorphid and solemyid bivalves and arguably the tube worms, display advanced adaptations to inhabiting hydrocarbon seeps, suggesting prolonged evolution of their respective lineages in chemosynthesis-based ecosystems. Hence, to seek insights into the actual, early stages of colonisation of cold seep environments by metazoan organisms, we should apparently focus rather on early Palaeozoic to mid-Silurian time. By the late Silurian, the seep ecosystems were already inhabited by at least some seep-specialised biota. Although the discussion of the possible degree of this specialisation will inevitably entail a degree of speculation, some inferences can be made based on the skeletal morphological features, occurrence mode of the fossils as well as characteristics of their host sediments.

16.5.2 Bivalves

Arguably, the most convincing indications of adaptation to seep-related environments can be found for the bivalves that inhabited both the Silurian and Middle Devonian seeps. This is particularly well supported for the solemyids of the Eifelian Hollard Mound, for which cooperation with chemosymbionts is suggested by their behaviour similar to their extant, chemosynthetic relatives (Hryniewicz et al. 2017). Accordingly, some morphological arguments imply that chemosymbiosis in Solemyidae dates back to the early Ordovician and may be as old as the family (Waller 1998; Cope 2000; Oliver and Taylor 2012).

The two species of the modiomorphid genus *Ataviaconcha*, *Ataviaconcha* sp. from the Ludfordian El Borj site, and *A. wendti* from the Eifelian Hollard Mound share a suite of characteristic features, many observed also in modern seep-dwelling bivalves. Both species attained a very large size, placing them among the largest Palaeozoic bivalves documented so far. A large size is a common distinctive feature of modern vent and seep molluscs and in modern vent and seep bivalves reflects primarily the presence of anomalously enlarged gills, adapted to harbour chemosymbionts (Childress and Fisher 1992; Duperron 2010). Likewise, chemosymbiotic representatives are among the largest forms known in their respective bivalve lineages. Further evidence for adaptation to seep habitats comes from the allometric growth of the mid-Palaeozoic seep modiomorphids and, in particular, the elongated, arcuate shape of the adult specimens. In their studies of the modiomorphids from the Hollard Mound and El Borj sites, Hryniewicz et al. (2017) and Jakubowicz et al. (2017) discussed a role of the boomerang-like shape observed in many members of modern, seep-obligate, chemosymbiotic Vesicomyidae and Mytilidae (Duperron 2010; Krylova et al. 2010; Taylor and Glover 2010), as well as Mesozoic Kalenteridae, another group of the order Modiomorphoida (Kelly et al. 2000; Jenkins et al. 2013, 2018; Kiel 2018). The arcuate shell represents an adaptation to a semi-infaunal habit, enabling the bivalve to orient its shell in a half-buried position and facilitating simultaneous access to oxygen and interstitial-reduced compounds. It is worth noticing that the inferred semi-infaunal lifestyle provides an argument after the presence of chemosymbiosis in *Ataviaconcha*, since, in the absence of microbial symbionts, seeking better access to sulphide-rich sediment pore fluids cannot be explained by metabolic requirements of the bivalve (Jakubowicz et al. 2017). Conversely, even low concentrations of sulphide typically prove lethal to metazoans lacking sulphide detoxification mechanisms or ability to shift to anaerobic metabolism (Powell and Somero 1986; Hourdez and Lallier 2007). Regardless of their position within the phylogenetic tree of the Bivalvia, bivalves appear generally well adapted to develop different forms of chemosymbioses, which appeared independently in several lineages of even distantly related bivalves, starting from their divergence in the early Palaeozoic (e.g. Solemyidae, Lucinidae; Taylor and Glover 2010).

Given that large, strongly elongated shells represent a derived feature that appeared relatively late in the evolution of the seep-related mytilids and

vesicomyids, Silurian *Ataviaconcha* seems to represent a relatively advanced stage in a continuous evolution of its modiomorphid lineage in the chemosynthesis-based communities. Indeed, by now the genus is not known from palaeoecosystems other than two studied fossil seeps. Unfortunately, the question of how widespread the modiomorphid-dominated seep ecosystems were in the middle Palaeozoic cannot be addressed until more mid-Palaeozoic seep communities are reported. It needs to be stressed that although the two *Ataviaconcha*occurrences, separated by some 20 Myr, are currently 250 km apart, their present proximity does not correspond to the original distance between the two seep sites, which was probably considerably larger. According to some palaeogeographic reconstructions, the Meseta area, with its El Borj and Khenifra seeps, could have, in fact, been separated from the main part of Gondwana, and thus the Hollard Mound, by a seaway a few thousand km wide (for discussions, see Hoepffner et al. (2005), Michard et al. (2010) and Stampfli et al. (2013)).

16.5.3 Tube Worms

Although the perception of seep specialisation of the inferred polychaete tube worms found in the Hollard Mound cannot be easily verified given their uncertain taxonomic position, some speculations appear justified based on the combination of their taphonomic characteristics and facies context. The fact that the tubes occur exclusively in carbonates dominated by isopachous fibrous and clotted cements, with very few fossils and low carbon isotope ratios, implies that the tube-forming organisms inhabited areas of increased fluid flow (Peckmann et al. 2005; Jakubowicz et al. 2015). This is consistent with the location of the tube worm limestone in the central part of the seep deposit, adjacent to a thick, near-vertical vein, which likely represents an important part of the former plumbing system (cf. Cavalazzi et al. 2007, 2012; Jakubowicz et al. 2015). This habitat was apparently unfavourable for the modiomorphid and solemyid bivalves, as fragments of bivalve shells are very rare in the tubeworm limestone facies. In general, association of the putative tube worms with fibrous and clotted cement-dominated – and commonly most ^{13}C-depleted – carbonates has been observed at many fossil seeps, including Palaeozoic and Mesozoic ones (e.g. Beauchamp and Savard (1992), Campbell et al. (2002), Buggisch and Krumm (2005), Himmler et al. (2008), Hryniewicz et al. (2015)). This is similar to the pattern observed at modern seeps and vents, where clusters of vestimentiferan tube worms, requiring hard substrates for anchorage, often occupy areas of increased flow and thus concentrations of reduced compounds (e.g. Van Dover (2000), Olu-Le Roy et al. (2004), Bowden et al. (2013)).

In general, the reconstructed habitat, together with the sessile benthic habit preventing the seep-related polychaetes from avoiding the environmental toxicity, may provide indirect arguments supporting their former cooperation with microbial chemosymbionts. This is particularly feasible if the relation of the Hollard Mound worms to the Siboglinidae is accepted (Peckmann et al. 2005; Haas et al. 2009;

Hilário et al. 2011), as all extant siboglinid taxa studied to date in modern chemosynthesis-based environments were documented to host chemoautotrophic microbes (Hilário et al. 2011). Interestingly, modern vestimentiferan siboglinids directly engineer their habitat by stimulating anaerobic oxidation of methane, and thus carbonate precipitation, within the sediment by pumping seawater-derived sulphate into the interstitial waters (Dattagupta et al. 2006; Cordes et al. 2009). A similar behaviour of the mid-Devonian tube worms might possibly account for the precipitation and unique characteristics of the 'carbonate with spheres' that rimmed the Hollard Mound tubes. Remarkably, this phase shows significant textural similarities to the carbonate collars embedding tubes of modern vestimentiferans (Haas et al. 2009) but otherwise seems to have no analogues among a variety of carbonate phases known from cold seep deposits. Indeed, a texturally very similar phase has been described as surrounding tube worms in another, Lower Jurassic seep deposit (Gómez-Pérez 2003). The involvement of the tube-forming organism in the formation of the 'carbonate with spheres' appears also consistent with the typical limitation of this phase to the external tube walls. Nevertheless, until the fossil record of the Siboglinidae is better resolved, the role of the tube worms in precipitation of tube-encrusting carbonates cannot be elucidated beyond doubt.

16.5.4 Brachiopods

The degree of seep specialisation in brachiopods inhabiting Palaeozoic and Mesozoic methane seeps has been a topic of ongoing discussion (see Kaim et al. (2010), Sandy (2010), Kiel and Peckmann (2019) and references therein; see also Baliński et al. this volume). Addressing this issue in general is beyond the scope of this review. Nonetheless, several aspects of the palaeoecology of the mid-Palaeozoic seep-inhabiting brachiopods need to be addressed here. Of the two groups of articulate brachiopods forming mass accumulations at the Moroccan seeps, the Silurian atrypids from El Borj have no documented relatives from other fossil seeps. The implications of this 'scarcity' of seep-related Atrypida should not be overemphasised, as the entire order became extinct during the Frasnian-Famennian extinctions. This limits the actual number of known chemosynthesis-based palaeoecosystems that remained uncolonised by atrypids to a single hydrocarbon seep (the Middle Devonian Hollard Mound) and two hydrothermal vents (Silurian and Middle Devonian of the Urals, Russia; Little et al. 1999). It needs to be noticed, however, that the genus *Septatrypa* has been documented also from various non-seep, both deep- and shallow-water settings, including Silurian reefs and biostromes (Copper 2004; Baliński 2012; Racki et al. 2012). In addition, the morphological characteristics of *S. lentenoisi* do not include traits indicative of an unusual life strategy; its relatively small, smooth, distinctly sulcate shell represents a suite of common adaptations to a deep-water habitat (e.g. Cooper (1972), Fürsich and Hurst (1974)). This may suggest that *S. lantenoisi* inhabiting the El Borj seep either represents a lineage with a comparatively short history in seep-related environments or was a species

applying an opportunistic strategy, which did not require advanced morphological modifications to colonise some chemosynthesis-based ecosystems.

The latest Devonian (Famennian) saw the onset of a new type of cold seep community, conspicuously different from the bivalve-rich assemblages present at the Silurian and Middle Devonian seeps. The role of the Late Devonian biotic crises, associated with dysaerobic events near the Frasnian-Famennian boundary (Wendt and Belka 1991), in restructuring the seep palaeoecosystems is unclear, as is the potential of anoxic events to entirely reset seep ecosystems worldwide in general (Jacobs and Lindberg 1998; Kiel and Little 2006; Vrijenhoek 2013; see also Baliński et al. this volume). A characteristic element of the few known Famennian seeps were brachiopods of the genus *Dzieduszyckia* (Campbell and Bottjer 1995a; Torres et al. 2003; Baliński and Biernat 2003; Peckmann et al. 2007; Canet et al. 2014), best known from the mass accumulations of the Moroccan Meseta. The genus represents the oldest-known representative of the Dimerelloidea, a group with long and successful history in chemosynthesis-based ecosystems, lasting until the Early Cretaceous (Gischler et al. 2003; Kaim et al. 2010; Sandy 2010; Kiel et al. 2014; Kiel and Peckmann 2019). Indeed, *Dzieduszyckia* displays some peculiar morphological features, the most notable of which is perhaps its often exceptionally large size, a trait recurring among dimerelloids during their evolutionary history at seeps (Baliński and Biernat 2003; Sandy 2010; Kiel et al. 2014). Unfortunately, given the absence of analogous brachiopod associations at Cenozoic seeps, it is uncertain as to what degree the very large, bisulcate, distinctly costate shells of *Dzieduszyckia* can be regarded as reflecting its seep-related habitat. Furthermore, it is not clear whether *Dzieduszyckia* and younger dimerelloids shared a common ancestor or colonisation of seeps occurred several times by dimerelloid taxa recruited from background deep-water faunas (cf. Kaim et al. 2010; Sandy 2010; Kiel et al. 2014). Members of *Dzieduszyckia* were reported also from non-seep, deep-water environments (Peckmann et al. 2007; Nie et al. 2016), and a moderate level of specialisation to seep habitats appears typical of the Dimerelloidea in general. This reflects possibly the low metabolic rates and low tissue densities generally typical of the Brachiopoda (James et al. 1992; Ballanti et al. 2012), the features making them successful ecological generalists able to thrive in a variety of marginal habitats, but probably not favourable for development of close chemosymbioses (for discussions, see Sandy (2010), Hryniewicz et al. (2017), Jakubowicz et al. (2017) and Kiel and Peckmann (2019)).

16.5.5 Corals

The presence of very dense, single-taxon assemblages of rugose corals is a peculiar feature of the Middle Devonian seep palaeoecosystem of the Hollard Mound and seems to have no analogues at either fossil or modern seeps known from elsewhere.

The ecological succession observed in the Hollard Mound, with the dominance of bivalves at an early stage, subsequent appearance of tube worms under the continuously high fluid flow and finally colonisation by corals during the terminal stage of the seep activity resemble successions known from modern seeps (Cordes et al. 2008, 2009; Becker et al. 2009; Bowden et al. 2013). At contemporary seeps, scleractinian corals are typically able to colonise hard substrates provided by seep carbonates only once fluid flow had ceased (León et al. 2007; Cordes et al. 2008; Becker et al. 2009; Liebetrau et al. 2010). In contrast, Berkowski (2006) and Jakubowicz et al. (2013) provided palaeontological, sedimentological and carbon isotope evidence that the '*Amplexus*' rugosans inhabited the Hollard Mound seep when seepage of methane remained at least periodically active. The hostile environmental conditions can likely explain the mass occurrence of the rugosan genus that normally constituted a subordinate component of Palaeozoic deep-water faunas but was a successful ecological opportunist able to grow rapidly under unfavourable environmental conditions (Jakubowicz et al. 2013). The latter characteristic was enabled by an unusual, extremely simplified skeletal architecture of the amplexoid corals, which resulted in their ability to rapidly increase their growth rate and change their growth direction, the features likely advantageous for non-specialised corals entering chemosynthesis-based ecosystems.

Within several km to the west of the Hollard Mound, both open surface and cryptic populations of '*Amplexus*' corals are found locally also in Devonian mound deposits (Berkowski 2006, Jakubowicz et al. 2013). In contrast to these mound-related '*Amplexus*' associations, the seep-dwelling corals of the Hollard Mound are typically stunted, having smaller diameters and lower number of septa, and display the peculiar, 'calice-in-calice' growth pattern sensu Berkowski (2004) typical of Devonian vent- and seep-related environments. Jakubowicz et al. (2013) proposed that the 'calice-in-calice' growth developed as a response to periodically increased concentrations of reduced compounds in near-bottom water layers, which resulted in periodic mortalities of larvae that settled too close to the sediment-water interface. While this mode of growth was also noted in some other marginal Palaeozoic environments (Berkowski 2004, 2006; Belka and Berkowski 2005; Jakubowicz et al. 2013), it is unknown in modern deep-water corals. It seems to be, in turn, broadly analogous to colonisation strategies reported from modern seeps for foraminifera, sea anemones, non-seep-obligate polychaetes and hydroids, which settle on elevated tubes of vestimentiferans as a means of simultaneously benefiting from diminished water toxicity and the firm substrate (Bergquist et al. 2003; Cordes et al. 2005; Sen Gupta et al. 2007).

16.6 Conclusions and Perspectives

Despite much scientific effort aimed over the past three decades to better constrain the fossil record of chemosynthesis-based communities, our understanding of their early evolution remains fragmentary. Until recently, a dominant perception was

that, unlike the Cenozoic, bivalve-dominated chemosynthetic ecosystems, the Palaeozoic to mid-Mesozoic methane seeps and hydrothermal vents were dominated by brachiopods. Similarly, the pattern of brachiopod vs. bivalve dominance at seeps and vents over the Phanerozoic was believed to have crudely followed that observed in normal-marine benthic shelly assemblages. Recent discoveries from the middle Palaeozoic of Morocco have questioned this simple perception, documenting the presence of late Silurian and Middle Devonian seeps dominated by mass accumulations of large, semi-infaunal, modiomorphid bivalves. While representing a lineage unrelated to modern seep-obligate bivalve taxa, the mid-Palaeozoic seep bivalves display morphological adaptations strikingly similar to those of their modern ecological counterparts and formed analogous, densely packed, nearly monospecific assemblages, both suggesting their chemosymbiotic lifestyle. The new documentation of Palaeozoic establishment of the bivalve-dominated seep communities shows that, despite the clear taxonomic differences, in morphological terms, the modern assemblages of seep-obligate, epifaunal and semi-infaunal bivalves represent a revival of an ancient theme in the evolution of chemosynthesis-based ecosystems.

The refined Palaeozoic record makes the factors responsible for the apparent scarcity of seep-related bivalves during the upper Devonian to early Mesozoic, an interval of remarkable success for brachiopod-dominated seep assemblages, ever more enigmatic. Starting from the Eocene, a characteristic element of chemosynthesis-based communities has become dense clusters of large, elongated, epifaunal to semi-infaunal bivalves: bathymodiolin mussels and vesicomyid clams (Kiel 2010). These bivalves closely cooperate with microbial, thiotrophic (vesicomyids, bathymodiolins) or methanotrophic (bathymodiolins) endosymbionts and convergently developed a set of morphological characters resembling those observed in seep-related mid-Palaeozoic modiomorphids and Mesozoic kalenterids (cf. Hryniewicz et al. 2017; Jenkins et al. 2013, 2018). In contrast, no seep-specialised brachiopods are known from modern oceans, and unlike the situation for *Ataviaconcha*bivalves, there are no morphological traits that would suggest that fossil brachiopods developed symbioses with chemosynthetic microbes. The controls on the changing fate of bivalves vs. brachiopods at seeps remain arguably the most pertinent question, and thus future research direction, in studies of pre-Cenozoic chemosynthetic communities; this issue is discussed in more detail in the Chap. 8 (Baliński et al., this volume) in this volume.

Acknowledgements Part of the work summarised in this contribution was supported by the National Science Centre, Poland, grants No. 2012/07/N/ST10/04044 (to MJ) and 2013/11/B/ST10/00243 (to BB); Polish Ministry of Science and Higher Education, grant No. N307 016237 (to BB); and German Research Council (DFG), grant No. Be 1296/7 (to ZB). The manuscript benefited from helpful reviews by L. Agirrezabala (University of the Basque Country) and B. Cavalazzi (University of Bologna).

References

Ager DV (1968) The supposedly ubiquitous Tethyan brachiopod *Halorella* and its relations. J Palaeontol Soc India 5−9:54–70

Ager DV, Cossey SPJ, Mullin PR et al (1976) Brachiopod ecology in mid-Palaeozoic sediments near Khenifra, Morocco. Palaeogeog Palaeoclimat Palaeoecol 20:171–185

Aitken SA, Collom CJ, Henderson CM et al (2002) Stratigraphy, paleoecology, and origin of Lower Devonian (Emsian) carbonate mud buildups, Hamar Laghdad, eastern Anti-Atlas, Morocco, Africa. Bull Can Petrol Geol 50:217–243

Anderson EJ, Makurath JH (1973) Palaeoecology of Appalachian gypidulid brachiopods. Palaeontology 16:381–389

Balinski A, Biernat G (2003) New observations on rhynchonelloid brachiopod *Dzieduszycki*a from the Famennian of Morocco. Acta Palaeontol Pol 48:463–474

Baliński A (2012) The Brachiopod Succession Through the Silurian—Devonian Boundary Beds at Dnistrove, Podolia, Ukraine. Acta Palaeontol Pol 57:897–924

Balinski A, Bitner A, Jakubowicz M (this volume) Brachiopods at Hydrocarbon Seeps. In: Kaim A, Cochran JK, Landman NH (eds) Ancient hydrocarbon seeps, Topics in geobiology, vol 50. Springer, Cham

Ballanti LA, Tullis A, Ward PD (2012) Comparison of oxygen consumption by *Terebratalia transversa* (Brachiopoda) and two species of pteriomorph bivalve molluscs: implications for surviving mass extinctions. Paleobiology 38:525–537

Barbieri R, Ori GG, Cavalazzi B (2004) A Silurian cold-seep ecosystem from the Middle Atlas, Morocco. PALAIOS 19:527–542

Bau M, Dulski P (1999) Comparing yttrium and rare earths in hydrothermal fluids from the Mid-Atlantic Ridge: implications for Y and REE behaviour during nearvent mixing and for the Y/Ho ratio of Proterozoic seawater. Chem Geol 155:77–90

Beauchamp B, Savard M (1992) Cretaceous chemosynthetic carbonate mounds in the Canadian Arctic. PALAIOS 7:434–450

Becker EL, Cordes EE, Macko SA et al (2009) Importance of seep primary production to *Lophelia pertusa* and associated fauna in the Gulf of Mexico. Deep-Sea Res Part I 56:786–800

Belka Z (1991) Conodont alteration patterns in Devonian rocks of the eastern Anti-Atlas, Morocco. J Afr Earth Sci 12:417–428

Belka Z (1998) Early Devonian Kess-Kess carbonate mud mounds of the eastern Anti-Atlas (Morocco), and their relation to submarine hydrothermal venting. J Sediment Res 68:368–377

Belka Z, Berkowski B (2005) Discovery of thermophilic corals in an ancient hydrothermal vent community, Devonian, Morocco. Acta Geol Pol 55:1–7

Belka Z, Berkowski B, Jakubowicz M et al (2015) Life of the dead mounds: an example from the Devonian mud mounds of Hamar Laghdad (Morocco). In: Abstracts, 31st IAS meeting of sedimentology, Polish Geological Society, Kraków, 22–25 June 2015, p 60

Bergquist DC, Andras JP, McNelis T et al (2003) Succession in Gulf of Mexico cold seep vestimentiferan aggregations: the importance of spatial variability. PSZNI: Mar Ecol 24:31–44

Berkowski B (2004) Monospecific rugosan assemblage from the Emsian hydrothermal vents of Morocco. Acta Palaeontol Pol 49:75–84

Berkowski B (2006) Vent and mound rugose coral associations from the Middle Devonian of Hamar Laghdad (Anti-Atlas, Morocco). Geobios 39:155–170

Berkowski B (2008) Emsian deep-water Rugosa assemblages of Hamar Laghdad (Devonian, Anti-Atlas, Morocco). Palaeontographica Abt A 284:17–68

Berkowski B, Weyer D (2012) *Hamaraxonia*, a new pseudocolumellate genus of Middle Devonian deep-water Rugosa (Anthozoa) from Morocco. Geol Belg 15:245–253

Birgel D, Himmler T, Freiwald A et al (2008) A new constraint on the antiquity of anaerobic oxidation of methane: late Pennsylvanian seep limestones from southern Namibia. Geology 36:543–546

Bowden DA, Rowden AA, Thurber AR et al (2013) Cold seep epifaunal communities on the Hikurangi Margin, New Zealand: composition, succession, and vulnerability to human activities. PLoS One 8:e76869

Brachert TC, Buggisch W, Flugel E et al (1992) Controls of mud mound formation – the Early Devonian Kess-Kess carbonates of the Hamar Laghdad, Antiatlas, Morocco. Geol Rundsch 81:15–44

Buggisch W, Krumm S (2005) Palaeozoic cold seep carbonates from Europe and North Africa – an integrated isotopic and geochemical approach. Facies 51:566–583

Calner M (2005) A late Silurian extinction event and anachronistic period. Geology 33:305–308

Campbell K (2006) Hydrocarbon seep and hydrothermal vent paleoenvironments and paleontology: past developments and future research directions. Palaeogeog Palaeoclimat Palaeoecol 232:362–407

Campbell KA, Bottjer DJ (1995a) Brachiopods and chemosymbiotic bivalves in Phanerozoic hydrothermal vent and cold seep environments. Geology 23:321–324

Campbell KA, Bottjer DJ (1995b) *Peregrinella*: an Early Cretaceous cold-seep-restricted brachiopod. Paleobiology 21:461–478

Campbell KA, Farmer JD, Des Marais D (2002) Ancient hydrocarbon seeps from the Mesozoic convergent margin of California: carbonate geochemistry, fluids and palaeoenvironments. Geofluids 2:63–94

Canet C, Anadón P, González-Partida E et al (2014) Paleozoic bedded barite deposits from Sonora (NW Mexico): evidence for a hydrocarbon seep environment of formation. Ore Geol Rev 56:292–300

Cavalazzi B (2007) Chemotrophic filamentous microfossils from the Hollard Mound (Devonian, Morocco) as investigated by focused ion beam. Astrobiology 7:402–415

Cavalazzi B, Barbieri R, Ori G (2007) Chemosynthetic microbialites in the Devonian carbonate mounds of Hamar Laghdad (Anti-Atlas, Morocco). Sediment Geol 200:73–88

Cavalazzi B, Barbieri R, Cady SL et al (2012) Iron-framboids in the hydrocarbon-related Middle Devonian Hollard Mound of the Anti-Atlas mountain range in Morocco: evidence of potential microbial biosignatures. Sediment Geol 263(264):183–193

Childress JJ, Fisher CR (1992) The biology of hydrothermal vent animals: physiology, biochemistry, and autotrophic symbioses. Oceanogr Mar Biol Annu Rev 30:337–441

Cooper GA (1972) Homeomorphy in recent deep-sea brachiopods. Smithson Contrib Paleobiol 11:1–25

Cope JCW (2000) A new look at early bivalve phylogeny. Geol Soc Spec Publ 177:81–95

Copper P (2004) Silurian (late Llandovery–Ludlow) atrypid brachiopods from Gotland, Sweden, and the Welsh borderlands, Great Britain. NRC Research Press, Ottawa

Cordes EE, Hourdez S, Predmore BL et al (2005) Succession of hydrocarbon seep communities associated with the long-lived foundation species Lamellibrachia luymesi. Mar Ecol Prog Ser 305:17–29

Cordes EE, McGinley MP, Podowski EL et al (2008) Coral communities of the deep Gulf of Mexico. Deep-Sea Res Part I 55:777–787

Cordes EE, Bergquist DC, Fisher CR (2009) Macro-ecology of Gulf of Mexico cold seeps. Annu Rev Mar Sci 1:143–168

Cohen KM, Finney SC, Gibbard PL, Fan JX (2013) The ICS International Chronostratigraphic Chart. Episodes 36:199–204

Dattagupta S, Miles LL, Barnabei MS et al (2006) The hydrocarbon seep tubeworm *Lamellibrachia luymesi* primarily eliminates sulfate and hydrogen ions across its roots to conserve energy and ensure sulfide supply. J Exp Biol 209:3795–3805

Denison RE, Koepnick RB, Burke WH et al (1997) Construction of the Silurian and Devonian seawater $^{87}Sr/^{86}Sr$ curve. Chem Geol 140:109–121

Duperron S (2010) The diversity of deep-sea mussels and their bacterial symbioses. In: Kiel S (ed) The vent and seep biota: aspects from microbes to ecosystems. Topics in geobiology, vol 33. Springer, Dordrecht, pp 137–167

Feng D, Chen D, Peckmann J (2009) Rare earth elements in seep carbonates as tracers of variable redox conditions at ancient hydrocarbon seeps. Terra Nova 21:49–56

Franchi F, Cavalazzi B, Pierre C et al (2015a) New evidences of hydrothermal fluids circulation at the Devonian Kess mounds, Hamar Laghdad (eastern Anti-Atlas, Morocco). Geol J 50:634–650

Franchi F, Hofmann A, Cavalazzi B et al (2015b) Differentiating marine vs hydrothermal processes in Devonian carbonate mounds using rare earth elements (Kess mounds, Anti-Atlas, Morocco). Chem Geol 409:69–86

Fürsich FT, Hurst JM (1974) Environmental factors determining the distributions of brachiopods. Palaeontology 17:879–900

Georgieva MN, Little CTS, Watson JS et al (2017) Identification of fossil worm tubes from Phanerozoic hydrothermal vents and cold seeps. J Syst Palaeontol 17(4):287–329

Gischler E, Sandy MR, Peckmann J (2003) Ibergirhynchia contraria (F. A. Roemer, 1850), an Early Carboniferous seep-related rhynchonellide brachiopod from the Harz Mountains, Germany - A possible successor to Dzieduszyckia? J Paleontol 77:293–303

Gómez-Pérez I (2003) An Early Jurassic deep-water stromatolitic bioherm related to possible methane seepage (Los Molles Formation, Neuquén, Argentina). Palaeogeog Palaeoclimat Palaeoecol 201:21–49

Griffin M, Pastorino G (2006) *Madrynomya bruneti* n. gen. and sp. (Bivalvia: ?Modiomorphidae): a Mesozoic survivor in the Tertiary of Patagonia? J Paleontol 80:272–282

Haas A, Little C, Sahling H et al (2009) Mineralization of vestimentiferan tubes at methane seeps on the Congo deep-sea fan. Deep-Sea Res Part I 56:283–293

Henriet JP, Hamoumi N, Da Silva AC et al (2014) Carbonate mounds: from paradox to World Heritage. Mar Geol 352:89–110

Hilário A, Capa M, Dahlgren TG et al (2011) New perspectives on the ecology and evolution of siboglinid tubeworms. PLoS One 6:e16309

Himmler T, Freiwald A, Stollhofen H et al (2008) Late Carboniferous hydrocarbon-seep carbonates from the glaciomarine Dwyka Group, southern Namibia. Palaeogeog Palaeoclimat Palaeoecol 257:185–197

Himmler T, Bach W, Bohrmann G et al (2010) Rare earth elements in authigenic methane-seep carbonates as tracers for fluid composition during early diagenesis. Chem Geol 277:126–136

Hoepffner C, Soulaimani A, Piqué A (2005) The Moroccan Hercynides. J Afr Earth Sci 43:144–165

Hollard H (1967) Maroc el du Sahara nord-occidental. In: Oswald DH (ed) Proceedings, international symposium on the Devonian System, Calgary, Alberta, Canada, pp 203–244

Hollard H (1974) Recherches sur la stratigraphie des formations du Dévonien moyen, de l'Emsien supérieur au Frasnien, dans le Sud du Tafilalt et dans le Ma'der (Anti-Atlas oriental). Notes Serv Géol Maroc 36:7–68

Hollard H (1981) Principaux caractères des formations dévoniennes de l'Anti-Atlas. Notes Serv Géol Maroc 42:15–22

Hollard H, Morin P (1973) Les gisements de Dzieduszyckia (Rhynchonellida) du Famennien inférieur du massif Hercynien central du Maroc. Notes Mém Serv Géol Maroc 249:7–14

Hourdez S, Lallier FH (2007) Adaptations to hypoxia in hydrothermal-vent and cold-seep invertebrates. Rev Env Sci Biotechnol 6:143–159

Hryniewicz K, Nakrem HA, Hammer Ø et al (2015) The palaeoecology of the latest Jurassic−earliest Cretaceous hydrocarbon seep carbonates from Spitsbergen, Svalbard. Lethaia 48:353–374

Hryniewicz K, Jakubowicz M, Belka Z et al (2017) New bivalves from a Middle Devonian methane seep in Morocco: the oldest record of repetitive shell morphologies among some seep bivalve molluscs. J Syst Palaeontol 15:19–41

Jacobs DK, Lindberg DR (1998) Oxygen and evolutionary patterns in the sea: onshore/offshore trends and recent recruitment of deep-sea faunas. Proc Natl Acad Sci 95:9396–9401

Jakubowicz M, Berkowski B, Belka Z (2013) Devonian rugose coral '*Amplexus*' and its relation to submarine fluid seepage. Palaeogeog Palaeoclimat Palaeoecol 386:180–193

Jakubowicz M, Belka Z, Berkowski B (2014a) Frutexites encrustations on rugose corals (Middle Devonian, southern Morocco): complex growth of microbial microstromatolites. Facies 60:631–650

Jakubowicz M, Berkowski B, Belka Z (2014b) Cryptic coral-crinoid 'hanging gardens' from the Middle Devonian of southern Morocco. Geology 42:119–122

Jakubowicz M, Dopieralska J, Belka Z (2015) Tracing the composition and origin of fluids at an ancient hydrocarbon seep (Hollard Mound, Middle Devonian, Morocco): a Nd, REE and stable isotope study. Geochim Cosmochim Acta 156:50–74

Jakubowicz M, Hryniewicz K, Belka Z (2017) Mass occurrence of seep-specific bivalves in the oldest-known cold seep metazoan community. Sci Rep 7:14292

James MA, Ansell AD, Collins MJ et al (1992) Biology of living brachiopods. In: Blaxter JHS, Southward AJ (eds) Advances in marine biology, vol 28. Academic Press, London, pp 175–387

Jarochowska E, Kozłowski W (2014) Facies development and sequence stratigraphy of the Ludfordian (Upper Silurian) deposits in the Zbruch River Valley, Podolia, western Ukraine: local facies overprint on the $\delta^{13}C_{carb}$ record of a global stable carbon isotope excursion. Facies 60:347–369

Jenkins R, Kaim A, Little C et al (2013) Worldwide distribution of the modiomorphid bivalve genus *Caspiconcha* in late Mesozoic hydrocarbon seeps. Acta Palaeontol Pol 58:357–382

Jenkins RG, Kaim A, Hikida Y et al (2018) Four new species of the Jurassic to Cretaceous seep-restricted bivalve *Caspiconcha* and implications for the history of chemosynthetic communities. J Paleontol 92(4):596–610

Jin J (2008) Environmental control on temporal and spatial differentiation of early Silurian pentameride brachiopod communities, Anticosti Island, eastern Canada. Can J Earth Sci 45:159–187

Johnson SB, Warén A, Tunnicliffe V et al (2015) Molecular taxonomy and naming of five cryptic species of *Alviniconcha* snails (Gastropoda: Abyssochrysoidea) from hydrothermal vents. Syst Biodivers 13:278–295

Kaim A, Bitner MA, Jenkins RG et al (2010) A monospecific assemblage of terebratulide brachiopods in the Upper Cretaceous seep deposits of Omagari, Hokkaido, Japan. Acta Palaeontol Pol 55:73–84

Kaim A, Tucholke BE, Warén A (2012) A new late Pliocene large provannid gastropod associated with hydrothermal venting at Kane Megamullion, Mid-Atlantic Ridge. J Syst Palaeontol 10:423–433

Kelly SRA, Blanc E, Price SP et al (2000) Early Cretaceous giant bivalves from seep-related limestone mounds, Wollaston Forland, northeast Greenland. Geol Soc Spec Publ 177:227–246

Kiel S (2010) The fossil record of vent and seep mollusks. In: Kiel S (ed) The vent and seep biota: aspects from microbes to ecosystems. Topics in geobiology, vol 33. Springer, Dordrecht, pp 255–277

Kiel S (2018) Three new bivalve genera from Triassic hydrocarbon-seep deposits in southern Turkey. Acta Palaeontol Pol 63(2):221–234

Kiel S, Dando PR (2009) Chaetopterid tubes from vent and seep sites: implications for fossil record and evolutionary history of vent and seep annelids. Acta Palaeontol Pol 54:443–448

Kiel S, Little CT (2006) Cold-seep mollusks are older than the general marine mollusk fauna. Science 313:1429–1431

Kiel S, Glodny J, Birgel D et al (2014) The paleoecology, habitats, and stratigraphic range of the enigmatic Cretaceous brachiopod *Peregrinella*. PLoS One 9:e109260

Kiel S, Peckmann J (2019) Resource partitioning among brachiopods and bivalves at ancient hydrocarbon seeps: A hypothesis. PLoS One 14:e0221887

Król JJ, Zapalski MK, Jakubowicz M et al (2016) Growth strategies of the tabulate coral Favosites bohemicus on unstable, soft substrates: an example from the Hamar Laghdad (Lower Devonian, Anti-Atlas, Morocco). Palaeogeog Palaeoclimat Palaeoecol 449:531–540

Krylova EM, Sahling H, Janssen R (2010) *Abyssogena*: a new genus of the family Vesicomyidae (Bivalvia) from deep-water vents and seeps. J Molluscan Stud 76:107–132

León R, Somoza L, Medialdea T et al (2007) Sea-floor features related to hydrocarbon seeps in deepwater carbonate-mud mounds of the Gulf of Cádiz: from mud flows to carbonate precipitates. Geo-Mar Lett 27:237–247

Li Y, Kocot KM, Whelan NV et al (2017) Phylogenomics of tubeworms (Siboglinidae, Annelida) and comparative performance of different reconstruction methods. Zool Scr 46:200–213

Liebetrau V, Eisenhauer A, Linke P (2010) Cold seep carbonates and associated cold-water corals at the Hikurangi Margin, New Zealand: new insights into fluid pathways, growth structures and geochronology. Mar Geol 272:307–318

Lietard C, Pierre C (2009) Isotopic signatures ($\delta^{18}O$ and $\delta^{13}C$) of bivalve shells from cold seeps and hydrothermal vents. Geobios 42:209–219

Little CTS, Maslennikov VV, Morris NJ et al (1999) Two Palaeozoic hydrothermal vent communities from the southern Ural Mountains, Russia. Palaeontology 42:1043–1078

Loydell DK, Frýda J (2011) At what stratigraphical level is the mid Ludfordian (Ludlow, Silurian) positive carbon isotope excursion in the type Ludlow area, Shropshire, England? Bull Geosci 86(2):197–208

Michard A, Soulaimani A, Hoepffner C et al (2010) The south-western branch of the Variscan Belt: evidence from Morocco. Tectonophysics 492:1–24

Mounji D, Bourque PA, Savard MM (1998) Hydrothermal origin of Devonian conical mounds (Kess-Kess) of Hamar Lakhdad Ridge, Anti-Atlas, Morocco. Geology 26:1123–1126

Mounji D, Bourque PA, Savard M (1999) The Hollard mound: complementary information. In: Bourque PA, Mounji D, Neuweiler F et al (eds) Carbonate mounds of Morocco. In: IGCP 380 field workshop, Morocco, October 24–November 1, pp 83–97

Naehr TH, Birgel D, Bohrmann G et al (2009) Biogeochemical controls on authigenic carbonate formation at the Chapopote 'asphalt volcano,' Bay of Campeche. Chem Geol 266:390–402

Nedoncelle K, Le Bris N, de Rafélis M et al (2014) Non-equilibrium fractionation of stable carbon isotopes in chemosynthetic mussels. Chem Geol 387:35–46

Newman WA (1985) The abyssal hydrothermal vent invertebrate fauna: a glimpse of antiquity? Bull Biol Soc Wash 6:231–242

Nie T, Guo W, Sun Y-L et al (2016) Age and distribution of the Late Devonian brachiopod genus *Dzieduszyckia* Siemiradzki, 1909 in southern China. Palaeoworld 25:600–615

Oliver PG, Taylor JD (2012) Bacterial symbiosis in the Nucinellidae (Bivalvia: Solemyida) with descriptions of two new species. J Molluscan Stud 78:81–91

Olu-Le Roy K, Sibuet M, Fiala-Médioni A et al (2004) Cold seep communities in the deep eastern Mediterranean Sea: composition, symbiosis and spatial distribution on mud volcanoes. Deep-Sea Res Part I 51:1915–1936

Peckmann J, Walliser OH, Riegel W et al (1999) Signatures of hydrocarbon venting in a Middle Devonian carbonate mound (Hollard Mound) at the Hamar Laghdad (Antiatlas, Morocco). Facies 40:281–296

Peckmann J, Little CTS, Gill F et al (2005) Worm tube fossils from the Hollard Mound hydrocarbon-seep deposit, Middle Devonian, Morocco: Palaeozoic seep-related vestimentiferans? Palaeogeog Palaeoclimat Palaeoecol 227:242–257

Peckmann J, Campbell KA, Walliser OH et al (2007) A Late Devonian hydrocarbon-seep deposit dominated by dimerelloid brachiopods, Morocco. PALAIOS 22:114–122

Pleijel F, Dahlgren TG, Rouse GW (2009) Progress in systematics: from Siboglinidae to Pogonophora and Vestimentifera and back to Siboglinidae. C R Biol 332:140–148

Powell MA, Somero GN (1986) Adaptations to sulfide by hydrothermal vent animals: sites and mechanisms of detoxification and metabolism. Biol Bull 171:274–290

Racki G, Baliński A, Wrona R, Małkowski K, Drygant D, Szaniawski H (2012) Faunal Dynamics Across the Silurian—Devonian Positive Isotope Excursions (δ13C, δ18O) in Podolia, Ukraine: Comparative Analysis of the Ireviken and Klonk Events. Acta Palaeontol Pol 57:795–832

Rongemaille E, Bayon G, Pierre C et al (2011) Rare earth elements in cold seep carbonates from the Niger Delta. Chem Geol 286:196–206

Roulleau R (1956) Découverte d'une Halorella (Brachiopode fossile) dans la région de Khatouat. CR Séances Mensuelles [Soc Sci Nat Phys Maroc] 1:26

Sandy MR (2010) Brachiopods from ancient hydrocarbon seeps and hydrothermal vents. In: Kiel S (ed) The vent and seep biota: aspects from microbes to ecosystems. Topics in geobiology, vol 33. Springer, Dordrecht, pp 279–314

Sen Gupta BK, Smith LE, Lobegeier MK (2007) Attachment of Foraminifera to vestimentiferan tubeworms at cold seeps: refuge from seafloor hypoxia and sulfide toxicity. Mar Micropaleontol 62:1–6

Stampfli GM, Hochard C, Vérard C et al (2013) The formation of Pangea. Tectonophysics 593:1–19

Taylor JD, Glover EA (2010) Chemosymbiotic bivalves. In: Kiel S (ed) The vent and seep biota: aspects from microbes to ecosystems. Topics in geobiology, vol 33. Springer, Dordrecht, pp 107–135

Termier H (1936) Etudes géologiques sur le Maroc central et le Moyen-Atlas septentrional, tome III: paléontologie, pétrographie. Notes Mém Serv Géol Maroc 33:1087–1421

Termier H (1938) Sur l'existence des *Halorella* au Dévonien supérieur. CR Sommaire Séances Soc Géol France 7:108

Termier H, Termier G (1948) Les phénomènes de spéciation dans le genre Halorella. Notes Mém Serv Géol Maroc 71:47–63

Termier H, Termier G (1949) Sur les genres *Halorella* et *Dzieduszyckia*. Notes Mém Serv Géol Maroc 74:113–115

Töneböhn R (1991) Bildungsbedingungen epikontinentaler Cephalopodenkalke (Devon, SE-Marokko). Gottinger Arb Geol Paleontol 47:3–114

Torres ME, Bohrmann G, Dubé TE et al (2003) Formation of modern and Paleozoic stratiform barite at cold methane seeps on continental margins. Geology 31(10):897–900

Van Dover CL (2000) The ecology of deep-sea hydrothermal vents. Princeton University Press, Princeton

van Geldern R, Joachimski MM, Day J et al (2006) Carbon, oxygen and strontium isotope records of Devonian brachiopod shell calcite. Palaeogeog Palaeoclimat Palaeoecol 240:47–67

Vrijenhoek RC (2013) On the instability and evolutionary age of deep-sea chemosynthetic communities. Deep-Sea Res Part II 92:189–200

Waller TR (1998) Origin of the molluscan class Bivalvia and a phylogeny of major groups. In: Johnston PA, Haggart JW (eds) Bivalves: an eon of evolution. University of Calgary Press, Calgary, pp 1–45

Walliser OH (1991) Hamar el Khdad (Hamar Laghdad). In: Walliser OH (ed) Morocco 1991, field meeting of the international subcommission on Devonian Stratigraphy, International Union of Geological Sciences, 28 November−5 December 1991. Guide-Book, pp 75–79

Walliser OH, El Hassani A, Tahiri M (2000) Mrirt: a key area for the Variscan Meseta of Morocco. Notes Mém Serv Géol Maroc 399:93–108

Wang S, Yan W, Chen Z et al (2014) Rare earth elements in cold seep carbonates from the southwestern Dongsha area, northern South China Sea. Mar Pet Geol 57:482–493

Wang Q, Tong H, Huang C-Y et al (2018) Tracing fluid sources and formation conditions of Miocene hydrocarbon-seep carbonates in the central western foothills, central Taiwan. J Asian Earth Sci 168:186–196

Wendt J, Belka Z (1991) Age and depositional environment of Upper Devonian (early Frasnian to early Famennian) black shales and limestones (Kellwasser Facies) in the eastern Anti-Atlas, Morocco. Facies 25:51–90

Chapter 17
Caribbean Ancient Seep Communities

Fiona L. Gill and Crispin T. S. Little

17.1 Introduction

Seep carbonates and associated fossils have been reported from six countries in the Caribbean Region (Fig. 17.1). This area is tectonically complex, due to the interactions between the Caribbean Plate, the North American plate, the South American plate and a number of smaller tectonic plates (Speed 1990; Iturralde-Vinent 1994; Audemard 2001; Flinch 2003; Escalona and Mann 2011; McNeill et al. 2012). Further details of the tectonic setting, as well as locality information, age and a summary of the petrography and fauna are provided for each of the ancient seep deposits described. No biomarker analysis has been published for the seep deposits reported here.

17.2 Cuba

Seep-associated material from Cuba has been described from two localities in the north-western part of Cuba (Fig. 17.1), close to Havana (Kiel and Hansen 2015). The seep material from Cuba is interpreted to have formed in a neo-autochthon that unconformably overlies a tectonically-complex fold-belt of pre-Miocene rocks (Iturralde-Vinent 1994).

Cooke (1919) described fossils from the asphalt beds of the Angela Elmira mine near Bejucal, Cuba, which he interpreted to represent a mixture of freshwater and marine species. Kiel and Peckmann (2007) reinterpreted these fossils to have a seep origin, due to taxonomic affinities with modern seep-dwelling, chemosymbiotic taxa and the carbon stable isotopic signature of associated carbonate. Kiel and

F. L. Gill (✉) · C. T. S. Little
School of Earth & Environment, University of Leeds, Leeds, UK
e-mail: f.gill@leeds.ac.uk; earctsl@leeds.ac.uk

A. Kaim et al. (eds.), *Ancient Hydrocarbon Seeps*, Topics in Geobiology 50,
https://doi.org/10.1007/978-3-031-05623-9_17

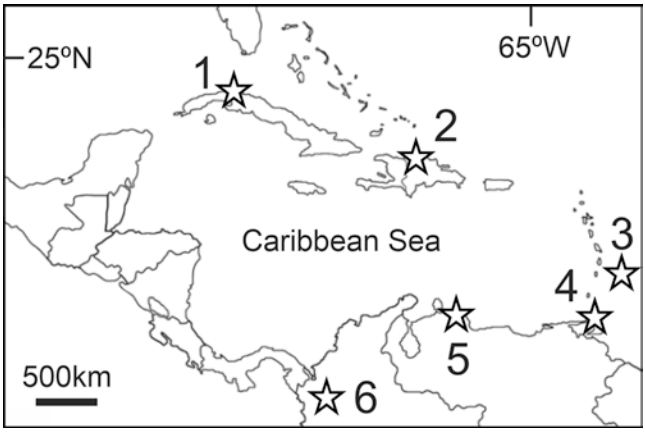

Fig. 17.1 General location of fossiliferous seep carbonates in the Caribbean region: *1*. Cuba. *2*. Dominican Republic. *3*. Barbados. *4*. Trinidad. *5*. Venezuela. *6*. Colombia

Hansen (2015) described material from a second Cuban locality, Cantera Portugalete, and interpreted it to have a seep origin, based on the presence of bivalves with modern chemosymbiotic relatives.

17.2.1 Location and Accessibility

The Angela Elmira asphalt mine corresponds to USGS localities 3652 and 5312 (Cooke 1919). The Cantera Portugalete locality is described as 'Habana Province, Cantera Portugalete, 1 km. N of Jamaica' (Palmer 1948). The material from this locality is attributed to the Husillo Formation (Kiel and Hansen 2015). No information is available on the accessibility of these localities.

17.2.2 Age

Cooke (1919) stated of the Angela Elmira asphalt mine that 'The fossils are doubtfully referred to the Oligocene', but strontium isotope measurements reported by Kiel and Hansen (2015) for three samples from this locality corresponded to an upper middle Eocene age in one case (Bartonian, 39.0 Ma) and an early Eocene age for the other two samples (Ypresian, 49.25 to 48.28 Ma). Kiel and Hansen (2015) reported an early Miocene age for the Cantera Portugalete material (basal Burdigalian, 19.4 to 19.5 Ma), based on strontium isotopic dating.

17.2.3 Brief Description of Sediments

Carbonate concretions associated with the material from the Angela Elmira asphalt mine comprise pyrite-bearing micrite, enclosing detrital quartz and foraminifera, with framboidal pyrite concentrated around the margin of the concretion (Kiel and Peckmann 2007). The Cantera Portugalete fossils are mainly internal moulds and are associated with indurated, dark grey, massive carbonates (Kiel and Hansen 2015).

17.2.4 Isotopes

Kiel and Peckmann (2007) reported $\delta^{13}C$ values of −32.2% and −23.5% for micrite from the Angela Elmira asphalt mine material, indicating a site of ancient methane seepage. Bivalve fossils at the same locality yielded $\delta^{13}C$ values of between 0.00% and −1.3%, interpreted to represent shell carbonate formed from ambient seawater rather than incorporating metabolic products from a methane carbon source (Kiel and Peckmann 2007).

Kiel and Hansen (2015) reported $\delta^{13}C$ values of −10% to −4.4% from bivalve internal moulds and associated carbonate from the Cantera Portugalete locality. These values are outside the range normally attributed to seep limestone but are interpreted to represent dilution of a methane seepage isotopic signature by marine bicarbonate, possibly indicating low seepage rates and diffuse fluid flow (Kiel and Hansen 2015).

17.2.5 Fauna

The Angela Elmira asphalt mine fauna consists of the lucinid *Cubatea asphaltica* (Cooke 1919), a solemyid and a possible vesicomyid bivalve, and a number of gastropod species, including *Elmira cornuatietis* Cooke, 1919, and a possible abyssochrysoid (Kiel and Peckmann 2007; Kiel et al. 2010; Kiel and Hansen 2015). The fauna at the Cantera Portugalte site comprises lucinids, including *Meganodontia* sp. and a smaller species, possibly of *Myrteopsis*; a vesicomyid resembling *Pleurophopsis lithophagoides* Olsson, 1931; and a mytilid bivalve, possibly a species of *Brachidontes* (Kiel and Hansen 2015).

17.3 Dominican Republic

The material described below is attributed to the Gurabo Formation, which formed in the Cibao Basin (Fig. 17.1), due to combined strike-slip and convergent motion at the boundary between the Caribbean and North American tectonic plates (McNeill et al. 2012).

17.3.1 Location and Accessibility

Kiel and Hansen (2015) described material interpreted to have a seep origin from the Gurabo Formation at Cañada de Zamba of the Río Cana, in the Cibao Valley in the northern Dominican Republic (NMB locality 16813). No information is available on the current accessibility of this locality.

17.3.2 Age

Kiel and Hansen (2015) reported that the Gurabo Fm. in the Río Cana section has an age between 5.7 and 4.3 Ma (McNeill et al. 2012) and (based on a personal communication to the aforementioned authors from Donald McNeill, 2015) that the material from NMB locality 16813 is from the lower part of the Gurabo Fm., close to the Miocene–Pliocene boundary and therefore latest Miocene or earliest Pliocene in age.

17.3.3 Brief Description of Sediments

The Dominican Republic material consists of a number of bivalves, some with associated hard micritic matrix (Kiel and Hansen 2015).

17.3.4 Isotopes

Kiel and Hansen (2015) reported $\delta^{13}C$ values of −28% to −20% for the micritic matrix of this material, which they interpreted to result from oxidation of hydrocarbons including methane during formation.

17.3.5 Fauna

The Dominican Republic fauna is composed solely of lucinid bivalves of *Anodontia* (*Pegophysema*) sp. (Kiel and Hansen 2015).

17.4 Barbados

Barbados represents the crest of an accretionary prism formed by subduction of the North Atlantic Plate beneath the Caribbean Plate (Speed 1990). Fossiliferous blocks of seep carbonate occur in the Scotland District, a 50 km^2 area in the northeast of the island (Fig. 17.1), but are rarely found in situ (Gill et al. 2005). The rocks of the Scotland District are tectonically complex and include the Eocene to Miocene Oceanic Series and accretionary prism sediments, the latter comprising the Eocene Basal Complex, Miocene prism cover and diapiric mélange (Torrini et al. 1985; Speed 1990). Fossils interpreted to have lived at seeps are found in two distinct contexts in Barbados: the Joe's River fauna associated exclusively with diapiric mélange, and the Sub-Oceanic Fault Zone (SOFZ) fauna, interpreted to have formed where the detachment surface between the Oceanic Series and the Basal Complex during the Miocene intersected the seafloor (Speed 1990).

The first mention of what is here referred to as the Joe's River fauna was by Senn (1940), who noted 'well preserved marine mollusca' in the fossiliferous zone of the Joe's River beds. However, Kugler et al. (1984) were the first to describe and figure the bivalves and gastropods of the Joe's River Formation. Kugler et al. (1984) also stated that 'the fauna appears to be a specialized one, perhaps requiring an unusual environment for its existence' and suggested that this unusual environment may have been a diapiric structure with associated mud volcano activity. Harding (1998) referred to the same fossil-bearing unit as the Joe's River mélange, which he also interpreted as a diapiric structure. Harding (1998) was the first to explicitly attribute a cold seep origin to this fauna, based on taxonomic affinities between the fossils of the Joe's River mélange and chemosymbiotic modern taxa. Gill et al. (2005) identified the fossil-bearing unit as the 'Frizers body diapiric mélange' of Speed (1998), and Kiel and Hansen (2015) referred to this unit as the 'diapiric mélange' and the fossils found within as the Joe's River fauna, a convention also followed here.

Harding (1998) described fossiliferous authigenic carbonates and carbonate chimneys interpreted to have a seep origin from the 'Sub-Oceanic Fault Zone' (SOFZ), a detachment surface between the Basal Complex of the accretionary prism and the over-thrusting Oceanic Series nappes (Speed 1990). The Basal Complex (Speed 1990) is equivalent to the Scotland Beds of Trechmann (1925) and the Scotland Formation of Senn (1940). Trechmann (1925) described fossils from 'Bed a' within the Scotland Beds, which he interpreted as a freshwater sandstone, but which could potentially have originated in the SOFZ. Senn (1940) assigned 'Bed a' of Trechmann (1925) to the Murphy Beds of the Upper Scotland Formation. Gill et al. (2005) interpreted the carbonates and fossils of the SOFZ to represent a series of seep ecosystems, separated in space and time, due to the sequential emplacement of numerous Oceanic Series nappes on top of accretionary prism sediments (Speed 1990). Kiel and Hansen (2015) referred to the fossils that Gill et al. (2005) and Harding (1998) attributed to the SOFZ as the 'Bath Cliffs fauna', but the material from the Bath Cliffs locality is not representative of the SOFZ material in general,

differing in faunal content and textural features from the remaining material attributed to the SOFZ (Gill et al. 2005). Therefore, we prefer to use the term 'SOFZ fauna' here.

17.4.1 Location and Accessibility

Kugler et al. (1984) included a map showing the Joe's River Formation Naturhistorisches Museum Basel (NMB) localities 10039–41, 10070, 10073–5, 10088–90, 10097 and 17482. Harding (1998) mentioned the Joe's River mélange locality 'Coconut Grove' and this locality is included in Gill et al. (2005: fig. 2), together with the 'Joe's River' locality of those authors.

Trechmann (1925: fig. 1) showed the location of 'Bed a', described as being found on the slope below Turner's Hall, and Senn (1940: fig. 1) later illustrated the location of Turner's Hall. Harding (1998) described SOFZ material from Bath Cliffs, Windy Hill, Belleplaine and Morgan Lewis, and Gill et al. (2005) included these same localities in their figure 2, together with Boscobelle, Bruce Vale, Cambridge and Cattlewash. No current information on the accessibility of any of these localities is available.

17.4.2 Age

Based on their molluscan fossil content, Trechmann (1925) considered the Scotland beds (equivalent to the Basal Complex of Speed 1990) 'of rather high Eocene aspect'. Senn (1940) considered the Joe's River Formation to be late Eocene in age and the Upper Scotland Formation (equivalent to the Basal Complex of Speed 1990) to be middle Eocene in age. Kugler et al. (1984) concurred on a late Eocene age for the Joe's River Formation. Harding (1998) regarded all the seep-related fossils of Barbados as Miocene, while Gill et al. (2005) specified only that they were between Eocene and middle Miocene in age. Kiel and Hansen (2015) used a strontium isotopic dating approach to derive an early Late Eocene age for the Joe's River fauna (basal Priabonian, 37.2–37.6 Ma) and an early Miocene (Aquitanian, 21.6–22.05 Ma) age for the SOFZ fauna.

17.4.3 Brief Description of Sediments

Senn (1940) described the Joe's River beds as 'dark gray silts with numerous angular, sharply delimited inclusions of greenish clay up to walnut size, giving them the typical aspect of pebbly silts'. Angular pebbles and irregular nests and wisps of dark brown tar sand are also commonly included. The pebbly silts are traversed by

numerous cleavage planes, showing slickensiding and containing free inspissated oil'. Kugler et al. (1984) described the Joe's River Formation as an 'incompetent, dark coloured, silty clay mass highly impregnated with oil'. Harding (1998) described the Joe's River mélange as 'a sandy, organic-rich mudstone, containing large angular exotic blocks'. Gill et al. (2005) described the diapiric mélange as 'foliated, bitumen-rich, sandy mudstone matrix containing angular blocks of sediments, green mudclasts and authigenic carbonate deposits'.

Trechmann (1925) described 'Bed a' as 'a very hard indurated sandstone a few feet thick, often impregnated with pitch or oil' and noted that the bed was not observed in situ but was 'found as isolated masses that seem to have travelled down the valley slopes some distance from their point of origin'. Senn (1940) described the rocks corresponding to 'Bed a' of Trechmann (1925) as 'hard, grey, sandy limestone'. Harding (1998) described two different types of seep-associated authigenic carbonates from the SOFZ: a 'calcitized radiolarian ooze protolith with an unusual early-formed fabric of coarse-grained calcite "spherules" <1.5 mm diameter' and 'polymict matrix-supported calcirudites'. Harding interpreted the complex carbonate fabrics to reflect fluctuations in fluid flow to the seafloor, resulting in cycles of brecciation, dissolution, cementation and infilling by sediment. Gill et al. (2005) described the SOFZ carbonates as 'strongly indurated, buff coloured and commonly displaying complex multi-phase precipitation histories'.

The majority of SOFZ material described by Harding (1998) and Gill et al. (2005) was collected as ex situ blocks. The only in situ SOFZ material collected by both Harding (1998) and Gill et al. (2005) was from the Bath Cliffs locality. Gill et al. (2005) described the carbonate blocks and chimneys from Bath Cliffs as 'manifesting a coarse, spherulitic calcite fabric'.

17.4.4 Isotopes

Gill et al. (2005) showed in their figure 3 that the $\delta^{13}C$ values of carbonate from the diapiric mélange and SOFZ lie between −15% and −54% PDB, strongly supporting the cold seep origin proposed for this fauna by Harding (1998).

17.4.5 Fauna

The Joe's River fauna consists of the nuculanid bivalve *Nuculana senni* Kugler, Jung, and Saunders, 1984, large lucinid bivalves, large bivalves of unknown but possibly vesicomyid affinity and the gastropods *Cantrainea* sp., *Calliotropis* sp. and *Ascheria* sp. (Kugler et al. 1984; Harding 1998; Gill et al. 2005; Kaim et al. 2014; Kiel and Hansen 2015).

The SOFZ fauna is rather more diverse and includes nuculid, nuculanid, solemyid, arcid, bathymodiolin, thyasirid, lucinid and vesicomyid bivalves (Harding

1998; Gill et al. 2005; Kiel and Hansen 2015). *Calliotropis* sp., *Homalopoma* sp., neritid, neolepetopsid, neomphalid, fissurellid, cataegid, hokkaidoconchid and mangeliid gastropods have also been reported, as well as possible vestimentiferan tubeworms (Harding 1998; Gill et al. 2005; Kiel and Hansen 2015).

17.5 Trinidad

Trinidad is situated within the boundary zone between the Caribbean and South American plates (Fig. 17.1), which is wide and structurally complex (Escalona and Mann 2011). The deposits described below are interpreted to have formed at cold seep sites on the Nariva accretionary prism (Gill et al. 2005). Maury (1912) described the finding of 'moulds of large shells', interpreted to have a freshwater origin, on the shore of the Gulf of Paria. Van Winkle (1919) described this material in more detail and noted 'the fauna is very peculiar and unlike any known'. Kugler (2001) provided a detailed bibliographic history of the Freeman's Bay Limestone member of the Lengua Formation, to which the material described by Maury (1912) and Van Winkle (1919) was attributed. Goedert et al. (2003) attributed the fauna described by Van Winkle (1919) to a seep origin, based on the occurrence of taxa with modern seep representatives. Gill et al. (2005) interpreted the Freeman's Bay limestone to represent cold seep deposits that formed within Nariva accretionary prism. Kugler (2001) described two distinct lithologies within the Freeman's Bay Limestone: one, an 'isolated, impure limestone block standing on the coastal mudflat', and the other 'in the adjoining coastal section, oil-impregnated calcareous mudstone lenses, some strongly brecciated'. Gill et al. (2005) interpreted the former lithology to represent an area of 'extensive carbonate formation, probably due to more focused fluid flow controlled by local structural features such as faults or fracture zones' and the latter lithology as 'diapiric structures that formed due to overpressuring in accreted sediments', analogous to the Joe's River Formation in Barbados. Kiel and Hansen (2015) noted the differences in preservation of the fossils associated with each of these two lithologies and proposed restricting the term 'Freeman's Bay fauna' to material from the impure limestone lithology, using the term 'Godineau River fauna' to refer to material from the brecciated mudstone lenses, a convention followed here. Kiel and Hansen (2015) also described additional material attributed to the Freeman's Bay fauna from the Bronte Estate and Jordan Hill localities.

17.5.1 Location and Accessibility

The majority of seep-associated material from Trinidad was collected as loose blocks on the beach in Freeman's Bay, on the shore of the Gulf of Paria (Maury 1912), on the west coast of the island, as illustrated by Gill et al. (2005) in their

figure 6. Kiel and Hansen (2015) described two further localities: Bronte Estate, equivalent to Naturhistorisches Museum Basel (NMB) locality 10228 and Jordan Hill at 10°15′22″N, 61°24′29″W. Gill et al. (2005) noted that the original Freeman's Bay outcrops were no longer present and that sea defences have been erected that obscure adjacent coastal exposures.

17.5.2 Age

Maury (1912) assigned a probable Oligocene age to the shells described that are now considered part of the Freeman's Bay fauna. Van Winkle (1919) considered that same material to be 'probably middle Tertiary' in age. The Freeman's Bay Limestone member of the Lengua Formation was ascribed a late middle Miocene age by Kugler (2001). Strontium isotope dating reported by Kiel and Hansen (2015) indicated a late Miocene age for the Godineau River fauna, the more reliable of the two samples analysed yielding a middle Messinian age (6.35 Ma).

17.5.3 Brief Description of Sediments

Maury (1912) described 'a whitish, decayed rock', which corresponds to the 'whitish and cream coloured, soft, cavernous, tufa-like impure limestone' described by Kugler (2001) from the type locality of the Freeman's Bay Limestone member of the Lengua Formation and is the host rock for the Freeman's Bay fauna. Kiel and Hansen (2015) observed that the lithology of the Jordan Hill material differs from that associated with the Freeman's Bay fauna at other localities in containing diverse carbonate phases, including vugs lined with banded rim cements.

The second lithology described by Kugler (2001) from the Freeman's Bay Limestone type locality is associated with the Godinaeu River fauna and is described as 'greenish, unctuous, slickensided clay with small lenses and boudinaged layers of dark and light calcareous mudstones. The dark mudstones are impregnated with inspissated oil'.

17.5.4 Isotopes

Kiel and Hansen (2015) reported $\delta^{13}C$ values from −25.8% to −20.2% from oil-impregnated calcareous mudstone associated with the Godineau River fauna, interpreted to represent a methane oxidation isotopic signature with some dilution from marine bicarbonate. $\delta^{13}C$ values from limestone associated with the Freeman's Bay fauna, from the Freeman's Bay, Bronte Estate and Jordan's Hill localities range

from −43.7% to −12.3%, indicating methane oxidation was involved in the formation of the carbonate (Kiel and Hansen 2015).

17.5.5 Fauna

The Freeman's Bay fauna comprises the bivalves *Pleurophopsis unioides* Van Winkle, 1919; *P. unioides.* var. *fernandensis* Van Winkle, 1919, lucinid bivalves including *Cubatea* sp., the thyasirid *Conchocele adoccasa* (Van Winkle 1919), two bathymodiolin species, a nuculanid and a possible vesicomyid bivalve as well as the gastropods *Cataegis godineauensis* (Van Winkle 1919), *Cantrainea* sp., *Provanna* sp., *Retiskenea* sp. and a limpet (Van Winkle 1919; Gill et al. 2005; Kiel and Hansen 2015). The Godineau River fauna consists of bivalves including the thyasirid *Conchocele adoccasa* Van Winkle, 1919, the lucinids *Nipponothracia* sp. and *Elliptiolucina* sp., and an unidentified possible vesicomyid species (Kiel and Hansen 2015).

17.6 Venezuela

The seep-associated material described below originated in the Falcon Basin (Fig. 17.1), within the active boundary zone between the Caribbean and South American plates, which is structurally very complex (Audemard 2001). A seep origin for the material from the Pozon Formation at the Puerto Escondido locality was suggested first by Gill et al. (2005), reiterated by Gill and Little (2013) and supported by carbon stable isotopic data by Kiel and Hansen (2015). Kiel and Hansen (2015) also attributed a seep origin to fossils from additional localities on or near the Caribbean coastline of Venezuela, namely Buenavista de Maicillal, Corro Colorado and La Piedra from the Pozon Formation and Caujarao from the Guacharaca Formation.

17.6.1 Location and Accessibility

The Puerto Escondido locality is shown in figure 8 by Gill et al. (2005) and identified as NMB locality 13968 by Kiel and Hansen (2015). The Buenavista de Maicillal locality in the Mirimire area and the La Piedra locality in the Isidro area of Estado Falcón correspond to NMB localities 15781 and 15780, respectively (Kiel and Hansen 2015). The Corro Colorado locality is not figured in any publications, but Kiel and Hansen (2015) quoted the original labels as reading 'Corro Colorado, near Maicillal de la Costa, due South on road' and '[unreadable] between Corro Colorado

onto road to San Francisco'. The Caujarao locality is described by Kiel and Hansen (2015) as being from Río Mirimire near Caujarao in the Aguide area in Estado Falcón (NMB locality 16626). The current accessibility of these localities is unknown.

17.6.2 Age

Gill et al. (2005) assigned a Miocene age to the Venezuelan seep material described from Puerto Escondido, due to its occurrence within the Huso Member of the Pozon Formation of the Agua Salada Group. Kiel and Hansen (2015) used strontium isotope dating to establish an early Miocene age for the material from Buenavista do Maicillal (Aquitanian, 22.3 to 21.25 Ma) and Corro Colorado (uppermost Aquitanian to lower Burdigalian, 20.3 to 19.1 Ma) and an upper late Miocene age for the material from Puerto Escondido (Tortonian/Messian, 7.2 Ma), with ages derived for the remaining localities considered unreliable due to likely diagenetic alteration.

17.6.3 Brief Description of Sediments

The Venezuelan seep fossils are mainly articulated casts of large bivalves and have very little matrix associated with them (Gill et al. 2005; Kiel and Hansen 2015). One specimen from Puerto Escondido attributed to the Huso Clay Member of the Pozon Formation had a matrix consisting of 'calcareous mud with some sparry calcite filling in pore spaces' (Gill et al. 2005). The Husite Member of the Pozon Formation, from which the material at Buenavista de Maicillal and Corro Colorado was collected, comprises 'marly clays interbedded with foraminifera marls, with scattered glauconite' (Kiel and Hansen 2015). The fossils from La Piedra were attributed to the Policarpo Member of the Pozon Formation, which is composed of marly limestones and clays, glauconitic beds and frequent iron concretions (Kiel and Hansen 2015). The material from Caujarao has been attributed to the Guacharaca Formation, although whether it originated from the Guayabal marls or the pelitic La Danta member of this Formation is uncertain (Kiel and Hansen 2015).

17.6.4 Isotopes

Kiel and Hansen (2015) reported $\delta^{13}C$ values from the Puerto Escondido, Buenavista de Maicillal, Corro Colorado and Caujarao localities ranging from −26.5% to −9.5%, which they interpreted as a signature for oxidation of seeping hydrocarbons, including methane, diluted by marine carbonate, due to the carbonate-rich middle to outer-shelf setting. The $\delta^{13}C$ values from the La Piedra material are quite different,

ranging from −11.5% to +12.4%, which Kiel and Hansen (2015) interpreted to represent two phases of carbonate precipitation, the first, with negative carbon isotope values, indicating oxidation of hydrocarbons and the second, with positive values, suggested to be associated with archaeal methanogenesis during early burial.

17.6.5 Fauna

Puerto Escondido fossils represent the most abundant and diverse Venezuelan assemblage with vesicomyid, bathymodiolin, thyasirid, solemyid and lucinid bivalves, including *Elongatolucina* sp. aff. *E. elassodyseides*, as well as naticid and trochid gastropods (Gill et al. 2005; Gill and Little 2013; Kiel and Hansen 2015). A lucinid and a possible vesicomyid bivalve were present at Buenavista de Maicillal (Kiel and Hansen 2015). The fauna at Caujarao consists of a species of moderately sized lucinid bivalves, possibly belonging to *Meganodontia* (Kiel and Hansen 2015). At Corro Colorado, the fauna includes lucinid bivalves, a possible vesicomyid bivalve and many callianassid shrimp fragments of the genus *Glypturus* (Kiel and Hansen 2015). At La Piedra, two species of lucinid are present, together with a mytilid assigned to *Brachidontes* (Kiel and Hansen 2015).

17.7 Colombia

The seep deposits described below are interpreted to have formed on the northern Colombia accretionary prism (Fig. 17.1), related to the subduction of the Caribbean Plate beneath the South American Plate (Flinch 2003). Based on the chemosymbiotic affinities of the fauna and their carbon stable isotope signatures, the Palmar-Molinera Road site in Colombia was identified as an ancient methane seep by Kiel and Peckmann (2007), and material from the Mata Cana and Sta. Clara localities was identified as seep related by Kiel and Hansen (2015).

17.7.1 Location and Accessibility

The Palmar-Molinera Road site corresponds to USGS locality 11253, 1/4 mile N of the junction of Arroyo Piadras Palmar and Palmar-Molinera Road (Kiel and Peckmann 2007). The Mata Cana locality was determined by Kiel and Hansen (2015) to refer to Mata de Caña, about 20 km south of Lorica in the Department Córdoba, along the Sinú River, at 9°04′30″ N, 75°49′30″W, Colombia. The Sta. Clara material was interpreted by Kiel and Hansen (2015) to be from the Sinú River

basin, possibly from Oligocene accretionary prism sediments referred to as the Floresanto Formation. The current accessibility of these localities is unknown.

17.7.2 Age

Kiel and Peckmann (2007) referred to a presumed Oligocene age of the Palmar-Molinera Road material, based on the original labels for the specimens, but Kiel and Hansen (2015) found an early Miocene age (upper Burdigalian, 17.3 to 16.85 Ma) for this material using strontium isotopic dating. Additional dates derived from strontium isotope ratios for material from Mata Cana and Sta. Clara were considered unreliable due to diagenetic alteration of the carbonate (Kiel and Hansen 2015).

17.7.3 Brief Description

The material from the Palmar-Molinera Road has a micritic matrix with glauconitic grains, faecal pellets, shell detritus and evidence of bioturbation, together with commonly occurring former voids showing banded and botryoidal rim cements and sparry calcite infilling (Kiel and Hansen 2015).

Most fossils from Mata Cana are preserved as internal moulds (Kiel and Hansen 2015). The carbonate associated with these fossils consists mainly of bioturbated peloidal micrite with microdetritus, with some small vugs containing sparry calcite but lacking rim cements (Kiel and Hansen 2015). Similarly, fossils from the Sta. Clara locality are preserved either as internal moulds with a chalky surface or with recrystallized shell (Kiel and Hansen 2015). Associated carbonates from Sta. Clara comprise fine peloidal and detrital micrite with evidence of bioturbation, and there are small voids that lack rim cement, as well as common pyrite-rimmed dissolution features (Kiel and Hansen 2015).

17.7.4 Isotopes

Kiel and Peckmann (2007) reported $\delta^{13}C$ values ranging from −51.3% to −45.6% for the Palmar-Molinera Road material, indicating incorporation of methane-derived carbon. Kiel and Hansen (2015) reported $\delta^{13}C$ values of −37.2% to −29.6% for the Mata Cana material and −24.5% to −22.9% for the material from Sta. Clara, indicating that hydrocarbon-derived carbon was incorporated into the carbonate.

17.7.5 Fauna

The fauna from the Palmar-Molinera Road locality comprises a solemyid bivalve, two lucinid bivalves species, including *Elongatolucina peckmanni* Kiel, 2013, and the mussel *Bathymodiolus palmarensis* Kiel, Campbell and Gaillard, 2010 (Kiel and Peckmann 2007; Kiel et al. 2010; Kiel 2013). The Mata Cana fauna consists of a solemyid, lucinids, including a species of *Elongatolucina* Gill and Little, 2013, a species of nuculid *Truncacila* Schenck, 1931, as well as a high-spired gastropod, a nautiloid and abundant crustacean claws and a crustacean carapace (Kiel and Hansen 2015). The Sta. Clara fauna includes the vesicomyid bivalves *Pliocardia* sp. and *Pleurophopsis* sp., the lucinid *Elongatolucina* sp., an unidentified bivalve that externally resembles *Nucinella* Wood, 1851, and the thyasirid *Conchocele adoccasa* (Van Winkle 1919), together with a neogastropod and the seguenzoid *Cataegis godineauensis* (Van Winkle 1919) (Kiel and Hansen 2015).

References

Audemard MFA (2001) Quaternary tectonics and present stress tensor of the inverted northern Falcon Basin, north-western Venezuela. J Struct Geol 23:431–453

Cooke CW (1919) Contributions to the geology and paleontology of the West Indies, IV: Tertiary mollusks from the Leeward Islands and Cuba. Carnegie Inst Wash Publ 291:103–156

Escalona A, Mann P (2011) Tectonics, basin subsidence mechanisms, and paleogeography of the Caribbean-South American plate boundary zone. Mar Pet Geol 28:8–39

Flinch J (2003) Structural evolution of the Sinu-Lower Magdalena area (northern Colombia). In: Bartolini C, Buffler RT, Blickwede J (eds) The circum-Gulf of Mexico and the Caribbean: hydrocarbon habitats, basin formation, and plate tectonics, vol 79. Am Ass Pet Geol Mem, pp 776–796

Gill FL, Little CTS (2013) A new genus of lucinid bivalve from hydrocarbon seeps. Acta Palaeontol Pol 58:573–578

Gill FL, Harding IC, Little CTS et al (2005) Palaeogene and Neogene cold seep communities in Barbados, Trinidad and Venezuela: an overview. Palaeogeog Palaeoclimat Palaeoecol 227:191–209

Goedert JL, Thiel V, Schmale O et al (2003) The late Eocene 'Whiskey Creek' methane-seep deposit (western Washington State), Part I: Geology, palaeontology, and molecular geobiology. Facies 48:223–240

Harding IC (1998) Miocene cold seep faunas and carbonates from Barbados. Cah Biol Mar 39:341–344

Iturralde-Vinent MA (1994) Cuban geology: a new plate tectonic synthesis. J Pet Geol 17:39–70

Kaim A, Jenkins RG, Tanabe K et al (2014) Mollusks from late Mesozoic seep deposits, chiefly in California. Zootaxa 3861:401–440

Kiel S (2013) Lucinid bivalves from ancient methane seeps. J Molluscan Stud 79:346–363

Kiel S, Hansen BT (2015) Cenozoic methane-seep faunas of the Caribbean region. PLoS One 10:e0140788

Kiel S, Peckmann J (2007) Chemosymbiotic bivalves and stable carbon isotopes indicate hydrocarbon seepage at four unusual Cenozoic fossil localities. Lethaia 40:345–357

Kiel S, Campbell KA, Gaillard C (2010) New and little known mollusks from ancient chemosynthetic environments. Zootaxa 2390:26–48

Kugler HG (2001) Treatise on the geology of Trinidad, Part 4. Museum of Natural History, Basel
Kugler HG, Jung P, Saunders JB (1984) The Joes River formation of Barbados and its fauna. Ecol Geol Helv 77:675–705
Maury CJ (1912) A contribution to the paleontology of Trinidad. J Acad Natl Sci Phila 15:24–112, 5–13
McNeill DF, Klaus JS, Budd AF et al (2012) Late Neogene chronology and sequence stratigraphy of mixed carbonate-siliciclastic deposits of the Cibao Basin, Dominican Republic. Geol Soc Am Bull 124:35–58
Palmer RH (1948) List of Palmer Cuban localities. Bull Am Paleontol 31:1–178
Senn A (1940) Palaeogene of Barbados and its bearing on the history and structure of the Antillean-Caribbean region. Bull Am Soc Pet Geol 24:1548–1610
Speed RC (1990) Volume loss and defluidization history of Barbados. J Geophys Res 95:8983–8996
Speed RC (1998) Diapirs of Barbados. Unpublished report, Conoco Inc
Torrini R, Speed RC, Mattioli GS (1985) Tectonic relationships between forearc-basin strata and the accretionary complex at Bath, Barbados. Geol Soc Am Bull 96:861–874
Trechmann C (1925) The Scotland beds of Barbados. Geol Mag 62:481–504
Van Winkle K (1919) Remarks on some new species from Trinidad. Bull Am Paleontol 8:19–27

Chapter 18
Ancient New Zealand Seep Limestones

Kristian P. Saether, Crispin T. S. Little, Kathleen A. Campbell, Campbell S. Nelson, and David A. Francis

18.1 Introduction

The East Coast Basin of eastern North Island, New Zealand, is one of a few places in the world that offers the opportunity to reconstruct a spatiotemporal record of long-lived (ca. 25 Myr duration from Neogene to the Recent) hydrocarbon seepage for both onshore, exhumed accretionary prism and forearc rocks and their adjacent, offshore, modern convergent tectonic settings (Campbell et al. 2008). Comparable settings, with analogous ancient and modern seeps, are found elsewhere on the Pacific Rim and include Japan, northwestern USA, and western South America (e.g., Olsson 1931; Goedert and Squires 1990; Kanie et al. 1992a, b; Asami et al. 1995; Goedert and Campbell 1995; Hattori et al. 1995; Naganuma et al. 1995a, b; Squires and Goedert 1995; Goedert and Kaler 1996; Kanie and Sakai 1997; Peckmann et al. 2002; Goedert et al. 2003; Majima et al. 2005; Campbell 2006; Kiel and Peckmann 2007; Kaim et al. 2014). The basin is also host to much older, Late Cretaceous allochthonous seep deposits, which are less numerous than the Miocene

K. P. Saether (✉)
Hull, UK
e-mail: kris.saether@gmail.com

C. T. S. Little
School of Earth and Environment, University of Leeds, Leeds, UK
e-mail: c.little@earth.leeds.ac.uk

K. A. Campbell
School of Environment, University of Auckland, Auckland, New Zealand
e-mail: ka.campbell@auckland.ac.nz

C. S. Nelson
School of Science (Earth Sciences), University of Waikato, Hamilton, New Zealand
e-mail: campbell.nelson@waikato.ac.nz

D. A. Francis
Lower Hutt, New Zealand

A. Kaim et al. (eds.), *Ancient Hydrocarbon Seeps*, Topics in Geobiology 50,
https://doi.org/10.1007/978-3-031-05623-9_18

seeps, and not as widely studied, but are similar lithologically and also contain rich faunal assemblages (Kiel et al. 2013).

18.2 Miocene New Zealand Seep Sites

18.2.1 Distribution

At least 16 geographically isolated Miocene hydrocarbon seep deposits occur as discrete pods or lenses of authigenic carbonate enclosed within thick siliciclastic bathyal mudstone deposits along a 300 km tract of the East Coast Basin, eastern North Island (Fig. 18.1 and Table 18.1; Campbell et al. 2008). They occur in two distinct areas—the northern (Gisborne) and southern (Dannevirke) sites—separated by approximately 200 km through the Hawke's Bay region (Fig. 18.1). By far, the largest of these deposits, at least in exposure, is at Rocky Knob in the Raukumara Peninsula, which also harbors the widest diversity of seep taxa and characteristic seep geological features such as tubular conduit concretions (e.g., Nelson et al. 2019). There is also evidence for other potential late Miocene seepage from the presence of tubular conduit concretions without associated development of seafloor seep carbonate at other sites in East Coast Basin (e.g., Nyman et al. 2010; Nelson et al. 2017), as well as in Taranaki Basin on the west coast of North Island (Nyman and Nelson 2011).

18.2.2 Geotectonic Setting

The East Coast Basin formed as the result of regional tectonism that has been ongoing since the Miocene (New Zealand Waitakian Stage; e.g., Ballance 1976; Barnes et al. 2002, 2010). Extending roughly 650 km north to south, the East Coast Basin varies in width from 60 to 110 km, bounded to the west by NNE–SSW trending axial mountain ranges and extending offshore to its eastern boundary along similarly trending troughs. It represents an exhumed forearc, its sediments having been generated during a period of oblique convergence along the Hikurangi subduction zone (HSZ, Fig. 18.1) throughout the late Cenozoic (e.g., Ballance 1976; Barnes et al. 2002), in correspondence with the onset of intense deformation, the appearance of andesitic volcanism, and abrupt changes in sedimentation rate and character (Rait et al. 1991).

Today, the margin constitutes the southern extremity of the Tonga–Kermadec–Hikurangi seismic zone, a west-facing subduction zone running roughly parallel to the east coast of North Island, along which the thick and bathymetrically elevated

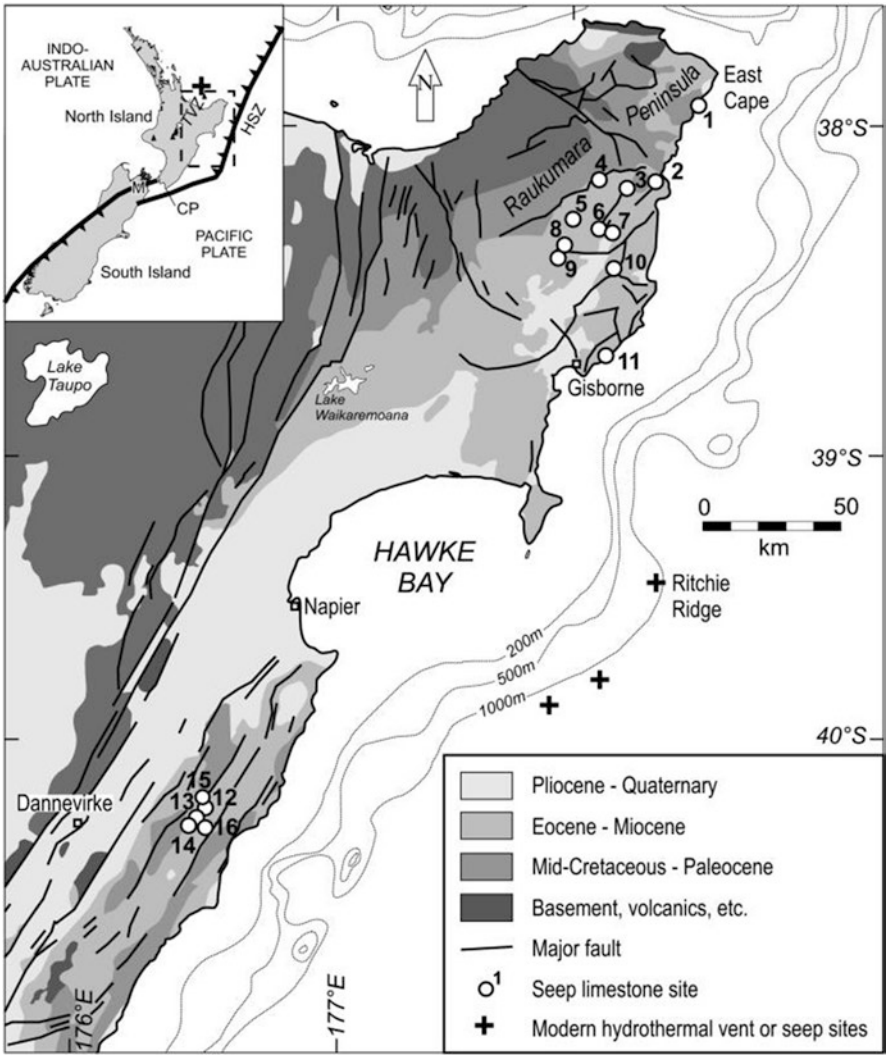

Fig. 18.1 Overview of the East Coast Basin in the Hawke's Bay area, east coast of North Island, showing the approximate locations of the majority of the known Miocene carbonate seep sites (see also Table 17.1). Numbers 1–11 correspond to the northern sites: 1 = Waiapu; 2 = Waipiro; 3 = Karikarihuata; 4 = Bexhaven; 5 = Tauwhareparae; 6 = Puketawa; 7 = Totaranui; 8 = Moonlight North; 9 = Rocky Knob; 10 = Waikairo; 11 = Turihaua. Numbers 12–16 correspond to the southern sites: 12 = Wanstead; 13 = Ugly Hill; 14 = Haunui; 15 = Ngawaka; 16 = Wilder. Also shown are some of the modern offshore hydrocarbon seep and hydrothermal vent sites on the Hikurangi margin. Inset shows the Hikurangi subduction zone (HSZ) as part of the transpressive boundary between the Indo-Australian and Pacific plates. CP = Cape Palliser; TVZ = Taupo Volcanic Zone. (Image modified from Campbell et al. 2008)

Table 18.1 Locality and age information for the main onshore Miocene seep limestone occurrences in East Coast Basin, North Island, New Zealand, arranged in roughly north to south order (see Fig. 18.1)

No.	Name	Approx. NZ Map Grid (NZMG) reference[a]	NZ stage	International epoch
1	Waiapu	Z15/917654	Tongaporutuan	Late Miocene
2	Waipiro	Z16/763394 and nearby	Otaian–Altonian	Early Miocene
3	Karikarihuata	Y16/657351	Lillburnian–Waiauan	Middle Miocene
4	Bexhaven	Y16/558332	Lillburnian	Middle Miocene
5	Tauwhareparae	Y16/463242	Lillburnian	Middle Miocene
6	Puketawa	Y16/557206	Clifdenian–Lillburnian	Middle Miocene
7	Totaranui	Y16/606192	Lillburnian	Middle Miocene
8	Moonlight North	Y16/433141	Waiauan	Middle Miocene
9	Rocky Knob	Y16/412103	Lillburnian	Middle Miocene
10	Waikairo	Y17/600065	Lillburnian	Middle Miocene
11	Turihaua	Y18/581745	Tongaporutuan	Late Miocene
12	Wanstead	V23/130107	Waitakian–Otaian	Early Miocene
13	Ugly Hill	U23/095076 and nearby	Waitakian	Early Miocene
14	Haunui	U23/072044-092070	Waitakian	Early Miocene
15	Ngawaka	U23/040075-044072	Waitakian–Clifdenian	Early to middle Miocene
16	Wilder	U23/063027	?	Miocene

[a]Based on existing series of NZMS260 1:50,000 topographic map sheets

oceanic Hikurangi Plateau (Pacific Plate) is subducting northwestward underneath the overriding Indo-Australian Plate (e.g., Ansell and Bannister 1996; Barnes et al. 2010). Along the Hikurangi margin, subduction occurs at a gentle dip angle of ca. 3° before steepening south of the North Island (Henrys et al. 2006) and at variable rates, from ~50 mMa^{-1} at the Kermadec Trench (northwest of North Island), decreasing southward to ~38 mMa^{-1} at the southern tip of the Hikurangi Trough (Beanland et al. 1998; Barnes et al. 2002).

The present forearc system can be divided into three major east–west components (Lewis and Pettinga 1993): an inner forearc located mostly onshore; an imbricated, frontal accretionary wedge lying mainly offshore; and a zone of trench slope sediments formed via offshore frontal accretion. West of the forearc lies a backstop, the axial ranges, of Mesozoic metasedimentary basement that comprises Torlesse terrane dominated by graywackes (Barnes et al. 2002), with older (Mid-Cretaceous to Paleogene) passive margin sediments underlying the Mio–Pliocene section, some of which are known organic-rich (gas and oil) source rocks (Field et al. 1997).

18.2.3 Localities

18.2.3.1 Northern (Gisborne) Sites

Waiapu A fossil-poor limestone described by McKay (1877) from near the mouth of the Waiapu River, probably on the south bank, contains a few poorly preserved, undescribed bivalves similar to those in the Waipiro locality (see below). It is hosted in a small outlier of Miocene mudstone, probably mid-upper Miocene (New Zealand Tongaporutuan Stage), but the age is uncertain.

Waipiro This site is a collection of several sublocalities, in the form of large, often slumped, boulders (~2 × 4 m) of moderately fossiliferous limestone, within a 1 km area on either side of the Waipiro Stream. Boulders of the same material can be found downstream. McKay (1877, p. 138) described "… a very peculiar yellow semi-crystalline limestone. This contains some fossils, which, from what I can make out, I believe to be the same as those that are found in the limestones near the mouth of the Waiapu River, and in coral beds in the cliff behind … Great quantities of this limestone, in large blocks, are found in the bed of the creek further up, …" This early Miocene (New Zealand Otaian–Altonian Stage) locality is set in a structurally complex, partly faulted Miocene outlier surrounded by Cretaceous–Eocene strata. The area is also affected by severe hillside slumping, which is locally more significant than faulting.

Karikarihuata The Karikarihuata site and surroundings are cyclically covered by pine forest that can make access difficult, but access is possible using a track south from Ihungia Road for about 2 km and then walking or, alternatively, traversing along Karikarihuata Stream (Fig. 18.2c). The main limestone is 4–8-m thick and pure (97% $CaCO_3$), with thick mudstone below and thin-bedded flysch above, all part of the Ihungia Formation (Mazengarb et al. 1991). Outcrops occur on both sides of the Karikarihuata Stream, extending in a north–south direction for up to 300 m along strike. The site is structurally set in a middle Miocene (New Zealand Lillburnian–Waiauan Stage), generally west-dipping sequence measured at 28° and 44° below and above the limestone, respectively. The base of the underlying thick mudstone is faulted against the Whangai Formation to the east, while a short distance up-section the flysch is faulted against Altonian Stage (early Miocene) strata to the west.

Bexhaven This site was mapped by Mazengarb et al. (1991), close to, and named for the nearby Bexhaven Farm. The deposit is up to 4 m thick in places and extends laterally for about 150 m above the road, but is concealed in part by slope colluvium (Fig. 18.2b). The rocks are probably middle Miocene (New Zealand Lillburnian Stage) in age and sit on the northwest limb of the Tutamoe Syncline, about 3 km southeast of a major normal fault terminating the Miocene strata.

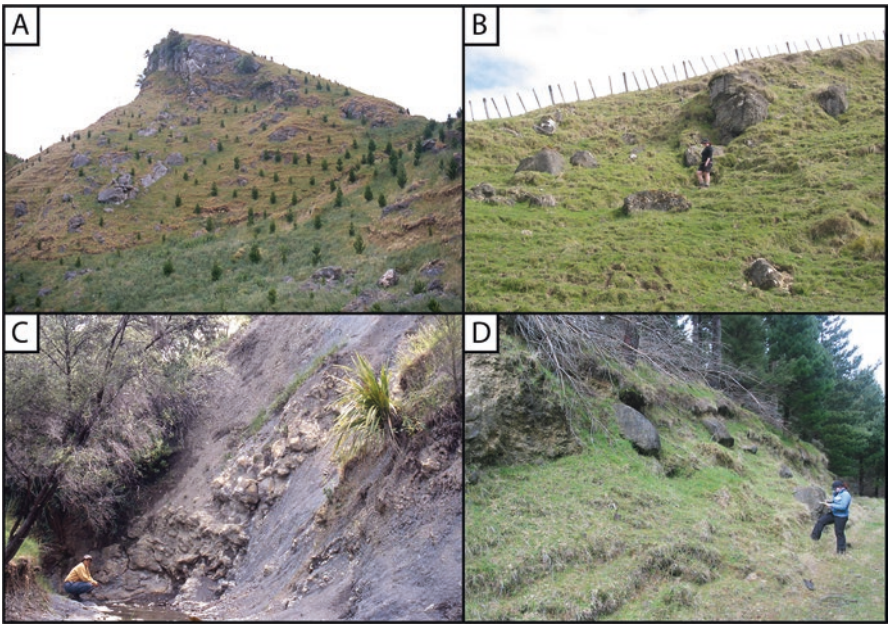

Fig. 18.2 Some of the larger northern (Gisborne) Miocene sites. (**a**) Rocky Knob, young trees (ca. 1 m tall) for scale; (**b**) Bexhaven, person for scale; (**c**) Karikarihuata, person for scale; (**d**) Moonlight North, person for scale. (Photographs taken on various field trips from 1997 to 2009 by the authors, Andrea C. Alfaro and Mike Collins)

Tauwhareparae This site is an abandoned (1985) limestone quarry site, named for the nearby Tauwhareparae Road. It is underlain by 2.5 km or more of middle Miocene (New Zealand Otaian–Lillburnian Stage) strata from a fault contact to the west, probably mostly mudstone, but this is uncertain. Overlying to the southwest are ca. 800 m of middle–late Miocene (New Zealand Lillburnian–Tongaporutuan Stage) strata, including ca. 500 m of shallow-facies late Miocene sandstone. It is probably a part of the Ihungia Formation, lying in the axis of the extensive northeast–southwest Tutamoe Syncline.

Puketawa This site is upstream of the Totaranui locality (see below) near the Upper Waiau River. It is a single large slumped limestone boulder in a creek bed, up to 1.8-m thick across bedding, with a 0.6-m-thick richly fossiliferous unit at one end. A strong fetid smell (as at Totaranui) is evident upon striking the rock. The surrounding geology consists of middle Miocene mudstone, so is dated to the middle Miocene (New Zealand Clifdenian Stage). Structurally, it is set near the axis of the Matanui Anticline, which plunges southward locally.

Totaranui The Totaranui locality comprises limestone boulders (the largest about 2-m thick through bedding) located ca. 800 m west of and named for Totaranui outstation, near a spur track 500 m north and 150 m above the Waiau River. It is

accessible via a forestry track down to the river, from where it is possible to drive further upstream, and is notable for a somewhat fetid sulfur smell, and radially recrystallized tubes, ca. 8-mm diameter and up to 100 mm long, which are worm tubes (Georgieva et al. 2019). Analysis indicates about 88% $CaCO_3$ content. It is situated within a fault-bounded segment of Miocene strata and is probably middle Miocene (New Zealand Lillburnian) in age.

Moonlight North This site consists of a single ca. 2-m-thick bed of richly fossiliferous limestone that crops out for about 200 m along strike that is located in a high tributary of the Waingaromia River, just east of a watershed created with Mangaorongo Stream (a tributary of the Waipaoa River), and south of the high escarpment forming the Tutamoe Plateau (Fig. 18.2d). Moonlight North is underlain by thick (>2 km) Miocene mudstone to the north of the Atarau Fault, and overlain by some 700 m of mudstone and flysch that is unconformably topped by late Miocene fossiliferous sandstone. Access is via Moonlight Station and farm or forestry tracks. The site includes the presence of tubular concretionary plumbing features observable in road cuts, and float blocks that occur in a nearby paddock which is under forestry management and cyclically covered in pine plantations. Probably middle Miocene (New Zealand Waiauan Stage) in age, the deposits at Moonlight North dip 28° NNE, within a north–northeast-dipping sequence north of the east–west trending Atarau Fault.

Rocky Knob The name "Moonlight Limestone" was first used informally by Kamp and Nelson (1988) for this locality. The name "Moonlight Limestone" was then formalized by Mazengarb et al. (1991) for an older, lithologically different limestone nearby, and the name "Bexhaven Limestone" was applied to the locality originally mentioned by Kamp and Nelson (1988). It is a large (roughly 15 × 200 m) and prominent fossiliferous limestone outcrop forming a minor north–northeast trending spur in the headwaters of an unnamed tributary of Tawa Stream, in turn a tributary of the Waingaromia River, at the end of a subsidiary track of Moonlight Station (Fig. 18.2a). The outcrop is currently within a pine plantation, but sporadic good exposures remain. Up to 15-m thick, Rocky Knob extends 200 m in strike direction. Part of the deposit has been quarried, and an oily odor is evident on freshly broken samples. A mudstone-dominant section to the south (about 1.5-km thick) underlies down to a ca. 100 m sandier phase near an unconformity at the base of the Miocene. It is overlain by about 500 m of mudstone followed by a sharp erosional unconformity by a late Miocene (Tongaporutuan Stage) sandstone to the north. Argillaceous sandstone blocks can be found in the adjacent stream (Adams 1910), containing abundant macrofossils. Rocky Knob is middle Miocene (New Zealand Lillburnian) in age and structurally dips at 20–25° WNW, with local complexities. It is situated 2 to 3 km from the northern end of Waitangi High (with its modern active oil and gas seeps), 2.5 km east of the northern faulted extension of this high, and 1.8 km south of the east–west trending Atarau Fault (e.g., Campbell et al. 2006; Nelson et al. 2017).

Waikairo This site consists of a single, large, spheroidal block (~0.8 × 1 m) of limestone located within Waikairo Stream, a tributary of Mangaheia River, that can be accessed through a plantation forest. It bears signatures typical of other seep limestones, such as a micritic lithology, yellow-orange weathering, and reports of a few mussels. It is situated within probable middle Miocene (New Zealand Lillburnian Stage) mudstone with some interbedded sandstone on the steeply dipping northern flank of a faulted anticline.

Turihaua Sometimes referred to as *Idasola* Limestone, Turihaua is a slumped site extending ca. 150 m laterally on the northeast side of Turihaua Stream on both sides of a farm access track, altitude ca. 80–100 m. With a thickness of 2 to 4 m, the lateral extent is difficult to assess due to slumping; it was probably originally less than 50 m. This broken outcrop extends over 150 m due to slumping. There are active modern gas seeps in the area, and notable features of the limestone include a mussel-dominated coquina, clotted microbialite, and anastomosing calcite veins. It is late Miocene (New Zealand Tongaporutuan Stage) in age, based on foraminiferal data from the surrounding mudstone, and situated in the axis of a syncline trending and plunging gently east–southeast.

18.2.3.2 Southern (Dannevirke) Sites

Wanstead First described by Lillie (1953), the Wanstead locality is a suite of brecciated limestones comprising several boulders in a field, close to nearby Manley Stream, which affords a variant name sometimes used for the site (Fig. 18.3d). The boulders are early Miocene (New Zealand Waitakian–Otaian Stage) in age and are situated on the west flank of Akitio Syncline, adjacent to the faulted margin of Whangai Range.

Ugly Hill The Ugly Hill locality contains moderately coherent small outcrops and/or boulders on the north and south sides of Ugly Hill Road (and, therefore, sometimes separated into North and South Ugly Hill localities), near to Epae Road. The main outcrop is the northern one, with localized common fossil horizons, occurring about 500 m north of the owner's house, across a small valley from a sheep graveyard, accessible by walking downhill through the owner's garden to the left, past a stable, through two gates, then bearing right over a ridge (Fig. 18.3c). Directly south across Ugly Hill Road from the northern deposits, entering through a roadside gate, involves a different landowner and consists of several isolated, small seep boulders and probably in situ outcrops. They occur within a few 100 m of the road and protrude through some of the knolls in the grassy paddocks; a small disused and overgrown quarry occurs in the limestone over the fence line in a bounding pine plantation. The site is early Miocene (New Zealand Otaian–Altonian, possibly Waitakian Stage) in age, sitting on the west flank of the Akitio Syncline, adjacent to the faulted margin of the Whangai Range.

Haunui Named for nearby Haunui Farm, this is a relatively extensive set of outcrops of fossiliferous limestone, covering a moderately sized, sparsely forested hill (an ancient pā site), approximately 300 m south of the farmhouse at the end of the farm entrance road, north of Mangawhero Stream and northeast of Motuotaraia Stream (Fig. 18.3a). With permission, the hill site is accessible on tracks across the farmland, by foot, or 4-wheel drive vehicle. Outcrops occur at the base, on the sides, and all over the summit, spanning approximately 200 × 100 × 30 m. The summit area is the site of a now disused, shallow quarry. Late early Miocene (New Zealand Altonian–Clifdenian Stage) in age, the site, like Ugly Hill, is situated on the west flank of the Akitio Syncline, adjacent to the faulted margin of the Whangai Range.

Ngawaka This locality comprises several outcrops across four paddocks on the eastern side of Ngawaka Road, yielding its name. To the west of the site are a few probably in situ outcrops in paddocks as well as the largest uninterrupted seep carbonate outcrop in southern Hawke's Bay, some 15 m long by 8 m high, composed of brecciated and veined limestone (Fig. 18.3b). Access is through a roadside gate on the east side of the road near the farm owner's house (on the west side of road) and then walk down the fence line to the main outcrop. Several 100 m southeast of these western deposits, and walkable from it, are float boulders of sparsely fossiliferous limestone ranging from small to large (>5 m) and exposed over a few 100 m of grassy hillside, from about 20 m above the edge of a small lake all the way up to the summit a few 100 m away, with the occasional cabbage tree interspersed between the rocks. Access, if not from the west of the site, is over a roadside fence across a barren strip of muddy ground that may have been a plantation but had no growth at the time of the last visit (July 2007), about a 50 m walk. The rocks are in general strongly veined, often in reticulate fashion and sometimes anastomosing, and a strong hydrocarbon odor is detectable upon striking them. The age of the site is probably early to middle Miocene (New Zealand Waitakian–Clifdenian Stage).

Wilder This site consists of about five separate outcrops found in the middle of a large complex of fields used for grazing sheep, located approximately 2 km down a farm track off Wilder Road (entrance at Gate No. 164), just past the cottage of the farmer who owns the land. This track can be quite treacherous and best navigated in a four-wheel-drive vehicle, then walking back downhill. Go through a significant dip in the track, and about a further 500 m as it trends to the right, and turn left through a gate then follow this straight, even track down a further 300–400 m. There is a large pond which will be unseen at this point out to the right, another 200 or so m into the field, with some nearby trees. No fossil material was observed, and its specific age (other than Miocene) is unknown.

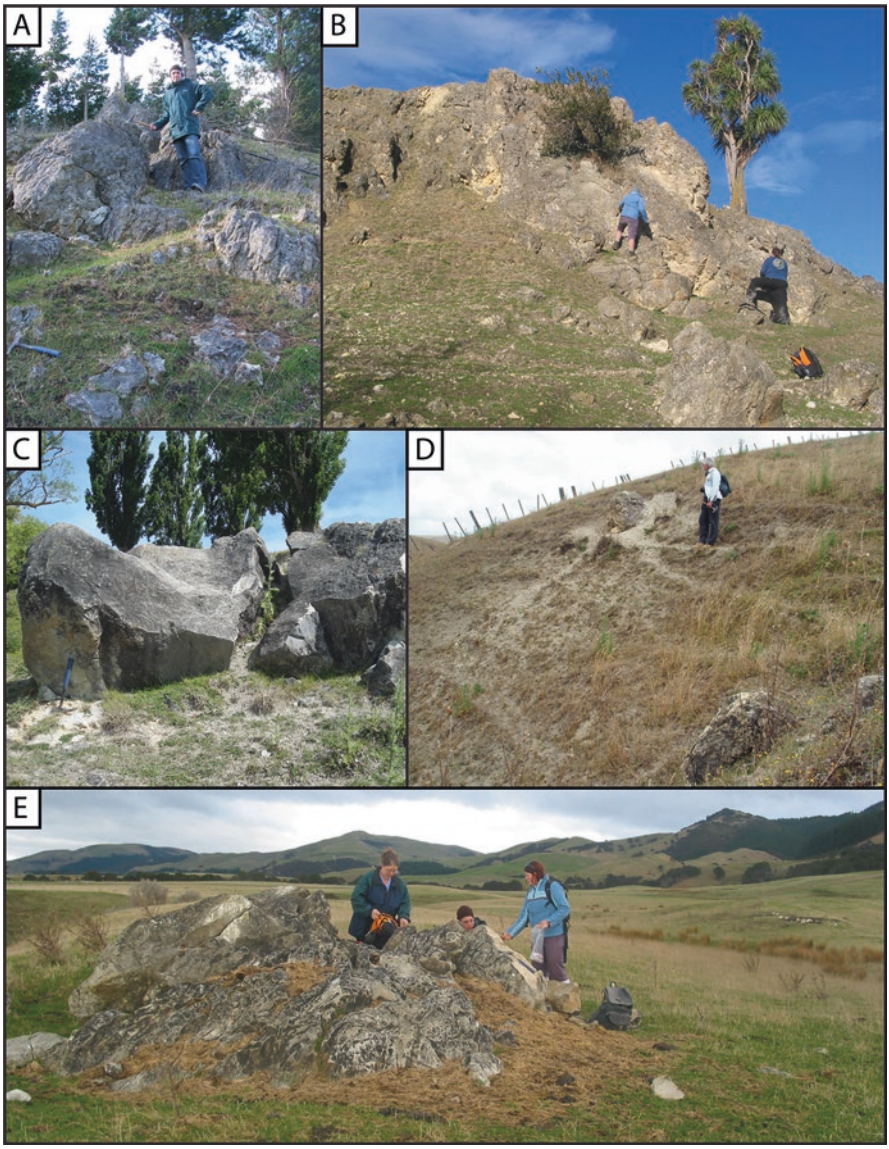

Fig. 18.3 Some of the larger southern (Dannevirke) Miocene sites. (**a**) Haunui, person for scale; (**b**) Ngawaka, people for scale; (**c**) Ugly Hill, geological hammer for scale; (**d**) Wanstead, person for scale. (All photographs taken on a 2008 field trip with CSN, KPS, Stephanie L. Nyman, Sarah M. Ewen, and Susan Nyman)

18.2.4 Fauna

For his PhD thesis, Saether (2011) identified numerous taxa at northern Miocene New Zealand hydrocarbon seep deposits (Table 18.2) and ranked this fauna among the most diverse known globally compared to other ancient fossil seeps. He observed around 39 taxa in at least 28 families (some of which are identified at suprafamilial levels but cannot be confamilial with any other New Zealand seep taxa), in nine classes, belonging to six phyla, not including ichnotaxa, microtaxa, and identifications of uncertain nature. However, further, more detailed work for formal completion of the taxonomy of these deposits is required, and therefore for the purposes of this chapter only, those reports from primary literature are recorded.

18.3 Cretaceous New Zealand Seep Sites

18.3.1 Distribution

Kiel et al. (2013) separated the Cretaceous (late Albian–middle Cenomanian) seep limestone concretions into three localities, namely the coastal Port Awanui and Waipiro Bay sites situated within the East Coast Allochthon (see Sect. 18.3.2), and a third locality located roughly 20 km inland, in situ and informally named "Owhena Stream" (Fig. 18.4). "Owhena Stream" represents a single deposit apparently devoid of macrofossils but was identified through isotopic and petrographic analyses as of seep origin. Port Awanui is identified as three distinct deposits, each of which is represented by shore-platform boulders almost certainly eroded from a well-exposed, calcareous mudstone unit that forms the onshore platform at this point (Kiel et al. 2013). Two of these boulders can be observed today, and a third was recognized as most likely a similar boulder based on literature study (see McKay 1887; Ongley and Macpherson 1928). The Waipiro Bay locality comprises two deposits which, as at Port Awanui, are represented by boulders found on the beach, and inferred to have been sourced from a mélange that formed in association with emplacement of the East Coast Allochthon (Kiel et al. 2013; Zwicker et al. 2021).

18.3.2 Geotectonic Setting

Adding to the complexity of the geology of the Raukumara Peninsula mentioned earlier (Sect. 18.2.1), there is also a significant Cretaceous–Paleogene allochthon that separates the Miocene strata (and hence, the Miocene seep deposits) into its northern and southern components (Figs. 18.1 and 18.6). This allochthon, called the East Coast Allochthon, is characterized by a succession of thrust sheets and folds and was emplaced in response to the development of the East Coast Basin in the

Table 18.2 Fossil distribution of Miocene New Zealand seep deposits

Taxon	Locality distribution	Reference
Bivalvia		
Bathymodiolus heretaunga	3, 4, 5, 6, 7, 8, 9, 11, 12, 13, 14, 15	Saether et al. (2010b)
Gigantidas coseli	6, 8, 9, 11	Saether et al. (2010b)
Pliocardia sp.	8	Amano et al. (2014)
Notocalyptogena neozelandica	13	Amano et al. (2014)
Thyasira (*Thyasira*) *beui*	4, 8	Amano et al. (2015)
Protobranchia indet.	4	Saether et al. (2016)
Solemyidae indet.	8	Saether et al. (2016)
Cf. *Pulvinites* sp.	8	Saether et al. (2016)
Acesta cf. *saginata*	9	Saether et al. (2016)
Parvamussium cf. *maorium*	8	Saether et al. (2016)
Pratulum quinarium	4, 5, 7, 8	Saether et al. (2016)
Semeloidea (s.l.) *bexhavenensis*	4, 8	Saether et al. (2016)
Meganodontia haunuiensis	12, 13, 14, 15	Amano et al. (2018)
Elliptiolucina neozelandica	8	Amano et al. (2018)
Lucinoma saetheri	4, 8, 9, 13, 14	Amano et al. (2018)
Lamellinucula sp.	8	Amano et al. (2018)
Nuculana sp.	8	Amano et al. (2018)
Leptomya sp.	14	Amano et al. (2018)
Gastropoda		
Buccinidae indet.	5	Campbell et al. (2008)
Provanna marshalli	6, 9, 13	Saether et al. (2010a)
Bathyacmaea kimberleyae	6, 7, 9	Saether et al. (2012) (as *Serradonta*)
Homalopoma	8	Amano et al. (2018)
Naticidae indet.	8	Amano et al. (2018)
Mitrella sp.	8, 9	Amano et al. (2018)
Other body fossils		
Vestimentiferan worm tubes	3, 4, 5, 7, 8, 9, 13	Campbell et al. (2008)
Decapod fragments	4, 9	Campbell et al. (2008)
Terebratulidae indet. (×3, including *Liothyrella*)	4, 8, 9	Campbell et al. (2008)
Cf. *Goniocorella* sp.	5, 8, 9, 12, 13, 15	Campbell et al. (2008)
Trace fossils		
Thalassinoides	4, 5, 9	Campbell et al. (2008)
Gastrochaenolites	15	Campbell et al. (2008)
Small circular borings	9	Campbell et al. (2008)

See Fig. 18.1 for locality key, and Figs. 18.4 and 18.5 for image of representative taxa

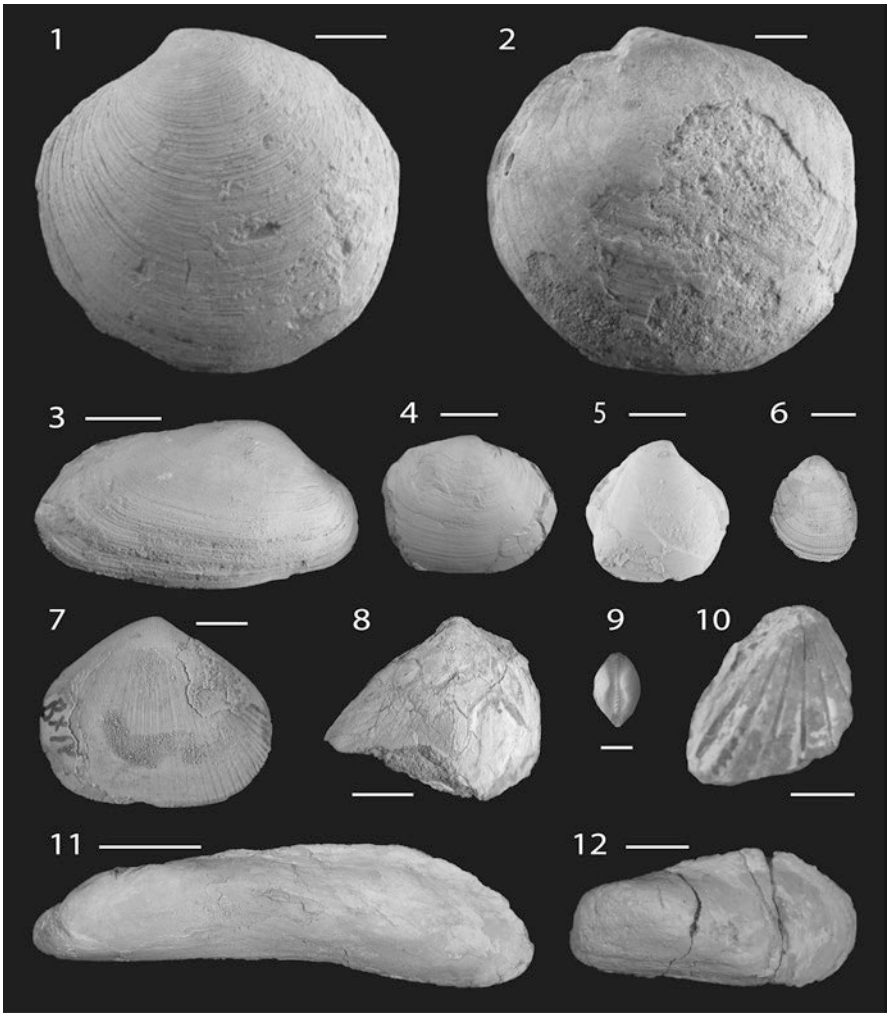

Fig. 18.4 Miocene bivalves from New Zealand ancient seep sites. 1. *Lucinoma saetheri* Amano et al., 2018, 2. *Meganodontia haunuiensis* Amano et al., 2018, 3. *Notocalyptogena neozelandica* Amano et al., 2014, 4. *Elliptiolucina neozelandica* Amano et al., 2018; 5. *Thyasira beui* Amano et al. 2015; 6. *Pratulum quinarium* (Marwick, 1944), 7. *Semeloidea bexhavenensis* Saether et al., 2016, 8. *Acesta* cf. *saginata* Marshall, 2001, 9. protobranch bivalve indet., 10. *Parvamussium* cf. *maorium* Dell, 1956, 11. *Gigantidas coseli* Saether et al., 2010, 12. *Bathymodiolus heretaunga* Saether et al., 2010. For 6–10, see Saether et al. 2016; for 11–12, see Saether et al. 2010b. Scale bars: 1, 2, 8, 11, 12 are 10 mm; 3 and 4 are 5 mm; 5 and 7 are 3 mm; 6 and 10 are 2 mm; 9 is 0.5 mm

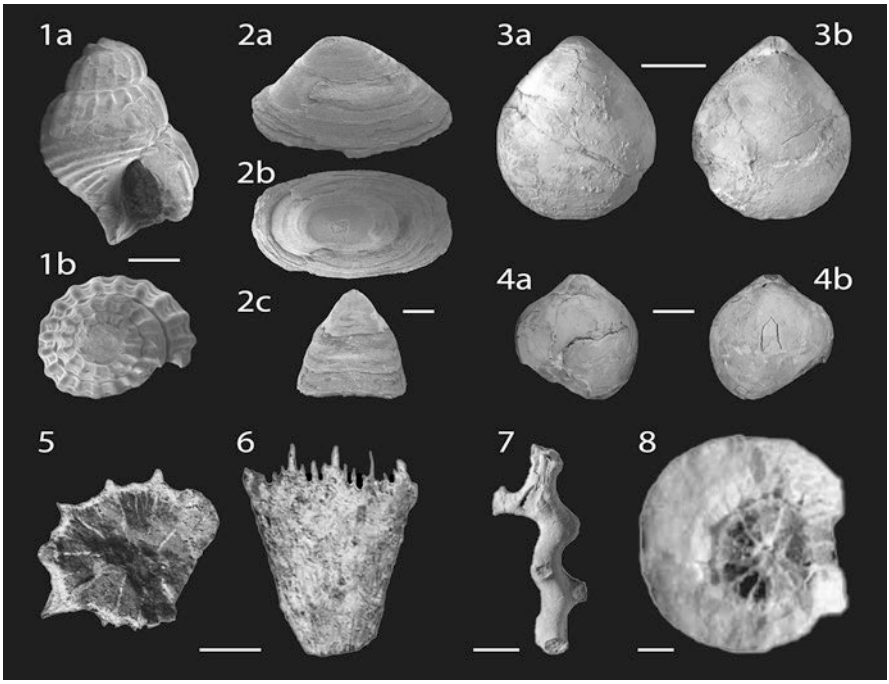

Fig. 18.5 Miocene fossils from New Zealand ancient seep sites. 1. *Provanna marshalli* Saether et al., 2010a, 2. *Bathyacmaea kimberleyae* (Saether et al., 2012), 3. *Liothyrella* sp. A, 4. *Liothyrella* sp. B, 5–6. *Caryophyllia clavus* Scacchi, 1835, 7–8. *Madrepora oculata* Linnaeus, 1758. All corals are from Moonlight North. *Liothyrella* sp. A is from Rocky Knob and *Liothyrella* sp. B is from Tauwhareparae. Scale bars: 1 is 2 mm; 2 is 1 mm; 3 is 20 mm; 4 is 10 mm; 5, 6 are 5 mm; 7 is 4 mm; 8 is 0.5 mm

early Miocene (Kiel et al. 2013). The allochthon strata are similar to the Miocene deposits (Sect. 18.2) in that thinly interbedded mudstones and sandstones can be found within vast successions of bathyal mudstone (Field et al. 1997), and are likely displaced by at least a few 10s of kilometers from their original position (Mazengarb and Speden 2000; Kiel et al. 2013). To the south and west of the East Coast Allochthon lie autochthonous Cretaceous strata that were deposited on the passive paleo-Pacific margin of New Zealand during early thermal subsidence following the separation of the New Zealand crustal block from Gondwanaland (Crampton et al. 2006; Kiel et al. 2013).

18.3.3 Localities

Owhena Stream Kiel et al. (2013) described a conspicuous concretionary mudstone exposed within the river bed at the mouth of Owhena Stream. Because of the nature of its occurrence, it is periodically covered by riverine gravelly deposits, but

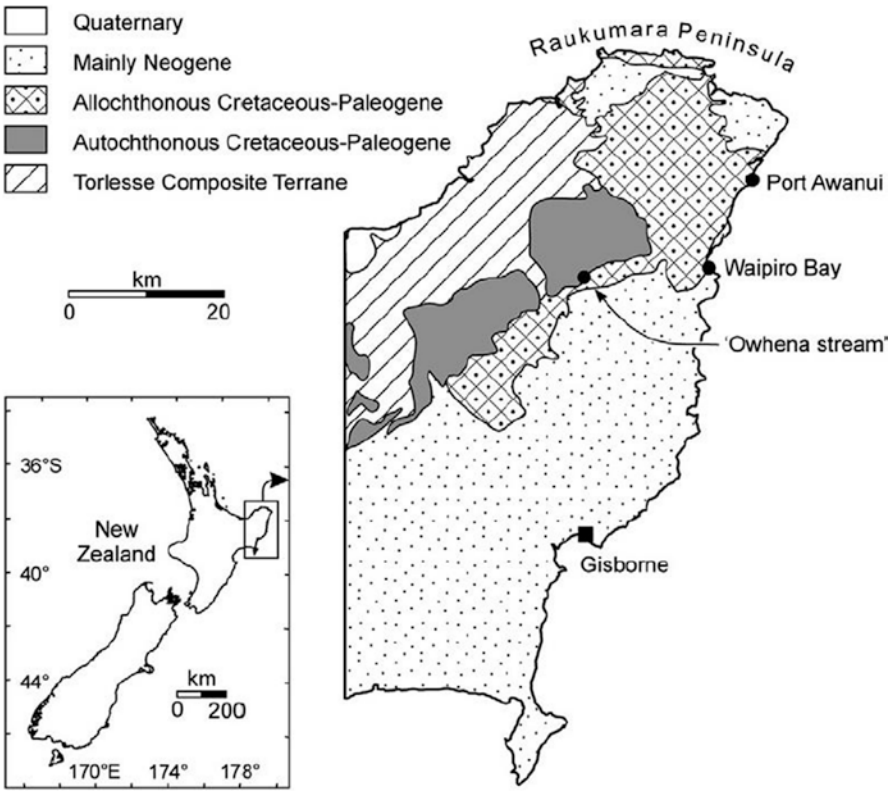

Fig. 18.6 Map of the Raukumara Peninsula (East Coast Basin) showing the locations of the three Cretaceous New Zealand seep localities. (Image modified from Kiel et al. 2013)

up to 2 m of laminated, concretionary sandy mudstone can occasionally be exposed. Distinctive pipe-like concretions extend at least 15 m up into the base of the overlying Whangai Formation. Owhena Stream remains the only known in situ Cretaceous seep locality in New Zealand, and Schiøler et al. (2000) established a middle Campanian (New Zealand early Haumurian) age for the site. Moore et al. (1988) placed a gradational contact between the Owhena and overlying Whangai formations at the level of the concretionary mudstone.

Port Awanui McKay (1877) first described this coastal locality, at the mouth of Waiotautu Stream, East Cape, as concretionary black shales with some Cretaceous fossils. Crampton (1998) noted that the geology to the south is entirely of Eocene age and shows a common trend of northward younging, but that the area is characterized by intensive faulting which may have juxtaposed the strata and locally reversed this trend, or else this could be an olisthostrome deposit. Kiel et al. (2013) identified three separate sites that they named Awanui I, Awanui II, and GS 688, all

Table 18.3 Locality and age information for the main onshore Cretaceous seep limestone occurrences in East Coast Basin, North Island, New Zealand, arranged in roughly north to south order (see Fig. 18.6)

No.	Name	Approx. NZ Map Grid (NZMG) reference[a]	NZ stage	International epoch
1	Port Awanui	Z15/f82–63, 7485	Motuan–Ngaterian	Late Albian–middle Cenomanian
2	Waipiro Bay	Z16/f83–84	Haumurian	Middle Campanian
3	Owhena Stream	Y16/f945	Early Haumurian	Middle Campanian

[a]Based on existing series of NZMS260 1:50,000 topographic map sheets

hard, medium gray, calcareous mudstone eroded from a well-exposed shore platform unit close to the headland of Whakariki Point and of late Albian–middle Cenomanian (New Zealand Motuan–Ngaterian) age.

Waipiro Bay Not to be confused with the Miocene Waipiro locality described earlier, which lies inland, Kiel et al. (2013) identified two loose boulders, designated Waipiro I and Waipiro III, on the beach at Pokurakura Point, immediately south of Waikawa Stream. The boulders comprise hard, medium gray, calcareous mudstone sourced from adjacent outcrops of undifferentiated mélange mentioned above in Sect. 18.3.1. They aged the boulders to the middle Campanian (New Zealand Haumurian Stage) (Table 18.3).

18.3.4 Fauna

The fauna of the Cretaceous New Zealand seep sites (Fig. 18.7 and Table 18.4) is similar to that of the Miocene sites in terms of being dominated by bivalves and gastropods. It is slightly less diverse among its bivalve content but perhaps more diverse among the gastropods, although many of the taxa are still in open nomenclature and require further study. This is particularly true of the gastropods many of which are still left in open nomenclature (e.g., Campbell et al. 2008; Kiel et al. 2013) with only two formally described species from the Miocene seep deposits and one from the Cretaceous sites (Saether et al. 2010b; Saether et al. 2012; Kaim et al. 2014). Coral and decapod fragments are present from both Miocene and Cretaceous deposits, and the Miocene deposits also contain at least two brachiopod species, and worm tubes that are well represented in number but also require further future work.

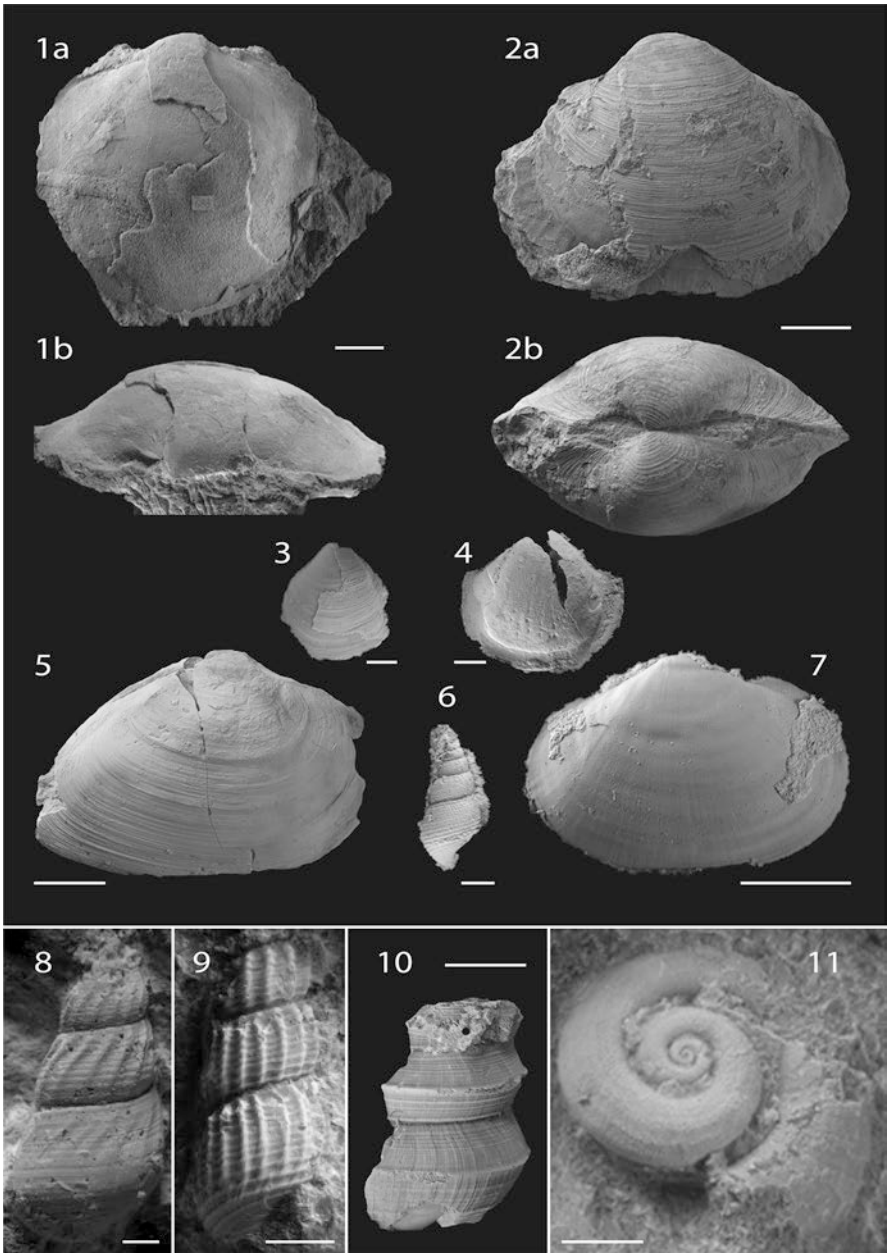

Fig. 18.7 Selected molluscs from the Cretaceous deposits. 1, *Amanocina raukumara* Kiel, 2013, from Port Awanui: 1a: Lateral view of right valve. 1b: Dorsal view. Scale bar is 10 mm. 2, *Ezolucina* sp. "Awanui": 2a: Lateral view of left valve. 2b: Dorsal view. Scale bar is 10 mm. 3. Thyasirid from Awanui II, lateral view of left valve. Scale bar is 2 mm. 4. *Ezolucina* "tall" from Awanui I, lateral view of right valve. Scale bar is 5 mm. 5. *Ezolucina* sp. "Waipiro" from Waipiro I, lateral view of

(continued)

right valve. Scale bar is 25 mm. 6. Fusiform gastropod from Awanui I, abapertural view. Scale bar is 1 mm. 7. Heterodont bivalve from Awanui I, lateral view of left valve. Scale bar is 5 mm. 8. *Abyssomelania cramptoni* Kaim et al., 2014, from Waipiro III, apertural view. Scale bar is 5 mm. 9. *Hokkaidoconcha* sp. 1 from Awanui GS 688, apertural view. Scale bar is 2 mm. 10. Aporrhaid gastropod from Awanui GS 688, lateral (abapertural) view. Scale bar is 3 mm. 11. *Aucellina* aff. *euglypha* Woods, 1917 from Awanui GS 688, lateral view of right valve. Scale bar is 5 mm. All specimens are illustrated by Kiel (2013), Kiel et al. (2013) and Kaim et al. (2014). Photographs courtesy of Steffen Kiel (Stockholm, Sweden). All specimens housed at GNS Sciences, Lower Hutt, New Zealand

Table 18.4 Fossil distribution of Cretaceous New Zealand seep deposits

Taxon	Locality distribution	Reference
Bivalvia		
Solemyidae indet.	AWII, WPIII	Kiel et al. (2013)
Nucinella sp.	AWI, AWII	Kiel et al. (2013)
Nuculanidae indet.	AWI, AWII, WPIII	Kiel et al. (2013)
Thyasiridae indet.	AWII, GS 688, WPIII	Kiel et al. (2013)
Inoceramidae indet.	AWI, AWII, GS 688	Kiel et al. (2013)
Aucellina aff. *euglypha*	GS 688	Kiel et al. (2013)
Carditiidae indet.	AWI	Kiel et al. (2013)
Caspiconcha sp.	AWII, GS 688	Kiel et al. (2013)
Veneridae indet.	AWI	Kiel et al. (2013)
Cubatea awanuiensis	AWII, GS 688	Kiel (2013)
Ezolucina sp. "ridge"	GS 688	Kiel et al. (2013)
Ezolucina sp. "Waipiro"	WPI	Kiel et al. (2013)
Ezolucina sp. "tall"	AWI	Kiel et al. (2013)
Amanocina raukumara	GS 688	Kiel (2013)
Gastropoda		
Bathyacmaea sp.	WPIII	Kiel et al. (2013) (as *Serradonta*)
Retiskenea sp.	GS 688	Kiel et al. (2013)
Hokkaidoconcha sp. 1	AWII	Kiel et al. (2013)
Hokkaidoconcha sp. 2	GS 688, WPIII	Kiel et al. (2013)
Fusiform gastropod	AWI	Kiel et al. (2013)
Low spired gastropod	AWII	Kiel et al. (2013)
Small globular gastropod	AWII	Kiel et al. (2013)
Aporrhaidae indet.	GS 688	Kiel et al. (2013)
Naticidae indet.	WPIII	Kiel et al. (2013)
Abyssomelania cramptoni	WPIII	Kaim et al. (2014)
Other		
Callianassa spp.	AWII, WPIII	Kiel et al. (2013)
Solitary coral	GS 688	Kiel et al. (2013)
Fish scales	AWI	Kiel et al. (2013)
Argentinid otolith	AWII	Kiel et al. (2013)

Localities are after Kiel et al. (2013). None are reported from "Owhena Stream," which is devoid of macrofossils

Awanui localities: AWI = Awanui I; AWII = Awanui II; GS 688. Waipiro Bay localities: WPI = Waipiro I; WPIII = Waipiro III

Acknowledgments We extend our gratitude to Andrzej Kaim (Warsaw, Poland) for inviting us to contribute a New Zealand chapter to this book, and two reviewers: Kazutaka Amano (Joetsu, Japan) and J. Kirk Cochran (Stony Brook, USA) for their helpful and constructive feedback. Many individuals assisted or accompanied the authors during visits to the New Zealand seep carbonate localities between 1983 and 2009. They include: Steven Hood, Steph Nyman, Sarah Ewen, Melissa Troup and Peter Kamp (University of Waikato, New Zealand), Mike Collins and Andrea Alfaro (University of Auckland, New Zealand), Alan Beu, Geoff Rait, Mike Johnston and Colin Mazengarb (GNS Science, Lower Hutt, New Zealand). Steffen Kiel (Swedish Museum of Natural History, Stockholm, Sweden) kindly allowed use of his images of Cretaceous molluscs. Neville Hudson and Louise Cotterall (University of Auckland, New Zealand) provided assistance in fossil preparation, photography, and graphics.

References

Adams JH (1910) The geology of the Whatatutu Subdivision, Raukumara Division, Poverty Bay. New Zealand Geological Survey Bulletin, no. 9. MacKay, Wellington

Amano K, Saether KP, Little CTS et al (2014) Fossil vesicomyid bivalves from Miocene hydrocarbon seep sites, North Island, New Zealand. Acta Palaeontol Pol 59(2):421–428

Amano K, Little CTS, Campbell KA et al (2015) Paleocene and Miocene *Thyasira* sensu stricto (Bivalvia: Thyasiridae) from chemosynthetic communities from Japan and New Zealand. Nautilus 129(2):43–53

Amano A, Little CTS, Campbell KA (2018) Lucinid bivalves from Miocene hydrocarbon seep sites of eastern North Island, New Zealand, with comments on Miocene New Zealand seep faunas. Acta Palaeontol Pol 63(2):371–382

Ansell JH, Bannister SC (1996) Shallow morphology of the subducted Pacific plate along the Hikurangi margin, New Zealand. Phys Earth Planet Inter 93:3–20

Asami S, Kanie Y, Takei H (1995) Chemosynthetic fossil communities discovered from fractured stones of the Miocene Hayama Group in the Miura Peninsula. Rep Cult Nat Treas Yokosuka City 29:19–22. (in Japanese)

Ballance PF (1976) Evolution of the Upper Cenozoic magmatic arc and plate boundary in northern New Zealand. Earth Planet Sci Lett 28:356–370

Barnes PM, Nicol A, Harrison T (2002) Late Cenozoic evolution and earthquake potential of an active listric thrust complex above the Hikurangi subduction zone, New Zealand. Geol Soc Am Bull 114:1379–1405

Barnes PM, Lamarche G, Bialas J et al (2010) Tectonic and geological framework for gas hydrates and cold seeps on the Hikurangi subduction margin, New Zealand. Mar Geol Spec Issue 272:26–48

Beanland S, Melhuish A, Nicol A et al (1998) Structure and deformational history of the inner forearc region, Hikurangi subduction margin, New Zealand. N Z J Geol Geophys 41:325–342

Campbell KA (2006) Hydrocarbon seep and hydrothermal vent palaeoenvironments: past developments and future research directions. Palaeogeog Palaeoclimat Palaeoecol 232:362–407

Campbell KA, Francis DA, Collins M et al (2008) Hydrocarbon seep-carbonates of a Miocene forearc (East Coast Basin), North Island, New Zealand. Sediment Geol 204:83–105

Crampton JS, Schiøler P, Roncaglia L (2006) Detection of Late Cretaceous eustatic signatures using quantitative biostratigraphy. Geol Soc Am Bull 118:975–990

Cuvier G (1797–1798) Tableau élémentaire de l'histoire naturelle des animaux. Baudouin, Paris

Dell RK (1956) The archibenthal Mollusca of New Zealand. Bull Dominion Mus Wellington 18:1–235

Field BD, Uruski CI, Beu AG et al (1997) Cretaceous–Cenozoic geology and petroleum systems of the East Coast region, New Zealand. Inst Geol Nucl Sci Monogr 19:1–301

Georgieva MN, Paull CK, Little CTS et al (2019) Discovery of an extensive deep-sea fossil serpulid reef associated with a cold seep, Santa Monica Basin, California. Front Mar Sci 6:115. https://doi.org/10.3389/fmars.2019.00115

Goedert JL, Campbell KA (1995) An Early Oligocene chemosynthetic community from the Makah Formation, northwestern Olympic Peninsula, Washington. Veliger 38:22–29

Goedert, JL, Squires, RL (1990) Eocene deep-sea communities in localized limestones formed by subduction-related methane seeps, southwestern Washington. Geology (Boulder), 18:1182–1186

Goedert JL, Kaler KL (1996) A new species of *Abyssochrysos* (Gastropoda: Loxonematoidea) from a middle Eocene cold-seep carbonate in the Humptulips Formation, western Washington. Veliger 39:65–70

Goedert JL, Thiel V, Schmale O et al (2003) The late Eocene 'Whiskey Creek' methane-seep deposit (western Washington State) Part I: Geology, palaeontology, and molecular geobiology. Facies 48:223–240

Hattori M, Kanie Y, Oba T (1995) Carbonates and chemosynthetic fossil community from the Miocene Hayama Group, central Miura Peninsula. Rep Cult Nat Treas Yokosuka City 29:89–96. (in Japanese)

Henrys S, Reyners M, Pecher I et al (2006) Kinking of the subducting slab by escalator normal faulting beneath the North Island of New Zealand. Geology 34:777–780

Kaim A, Jenkins RG, Tanabe K et al (2014) Mollusks from late Mesozoic seep deposits, chiefly in California. Zootaxa 3861:401–440

Kamp PJJ, Nelson CS (1988) Nature and occurrence of modern and Neogene active margin limestones in New Zealand. N Z J Geol Geophys 31:1–20

Kanie Y, Sakai T (1997) Chemosynthetic thraciid bivalve *Nipponothracia*, gen. nov. from the Lower Cretaceous and middle Miocene mudstones in Japan. Venus 56:205–220

Kanie Y, Asami S, Okada H et al (1992a) White clam community discovered from fractured claystone of the Miocene Hayama Group, Miura Peninsula, south-central Japan. Sci Rep Yokosuka City Mus 40:31–35. (in Japanese)

Kanie Y, Hattori M, Sasahara Y (1992b) Two types of white clam communities in Sagami Bay, central Japan: geologic settings and the Tertiary records in the Miura and Boso peninsulas. Sci Rep Yokosuka City Mus 40:37–43

Kiel S (2013) Lucinid bivalves from ancient methane seeps. J Molluscan Stud 79:346–363

Kiel S, Peckmann J (2007) Chemosymbiotic bivalves and stable carbon isotopes indicate hydrocarbon seepage at four unusual Cenozoic fossil localities. Lethaia 40:345–357

Kiel S, Birgel D, Campbell KA et al (2013) Cretaceous methane seep deposits from New Zealand and their fauna. Palaeogeog Palaeoclimat Palaeoecol 390:17–34

Lewis KB, Pettinga JR (1993) The emerging, imbricate frontal wedge of the Hikurangi margin. In: Ballance PF (ed) Sedimentary basins of the world 3: basins of the South West Pacific. Elsevier Science, Amsterdam, pp 225–250

Lillie AR (1953) The geology of the Dannevirke subdivision. N Z Geol Surv Bull 46:1–156

Linnaeus C (1758) Systema naturae per regna tria naturae, secundum classes, ordines, genera, species, cum characteribus, differentiis, synonymis, locis, 10th edn. Salvius, Stockholm

Majima R, Nobuhara T, Kitazaki T (2005) Review of fossil chemosynthetic assemblages in Japan. Palaeogeog Palaeoclimat Palaeoecol 227:86–123

Marshall BA (2001) The genus *Acesta* H. and A. Adams, 1858 in the south-west Pacific (Bivalvia: Limidae). In: Bouchet P, Marshall BA (eds) Tropical deep-sea benthos, vol 22. Mém Mus Natl Hist Nat 185, pp 97–109

Marwick J (1944) New Zealand fossil and Recent Cardiidae (Mollusca). Trans R Soc N Z 74:255–272

Mazengarb C, Speden IG (2000) Geology of the Raukumara area. Institute of Geological and Nuclear Sciences 1:250 000. Geological Map 6

Mazengarb C, Francis DA, Moore PR (1991) Sheet Y16 Tauwhareparae. Geological Map of New Zealand 1:50 000. DSIR, Wellington

McKay A (1887) On the geology of East Auckland and the northern district of Hawke's Bay. N Z Geol Surv Rep Geol Explor 18:182–219

Moore PR (1988) Stratigraphy, composition and environment of deposition of the Whangai Formation and associated Late Cretaceous–Paleocene rocks, eastern North Island, New Zealand. N Z Geol Surv Bull 100:1–82

Naganuma T, Hattori M, Kanie Y (1995a) Worm tubes from the Miocene Hayama Group, central Miura Peninsula. Rep Cult Nat Treas Yokosuka City 29:77–87. (in Japanese)

Naganuma T, Okayama Y, Hattori M et al (1995b) Fossil worm tubes from the presumed cold-seep carbonates of the Miocene Hayama Group, central Miura Peninsula, Japan. Island Arc 4:199–208

Nelson CS, Nyman SL, Campbell KA et al (2017) Influence of faulting on the distribution and development of cold seep-related dolomitic conduit concretions at East Cape, New Zealand. N Z J Geol Geophys 60:478–496. https://doi.org/10.1080/00288306.2017.1372489

Nelson CS, Campbell KA, Nyman SL et al (2019) Genetic link between Miocene seafloor methane seep limestones and underlying carbonate conduit concretions at Rocky Knob, Gisborne, New Zealand. N Z J Geol Geophys 62(3):318–340. https://doi.org/10.1080/00288306.2018.1561474

Nyman SL, Nelson CS (2011) The place of tubular concretions in hydrocarbon cold seep systems: late Miocene Urenui Formation, Taranaki Basin, New Zealand. Am Assoc Pet Geol Bull 95:1495–1524

Nyman SL, Nelson CS, Campbell KA (2010) Miocene tubular concretions in East Coast Basin, New Zealand: analogue for the subsurface plumbing of cold seeps. Mar Geol 272:319–336. https://doi.org/10.1016/j.margeo.2009.03.021

Olsson AA (1931) Contributions to the Tertiary paleontology of northern Peru: part 4, the Peruvian Oligocene. Bull Am Paleontol 17:97–264

Ongley M, Macpherson EO (1928) The geology of the Waiapu Subdivision, Raukumara Division. N Z Geol Surv Bull 30:1–79

Peckmann J, Goedert JL, Thiel V et al (2002) A comprehensive approach to the study of methane-seep deposits from the Lincoln Creek Formation, western Washington State, USA. Sedimentology 49:855–873

Rait G, Chanier F, Waters DW (1991) Landward and seaward-directed thrusting accompanying the onset of subduction beneath New Zealand. Geology 19:230–233

Saether KP (2011) A taxonomic and palaeobiogeographic study of the fossil fauna of Miocene hydrocarbon seep deposits, North Island, New Zealand. Dissertation, University of Auckland

Saether KP, Little CTS, Campbell KA (2010a) A new fossil provannid gastropod from Miocene hydrocarbon seep deposits, East Coast Basin, North Island, New Zealand. Acta Palaeontol Pol 55:507–517

Saether KP, Little CTS, Campbell KA et al (2010b) New fossil mussels (Bivalvia: Mytilidae) from Miocene hydrocarbon seep deposits, North Island, New Zealand, with general remarks on vent and seep mussels. Zootaxa 2577:1–45

Saether KP, Little CTS, Marshall BA et al (2012) Systematics and palaeoecology of a new fossil limpet (Patellogastropoda: Pectinodontidae) from Miocene hydrocarbon seeps deposits, East Coast Basin, North Island, New Zealand with an overview of known fossil seep pectinodontids. Molluscan Res 32:1–15

Saether KP, Sha J, Little CTS et al (2016) New records and a new species of bivalve (Mollusca: Bivalvia) from Miocene hydrocarbon seep deposits, North Island, New Zealand. Zootaxa 4154:1–26

Schiøler P, Crampton JS, King P (2000) Palynostratigraphic analysis of a measured section through the Karekare, Owhena and Whangai formations (Upper Cretaceous) at Waitahaia River-'Owhena Stream' (Raukumara Peninsula). Inst Geol Nucl Sci Rep 31:1–24

Squires RL, Goedert JL (1995) An extant species of *Leptochiton* (Mollusca: Polyplacophora) in Eocene and Oligocene cold-seep limestones, Olympic Peninsula, Washington. Veliger 38:47–53

Woods H (1917) The Cretaceous faunas of the north-eastern part of the South Island of New Zealand. N Z Geol Surv Paleontol Bull 4:1–41

Zwicker J, Smrzka D, Steindl F et al (2021) Mineral authigenesis within chemosynthetic microbial mats: coated grain formation and phosphogenesis at a Cretaceous hydrocarbon seep, New Zealand. Depos Rec 7:294–310

Chapter 19
Fossil Methane Seep Deposits and Communities from the Mesozoic of Antarctica

James D. Witts and Crispin T. S. Little

19.1 Introduction

Fossil methane seep deposits are rare in the Mesozoic of the Southern Hemisphere and especially in the high palaeolatitudes of Antarctica. This rarity is also reflected in the relatively small number of present-day methane seep and hydrothermal vent communities known from around the continent, which is the subject of ongoing research (e.g. Römer et al. 2014; Bell et al. 2016; Linse et al. 2019). Perhaps unsurprisingly, given the relatively small area of the continent that is ice-free and permits geological study, only two occurrences of fossil methane seep deposits have been reported from Antarctica (Fig. 19.1). Both are located on islands surrounding the Antarctic Peninsula region, which because of the lack of significant vegetation at this latitude offers exceptional outcrop conditions. These seep deposits are related to the accumulation of thick sedimentary sequences deposited in forearc and back-arc settings during the Jurassic (Tithonian) and Cretaceous (Maastrichtian), adjacent to a long-lived active magmatic arc.

19.2 Alexander Island

The fossil methane seep from the uppermost Jurassic (Tithonian) Fossil Bluff Group exposed on Alexander Island (AI) (Fig. 19.1b), Antarctica, is of interest given its remoteness from other Jurassic seep faunas. The seep locality was initially described

J. D. Witts (✉)
School of Earth Sciences, University of Bristol, Bristol, UK
e-mail: james.witts@bristol.ac.uk

C. T. S. Little
School of Earth & Environment, University of Leeds, Leeds, UK
e-mail: earctsl@leeds.ac.uk

A. Kaim et al. (eds.), *Ancient Hydrocarbon Seeps*, Topics in Geobiology 50,
https://doi.org/10.1007/978-3-031-05623-9_19

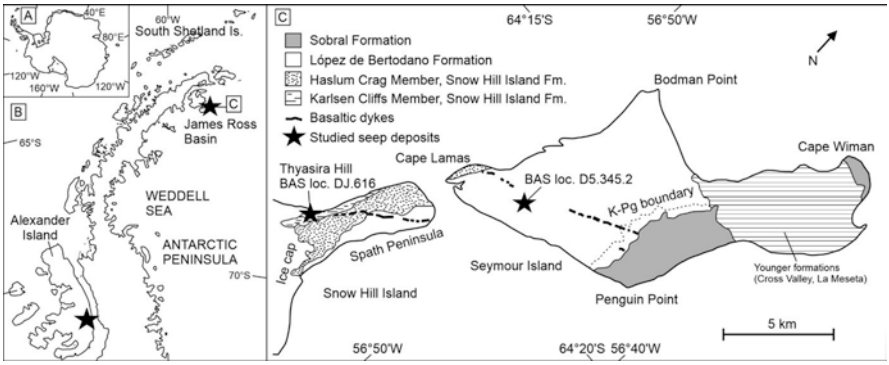

Fig. 19.1 Locality map of Antarctica (**a**) and Antarctic Peninsula Region (**b**), showing general location of fossiliferous methane seep deposits (black stars) on Alexander Island and the James Ross Basin. (position of (**c**) indicated). (**c**) Outline geological map of Seymour Island and the NE tip of Snow Hill Island, James Ross Basin. (Modified from Crame et al. (2004), Little et al. (2015), and Tosolini et al. (2021))

by Kelly et al. (1995) who provided lithological and preliminary faunal descriptions, as well as taphonomic and geochemical data. The seep carbonates form a laterally discontinuous limestone body known as the Gateway Pass Limestone Bed (GPLB). A description of hokkaidoconchid gastropods, the dominant faunal element at the seep, was provided by Kaim and Kelly (2009). Beyond these two papers, this locality is unstudied, and we provide only a brief overview here.

19.2.1 Location and Geological Setting of AI

The >7000-m-thick Fossil Bluff Group outcrops across the eastern coast of AI, bounded to the east by the present George VI Ice Shelf and to the west by the accretionary complex Le May Group, which it is faulted against and unconformably overlies. It represents the clastic fill of a forearc basin succession to the west of the active magmatic arc of the Antarctic Peninsula during the late Jurassic and early Cretaceous (Doubleday et al. 1993). Rifting in the Kimmeridgian formed a deep-marine basin, filled initially by hemipelagic muds, overlain in places by a large-scale (tens of km) slope mass-transport complex and succeeded by deep-marine channel-levee complexes (Butterworth and Macdonald 2007).

The Fossil Bluff Group is divided into five formations (Doubleday et al. 1993). The ~1.1-km-thick Atoll Nunatacks Formation (ANF) occurs towards the base of the group and comprises thinly bedded mudstones and silty mudstones representing a marine transgression followed by deposition of turbidites in a trench-slope setting. It probably indicates a phase of subsidence in response to contemporaneous tectonic events in the adjacent accretionary prism (Doubleday et al. 1993). This area may have been located at 60–70°S during the Tithonian (Lawver et al. 1992), but

complex terrane tectonics in this region place some doubt as to the palaeolatitude of AI prior to the mid-Cretaceous (Vaughan and Storey 2000).

19.2.2 Age of ANF

The precise age of the seep locality within the ANF is not well constrained. Faunal data from radiolaria (Holdsworth and Nell 1992) and a sparse molluscan fauna containing buchiid bivalves and belemnopsid belemnites constrain deposition to the Bathonian–Tithonian (Doubleday et al. 1993). The seep carbonates occur towards the upper part of the succession and are, therefore, considered Tithonian in age.

19.2.3 Brief Description of Seep Localities on ALI

The GPLB is exposed discontinuously for around 200 m between scree-filled gullies on Offset Ridge, AI (68°39′W, 71°38′S), ~2 km east of the LeMay Range Fault Zone, which represents the boundary between forearc and accretionary prism deposits (Kelly et al. 1995). It varies from 3 m at its thickest at the east end of the outcrop where the base is not exposed, pinching out westwards. The seep carbonates themselves are composed of calcite-cemented mudstones and sandstones covered by irregular laminated crusts up to 2-m wide and 20-cm thick, which are in places brecciated (Kelly et al. 1995; Kaim and Kelly 2009). Mass aggregations of fossils occur in mudstone interbeds associated with the crusts. Four phases of calcite and silica cement formed within the crusts. The cemented crusts exhibit depleted $\delta^{13}C$ values of −40.8% to −44.6%, while sparry cement infills range from −33.5% to −40.5%, both typical of the anaerobic oxidation of methane (AOM).

Kelly et al. (1995) interpreted the seep as potentially forming on a palaeobathymetric high, but within a pockmark structure on the seafloor with carbonate crusts forming around the mouth of the seep. The source of the methane is unclear, but up to 2 km of the Fossil Bluff Group underlies the horizon containing the seep. Kelly et al. (1995) speculated that structural features and faulting focused methane migration within the basin, and identified a nearby synsedimentary normal fault as a conduit, with brecciation evidence for occasional gas ponding and explosions.

19.2.4 Fauna of the GPLB

The GPLB is characterized by increased faunal abundance compared to the rest of the relatively unfossiliferous ANF. The seep fauna is dominated by high-spired gastropods, originally described as ‘cerithiforms’ by Kelly et al. (1995). Kaim and Kelly (2009) redescribed these as a new species of seep obligate hokkaidoconchid,

Hokkaidoconcha hignalli. These gastropods are associated with large lucinids, protobranch bivalves, as well as rare limpets, crinoids, belemnites and ammonites (Kelly et al. 1995; Kaim and Kelly 2009). Microfossils (ostracods and foraminifera) are also present. *Thalassinoides* burrows and *Trypanites* borings occur in the limestone crusts (Kelly et al. 1995). Abundant gastropod faecal pellets were documented by Kaim and Kelly (2009). Dark-clotted laminae and blebs within the crusts themselves may represent fossilized *Beggiatoa*-type bacterial mats.

The faunal association of hokkaidoconchids and lucinids in the AI seep is very reminiscent of Jurassic and Cretaceous fossil seep communities from Japan (Kaim et al. 2008) and the US Pacific Coast (Kiel et al. 2008), suggesting that a widespread seep fauna was present around the margins of the Pacific during this part of the Mesozoic.

19.3 James Ross Basin

Methane seeps from uppermost Cretaceous (Maastrichtian) volcaniclastic shallow shelf sediments exposed on Snow Hill and Seymour Islands, James Ross Basin (JRB) (Fig. 19.1b), Antarctica were documented in detail by Little et al. (2015). The seeps are manifest as large, cement-rich carbonate bodies on Snow Hill Island and micrite-cemented burrow systems on Seymour Island (Fig. 19.1c). They are associated with a low diversity fauna of thyasirid, solemyid and lucinid bivalves.

19.3.1 Location and Geological Setting of the JRB

The JRB is a large extensional sedimentary basin that formed behind the magmatic arc of the Antarctic Peninsula from the late Mesozoic to early Cenozoic (e.g. Pirrie et al. 1997; Crame et al. 2004; Olivero 2012). The volcaniclastic sediments deposited in this basin are now exposed on various islands in the James Ross Island area, including Snow Hill and Seymour Islands (subsequently SHI and SI, respectively; Fig. 19.1), and represent the best onshore sedimentary sequence of its age in the southern high latitudes. Because of its importance and fossiliferous nature, this region has been the focus of a large number of studies (see Crame 2019 for a recent review).

The Late Cretaceous-Paleogene infill of the JRB comprises >2500 m of fine-grained sediments, part of which forms the Coniacian to Danian aged Marambio Group (Pirrie et al. 1997; Crame et al. 2004; Olivero 2012; Milanese et al. 2020). The middle-upper part of the Group comprises most of the Snow Hill Island Formation (SHIF) and overlying López de Bertodano (LBF) and Sobral (SF) formations (Fig. 19.2). Tectonic reconstructions and magnetostratigraphic data suggest that the JRB was located at ~65°S during the Late Cretaceous-Paleogene (Lawver et al. 1992; Milanese et al. 2019a).

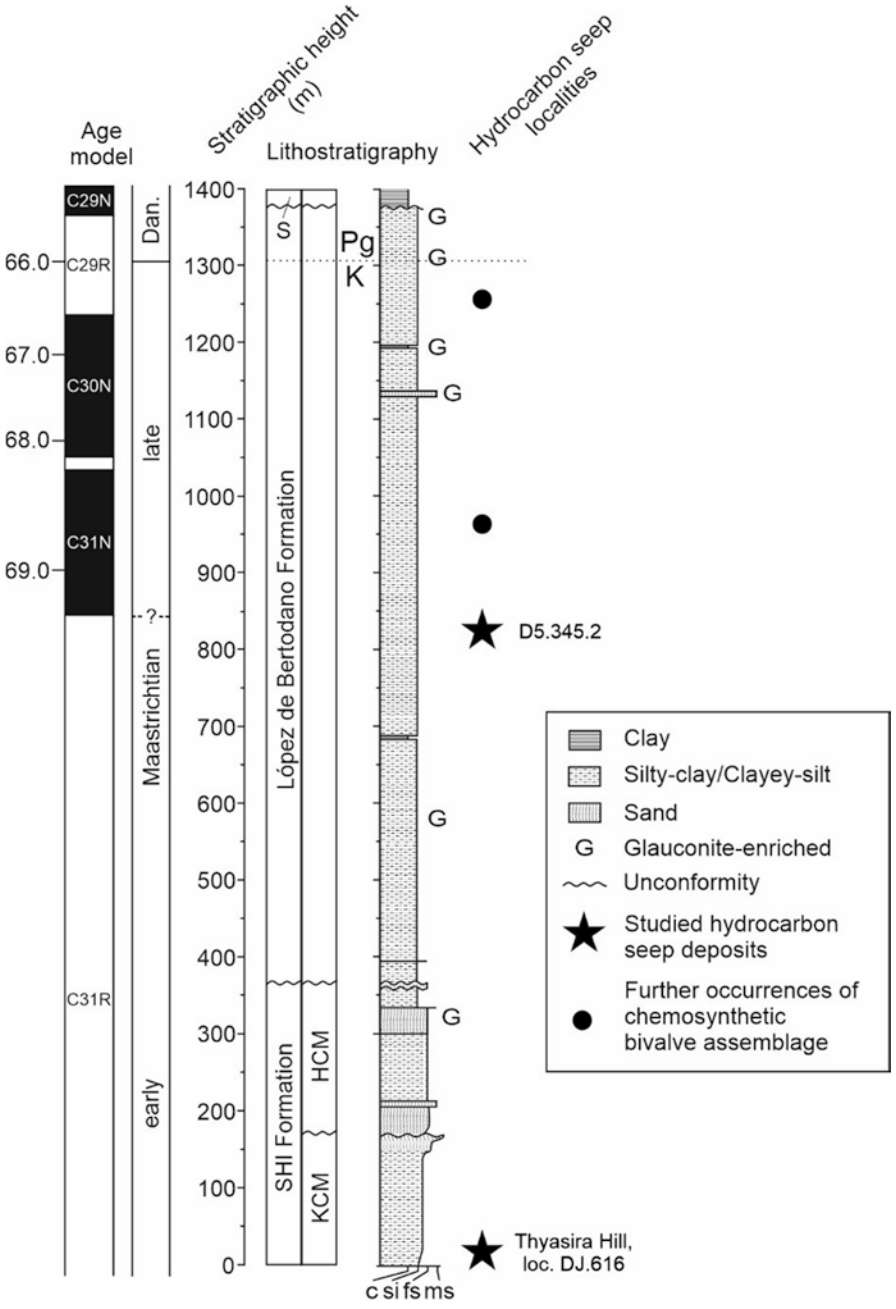

Fig. 19.2 Composite stratigraphy of the Maastrichtian part of the Marambio Group on Snow Hill and Seymour Islands, following Pirrie et al. (1997), Crame et al. (2004) and Bowman et al. (2013) for lithostratigraphy and biostratigraphy, and Tobin et al. (2012), Bowman et al. (2013), Montes et al. (2019) and Milanese et al. (2019b) for age model. Stars mark the approximate positions of the studied hydrocarbon seep deposits. Black circles indicate other occurrences of chemosynthetic bivalve assemblage ('*Thyasira*'; '*Lucina*'; *Solemya*) collected during British Antarctic Survey (BAS) expeditions in 1999 and 2006 (see Witts et al. (2016) for details). Abbreviations: *SHI* Snow Hill Island, *KCM* Karlsen Cliffs Member, *HCM* Haslum Crag Member, *S* Sobral Formation, *K* Cretaceous, *Pg* Paleogene, *Dan* Danian

The top two units of the SHIF on SHI are the Karlsen Cliffs Member (KCM) below and the Haslum Crag Member (HCM) above (Fig. 19.2). These two units crop out on the Spath Peninsula at the northern tip of SHI, and along strike on the southwestern tip of SI. The KCM consists of mudstones, sandy mudstones and heavily bioturbated fine sandstones with abundant early diagenetic concretions (Pirrie et al. 1997), interpreted by Olivero (2012) as representing sediments formed in a coarsening upwards prograding deltaic wedge. The HCM of Pirrie et al. (1997) is roughly equivalent to the Haslum Crag Sandstone of Olivero (2012) and comprises medium- to coarse-grained cross-stratified and channelized sandstones, passing upwards into intensely bioturbated fine-grained sandstones and siltstones, containing fossiliferous concretions (Pirrie et al. 1997). The HCM is separated from the KCM and overlying LBF by unconformities (Pirrie et al. 1997; Crame et al. 2004). Olivero (2012) interpreted the Haslum Crag Sandstone as being forced regressive tidal deposits (Olivero 2012; fig. 2). The LBF crops out on the eastern side of the Spath Peninsula of SHI (lower part only) and extensively on the western side of SI (full thickness; Fig. 19.2). The LBF contains the Cretaceous-Paleogene (K-Pg) boundary and mass extinction event near its top (Fig. 19.2; Zinsmeister 1998; Crame et al. 2004; Witts et al. 2016). Lithologically, the LBF is dominated by intensely bioturbated muddy siltstones, with thin intercalated sandstones and discontinuous concretionary levels. The LBF coarsens upwards slightly towards the top of the section where there are some prominent glauconitic sandstones (Crame et al. 2004). According to Olivero (2007), the lower part of the LBF comprises estuarine and shallow marine deposits, the middle part transgressive shelf deposits and the top part regressive shelf deposits (Olivero 2012; fig. 2). The LBF is overlain by the Sobral Formation (SF), which out crops on the eastern and northern sides of SI and records deposition in a range of prodelta and shallow deltaic environments (Marenssi et al. 2012; Bowman et al. 2016; Whittle et al. 2019).

19.3.2 Age of the JRB Sequence

Ammonites provide the best biostratigraphic zonation of the JRB Cretaceous sequence (Macellari 1986; Olivero 2012; Witts et al. 2015). Olivero and Medina (2000) and Olivero (2012) divided the Cretaceous succession into 14 ammonite assemblages, based mainly on the stratigraphic distribution of the family Kossmaticeratidae. The KCM and HCM occur in assemblage 10, while the overlying LBF contains assemblages 11 to 14. Ammonite taxa from the KCM, HCM and LBF are all indicative of a Maastrichtian age (Macellari 1986; Olivero 2012; Witts et al. 2015). This is in agreement with microfossil data from dinoflagellate cysts (Bowman et al. 2012). Palynological data also support assignment of the upper part of the LBF above the K-Pg boundary and most of the overlying Sobral Formation on SI to the Danian (Elliot et al. 1994; Bowman et al. 2016).

Magnetostratigraphic study of the JRB Cretaceous and early Paleogene sequence has recently been completed (Fig. 19.2). These data suggest the KCM on SHI

correlates in its entirety to magnetochron C31R (Milanese et al. 2019b). The LBF on SI spans chrons C31R through C29N and was, therefore, deposited between ~70 and 65.7 Ma (Tobin et al. 2012). The overlying SF contains chrons C29N to C26R and was deposited between 65.7 and ~62 Ma (Montes et al. 2019).

19.3.3 Description of Fossil Seep Localities in the JRB

19.3.3.1 Carbonate Bodies and 'Thyasira' Occurrences on Snow Hill Island

As reported in Little et al. (2015), specimens of the large thyasirid bivalve *'Thyasira' townsendi* are common in the lower part of the type section of the KCM on the Spath Peninsula, SHI, especially at the locality known as '*Thyasira* Hill' (British Antarctic Survey (BAS) locality DJ.616) (64.37°48'S, 56.98°07'W) (Pirrie et al. 1997) (Figs. 19.3, 19.4, and 19.5g). In places at this locality, thyasirid fossils reach an estimated density of >120/m^2 (Fig. 19.3c). Clusters of *'T.' townsendi* are associated with patches of pale blue-grey carbonate cementation which serve to accentuate the regular, planar bedding (Fig. 19.3b, d). At the bottom of the section, the cemented regions are 20 to 30 cm thick and 50 to 100 cm in width, but at higher levels in the succession, the beds are more continuous and weather out to form the peak of a prominent structure 60 m in height that forms the summit of *Thyasira* Hill (Figs. 19.3a and 19.4a, c). This feature is located approximately 500 m SW of 'Nordenskjöld's Hut', a historic structure erected as a winter station by the Swedish South Polar Expedition in the early twentieth century (see Zinsmeister 1988; Almevik et al. 2021).

At *Thyasira* Hill, carbonate-cemented, sheet-like shell beds are 30 to 75 cm thick (Figs. 19.3e and 19.4c). Many '*T.*' *townsendi* shells are in growth position but rarely touch each other (Figs. 19.4c and 19.5a); others are clearly *ex situ* and broken. Small specimens of ammonites (*Gunnarites antarcticus* and indeterminate lytoceratids) are also preserved in the cemented layers (Fig. 19.3e). Interbeds have yielded isolated specimens of '*T.*' *townsendi* together with ammonites, including *Jacobites anderssoni* (Fig. 19.5f), *Gunnarites bhavaniformis* (Fig. 19.5e) and scattered specimens of the serpulid worm *Austrorotularia* sp. About 200 m across a small valley to the South of *Thyasira* Hill at the same stratigraphic level are approximately 12 topographic knolls up to 10 m tall and ~5 m wide (Fig. 19.4b, d), which represent carbonate-cemented patches that have been exhumed by weathering from the enclosing fine-grained sediments. These knolls have similar lithologies and faunal content to *Thyasira* Hill, including the ammonite *Gunnarites antarcticus*, the solemyid bivalve *Solemya rossiana* and indeterminate gastropods. Well-cemented '*Thyasira*' patches and carbonate layers are discontinuous both laterally and vertically within the KCM, occurring through an approximately 50-m-thick section, and over 100 m horizontally.

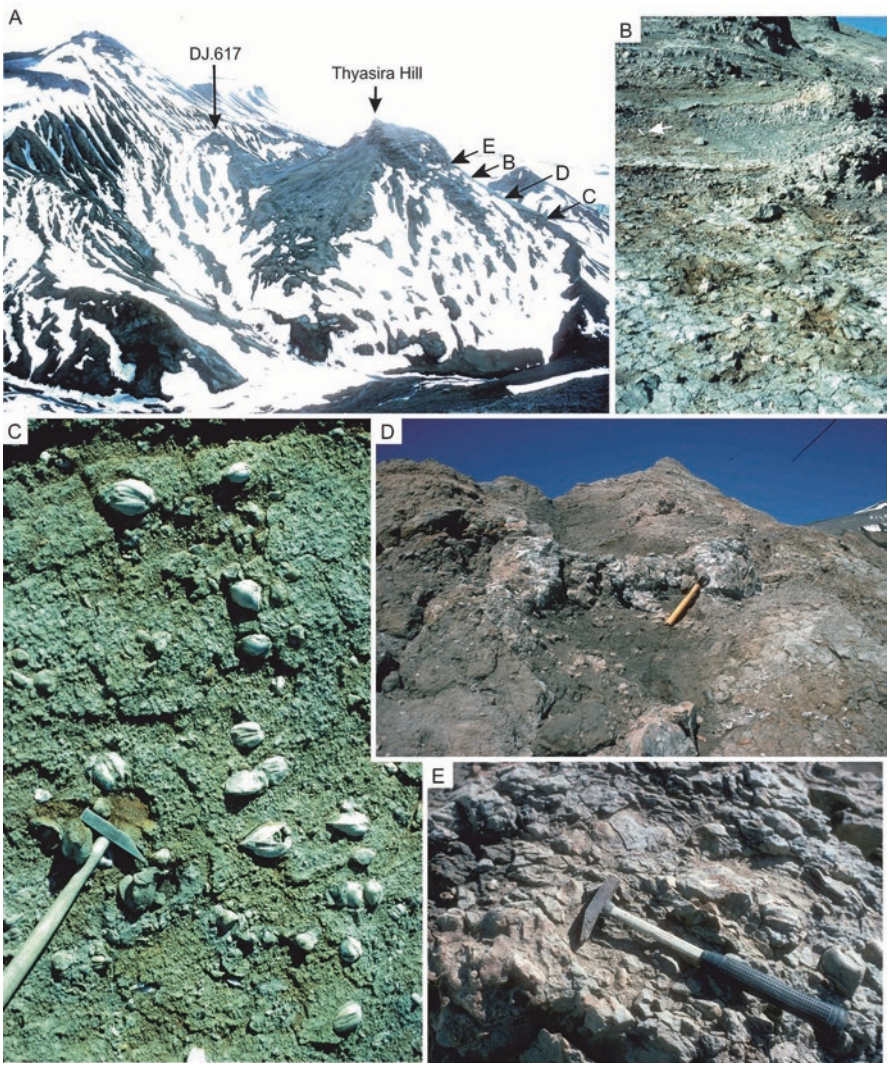

Fig. 19.3 Field images of carbonate-cemented sediments and associated fossils from the Karlsen Cliffs Member, near Nordenskjolds Hut, Snow Hill Island, looking toward the SW. Section (**a**) runs from the base of the hill, bottom right of the photograph, up the slope through points where photographs (**c**–**e**) were taken, over Thyasira Hill. Cliffs at the top left of photograph **a** are the Haslum Crag Member. The white arrow points in the younging direction, perpendicular to dip of the beds. (**b**) and (**d**) Irregularly shaped patches of carbonate-cemented sediments. (**c**) *In-situ* articulated '*Thyasira*' *townsendi* specimens in plain view on the surface of an exposed bedding plane. (**e**) Ammonites and articulated '*Thyasira*' *townsendi* specimens, base of Thyasira Hill. Geological hammers are for scale in (**b**) (see white arrow), (**c**), (**d**) and (**e**) approximately 40 cm long

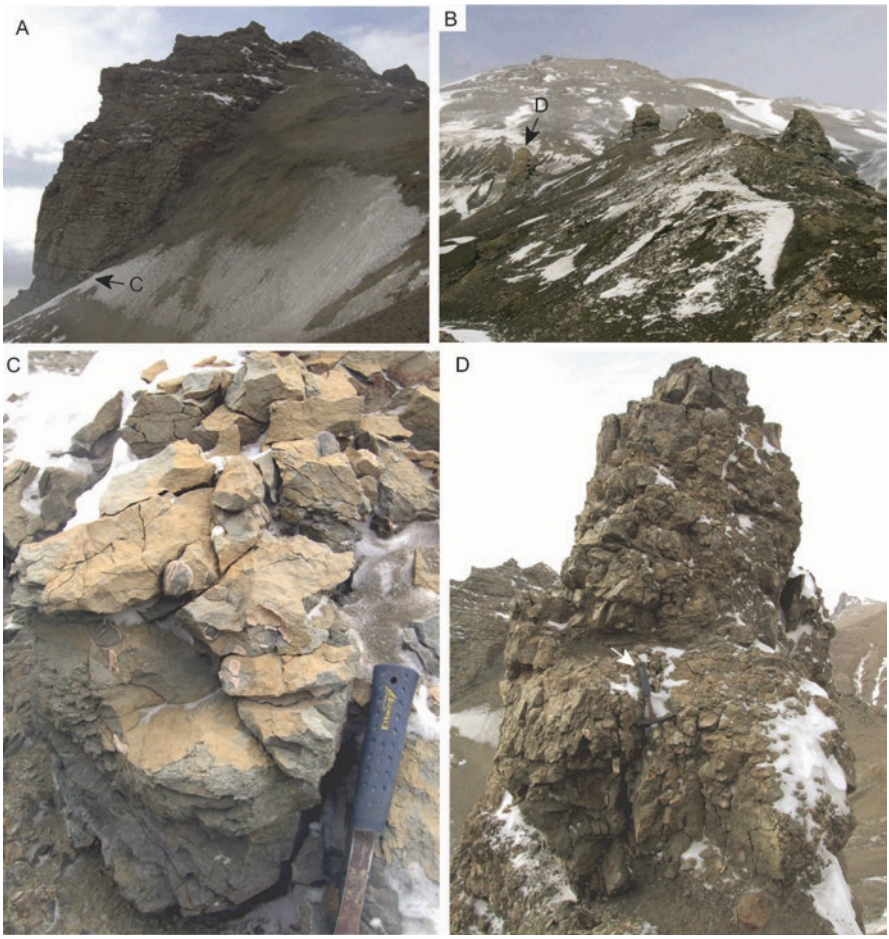

Fig. 19.4 Field images of carbonate-cemented sediments and associated fossils from Karlsen Cliffs Member, Snow Hill Island. (**a**) Thyasira Hill; arrows show position of image (**c**). (**b**) Knolls of exhumed carbonate-cemented sediment, approximately 200 m East of Thyasira Hill; arrow shows position of photo (**d**). Outcrops in the hills in background are Haslum Crag Member. (**c**) Detail of (**a**) showing carbonate-cemented sediment enclosing weathered articulated '*Thyasira*' *townsendi* specimens. (**d**) Detail of knoll in (**b**) with Thyasira Hill in background, to left; arrow points to hammer scale. Geological hammers are for scale in (**c**) and (**d**) approximately 30 cm long

Little et al. (2015) interpreted the laterally discontinuous carbonate-cemented sediments at the *Thyasira* Hill locality on SHI as representing methane seeps formed during a period of increasingly concentrated hydrocarbon seepage. Cement phases from the SHI carbonates and infill within articulated '*T.*' *townsendi* fossils exhibit $\delta^{13}C$ values between -20.4% and -10.7%. Molecular fossils extracted from the seep carbonates are indicative of micro-organisms involved in AOM such as methanotrophic archaea and suggest dominance of thermogenic methane over other hydrocarbons (Little et al. 2015).

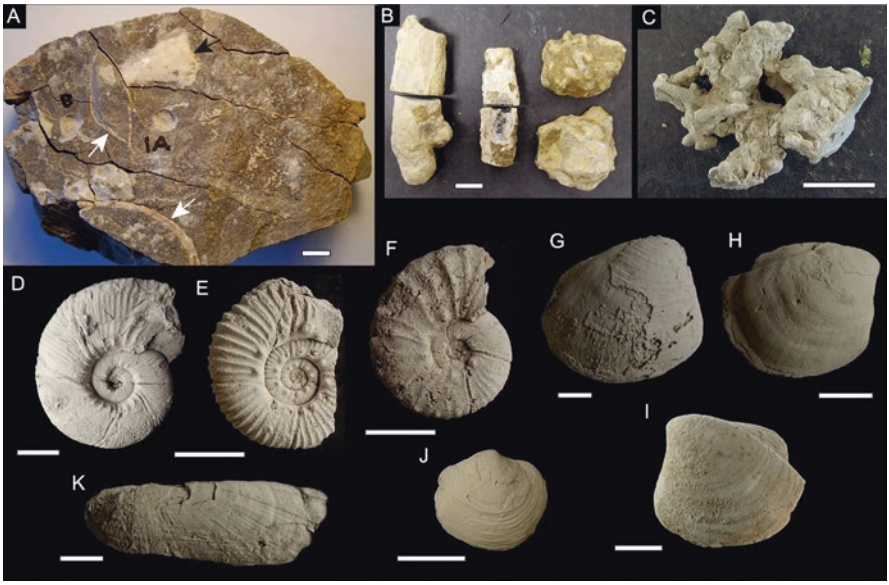

Fig. 19.5 Fossils and carbonate concretions from methane seep deposits on Snow Hill and Semyour Islands, Antarctica. (**a**) Hand specimen of carbonate-cemented siltstone from Thyasira Hill, Karlsen Cliffs Member, Snow Hill Island. White arrows point to articulated '*Thyasira*' *townsendi* specimens in various sections. Black arrow points to sparry calcite cement patch. Codes 1A and B are sites drilled for isotopic analysis in Little et al. (2015). (**b**) Cut tubular carbonate concretion from BAS locality D5.345.2, López de Bertodano Formation, Seymour Island. Note the presence of small *Planolites*-like burrows on the surface of the concretion. (**c**) Carbonate concretion of cemented large burrows with smaller burrows on their surfaces; from Hydrate Hole seep site, 3100 m water depth, Congo deep-sea fan (Haas et al. 2010). (**d**) Ammonite *Maorites seymourianus* from BAS locality D5.347.2, López de Bertodano Formation, Seymour Island. (**e**) Ammonite *Gunnarites* sp. (possibly *G. bhavaniformis*) from Thyasira Hill, Snow Hill Island. (**f**) Ammonite *Jacobites anderssoni* from BAS locality DJ.633.1, Thyasira Hill, Karlsen Cliffs Member, Snow Hill Island. (**g**) Right valve of articulated '*Thyasira*' *townsendi* from Thyasira Hill, Snow Hill Island. (**h**) Right valve of articulated specimen of bivalve '*Thyasira*' *townsendi* from BAS locality D5.345.2, López de Bertodano Formation, Seymour Island; internal mould. (**i**) Left valve of articulated large thyasirid bivalve from Deception Island, Antarctica (specimen 1464 from PRI, New York). (**j**) Right valve of articulated specimen of bivalve '*Lucina*' *scotti* from BAS locality D5.345.2, López de Bertodano Formation, Seymour Island. (**k**) Right valve of bivalve *Solemya rossiana,* BAS locality D5.345.2, López de Bertodano Formation, Seymour Island. All fossils are whitened with ammonium chloride powder. Scale bars **a**–**c** = 10 mm; **d**–**k** = 20 mm

19.3.3.2 Carbonate Concretions and 'Thyasira' Occurrences on Seymour Island

'*Thyasira' townsendi* itself occurs intermittently in laterally discontinuous layers, usually within a distinctive dark sulphurous mudstone facies, throughout the rest of the nearly 1500-m-thick Maastrichtian succession on SHI and SI (Fig. 19.2), often in association with articulated specimens of the lucinid '*Lucina*' *scotti* (Fig. 19.5j) and/or the solemyid *Solemya rossiana* (Fig. 19.5k). Stratigraphically, later *'T.'*

townsendi layers in the HCM and LBF are, however, not associated with well-cemented large carbonate deposits like those in the KCM.

Little et al. (2015) studied one of these horizons from the LBF of SI (BAS locality D5.345.2), ~458 m above the basal unconformity with the HCM (Fig. 19.2). This locality contains scattered cylindrical and carbonate-cemented concretions up to 39 mm in length composed of dark fine-grained sediments cemented by micrite with a later, weathering rind of gypsum (Fig. 19.5b). Some concretions have internal infillings of fibrous calcite cements. Others are roughly circular and have pale-coloured *Planolites*-like burrows on their surfaces, strongly resembling modern seep-associated concretions (Fig. 19.5c) (Haas et al. 2010). Associated with these are abundant specimens of *'T.' townsendi* (Fig. 19.5h), *S. rossiana* (Fig. 19.5k) and some examples of the ammonites *Maorites seymourianus* (Fig. 19.5d) and *M. weddelliensis.* Benthic molluscs are also associated with this concretionary layer, such as the nuculid and trigoniid bivalves *Leionucula suboblonga* and *Oistotrigonia pygoscelium*, and the gastropod '*Cassidaria*' mirabilis. These are typical of the 'background' benthic molluscan fauna found throughout the LBF on SI (Zinsmeister and Macellari 1988; Crame et al. 2014; Witts et al. 2016). The last occurrence of the distinctive '*T.*' *townsendi* facies is a prolifically fossiliferous bedding plane ~48 m below the K-Pg boundary in the upper levels of the LBF (Fig. 19.2) (Witts et al. 2016).

Little et al. (2015) concluded that the laterally discontinuous concretionary layers with putatively chemosymbiotic bivalves present throughout the LBF on SI were methane seeps that formed during repeated periods of diffuse methane flux to the sediment. Depleted carbon isotope values within concretionary matrix and cements range from -58.0% to -24.6% and suggest AOM together with an increased contribution of biogenic methane compared to the older SHI seeps. Geochemical data (specifically depleted $\delta^{13}C$ values) derived from shell material of well-preserved bivalves and ammonites at discrete intervals throughout the LBF also suggest that these periodic intervals of increased methane flux may have influenced the chemistry of the sediments, overlying water column and organisms inhabiting these environments (Tobin and Ward 2015; Hall et al. 2018; Ivany and Artruc 2020).

19.3.4 Fauna of the JRB Methane Seeps

The JRB methane seep fauna is dominated by the large thyasirid bivalve '*T.*' *townsendi*, often co-occurring together with the lucinid bivalve *'Lucina' scotti* and/or the solemyid bivalve *Solemya rossiana* (Zinsmeister and Macellari 1988; Crame et al. 2014; Witts et al. 2016). Little et al. (2015) suggested that these taxa very likely had symbionts like many living representatives of these families, and that association of these species with the seep carbonates in the KCM and LBF indicated the presence of AOM-derived hydrogen sulphide. Other studies have found petrological and geochemical evidence for fluctuating redox conditions in these sections, possibly on a seasonal scale (Schoepfer et al. 2017). However, the presence of a

diverse 'background' benthic molluscan fauna, both epi- and infauna, associated with the chemosymbiotic taxa in the KCM and LBF indicates that environmental conditions in the sediment were not persistently challenging.

Interestingly, the JRB methane seep fauna does not include representatives of other common Mesozoic and Cenozoic seep obligate taxa, such as *Paskentana*, hokkaidoconchids, *Peregrinella*, *Caspiconcha*, vesicomyids or bathymodiolins. The reasons for this are unclear, but may be related to the high palaeolatitude of the JRB, the relatively shallow (<200 m) water depths in the basin, palaeoecology, or simply that the Maastrichtian age of the succession is earlier than the evolution of some of these taxa (see discussion in Little et al. 2015).

'Thyasira' townsendi specimens from SHI were first described by Weller (1903) and identified as being conspecific with White's (1890) species *Lucina townsendi* from Cretaceous sediments on St. Paul's and St. Peter's Islands in the Magellan Strait. Wilckens (1910) later suggested that *Lucina townsendi* (White) 1890 is not a lucinid and transferred the species to the genus *Thyasira*. However, as noted by Zinsmeister and Macellari (1988), '*Thyasira' townsendi* is much larger than other *Thyasira* species, and in size and shape more resembles species belonging to *Conchocele* (Kamenev et al. 2001; Okutani, 2002; Oliver and Sellanes, 2005), hence the placement of the genus name '*Thyasira*' in quotation marks here and in Little et al. (2015). Large thyasirid bivalves with very similar morphologies to '*T.' townsendi* are also found in other Cretaceous deposits in the high Southern latitudes, including specimens from Deception Island, Antarctica (Fig. 19.5i) and the species *T. bullpointensis* (Stilwell) from North Island, New Zealand.

Similarly, the shell morphology of '*Lucina*' *scotti* (Wilckens) (Fig. 19.5j) 1910 does not correspond well to this genus (or to Wilckens' original genus *Phacoides*). The Antarctic species very likely belongs to the extinct lucinid genus *Nymphalucina* Speden, 1970 (Kiel 2013), which is particularly well known from seep and non-seep environments in the Cretaceous Western Interior Seaway in North America (Kauffman et al. 1996; Ryan et al. 2020), because of the external characters, and the shape of the cardinal teeth that can be seen in some weathered articulated JRB specimens.

It seems unlikely that any of the three bivalve taxa common at JRB seep localities were seep obligates. Both *'L.' scotti* (commonly) and *S. rossiana* (rarely) occur throughout the LBF, apparently not always in association with seep carbonates (Zinsmeister and Macellari, 1988). A single specimen of *'T.' townsendi* was also recently documented from the 237- to 250-m level in the Palaeocene SF, i.e., ~315 m above the K-Pg boundary. The upper levels of the SF have also yielded several small specimens of a solemyid that appears to represent a new species (Crame et al. 2014; Whittle et al. 2019). Other lucinid bivalves (previously assigned to *Saxolucina*) occur sporadically throughout the LBF and SF (Stilwell et al. 2004; Beu 2009; Crame et al. 2014; Whittle et al. 2019). The precise taxonomic placement of these bivalves, and whether their occurrence coincides with additional periods of hydrocarbon seepage in the JRB, remains to be elucidated.

Acknowledgements We thank Alistair Crame, Jane Francis, Rowan Whittle and Vanessa Bowman (British Antarctic Survey) for assistance and useful discussions about the JRB and Antarctic palaeontology. Thanks also to the co-authors of the Little et al. (2015) study (Daniel Birgel, Adrian Boyce, Steffen Kiel, Jörn Peckmann, Duncan Pirrie and Gavyn Rollinson). Hilary Blagborough is thanked for providing access to BAS specimens and collections. We are grateful to Neil Landman (AMNH) and Kirk Cochran (Stony Brook University) for their encouragement and opportunity to write this contribution and helpful reviews.

References

Almevik G, Avango D, Contissa V et al (2021) Built cultural heritage in Antarctica. Remains and uses of the first Swedish South Polar expedition 1901–1903. Report from the Expert and Research Expedition CHAQ2020, Swedish National Heritage Board, p 169

Bell JB, Aquilina A, Woulds C et al (2016) Geochemistry, faunal composition and trophic structure in reducing sediments on the southwest South Georgia margin. Roy Soc Open Sci 3:160284

Beu AG (2009) Before the ice: biogeography of Antarctic Paleogene molluscan faunas. Palaeogeogr Palaeoclim Palaeoecol 284:191–226

Bowman VC, Francis JE, Riding JB et al (2012) A latest Cretaceous to earliest Paleogene dinoflagellate cyst zonation from Antarctica, and implications for phytoprovincialism in the high southern latitudes. Rev Palaeobot Palynol 171:40–56

Bowman VC, Francis, JE, Riding, JB (2013) Late Cretaceous winter sea ice in Antarctica? Geology 41:1227–1230

Bowman V, Ineson J, Riding J et al (2016) The Paleocene of Antarctica: Dinoflagellate cyst biostratigraphy, chronostratigraphy and implications for the palaeo-Pacific margin of Gondwana. Gondwana Res 38:132–148

Butterworth P, Macdonald D (2007) Channel-levee complexes of the Fossils Bluff Group, Antarctica. In: Nilson T, Shew R, Steffens G, Studlick J (eds) AAPG Atlas of deepwater outcrops. American Association of Petroleum Geologists Special Publication, Tulsa, pp 36–41

Crame JA (2019) Paleobiological significance of the James Ross Basin. Adv Polar Sci 30:186–198

Crame JA, Francis JE, Cantrill DJ, Pirrie D (2004) Maastrichtian stratigraphy of Antarctica. Creta Res 25:411–423

Crame JA, Beu AG, Ineson JR et al (2014) The Early Origin of the Antarctic Marine Fauna and Its Evolutionary Implications. PLoS One 9:e114743

Doubleday PA, Macdonald DIM, Nell PAR (1993) Sedimentology and structure of the trench-slope to forearc basin transition in the Mesozoic of Alexander Island, Antarctica. Geol Mag 130:737–754

Elliot DH, Askin RA, Kyte FT, Zinsmeister WJ (1994) Iridium and dinocysts at the Cretaceous-Tertiary boundary on Seymour Island, Antarctica: implications for the K-T event. Geology 22:675–678

Haas A, Peckmann J, Elvert M et al (2010) Patterns of carbonate authigenesis at the Kouilou pockmarks on the Congo deep-sea fan. Mar Geol 268:129–136

Hall JLO, Newton RJ, Witts JD et al (2018) High benthic methane flux in low sulfate oceans: Evidence from carbon isotopes in Late Cretaceous Antarctic bivalves. Earth Planet Sci Lett 497:113–122

Holdsworth BK, Nell PR (1992) Mesozoic radiolarian faunas from the Antarctic Peninsula: age, tectonic and palaeoceanographic significance. J Geol Soc (London) 149:1003–1020

Ivany LC, Artruc EG (2020) Lifespan, growth rate, and ecology of a giant heteromorph ammonite from Antarctica. Paper presented at the Annual Meeting of the Geological Society of America, GSA Connects Online, 25–28 October 2020

Kaim A, Kelly SRA (2009) Mass occurrence of hokkaidoconchid gastropods in the Upper Jurassic methane seep carbonate from Alexander Island, Antarctica. Antarct Sci 21:279–284

Kaim A, Jenkins RG, Warén A (2008) Provannid and provannid-like gastropods from the Late Cretaceous cold seeps of Hokkaido (Japan) and the fossil record of the Provannidae (Gastropoda: Abyssochrysoidea). Zool J Linne Soc 154:421–436

Kamenev GM, Nadtochy VA, Kuznetsov AP (2001) *Conchocele bisecta* (Conrad, 1849) (Bivalvia: Thyasiridae) from cold-water methane-rich areas of the Sea of Okhotsk. Veliger 44:84–94

Kauffman EG, Arthur MA, Howe B, Scholle PA (1996) Widespread venting of methane-rich fluids in Late Cretaceous (Campanian) submarine springs (Tepee Buttes), Western Interior seaway, U.S.A. Geology 24:799–802

Kelly SRA, Ditchfield PW, Doubleday PA, Marshall JD (1995) An Upper Jurassic methane-seep limestone from the Fossil Bluff Group forearc basin of Alexander Island, Antarctica. J Sed Res 65:274–282

Kiel S (2013) Lucinid bivalves from ancient methane seeps. J Molluscan Stud 79:346–363

Kiel S, Campbell KA, Elder WP, Little CTS (2008) Jurassic and cretaceous gastropods from hydrocarbon seeps in forearc basin and accretionary prism settings, California. Acta Palaeontol Polonica 53:679–703

Lawver LA, Gahagan LM, Coffin MF (1992) The development of Paleoseaways around Antarctica. In: Kennet JP, Warnke DA (eds) The Antarctic paleoenvironment: a perspective on global change: part one, vol 56. American Geophysical Union (AGU), Washington, DC, pp 7–30

Linse K, Copley JT, Connelly DP et al (2019) Fauna of the Kemp Caldera and its upper bathyal hydrothermal vents (South Sandwich Arc, Antarctica). Roy Soc Open Sci 6:91501

Little CTS, Birgel D, Boyce AJ et al (2015) Late Cretaceous (Maastrichtian) shallow water hydrocarbon seeps from Snow Hill and Seymour Islands, James Ross Basin, Antarctica. Palaeogeog Palaeoclim Palaeoecol 418:213–228

Macellari CE (1986) Late Campanian–Maastrichtian Ammonite Fauna from Seymour Island (Antarctic Peninsula). J Paleontol 60:1–55

Marenssi S, Santillana S, Bauer M (2012) Stratigraphy, sedimentary petrology and provenance of the Sobral and Cross Valley formations (Paleocene), Marambio (Seymour) Island, Antarctica. Andean Geol 39:67–91

Milanese F, Rapalini A, Slotznick SP, Tobin TS (2019a) Late Cretaceous paleogeography of the Antarctic Peninsula: new paleomagnetic pole from the James Ross Basin. J South Am Earth Sci 91:131–143

Milanese FN, Olivero EB, Raffi ME et al (2019b) Mid Campanian-Lower Maastrichtian magnetostratigraphy of the James Ross Basin, Antarctica: chronostratigraphical implications. Basin Res 31:562–583

Milanese FN, Olivero EB, Slotznick SP, Tobin TS, Raffi ME, Skinner, SM, Kirschvink, JL, Rapalini AE (2020) Coniacian-Campanian magnetostratigraphy of the Marambio Group: The Santonian-Campanian boundary in the Antarctic Peninsula and the complete Upper Cretaceous-Lowermost Paleogene chronostratigraphical framework for the James Ross Basin. Palaeogeog Palaeoclim Palaeoecol 555:109871

Montes M, Beamud E, Nozal F, Santillana S (2019) Late Maastrichtian–Paleocene chronostratigraphy from Seymour Island, James Ross Basin, Antarctic Peninsula: eustatic controls on sedimentation. Adv Polar Sci 61:303–327

Okutani T (2002) A new thyasirid *Conchocele novaeguinensis* n. sp. from a thanatocoenosis associated with a possible cold seep activity off New Guinea. Venus (J Malacol Soc Jpn) 61:141–145

Oliver PG, Sellanes J (2005) New species of Thyasiridae from a methane seepage area off Concepción, Chile. Zootaxa 1092:1–20

Olivero EB (2012) Sedimentary cycles, ammonite diversity and palaeoenvironmental changes in the Upper Cretaceous Marambio Group, Antarctica. Cretaceous Res 34:348–366

Olivero EB, Medina FA (2000) Patterns of Late Cretaceous ammonite biogeography in southern high latitudes: the family Kossmaticeratidae in Antarctica. Cretaceous Res 21:269–279

Olivero EB, Ponce JJ, Marsicano CA, Martinioni DR (2007) Depositional Settings of the basal López de Bertodano Formation, Maastrichtian, Antarctica. Revista de la Asociación Geológica Argentina 62:521–529

Pirrie D, Crame JA, Lomas SA, Riding JB (1997) Late Cretaceous stratigraphy of the Admiralty Sound region, James Ross Basin, Antarctica. Cretaceous Res 18:109–137

Römer M, Torres M, Kasten S et al (2014) First evidence of widespread active methane seepage in the Southern Ocean, off the sub-Antarctic island of South Georgia. Earth Planet Sci Lett 403:166–177

Ryan DR, Witts JD, Landman NH (2020) Palaeoecological analysis of a methane seep deposit from the Upper Cretaceous (Maastrichtian) of the U.S. Western Interior. Lethaia 54:185–203

Schoepfer SD, Tobin TS, Witts JD, Newton RJ (2017) Intermittent euxinia in the high-latitude James Ross Basin during the latest Cretaceous and earliest Paleocene. Palaeogeog Palaeoclim Palaeoecol 477:40–54

Speden IG (1970) The type Fox Hills Formation, Cretaceous (Maestrichtian), South Dakota. Systematics of the Bivalvia, Bulletin of the Peabody Museum 33. Yale University, p 222

Stilwell JD, Zinsmeister WJ, Oleinik AE (2004) Early paleocene Mollusks of Antarctica: systematics, paleoecology and paleobiogeographic significance, 367th edn. Allen Press, Lawrence, p 89

Tobin TS, Ward PD (2015) Carbon isotope ($\delta^{13}C$) differences between Late Cretaceous ammonites and benthic mollusks from Antarctica. Palaeogeog Palaeoclim Palaeoecol 428:50–57

Tobin TS, Ward PD, Steig EJ et al (2012) Extinction patterns, $\delta^{18}O$ trends, and magnetostratigraphy from a southern high-latitude Cretaceous–Paleogene section: links with Deccan volcanism. Palaeogeog Palaeoclim Palaeoecol 350–352:180–188

Tosolini A-MP, Cantrill DJ, Francis JE (2021) Paleocene high-latitude leaf flora of Antarctica Part 1: entire-margined angiosperms. Rev Palaeobot Palynol 285:104317

Vaughan APM, Storey BC (2000) The eastern Palmer Land shear zone: a new terrane accretion model for the Mesozoic development of the Antarctic Peninsula. J Geolog Soc (London, U.K.) 157:1243–1256

Weller S (1903) The stokes collection of Antarctic fossils. J Geolog 11:413–419

White CA (1890) On certain Mesozoic fossils from the Islands of St. Paul's and St. Peter's in the Straits of Magellan. Proc US Nat Mus 13:13–14

Whittle RJ, Witts JD, Bowman VC et al (2019) Nature and timing of biotic recovery in Antarctic benthic marine ecosystems following the Cretaceous–Palaeogene mass extinction. Palaeontology 62:919–934

Wilckens O (1910) Die Anneliden, Bivalven, und Gastropoden der Antarktischen Kreideformationen Wissenschaftliche Ergebnisse der Schwedischen Südpolar-Expedition, 1901–1903, vol 3, p 1–132

Witts JD, Bowman VC, Wignall PB et al (2015) Evolution and extinction of Maastrichtian (Late Cretaceous) cephalopods from the López de Bertodano Formation, Seymour Island, Antarctica. Palaeogeog Palaeoclim Palaeoecol 418:193–212

Witts JD, Whittle RJ, Wignall PB et al (2016) Macrofossil evidence for a rapid and severe Cretaceous–Paleogene mass extinction in Antarctica. Nat Commun 7:11738

Zinsmeister WJ (1988) Early geological exploration on Seymour Island, Antarctica. In: Feldmann RM, Woodburne MO (eds) Geology and paleontology of Seymour Island, Antarctic Peninsula, Memoir 169. Geological Society of America, Boulder, pp 1–16

Zinsmeister WJ (1998) Discovery of fish mortality horizon at the K-T Boundary on Seymour Island: re-evaluation of events at the end of the Cretaceous. J Paleontol 72:556–571

Zinsmeister WJ, Macellari CE (1988) Bivalvia (Mollusca) from Seymour Island, Antarctic Peninsula. In: Feldmann RM, Woodburne MO (eds) Geology and paleontology of Seymour Island, Antarctic Peninsula, Memoir 169. Geological Society of America, Boulder, pp 253–284

Chapter 20
Ancient Hydrocarbon Seeps of the World

Krzysztof Hryniewicz

20.1 Introduction

This chapter summarizes information about ancient hydrocarbon seeps from around the globe. The information is organized into two tables, one comprising both Americas and Antarctica, the other comprising Africa, the Arctic, Asia, Australia, Europe, and New Zealand (Tables 20.1 and 20.2 respectively). Two cornerstones for this summary were earlier reviews of ancient seep deposits around the world by Campbell (2006) and within Japan by Majima et al. (2005), supplemented by subsequently published literature on this topic. Included in the table are only the occurrences that could be confidently interpreted as ancient seep deposits due to the two basic criteria:

(i) Presence of authigenic carbonates formed due to anaerobic oxidation of methane, as indicated by isotopic, biomarker, or other geochemical evidence (cf. Peckmann and Thiel 2004)
(ii) Presence of authigenic carbonates for which methanogenic origin due to anaerobic oxidation of methane has not been confirmed geochemically but which contain accumulation of fauna frequently associated with coeval seep deposits and which is otherwise rare, smaller-sized, or absent in coeval ambient marine sediments.

Not included are the sites where such fauna has been found, but no carbonate cementation of any kind has been reported (e.g., Kiel and Amano 2010; Amano et al. 2014a; cf. Majima et al. 2005) or carbonate was reported but turned out to be not of methanogenic origin (e.g., Amano et al. 2008). Such occurrences likely represent either chemosynthesis-based environment not affected by methane seepage or a seep fauna that has been transported from a seep and deposited elsewhere.

K. Hryniewicz (✉)
Institute of Paleobiology, Polish Academy of Sciences, Warszawa, Poland
e-mail: krzyszth@twarda.pan.pl

A. Kaim et al. (eds.), *Ancient Hydrocarbon Seeps*, Topics in Geobiology 50,
https://doi.org/10.1007/978-3-031-05623-9_20

Table 20.1 Compilation of ancient hydrocarbon seeps in South America, North America and Antarctica

Site	Age	Geological context	Inferred water depth	Deposits: size and geometry	Carbonate stable C isotopes[a], biomarkers	Macrofossils	References
Central and southern South America							
Brazil							
Serra Alta Fm. seep deposit	Permian (Guadalupian)	Epicontinental sea	Shallow(?)	Numerous small to medium *in situ* concretions	$\delta^{13}C$ as low as −7.6‰[b], no biomarkers reported	Low diversity (3 sp.)	Matos et al. (2017)
Irati Fm. seep deposit	Permian (Cisuralian)	Epicontinental sea	Shallow(?)	153 medium *in situ* domes	$\delta^{13}C$ as low as −4.4‰[b], no biomarkers reported	None reported	Warren et al. (2017)
Argentina							
La Elina seep deposit, Neuquén Basin	Early Jurassic (Toarcian)	Backarc basin	Deep	Large *in situ* boulders forming a composite very large deposit	$\delta^{13}C$ as low as −33.0‰, no biomarkers reported	Medium diversity (13 sp., S, L, N, A)	Gómez-Pérez (2001, 2003) and Kaim et al. (2015a, b, 2016)
Western South America							
Peru							
Lomitos chert, Talara Basin	early Oligocene	Forearc/linear downwarp basin	Shallow(?)–deep	*In situ*, size and shape unknown	$\delta^{13}C$ as low as −25.3‰, no biomarkers reported	Medium diversity (9 sp., K, T, L, V?)	Kiel and Peckmann (2007) and Olsson (1931)

Site	Age	Geological context	Inferred water depth	Deposits: size and geometry	Carbonate stable C isotopes[a], biomarkers	Macrofossils	References
Cerro La Saline seep deposit, Talara Basin	early Oligocene	Forearc/linear downwarp basin	Shallow(?)–deep	9 *ex situ* blocks, size unknown	$\delta^{13}C$ as low as −46.0‰, biomarkers reported	High diversity (18 sp., K, T, L, V, N?, A)	Kiel et al. (2019, 2020a), Kiel and Peckmann (2007) and Olsson (1931)
Belén seep deposit, Heath Shale, Talara Basin	early Oligocene	Forearc/linear downwarp basin	Shallow(?)–deep	*in situ*, carbonate crust, size unknown	$\delta^{13}C$ as low as −25.9‰, biomarkers reported	Low diversity (4 sp., V, A)	Kiel et al. (2019, 2020a) and Olsson (1931)
Cerros El Pelado seep deposit, Talara Basin	late Eocene–early Oligocene	Forearc/linear downwarp basin	Shallow(?)–deep	Size and number unknown, *ex situ*, blocks, size unknown	$\delta^{13}C$ as low as −42.4‰, biomarkers reported	Low diversity (5 sp., K, L, A)	Kiel et al. (2019, 2020a) and Olsson (1931)
Ecuador							
Punta Montañita seep deposit, Dos Bocas Fm., Progreso Basin	Oligocene/Miocene boundary	Forearc basin	Shallow	3 *in situ* medium domes	$\delta^{13}C$ as low as −52.6‰, biomarkers reported	Low diversity (3 sp., T)	Kiel et al. (2021)
Colombia							
Palmar–Molinera Road seep deposit, Sinú–San Jacinto belt	Oligocene–Early Miocene	Accretion wedge/piggy-back basin	Deep(?)	Unknown	$\delta^{13}C$ as low as −52.5‰, no biomarkers reported	Medium diversity (6 sp., S, B, L)	Boss and Turner (1980), Kiel (2013), Kiel et al. (2010), Kiel and Peckmann (2007) and Kiel and Hansen (2015)

(continued)

Table 20.1 (continued)

Site	Age	Geological context	Inferred water depth	Deposits: size and geometry	Carbonate stable C isotopes[a], biomarkers	Macrofossils	References
Sta. Clara seep deposit, Floresanto Fm., Sinú–San Jacinto belt	Oligocene	Accretion wedge/ piggy-back basin	Deep(?)	Unknown	$\delta^{13}C$ as low as −24.5‰, no biomarkers reported	Medium diversity (7 sp., T, L, 2V, N?)	Kiel and Hansen (2015) and Olsson (1940)
Mata Cana seep deposit, Sinú–San Jacinto belt	early Oligocene	Accretion wedge/ piggy-back basin	Deep(?)	Unknown	$\delta^{13}C$ as low as −37.2‰ no biomarkers reported	Medium diversity (8 sp., S, 2L)	Kiel and Hansen (2015)
Venezuela							
Puerto Escondido seep deposit, Pozon Fm., Falcon Basin	Middle–Late Miocene	Foreland basin	Shallow	Unknown	$\delta^{13}C$ −26.5‰, no biomarkers reported	Medium diversity (10 sp., S, T, V, L, B)	Gill et al. (2005), Gill and Little (2013), Kiel (2013) and Kiel and Hansen (2015)
Corro Colorado seep deposit, Pozon Fm., Falcon Basin	Early–Middle Miocene	Backarc basin	Shallow	Unknown	$\delta^{13}C$ −22.0‰, no biomarkers reported	Low diversity (4 sp., 2L, V?)	Kiel and Hansen (2015)
Buenavista de Maicillal seep deposit, Pozon Fm., Falcon Basin	Early–Middle Miocene	Backarc basin	Shallow	Unknown	$\delta^{13}C$ as low as −21.8‰, no biomarkers reported	Low diversity (2 sp.; L, V)	Kiel and Hansen (2015)

Site	Age	Geological context	Inferred water depth	Deposits: size and geometry	Carbonate stable C isotopes[a], biomarkers	Macrofossils	References
La Piedra seep deposit, Pozon Fm., Falcon Basin	Early Miocene	Backarc basin	Shallow–deep	Unknown	$\delta^{13}C$ as low as −11.5‰, no biomarkers reported	Low diversity (3 sp., 2L)	Kiel and Hansen (2015)
Caujarao seep deposit, Guacharaca Fm., Falcon Basin	Oligocene–Early Miocene	Backarc basin(?)	Shallow	Unknown	$\delta^{13}C$ as low as −23.0‰, no biomarkers reported	Low diversity (1 sp., L)	Kiel and Hansen (2015)
Caribbean							
Trinidad							
Jordan's Hill seep deposit, Cipero Fm./ Lengua Fm., Trinidad	Late Miocene	Accretion wedge/ Foredeep	Shallow–deep	Unknown	$\delta^{13}C$ as low as −43.7‰, no biomarkers reported	Low diversity (5 sp., B, 2V)	Kiel and Hansen (2015)
Gordineau River seep deposit, Lengua Fm., Trinidad	Late Miocene	Foredeep	Deep	Unknown	$\delta^{13}C$ as low as −25.8‰, no biomarkers reported	Low diversity (4 sp., T, K, 2L)	Kiel and Hansen (2015)

(continued)

Table 20.1 (continued)

Site	Age	Geological context	Inferred water depth	Deposits: size and geometry	Carbonate stable C isotopes[a], biomarkers	Macrofossils	References
Freeman's Bay seep deposit, Lengua Fm., Trinidad	Late Miocene	Foredeep	Deep	Size unknown; isolated limestone block and surrounding calcareous limestone lenses	$\delta^{13}C$ as low as −20.0‰, no biomarkers reported	Medium diversity (9 sp. (T, L, 2V, A)	Gill et al. (2005), Kiel (2007), Kiel and Hansen (2015), Kugler (2001), Maury (1912) and Van Winkle (1919)
Bronte Estate seep deposit, Lengua Fm., Trinidad	Late Miocene	Foredeep	Deep	Unknown	$\delta^{13}C$ as low as −30.2‰, no biomarkers reported	Low diversity (3 sp., 2B, V)	Kiel and Hansen (2015)
Barbados							
Suboceanic Fault Zone seep deposit, Oceanic Fm.	Early Miocene	Accretion wedge/forearc basin	Deep/very deep	Size unknown; blocks, lenses, chimneys	$\delta^{13}C$ as low as approx. −45‰, no biomarkers reported	Medium diversity (15 sp., S, T, L, V, A)	Gill et al. (2005), Harding (1998), Kiel and Hansen (2015) and Torrini Jr et al. (1990)
Diapiric mélange seep deposit, Joes River Fm.	late Eocene	Accretion wedge	Very deep	Size unknown; blocks, fossils, nodules, chimneys	$\delta^{13}C$ as low as approx. −40‰, no biomarkers reported	Medium diversity (7 sp., K, L, A, T)	Gill et al. (2005), Kaim et al. (2014), Kiel and Hansen (2015), Kiel et al. (2020a) and Kugler et al. (1984)

Site	Age	Geological context	Inferred water depth	Deposits: size and geometry	Carbonate stable C isotopes[a], biomarkers	Macrofossils	References
Dominican Republic							
Cañada de Zambia seep deposit, Gurabo Fm.	Early Pliocene	Strike-slip plate boundary basin	Shallow–deep	Unknown	$\delta^{13}C$ as low as −28.0‰, no biomarkers reported	Low diversity (1 sp., L)	Kiel and Hansen (2015)
Cuba							
Cantera Portugalete seep deposit, Husillo Fm.	Early Miocene	Postorogenic basin (epicontinental sea)	Deep	Unknown	$\delta^{13}C$ as low as −10.0‰, no biomarkers reported	Low diversity (4 sp, L, V)	Kiel and Hansen (2015) and Palmer (1948)
Elmira asphalt mine seep deposit, Bejucal	Eocene	Piggy-back basin (?)	Unknown	Unknown	$\delta^{13}C$ as low as −32.2‰, no biomarkers reported	Medium diversity (8 sp. (S, K, L, V, A)	Cooke (1919), Kiel et al. (2010, 2020a), Kiel and Hansen (2015), Kiel and Peckmann (2007)
North America							
Western Interior							
Beecher Island Shale Member seep deposit, Pierre Shale, Wallace County, Kansas, USA	Late Cretaceous (early Maastrichtian)	Foreland basin	Shallow	Unknown	Unknown	Unknown	Elias (1933), Landman et al. (this volume) and Metz (2000)

(continued)

Table 20.1 (continued)

Site	Age	Geological context	Inferred water depth	Deposits: size and geometry	Carbonate stable C isotopes[a], biomarkers	Macrofossils	References
Pierre Shale seep deposits, Dawson County, Montana, USA	Late Cretaceous (early Maastrichtian)	Foreland basin	Shallow	Numerous *in situ* and *ex situ* small to medium	$\delta^{13}C$ as low as −51.5‰, no biomarkers reported	High diversity (up to 42 sp./seep, L)	Landman et al. (2019, 2020) and Ryan (2020)
Pierre Shale seep deposits, Niobrara County, Wyoming, USA	Late Cretaceous (early Maastrichtian	Foreland basin	Shallow	Large	Unknown	Unknown	Gill and Cobban (1966) and Landman et al. (this volume)
Pierre Shale seep deposits, Crook and Weston Counties, Wyoming, USA	Late Cretaceous (middle–late Campanian)	Foreland basin	Shallow	Numerous *in situ* and *ex situ*, small to large deposits	Unknown	Unknown	Landman et al. (this volume), Metz (2010) and Robinson et al. (1959, 1964)
Pierre Shale seep deposits, near Longmont, Colorado, USA	Late Cretaceous (late Campanian)	Foreland basin	Shallow	Unknown	Unknown	Unknown	Landman et al. (this volume) and Scott and Cobban (1965)
Bearpaw Shale seep deposits, Porcupine Dome, Montana, USA	Late Cretaceous (late Campanian)	Foreland basin	Shallow	Unknown	Unknown	Unknown	Landman et al. (this volume)

Site	Age	Geological context	Inferred water depth	Deposits: size and geometry	Carbonate stable C isotopes[a], biomarkers	Macrofossils	References
Pierre Shale seep deposits, southwestern South Dakota and Sioux County, Nebraska, USA	Late Cretaceous (middle–late Campanian)	Foreland basin	Shallow	Numerous *in situ* and *ex situ* small to large deposits	$\delta^{13}C$ as low as −46.9‰, no biomarkers reported	High diversity (up to 18 sp./seep; L)	Cochran et al. (2015), Darton (1902, 1919), Elias (1933), Hunter et al. (2016), Kato et al. (2017), Larson et al. (2014), Landman et al. (2012, 2018), Meehan and Landman (2016) and Thuy et al. (2018)
Pierre Shale seep deposits, Carter County, Montana, USA	Late Cretaceous (late Campanian)	Foreland basin	Shallow	Unknown	Unknown	Unknown	Landman et al. (this volume)

(continued)

Table 20.1 (continued)

Site	Age	Geological context	Inferred water depth	Deposits: size and geometry	Carbonate stable C isotopes[a], biomarkers	Macrofossils	References
"Tepee Butte Zone" in Pierre Shale seep deposits, near Pueblo, Colorado, USA	Late Cretaceous (middle–late Campanian)	Foreland basin	Shallow	Numerous *in situ* and *ex situ* small to large deposits	$\delta^{13}C$ as low as −49.7‰, biomarkers reported	High diversity (up to 30 sp./seep; L, T)	Birgel and Peckmann (2008), Birgel et al. (2006a), Bishop and Williams (2000), Darton (1902), Darton (1919), Gilbert and Gulliver (1895), Howe (1987), Howe andf Kauffman (1986), Hryniewicz et al. (2017a), Hunter et al. (2016), Kato et al. (2017), Kauffman (1967), Kauffman et al. (1996), Krause et al. (2009), Lavington (1933), Meehan and Landman (2016), Scott (1969), Scott and Cobban (1965, 1986a, 1975), Shapiro (2004), Shapiro and Fricke (2002) and Landman et al. (2012, 2013, 2014)
Pierre Shale seep deposits, Larimer County, Colorado, USA	Late Cretaceous (middle Campanian)	Foreland basin	Shallow	Unknown	Unknown	Unknown	Gill and Cobban (1966), Kauffman (1967), Landman et al. (this volume) and Scott and Cobban (1986b)

Site	Age	Geological context	Inferred water depth	Deposits: size and geometry	Carbonate stable C isotopes[a], biomarkers	Macrofossils	References
Ojinaga Fm. seep deposit, Vieja Region, Presidio County, Texas, USA	Late Cretaceous (early Campanian)	Foreland basin	Shallow	2 *in situ* medium deposits	$\delta^{13}C$ as low as −37.6‰, no biomarkers reported	Medium diversity (8 sp.)	Landman et al. (this volume) and Metz (2000)
Iron oolites in Bad Heart Fm., Alberta, Canada	Late Cretaceous (late Coniacian)	Foreland basin	Shallow	Unknown	Unknown	Unknown	Collom and Johnston (2000)
Tropic Shale seep deposits, Alton Sink and Cottonwood Canyon, Utah, USA	Late Cretaceous (late Cenomanian)	Foreland basin	Shallow	Small to medium *in situ* blocks and concretions	$\delta^{13}C$ as low as −37.2‰, no biomarkers reported	Medium diversity (11 sp, L)	Kiel et al. (2012) and Landman et al. (this volume)
Cascadia Margin							
Washington State, USA							
Quinault seep deposit, Quinault Fm.	Pliocene	Accretion wedge/forearc basin	Shallow	Large, composite deposit, *in situ* to *ex situ*	$\delta^{13}C$ −33.6‰ to 0.2‰, no biomarkers reported	Medium diversity (5 sp., S, L)	Campbell (1992, 2006), Campbell et al. (2006), Joseph et al. (2012, 2013), Martin et al. (2007) and Torres et al. (2010)
Frankfort seep deposit, Astoria Fm.	Early–Middle Miocene	Retroforearc basin	Shallow/ deep	Small blocks, *ex situ* to rare *in situ*	$\delta^{13}C$ as low as −37.6‰, biomarkers reported	High diversity (18 sp. in total, S, T, L, V)	Amano and Kiel (2007), Kiel (2010a, b) and Kuechler et al. (2012)

(continued)

Table 20.1 (continued)

Site	Age	Geological context	Inferred water depth	Deposits: size and geometry	Carbonate stable C isotopes[a], biomarkers	Macrofossils	References
Knappton seep deposit, Lincoln Creek Fm.	latest Oligocene	Retroforearc basin	Deep	Medium *ex situ* blocks	$\delta^{13}C$ −22.4‰, no biomarkers reported	High diversity (27 sp. in total, b, T, L, V)	Amano and Kiel (2007), Goedert and Squires (1993), Kiel (2010a, b), Kiel and Amano (2013) and Moore (1984)
Murdock Creek seep deposit, Pysht Fm.	late early Oligocene	Retroforearc basin	Deep–very deep	Medium *ex situ* blocks	$\delta^{13}C$ as low as −33.7‰, no biomarkers reported	Medium diversity (11 sp. in total, B, T, V, A)	Squires (1989), Georgieva et al. (2019), Goedert and Squires (1993), Hryniewicz et al. (2017a), Kiel and Amano (2013) and Vinn et al. (2013)
Shipwreck Point seep deposit, Makah Fm.	early Oligocene	Retroforearc basin	Shallow(?), redeposited into deep to very deep setting	One large *in situ* and several small to medium *ex situ*	$\delta^{13}C$ as low as −34.47‰, no biomarkers reported	High diversity (15 sp., S, B, L, V, N, A)	Campbell (2006), Goedert and Campbell (1995), Kiel (2010b), Kiel & Amano (2013) and Squires and Goedert (1995)
West Fork of the Satsop River seep deposit, Lincoln Creek Fm.	Oligocene	Retroforearc basin	Deep	One very large *in situ* ("Little River seep deposit") and numerous small to medium *ex situ* deposit	Unknown	Medium diversity (9 sp., B, L, V, A)	Amano and Kiel (2007), Campbell and Bottjer (1993), Georgieva et al. (2019), Kiel (2006), Kiel (2010b, 2013)

Site	Age	Geological context	Inferred water depth	Deposits: size and geometry	Carbonate stable C isotopes[a], biomarkers	Macrofossils	References
Whiskey Creek Beach seep deposit, Makah Fm.	Oligocene	Retroforearc basin	Unknown	Numerous small *in situ* nodules, blebs and fracture fills	$\delta^{13}C$ as low as −25.1‰, no biomarkers reported	None reported	Nesbitt et al. (2013)
Restoration Point seep deposit, Blakeley Fm.	Oligocene	Retroforearc basin	Deep	Numerous small *in situ* nodules, burrow and shell fills	$\delta^{13}C$ as low as −48.6‰, no biomarkers reported	Low diversity, bivalve-dominated (3 sp., S, T, L)	Nesbitt et al. (2013)
Pysht Quarry seep deposit, Pysht Fm.	Oligocene	Retroforearc basin	Deep	Numerous small *in situ* nodules, blebs and shell fills	$\delta^{13}C$ as low −21.7‰, no biomarkers reported	Low diversity, bivalve-dominated (4 sp., S, T, L, V)	Joseph et al. (2012, 2013), Torres et al. (2010) and Nesbitt et al. (2013)
Pysht Twin Rivers seep deposit, Pysht Fm.	Oligocene	Retroforearc basin	Deep	Numerous small to medium *in situ* fracture fills, blebs, burrow fills and glendonite	$\delta^{13}C$ as low as −24.4‰, no biomarkers reported	Low diversity (3 sp., S, T, L)	Torres et al. (2010) and Nesbitt et al. (2013)
Pysht Tree Farm seep deposit, Pysht Fm.	Oligocene	Retroforearc basin	Deep	Numerous small to medium *in situ* fracture fills and blebs	$\delta^{13}C$ as low as −29.9‰, no biomarkers reported	Low diversity, bivalve-dominated (3 sp., S, T, L)	Torres et al. (2010) and Nesbitt et al. (2013)

(continued)

Table 20.1 (continued)

Site	Age	Geological context	Inferred water depth	Deposits: size and geometry	Carbonate stable C isotopes[a], biomarkers	Macrofossils	References
Fiddlers Bluff seep deposit, Blakeley Fm.	Oligocene	Retroforearc basin	Shallow	Numerous small to medium *in situ* nodules, burrow fills and glendonite	$\delta^{13}C$ as low as −20.7‰, no biomarkers reported	Low diversity (3 sp., S, T, L)	Nesbitt et al. (2013)
Canyon River seep deposit, Lincoln Creek Fm.	Oligocene	Retroforearc basin	Deep	Numerous medium *ex situ* and one *in situ* deposit	$\delta^{13}C$ –as low as −48.1‰, biomarkers reported	High diversity (36 sp. in total, B, T, L, V, A)	Amano and Kiel (2007), Georgieva et al. (2019), Goedert and Benham (2003), Goedert and Kiel (2016), Hryniewicz et al. (2017a), Kiel (2006, 2010b), Kiel and Amano (2013), Nesbitt et al. (2013), Smrzka et al. (2015), Squires (1995), Squires and Goedert (1995), Zwicker et al. (2018), Goedert et al. (2000), Hagemann et al. (2013) and Rigby and Goedert (1996)
Mt. Appleton seep deposit, Olympic Subduction Complex	Oligocene(?)	Accretion wedge (?)	Deep	Limestone lens; details unknown	Unknown	Diversity unknown (S, T, V)	Harvey (1959) and Kiel (2010b)

Site	Age	Geological context	Inferred water depth	Deposits: size and geometry	Carbonate stable C isotopes[a], biomarkers	Macrofossils	References
Middle Fork of the Satsop River seep deposit, Lincoln Creek Fm.	late Eocene–Oligocene	Retroforearc basin	Deep	Several small to large *in situ* and *ex situ* deposits, some already eroded away	$\delta^{13}C$ as low as −51.3‰, biomarkers reported	High diversity (31 sp. in total, S, L, T, V, N, A)	Peckmann et al. (2002), Nesbitt et al. (2013), Goedert and Kiel (2016), Goedert and Peckmann (2005), Hryniewicz et al. (2017a), Kiel (2010a, b), Smrzka et al. (2016) and Zwicker et al. (2015, 2018)
Menlo seep deposit, Lincoln Creek Fm.	late Eocene–(?) early Oligocene	Retroforearc basin	Deep	Several medium to large *in situ*(?) deposits	Unknown	Low diversity (4 sp., B, T, V)	Campbell and Bottjer (1993), Danner (1966), Goedert and Benham (2003), Goedert and Squires (1990) and Squires and Goedert (1991)
Knappton, "Siltstone of Shoalwater Bay" seep deposit, Lincoln Creek Fm.	late Eocene(?)	Retroforearc basin	Deep	Several outcrops, details unknown	$\delta^{13}C$ −27.6‰, biomarkers reported	Low diversity (4 sp., S, B, A)	Goedert and Benham (2003), Kiel and Amano (2013) and Smrzka et al. (2015)
Whiskey Creek seep deposit, Pysht Fm.	late Eocene	Retroforearc basin	Deep	Several large *ex situ* boulders	$\delta^{13}C$ as low as −36.0‰, biomarkers reported	Medium diversity (12 sp., S, B, T, L, V)	Goedert and Squires (1990), Goedert et al. (2003), Hryniewicz et al. (2017a), Kiel (2006, 2007), Kiel and Goedert (2007), Peckmann et al. (2003) and Squires and Goedert (1991)

(continued)

Table 20.1 (continued)

Site	Age	Geological context	Inferred water depth	Deposits: size and geometry	Carbonate stable C isotopes[a], biomarkers	Macrofossils	References
Bear River, "Siltstone of Cliff Point" seep deposit	late Eocene	Retroforearc basin	Deep	Single very large *in situ* carbonate body	$\delta^{13}C$ as low as −36.0‰, no biomarkers reported	High diversity (15 sp., S, B, T, V, A)	Danner (1966), Georgieva et al. (2019), Goedert and Benham (2003), Goedert and Squires (1990), Hryniewicz et al. (2017a), Kiel (2006), Kiel and Amano (2013), Kiel et al. (2013a, 2014b), Rigby and Jenkins (1983), Saul et al. (1996), Squires (1995), Squires and Goedert (1991), Treude et al. (2011) and Vinn et al. (2012, 2013)
West Fork of Grays River, "Siltstone of Unit B" seep deposit	middle/upper Eocene	Retroforearc basin	Deep	Several *ex situ* blocks, details unknown	Unknown	Low diversity (1 sp., T)	Hryniewicz et al. (2017a)
Satsop Weatherwax seep deposit, Humptulips Fm.	middle Eocene	Retroforearc basin	Deep	Single *ex situ* boulder, size unknown	$\delta^{13}C$ as low as −43.5‰, no biomarkers reported	Medium diversity (14 sp., T, V, A)	Hybertsen and Kiel (2018)

Site	Age	Geological context	Inferred water depth	Deposits: size and geometry	Carbonate stable C isotopes[a], biomarkers	Macrofossils	References
Humptulips River seep deposit, Humptulips Fm.	middle Eocene	Retroforearc basin	Deep	Two, large (CSUN 1583 aka Raui site) and very large (LACMIP loc. 12385 aka Humptulips Main site) *in situ* deposits	$\delta^{13}C$ as low as −26.7‰, biomarkers reported	Medium diversity (14 sp., B, T, L, V, N, A)	Amano and Kiel (2007), Campbell (2006), Campbell and Bottjer (1993), Danner (1966), Gill and Little (2013), Goedert and Benham (2003), Goedert and Kaler (1996), Goedert et al. (2013), Goedert and Squires (1990), Hryniewicz et al. (2017a), Jakubowicz et al. (2020), Kaim et al. (2014), Kiel (2006, 2008a, 2010a, b), Kiel and Amano (2013), Peckmann et al. (2003, 2007b), Saul et al. (1996), Schweitzer and Feldmann (2008), Squires and Goedert (1991, 1995, 1996) and Vinn et al. (2012, 2013)

(continued)

Table 20.1 (continued)

Site	Age	Geological context	Inferred water depth	Deposits: size and geometry	Carbonate stable C isotopes[a], biomarkers	Macrofossils	References
East Fork Bridge seep deposit, Humptulips River, Humptulips Fm	middle Eocene	Retroforearc basin	Deep	Single *ex situ* boulder, details unknown	$\delta^{13}C$ as low as −24.0‰, no biomarkers reported	Low diversity (1 sp., L)	Jakubowicz et al. (2020)
Oregon, USA							
Nehalem River basin seep deposits, Keasey Fm.	late Eocene	Forearc basin	Deep	Three, large and several smaller *in situ* deposits (Vernonia-Timber deposit), and several small to medium blocks (Rock Creek deposit)	$\delta^{13}C$ as low as −13.7‰ (Vernonia-Timber Road), no biomarkers reported	Medium diversity (10 sp., S, T, L)	Campbell (2006), Campbell and Bottjer (1993), Hickman (1980, 2015) and Martin (2010)
Clatskanie River basin seep deposit, Pittsburg Bluff Fm.	Oligocene	Forearc basin	Shallow	Two *in situ* beds up to 1 m thick	Unknown	Low diversity (4 sp., T)	Eriksson (2002)
Seneca seep deposit, Aldrich Mountains	Early Jurassic (Sinemurian)	Melange (serpentinite diapir?)	Deep(?)	At least 3 large *in situ* blocks	$\delta^{13}C$ as low as −23.5‰, no biomarkers reported	Low diversity (2 sp., D)	Ager (1968) and Peckmann et al. (2013)

Site	Age	Geological context	Inferred water depth	Deposits: size and geometry	Carbonate stable C isotopes[a], biomarkers	Macrofossils	References
Graylock Butte seep deposit, Rail Cabin Member, Vester Fm.	Late Triassic (Norian)	Forearc basin	Deep(?)	Two large to very large *in situ* lenses	$\delta^{13}C$ as low as −35.6‰, no biomarkers reported	Low diversity (4 sp., D, Nu, K)	Ager (1968), Peckmann et al. (2011), Smrzka et al. (2015) and Kiel (2018)
Alaska							
Bonanza Creek seep deposit, Chisana Fm., Wrangellia Terrange	Early Cretaceous (Valanginian–Hauterivian)	Vicinity of volcanic island arc	Deep	Unknown	$\delta^{13}C$ as low as −22.3‰, no biomarkers reported	Low diversity (1 sp., D)	Kiel et al. (2014a) and Sandy and Blodgett (1996)
California							
Monterey Bay region seep deposits, Santa Cruz Mudstone	Late Miocene	Strike-slip plate boundary basin	Shallow–deep(?)	Numerous, small to medium *in situ* to *ex situ* concretions	$\delta^{13}C$ as low as −9.3‰[b], biomarkers not reported	None reported	Aiello (2005) and Aiello et al. (2001)

(continued)

Table 20.1 (continued)

Site	Age	Geological context	Inferred water depth	Deposits: size and geometry	Carbonate stable C isotopes[a], biomarkers	Macrofossils	References
Wagonwheel Mountain seep deposit, Wagonwheel Fm.	late Eocene	Forearc basin	Shallow/ deep	Two very large *in situ* lenticular bodies	$\delta^{13}C$ as low as −12.2‰, no biomarkers reported	Medium diversity (7 sp., T, L, V)	Amano and Kiel (2007), Hryniewicz et al. (2017a), Kiel and Peckmann (2007) and Squires and Gring (1996)
Panoche and Tumey Hills seep deposits, Great Valley Group	early Paleocene	Forearc basin	Shallow	Numerous small to very large *in situ* to *ex situ* concretions, sills and dykes	$\delta^{13}C$ as low as −50.9‰, no biomarkers reported	Medium diversity (8 sp., S, L)	Blouet et al. (2017), Campbell (2006), Kaim et al. (2008a), Kiel (2013), Minisini and Schwartz (2007) and Schwartz et al. (2003)
Guenoc Ranch seep deposit, Great Valley Group	Late Cretaceous (Campanian–Maastrichtian)	Forearc basin	Deep(?)	Numerous, small to medium *ex situ* blocks	$\delta^{13}C$ as low as −24.5‰, no biomarkers reported	Low diversity (5 sp., L)	Hepper (2004), Hepper et al. (2003) and Keenan (2010)
Romero Creek seep deposit, Great Valley Group	Late Cretaceous (Campanian)	Forearc basin	Deep(?)	Unknown	$\delta^{13}C$ as low as −20.6‰, no biomarkers reported	Low diversity (3 sp., A)[C]	Elder and Miller (1993), Keenan (2010) and Kiel et al. (2008a)
Harrington Flat Road seep deposit, Great Valley Group	Late Cretaceous (Campanian)	Forearc basin	Deep(?)	20 medium to large mounds	$\delta^{13}C$ as low as −28.6‰, no biomarkers reported	Medium diversity (6 sp., T, A)	Keenan (2010)

Site	Age	Geological context	Inferred water depth	Deposits: size and geometry	Carbonate stable C isotopes[a], biomarkers	Macrofossils	References
Moreno Gulch seep deposit, Great Valley Group	Late Cretaceous (Santonian)	Forearc basin	Deep(?)	Two carbonates, details unknown	Unknown	Medium diversity[c] (6 sp., S, T, A)	Kiel et al. (2008a)
Cold Fork of Cottonwood Creek seep deposit, Great Valley Group	Early Cretaceous (Albian)	Forearc basin	Deep	Numerous medium *in situ* lenses cropping out along 260 m of outcrop	$\delta^{13}C$ as low as −24.9‰, biomarkers reported	Medium diversity (10 sp., S, K, N, A)	Birgel et al. (2006b), Campbell (2006), Campbell and Bottjer (1993), Campbell et al. (2002, 2008a), Georgieva et al. (2019), Jenkins et al. (2013), Kaim et al. (2014), Keenan (2010), Kiel (2013), Kiel et al. (2008a), Kiel and Peckmann (2019) and Stanton (1895)
Eagle Creek seep deposit, Great Valley Group	Early Cretaceous (late Barremian)	Forearc basin	Deep(?)	Numerous medium *in situ* and *ex situ* carbonate deposits scattered along ca. 40 m of outcrop	$\delta^{13}C$ as low as −46.3‰, no biomarkers reported	Medium diversity (9 sp., S, Nu, K, L)	Jenkins et al. (2013), Kaim et al. (2014), Kiel et al. (2014a, b), Kiel and Peckmann (2019) and Stanton (1895)
Wide Awake Mine seep deposit, Great Valley Group	Early Cretaceous (Hauterivian)	Forearc basin	Deep(?)	Small *ex situ* cobbles	$\delta^{13}C$ as low as −22.3‰, no biomarkers reported	Low diversity, (4 sp., D, N, A)	Keenan (2010)

(continued)

Table 20.1 (continued)

Site	Age	Geological context	Inferred water depth	Deposits: size and geometry	Carbonate stable C isotopes[a], biomarkers	Macrofossils	References
Gravelly Flat seep deposit, Great Valley Group	Early Cretaceous (late Berriassian–Hauterivian)	Forearc basin	Deep(?)	Unknown	Unknown	Low diversity (4 sp., D, K, A)	Kiel et al. (2008a)
Foley Canyon seep deposit, Great Valley Group	Early Cretaceous (Valanginian–Hauterivian)	Forearc basin	Deep(?)	Quarried *in situ* lens, details unknown	Unknown	Low diversity (5 sp., D, K, A)	Kiel et al. (2008a)
Rice Valley seep deposit, Great Valley Group	Early Cretaceous (late Valanginian/early Hauterivian)	Forearc basin	Deep	Several medium to large *ex situ* blocks	$\delta^{13}C$ as low as −21.5‰, no biomarkers reported	Medium diversity (6 sp., D, K, N, A)	Campbell and Bottjer (1995), Campbell et al. (2008a), Kaim et al. (2014), Keenan (2010), Kiel et al. (2008a, 2014a) and Kiel and Peckmann (2019)
Wilbur Springs seep deposit, Great Valley Group	Early Cretaceous (late Valanginian/early Hauterivian)	Forearc basin (serpentinite diapir)	Deep	Very large outcrops of *in situ* quarried carbonate	$\delta^{13}C$ as low as −24.4‰, biomarkers reported	Medium diversity (10 sp., D, S, L, N, A)	Birgel et al. (2006b), Campbell and Bottjer (1993, 1995), Campbell et al. (2002), Georgieva et al. (2019), Jenkins et al. (2013), Kaim et al. (2014), Kiel (2013), Kiel et al. (2008a, 2014a), Kiel and Peckmann (2019) and Stanton (1895)
West Berryessa seep deposit, Great Valley Group	Early Cretaceous (Valanginian?)	Forearc basin	Deep	3 large to very large *in situ* pseudobioherms (emerging from Lake Berryessa only at low water)	Unknown	Low diversity (4 sp., K, A)	Kaim et al. (2014), Kiel et al. (2008a) and Kiel and Peckmann (2019)

Site	Age	Geological context	Inferred water depth	Deposits: size and geometry	Carbonate stable C isotopes[a], biomarkers	Macrofossils	References
Little Indian Valley seep deposit, Great Valley Group	Early Cretaceous (Valanginian?)	Accretion wedge (?)	Deep(?)	*In situ*(?) concretions, details unknown	$\delta^{13}C$ as low as −23.4‰, no biomarkers reported	Medium diversity (6 sp., S, A)	Kaim et al. (2014), Kiel et al. (2008a), McLaughlin and Ohlin (1984) and McLaughlin et al. (1990)
Rocky Creek seep deposit, California, Great Valley Group	Early Cretaceous (Valanginian)	Forearc basin	Deep	Several medium to large *in situ* to *ex situ* boulders	$\delta^{13}C$ as low as −19.4‰, no biomarkers reported	Medium diversity (10 sp., S, L, N?, A?)	Campbell (2006), Kaim et al. (2014), Keenan (2010), Kiel and Campbell (2005), Kiel (2013), Kiel et al. (2008a), Kiel et al. (2010) and Vinn et al. (2012, 2013)
Knoxville seep deposit, Great Valley Group	Early Cretaceous(?)	Forearc basin	Deep(?)	Unknown	Unknown	Low diversity (3 sp., K, A)	Kaim et al. (2014), Kiel et al. (2008a) and Stanton (1895)

(continued)

Table 20.1 (continued)

Site	Age	Geological context	Inferred water depth	Deposits: size and geometry	Carbonate stable C isotopes[a], biomarkers	Macrofossils	References
Bear Creek seep deposit, Great Valley Group	Early Cretaceous (Valanginian)	Forearc basin	Deep	Numerous large *in situ* to *ex situ* blocks	$\delta^{13}C$ as low as −26.8‰, no biomarkers reported	Medium diversity (9 sp., S, L, N?, A)	Campbell (2006), Jenkins et al. (2013), Kaim et al. (2014), Keenan (2010), Kiel (2013), Kiel and Campbell (2005), Kiel et al. (2008a, 2010) and Vinn et al. (2012, 2013)
Charlie Valley seep deposit, Great Valley Group	Late Jurassic (Tithonian?)	Forearc basin	Deep	*In situ* lens, details unknown	Unknown	Medium diversity (9 sp., S, L)	Easton and Imlay (1955) and Kiel et al. (2008a)
NW Berryessa seep deposit, Great Valley Group	Late Jurassic (Tithonian?)	Forearc basin	Deep	Numerous small lenses, details unknown	Unknown	Medium diversity (11 sp., D, L, A)	Kiel et al. (2008a), Klosterman et al. (2001) and Stanton (1895)
East Berryessa seep deposit, Great Valley Group	Early Cretaceous	Forearc basin	Deep(?)	Unknown (currently flooded by Lake Berryessa)	Unknown	Low diversity (3 sp., K, A)	Kaim et al. (2014) and Kiel et al. (2008a)
Paskenta seep deposit, Great Valley Group	Late Jurassic (Tithonian)	Forearc basin	Deep	Two, large to very large, *in situ* lenses	$\delta^{13}C$ as low as −43.7‰, biomarkers reported	High diversity (17 sp., D, S, K, L, A)	Birgel et al. (2006b), Campbell and Bottjer (1993), Campbell et al. (2002), Campbell (2006), Jenkins et al. (2017), Kaim et al. (2014), Keenan (2010), Kiel (2010a), Kiel (2013), Kiel et al. (2008a, 2014b), Sandy and Campbell (1994), Stanton (1895), Vokes (1955) and Zakharov and Rogov (2020)

Site	Age	Geological context	Inferred water depth	Deposits: size and geometry	Carbonate stable C isotopes[a], biomarkers	Macrofossils	References
Bedford Canyon seep deposit, "pre-batholith series", Santa Ana Mountains	Middle Jurassic	Pre-arc continental margin	Deep(?)	Numerous small *ex situ* boulders	Unknown	Low diversity (1 sp., D)	Ager (1968), Imlay (1964, 1980), Sandy (2001, 2010), Sandy and Campbell (2003) and Silberling et al. (1961)
British Columbia							
Sombrio Beach seep deposit, Sooke Fm., Vancouver Island	Oligocene	Retroforearc basin	Shallow	Fracture fills and nodules	$\delta^{13}C$ as low as −5.6‰[d], no biomarkers reported	None reported	Joseph et al. (2012, 2013), Nesbitt et al. (2013) and Torres et al. (2010)
Hornby Island seep deposit, Nurthumberland Fm., Nanaimo Group, Vancouver Island	Late Cretaceous (Campanian)	Foreland basin	Shallow(?)–deep	At least 2 large *in situ* concretions	$\delta^{13}C$ as low as −45.5‰, no biomarkers reported	None reported	Jenkins et al. (2017)
Cooper Island seep deposit, Inklin Fm., Atlin Lake	Early Jurassic? (Pliensbachian?)	Forearc basin	Deep(?)	Single medium boulder	$\delta^{13}C$ as low as −39.8‰, no biomarkers reported	Low diversity, brachiopod dominated (2 sp., D)	Johannson et al. (1997) and Pálfy et al. (2017)

(continued)

Table 20.1 (continued)

Site	Age	Geological context	Inferred water depth	Deposits: size and geometry	Carbonate stable C isotopes[a], biomarkers	Macrofossils	References
Antarctica							
Seymour Island seep deposit, López de Bertodano Fm., James Ross Basin	Late Cretaceous (Maastrichtian)	Backarc basin	Shallow	Numerous *in situ* small concretions	$\delta^{13}C$ as low as −58.0‰, biomarkers not reported	Medium diversity (9 sp., S, T, L)	Hryniewicz et al. (2017a), Little et al. (2015) and Wilckens (1910)
Snow Hill Island seep deposit, Snow Hill Island Fm., James Ross Basin	Late Cretaceous (early Maastrichtian)	Backarc basin	Shallow	Dozens of medium to very large *in situ* lenses and chimneys	$\delta^{13}C$ as low as −20.4‰, biomarkers reported	Low diversity (5 sp., S, T)	Little et al. (2015), Wilckens (1910) and Zinsmeister and Macellari (1988)
Gateway Pass Limestone seep deposit, Fossil Bluff Group, Alexander Island	Late Jurassic (Tithonian)	Forearc basin	Deep	Very large *in situ* discontinuous lens	$\delta^{13}C$ as low as −44.6‰, no biomarkers reported	Low diversity (3 sp., L, A?)	Kaim and Kelly (2009) and Kelly et al. (1995)

[a] Values of $\delta^{13}C$ in ‰ VPDB

[b] Carbonate carbon isotope values are somewhat high for a seep deposit and, in the absence of biomarker or faunal data, should not be taken as definitive evidence for a seep origin of the deposit

[c] In Kiel et al. (2008a), the faunal list for the Romero Creek seep deposit has been erroneously listed under the "Moreno Gulch" site, and vice versa (pers. obs.), the data provided in this table are corrected

[d] The depleted values from the Sombrio Beach deposit are exclusively from calcareous foraminifera; the carbonate $\delta^{13}C$ values from the Sombrio Beach deposit vary between 6.98‰ and 7.37‰ VPDB, thus point toward methanogenesis rather than to anaerobic methane oxidation as an important factor in their formation

Table 20.2 Compilation of ancient hydrocarbon seeps in Africa, the Arctic, Asia, Australia, Europe and New Zealand

Site	Age	Geological context	Inferred water depth	Deposits: size and geometry	Carbonate stable C isotopes[a], biomarkers	Macrofossils	References
Africa							
Morocco							
Amma Fatma seep deposit, Tarfaya Basin	Late Cretaceous (early Turonian)	Basin on a passive margin	Shallow	Single large *in situ* columnar carbonate body	$\delta^{13}C$ as low as –23.5‰, biomarkers reported	Medium diversity (7 sp., L)	Smrzka et al. (2017)
Moroccan Meseta seep deposits	Late Devonian (Famennian)	Tectonic melange	Deep	Large *ex situ* blocks	$\delta^{13}C$ as low as –12.3 ‰, no biomarkers reported	Low diversity (2 sp., D)	Ager et al. (1976), Baliński and Biernat (2003), Biernat (1967), Campbell and Bottjer (1995a) and Peckmann et al. (2007)
Hollard Mound seep deposit, Hamar Laghdad	Middle Devonian (early Eifelian)	Intracratonic basin	Shallow/ deep	Two large *in situ* lenses	$\delta^{13}C$ as low as –23.2 ‰, no biomarkers reported	Medium diversity (8 sp., S, M)	Aitken et al. (2002), Berkowski (2006), Buggisch and Krumm (2005), Campbell (2006), Cavalazzi (2007), Cavalazzi et al. (2007, 2012), Hryniewicz et al. (2017b), Jakubowicz et al. (2013, 2015), Peckmann et al. (1999b, 2005)

(continued)

Table 20.2 (continued)

Site	Age	Geological context	Inferred water depth	Deposits: size and geometry	Carbonate stable C isotopes[a], biomarkers	Macrofossils	References
Kess-Kess mounds seep deposits, Hamar Laghdad	Early Devonian (Emsian) mud mounds and Early–Late Devonian (Emsian–Fammenian) neptunian dykes	Intracratonic basin, volcanic high	Shallow–deep(?)	Numerous very large mounds cross-cut by neptunian dykes	$\delta^{13}C$ as low as –17.63‰[c][b], no biomarkers reported	High diversity, full composition unknown	Aitken et al. (2002), Belka (1998), Berkowski (2008), Cavalazzi (2006), Cavalazzi et al. (2007), Feist and Belka (2018), Franchi et al. (2015) and Mounji et al. (1998)
El-Borj seep deposit, Moroccan Meseta	late Silurian (Ludfordian)	Tectonic melange	Deep	One very large carbonate	$\delta^{13}C$ as low as –2.8‰, no biomarkers reported	Low diversity (2 sp., M)	Ager et al. (1976), Barbieri et al. (2005), Buggisch and Krumm (2005), Campbell (2006), Campbell and Bottjer (1995a) and Jakubowicz et al. (2017)
Namibia							
Ganigobis seep deposit	Carboniferous (Pennsylvanian, Gzhelian)	Intracratonic rift basin	Deep	11 medium to large *in situ* carbonates	$\delta^{13}C$ as low as –51.4 ‰, biomarkers reported	Low diversity (5 sp.)	Bangert et al. (2000), Birgel et al. (2008), Himmler et al. (2008), Smrzka et al. (2015) and Zwicker et al. (2018)
Arctic							
Basilika Fm. seep deposits, Central Cenozoic Basin, Spitsbergen	Late Paleocene	Strike-slip plate boundary basin	Shallow	Numerous small to medium *ex situ* boulders	$\delta^{13}C$ as low as –49.4‰, biomarkers reported	High diversity (22 sp., S, T)	Hägg (1925), Hryniewicz et al. (2016, 2017a, 2019) and Rosenkrantz (1942 and 1970)

Site	Age	Geological context	Inferred water depth	Deposits: size and geometry	Carbonate stable C isotopes[a], biomarkers	Macrofossils	References
Prince Patrick Island seep deposit, Sverdrup Basin, Canada	Early Cretaceous (late Aptian–late Albian)	Active half graben	Shallow(?)–deep	2 large to very large *in situ* mounds	$\delta^{13}C$ as low as –50.2‰, no biomarkers reported	Low diversity (4 sp.)	Beauchamp et al. (1989), Beauchamp and Savard (1992), Georgieva et al. (2019), Sandy (1990) and Savard et al. (1996)
Ellef Ringes Island seep deposits, Sverdrup Basin, Canada	Early Cretaceous (late Aptian–late Albian)	Seabed affected by salt diapirism	Shallow(?)–deep	137 *in situ* to *ex situ*, small to very large mounds, beds and crusts	$\delta^{13}C$ as low as –52.6‰, biomarkers reported	Medium diversity (14 sp., S, Nu, T, L)	Beauchamp et al. (1989), Beauchamp and Savard (1992), Georgieva et al. (2019), Savard et al. (1996) and Williscroft et al. (2017)
Kuhnpasset seep deposits, Wollaston Forland, Greenland	Early Cretaceous (early?–late Barremian)	Basin on a passive margin	Shallow/deep	Over 30 small to medium, *in situ* and *ex situ* deposits	Unknown	Medium diversity (10 sp., S, K, L)	Bang et al. (2022), Kelly et al. (2000) and Maync (1949)
Sassenfjorden area seep deposits, Central Spitsbergen, Svalbard	Late Jurassic–Early Cretaceous (Tithonian–Berriasian)	Epicontinental sea	Shallow	15 small to medium *in situ* and *ex situ* deposits	$\delta^{13}C$ as low as –43.22‰, no biomarkers reported	High diversity (54 sp., in total, S, Nu, T, L, A)	Dalseg et al. (2016), Georgieva et al. (2019), Hammer et al. (2011, 2013), Hryniewicz et al. (2012, 2014, 2015b), Kaim et al. (2017), Sandy et al. (2014), Vinn et al. (2014) and Wierzbowski et al. (2011)
Novaya Zemlya seep deposits, Russia	Late Jurassic–Early Cretaceous (Oxfordian–Valanginian)	Unknown	Unknown	Pleistocene glacial erratics of small size	$\delta^{13}C$ as low as –41.3‰, no biomarkers reported	High diversity (at least 33 sp., S, Nu, A)	Beisel (1983), Guzhov (2017), Hryniewicz et al. (2015a), Kaim et al. (2004) and Tullberg (1881)

(continued)

Table 20.2 (continued)

Site	Age	Geological context	Inferred water depth	Deposits: size and geometry	Carbonate stable C isotopes[a], biomarkers	Macrofossils	References
Asia							
China							
Quiangdong section seep deposits, southern Tibet	mid-Cretaceous (Albian–Turonian)	Basin in a rift/ passive margin	Shallow	Numerous *in situ*, stacked, small to large boulders and nodules	$\delta^{13}C$ as low as –30.5‰, no biomarkers reported	None reported	Yao et al. (2022), Zhang et al. (2016)
Yongzhu Bridge seep deposit, Chebo Fm., northern Tibet	Early Cretaceous (Valanginian)	Tectonic melange	Unknown	Dark grey limestone, 15 m thick, details unknown	$\delta^{13}C$ as low as –24.5‰, no biomarkers reported	Low diversity (1 sp., D)	Sandy and Peckmann (2016) and Sun (1986)
Angie Fm. seep deposits, Central Lhasa Block, Tibet	early Permian (Cisuralian, Kugurian)	Basin in a rift/ passive margin	Shallow	Small to medium *in situ* layers and lenticular nodules, few pipes	$\delta^{13}C$ as low as –34.7‰, no biomarkers reported	None reported	Liu et al. (2021)
Australia							
Holmwood Shale seep deposits, Irwin Basin, Western Australia	early Permian (Cisuralian, Sakmarian)	Marginal rift basin	Shallow	At least three nodular limestone beds and associated nodules dispersed in the shale	$\delta^{13}C$ as low as -45.1.5‰, no biomarkers reported	Medium–high diversity (at least 12 sp.)	Clarke et al. (1951), Playford (1959) and Haig et al. (2022)

Site	Age	Geological context	Inferred water depth	Deposits: size and geometry	Carbonate stable C isotopes[a], biomarkers	Macrofossils	References
Indonesia							
Buton Asphalt seep deposit Buton Island off Celebes (Sulawesi)	Late Miocene	Foreland basin(?)	Shallow(?)–Deep	Unknown	Unknown	High diversity (up to 40 sp.;, B?, L, V)	Beets (1942, 1953), Boss (1968), Janssen (1999), Kiel (2013), Kiel et al. (2020b) and Martin (1933, 1937)
Japan							
Kyushu							
Kuge Shrine seep deposit, Takanabe Fm., Miyazaki Prefecture	Late Pliocene	Forearc basin	Shallow	Several large carbonate concretions	$\delta^{13}C$ as low as –53.2‰, no biomarkers reported	High diversity (19 sp., L)	Ikeda et al. (2003) and Majima et al. (2003, 2005)
Shikoku							
Mitsu Matsuyama seep deposit, Hioki Complex, Muroto City, Kochi Prefecture	late Oligocene–Early Miocene	Forearc basin/trench-slope basin	Deep	Carbonate concretion, details unknown	Unknown	Low diversity (2 sp.; T, V)	Amano and Kiel (2011), Amano et al. (2019), Majima et al. (2005) and Matsumoto and Hirata (1972)
Sada Limestone seep deposit, Shimanto Belt, Kochi Prefecture	Late Cretaceous (Campanian–Maastrichtian)	Accretionary wedge	Shallow–deep(?)	Numerous *in situ* small to very large blocks	$\delta^{13}C$ as low as –16.4‰, no biomarkers reported	Medium diversity (at least 7 sp., S, T, L, A)	Kaim et al. (2014), Katto and Hattori (1964), Nobuhara et al. (2008b, 2016) and Tsujino and Iwata (2009)

(continued)

Table 20.2 (continued)

Site	Age	Geological context	Inferred water depth	Deposits: size and geometry	Carbonate stable C isotopes[a], biomarkers	Macrofossils	References
Honshu							
Kawayatsu area seep deposit (Loc. 73 of Majima et al. (2005), Kakinokidai Fm., Boso Peninsula, Chiba Prefecture	Middle Pleistocene	Forearc basin	Shallow	Large outcrop of carbonate-cemented siltstone	$\delta^{13}C$ as low as –62.3‰, no biomarkers reported	Low diversity (5 sp., S, T, L)	Majima et al. (2005) and Shibasaki and Majima (1997)
Anden seep deposit, Wakimoto Fm., Akita Prefecture	Middle Pleistocene	Backarc basin	Shallow(?)	Small to medium sized carbonate concretions	$\delta^{13}C$ as low as –64.7‰, biomarkers reported	Low diversity (1 sp., T)	Miyajima et al. (2020)
Zushi Senior High School seep deposit, Loc. 3 of Niitsuma et al. (1989) and Utsunomiya et al. (2015), Urago Fm., Kanagawa Prefecture	Early Pleistocene	Forearc basin	Deep	Large outcrop of carbonate-cemented sandstone	$\delta^{13}C$ as low as –37.8‰, no biomarkers reported	Low diversity (2 sp., T, V)	Hirata et al. (1991), Majima et al. (2005), Niitsuma et al. (1989), Shikama and Masujima (1969) and Utsunomiya et al. (2015)
Kamigou High School paleoseep, Ofuna and Koshiba Fms, Yokohama City, Kanagawa Prefecture	Early Pleistocene	Forearc basin	Shallow	Carbonate concretions in a vertical interval of at least 37 m straddling formation boundary	$\delta^{13}C$ as low as –55.1‰, biomarkers reported	High diversity (20 sp., S, T, V)	Kitazaki and Majima (2003), Majima et al. 1996, 2005), Tate and Majima (1998) and Tsuboi et al. (2010)

Site	Age	Geological context	Inferred water depth	Deposits: size and geometry	Carbonate stable C isotopes[a], biomarkers	Macrofossils	References
Shirahama area seep deposits, Shiramazu Fm., Boso Peninsula, Chiba Prefecture,	Pliocene	Forearc basin	Deep	Medium concretions and large-size breccia pockets	$\delta^{13}C$ as low as –35.2‰, no biomarkers reported	Low diversity (2 sp., V)	Futakami et al. (2001), Kanie et al. (1997), Kanie and Kuramochi (2001) and Majima et al. 1992, 2005)
Carbonate blocks in the Takatoriyama Pyroclastic Member, Ikego Fm., Kanagawa Prefecture	Pliocene	Forearc basin	Deep	Limestone blocks within slump structures, details unknown	$\delta^{13}C$ between −30‰ and −40‰, no biomarkers reported	Medium diversity (6 sp., S, T, L, V)	Kondo et al. (1996), Majima et al. (2005) and Niitsuma et al. (1989)
Sagara-Kakegawa seep deposits, Tamari and Hijikata Fms, Shizuoka Prefecture	Pliocene	Forearc basin	Deep	Several large *in situ* mounds, medium barrel-shaped concretions and carbonate blebs	$\delta^{13}C$ as low as −54.5‰, no biomarkers reported	Medium diversity (6 sp., in total, S, B?, T, L, V)	Amano and Jenkins (2011a), Amano and Kiel (2010), Campbell (2006), Kanie et al. (1992a, b), Majima et al. (1990), Nobuhara (2003) and Nobuhara and Tanaka (1993)
Calcareous siltstones of the Ogikubo Fm., Nagano Prefecture	Early Pliocene	Intra-arc/ backarc basin	Shallow	Sandy siltstone cemented by carbonate; details unknown	$\delta^{13}C$ as low as −58.8‰, no biomarkers reported	Medium diversity (7 sp., T, L)	Amano and Karasawa (1993) and Majima et al. (2005)
Matsunoyama seep deposit, Tamugigawa Fm., Niigata Prefecture	Early Pliocene	Intra-arc/ backarc basin	Deep	Scattered small-sized carbonate concretions	$\delta^{13}C$ as low as −41.1‰, biomarkers reported	High diversity (up to 24 sp., S, T, L, V)	Amano and Kanno (2005) and Miyajima et al. (2018b, 2020)

(continued)

Table 20.2 (continued)

Site	Age	Geological context	Inferred water depth	Deposits: size and geometry	Carbonate stable C isotopes[a], biomarkers	Macrofossils	References
Nakanomata seep deposit, Nodani Fm., Niigata Prefecture	Late Miocene	Intra-arc/ backarc basin	Deep	Medium-sized *ex situ* blocks	$\delta^{13}C$ as low as −41.1‰, biomarkers reported	Low–Medium diversity (4–9 sp., B, V, A)	Miyajima et al. (2016, 2018a, 2020)
"another seep deposit" of Miyajima et al (2016), Nodani Fm., Niigata Prefecture	Late Miocene	Intra-arc/ backarc basin	Deep	Unknown	Unknown	Low diversity (1 sp., V)	Miyajima et al. (2016)
Kita-Kuroiwa seep deposits, Ogaya Fm., Niigata Prefecture	Middle–Late Miocene	Intra-arc/back arc basin	Deep	Two large *in situ* carbonate bodies ca. 250 m apart	$\delta^{13}C$ as low as –38.0‰, biomarkers reported	Medium diversity (6 sp. in total, B, V, A)	Amano et al. (2010), Amano and Kanno (2005), Amano and Kiel (2011), Amano and Little (2014), Amano et al. (2019) and Miyajima et al. (2020)
Shinhemi Tunnel seep deposits, Ikegami, Hayama Group; Yokusuka City	Middle Miocene	Forearc basin	Deep	Carbonate along the fault zone, details unknown	$\delta^{13}C$ as low as –23.0‰, no biomarkers reported	Medium diversity (6 sp., S, T, L, V)	Kanie and Kuramochi (1995), Kanie and Sakai (1997), Majima et al. (2005), Naganuma et al. (1995) and Shikama (1968)
Tonohara seep deposit, Bessho Fm., Nagano Prefecture	Middle Miocene	Intra-arc/ backarc basin	Deep(?)	Medium to large boulder in unknown situation exposed on the slope	$\delta^{13}C$ as low as –29.8‰, no biomarkers reported	Low diversity (4 sp., T, V)	Miyajima et al. (2017)

Site	Age	Geological context	Inferred water depth	Deposits: size and geometry	Carbonate stable C isotopes[a], biomarkers	Macrofossils	References
Sorimachi seep deposit, Bessho Fm., Nagano Prefecture	Middle Miocene	Intra-arc/ backarc basin	Deep(?)	Scattered numerous small *in situ* concretions	$\delta^{13}C$ as low as –34.6‰, biomarkers reported	Low diversity (5 sp., S, L, V)	Miyajima et al. (2017, 2018b, 2020)
Carbonate nodules within Haratajino Fm., Annaka-Tomioka area, Gunma Prefecture	Middle Miocene	Forearc basin	Deep	Elongated small to medium concretions	Unknown[c]	Low diversity (2 sp., S)	Amano and Ando 2011), Kanie et al. (1999), Kurihara (2000) and Majima et al. (2005)
Akanuda-Anazawa limestone, Bessho Fm., Nagano Prefecture	Middle Miocene	Intra-arc/ backarc basin	Deep(?)	Two large *in situ* carbonate outcrops ca. 250 m apart	$\delta^{13}C$ as low as –42.2‰, biomarkers reported	Medium diversity (10 sp. in total, B, T, L, V, A)	Amano and Kiel (2011), Amano et al. (2010, 2019), Kuroda (1931), Miyajima et al. (2016, 2017, 2018a, 2018b, 2020), Nobuhara (2010), Nobuhara and Ohtori (2010), Nobuhara et al. (2008a), Saether et al. (2012), Sato et al. (1993) and Tanaka (1959)
Limestone lenses, nodules and calcareous deposits of Setogawa Group, Shizuoka Prefecture	Early Miocene	Subduction complex	Deep	Unknown	Unknown	Diversity unknown (S, T, L, V)	Amano et al. (2015), Majima et al. (2005), Matsumoto (1966, 1971) and Matsumoto and Hirata (1972)

(continued)

Table 20.2 (continued)

Site	Age	Geological context	Inferred water depth	Deposits: size and geometry	Carbonate stable C isotopes[a], biomarkers	Macrofossils	References
Izura Hanko Hotel seep deposit, Kokozura Fm., Takaku Group, Kitaibaraki City, Ibaraki Prefecture	Early Miocene	Forearc basin	Shallow	Small to very large carbonate concretions	$\delta^{13}C$ as low as –29.4‰, no biomarkers reported	Medium diversity (10 sp., S, T, L, V)	Amano and Ando (2011) and Ueda et al. (1995)
Carbonate nodules within Aokiyama Fm., Boso Peninsula, Arakawa, Chiba Prefecture	Early Miocene	Forearc basin	Deep	Concretions within mudstones, details unknown	Unknown	High diversity (16 sp., S, T, L, V)	Isaji (2013), Kuramochi et al. (1999) and Majima et al. (2005)
Carbonate olistolith in Aokiyama Fm., Boso Peninsula, Ishidohara, Chiba Prefecture	Early Miocene	Forearc basin	Deep	Slumped siltstone block in the mudstone	Unknown	Low diversity (2 sp., S, V)	Majima et al. (2005) and Ogasawara et al. (1994)
Tanami seep deposit, Tanamigawa Fm., Wakayama Prefecture	late Eocene–early Oligocene	Accretionary wedge	Deep	Single large *in situ* carbonate block	$\delta^{13}C$ as low as –35.3‰, no biomarkers reported	Medium diversity (8 sp., S, Nu, B, T, V)	Amano et al. (2013) and Katto and Masuda (1978)
Hokkaido							
Morai seep deposit, Morai Fm., central Hokkaido	Late Miocene	Backarc basin	Shallow	Several large laminar to columnar carbonate concretions	$\delta^{13}C$ as low as –55.3‰, biomarkers reported	Medium diversity (7 sp., S, T, L, V)	Amano (2003), Amano and Jenkins (2011a), Ishimura et al. (2005), Amano et al. (2019), Campbell (2006) and Ogihara (2005)

Site	Age	Geological context	Inferred water depth	Deposits: size and geometry	Carbonate stable C isotopes[a], biomarkers	Macrofossils	References
Takinoue seep deposit, Takinoue Fm., Yamayosawa Creek	Middle Miocene	Foreland basin	Deep	Scattered small to medium sized carbonate concretions	$\delta^{13}C$ as low as –41.7‰, biomarkers reported	Low diversity (1 sp., V)	Amano and Kiel (2011), Amano et al. (2019), Kanno and Ogawa (1964) and Miyajima et al. (2020)
Kami-Atsunai seep deposit, Nuibetsu Fm., Urahoro Town area	early Oligocene	Forearc basin	Unknown	Several large carbonate bodies and associated scree	$\delta^{13}C$ as low as –49.0‰, no biomarkers reported	Medium diversity (8 sp., S, B, T, L, V, A)	Amano and Jenkins (2011b, 2013), Amano and Kiel (2007), Hryniewicz et al. (2017a) and Kiel et al. (2016)
Yayoi town seep deposit, Poronai Fm., Mikasa City area	late Eocene	Forearc basin	Shallow/ deep	A few *in situ* medium-sized concretions	$\delta^{13}C$ as low as –44.7‰, no biomarkers reported	Medium diversity (7 sp., T, V)	Amano and Jenkins (2007), Amano et al. (2013), Amano and Oleinik (2016), Campbell (2006) and Hryniewicz et al. (2017a)
Kiritachi seep deposit, Sakasagawa Fm.	late Eocene	Forearc basin	Unknown	Siltstone with chemosymbiotic fauna; details unknown	Unknown	Low diversity (2 sp., T)	Amano and Oleinik (2016) and Hryniewicz et al. (2017a)
Eikou Bridge seep deposit, Tappu Fm., Obira Town area	late Eocene	Forearc basin	Unknown	Floats, details unknown	Unknown	Medium diversity (8 sp., T, V)	Amano et al. (2013), Amano and Kiel (2007), Hryniewicz et al. (2017a), Ohara (1966) and Ohara and Kanno (1973)

(continued)

Table 20.2 (continued)

Site	Age	Geological context	Inferred water depth	Deposits: size and geometry	Carbonate stable C isotopes[a], biomarkers	Macrofossils	References
Yasukawa seep deposit, Yezo Supergroup, Nakagawa Town area	Late Cretaceous (Campanian)	Forearc basin	Shallow/ deep	Four *in situ* medium boulders, numerous smaller concretions	$\delta^{13}C$ as low as –43.5‰, biomarkers reported	High diversity (15 sp., S, Nu, T, A)	Amano et al. (2007), Jenkins et al. (2007a, b, 2008) and Kaim et al. (2008a, b, 2009)
Tannosawa seep deposit, Yezo Supergroup, Nakagawa Town area	Late Cretaceous (Campanian)	Forearc basin	Shallow/ deep	Blocks and conduits, details unknown	$\delta^{13}C$ as low as –47.27‰, no biomarkers reported	Low diversity (at least 4 sp., L)	Kaim et al. (2009) and Walliser et al. (2019)
Omagari seep deposit, Yezo Supergroup, Nakagawa Town area	Late Cretaceous (Campanian)	Forearc basin	Shallow/ deep	Large *in situ* seep deposit in the riverbed	$\delta^{13}C$ as low as –45.3‰, biomarkers reported	Medium diversity (at least 14 sp.; K, L, A)	Campbell (2006), Hashimoto et al. (1967), Hikida et al. (2003), Jenkins et al. (2007a, b, 2013, 2018), Kaim et al. (2008a, b, 2009, 2010), Kiel et al. (2008b), Majima et al. (2005) and Ogihara (2004, 2005)
Niosawa seep deposit, Yezo Supergroup, Nakagawa Town area	Late Cretaceous (Campanian)	Forearc basin	Shallow/ deep	Unknown	Unknown	Unknown	Kaim et al. (2009)

Site	Age	Geological context	Inferred water depth	Deposits: size and geometry	Carbonate stable C isotopes[a], biomarkers	Macrofossils	References
Gakkonosawa seep deposit, Yezo Supergroup, Nakagawa Town area	Late Cretaceous (Campanian)	Forearc basin	Shallow/ deep	One large *ex situ* boulder	$\delta^{13}C$ as low as –30.9‰, no biomarkers reported	Low diversity (at least 4 sp., A)	Kaim et al. (2008a, b) and Kato (2019)
Kanajirisawa seep deposit, Yezo Supergroup, Obira Town area	Late Cretaceous (Cenomanian)	Forearc basin	Deep	Several small to large *in situ* boulders	$\delta^{13}C$ as low as –43.4‰, biomarkers reported	Medium diversity (at least 12 sp., Nu, T, L, A)	Asai and Hirano (1990), Campbell (2006), Kaim et al. (2008a, 2009,), Kanie and Kuramochi (1996), Kanie et al. (1996), Karasawa and Kano (2021), Kiel (2013), Kiel et al. (2008b), Majima et al. (2005), Ogihara (2004, 2005, 2008) and Tanabe et al. (1977)
Utagoesawa seep deposit, Yezo Supergroup, Mikasa City area	Early Cretaceous (Albian)	Forearc basin	Shallow/ deep	Several medium to large *in situ* and *ex situ* carbonate boulders	$\delta^{13}C$ as low as –47‰, biomarkers reported	Diversity unknown (at least 3 sp., K, A)	Jenkins et al. (2013, 2018), Kaim et al. (2009) and Ogihara (2004, 2005)
Shikorozawa seep deposit, Yezo Supergroup, Mikasa City area	Early Cretaceous (Albian)	Forearc basin	Shallow/ deep	Several semi *in situ* boulders, details unknown	δ13C as low as ca. –39‰, biomarkers reported	Unknown	Ogihara (2004, 2005)

(continued)

Table 20.2 (continued)

Site	Age	Geological context	Inferred water depth	Deposits: size and geometry	Carbonate stable C isotopes[a], biomarkers	Macrofossils	References
Pombetsu seep deposit, Yezo Supergroup, Mikasa City area	Early Cretaceous (Albian)	Forearc basin	Shallow/ deep	Two *in situ* medium to large carbonate lenses currently flooded)	Carbonate carbon isotopes not reported, biomarkers reported	Diversity unknown (at least 3 sp., S, T, L)	Kaim et al. (2009), Kanie and Sakai (1997), Kanie et al. (1993), Karasawa (2011), Kiel et al. (2008b), Majima et al. (2005) and Ogihara (2005)
other Japanese Islands							
Tanohama limestone, Taishu Group, Tsushima	Early Miocene	Pull-apart basin	Deep	Single *in situ* large lenticular body and numerous smaller concretions	$\delta^{13}C$ as low as –52.8‰, biomarkers reported	Low diversity (4 sp., B, L, V, A?)	Hryniewicz et al. (2021) and Ninomiya (2011, 2012)
Nita limestone, Taishu Group, Tsushima	Early Miocene	Pull-apart basin	Deep	Unknown	Unknown	Low diversity (1 sp., V)	Aoki and Nishida (1999) and Ninomiya (2011, 2012)
Kanoura limestone, Taishu Group, Tsushima	Early Miocene	Pull-apart basin	Deep	Several *ex situ* small to medium blocks	$\delta^{13}C$ as low as –41.8‰, biomarkers reported	Low diversity (2 sp., V)	Hryniewicz et al. (2021) and Ninomiya (2011, 2012)
Fukuzaki limestone, Taishu Group, Tsushima	Early Miocene	Pull-apart basin	Deep	A single *in situ* large lenticular carbonate body and numerous small to medium boulders	$\delta^{13}C$ as low as –40.2‰, biomarkers reported	Low diversity (2 sp., B)	Hryniewicz et al. (2021), Ninomiya (2011, 2012) and Ninomiya et al. (2020)

Site	Age	Geological context	Inferred water depth	Deposits: size and geometry	Carbonate stable C isotopes[a], biomarkers	Macrofossils	References
Philippines							
Cambantung Point seep deposit, Bata Fm., Leyte	Early Pleistocene	Backarc basin	Deep	Numerous small to medium *in situ* concretions on the wavecut platform	$\delta^{13}C$ as low as –37.2‰, no biomarkers reported	Medium diversity (14 sp., T, L, V)	Kiel et al. (2020b) and Majima et al. (2010)
Buhoc Point seep deposit, Bata Fm., Leyte	Early Pleistocene	Backarc basin	Deep	*Ex situ* concretions on the wavecut platform	Unknown	Low diversity (4 sp., L)	Kiel et al. (2020b) and Majima et al. (2007)
Antipolo Point seep deposit, Bata Fm., Leyte	Early Pleistocene	Backarc basin	Deep	Numerous variable-sized and shaped concretions	Unknown	Medium diversity (9 sp., B, T, L)	Kiel et al. (2020b) and Majima et al. (2007)
Liog-Liog Point seep deposit, Bata Fm., Leyte	Late Pliocene	Backarc basin	Deep	At least four large to very large blocks, tubular conduits	$\delta^{13}C$ as low as –42.3‰, no biomarkers reported	High diversity (27 sp., B, T, L, V, N?, A)	Kase et al. (2019), Kiel et al. (2020b) and Majima et al. (2007)
Taiwan							
Gutinkeng Fm. seep deposit, Southern Taiwan	Pleistocene	Foreland basin	Shallow	Small to large boulders, cobbles and pipes	$\delta^{13}C$ as low as –53.7‰, no biomarkers reported	Low diversity (5 sp., L)	Wang et al. (2006)

(continued)

Table 20.2 (continued)

Site	Age	Geological context	Inferred water depth	Deposits: size and geometry	Carbonate stable C isotopes[a], biomarkers	Macrofossils	References
Chiansien seep deposit, Tenshuiken Fm., Western Foothills	Pliocene	Foreland basin	Shallow	Numerous medium to large *in situ* carbonate blocks, chimneys and pipes	$\delta^{13}C$ as low as –49.6‰, no biomarkers reported	Low diversity (2 sp., L)	Blouet et al. (2021b), Chien et al. (2013, 2018), Wang et al. (2019) and Zhao et al. (2021)
Hunghuatzu seep deposit, Hunghuatzu Fm., Western Foothills	Early Miocene	Passive margin	Shallow	Very large *in situ* carbonate mound	$\delta^{13}C$ as low as –51.8‰, no biomarkers reported	Low diversity (1 sp., L)	Chien et al. (2012)
Kuohsing seep deposits, Huodongkeng Fm., Western Foothills	Miocene	Passive margin	Shallow	Small to large blocks, chimneys and nodules	$\delta^{13}C$ as low as –47.6‰, no biomarkers reported	Low diversity (1 sp., L)	Wang et al. (2018)
Turkey							
Dumanlı and Terziler seep deposits, Kasımlar Basin	Late Triassic (late Carnian–middle Norian)	Inter-platform basin	Shallow(?)–deep	Five large carbonate deposits, one *in situ*, the remainder *ex situ*	$\delta^{13}C$ as low as –12.0‰, no biomarkers reported	High diversity (18 sp., D)	Ager et al. (1978), Kiel (2018) and Kiel et al. (2017)

Site	Age	Geological context	Inferred water depth	Deposits: size and geometry	Carbonate stable C isotopes[a], biomarkers	Macrofossils	References
Europe							
Italy							
Stirone River seep deposit, Castell' Arquato Basin, Northern Apennines	Late Pliocene	Foreland basin	Deep	Chemosymbiotic fauna and variously sized carbonate nodules	$\delta^{13}C$ as low as −37.5‰, no biomarkers reported	Diversity unknown (S, L, V)	Barbieri and Cavalazzi (2005), Cau et al. (2016), Capozzi et al. (2013), Capozzi (2017), Kiel and Taviani (2018), Monegatti et al. (2001), Taviani (2011, 2014) and Taviani et al. (1997)
Verzino seep deposit, Crotone Basin, Southern Apennines	Late Miocene	Forearc basin	Deep	Small isolated outcrops, details unknown	Unknown	Low diversity (2 sp., B, V)	Kiel and Taviani (2017)
Santa Sofia seep deposits, Verghereto Marls, Northern Apennines	Late Miocene	Thrust-wedge front	Deep	Numerous lens- to irregular-shaped carbonate bodies	$\delta^{13}C$ as low as –36.4‰, no biomarkers reported	Medium diversity (7 sp., L)	Conti et al. (2021), Kiel and Taviani (2017) and Moroni (1966)
Poggio Campane seep deposit, Verghereto Marls, Northern Apennines	Late Miocene	Thrust-wedge front	Deep	Three lenses and several pinnacles, all large to very large, and associated scree	$\delta^{13}C$ as low as –32.2‰, no biomarkers reported	Unknown	Conti et al. (2021)

(continued)

Table 20.2 (continued)

Site	Age	Geological context	Inferred water depth	Deposits: size and geometry	Carbonate stable C isotopes[a], biomarkers	Macrofossils	References
Pietralunga seep deposit, Tossignano Marls, Northern Apennines	Late Miocene	Foredeep	Deep	Large sized carbonate remnant within abandoned quarry	$\delta^{13}C$ as low as –51.5‰, biomarkers reported	Diversity unknown (L)	Barbieri and Cavalazzi (2005), Birgel and Peckmann (2008), Conti and Fontana (1998), Peckmann et al. (2004) and Terzi (1993)
Monticino-Limisano seep deposit, Marnoso-Arenacea Fm., Northern Appenines	Late Miocene	Foreland basin (thrust-wedge front?)	Deep	Few scattered blocks	See[d]	Diversity unknown (B)	Conti et al. (2021) and Kiel and Taviani (2017)
Montepetra seep deposit, Ghioli de letto Fm., Northern Apennines	Late Miocene	Thrust-wedge front	Deep	Several large to very large seep blocks of various morphologies	$\delta^{13}C$ as low as –52.7‰, no biomarkers reported	Diversity unknown (3 sp., B, L)	Clari et al. (2004b), Conti et al. (2021), Conti and Fontana (1998), Conti et al. (2010), Kiel and Taviani (2017) and Taviani (1994)
Marmorito seep deposit, Monferrato Hills, Piedmont Basin, Italy	Late Miocene	Foreland basin	Deep	Carbonate cemented sandstone layers up to 20 m thick	$\delta^{13}C$ as low as –40.2‰, biomarkers reported	Diversity unknown (V)	Birgel and Peckmann (2008), Campbell (2006), Cavagna et al. (1999), Clari et al. (1988, 1994), Kiel and Taviani (2017), Martire et al. (2010) and Peckmann et al. (1999a)
Case Rovereti seep deposit, San Paolo Marls(?), Northern Apennines	Late Miocene	Foreland basin	Deep	One large and several smaller boulders	$\delta^{13}C$ as low as –32.7‰, no biomarkers reported	Low diversity (4 sp., B, L, V)	Clari et al. (2004a), Kiel and Taviani (2017), Moroni (1966), Taviani (1994), Terzi et al. (1994) and Vinn et al. (2012, 2013)

Site	Age	Geological context	Inferred water depth	Deposits: size and geometry	Carbonate stable C isotopes[a], biomarkers	Macrofossils	References
Ca' Pianté seep deposit, Northern Apennines	Late Miocene	Foreland basin (thrust-wedge front?)	Deep	Scattered limestone blocks; details unknown	See[d]	Diversity unknown (V)	Conti et al. (2021), Conti and Fontana (1998) and Kiel and Taviani (2017)
Ca' Fornace seep deposit, Sintria creek valley, Northern Apennines	Late Miocene(?)	Foreland basin	Deep	Floats, details unknown	$\delta^{13}C$ as low as –57.6‰, no biomarkers reported	Medium diversity (14 sp., B, L, V)	Conti et al. (2021), Kiel and Taviani (2017), Kiel et al. (2018) and Vai et al. (1997)
Ca' Carnè seep deposits[e], Tossignano Marls, Northern Apennines	Late Miocene	Foreland basin (thrust-wedge front?)	Deep	Unknown	See[d]	Medium diversity (9 sp., L)	Kiel and Taviani (2017) and Sami and Taviani (2015)
Abisso "Mornig" seep deposits, Tossignano Marls, Northern Apennines	Late Miocene	Foreland basin	Deep	Micritic carbonate blocks, details unknown	See[d]	Medium diversity (6 sp., B, L, V)	Conti et al. (2021)[d], Kiel and Taviani (2017) and Sami and Taviani (2015)
Montebaranzone seep deposits (including Sasso di Streghe pinnacle), Termina Fm., Northern Apennines	Middle–Late Miocene	Wedge-top basin	Shallow(?)–deep	Numerous small to very large carbonate bodies	$\delta^{13}C$ as low as –39.1‰, no biomarkers reported	Diversity unknown (L, V)	Clari et al. (2004b), Conti et al. (2021), Conti and Fontana (2011), Conti et al. (2010, 2014), Russo et al. (2012) and Taviani (1994, 2011)
Le Colline seep deposit, Marnoso-arenacea Fm., Northern Apennines	Middle Miocene	Thrust-wedge front	Deep	Scattered carbonate blocks; details unknown	Unknown	Diversity unknown (B)	Conti and Fontana (1998) and Kiel and Taviani (2017)

(continued)

Table 20.2 (continued)

Site	Age	Geological context	Inferred water depth	Deposits: size and geometry	Carbonate stable C isotopes[a], biomarkers	Macrofossils	References
Fosso Riconi seep deposit, Vicchio Fm., Northern Apennines	Middle Miocene	Thrust-wedge front	Deep	Up to 80 large to very large carbonate bodies	$\delta^{13}C$ as low as –39.0‰, no biomarkers reported	Medium diversity (8 sp. in total, L, V)	Conti et al. (2021), Fontana et al. (2013) and Grillenzoni et al. (2017)
Deruta seep deposit, Marnoso-arenacea Fm., Northern Apennines	Middle Miocene	Thrust-wedge front	Deep	Numerous small to very large nodules, boulders and lenses	$\delta^{13}C$ as low as –46.0‰, no biomarkers reported	Diversity unknown (B, L, V)	Clari et al. (2004b), Conti et al. (2008, 2021) and Kiel and Taviani (2017)
Corella seep deposit, Marnoso-arenacea Fm., Northern Apennines	Middle Miocene	Foredeep	Deep	Six very large and several smaller carbonate deposits	$\delta^{13}C$ as low as –42.3‰, no biomarkers reported	Unknown	Argentino et al. (2019) and Conti et al. (2017, 2021)
Castagno D'Andrea seep deposit, Marnoso-arenacea Fm., Northern Apennines	Middle Miocene	Foredeep	Deep	Large pinnacle to stratiform carbonate bodies	Unknown	Diversity unknown (L?)	Argentino et al. (2019) and Conti et al. (2004, 2017, 2021)
Castelvecchio seep deposit, Marnoso-Arenacea Fm., Northern Apennines	Middle Miocene	Thrust-wedge front	Deep	Calcarenitic deposit	Unknown	Diversity unknown (V)	Kiel and Taviani (2017)

Site	Age	Geological context	Inferred water depth	Deposits: size and geometry	Carbonate stable C isotopes[a], biomarkers	Macrofossils	References
Ca' Cavalmagra seep deposit, Marnoso-Arenacea Fm., Northern Apennines	Middle Miocene	Thrust-wedge front	Deep	Unknown	Unknown	Diversity unknown (T, V)	Kiel and Taviani (2017)
Brasimone-Suviana seep deposit, Cervarola Fm., Northern Apennines	Middle Miocene	Intrabasinal high within a foredeep	Deep	Numerous small to large carbonate lenses	$\delta^{13}C$ as low as –29.5‰, no biomarkers reported	Diversity unknown (L)	Conti et al. (2021) and Conti and Fontana (2002, 2011)
Acquadalto seep deposits, Marnoso-arenacea Fm., Northern Apennines	Middle Miocene	Foredeep	Deep	Medium sized to large lenticular carbonates	$\delta^{13}C$ as low as –15.8‰, no biomarkers reported	Unknown	Argentino et al. (2019) and Conti et al. (2021)
Moggiona seep deposits, Vicchio Fm., Northern Apennines	Early Miocene	Thrust-wedge front	Deep	Several very large seep deposits	$\delta^{13}C$ as low as –37.5‰, no biomarkers reported	Unknown	Argentino et al. (2019), Conti et al. (2017, 2021)
Other countries							
Pobiti Kamani seep deposit, Dikilitash Fm., Bulgaria	Eocene	Shelf	Shallow	Numerous small to large vertical tubular concretions	$\delta^{13}C$ as low as –44.8‰, biomarkers reported	Low diversity (3 sp.)[f]	De Boever et al. (2006, 2011a, b, 2009a, b)

(continued)

Table 20.2 (continued)

Site	Age	Geological context	Inferred water depth	Deposits: size and geometry	Carbonate stable C isotopes[a], biomarkers	Macrofossils	References
Buje seep deposit, Istria, Dynaridic Foredeep, Croatia	Eocene	Foreland basin	Deep	Three large to very large *in situ* lenticular carbonate bodies	$\delta^{13}C$ as low as –44.8‰, biomarkers reported	Low diversity (4 sp., S, T, L)	Natalicchio et al. (2015) and Venturini et al. (1998)
Świątkowa Wielka seep deposit, Krosno Fm., Grybów Nappe, Poland	Oligocene	Flysch basin	Deep	Large carbonate mound and associated fossil talus	$\delta^{13}C$ as low as –39.0‰, no biomarkers reported	None reported	Bojanowski (2007)
Kardala seep deposit, Black Flysch Group, Basque-Cantabrian Basin, Spain	Early Cretaceous (Albian)	Peri-cratonic rift	Deep	Stacked medium to large carbonate lenses, nodules, and breccias	$\delta^{13}C$ as low as −20.7‰, biomarkers reported	Low diversity (5 sp., L)	Agirrezabala (2009) and Jakubowicz et al. (2021)
Ispaster seep deposit, Black Flysch Group, Basque-Cantabrian Basin, Spain	Early Cretaceous (Albian)	Peri-cratonic rift	Deep	Numerous small to large *in situ* carbonate lenses and associated *ex situ* boulders	$\delta^{13}C$ as low as –41.6‰, biomarkers reported	Medium diversity (9 sp., K, L, A)	Agirrezabala et al. (2013), Jakubowicz et al. (2021), Jenkins et al. (2018) and Wiese et al. (2015)
Gorliz seep deposit, Black Flysch Group, Basque-Cantabrian Basin, Spain	Early Cretaceous (Albian)	Peri-cratonic rift	Deep	Numerous small carbonate lenses and concretions	$\delta^{13}C$ as low as –38.8‰, no biomarkers reported	Low diversity (2 sp.)	Agirrezabala (2015), Agirrezabala et al. (2014) and Jakubowicz et al. (2021, 2022)

Site	Age	Geological context	Inferred water depth	Deposits: size and geometry	Carbonate stable C isotopes[a], biomarkers	Macrofossils	References
Alkolea seep deposit, Black Flysch Group, Basque-Cantabrian Basin, Spain	Early Cretaceous (Albian)	Peri-cratonic rift	Deep	Stacked medium to large carbonate lenses and associated concretions	$\delta^{13}C$ as low as –41.5‰, no biomarkers reported	Low diversity (2 sp.)	Agirrezabala (2009) and Jakubowicz et al. (2021, 2022)
Salinac seep deposit, Vocontian Basin, France	Early Cretaceous (Aptian)	Basin on a passive margin	Deep	Small to medium-sized *in situ* concretions	$\delta^{13}C$ as low as –25.9‰, biomarkers reported	None reported	Reitner et al. (2015)
Baška seep deposit, Carpathians, Czech Republic	Early Cretaceous (Barremian)	Failed continental rift	Deep	Small concretions dispersed in mudstone on a few square meters	$\delta^{13}C$ as low as –28.4‰, no biomarkers reported	Low diversity (3 sp., L, A)	Jakubowicz et al. (2019) and Kaim et al. (2013)
Archival localities of Ascher (1906), Carpathians	Early Cretaceous (Hauterivian?)	Unknown	Unknown	Unknown	Unknown	High diversity (17 sp., D, K, L, T, A)	Ascher (1906) and Kaim et al. (2013)

(continued)

Table 20.2 (continued)

Site	Age	Geological context	Inferred water depth	Deposits: size and geometry	Carbonate stable C isotopes[a], biomarkers	Macrofossils	References
Rottier seep deposit, Vocontian Basin, France	Early Cretaceous (Hauterivian)	Basin on a passive margin	Deep	Very large seep deposit and associated scree	$\delta^{13}C$ as low as –5.6‰, no biomarkers reported	Low diversity (3 sp., D, L)	Campbell and Bottjer (1995b), Kiel (2013), Kiel et al. (2014a) and Thieuloy (1972)
Raciborsko seep deposit, Carpathians, Poland	Early Cretaceous (Hauterivian)	Failed continental rift	Deep	Unknown	$\delta^{13}C$ as low as –33.7‰, no biomarkers reported	Low diversity (1 sp., D)	Biernat (1957), Campbell and Bottjer (1995b), Kiel et al. (2014a)
Curnier seep deposit, Vocontian Basin, France	Early Cretaceous (Hauterivian)	Basin on a passive margin	Deep	One large *ex situ* boulder	$\delta^{13}C$ as low as –6.9‰, biomarkers reported	Low diversity (2 sp., D, L)	Campbell and Bottjer (1995b), Kiel (2013) and Kiel et al. (2014a)
Planerskoje seep deposit, Crimea, Ukraine	Early Cretaceous (Berriasian)	Basin on a passive margin	Shallow(?)–deep	Medium *in situ* carbonate lens	$\delta^{13}C$ as low as –13.6‰, biomarkers reported	Medium diversity (11 sp., D, K, L, A)	Kiel (2008b, 2013), Jenkins et al. (2013), Kiel et al. (2010, 2014a), Kiel and Peckmann (2008), Peckmann et al. (2009), Sarycheva (1960) and Smirnova (1972)
Beauvoisin seep deposits, Terres Noires Fm., Drome, France	Middle(?)–Late Jurassic (Bathonian?–Oxfordian)	Basin on a passive margin	Deep	ca. 40 medium to very large *in situ* pseudobioherms	$\delta^{13}C$ as low as –26.5‰, biomarkers reported	Low diversity (5 sp, L, A)	Blouet et al. (2021a), Campbell (2006), Gaillard et al. (1985, 1992, 2011), Gaillard and Rolin (1986, 1988), Gay et al. (2020), Kiel et al. (2010), Peckmann et al. (1999a), Rolin et al. (1990) and Senowbari-Daryan et al. (2007)

Site	Age	Geological context	Inferred water depth	Deposits: size and geometry	Carbonate stable C isotopes[a], biomarkers	Macrofossils	References
Kilve seep deposit, Blue Lias Fm., Somerset, UK	Early Jurassic (Sinemurian)	Intra-platform extensional basin	Shallow(?)	Four large *in situ* coniform mounds	$\delta^{13}C$ as low as –26.2‰, no biomarkers reported	Low diversity (3 sp.)	Alisson et al. (2008)
Tantes Mound seep deposit, Pyrenees, France	Carboniferous, early Mississippian–Pennsylvanian (Moscovian)	Flysch basin	Deep(?)	Very large carbonate body	$\delta^{13}C$ as low as –50.0 ‰, no biomarkers reported	Low diversity (3 sp.)	Buggisch and Krumm (2005) and Kiel et al. (2014b)
Iberg Reef, Harz Mountains, Germany	Carboniferous, Mississippian (latest Viséan)	Seamount (drowned reef)	Shallow	Small to very large depressions and neptunian dykes	$\delta^{13}C$ as low as –32.0 ‰, no biomarkers reported	Low diversity (4 sp., D, S)	Buggisch and Krumm (2005), Campbell (2006), Campbell and Bottjer (1995a), Gischler et al. (2003) and Peckmann et al. (2001)
Australia							
Holmwood Shale seep deposits, Irwin Basin, Western Australia	early Permian (Cisuralian, Sakmarian)	Marginal rift basin	Shallow	At least three nodular limestone beds and associated nodules dispersed in the shale	$\delta^{13}C$ as low as -45.1.5‰, no biomarkers reported	Medium–high diversity (at least 12 sp.)	Clarke et al. (1951), Playford (1959) and Haig et al. (2022)
New Zealand							
Wilder seep deposit, East Coast Basin, North Island	Miocene	Forearc basin	Shallow/ deep	Five outcrops, details unknown	Unknown	None reported	Campbell et al. (2008b), Saether (2011), and Saether et al. (this volume)

(continued)

Table 20.2 (continued)

Site	Age	Geological context	Inferred water depth	Deposits: size and geometry	Carbonate stable C isotopes[a], biomarkers	Macrofossils	References
Waiapu seep deposit, East Coast Basin, North Island	Late Miocene	Forearc basin	Deep	Unknown	Unknown	Low diversity (1 sp.)	Campbell et al. (2008b), Saether (2011) and Saether et al. (this volume)
Turihaua seep deposit, East Coast Basin, North Island	Late Miocene	Forearc basin	Deep	Partially *ex situ*, very large lenticular carbonate	$\delta^{13}C$ as low as –49.2‰, no biomarkers reported	Low diversity (2 sp., B)	Campbell et al. (2008b), Saether (2011) and Saether et al. (2010b, this volume)
Karikahiruata seep deposit, East Coast Basin, North Island	Middle Miocene	Forearc basin	Deep	Very large *in situ* lenticular carbonate	Unknown	Low diversity (2 sp., B)	Campbell et al. (2008b), Saether (2011) and Saether et al. (2010b, this volume)
Bexhaven seep deposit, East Coast Basin, North Island	Middle Miocene	Forearc basin	Deep	Very large *in situ* lenticular carbonate	$\delta^{13}C$ as low as –48.5‰, no biomarkers reported	Medium diversity (9 sp., B, T, L)	Amano et al. (2015, 2018), Georgieva et al. (2019), Campbell et al. (2008b), Saether (2011) and Saether et al. (2010b, 2016, this volume)
Tauwhareparae seep deposit, East Coast Basin, North Island	Middle Miocene	Forearc basin	Deep	Very large hill (an abandoned quarry) with associated scree	$\delta^{13}C$ as low as –48.8‰, no biomarkers reported	Low diversity (5 sp., B)	Amano et al. (2018), Campbell et al. (2008b), Saether (2011) and Saether et al. (2010b, 2016, this volume)
Puketawa seep deposit, East Coast Basin, North Island	Middle Miocene	Forearc basin	Deep	Single large *ex situ* boulder	$\delta^{13}C$ as low as –51.7‰, no biomarkers reported	Low diversity (4 sp., B, A)	Campbell et al. (2008b), Saether (2011) and Saether et al. (2010a, b, 2012, this volume)

Site	Age	Geological context	Inferred water depth	Deposits: size and geometry	Carbonate stable C isotopes[a], biomarkers	Macrofossils	References
Totaranui seep deposit, East Coast Basin, North Island	Middle Miocene	Forearc basin	Deep	Several medium to large *ex situ* boulders	$\delta^{13}C$ as low as –45.0‰, no biomarkers reported	Low diversity (4 sp., B)	Campbell et al. (2008b), Saether (2011) and Saether et al. (2010b, 2012, this volume)
Ngawaka seep deposit, East Coast Basin, North Island	Middle Miocene	Forearc basin	Shallow/ deep	Several large to very large *in situ* seep deposits	Unknown	Low diversity (3 sp., B, L)	Amano et al. (2018), Campbell et al. (2008b), Saether (2011) and Saether et al. (2010b, this volume)
Moonlight North seep deposit, East Coast Basin, North Island	Middle Miocene	Forearc basin	Deep	Single very large lenticular seep deposit	$\delta^{13}C$ as low as –31.1‰, no biomarkers reported	High Diversity (17 sp., S, B, T, L, A)	Amano et al. (2015, 2018), Campbell et al. (2008b), Saether (2011), Saether et al. (2010a, b, 2016, this volume)
Rocky Knob seep deposit, East Coast Basin, North Island	Middle Miocene	Forearc basin	Deep	Very large limestone outcrop forming a vertical wall	$\delta^{13}C$ as low as –48.3‰, no biomarkers reported	Medium diversity (11 sp., B, L, A)	Amano et al. (2018), Georgieva et al. (2019), Campbell et al. (2008b) and Saether et al. (2010a, b, 2012, this volume)
Waikairo seep deposit, East Coast Basin, North Island	Middle Miocene	Forearc basin	Deep	A single large *ex situ* boulder in the riverbed	Unknown	Unknown	Campbell et al. (2008b), Saether (2011) and Saether et al. (this volume)

(continued)

Table 20.2 (continued)

Site	Age	Geological context	Inferred water depth	Deposits: size and geometry	Carbonate stable C isotopes[a], biomarkers	Macrofossils	References
Wanstead seep deposit, East Coast Basin, North Island	Early Miocene	Forearc basin	Shallow/ deep	Several boulders	$\delta^{13}C$ as low as –22.9‰, no biomarkers reported	Low diversity (4 sp., B, L)	Amano et al. (2018), Campbell et al. (2008b), Saether (2011) and Saether et al. (2010b, this volume)
Waipiro seep deposit, East Coast Basin, North Island	Early Miocene	Forearc basin	Deep	Several large *ex situ* boulders	Unknown	Low diversity (1 sp., B)	Campbell et al. (2008b), Saether (2011) and Saether et al. (this volume)
Ugly Hill seep deposit, East Coast Basin, North Island	Early Miocene	Forearc basin	Shallow/ deep	At least two separate localities composed of outcrops and *ex situ* boulders	Unknown	Medium diversity (7 sp., B, L, V, A)	Amano et al. (2018), Amano et al. (2014b), Campbell et al. (2008b), Saether (2011) and Saether et al. (2010a, b, this volume)
Haunui seep deposit, East Coast Basin, North Island	Early Miocene	Forearc basin	Shallow/ deep	A set of outcrops of a very large *in situ* deposit	$\delta^{13}C$ as low as –11.1‰, no biomarkers reported	Low diversity (4 sp., B, L)	Amano et al. (2018), Campbell et al. (2008b), Saether (2011) and Saether et al. (this volume)
Waipiro Bay seep deposit (including Waipiro I and Waipiro III boulders), Raukumara Peninsula, North Island	Late Cretaceous (Campanian)	Unknown	Shallow–deep(?)	*Ex situ* boulders on the beach	$\delta^{13}C$ as low as –25.4‰, biomarkers reported	Medium diversity (8 sp., S, T, L, A)	Kaim et al. (2014), Kiel et al. (2013b), Saether et al. 2010b, this volume) and Zwicker et al. (2021)

Site	Age	Geological context	Inferred water depth	Deposits: size and geometry	Carbonate stable C isotopes[a], biomarkers	Macrofossils	References
Owhena Stream seep deposit, Raukumara Peninsula, North Island	Late Cretaceous (Campanian)	Passive margin	Unknown	Concretionary mudstone with tubular conduits	$\delta^{13}C$ as low as –20.0‰, no biomarkers reported	None reported	Kiel et al. (2013b) and Saether et al. (this volume)
Port Awanui seep deposits (including Awanui I, Awanui II and GS 688 boulders), Raukumara Peninsula, North Island	mid-Cretaceous (late Albian–middle Cenomanian	Unknown	Shallow–deep(?)	Three large *ex situ* boulders on the shore	$\delta^{13}C$ as low as −29.2‰, biomarkers reported	High diversity (24 sp., S, Nu, K, T, L, N?, A)	Jenkins et al. (2018), Kiel (2013), Kiel et al. (2013b) and Saether et al. this volume)

Notes

[a] Carbon isotope values reported as per mil (‰) relative to VPDB

[b] The depleted $\delta^{13}C$ values indicative of hydrocarbon seepage and oxidation come from the carbonate filling the neptunian dykes within Kess Kess mounds; the $\delta^{13}C$ of carbonate sediment forming the mounds themselves is within the range of normal marine Devonian carbonates

[c] Biogenic $\delta^{34}S$ data reported by Kanie et al. (1999) ($\delta^{34}S$ CDT = −17.2‰) indicate that sulfide supplied to site was produced due to biogenic sulfate reduction, likely coupled with anaerobic oxidation of methane as indicated by prolific carbonate nodular cementation

[d] This seep deposit is located close to the town of Brisighella. Conti et al. (2021) report several cold seep carbonate deposits near Brisighella, with collective $\delta^{13}C$ values ranging as low as −51.7‰. The Abisso "Mornig," Ca' Carnè, Ca' Fornace, Ca' Pianté, and Monticino-Limisano seep deposits listed by Kiel and Taviani (2017) are located near Brisighella, and it was not possible to confidently assign $\delta^{13}C$ values given by Conti et al. (2021) to any of these deposits. $\delta^{13}C$ values from Ca' Fornace seep deposit provided by Kiel et al. (2018) are as low as −57.6‰, thus lower than the lowest value provided by Conti et al. (2021)

[e] Sami and Taviani (2015) list three different sites called "Ca' Carnè"

[f] De Boever et al. (2009b) mention infrequent bivalves, gastropods, and serpulids among bioclasts; they were likely not members of the seep community

Within each table, entries are organized by continent, and within the continent, by country, region, and state. Each entry contains the following information: the site, including locality information and geological formation, the age (period, etc.), the geologic context (e.g., forearc basin), the inferred water depth at which the seeps developed (shallow <300 m; deep >300 m), a description of the deposits, the lowest reported value of the carbon isotope composition ($\delta^{13}C‰$ VPDB) of the seep carbonates (if they have been analyzed), whether biomarkers have been reported, and a list of the fauna with most important obligate or seep-associated groups indicated (A = abyssochryssoid gastropod; B = bathymodiolin mussel; D = dimerelloid brachiopod; K = kalenterid bivalve; L = lucinid bivalve; M = modiomorphid bivalve; N = neomphalid gastropod; Nu = *Nucinella*; S = solemyid bivalve; T = thyasirid bivalve; V = vesicomyid bivalve) and relevant references.

Acknowledgments First, I would like to thank Volume editors: Andrzej Kaim (Institute of Paleobiology, Warsaw), Kirk J. Cochran (Stony Brook University, New York), and Neil H. Landman (American Museum of Natural History, New York) for an opportunity to prepare this contribution and for their patience during the time it was compiled. I would also like to heartily thank Hans Arne Nakrem and Øyvind Hammer (both Natural History Museum, Oslo) and Crispin T.S. Little (School of Earth and Environment, University of Leeds) thanks to whom started to study ancient seeps. Company of Hans Arne, Øyvind, Jörn H. Hurum (Natural History Museum, Oslo), Cris TS Little, and my other colleagues from Svalbard Jurassic Research Group was invaluable on Svalbard and during the time materials were studied in Oslo. Kazutaka Amano (Joetsu University of Education, Joetsu), Robert G. Jenkins (Kanazawa University, Kanazawa), and Yusuke Miyajima (Geological Survey of Japan, Tsukuba) have guided me to several sites in Japan, especially Hokkaido. Jamie Brezina (Rapid City, South Dakota) has been a companion in the fieldwork in the USA and Japan. Russell Shapiro (California State University, Chico) has shown me around some localities in California. Petr Skupien (Technical University of Ostrava) has accompanied me to Baška site in Czech Republic. Steffen Kiel (Naturhistoriska riksmuseet, Stockholm) and I have visited Buje in Croatia together and spend many good days prospecting for more seep deposits in the area. The biggest thanks perhaps should go to Andrzej Kaim, with whom we visited numerous seep deposits in the Americas, Arctic, Asia, and Europe. Many fruitful discussions with Kazutaka Amano, Michał Jakubowicz (Adam Mickiewicz University, Poznań), Robert G. Jenkins, Andrzej Kaim, Steffen Kiel, Yusuke Miyajima, and Crispin TS Little are acknowledged. Final thanks go to my family for showing a lot of understanding when I was preparing this chapter during numerous long evenings.

References

Ager DV (1968) A supposedly ubiquitous Tethyan brachiopod *Halorella* and its relations. J Palaeontol Soc Ind 5–9:54–70

Ager DV, Cossey SPJ, Mullin PR et al (1976) Brachiopod ecology in mid-Paleozoic sediments near Khenifra, Morocco. Palaeogeogr Palaeoclimatol Palaeoecol 20:171–185

Ager DV, Gutnic M, Juteau T et al (1978) New early Mesozoic brachiopods from southern Turkey. Bull Miner Res Explor 91:59–75

Agirrezabala LM (2009) Mid-Cretaceous hydrothermal vents and authigenic carbonates in a transform margin, Basque-Cantabrian Basin (western Pyrenees): a multidisciplinary study. Sedimentology 56:969–996

Agirrezabala LM (2015) Syndepositional forced folding and related fluid plumbing above a magmatic laccolith: Insights from outcrop (Lower Cretaceous, Basque-Cantabrian Basin, western Pyrenees). Geol Soc Am Bull 127:982–1000

Agirrezabala LM, Kiel S, Blumenberg M et al (2013) Oucrop analogues of pockmarks and associated methane-seep carbonates: a case study from the Lower Cretaceous (Albian) from the Basque-Cantabrian Basin, western Pyrenees. Palaeogeogr Palaeoclimatol Palaeoecol 390:94–113

Agirrezabala LM, Permanyer A, Suárez-Ruiz I et al (2014) Contact metamorphis of organic-rich mudstones and carbon release around a magmatic sill in Basque-Cantabrian Basin, western Pyrenees. Org Geochem 69:26–35

Aiello IW (2005) Fossil seep structures of the Monterey Bay region and tectonic/structural controls on fluid flow in an active transform margin. Palaeogeogr Palaeoclimatol Palaeoecol 227:124–142

Aiello IW, Garrison RE, Moore JC et al (2001) Anatomy and origin of carbonate structures in a Miocene cold-seep field. Geology 29:1111–1114

Aitken SA, Henderson CM, Collom CJ et al (2002) Stratigraphy, paleoecology, and origin of Lower Devonian (Emsian) carbonate mud buildups, Hamar Laghdad, eastern Anti–Atlas, Morocco, Africa. Bull Can Pet Geol 50:217–243

Alisson PA, Hasselbo SP, Brett CE (2008) Methane seeps on an Early Jurassic dysoxic seafloor. Palaeogeogr Palaeoclimatol Palaeoecol 270:230–238

Amano K (2003) Predatory gastropod drill holes in Upper Miocene cold seep bivalves, Hokkaido, Japan. Veliger 46:90–96

Amano K, Ando H (2011) Giant fossil *Acharax* (Bivalvia: Solemyidae) from the Miocene of Japan. Nautilus 125:207–212

Amano K, Jenkins RG (2007) Eocene drill holes in cold seep bivalves from Hokkaido, Japan. Mar Ecol 28:108–114

Amano K, Jenkins RG (2011a) Fossil records of extant vesicomyid species from Japan. Venus 69(3–4):163–176

Amano K, Jenkins RG (2011b) New fossil *Bathymodiolus* (sensu lato) (Bivalvia: Mytilidae) from Oligocene seep carbonates in Eastern Hokkaido, Japan, with remarks on the evolution of the genus. Nautilus 125:29–35

Amano K, Jenkins RG (2013) A new species of *Provanna* (Gastropoda: Provannidae) from an Oligocene seep deposit in Eastern Hokkaido. Paleontol Res 17:325–329

Amano K, Kanno S (2005) *Calyptogena* (Bivalvia: Vesicomyidae) from Neogene strata in the Joetsu District, Niigata Prefecture, central Japan. Veliger 47:202–212

Amano K, Karasawa S (1993) Molluscan fauna and paleoenvironment of the Pliocene Ogikubo Formation in the Northern Part of the Nagano Prefecture, Central Japan. J Geograph 102:572–582

Amano K, Kiel S (2007) Fossil vesicomyid bivalves from the North Pacific Region. Veliger 49:270–293

Amano K, Kiel S (2010) Taxonomy and distribution of fossil *Archivesica* (Bivalvia: Vesicomyidae) in Japan. Nautilus 124:155–165

Amano K, Kiel S (2011) Fossil *Adulomya* (Vesicomyidae, Bivalvia) from Japan. Veliger 51:76–90

Amano K, Little CTS (2014) Miocene abyssochrysoid gastropod *Provanna* from Japanese seep and whale-fall sites. Acta Palaeontol Pol 59:163–172

Amano K, Oleinik A (2016) Ancistrolepidine gastropods (Buccinidae) from the upper Eocene hydrocarbon seep deposits in Hokkaido, northern Japan. Nautilus 130:158–163

Amano K, Jenkins RG, Hikida Y (2007) A new gigantic *Nucinella* (Bivalvia: Solemyioida) from the Cretaceous cold-seep deposit in Hokkaido, northern Japan. Veliger 49:84–90

Amano K, Jenkins RG, Kurihara Y et al (2008) A new genus for *Vesicomya inflata* Kanie & Nishida, a lucinid shell convergent with that of vesicomyids, from Cretaceous strata of Hokkaido, Japan. Veliger 50:255–262

Amano K, Jenkins RG, Aikawa M et al (2010) A Miocene chemosynthetic community from the Ogaya Formation in Joetsu: Evidence for depth-related ecologic control among fossil seep communities in the Japan sea back-arc basin. Palaeogeogr Palaeoclimatol Palaeoecol 286:164–170
Amano K, Jenkins RG, Sako Y et al (2013) A Paleogene deep-sea methane-seep community from Honshu, Japan. Palaeogeogr Palaeoclimatol Palaeoecol 387:126–133
Amano K, Jenkins RG, Ohara M et al (2014a) Miocene vesicomyid species (Bivalvia) from Wakayama in southern Honshu, Japan. Nautilus 128:9–17
Amano K, Saether KP, Little CTS et al (2014b) Fossil vesicomyid bivalves from Miocene hydrocarbon seep sites, North Island, New Zealanad. Acta Palaeontol Pol 59:421–428
Amano K, Little CTS, Campbell KA et al (2015) Paleocene and Miocene *Thyasira* sensu stricto (Bivalvia: Thyasiridae) from chemosynthetic communities from Japan and New Zealand. Nautilus 129:43–53
Amano K, Little CTS, Campbell KA (2018) Lucinid bivalves from Miocene hydrocarbon seep sites of eastern North Island, New Zealand, with comments on Miocene New Zealand seep faunas. Acta Palaeontol Pol 63:371–382
Amano K, Miyajima Y, Jenkins RG et al (2019) The Miocene to Recent biogeographic history of vesicomyid bivalves in Japan, with two new records of the family. Nautilus 133:48–56
Aoki T, Nishida T (1999) Chemosynthetic molluscan fauna from the basal part of the Middle Formation of the Taishu Group. Proc Nishinhon Branch Geol Soc Japan 114:19–20. [in Japanese]
Argentino C, Conti S, Crutchley GJ et al (2019) Methane-derived authigenic carbonates on accretionary ridges: Miocene case studies in the Northern Apennines (Italy) compared with modern submarine counterparts. Mar Pet Geol 102:860–872
Asai A, Hirano H (1990) Stratigraphy of the Upper Cretaceous of the Obira area, Northwestern Hokkaido. Gakujitsu Kekyu, School of Education, Waseda University, Series Biology and Geology 39:37–50 [in Japanese]
Ascher E (1906) Die Gastropoden, Bivalven und Brachiopoden der Grodischter Schichten. Beitr zur Paläontol Österreich-Ungarns und des Orients 19:135–167
Bang E, Nakrem HA, Little CTS et al (2022) Palynology of Early Cretaceous (Barremian to Aptian) hydrocarbon (methane) seep carbonates and associated mudstones, Wollaston Forland, Northeast Greenland. Acta Palaeobotanica 62:11–23
Baliński A, Biernat G (2003) New observations on rhynchonellid brachiopod *Dzieduszyckia* from the Famennian of Morocco. Acta Palaeontol Pol 48:463–474
Bangert B, Stollhofen H, Geiger M et al (2000) Fossil record and high resolution tephrostratigraphy of Carboniferous glaciomarine mudstones, Dwyka Group, southern Namibia. Commun Geol Surv Namibia 12:265–276
Barbieri R, Cavalazzi B (2005) Microbial fabrics from Neogene cold seep carbonates, Northern Apennine, Italy. Palaeogeogr Palaeoclimatol Palaeoecol 227:143–155
Barbieri R, Ori GG, Cavalazzi B (2005) A Silurian cold-seep ecosystem from the Middle Atlas, Morocco. Palaios 19:527–542
Beauchamp B, Savard M (1992) Cretaceous Chemosynthetic Carbonate Mounds in the Canadian Arctic. Palaios 7:434–450
Beauchamp B, Krouse HR, Harrison JC et al (1989) Cretaceous cold-seep communities and methane-derived carbonates in the Canadian Arctic. Science 244:53–56
Beets C (1942) Beiträge zur kenntnis der angeblich oberoligocänen Mollusken-Fauna der Insel Buton, Niederländisch-Ostindien. Leidsche Geol Meded 13:255–328
Beets C (1953) Reconsideration of the so-called Oligocene fauna in the asphaltic deposits of Buton (Malay Archipelago). Leidsche Geol Meded 17:237–258
Beisel AL (1983) Pozdniejurskije i ranniemielovyje gastropody seviera sredniej Sibirii. Trudy Instituta Geologii i Geofizyki ANSSSR 484:1–94
Belka Z (1998) Early Devonian Kess-Kess Carbonate mud mounds in the eastern Anti-Atlas (Morocco), and their relation to submarine hydrothermal venting. J Sediment Res 68:368–377

Berkowski B (2006) Vent and mound rugose coral associations from the Middle Devonian of Hamar Laghdad (Anti-Atlas, Morocco). Geobios 39:155–170
Berkowski B (2008) Emsian deep-water Rugosa assemblages of Hamar Laghdad (Devonian, Anti-Atlas, Morocco). Palaeontographica A 284:17–68
Biernat G (1957) On *Peregrinella multicarinata* (Lamarck)(Brachiopoda). Acta Palaeontol Pol 2:19–52
Biernat G (1967) New data on the genus *Dzieduszyckia* Siemiradzki, 1909 (Brachiopoda). Acta Palaeontol Pol 12:133–155
Birgel D, Peckmann J (2008) Aerobic methanotrophy at ancient marine methane seeps: a synthesis. Org Geochem 39:1659–1667
Birgel D, Peckmann J, Klautzch S et al (2006a) Anaerobic and aerobic oxidation of methane at Late Cretaceous seeps in the Western Interior Seaway, USA. Geomicrobiol J 23:565–577
Birgel D, Thiel V, Hinrichs K-U et al (2006b) Lipid biomarker patterns of methane-seep microbialites from the Mesozoic convergent margin of California. Org Geochem 37:1289–1302
Birgel D, Himmler T, Freiwald A et al (2008) A new constraint on the antiquity of anaerobic oxidation of methane: late Pennsylvanian seep limestones from southern Namibia. Geology 36:543–546
Bishop GA, Williams AB (2000) Fossil crabs from Tepee Buttes, submarine seeps of the Late Cretaceous Pierre Shale, South Dakota and Colorado, USA. J Crustac Biol 20:286–300
Blake DB, Halligan WK, Larson NL (2018) A new species of the asteroid genus *Betelgeusia* (Echinodermata) from methane seep settings, Late Cretaceous of South Dakota. J Paleontol 92(2):196–206
Blouet J-P, Imbert P, Foubert A (2017) Mechanisms of biogenic gas migration revealed by seep carbonate paragenesis, Panoche Hills, California. Am Assoc Pet Geol Bull 101:1309–1340
Blouet J-P, Imbert P, Ho S et al (2021a) What makes seep carbonates ignore self-sealing and grow vertically: the role of burrowing decapod crustaceans. Solid Earth 12:2439–2466
Blouet J-P, Wetzel A, Ho S (2021b) Fluid conduits formed along burrows of giant bivalves at the cold seep site, Southern Taiwan. Mar Petrol Geol 131:105123
Bojanowski MJ (2007) Oligocene cold-seep carbonates from the Carpathians and their inferred relation to gas hydrates. Facies 53:347–360
Boss KJ (1968) New species of Vesicomyidae from the Gulf of Darien, Caribbean Sea (Bivalvia, Mollusca). Bull Mar Sci 18:731–748
Boss KJ, Turner RD (1980) The giant while clam from the Galapagos Rift, *Calyptogena magifica* species novum. Malacologia 20:161–194
Buggisch W, Krumm S (2005) Palaeozoic cold seep carbonates from Europe and North Africa—integrated isotopic and geochemical approach. Facies 51:566–583
Campbell KA (1992) Recognition of Mio-Pliocene cold seep setting from the Northeast Pacific convergent margin, Washington, USA. Palaios 7:422–433
Campbell KA (2006) Hydrocarbon seep and hydrothermal vent paleoenvironments and paleontology: past developments and future research directions. Paleogeogr Paleoclimatol Palaeoecol 232:362–407
Campbell KA, Bottjer D (1993) Fossil cold seeps. Natl Geogr Res Explor 9:326–343
Campbell KA, Bottjer D (1995a) Brachiopods and chemosymbiotic bivalves in Phanerozoic hydrothermal vent and cold seep environments. Geology 23:321–324
Campbell KA, Bottjer D (1995b) *Peregrinella*: an Early Cretaceous cold-seep-restricted brachiopod. Paleobiology 21:461–478
Campbell KA, Farmer JD, Des Marais D (2002) Ancient hydrocarbon seeps from Mesozoic convergent margin of California: carbonate geochemistry, fluids and palaeoenvironments. Geofluids 2:63–94
Campbell KA, Nesbitt EA, Bourgeois J (2006) Signatures of storms, oceanic floods and forearc tectonism in marine shelf strata of the Quinault Formation (Pliocene), Washington, USA. Sedimentology 53:945–969

Campbell KA, Peterson DE, Alfaro AC (2008a) Two new species of *Retiskenea*? (Gastropoda: Neomphalidae) from Lower Cretaceous hydrocarbon-seep carbonates of Northern California. J Paleontol 82:140–153

Campbell KA, Francis DA, Collins M et al (2008b) Hydrocarbon seep-carbonates of Miocene forearc (East Coast Basin, New Zealand). Sed Geol 204:83–105

Capozzi R, Oppo D, Taviani M (2017) Cold seepages: an economic tool for hydrocarbon appraisal. Am Assoc Pet Geol Bull 101:617–623

Capozzi R, Negri A, Reitner J et al (eds) (2013) Carbonate Conduits Linked to Hydrocarbon-enriched Fluid Escape, Workshop and Field Seminar, Bologna, June 28th–July 1st, 2013. ISMAR, Bologna, 51 pp

Cavagna S, Clari P, Martire L (1999) The role of bacteria in the formation of cold seep carbonates: geological evidence from Monferrato (Tertiary, NW Italy). Sed Geol 126:253–270

Cavalazzi B (2006) Kess Kess carbonate mounds, Hamar Laghdad, Anti-Atlas. SE Morocco – Field Guide, UNESCO Field Action Guide, 19 pp

Cavalazzi B (2007) Chemotrophic filamentous microfossils from the Hollard Mound (Devonian, Morocco) as investigated by focus ion beam. Astrobiology 7:402–415

Cavalazzi B, Barbieri R, Ori GG (2007) Chemosynthetic microbialites in the Devonian carbonate mounds of Hamar Laghdad (Morocco). Sediment Geol 200:73–88

Cavalazzi B, Barbieri R, Cady SJ et al (2012) Iron framboids in the hydrocarbon-related Middle Devonian Hollard Mound of the Anti-Atlas mountain range in Morocco: evidence for potential microbial biosignatures. Sediment Geol 263–264:183–193

Cau S, Franchi F, Roveri M et al (2016) The Pliocene-age Stirone River hydrocarbon chemoherm complex (Northern Apennines, Italy). Mar Petrol Geol 66:582–595

Chien C-W, Huang C-Y, Chen Z et al (2012) Miocene shallow-marine cold seep carbonate in fold-and-thrust Western Foothills, SW Taiwan. J Asian Earth Sci 56:200–211

Chien C-W, Huang C-Y, Lee H-C et al (2013) Patterns and sizes of authigenic carbonate formation in the Pliocene foreland of southwestern Taiwan: implications of an ancient methane seep. Terr Atmospheric Ocean Sci 24:971–984

Chien C-W, Huang C-Y, Luo S-D et al (2018) Calcareous and agglutinated foraminifera ratio: Chemical interface tracer for Pliocene Chiahsien Paleoseep, SW Taiwan. Terr Atmospheric Ocean Sci 29:417–428

Clarke E de C, Prendergast KL, Teichert C et al (1951) Permian succession and structure in the northern part of the Irwin Basin, western Australia. J Royal Soc West Aust 35:31–84

Clari PA, Gagliardi C, Governa ME et al (1988) I Calcari di Marmorito: una testimonianza di processi diagenetici in presenza di metano. Boll Mus Reg Sci Nat Torino 5:197–216

Clari PA, Fornara L, Ricci B et al (1994) Methane-derived carbonates and chemosymbiotic communities of Piedmont (Miocene), Northern Italy: an update. Geo-Mar Lett 14:201–209

Clari P, Cavagna S, Martire L et al (2004a) A Miocene mud volcano and its plumbing system: a chaotic complex revisited (Monferrato, NW Italy). J Sedimenary Res 74:662–676

Clari P, Conti S, Fontana D et al (2004b) Fluid expulsion and authigenic products in the Miocene foredeep and satellite basins of the Northern Apennines, Italy. Field Guide Book-Post-Congress P07, 32nd IGC, August 20–28. Florence, Italy, 16 pp

Cochran JK, Landman NH, Larson NL et al (2015) Geochemical evidence (C and Sr isotopes) for methane seeps as ammonite habitats in the Late Cretaceous (Campanian) Western Interior Seaway. Swiss J Paleontol 134:153–165

Collom CJ, Johnston PA (2000) Late Cretaceous seep facies in the Western Interior of Canada and the United States: iron ooids, carbonate mounds, and associated tectonism. In: Program with extended abstracts (CD), GeoCanada 2000 Millenium Geoscience Summit, University of Calgary, Alberta, 29 May–2 June 2000

Conti S, Fontana D (1998) Recognition of primary and secondary Miocene lucinid deposits in the Apennine chain. Mem Sci Geol 50:101–131

Conti S, Fontana D (2002) A pelitic interval enclosing primary chemoherms in the M. Cervarola Formation (Northern Apennines): Evidence for synsedimentary tectonics during the Miocene. Boll Soc Geol Ital 1:499–508

Conti S, Fontana D (2011) Possible relationships between seep carbonates and gas hydrates in the Miocene of the Northern Apennines. J Geol Res 2011:20727
Conti S, Fontana D, Gubertini A (2004) A multidisciplinary study of middle Miocene seep-carbonates from the northern Apennine foredeep (Italy). Sed Geol 169:1–19
Conti S, Fontana D, Lucente CC (2008) Sedimentary filling of a wedge-top basin and relationship with a foredeep (Middle Miocene, Marnoso-arenacea Formation, northern Apennines). Facies 54:479–498
Conti S, Fontana D, Mecozzi S et al (2010) Late Miocene seep-carbonates and fluid migration on top of the Montepetra intrabasinal high (Northern Apennines, Italy): relations with synsedimentary folding. Sed Geol 231:41–54
Conti S, Fontana D, Lucente CC et al (2014) Relationships between seep-carbonates, mud volcanism and basin geometry in the Late Miocene of the northern Apennines of Italy: the Montardone mélange. Int J Earth Sci 103:281–295
Conti S, Fioroni C, Fontana D (2017) Correlating shelf carbonate evolutive phases with fluid expulsion episodes in the foredeep (Miocene, northern Apennines, Italy). Mar Pet Geol 71:351–359
Conti S, Argentino C, Fioroni C et al (2021) Miocene seep carbonates of the northern Apennines (Emilia to Umbria, Italy): An overview. Geosciences 11:53
Cooke CW (1919) Contributions to the geology and paleontology of West Indies IV. Tertiary mollusks from the leeward islands and Cuba. Carnegie Inst Wash Publ 291:103–156
Dalseg TS, Nakrem HA, Smelror M (2016) Organic-walled microfossils and palynodebris in cold seep carbonate deposits: The upper Jurassic–Lower Cretaceous Agardhfjellet Formation on Svalbard (Arctic Norway). Nor J Geol 96:1–12
Danner WR (1966) Limestone resources of Western Washington. Wash Div Min Geol Bull 52:1–474
Darton NH (1902) Oelrichs folio: South Dakota–Nebraska. United States Geologic Survey Geologic Atlas of the United States 85. United States Geological Survey, Reston, Virginia
Darton NH (1919) Newell folio: South Dakota. United States Geological Survey Geologic Atlas of the United States 209. United States Geological Survey, Reston, Virginia
David W., Haig Antoine, Dillinger Geoffrey, Playford Rosine, Riera Aleksey, Sadekov Grzegorz, Skrzypek Eckart, Håkansson Arthur J., Mory Daniel, Peyrot Charmaine, Thomas (2022) Methane seeps following Early Permian (Sakmarian) deglaciation interior East Gondwana Western Australia: Multiphase carbonate cements distinct carbon-isotope signatures extraordinary biota. Palaeogeography Palaeoclimatology Palaeoecology 591110862-10.1016/j.palaeo.2022.110862
De Boever E, Swennen R, Dimitrov L (2006) Lower Eocene carbonate-cemented “chimney” structures (Varna, Bulgaria)—Control of seepage rates on their formation and stable isotopic signatures. J Geochem Explor 89:78–82
De Boever E, Birgel D, Thiel V et al (2009a) The formation of giant tubular concretions triggered by anaerobic oxidation of methane as revealed by archaeal molecular fossils (Lower Eocene, Varna, Bulgaria). Palaeogeogr Palaeoclimatol Palaeoecol 280:23–36
De Boever E, Huysmans M, Muchez P et al (2009b) Controlling factors on the morphology and spatial distribution of methane-related tubular concretions – Case study of an Early Eocene seep system. Mar Pet Geol 26:1580–1591
De Boever E, Birgel D, Muchez P et al (2011a) Fabric and formation of grapestone concretions within an unusual ancient methane seep system (Eocene, Bulgaria). Terra Nova 23:56–61
De Boever E, Muchez P, Swennen R et al (2011b) Evolution of deformation and fault-related fluid flow within an ancient methane-seep system (Eocene, Varna, Bulgaria). Geofluids 11:166–183
Easton WH, Imlay RW (1955) Upper Jurassic fossil localities in Franciscan and Knoxville Formations in southern California. Am Assoc Pet Geol Bull 39:2336–2340
Elder WP, Miller JW (1993) Map and checklists of Jurassic and Cretaceous macrofossil localities within the San Jose 1:100, 000 quadrangle, California, and discussion of paleontological results. US Geol Surv Open-File Rep 93–503:1–49
Elias MK (1933) Cephalopods of the Pierre Formation of Wallace County, Kansas, and adjacent area. Univ Kansas Sci Bull 21(9):289–363

Eriksson A (2002) Stratigraphy, structure and natural gas potential of Tertiary Sedimentary and Volcanic Units, Clatskanie 7.5-minute Quadrangle, Northwest Oregon. MSc thesis, Oregon State University, 215 pp.

Feist R, Belka Z (2018) Late Emsian (Devonian) trilobite communities from the Kess-Kess mounds, Hamar Laghdad, Morocco. Neues Jahrb Geol Palaontol Abh 290:277–290

Fontana D, Conti S, Fioroni C et al (2013) Evidence of climatic control on hydrocarbon seepage in the Miocene of northern Apennines: The case study of the Vicchio Marls. Mar Pet Geol 48:90–99

Franchi F, Cavalazzi B, Pierre C (2015) New evidence of hydrothermal fluid circulation at the Devonian Kess-Kess mounds, Hamar Laghdad, Morocco. Geol J 50:634–650

Futakami M, Ito M, Matsukawa M (2001) Conglomerates with vesicomyid Bivalvia (*Calyptogena*) of the Shiramazu Formation of the Chikura Group in Shirahama, Chiba—An example of mud diapirs. J Geol Soc Japan 107:611–619. [in Japanese with English abstract]

Gaillard C, Rolin Y (1986) Paléobiocenoses susceptibles d'être liées à des sources sous-marines en milieu sédimentaire. L'exemple des Terres Noires (SE France) et des tepee buttes de la Pierre Shale Formation (Colorado, USA). CR Acad Sci II 303:1503–1508

Gaillard C, Rolin Y (1988) Rélation entre tectonique synsédimentaire et pseudobiohermes (Oxfordien de Beauvoisen – Drôme – France). Un argument supplémentaire pour interpréter les pseudobiohermes comme formés au droit de sources sous-marines. CR Acad Sci II II 307:1265–1270

Gaillard C, Bourseau JP, Boudelle M et al (1985) Les pseudobiohermes de Beauvoisin (Drôme): Un site hydrothermal sur la marge téthysienne à l'Oxfordien? Bull Soc Géol Fr 1:69–78

Gaillard C, Rio M, Rolin Y et al (1992) Fossil chemosynthetic communities related to vents and seeps in sedimentary basins: the pseudobioherms of southeastern France compared to other world examples. Palaios 7:451–465

Gaillard C, Néraudeau D, Thierry J (2011) *Tithonia oxfordiana*, a new irregular echinoid associated with Jurassic seep deposits in south-east France. Palaeontology 54:735–752

Gay A, Favier A, Potevin J-L et al (2020) Poly-phased fluid flow in the giant fossil pockmark of Beavoisin, SE Basin of France. BSGF – Eart Sci B 191:35

Georgieva MN, Little CTS, Watson JS et al (2019) Identification of fossil worm tubes from Phanerozoic hydrothermal vents and cold seeps. J Syst Palaeontol 17:287–329

Gilbert GK (1897) Pueblo folio: Colorado. United States Geological Survey Geologic Atlas of the United States 36. United States Geologic Survey, Reston, Virginia

Gilbert GK, Gulliver FR (1895) Tepee Buttes. Geol Soc Am Bull 6:333–342

Gill JR, Cobban WA (1966) The Red Bird section of the Upper Cretaceous Pierre Shale in Wyoming. US Geol Surv Prof Pap 393-A:1–73

Gill FL, Little CTS (2013) A new genus of lucinid bivalve from hydrocarbon seeps. Acta Palaeontol Pol 58:573–578

Gill FL, Harding IC, Little CTS et al (2005) Palaeogene and Neogene cold seep communities in Barbados, Trinidad and Venezuela: an overview. Palaeogeogr Palaeoclimatol Palaeoecol 227:191–209

Gischler E, Sandy MR, Peckmann J (2003) *Ibergirhynchia contraria* (F.A. Roemer, 1850), an Early Carboniferous seep-related rhynchonellide brachiopod from the Harz Mountains, Germany—a possible successor to *Dzieduszyckia*? J Paleontol 77:293–303

Goedert JL, Benham SR (1999) A new species of *Depressigyra*? (Gastropoda: Peltospiridae) from cold-seep carbonates in Eocene and Oligocene rocks of Western Washington. Veliger 42:112–116

Goedert JL, Benham SR (2003) Biogeochemical processes at ancient methane seeps: the Bear River site in southwestern Washington. In: Swanson TW (ed) Western Cordillera and adjacent areas. Geological Society of America Field Guide, Boulder, Colorado, vol. 4, pp 201–208

Goedert JL, Campbell KA (1995) An Early Oligocene chemosynthetic community from the Makah Formation, northwestern Olympic Peninsula, Washington. Veliger 38:22–29

Goedert JL, Kaler KL (1996) A new species of *Abyssochrysos* (Gastropoda: Loxonematoidea) from a middle Eocene cold-seep carbonate in the Humptulips Formation, western Washington. Veliger 39:65–70

Goedert JL, Kiel S (2016) A lower jaw of the nautiloid *Aturia angu*stata (Conrad, 1849) from Oligocene cold seep limestone, Washington State, U.S.A. PaleoBios 33:1–6

Goedert JL, Peckmann J (2005) Corals from deep-water methane-seep deposits in Paleogene strata of western Oregon and Washington, USA. In: Freiwald A, Robert JM (eds) Cold-water corals and ecosystems. Springer, Berlin, pp 27–40

Goedert JL, Squires RL (1990) Eocene deep-sea communities in localized limestones formed by subduction-related methane seeps, southwestern Washington. Geology 18:1182–1185

Goedert JL, Squires RL (1993) First Oligocene record of *Calyptogena* (Bivalvia: Vesicomyidae). Veliger 36:72–77

Goedert J, Peckmann J, Reitner J (2000) Worm tubes in an allochthonous cold-seep carbonate from Lower Oligocene rocks of western Washington. J Paleontol 74:992–999

Goedert JL, Thiel V, Schmale O et al (2003) The Late Eocene 'Whiskey Creek' Methane-Seep Deposit (Western Washington State) Part I: Geology, Palaeontology and Molecular Geobiology. Facies 48:223–240

Goedert JL, Peckmann J, Benham SR et al (2013) First record of the Eocene pteropod *Heliconoides nitens* (Gastropoda: Thecosomata: Limnacinidae) from the Pacific Basin. Proc Biol Soc Wash 126:72–82

Gómez-Pérez I (2001) Estromatolitos de aguas profundas en la Formación Los Molles (Neuquén, Argentina): ¿chimeneas de metano en le fondo marino jurasico? Rev Asoc Argent Sedimentol 8:1–14

Gómez-Pérez I (2003) An Early Jurassic deep-water stromatolitic bioherm related to possible methane seepage (Los Molles Formation, Neuquén, Argentina). Palaeogeogr Palaeoclimatol Palaeoecol 201:21–49

Grillenzoni C, Monegatti P, Turco E et al (2017) Paleoenvironmental evolution in a high-stressed cold-seep system (Vicchio Marls, Miocene, northern Apennines, Italy). Palaeogeogr Palaeoclimatol Palaeoecol 487:37–50

Guzhov AV (2017) On new Jurassic Rissooidea and Zygopleuroidea convergently similar to them (Gastropoda: Pectinibranchia). Paleontol J 51:1375–1394

Hagemann A, Leefman T, Peckmann J et al (2013) Biomarkers from individual carbonate phases of an Oligocene cold-seep deposit, Washington State, USA. Lethaia 46:7–18

Hägg R (1925) A new Teritary fauna from Spitsbergen. Bull Geol Inst Univ Uppsala 20:39–55

Haig DW, Dillinger A, Playford G et al (2022) Methane seeps following Early Permian (Sakmarian) deglaciation, interior East Gondwana, Western Australia: Multiphase carbonate cements, distinct carbon-isotope signatures, extraordinary biota. Paleogeogr Paleoclimatol Palaeoecol 591:110862

Hammer Ø, Nakrem HA, Little CTS et al (2011) Hydrocarbon seeps from close to the Jurassic–Cretaceous boundary, Svalbard. Palaeogeogr Palaeoclimatol Palaeoecol 306:15–26

Hammer Ø, Hryniewicz K, Hurum JH et al (2013) Large onychites (cephalopod hooks) from Upper Jurassic of Boreal Realm. Acta Palaeontol Pola 58:827–835

Harding IC (1998) Miocene cold seep faunas and carbonates from Barbados. Cah Biol Mar 39:341–344

Harvey JL (1959) A geologic reconnaissance in the southwestern Olympic Peninsula. MSc thesis, University of Washington, 53 pp

Hashimoto W, Nagao S, Kanno S et al (1967) Geology and underground resources of Nakagawa-cho, Hokkaido. Nakagawa-cho, Nakagawa, 48 pp. [in Japanese]

Hepper K (2004) A new hydrocarbon seep locality in the Mesozoic Great Valley Group, Guenoc Ranch, northern California. San Francisco State University, San Francisco, MSc Thesis, 154 pp

Hepper K, Whyte L, Campbell KA (2003) Isotopic analysis of a new cold seep locality, Guenoc Ranch, Great Valley Group, Northern California. EOS Fall Meeting Supplement 84:F310

Hickman CS (1980) Paleogene marine gastropods of the Keasey Formation in Oregon. Bull of Am Paleontol 78:1–112
Hickman CS (2015) Paleogene marine bivalves of the deep-water Keasey Formation in Oregon, part III: The heteroconchs. PaleoBios 32:1–44
Hikida Y, Suzuki S, Togo Y et al (2003) An exceptionally preserved fossil seep community from the Yezo Group in the Nakagawa area, Hokkaido, Japan. Paleontol Res 7:329–342
Himmler T, Freiwald A, Stollhofen H et al (2008) Late Carboniferous hydrocarbon seep carbonates from the glaciomarine Dwyka Group, southern Namibia. Palaeogeogr Palaeoclimatol Palaeoecol 257:185–197
Hirata D, Matsushima Y, Asaga S (1991) Distributions and mode of occurrences of fossil *Calyptogena* in Miura and Boso Peninsulas. Chikyu Montly 139:47–52 [in Japanese, title translated]
Howe B (1987) Tepee Buttes: a petrological, paleontological, paleoenvironmental study of Cretaceous submarine spring deposits. MSc thesis, University of Colorado, 217 pp
Howe B, Kauffman EG (1986) Tepee Buttes, late Campanian submarine springs and the biofacies, between Colorado Springs and Boone, Colorado. In: Kauffman EG (ed), Cretaceous biofacies of the central part of the Western Interior Seaway: a field guidebook. 4th North American Paleontological Convention, University of Colorado, Boulder, pp 155–175
Hryniewicz K, Hammer Ø, Nakrem HA et al (2012) Microfacies of the Volgian–Ryazanian (Jurassic–Cretaceous) hydrocarbon seep carbonates from Sassenfjorden, central Spitsbergen, Svalbard. Nor J Geol 92:113–131
Hryniewicz K, Little CTS, Nakrem HA (2014) Bivalves from the latest Jurassic–earliest Cretaceous hydrocarbon seep carbonates from central Spitsbergen, Svalbard. Zootaxa 3859:1–66
Hryniewicz K, Hagström J, Hammer Ø et al (2015a) Late Jurassic–Early Cretaceous hydrocarbon seep boulders from Novaya Zemlya and their faunas. Palaeogeogr Palaeoclimatol Palaeoecol 436:231–244
Hryniewicz K, Nakrem HA, Hammer Ø et al (2015b) Palaeoecology of the latest Jurassic–earliest Cretaceous hydrocarbon seep carbonates from Spitsbergen, Svalbard. Lethaia 48:353–374
Hryniewicz K, Bitner MA, Durska E et al (2016) Paleocene methane seep and wood-fall marine environments from Spitsbergen, Svalbard. Palaeogeogr Palaeoclimatol Palaeoecol 462:41–56
Hryniewicz K, Amano K, Jenkins RG et al (2017a) Thyasirid bivalves from Cretaceous and Paleogene cold seeps. Acta Palaeontol Pol 62:705–728
Hryniewicz K, Jakubowicz M, Belka Z et al (2017b) New bivalves from Middle Devonian methane seep in Morocco: the oldest record of repetitive shell morphologies among some seep bivalve molluscs. J Syst Palaeontol 15:19–41
Hryniewicz K, Amano K, Bitner MA et al (2019) A late Paleocene fauna from shallow-water chemosynthesis-based ecosystems, Spitsbergen, Svalbard. Acta Paleontol Pol 64:101–141
Hryniewicz K, Miyajima Y, Amano K et al (2021) Formation, diagenesis and fauna of cold seep carboanates from the Miocene Taishu Group of Tsushima (Japan). Geol Mag 158:964–984
Hunter AW, Larson NL, Landman NH et al (2016) A new crinoid from cold methane seep deposits in the Upper Cretaceous Pierre Shale. J Paleontol 90:506–524
Hybertsen F, Kiel S (2018) A middle Eocene seep deposit with silicified fauna from the Humptulips Formation in western Washington State, USA. Acta Palaeontol Pol 63:751–768
Ikeda K, Majima R, Wada H et al (2003) A cold seep assemblage from the Takanabe Formation, Miyazaki Group, Kyushu, Japan. Fossils 73:1–2. [In Japanese]
Imlay RW (1964) Middle and Upper Jurassic fossils from Southern California. J Paleontol 38:505–509
Imlay RW (1980) Jurassic palaeobiogeography of the conterminous United States and its continental setting. Geol Sur Prof Pap 1062:1–134
Isaji S (2013) *Adulomya* from the Miocene Aokiyama Formation, Hota Group, in the Boso Peninsula, Japan. Paleontol Res 17:196–199
Ishimura T, Ijiri A, Abe K et al (2005) Characteristics of calcareous concretions with *Calyptogena* sp. in the Miocene Morai Formation, Hokkaido. J Geol Soc Japan 111:VII–VIII [in Japanese]

Jakubowicz M, Berkowski B, Belka Z (2013) Devonian rugose coral '*Amplexus*' and its relations to submarine fluid seepage. Palaeogeogr Palaeoclimatol Palaeoecol 386:180–193

Jakubowicz M, Dopieralska J, Belka Z (2015) Tracing the composition of original fluids at the ancient hydrocarbon seep (Hollard Mound, Middle Devonian, Morocco): a Nd, REE and stable isotope study. Geochim Cosmochim Acta 156:50–74

Jakubowicz M, Hryniewicz K, Belka Z (2017) Mass-occurrence of seep-specific bivalves in the oldest-known cold seep metazoan community. Sci Rep 7:14292

Jakubowicz M, Dopieralska J, Kaim A et al (2019) Nd isotope composition of seep carbonates: Towards a new approach for constraining subseafloor fluid circulation at hydrocarbon seeps. Chem Geol 503:40–51

Jakubowicz M, Kiel S, Goedert JL et al (2020) Fluid expulsion system and tectonic architecture of the incipient Cascadia convergent margin as revealed by Nd, Sr and stable isotope composition of mid-Eocene methane seep carbonates. Chem Geol 558:119872

Jakubowicz M, Agirrezabala L, Dopieralska J et al (2021) The role of magmatism in hydrothermal generation in sedimented rifts: a Nd isotope perspective from mid-Cretaceous methane-seep deposits of the Basque-Cantabrian Basin, Spain. Geochim Cosmochim Acta 303:223–248

Jakubowicz M, Agirrezabala L, Belka Z et al (2022) Sr–Nd isotope decoupling at Cretaceous hydrocarbon seeps of Basque-Cantabrian Basin (Spain): Implications for tracing volcanic-influenced fluids in sedimented rifts. Mar Pet Geol 135:105430

Janssen AW (1999) Euthecosomatous gastropods (Mollusca: Heterobranchia) from Buton (SE Sulawesi, Indonesia) with notes on species from Viti Levu, Fiji: systematics, biostratigraphy. Neth J Geosci 78:179–189

Jenkins RG, Kaim A, Hikida Y (2007a) Antiquity of substrate choice among acmaeid limpets from Late Cretaceous chemosynthesis-based communities. Acta Paleontol Pol 52:369–373

Jenkins RG, Kaim A, Hikida Y et al (2007b) Methane flux dependent lateral faunal changes in a Late Cretaceous chemosymbiotic assemblage in the Nakagawa area of Hokkaido, Japan. Geobiology 5:127–139

Jenkins RG, Hikida Y, Chikaraishi Y et al (2008) Microbially induced formation of ooid-like coated grains in the Late Cretaceous methane-seep deposit of the Nakagawa area, Hokkaido, northern Japan. Island Arc 17:261–269

Jenkins RG, Kaim A, Little CTS et al (2013) Worldwide distribution of modiomorphid bivalve genus *Caspiconcha* in late Mesozoic hydrocarbon seeps. Acta Palaeontol Pol 58:357–382

Jenkins RG, Hasegawa T, Haggart JW et al (2017) Cool eastern rim of the North Pacific during Late Cretaceous time: a seep carbonate paleothermometry from the Nanaimo Group, British Columbia, Canada. Palaeogeogr Palaeoclimatol Palaeoecol 487:407–415

Jenkins RG, Kaim A, Hikida Y et al (2018) Four new species of Jurassic to Cretaceous seep-restricted bivalve *Caspiconcha* and implications for the history of chemosynthetic communities. J Paleontol 92:596–610

Johannson GC, Smith PL, Gordey SP (1997) Early Jurassic evolution of the northern Stikinian arc: evidence from the Laberge Group, northwestern British Columbia. Can J Earth Sci 3:1030–1057

Joseph C, Torres ME, Martin RA et al (2012) Using the $^{87}Sr/^{86}Sr$ of modern paleoseep carbonates from northern Cascadia to link modern fluid flow to the past. Chem Geol 334:122–130

Joseph C, Campbell KA, Torres ME et al (2013) Methane-derived authigenic carbonates from modern and paleoseeps on the Cascadia margin: mechanisms of formation and diagenetic signals. Palaeogeogr Palaeoclimatol Palaeoecol 390:52–67

Karasawa H (2011) New axiidean Decapoda from the Albian (Lower Cretaceous) chemosynthetic community from Hokkaido, Japan. Bull Mizun Fossil Mus 37:27–29

Kaim A, Kelly SRA (2009) Mass occurrence of hokkaidoconchid gastropods in the Upper Jurassic methane seep carbonate from Alexander Island, Antarctica. Antarct Sci 21:279–284

Kaim A, Beisel AL, Kurushin NI (2004) Mesozoic gastropods from Siberia and Timan (Russia). Part 1: Vetigastropoda and Caenogastropoda (exclusive of Neogastropoda). Pol Polar Res 25:241–266

Kaim A, Jenkins RG, Warén A (2008a) Provannid and provannid-like gastropods from Late Cretaceous cold seeps of Hokkaido (Japan) and the fossil record of the Provannidae (Gastropoda: Abyssochrysoidea). Zool J Linn Soc 154:421–436

Kaim A, Kobayashi Y, Echizenya H et al (2008b) Chemosynthesis-based associations on Cretaceous plesiosaurid carcasses. Acta Paleontol Pol 53:97–104

Kaim A, Jenkins RG, Hikida Y (2009) Gastropods from Late Cretaceous Omagari and Yasukawa hydrocarbon seep deposits in the Nakagawa area, Hokkaido, Japan. Acta Paleontol Pol 54:463–490

Kaim A, Skupien P, Jenkins RG (2013) A new Lower Cretaceous hydrocarbon seep locality from the Czech Carpathians at its fauna. Palaeogeogr Palaeoclimatol Palaeoecol 390:42–51

Kaim A, Jenkins RG, Tanabe K et al (2014) Mollusks from late Mesozoic seep deposits, chiefly in California. Zootaxa 3861:401–440

Kaim A, Jenkins RG, Parent H et al (2015a) Early Jurassic seep from Argentina displays faunal composition of modern aspect. In: Abstract volume, Jahrestagung der Paläontologischen Gesellschaft, 14–16 September 2015, Schiffweiler-Reden, Germany

Kaim A, Jenkins R, Parent H et al (2015b) The earliest mollusc dominated seep fauna from the Early Jurassic of Argentina. Geophysical Research Abstracts 17, EGU 2015–13280

Kaim A, Jenkins R, Hryniewicz K et al (2016) Early Mesozoic seeps and the advent of modern seep faunas. 1st International Workshop on Ancient hydrocarbon seep and cognate communities 2016, Warsaw, Poland, book of abstracts: 20

Kaim A, Hryniewicz K, Little CTS et al (2017) Gastropods from the Late Jurassic–Early Cretaceous seep deposits in Spitsbergen, Svalbard. Zootaxa 4329:351–374

Kanie Y, Kuramochi T (1995) *Acharax yokosukensis* n. sp. (gigantic Bivalve) from the Miocene Hayama Formation of the Miura Peninsula, south-central Japan. Sci Rep Yokosuka City Mus 43:51–57

Kanie Y, Kuramochi T (1996) Description of possibly chemosynthetic bivalves from the Cretaceous deposits of Obira-cho, northwestern Hokkaido. Sci Rep Yokosuka City Mus 44:63–68

Kanie Y, Kuramochi T (2001) Two new species of Vesicomyidae (Bivalvia: Mollusca) from the Pliocene Shiramazu Formation of the Chikura Group in the Boso Peninsula, Japan. Sci Rep Yokosuka City Mus 48:1–9

Kanie Y, Sakai T (1997) Chemosynthetic thraciid bivalve *Nipponothracia*, gen. nov. from the Lower Cretaceous and Middle Miocene Mudstones in Japan. Venus 56:205–220

Kanie Y, Asami M, Okada H et al (1992a) White clam community discovered from fractured claystone of the Miocene Hayama Group, Miura Peninsula, south-central Japan. Sci Rep Yokusuka City Mus 39:31–35. [in Japanese]

Kanie Y, Hattori M, Sasahara Y (1992b) Two types of white clam communities in Sagami Bay, central Japan: geologic settings and the Tertiary records in the Miura and Boso Peninsula. Sci Rep Yokusuka City Mus 40:37–43

Kanie Y, Yoshikawa Y, Sakai T et al (1993) The Cretaceous chemosynthetic cold-water dependant molluscan community discovered from Mikasa City, central Hokkaido. Sci Rep Yokusuka City Mus 41: 31–36[in Japanese]

Kanie Y, Yoshikawa Y, Sakai T et al (1996) Cretaceous chemosynthetic fauna from Hokkaido. Sci Rep Yokosuka City Mus 44:69–74

Kanie Y, Hattori M, Kuramochi T et al (1997) Two vesicomyid Bivalvia from the Shiramazu Formation of the Chikura Group in the southernmost part of the Boso Peninsula. J Geol Soc Japan 103:794–797. [in Japanese]

Kanie Y, Kuramochi T, Kanno S et al (1999) New occurrence and the shell form of the of the Middle Miocene *Acharax gigas* (Bivalvia: Solemyidae) in Gunma Prefecture. Bull Gunma Mus Nat Hist 3:17–23

Kanno S, Ogawa H (1964) Molluscan fauna from the Momijiyama and Takinoue districts, Hokkaido, Japan. Sci Rep Tokyo Kyoiku Daigaku, C 8:269–294

Kanno S, Tanaka K, Koike H et al (1998) *Adulomya uchimuraensis* Kuroda (Bivalvia) from the Middle Miocene Bessho Formation in Shiga-mure, Nagano Prefecture, Japan. Res Rep Shinshushinmachi Fos Mus 1:17–28

Karasawa H, Kano M (2021) A first notice of the goniodromitid crab from the Cenomanian (Upper Cretaceous) cold seep deposit of Hokkaido, Japan, with the redescription of *Sabellidromites inflata* (Collins and Karasawa, 1993) (Decapoda: Goniodromitidae). B Soc Geol Mexic 73:A020121

Kase T, Isaji S, Aguilar Y et al (2019) A large new *Wareniconcha* (Bivalvia: Vesciomyidae) from a Pliocene methane seep deposit in Leyte, Philippines. Nautilus 133:26–30

Kato M (2019) Crinoids lived around the Cretaceous seeps: the second example from cold-seep deposit in the Yezo Group in Hokkaido, Japan. Zoosymposia 15:88–97

Kato M, Oji T, Shirai K (2017) Paleoecology of echinoderms in cold seep environments revealed by isotope analysis in the Late Cretaceous Western Interior Seaway. Palaios 32:218–230

Katto J, Hattori M (1964) Some Veneridae from the Shimantogawa Group in the Outer Zone of Shikoku, Japan. Res Rep Kochi Univ 52:1–24

Katto J, Masuda K (1978) Tertiary mollusca from southern part of Kii Peninsula, Wakayama Prefecture, southwest Japan. Res Repo Kochi Univ Nat Sci 27:97–111

Kauffman EG (1967) Cretaceous *Thyasira* from the western interior of North America. Smith Misc Coll 151:1–159

Kauffman EG, Arthur MA, Howe B et al (1996) Widespread venting of methane-rich fluids in Late Cretaceous (Campanian) submarine springs (Tepee Buttes), Western Interior Seaway, U.S.A. Geology 24:799–802

Keenan KE (2010) Hydrocarbon seeps of the Mesozoic Great Valley Forearc Strata and Franciscan Complex, Northern and Central California, USA. Unpublished PhD Thesis, University of California, Riverside, 247 pp

Kelly SRA, Ditchfield PW, Doubleday PA et al (1995) An Upper Jurassic methane-seep limestone from the Fossil Bluff Group forearc basin of Alexander Island, Antarctica. J Sediment Res A65:274–282

Kelly SRA, Blanc E, Price SP et al (2000) Early Cretaceous giant bivalves from seep-related limestone mounds, Wollaston Forland, Northeast Greenland In: Harper EM, Taylor JD, Crame JA (ed), The Evolutionary Biology of Bivalvia. Geological Society of London Special Publication 177, The Geological Society, London, pp. 227–246

Kiel S (2006) New records and species of molluscs from Tertiary cold-seep carbonates in Washington State, USA. J Paleontol 80:121–137

Kiel S (2007) Status of the enigmatic fossil vesciomyid bivalve *Pleurophopsis*. Acta Palaeont Pol 52:639–642

Kiel S (2008a) An unusual new gastropod from an Eocene hydrocarbon seep in Washington. J Paleontol 82:188–191

Kiel S (2008b) Parasitic polychaetes in the Early Cretaceous hydrocarbon seep-restricted brachiopod *Peregrinella multicarinata*. J Paleontol 82:1215–1217

Kiel S (2010a) On the potential generality of depth-related ecologic structure in cold-seep communities: Evidence from Cenozoic and Mesozoic examples. Palaeogeogr Palaeoclimatol Palaeoecol 295:245–257

Kiel S (2010b) An Eldorado for palaeontologists: the Cenozoic seeps of western Washington State, USA. In: Kiel S (ed) The vent and seep biota. Springer, Heidelberg, pp 433–448

Kiel S (2013) Lucinid bivalves from ancient methane seeps. J Molluscan Stud 79:346–363

Kiel S (2018) Three new bivalve genera from Triassic hydrocarbon seep deposits in southern Turkey. Acta Paleontol Pol 63:221–234

Kiel S, Amano K (2010) Oligocene and Miocene vesicomyid bivalves from the Katalla District, Southern Alaska. Veliger 51:76–84

Kiel S, Amano K (2013) The earliest bathymodiolin mussels: an evaluation of Eocene and Oligocene taxa from deep-sea methane seep deposits in western Washington State, USA. J Paleontol 87:589–602

Kiel S, Campbell KA (2005) *Lithomphalus enderlini* gen. et sp. nov. from cold-seep carbonates in California—a Cretaceous neomphalid gastropod? Palaeogeogr Palaeoclimatol Palaeoecol 227:232–241
Kiel S, Goedert JL (2007) New mollusks associated with biogenic substrates in Cenozoic deep-water sediments of Washington State. Acta Palaeontol Pol 52:41–52
Kiel S, Hansen B (2015) Cenozoic methane-seep faunas of the Caribbean Region. PLoS ONE:e0140788
Kiel S, Peckmann J (2007) Chemosymbiotic bivalves and stable carbon isotopes indicate hydrocarbon seepage at four unusual Cenozoic fossil localities. Lethaia 40:345–357
Kiel S, Peckmann J (2008) Paleoecology and evolutionary significance of an Early Cretaceous *Peregrinella*-dominated hydrocarbon seep deposit on the Crimean Peninsula. Palaios 23:751–759
Kiel S, Peckmann J (2019) Resource partitioning among brachiopods and bivalves at ancient hydrocarbon seeps: a hypothesis. PLoS ONE 14:e0221887
Kiel S, Taviani M (2017) Chemosymbiotic bivalves from Miocene methane-seep carbonates in Italy. J Paleontol 91:444–466
Kiel S, Taviani M (2018) Chemosymbiotic bivalves from the late Pliocene Stirone River hydrocarbon seep complex in northern Italy. Acta Palaeontol Pol 63:557–568
Kiel S, Campbell KA, Elder WP et al (2008a) Jurassic and Cretaceous gastropods from hydrocarbon seeps in forearc basin and accretionary prism settings, California. Acta Palaeontol Pol 53:679–703
Kiel S, Amano K, Jenkins RG (2008b) Bivalves from Cretaceous cold-seep deposits on Hokkaido, Japan. Acta Paleontol Pol 53:525–537
Kiel S, Campbell KA, Gaillard C (2010) New and little known mollusks from ancient chemosynthetic environments. Zootaxa 2390:26–48
Kiel S, Wiese F, Titus A (2012) Shallow-water methane-seep faunas in the Cenomanian Western Interior Seaway: no evidence for onshore-offshore adaptations to deep-sea vents. Geology 40:839–842
Kiel S, Peckmann J, Simon K (2013a) Catshark egg capsules from a Late Eocene deep-water methane-seep deposit in Western Washington State, USA. Acta Palaeontol Pol 58:77–84
Kiel S, Birgel D, Campbell KA et al (2013b) Cretaceous methane-seep deposits from New Zealand and their fauna. Palaeogeogr Palaeoclimatol Palaeoecol 390:17–34
Kiel S, Glodny J, Birgel D (2014a) The paleoecology, habitats, and stratigraphic range of the enigmatic Cretaceous brachiopod *Peregrinella*. PLoS ONE 9:e109260
Kiel S, Hansen C, Nitzsche KN et al (2014b) Using $^{87}Sr/^{86}Sr$ Ratios to date fossil methane seep deposits: methodological requirements and an example from the Great Valley Group, California. J Geol 122:353–366
Kiel S, Amano K, Jenkins RG (2016) Predation scar frequencies in chemosymbiotic bivalves at an Oligocene seep deposit and their potential relation to inferred sulfide tolerances. Palaeogeog Palaeoclimatol Palaeoecol 453:139–145
Kiel S, Krystyn L, Demirtaş F et al (2017) Late Triassic mollusc-dominated hydrocarbon-seep deposits from Turkey. Geology 45:751–754
Kiel S, Sami M, Taviani M (2018) A serpulid-*Anodontia*-dominated methane-seep deposit from the upper Miocene of northern Italy. Acta Palaeontol Pol 63:569–577
Kiel S, Altamirano A, Birgel D et al (2019) Fossiliferous methane seep deposits from the Cenozoic Talara Basin in northern Peru. Lethaia 53:166–182
Kiel S, Hybertsen F, Hyžný M et al (2020a) Mollusks and a crustacean from early Oligocene methane-seep deposits in the Talara Basin, northern Peru. Acta Palaeontol Pol 65:109–138
Kiel S, Aguilar YM, Kase T (2020b) Mollusks from Pliocene and Pleistocene seep deposits in Leyte, Philippines. Acta Paleontol Pol 65:589–627
Kiel S, Birgel D, Lu Y et al (2021) A thyasirid-dominated methane-seep deposit from Montañita, southwestern Ecuador, from the Oligocene–Miocene boundary. Palaeogeogr Palaeooclimatol Palaeoecol 575:110477
Kitazaki T, Majima R (2003) A slope to outer-shelf cold-seep assemblage in the Plio-Pleistocene Kazusa Group, Pacific side of central Japan. Paleontol Res 7:279–296

Klosterman SL, Sandy MR, Campbell KA (2001) A new occurrence of the Late Jurassic rhynchonellid *Cooperrhynchia* (Brachiopoda) from the Great Valley Group, California—confirming a cold-seep community association. Geological Society of America: Abstracts with Program 33:a24

Kondo Y, Chinzei K, Kanno S et al (1996) *Calyptogena* fossil associations in the Pliocene of Ikego, Kanagawa Prefecture: composition, mode of occurrence and taphonomy. Fossils 61:55–58. [In Japanese with English abstract]

Krause FF, Clark J, Sayegh SG et al (2009) Tube worm fossils or relic methane expulsing conduits? Palaios 24:41–50

Kuechler R, Birgel D, Kiel S et al (2012) Miocene methane-derived carbonates from southwestern Washington, USA and a model for silicification at seeps. Lethaia 45:259–273

Kugler HG (2001) Treatise on the Geology of Trinidad: Part 4. Museum of Natural History, Basel, 309 pp

Kugler HG, Jung PM Saunders JB (1984) The Joes River Formation of Barbados and its fauna. Eclogae Geol Helv 77:675–705

Kuramochi T, Kanie Y, Akimoto K et al (1999) *Calyptogena* (*Ectenagena*) sp. from the Miocene Hota Group in the south-central part of the Boso Peninsula. Sci Rep Yokosuka City Mus 46:55–56

Kurihara Y (2000) Middle Miocene deep water mollusks of the Haratajino Formation in the Isobe District, the Annaka-Tomioka area, Gunma Prefecture, central Japan. Bull Gunma Mus Nat Hist 4:1–22

Kuroda T (1931) Mollusca In: F Homma (ed) Geology of the central part of Shinano, Part 4. Kokin Shoin, Tokyo, pp. 1–90. [in Japanese, title translated]

Landman NH, Cochran JK, Larson NL et al (2012) Methane seeps as ammonite habitats in the U.S. Western Interior Seaway revealed by isotopic analyses of well-preserved shell material. Geology 40(6):507–510

Landman NH, Kennedy WJ, Cobban WA et al (2013) A new species of *Hoploscaphites* (Ammonoidea: Ancyloceratina) from cold methane seeps in the Upper Cretaceous of the U.S. Western Interior. Am Mus Novit 3881:1–39

Landman NH, Jicha BR, Cochran JK et al (2018) $^{40}Ar/^{39}Ar$ date of a bentonite associated with a methane seep deposit in the upper Campanian *Baculites compressus* Zone, Pierre Shale, South Dakota. Cret Res 90:90–96

Landman NH, Kennedy WJ, Larson NL et al (2019) Description of two species of *Hoploscaphites* (Ammonoidea: Ancyloceratina) from the Upper Cretaceous (lower Maastrichtian) of the U.S. Western Interior. Bull Am Mus Natl Hist 427:1–72

Landman NH, Kennedy WJ, Grier J et al (2020) Large scaphitid ammonites (*Hoploscaphites*) from the Upper Cretaceous (upper Campanian–lower Maastrichtian) of North America: endless variation on a single theme. Bull Am Mus Natl Hist 441:1–131

Landman NH, Cochran JK, Brezina J et al (this volume) Methane seeps in the Late Cretaceous Western Interior Seaway. In: Kaim A, Cochran JK, Landman NH (eds) Ancient hydrocarbon seeps. Topics in geobiology, vol. 50, Springer, New York

Larson NL, Brezina J, Landman NH et al (2014) Hydrocarbon seeps: unique habitats that preserved the diversity of fauna in the Late Cretaceous Western Interior Seaway. Wyoming Geological Society Guidebook, Caspar, Wyoming

Lavington CS (1933) Montana Group in eastern Colorado. Am Assoc Pet Geol Bull 17:397–410

Little CTS, Birgel D, Boyce AJ et al (2015) Late Cretaceous (Maastrichtian) shallow water hydrocarbon seeps from Snow Hill and Seymour Islands, James Ross Basin, Antarctica. Palaeogeogr Palaeoclimatol Palaeoecol 418:213–228

Liu C, Xianyin A, Algeo T et al (2021) Hydrocarbon-seep deposits in the lower Permian Angie Formation, Central Lhasa Block, Tibet. Gondwana Res 90:258–272

Majima R, Imai S, Uchimura R et al (1990) Finding of *Calyptogena* sp. (Bivalvia) from the Late Pliocene Hijikata Formation, Kakegawa City, Shizuoka Prefecture, central Japan. J Geol Soc Japan 96:553–556. [in Japanese]

Majima M, Tanase S, Uchimura R et al (1992) Finding of *Calyptogena* sp. (Bivalvia) in the Neogene of the southern end in the Boso Peninsula. J Geol Soc Japan 98:373–376

Majima R, Tato Y, Shibasaki T (1996) In situ fossil chemosynthetic community found from the lower Pleistocene Kazusa Group, Yokohama City, central Japan. Fossils 61:47–54
Majima R, Ikeda K, Wada H et al (2003) An outer-shelf cold-seep assemblage in forearc basin fill, Pliocene Tanakabe Formation, Kyushu, Japan. Paleontol Res 7:297–311
Majima R, Nobuhara T, Kitazaki T (2005) Review of fossil chemosynthetic assemblages in Japan. Paleogeogr Paleoclimatol Palaeoecol 227:86–123
Majima R, Kase T, Kawagata S et al (2007) Fossil cold seep assemblages from Leyte Island, Philippines. J Geogr 116: 643–652 (+ pictorial). [in Japanese with English abstract]
Majima R, Jenkins RG, Kase T et al (2010) In situ *Calyptogena* colonies from Pliocene back-arc basin fills in Leyte Island, Philippines. J Geol Soc Japan 116:15–16
Martin K (1933) Eine neue tertiäre Molluskenfauna aus dem indischen Archipel. Leidsche Geol Meded 6:7–32
Martin K (1937) Die Oligocaenen mollusken von Buton als Auswürflinge eines Schlammsprudels betrachtet. Leidsche Geol Meded 8:311–314
Martin RA (2010) Accessing the Records of Methane Passage in Ancient Sediments. PhD thesis, University of Washington, 219 pp
Martin RA, Nesbitt EA, Campbell KA (2007) Carbon stable isotopic composition of benthic foraminifera from Pliocene cold methane seeps, Cascadia accretionary margin. Palaeogeogr Palaeoclimatol Palaeoecol 246:260–277
Martire L, Natalicchio M, Petrea C et al (2010) Petrographic evidence of the past occurrences of gas hydrates in the Tertiary Piedmont Basin (NW Italy). Geo-Marine Lett 30:461–476
Matos S, Warren LV, Fürsich FT et al (2017) Paleoecology and paleoenvironments of Permian bivalves of the Serra Alta Formation, Brazil: ordinary suspension feeders of Late Paleozoic Gondwana seep organisms? J South Am Earth Sci 77:21–42
Matsumoto E (1966) Geology of Palaeogene and lower Neogene formations in the lower course of the River Ooigawa, Shizuoka Prefecture, central Japan. Part I, Stratigraphical Succession and Geological Structure. Mem Fac Sci Kyoto Univ Ser B 33:115–133
Matsumoto E (1971) Oligocene mollusks from the Setogawa Group in central Japan. Bull Natl Sci Mus Tokyo 14:661–669
Matsumoto E, Hirata M (1972) *Akebiconcha uchimuraensis* (Kuroda) from the Oligocene formations of the Shimanto Terrain. Bull Natl Sci Mus Tokyo 15:754–760
Maury CJ (1912) A contribution to the paleontology of Trinidad. J Acad Nat Sci Philadelphia 15:24–112
Maync W (1949) The Cretaceous beds between Kuhn Island and Cape Franklin (Gauss Peninsula) northern East Greenland. Medd Grønl 133:1–291
McLaughlin RJ, Ohlin HN (1984) Tectonostratigraphic framework of the Geysers–Clear Lake region, California. In: Blake MCJ (ed) Franciscan Geology of Northern California. Society of Economic Paleontologists and Mineralogists, Pacific Section, Los Angeles, pp 221–254
McLaughlin RJ, Oglin HN, Thormahlen DJ (1990) Geologic map and structure sections of the Little Indian Valley—Wilbur Springs geothermal area, northern Coast Ranges, California. 1 map. Scale 1:24000, structure sections, explanation and interpretive text (2 sheets). US Geological Survey, Map I-1706
Meehan KC, Landman NH (2016) Faunal associations in cold-methane seep deposits from the Upper Cretaceous Pierre Shale, South Dakota. Palaios 31:291–301
Metz CL (2000) Upper Cretaceous (Campanian) sequence and biostratigraphy, west Texas to east-central Utah and development of cold-seep mounds in the Western Interior Cretaceous basin. Texas A & M University, Dissertation, 256 pp
Metz CL (2010) Tectonic controls on the genesis and distribution of Late Cretaceous, Western Interior Basin hydrocarbon-seep mounds (Tepee Buttes) of North America. J Geol 118:201–213
Minisini D, Schwartz H (2007) An Early Paleocene cold seep system in the Panoche and Tumey Hills, Central California. In: Hurst A and Cartwright J (eds) Sand injectites: implications for hydrocarbon exploration and production: Am Ass Pet Geol Bull 87:185–197

Miyajima Y, Watanabe Y, Yanagisawa Y et al (2016) A late Miocene methane-seep deposit bearing methane-trapping silica minerals at Joetsu, central Japan. Palaeogeogr Palaeoclimatol Palaeoecol 455:1–15

Miyajima Y, Nobuhara T, Koike H (2017) Taxonomic reexamination of three vesicomyid species (Bivalvia) from the Middle Miocene Bessho Formation in Nagano Prefecture, central Japan, with notes on vesicomyid diversity. Nautilus 131:51–56

Miyajima Y, Ijira A, Miyake A et al (2018a) Origin of methane and heavier hydrocarbons entrapped within Miocene methane-seep carbonates from central Japan. Chem Geol 498:83–95

Miyajima Y, Watanabe Y, Jenkins RG et al (2018b) Diffusive methane seepage in ancient deposits: Examples from Neogene Shin'etsu sedimentary basin, central Japan. J Sediment Res 88:449–466

Miyajima Y, Watanabe Y, Goto A et al (2020) Archaeal lipid biomarker as a tool to constrain the origin of methane at ancient methane seeps: insight into subsurface fluid flow in the geological past. J Asian Earth Sci 189:104134

Monegatti P, Raffi S, Roveri M, Taviani M (2001) One day trip in the outcrops of Castell'Arquato Plio-Pleistocene Basin: from the badland of Monte Giogo to the Stirone River. In: Monegatti P, Cecca F, Raffi S (eds) International Conference Paleobiogeography and Paleoecology (2001: Piacenza, Italy, and Castell'Arquato, Italy), May 31–June 2 2001. Excursion Guidebook, Elsevier, Paris, pp 1–22

Moore EJ (1984) Molluscan paleontology and biostratigraphy of the lower Miocene upper part of the Lincoln Creek Formation in southwestern Washington. Contrib sci Los Angel Calif 351:1–42

Moroni MA (1966) Malacofauna del "Calcare a Lucine" di Santa Sofia–Forlì. Paleontogr Italica 60:69–87

Mounji D, Bourque P-A, Savard MM (1998) Hydrothermal origin of Devonian conical mounds (kess-kess) of Hamar Laghdad ridge, Anti-atlas, Morocco. Geology 26:1123–1126

Naganuma T, Okayama Y, Hattori M et al (1995) Fossil worm tubes from the presumed cold-seep carbonates of the Miocene Hayama Group, Central Miura Peninsula, Japan. Island Arc 4:199–208

Natalicchio M, Peckmann J, Birgel D et al (2015) Seep deposits from northern Istria, Croatia: a first glimpse into the Eocene seep fauna of the Tethys region. Geol Mag 152:444–459

Nesbitt EA, Martin RA, Campbell KA (2013) New records of Oligocene diffuse hydrocarbon seeps, northern Cascadia margin. Palaeogeogr Palaeoclimatol Palaeoecol 90:116–129

Niitsuma N, Matsushima Y, Hirata D (1989) Abyssal molluscan colony of *Calyptogena* in the Pliocene strata of the Miura Peninsula, central Japan. Palaeogeogr Palaeoclimatol Palaeoecol 71:193–203

Ninomiya T (2011) Chemosynthetic fossil molluscan faunas from the Neogene Taishu Group, distributed in Tsushima Islands, Nagasaki Prefecture, the south-west Japan. Mem Fac Sci Kyushu Univ Ser D, Earth Planet Sci 32:11–26

Ninomiya T (2012) Seep limestone and chemosynthetic fossil assemblages dependent on the seep from the Neogene Taishu Group, Tsushima Island, Nagasaki Prefecture, the southwest Japan. Sci Rep Kyushu Univ, Dept Earth Planet Sci 23:13–21. [in Japanese]

Ninomiya T, Shimoyama S, Miyata Y et al (2020) Origin and water depth of a newly identified seep carbonate and paleoecology of *Bathymodiolus* in the Miocene Taishu Group, southwestern Japan. Palaeogeogr Palaeoclimatol Palaeoecol 546:109655

Nobuhara T, Onda D, Sato T et al (2016) Mass occurrence of the enigmatic gastropod Elmira in the Late Cretaceous Sada Limestone seep deposit in southwestern Shikoku, Japan. PalZ 90:701–722

Nobuhara T (2003) Cold seep carbonate mounds with *Vesicomya* (*Calyptogena*) *kawamurai* (Bivalvia: Vesicomyidae) in slope-mud facies of the Pliocene forearc basin of Sagara-Kakegawa area, central Japan. Paleontol Res 7:313–328

Nobuhara T (2010) Searching for the background of flourishing of vesicomyid bivalves by investigating underground cross sections of methane seep sites. Biol Sci Inheritance 64:21–32 [in Japanese, title translated]
Nobuhara T, Ohtori Y (2009) Data report: lithological description of boring core samples of the lower Middle Miocene methane-seep carbonate mound (the Anazawa limestone) in the Bessho Formation, Nagano Prefecture, central Japan. Geosci Rep Shizuoka Univ 36:9–26. [in Japanese]
Nobuhara T, Tanaka T (1993) Palaeoecology of *Akebiconcha kawamurai* (Bivalvia: Vesicomyidae) from the Pliocene Tamari Silt Formation in the Kakegawa area, central Japan. Palaeogeogr Palaeoclimatol Palaeoecol 102:27–40
Nobuhara T, Imaizumi T, Kaneko H et al (2008a) Mode of fossil occurrence and taxonomical re-examination of modiolid bivalves from the lower Middle Miocene cold seep carbonates in the Bessho Formation, Nagano Prefecture, central Japan. Venus 67:102. [in Japanese]
Nobuhara T, Onda N, Kikuchi I et al (2008b) Lithofacies and fossil assemblages of the Upper Cretaceous Sada Limestone, Shimanto City, Kochi Prefecture, Shikoku, Japan. Fossils 84:47–60. [in Japanese with English abstract]
Ogasawara K, Hisada K, Kitada N (1994) Early Miocene *Calyptogena* from the Miocene Aokiyama Formation, Hota Group, Boso Peninsula, Japan. Ann Rep Inst Geosci Univ Tsukuba 20:33–37
Ogihara S (2004) Biomarker composition for anaerobic methane oxidation in cold-seep carbonates. Chikyukagaku (Geochemistry) 38:45–55[in Japanese with English abstract]
Ogihara S (2005) The evolution of chemosynthetic biological community at the site of cold-seep carbonate precipitation. Fossils 78:40–46. [in Japanese with English abstract]
Ogihara S (2008) Acyclic hydrocarbons and ketones in cold-seep carbonates from central Hokkaido, Japan. Geochem J 42:421–427
Ohara S (1966) Stratigraphic and geologic structures of the Tertiary deposits in the Uryu coal-field, Hokkaido, Japan. J Coll Arts Sci Chiba Univ 4:599–615
Ohara S, Kanno S (1973) Mid-Tertiary molluscan fauna from the Uryu coal-field of central Hokkaido, Japan. Tohoku Univ Sci Rep 2nd series Special Volume 6: 125–135
Olsson AA (1931) Contributions to the Tertiary paleontology of northern Peru. Part 4, The Peruvian Oligocene. Bull Am Paleontol 17:97–264
Olsson AA (1940) Tertiary deposits of northwestern South America and Panama. 8th Am Sci Congr; Proc Geol Sci Washington 4:231–287
Pálfy J, Kovács Z, Price GD et al (2017) A new occurrence of the Early Jurassic brachiopod *Anarhynchia* from the Canadian Cordillera confirms its membership in chemosynthesis-based ecosystems. Can J Earth Sci 54:1179–1193
Palmer RH (1948) List of Palmer Cuban localities. Bull Am Paleont 31(128):1–178
Peckmann J, Thiel V (2004) Carbon cycling at ancient methane–seeps. Chem Geol 205:443–467
Peckmann J, Thiel V, Michaelis W et al (1999a) Cold seep deposits of Beauvoisin (Oxfordian; southeastern France) and Marmorito (Miocene, northern Italy): microbially induced authigenic carbonates. Int J Earth Sci 88:60–75
Peckmann J, Walliser O, Riegel W et al (1999b) Signatures of hydrocarbon venting in the Middle Devonian carbonate mound (Hollard Mound) at the Hamar Laghdad (Morocco). Facies 40:281–296
Peckmann J, Gischler E, Oschmann W et al (2001) An Early Carboniferous seep community and hydrocarbon-derived carbonates from the Harz Mountains, Germany. Geology 29:271–274
Peckmann J, Goedert JL, Heinrichs T et al (2003) The Late Eocene 'Whiskey Creek' methane-seep deposit (Western Washington State). Part II: petrology, stable isotopes, and biogeochemistry. Facies 48:241–254
Peckmann J, Thiel V, Reitner J et al (2004) A microbial mat of a large sulfur bacterium preserved in a Miocene methane-seep limestone. Geomicrobiol J 21:247–255
Peckmann J, Little CTS, Gill F et al (2005) Worm tube fossils from the Hollard Mound hydrocarbon-seep deposit, Middle Devonian, Morocco: Palaeozoic seep-related vestimentiferans? Palaeogeogr Palaeoclimatol Palaeoecol 227:242–257

Peckmann J, Campbell KA, Walliser OH et al (2007a) A Late Devonian hydrocarbon-seep deposit dominated by dimerelloid brachiopods, Morocco. Palaios 22:114–122
Peckmann J, Senowbari-Daryan B, Birgel D et al (2007b) The crustacean ichnofossil *Palaxius* associated with callianassid body fossils in an Eocene methane-deep limestone, Humptulips Formation, Olympic Peninsula, Washington. Lethaia 40:273–280
Peckmann J, Birgel D, Kiel S (2009) Molecular fossils reveal fluid composition and flow intensity at a Cretaceous seep. Geology 37:847–850
Peckmann J, Kiel S, Sandy MR et al (2011) Mass occurrence of the brachiopod *Halorella* in Late Triassic methane-seep deposits, eastern Oregon. J Geol 119:207–220
Peckmann J, Sandry MR, Taylor DG et al (2013) An Early Jurassic brachiopod-dominated seep deposit enclosed by serpentinite, eastern Oregon, USA. Palaeogeogr Palaeoclimatol Palaeoecol 390:4–16
Playford G (1959) Permian stratigraphy of the Woolaga Creek area, Mingenew District, Western Australia. J Soc West Aust 42:7–29
Reitner J, Blumenberg M, Walliser E-O et al (2015) Methane-derived carbonate conduits from the late Aptian of Salinac (Marnes Bleues, Vocontian Basin, France): Petrology and biosignatures. Mar Pet Geol 66:641–652
Rigby K, Goedert J (1996) Fossil sponges from localized cold-seep limestone in Oligocene rocks of the Olympic Peninsula, Washington. J Paleontol 70:900–908
Rigby JK, Jenkins DE (1983) The Tertiary sponges *Aphrocallistes* and *Eurete* from western Washington and Oregon. Los Angeles County Mus Contr Sci 344:1–13
Robinson CS, Mapel WJ, Cobban WA (1959) Pierre Shale along western and northern flanks of Black Hills, Wyoming and Montana. Am Ass Pet Geol Bull 43:101–123
Robinson CS, Mapel WJ, Bergendahl MH (1964) Stratigraphy and structure of the northern and western flanks of the Black Hills Uplift, Wyoming, Montana, and South Dakota. Geol Surv Prof Pap 404:1–134
Rolin Y, Gaillard C, Roux M (1990) Ecologie des pseudobiohermes des Terres Noires jurrasiques liés à des paléo-sources sous-marines. Le site oxfordien de Beauvoisin (Drôme, Bassin du Sud-Est, France). Palaeogeogr Palaeoclimatol Palaeoecol 80:79–105
Rosenkrantz A (1942) Slaegten Thyasiras geologiske Optræden. Medd Dan Geol Foren 10:277–278
Rosenkrantz A (1970) Marine Upper Cretaceous and lowermost Tertiary deposits in West Greenland. Investigations before and since 1938. Medd Dan Geol Foren 19:406–453
Russo A, Pugliese N, Serventi P (2012) Miocene ostracodes of cold-seep settings from northern Apennines (Italy). Rev de Micropaleontol 55:29–38
Ryan D, Witts JD, Landman NH (2020) Paleoecological analysis of a methane seep in the Late Cretaceous (Maastrichtian) Western Interior, USA. Lethaia 54:185–203
Saether KP (2011) A taxonomic and palaeobiogeographic of the fossil fauna of Miocene hydrocarbon seep deposits, North Island, New Zealand. PhD thesis, University of Auckland, New Zealand, 479 pp
Saether KP, Little CTS, Campbell KA (2010a) A new fossil provannid gastropod from Miocene hydrocarbon seep deposits, East Coast Basin, North Island, New Zealand. Acta Paleontol Pol 55:507–517
Saether KP, Little CTS, Campbell KA et al (2010b) New fossil mussels (Bivalvia: Mytilidae) from Miocene hydrocarbon seep deposits, North Island, New Zealand, with general remarks on vent and seep mussels. Zootaxa 2577:1–45
Saether KP, Little CTS, Marshall B et al (2012) Systematics and palaeoecology of a new fossil limpet (Patellogastropoda: Pectonodontidae) from Miocene hydrocarbon seep deposits, East Coast Basin, North Island, New Zealand with an overview of known fossil pectinodontids. Moll Res 32:1–15
Saether KP, Jingeng S, Little CTS et al (2016) New records and new species of bivalvie (Mollusca: Bivalvia) from Miocene hydrocarbon seep deposits, North Island, New Zealand. Zootaxa 4154:1–26

Saether KP, Little CTS, Campbell KA et al (this volume) Ancient New Zealand Seep Limestones. In: Kaim A, Cochran JK, Landman NH (eds) Ancient hydrocarbon seeps. Topics in geobiology, vol. 50, Springer, New York

Sami M, Taviani M (2015) I Calcari a Lucina e I gessi di Rontana. Memorie dell'Istituto Italiano di Speleologia 28:39–56

Sandy MR (1990) A new Early Cretaceous articulate brachiopod from the Northwest Territories, Canada, and its paleobiogeographic significance. J Paleontol 64:367–372

Sandy MR (2001) Mesozoic articulated brachiopods from the Western Cordillera of North America: their significance for palaeogeographic and tectonic reconstruction, palaeobiogeography and palaeoecology. In: Brunton CHC, Cocks LRM, Long SL (eds) Brachiopods past and present. The Systematics Associations Special Volume 63, Taylor & Francis, London, pp. 394–410

Sandy MR (2010) Brachiopods from Ancient Hydrocarbon Seeps and Hydrothermal Vents. In: S. Kiel (ed) The Vent and Seep Biota, Aspects from Microbes to Ecosystems. Topics in Geobiology 33, Springer, Dordrecht, Heidelberg, London, New York, pp. 394–410

Sandy MR, Blodgett RB (1996) *Peregrinella* (Brachiopoda: Rhynchonellida) from the Early Cretaceous Wrangellia Terrane, Alaska In: Cooper P, Jin J (eds) Brachiopods. Proceedings of the Third International Brachiopod Congress, Sudbury, Ontario, Canada, 2–5 September 1995, AA Balkema, Rotterdam, Brookfield, pp. 239–242

Sandy MR, Campbell KA (1994) New rhynchonellid brachiopod genus from Tithonian (Upper Jurassic) cold seep deposits of California and its paleoenvironmental setting. J Paleontol 68:1243–1252

Sandy MR, Campbell KA (2003) *Anarhynchia* (Jurassic Brachiopoda) in a possible seep deposit from Bedford Canyon, California, USA. GSA Abstracts with Programs 33, A-53

Sandy MR, Hryniewicz K, Hammer Ø etc. (2014) Brachiopods from Late Jurassic–Early Cretaceous hydrocarbon seep deposits, central Spitsbergen, Svalbard. Zootaxa 3884:501–532

Sandy M, Peckmann J (2016) The Early Cretaceous brachiopod *Peregrinella* from Tibet: a confirmed hydrocarbon-seep occurrence for a seep-restricted genus. PalZ 90:691–699

Sandy MR, Hryniewicz K, Hammer Ø et al (2014) Brachiopods from Late Jurassic–Early Cretaceous hydrocarbon seep deposits, central Spitsbergen, Svalbard. Zootaxa 3884:501–532

Sarycheva TGE (1960) Treatise of Paleontology. Handbook for Paleontologists and Geologists of the USSR in 15 Volumes. Bryozoans, Brachiopods. Addendum (Appendix): Phoronids. Nauka, Moscow., 343 pp. [in Russian]

Sato H, Endo T, Nikaido M (1993) Isotope geochemistry of the limestone bodies scattered in shales of the Bessho Formation in Akanuda area, Shiga-mura, Nagano Precefecture. The Mining, Geological and Mineralogical, Petrological and Economic Geological Society Union Meeting, p. 108 [Abstract, in Japanese, title translated]

Saul LR, Squires RL, Goedert JL (1996) A new genus of cryptic lucinid? bivalve from Eocene cold seeps and turbidite-influenced mudstone, western Washington. J Paleontol 70:788–794

Savard MM, Beauchamp B, Veizer J (1996) Significance of aragonite cements around Cretaceous marine methane seeps. J Sediment Petrol 66:430–438

Schwartz H, Sample J, Weberling KD et al (2003) An ancient linked fluid migration system: cold-seep deposits and sandstone intrusions in the Panoche Hills, California, USA. Geo-Mar Lett 23:340–350

Schweitzer CE, Feldmann RM (2008) New Eocene hydrocarbon seep decapod crustacean (Anomura: Galatheidae: Shinkaiinae) and its paleobiology. J Paleontol 82:1021–1029

Scott GR (1969) General and engineering geology of the northern part of Pueblo, Colorado. Geol Surv Bull 1262:1–131

Scott GR, Cobban WA (1965) Geologic and biostratigraphic map of the Pierre Shale between Jarre Creek and Loveland, Colorado. Geol Surv Misc Geol Invest Map Ser I-439, scale 1:48, 000

Scott GR, Cobban WA (1975) Geology and biostratigraphic map of the Pierre Shale in the Canon City-Florence Basin and the Twelvemile Park area, south-central Colorado. Geol Surv Misc Geol Invest Map Ser I-937. scale 1:48, 000

Scott GR, Cobban WA (1986a) Geologic and biostratigraphic map of the Pierre Shale in the Colorado Springs-Pueblo area, Colorado. Geol Surv Misc Geol Invest Map Ser I-1627. scale 1:100, 000

Scott GR, Cobban WA (1986b) Geology, biostratigraphy, and structure map of the Pierre Shale between Loveland and Round Butte. Colorado. US Geol Surv Misc Geol Invest Map Ser I-1700. scale 1:50, 000

Senowbari-Daryan B, Gaillard C, Peckmann J (2007) Crustacean microcoprolites from Jurassic (Oxfordian) hydrocarbon-seep deposits of Beauvoisin, southeastern France. Facies 53:229–238

Shapiro RS (2004) Recognition of fossil prokaryotes in Cretaceous methane seep carbonates: relevance to astrobiology. Astrobiology 4:438–449

Shapiro RS, Fricke H (2002) Tepee Buttes: fossilized methane-seep ecosystems. In: Leonard EM et al (eds), High Plains to Rio Grande Rift: late Cenozoic evolution of central Colorado. Geol Soc Am Field Guide 3:94–101

Shibasaki T, Majima R (1997) A fossil chemosynthetic community from outer shelf environment of the Middle Pleistocene Kakinokidai Formation, Kazusa Group in Boso Peninsula, Chiba Prefecture, central Japan. J Geol Soc Japan 103:1065–1080

Shikama T (1968) On a giant *Thracidora* from the Hayama Group. Miura Peninsula. Sci Rep Yokohama Nat Univ 2(14):13–16

Shikama T, Masujima A (1969) Quantitative studies of the molluscan assemblages in the Ukego-Nojima Formations. Sci Rep Yokohama Natl Univ Sec II 15:61–94

Silberling NJ, Schoellhamer JE, Gray CH Jr et al (1961) Upper Jurassic fossils from Bedford Canyon Formation, southern California. Am Ass Pet Geol Bull 45:1746–1765

Smirnova TN (1972) Early Cretaceous brachiopods of Crimea and Northern Caucasus. Nauka, Moscov, 143 pp. [In Russian]

Smrzka D, Kraemer SM, Zwicker J et al (2015) Constraining silica diagenesis in methane-seep deposits. Palaeogeogr Palaeoclimatol Palaeoecol 420:113–126

Smrzka D, Zwicker J, Klüge A, Monien P, Back W, Bohrmann G, Peckmann J (2016) Establishing criteria to distinguish oil-seep from methane-seep carbonates. Geology 44:667–670

Smrzka D, Zwicker J, Kolonic S et al (2017) Methane seepage in a Cretaceous greenhouse world recorded by an unusual carbonate deposit in the Tarfaya Basin, Morocco. Depos Rec 3:4–37

Squires RL (1989) Pteropods (Mollusca: Gastropoda) from Tertiary formations of Washington and Oregon. J Paleontol 63:443–448

Squires RL (1995) First fossil species of the chemosynthetic-community gastropod *Provanna*: localized cold-seep limestones in upper Eocene and Oligocene rocks, Washington. Veliger 38:30–36

Squires RL, Goedert JL (1991) New late Eocene mollusks from localized limestone deposits formed by subduction-related methane seeps, southwestern Washington. J Paleontol 65:412–416

Squires RL, Goedert JL (1995) An Extant Species of *Leptochiton* (Mollusca: Polyplacophora) in Eocene and Oligocene cold-seep limestones, Olympic Peninsula, Washington. Veliger 38:47–53

Squires RL, Goedert JL (1996) A new species of *Thalassonerita*? (Gastropoda: Neritidae?) from a middle Eocene cold-seep carbonate in the Humptulips Formation western Washington. Veliger 39:270–273

Squires RL, Gring MP (1996) Late Eocene chemosynthetic? bivalves from suspect cold seeps, Wagonwheel Mountain, central California. J Paleontol 70:63–73

Stanton TW (1895) Contributions to the Cretaceous paleontology of the Pacific coast: the fauna of the Knoxville beds. United States Geol Surv Bull 133:1–132

Sun D (1986) Discovery of Early Cretaceous *Peregrinella* (Brachiopoda) from Hizang (Tibet) and its significance. Palaeontol Cathay 2:211–227

Tanabe K, Hirano H, Matsumoto T et al (1977) Stratigraphy of the Upper Cretaceous deposits of the Obira area, northwestern Hokkaido. Mem Fac Sci, Kyushu Univ Ser D Geol 12:181–202

Tanaka K (1959) Molluscan fossils from central Shinano, Nagano Prefecture, Japan. (Part 1) Fossils from the Akanuda Limestone. J Shinshu Univ Fac Educ 8:115–133

Tate Y, Majima R (1998) A chemosynthetic fossil community related to cold seeps in the outer shelf environment—A case study in the Lower Pleistocene Koshiba Formation of the Kazusa Group, central Japan. J Geol Soc Japan 104:24–41

Taviani M (1994) The "Calcari a *Lucina"* macrofauna reconsidered: deep sea fauna oases from Miocene-aged cold vents in the Romagna Apennines, Italy. Geo-Mar Lett 14:185–191

Taviani M (2001) Fluid venting and associated processes. In: Vai GB, Martini IP (eds) Anatomy of an Orogen: the Apennines and Adjacent Mediterranean Basins. Kluwer Academic Publishers, Dordrecht, pp 351–366

Taviani M (2011) The deep-sea chemoautotroph microbial world as experienced by the Mediterranean metazoans through time. In: Reitner J, Quéric N-V, Arp G (eds) Advances in Stromatolite Geobiology, Lecture Notes in Earth Sciences, vol 131. Springer, Berlin, pp 277–295

Taviani M (2014) Marine chemosynthesis in the Mediterranean Sea. In: S Goffredo Z. Dubinsky (eds.), The Mediterranean Sea: its history and present challenges, Springer, Dordrecht, pp. 69–83

Taviani M, Roveri M, Aharon P et al (1997). A Pliocene deepwater cold seep (Stirone River, N. Italy). In: GB Vai, M Taviani, S Conti et al (eds.), Cold-E-Vent. Hydrocarbon Seepage and Chemosynthesis in Tethyan Relic Basins: Products, Processes and Causes. An International Field Workshop to be held in Bologna and nearby Apennines. June 23–26/1997. Abstract with Program ISMAR, Bologna, pp. 20.

Terzi C (1993) The "Calcari a Lucina" (Lucina Limestones) of the Tuscan-Romagna Apennines as indicators of Miocene cold seep activity (Northern Apennines, Italy). Giorn Geol 55:71–81

Terzi C, Aharon P, Ricci Lucchi F et al (1994) Petrography and stable isotope aspects of cold-vent activity imprinted on Miocene-age "Calcari a Lucina" from Tuscan and Romagnan Apennines, Italy. Geo-Mar Lett 14:177–184

Thieuloy J-P (1972) Biostratigraphie des lentilles a peregrinelles (Brachiopodes) de l'Hauterivien de Rottier (Drôme, France). Geobios 5:5–53

Thuy B, Landman NH, Larson NL et al (2018) Brittle-star mass occurrence on a Late Cretaceous methane seep from South Dakota, USA. Sci Rep 9:9617

Torres ME, Martin RA, Klinkhammer GP et al (2010) Post-depositional alteration of foraminiferal shells in cold-seep settings: new insights from flow-through time-resolved analyses of biogenic and inorganic seep carbonates. Earth Planet Sci Lett 299:10–22

Torrini R Jr, Speed RC, Claypool GE (1990) Origin and geologic implications of diagenetic limestone in fault zones of Barbados. In: D.K. Larue DK and G. Draper (eds), Transactions of the 12th Caribbean Geological Conference St Criox, pp. 366–370

Treude T, Kiel S, Linke P et al (2011) Elasmobranch egg capsules associated with modern and ancient cold seeps: a nursery for marine deep-water predators. Mar Ecol Prog 437:175–181

Tsuboi M, Nakamura E, Majima R et al (2010) Reconstruction of ancient cold-seep activities based on biomarkers—A case study of Lower Pleistocene Ofuna and Koshiba Formation, central Japan. Fossils 87:5–21

Tsujino Y, Iwata H (2009) *Aturoidea* (Nautilida) from the Upper Cretaceous Sada Limestone in Shimanto City, Kochi Prefecture, Japan. Cret Res 30:911–916

Tullberg SA (1881) Ueber versteinerungen aus den Aucellen-Schichten Novaja-Semljas. Bih Kongl Svenska Vetensk-Akad Handlr 6:1–25

Ueda Y, Jenkins RG, Ando H et al (1995) Methane-induced calcareous concretions and chemosynthetic community on an outer shelf of the Joban forearc basin: an example from the Miocene Kokozura Formation, Takaku Group, northern Honshu. Fossils 78:47–58 [in Japanese with English abstract]

Utsunomiya M, Majima R, Taguchi K et al (2015) An *in situ* vesicomyid-dominated cold-seep assemblage from the lowermost Pleistocene Urago Formation, Kazusa Group, forearc basin fill on the northern Miura Peninsula, Pacific side of central Japan. Paleontol Res 19:1–20

Vai GB, Taviani, M, Conti S (1997) Cold-E-Vent. Hydrocarbon seepage and chemosynthesis in Tethyan relic basins: prod-ucts, processes and causes. In: An international field workshop to be held in Bologna and nearby Apennines. June 23–26/1997. Abstract with Program, Bologna, 58 pp.

Van Winkle K (1919) Remarks on some new species from Trinidad. Bull Am Paleont 8:19–27

Venturini S, Selmo E, Tarlao A et al (1998) Fossiliferous methanogenic limestones in the Eocene flysch of Istria (Croatia). Giorn Geol 60:219–234

Vinn O, Kupriyanova E, Kiel S (2012) Systematics of serpulid tubeworms (Annelida, Polychaeta) from Cretaceous and Cenozoic hydrocarbon-seep deposits in North America and Europe. Neues Jahrb Geol Palaontol Abh 265(3):315–325

Vinn O, Kupriyanova E, Kiel S (2013) Serpulids (Annelida, Polychaeta) at Cretaceous to modern hydrocarbon seeps: ecological and evolutionary patterns. Palaeogeogr Palaeoclimatol Palaeoecol 390:35–41

Vinn O, Hryniewicz K, Little CTS et al (2014) A Boreal serpulid fauna from Volgian-Ryazanian (latest Jurassic-earliest Cretaceous) shelf sediments and hydrocarbon seeps from Svalbard. Geodiversitas 36:527–540

Vokes HE (1955) Notes on Tertiary and Recent Solemyacidae. J Paleontol 29:34–545

Walliser EO, Tanabe K, Hikida Y et al (2019) Sclerochronological studies of gigantic inoceramids *Sphenoceramus schmidti* and *S. sachaliniensis* from Hokkaido, northern Japan. Lethaia 52:410–428

Wang S-W, Gong S-Y, Mii H-S et al (2006) Cold seep carbonate hardgrounds as the initial substrata of coral reef development in a siliciclastic paleoenvironment of southwestern Taiwan. Terr Atmospheric Ocean Sci 17:405–421

Wang Q, Tong H, Huang C-Y et al (2018) Tracing fluid sources and formation conditions of Miocene hydrocarbon-seep carbonates in the central Western Foothils, Central Taiwan. J Asian Earth Sci 168:186–196

Wang Q, Chen D, Peckmann J (2019) Iron shuttle controls on molybdenium, arsenic, and antimony enrichment in Pliocene methane-seep carbonates from the southern Western Foothills, Taiwan. Mar Petrol Geol 100:263–269

Warren LV, Quaglio F, Simões MG et al (2017) A Permian methane-seep system as a paleonenvironmental analogue for the pre-metazoan carbonate platforms. Braz J Geol 47:722–733

Wierzbowski A, Hryniewicz K, Hammer Ø et al (2011) Ammonites from the hydrocarbon seep carbonate bodies from the uppermost Jurassic–lowermost Cretaceous of Spitsbergen and their biostratigraphical importance. Neues Jahrb Geol Palaontol Abh 262:267–288

Wiese F, Kiel S, Pack A et al (2015) The beast burrowed, the fluid followed—Crustacean burrows as methane conduits. Mar Petrol Geol 66:631–640

Wilckens O (1910) Die Anneliden, Bivalven und Gastropoden der antarktischen Kreideformation. Wissenschaftliche Egebnisse der Schwedischen Südpolar-Expedition 1901–1903 3(12):1–132

Williscroft K, Grasby SE, Beauchamp B et al (2017) Extensive Early Cretaceous (Albian) methane seepage on Ellef Ringnes Island Canadian High Arctic. Geol Soc Am Bull 129:788–805

Yao H, Chen X, Brunner B et al (2022) Hydrocarbon seepage in the mid-Cretaceous greenhouse world: a new perspective from southern Tibet. Gondwana Res 208:103683

Zhang X, Chen K, Hu D et al (2016) Mid-Cretaceous carbon cycle perturbations and Oceanic Anoxic Events recorded in southern Tibet. Sci Rep 6:39643

Zakharov VA, Rogov MA (2020) High-resolution stratigraphy of buchiid bivalves and ammonites from the Jurassic–Cretaceous boundary beds in the Paskenta area (California). Cret Res 110:104422

Zhao R, Wang Q, Chen D (2021) Geochemical characteristics of the Early Pliocene cold seep dolomite at Chiahsien, Taiwan and their implications for fluid sources and sedimentary environment. Mar Geol Quat Geol 41:85–94. [in Chinese with English abstract]

Zinsmeister WJ, Macellari CE (1988) Bivalvia (Mollusca) from Seymour Island, Antarctic Peninsula. Mem Geol Soc 169:253–284

Zwicker J, Smrzka D, Gier S et al (2015) Mineralized conduits are parts of the uppermost plumbing system of Oligocene methane-seep deposits, Washington State, USA. Mar Pet Geol 66:616–630

Zwicker J, Smrzka D, Himmler T et al (2018) Rare earth elements as tracers for microbial activity and early diagenesis: a new perspective from carbonate cements of ancient methane-seep deposits. Chem Geol 501:77–85

Zwicker J, Smrzka D, Steindl F et al (2021) Mineral authigenesis within chemosynthetic microbial mats: Coated grain formation and phosphogenesis at a Cretaceous hydrocarbon seep, New Zealand. Depos Rec 7:294–310

Glossary

Kristian P. Saether

Abstract This glossary includes predominantly geological, palaeontological and ecological terms in relation to the hydrocarbon seep environment. Definitions of commonly associated taxa and geographical locations are avoided, and abbreviations provide only a limited number of entries, since each of these areas is too broad for the scale and purposes of this appendix. Moreover, taxonomic terms used in the detailed descriptions of the morphology of various seep-associated groups are highly diverse, numerous and proliferative, and therefore their inclusion here is limited only to those most commonly found in the literature and this book.

Those readers interested in learning more about the strict definitions of such terms might refer to the various glossaries scattered throughout the *Treatise on Invertebrate Paleontology*. Pluralization guides are provided for terms that do not simply end in a suffix *-es*, *-ies* or *-s*. Sometimes, commonly used derivative terms are included beneath each core entry, as applicable. The orthographic system that provides the basis for the core entries is Oxford English, but alternative spellings are cross-referenced. Where Oxford English does not accommodate a specialist term, the core spelling is provided at the discretion of the author. Alphabetization follows that of Pearsall (1998), e.g., as if spaces in compound terms do not exist, etc. References to pronunciation employ standard International Phonetic Alphabet notation. The following references have proved useful in the compilation of this glossary: Gary et al. (1972), Bates and Jackson (1980, 1987), Lapidus and Winstanley (1990), Allaby and Allaby (1999).

K. P. Saether
Hull, UK

A. Kaim et al. (eds.), *Ancient Hydrocarbon Seeps*, Topics in Geobiology 50,
https://doi.org/10.1007/978-3-031-05623-9

Aa

abiogenic adjective: applied to processes that do not involve, or fluids, rocks or other physical phenomena that are not derived as a result of the activity of living organisms.

compare with: **biogenic**.
related adverb: **abiogenically**.

abiotic adjective: characterized by or produced in the absence of life.

related noun: **abiosis** (plural: **abioses**).
related adverb: **abiotically**.

abyssal adjective: applied to a deep ocean zone; definition varies but is generally taken to be 2000–6000 m, and covers the majority of the ocean floor (ca. 75%), constituting ca. 50% of the entire Earth's surface.

compare with: **bathyal**; **hadal**; **neritic**.
related adverb: **abyssally**.

abyssalbenthic variant term: **abyssobenthic.**
abyssalpelagic variant term: **abyssopelagic.**
abyssal zone see: **abyssal.**
abyssobenthic adjective: pertaining to the sea floor at abyssal depths, especially in reference to organisms endemic to such environments, or to those conditions considered as a habitat.
abyssobenthos noun: the organisms that occupy the sea floor at abyssal depths, considered collectively.
abyssopelagic adjective: pertaining to the open ocean in the abyssal zone.
accretionary prism noun: a tectonically thickened wedge of sediment found on the landward side of some trenches. It is formed by oceanic sediment being scraped off from the subducting plate, together with terrigenous sediments deposited in the trough.

variant term: **accretionary wedge**.
accretionary wedge variant term: **accretionary prism.**
allochthonous adjective: describing a large block of rock that originates from an area other than where it is now found, having been transported by some post-depositional process; *ex situ*.

compare with: **autochthonous**.
related noun: **autochthon**.

allometric adjective: describing the growth of an organism, e.g., a coral, during which the relative dimensions, features and overall shape change significantly throughout ontogeny.

compare with: **isometric**.
related adverb: **allometrically**.

allopatry noun: the occurrence of two or more species (or higher taxa) that are always found in geographically separate habitats, and never together.

compare with: **sympatry**.
related adjective: **allopatric**.

AMO abbreviation for: **anaerobic methane oxidation**.

anaerobic methane oxidation variant term for: **anaerobic oxidation of methane**.

abbreviation: **AMO**.

anaerobic oxidation of methane noun: a biogeochemically significant, microbially mediated process that occurs predominantly in anoxic marine sediments, during which methane (CH_4) is oxidized with sulfate (SO_4^{2-}) as the terminal electron receptor in the following reaction: $CH_4 + SO_4^{2-} \rightarrow HCO_3^- + HS^- + H_2O$. It is thought to be controlled by consortia of methane-oxidizing archaea and sulfate-reducing bacteria that operate syntrophically.

abbreviation: **AOM**.
variant term: **anaerobic methane oxidation**.

anoxia noun: a lack of respiratorily available oxygen.

related adjective: **anoxic**.
related adverb: **anoxically**.

AOM abbreviation: **anaerobic oxidation of methane**.

aragonite noun: orthorhombic calcium carbonate, differing in crystalline structure from, and dimorphic with, calcite. It varies in colour from white, pink, grey, yellowish, to colourless; the lustre is vitreous, and the crystal form is variable, usually prismatic but also acicular, tabular, pseudo-hexagonal, fibrous or stalactitic.

chemical formula: $CaCO_3$.
related adjective: **aragonitic**.

arc–trench gap noun: the region at a destructive plate boundary between the oceanic trench and island arc, usually at least 50 km in extent and increasing with time with the formation of an accretionary wedge and fore-arc basin. The larger arc–trench gaps appear to be related to higher rates of plate convergence.

variant term: **forearc**.

articulated adjective: (of a fossil) preserved with the body parts still in the relative positions they were in life.

compare with: **disarticulated**.
related noun: **articulation**.

authigenic adjective: describing the process by which rock sediments were deposited in the same position as where they are now found; similar to *autochthonous*.

related noun: **authigenesis** (plural: **authigeneses**).

autochthonous adjective: describing a large block of rock that is found in the same location where it was originally deposited; *in situ*.

compare with: **allochthonous**.
related noun: **allochthon**.

autotrophic adjective: describing a primary producer able to directly utilize light or chemical energy for nutrition, thus forming the basis of an ecosystem.

related noun: **autotroph**.
related noun: **autotrophy**.

Bb

backarc basin noun: a zone of thickened sedimentation and extensional tectonics on the overriding plate that lies behind an island arc.

variant spelling: **back-arc basin**.
variant term: **marginal basin**.
compare with: **forearc basin**.

back-arc basin variant spelling: **backarc basin**.

background adjective (usually used in combination): describing those organisms that might commonly be found in a certain environment but are not obligate to it, and are commonly found in other environments.

compare with: **obligate**; **opportunistic**.

bacterial mat noun: a microbial mat comprising only bacteria as opposed to one with archaea.

bacteriocyte noun: a cell in a host symbiont that contains symbiotic bacteria.

related adjective: **bacteriocytic**.

bathyal adjective: applied to a depth zone of the ocean from 200–2000 m (sometimes the definition has the lower boundary deeper, e.g., 4000 m), in which the continental shelf slopes from shallower waters towards deeper realms.

compare with: **abyssal**; **hadal**; **neritic**.
related adverb: **bathyally**.

bathybenthic adjective: inhabiting a life position upon the sediment–water interface in the bathyal zone of the oceans.

bathypelagic adjective: living in the water column at bathyal depth.

benthic adjective: relating to the sea floor, especially in reference to the life positions or habitats of metazoans.

related adverb: **benthically**.

benthon variant term: **benthos**.

benthos noun: a term for the organisms, considered as a group, that inhabit the sediment–water interface (attached to, locomoting, or resting upon it), at various depths in both freshwater and marine environments.

variant term: **benthon**.

biocenose variant term: **biocoenosis**.

biocenosis variant spelling (plural: **biocenoses**) for: **biocoenosis**.

bioclast noun: a fragment of a fossil.

related adjective: **bioclastic**.

biocoenose variant term: **biocoenosis**.

biocoenosis noun (plural: **biocoenoses**): the living part of a biogeocoenosis, i.e., all the fossil material that is available within a rock unit which can be used to reconstruct the biological component of the ancient environment it represents, and consisting of the microbiocoenosis, phytocoenosis and zoocoenosis. It is equivalent to the *biome* in an ecosystem.

variant spelling: **biocenosis**.
variant term: **bioc(o)enose**.

biodegradation noun: the breakdown of materials (especially organic) by the action of micro-organisms.

related adjective: **biodegradable**.
related verb: **biodegrade**.

bioerosion noun: the action of an organism upon a hard substrate, in which it sculpts and penetrates the surface via a variety of mechanisms such as boring, corroding and leaving attachments scars.

compare with: **bioturbation**.
related adjective: **bioerosive**.

biogenic adjective: occurring as a result of the behaviour or activities of living organisms, e.g., fluids, lebensspuren, rocks or other structures.

compare with: **abiogenic**.
related adverb: **biogenically**.

biogenic sedimentary structure variant term for: **lebensspur**.

biogeocenose variant term for: **biogeocoenosis**.

biogeocenosis variant spelling (plural: **biogeocenoses**) for: **biogeocoenosis**.

biogeocoenose variant term: **biogeocoenosis**.

biogeocoenosis noun (plural: **biogeocoenoses**): a term, equivalent to *ecosystem*, used for a rock unit considered from the palaeoecological perspective, which includes all fossils along with the evidence for the environment in which they lived; the biocoenosis plus its ecotope.

variant spelling: **biogeocenosis**.
variant term: **biogeoc(o)enose**.

bioherm noun: a build-up of largely *in situ* organisms (e.g. calcareous algae, colonial corals or stromatoporoids) that produces a reef or mound of organic origin.

compare with: **biostrome**.

biohieroglyph variant term for: **ichnofossil**.

related adjective: **biohieroglyphic**.

biological marker variant term for: **biosignature**.

biomarker variant term: **biosignature**.

biorrigation noun: the introduction of ambient water into a sediment through biogenic conduits, e.g., burrows.

biosignature noun: any molecular evidence indicating the presence of past living organisms in a given rock unit, especially those that indicate the presence of a particular taxon.

variant terms: **biological marker**; **biomarker**; **molecular fossil**.

biostratigraphy noun: a branch of stratigraphy in which rock ages are established based upon the fossil(s) found within them. Of particular importance in this area is the use of zone fossils.

related adjective: **biostratigraphic**.
related adjective: **biostragraphical**.
related adverb: **biostratigraphically**.

biostrome noun: a flat, extensive biocoenosis, composed of sedentary organisms that have mineral skeletons or hard shelly parts, and the sediments derived from them.

compare with: **bioherm**.
related adjective: **biostromal**.

biosynthesis noun: an enzymatically controlled process by which living organisms convert simple molecules into more complex ones.

related adjective: **biosynthetic**.
related adjective: **biosynthetically**.

biotope noun: a region of uniform environmental conditions and animal populations.

related adjective: **biotopic**.

bioturbation noun: disruption to soft sediment by an organism, typically infaunal. Most rocks are effectively homogeneous with very few features due to complete bioturbation, but sometimes isolated pockets of such activity leave recognizable trace fossils.

compare with: **bioerosion**.
related verb: **bioturbate**.
related adjective: **bioturbational**.

body fossil noun: the physical fossilized remains of an organism; the preserved body part(s).

variant term: **somatofossil**.

boring noun: a bioerosive trace fossil in the form of a cavity in a hard substrate such as a shell or hardground, caused by the rasping action of the progenitor.

related verb: **bore**.
related adjective: **bored**.

brine lake variant term: **brine pool**.

brine pool noun: a sea-floor crater-like depression containing very dense concentrations of highly saline fluids, giving the impression of an underwater 'lake' with a distinct shoreline. Such pools often contain a large quantity of methane gas that typically supports communities of mytilids that aggregate around the periphery. Brine pools have been found in greatest number in the Gulf of Mexico, where they range in size from less than a metre across to over 20 km in length. They occur where large salt deposits rise to the sea floor from within underlying oceanic sediments.

variant terms: **brine lake**; **brine seep**.

brine seep variant term: **brine pool**.

burrow noun: a bioturbational trace fossil, which can take a variety of morphological forms, from straight and unbranching to complexly branching and bifurcating, formed by the action of the progenitor tunnelling through soft sediment.

Cc

calcareous adjective: resembling, containing or entirely composed of calcium carbonate.

related adverb: **calcareously**.

calcicole noun: an organism with a preference for or requirement of a habitat that is rich in calcium, usually calcium carbonate.

compare with: **calcifuge**.
related adjective: **calcicolous**.

calcifuge noun: an organism that requires, or at least prefers, a habitat that is poor in calcium (especially calcium carbonate).

compare with: **calcicole**.
related adjective: **calcifugous**.

calcite noun: a very common and widespread rhombohedral crystalline form of calcium carbonate, dimorphic with aragonite. It is usually colourless or white, but can range from green, grey, red, yellow and sometimes black or brown. It is a common constituent of shells.

related adjective: **calcitic**.

Calvin–Benson cycle noun: a biochemical fixation cycle in chloroplasts, in which carbon dioxide is incorporated into ribulose–1,5–biphosphate, subsequently to form sucrose.

variant term: **carbon fixation**.

carbon fixation variant term for: **Calvin–Benson cycle**.

chemoautosynthesis variant term for: **chemosynthesis**.

related adjective: **chemoautosynthetic**.

chemoautotrophic adjective: describing a type of chemotrophy in which the microorganism, in addition to obtaining energy from chemical reactions, synthesizes all other organic compounds necessary to fuel its life processes from carbon dioxide (CO_2).

variant term: **chemolithoautotrophy**.
compare with: **chemoheterotrophy**.
related noun: **chemoautotroph**.
related noun: **chemoautotrophy**.

chemoherm noun: a build-up of chemical carbonates and the calcareous skeletal debris of those chemosymbiotic fauna whose carbon is primarily derived from microbial processes in areas of ambient hydrocarbon fluid venting. A major characteristic of these phenomena is the anomalously negative carbon isotope composition relative to the carbon signature of the surrounding sea water.

chemoheterotrophy noun: a microbial process in which the organism ingests organic building blocks (e.g. glucose) for the reactions they mediate in the production of energy to fuel their life processes, because they are unable to synthesize the compounds themselves.

compare with: **chemoautotrophy**.

chemolithoautotrophy variant term for: **chemoautotrophy**.

chemolithotrophy variant term: **chemotrophy**.

chemosymbiosis noun (plural: **chemosymbioses**): a symbiosis based upon a microbial primary producer that utilizes chemotrophic processes to provide energy for its host, as in all known Lucinidae.

related adjective: **chemosymbiont**.
related adjective: **chemosymbiotic**.

chemosynthesis noun (plural: **chemosyntheses**): the process by which certain microbes create energy by mediating chemical reactions.

compare with: **photosynthesis**.
related adjective: **chemosynthetic**.

chemotrophy noun: a microbial process through which energy is obtained via the oxidation of inorganic chemical compounds.

variant term: **chemolithotrophy**.

related noun: **chemotroph**.
related adjective: **chemotrophic**.

chitin noun: a substance $(C_8H_{13}O_5N)_n$ derived from glucose that is a common component in the hard parts of a wide range of organisms, e.g., the exoskeletons of arthropods such as crustaceans, or in the tubes of some tubeworms.

related adjective: **chitinous**.

chronostratigraphy noun: a branch of stratigraphy in which the concept of time is used both locally and globally to gauge the relative ages of rocks, with the ultimate aim of compiling a definitive timescale over geological history.

related adjective: **chronostratigraphic**.
related adjective: **chronostragraphical**.
related adverb: **chronostratigraphically**.

cenose variant term: **coenosis**.

cenosis variant spelling (plural: **cenoses**): **coenosis**.

coenose variant term: **coenosis**.

coenosis noun (plural: **coenoses**): an assemblage or association, e.g., of fossils in a rock facies, or living organisms in an ecosystem.

variant spelling: **cenosis**.
variant term: **c(o)enose**.

cold seep variant term: **hydrocarbon seep**.

concretion noun: a hard, solid mass of accumulated matter, typically subspherical in shape, found within sediment.

related adjective: **concretionary**.

consortium noun (plural: **consortia**): see **microbial consortium**.

Cope's rule noun: a trend seen in many animal groups whereby there is a tendency towards an increase in size with evolution. It is not a 'rule' sensu stricto, as the opposite trend has been shown in many lineages.

coprolite noun: fossilized faeces or excreta.

related adjective: **coprolitic**.

cosmopolitan adjective: (of an organism) having a worldwide distribution, or at least occurring in several widely separated areas.

Dd

demersal adjective: in the proximity of the sediment–water interface, applied especially to fish that live in this area in freshwater and marine environments, but also in other contexts (e.g. trawling activities).

related adverb: **demersally**.

diagenesis noun (plural: **diageneses**): any combination of several processes that occur at low temperature and pressure in order to change loose sediment into a sedimentary rock. Such processes include cementation, compaction, dissolution, recrystallization and replacement. In the case of trace fossils, these processes may either skew their preservational potential or enhance it (e.g. by pyritization). There are three main stages recognized in the diagenetic process: *eogenesis* (early diagenesis, dominated by the effects of surface chemistry of the depositional environment); *mesogenesis* (the middle phase where sediments are subject to changes in subsurface conditions during burial); and *telogenesis* (changes that occur upon weathering out and exposure to surface conditions).

related adjective: **diagenetic**.
related adverb: **diagenetically**.

disarticulated adjective: (of a fossil) preserved with multiple body parts present but not in the relative positions they were in life.

compare with: **articulated**.
related noun: **disarticulation**.

dissoconch noun [plural: **dissoconches** when pronounced -kɒn(t)ʃɪz; **dissoconchs** when pronounced -kɒŋks]: (in bivalves) a postlarval shell.

Dissolved inorganic carbon; DIC noun Sum of the forms of inorganic carbon dissolved in seawater (carbonate, CO_3^{2-}; bicarbonate, HCO_3^-; carbon dioxide, H_2CO_3, CO_2)

distal adjective: away from the centre or origin of (e.g. an area of seepage).

compare with: **proximal**.
related adverb: **distally**.

durophagous adjective: feeding on organisms with hard parts such as corals, or animals with shells or exoskeletons.

related noun: **durophage**.
related noun: **durophagy**.

dysoxic adjective: describing an environment heavily depleted in a regular supply of respiratorily available oxygen.

dysphotic adjective: poorly illuminated, especially in reference to that region of the photic zone in a body of water that lies below the compensation level.

Ee

ecotope noun: that part of a biogeocoenosis that comprises evidence for the ancient habitat.

related adjective: **ecotopic**.

ectosymbiosis noun (plural: **ectosymbioses**): a type of symbiosis in which one of the symbionts (typically a parasite) lives on the body surface of the other.

compare with: **endosymbiosis**.
related noun: **ectosymbiont**.
related adjective: **ectosymbiotic**.

encrust verb: (of a shell) tightly attach to a rock or other solid substrate. Curiously, as a verb this is the more common spelling (see variant below), however as a noun *incrustation* is preferred to *encrustation*.

variant spelling: **incrust**.

encrustation variant spelling for: **incrustation**.

endemism noun: the condition of a taxon that is restricted to a particular habitat or environment, either in a geographical sense or in the sense of being unable to survive without a particular combination of prevailing conditions (e.g. endemic to New Zealand or endemic to the deep sea).

related adjective: **endemic**.
related noun: **endemicity**.

endolithic adjective: living within rock or other hard substrate.

endosymbiosis noun (plural: **endosymbioses**): a type of symbiosis in which one of the symbionts lives within the other.

compare with: **ectosymbiosis**.
related noun: **endosymbiont**.
related adjective: **endosymbiotic**.

eogenesis noun (plural: **eogeneses**): see **diagenesis**.

related adjective: **eogenetic**.

epifaunal adjective: living upon the sediment.

compare with: **infaunal**; **semi-infaunal**.
related noun: **epifauna** (plural: **epifauna**; **epifaunas**).
related adverb: **epifaunally**.

ex situ adverb: not in the original position or location. This term commonly occurs as *ex-situ* in the literature. It is not necessary to write it this way but not incorrect to do so if used in combination with a succeeding term to form a compound noun (e.g. *ex-situ occurrence* but never *occurring ex-situ*).

compare with: ***in situ***.
related adjective: ***ex situ***.

extremophilic adjective: describing organisms that can survive or even thrive in environments that are particularly harsh (e.g. high/low-temperature, radioactive, hypersaline, etc.) and can only support a relatively low biodiversity.

related noun: **extremophile**.

Ff

fabric noun: the arrangement of the features within a rock (e.g. minerals, fossils, strata, flow indicators) and the pattern they represent.

facies noun (plural: **facies**): the various attributes (e.g. compositional, biological, preservational condition) of a rock unit, series, etc. considered collectively in its description.

fauna noun (plural: **faunae**; **faunas**): the animals typical of a particular geographical region or a certain environment, habitat, etc., at any specified period of Earth history, considered as a group.

related adjective: **faunal**.
related adjective: **faunistic**.

favoured adjective: not obligate, i.e., regularly found also in other biotopes, but occurring in much larger densities in chemosynthetic environments.

compare with: **background; obligate; opportunistic**.

filter feeder noun: an organism that derives its nutrition from water by allowing seston to get caught in a filter-like structure, e.g., a crinoid pinna, as the water harbouring it passes through. Commonly such organisms occupy environments of adequate energy for water currents to naturally move the suspended material into their traps, but filter feeders do occupy quieter conditions, setting up their own water currents with structures such as flicking cilia.

variant term: **suspension feeder**.

forearc variant term: **arc–trench gap**.

variant spelling: **fore-arc**.

fore-arc variant spelling: **forearc**.

forearc basin noun: that part of the arc–trench gap that is adjacent to the island arc, characterized by flat-lying sediments which contrast starkly with the highly deformed accretionary wedge on the seaward side.

variant spelling: **fore-arc basin**.
compare with: **backarc basin**.

fore-arc basin variant spelling: **forearc basin**.

fossiliferous adjective: abounding in fossils.

Gg

gammaproteobacteria noun: a diverse class of Gram-negative proteobacteria.

geochemistry noun: the study of the chemical composition of rocks, water or air.

related adjective: **geochemical**.

related adverb: **geochemically**.

geomorphology noun: the study of the composition and morphology of landforms at the Earth's surface.

related adjective: **geomorphologic**.
related adjective: **geomorphological**.
related adverb: **geomorphologically**.

geopetal indicator noun: a feature within a rock unit that yields evidence for the upward direction in which the original sediment accumulated (the younging direction). Intuitively one would imagine a unit too young upwards, but tectonic events can fold large areas of the land and turn it upside-down completely, so geopetal indicators are very useful tools if present. Such indicators are often trace fossils and might be a U-shaped burrow, or rhizoliths extending from a particular boundary.

variant terms: **way-up indicator**; **younging indicator**.

grazer noun: an organism that feeds upon the surface of a soft sediment or mineral substrate, scraping away any nutritious material that crosses its path. Such organisms usually exhibit phobotactic behaviour to optimize their ability to obtain nutrients against energy expended.

related verb: **graze**.
related adjective: **grazing**.

guide fossil variant term: **zone fossil**.

Hh

hadal adjective: the deepest of the oceanic depth zones at >6000 m, lying mostly within the major trenches, extending down to the deepest known point, Challenger Deep (about 11,033 m) in the Mariana Trench, south-east of the Mariana Islands in the western Pacific.

compare with: **abyssal**; **bathyal**; **neritic**.
related adverb: **hadally**.

hadalbenthic variant term: **hadobenthic**.
hadalpelagic variant term: **hadopelagic**.
hadal zone see: **hadal**.
hadobenthic adjective: relating to the sea floor at hadal depths.

variant term: **hadalbenthic**.

hadopelagic adjective: relating to the open ocean in the hadal zone.

variant term: **hadalpelagic**.

heterotrophic adjective: describing those organisms that derive nutrition from the consumption of other organisms.

related noun: **heterotroph**.
related noun: **heterotrophy**.

homoplastic adjective: describing traits, such as the wings of birds and insects, that are similar in structure and function, but not in origin.

related noun: **homoplasy**.

hydrocarbon seep noun: a geological feature characterized by the release of fluids rich in methane and hydrogen sulfide from predominantly continental-margin sediments, usually diffusely over extensive areas, and at ambient temperatures.

variant term: **cold seep**.
compare with: **hydrothermal vent**.

hydrothermal vent noun: a geological feature characterized by the release of superheated fluids at sea-floor spreading centres, often from a sharply defined outlet such as a localized fissure or chimney-like conduit.

compare with: **hydrocarbon seep**.

Ii

ichnofossil noun: evidence for the behaviour of a once-living organism (especially a metazoan but also plants, fungi and other kingdoms) as preserved in the rock record. This evidence may come in the form of a boring, burrow, impression, track, trail, etc. It is not always clear as to the progenitor of a particular ichnofossil, and even when one can be identified (e.g. when accompanied by a somatofossil) it cannot be ruled out that another organism might produce the same sedimentary disruption.

variant terms: **biohieroglyph**; **trace fossil**.

ichnolithology variant term: **ichnology**.

ichnology noun: the study of trace fossils in their various aspects, e.g., nomenclature and/or palaeoenvironmental interpretation.

variant term: **ichnolithology**.
related adjective: **ichnologic**.
related adjective: **ichnological**.

incrust variant spelling: **encrust**.

incrustation noun: tight attachment of the shell or other hard part (e.g. a corallum) of a sedentary organism to a rock or other solid substrate, often resulting in the margin of the hard part moulding to the shape of the substrate surface and follow-

ing its irregularities. Curiously, as a noun this is the more common spelling (see variant below), however as a verb *encrust* is preferred to *incrust*.

variant spelling: **encrustation**.

index fossil variant term: **zone fossil**.

infaunal adjective: occupying a life position within a soft sediment. Those animals that inhabit soft sediments and only very rarely breach the surface, usually maintaining contact with the external environment (for respiratory purposes) with an elongated appendage such as a siphon. The vast majority are invertebrates that adopted this strategy chiefly in order to avoid predation.

compare with: **epifaunal**; **semi-infaunal**.
related noun: **infauna** (plural: **infauna**; **infaunas**).
related adverb: **infaunally**.

in situ adverb: in the original position or location.

compare with: ***ex situ***.

internal mould variant term: **steinkern**.

island arc noun: a series of subduction-related volcanoes lying landward of an oceanic trench, typically located roughly 100 km above the plate being subducted.

isometric adjective: describing the growth of an organism, e.g., a typical bivalve, that does not result in any significant change in relative dimensions throughout ontogeny.

compare with: **allometric**.
related adverb: **isometrically**.

isopachous adjective: having consistent thickness, e.g., of rock strata.

Kk

kelp fall noun: the organic loading of the sea floor by a large mat of fallen algal material, which may support a small and non-diverse ecosystem at depth for a short period.

compare with: **whale fall**; **wood fall**.

Ll

larval shell adjective: (in Mollusca) the hard parts of a pelagic larva before it settles down and undergoes metamorphosis.

lebensspur noun (plural: **lebensspuren**): a sedimentary structure of organic origin, having been created by a living organism as it interacted with the sediment and

including bioturbation structures such as various trace fossils and biostratification structures such as stromatolites. For many workers this term is restricted to modern traces.

variant terms: **biogenic sedimentary structure**; **organic sedimentary structure**.

lecithotrophic adjective: of larvae that depend on a reserve of egg-yolk nutrition supplied by the mother as they develop through metamorphosis.

related noun: **lecithotroph**.
related noun: **lecithotrophy**.

limestone noun: essentially, a rock made up of calcium carbonate ($CaCO_3$), usually calcite or aragonite. For a more specific description of the limestones discussed in this book, see: **seep carbonate**.

lithofacies noun (plural: **lithofacies**): the overall clastic and/or chemical signature of a given sedimentary environment.

lithogenic adjective: describing a substance derived from pre-existing terrigenous rock.

related noun: **lithogenesis** (plural: **lithogeneses**).
related adverb: **lithogenically**.

Mm

macrofauna noun (plural: **macrofauna**; **macrofaunas**): a category into which larger animals are placed, including most Aves, Amphibia, Mammalia, Reptilia, etc., and also sometimes includes the larger Insecta.

compare with: **megafauna**; **meiofauna**; **mesofauna**; **microfauna**.
related adjective: **macrofaunal**.

macrofossil noun: a fossil that can be seen with the naked eye, without the need for a microscope.

compare with: **microfossil**.
related adjective: **macrofossiliferous**.

marginal basin variant term for: **back-arc basin**.

matrix noun (plural: **matrices**): the fine-grained background constituent of a rock that supports larger grains in place.

megafauna noun (plural: **megafauna**; **megafaunas**): a category into which mostly Mammalia, and certain Reptilia are placed, especially in reference to that of the savannah in Africa were gigantism appears to be an evolutionary trait.

compare with: **macrofauna**; **meiofauna**; **mesofauna**; **microfauna**.
related adjective: **megafaunal**.

meiofauna noun (plural: **meiofauna; meiofaunas**): a term applied to minute organisms (0.063–0.5 mm in size) living in soil or benthic sediments.

compare with: **macrofauna**; **megafauna**; **mesofauna**; **microfauna**.
related adjective: **meiofaunal**.

mesofauna noun (plural: **mesofauna**; **mesofaunas**): a term applied to very small organisms (0.1–2 mm in size) living in soil or benthic sediments.

compare with: **macrofauna**; **megafauna**; **meiofauna**; **microfauna**.
related adjective: **macrofaunal**.

mesogenesis noun (plural: **mesogeneses**): see **diagenesis**.

related adjective: **mesogenetic**.

mesophilic adjective: describing organisms that thrive in environments with moderate temperature.

related noun: **mesophile**.

methane-oxidizing adjective: describing methanotrophic micro-organisms (bacteria or archaea) that metabolize methane as their source of carbon and unlock the energy of oxygen, nitrate, sulfate or other oxidized species.

methane seep noun: a commonly used term more or less interchangeable with *hydrocarbon seep*, where methane is the dominant hydrocarbon involved, as is typical.

methanogenic adjective: producing methane.

related noun: **methanogen**.

methanotrophic adjective: describing those bacteria or archaea that directly utilize methane for nutrition.

related noun: **methanotroph**.
related noun: **methanotrophy**.

microbial consortium noun (plural: **microbial consortia**): a community of two or more microbial groups living in symbiosis with one another.

microbial mat noun: a thin layer of bacteria and archaea (sometimes just bacteria) that forms at the interface of distinct materials in a variety of environments.

microfossil noun: a fossil that is only visibly recognizable and describable through employment of a microscope.

compare with: **macrofossil**.
related adjective: **microfossiliferous**.

microstucture noun: the fine layered structure observable in cross section of, e.g., a shell or worm tube at the microscopic level.

related adjective: **microstructural**.

mineralogy noun: **1.** the study of minerals, with particular attention paid to chemical, structural (crystal) and physical properties. **2.** the mineral composition of a given rock, unit, etc.

related adjective: **mineralogic**.
related adjective: **mineralogical**.
related adverb: **mineralogically**.

mixotrophic adjective: describing organisms that derive nutrition from a variety of energy sources, and are not reliant upon one particular trophic mode.

related noun: **mixotroph**.
related noun: **mixotrophy**.

molecular fossil variant term for: **biosignature**.

monophyletic adjective: belonging to a group in which the members are all descended from a single ancestor.

compare with: **paraphyletic**.
related noun: **monophyly**.

morphogenesis variant term (plural: **morphogeneses**) for: **ontogeny**.

related adjective: **morphogenetic**.

motile adjective: able to move freely between life sites.

related noun: **motility**.

mud volcano noun: a dome-shaped feature formed as a result of the ejection of fine solids suspended in water from deep within the sediment. Gases are also expelled in the process, predominantly methane.

muscle scar noun: the impression left on the interior of a shell (e.g. of a bivalve), reflecting the position of the muscle in life. Since soft tissues are rarely preserved in fossils, muscle scars are very important in identifications of many fossil groups.

mutualism noun: an interaction between members of two different species that benefits both.

compare with: **commensalism**; **neutralism**; **parasitism**.
related adjective: **mutualistic**.

Nn

nektobenthic adjective: applied to organisms that can swim freely but maintain a life position on or near the sediment–water interface (sea or lake floor).

related noun: **nektobenthos**.

nekton noun: those organisms that are able to swim freely within a body of water.

related adjective: **nektonic**.

neritic adjective: applied to that part of the ocean extending down to 200 m, with the upper limit governed by the level of low tide. It is the zone that is most

densely and diversely populated by marine benthos, due to the ability of sunlight to penetrate it.

compare with: **abyssal**; **bathyal**; **hadal**.
related adverb: **neritically**.

Oo

obligate adjective: confined to living in one particular type of environment.

compare with: **background**; **opportunistic**.

oligotrophic adjective: describing an environment that has a poor supply of nutrients, or an organism capable of surviving in such environments.

related noun: **oligotroph**.
related noun: **oligotrophy**.

ontogenesis variant term (plural: **ontogeneses**) for: **ontogeny**.

related adjective: **ontogenetic**.

ontogeny noun: the development of an organism from the time of fertilization through to maturity, e.g., the various stages in the life of a frog.

variant terms: **morphogenesis**; **ontogenesis**.
related adjective: **ontogenic**.

opportunistic adjective: describing an organism that is not obligate/specialized to a particular environment, but can still take advantage of its resources.

compare with: **background**; **obligate**.
related adverb: **opportunistically**.

organic fall noun: an umbrella term for any relatively large sunken mass of organic origin that can support an ecosystem, e.g., whale falls, wood falls and kelp falls.

organic sedimentary structure variant term for: **lebensspur**.

organoclastic adjective: relating to chemical breakdown by reaction with organic matter. The term is used almost exclusively in reference to organoclastic sulfate reduction, compared to anaerobic oxidation of methane.

see also: **anoxia**.

oxic adjective: characterized by the presence of respiratorily available oxygen.

see also: **anoxia**.

Pp

palaeo-combining form: meaning ancient, and used chiefly to describe something studied in the context of Earth history which has modern day analogues (e.g. palaeoenvironment; palaeomagnetism.

variant spelling: **paleo-** (applicable to all following **palaeo-** entries).

palaeobathymetry noun: **1.** ancient water depth; the estimated depth on the floor of a body of water at which the sediments creating a rock unit were deposited.

see also: **palaeodepth**.

2. a scientific discipline aimed towards the measurement of past bodies of water, useful in reconstructing palaeogeographic maps of the Earth over time. This is done chiefly by identifying which rocks were laid down in a subaqueous environment and gauging the likely time of their occurrence, plus their original position.

related adjective: **palaeobathymetric**.

palaeobiogeography see: **palaeogeography**.

related adjective: **palaeobiogeographic**.
related adjective: **palaeobiogeographical**.

palaeodepth noun: the depth at which sediments (usually marine) are inferred to have been deposited. This term is more or less a synonym of *palaeobathymetry* (sense 1), but is generally considered as a less precise term, e.g., the palaeodepth may be described as bathyal, but not given a more precise depth range.

palaeoecology noun: the application of ecological concepts to fossil and sedimentary evidence in order to study the interactions of the Earth's surface, atmosphere and biosphere at a given prehistoric time and location.

related adjective: **palaeoecologic**.
related adjective: **palaeoecological**.

palaeoenvironment noun: a past environment, usually in reference to a particular geographical region, which can be inferred from a wide range of palaeontological evidence.

related adjective: **palaeoenvironmental**.

palaeogeography noun: the study of changes in the distribution of landmasses and organisms, which have occurred over geological history. The physical elements of this research field are more specifically called *palaeogeomorphology*, and the biological aspects are called *palaeobiogeography*.

related adjective: **palaeogeographic**.
related adjective: **palaeogeographical**.

palaeogeomorphology see: **palaeogeography**.

related adjective: **palaeogeomorphologic**.

related adjective: **palaeogeomorphological**.

palaeoceanography noun: the study of the distribution and composition of ancient oceans.

related adjective: **palaeoceanographic**.
related adjective: **palaeoceanographical**.

palaeontology noun: the study of fossil remains.

compare with: **neontology**.
related adjective: **palaeontologic**.
related adjective: **palaeontological**.

paleo**-** variant spelling: **palaeo-**.

paragenesis noun (plural: **parageneses**): the sequence in which minerals form within a rock; it is an important concept in tracking the geological history of rock alteration and formation.

related adjective: **paragenetic**.

paraphyletic adjective: belonging to a group in which the members are mostly descended from one single ancestor but for the exception of a small number of outlying monophyletic subgroups.

compare with: **monophyletic**.
related noun: **paraphyly**.

periostracum noun (plural: **periostraca**): a protective outer layer of chitin found on the exterior of the shells of many mollusc groups, serving as protection from corrosion.

related adjective: **periostracal**.

petrography noun: the study of the mineral composition of rocks by use of thin section observation under a microscope.

related adjective: **petrographic**.
related adjective: **petrographical**.
related adverb: **petrographically**.

petrology noun: the study of rocks, its various subdisciplines considered as a whole.

related adjective: **petrologic**.
related adjective: **petrological**.
related adverb: **petrologically**.

photic zone noun: that relatively shallow part of a body of water that allows sunlight to penetrate; the depth of the photic zone varies according to different qualities of the water but typically goes no deeper than c. 200 m.

photoautotrophic adjective: describing a type of autotrophy in which the organism directly utilizes light and inorganic carbon for nutrition and the synthesis of more complex, organic molecules.

related noun: **photoautotroph**.
related noun: **photoautotrophy**.

phylogenetic adjective: relating to the evolutionary history and diversification/proliferation of a group of organisms.

related adverb: **phylogenetically**.
related noun: **phylogeny**.

phytoplankton noun: that part of the plankton that is made up of plants or plant-like organisms. They are a very important component of the global autotrophic community.

compare with: **zooplankton**.
related noun: **phytoplankter**.
related adjective: **phytoplanktonic**.

plankton noun: a collective term for those organisms without the means to locomote independently and are carried along with tides and currents as drifters.

related noun: **plankter**.
related adjective: **planktonic**.

planktotrophic adjective: of larvae that feed on plankton as they develop through metamorphosis.

related noun: **planktotroph**.
related noun: **planktotrophy**.

prodissoconch noun [plural: **prodissoconches** when pronounced -kɒn(t)ʃɪz; **prodissoconchs** when pronounced -kɒŋks]: (in bivalves) a shell secreted by the larva or embryo and preserved at the umbo of some adult shells. It is separated into two stages: *prodissoconch I* (or *protostracum*) being the earlier-formed part, secreted by a shell gland of the larva, and *prodissoconch II* being the later-formed part, secreted by the mantle edge.

protoconch noun [plural: **protoconches** when pronounced -kɒn(t)ʃɪz; **protoconchs** when pronounced -kɒŋks]: (in gastropods) a collective term for the earlier, apical whorls of the shell, especially where clearly demarcated from the later ones.

compare with: **teleoconch**.

protostracum noun (plural: **protostraca**): see **prodissoconch**.

related adjective: **protostracal**.

pseudofossil adjective: a feature in the rock record that is an artefact of inorganic processes but coincidentally mirrors a true fossil, and is often taken to be one under such ostensible evidence.

Rr

rare earth elements noun: one of the set of elements of the lanthanide group with atomic numbers ranging from 57 to 71. abbreviation: **REE**.

recrystallization noun: the process by which the original material the body parts of a fossilized organism were composed of has been altered during diagenetic and taphonomic processes into another material, which obliterates its microstructure; this process is very common among vent and seep fossils.

related verb: **recrystallize**.
related adjective: **recrystallized**.

reducing adjective: describing an environment where oxygen is removed by any of various processes, thus preventing any significant oxidation.

REE abbreviation: **rare earth elements**.

refugium noun (plural: **refugia**): a climatically and/or environmentally stable, isolated location that undergoes or has undergone little change whilst contemporaneous habitats have, providing its flora and fauna with effective shelter from extinction or mass migration events;

related adjective: **refugial**.

Ss

SAC abbreviation: **seep-associated concretion**.

sclerochronology noun: an analysis that focuses on the growth patterns of the hard parts of organisms, observing changes over time in varying increments according to the aims of the study and material used.

related adjective: **sclerochronological**.

seagrass noun: a grass-like plant that grows in the marine environment; the term usually refers to the underwater 'fields' or 'beds' that they form, which are commonly able to support a chemosynthetic fauna.

variant spelling: **sea grass**.

sea grass variant spelling of: **seagrass**.

sediment–water interface noun: the boundary between bottom sediments and the overlying water; essentially, the ocean, sea or lake floor.

abbreviation: **SWI**.

seep-associated concretion noun: a calcium carbonate concretion associated with seep deposits. These range widely in shape but generally are spherical to subspherical and are relatively small in size.

abbreviation: **SAC**.

sedentary adjective: applied to an organism that lives attached to a substrate but is still capable of a range of limited movement.

compare with: **sessile**; **vagile**.
related adverb: **sedentarily**.

sedimentology noun: the study of the various attributes of sedimentary rocks (e.g. physical and chemical make-up, formation, depositional environment, etc.).

related adjective: **sedimentologic**.
related adjective: **sedimentological**.
related adverb: **sedimentologically**.

seep carbonate noun: a limestone pod, of variable extent from a boulder to several kilometres of outcrop, usually occurring within a larger extent of surrounding mudstone, that represents a calcareous hardground that was formed in a hydrocarbon seep environment on the palaeocean floor. They are commonly marked by distinctive palaeontological and petrographic features, such as chemosynthetic faunal content and fibrous aragonite. They also have distinct isotopic features associated with reduced methane, and are sometimes recognized in the field by the release of a strong hydrocarbon smell upon striking.

variant spelling: **seep-carbonate**.

seep-carbonate variant spelling: **seep carbonate**.

semi-infaunal adjective: occupying a life position that is partially infaunal and partially epifaunal.

related adverb: **semi-infaunally**.

sessile adjective: (of an organism) not able to locomote freely; permanently attached to a solid substrate.

compare with: **sedentary**; **vagile**.
related noun: **sessility**.

siliceous adjective: composed primarily of silica.

SMTZ abbreviation: **sulfate–methane transition zone**.

somatofossil variant term: **body fossil**.

steinkern noun [plural: **steinkerne**; (less correctly) **steinkerns**]: a type of fossil in which the internal features are preserved, but the outer layers (e.g. shelly material) is mostly absent.

variant term: **internal mould**.

stratigraphy noun: the study of rock strata, i.e., the changes in mineral, chemical and biological composition observable throughout a sequence of rock layers. It is an essential aspect of geology in determining the age and palaeoenvironmental shifts through geological time, among many other applications.

related adjective: **stratigraphic**.
related adjective: **stratigraphical**.
related adverb: **stratigraphically**.

subduction zone noun: the zone, at an angle to the Earth's surface, down which a lithospheric plate descends beneath an adjacent plate.

subfossil noun: the partially preserved bodily remains of an organism, for which the fossilization process has not been fully completed, usually due to time constraints as opposed to the absence of appropriate preservation conditions. Subfossils tend not to occur in sediments any older than the Pleistocene because if fossilization conditions were inadequate, all traces of the organism would be obliterated over longer time frames.

substrate noun: the living environment of an organism or ecosystem, usually used in reference to the surface of a medium (e.g. a hardground or softground) on which the organism grows.

variant term: **substratum**.
related adjective: **substratal**.

substratum variant term (plural: **substrata**) for: **substrate**.

sulfate noun: a polyatomic anion, SO^{2-}.

variant spelling: **sulfate** (the non-IUPAC spelling).
related adjective: **sulfatic**.

sulfate-reduction noun: a term applied to the process by which micro-organisms perform anaerobic respiration utilizing sulphate as a terminal electron acceptor, reducing it to hydrogen sulphide. Also termed **organoclastic sulphate reduction (OSR)**

sulfate–methane transition zonenoun: zone in anoxioc sediments or water column in which both dissolved sulphate and methane co-exist and anaerobic oxifation of methane can occur.

abbreviation: **SMTZ**.

sulphate variant spelling for: **sulfate**.

related adjective: **sulphatic**.

suspension feeder variant term: **filter feeder**.

SWI abbreviation: **sediment-water interface.**

symbiosis noun (plural: **symbioses**): a close and often life-long biological association between organisms of different species.

related noun: **symbiont**.
related noun: **symbiotic**.
related adverb: **symbiotically**.

sympatry noun: the phenomenon of different species (or higher taxa) being found together in the same area. The differences between closely related species usually increase (diverge) when they occur together, in a process called character displacement, which may be ecological or morphologic.

compare with: **allopatry**.
related adjective: **sympatric**.

syntrophic noun: describing a trophic relationship in which one or more organisms feeds off the nutrients provided by the other(s).

related noun: **syntroph**.
related noun: **syntrophy**.

systematics noun: the science of classification of organisms through observations of their genetic, morphological and evolutionary relationships; similar to *taxonomy*.

related adjective: **systematic**.
related adjective: **systematical**.
related adverb: **systematically**.

Tt

taphonomy noun: a term used for any of the multitude of pathways by which an organism might decay upon burial, a detailed understanding of which is essential in drawing conclusions as to the biology, ecology, etc., of extinct specimens.

related adjective: **taphonomic**.
related adverb: **taphonomically**.

taxonomy noun: the theory and practice of classifying organisms. Despite being a well-accepted universal term amongst authors often proficient in Latin, in fact, from its base roots it should more correctly be spelled *taxinomy*, but this has never been the more popular choice.

related adjective: **taxonomic**.
related adverb: **taxonomically**.

teleoconch noun [plural: **teleoconches** when pronounced -kɒn(t)ʃɪz; **teleoconchs** when pronounced -kɒŋks]: (in gastropods) the entire shell, exclusive of the protoconch.

compare with: **protoconch**.

telogenesis noun (plural: **telogeneses**): see **diagenesis**.

related adjective: **telogenetic**.

terrigenous adjective: describing a marine sediment that was derived from deposits originally formed in a terrestrial environment (onland), usually by erosion.

thermogenic adjective: produced as a result of reactions driven by elevated temperatures. In seep parlance this term is usually found in reference to the formation of methane.

related adverb: **thermogenically**.

thermophilic adjective: describing organisms that can survive or even thrive in relatively high-temperature environments.

related noun: **thermophile**.

thiotrophic adjective: describing those bacteria that directly utilize sulfate for nutrition.

related noun: **thiotroph**.
related noun: **thiotrophy**.

trace fossil a variant term for: **ichnofossil**.

tubicolous adjective: living within a self-constructed tube or tube-like structure, as in tubeworms; tube-dwelling.

related noun: **tubicole**.

Vv

vagile adjective: tending to move around within a given environment; free-moving, as an animal that is not fixed in a particular life position.

compare with: **sedentary**; **sessile**.
related noun: **vagility**.

VPDB (Vienna Peedee Belemnite) noun: an international standard established for carbon and oxygen isotope analyses of carbonates and carbon in other carbon reservoirs such as dissolved inorganic carbon, organic matter and methane. It is based on a Cretaceous fossil, *Belemnitella americana,* known from the Peedee Formation in South Carolina, USA.

VSMOW (Vienna Standard Mean Ocean Water) noun: an international standard established for oxygen (and hydrogen) isotope analyses, principally of water.

Ww

way-up indicator variant term for: **geopetal indicator**.

whale fall noun: a whale that has perished in the open ocean and sunk to the sea floor, providing a point source of organic enrichment to an otherwise relatively oligotrophic environment. The sudden availability of such nutrients is typically taken advantage of by a diverse range of organisms, that often establish complex communities based upon chemosynthesis with bacteria that are able to utilize bone lipids, especially on larger carcasses (e.g. adult blue whales).

compare with: **kelp fall**; **wood fall**.

wood fall noun: an instance of large organic loading of the sea floor, where a tree or log has fallen through the water column, coming to rest on the sediment. Wood falls are able to support small biological communities, which colonize the area over a period of years to decades, taking advantage of the reducing and sulfide-rich environment that is produced at such sites.

compare with: **kelp fall**; **whale fall**.

Yy

younging indicator variant term: **geopetal indicator**.

Zz

zone fossil noun: a type of fossil that can be used to gauge the age of the unit in which it is found, due to its properties of being temporally restricted in its occurrence within the rock record. Such fossils usually also have to be relatively abundant in order to be useful. Many zone fossils are ammonites, which have relatively good preservational potential and shell patterns that are accurately traceable through time.

variant terms: **guide fossil**; **index fossil**.

zoocenose variant term: **zoocoenosis**.

zoocenosis variant spelling (plural: **zoocenoses**): **zoocoenosis**.

zoocoenose variant term: **zoocoenosis**.

zoocoenosis noun (plural: **zoocoenoses**): the part of a biocoenosis that is represented by metazoans.

variant spelling: **zoocenosis**.
variant term: **zooc(o)enose**.

zooplanktonnoun: that part of the plankton that is made up of heterotrophic organisms.

compare with: **phytoplankton**.
related noun: **zooplankter**.
related adjective: **zooplanktonic**.

References

Allaby A, Allaby M (1999) Oxford Dictionary of Earth sciences. Oxford University Press, Oxford, vii + 619 pp

Bates RL, Jackson JA (1980) Glossary of geology, 2nd edn. American Geological Institute, Falls Church, x + 715 pp

Bates RL, Jackson JA (1987) Glossary of geology—Third edition. American Geological Institute, Alexandria, Virginia, x + 788 pp

Gary M, McAfee R Jr, Wolf CL (1972) Glossary of geology. American Geological Institute, Washington, DC, xiv + 805 + A-52 pp

Lapidus DF, Winstanley I (1990) Collins Dictionary of Geology. HarperCollins, London, 565 pp

Pearsall J (1998) The New Oxford Dictionary of English. Oxford University Press, Oxford, xxi + 2152 pp

Index

A. Kaim et al. (eds.), *Ancient Hydrocarbon Seeps*, Topics in Geobiology 50,
https://doi.org/10.1007/978-3-031-05623-9

N